University of Ghana http://ugspace.ug.edu.gh

STUDIES ON THE ARTEMISININ RESISTOME OF *PLASMODIUM FALCIPARUM* AND THE ROLE OF EXTRACELLULAR VESICLES IN THE DEVELOPMENT OF ANTIMALARIAL DRUG RESISTANCE

THIS THESIS IS SUBMITTED TO THE UNIVERSITY OF GHANA, LEGON IN PARTIAL FULFILMENT OF THE REQUIREMENT FOR THE AWARD OF PHD IN MOLECULAR CELL BIOLOGY OF INFECTIOUS DISEASE DEGREE

BY

KWESI ZANDOH TANDOH
(10172044)

OCTOBER 2022

University of Ghana http://ugspace.ug.edu.gh

DECLARATION

I, Kwesi Zandoh Tandoh, declare that the work presented in this thesis was done by me at the Department of Biochemistry of Cell and Molecular Biology, University of Ghana, under the supervision of Prof. Nancy O. Duah Quashie (Department of Epidemiology, Noguchi Memorial Institute for Medical Research, College of Health Sciences, University of Ghana, Legon), Professor Michael D. Wilson (Department of Parasitology, Noguchi Memorial Institute for Medical Research, College of Health Sciences, University of Ghana, Legon), and Professor Neils B. Quashie (Centre for Tropical Clinical Pharmacology and Therapeutics, University of Ghana Medical School, College of Health Sciences, University of Ghana, Legon); and at the Institute for Bioengineering of Catalonia (IBEC) Nanomalaria joint group under the invitation of Professor Xavier Fernandez-Busquets. All references have been duly cited.

……10th November, 2022……..

Kwesi Zandoh Tandoh — Date

(Candidate)

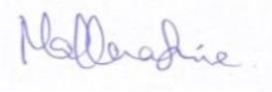

……. ……10th November, 2022……..

Professor Nancy O. Duah Quashie — Date

(Supervisor)

……10th November, 2022……..

Professor Michael D. Wilson — Date

(Supervisor)

……..7TH December 2022 ……

Professor Neils B. Quashie — Date

(Supervisor)

University of Ghana http://ugspace.ug.edu.gh

ACKNOWLEDGMENTS

I owe the accomplishment of this work to several people who helped me to complete this thesis. I am forever indebted and deeply grateful for their supervision, mentorship, friendship, and acquaintance. First, I am deeply grateful to my supervisorial team: Prof. Nancy O. Duah Quashie, Prof. Michael D. Wilson, and Prof. Neils B. Quashie. This bespoke team was the ideal composition for me to explore that creative side of my skills set within the supervised latitude they gifted me. With this team, I easily discussed ideas and shared the burden of troublesome experiments during my PhD journey. No matter the problem, they helped me remain focused and deliver on set goals. I am deeply grateful to them. Secondly, I am deeply indebted to Prof. Gordon Awandare who officially introduced me to my lead supervisor Prof. Nancy Quashie at the beginning of what has turned out to be my PhD project. I thank him deeply for his generous spirit. In hindsight, it was after my first meeting with Prof. Awandare that I decided to commit to a post graduate course in molecular cell biology of infectious diseases. I will always be in his debt. I wish to also express my gratitude to Prof. Amos Laar (School of Public Health) who introduced me to Prof. Gordon Awandare in 2016.

To the members of the molecular epidemiology laboratory (room 121, NMIMR), I say thank you especially to Mr. Felix Zoiku, who introduced me to *in vitro* cultures. I also thank Mr. Prince Ato Donkor, Mr. Prince Fordjour and Mr. Bright Asare. My deepest gratitude also goes to Mrs. Sena Matrevi, Mr. Philip Opoku-Agyemang, Ms. Selasie Bruku and Ms. Tryphena Adams. I also thank Dr. Oheneba C. Hagan for generating the transgenic parasite lines I used in objective 2 of my work, and Dr. Samuel Y. Ahorhorlu and Dr. Charles Ejiofor for their encouragement and support throughout my program. I thank the staff, faculty and students of BCMB, WACCBIP and BANGA. Coming from an MPhil to a PhD upgrade, I am a product of the quality of tutelage and mentorship that drives BCMB and WACCBIP. In this regard, I am especially grateful to Prof. Osbourne Quaye, Dr Kwadwo Asamoah Kusi, Dr.

University of Ghana http://ugspace.ug.edu.gh

Lydia Mosi, Dr Y. Aniweh, Dr. E. Amlabu and Dr. P. Arthur. As lecturers they indelibly influenced me into the product I am today. I thank them deeply. I am also grateful to Prof. David Conway and Dr. Lucas Amenga-Etego who sparked my interest in parasite population genetics. I am also deeply grateful to the members of the cell biology and immunology laboratory. I thank Dr. Y. Aniweh again for his generosity in accommodating me. I also owe the utmost gratitude to Mr. Jersley D. Chirawurah, Ms. Bridget Adikah, Mr. Daniel Dosoo, and Mr. Jacob Donkor. I also thank the following members of the Bioinformatics laboratory: Mr. Collins M. Morang'a and Mr. Vincent Appiah for helping me get a working knowledge of next generation sequencing data analysis. I am also deeply grateful to Ms. Sika Menka, Ms. Marian Nanor and Ms. Sarah Ofori for doing their jobs so well and lightening the burden of a PhD for some of us. I would also like to thank my PhD class mates for their camaraderie during this PhD journey.

I wish to thank Prof. Xavier Fernàndez Busquets (head of Nanomalaria joint unit), Institute for Bioengineering of Catalonia (IBEC) for giving me opportunity to visit his laboratory for objective three of my PhD work. In this regard, I also thank Dr. Yunuen Avalos Padilla and Ms. Miriam Ramirez for making my stay and work in their laboratory fruitful. I am also grateful to have made the acquaintance of Dr. Valentin Iglesias, Ms. Lucia Roman, Mr. Omar Prades, Ms. Emma Portabella, Ms. Federica Fulgheri and Mr. Timen Mooren – who made my stay in Barcelona memorable. I am grateful to Professor David A. Fidock and his team, of Columbia University Irving Medical Center, for gifting me the transgenic parasite lines I used for objective 3 of my work. I am also deeply grateful for the generosity of Dr. Mauro Muraro of Single cells discovery, The Netherlands and Dr. Abel Vertesy for introducing me to RNA sequencing data analysis in 2018.

Finally, and most importantly, I thank God for his goodness and grace; and my wife, Akua Tandoh, for her unyielding support throughout this journey.

TABLE OF CONTENTS

University of Ghana http://ugspace.ug.edu.gh

DECLARATION…….. i
ACKNOWLEDGMENT…….. ii
TABLE OF CONTENTS……. iv
LIST OF FIGURES……. viii
LIST OF TABLES……. x
LIST OF ABBREVIATIONS……... xi
ABSTRACT……. xv
CHAPTER ONE……. 1
GENERAL INTRODUCTION……....1
1.1 Introduction……... 1
1.2 Problem Statement…… 6
1.3 Justification……... 7
1.4 Hypotheses……... 8
1.5 General Objective …… 9
1.5.1 Specific Objectives…… 9
CHAPTER TWO…….. 10
LITERATURE REVIEW……. 10
2.1 Malaria Burden and Epidemiology…… 10
2.2 Life Cycle And Biology of *Plasmodium falciparum*…… 13
2.3 Malaria Case Management, Vector Control and Molecular Surveillance…….. 17
2.4 Greater Mekong Subregion of Southeast Asia: The Ground Zero of Antimalarial Drug Resistance development …… 19
2.4.1 What Factors May Contribute to the GMS Hotbed for Antimalarial Drug Resistance? …… 20
2.5 *Plasmodium falciparum* Population Genomics and Genetics…… 24
2.5.1 Measures of population variation…… 26
2.5.2 The *Plasmodium falciparum* genome…….. 32
2.5.3 Leveraging population genetics and genomics for molecular surveillance of ART resistance…… 33
2.6 Artemisinin: Mechanism of Action and Targets…… 35
2.7 Artemisinin Resistance……..... 38
2.7.1 *PfK13* variants take center-stage as molecular markers of artemisinin resistance…….. 40
2.7.2 Patterns in the geographic distribution of *PfK13* variants have been observed in the GMS of SEA……... 43
2.8 Molecular Mechanisms Undergirding Artemisinin Resistance…….. 45
2.8.1 The *PfK13* interactome: a window into the multiple cellular processes undergirding artemisinin resistance…….. 51
2.8.2 The digestive food vacuole and artemisinin resistance…… 54
2.9 The Artemisinin Resistome…… 56
2.9.1 *Plasmodium falciparum* ubiquitin carboxyl-terminal hydrolase 1…….. 56
2.9.2 Adaptor protein complex 2 mu subunit……... 57
2.9.3 *Plasmodium falciparum* kelch 13……... 57
2.9.4 Artemisinin Resistance Outside *Pfk13* Variants…….. 59
2.9.5 Background Art Resistome…….. 60
2.10 Extracellular Vesicles……... 61
2.10.1 EVs biogenesis in *Plasmodium falciparum*……... 66
CHAPTER THREE……. 69
Plasmodium falciparum Malaria Parasites in Ghana Show Signatures of Balancing Selection at Artemisinin Resistance Predisposing Background Genes……... 69
3.1 Abstract……71
3.2 Introduction……..72
3.3 Results……..76
3.3.1 Multiplicity of infection……76
3.3.2 *P. falciparum* population structure…….. 78
3.3.3 Summary of genomic diversity among single clone infections……... 80
3.3.4 *PfK13* ARTr genome background loci under balancing selection……... 83
3.4 Discussion……90
3.5 Methods……... 94
3.5.1. Sequencing and genotyping…… 94
3.5.2. Hard filtering pipeline of Ghana 2009/2010 clinical isolates variants……95

3.5.3. Evaluation of multiplicity of infection (MOI) and population structure…… 96
3.5.4 Tests for departures from neutrality……96
CHAPTER FOUR…… 98
Implicating Extracellular Vesicles in *Plasmodium falciparum* Artemisinin Resistance Development……... 98
4.1 Abstract…… 100
4.2 Introduction…….. .101
4.3 Extracellular Vesicles in Malaria Pathogenesis and *P. falciparum* Biology……103
4.4 Implicating EVs in *P. falciparum* ARTr Development……105
4.5 Conclusion……108
CHAPTER FIVE……110
Transcriptome-Module Phenotype Association Study Implicates Extracellular Vesicles Biogenesis in *Plasmodium falciparum* Artemisinin Resistance…… 110
5.1 Abstract…… 112
5.2 Introduction……... 113
5.3 Method…….. 116
5.3.1. Parasite lines and culture conditions…… 116
5.3.2. Parasite sensitivity assays to dihydroartemisinin…….. 117
5.3.3. DHA and DMSO exposures to parasite cultures……...119
5.3.4. RNA extraction, Library preparation and Next-Generation Sequencing…….. 120
5.3.5. Data Analysis…… 121
5.3.6 Modular analysis…… 122
5.3.7 Identification of differentially expressed genes between conditions…… 125
5.3.8 Gene ontology analysis…….. 125
5.4 Results……... 126
5.4.1 *P. falciparum* parasites susceptibility to DHA…….. 126
5.4.2 Quality check for integrity of extracted RNA and mapped reads of samples analyzed……...127
5.4.3 A module of EVs interest is associated with ART resistance in *P. falciparum*……...126
5.4.4 Analysis of differentially expressed genes reveals little insight into the role of EVs in *P. falciparum*……135
5.4.5 A complex heterogeneous transcript profile characterizes *P. falciparum* ARTr parasites……..144
5.5 Discussion……..147
CHAPTER SIX……153
Malaria Artemisinin Resistance: An Extracellular Vesicles Export Hypothesis……153
6.1 Abstract……..155
6.2 The burden of *P. falciparum* malaria and importance of artemisinin resistance……...156
6.3 The missing piece in the portrait of artemisinin resistance……157
6.4 Extracellular vesicles may play a role in artemisinin resistance……159
6.5 An extracellular vesicles export model of artemisinin resistance……..161
CHAPTER SEVEN……165
Extracellular vesicles abundance is positively correlated with dihydroartemisinin exposure in *Plasmodium falciparum* parasites……165
7.1 Abstract……..166
7.2 Introduction……167
7.3 Method……...169
7.3.1 *P. falciparum in vitro* parasite culture and treatment conditions……169
7.3.2 Ring stage survival analysis……170
7.3.3 EVs extraction and purification…… 171
7.3.4 EV size and abundance measurements……...173
7.4 Results……174
7.4.1 Determination of parasite sensitivity to artemisinin……...174
7.4.2 Size distribution of enriched EVs is similar among parasite lines for all conditions…….175
7.4.3 Treatment condition is a better predictor of EVs abundance compared to parasite line…… 177
7.4.4 DHA exposure is the strongest predictor of EVs abundance……..184
7.5 Discussion…… 187
CHAPTER EIGHT……..190
GENERAL DISCUSSION, CONCLUSIONS AND FUTURE DIRECTIONS……190
8.1 General Discussion……190
8.2 General Conclusions and Future Directions……..198
REFERENCES……199
APPENDICES……261
Appendix I……...261
Supplementary Table 3.1 Genome wide scan of all genes under balancing selection……267
Supplementary Table 3.2 Top ten percent of *P. falciparum* genomic positions

University of Ghana http://ugspace.ug.edu.gh

under balancing selection……297
Supplementary Table 3.3 Variants identified in genes of interest……301
Supplementary Table 3.4 Distribution of polymorphic sites for determination of McDonald–Kreitman test……...302
Supplementary Table 3.5 List of genes reported and known to be under balancing selection in *P. falciparum*……303
Supplementary Figure 3.1 PCA analysis for all samples (N = 617) ……. 304
Supplementary Figure 3.2 PCA analysis for samples with multiplicity of infections (N=344) ……305
Appendix II……306
Supplementary Table 5.1 Sample annotation file containing phenotype data for the twenty-seven samples used……306
Supplementary Table 5.2 Genes composition of modules identified using the WGCNA R package……307
Supplementary Table 5.3 Gene ontology tabular summary of module 0…….. 332
Supplementary Table 5.4 Gene ontology tabular summary of module 1…….. 336
Supplementary Table 5.5 Gene ontology tabular summary of module 3……...339
Supplementary Table 5.6 Gene ontology tabular summary of module 17……346
Supplementary Table 5.7 Gene ontology tabular summary of module 7……...349
Supplementary Table 5.8 List of differentially expressed genes (up- and down-regulated) between the conditions R539T_DMSO treated compared with R539T_DHA treated……..353
Supplementary Table 5.9 Gene ontology enrichment analysis for up/downregulated genes between R539T DMSO_treated and DHA_treated condition……. 354
Supplementary Table 5.10 List of differentially expressed genes (up- and down-regulated) between the conditions R539T_untreated compared with R539T_DHA treated…….. 357
Supplementary Table 5.11 Gene ontology enrichment analysis for up/down-regulated genes between R539T untreated and DHA_treated condition……364
Supplementary Table 5.12 List of differentially expressed genes (up- and down-regulated) between the conditions C580R_DMSO treated compared with C580R_DHA treated…….. 390
Supplementary Table 5.13 Functional prediction and gene ontology enrichment analysis for up/down-regulated genes between C580R DMSO_treated and DHA_treated condition……... 391
Supplementary Table 5.14 List of differentially expressed genes (up- and down-regulated) between the conditions C580R_untreated compared with C580R_DHA treated……... 395
Supplementary Table 5.15 Gene ontology enrichment analysis for up/downregulated genes between C580R untreated and DHA_treated condition……405
Supplementary Table 5.16 List of differentially expressed genes (up- and downregulated) between the conditions Dd2_DMSO_treated compared with Dd2_DHA treated……435
Supplementary Table 5.17 Gene ontology enrichment analysis for up/downregulated genes between Dd2 DMSO_treated and DHA_treated condition……..441
Supplementary Table 5.18 List of differentially expressed genes (up- and downregulated) between the conditions Dd2 untreated compared with Dd2_DHA treated……449
Supplementary Table 5.19 Gene ontology enrichment analysis for up/downregulated genes between Dd2 untreated and DHA_treated condition……...464
Supplementary Figure 5.1 Map of the plasmid vector pDC2-cam-co.Cas9-U6-hDHFR……500
Supplementary Figure 5.2 Design of donor DNA for *PfK13* genome editing……501
Supplementary Figure 5.3 Chromatographs showing analyses of genotyped transfectants……502
Supplementary Figure 5.4 *In vitro* RSA_{0-3} survival rates (%) for the ART Susceptible wild type *Plasmodium falciparum* strain (Dd2) and two *P. falciparum PfK13* ARTr variants (C580R and R539T) used in this study……503
Supplementary Figure 5.5 IC50 values for DHA for the ART susceptible wild type *Plasmodium falciparum* strain (Dd2) and two *P. falciparum PfK13* ARTr variants (C580R and R539T) used in this study……504
Supplementary Figure 5.6 Quality of extracted RNA integrity from the 27 samples used in this study……...505
Supplementary Figure 5.7 Quality of reads mapped to reference genome for all samples…….506
Supplementary Figure 5.8 Identification of surrogate variables……. 507
Supplementary Figure 5.9 Summary findings following interrogation of validity of the RNA sequenced data…..……. 508
Supplementary Figure 5.10 Properties of EVs module of interest module 1……. 509
Supplementary Figure 5.11 Properties of EVs module of interest module 3……. 510
Supplementary Figure 5.12 Properties of EVs module of interest module 17……... 511
Supplementary Data 5.1 Summary of GSEA output for R539T_DHA_treated

University of Ghana http://ugspace.ug.edu.gh

versus R539T_untreated showing association with module 0…… 512
Supplementary Data 5.2 Summary of GSEA output for R539T_DHA_treated versus R539T_DMSO_treated showing association with module 0…….. 513
Supplementary Data 5.3 Summary of GSEA output for R539T_DHA_treated versus Dd2_DHA_treated showing association with module 0…… 514
Supplementary Data 5.4 Summary of GSEA output for C580R_DHA_treated versus C580R_untreated showing association with module 0……... 515
Supplementary Data 5.5 Summary of GSEA output for C580R_DHA_treated versus C580R_DMSO_treated showing association with module 0……. 516
Supplementary Data 5.6 Summary of GSEA output for C580R_DHA_treated versus Dd2_DHA_treated showing association with module 0……... 517
Supplementary Data 5.7 Summary of GSEA output for Dd2_DHA_treated versus Dd2_untreated showing association with module 0…….. 518
Supplementary Data 5.8 Summary of GSEA output for Dd2_DHA_treated versus Dd2_DMSO_treated showing association with module 0……. 519
Supplementary Data 5.9 Summary of GSEA output for R539T_DHA_treated versus R539T_untreated showing association with module 7……... 520
Supplementary Data 5.10 Summary of GSEA output for R539T_DHA_treated versus R539T_DMSO_treated showing association with module 7……. 521
Supplementary Data 5.11 Summary of GSEA output for R539T_DHA_treated versus Dd2_DHA_treated showing association with module 7…… 522
Supplementary Data 5.12 Summary of GSEA output for C580R_DHA_treated versus C580R_untreated showing association with module 7……... 523
Supplementary Data 5.13 Summary of GSEA output for C580R_DHA_treated versus C580R_DMSO_treated showing association with module 7……. 524
Supplementary Data 5.14 Summary of GSEA output for C580R_DHA_treated versus Dd2_DHA_treated showing association with module 7…… 525
Supplementary Data 5.15 Summary of GSEA output for Dd2_DHA_treated versus Dd2_untreated showing association with module 7…….. 526
Supplementary Data 5.16 Summary of GSEA output for Dd2_DHA_treated versus Dd2_DMSO_treated showing association with module 7……. 527
Supplementary Data 5.17 Summary of gene ontology enrichment in the biological processes terms for DHA_treated condition compared to the untreated condition baseline……528
Appendix III…… 529
Supplementary Table 7.1 Summary data of EVs extraction experiment for all parasite lines and treatment conditions…… 529
Supplementary Table 7.2 Post-hoc Dunn's test for the RSA analysis for 3D7, Vps60 and R561H…… 531
Supplementary Table 7.3 Analysis of EVs size distribution by parasite lines……... 532
Supplementary Table 7.4 Tabular summary of simple linear regression model to determine strength of the association between parasite line (predictor/independent factors) and EVs abundance (response/dependent factor) for the untreated condition…….. 533
Supplementary Table 7.5 Tabular summary of simple linear regression model to determine strength of the association between parasite line (predictor/independent factors) and EVs abundance (response/dependent factor) for the 0.1% DMSO treated condition……534
Supplementary Table 7.6 Tabular summary of simple linear regression model to determine strength of the association between parasite line (predictor/independent factors) and EVs abundance (response/dependent factor) for the 700nM DHA treated condition……535
Supplementary Table 7.7 Tabular summary of simple linear regression model to determine strength of the association between treatment condition (predictor/independent factors) and EVs abundance (response/dependent factor) for the Vps60_KO parasite line……536
Supplementary Table 7.8 Tabular summary of simple linear regression model to determine strength of the association between treatment condition (predictor/independent factors) and EVs abundance (response/dependent factor) for the 3D7 parasite line……537
Supplementary Table 7.9 Tabular summary of simple linear regression model to determine strength of the association between treatment condition (predictor/independent factors) and EVs abundance (response/dependent factor) for the R561H parasite line……..538

University of Ghana http://ugspace.ug.edu.gh

LIST OF FIGURES

Figure		Page
Figure 2.1	*Plasmodium falciparum* life cycle showing targets of ACTs	15
Figure 3.1	Distribution of multiplicity of infection in the analyzed Ghanaian *P. falciparum* samples analyzed (n = 617).	77
Figure 3.2	*P. falciparum* population structure analysis of Ghana samples	79
Figure 3.3	Summary of SNPs characteristics	81
Figure 3.4	Distribution of SNPs effect across all genomic positions analyzed.	82
Figure 3.5	Genome-wide distribution of Tajima's D values summarizing the site frequency spectra for *P. falciparum* genes	84
Figure 4.1	The emergence of the ARTr phenotype depends on the presence of an ARTr conferring variant that is selected and successfully transmitted.	109
Figure 5.1	Properties of EVs module of interest module 0 (ME0).	130
Figure 5.2	Enrichment score behavior showing the distribution of module 0 (ME0) in the input list of ranked genes for the three compared treatment conditions with FDR < 0.25	134
Figure 5.3	Properties of EVs module 7 (ME7)	138
Figure 5.4	Enrichment score behavior showing the distribution of module 7 (ME7) in the input list of ranked genes for the three compared treatment conditions with FDR < 0.25	139
Figure 5.5	Differentially expressed genes (DEG) between compared conditions for the R539T parasite line.	141
Figure 5.6	Differentially expressed genes (DEG) between compared conditions for the C580R parasite line.	142
Figure 5.7	Differentially expressed genes (DEG) between compared conditions for the Dd2 parasite line.	143
Figure 5.8	Scatter plots showing the strength of the correlation between the two ARTr biological replicates (C580R and R539T) for the compared conditions	145
Figure 5.9	Principal component analysis (PCA) highlight the transcriptional heterogeneity undergirding the ARTr phenotype	146
Figure 6.1	Schematic summary of the extracellular vesicles export model of artemisinin resistance in *Plasmodium falciparum*.	162

University of Ghana http://ugspace.ug.edu.gh

Figure 7.1 Workflow for extracellular vesicles (EVs) extraction, purification, and abundance estimation 172

Figure 7.2 *In vitro* RSA0–3 parasite survival rates (%) for the ART susceptible WT *Plasmodium falciparum* strain (3D7), the *P. falciparum* PfK13 ARTr variants (R561H) and the *P. falciparum* Vps60 knock out (Vps60_KO) used in this study 175

Figure 7.3 Analysis of EVs size by parasite line and treatment condition factors. 176

Figure 7.4 Comparison of extracellular vesicles (EVs) abundance among parasite lines for each of the three conditions studied. 181

Figure 7.5 Comparison of extracellular vesicles (EVs) abundance between treatment conditions for each parasite line studied. 182

Figure 7.6 The strength of the association between treatment condition and parasite line and EVs abundance. 186

University of Ghana http://ugspace.ug.edu.gh

LIST OF TABLES

Table		Page
Table 2.1	The armamentarium of metrics for population diversity, selection, and linkage disequilibrium	30
Table 3.1	List of genes of interest reported to be associated with the genomic background for artemisinin resistance in *P. falciparum*	86
Table 3.2	Tests of neutrality on four genes of interest under balancing selection in Ghana population of *Plasmodium falciparum*.	87
Table 3.3	Summary of the number of SNPs and effect at loci of interest	89
Table 5.1	Genes of interest (GOI) involved in the biogenesis and export of extracellular vesicles (EVs) in *P. falciparum*	129
Table 5.2	Association of module 0 with the ARTr phenotype.	133
Table 5.3	Summary of gene ontology enrichment analysis of differentially expressed genes	140
Table 6.1	Summary of evidence from several studies and how they fit into the EVs export hypothetical model of ARTr compared to the two mainstream organizing principles of ARTr.	164
Table 7.1	Analysis of EVs abundance by parasite line and treatment condition factors.	178
Table 7.2	Post-hoc Dunn's test for the factors: parasite lines (3D7, Vps60 and R561H0) and treatment condition (untreated, DMSO treated, and DHA treated)	183
Table 7.3	Simple linear regression model to determine the strength of the association between parasite line and treatment condition (predictor/independent factors) and EVs abundance (response/dependent factor).	185

University of Ghana http://ugspace.ug.edu.gh

University of Ghana http://ugspace.ug.edu.gh

LIST OF ABBREVIATIONS

ACT	Artemisinin-based combination therapy
AL	Artemether-lumefantrine
ARMD	Accelerated resistance to multiple drugs
ART	Artemisinin
ARTr	Artemisinin resistant
AS-AQ	Artesunate-amodiaquine
AS-MQ	Artesunate-mefloquine
AS-PND	Artesunate-pyronaridine
AS-SP	Artesunate-sulfadoxine/pyrimethamine
ATP	Adenosine triphosphate
BLAST	Basic local assignment search tool
BWA	Burrows-Wheeler Aligner
CELTOS	Cell traversal protein for ookinetes and sporozoites
CQ	Chloroquine
CRISPR	Clustered regularly interspaced short palindromic repeats
CRT	Chloroquine resistance transporter
CSP	Circumsporozoite protein
DEG	Differentially expressed gene
DHA	Dihydroartemisinin
DHA-PQ	Dihydroartemisinin-piperaquine
DHFR	Dihydrofolate reductase
DMSO	Dimethyl sulfoxide
DNA	Deoxyribonucleic acid
ER	Endoplasmic reticulum
ERCC	External RNA Controls Consortium
ESCRT	Endosomal sorting complex required for transport
EVs	Extracellular vesicles
FDR	False discovery rate
FV	Food vacuole
G6PD	Glucose-6-phosphate dehydrogenase
GATK	Genome Analysis Tool Kit

University of Ghana http://ugspace.ug.edu.gh

GEST	Gamete egress and sporozoite traversal protein
GFP	Green fluorescent protein
GLM	Generalized linear model
GMS	Greater Mekong subregion
GO	Gene ontology
GOI	Genes of interest
GSEA	Gene set enrichment analysis
GTP	Guanosine triphosphate
GTS	Global technical strategy
GWAS	Genome wide association study
HEPES	4-(2-hydroxyethyl)-1-piperazineethanesulfonic acid
HKA	Hudson–Kreitman–Aguade test
HSPG	Highly sulfated proteoglycans
IBEC	Institute for Bioengineering of Catalonia
IC50	50% inhibitory concentration
ILV	Intraluminal vesicles
IQR	Interquartile range
IRE1	Inositol requiring enzyme 1α/β
ISEV	International Society for Extracellular Vesicles
ISGlobal	Barcelona Institute for Global Health
KO	Knock out
KW	Kruskal-Wallis test
LCR	Low-complexity regions
ME	Module
MK	McDonald–Kreitman test
MOI	Multiplicity of infections
MVB	Multivesicular body
NES	Normalised enrichment score
NGS	Next generation sequencing
NMCP	National Malaria Control Program
NS	Non-synonymous
PBS	Phosphate Buffered Saline
PC	Principal components

University of Ghana http://ugspace.ug.edu.gh

PCA	Principal component analysis
PCR	Polymerase chain reaction
PDR	People's Democratic Republic
PFA	Paraformaldehyde
PfEMP1	*Plasmodium falciparum* erythrocyte membrane protein
PfKIP	PfK13 interacting partners
PfK13	*P. falciparum* kelch 13 gene
PfPTP	PfEMP1 trafficking protein
PfUBP-1	*P. falciparum* ubiquitin carboxyl-terminal hydrolase 1
PI3K	Phosphatidylinositol-3-kinase
PI3P	Phosphatidylinositol-3-phosphate
PI4K	Phosphatidylinositol 4-kinase
PL	Phospholipase
PLP1	Perforin-like protein 1
PSV	Parasitophorous vacuole
PTEX	*Plasmodium* translocon of exported proteins
RBC	Red blood cell
RIN	RNA integrity number
RNA	Ribonucleic acid
ROS	Reactive oxygen species
RPMI	Roswell Park Memorial Institute 1640 medium
RSA	Ring-stage survival assay
SDS	Sodium Dodecyl Sulphate
SEA	South-East Asia
SENP2	Sentrin-specific protease 2, putative
SIF	Stumpy induction factor
SNP	Single nucleotide polymorphism
SPECT	Sporozoite microneme protein essential for traversal
SSA	Sub-Saharan Africa
TCTP	*P. falciparum* translationally controlled tumor protein
TMPAS	Transcriptome-module phenotype association study
TPM	Transcripts per million
TSR	Type I thrombospondin repeat

University of Ghana http://ugspace.ug.edu.gh

UPR	Unfolded protein response
UPS	Ubiquitin-proteasome system
UTR	Untranslated region
VCF	Variant Calling format
WGCNA	Weighted gene correlation network analysis
WHO	World Health Organization
WSAF	Within-sample allele frequencies
WT	Wild type
WWARN	Worldwide Antimalarial Resistance Network

University of Ghana http://ugspace.ug.edu.gh

ABSTRACT

The development of antimalarial drug resistance by *Plasmodium falciparum* has historically derailed efforts at effective control of malaria especially in sub-Saharan Africa (SSA). Presently, this risk has resurfaced following the emergence of artemisinin (ART) resistant (ARTr) *P. falciparum* parasites in the Greater Mekong subregion (GMS) of Southeast Asia (SEA). To mitigate the risk of the spread of ARTr *P. falciparum* parasites to SSA, molecular surveillance is indispensable. This need has partly been met by the identification of *P. falciparum* kelch 13 (*PfK13*) variants associated with ART resistance. However, the genomic architecture of ART resistance is complex and multiple layers of evidence have shown that *PfK13*-driven ARTr is not the universally exclusive molecular marker(s) of ARTr *P. falciparum* parasites. This fluidity of the molecular marker associated with ARTr parasites is linked to the genetic background of the regional *P. falciparum* parasite population and the promiscuous mechanism of action of ART that makes possible a plurality of molecular mechanisms to drive the evolution of ART resistance. Therefore, in regions at risk of ARTr *P. falciparum* parasites emerging, interrogating the artemisinin resistome (all resistance genes including the precursor genes capable of contributing to ART resistance) may shed light on the topology of ART resistance evolution - *PfK13* dependent or not. This paradigm has the long-term potential to be retrofitted into a molecular surveillance forecasting tool for ARTr *P. falciparum* parasites. Furthermore, the impact of ARTr *P. falciparum* parasites emerging in SSA can be mitigated by deepening our understanding of the molecular mechanisms undergirding ART resistance development and translating that knowledge into the discovery of novel antimalarial drug targets. With mounting evidence implicating *PfK13* gene variants in the emergence of the ARTr phenotype in *P. falciparum* parasites, efforts to understand its underlying molecular mechanisms have progressed swiftly. Presently, two mechanistic

University of Ghana http://ugspace.ug.edu.gh

propositions capture our understanding of the molecular mechanisms of ART resistance in *P. falciparum*.

These are reduced hemoglobin endocytosis into the digestive food vacuole and increased tolerance to ART-induced oxidative stress. This model of ART resistance may also accommodate a role for extracellular vesicles (EVs), which are ubiquitously expressed in the parasite and have been already reported to play a role in the transfer of the ARTr phenotype in *P. falciparum* parasites. However, a role for EVs in developing ART resistance outside this motif of parasite-parasite communication is yet to be explored. To approach these problems, it was hypothesized that *PfK13*-dependent ARTr parasites will evolve in Ghana if there are signatures of balancing selection at genomic loci that have been reported to serve as genetic background on which the ART resistance-conferring *PfK13* variant(s) emerges. Diversity at these loci will suggest that the population of *P. falciparum* parasites were primed for a fast selection sweep under ART pressure. Secondly, it was hypothesized that extracellular vesicles (EVs) are implicated in the development of ART resistance as actively secreted organelles involved in the export of toxic proteinopathic molecules, to maintain cellular homeostasis under ART pressure. This is the EVs export hypothesis. Therefore, the transcriptome of ARTr parasites under ART pressure will be enriched with genes known to be involved in *P. falciparum* EVs biogenesis. Finally, the EVs export hypothesis predicts an alteration in EVs abundance under ART exposure. In this thesis, the power of population genomic tools has been leveraged to show that two genes, previously reported as background loci for ART resistance, were under balancing selection in clinical isolates of *P. falciparum* from Ghana in 2010. This finding demonstrates the potential utility of looking for signatures of selection in ART resistance background genes as an early warning molecular surveillance tool and argues for a further exploration of this approach as an addendum to existing tools for molecular surveillance of ARTr *P. falciparum* parasites. This finding also provides empirical evidence for malaria

University of Ghana http://ugspace.ug.edu.gh

molecular surveillance in Ghana to continue to use *PfK13* as the marker for ARTr despite the possibility of *PfK13* independent emergence of ARTr parasites in Ghana.

Secondly, an EVs module (set of genes with correlated expression) associated with the transcriptome of ARTr *P. falciparum* parasites was reported. This implicates EVs in the molecular mechanisms undergirding ART resistance and warrants further exploration of the EVs export hypothesis. Finally, the EVs export hypothesis was tested, and it was observed that a positive correlation between DHA exposure and EVs abundance which suggests that EVs biogenesis is one of the *P. falciparum*'s response pathways to ART and implicates EVs in the ARTr phenotype.

INTEGRI PROCEDAMUS

University of Ghana http://ugspace.ug.edu.gh

CHAPTER ONE

GENERAL INTRODUCTION

1.1 Introduction

Malaria remains a disease of significant public health importance today. In 2020, there were 228 million cases of malaria in the WHO African region with an estimated 602 000 deaths due to malaria. Although many gains have been made in the fight against malaria, since 2015 the global incidence of malaria have taken a troubling slowing-down trend (WHO, 2021a). The disease is caused by the apicomplexan parasites *Plasmodium falciparum, P. knowlesi, P. vivax, P. ovale, P. malariae* and *P. cynomolgi* (Carter et al., 2002; Imwong et al., 2019). *P. falciparum* is responsible for the highest toll in morbidity and mortality as it causes the most virulent form of malaria (WHO, 2021a; Wassmer et al., 2017; Jensen et al., 2020).

Intervention measures to control malaria employ vector control tools, early efficient case detection and management, and surveillance for the emergence of drug resistance (WHO, 2015). Even though significant strides have been made in malaria control, concerns about emerging artemisinin (ART) resistance combined with the low efficacy of the only licensed malaria vaccine have highlighted the risk of losing grounds on successes achieved especially in developing countries (WHO, 2021a; Mahmoudi et al., 2017; Olotu et al., 2016). These facts propel the need for further studies on *P. falciparum* biology to deepen our understanding of ART resistance and translate that knowledge into molecular surveillance tools and novel antimalarial drugs. This need has even become direr in the wake of the COVID-19 pandemic that has the potential to sweep malaria control efforts into its penumbra.

University of Ghana http://ugspace.ug.edu.gh

The emergence of *P. falciparum* parasites resistant to antimalarial drugs has historically had its epicenter in the Mekong delta area bordered by Thailand, Vietnam, and Cambodia. This region has served as ground zero for the development of *P. falciparum* resistance to antimalarial drugs like chloroquine, sulphadoxine-pyrimethamine and quinine (Fairhurst, 2015). Following the worldwide use of artemisinin (ART)-based combination therapies (ACT), ART-resistant (ARTr) *P. falciparum* parasites were first reported in Western Cambodia in 2008 (Noedl et al., 2008; Dondorp et al., 2009).

Resistance to ART and its derivatives has been defined as an *in vivo* reduction in parasite clearance rate (parasite clearance half-life greater than 5 hours) and increased *in vitro* survival of early ring stages in the presence of optimum concentrations of dihydroartemisinin (DHA) – the active metabolite of ART and its derivatives *in vivo* (Fairhurst, 2015; Noedl et al., 2008; Witkowski et al., 2013a; Dai et al., 2021; Klayman, 1985). Since the identification of the ARTr phenotype in Western Cambodia, epidemiological studies have further uncovered the *P. falciparum* ARTr phenotype in Myanmar, Thailand and Vietnam (Ashley et al., 2014; Thriemer et al., 2014; Phyo et al., 2012). Against this backdrop, the report of artemether-lumefantrine (AL) cure rate of 97.2% and some molecular markers associated with artemisinin delayed clearance in sentinel sites in Ghana has brought to the fore the need to interrogate the ART resistome in Ghana *P. falciparum* parasites (Abuaku et al., 2012; Adams et al., 2018). Additionally, the *de novo* emergence and clonal expansion of ARTr *P. falciparum* parasites in Rwanda and Uganda add further impetus to this problem (Uwimana et al., 2020; Balikagala et al., 2021). *P. falciparum* kelch 13 (*PfK13)* propeller domain polymorphisms strongly associate with ARTr (Ashley et al., 2014; Ariey et al., 2014).

University of Ghana http://ugspace.ug.edu.gh

Presently, active molecular surveillance efforts to monitor the emergence of *PfK13* in Africa have been spurred (WHO, 2021a; Talisuna et al., 2012; Mita et al., 2012). However, this strategy is entirely hinged on the assumption of a *PfK13*-dependent evolution of ART resistance and a universal concordance with the *PfK13* variants associated with ART resistance in SEA. This begs the following questions: will *PfK13*-dependent ARTr emerge in Africa? How can this be forecasted? (Demas et al., 2018; Sutherland et al., 2017; Henriques et al., 2014; Breglio et al., 2018).

Furthermore, current surveillance for ARTr *P. falciparum* parasites is built on a platform that announces the presence of the drug-resistant parasite (Hassett et al., 2019; Mita et al., 2016). Drawing from the principles of the emerging theme of precision medicine (König et al., 2017), I believe that surveillance for ART resistance will be better delivered when it is shifted into a forecasting motif. I refer here to the ability of surveillance to predict the emergence of drug-resistant parasites in a region, with well-defined margins of uncertainty and account for local transmission factors, parasite genetic background and host immune protection. Efforts towards this paradigm shift will benefit the malaria control campaign immensely.

The ART resistome refers to the gamut of genetic variants, including background fitness-compensatory variants, that determine and/or associate with the ARTr phenotype (Kümpornsin et al., 2019; Carolino et al., 2020; Cowell et al., 2018). In *P. falciparum*, *PfK13* variants are the most established variants associated with ART resistance and known *PfK13*-independent variants are yet to be validated as much (Siddiqui et al., 2021).

University of Ghana http://ugspace.ug.edu.gh

Background multigenetic variants, at certain loci, have been reported as prerequisites for the emergence of *PfK13*-dependent ART resistance (Cerqueira et al., 2017; Miotto et al., 2015). Whether these genetic loci, that constitute this *PfK13*-dependent ART resistance background, is under selection in clinical isolates of *P. falciparum* in Ghana is not known (Project, 2016). The molecular mechanism of ARTr has also been explored on a *PfK13*-driven motif. The current evidence amalgamates into two mechanistic arms that undergird ART resistance: reduced hemoglobin endocytosis into the digestive food vacuole and increased tolerance to ART-induced oxidative stress (Siddiqui et al., 2021). This model of ART resistance suggests a role for extracellular vesicles as well. A seminal study has already implicated EVs in the transfer of the ARTr phenotype from the resistant to susceptible parasite under a parasite-parasite communication theme (Regev-Rudzki et al., 2013). However, outside this parasite-parasite communication theme, the possible contribution of EVs to the emergence of the ARTr phenotype is yet to be explored.

In this PhD thesis, the foundations of a molecular surveillance tool for forecasting ARTr was first explored. This was approached by using population diversity metrics to identify the presence of signatures of balancing selection on background loci, on which definitive *PfK13*-driven ARTr-conferring variants have been known to emerge. This approach has the potential to be leveraged into a forecasting model on account of the unique genetic architecture of ART resistance.

University of Ghana http://ugspace.ug.edu.gh

Secondly, the discovery power of bulk RNA sequencing was leveraged to explore whether EVs are implicated in developing ART resistance in *P. falciparum* parasites. A modular analysis pipeline was employed to bypass the inherent limitation, to novel discovery, in traditional differential gene expression and gene ontology analysis. This involved identification of modules or sets of genes with correlated expression and defining EVs modules of interest as the modules that contain known EVs biogenesis genes. Subsequently, these EVs modules of interest were used as the query list in a gene set enrichment analysis of the bulk RNA sequencing data.

Finally, EVs were enriched, quantified and compared among three parasite lines and treatment conditions to test the EVs export hypothetical model of ART resistance. This model was built from review of the literature on the molecular mechanisms undergirding the development of ART resistance and the findings of specific objective two.

University of Ghana http://ugspace.ug.edu.gh

1.2 Problem Statement

The risk of the emergence of ARTr *P. falciparum* parasites in SSA has been portended by their discovery in SEA. To mitigate this risk, molecular surveillance is key. However, against the backdrop of the unique genetic architecture of ARTr *P. falciparum* parasites, the utility of the SEA molecular marker of ART resistance – *PfK13,* must be interrogated. This problem presents a unique solution as the presence of signatures of balancing selection in known background genes of *PfK13*-dependent ART resistance may suggest, for a regionally defined population of *P. falciparum* parasites, the likelihood of *PfK13*-dependent ARTr parasites emerging. Another mitigating measure for the risk of ARTr *P. falciparum* parasites in SSA is deepening our understanding of the molecular mechanisms of ART resistance. EVs are biological nanoparticles that have been previously reported to play a role in developing ART resistance within the context of parasite-parasite communication. However, how EVs fit into the evidence portrait, outside the theme of parasite-parasite communication, and within the larger context of the accumulated wet-lab findings on ART resistance is yet to be explored. Here, I present the EVs export hypothesis and explore answers to the question: do EVs play a role in developing ART resistance?

University of Ghana http://ugspace.ug.edu.gh

1.3 Justification

This study will help provide evidence to support the use of the *PfK13* molecular marker for ART resistance molecular surveillance in Ghana. Additionally, it will lay down the platform for efforts to shift molecular surveillance for ARTr parasites into a forecasting motif. This study will also add to the body of knowledge on the molecular mechanisms of ART resistance by exploring whether EVs play a role in the development of the ARTr phenotype. By implicating EVs in ARTr development, this study will open a new target for antimalarial drug discovery purposes.

INTEGRI PROCEDAMUS

University of Ghana http://ugspace.ug.edu.gh

1.4 Hypotheses

I. To mitigate the risk of ARTr spreading and taking hold in SSA, molecular surveillance for parasites with ARTr is critical and a molecular-based early warning metric that predicts ARTr will be desirable. A tool that may serve this purpose is the detection of signatures of balancing selection on loci demonstrated to act as a background for ARTr emergence. To explore this, I hypothesized that the background *PfK13* genetic variants is present before the *PfK13* ARTr-conferring variant is selected and that signatures of balancing selection on these loci (the *PfK13* ARTr background genome) serve as an early warning signal of the likelihood of *PfK13*-dependent evolution of ARTr.

II. The role of extracellular vesicles (EVs) in the biology of malaria parasites is yet to be fully understood. Some studies have suggested that EVs may play a role in the development of the ARTr phenotype. However, empirical evidence supporting conceptual answers are inadequate. One of these gaping questions is the gene set (module) representative of EVs biogenesis and whether an association with ARTr in *P. falciparum* can be implicated. Here, I hypothesize that an EVs module of interest (a set of genes with correlated expression including genes involved in biogenesis of EVs) is associated with the ARTr phenotype and that EVs abundance is altered by ART exposure in *P. falciparum* parasites

University of Ghana http://ugspace.ug.edu.gh

1.5 General Objective

To study the ART resistome of *Plasmodium falciparum* clinical isolates from Ghana and investigate the role of EVs in the development of ARTr

1.5.1 Specific Objectives

I. To determine whether there are signatures of selection in the genome of Ghanaian clinical isolates of *P. falciparum* that suggest likelihood of emergence of *PfK13*-dependent ARTr.

II. To determine whether an EVs module of interest is associated with ARTr *P. falciparum* parasites.

III. To investigate a prediction of the EVs export hypothetical model of ART resistance by determining whether the biophysical profile of EVs from *P. falciparum* is altered by exposure to dihydroartemisinin (DHA).

University of Ghana http://ugspace.ug.edu.gh

CHAPTER TWO

LITERATURE REVIEW

2.1 Malaria Burden and Epidemiology

Malaria is the most important disease in SSA today . This is despite decades of control efforts erected on principles and practices of public health, biomedical research, and clinical care. As of 2020, an estimated 241 million cases of malaria was reported globally according to the World Health Organization (WHO). Additionally, the malaria related mortality rate was reported as 627 000 in 2020 with children under 5 years old bearing the highest brunt of the disease's impact. Since 2015, a slowing down and reversal in downward trends of malaria morbidity has provided cause for worry (WHO, 2021a). Malaria is caused by six *Plasmodium* species: *P. falciparum, P. knowlesi, P. vivax, P. malariae, P. ovale curtisi,* and *P. ovale wallikeri* (Garrido-Cardenas et al., 2019). *P. falciparum* is the most important malaria parasite because it accounts for the highest toll in cases of morbidity. The impact of *P. falciparum* malaria on the world stage is not uniform. Of the approximately ninety seven countries with malaria transmission, the majority of the disease's burden is in SSA and South East Asia (SEA) regions (WHO, 2021a; Cowman et al., 2016).

Transmission of the disease is influenced by factors such as temperature, humidity, and altitude (Rossati et al., 2016). Within these dynamic environmental factors, the frequency of contact between the infected mosquito and the susceptible human host determines the actual transmission rate of the malaria parasites. Transmission can be therefore unstable or stable in an area supporting malaria transmission. Unstable transmission means a fluctuating low to a high incidence of malaria annually.

University of Ghana http://ugspace.ug.edu.gh

On the other hand, a stable transmission means a consistently high incidence of malaria over successive years (WHO, 2021b).

The WHO classifies malaria endemicity by spleen rates in children aged 2–9 years as hypoendemic (0–10%), mesoendemic (10–50%), hyperendemic (constantly > 50%) and holoendemic (constantly ≥ 75%) with a low adult spleen rate (WHO, 2021b).

The burden of malaria is also seen in its economic ramifications as a sequela of the disease is the reduction in the productivity of the affected population. It also increases the health care burden of the individual or family because of the purchase of drugs and the unplanned costs of hospital admissions. This in turn translates into a reduction in the country's gross domestic product. Therefore, malaria is costly to both governments and individuals (Alonso et al., 2019; Nonvignon et al., 2016).

The goal of all malaria control efforts is platformed on the strategic aim of regional elimination and eventual global eradication of the disease. The global technical strategy (GTS) for malaria control outlines three pillars and two supporting elements. The three pillars are: ensure universal access to malaria prevention, diagnosis and treatment; accelerate efforts towards elimination and attainment of malaria-free status; and transform malaria surveillance into a core intervention (WHO, 2015). Therefore, chemotherapy and molecular surveillance for ARTr parasites are key to malaria control efforts especially in SSA.

University of Ghana http://ugspace.ug.edu.gh

In Ghana, malaria transmission is holoendemic with peak transmission occurring during the rainy seasons and reduced transmission during the dry season. The incidence of malaria in Ghana is estimated to account for 40% of all out-patient department visits especially in the under 5-year age group (Ameme et al., 2014; Awine et al., 2017). Although molecular surveillance has reported some variants associated with ARTr, *in vivo* or *ex vivo* ARTr is yet to emerge in Ghana (Adams et al., 2018; Matrevi et al., 2019).

INTEGRI PROCEDAMUS

University of Ghana http://ugspace.ug.edu.gh

2.2 Life Cycle and Biology of *Plasmodium falciparum*

The malaria parasites are pathogens with a complex life cycle that involves the invertebrate female *Anopheles* mosquito and the human host. This life cycle requires the formation of special parasite forms at different stages. These zoite forms of the parasite are responsible for the invasion of the different host cell types at the various stages in the parasite's life cycle (Cowman et al., 2016).

Sporozoites are introduced into the human host's dermis by the bite of an infected female *Anopheles* mosquito during a blood meal. These invasive forms of the parasite use gliding motion to exit the dermis and enter a blood vessel (Sultan et al., 1997; Keeley et al., 2004). The remaining sporozoites in the dermis are drained by lymphatics and can be destroyed by the host's immune response. A trap-like protein has been implicated as vital to this phase of sporozoite activity (Hopp et al., 2015). Once in the bloodstream, the sporozoites home into the liver and cross the sinusoidal fenestrated endothelial cell barrier by a process known as traversal (Tavares et al., 2013). Perforin-like protein 1 (PLP1), sporozoite microneme protein essential for traversal (SPECT) , cell traversal protein for ookinetes and sporozoites (CelTOS), phospholipase (PL) and gamete egress and sporozoite traversal protein (GEST) are some of the parasite proteins implicated as vital to liver stage infection in the host (Ishino et al., 2004; Risco-Castillo et al., 2015; Bhanot et al., 2005).

The sporozoite circumsporozoite protein (CSP) also plays a key role in liver cell invasion by binding to highly sulfated proteoglycans (HSPGs). CSP is made up of a highly repetitive region and a type I thrombospondin repeat (TSR). The N-terminus of CSP is processed and removed, on binding to HSPGs, exposing the TSR domain. This enables hepatocyte invasion (Herrera et al., 2015). The established sporozoite infection in the liver cell then transforms over 2-10 days, to a liver stage.

University of Ghana http://ugspace.ug.edu.gh

This culminates in the release of up to 40,000 merozoites per infected hepatocyte into the bloodstream. The release of these merozoites is done by budding of parasite-filled vesicles known as merosomes (Sturm et al., 2006). The release of the merozoites from the liver shifts the invasion phase to the red blood cells. Here erythrocyte invasion takes place in a speedy, multi-step and dynamic process. This is completed within 2 minutes and includes pre-invasion, active invasion and echinocytosis (Weiss et al., 2015).

INTEGRI PROCEDAMUS

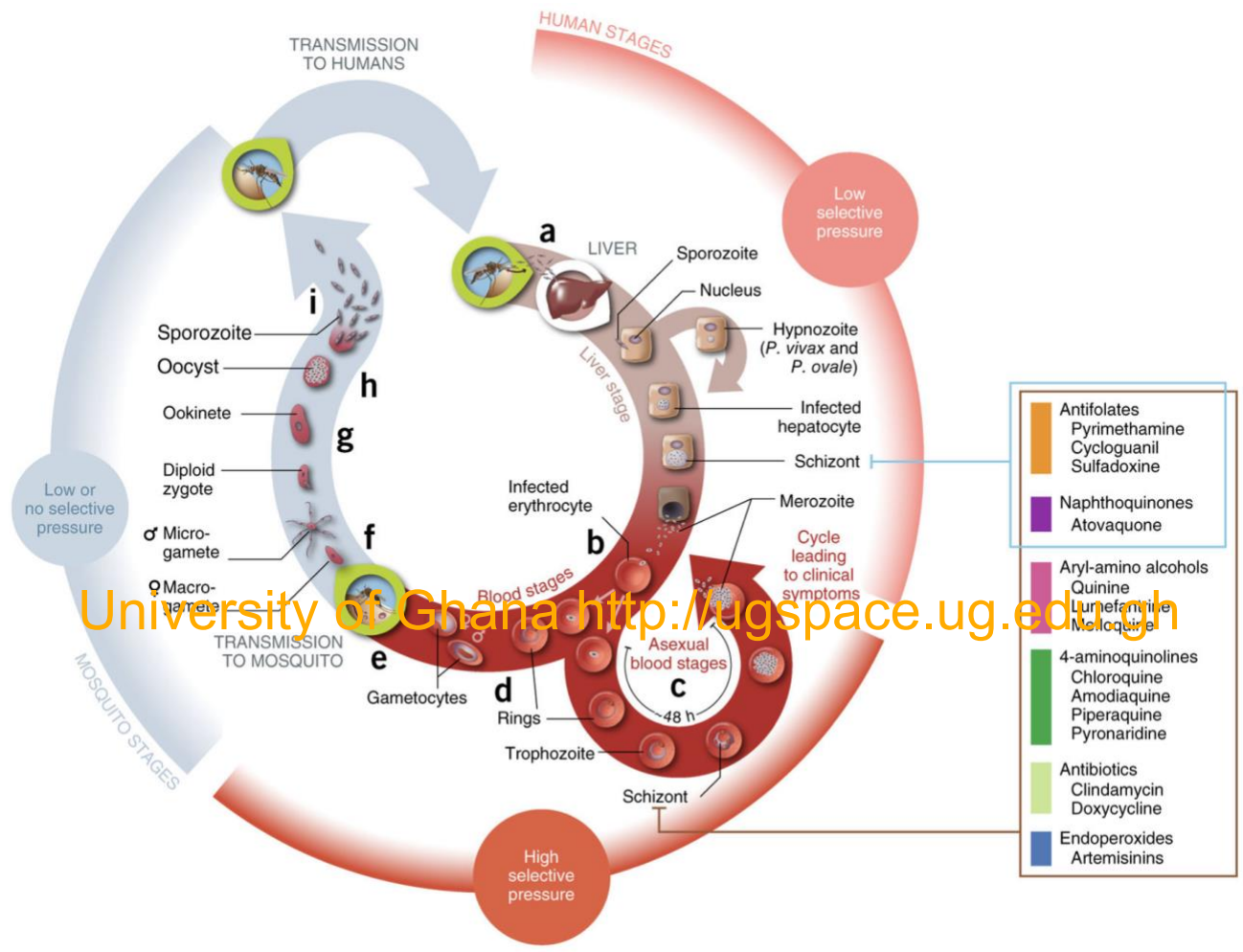

University of Ghana http://ugspace.ug.edu.gh

Figure 2.1 ***Plasmodium falciparum*** **life cycle showing targets of ACTs (Blasco et al., 2017). This figure and figure legend has been reproduced with permission from Springer Nature through Copyright Clearance Center's RightsLink® service (Order Number: 5423011199517)**

Plasmodium's life cycle and its relationship to drug resistance. (a) Human infection begins when infective female Anopheles mosquitoes deliver fewer than 100 sporozoites into the dermis during blood feeding (Douglas et al., 2015). These motile forms migrate rapidly into the bloodstream and to the liver, where they invade hepatocytes. A prodigious phase of replication over a week results in an estimated 10,000–30,000 merozoite progeny per intracellular parasite. (b) Liberated merozoites (~105–106 in total) then invade human mature red blood cells, developing inside a parasitophorous vacuole and initiating ~48-h cycles of asexual blood stage parasite growth, egress and reinvasion. (c) Asexual blood stage parasites, typically 10^8–10^{12}, are responsible for disease manifestations. (d) About 1–2% of intra-erythrocytic parasites enter an alternative program of sexual development, a process that over ~10–12 days produces mature male and female gametocytes that are transmissible to Anopheles mosquitoes. (e) An estimated 10^3–10^4 mature gametocytes are taken up during a blood meal. (f–i) These gametocytes then form male and female gametes (~10^2–10^3) that undergo sexual recombination (f), forming ookinetes (<100; g) and then oocysts (typically 1–2; h) before completing their life cycle by forming 10^3 to 10^4 sporozoites that migrate to salivary glands (i), ready for further human infection. In acute cases, ABS parasites can infect up to 10–20% of all erythrocytes (i.e., >10^{12}). Primary causes of death include severe malaria anemia, or cerebral malaria that causes brain herniation and respiratory arrest (Seydel et al., 2015). Immunity is acquired slowly and is non-sterilizing; its maintenance is dependent on continued infection (Fowkes et al., 2016). Selective forces that drive the emergence and spread of drug resistance differ throughout the life cycle. Important factors include the parasite numbers and drug pressure at different stages, stage specificity of drug action, the essentiality of the targeted pathways in the mosquito vector and vertebrate host, host immunity, multiplicity of infection, and local factors that affect therapeutics use and compliance. The pathogenic asexual blood stage reproduction cycle experiences the highest parasitemia and drug pressure, whereas the lower numbers of clinically silent liver-stage parasites provide much less fertile ground for the emergence of resistance (White, 2004). Human-to-mosquito transmission is possible only if sufficient densities of mutant gametocytes are produced, which can be triggered in some instances by drug treatment (Bousema et al., 2011). Parasite number estimates were derived from refs. (Bejon et al., 2005; Pongtavornpinyo et al., 2009; Vanaerschot et al., 2014; White et al., 2014). Stages targeted by current and former first-line drugs used to treat *P. falciparum* are shown.

University of Ghana http://ugspace.ug.edu.gh

Once established within the red blood cell, schizogony occurs and is completed after 48 hours. This results in the release of 16-32 merozoites from each infected red blood cell (RBC). The egress of the merozoites from the infected RBC destroys the red cell membrane. These merozoites in turn invade new RBCs for the erythrocytic stage of the infection cycle to continue (Cowman et al., 2016).

As schizogony occurs, some parasites undergo a developmental switch to male and female gametocytes. This is a vital step for the transmission by the mosquito vector to continue. It is a thus a veritable bottleneck that can be explored to augment current control efforts. Thus, there is significant effort at developing transmission-blocking vaccine and drugs that will target vital proteins in this key developmental stage switch (Patel et al., 2021; Duffy, 2021; Coelho et al., 2019). Extracellular vesicles, epigenetic control and the transcription factor AP2-G have been identified as key elements in the developmental switch to produce gametocytes (Regev-Rudzki et al., 2013; Mantel et al., 2013; Kafsack et al., 2014). This irreversible commitment to the sexual form takes about 11 days for the mature forms capable of infecting mosquitoes to develop. The immature gametocyte developmental stages are sequestered in the bone marrow and thus protected from the filtering action of the spleen (Cowman et al., 2016; Joice et al., 2014).

When a female anopheline mosquito takes a blood meal, the male and female gametocytes are ingested. Within the gut of the mosquito, they fuse and develop into the ookinete. This ookinete migrates through the gut wall and attaches itself to the basal lamina of the gut epithelium. There, it develops into the matured oocyst and eventually releases the human infective form called the sporozoites. These migrate to the salivary glands of the mosquito. They are introduced into the skin of a susceptible human by the biting action of the female anopheline mosquito (Cowman et al., 2016) – thus completing the malaria parasite's life cycle (Figure 2.1).

University of Ghana http://ugspace.ug.edu.gh

2.3 Malaria Case Management, Vector Control and Molecular Surveillance

The clinical presentation of malaria is characterized by a febrile illness associated with non-specific symptoms such as headache, chills, rigors, malaise and fatigue, and myalgia. Clinical signs may include an axilla temperature of 37.5°C or greater, pallor, tachycardia, tachypnoea, hepatomegaly or splenomegaly and reduced consciousness. Based on the presentation, malaria is classified as either uncomplicated or complicated (WHO, 2021c).

Uncomplicated malaria is defined as a presentation with clinical features of malaria and a positive parasitological test without features of severe malaria. The goal of treatment here is the elimination of all parasites following the administration of an appropriate ACT. Once promptly diagnosed and treated with ACTs, clinical features of uncomplicated malaria resolve in a couple of days. Complicated or severe malaria is characterized by features such as coma (cerebral malaria), respiratory distress (typically with metabolic acidosis), and reduced kidney function. Severe malaria is managed with parenteral artesunate or quinine monotherapy until the patient can tolerate orally administered ACTs (WHO, 2021c).

The World Health Organization (WHO) presently endorses the usage of the following ACTs; artesunate-amodiaquine (AS-AQ), artemether-lumefantrine (AL) artesunate-mefloquine (AS-MQ), dihydroartemisinin-piperaquine (DHA-PPQ), artesunate-sulfadoxine/pyrimethamine (AS-SP), and artesunate-pyronaridine (AS-PND) (WHO, 2021c). The ACT strategy allows for the rapid reduction in malaria parasite mass (approximately 10,000-fold over the 48-hour asexual life cycle) by the fast-acting ART compound. After this, any remaining parasites are mopped up by the relatively slower-acting partner drug (White, 2008). This has made ACTs, the most important and effective chemotherapeutic agents in the global malaria control fight.

University of Ghana http://ugspace.ug.edu.gh

Since the clinical features of malaria are non-specific, case identification can only be validated by laboratory tests to confirm malaria and rule out other causes of acute febrile illness presentation. Laboratory parasitological diagnosis is typically achieved with light microscopy of Giemsa-stained thick and thin blood films and/or by an immunochromatographic rapid diagnostic test (Warhurst et al., 1996; Tangpukdee et al., 2009). Laboratory tests are also important for the identification of recrudescence and treatment failure (will need a nucleic acid amplification assay) after initiation of treatment with ACTs. The effectiveness of light microscopy is hinged on the technical expertise of trained laboratory technicians in the clinic.

Vector control for malaria is achieved by targeting the anopheline mosquito and has also been plagued by the percolating problem of insecticide resistance (Rubert et al., 2016). Researchers are exploring novel ways to target the *Anopheles* mosquito vector. One of such current research aims to target the mosquito vector with nanoparticles delivered drug agents to mitigate the risk of insecticide resistance emerging (Neves Borgheti-Cardoso et al., 2020).

University of Ghana http://ugspace.ug.edu.gh

2.4 Greater Mekong Subregion of Southeast Asia: The Ground Zero of Antimalarial Drug Resistance Development

Historically, the ground zero of antimalarial drug resistance emergence in *P. falciparum* parasites has been the Greater Mekong Subregion (GMS) of Southeast Asia (SEA) (Fairhurst, 2015; Siddiqui et al., 2021). The GMS is an economic cooperation program of countries along the Mekong River and comprises Cambodia, China's Yunnan Province, Lao's People's Democratic Republic, Myanmar (Burma), Thailand and Vietnam Cui et al. (2012a). Chloroquine (CQ), sulphadoxine-pyrimethamine (SP) and mefloquine (MQ) resistance emerged in *P. falciparum* parasites in the GMS (Eyles et al., 1963; Hurwitz et al., 1981; Powell et al., 1964; Boudreau et al., 1982; Mockenhaupt, 1995; Wongsrichanalai et al., 2002).

Between 2006 and 2007, *in vivo* clinical resistance to ART was reported for the first time in SEA (Noedl et al., 2008; Dondorp et al., 2009). Subsequently, ARTr malaria parasites have emerged in all countries in the GMS either due to the direct spread of ARTr *P. falciparum* parasites or independent emergence of the ARTr phenotype (Ashley et al., 2014; Bustos et al., 2013; Kyaw et al., 2013). Following the emergence of ARTr, partner drugs in ACTs also fell to drug resistance and forced a revision of the first-line chemotherapeutic ACT for *P. falciparum* malaria (Hassett et al., 2019; Amaratunga et al., 2016; Leang et al., 2015; Saunders et al., 2014; Spring et al., 2015).

University of Ghana http://ugspace.ug.edu.gh

2.4.1 What factors may contribute to the GMS hotbed for antimalarial drug resistance?

Host, parasite and epidemiological factors may contribute to the recurrence of antimalarial drug resistance in the GMS of SEA (Siddiqui et al., 2021). Host factors like hemoglobinopathies and erythrocyte glucose-6-phosphate dehydrogenase (G6PD) deficiency have been reported to be highly prevalent in the GMS of SEA and are known to provide some level of innate immune resistance to malaria infection. Therefore, it is likely that this background pseudo-resistance to malaria parasites in the human hosts of the GMS acts as the first selection pressure that drives the evolution of parasites with tolerance to higher oxidative states that are found in these erythrocytes (Roberts et al., 2003; Kariuki et al., 2020; Taylor et al., 2012; Ginsburg et al., 1996). Another host factor that may drive the evolution of antimalarial drug resistance is parasite-directed natural immunity (Rogerson et al., 2010). Immunity to malaria is acquired following repeated exposures and ultimately is mounted to mitigate disease severity. This anti-disease immunity allows strain-specific parasite tolerance without the clinical manifestation of disease and is maintained by recurrent exposure to malaria parasites. It is reported to wane in the absence of such exposure and with a lowering of malaria transmission (Cowman et al., 2016; Hviid et al., 2015). In SEA, the hypoendemic nature of malaria transmission does not favor the maintenance of acquired malaria immunity and may contribute to the selection of ARTr variants because of the absence of the mopping clearing action of such immune pressure on any cohort of initially selected parasites. Thirdly, the human culture of self-treatment with antimalarial drugs (especially if monotherapy) and the culture of poor compliance to standard effective dosing and duration regimes may also contribute to the evolution of drug resistant malaria parasites in SEA (Roosihermiatie et al., 2017; Espino et al., 2000; Sonkong et al., 2015).

University of Ghana http://ugspace.ug.edu.gh

Finally, access to fake and/or substandard medications in the countries of the GMS have been implicated as a contributing factor to the perennial observation of the emergence of drug-resistant malaria parasites (Guo et al., 2017; Newton et al., 2008; Dondorp et al., 2004).

Under parasite factors, the first worth considering is the genetic background of the circulating population of *P. falciparum* parasites. If such a background favors the acquisition of new variants at drug-resistant conferring loci without sacrificing fitness, then it will promote the evolution of drug-resistant parasites (Beez et al., 2011). Such an antimalarial drug resistance development background may be present in the *P. falciparum* parasite population circulating in the GMS. This idea helped shaped the definition of the accelerated resistance to multiple drugs (ARMD) phenotype (Rathod et al., 1997). In the GMS, *in vitro* studies have established an association between circulating *P. falciparum* parasites and the ARMD phenotype which is related to the expression of DNA repair genes that alter DNA repair mechanisms to favor the evolution of drug-resistant parasites (Castellini et al., 2011; Gupta et al., 2016; Trotta et al., 2004). Variants in up to six genes involved in DNA repair was reported in ARTr parasites circulating in the GMS (Miotto et al., 2013; Xiong et al., 2020). A mild mutator phenotype was also discovered in parasites from the GMS that conferred the ability to withstand DNA damage much more effectively without sacrificing fitness (Lee et al., 2016). Finally, a laboratory strain of *P. falciparum*, Dd2, from the SEA region, has been observed to develop resistance to dihydroartemisinin (DHA) quicker than laboratory parasite lines from other malaria endemic regions. Thus, suggesting a genetic background predilection of Dd2 for evolving drug resistance (Cui et al., 2012b).

University of Ghana http://ugspace.ug.edu.gh

The second element to consider under parasite factors is the fitness (index of gametocytogenesis ability in the asexual parasites) resulting from the emergence of a drug-resistant conferring variant. As drug-resistant parasites have been shown to have reduced fitness in the absence of the drug selection pressure, the emerging novel drug-resistant variant is unlikely to thrive. This fact may reduce the likelihood of drug-resistant variants emerging. However, this potential bottleneck to the emergence of drug-resistant parasites is effectively neutralized by variants that compensate for the loss of fitness. For the asexual *P. falciparum* parasite, fitness is intricately linked to within-host competition among various parasite strains which is indexed by the multiplicity of infection (MOI) within the human host. MOI refers to the number of parasite strains with distinct genetic lineages infecting the human host at a particular time (Duah et al., 2016; Vafa et al., 2008). MOI is expected to be relatively higher in regions with higher malaria parasites transmissions (Sondo et al., 2020; Nkhoma et al., 2013). Within the context of MOI, it is conceivable that parasites with the drug-resistant conferring variant, evolving in a host with MOI will face stiffer opposition in the race for nutrient competition and gametocytogenesis. Therefore, it is highly likely that without the selective agent (drug) these variants will be less fit and will not survive. However, in the presence of the drug, parasites carrying these variants will be more fit and therefore, will survive.

Multiplicity of infection also affects the likelihood of transmission of multi-loci drug-resistant variants to other human hosts via the mosquito vector. This is because of the possibility of sexual recombination, in the mosquito vector, breaking down the multi-loci drug-resistant variant(s) when outcrossing (as opposed to selfing) occurs. As outcrossing is most likely to occur when MOI is high in the human host population, it is widely held that regions with low or absent MOI (MOI equal to 1) are likely to serve as better seedbeds for the evolution of drug-resistant malaria parasites.

University of Ghana http://ugspace.ug.edu.gh

In the absence of MOI, self-fertilization in the sexual vector will keep the multi-loci drug-resistant variants and is the more favorable scenario that can drive the emergence of drug resistant parasites (Cerqueira et al., 2017). This is most likely the picture in the GMS. Although high MOI in high transmission regions are likely to negatively impact the probability of drug-resistant parasites emerging *de novo*, it is still possible for such multi-loci drug-resistant variants to be maintained, following sexual recombination, in the mosquito vector (Mackinnon, 1997). Here, the determining factor may be the sheer force of the number of transmissions occurring. This framework is the reason the *de novo* emergence of drug-resistant parasites may still occur in the SSA subregion despite relatively high transmission and MOI. Finally, epidemiological factors that affect transmission rates and in turn the estimates of the within-host infection complexity (MOI). Concerning transmission rates, low endemicity favors drug resistance development as already discussed.

University of Ghana http://ugspace.ug.edu.gh

2.5 Plasmodium falciparum Population Genomics and Genetics

Population genetics and genomics studies examine the changes in allele frequencies in a population's gene pool over time with the objective to understand population variation and molecular evolution from the population perspective. Its theoretical framework is distilled from the central motif that variation between species is the cause of intraspecies variation and factors such as selection and genetic drift shape population diversity over time. Furthermore, population genetics/genomics has successfully integrated the principles of Mendelian inheritance into the study of variation (genetic and phenotypic) within and between populations (Casillas et al., 2017).

Since the advent of next-generation sequencing, the focus has shifted from samples of genetic loci in population genetics to the study of the entire gamut of variation within and between populations of organisms viz population genomics. Thus, the field has seen great advances in data acquisition as well as the theoretical models that frame how the data is interpreted and translated into public health solutions. Today, the field is characterized by an inundation with big data and largely governed by the theoretical frameworks of natural selection and the (near) neutral theory of molecular evolution (Casillas et al., 2017). However, since the inception of the field in the 1950s, the rudimentary tenets of evolution (natural selection, genetic drift, mutation, recombination, and gene flux) are still the concepts and principles used to explain evolutionary change through the population perspective (Fisher, 1930; Haldane, 1932; Kimura, 1954; Lynch et al., 2007; Charlesworth, 2010).

University of Ghana http://ugspace.ug.edu.gh

Historically, the modern synthesis of evolutionary theory predicated the natural/classical versus balance/neutral hypothesis of the evolutionary theory divide. The classical hypothesis (selectionist) postulates that natural selection drives the positive selection of the fittest variant under existing selection pressure. Thus, it predicts that populations should be less diverse and more uniform at such genetic loci of interest. An extension of this model is the fact that in the event of changes in selection forces, the absence of a standing variation will slow the pace at which evolution occurs.

On the other hand, the balance (neutral) hypothesis intimates the maintenance of a standing variation by natural selection, as multiple variants exhibit equal competitive fitness under the given selection pressure. This translates into a high diversity index at genetic loci of interest in populations. This translates into the phenomenon of a soft selection sweep on the standing variation, in the event of changes in selection pressure. Much of the evidence gathered today supports the latter balanced hypothesis (Casillas et al., 2017). The neutral and near-neutral theories of evolution have emerged under the motif of the balancing hypothesis to model the observation of naturally high diversity in populations even under natural selection.

University of Ghana http://ugspace.ug.edu.gh

2.5.1 Measures of population variation

The earliest measures of population variation were done using electrophoresis to measure allozyme activity and analysis of restriction enzymes sites. This approach was extensively used in *Drosophilia* (Langley et al., 1993; Langley et al., 1982; Langley et al., 1988; Langley et al., 2012; Aguadé et al., 1989; Aquadro et al., 1986; Miyashita et al., 1988; Schaeffer et al., 1988; Stephan et al., 1989). Restriction enzyme analysis and mapping saw the genesis of the use of new summary statistics to represent DNA sequence genetic diversity such as the nucleotide site diversity (π) (Nei et al., 1979; Begun et al., 1992).

Such extensive studies in *Drosophilia* led to the discovery that regions of the genome with low recombination also have low levels of genetic variability (Langley et al., 1993; Stephan et al., 1989; Begun et al., 1992; Aguade et al., 1989; Berry et al., 1991; Martín-Campos et al., 1992; Stephan et al., 1992). In particular, the seminal study by Begun and Aquadro in 1992 highlighted and cemented this observation by reporting a strong positive correlation between the rate of recombination and mutation rate (Begun et al., 1992). This finding did not fit the established observation that interspecies DNA sequence diversion was independent of local recombination rate. This discordance threatened the neutral theory of molecular evolution as it posited, under the assumption that recombination was mutagenic, that advantageous variants were fixed, and that levels of polymorphic diversity were driven by the hitchhiking effect. However, we know today that the assumption that recombination is mutagenic is flawed and that diversity at a DNA locus is in part driven by the recombination rate, and the selection and fixation of variants are largely driven by the corresponding competitive fitness of their phenotype under the selection pressure. In this regard, Kimura's neutral theory of molecular evolution fits observed data and is the better model.

University of Ghana http://ugspace.ug.edu.gh

The era of nucleotide sequencing pioneered by Sanger sequencing brought into the field of molecular population genetics higher resolution power to detect DNA sequence diversity and index population diversity and interspecies divergence. The first study to look at nucleotide sequence variation used the cumbersome Maxam-Gilbert approach in resequencing the *Adh* gene of *D. melanogaster* and discovered 43 single nucleotide variants, previously unseen by protein gel electrophoresis studies, of which only one accounted for the allozyme diversity (Kreitman, 1983). These data showed the higher resolution power of nucleotide sequencing and established the wide gamut of genetic variants segregating in a population. It also supported the view that most amino acid changes are likely to be selectively deleterious as only few such variants keep enzyme activity intact.

Today, with the power of next-generation sequencing, a plethora of DNA sequence variants have been identified such as insertions and deletions, frameshift variants, copy number variations and a bewildering number of nucleotide sequences-derived metrics for molecular population genetics (Table 2.1). In addition, the advent of whole genome sequencing has further pushed the boundaries of the power to detect signatures of selection in a population at the molecular level (Table 2.1) (Casillas et al., 2017).

Using the neutral model as the null hypothesis, it is possible to test for natural selection using statistical metrics derived from computations on population polymorphism or divergence data, site frequency spectrum and linkage disequilibrium analysis (Casillas et al., 2017; Conway, 2019).

University of Ghana http://ugspace.ug.edu.gh

Site frequency spectrum-based tests like Tajima's D, Fu and Li's F and Fu and Li's D statistic can be computed by comparing the observed allele frequency distribution within a population with the expected distribution under the infinite neural alleles model of mutation and drift. The infinite alleles model of population genetics assumes that for any possible site at which mutation can occur and given a low rate of occurrence of mutation per site, the likelihood of a new mutation resulting in a distinct allele rather than reverting by 'back-mutation' to a previous one is high. Fundamentally, both Tajima's D and Ewens-Watterson test assume a constant population size (Conway, 2019).

Tajima's D measures the difference between the average pair-wise nucleotide diversity between sequences (π) and Watterson's population nucleotide diversity (θ) (Casillas et al., 2017; Tajima, 1989). This will make the expected value of Tajima's D for populations under neutrality to be zero. When conditions of neutrality are violated, Tajima's D will capture a skew in the allele frequency distribution. These significant deviations from zero can either be positive or negative. Positive values of Tajima's D indicate an excess of intermediate frequency alleles. This can be caused by population bottlenecks, population structure, and/or balancing selection (Casillas et al., 2017). Fu and Li's F statistic is determined by the difference between the number of single nucleotide variants observed only once in a sample and the total number expected under neutrality given the number of segregating sites and Watterson's estimate of nucleotide diversity (θ); Fu and Li's D is the difference between the number of derived nucleotide variants observed only once in a sample with the total number of derived nucleotide variants (Casillas et al., 2017; Fu et al., 1993).

University of Ghana http://ugspace.ug.edu.gh

Comparison of polymorphism within species and divergence data between species, for different loci or different polymorphic site types is used to generate metrics such as the McDonald Kreitman (MK) and Hudson-Kreitman-Aguade (HKA) test. The MK test is computed using the ratios of synonymous to nonsynonymous polymorphisms in species and substitutions between species. The HKA test ignores the coding status of polymorphisms and compares the pairwise nucleotide polymorphism (π) and inter-species divergence (K) across loci. These are essentially very simple contingency-based tests (with output such as a Fisher's exact test computed on a 2×2 contingency table) that are useful for screening for evidence of selection (Conway, 2019; McDonald et al., 1991; Innan, 2006).

Table 2.1 | The armamentarium of metrics for population diversity, selection, and linkage disequilibrium. Adopted from (Casillas et al., 2017).

University of Ghana http://ugspace.ug.edu.gh

Measure/test	Description	References
Nucleotide diversity measures (uni-dimensional measures)		
S, s	Number of segregating sites (per DNA sequence or per site, respectively)	Nei (1987)
H, η	Minimum number of mutations (per DNA sequence or per site, respectively)	Tajima (1996)
k	Average number of nucleotide differences (per DNA sequence) between any two sequences	Tajima (1983)
π	Nucleotide diversity: average number of nucleotide differences per site between any two sequences	Jukes and Cantor (1969); Nei and Gojobori (1986); Nei (1987)
θ, θ_W	Nucleotide polymorphism: proportion of nucleotide sites that are expected to be polymorphic in any suitable sample	Watterson (1975); Tajima (1993, 1996)
SFS	Site/allele frequency spectrum: distribution of allele frequencies at a given set of loci in a population or sample	Ronen *et al.* (2013)
LD (multi-dimensional association among variable sites) and recombination		
D	Coefficient of LD whose range depends of the allele frequencies	Lewontin and Kojima (1960)
D'	Normalized D, independent of allele frequencies	Lewontin (1964)
R, R^2	Statistical correlation between pairs of sites	Hill and Robertson (1968)
Z_{nS}	Average of R^2 over all pairwise comparisons	Kelly (1997)
Z_A/ZZ	Z_A is the average of R^2 only between adjacent polymorphic sites. ZZ is Z_A minus Z_{nS}, which is an estimate of the recombination parameter r	Rozas *et al.* (2001)
Four-gamete test	Measure of historical recombination under the infinite-sites model	Hudson and Kaplan (1985)
ρ	Population-scaled recombination rate $\rho = 4N_e r$ [computed, *e.g.*, by LDhat (Auton and McVean 2007) and LDhelmet (Chan *et al.* 2012)]	Hudson (1987)
Selection tests based on the allele frequency spectrum and/or levels of variability		
Tajima's D	Number of nucleotide polymorphisms with the mean pairwise difference between sequences	Tajima (1989)
Fu and Li's D, D^*	Number of derived nucleotide variants observed only once in a sample with the total number of derived nucleotide variants	Fu and Li (1993)
Fu and Li's F, F^*	Number of derived nucleotide variants observed only once in a sample with the mean pairwise difference between sequences	Fu and Li (1993)
Fay and Wu's H	Number of derived nucleotide variants at low and high frequencies with the number of variants at intermediate frequencies	Fay and Wu (2000)
Zeng's E, θ_L, DH	Difference between θ_L and θ_W: the first is sensitive to changes in high-frequency variants. DH is a joint test including Tajima's D and Fay and Wu's H	Zeng *et al.* (2006)
Achaz's Y	Unified framework for θ estimators on the basis of the allele frequency spectrum	Achaz (2009)
Fu's F_S	Test based on the allele frequency spectrum	Fu (1997)
Ramos-Onsins' and Rozas' R_2, R_3, R_4, R_{2E}, R_{3E}, R_{4E}	Tests based on the difference between the number of singleton mutations and the average number of nucleotide differences	Ramos-Onsins and Rozas (2002)
CL, CLR	Genome scan for candidate regions of selective sweeps based on aberrant allele frequency spectrum	Nielsen *et al.* (2005)
Selection tests based on comparisons of polymorphism and/or divergence between different classes of mutation		
d_N/d_S, K_a/K_s	Ratio of nonsynonymous to synonymous nucleotide divergence/ polymorphism (ω)	Li *et al.* (1985); Nei and Gojobori (1986)
HKA	Degree of polymorphism within and between species at two or more loci	Hudson *et al.* (1987)
MK	Ratios of synonymous and nonsynonymous nucleotide divergence and polymorphism	McDonald and Kreitman (1991)
Estimators derived from extensions of the MK test or the DFE		
NI	Neutrality index that summarizes the four values in an MK test table as a ratio of ratios	Rand and Kann (1996)
DoS	Direction of selection: difference between the proportion of nonsynonymous divergence and nonsynonymous polymorphism	Stoletzki and Eyre-Walker (2011)

University of Ghana http://ugspace.ug.edu.gh

Measure/test	Description	References
α	Proportion of substitutions that are adaptive	Charlesworth (1994); Smith and Eyre-Walker (2002)
DFE-α	Fraction of adaptive nonsynonymous substitutions, robust to low recombination	Eyre-Walker and Keightley (2009)
ω_A	Rate of adaptive evolution relative to the mutation rate	Gossmann *et al.* (2010)
K_{a+}	Rate of adaptive amino acid substitution ($K_{a+} = \alpha K_a$)	Gossmann *et al.* (2010); Castellano *et al.* (2016)
$\hat{d}$, $\hat{b}$, $\hat{f}$, $\hat{\gamma}$, $\hat{\alpha}$	Fractions of five different selection regimes derived from an extension of the MK test: $\hat{d}$, fraction of new mutations that are strongly deleterious and do not segregate in the population; $\hat{b}$, fraction of new mutations that are slightly deleterious and segregate at minor allele frequency (MAF) <5%; $\hat{f}$, fraction of new mutations that are neutral, calculated after removing the excess of sites at MAF <5% due to slightly deleterious mutations; $\hat{\gamma}$, subset of $\hat{f}$ corresponding to recently neutral sites; $\hat{\alpha}$, fraction of new mutations that are adaptive, calculated after removing slightly deleterious mutations	Mackay *et al.* (2012)
L_{HRi}	Proportion of adaptive substitutions lost due to HRi	Castellano *et al.* (2016)
r_{opt}	Optimal baseline recombination, above which the genome is free of the HRi and thus $L_{HRi} = 0$	Mackay *et al.* (2012); Castellano *et al.* (2016)
Selection tests based on LD		
Hudson's haplotype test	Detection of derived and ancestral alleles on unusually long haplotypes	Hudson *et al.* (1994)
B/Q	Based on LD between adjacent pairs of segregating sites, under the coalescent model with recombination	Wall (1999)
iHS	Integrated haplotype score, based on the frequency of alleles in regions of high LD	Voight *et al.* (2006)
LRH	Long-range haplotype test, based on the frequency of alleles in regions of long-range LD	Sabeti *et al.* (2002)
HS	Haplosimilarity score: long-range haplotype similarity	Hanchard *et al.* (2006)
EHH	Extended haplotype homozygosity: measurement of the decay of LD between loci with distance	Sabeti *et al.* (2002)
LDD	LD decay: expected decay of adjacent SNP LD at recently selected alleles	Wang *et al.* (2006)
SGS	Shared genomic segment analysis: detection of shared regions across individuals within populations	Cai *et al.* (2011)
GIBDLD	Detection of genomic loci with excess of identity-by-descent sharing in unrelated individuals as signature of recent selection	Han and Abney (2013)
XP-EHH	Long-range haplotype method to detect recent selective sweeps	Sabeti *et al.* (2007)
H12, H2/H1	Haplotype homozygosity	Garud *et al.* (2015)
Population differentiation and associated selection tests		
G_{ST}	Analysis of gene diversity (heterozygosity) within and between subpopulations	Nei (1973)
F_{ST}	Average levels of gene flow based on allele frequencies, under the infinite-sites model	Hudson *et al.* (1992b)
Bayesian F_{ST}	Probability that a locus is subject to selection based on locus-specific population differentiation, using a Bayesian method	Foll and Gaggiotti (2008)
G_{ST}, H_{ST}, K_{ST}	Different test statistics based on haplotype frequencies and/or the number of nucleotide differences between sequences	Hudson *et al.* (1992a)
S_{nn}	Genetic differentiation of subpopulations based on haplotypic data	Hudson (2000)
Phi_{ST}	Correlation of haplotypic diversity at different levels of hierarchical subdivision	Excoffier *et al.* (1992)
Strobeck's *S*	Measure of population structure based on the comparison of the observed number of alleles in a sample to that expected when θ is estimated from the average number of nucleotide differences	Strobeck (1987)
XP-CLR	Cross-population composite likelihood ratio test, based on allele frequency differentiation across populations	Chen *et al.* (2010)
TLK, TF-LK	Original Lewontin–Krakauer test (TLK) and an extension (TF-LK), aimed at detecting selection based on the variance of F_{ST} across loci	Lewontin and Krakauer (1973); Bonhomme *et al.* (2010)
LSBL	Locus-specific branch length, based on pairwise F_{ST} distances	Shriver *et al.* (2004)
hapFLK	Detecting of selection based on differences in haplotype frequencies among populations with a hierarchical structure	Fariello *et al.* (2013)

This table is reproduced here in tandem with its open access designation under the Creative Commons Attribution 4.0 International License (http://creativecommons.org/licenses/by/4.0/)

University of Ghana http://ugspace.ug.edu.gh

2.5.2 The *Plasmodium falciparum* genome

The first draft of the *P. falciparum* genome was completed in 2002 (Gardner et al., 2002; Aravind et al., 2003). The *P. falciparum* genome is a 23Mb nuclear genome packaged into 14 linear chromosomes, a circular plastid and multiple mitochondria. Its proteome, comprising a large proportion of proteins devoted to immune evasion and host-parasite interactions, is encoded by approximately 5300 genes. The *P. falciparum* genome is the most AT-rich (~80%) among all species of the genus *Plasmodium* (Gardner *et* al., 2002).

Additionally, approximately one-third of the *P. falciparum* proteome is characterized by low-complexity regions (LCRs) enriched in asparagine residues (Aravind et al., 2003; Singh et al., 2004; Feng et al., 2006; DePristo et al., 2006). As these proteins with large LCRs have abundant glutamine/asparagine (Q/N) repeats, they also have a high likelihood to form insoluble intracellular aggregates (Tartaglia et al., 2005; Halfmann et al., 2011). The subtelomere of *P. falciparum* chromosomes encode the highly polymorphic genes devoted to antigenic variation. Additionally, many of its nucleus-encoded proteins are shipped to its apicoplast which serves as the organelle for isoprenoid and fatty acid metabolism (Gardner et al., 2002).

Since 2002, the increasing access to next-generation sequencing (NGS) and its reduced cost has made many interrogations of the *P. falciparum* genome possible. Much interest has been dedicated to multi-gene families involved in antigenic variation to evade host immune responses, host red cell organization, protein trafficking and host vascular bed adhesion. Of these, the PfEMP1 (*P. falciparum* erythrocyte membrane protein 1) gene family is the most studied. This gene is part of the var family of genes located in the subtelomeric regions of the chromosome.

University of Ghana http://ugspace.ug.edu.gh

It is important for adhesion of the infected erythrocyte to the vascular bed of the host and has been implicated as vital to the pathogenesis of cerebral malaria, a severe manifestation of *P. falciparum* malaria (Jensen et al., 2020; Hviid et al., 2015). Additionally, recent evidence suggests that it may play a role in the biogenesis of EVs as parasite strains null for its expression do not produce EVs (Regev-Rudzki et al., 2013; Maier et al., 2008).

2.5.3 Leveraging population genetics and genomics for molecular surveillance of ART resistance

Since the publication of the reference *P. falciparum* genome more than 20 years ago, the foundation for population genomics and genetics studies to advance our understanding of *P. falciparum* biology was laid. In single-cell protozoan parasites like *Plasmodium sp.*, population genomics has been used to guide the evaluation of control interventions such as ACT use and vector control (Neafsey et al., 2021) and has led to advancement in our understanding of parasite drug resistance, population structure, drug and vaccine targets and host-parasite interactions. In principle, population genomics has the potential to shift molecular surveillance for ART drug resistance beyond the realm of pronunciation to forecasting. This new paradigm is likely to emerge, in tandem with the increasing waves of precision medicine in the clinical arena (König et al., 2017). Traditional molecular surveillance for drug resistance in malaria parasites relies on the analysis of genes of interest for known resistant conferring variants and looks for such variants in parasite samples circulating in the human population. At best, this kind of molecular surveillance merely announces the presence of the resistant parasite and is not powered to predict their emergence.

University of Ghana http://ugspace.ug.edu.gh

However, the unique genetic architecture of *PfK13*-driven ARTr presents a novel opportunity for scanning for background signatures of selection on ARTr predisposing loci to determine whether there are signatures of selection to suggest the evolution of *PfK13*-driven ARTr. The potential future direction of such an approach can bring to fruition the forecasting of ARTr parasites in a geographically defined population of malaria parasites. In this regard, looking for signatures of selection in these background loci may serve to give an early warning signal for the eventual emergence of ARTr.

University of Ghana http://ugspace.ug.edu.gh

2.6 Artemisinin: Mechanism of Action and Targets

Discovered in the 1970s by Youyou Tu, who won the Nobel Prize in Medicine and Physiology in 2015, artemisinin (ART) belongs to the sesquiterpene lactone group of antimalarial drugs and was isolated from *Artemisia annua*, a Chinese medicinal herb (Tu, 2016, 2011; Wang et al., 2018). The mode of action of ART is considered to involve heme-generated Fe2+ (ferrous iron) catalyzed reductive scission of the endoperoxide bridge. This produces carbon-centered radical species that target and alkylate cellular macromolecules, especially, proteins, killing the parasite (Haynes et al., 2013; Heller et al., 2019; Klonis et al., 2013a; Meshnick, 2002). Heme-generated Fe2+ is known to be produced by the digestion of hemoglobin in the parasite's food vacuole (Siddiqui et al., 2021; Meunier et al., 2010). This is the explanation behind the observation of high parasite sensitivity to ART at the trophozoite stage of intra-erythrocytic development as this stage is when heme-digestion is at its zenith (Abu Bakar et al., 2010; Klonis et al., 2013b; Tilley et al., 2016). However, and rather paradoxically, 2–4-hour post-invasion rings have been reported to also exhibit high sensitivity to ART (Klonis et al., 2013b; Xie et al., 2016). This observation is not due to hemoglobin digestion but has been suggested to be driven by *de novo* synthesis of heme (Klonis et al., 2013a; Wang et al., 2015a). Iron may also be obtained from other sources such as non-polymerized heme yet to be acted on by glutathione (Ginsburg et al., 1998), free heme from peroxidative decomposition in the FV (Loria et al., 1999) and ferrous iron from a labile pool in the parasite cytoplasm (Clark et al., 2013).

University of Ghana http://ugspace.ug.edu.gh

Once activated, ART-produced free radicals causes the alkylation of proteins, lipids and even heme (O'Neill et al., 2010; Yang et al., 1994). To identify the protein targets of ART, an early study treated *P. falciparum*-infected erythrocytes with a radiolabeled antimalarial endoperoxide (study used artether, dihydroartemisinin and arteflene), and employed SDS-polyacrylamide gels to identify six radioactively labeled malarial proteins (Asawamahasakda et al., 1994). Subsequently, one of these proteins was identified as the translationally controlled tumor protein *PfTCTP* (Bhisutthibhan et al., 2001; Li et al., 2016).

Following attempts to elucidate the mechanism of action of ART from the central action of *PfTCTP*, it emerged that the alkylation action of ART-induced free radicals is promiscuous and targets a wide range (more than the 6 identified earlier) of proteins in the parasite-infected erythrocyte (Wang et al., 2015a; Ismail et al., 2016a; Ismail et al., 2016b; Jourdan et al., 2019). This conclusion was reached following a proteomic study that used a suite of ART activity-based protein profiling probes to identify parasite protein drug targets using *in vitro* culture. The probes were designed to retain biological activity and alkylate the molecular target(s) for subsequent isolation using click chemistry. Liquid chromatography-tandem mass spectrometry proteomic analysis was used to identify the protein targets alkylated by ART. This defined an ART proteome with many targets in the glycolytic, hemoglobin degradation, antioxidant defense, and protein synthesis pathways. Thus, Ismail et al. revealed the pleiotropic gamut of the biological functions targeted by ART (Ismail et al., 2016a). A limitation of the Ismail et al. study was a lack of experimental design to identify non-covalent targets of ART action. Therefore, it is highly suggestive that the protein targets of ART may be broader.

University of Ghana http://ugspace.ug.edu.gh

Apart from the protein targets identified, several studies have also implicated heme as a target of ART action (Meunier et al., 2010; Asawamahasakda et al., 1994; Robert et al., 2002; Robert et al., 2001). Additionally, it has been reported that the accumulation of non-polymerizable redox-active ART-heme adducts (Hong et al., 1994; Heller et al., 2018a) intimate at a mechanism of action similar to 4-aminoquinoline drugs that preclude heme detoxification (Meunier et al., 2010; Pandey et al., 1999). In tandem with this view, ARTr parasites have showed lower levels of ART-heme adduct in comparison to ART-sensitive parasites (Heller et al., 2018a; Heller et al., 2018b). A final mechanism of action motif for ART involves the generation of reactive oxygen species (ROS) following the activation of ART. The ROS damages parasite DNA and mitochondria and causes a reduction in the cellular antioxidant capacity of the parasite-infected erythrocyte (Meshnick, 2002; Gopalakrishnan et al., 2015; Krungkrai et al., 1987; Wang et al., 2010).

University of Ghana http://ugspace.ug.edu.gh

2.7 Artemisinin Resistance

Artemisinin (ART) resistance was initially defined microscopically as a high proportion of persisting parasitemia on the third day after ART treatment (Noedl et al., 2008; Dondorp et al., 2009; Stepniewska et al., 2010). The cut-off day 3 parasitemia indicative for this clinical definition of ART resistance is 10% in SEA and 5% in SSA (White et al., 2015; Group. et al., 2015). This definition was subsequently improved by estimating the parasite clearance half-life ($PC_{1/2}$) and defining ART resistance as a $PC_{1/2}$ greater than 5 hours in comparison to the known $PC_{1/2}$ of ART-sensitive parasites estimated at ~ 2 hours. Presently, this is the ideal way to determine ART resistance *in vivo* (Ashley et al., 2014; Phyo et al., 2012; Uwimana et al., 2020; Balikagala et al., 2021; Amaratunga et al., 2012). Interestingly, the standard 72-hour IC50 drug sensitivity assay cannot distinguish ART-sensitive and resistant parasites (Dondorp et al., 2009; Amaratunga et al., 2012). This unclassical definition of ARTr has reportedly sparked numerous debates (Dondorp et al., 2013; Ferreira et al., 2013; Krishna et al., 2013; Wellems et al., 2020).

Another interesting point is the fact that, before the widespread use of ACTs, ART monotherapies have been known to effectively clear parasites from the blood within 7 days with many cases of parasite recrudescence reported within 28 days. This is consistent with the WHO definition of the R1 resistance phenotype that details an initial greater than 25% reduction in parasitemia by day 2 of treatment followed by parasite recrudescence reported as parasitemia persisting after 3 days of completing full course treatment. RII resistance phenotype is defined as an initial greater than 25% reduction in parasitemia by day 2 of treatment followed by parasitemia persisting after 4-7 days of completing full course treatment. RIII resistance phenotype is defined as no reduction in parasitemia after full course treatment (WHO, 1965).

University of Ghana http://ugspace.ug.edu.gh

Currently, concerning ART resistance, RII and RIII resistance is yet to be reported (Siddiqui et al., 2021). This makes ART resistance different from previous events of antimalarial drug resistance. This notwithstanding, present efforts to prevent the spread of ART resistance serve as a good strategy to mitigate, at a very early stage, the risk of full-blown ART resistance emerging (WHO, 2021a, 2015).

The ring stage of the intra-erythrocytic developmental cycle of *P. falciparum* has been identified as the most resistant to ART (Dondorp et al., 2009; Saralamba et al., 2011). The mechanism identified to explain this observation is one that suggests that the ring stage is ideal for parasites to enter dormancy and reduce cellular metabolic activities to culminate in the emergence of the ART resistance phenotype (Witkowski et al., 2010; Teuscher et al., 2010). Several studies have also reported an association between decelerated intra-erythrocytic developmental cycle at the ring stage and the expression of ARTr in *P. falciparum* parasites (Cheng et al., 2012; Witkowski et al., 2013b). Therefore, it has been extrapolated that ARTr in *P. falciparum* emerges on an increased predilection of the ring stage parasites to enter dormancy under ART pressure and resume normal growth once this pressure is removed (Siddiqui et al., 2021). Another explanation for this observation is that the propensity for dormancy at the ring stage is hinged on the underlying mechanisms that are the main drivers of the ARTr phenotype.

University of Ghana http://ugspace.ug.edu.gh

The *in vitro* and *ex-vivo* ring-stage survival assay (RSA) was designed on this observation of delayed intra-erythrocytic development at the ring stage. In principle, the assay treats 0–3-hour ring-stage parasites with 700nM DHA (the pharmacological equivalent for optimal *in vivo* treatment) for six hours and measures their survival after sixty-six hours (Witkowski et al., 2013a). The read-out of the assay is centered on an RSA value of 1%. Above 1% correlates with ARTr and below 1% with ART sensitivity. The RSA has been demonstrated to show a strong correlation with low- and fast-clearing parasites after ART therapy and its utility as a tool in surveillance of ARTr is indispensably practical.

2.7.1 *PfK13* variants take center-stage as molecular markers of artemisinin resistance

Initial studies into the molecular determinants of ART resistance in *P. falciparum* relied on the *in vivo* definition of reduced parasite clearance rate (Amaratunga et al., 2012; Takala-Harrison et al., 2013). In 2010, a study reported findings to suggest that the delayed parasite clearance phenotype was heritable (Anderson et al., 2010) and laid the foundation for further enquiries into the genetic underpinnings of its expression. Subsequently, genome-wide association studies (GWAS) determined an association between delayed parasite clearance and genomic regions on chromosome 13 of the *P. falciparum* genome (Takala-Harrison et al., 2013; Cheeseman et al., 2012). In 2014, a study reported the long-term *in vitro* selection with dihydroartemisinin (for about 5 years) of an ARTr parasite from a Tanzanian parasite strain (F32) and used comparative whole genome sequencing to identify a *PfK13* variant associated with the ARTr phenotype (Ariey et al., 2014).

University of Ghana http://ugspace.ug.edu.gh

Ariey et al. further conducted a retrospective analysis of clinical isolates from Cambodia and identified many variants in the *PfK13* propeller domain that were significantly associated with the ARTr phenotype as defined by *in vivo* delayed parasite clearance rates and *in vitro* ring-stage survival assays (Ariey et al., 2014). This centrally placed *PfK13* as the key molecular marker of ARTr in *P. falciparum* parasites.

Since the discovery of the *PfK13* molecular marker, many studies have validated its association with ART resistance *in vivo* clinical efficacy studies (Ashley et al., 2014; Miotto et al., 2015; Huang et al., 2015). Furthermore, several of the commonest *PfK13* variants (C580Y, R539T, I543T, N458Y and Y493H) were genetically engineered into laboratory parasite strains to validate their association with ARTr *in vitro* (Ghorbal et al., 2014; Siddiqui et al., 2020; Straimer et al., 2015). All these validation studies paved the way for the global utilization of *PfK13* variants as molecular markers for ARTr surveillance. Presently, more than two hundred non-synonymous *PfK13* variants have been reported globally (Project, 2016; Chhibber-Goel et al., 2019; Ménard et al., 2016; Taylor et al., 2015).

To help focus ARTr surveillance efforts, especially in SSA, the WHO issued a validated set of *PfK13* variants associated with ART resistance. This list includes: F446I, N458Y, M476I, Y493H, R539T, I543T, P553L, R561H, P574L, and C580Y (WHO, 2020a). In Africa multiple *PfK13* variants have been reported, however, the *PfK13* variants that correlate with *in vivo* delayed parasite clearance phenotype in the GMS are relatively rare in Africa (Uwimana et al., 2020; Balikagala et al., 2021; Ménard et al., 2016; Taylor et al., 2015; Bergmann et al., 2021; Bayih et al., 2016; Conrad et al., 2014; L'Episcopia et al., 2020; Raman et al., 2019).

University of Ghana http://ugspace.ug.edu.gh

For example, the most frequent *PfK13* variant in Africa is A578S and this variant was not associated with *in vitro* ARTr when engineered into a Dd2 parasite strain (Menard et al., 2016). Recent evidence has highlighted the emergence of *PfK13* conferring ARTr variants in regions outside the GMS in SEA and this imminent threat has been cast over the SSA sub-region by two recent publications (Uwimana et al., 2020; Balikagala et al., 2021). In Rwanda, the R561H variant was found in 7.4% of patients in the study population. Although the ACTs cure rate was greater than 95%, the prevalence of this variant is of concern as the phylogenetic analysis indicate that it represents the independent expansion of a local line. Furthermore, when the R561H variant was engineered into a Dd2 line, it manifested the ARTr phenotype indexed by the *in vitro* RSA assay (Uwimana et al., 2020). Additionally, Fernando et al. published a case report of AL treatment failure of a parasite with the R561H variant (Fernando et al., 2020). This association of the R561H variant with clinical delayed parasite clearance is not surprising because it has been previously validated to be associated with delayed parasite clearance in the GMS (WWARN Artemisinin-based Combination Therapy Africa Baseline Study Group et al., 2015).

In the Caribbean, the most prevalent *PfK13* variant is C580Y with evidence that it independently emerged in the *P. falciparum* populations in Guyana and Papua New Guinea (Chenet et al., 2016; Mathieu et al., 2020; Miotto et al., 2020). It has been reported that since 2010, this variant has been circulating at low frequency and that the reason for this is most likely due to the high fitness cost of the variant. This was confirmed by gene editing in two parasite strains from the French Guiana (Chenet et al., 2016; Mathieu et al., 2020). In Papua New Guinea, *P. falciparum* parasites with the C580Y variant were also detected at a low prevalence (2.3%) from samples collected in 2017 (Miotto et al., 2020).

University of Ghana http://ugspace.ug.edu.gh

In all these regions outside SEA where ARTr variants have emerged, it is probable that the levels of human immunity to malaria, the fitness cost of the ARTr parasites, the transmission intensities and within-host competition from the multiplicity of infections, as discussed earlier, are responsible for the relatively low frequencies of the ARTr variants observed.

2.7.2 Patterns in the geographic distribution of *PfK13* variants have been observed in the GMS of SEA.

C580Y has the highest prevalence in the eastern part of the GMS (Cambodia, Laos, Vietnam, and eastern Thailand) and is almost fixed in some regions. In the western part of the GMS, F446I is most prevalent (western Thailand, Yunnan province of China, and Myanmar) (Ménard et al., 2016; Kobasa et al., 2018; Tun et al., 2015; Wang et al., 2015b; Ye et al., 2016). Some factors that may explain this observed variation along geographical lines are the idiosyncratic demographic factors (age, hemoglobinopathies, malaria immunity), ART drug usage (monotherapy, compliance to dosing and duration regimens, access to quality drugs), parasite genetic background and makeup, and transmission activities of the female anopheline vector (Siddiqui et al., 2020; Straimer et al., 2015).

Another point to note is that ART resistance in the GMS arose from multiple founder populations with variants in ferredoxin, apicoplast ribosomal protein S10 (*arps10*), multidrug resistance protein 2 (*mrp2*), and *P. falciparum* chloroquine resistance transporter (*Pfcrt*) as genetic background (Miotto et al., 2015; Miotto et al., 2013). This may also account for the variation in *PfK13* variants along geographical lines globally. These background variants on which ARTr emerged in SEA are likely to serve a fitness compensatory role to offset the fitness cost for the ARTr-conferring *PfK13* variant.

University of Ghana http://ugspace.ug.edu.gh

For example, the *PfK13* C580Y variant in different genetic backgrounds had varied fitness costs as measured using *in vitro* fitness assays (Siddiqui et al., 2020; Li et al., 2019; Nair et al., 2018; Tirrell et al., 2019; Straimer et al., 2017).

In the grand scheme of affairs, the evolved asexual ARTr parasites in the human host must be transmitted to the female anopheline mosquito vector to achieve spread in the larger human population. For this to happen, the effect of the ARTr conferring variant on gametocytogenesis is important. It has been shown, by clinical *in vivo* and laboratory *in vitro* studies, that ARTr parasites have higher gametocytes and thus a greater potential for transmission to the mosquito vector (Ashley et al., 2014; Witmer et al., 2020). Additionally, the exposure of trophozoites to low dihydroartemisinin concentrations has been reported to promote gametocytogenesis and further adds evidence to support the transmission of ARTr parasites (Portugaliza et al., 2020). Finally, ARTr parasites have been demonstrated to readily infect the diverse *Anopheles* mosquito population (including the primary African vector *Anopheles gambiae*) and indicate the lack of a biological barrier for the spread of ARTr to Africa (St Laurent et al., 2015). This is unlike atovaquone resistance which is conferred by variants in cytochrome b of the mitochondria and cannot be transmitted to mosquitoes (Goodman et al., 2016).

University of Ghana http://ugspace.ug.edu.gh

2.8 Molecular Mechanisms Undergirding Artemisinin Resistance

The mounting evidence on the molecular mechanisms undergirding ART resistance span multiple organelles and biological pathways consistent with the pleiotropic nature of the action of ART. However, two main themes emerge following a review of the literature. ARTr emerges when *P. falciparum* parasites under ART pressure, reduce hemoglobin endocytosis into the digestive food vacuole and/or maintain redox homeostasis under the ART-induced oxidative stress (Siddiqui et al., 2021). The expression of both motifs undergirding ARTr is primarily centered on the *PfK13* variant which is a structural homolog of the human Kelch-like ECH-associated protein 1 (Keap 1) (Ariey et al., 2014) that is known to bind and ubiquitylate the nuclear factor erythroid 2-related factor 2 (Nrf2) (Hayes et al., 2006) which is involved in regulating the oxidative stress response pathway. BLAST analysis of the *Plasmodium* genome and proteome reveals that it does not have an Nrf2 homolog. However, *PfK13* is thought to function as a ubiquitin ligase adaptor to control the degradation of other proteins (Haldar et al., 2018).

PfK13 is primarily localized to the endoplasmic reticulum (ER), cytostomes, intracellular vesicles (endocytic and secretory), and to a lesser extent, cytoplasm, food vacuole and apicoplast (Siddiqui et al., 2020; Xie et al., 2020; Bhattacharjee et al., 2018; Birnbaum et al., 2020; Gnädig et al., 2020; Yang et al., 2019) suggesting pleiotropic roles in multiple biological pathways. Additionally, and of significant importance, was the finding that *PfK13* variants also localized to vesicular structures marked by phosphatidylinositol-3-phosphate (PI3P) and were greatly expanded in the C580Y variant (Bhattacharjee et al., 2018). A possible function of *PfK13*-associated PI3P vesicles is for *PfEMP1* export under ART pressure and the observation that parasite lines with *PfPTP* (*Plasmodium* translocon of exported proteins) knocked out do no transport *PfEMP1* and do not produce extracellular vesicles (EVs), suggests a role for EVs in the molecular mechanisms undergirding ARTr. Another proposed importance of this

University of Ghana http://ugspace.ug.edu.gh

association between ARTr parasites and *PfEMP1* is the conceptualized *in vivo* survival advantage from adherence to host capillary receptors to evade the clearance power of the spleen (Regev-Rudzki et al., 2013; Maier et al., 2008; Bhattacharjee et al., 2018).

The kaleidoscopic nature of the many *PfK13* variants associated with ART resistance suggests that it is likely mediated by a loss of function of the variant *PfK13* (Xie et al., 2020). Multiple studies have shown that *PfK13* variants do not affect *PfK13* cellular localization and interaction partners but are associated with decreased protein levels (Birnbaum et al., 2020; Gnädig et al., 2020; Yang et al., 2019; Siddiqui et al., 2017). *PfK13* is an essential parasite protein and when knocked out, parasites lose viability. However, the asexual intra-erythocytic developmental cycle of the parasite can tolerate up to 50% loss in *PfK13* levels (Birnbaum et al., 2020).

In vitro genetic manipulations of the expression level and localization of *PfK13* proteins have produced, as a corollary, changes in the ARTr phenotype independent of the presence of the *PfK13* ART conferring genetic variant (Birnbaum et al., 2020; Gnädig et al., 2020; Yang et al., 2019). Interestingly, a study that analyzed the transcriptome of a large sample of clinical parasites from the GMS did not report an association between the ARTr phenotype and transcript levels of *PfK13* (Mok et al., 2015). However, a temporal analysis of *PfK13* transcript levels after AL exposure reported an inverse relationship between *PfK13* gene expression and parasite clearance half-life (Silva et al., 2019). A recent multi-omics study compared the transcriptome and proteome of isogenic parasites and determined that the effect of the *PfK13* genetic variant on its protein levels depends on the variant type and the developmental stage of the asexual parasite. However, all ARTr conferring *PfK13* variants showed elevated *PfK13* transcripts levels at the ring stage (Mok et al., 2021).

University of Ghana http://ugspace.ug.edu.gh

What remains to be elucidated is what accounts for the reduced protein levels of *PfK13* variants. Some studies have implicated a reduction in variant PfK13 protein stability (Xie et al., 2020; Birnbaum et al., 2020). Additionally, *in silico* molecular simulations of the *PfK13* variants R539T and C580Y protein structures have shown some local structural destabilization in the propeller domain (Coppée et al., 2019).

The second overarching theme in the evidence gathered towards understanding the molecular mechanisms undergirding ART resistance in *P. falciparum* is increased tolerance towards ART-induced proteinopathic and oxidative stress. ART activation, following heme-mediated scission of the endoperoxide bridge, results in the production of carbon-centered radicals that promiscuously alkylate parasite proteins, lipids and membranes. The resulting cellular damage leads to cellular death. An increased cellular response to the resulting ART-induced proteotoxic and oxidative stress has been seen in ARTr parasites (Mok et al., 2021; Mok et al., 2015; Rocamora et al., 2018).

Mok and others conducted a transcriptomic analysis of clinical isolates of ARTr *P. falciparum* parasites and reported an increased expression of genes involved in modulating tolerance to the proteotoxic and oxidative stress mounted under ART pressure. This study showed an upregulation of genes involved in the unfolded protein response (UPR) such as the endoplasmic reticulum-located reactive oxidative stress complex BiP and ERp72; and the cytoplasmic T-complex protein 1 ring complex (TRiC) (Mok et al., 2015). Mok and others further used proteomic analysis of genetically engineered laboratory parasite strains to confirm the association between *PfK13* and upregulated chaperones, such as cyclophilin 19B protein (Mok et al., 2021).

University of Ghana http://ugspace.ug.edu.gh

To further support the association between increased tolerance to oxidative stress and ART resistance, a long-term *in vitro* selection of ARTr study also reported a transcriptome with upregulated genes in the cellular adaptive responses to stress (Rocamora et al., 2018). The ensuing proteinopathy from ART action results in the damming of unfolded and polyubiquitinated proteins in the endoplasmic reticulum. This in turn leads to an endoplasmic reticulum stress activation response that drives phosphorylation of the ER stress sensor eIF2α by the PK4 protein kinase and culminates in cellular translational arrest. ARTr *PfK13* variants were found to have high levels of eIF2 α phosphorylation in early rings and this is likely to account for the ring stage dormancy associated with ARTr (Zhang et al., 2017). Another arm of evidence that associates ARTr with ring stage dormancy is the ability of *PfK13* variant parasites to reduce tRNA expression under ART pressure. This is similar to what happens in a cell under amino acid starvation and promotes eventual recovery from the cell cycle quiescence (Mok et al., 2021; McLean et al., 2017). ARTr-conferring *PfK13* variant parasites have been reported to have less ubiquitination of proteins and thus a lower burden on the proteasomal response pathway. This likely contributes to mitigating the collapse of the proteasomal response pathway (Siddiqui et al., 2020; Bridgford et al., 2018; Dogovski et al., 2015). Furthermore, Yang and others have reported that ARTr parasites achieved protein turnover much earlier than ART-sensitive parasites although both sensitive and resistant parasites showed equal initial responses to ART oxidative stress. This reported discrepancy may be explained by the action of an ARTr proteotoxic vehicular transport system. Such a system if present is likely to be driven by an extracellular vesicle connection to the endovesicular trafficking system. Finally, a recent study by Zhang and others suggested that upregulation of the UPR and down-regulating ubiquitination are the overarching mechanisms used to mitigate the accumulation of proteotoxic waste (Zhang et al., 2021).

University of Ghana http://ugspace.ug.edu.gh

Two studies that investigated the *PfK13* interactome identified BiP (an ER-resident chaperone) as one of the interacting partners of *PfK13* and further strengthened the association between *PfK13* ARTr and the ER proteostatic response (Siddiqui et al., 2020; Gnädig et al., 2020). In addition to this, Bhattacharjee and others found a preponderance of *PfK13*-associated PI3P vesicles in the ER of an ARTr parasite under ART stress (Bhattacharjee et al., 2018). This finding suggests a nexus between the endomembranous vesicular pathway and the oxidative stress response arm. Likely, the bridging process between these two molecular mechanistic arms of ARTr is the putative role of EVs as vehicles mediating cellular redox homeostasis by actively removing proteinopathic waste in tandem with the proteasomal system. As it is known that ARTr parasites exhibit a heightened antioxidant response to ART-induced oxidative stress, this cellular redox homeostasis function of EVs may add to the ARTr parasite's armamentarium that deals with ART-induced oxidative stress (Gopalakrishnan et al., 2015; Krungkrai et al., 1987; Kavishe et al., 2017). Further evidence in support of this position was reported by Cui and others who showed that ARTr parasites (selected by long-term *in vitro* exposure to serial escalating doses of DHA) have increased transcripts of more than 20 genes involved in cellular antioxidant responses and had increased levels of cellular antioxidants such as glutathione and thioredoxin Cui et al. (2012b). Additionally, it is a known fact that ART activation in the *P. falciparum*-infected erythrocyte also produces reactive oxygen species (ROS) that target the parasite's DNA and mitochondria (Gopalakrishnan et al., 2015). Therefore, the variants in genes associated with improving DNA damage repair under ART-oxidative injury are needed for parasites to tolerate ART. Clinical isolates of ARTr parasites in the GMS have been reported to harbor such DNA repair variants that endow them with the ability to thrive under ART-oxidative stress (Miotto et al., 2013; Xiong et al., 2020; Takala-Harrison et al., 2013).

University of Ghana http://ugspace.ug.edu.gh

The apicoplast and mitochondria have also been implicated in the development of ARTr (Mok et al., 2021; Zhang et al., 2021). Wang and others reported that mitochondria are one of the cellular targets of ART and that the mitochondrial response to ART is critical for the survival of ARTr parasites (Wang et al., 2010; Peatey et al., 2015). Using monoclonal antibodies of *PfK13* to interrogate its interacting partners, Gnadig and others reported mitochondrial proteins associated with PfK13 protein (Gnädig et al., 2020). This association was further validated by a multi-omics study that exposed *PfK13* ARTr parasites to ART and unveiled a correlation of the phenotype with upregulated mitochondrial metabolism (Mok et al., 2021). Finally, it has been demonstrated that atovaquone (an inhibitor of cytochrome bc1 in the mitochondria) can impede the reversal of quiescence in *PfK13* ARTr parasites under ART pressure and in effect prevent the ARTr phenotype from emerging (Mok et al., 2021; Peatey et al., 2015).

The apicoplast has also been implicated in ARTr. Its role in developing ARTr had been initially suggested by the finding that fatty acid synthesis in this bacteria-originating organelle was not turned off in quiescent parasites under DHA pressure (Chen et al., 2014). This association between the apicoplast and ARTr was further entrenched by a genetic screening study that showed its contribution to heat shock responses of *PfK13* ARTr parasites (Zhang et al., 2021). Of particularly interesting note was the finding that the isoprenoid biosynthesis pathway in the apicoplast remains unhindered under ART pressure in the *PfK13* ARTr parasite. This allows for the prenylation of an important class of proteins (the Rab GTPases) involved in the endocytic vesicular trafficking system (transport of hemoglobin into the DFV and maintenance of the DFV integrity) (Suazo et al., 2016; Howe et al., 2013; Kennedy et al., 2019). This is another fact that can accommodate a putative role of EVs in ARTr.

University of Ghana http://ugspace.ug.edu.gh

The genomic architecture of ARTr is complex. This multi-locus spanning resistome is centered on *PfK13* variants with molecular mechanisms spanning multiple parasite organelles including the digestive food vacuole, ER, mitochondria and apicoplast. However, two organizing motifs emerge from this quagmire of evidence on ARTr: reduced endocytosis of hemoglobin to the DFV and increased tolerance to oxidative stress. Within this milieu, the ubiquitous EVs may fit into a hypothetical model of ARTr by acting as the bridge between these two organizing motifs: their putative role as the vehicles originating from the endovesicular system that mediate cellular oxidative homeostasis under ART pressure in the *P. falciparum*-infected erythrocyte.

2.8.1 The *PfK13* interactome: a window into the multiple cellular processes undergirding artemisinin resistance

To understand the molecular mechanisms that contribute to the emergence of the ARTr phenotype, many studies have employed the experimental approach that determines the interacting partners of *PfK13* and gleans its function from this identified interactome. These interactome studies have identified a plethora of proteins that interact with *PfK13* and inferred its contribution to the ARTr phenotype using functional studies. However, there is only partial concordance in the varied findings of these studies most likely because of the different techniques employed or the fluctuating nature of the *PfK13* interaction partners (Siddiqui et al., 2020; Birnbaum et al., 2020; Gnädig et al., 2020).

University of Ghana http://ugspace.ug.edu.gh

Birnbaum et al. approached the identification of the *PfK13* interacting partners using the dimerization-induced quantitative BioID (DiQ-BioID) technique. The DiQ-BioID technique employs the addition of rapalog for the induction of dimerization and recruitment of the biotinylizer (BirA) to the F1-tagged *PfK13* protein. A streptavadin pull down is subsequently used to trap *PfK13* and its interacting partners. Then mass spectrometry was used to identify the peptides and report on the interacting partners of *PfK13*. With this technique, approximately ten *PfK13* interacting proteins were identified. These included the known endocytic factor Eps15 (epidermal growth factor receptor substrate 15), and a putative ubiquitin hydrolase ubiquitin-binding protein-1 (UBP-1) (Birnbaum et al., 2020).

Following this finding, a co-localization study was done using the top ten hits that showed that *PfK13* interacts with Eps15. The study then proceeded with the hypothesis that the *PfK13* interacting partners (PfKIP) are involved in endocytosis because Eps15 has been reported to be involved in endocytosis in other organisms. To test whether *PfK13*-Eps15 marks an endocytic structure, another co-localization experiment with endogenously GFP-tagged clathrin heavy chains (CHC) and AP2µ was done. This brought the conclusion that *PfK13*+Eps15 marks a clathrin-independent AP2µ endocytic pathway (Birnbaum et al., 2020; Henrici et al., 2020). This finding was unique in the fact that all previously known AP2µ complexes involved in endocytosis were clathrin-dependent (Yap et al., 2015).

University of Ghana http://ugspace.ug.edu.gh

Finally, using high-resolution microscopy techniques and a battery of functional assays, Birnbaum et al. implicated the *PfK13* interactome in endocytic uptake of hemoglobin to the digestive food vacuole as the key molecular mechanism undergirding *PfK13* ART resistance in *P. falciparum* (Birnbaum et al., 2020). One of these functional assays was a knock sideways of eight proteins (UBP-1,AP-2 μ, KIC4, KIC5, KIC7, KIC9, MCA2 (metacaspase 2), and Eps15) of the PfKIP, which caused the ARTr phenotype to emerge in parasites. This was characterized by reduced endocytosis of heme into the food vacuole (absence of bloating in the food vacuole assay utilized) (Birnbaum et al., 2020).

The second seminal study that interrogated the *PfK13* interactome was Siddiqui and others (Siddiqui et al., 2020). This study pulled down GFP-tagged *PfK13* interacting proteins, from transgenic parasites, using GFP-Trap beads. They reported that *PfK13* was associated with the unfolded protein response (UPR) pathway and elements of the reactive oxidative stress complex of the parasite (BiP (binding immunoglobulin protein), a protein disulfide isomerase (ERp72), and the putative endoplasmin (GRP94)) (Siddiqui et al., 2020). This implicated *PfK13* as a player in the oxidative stress response to ART. The third study was conducted by Gnadig and others and used an array of monoclonal antibodies targeting *PfK13* to identify an interactome enriched with Rab GTPases. This study also identified other proteins associated with endocytic vesicular transport, protein folding, the food vacuole and the mitochondrion (Gnädig et al., 2020). The finding of Rab GTPases (PfKIP) that are known to be involved in vesicular secretion and transport also suggests a role for extracellular vesicles in ARTr development. Therefore, studies into the *PfK13* interactome implicates *PfK13* in cellular endovesicular transport and suggest a role for EVs in ART resistance.

University of Ghana http://ugspace.ug.edu.gh

2.8.2 The digestive food vacuole and artemisinin resistance

The digestive food vacuole (DFV) of *P. falciparum* has become the center of our current understanding of the molecular mechanisms undergirding ARTr revolves. Heme, produced from endocytosed hemoglobin in the food vacuole, is considered the main activator of ART in the parasite. Therefore, any alteration in hemoglobin endocytosis, heme production, heme activation of ART, heme detoxification or the functional/structural integrity of the food vacuole can contribute to the emergence of the ARTr phenotype (Siddiqui et al., 2021; Birnbaum et al., 2020).

Several studies have mounted evidence to implicate the DFV and changes in its processing of heme with ARTr. In this vein, most of the proteins associated with ARTr such as PfK13, PfPI3K, UBP-1 and AP-2μ have been shown to play a role in the endocytic pathway for trafficking hemoglobin into the DFV (Xie et al., 2020; Sutherland et al., 2021). Additionally, genetic variants of falcipain-2, an enzyme responsible for the digestion of hemoglobin and the release of heme may also contribute to ARTr. In concordance with this view, an earlier proteomics experiment suggested that ARTr-conferring *PfK13* variants were characterized by reduced amounts of hemoglobin peptides in comparison to ART-sensitive parasites at the trophozoite stage (Siddiqui et al., 2017). However, a much recent study did not replicate these findings in the ring stage of the *P. falciparum* parasite (Mok et al., 2021).

Birnbaum et al.'s investigation of the *PfK13* interactome, as described earlier, provided overwhelming evidence to implicate *PfK13* in reduced hemoglobin endocytosis in the food vacuole. Their findings situated the quest for the function of *PfK13* in the arena of the parasite's endomembranous vesicular pathway. Using high-resolution microscopy and a parasite line expressing GFP-tagged *PfK13*, Yang and others also showed that *PfK13* is associated with doughnut shape structures near the parasite's cell membrane which take on the dimension of a cytostome (Yang et al., 2019). A similar finding to this was also reported by a study that used

University of Ghana http://ugspace.ug.edu.gh

electron microscopy (Gnädig et al., 2020). A common thread in all these research findings is the circumscribing of an arena suggestive of a role for EVs in ART resistance.

University of Ghana http://ugspace.ug.edu.gh

2.9 The Artemisinin Resistome

The ART resistome refers to the entire gamut of molecular markers associated with the ARTr phenotype including variants in background loci involved in fitness compensation or that may have arisen from founder populations (Kümpornsin et al., 2019; Miotto et al., 2015). The ART resistome comprise several functionally different and phenotypically varied set of genetic molecular markers.

2.9.1 *Plasmodium falciparum* ubiquitin carboxyl-terminal hydrolase 1

P. falciparum ubiquitin carboxyl-terminal hydrolase 1 (*PfUBP-1*), one of the PfKIP's identified by Birnbaum et al. was previously reported to be associated with ART resistance in *in vitro* selected *Plasmodium chabaudi,* a rodent malaria parasite (Hunt et al., 2007). Furthermore, surveillance of clinical populations of *P. falciparum* in SSA have reported multiple variants in *PfUBP-1* (Adams et al., 2018; Henriques et al., 2014). *PfUBP-1* has also been associated with ARTr following genome wide association studies (GWAS) and *in vitro* selection of ART resistant *P. falciparum* (Borrmann et al., 2013). A retrospective longitudinal genomic surveillance study of clinical isolates from Thailand showed that the *PfUBP*-1 R3138H variant exhibited temporal changes in frequencies that correlated with the *PfK13* C580Y variant (Cerqueira et al., 2017) and has been validated by *in vitro* assessments of ARTr (Birnbaum et al., 2020). Finally, the *PfUBP*-1 V3275F variant, first discovered in the non-human *Plasmodium* parasite *P. chabaudi*, was genetically engineered into a *P. falciparum* strain to confirm its association with ARTr (Simwela et al., 2020a; Simwela et al., 2020b; Henrici et al., 2019).

University of Ghana http://ugspace.ug.edu.gh

2.9.2 Adaptor protein complex 2 mu subunit

Adaptor protein complex 2 mu subunit (AP2µ) is known to be important for a functional endocytic vesicular system (Henrici et al., 2020). Two reports first discovered that the mutant *P. chabaudi* malaria parasite with the I562T variant in the AP2µ gene was associated with ARTr (Henriques et al., 2014; Hunt et al., 2007). Since then, several variants in the AP2µ gene have been reported in varied *P. falciparum* clinical isolates in East and West Africa (Adams et al., 2018; Henriques et al., 2014). This variant was validated as associated with the ARTr phenotype when upon genetically engineering it into the 3D7 strain using CRISPR/cas9, *in vitro* ARTr emerged. Additionally, Rocomara and others used long-term *in vitro* selection to show that the AP2µ H1298Q variant was associated with the ARTr phenotype. Interestingly, this study did not identify any variant in *PfK13 (*Rocamora et al*.,* 2018*)*.

2.9.3 *Plasmodium falciparum* kelch 13

Insight into the molecular marker of ARTr was first discovered by the seminal paper that associated *P. falciparum* kelch 13 (*PfK13)* with the ARTr phenotype (Ariey et al., 2014). K13 was predicted to be a substrate adapter of an E3 ligase and its mammalian orthologue, Keap1, was reported to bind specific substrates to ubiquitin and tag them for proteasomal degradation. Mbengue et al., as already discussed earlier, unraveled the association between ARTr conferring *PfK13* variants and phosphatidyl inositol-3-phosphate (PI3P), which is a major component of endosomal membranes (Mbengue et al., 2015; Jonscher et al., 2019; Tawk et al., 2010).

University of Ghana http://ugspace.ug.edu.gh

To recapitulate, the group had earlier identified PI3P as important to the role of parasite export of proteins from the endoplasmic reticulum to the host red cell surface in the early ring stage. Using a cell-based assay, they found that a low-dose DHA inhibited PI3P function.

Their findings suggested that DHA had specificity for PI3P and therefore against the only phospho-inositol-3-kinase (PfPI3K) in the parasite. Since PfPI3K catalyzes the formation of PI3P, their data suggested that PI3K is the target of DHA. Additionally, it was identified that DHA is not a 'promiscuous kinase inhibitor' by showing that it does not inactivate other kinases including the closely related orthologue of PfPI3K, VPS34 (Hassett et al., 2017). The final model of *PfK13* ARTr suggested that variant PfK13 acts as a weaker substrate adaptor for an E3 ligase that poorly ubiquitinates PfPI3K resulting in its reduced loss and subsequent accumulation. This increases the cellular amounts of PI3P that confers ARTr. In correlation with this model, ARTr parasites with the PfK13 variants (C580Y and R539T) showed elevated cellular levels of PI3P (Mbengue et al., 2015). However, this model of ARTr that showed elevated PfPI3K and PI3P was not replicated by other studies (Yang et al., 2019; Siddiqui et al., 2017). Furthermore, *PfK13* has been shown to localize with the digestive food vacuole and with PI3P-labelled vesicular structures in the endoplasmic reticulum (Bhattacharjee et al., 2018; Gnädig et al., 2020).

This intimates a connection between *PfK13* variants, PfPI3K and endosomal vesicle transport with ARTr (Siddiqui et al., 2021). Amalgamating this evidence paints the portrait that suggests that elevated amounts of PI3P lead to ARTr by reducing the endocytic transport of hemoglobin to the food vacuole. However, this model sharply contrasts with an earlier study that showed that inhibition of PfPI3K failed hemoglobin-filled endocytic vesicles transportation to the DFV (Vaid et al., 2010).

University of Ghana http://ugspace.ug.edu.gh

2.9.4 Artemisinin resistance outside *Pfk13* variants

The complexity of the genomic landscape that defines ARTr is further highlighted by variants outside the *PfK13* loci associated with the phenotype. Several such non-*PfK13* variants have been reported to play a role in the emergence of the ARTr phenotype. Despite their multi-locus architecture, almost all these non-*PfK13* variants have been intimated to contribute to ARTr via one of the two main motifs already discussed: reduced hemoglobin endocytosis to the FV and increased tolerance to ART-induced oxidative stress.

In 2018, Demas and others reported ARTr-conferring variants in the *P. falciparum* actin-binding protein *pfcoronin* gene after long-term *in vitro* selection on a parasite strain from Senegal (Demas et al., 2018). Following the engineering of these *pfcoronin* variants into a Dd2 line, they were validated as genetic markers of ARTr in the ring stage (Demas et al., 2018). Coronin shares a propeller-like structure with *PfK13* and has also been implicated in the endovesicular transport of hemoglobin (Xie et al., 2020; Olshina et al., 2015). Interestingly, in the presence of the ARTr-conferring *PfK13* C580Y variant, the ARTr-conferring *pfcoronin* variants did not produce the ARTr phenotype (Sharma et al., 2020). This suggests that their individual mechanisms of ARTr may overlap and the effect of the *PfK13* loci is likely dominant or epistatically modifying on the *pfcoronin* variants. Other non-*PfK13* loci that have been implicated in ARTr include ATG18, falcipain 2a, and UBP-2 as has been earlier discussed (Siddiqui et al., 2021).

University of Ghana http://ugspace.ug.edu.gh

2.9.5 Background of artemisinin resistome

Considering the ART resistome involves multiple loci, the ART background resistome can be conceptualized as the variants in loci that emerge before the ARTr conferring variant(s). These background resistome variants may act as the seedbed for the ARTr conferring variant(s) in multiple ways such as exerting epistatic effects to weather fitness costs. The background resistome also acts as a modifier of the expressed ARTr phenotype and may account for the plasticity of the ARTr phenotype for the same *PfK13* variant in different genetic backgrounds, and among different *PfK13* variants (Straimer et al., 2015). In the GMS, the emergence of ARTr parasites occurred on a seedbed of background resistome from founder populations comprising variants in *P. falciparum* multidrug resistance gene (*pfmdr1_T484I*), *P. falciparum* ferredoxin gene *(D193Y)*, autophagy-related protein 18 (*atg 18*), *P. falciparum* Chloroquine Resistance Transporter gene (*N*326S, I356T) and *P. falciparum* Apicoplast Ribosomal Protein S10 gene (V127M, D128Y/H) (Miotto et al., 2015).

University of Ghana http://ugspace.ug.edu.gh

2.10 Extracellular Vesicles

Parasite-parasite communication is a central motif in the biology, virulence, host immunity, and drug pressure adaptation mechanisms of many infectious agents (Coakley et al., 2015). Extracellular vesicles (EV) have been reported to mediate communication between single-celled protozoans such as *Leishmania sp., Toxoplasma sp.,* and *Trypanosoma sp.* (Sampaio et al., 2017; Valadi et al., 2007; Babatunde et al., 2020); and have been shown to shuttle the transfer of vital factors necessary for population growth and adaptation.

Microbial-microbial communication is exemplified by the ability of bacteria to use quorum-sensing to switch from planktonic to biofilm forms (Hammer et al., 2003). This morphological switch confers on bacteria the ability to withstand antimicrobial action and host immune defenses. Additionally, microbial-microbial communication is used in bacteria to propagate antibiotic resistance via the horizontal transfer of plasmids (Bennett, 2008). In single-cell eukaryotic protozoans such as trypanosomes, parasite-parasite communication (P-PC) has a ubiquitous utility. In the human host, the stumpy induction factor (SIF) serves a quorum-sensing-like function. SIF activates the development of stumpy forms from the proliferative slender forms. This allows the transmission to the tsetse fly and perpetuation of the infectious cycle (McDonald et al., 2018; Szempruch et al., 2016).

Thus, the theme of P-PC is ubiquitous in parasite biology. This is the context in which EVs have emerged as a plausible mechanism underlying P-PC in *P. falciparum* biology (Roditi, 2016; Marti et al., 2016; Mantel et al., 2014). Whether EVs have functional utility in the life cycle and virulence of the apicomplexan parasite *P. falciparum* is yet to be satisfactorily established (Mantel et al., 2014).

University of Ghana http://ugspace.ug.edu.gh

Some studies have reported on the role of EVs in malaria parasite maturation, host immunomodulation, and pathophysiological development of cerebral malaria (Babatunde et al., 2020; Babatunde et al., 2018; Sahu et al., 2013a; Shrivastava et al., 2017; Sahu et al., 2013b).

In this context, EVs have been implicated as the biological vehicles mediating the transfer of molecules conferring antimalarial drug resistance to malaria parasites (Regev-Rudzki et al., 2013). Furthermore, EVs have been suggested to be the carriers of signals for the vital switch of asexual malaria parasites to gametocytes (Regev-Rudzki et al., 2013).

Contemporary work on EVs is pacing to uncover their role in molecular mechanisms undergirding the biology and virulence of *P. falciparum* (Sierro et al., 2019; Correa et al., 2019; Mantel et al., 2016; Antwi-Baffour et al., 2020; Ankarklev et al., 2014). This has the potential to transform the malaria research landscape by discovering novel drug targets for malaria drug development. Besides, EV research has parallel promising applications in the field of gene delivery vectors (Saari et al., 2020). Therefore they may become the utilitarian vehicle needed to translate gene therapy into clinical practice (Andaloussi et al., 2013).

The study of the role of EVs in *P. falciparum* biology is however plagued by a lack of consensus on the extraction and purification of parasite-derived EVs (Sampaio et al., 2017; Théry et al., 2018). This has cast a shadow on the findings and claims of the biological role imputed to EVs (Brancucci et al., 2017). Currently, the International Society for Extracellular Vesicles (ISEV) has proposed a set of stringent measures that will help standardize EV research (Théry et al., 2018). Broadly, these considerations touch on three themes: processing of preanalytical variables, EVs enrichment; and determining functional attributes of EVs.

University of Ghana http://ugspace.ug.edu.gh

A well-designed EVs study utilizing cell culture conditioned media should characterize the cellular identity of the EVs-releasing cells and the proportion of viable cells in the culture mix. The duration of the culture before harvesting EVs, the culture density (parasitemia), and the absence of microbial contamination must be evaluated and reported. Additionally, all media composition and preparation must be stated. It is recommended that culture medium components like serum that naturally contain EVs be avoided as they can be a source of bias in the study.

If serum use is inevitable, a serum-free media control should be used to assess the contribution of serum to EV production. Alternatively, EVs depleted serum if available can be used. Storage conditions and duration of the culture media and/or source of EVs may affect downstream functional analysis and thus must be reported. EV enrichment is another important factor to consider in EV studies. Independent of the method of EVs purification used (Théry et al., 2006; Livshits et al., 2015; Szatanek et al., 2015), characterization of EVs enrichment must be evaluated and reported. This is of particular importance in studies of functional inquiry where highly pure EVs fractions are required. EVs quantification should state the volumes of each purification step and evaluate the concentration of EVs (e.g. counts of EVs per volume) at the end of each step. Furthermore, the numbers of EVs at the end of the enrichment cycle must be enumerated by light scattering techniques such as nanoparticle tracking systems, or by high-resolution flow cytometry. Any attribution of EVs to a functional role must demonstrate that the activity occurs in absence of direct cell-cell contact; and that the activity is predominantly associated with EVs rather than any other soluble mediator. Following these standards in the design of EVs studies will augur well for the field. It will make comparisons and pooling of findings among EV studies feasible to help deepen our collective understanding of their role (Théry et al., 2018).

University of Ghana http://ugspace.ug.edu.gh

Juxtaposed to this proposed methodology, many important questions on EVs are yet to be answered. These include questions such as: what parasite molecules correlate unambiguously as markers of parasite-derived EVs (Théry et al., 2018)?; are parasite-derived EVs actively produced by the parasite in the infected red blood cell?; if they are, what pathways of the parasite's biology are important for this?; if they are not actively produced, does this singularly remove their significance to the parasite's biology?; could EVs unequivocally mediate horizontal nucleic acids transfer between malaria parasites?

EVs are a versatile population of vehicles that mediate cell-cell communication (Andaloussi et al., 2013; Tkach et al., 2016). They are membrane-bound vesicles released by cells. Structurally, EVs are made of single lipid membrane bilayers enclosing a cargo of cytosolic proteins, lipids, metabolites, and nucleic acids (Tkach et al., 2016). They represent a heterogeneous population (Zaborowski et al., 2015; Willms et al., 2016) that can range in size from 30nm to 2000nm. Broadly, EVs have been previously classified into microvesicles and exosomes based on their size and biogenesis. Microvesicles are formed by evagination of the plasma membrane, and typically have a diameter between 0.3 and 1µm. Exosomes have a smaller size (50-200nm) and are formed by the fusion of multivesicular bodies from the endosomal pathway with the external cell membrane (Maas et al., 2017). EVs are distinct from apoptotic bodies as their formation and release are independent of cell death (Raposo et al., 2013). However, the current consensus in the field is shifting away from these terms (Théry et al., 2018). This is on account of the difficulty in providing evidence on the biosynthetic source of harvested EVs.

University of Ghana http://ugspace.ug.edu.gh

The ISEV has recommended that empirical descriptions should be used in EV nomenclature. This utilizes size, biochemical composition (presence or absence of protein markers like CD63 and CD81), and cell origin descriptions to name EVs (Théry et al., 2018). Thus, EVs are now referred to as small, medium, or large. Small EVs (sEVs) have a size between 100nm and 200nm. Medium and large EVs (m/lEVs) are larger than 200nm in diameter (Théry et al., 2018). The known cargo diversity in EVs underpins the plurality of biological functions ascribed to EVs. The origin of EVs from *P. falciparum*-infected red blood cells (PfiRBCs) has been suggested to be from the cell's interior and not the cell surface (Sampaio et al., 2018; Taraschi et al., 2003).

A study characterizing the composition of m/lEVs from PfiRBC*s* reported the preponderance of parasite antigens associated with red cell invasion, host immunomodulation, and gametocytogenesis (Mantel et al., 2013). Another study, using clinical isolates from a child with cerebral malaria in Kenya, reported that EVs are rich in immunogenic proteins found in the exomembrane compartment and endomembrane secretory systems of PfiRBCs (Abdi et al., 2017). EVs from PfiRBCs can be internalized by monocyte-derived microglia cells (Mbagwu et al., 2019). This supports the hypothetical role of EVs in the pathogenesis of cerebral malaria. Another study showed that EVs contain a large amount of hemoglobin from the host red blood cell (Antwi-Baffour et al., 2016). This may suggest that EVs are the vehicles of vesiculation that mediate hemoglobin waste disposal in PfiRBCs. EVs have also been suggested to correlate with severe *P. falciparum* malaria (Nantakomol et al., 2011).

University of Ghana http://ugspace.ug.edu.gh

EVs from PfiRBCs have also been shown to contain functional miRNA-Argonaute 2 complexes, which can be internalized by human endothelial cells, and may play a role in the ability of the parasite to sequester in the microvasculature (Mantel et al., 2016; Wang et al., 2017). EVs from PfiRBCs have been shown to shuttle parasite nucleic acids to cytosolic immune cell receptors to activate the innate immune response of the host (Sisquella et al., 2017; Ye et al., 2018). Furthermore, EVs from PfiRBCs have been shown to carry a host of small regulatory RNAs that could be transferred to host endothelial cells (Babatunde et al., 2018).

2.10.1 EVs biogenesis in *Plasmodium falciparum*

Until recently, very little was known about the biogenesis of EVs in *P. falciparum*. In most eukaryotes, EV biogenesis and transport are achieved by the endomembrane system (Akers et al., 2013). The nano-sized (30-50nm) EVs referred to as exosomes are produced by the fusion of multi-vesicular bodies (MVBs) with the plasma membrane (van Niel et al., 2018). MVBs are produced from intraluminal vesicles (ILVs) derived from early endoscopes (Raposo et al., 2013). ILVs production is achieved by the action of the endosomal sorting complex required for transport (ESCRT). The ESCRT is composed of four protein complexes denoted ESCRT-0, ESCRT-I, ESCRT-II, ESCRT-III and a complement of accessory proteins (Winter et al., 2006; Katzmann et al., 2002). ESCRT action starts with the recognition of mono-ubiquitinated proteins by ESCRT-0 (Raiborg et al., 2009), which activates the recruitment of ESCRT-I and ESCRT-II that drive membrane deformation into buds (Katzmann et al., 2003; Gill et al., 2007; Im et al., 2009; Boura et al., 2012).

University of Ghana http://ugspace.ug.edu.gh

Eventually, polymerization of ESCRT-III is initiated with the binding of Vps20 to the invaginated membrane and recruits the rest of the ESCRT-III members to the bud neck resulting in the closure of the nascent vesicle (Im et al., 2009; Babst et al., 2002; Teis et al., 2010). This process involves membrane fission, protein dissociation and recycling of the ESCRT machinery and is achieved by the participation of a Vps4 AAA-ATPase enzyme (Obita et al., 2007).

The ESCRT-III complex, comprising Vps20, Snf7/Vps32, Vps24 and Vps2, and its accessory proteins Vps4, Vta1, Vps60, and Alix, have been shown to partake in other important membrane-scission mechanisms such as virus budding, cytokinesis, nuclear envelope remodeling and exosome biogenesis among others (Hurley, 2015). These processes are similar in the fact that they share the same topology where the nascent vesicle buds away from the cytosol, contrary to the topology observed in clathrin-coated vesicles (Henne et al., 2013).

Although the ESCRT machinery is reported to be highly conserved across eukaryotic lineages, strictly intracellular protists, like *P. falciparum*, are devoid of ESCRT-0, -I and -II sub complexes (Leung et al., 2008). Therefore, it is likely that nanoparticle EVs biogenesis in *P. falciparum* is achieved by alternative pathways. A well-studied alternative pathway in humans is Alix, a Bro1-domain protein, that binds directly to Vps32 and activates the production of ESCRT-III polymers, leading to ILVs generation (Dores et al., 2012). Earlier in silico assays had shown that *P. falciparum* had two putative proteins from the ESCRT-III complex: Vps2 and Vps32/Snf7 (Leung et al., 2008; Jimenez-Ruiz et al., 2016). Furthermore, the ATPase Vps4, an accessory protein of the ESCRT-III complex, was found in the *P. falciparum* cytoplasm at the trophozoite blood stage (Yang et al., 2004).

University of Ghana http://ugspace.ug.edu.gh

Avalos-Padilla and others showed that *P. falciparum* possesses functional ESCRT-III machinery activated by an alternative recruitment pathway involving the action of PfBro1 and PfVps32/PfVps60 proteins. They also reported the presence of PfVps32, PfVps60 and PfBro1 in EVs purified from a *P. falciparum in vitro* culture. Finally, the knockout of the PfVps60 gene resulted in reduced EV formation in *P. falciparum* (Avalos-Padilla et al., 2021).

This most recent evidence on EVs biogenesis in *P. falciparum* helps frame a model built on the endomembranous system that involves pathways for *PFEMP1* trafficking and EVs biogenesis. Thus, the question that emerges is this: can EVs play a role in the emergence of ARTr? Can they function as vehicles that aid the increased tolerance of ART oxidative stress, by actively removing the products of proteinopathic stress? These are questions worth looking into.

University of Ghana http://ugspace.ug.edu.gh

CHAPTER THREE

Plasmodium falciparum Malaria Parasites in Ghana Show Signatures of Balancing Selection at Artemisinin Resistance Predisposing Background Genes

Kwesi Z. Tandoh[1*], Lucas Amenga-Etego[1] , Neils B. Quashie[2,3] , Gordon Awandare[1], Michael Wilson[4], Nancy O. Duah-Quashie[2*]

Affiliations

1. West African Center for Cell Biology of Infectious Pathogens, Department of Biochemistry, Cell and Molecular Biology, College of Basic and Applied Sciences, University of Ghana, Accra, Ghana
2. Department of Epidemiology, Noguchi Memorial Institute for Medical Research, College of Health Sciences, University of Ghana, Accra, Ghana.
3. Center for Tropical Clinical Pharmacology and Therapeutics, School of Medicine and Dentistry, College of Health Sciences, University of Ghana, Accra, Ghana
4. Department of Parasitology, Noguchi Memorial Institute for Medical Research, College of Health Sciences, University of Ghana, Accra, Ghana

*Corresponding authors: Nancy O. Duah-Quashie, NDuah@noguchi.ug.edu.gh; Kwesi Z. Tandoh, kztandoh@st.ug.edu.gh

University of Ghana http://ugspace.ug.edu.gh

Tandoh KZ, Amenga-Etego L, Quashie NB, Awandare G, Wilson M, Duah-Quashie NO. *Plasmodium falciparum* Malaria Parasites in Ghana Show Signatures of Balancing Selection at Artemisinin Resistance Predisposing Background Genes. Evol Bioinform Online. 2021 Mar 3;17:1176934321999640. doi:10.1177/1176934321999640. PMID: 33746510; PMCID: PMC7940735.

This manuscript has been published in journal of Evolutionary Bioinformatics and has been reproduced in this thesis in concordance with the Open Access license (CC BY-NC 4.0) that allows the use and sharing of the manuscript for non-commercial purposes.

University of Ghana http://ugspace.ug.edu.gh

3.1Abstract

Sub-Saharan Africa is courting the risk of ART resistance emerging in *Plasmodium falciparum* malaria parasites. Current molecular surveillance efforts for ARTr have been built on the utility of *P. falciparum* kelch13 (*PfK13*) validated molecular markers. However, whether these molecular markers will serve the purpose of early detection of ARTr parasites in Ghana is hinged on a PfK13-dependent evolution. Here, we tested the hypothesis that the background *PfK13* genome may be present before the *PfK13* ARTr-conferring variant(s) is selected and that signatures of balancing selection on these genomic loci may serve as an early warning signal of ARTr. We analyzed 12198 single nucleotide polymorphisms (SNPs) in Ghanaian clinical isolates in the Pf3K MalariaGEN dataset that passed a stringent filtering regimen. We identified signatures of balancing selection in two genes (phosphatidylinositol 4-kinase and chloroquine resistance transporter) previously reported as background loci for ARTr. These genes showed statistically significant and high positive values for Tajima's D, Fu and Li's F, and Fu and Li's D. This indicates that the biodiversity required to establish a PfK13 background genome may have been primed in clinical isolates of *P. falciparum* from Ghana as of 2010. Despite the absence of ARTr parasites in Ghana to date, our finding supports the current use of PfK13 for molecular surveillance of ARTr parasites in Ghana and highlights the potential utility of monitoring malaria parasite populations for balancing selection in ARTr precursor background genes as early warning molecular signatures for the emergence of ARTr.

Keywords: population genomics, artemisinin resistance, molecular surveillance, malaria, *Plasmodium falciparum*, signatures of balancing selection

University of Ghana http://ugspace.ug.edu.gh

3.2 Introduction

The global *Plasmodium falciparum* malaria burden is highest in sub-Saharan Africa (SSA). In 2018, the World Health Organization (WHO) estimated that 213 million people in SSA suffered from malaria, with an estimated 380,000 deaths (WHO, 2020b). In Ghana, malaria transmission is hyperendemic, with a high malaria attributable morbidity and mortality, particularly among pregnant women and children under five years of age (Ministry of Health, 2017). Until 2005, chloroquine was the main drug used for malaria treatment in Ghana, however, widespread *P. falciparum* resistance led to the replacement of chloroquine with artemisinin-based combination therapy (ACT) as the first-choice antimalarial chemotherapy for the management of uncomplicated malaria in line with the WHO recommendations (Koram et al., 2005; Quashie et al., 2007; WHO, 2006). Currently, ACTs recommended by the national malaria control program (NMCP) of Ghana include artesunate–amodiaquine (AS AQ), artemether-lumefantrine (AL) and dihydroartemisinin-piperaquine (DHAPQ) (Quashie et al., 2010). Although artemisinin-resistant (ARTr) *P. falciparum* has not been confirmed in Ghana or SSA yet, there is a real risk of such parasites emerging and severely undermining malaria control efforts (Taylor et al., 2015; Amambua-Ngwa et al., 2019; Conrad et al., 2019).

Since the discovery of ARTr parasites in South-East Asia (SEA) (Noedl et al., 2008; Dondorp et al., 2009), there is global concern about the spread of these parasites to SSA. Currently, molecular surveillance for ARTr is achieved with validated *P. falciparum* kelch-13 (*PfK13*) molecular markers (Ariey et al., 2014; Nyunt et al., 2017; Mvumbi et al., 2017). However, with the possibility of involvement of multiple mechanisms in ARTr development, there are concerns about the universal utility of *PfK13* as a marker of ARTr (Project, 2016; Bhattacharjee et al., 2018; Birnbaum et al., 2020; Mok et al., 2015; Rocamora et al., 2018; Mbengue et al., 2015; Suresh et al., 2018).

University of Ghana http://ugspace.ug.edu.gh

Additionally, SSA has been shown to harbor a biodiverse *P. falciparum* population with sufficient variation at the *PfK13* locus to allow a soft selection sweep under ART drug pressure (Project, 2016; Taylor et al., 2015; Manske et al., 2012). Despite this, ARTr malaria parasites are yet to emerge in SSA (Taylor et al., 2015; Conrad et al., 2019).

A possible explanation for the delay of artemisinin resistance emergence in SSA, is the prerequisite for a *PfK13* ARTr-conferring background genome. This model is framed on the hypothesis that the *PfK13* ARTr-conferring variants only express the phenotype in the presence of a particular *PfK13* genomic background that weathers any fitness cost of the *PfK13* ARTr conferring variant(s) and may augment any baseline partner drug resistance required for the parasites to be transmitted (Cerqueira et al., 2017; Miotto et al., 2015). Whether this *PfK13* genome background evolves before, with, or after the PfK13 ARTr variant is selected remains unclear (Project, 2016). This ARTr genomic model presents a high genetic barrier to the emergence of ARTr and may explain the delay in the manifestation of the phenotype in SSA.

University of Ghana http://ugspace.ug.edu.gh

The *PfK13* background genome has been characterized by population association studies to involve single nucleotide polymorphisms (SNPs) in the following loci: ferredoxin (fd-D193Y), apicoplast ribosomal protein S10 (arps10-V127M), multidrug resistance protein2 (mdr2-T484I), and chloroquine resistance transporter(crt-N326S) (Miotto et al., 2015). A retrospective longitudinal genomic study also identified background SNPs that were associated with the ARTr phenotype in malaria parasites from North-Western Thailand (Cerqueira et al., 2017). This study used genotype-phenotype association tests and genomic scans for signals of selection to determine genomic loci in *P. falciparum* that may contribute to the *PfK13* ARTr background genome.

These variants followed a similar non-reference allele frequency temporal trajectory as the dominant *PfK13* ARTr conferring variant C580Y in SEA and included SNPs in the following genes: Phosphatidylinositol 4-kinase (S915G), Sec14 domain-containing protein (L498F and N615D), Ubiquitin-protein ligase (S57T), Ubiquitin carboxyl-terminal hydrolase (R3138H), and Sentrin-specific protease 2, putative protein (H423Y) (Cerqueira et al., 2017).

To mitigate the risk of ARTr spreading and taking hold in SSA, molecular surveillance for parasites with ARTr is critical and a molecular-based early warning metric that predicts ARTr will be desirable. A tool that may serve this purpose is the detection of signatures of balancing selection on loci demonstrated to act as a background for ARTr emergence. To explore this, here we hypothesized that the background *PfK13* genome may be present before the *PfK13* ARTr-conferring variant is selected and that signatures of balancing selection on these genomic loci may serve as an early warning signal. Our analysis has identified loci previously reported as *PfK13* background mutations required for the emergence of ARTr to be under balancing selection in *P. falciparum* clinical samples from Ghana.

University of Ghana http://ugspace.ug.edu.gh

Our findings show that two of these genomic loci required for ARTr to emerge have sufficient standing variation to allow a soft selective sweep and emergence of ART-tolerant parasites under ART pressure. Our data also provides empirical evidence for malaria molecular surveillance in Ghana continue to use *PfK13* as the marker for ARTr despite the possibility of *PfK13* independent emergence of ARTr parasites in Ghana.

University of Ghana http://ugspace.ug.edu.gh

3.3 Results

3.3.1 Multiplicity of infection

Multiplicity of infection (MOI) can result in spurious signatures of selection metrics if it is not evaluated (Manske et al., 2012). The proportion of samples with multiple infections was determined by calculating the genome-wide within sample F statistic (F_{ws}). We found 56% (343) of sample to have $F_{ws} < 0.95$, which is indicative of multi-genomic infection (Figure 3.1). These samples were excluded from tests of neutrality analysis to determine signatures of balancing selection.

University of Ghana http://ugspace.ug.edu.gh

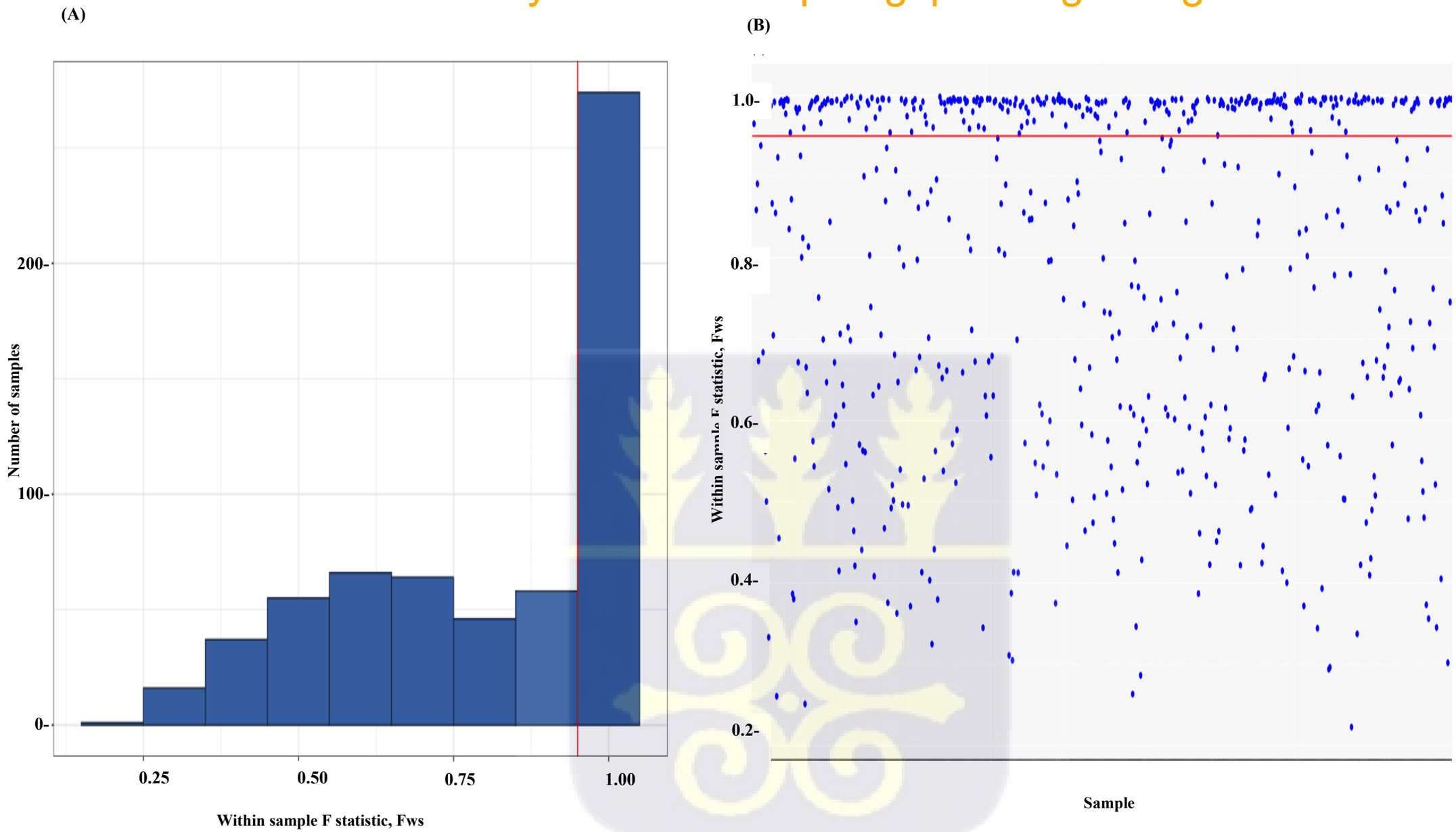

Figure 3.1 Distribution of multiplicity of infection in the analysed Ghanaian *P. falciparum* isolates (n = 617). (A) is a histogram showing the number of samples with within sample F statistic (Fws) on the vertical axis within the range specified on the horizontal axis. (B) is a scatter plot that shows the distribution of the samples with Fws. The red line is at Fws = 0.95 , the cutoff point for MOI

3.3.2 *P. falciparum* population structure

Next, we interrogated the hypothesis that there is no population structure in the malaria parasite

University of Ghana http://ugspace.ug.edu.gh

population in Ghana. Population structure analysis was undertaken using principal component analysis (PCA). We sought to uncover any effect of varying local transmission and geographical distribution on the parasite population structure. We adopted an approach that evaluates population structure by utilizing within-sample allele frequencies (WSAF) across all variable genomic loci (Verity et al., 2020). Principal components were plotted using the ggplot2 package in R version 4.0. No significant parasite population structure was observed (Figure 3.2).

University of Ghana http://ugspace.ug.edu.gh

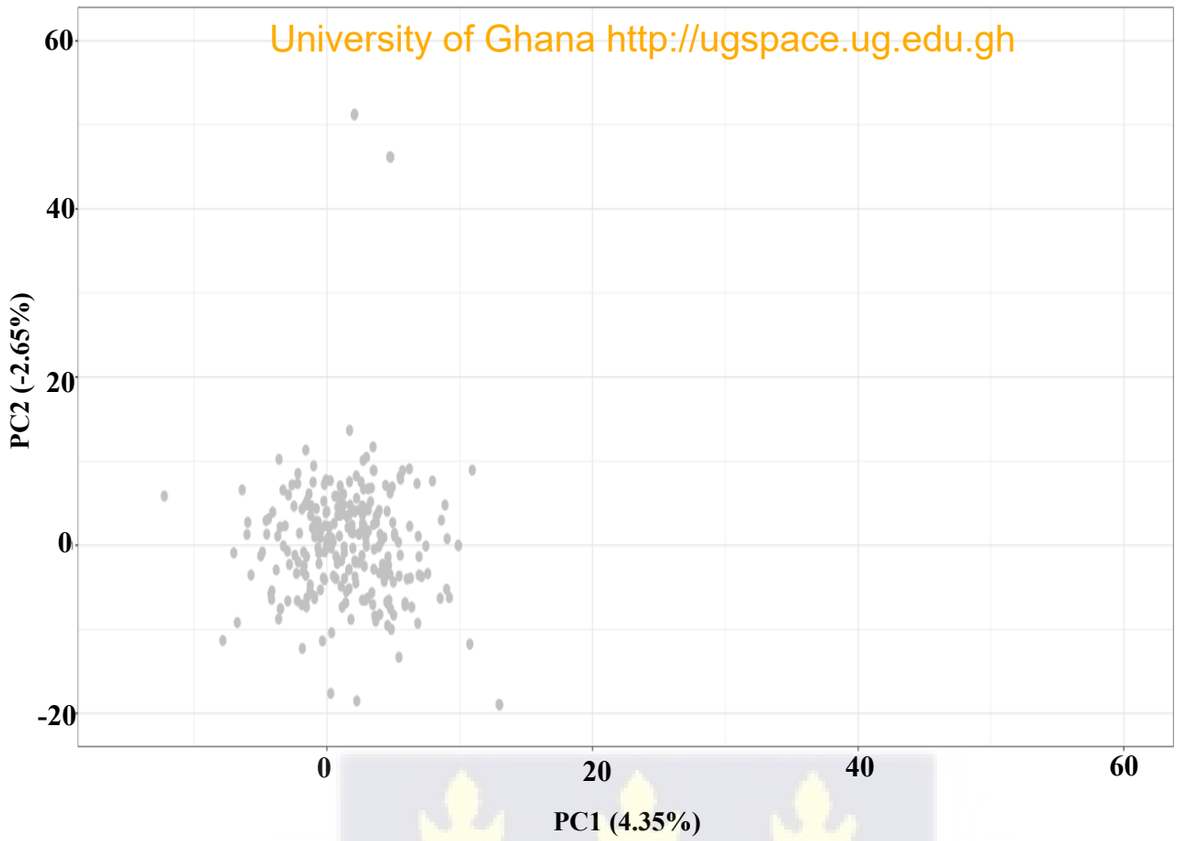

Figure 3.2 ***P. falciparum*** **population structure analysis of Ghana samples. PCA analysis for samples with a single clonal infection (N=274). Sample coordinates for PCA were obtained using vcfdo. A subsequent plot was generated in R.4.0 with the ggplot2 package. Principal components 1 and 2 show no genetic differentiation within the Ghana samples of** ***P. falciparum***

3.3.3 Summary of genomic diversity among single clone infections

We subsequently only analyzed sequence data for samples with single clone infections (F_{ws} > 0.95, N = 274) with 12198 biallelic SNPs. 60% of SNPs in the population had a non-reference allele frequency of less than 25% (Figure 3.3). 45% of SNPs were missense variants, 28% of SNPs were in intergenic regions, 22% of SNPs were synonymous variants, and 4% were in intronic regions (Figure 3.4). The SNPs analyzed were distributed across 2256 protein-coding genes.

University of Ghana http://ugspace.ug.edu.gh

University of Ghana http://ugspace.ug.edu.gh

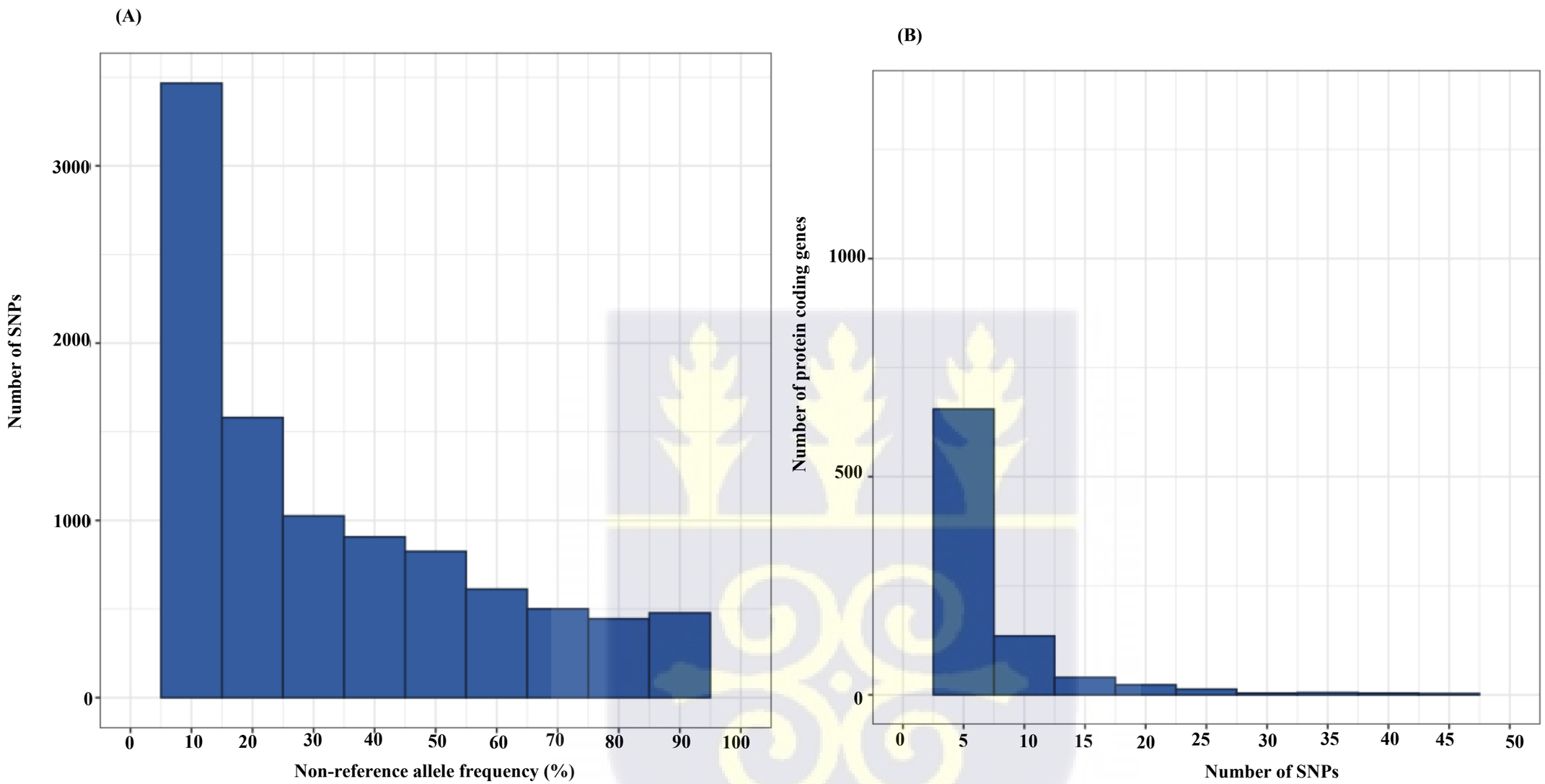

Figure 3.3 Summary of SNPs characteristics. (A) Frequency distribution of the non-reference allele for each of the biallelic SNPs in the sample of *P. falciparum* clinical isolates from Ghana (N = 274). (B) Distribution of numbers of protein-coding genes (N = 2256) with each given number of SNPs in the Ghana population sample of *P. falciparum* clinical isolates.

University of Ghana http://ugspace.ug.edu.gh

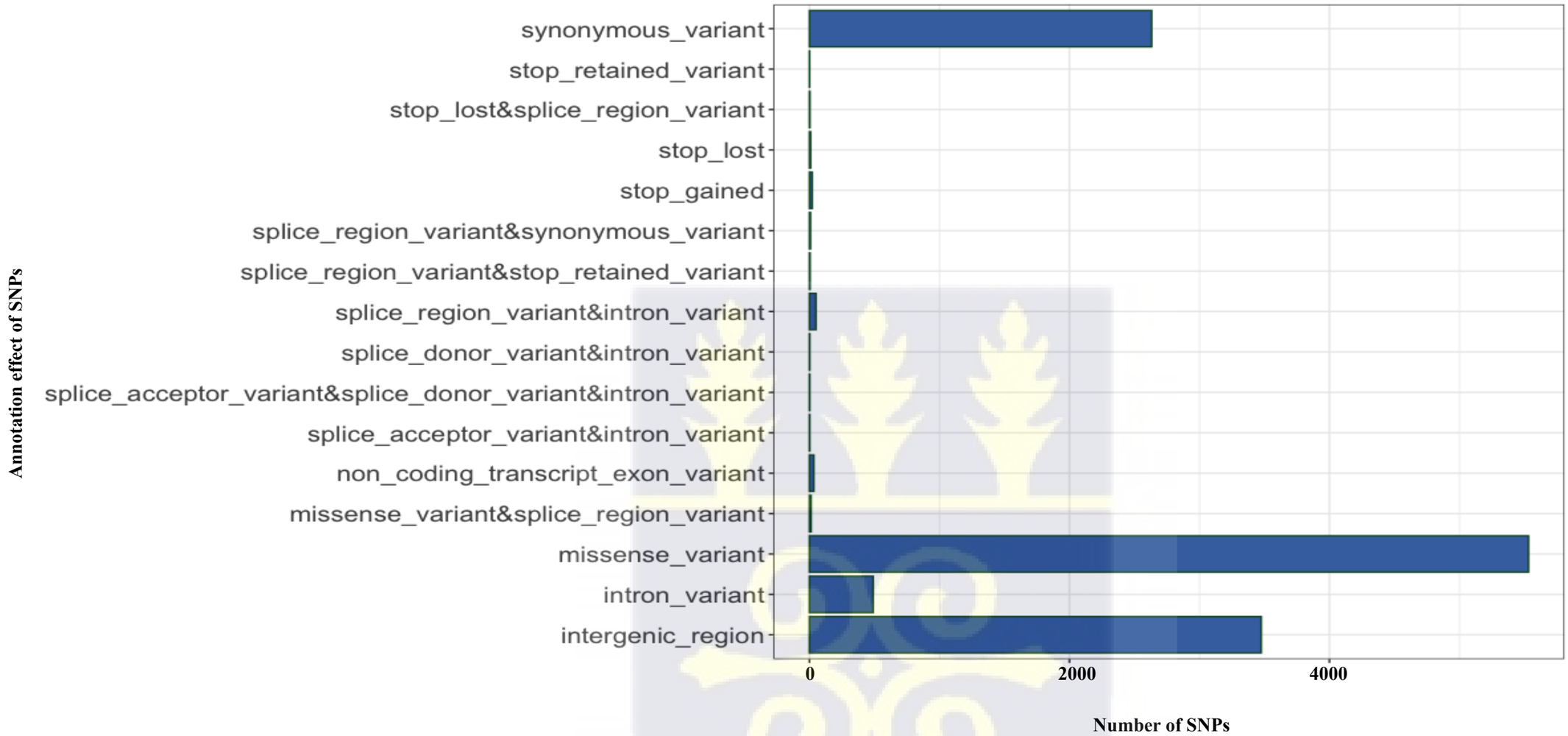

Figure 3.4 Distribution of SNPs effect across all genomic positions analyzed. The most abundant biological effect of the SNPs analyzed were missense variants, variants in intergenic regions, synonymous variants, and intron variants in decreasing order.

University of Ghana http://ugspace.ug.edu.gh

3.3.4 *PfK13* ARTr genome background loci under balancing selection

We used clonal samples ($F_{ws} > 0.95$) to screen for signatures of selection in the *P. falciparum* genome. We found 579 *P. falciparum* genes with Tajima's D greater than one (Figure 3.5, Supplementary Table 3.1) (Ochola et al., 2010; Ochola-Oyier et al., 2019; Amambua-Ngwa et al., 2012). Of these, genomic positions above the 90th percentile of the Tajima's D distribution showed gene ontology biochemical processes spanning multiple pathways (Supplementary Table 3.2). There were no SNPs in the PfK13 gene and none of the reported SNPs that form the background genome for ARTr to emerge was identified in this analysis (Supplementary Table 3.3).

University of Ghana http://ugspace.ug.edu.gh

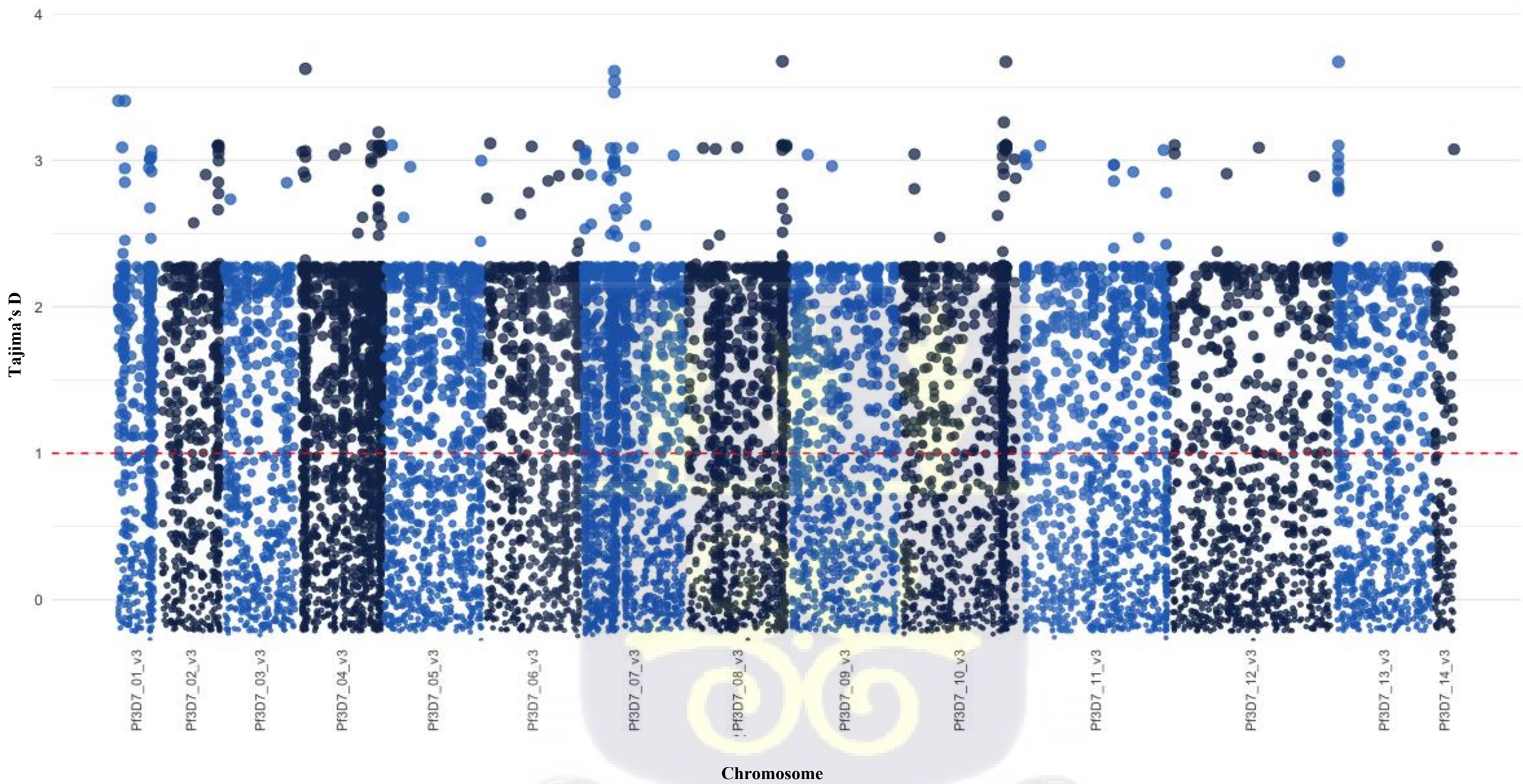

Figure 3.5 Genome-wide distribution of Tajima's D values summarizing the site frequency spectra for *P. falciparum* genes. 579 *P. falciparum* genes had Tajima's D > 1. Chromosomes are identified by the alternate black and blue coloring, with SNPs plotted as individual points based on their position in the chromosome. The red dashed line marks Tajima's D = 1.

University of Ghana http://ugspace.ug.edu.gh

Among the genes under balancing selection, we looked for loci previously reported to be part of the required multi-locus genomic background on which ARTr-conferring PfK13 variants emerged (Cerqueira et al., 2017; Miotto et al., 2015). Among the nine genomic loci implicated in this background phenomenon (Table 1), two were found to be under balancing selection in the Ghana sample set collected in 2010 (Table 2). One of these genes (phosphatidylinositol 4-kinase) stand out in their gene ontology terms (http://plasmodb.org) as directly connected to the molecular mechanisms of ARTr development(Suresh et al., 2018).

University of Ghana http://ugspace.ug.edu.gh

Table 3.1 List of genes of interest reported to be associated with the genomic background for artemisinin resistance in *P. falciparum*

Gene Name	Gene ID	SNP
ferredoxin	PF3D7_1318100	D193Y
apicoplast ribosomal protein S10	PF3D7_1460900	V127M
multidrug resistance protein 2	PF3D7_1447900	T484I
chloroquine resistance transporter	PF3D7_0709000	N326S
Phosphatidylinositol 4-kinase	PF3D7_0419900	S915G
Sec14 domain-containing protein	PF3D7_0626400	L498F, N615D
Ubiquitin-protein ligase	PF3D7_1448400	S57T
Ubiquitin carboxyl-terminal hydrolase	PF3D7_0104300	R3138H
Sentrin-specific protease 2, putative	PF3D7_0801700	H423Y

Table 3.2 Tests of neutrality on four genes of interest under balancing selection in Ghana population of *Plasmodium falciparum*.

Gene Name	Genomic length (bp)	sites[1]	π ($x 10^{-5}$)	K ($x10^{-3}$)	T' D	F	D	HKA (π/K)	MK P value
chloroquine resistance transporter	3096	6	64	559.71	2.7 *	1.96*	1.04	0.11	0.68
Phosphatidylinositol 4-kinase	15845	38	67	645.02	2.2 *	2.6*	2.18*	0.10	0.32
Ubiquitin carboxyl-terminal hydrolase	10962	6	17	615.51	1.8	1.5	1.04	0.03	0.64
Sentrin-specific protease 2, putative	5579	2	0.07	591.25	1.1	0.9	0.62	$11 x10^{-3}$	1

[1]number of polymorphic sites; π is nucleotide diversity index.

K is nucleotide divergence; T'D is Tajima's D; F is Fu and Li's F; D is Fu and Li's D; *P value < 0.05

University of Ghana http://ugspace.ug.edu.gh

The phosphatidylinositol 4-kinase (PI4K) gene product shares similar gene ontology terms (phosphatidylinositol metabolic process, kinase activity and cellular membrane component) with phosphatidylinositol 3-kinase (PI3K), which has been associated with the primary ARTr-conferring variant PfK13 C580Y. The gene is located on chromosome 4 and has six exons that encode a protein with 5035 amino acid residues. We found 38 SNPs in this gene of which 16 were synonymous, 20 missense variants, and two intron variants. The ubiquitin carboxyl-terminal hydrolase 1 locus (UBP1) gene is located on chromosome 1 and has three exons that encode a protein with 3499 amino acid residues. We found six SNPs in this gene of which two were synonymous and four missense variants. The chloroquine resistance transporter (CRT) gene is located on chromosome 7 and has 13 exons that encode a protein with 424 amino acid residues. We found 6 SNPs in this gene of which three were missense variants and three were intron variants. One missense variant was the chloroquine-resistance K76T mutation with an allele frequency of 0.57 percent (Wellems et al., 2001). The Sentrin-specific protease 2, putative (SENP2) gene is located on chromosome 8 and has three exons that encode a protein with 1784 amino acid residues. We found two SNPs in this gene of which one was a missense variant and the other a synonymous variant (Table 3.3).

University of Ghana http://ugspace.ug.edu.gh

Table 3.3 Summary of the number of SNPs and effect at loci of interest

	Annotation Effect		
Gene Name	**missense variant**	**synonymous variant**	**intron variant**
chloroquine resistance transporter (crt)	3	0	3
Phosphatidylinositol 4-kinase (PI4K)	20	16	2
Ubiquitin carboxyl-terminal hydrolase (ubp1)	4	2	0
Sentrin-specific protease 2, putative (senp2)	1	1	0

University of Ghana http://ugspace.ug.edu.gh

3.4 Discussion

It is important to improve malaria molecular surveillance, particularly detection and monitoring of *P. falciparum* parasites with ARTr genotypes. Given the absence of confirmed ARTr in SSA and complex evolution of ARTr, which includes precursor genomic background, we explored the plausibility of using molecular early warning signatures of balancing selection in nine genes associated with the genomic background on which ARTr conferring variants may emerge (Cerqueira et al., 2017; Miotto et al., 2015; Project, 2016). We found signatures of balancing selection in two loci reported to contribute to the genomic background on which definitive ARTr-conferring variants arise (Table 3.2). Genomic loci under balancing selection provide standing variation on which a soft selective sweep can occur, especially in the presence of high transmission rates, which is common in Ghana (Barrett et al., 2008; Botwe et al., 2017; Lamptey et al., 2018). Although we did not find any of the reported multi-loci ARTr predisposing background SNPs (Supplementary Table 3.3) and none of the variants identified at these loci has been reported to be associated with ARTr (Anonymous, 2019), the increased genetic diversity observed at these loci as of 2010 (Table 3.2) suggests that the biodiversity required to establish a PfK13 background genome may be primed in Ghana. Since balanced alleles may be randomly lost over long periods, whether these variants will be maintained, increase in frequency, or be lost over time remains unclear. Against the backdrop of the absence of ARTr in Ghana despite this background, the delay may be attributed to use of ACTs or breakdown of standing variation by rampant recombination due to the high transmission intensity in Ghana.

University of Ghana http://ugspace.ug.edu.gh

PI4K may have an impact on the levels of phosphatidylinositol-3-phosphate (PI3P) which has been associated with ARTr *in vitro* (Mbengue et al., 2015). PI4K may also contribute to ARTr development by modulating the activity of members of the phosphoinositol pathways in triggering the unfolded protein response to ART stress via the inositol-requiring enzyme 1α/β (IRE1) (Cerqueira et al., 2017; Adams et al., 2019). UBP1 is a putative protein predicted to function in a ubiquitin-dependent protein catabolic process (https://plasmodb.org/plasmo/app/record/gene/PF3D7_0104300#category:function-analysis).The ubiquitination/proteasome pathway has been associated with ARTr (Rocamora et al., 2018; Dogovski et al., 2015; Mbengue et al., 2015) via the cellular stress response to ART assault. Thus, our finding of signatures of balancing selection in UBP1 gene suggests an association with these pathways related to the molecular mechanisms of ARTr. Our data support the point conveyed by Cerqueira et al. that the complex multi-loci nature of ARTr makes it less likely to occur *de novo* in SSA (Cerqueira et al., 2017). This is because of the high rate of outcrossing and recombination that may derail the stability of the required complex genomic background. However, the presence of signatures of balancing selection in loci, that predispose to the emergence of PfK13-dependent ARTr, highlights the need for molecular surveillance of parasite populations in SSA to generate data for interrogating the risk of ARTr emerging in SSA whether *de novo* or imported by gene flow from SEA. Regardless of how ARTr arises in SSA, our analysis suggests that the requisite adaptation for ARTr in Ghana has occurred and conditions are ripe for a soft selective sweep either via importation or independent emergence to occur sooner than later. It is in light of this that we recommend prospective genomic surveillance for signatures of balancing selection in ARTr precursor background genes as they accumulate more variation and could serve as a molecular early warning system for ARTr emergence.

University of Ghana http://ugspace.ug.edu.gh

However, it is worth noting some limitations of the current study. A key weakness of this study is the absence of statistical power evaluations to ascertain whether the hard filtering pipeline and the resulting number of SNPs were sufficient to interrogate the central hypothesis for this analysis. It may be argued that the size of the relatively small variant set was not powered enough to capture the veracity or otherwise of our hypothesis. In addition, the evidence from Africa on PfK13 ARTr suggest that different variants from those seen in SEA may emerge (Uwimana et al., 2020). However, we are confident, the absence of any known ARTr–conferring variants in the samples analyzed is a strong indication that the background genome may be established before the emergence of the definitive ARTr-conferring variant(s). Although tests of departures from neutrality are best suited for evaluating deviations of nucleotide diversity from expectations under a neutral model of population evolution, they may also suggest a demographically driven change such as population bottleneck (e.g. drug pressure) (Kloch et al., 2018; Ramírez-Soriano et al., 2008).

What remains unknown and merits further investigation is the time scale between these events. Given that the effective population size is greater in SSA compared to SEA, the high recombination rates in SSA may prolong the evolutionary time scale to ARTr emergence. Therefore, the departures from neutrality from different complementary approaches observed in this study, though indicative of balancing selection in some of these genes, are restricted by this fact. However, the evidence of balancing selection supported by Tajima's D, Fu and Li's D, Fu and Li's F is quite strong for two of our genes of interest (Table 3.2). The lack of concordance between Tajima's D and HKA in our analysis is consistent with previous findings for genes widely reported to be under balancing selection in African parasite populations (Supplementary Table 5) (Ochola et al., 2010; Ochola-Oyier et al., 2019).

University of Ghana http://ugspace.ug.edu.gh

This may be attributed to high recombination rates, changing effective population size, and the presence of mutations that may not be selectively neutral (Hudson, 1990; Hudson et al., 1987).

In general, we have detected loci under balancing selection, in Ghanaian *P. falciparum* isolates, which intersect with the genome background required for ARTr to emerge in SEA. Although Ghana and SSA are yet to report solid evidence of ARTr, our analysis shows that molecular surveillance efforts may be improved by scanning the background of such loci associated with PfK13 ARTr. This approach can signal the emergence of the ARTr phenotype but may require optimization to serve as the missing tool needed in the current landscape of ARTr surveillance of *P. falciparum* malaria parasites in Africa. Thus, we have suggested the potential utility of surveying the genome of parasites for balancing selection in ARTr precursor background genes as a potential molecular early warning system for ARTr surveillance efforts.

INTEGRI PROCEDAMUS

University of Ghana http://ugspace.ug.edu.gh

3.5 Methods

3.5.1. Sequencing and genotyping

DNA sequences were retrieved from the Malaria Genomic Epidemiology Network (MalariaGEN) Pf3k data repository (https://www.malariagen.net/projects/parasite/pf3k). Paired-end sequencing was done using the Illumina HiSeq platform (Bentley et al., 2008) by Sanger sequencing core. Read lengths ranged between 200–300 bp and approximately 1 Gbp of data per sample was produced as described (Project, 2016). Quality control, variant discovery and sample genotyping were done using custom pipelines details of which may be reviewed in (Manske et al., 2012). Briefly, short sequence reads from *P. falciparum* isolates that passed stringent quality filters were aligned against the *P. falciparum* 3D7 reference sequence V3 (ftp://ftp.sanger.ac.uk/pub/pathogens/*Plasmodium*/*falciparum*/3D7/3D7.latest_version/version3/), using the bwa program (Li and Durbin, 2009) (http://bio-bwa.sourceforge.net/) as previously described (Manske et al., 2012).

Genotyping was done with the Genome Analysis Tool Kit (GATK 3.3-46) best practices pipeline for *de novo* variant discovery. After mapping each sample to the 3D7 reference genome, PCR and sequencing duplicates were marked using Picard SortSam and the MarkDuplicates function of GATKs pipeline. Realignment around InDels (insertion and deletion sequence variants) was done using GATK's RealignerTargetCreator/IndelRealigner. The base quality score recalibration was done with GATK's BaseRecalibrator. The following *P. falciparum* genetic crosses 1.0 databases were used for the base quality recalibration: ftp://ngs.sanger.ac.uk/production/malaria/pf-crosses/1.0/7g8_gb4.combined.final.vcf.gz; ftp://ngs.sanger.ac.uk/production/malaria/pf-crosses/1.0/hb3_dd2.combined.final.vcf.gz; and ftp://ngs.sanger.ac.uk/production/malaria/pf-crosses/1.0/3d7_hb3.combined.final.vcf.gz.

University of Ghana http://ugspace.ug.edu.gh

Variants calling was done using GATK's CombineGVCFs and GenotypeGVCFs. This was followed by variant quality score recalibration using GATKs VariantRecalibrator/ApplyRecalibration functions. The same set of *P. falciparum* crosses 1.0 databases above were used. Finally, variants annotation was done using SnpEff (v4.1) with a database created from ftp://ftp.sanger.ac.uk/pub/project/pathogens/gff3/2015-08/P*falciparum*.gff3.gz; annotate variants by regions identified in Pf crosses 1.0 data (ftp://ngs.sanger.ac.uk/production/malaria/pf-crosses/1.0/regions-20130225.onebased.txt). Variants were filtered out where VQSLOD <= 0 or RegionType!= "Core" to generate a final VCF file available at the MalariaGEN Pf3k data repository.

3.5.2. Hard filtering pipeline of Ghana 2009/2010 clinical isolates variants

Bcftools was used in a custom bash script to extract the Ghana 2009/2010 samples and concatenate all the variant information into a single VCF without structural variants such as InDels. Quality hard filtering of single nucleotide polymorphisms (SNPs) was done to filter out SNPs with the following features: SNPs with very poor sequencing depth (<10 reads in one sample) and coverage across samples; SNPs that had more than two alleles; and SNPs located in the highly polymorphic var, rifin and stevor regions (Manske et al., 2012). Further snpEFF annotation was done using the global barcode SNPs from a genome-wide study of *P. falciparum* population divergence by natural selection (Neafsey et al., 2008). The final VCF file was filtered again using the default parameters of the GATK SelectVariants function. Samples with missing genotype calls of >5% were filtered out. VCFtools (0.1.16) was used to determine the genome-wide average nucleotide diversity.

University of Ghana http://ugspace.ug.edu.gh

3.5.3. Evaluation of multiplicity of infection (MOI) and population structure

We used the within-sample F statistic (F_{ws}) to determine MOI in the Ghana cohort of clinical isolates of *P. falciparum* (Manske et al., 2012; Auburn et al., 2012). The moimix package (Lee, 2016) was used to determine the F_{ws} in R version 4.0.Principal component analysis (PCA) was done using vcfdo (https://github.com/IDEELResearch/vcfdo) function 'pca'.

3.5.4 Tests for departures from neutrality

We used the R package PopGenome for genome scans and determination of the allele frequency distribution selection metric Tajima's D at each SNP site (Pfeifer et al., 2014). Subsequently, we used custom bash scripts to extract the DNA sequences of the nine genes of interest (Supplementary Table_1). DnaSP6.0 was used to determine departures from neutrality, for the nine genes of interest, using allele frequency distribution measures Tajima's D, Fu and Li's F and Fu and Li's D, and comparisons of variations within and between species with Hudson–Kreitman–Aguade (HKA) and McDonald–Kreitman (MK) ratios (Rozas et al., 2017). Tajima's D measures the difference between the average pairwise nucleotide diversity between sequences (π) and Watterson's population nucleotide diversity (q) (Tajima, 1989; Ochola et al., 2010). This will make the expected value of Tajima's D for populations under neutrality to be zero. When conditions of neutrality are violated, Tajima's D will capture a skew in the allele frequency distribution. These significant deviations from zero can either be positive or negative. Positive values of Tajima's D indicate an excess of intermediate frequency alleles. This can be caused by population bottlenecks, population structure, and/or balancing selection (Casillas et al., 2017).

Fu and Li's F statistic is determined by the difference between the number of single nucleotide variants observed only once in a sample and the total number expected under

University of Ghana http://ugspace.ug.edu.gh

neutrality given the number of segregating sites and Watterson's estimate of nucleotide diversity (q); Fu and Li's D is the difference between the number of derived nucleotide variants observed only once in a sample with the total number of derived nucleotide variants (Casillas et al., 2017; Fu et al., 1993). HKA ratio was used to determine *P. falciparum* genes with high ratios of polymorphism(p) over divergence(K) from the closely related chimpanzee parasite *Plasmodium reichenowi* (Innan, 2006; Hudson et al., 1987).

The MK test is based on the ratios of non-synonymous (NS) and synonymous (S) nucleotide divergence and polymorphism within species and a closely related species, using a Fisher's exact test on the 2x2 contingency table (McDonald et al., 1991). Finally, we used the PlasmoDB Gene Ontology (GO) analysis tool (http://plasmodb.org) to identify the biological processes of genes significantly deviating from neutrality.

University of Ghana http://ugspace.ug.edu.gh

CHAPTER FOUR

Implicating Extracellular Vesicles in *Plasmodium falciparum* Artemisinin Resistance Development

Kwesi Z. Tandoh[1], Michael D. Wilson[2], Neils B. Quashie[3,4], Nancy O. Duah-Quashie[3]

Affiliations

1. West African Center for Cell Biology of Infectious Pathogens, Department of Biochemistry, Cell and Molecular Biology, College of Basic and Applied Sciences, University of Ghana, Accra, Ghana
2. Department of Parasitology, Noguchi Memorial Institute for Medical Research, College of Health Sciences, University of Ghana, Accra, Ghana
3. Department of Epidemiology, Noguchi Memorial Institute for Medical Research, College of Health Sciences, University of Ghana, Accra, Ghana.
4. Center for Tropical Clinical Pharmacology and Therapeutics, School of Medicine and Dentistry, College of Health Sciences, University of Ghana, Accra, Ghana

Corresponding author: Nancy O. Duah-Quashie, NDuah@noguchi.ug.edu.gh;

Kwesi Z. Tandoh, kztandoh@st.ug.edu.gh.

University of Ghana http://ugspace.ug.edu.gh

Tandoh KZ, Wilson MD, Quashie NB, Duah-Quashie NO. Implicating extracellular vesicles in *Plasmodium falciparum* artemisinin resistance development. Traffic. 2021 Jun;22(6):194-200. doi: 10.1111/tra.12787. Epub 2021 Apr 24. PMID: 33860593.

This manuscript has been published in Traffic journal (Wiley) and has been reproduced in this thesis with permission from the journal.

University of Ghana http://ugspace.ug.edu.gh

4.1 Abstract

Plasmodium falciparum malaria remains a disease of significant public health impact today. With the risk of emerging artemisinin resistance (ARTr) stalling malaria control efforts, the need to deepen our understanding of the parasite's biology increases. Extracellular vesicles (EVs) are vital to the biology of *P. falciparum* and play a role in the pathogenesis of malaria. Recent studies have also shown that EVs may play a role in the development of ARTr in *P. falciparum*. In this review, we highlight evidence on EVs, *P. falciparum* biology, and malaria pathogenesis and argue that there are sufficient grounds to propose a role for EVs in the development of *P. falciparum* ARTr. We also re-visit the idea of EVs as parasite waste disposal vehicles within the context of their role as actively secreted functioning organelles mediating cellular redox homeostasis in the *P. falciparum*-infected red blood cell. A deeper understanding of the mechanisms underpinning ARTr development will, in the short to medium term, help in the formulation of ARTr containment measures to mitigate the global spread of ARTr.

Keywords: malaria, *Plasmodium falciparum*; extracellular vesicles, parasite waste management, cellular redox homeostasis, artemisinin drug resistance

University of Ghana http://ugspace.ug.edu.gh

4.2 Introduction

Extracellular vesicles (EVs) are a diverse and versatile group of cell-derived membranous structures that function as vehicles of intercellular communication in prokaryotes and eukaryotes (van Niel et al., 2018; Yáñez-Mó et al., 2015). Structurally, EVs are single lipid membrane-bound vesicles enclosing a cargo suite of proteins, lipids, metabolites, and nucleic acids (Babatunde et al., 2020; Babatunde et al., 2018; Sahu et al., 2013a; Shrivastava et al., 2017; Sahu et al., 2013b). EVs represent a heterogeneous population that can range in size from 30nm to 2000nm and have been previously classified into microvesicles and exosomes based on their size and biogenesis (Willms et al., 2016; Yáñez-Mó et al., 2015; Willms et al., 2018; Greening et al., 2018).

Microvesicles are formed from outward budding of the plasma membrane, and typically have a diameter between 0.3 and 1µm. Exosomes have a smaller size (50-200nm) and are formed by the fusion of multivesicular bodies from the endosomal pathway with the external cell membrane that occurs via the endosomal sorting complex required for transport (ESCRT) pathway (Maas et al., 2017; Abels et al., 2016; Latifkar et al., 2019). EVs are distinct from apoptotic bodies as their formation and release are independent of cell death (Raposo et al., 2013).

EVs mediate parasite-parasite communication (P-PC) between single-celled protozoans such as *Leishmania* sp., *Toxoplasma* sp., and *Trypanosoma* sp., and have been shown to transfer factors necessary for population growth and host adaptation (Coakley et al., 2015). In *P. falciparum* biology and malaria pathogenesis, EVs have been established as the vehicles mediating P-PC in host immunomodulation, pathophysiological development of cerebral malaria, antimalarial drug resistance, and gametocytogenesis (Regev-Rudzki et al., 2013; Babatunde et al., 2020; Babatunde et al., 2018; Sahu et al., 2013a; Shrivastava et al., 2017; Sahu et al., 2013b).

University of Ghana http://ugspace.ug.edu.gh

Contemporary work on EVs is pacing to furnish details on their role in molecular mechanisms undergirding the biology and virulence of *P. falciparum* (Sierro et al., 2019; Correa et al., 2019; Mantel et al., 2016; Antwi-Baffour et al., 2020; Ankarklev et al., 2014). This has the potential to transform the malaria research landscape by discovering novel drug targets for malaria drug development. Additionally, EV research has parallel promising applications in the field of gene delivery vectors (Saari et al., 2020). Therefore they may become the utilitarian vehicle needed to translate gene therapy into clinical practice (Andaloussi et al., 2013). Here, we present a synopsis of the evidence supporting the role of EVs in the biology of *P. falciparum* and the pathogenesis of malaria. We highlight the plausible role of EVs in the development of artemisinin resistance (ARTr) in *P. falciparum* and re-visit the idea of EVs as parasite waste disposal vehicles within the context of functioning organelles involved in maintaining cellular redox homeostasis in *P. falciparum*-infected red blood cells.

University of Ghana http://ugspace.ug.edu.gh

4.3 Extracellular vesicles in malaria pathogenesis and *P. falciparum* biology

Several studies have shown that EVs are released from infectious organisms and infected host cells and that these EVs modulate both the infectious process and the host immune response, and are vehicles of P-PC (Sampaio et al., 2017; Babatunde et al., 2020). EVs, as functionally relevant biological organelles in PfiRBCs, have been firmly established and are actively secreted in quantitatively larger amounts in comparison to uninfected RBCs (Sampaio et al., 2017; Nantakomol et al., 2011).

In *P. falciparum*, EVs have been shown to associate with malaria severity through host immune modulation, drug resistance development, and gametocytogenesis. For example, the composition of EVs from *P. falciparum*-infected red blood cells (PfiRBCs) was reported to contain parasite antigens and nucleic acids that aid red cell invasion, host immunomodulation, and gametocytogenesis (Mantel et al., 2013; Babatunde et al., 2018; Sisquella et al., 2017; Ye et al., 2018). EVs from PfiRBCs have also been shown to contain functional miRNA-Argonaute 2 complexes, and can be internalized by human endothelial cells, and may play a role in the ability of the parasite to sequester in the microvasculature (Mantel et al., 2016; Wang et al., 2017).

Accumulating evidence on EVs from PfiRBCs suggests a role for EVs in the pathogenesis of cerebral malaria. Increased levels of endothelial-derived EVs have been reported to associate with cerebral malaria and activate brain microglial cells, thus contributing to the enhanced inflammation seen in cerebral malaria (Mbagwu et al., 2019; Combes et al., 2004). Abdi et al. also reported that the cargo of EVs from a clinical case of cerebral malaria was rich in immunogenic proteins found in the exomembrane compartment and endomembrane secretory systems of PfiRBCs (Abdi et al., 2017). These studies implicate EVs in the pathogenesis and severity of malaria.

University of Ghana http://ugspace.ug.edu.gh

Intercellular communication between malaria parasites is made cumbersome by the presence of three lipid membranes that must be traversed for such communication to be achieved. First is the parasite membrane, then the parasitophorous vacuole (PSV) membrane, and finally the red blood cell (RBC) membrane. However, extensive host PfiRBC remodeling achieves active transportation of parasite antigens across all membranes and suggests that EVs from PfiRBCs may act as vehicles that mediate intercellular communication in *P. falciparum* (Bhattacharjee et al., 2018; Warncke et al., 2019). In support of this idea, it has been reported that EVs serve as the carriers of signals for the vital switch of asexual malaria parasites to gametocytes and the plausible vehicles mediating the transfer of molecules conferring antimalarial drug resistance to malaria parasites (Regev-Rudzki et al., 2013, Mantel et al., 2013). It has also been shown that EVs contain a large amount of hemoglobin from the host red blood cell, and this suggests that EVs are the vehicles of vesiculation that mediate hemoglobin waste disposal in PfiRBCs (Antwi-Baffour et al., 2016).

University of Ghana http://ugspace.ug.edu.gh

4.4 Implicating EVs in *P. falciparum* ARTr development

Population genetics and genomics studies have detailed the historical precision with which *P. falciparum* resistance to anti-malarial drugs emerge. Against the backdrop of a life cycle delicately balanced between the human host and the invertebrate mosquito, the odds that drug resistance will emerge should be tenuous. However, this is not the case. The parasite population navigates significant odds to arrive at the endpoint of drug resistance and the success of this process may be significantly enhanced by P-PC that may be mediated via EVs.

We outline below the processes that lead to antimalarial drug resistance development of any kind. This highlights the population paradigm as opposed to a single infected red blood cell perspective. The development of any form of antimalarial drug resistance requires that the natural diversity of the malaria parasites in the human host be able to absorb and outstrip the drug selection pressure. Here, we utilize the selection on standing variation model of evolution (Barrett et al., 2008) that removes the need for advantageous *de novo* variants to be formed before selection can occur under the drug selection pressure. This drug selection pressure typically takes the form of sub-lethal doses of the drug and/or sub-optimum drug duration of exposure in the human host. This sets the milieu that caters for the selection of the parasite clones with a fitness advantage over the wild type (Cerqueira et al., 2017). For the process of drug resistance development to continue, the selected minority population of parasites in the human host must be transmitted to the mosquito vector. The genomic variant (that confers the selective advantage) must keep the parasite's competency to form gametocytes. Such that, any fitness cost that may have arisen from the selection pressure must be compensated for. This compensation usually takes the form of a selection of additional genomic variants on the advantage-conferring genomic variant (Cerqueira et al., 2017).

Having successfully produced gametocytes, they are taken up during the blood meal of a female anopheline mosquito. Within the mosquito, the genetic variant conferring selective

University of Ghana http://ugspace.ug.edu.gh

advantage (without fitness cost) must not be neutralized by recombination during the sexual phase. If this hurdle is traversed, the sporozoites for this clone are then transmitted to another human host and the cycle is perpetuated. Upon re-entry into a human host, another difficulty arises. This minor population of selected drug-resistant parasites must compete with the wild type in the human host (Bushman et al., 2018). Their competitive advantage is drug pressure. Given the interval for the manifestation of malaria in the human host, there seems to be enough time for the wild-type parasites to drown out the minor advantageous parasites. The telling question remains: what are the odds that all these events will occur without the role of signaling? (Bushman et al., 2016)

Within the invertebrate vector and the human host, there may be the transfer of selection pressure conferring advantage between parasites. This can occur via EVs from the resistant parasite clone to the susceptible ones (Regev-Rudzki et al., 2013). This EVs-mediated P-PC improves the odds of what we empirically observe in antimalarial drug resistance development. In ARTr development, EVs may play a vital role in transferring resistant factors from the selected resistant parasites to the susceptible parasites (Regev-Rudzki et al., 2013). Regev-Rudzki et al. demonstrated the unidirectional movement of EVs from the resistant to the susceptible parasites which subsequently resulted in the latter becoming resistant and thus providing proof that the transfer of resistance was mediated by EVs. EVs may also carry in their cargo the molecules that signal gametocyte switch. This is an important bottleneck in the ARTr development process. This stage has higher odds of success if it is aided by intercellular signaling molecules.

University of Ghana http://ugspace.ug.edu.gh

Thus, we single out EVs as the biologically plausible vehicles for this switch. Two seminal studies have suggested that EVs may be responsible for mediating the switch of *P. falciparum* asexual forms to gametocytes (Regev-Rudzki et al., 2013; Mantel et al., 2013).

ARTr is driven by an enhanced stress response to cellular oxidative and proteotoxic injury induced by the activation of ART and has been associated with an upregulation of unfolded protein response, and longer duration in the ring stage of asexual development (Mok et al., 2015; Rocamora et al., 2018). Endoplasmic reticulum-related phosphatidylinositol-3-phosphate (PI3P) vesicular amplification has also been implicated as a molecular mechanism undergirding ARTr (Bhattacharjee et al., 2018; Mbengue et al., 2015; Suresh et al., 2018). Within this hypothetical framework of ARTr development in *P. falciparum*, we suggest that EVs may play a role in the maintenance of protein homeostasis in the PfiRBC by removing unwanted proteotoxic damage of ART assault from the PfiRBC. Here, we propose that EVs are crucial for maintaining cellular redox homeostasis in PfiRBCs especially under ART assault. This EV secretion theme is not new, although it remains less studied (Correa et al., 2019; Yáñez-Mó et al., 2015; Vidal, 2019). Therefore, conferring on EVs the role of waste disposal vehicles is a biologically plausible hypothesis.

Rocamora et al. described an *in vitro* selection regime, that mimicked *in vivo* parasite-dihydroartemisinin interactions, was used to derive the ARTr phenotype from two clones of 3D7. ART drug sensitivity and transcriptomic profiling of the selected ARTr parasite lines showed that adaptive responses against oxidative stress and proteotoxic damage correlated with ARTr (Rocamora et al., 2018). This established that the unfolded protein response (UPR) is associated with ARTr development. UPR is characterized by enhanced PI3P ER vesiculation (Bhattacharjee et al., 2018; Dogovski et al., 2015; Suresh et al., 2018).

University of Ghana http://ugspace.ug.edu.gh

Furthermore, Dogovski et al. profiled the dynamic responses of ART-resistant and susceptible *P. falciparum* parasites and reported that ART induces growth retardation and accumulation of ubiquitinated proteins (Dogovski et al., 2015). Juxtaposing this observation next to the fact that ARTr develops at the early ring stage of intra-erythrocyte development (Mok et al., 2011) may suggest that the early ring stage is the optimum time for waste disposal of accumulated damaged proteins from ART action. Having stated these facts, we suggest that EVs can be implicated as biologically plausible vehicles that shed the proteotoxic damage off the infected red blood cell. This EVs driven waste disposal system will help maintain cellular redox homeostasis under ART assault and thus ART tolerance. An experimental design that further interrogates these hypotheses will help the field immensely.

4.4.1 Conclusion

In this review, we have highlighted a plausible role of EVs in the development of ARTr in *P. falciparum* and suggested that this role could be centered around a vehicular waste disposal system for maintaining cellular redox homeostasis under ART pressure. We recommend further studies to test this hypothesis as understanding the role of EVs in *P. falciparum* biology is crucially needed, especially within the research arena searching for novel druggable targets for alternative antimalarial drug discovery purposes.

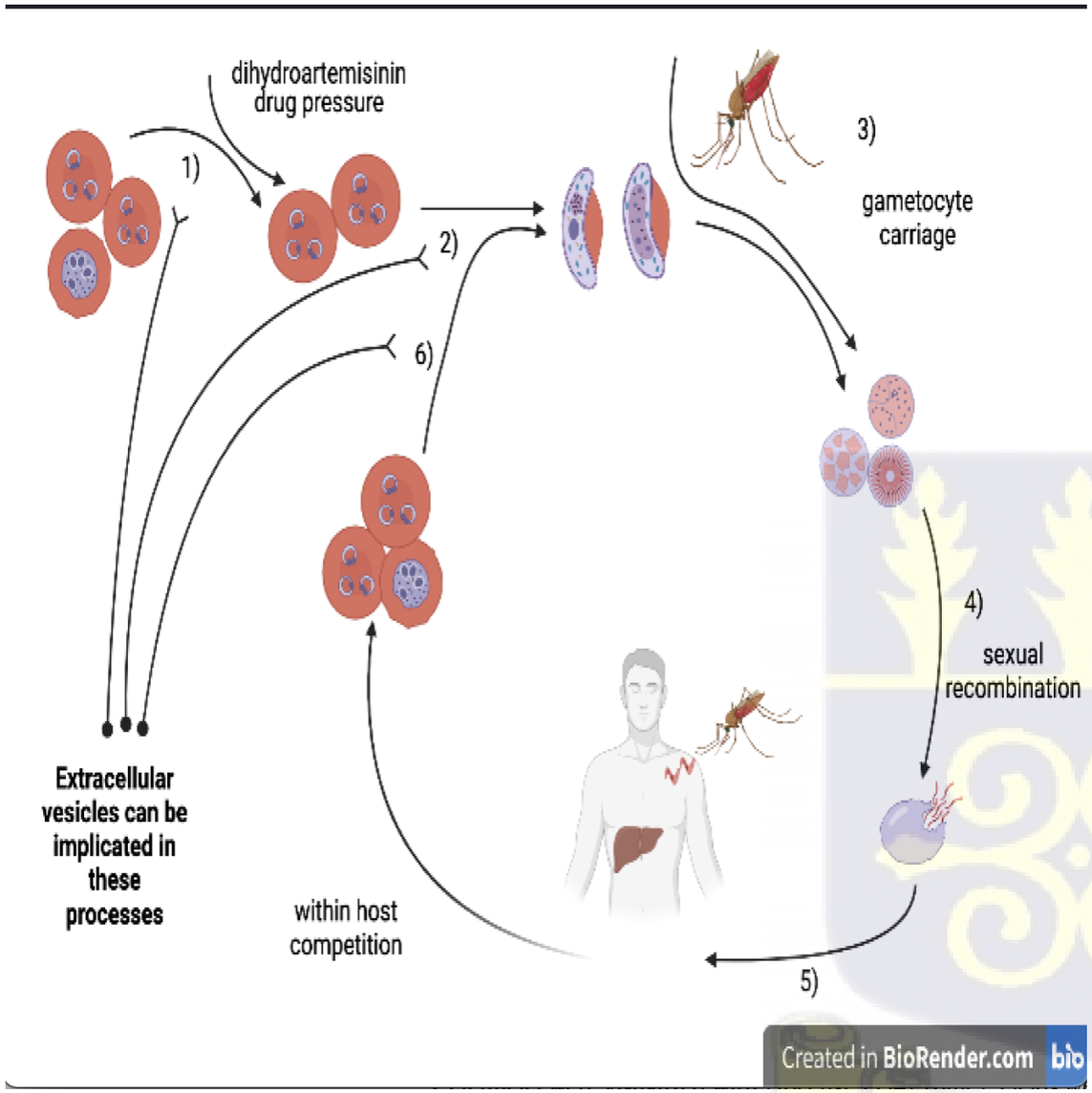

Figure 4.1 The emergence of the ARTr phenotype depends on the presence of an ARTr conferring variant that is selected and successfully transmitted. The many bottlenecks that must be traversed suggest a role for P-PC, which may be achieved by EVs.

1. Assuming a standing diversity in the asexual parasite population within the human host, which has a high prior probability in malaria endemic zones like SSA, a parasite subpopulation with the ARTr conferring variant(s) may already in circulation but kept in check from expansion by immune pressure. Repeated exposure to sub-lethal concentrations of dihydroartemisinin selects for these ARTr variants against a backdrop of improving malaria control efforts related waning of natural immunity. EVs may play a role here as the actively secreted vehicles involved in maintaining cellular homeostasis under ART action.

2. Assuming there is no fitness disadvantage of the ARTr conferring variant(s), then sufficient gametocyte carriage will be reached to enable transmission to the female anopheline mosquito vector. EVs have been suggested to play a role here by acting as signaling vehicles mediating gametocytogenesis.

3,4. Once in the mosquito vector, the ARTr conferring variant(s) must not be reversed by the sexual recombination phase. The ARTr conferring variant must not negatively affect the developmental phase in the mosquito vector.

5. On completion of the sexual phase, the transmission of sporozoites of the ARTr conferring variant into another human host is vital to continuing the cycle and propagating the newly selected ARTr parasite.

6. Finally, within-host competition between the ARTr and wild-type ART susceptible parasites is the last bottleneck for the onward transmission of the emerging ARTr parasites in the human population. Here, EVs may be implicated as vehicles transferring the ARTr phenotype from ARTr to ART susceptible parasites.

University of Ghana http://ugspace.ug.edu.gh

CHAPTER FIVE

Transcriptome-Module Phenotype Association Study Implicates Extracellular Vesicles Biogenesis in *Plasmodium falciparum* Artemisinin Resistance

Kwesi Z. Tandoh[1*], Oheneba C. Hagan[1], Michael Wilson[2], Neils B. Quashie[3,4], Nancy O. Duah-Quashie[3*]

Affiliations

1. West African Center for Cell Biology of Infectious Pathogens, Department of Biochemistry, Cell, and Molecular Biology, College of Basic and Applied Sciences, University of Ghana, Accra, Ghana
2. Department of Parasitology, Noguchi Memorial Institute for Medical Research, College of Health Sciences, University of Ghana, Accra, Ghana
3. Department of Epidemiology, Noguchi Memorial Institute for Medical Research, College of Health Sciences, University of Ghana, Accra, Ghana.
4. Center for Tropical Clinical Pharmacology and Therapeutics, School of Medicine and Dentistry, College of Health Sciences, University of Ghana, Accra, Ghana

*Corresponding authors:

Nancy O. Duah-Quashie, NDuah@noguchi.ug.edu.gh;

Kwesi Z. Tandoh, kztandoh@st.ug.edu.gh

University of Ghana http://ugspace.ug.edu.gh

Tandoh KZ, Hagan OC, Wilson MD, Quashie NB, Duah-Quashie NO. Transcriptome-module phenotype association study implicates extracellular vesicles biogenesis in *Plasmodium falciparum* artemisinin resistance. Front Cell Infect Microbiol. 2022 Aug 19;12:886728. doi: 10.3389/fcimb.2022.886728. PMID: 36061874; PMCID: PMC9437462.

This manuscript has been published in Frontiers in Cellular & Infection Microbiology and has been reproduced in this thesis with permission from the journal.

5.1 Abstract

Plasmodium falciparum malaria is still an important disease in sub-Saharan Africa (SSA). Great strides have been made in its control spear-headed by artemisinin(ART)-based combination therapies (ACTs). However, concerns about the imminent spread of ART-resistant(ARTr) malaria parasites to SSA threaten gains already made. Attempts to mitigate this risk have highlighted the need to discover novel *P. falciparum* drug targets. Therefore, studies to deepen our understanding of the biology of *P. falciparum* are needed. The role of extracellular vesicles (EVs) in the biology of malaria parasites is not fully understood. Recently, the ART resistance-associated transcriptional profile has been reported to involve several biological processes connected to vesicular trafficking, proteotoxic stress, erythrocyte remodeling, and mitochondrial metabolism. We explored a role for EVs in developing the *P. falciparum* ARTr phenotype using bulk RNA sequencing of unsynchronized parasite cultures under untreated, 0.1% dimethyl sulfoxide and 700nM dihydroartemisinin treatment conditions for six hours. As pathway and gene ontology analysis is limited in its curated knowledge repertoire on EVs biogenesis in *P. falciparum*, we used a modular (gene set) analysis approach to explore whether an EVs biogenesis module is associated with the ARTr phenotype in *P. falciparum*. We first generated well-defined EV modules of interest and used statistical tools to determine differences in their expression among the parasite and treatment conditions. Then, we used gene set enrichment analysis to determine the strength of the association between each EVs module of interest and the ARTr phenotype. This transcriptome-module phenotype association study (TMPAS) represents a well-powered approach to making meaningful discoveries out of bulk gene expression data. We identified four EV module of interest and report that one module representing gene sets with correlated expression to PF3D7_1441800 – involved with EVs biogenesis in *P. falciparum* - is associated with the ARTr phenotype (R539T_DHA_treated versus R539T_untreated: normalized enrichment score (NES) = 1.1830174, FDR q-value < 0.25; C580R_DHA_treated versus C580R_untreated: NES = 1.2457103, FDR q-value < 0.25). PF3D7_1441800 has been reported to reduce EV production when knocked out in *P. falciparum*. Altogether, our findings suggest a role for EVs in developing ART resistance and warrant further studies interrogating this association.

Keywords: transcriptomics, modules, association, artemisinin resistance, *Plasmodium falciparum*, extracellular vesicles, malaria

University of Ghana http://ugspace.ug.edu.gh

University of Ghana http://ugspace.ug.edu.gh

5.2 Introduction

One of the pillars driving malaria control in sub-Saharan Africa (SSA) is the use of artemisinin-based combination therapies (ACTs) for effective management of identified malaria cases (WHO, 2015, 2021c). Although ACTs are still effective today, grave concerns have risen about their future efficacy because of the emergence of artemisinin-resistant (ARTr) parasites in South-East Asia (SEA) (Noedl et al., 2008; Dondorp et al., 2009) and their recent independent emergence in Rwanda and Uganda (Uwimana et al., 2020; Balikagala et al., 2021; Bergmann et al., 2021; Uwimana et al., 2021). This trajectory of events has made dire the need for efforts to provide alternatives to current ACTs. The preemptive risk mitigation activities spectrum includes active molecular surveillance and discovering novel antimalarial drug targets (WHO, 2021a). Therefore, to spur efforts toward novel malaria drug discovery and active molecular surveillance, our current understanding of the molecular mechanisms underpinning ARTr must be deepened.

Extracellular vesicles (EVs) are a heterogeneous group of membrane-bound vehicles reported to be important to the biology of *P. falciparum*, mainly within the context of parasite-parasite communication (Roditi, 2016; Marti et al., 2016; Mantel et al., 2014). As very little was previously known about EVs biogenesis pathways in *P. falciparum*, exploratory transcriptome-phenotype association studies yielded little or no power to explore their role in ART resistance. Recently, Avalos-Padilla et al. reported that *P. falciparum* EVs biogenesis is accomplished by a functional endosomal sorting complex required for transport (ESCRT) activated by an alternative recruitment pathway involving the action of PfBro1 and PfVps32/PfVps60 proteins (Avalos-Padilla et al., 2021). This finding has made it possible for direct and targeted interrogation of the role of EVs in *P. falciparum* ART resistance.

University of Ghana http://ugspace.ug.edu.gh

ART resistance is understood to be undergirded by two broad molecular mechanistic motifs: an increased tolerance to ART-induced oxidative stress and reduced hemoglobin endocytosis to the digestive food vacuole. Both motifs are causally associated with variants in the propeller region of the *P. falciparum* kelch 13 gene (*PfK13*) and have been extensively reviewed recently by (Siddiqui et al., 2021). Whether EVs can be implicated in the expression of the ARTr phenotype is yet to be empirically explored (Tandoh et al., 2021). The closest sliver of evidence was established within the context of parasite-parasite communication and suggested that EVs may be able to transfer the ARTr phenotype to ART-susceptible parasites (Regev-Rudzki et al., 2013). Additionally, recently conducted gene expression studies to gain insight into the molecular mechanisms undergirding ART resistance reported the involvement of many biological processes that included cell-cycle periodicity, the unfolded protein response, protein degradation, mitochondrial and redox metabolism, erythrocyte remodeling and vesicular trafficking (Mok et al., 2021; Zhu et al., 2022).

In this study, we posed the research question: is EVs biogenesis associated with the ARTr phenotype? We conducted an EVs targeted exploratory analysis of the transcriptome of two ARTr and one ART susceptible parasite line under three conditions (untreated, 0.1% dimethyl sulfoxide (DMSO) and 700nM dihydroartemisinin (DHA) treatment conditions for six hours) to interrogate this question. Using the higher discovery power of a transcriptome-module phenotype association study (TMPAS), we show that an EVs module of interest is associated with the ARTr phenotype R539T_DHA_treated versus R539T_untreated: NES =1.1830174, FDR < 0.25; C580R_DHA_treated versus C580R_untreated: NES = 1.2457103, FDR < 0.25). We also report on the heterogeneous nature of the ARTr population of *P. falciparum* parasites.

University of Ghana http://ugspace.ug.edu.gh

Our findings add knowledge that will help shape future studies into EVs biogenesis and ART resistance and will contribute to novel antimalarial drug discovery efforts. Most importantly, our data implicate EVs in developing the ARTr phenotype outside the already reported theme of parasite-parasite communication. Further studies interrogating this motif are merited.

INTEGRI PROCEDAMUS

University of Ghana http://ugspace.ug.edu.gh

5.3 Method

5.3.1. Parasite lines and culture conditions

Transgenic parasite lines (C580R and R539T) were generated by OCH using CRISPR/Cas9 genome editing of the *PfK13* locus in a Dd2 parental line. The plasmid utilized for the genome editing targeting the *P. falciparum* kelch 13 gene, pDC2-cam-co.Cas9-U6-hDHFR was originally designed by Marcus Lee of Sanger Institute. The components included a codon-optimized Cas9 sequence with a nuclear localization sequence driven by the *P. falciparum* calmodulin promoter and Pfhsp86 3' UTR (untranslated region) terminator. It had a *P. falciparum* U6 cassette for gRNA (guide RNA) expression with a *BbsI* restriction site for cloning in the gRNA. A human dihydrofolate reductase (*hdhfr*) gene sequence expressed using the *P. chabaudi* dihydrofolate reductase-thymidylate synthase (*PcDT*) 5' UTR and *P. falciparum* histidine-rich protein 2 (*Pfhrp2*) 3' UTR was used for selection during transfection using WR22910 - an ampicillin resistance cassette for selecting successfully transformed *Escherichia coli* after the plasmid transformation. It also possesses an *EcoR1/AatII* restriction site for cloning in the donor DNA sequence. Successfully genome-edited parasites were confirmed using Sanger sequencing of polymerase chain reaction (PCR) products, with the primers for the PCR designed to amplify beyond the donor DNA to preclude amplification of episomally retained plasmids. Additionally, whole-genome sequencing was performed, and the sequence was compared with the parental genome (Supplementary Figures 5.1 – 5.3).

University of Ghana http://ugspace.ug.edu.gh

We used the known R539T ARTr variant found in SEA and the C580R *PfK13* variant first reported to be present in the forest and coastal zones of Ghana (Ariey et al., 2014; Miotto et al., 2015; Ménard et al., 2016; Matrevi, 2017). Our rationale was to validate that the *PfK13* variant (C580R) of Ghanaian provenance did confer the ARTr phenotype.

Plasmodium falciparum parasites were cultured at 5% hematocrit in human O- red blood cells (RBCs) and culture media comprising RPMI 1640 (Thermo Fisher Scientific) supplemented with 0.5% (w/v) Albumax II (Invitrogen), 50 mg/L hypoxanthine, 0.225% NaHCO3, 25 mM HEPES, and 10 mg/L gentamycin. Parasites were cultured at 37°C in 5% O2, 5% CO2, and 90% N2 (Quashie et al., 2013).

5.3.2. Parasite sensitivity assays to dihydroartemisinin

The SYBR Green 1 fluorescent-based *in vitro* drug sensitivity assay was used to assess the susceptibility of the *P. falciparum* parasites, used in this study, to ART. This assay was used to determine the 50% inhibitory concentrations (IC50) defined as the concentration of dihydroartemisinin (DHA) (the *in vivo* metabolically active form of ART) inhibiting parasite growth by 50% (Johnson et al., 2007; Machado et al., 2016). Briefly, we exposed unsynchronized *in vitro* parasite cultures, in triplicate, across a range of dihydroartemisinin concentrations (62.5pM to 16nM) for 72 hours. Parasites were diluted to 1% parasitemia in 2% hematocrit, and a 100µl parasite culture mix was pipetted into a drug-prefilled 96-well plate in triplicates to obtain a final volume of 200µl in each well. The control parasite cultures devoid of the drug were referred to as having 100% growth. The plates were incubated for 72 hours with a gas mixture of 93% nitrogen, 5% CO2, and 2% oxygen.

University of Ghana http://ugspace.ug.edu.gh

We measured growth by SYBR Green I staining (ThermoFisher, https://www.thermofisher.com) and performed a photometric assessment using a SpectraMax M5 plate reader (Molecular Devices) to measure fluorescence with excitation and emission wavelength bands at 485 and 530nm, respectively. IC50 for DHA was estimated using nonlinear regression with the log drug concentration versus growth rate response in a 4-parameter variable slope fitting dose-response curve (generated from the nine-point dilution series carried out in triplicates) using the R package drc (https://cran.r-project.org/web/packages/drc/drc.pdf) , version 3.0-1 (Ritz et al., 2015) and comparison between parasite lines was done by Student t-test. All analysis were performed in R version 4.0 (Core Team, 2021). A p-value of less than 0.05 was considered indicative of statistical significance.

The 0–3 hour ring-stage survival assay (RSA) was performed as described previously (Witkowski et al., 2013a) with few modifications. The RSA is an *in vitro* assay for measuring ART resistance and is of very practical utility in this regard because IC50s for both ARTr and susceptible parasites tend to have no statistically significant differences (Witkowski et al., 2013a; Ariey et al., 2014). In brief, highly synchronized 0–3 hour post-invasion rings were exposed to 700nM DHA for 6 hours, followed by removal of the drug. A parallel non-DHA exposed (0.1% DMSO exposed) set of isolates were used as controls. After 72 hours after initial drug treatment, parasitemia was assessed by Giemsa-stained smear microscopy of thin smears (parasite density per ≥ 10,000 red blood cells). The ring-stage survival percentage was calculated as the fraction of surviving DHA-treated parasites over the DMSO-treated control of the same parasite line (with a parasite growth rate of > 1.5%). An RSA survival percentage >1% is indicative of ART resistance. The RSA for each parasite line was determined with triplicates.

University of Ghana http://ugspace.ug.edu.gh

5.3.3. DHA and DMSO exposures to parasite cultures

We harvested a total of 27 samples from three *P. falciparum* lines *in vitro* cultures (Supplementary Table 1). We used a Dd2 parent line, and two engineered ART resistant lines on the Dd2 background (R539T and C580R). We cultured *P. falciparum* parasites in human O-negative RBCs using standard methods (Trager et al., 1976). Once parasitemia reached 3-5%, unsynchronized parasite cultures were exposed to 700nM DHA or 0.1% (v/v) DMSO solvent control for six hours. Parallel culture plates were also left untreated. After 6 hours of DHA or DMSO treatment, we centrifuged the parasite culture mix at 2500rpm for five minutes to harvest the infected erythrocytes. Subsequently, parasites were liberated from host erythrocytes by treatment with 0.015 % (w/v) saponin for five minutes at room temperature (Gibbons et al., 2018). After that, liberated parasites were washed twice with 1x PBS (137mM NaCl, 8mM KCl, 10mM Na2HPO4, 2mM KH2PO4, pH 7.4) to remove any host cell debris and residual drug. The parasites were then pelleted and stored at -80°C in an Eppendorf tube (1.5ml) containing 1mL Trizol reagent (Fisher Scientific, Hampton, NH) before RNA extraction (Gibbons et al., 2018).

University of Ghana http://ugspace.ug.edu.gh

5.3.4. RNA extraction, Library preparation and Next-Generation Sequencing

Sequencing was performed at Single Cell Discoveries, a sequencing service provider located in the Netherlands using an adapted version of the CEL-seq protocol. Total ribonucleic acid (RNA) was extracted from TRIzol-preserved parasites after thawing at room temperature using the standard TRIzol (Invitrogen) protocol and used for library preparation and sequencing. The extracted RNA was dissolved in 100µl RNase-free water and DNA removed by DNase I digestion, after which the purified RNA was eluted into 50µl RNase-free water. Qubit High Sensitivity RNA assay (Thermo Fisher Scientific) was used to quantify the purified RNA, and RNA integrity was determined on an Agilent Bioanalyzer (Agilent Genomics, Waldbronn, Germany). Messenger RNA (mRNA) was processed as described previously, following an adapted version of the single-cell mRNA sequencing protocol of CEL-Seq (Hashimshony et al., 2012; Simmini et al., 2014). In brief, samples were barcoded with CEL-seq primers during reverse transcription and pooled after second strand synthesis. The resulting complementary DNA (cDNA) was amplified with an overnight *in vitro* transcription reaction. From this amplified RNA, sequencing libraries were prepared with Illumina Truseq small RNA primers. The DNA library was paired end sequenced on an Illumina NextseqTM 500, high output, with a 1x75 bp Illumina kit (R1: 26 cycles, index read: 6 cycles, R2: 60 cycles). Read 1 was used to identify the Illumina library index and CEL-Seq sample barcode. Read 2 was aligned to the *Plasmodium falciparum* ASM276v2 reference transcriptome using BWA, version 0.7.17-r1188 (Li et al., 2009).

University of Ghana http://ugspace.ug.edu.gh

We aligned sequence reads to the *P. falciparum* transcriptome because our objective was to explore the well-annotated reference transcriptome and perform differential expression analysis within known genes (Conesa et al., 2016). Reads that mapped equally well to multiple locations were discarded. Mapping and generation of count tables were done, after quality control using *fastqc* (https://www.bioinformatics.babraham.ac.uk/projects/fastqc/) version 0.11.9, and converted to "bam" format using *samtools* (https://github.com/samtools/samtools) version 1.10, using the MapAndGo script (https://github.com/anna-alemany/transcriptomics/tree/master/mapandgo).

5.3.5. Data Analysis

The R package DaMiRseq version 2.0.0 (Chiesa et al., 2018) was used to explore the raw count data for batch effect, identify surrogate variables that may act as confounders and adjust the count data for downstream analysis. Lowly expressed genes (minimum count of 10) and samples with less than 70% of genes expressed were filtered out before normalization using variance stabilizing transformation (vst). The variance stabilizing transformation (vst) function to normalize and transform the count matrix. The vst is computed from the fitted relationship between the variance and the mean. This is used to normalize the count data to generate values of approximately equal variance along with the range of mean values. The vst transformation also normalizes for library size. Its use precludes the need for the generation of TPM (transcripts per million) normalized count data. Following pre-processing and transformation of the count data filtering by the coefficient of variation, set at a correlation coefficient of greater than or equal to 0.7, was done. Sample filtering was done using a cut-off spearman correlation coefficient of $\rho > 0.8$. The normalized and transformed count data was used for the exploratory data analysis for examining the quality of the data before downstream modular and differential gene expression analysis.

University of Ghana http://ugspace.ug.edu.gh

5.3.6 Modular analysis

Modular analysis involves the generation of a gene set (module) comprised of gene members with correlated expression and the determination of whether the module of interest is associated with the biological process (phenotype) of interest. The generated "repertoire of co-clustering gene sets" or the transcriptional module is used to "simplify" large-scale analysis and interpretation of transcriptional data (Chaussabel et al., 2014). It is a strategy largely borrowed from the field of immunology and was leveraged here to explore any association between EVs and ARTr.

We used the R package Weighted correlation network analysis (WGCNA version 1.70-3, http://www.genetics.ucla.edu/labs/horvath/CoexpressionNetwork/Rpackages/WGCNA) for our modular analysis using customized scripts (Langfelder et al., 2008). The WGCNA R software package is a compendium of R functions for performing various aspects of weighted correlation network analysis. It highlights a systems biology approach for describing the correlation patterns among genes in a gene expression data set. It can identify clusters/modules of highly correlated genes that can be used as the gene sets for determining associations with a biological phenotype of interest.

University of Ghana http://ugspace.ug.edu.gh

Biological meaning was distilled from our EVs modules of interest by using the gene sets as our *a priori* list for functional class scoring in the Gene Set Enrichment Analysis (GSEA) software (version 4.1.0) for enrichment analysis and gene ontology (GO) analysis (Subramanian et al., 2005). GSEA is a powerful analytical method for distilling biological meaning from gene expression datasets. Unlike traditional differentially expressed gene (DEG) and GO analysis pipelines, GSEA's discovery power is hinged on its use of gene sets instead of single gene units. Its approach to gene expression analysis keeps pace with the systems biology motif that biological phenomenon and/or phenotypes are results of multiple genes working in concert as opposed to the reductionist motif that assumes a single or few genes largely account for the biological phenomenon of interest (Bruggeman et al., 2007). It uses an *a priori* defined gene set(s) (we used EVs module of interest defined as sets of genes with correlated expression with known EVs biogenesis genes. These EVs modules of interest do not necessarily belong to the same biological pathway) to interrogate the ordered count data of an RNA sequencing experiment and outputs the gene set with significant association to the biological phenomenon of interest.

GSEA highlights the following deficiencies of the traditional DEG analysis pipeline and bypasses them. Traditional analysis approaches the problem of distilling meaning from the gene expression data set by focusing on a few genes that show the largest differences in expression. The over-representation analytical methods are seminal examples of this conventional approach. However, the sensitivity of this approach is stymied by the following problems: If the relevant gene(s) responsible for the biological phenomenon of interest do so by small changes in gene expression, then it will not be detected at all or will be detected with no statistical significance. On the other hand, this approach can output a tall list of statistically significant genes involved in a plethora of divergent biological processes. This lack of a unifying biological theme may make meaningful interpretation impossible.

University of Ghana http://ugspace.ug.edu.gh

Finally, precision has been reported to be a problem with the traditional gene expression approach as subsequent analysis by different groups, of the same data set, may yield strikingly discordant results (Subramanian et al., 2005). GSEA, as a functional class scoring method, is designed to overcome these challenges by inputting a gene set defined *a priori* and determining whether members of the gene set tend to occur at the top or bottom of the ordered list (or whether they are randomly distributed) of genes in the count data. If they do, then the gene set is associated with the phenotypic distinction used.

GSEA calculates three key elements: 1) the calculated enrichment score (ES) indexes the strength of the correlation between a gene set and the entire ranked list of count data. ES is calculated by walking down the ranked list of count data and assigning an increasing running-sum statistic when a gene in the gene set is encountered and decreasing the running-sum statistic when genes not in the gene set are encountered. The magnitude of the running-sum statistic depends on the strength of the gene set-phenotype correlation. Thus the ES is the maximum deviation from zero assigned during the random walk down the ranked count list and corresponds to a weighted Kolmogorov–Smirnov-like statistic (Subramanian et al., 2005) 2) the significance level of the calculated ES is estimated using an empirical phenotype-based permutation test and calculates the P-value of the ES. 3) adjustment is made for multiple testing and normalizes for variance in the gene sets used to yield the normalized ES (NES). Finally, the false discovery rate (FDR) (estimate of the probability that an NES represents a false positive finding) is calculated to control the proportion of false discoveries (Subramanian et al., 2005).

University of Ghana http://ugspace.ug.edu.gh

5.3.7 Identification of differentially expressed genes between conditions

The raw count data was fed into the DESeq2 R package (version 1.28.1) (Love et al., 2014) for the differential expression analysis. Following the generation of the DESEq2 object, the result function was used to generate the differentially expressed genes for each paired condition. This function uses a generalized linear model (GLM) to model the contribution of each gene to the conditions. This GLM is modelled using a discrete probability distribution such as negative binomial or Poisson's distribution. This is because RNA sequencing data is discrete count data and does not follow a normal distribution as negative integers are not expected. Then Wald's statistic and t-test (with p-value) are used to weight the contribution of each gene in the model as significant or insignificant.

5.3.8 Gene ontology analysis

Was done by uploading modules and DEG to PlasmoDB (https://plasmodb.org/plasmo/app, release 58) and using the site's GO pipeline for analysis. REVIGO was used to generate the GO summaries. REVIGO is a web server that summarizes the enriched gene functional categories lists of GO terms by finding a representative subset of the terms using a simple clustering algorithm that relies on semantic similarity measures (Supek et al., 2011).

University of Ghana http://ugspace.ug.edu.gh

5.4 Results

5.4.1 *P. falciparum* parasites susceptibility to DHA

We first used the RSA and IC50 assays, described earlier, to confirm the drug susceptibility of the parasite strains to DHA. The *in vitro* RSA was used to measure the susceptibility of the parasite lines to DHA. A read out of greater than 1% is indicative of resistance to ART. The RSA assay showed that C580R and R539T were ARTr, with median RSA survival rates of 3.5% (IQR, C580R = 3.25-3.75; IQR, R539T=3.5-4.05). Dd2 was artemisinin susceptible with a median survival rate of 0.5% (IQR, = 0.5 – 0.65) (Supplementary Figure 5.4). The IC50 assay measures the drug concentration at which 50% of parasites are killed by ART. Drug susceptibility by IC50 assay showed no statistically significant differences among the three parasite lines (p-value, Kruskal-Wallis test = 0.37). (Supplementary Figure 5.5).

5.4.2 Quality check for integrity of extracted RNA and mapped reads of samples analyzed

For each of the three parasite lines (Dd2, C580R and R539T), the following replicates were used for the three treatment conditions studied: four replicates per parasite line for the 700nM DHA condition, three replicates per parasite line for the 0.1% DMSO control condition and two replicates per parasite line for the untreated condition (Supplementary Table 5.1). Following ribonucleic acid (RNA) extraction, the quality of RNA was assessed using the RNA integration number (RIN) metric. RIN is determined, following bioanalyzer electrophoretic assay, by the ratio of the 18s and 28s ribosomal peaks to the total area under the curve. Most of the RNA extracted from samples was of good quality (Supplementary Figure 5.6). The overall mapping quality across all samples was good.

University of Ghana http://ugspace.ug.edu.gh

The mapping depth (mean read counts per sample) was 3035536.93, and reads were mapped to at least 5000 genes for each of the samples. External RNA Controls Consortium (ERCC) spike-in control levels were similar across all samples. ERCC helps control for variation in RNA expression data arising from factors such as RNA quality and yield and sequencing errors (Tong et al., 2016) (Supplementary Figure 5.7).

Lowly expressed genes (minimum count = 10) and samples with less than 70% of genes expressed were filtered out (997 features removed) after data pre-processing and normalization using DaMiRseq (Chiesa et al., 2018). Finally, two surrogate variables (Sv) that explained 95% of the variance in the data set were identified and adjusted for in the data. Sv's are covariates generated from high-dimensional data and used to adjust for hidden sources of variation. The DaMiR.corrplot function produced a correlation plot where significant correlations (significance level = 0.01) are shown within colored circles (blue or red gradient). As expected, the correlation between class, and the other covariates, was not significant (Supplementary Figure 5.8). Overall variation in relative log expression across samples was identical and the effect of surrogate variables on the count data set was adjusted (Supplementary Figure 5.9).

5.4.3 A module of EVs interest is associated with ART resistance in *P. falciparum*

The transcript count data was fed into the R package, WGCNA (Langfelder et al., 2008) to generate modules made up of gene transcripts with correlated expression profiles. Seventeen modules were then selected based on the statistical significance (adjusted p-value < 0.05) of their expression profile correlation. Gene transcripts were converted to gene identities for each of these seventeen modules (Supplementary Table 5.2).

University of Ghana http://ugspace.ug.edu.gh

As relatively little is known about EVs biogenesis in *P. falciparum* biology, we approached the problem of determining whether the transcript profile of ART-resistant *P. falciparum* is associated with EVs biogenesis by defining EVs biogenesis modules. Four modules (modules 0, 1, 3 and 17) contained our genes of interest implicated in the biogenesis and export of EVs (Table 5.1, Supplementary Table 5.2) (Regev-Rudzki et al., 2013; Avalos-Padilla et al., 2021). We refer to these modules as our modules of EVs interest and they comprise genes with correlated expression to known genes in the *P. falciparum* EVs biogenesis pathway (Table 5.1).

Module 0 comprised 693 genes (Supplementary Table 5.2) and showed differences in expression between treatment conditions (0.05 < p-value < 0.1) (Figure 5.1). GO analysis using the online PlasmoDB (https://plasmodb.org/plasmo/app) and REVIGO (http://revigo.irb.hr) platform (Supek et al., 2011) showed enrichment for biological processes related to vesicle-mediated transport (p-value = 0.00327114166063; adjusted p-value = 0.474821139088) (Figure 5.1 and Supplementary Table 5.3). Modules 1 (ME1), 3 (ME3) and 17 (ME17) were made of 1119, 363 and 67 genes respectively (Supplementary Table 5.2) and showed differences in expression between treatment conditions (0.05 < p-value < 0.1). GO analysis showed enrichment for translation and proteasomal ubiquitin-independent protein catabolic process in ME3 and cell cycle, nuclear chromosome segregation processes and phosphatidylinositol-3-phosphate biosynthetic process in ME17 (Supplementary Figures 5.10 – 5.12; Supplementary Tables 5.4 – 5.6).

University of Ghana http://ugspace.ug.edu.gh

Table 5.1 Genes of interest (GOI) involved in the biogenesis and export of extracellular vesicles, (EVs) in *P. falciparum*. GOI were identified by review of the literature on EVs in *P. falciparum*. The module of EVs interest was determined using the weighted correlation network analysis (WGCNA) R package by first generating modules of genes with statistically significant correlated expression across all samples (p-value < 0.05) and then identifying the modules containing the GOI.

Gene of interest	Protein ID	Alternative name	Literature source	The module of EVs interest
PF3D7_1224200	CZT99401	*PfBRO1*	(Avalos-Padilla et al., 2021)	Not found
PF3D7_1243500	CZT99591	*PfVps32*		ME 1*
PF3D7_1441800	CZU00114	*PfVps60*		ME0
PF3D7_0816200	CAD51211	*PfVps2*		ME0
PF3D7_0906100	CAD51746	*PfVps46*		ME3*
PF3D7_1121600	CZT98878	*PfPTP*	(Regev-Rudzki et al., 2013)	ME17**

*0.05 < p-value < 0.1

** p-value < 0.05

P-values were determined by comparing the module of EVs interest expression among the various treatment conditions of the parasite lines using the Kruskal-Wallis test.

University of Ghana http://ugspace.ug.edu.gh

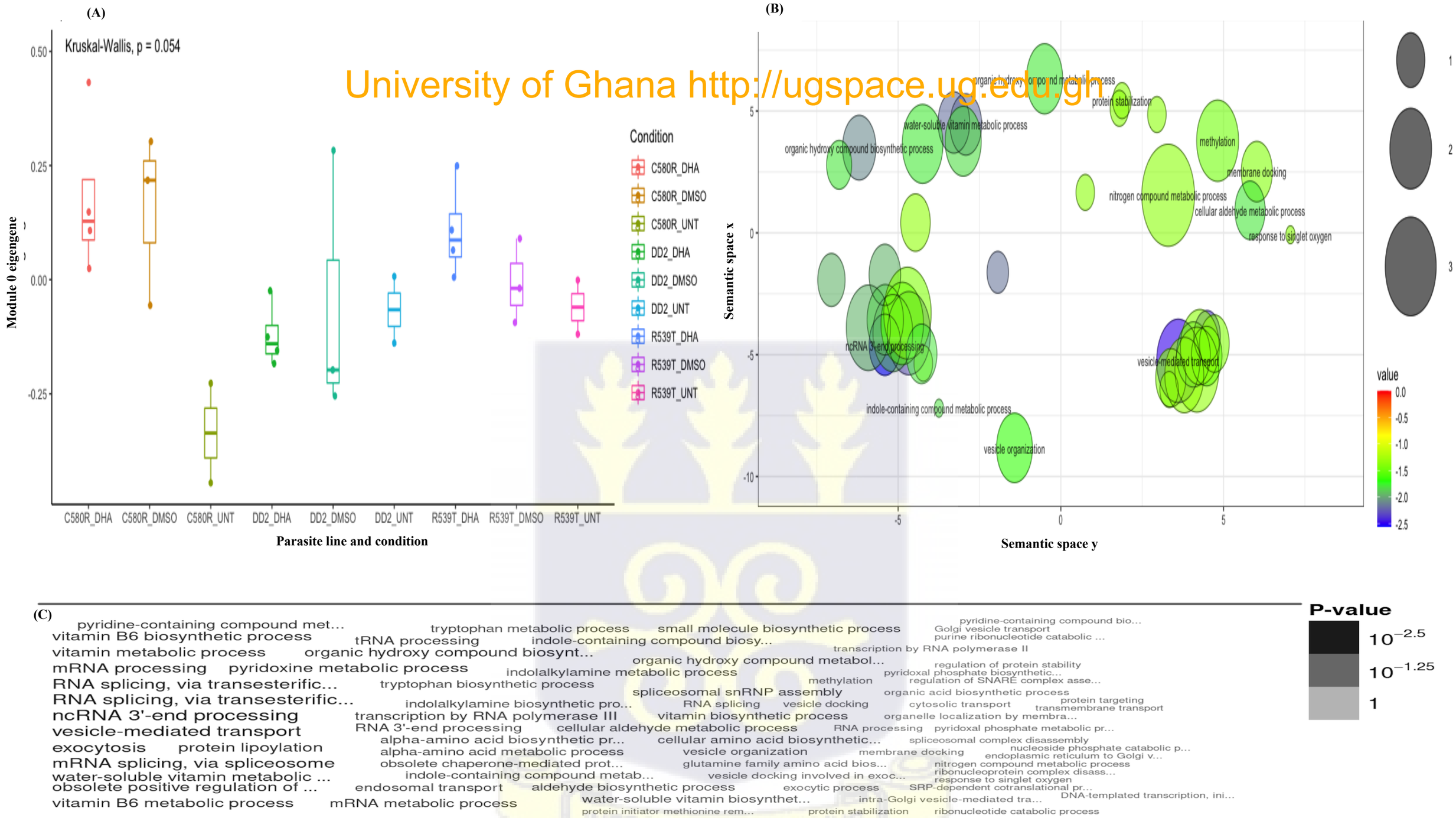

Figure 5.1 Properties of EVs module of interest module 0 (ME0). ME0 was uploaded to Plasmodb (https://plasmodb.org/plasmo/app) and analyzed with the platform's gene ontology (GO) pipeline. A) Comparison of ME0 between the three treatment conditions pooled for all parasite lines (Dd2, C580R and R539T). The Kruskal-Wallis test was used to determine the statistical significance of the difference in expression of ME0 among the conditions (0.05 < p-value < 0.1). B) GO (biological processes) output for ME0 summarized using REVIGO (http://revigo.irb.hr) scatterplot visualization option. Each circle denotes the representative cluster of the GO biological process associated with the ARTr phenotype and is derived by multidimensional scaling and redundancy reduction of the GO sematic similarities. The size of the circles denote the frequency of the GO term in the *P. falciparum* GO database (updated in November 2021) with larger circles denoting more general terms. The colors (red to blue range) indicate the statistical significance of the association's strength. "Vesicle-mediated transport" was one of the biological processes enriched C) Word cloud summary of the GO biological processes associated with the ARTr phenotype. EVs – extracellular vesicles, ARTr – artemisinin resistant

University of Ghana http://ugspace.ug.edu.gh

Next, we used the functional class scoring GSEA version 4.1.0 software (Subramanian et al., 2005) in a TMPAS analysis to determine the association of each of the 17 modules (including the four EVs modules of interest) with the ARTr phenotype. We leveraged on the ability of this method to determine even a small association of our modules (in particular our EVs modules of interest) with the ART resistance phenotype of interest. GSEA requires 3 files as input: a phenotype data file, a gene set file, and an expression data file (https://www.gsea-msigdb.org/gsea/doc/GSEAUserGuideFrame.html). Phenotype data was generated from Supplementary Table 1 and formatted in the categorical class format (*.cls). Supplementary Table 2 was formatted in the gene matrix file format (*.gmx) to generate the gene set file. Finally, we entered a normalized and *vst* transformed (using DESeq2 version 1.28.1) count matrix with gene expression ranked according to their correlation with the ART resistance phenotype of interest as our expression data set or gene list. The expression data set was formatted in gene cluster text file format (*.gct).

GSEA determines whether members of our modules are randomly distributed throughout the expression data or are differentially found at the top or bottom (indicative of association to ARTr). An enrichment score (ES) is calculated for each module that captures the strength of its association with the ARTr phenotype. The ES is calculated by the GSEA program and reflects the maximum deviation from zero in its random walk through the ranked genome-wide expression list. The ES corresponds to a weighted Kolmogorov–Smirnov-like statistic. GSEA also estimates the statistical significance of the association using an empirical phenotype-based permutation test procedure and corrects for the varied sizes of the modules of interest and multiple hypothesis testing by calculating the normalized enrichment score (NES) and false discovery rate (FDR), respectively (Subramanian et al., 2005). GSEA returns the strength of the association between each module of interest and the ART resistance phenotype.

University of Ghana http://ugspace.ug.edu.gh

We identified module 0 (containing the EVs biogenesis genes PF3D7_1441800 and PF3D7_0816200) (Table 1) and module 7 as associated with the ARTr phenotype in *P. falciparum* (Table 2).

Module 0 was significantly upregulated in the DHA-treated condition in both ARTr (C580R and R539T) and ART sensitive (Dd2) parasite lines for the DHA-treated versus untreated condition. For the condition DHA treated versus DMSO-treated, module 0 was upregulated in the DMSO-treated condition for R539T and Dd2 parasite lines, and in the DHA-treated condition for C580R line. Comparison of the Dd2_DHA_treated condition with C580R_DHA_treated and R539T_DHA_treated treatment conditions showed that module 0 was upregulated in the C580R_DHA_treated condition and the Dd2_DHA_treatment conditions respectively. (Table 2, Figure 2, Supplementary Data 1 - 8).

Module 7 comprised 182 genes (Supplementary Table 2) and showed differences in expression between treatment conditions which were not statistically significant (p-value = 0.3606) (Figure 5.3). GO analysis using the online PlasmoDB (https://plasmodb.org/plasmo/app, release 58) and REVIGO (http://revigo.irb.hr) platform (Supek et al., 2011) showed enrichment for biological processes related to modulation by symbiont of host erythrocyte aggregation (adjusted p-value = 1.17×10^{-70}) (Figure 5.3 and Supplementary Table 5.7). Module 7 was significantly upregulated in the untreated condition for both ARTr (C580R and R539T) and ART sensitive (Dd2) parasite lines for the DHA-treated versus untreated condition. For the condition DHA treated versus DMSO-treated, module 7 was upregulated in the DMSO-treated condition for R539T and Dd2 parasite lines, and in the DHA-treated condition for C580R line. Comparison of the Dd2_DHA_treated condition with C580R_DHA_treated and R539T_DHA_treated treatment conditions showed that module 7 was upregulated in the R539T_DHA_treated and the C580R_DHA_treated conditions. (Table 5.2, Figure 5.4, Supplementary Data 5.9 – 5.16).

University of Ghana http://ugspace.ug.edu.gh

Table 5.2 Association of modules with the ARTr phenotype. Only 2 out of the 17 modules tested – modules 0 and 7- were associated with the ARTr phenotype. Module 0 is an EVs module of interest comprising 693 genes with correlated expression with the PF3D7_1441800 gene (*PfVps60*) involved in EVs biogenesis in *P. falciparum*. Module 7 is made up of 182 genes. The normalized enrichment score (NES) is calculated by normalizing the enrichment score for gene set size and represents the association of the modules with the treatment conditions compared. A positive NES indicates module enrichment and association with the first treatment condition and a negative NES indicates module enrichment and association with the second treatment condition. The higher the NES the stronger the association with the module. The false discovery rate (FDR) was used to correct multiple testing. Statistical significance was designated at an FDR q-value < 0.25. Module 0 was significantly upregulated in the DHA-treated condition for both ARTr (C580R and R539T) and ART sensitive (Dd2) parasite lines for the DHA-treated versus untreated condition. For the condition DHA-treated versus DMSO-treated, module 0 was upregulated in the DMSO-treated condition for R539T and Dd2 parasite lines, and in the DHA-treated condition for C580R line. Comparison of the Dd2_DHA_treated condition with C580R_DHA_treated and R539T_DHA_treated treatment conditions showed that module 0 was upregulated in the C580R_DHA_treated condition and the Dd2_DHA_treatment conditions respectively. Module 7 was significantly upregulated in the untreated condition for both ARTr (C580R and R539T) and ART sensitive (Dd2) parasite lines for the DHA-treated versus untreated condition. For the condition DHA treated versus DMSO-treated, module 7 was upregulated in the DMSO-treated condition for R539T and Dd2 parasite lines, and in the DHA-treated condition for C580R line. Comparison of the Dd2_DHA_treated condition with C580R_DHA_treated and R539T_DHA_treated treatment conditions showed that module 7 was upregulated in the R539T _DHA_treated and the C580R_DHA_treated conditions.

Treatment conditions compared	Module	Upregulated in condition	Normalized enrichment score (NES)	False discovery rate q-value
R539T_DHA_treated versus R539T_untreated	**Module 0**	**R539T_DHA_treated**	**1.1830174**	**0.23794872***
	Module 7	**R539T_untreated**	**-1.2690192**	**0.14516129***
R539T_DHA_treated versus R539T_DMSO_treated	Module 0	R539T_DMSO_treated	-0.78877187	0.859322
	Module 7	R539T_DMSO_treated	1.141659	0.43728814
R539T _DHA_treated versus Dd2_DHA_treated	Module 0	Dd2_DHA_treated	-1.1220989	0.28233033
	Module 7	R539T _DHA_treated	0.6829786	0.9447514
C580R_DHA_treated versus C580R_untreated	**Module 0**	**C580R_DHA_treated**	**1.2457103**	**0.14403293 ***
	Module 7	**C580R_untreated**	**-2.4335837**	**0.0***
C580R_DHA_treated versus C580R_DMSO_treated	Module 0	C580R_DHA_treated	0.7299921	0.891
	Module 7	C580R_DHA_treated	1.2448145	0.253
C580R_DHA_treated versus Dd2_DHA_treated	Module 0	C580R_DHA_treated	1.0806667	0.35456595
	Module 7	C580R_DHA_treated	1.088161	0.686584
Dd2_DHA_treated versus Dd2_untreated	**Module 0**	**Dd2_DHA_treated**	**1.1802711**	**0.22940503***
	Module 7	**Dd2_untreated**	**-2.2366247**	**0.0***
Dd2_DHA_treated versus Dd2_DMSO_treated	Module 0	Dd2_DMSO_treated	-1.1928045	0.33333334
	Module 7	Dd2_DMSO_treated	-0.9836254	0.51960784

University of Ghana http://ugspace.ug.edu.gh

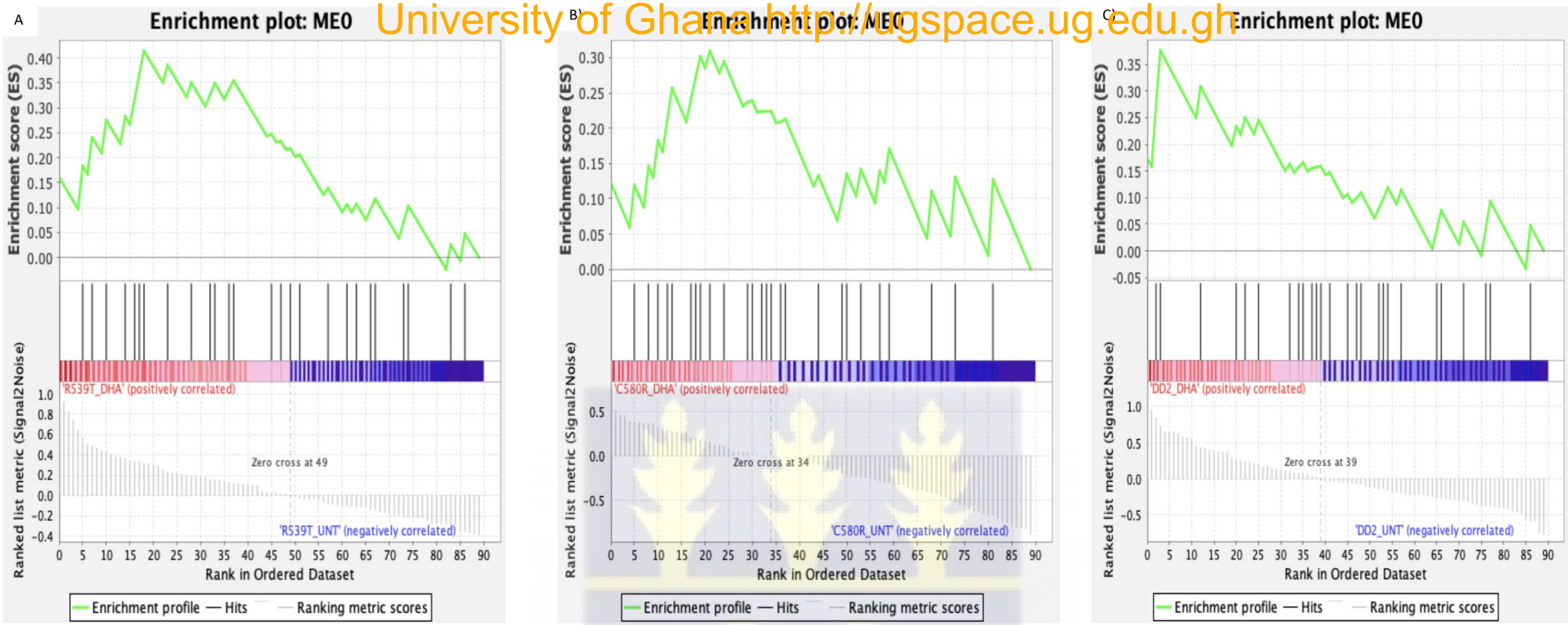

Figure 5.2 Enrichment score behavior showing the distribution of module 0 (ME0) in the input list of ranked genes for the three compared treatment conditions with FDR q-value < 0.25. Module 0 is the EVs module of interest comprising 693 genes with correlated expression with the PF3D7_1441800 gene (PfVps60) and PF3D7_0816200 (PfVps2) involved in EVs biogenesis in *P. falciparum*. The enrichment plots were generated by GSEA. Enrichment scores (ES) were calculated by strolling down the input list of ranked genes, increasing a running-sum statistic when a gene is in ME0 and decreasing it when it is not. The magnitude of the increment depends on the correlation of the gene with the treatment condition. The ES is the maximum deviation from zero encountered in walking the list. The normalized enrichment score (NES) is calculated by normalizing the enrichment score for gene set size and represents the association of the modules with the treatment conditions compared. A positive NES indicates module enrichment and association with the first treatment condition. The higher the NES the stronger the association with the module. The false discovery rate (FDR) was used to correct multiple testing. Statistical significance was designated at a FDR q-value < 0.25.

A) R539T_DHA_treated versus R539T_untreated condition; ME0 was upregulated in the R539T_DHA_treated condition (NES = 1.18, FDR q-value = 0.24)

B) C580R_DHA_treated versus C580R_untreated; ME0 was upregulated in the C580R_DHA_treated condition (NES = 1.25, FDR q-value = 0.14)

C) Dd2_DHA_treated versus Dd2_untreated; ME0 was upregulated in the Dd2_DHA_treated condition (NES = 1.18, FDR = 0.23)

ME0- module 0; ES - enrichment score; NES – normalized enrichment score; FDR - False discovery rate; GSEA – gene set enrichment analysis

University of Ghana http://ugspace.ug.edu.gh

5.4.4 Analysis of differentially expressed genes reveals little insight into the role of EVs in *P. falciparum*

Next, we employed the traditional differentially expressed genes (DEGs) analysis pipeline to explore our research question of whether EVs play a role in the ARTr phenotype. DEGs were identified as genes with a log2 fold expression change > 2 (translating into more than a fourfold difference) and with a p-value < 0.05. For each DEGs list, gene ontology analysis for biological pathway enrichment was done using the online platforms PlasmoDB (https://plasmodb.org/plasmo/app, release 58) and REVIGO (Supek et al., 2011).

Comparison of the treatment condition R539T_DMSO_treated versus R539T _DHA treated identified 2 upregulated genes and 15 downregulated genes (Figure 5.5A and Supplementary Table 5.8). Gene ontology enrichment analysis showed upregulation of molecular function, under DHA_treated condition, related to acyl-CoA binding, fatty-acyl-CoA binding, and fatty acid derivative binding; and downregulation of molecular function related to cholesterol binding (Table 5.3, Supplementary Table 5.9). Comparison of the treatment condition R539T_untreated versus R539T_DHA_treated identified 70 upregulated genes and 217 downregulated genes (Figure 5.5B and Supplementary Table 5.10). Gene ontology enrichment analysis showed downregulation of 18 biological processes, under DHA_treated condition, related to movement and entry into host environment, and downregulation of cellular components related to apical complex, extracellular vesicle, and extracellular membrane-bound organelle (Table 5.3, Supplementary Table 5.11).

University of Ghana http://ugspace.ug.edu.gh

Comparison of the treatment condition C580R_DMSO_treated versus C580R_DHA treated identified one upregulated gene and 21 downregulated genes (Figure 5.6A and Supplementary Table 5.12). Gene ontology enrichment analysis showed downregulation of molecular function, under DHA_treated condition, related to response to heat, temperature, and abiotic stimulus; and of cellular components related to the host (Table 5.3, Supplementary Table 5.13). Comparison of the treatment condition C580R_untreated versus C580R_DHA treated identified 150 upregulated genes and 269 downregulated genes (Figure 5.6B and Supplementary Table 5.14). Gene ontology enrichment analysis showed upregulation of biological processes, under DHA_treated condition, related to cytoadherence to the host microvasculature and antigenic variation; and downregulation of biological processes related to movement and entry into host environment. It also showed downregulation of cellular components related to apical complex, extracellular vesicle, and extracellular membrane-bound organelle (Table 5.3, Supplementary Table 5.15).

Comparison of the treatment condition Dd2_DMSO treated versus Dd2_DHA treated identified 13 upregulated genes and 55 downregulated genes (Figure 5.7A and Supplementary Table 5.16). Gene ontology enrichment analysis showed downregulation, under DHA_treated condition, of biological processes related to chaperone cofactor-dependent protein refolding, '*de novo*' posttranslational protein folding and chaperone-mediated protein folding (Table 5.3, Supplementary Table 5.17). Comparison of the treatment condition Dd2_untreated versus Dd2_DHA treated identified 403 upregulated genes and 247 downregulated genes (Figure 5.7B and Supplementary Table 5.18). Gene ontology enrichment analysis showed under downregulation, under DHA_treated condition, of biological processes related to entry and movement into host; and downregulation of cellular components related to apical complex, extracellular vesicle, and extracellular membrane-bound organelle (Table 5.3, Supplementary Table 5.19).

University of Ghana http://ugspace.ug.edu.gh

In summary, the largest number of DEGs were found in the DHA treatment condition, when compared to the untreated condition baseline, and was associated with an upregulation of 70 and 150 genes and down regulation of 217 and 269 genes in the ARTr parasite lines R539T and C580R respectively. DHA treatment, in the ART sensitive Dd2 parasite line, was associated with 247 unregulated genes and 403 down regulated genes (Table 5.3, Supplementary Tables 5.10 -5.19, Supplementary Data 5.17).

University of Ghana http://ugspace.ug.edu.gh

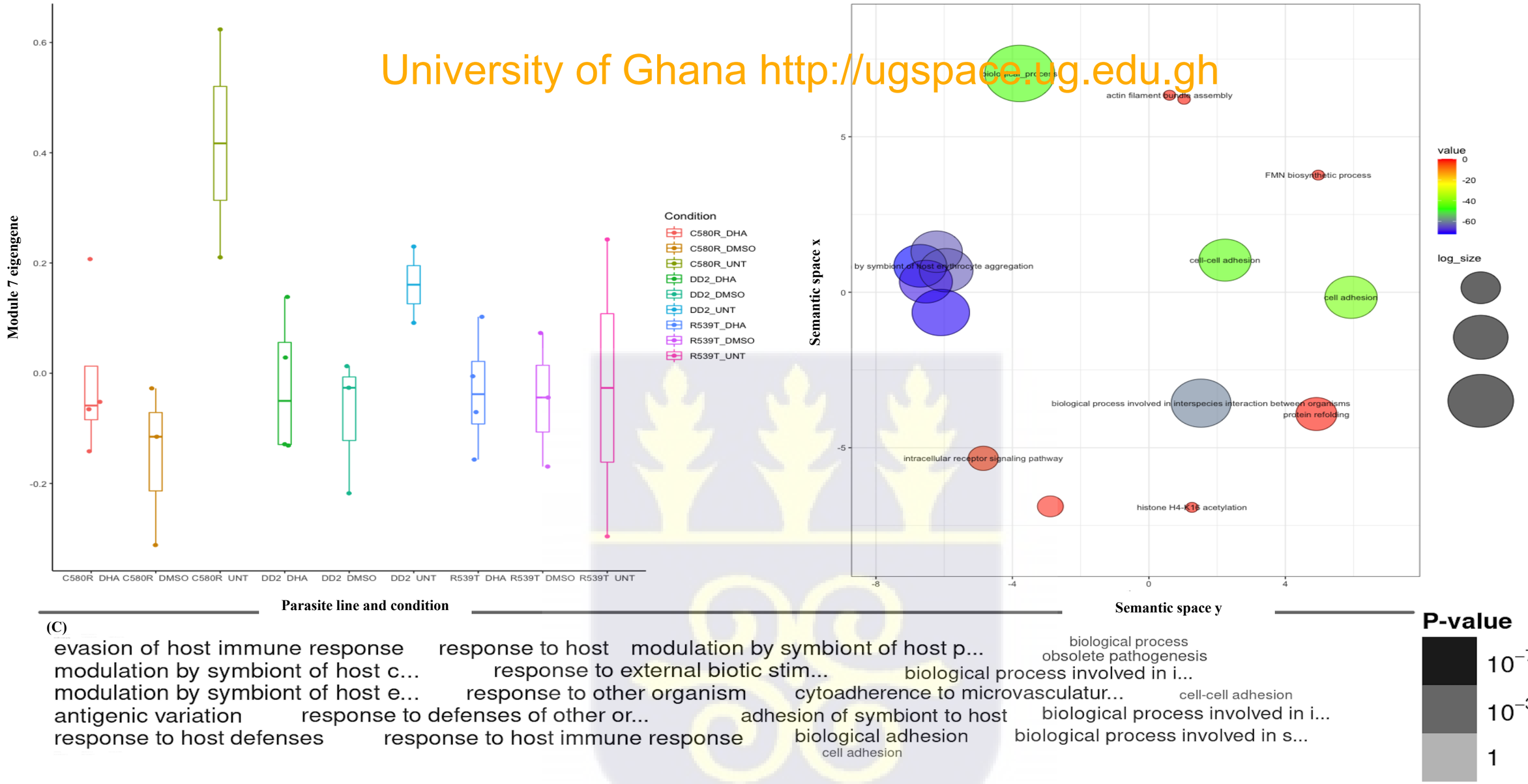

Figure 5.3 Properties of EVs module 7 (ME7). ME7 was uploaded to Plasmodb (https://plasmodb.org/plasmo/app) and analyzed with the platform's gene ontology (GO) pipeline. A) Comparison of ME1 between the three treatment conditions pooled for all parasite lines (Dd2, C580R and R539T). The Kruskal-Wallis test was used to determine the statistical significance of the difference in expression of ME7 among the conditions (p-value = 0.3606). B) GO (biological processes) output for ME7 summarized using REVIGO (http://revigo.irb.hr) scatterplot visualization option. Each circle denotes the representative cluster of the GO biological process associated with the ARTr phenotype and is derived by multidimensional scaling and redundancy reduction of the GO sematic similarities. The size of the circles denote the frequency of the GO term in the *P. falciparum* GO database (updated in November 2021) with larger circles denoting more general terms. The colors (red to blue range) indicate the statistical significance of the association's strength. "modulation by symbiont of host erythrocyte aggregation" was one of the biological processes enriched C) Word cloud summary of the GO biological processes associated with the ARTr phenotype. EVs – extracellular vesicles, ARTr – artemisinin resistant

University of Ghana http://ugspace.ug.edu.gh

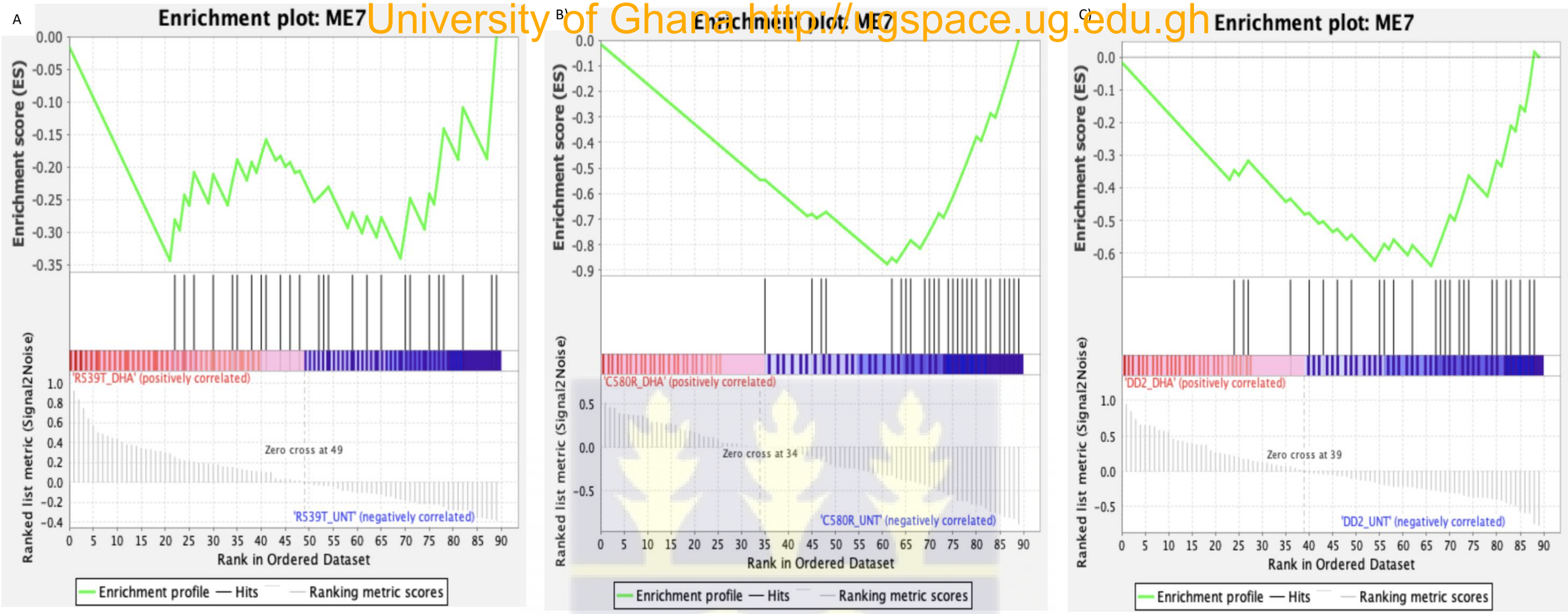

Figure 5.4 Enrichment score behavior showing the distribution of module 7 (ME7) in the input list of ranked genes for the three compared treatment conditions with FDR q-value < 0.25. Module 7 comprises 182 genes with correlated expression in *P. falciparum*. The enrichment plots were generated by GSEA. Enrichment scores (ES) were calculated by strolling down the input list of ranked of genes, increasing a running-sum statistic when a gene is in ME7 and decreasing it when it is not. The magnitude of the increment depends on the correlation of the gene with the treatment condition. The ES is the maximum deviation from zero encountered in walking the list. The normalized enrichment score (NES) is calculated by normalizing the enrichment score for gene set size and represents the association of the modules with the treatment conditions compared. A positive NES indicates module enrichment and association with the first treatment condition and a negative NES indicates module enrichment and association with the second treatment condition. The higher the NES the stronger the association with the module. The false discovery rate (FDR) was used to correct multiple testing. Statistical significance was designated at a FDR q-value < 0.25.

A) R539T_DHA_treated versus R539T_untreated condition; ME7 was upregulated in the R539T_untreated condition (NES = -1.27, FDR q-value = 0.15)

B) C580R_DHA_treated versus C580R_untreated; ME7 was upregulated in the C580R_DHA_treated condition (NES = -2.43, FDR q-value = 0.0)

C) Dd2_DHA_treated versus Dd2_untreated; ME7 was upregulated in the Dd2_untreated condition (NES = -2.24, FDR = 0.0)

ME7- module 7; ES - enrichment score; NES – normalized enrichment score; FDR - False discovery rate; GSEA – gene set enrichment analysis

University of Ghana http://ugspace.ug.edu.gh

Table 5.3 Summary of gene ontology enrichment analysis of differentially expressed genes, identified a number of significantly enriched (bonferroni adjusted p-value < 0.05) biological processes, molecular function and cellular components among the up/down-regulated genes of the compared treatment conditions.

Parasite Line	Treatment conditions compared	Number of genes (up/down-regulated)	Number upregulated in DHA_treated condition			Number down-regulated in DHA_treated condition		
			Biological process	Molecular function	Cellular component	Biological process	Molecular function	Cellular component
R539T	R539T_DHA_treated versus R539T_DMSO_treated	2/15	0	4	0	0	1	0
	R539T_DHA_treated versus R539T_untreated	70/217	0	0	1	18	7	29
C580R	C580R_DHA_treated versus C580R_DMSO_treated	1/21	0	0	0	3	0	2
	C580R_DHA_treated versus C580R_untreated	150/269	20	3	12	21	11	41
Dd2	Dd2_DHA_treated versus Dd2_DMSO_treated	13/55	0	0	0	6	0	10
	Dd2_DHA_treated versus Dd2_untreated	247/403	0	0	2	14	11	30

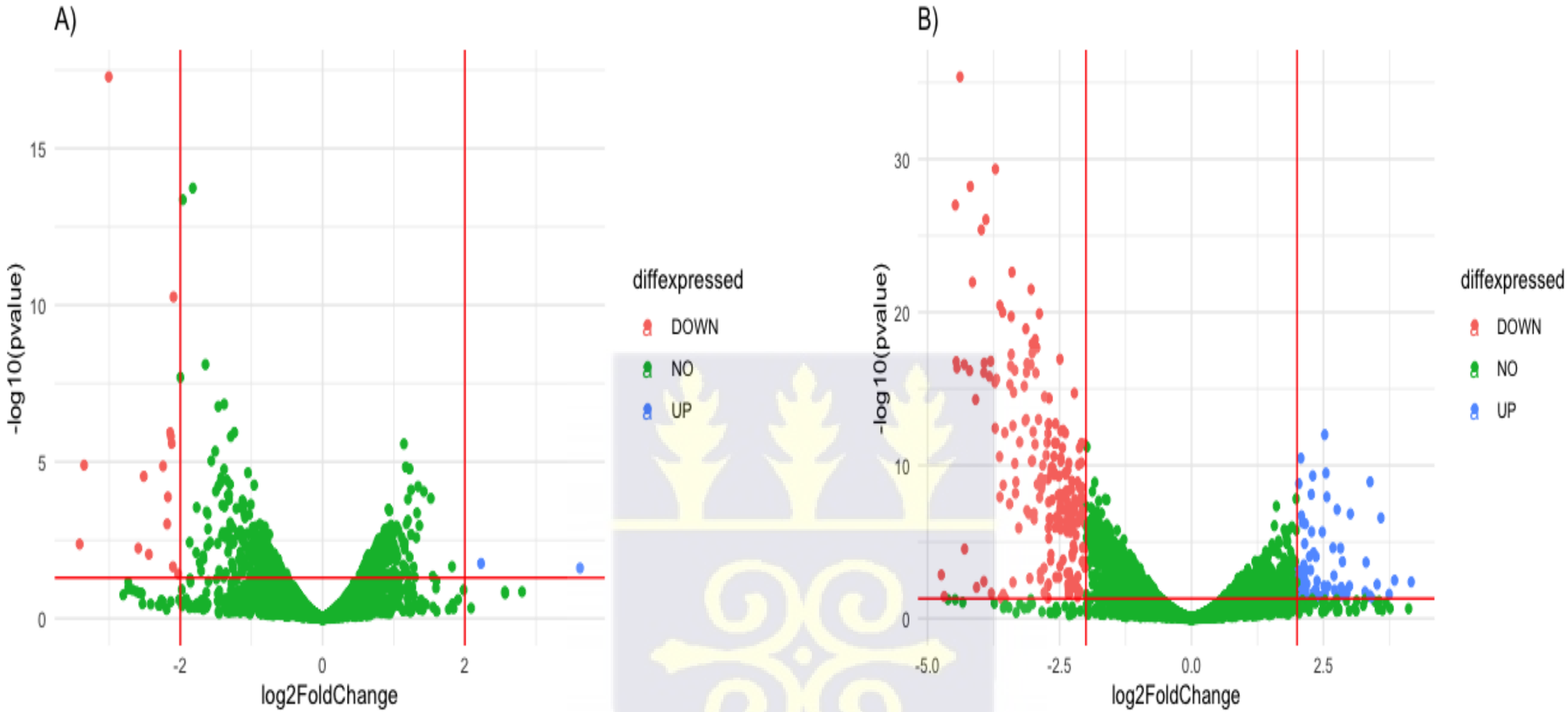

Figure 5.5 Differentially expressed genes (DEG) between compared conditions for the R539T parasite line. Scatter plots indicate the genes differentially expressed (log2 fold expression change > 2 and with a p-value < 0.05). Red vertical lines indicate absolute log2 fold change >2 and red horizontal line indicates p-value < 0.05. A) Volcano plot for R539T_DMSO treated versus R539T_DHA treated; 15 genes were downregulated and 2 genes upregulated B) Volcano plot for R539T_untreated compared with R539T_DHA; 70 genes upregulated and 217 genes were downregulated

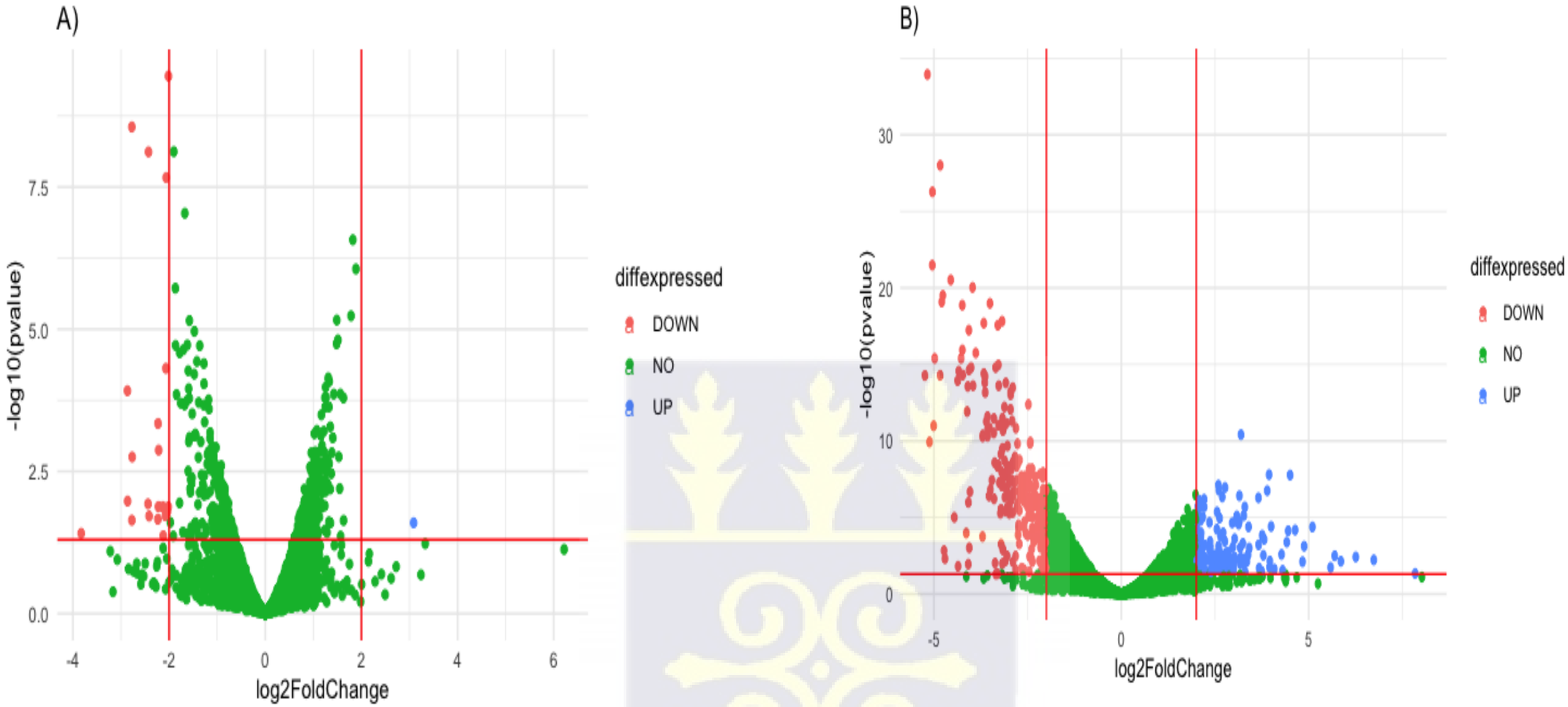

Figure 5.6 Differentially expressed genes (DEG) between compared conditions for the C580R parasite line. Scatter plots indicate the genes differentially expressed (log2 fold expression change > 2 and with a p-value < 0.05). Red vertical lines indicate absolute log2 fold change >2 and red horizontal line indicates p-value < 0.05. A) Volcano plot for C580R_DMSO treated versus C580R_DHA treated. One gene was upregulated, and 21 genes were downregulated. B) Volcano plot for C580R_untreated compared with C580R_DHA. 150 genes were upregulated, and 269 genes were downregulated genes.

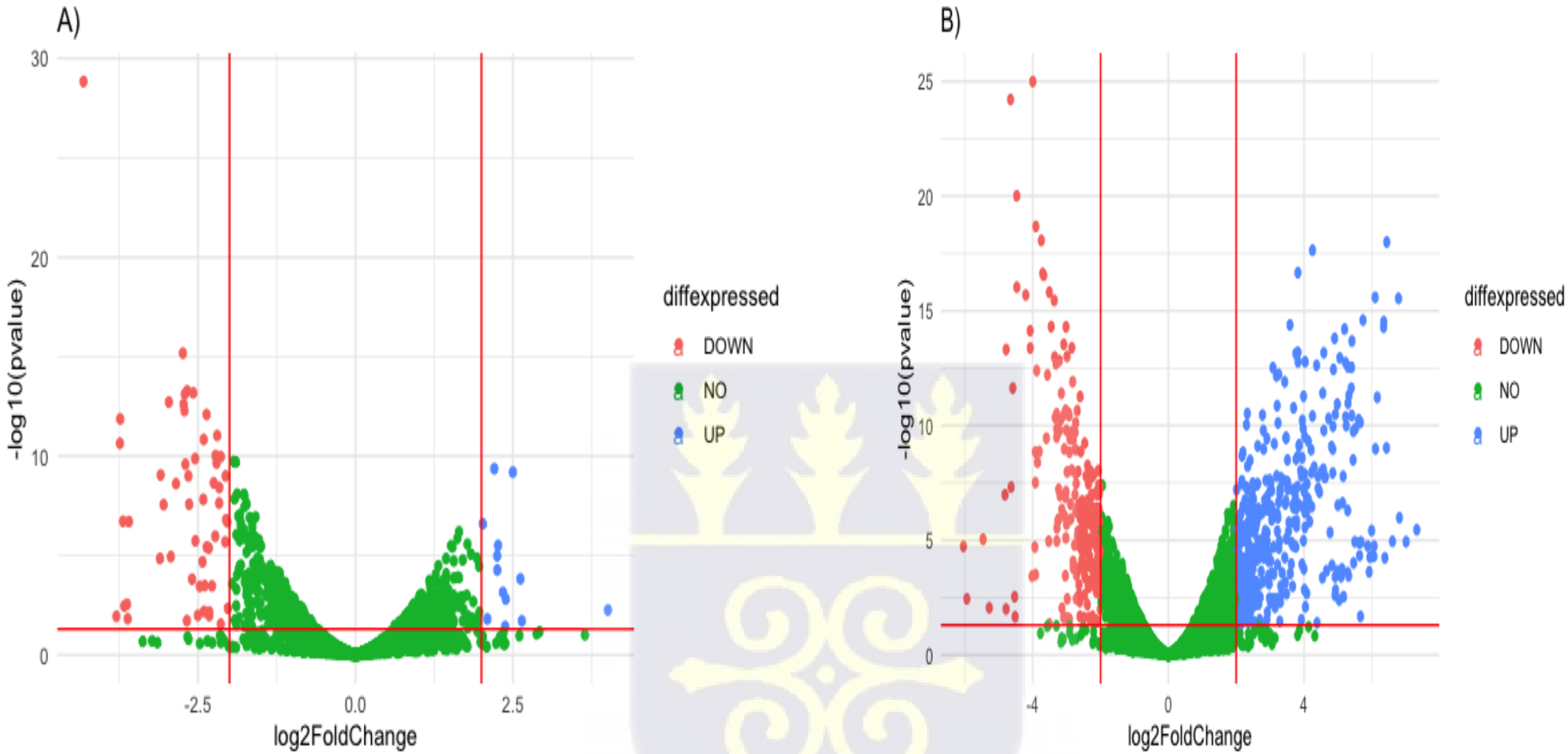

Figure 5.7 Differentially expressed genes (DEG) between compared conditions for the Dd2 parasite line. Scatter plots indicate the genes differentially expressed (log2 fold expression change > 2 and with a p-value < 0.05). Red vertical lines indicate absolute log2 fold change >2 and red horizontal line indicates p-value < 0.05. A) Volcano plot for Dd2_DMSO treated versus Dd2_DHA treated; 13 genes were upregulated, and 55 genes were downregulated B) Volcano plot for Dd2_untreated compared with Dd2_DHA; 403 genes were upregulated and 247 downregulated genes

5.4.5 A complex heterogeneous transcript profile characterizes *P. falciparum* ARTr parasites

University of Ghana http://ugspace.ug.edu.gh

Against the backdrop of the known heterogeneity in the ARTr phenotype (Siddiqui et al., 2021), we compared the gene expression profile between the two ARTr parasite lines (C580R and R539T) for the paired conditions of untreated versus DHA treated and DMSO treated versus DHA treated to determine whether the gene expression profiles were heterogeneous too. We expected that, given the ARTr phenotype heterogeneity, the gene expression profiles between the C580R and R539T parasite lines will not be well correlated. For the condition – DMSO versus DHA treated, between the ARTr parasite lines C580R and R539T the Spearman correlation coefficient was $\rho = 0.6$, p-value $< 2.2 \times 10^{-16}$ (Figure 5.8A). For the condition – untreated versus DHA treated, between the ARTr parasite lines C580R and R539T the Spearman correlation coefficient was $\rho = 0.79$, p-value $< 2.2 \times 10^{-16}$ (Figure 5.8B). This showed that the expression profile of ARTr parasite lines was poorly correlated and hinted at a transcriptionally heterogeneous ARTr parasite population. Additionally, this discordance in gene expression profile was further highlighted by principal component analysis (PCA) using- *vst* transformed data as input- for both ARTr parasite strains under DHA and DMSO treatment conditions, as only untreated ARTr samples clustered together (Figure 5.9). The presence of multiple clusters of ARTr parasite strains under DHA and DMSO treatment conditions adds to evidence for a complex heterogeneous transcript profile undergirding the known heterogeneity of the ARTr phenotype.

University of Ghana http://ugspace.ug.edu.gh

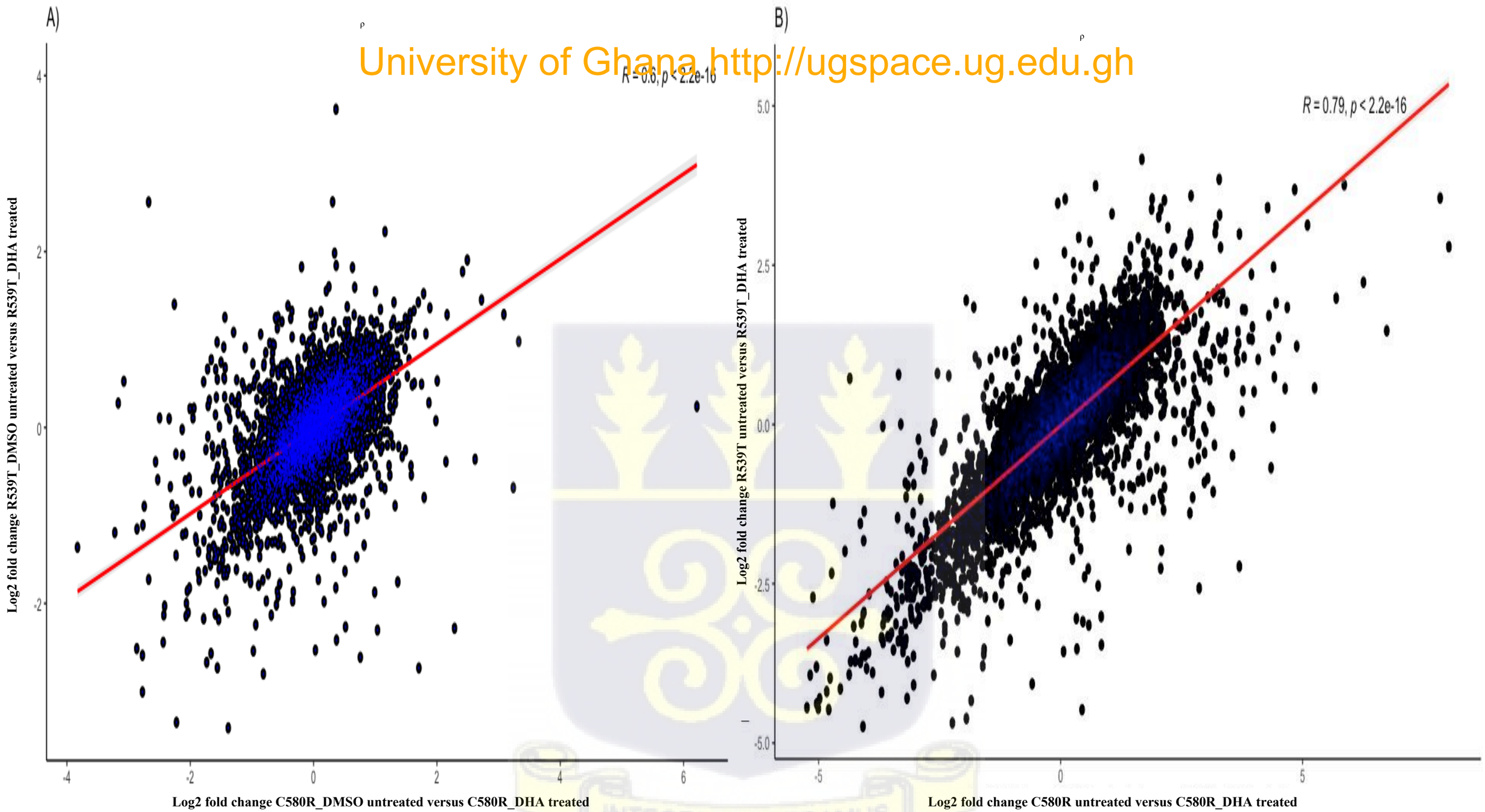

Figure 5. 8 Scatter plots showing the strength of the correlation between the two ARTr biological replicates (C580R and R539T) for the compared conditions: A) DMSO_treated versus DHA_treated and B) untreated versus DHA_treated. The analysis explored the underlying heterogeneity in the gene expression profile between C580R and R539T and shows poor to moderate correlation in gene expression profile. The spearman rank correlation plot was constructed using the log2 fold change values between the compared conditions. ρ is the Spearman coefficient of correlation.

University of Ghana http://ugspace.ug.edu.gh

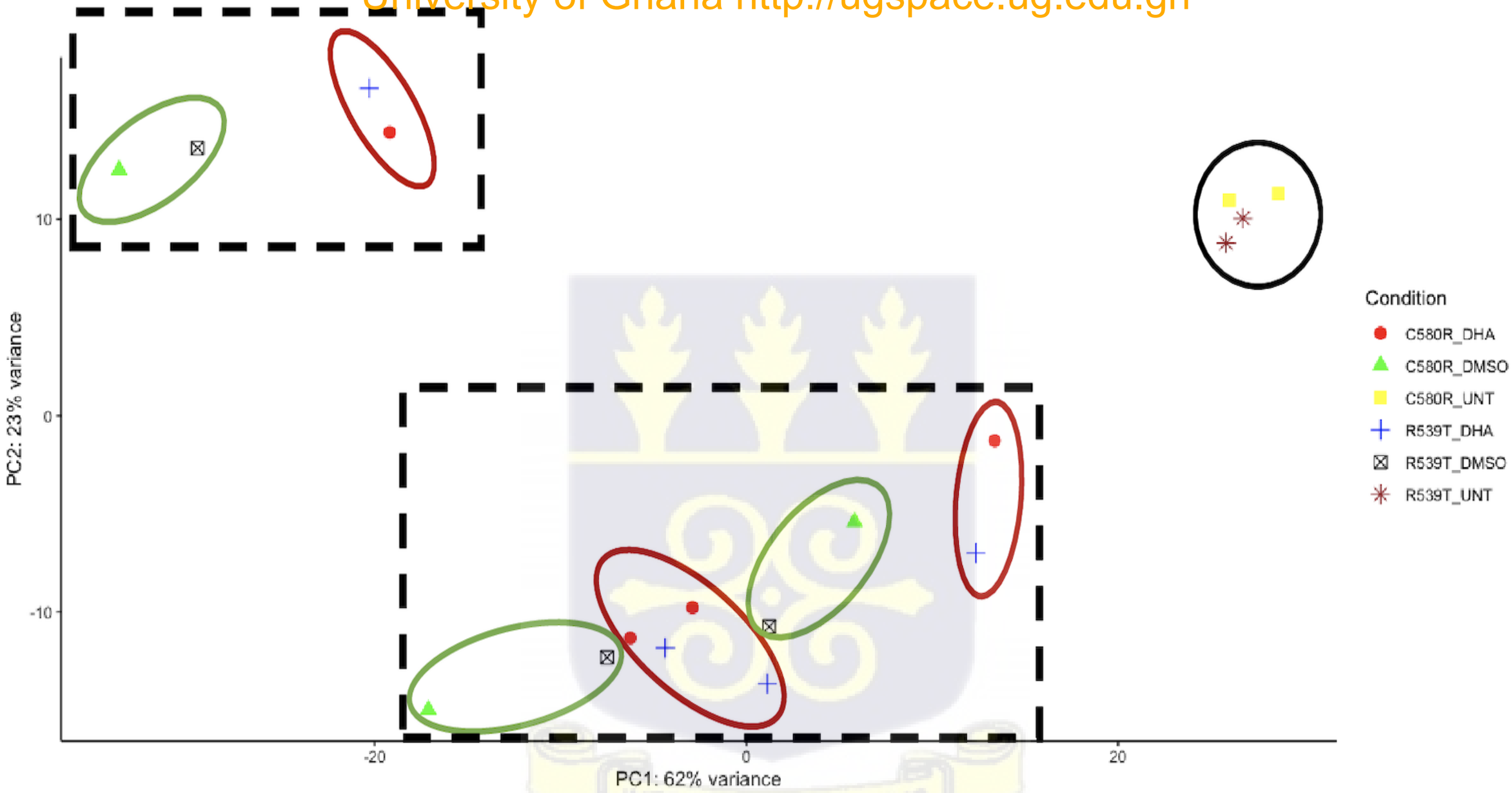

Figure 5.9 Principal component analysis (PCA) intimating at the transcriptional heterogeneity undergirding the ARTr phenotype. The dimensionality reducing technique PCA was used to explore the heterogeneity in gene expression profile under DMSO and DHA treatment conditions for the two ARTr parasite lines (C580R and R539T) used in this study. The black circle shows the untreated ARTr samples. The black dashed squares outlines the two clusters of DMSO and DHA-treated samples. In each square, the red circles show the different clusters for the C580R, and R539T DHA treated samples, and the green circles show the different clusters for the C580R and R539T DMSO treated samples.

University of Ghana http://ugspace.ug.edu.gh

5.5 Discussion

Against the backdrop of the need to deepen our understanding of the molecular mechanisms undergirding ARTr in *P. falciparum*, we sought to determine whether the gene expression profile of artemisinin-resistant parasites suggested the involvement of EVs. The mechanism of action of ART is known to involve the production of carbon-centered radicals, following reductive scission of the endoperoxide bridge, that promiscuously target proteome and nucleic acid and mediate cell-wide oxidative injury (Meshnick, 2002; O'Neill et al., 2010; Gopalakrishnan et al., 2015). This is unlike many antimalarial drugs that have well-defined drug targets and delineated mechanisms of action. This background accounts for the plethora of multiple molecular mechanisms reported to account for ARTr and is currently grouped under the organizing principles of increased tolerance to oxidative stress, reduced hemoglobin endocytosis and delay in the ring stage of the intra-erythrocytic developmental cycle (Siddiqui et al., 2021). Therefore, leveraging the power of RNA sequencing emerges as apt for interrogating the likely heterogeneous molecular mechanisms milieu of ARTr. This informed our choice to pivot the power of RNA sequencing to interrogate the role of EVs in *P. falciparum* ARTr. The novelty of our RNA sequencing experimental design, conduct and analysis lies in the research question posed, and the association testing method employed using modular analysis and gene set enrichment analysis.

We posited a molecular mechanistic model of ART resistance involving EVs as vehicles responsible for the active removal of ART-induced proteotoxic waste from the *P. falciparum*-infected erythrocyte (Tandoh et al., 2022). To test this model, we designed a targeted transcriptome exploratory analysis of two ARTr and one ART-sensitive parasite (with three replicates each) under the three conditions: untreated, 0.1% DMSO treated and 700nM DHA treated for six hours.

University of Ghana http://ugspace.ug.edu.gh

Therefore, the research question we explored was: does the gene expression profile of an ARTr parasite under ART pressure implicate a role for EVs? To explore this question, we designed a transcriptome-module phenotype association study (TMPAS). Our approach involved generating EV modules of interest made of genes with correlated expression to known genes involved in the *P. falciparum* EVs biogenesis pathway. Next, we used these modules as *a priori* gene sets in a gene set enrichment analysis of the normalized and ranked gene expression data. We implicated EVs in ARTr phenotype because we found a module (module 0) associated with the ARTr phenotype (Table 5.1 and 5.2, Figure 5.1 and 5.2).

An ever-present limitation for RNA sequencing analysis is the reliance on the known body of evidence (curated or computed) for GO analysis and the distillation of meaning from the transcriptome data. If the research question borders on a biological phenomenon that little is known about, current GO analysis pipelines are poorly powered to detect any associations between the transcript data and the biological phenotype of interest. In this regard, very little insight was made by traditional GO analysis. As GO discovery is limited to what is already known, querying ontologies that lack data on EVs biogenesis expectedly revealed little insight (Figures 5.4 - 5.6, Supplementary Tables 5.8 – 5.19). We had anticipated this during our experimental design, hence our use of a TMPAS approach to distil meaning from the gene expression data.

First, we generated gene lists (EVs modules of interest) of known EVs biogenesis genes and genes with correlated expression (known interacting partners data was not found). By expanding the analytical power, a modular analysis approach increases the chance of distilling meaningful information from gene expression data.

University of Ghana http://ugspace.ug.edu.gh

As it does not focus on one gene alone, a unit which by itself is unlikely to cause the biological phenomenon of interest to emerge, the modular analysis looks at the set of correlated genes that are likely to carry all the significant players associated or causal to the biological interest (Chaussabel et al., 2014; Bediako et al., 2019). The novelty in our analysis pipeline was to use our EVs modules of interest as our *a priori* gene list in our search for enrichment within the count data for the various paired conditions. We also analyzed the gene ontology signatures of our modules of EVs interest.

We report that out of the four EVs modules of interest generated, module 0 (ME0) was significantly associated with ARTr in *P. falciparum* (R539T_DHA_treated versus R539T_untreated: NES =1.18, FDR q-value = 0.24; C580R_DHA_treated versus C580R_untreated: NES = 1.25, FDR q-value = 0.14) (Table 5.2, Figure 5.2). GO analysis of ME0 showed enrichment for biological processes that included RNA processing, vesicle-mediated transport and exocytosis (Figure 5.1, Supplementary Table 5.3). GO analysis of the other three EVs modules of interest (modules 1, 3 and 17) showed enrichment for biological processes related to movement in host environment, entry and exit into host (for module 1); translation and the proteasomal ubiquitinin system (module 3); and cell cycle, nuclear chromosome segregation processes and phosphatidylinositol-3-phosphate biosynthetic processes (module 17) (Supplementary Tables 5.4 – 5.6, Supplementary Figures 5.10 – 5.12).

The EVs gene of interest in module 0 was *PfVps60* implicated in EVs biogenesis (Avalos-Padilla et al., 2021). It was the only gene that was successfully knocked out to yield a parasite line with significantly reduced EV production. That the module containing such a gene was found to be upregulated under DHA pressure in ARTr suggests a role for EVs in ARTr. We opine that such a role for EVs in ARTr is likely hinged on the increased tolerance to oxidative stress arm of evidence explaining the molecular mechanisms of ARTr (Tandoh et al., 2022).

University of Ghana http://ugspace.ug.edu.gh

Within this framework, we suggest that EVs may act as vehicles mediating the active removal of built-up and accumulating proteotoxic waste of ART action. Our data finds concordance with a recent multi-omics study that identified that ARTr involves a plethora of molecular mechanisms that included proteasome-mediated turnover, protein folding pathways and vesicular trafficking (Mok et al., 2021); and a transcriptome-phenotype association study that highlighted an association of the ARTr phenotype with proteotoxic stress, host cytoplasm remodeling and redox metabolism (Zhu et al., 2022). Further studies interrogating the members of this gene list are merited to further insights into the role of EVs in *P. falciparum* ARTr.

Our DEG analysis revealed that in the presence of DHA, approximately 400-600 genes were differentially expressed. These observations were similar to that reported earlier by (Mok et al., 2021). We observed that relatively smaller DEGs were found in the DHA treated condition when normalized to the DMSO treated condition (Table 5.3). This was not expected. We found non-statistically significant GO enrichment of biological processes related to the unfolded protein response (UPR) in C580R_DMSO treated versus C580R_DHA treated and Dd2_DMSO treated versus Dd2_DHA treated (Supplementary Table 5.14 and 5.18). We found this process downregulated under DHA treatment unlike earlier studies that reported upregulation of this biological process (Mok et al., 2021; Rocamora et al., 2018; Zhang et al., 2017; Zhu et al., 2022). Similarly downregulated and statistically not significant, were GO biological processes related to mitochondrial processes in R539T_DMSO treated versus R539T_DHA treated (Supplementary Table 5.10), unlike the findings of (Mok et al., 2021). Thus, our traditional DEG analysis did not recapitulate a statistically significant portrait in concordance with recent earlier findings (Mok et al., 2021; Zhu et al., 2022).

University of Ghana http://ugspace.ug.edu.gh

Finally, we report that the gene expression profile of ARTr *P. falciparum* parasites under ART exposure is complex and heterogeneous. This evidence for this heterogeneity in gene expression profile is seen in the low correlation plots between the two ARTr parasite strains (Figure 5.8). We also observed that PCA analysis of parasite treatment condition showed multiple clusters suggestive of a heterogeneous gene expression profile (Figure 5.9). Therefore, we concluded that the transcript profile of ARTr parasites under DHA pressure is complex and likely harbors a heterogeneous cell population. This finding is expected as it is known that the expression of the ARTr phenotype is undergirded by a plethora of molecular mechanisms currently broadly fitted into two motifs viz reduced hemoglobin endocytosis into the digestive food vacuole and increased tolerance to oxidative stress (Siddiqui et al., 2021). Within this framework, it is plausible that genetically identical ARTr parasites might have significantly different expression profiles. Further transcriptomic and epigenetic studies investigating this observation will be needed. In this vein, future studies may employ a transcriptomics study at single-cell resolution to deconvolute this suspected transcriptional heterogeneity of ARTr parasites.

We recognize the following limitations in our study. Our experimental design used two to four replicates for each parasite line under each different condition. Increasing the replicate number could have increased the power of the study to determine the role of EVs in ARTr (Tarr et al., 2018). Secondly, we had to conduct the experiments in four different batches that may have introduced hard to control for technical variations. Although we tried to detect and control for this using the surrogate variables adjustment option in DaMiRseq, its effect on our data analysis pipeline cannot be fully discounted. Thirdly, our experimental design did not control for parasite age and asexual stage. These factors may have acted as confounders to some of our conclusions such as our intimation of heterogeneous gene expression profiles in the ARTr parasite lines.

University of Ghana http://ugspace.ug.edu.gh

This limitation may explain the intermingling of the DMSO_treated and DHA_treated samples and why we saw a better correlation when we normalized to the untreated condition instead of the DMSO_treated condition (Figure 5.8 and 5.9). Finally, we noticed that most of the EVs modules of interest (three out of four) did not show an association with the ARTr phenotype in the gene set enrichment analysis (Table 5.1 and 5.2, Supplementary Data 5.1 – 5.16). We opine that this does not conclusively rule out the alternative hypothesis that these EV module of interest are correlated with ARTr. This is because, a critique of the frequentist as opposed to the Bayesian approach to hypothesis testing is the assumption of only one alternative to the null hypothesis. Thus, by failing to accept the null, it is implied that the alternative hypothesis is acceptable or correct. We recognize this is an overly simplistic heuristic approach to hypothesis testing by falsification. A rather conceivable alternative is that the alternative hypothesis are more than one and failing to accept the null hypothesis raises the question of which alternative hypothesis is acceptable. As our entire analytical framework was done within the enclave of this frequentist approach limitation, it will be interesting for future studies to explore a Bayesian approach to the data analysis hypothesis testing. Overall, further high-powered studies and replicates, correcting for these limitations, will be needed to interrogate our findings further.

In conclusion, our data has shown that an EV module (module 0, containing the *PfVps60* gene) is associated with ART resistance and highlighted the complex and heterogeneous gene expression profile of ARTr parasites. This suggests that EV biogenesis may play a critical role in mitigating proteotoxic injury in *P. falciparum*-infected erythrocytes. Therefore, further studies interrogating the implications of this study (EVs export hypothesis for ARTr in malaria parasites) are needed. Additionally, exploring further deconvolution of the heterogenous ARTr population of *P. falciparum* with single-cell transcriptomics is merited. We envisage that the findings reported here will aid future novel antimalarial drug discovery efforts.

University of Ghana http://ugspace.ug.edu.gh

CHAPTER SIX

Malaria Artemisinin Resistance: An Extracellular Vesicles Export Hypothesis

Kwesi Z. Tandoh[1*], Collins M. Morang'a[1], Michael Wilson[2], Neils B. Quashie[3,4] , Nancy O. Duah-Quashie[3]

[1] West African Center for Cell Biology of Infectious Pathogens, Department of Biochemistry, Cell and Molecular Biology, College of Basic and Applied Sciences, University of Ghana, Accra, Ghana

[2] Department of Parasitology, Noguchi Memorial Institute for Medical Research, College of Health Sciences, University of Ghana, Accra, Ghana

[3] Department of Epidemiology, Noguchi Memorial Institute for Medical Research, College of Health Sciences, University of Ghana, Accra, Ghana.

[4] Center for Tropical Clinical Pharmacology and Therapeutics, School of Medicine and Dentistry, College of Health Sciences, University of Ghana, Accra, Ghana

* Correspondence: kztandoh@st.ug.edu.gh (K. Z. Tandoh)

Keywords: artemisinin resistance, extracellular vesicles, hypothetical model

University of Ghana http://ugspace.ug.edu.gh

Tandoh KZ, Morang'a CM, Wilson M, Quashie NB, Duah-Quashie NO. Malaria artemisinin resistance: an extracellular vesicles export hypothesis. Trends Parasitol. 2022 Aug;38(8):614-617. doi: 10.1016/j.pt.2022.05.004. Epub 2022 Jun 2. PMID: 35661626.

This manuscript has been published in Trends in Parasitology journal and has been reproduced in this thesis with permission from the journal.

University of Ghana http://ugspace.ug.edu.gh

6.1 Abstract

Plasmodium falciparum causes malaria and is threatened by resistance to artemisinin (ART) - the drug for its effective management. ART resistance is driven by increased tolerance to oxidative stress and reduced hemoglobin trafficking to the food vacuole. We discuss how extracellular vesicles may play a role in developing ART resistance.

University of Ghana http://ugspace.ug.edu.gh

6.2 The burden of *P. falciparum* malaria and importance of artemisinin resistance

Malaria is responsible for a significant disease burden, especially in sub-Saharan Africa (SSA). In 2020, malaria cases reported globally were approximated at 214 million, with up to 627 thousand deaths (WHO, 2021a). Control of the mosquito vector and effective case management with artemisinin (ART)-based combination therapies (ACTs) are two pillars of malaria control efforts. ACTs pair a derivative of the fast-acting ART with a partner drug such as lumefantrine and piperaquine and have significantly reduced the malaria burden, especially in SSA. Since ART resistance in *P. falciparum* parasites emerged in South-East Asia (SEA), it has increasingly become the single biggest threat to stalling gains made in malaria control, especially in SSA (WHO, 2021a; Siddiqui et al., 2021).

University of Ghana http://ugspace.ug.edu.gh

6.3 The missing piece in the portrait of artemisinin resistance

ART is a sesquiterpene lactone with a mechanism of action that involves heme-mediated scission of its endoperoxide bridge, resulting in carbon-centered radicals. These active redox molecules target multiple proteins resulting in oxidative stress and parasite death. Additionally, activated ART contributes to offsetting parasite cellular redox homeostasis and antagonizes hemozoin production. This promiscuous targeting and alkylation of proteins trigger the activation of the unfolded protein response (UPR). The UPR is characterized by reduced production of new proteins and upregulation of protein-folding enzymes. This results in an accumulation of misfolded proteins, and increased protein destruction by the ubiquitin-proteasome system (UPS) which is achieved by elevated ubiquitination of proteins and trafficking to the proteasome/lysosomal complex (Siddiqui et al., 2021).

Our current understanding of ART resistance hinges on two motifs: increased tolerance to oxidative stress and reduced hemoglobin trafficking to the food vacuole (Siddiqui et al., 2021). However, not all observations of the ART resistant (ARTr) phenotype are explained by these broad organizing principles. Additionally, whether these mechanisms are independent and mutually exclusive of each other has not been determined. It is possible that in an ARTr parasite, reduced hemoglobin endocytosis to the food vacuole and resulting reduced activation of ART may underlie the expression of the reduced oxidative stress observed. ARTr parasites should also have little or no oxidative stress if this were the case.

University of Ghana http://ugspace.ug.edu.gh

This is not so as what has been observed is that both ART resistant and susceptible parasites exhibit a similar initial response to ART-induced oxidative stress. However, the ARTr parasite eventually achieves redox homeostasis and outstrips the ART-sensitive parasite in its tolerance to ART-induced proteinopathy (Yang et al., 2019). This observation suggests the switching on of a non-constitutive mechanism under ART pressure to deal with mounting ART-induced oxidative stress and hints at a yet incomplete model of our understanding of ARTr in *P. falciparum*. Additionally, it is known that ART action causes the alkylation of parasite macromolecules and disables the proteasomal system (Bridgford et al., 2018). What happens to this cargo of alkylated proteins is yet to be interrogated. Does it remain in the infected erythrocyte? Is it biologically harmful to the parasite? How is it removed? Can extracellular vesicles (EVs) be implicated as the vehicles responsible for their excretion? Whether there is an association between *P. falciparum* endomembranous vesicular network, EVs and ARTr is the question to explore. The current research landscape into ARTr is yet to thoroughly examine the role of EVs in developing ARTr in *P. falciparum*.

University of Ghana http://ugspace.ug.edu.gh

6.4 Extracellular vesicles may play a role in artemisinin resistance

EVs are nanoparticles generated in *P. falciparum* by an ESCRT-III (endosomal sorting complex required for transport) complex activated by an alternate pathway involving *PfBro1* and *PfVps32*/*PfVps60* proteins (Avalos-Padilla et al., 2021). EVs have been reported to be involved in many processes of the biology of *P. falciparum* and malaria pathogenesis and multiple lines of evidence suggest a role for EVs in ART resistance (Bhattacharjee et al., 2018; Yang et al., 2019; Mok et al., 2021; Tandoh et al., 2021). Across eukaryotic organisms, EVs are ubiquitous and play diverse roles including mediating drug resistance development (Tandoh et al., 2021).

However, the evidence presented by two studies make the most suggestive argument in implicating EVs and the endomembranous vesicular trafficking system in developing ART resistance.

Following the thread of established evidence that showed that ART resistance emerged when phosphatidyl inositol-3-phosphate (PI3P) levels in the parasite were elevated and that the phenotype was also characterized by the unfolded protein response (UPR), a connection between these two arms of evidence was sought (Siddiqui et al., 2021). Bhattacharjee and others used cryoimmunoelectron microscopy to delineate the *PfK13* interactome and showed that PfK13 colocalizes with PI3P vesicles close to the ER- the primary site of the UPR (Bhattacharjee et al., 2018). Additionally, they reported that PfK13 interacts with *P. falciparum* erythrocyte membrane protein 1 (*PfEMP1*) and that the PfK13-PfEMP1 interactome is enriched for a proteome involved in the proteostatic UPR pathway. This evidence linked PI3P and proteostasis and highlighted the role of the endomembranous system in ART resistance by connecting it to host erythrocyte remodeling and trafficking of *PfEMP1*.

University of Ghana http://ugspace.ug.edu.gh

Furthermore, these investigators showed increased PI3P vesicles and export throughout the parasite, and the infected erythrocyte characterized parasites with the PfK13 C580Y variant. They finally concluded that PI3P vesicle amplification spread the needed proteostasis capacity to neutralize ART-induced oxidative stress. Their finding suggested that PI3P elevation drives an ER vesicle expansion that offsets ART-induced oxidative injury by engaging the endomembranous trafficking system and remodeling the infected erythrocyte. Thus, EVs may function as vehicles to disseminate proteostatic capacity to neutralize ART toxic proteinopathy (Bhattacharjee et al., 2018).

Secondly, a multi-omics study that was designed to unravel insight into the molecular mechanisms of ART resistance reported an ART resistance proteome differentially enriched for chaperones, ubiquitin ligase, proteasome function, redox activities, and processes within intracellular vesicles upon functional enrichment analysis. They also identified mitochondrial factors as interacting partners of *PfK13* (Mok et al., 2021). The transcriptomics arm of this study reported that proteasome-mediated turnover and protein folding pathways were differentially expressed and associated with ARTr parasite lines. They also implicated vesicular trafficking as a means for removing this accumulated ART proteinopathy as part of the rewiring of the *P. falciparum* intra-erythrocytic metabolic program to enhance survival, a process which they surmised converged on the mitochondria (Mok et al., 2021). Finally, a recent transcriptomic-phenotype analysis of clinical isolates from SEA identified a complex ART resistance-associated transcript profile that included pathways related to proteotoxic stress, host cytoplasm remodeling and redox metabolism (Zhu et al., 2022). These findings are accommodated by the EVs export hypothetical model (Table 6.1).

University of Ghana http://ugspace.ug.edu.gh

6.5 An extracellular vesicles export model of artemisinin resistance

We propose a novel role for extracellular vesicles as an extension of the involvement of the endomembranous vesicular trafficking network to manage ART-induced oxidative stress-related proteotoxicity in the parasite-infected erythrocyte. We suggest that ART resistance can emerge in any parasite that can withstand ART's oxidative and proteotoxic assault by actively removing damaged proteins from the infected erythrocyte to maintain cellular homeostasis under ART pressure (Figure 6.1). This EVs exports model complements the two, earlier mentioned, established organizing principles of ART resistance and explains certain observations about the phenotype not accommodated by the conventional two organizing principles (Table 6.1).

Our model implicates EVs as the vehicles that mediate the active removal of misfolded and ubiquitinated proteins in the *P. falciparum*-infected erythrocyte under ART pressure. It is frame worked by the following evidence: the central role of the UPR to ARTr development; the attending PI3P vesicle amplification and host erythrocyte remodeling by the endomembranous trafficking system; the associated transport of parasite proteins; and the ubiquity of EVs in the biology of the parasite and the pathophysiology of malaria (Table 6.1).

University of Ghana http://ugspace.ug.edu.gh

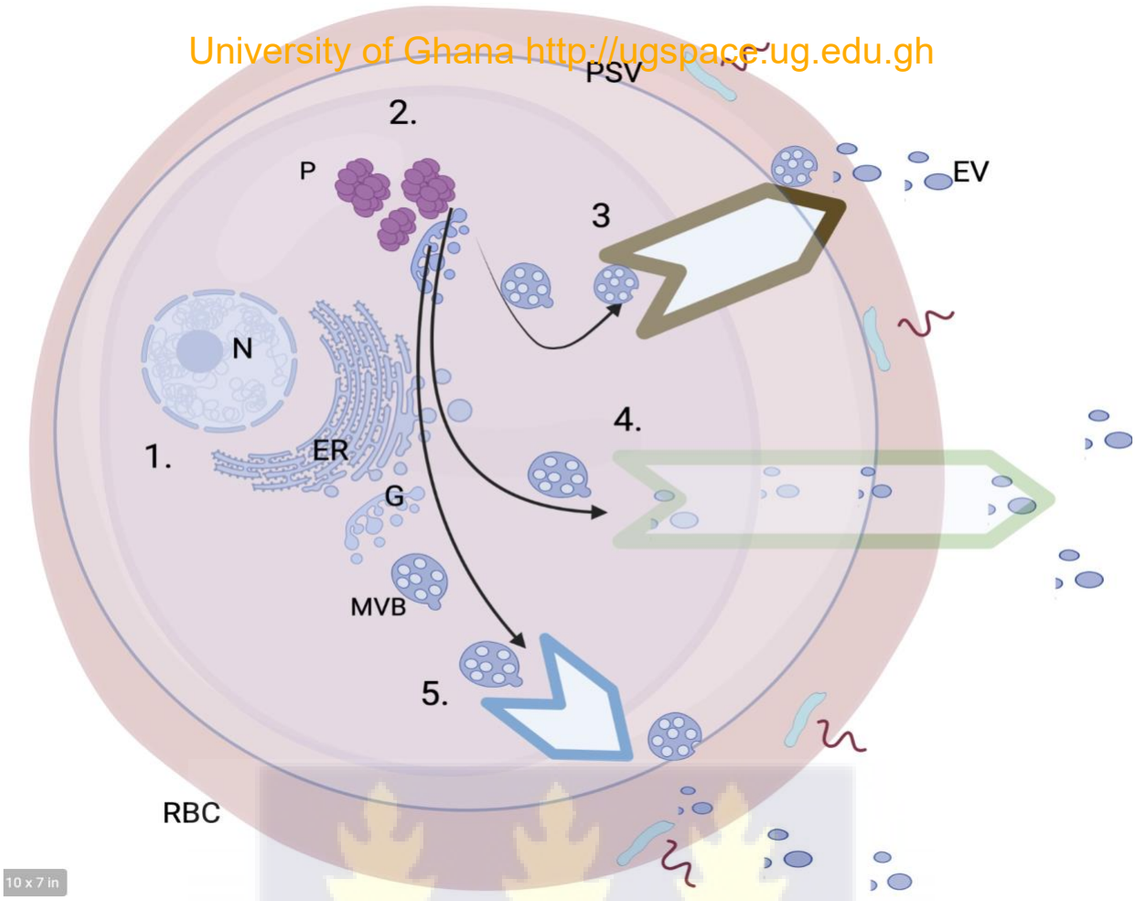

Figure 6.1 | Schematic summary of the extracellular vesicle export model of artemisinin resistance in *Plasmodium falciparum*. The model is platformed on the increased tolerance to oxidative stress motif of artemisinin resistance. 1. Under artemisinin pressure, *P. falciparum* Kelch 13 artemisinin-resistant conferring variants mount a cellular response characterized by increased endoplasmic reticulum PI3P vesiculation and protein misfolding. 2. This increased proteostasis engages the proteo-lysosomal system of the unfolded protein response and leads to the formation of intraluminal vesicles (ILVs). The formation of multivesicular bodies (MVBs), most likely under the influence of *PfBro1*, is in turn formed from ILVs. These MVBs with their cargo of extracellular vesicles are exported out of the parasite in one of the following ways. 3. From the *P. falciparum* cell into the infected erythrocyte cytoplasm for transfer of the MVBs cargo to the extracellular space via the remodeled exo-membranous trafficking system. 4. From the *P. falciparum* cell to the extracellular space via a yet to be defined export pathway. 5. From the *P. falciparum* cell into the parasitophorous vacuolar space via a yet to be defined export pathway. Then subsequently via a *Plasmodium* translocon of exported proteins (PTEX) transporter through the parasitorous vacuolar membrane into the infected erythrocyte cytoplasm. And finally, to the extracellular space via the remodeled exo-membranous trafficking system.

N- nucleus
P- proteasome
ER- endoplasmic reticulum
G- Golgi
MVB- multivesicular bodies
PSV- parasitophorous vacuolar membrane
RBC- red blood cell membrane
EV – extracellular vesicle; PI3P – phosphatidyl inositol-3-phosphate

University of Ghana http://ugspace.ug.edu.gh

In this model, the goal of EV export is to return the offset oxidative homeostasis to normal by the excretion of the oxidative proteotoxic waste. The plausibility of this model is further supported by the recent finding that EVs biogenesis in *P. falciparum* is accomplished via ESCRT-III machinery activated by an alternative pathway involving the action of *PfBro1* and *PfVps32*/*PfVps60* proteins (Avalos-Padilla et al., 2021).

Our model predicts that EVs from ART-exposed infected erythrocytes will carry a relatively larger cargo of misfolded and ubiquitinated parasite proteins compared to EVs from uninfected RBCs. Our model also suggests that inducing ARTr by *in vitro* selection in an EVs-deficient parasite line may not be possible and that knocking out *PfBro1*, *PfVps32* or *PfVps60* in an ARTr parasite will recapitulate the ART susceptible phenotype. Finally, our model predicts that comparative transcriptome analysis between ART resistant and an EVs-deficient parasite line may give insight into druggable targets of EVs biosynthesis critical for the expression of the ARTr phenotype. Further studies investigating the molecular mechanisms of ARTr under this model are merited.

Table 6.1 | Summary of evidence from several studies and how they fit into the EVs export hypothetical model of ARTr compared to the two mainstream organizing principles of ARTr.

University of Ghana http://ugspace.ug.edu.gh

Evidence characterizing ARTr	Models of ARTr in *P. falciparum*			Discussion
	Trafficking model	**Oxidative model**	**EVs model**	
A plurality of molecular markers associated with ART resistance (Siddiqui et al., 2021)	√	√	√	All models accommodate this evidence as each recognizes that multiple genes could drive the ARTr phenotype
PI3P elevation confers ART resistance even in the absence of PfK13 ART resistance-conferring genetic variants (Bhattacharjee et al., 2018)	√	√	√	Models recognize that *PfK13* (a marker of endosomes) drives the elevation of PI3P (reduced levels of ubiquitinated PI3K and subsequent lower turnover by the ubiquitin-proteasomal system) and that such elevation may also be *PfK13* independent.
PfK13 interactome studies show that reduced hemoglobin endocytosis to FV is the molecular mechanism of ART resistance (Birnbaum et al., 2020)	√	X	X	A seminal study. Discovered reduced trafficking of hemoglobin to the FV model of ART resistance. However, it did not explore a connection between PI3K and the ubiquitin proteasomal pathway.
Increased isoprenoid production was observed in ARTr parasites under ART-induced oxidative stress. Important for prenylation of Rab GTPases involved in endovesicular transport to the FV (Zhang et al., 2021)	X	X	√	This does not fit the oxidative model as it recognizes no connection to vesicular trafficking and clashes with the expectations of the trafficking model. It is accommodated by the EVs model because it recognizes that this observation will drive the proposed exo-vesicular transport to the infected erythrocyte cytoplasm and beyond,
Upregulation of genes involved in the UPR pathway and increased expression of genes involved in adaptive responses against cellular damage; and attending build-up of unfolded and polyubiquitinated proteins under ART which activates the ER stress response with eIF2α phosphorylation (by the PK4 protein kinase) and global translational arrest (Mok et al., 2021; Rocamora et al., 2018; Zhang et al., 2017; Zhu et al., 2022)	X	√	√	This is the central motif of the oxidative model and forms a nexus with the EVs export model which will use PfK13-PI3P vesicles as vehicles for the removal of the oxidative/proteinopathic waste of ART action. Under the reduced Hb trafficking model which proposes a final reduction in ART activation, it will be expected that no or little ART-induced stress is meted to the parasite. This expectation is contrary to what has been observed.
Reduced levels of ubiquitinated proteins in ARTr parasites help alleviate pressure on the proteasomal system under ART pressure (Siddiqui et al., 2021; Siddiqui et al., 2020; Bridgford et al., 2018); no differences in proteasomal response in the PfK13 mutant and wildtype parasites against ART-induced oxidative stress but ARTr parasite regain protein turnover quicker (Yang et al., 2019)	√	X	√	This is another point where the oxidative model and the EV model differ. The oxidative model cannot explain why there will be reduced levels of ubiquitinated proteins in ARTr parasites. The EVs model hypothesizes that this observation is due to the active removal of these proteins by EVs and predicts that the proteome of EVs from ARTr parasites under ART pressure will be enriched for ubiquitinated proteins. This will explain why ARTr parasites eventually outstrip ART sensitive parasites in tolerance to ART-induced proteinopathy/oxidative stress even though they both start from a similar baseline.
PfK13 close to the FV and PI3P-labeled vesicular structures linking PfK13 with PI3K in vesicle transport and ARTr (Siddiqui et al., 2021; Bhattacharjee et al., 2018; Gnädig et al., 2020)	√	X	√	As discussed in main text.

EVs – extracellular vesicles Trafficking model - Reduced trafficking of hemoglobin to digestive food vacuole
Oxidative model - Increased tolerance to ART-induced oxidative stress and proteinopathy EVs model - EVs export hypothesis FV – food vacuole ART – artemisinin ARTr - artemisinin resistant PI3P – phosphatidylinositol-3-phosphate *PfK13* – *Plasmodium falciparum* kelch 13 gene PI3K - phosphatidylinositol-3-kinase

University of Ghana http://ugspace.ug.edu.gh

CHAPTER SEVEN

Extracellular vesicles abundance is positively correlated with dihydroartemisinin exposure in *Plasmodium falciparum* parasites

Kwesi Z. Tandoh[1], Yunuen Avalos-Padilla[2,3], Michael Wilson[4], Neils B. Quashie[5,6], Xavier Fernàndez-Busquets[2,3] , Nancy O. Duah-Quashie[6]

Affiliations

1. West African Center for Cell Biology of Infectious Pathogens, Department of Biochemistry, Cell and Molecular Biology, College of Basic and Applied Sciences, University of Ghana, Accra, Ghana

2. Institute for Bioengineering of Catalonia (IBEC), The Barcelona Institute of Science and Technology (BIST), Barcelona, Spain,

3. Barcelona Institute for Global Health (ISGlobal, Hospital Clınic-Universitat de Barcelona), Barcelona, Spain

4. Department of Parasitology, Noguchi Memorial Institute for Medical Research, College of Health Sciences, University of Ghana, Accra, Ghana

5. Center for Tropical Clinical Pharmacology and Therapeutics, School of Medicine and Dentistry, College of Health Sciences, University of Ghana, Accra, Ghana

6. Department of Epidemiology, Noguchi Memorial Institute for Medical Research, College of Health Sciences, University of Ghana, Accra, Ghana.

*Corresponding authors: Nancy O. Duah-Quashie, NDuah@noguchi.ug.edu.gh; Xavier Fernàndez-Busquets, xfernandez_busquets@ub.edu

This manuscript is currently under preparation for publication.

University of Ghana http://ugspace.ug.edu.gh

7.1 Abstract

Our understanding of the molecular mechanisms undergirding ART resistance in *Plasmodium falciparum* is represented by two organizing principles today: reduced hemoglobin trafficking to the digestive food vacuole resulting in lower levels of activated artemisinin (ART), and increased tolerance to ART-induced oxidative stress in the infected erythrocyte. Under the motif of increased tolerance to ART-induced oxidative stress, there is evidence that the parasite suffers a buildup of proteinopathic toxic waste that accumulates from the activation of the unfolded protein response and an overwhelming of the ubiquitin-proteasomal system. How this cargo of proteinopathic toxic waste is actively eliminated from the parasite is yet to be detailed. As evidence implicates the endomembranous vesicular system of the parasite in developing ART resistance, we hypothesized that extracellular vesicles (EVs) may be involved in developing ART resistance in *P. falciparum* by acting as vehicles mediating the excretion of ART-induced proteinopathic waste to maintain cellular homeostasis. This EVs model of ART resistance predicts that EVs abundance will be altered under ART pressure and that their cargo is likely to be enriched for ubiquitination and misfolded proteins. In this study we tested the first of these predictions using an ARTr transgenic line engineered on a 3D7 background and a 3D7 PfVps60 knock-out with a deficient EV production phenotype. We report that DHA exposure was positively correlated with EVs abundance (coefficient estimate = 1038.58, confidence interval of 194.86 – 1882.30 and p-value = 0.018) and suggests EVs biogenesis is part of the parasite's response to ART. This finding implicates a role for EVs in developing the ARTr phenotype and warrants further exploration.

Keywords: artemisinin resistance; extracellular vesicles export model

University of Ghana http://ugspace.ug.edu.gh

7.2 Introduction

Since the evolution of artemisinin (ART) resistance in *Plasmodium falciparum* parasites of South-East Asia (SEA), the risk of spread to sub-Saharan Africa (SSA) has become a significant concern for global malaria control efforts (Noedl et al., 2008; Dondorp et al., 2009; WHO, 2020b). To mitigate this risk, deepening our understanding of the molecular mechanisms underpinning ART resistance in *P. falciparum* parasites is needed. Such knowledge will drive translational agendas for novel antimalarial drug discovery efforts and improve existing molecular surveillance approaches (Siddiqui et al., 2021; Nsanzabana, 2021; Nsanzabana et al., 2018).

Our knowledge and understanding of ART resistance have primarily centered on the *P. falciparum* kelch 13 (*PfK13*) gene. This *PfK13* model of ARTr highlights two components: reduced endocytosis of hemoglobin into the digestive food vacuole and increased tolerance to artemisinin (ART) induced oxidative stress. We hypothesized a novel role for extracellular vesicles (EVs), as an extension of the involvement of the endomembranous network, to manage ART-induced proteinopathy and oxidative stress in the infected erythrocyte (Tandoh et al., 2022) . This EVs export hypothesis posits that ART resistance emerges in parasites that can withstand ART's oxidative and proteotoxic assault by actively removing damaged proteins from the infected erythrocyte to maintain cellular homeostasis under ART pressure. We suggest that this proteinopathic export is achieved by nanoparticle EVs expressed by the *P. falciparum*-infected erythrocyte. The EVs export model of ARTr further predicts that EVs abundance will be altered in ARTr parasites under ART pressure. To test this hypothesis, we exposed 3D7, 3D7_R561H (ART resistant) and 3D7_PfVps60_KO (EVs biogenesis-deficient line) to 0.1% DMSO and 700nm of dihydroartemisinin (Tebu) and measured the EVs abundance for each parasite line under each condition.

University of Ghana http://ugspace.ug.edu.gh

We report that DHA treatment was positively correlated with EVs abundance (coefficient estimate = 1038.58, confidence interval of 194.86 – 1882.30 and p-value = 0.018) and suggests that EVs biogenesis is part of the parasite's response to ART. Our findings provide evidence to support the EVs export hypothesis of ART resistance in *P. falciparum* parasites.

INTEGRI PROCEDAMUS

University of Ghana http://ugspace.ug.edu.gh

7.3 Method

7.3.1 *P. falciparum in vitro* parasite culture and treatment conditions

Asexual stages of *P. falciparum* parasites were cultured in group B human erythrocytes at 3% hematocrit using complete Roswell Park Memorial Institute (RPMI) medium supplemented with 0.5% (w/v) Albumax II (Life Technology, Auckland, New Zealand) and 200 mM L-glutamine. Parasites were maintained at 37℃ under an atmosphere of 5% O2, 5% CO2 and 90% N2. We exposed triplicates of the parasite lines 3D7, 3D7_R561H (ART resistant) and 3D7_PfVps60_KO (EVs biogenesis-deficient line) to 0.1% DMSO and 700nm of dihydroartemisinin (Tebu Bio) for 6 hours before harvesting the culture supernatant for EVs extraction (Figure 7.1). Before EVs extraction, parasite cultures were first synchronized in the ring stage with a 5% sorbitol lysis (Lambros et al., 1979). Subsequently after 36 hours, parasites were synchronized in the schizont stages by treatment in 70% Percoll (GE Healthcare, Uppsala, Sweden). Finally, a final 5% sorbitol lysis was done to yield ring-stage parasites tightly synchronized at 8 hours post-infection (hpi) (Figure 7.1). Parasite culture supernatant was then harvested at 40 hpi for EVs extraction. Final culture parasitemia was at least 1% for all conditions except DHA-treated samples (Supplementary Table 7.1).

University of Ghana http://ugspace.ug.edu.gh

7.3.2 Ring stage survival analysis

The 0–3 hour ring-stage survival analysis (RSA) was performed as described previously (Witkowski et al., 2013a; Ariey et al., 2014). In brief, highly synchronized 0–3 h post-invasion rings were exposed to 700 nM DHA for 6 hours, followed by removal of the drug. At 72 hours after initial drug treatment, parasitemia was assessed by Giemsa-stained smear microscopy of thin smears. The ring-stage survival percentage was calculated as the fraction of surviving DHA-treated parasites over the DMSO-treated control of the same parasite line (with a parasite growth rate of > 1.5%). An RSA survival percentage >1% is considered to indicate ART resistance. The RSA for each parasite line was determined with at least three technical replicates per biological replicate.

University of Ghana http://ugspace.ug.edu.gh

7.3.3 EVs extraction and purification

For the purification of EVs, parasite culture media was collected from *in vitro P. falciparum* culture. EVs extraction and purification were carried out as previously described (Borgheti-Cardoso et al., 2018). Briefly, parasite culture media samples were initially prepared by sequential centrifugations to remove large aggregates. First, cultures were centrifuged for 10 min at 400× g, the cell pellet was discarded, and supernatant was further centrifuged at 2,000× g for 10 min twice. In both cases, a small pellet was discarded. Finally, 25 ml of the supernatant was placed in an Amicon Ultra-15 centrifugal filter (100 kDa cut-off, Millipore-Merck, Cork, Ireland) and centrifuged for 10 min at 3,000× g. 1 ml of the resulting concentrated solution was collected and transferred to a 10 ml homemade Sepharose CL-4B column previously equilibrated with PBS. EV purification was performed by gravity flow at room temperature and 0.5-ml fractions were collected. EVs were enriched in fractions 7, 8, 9 and 10, which were combined, concentrated (placed in an Amicon Ultra-4 centrifugal filter (100 kDa cut-off, Millipore-Merck, Cork, Ireland) and centrifuged for 10 min at 5,000× g) and resuspended to a final volume of 200 µl to be used for the EVs abundance determination experiment (Avalos-Padilla et al., 2021). (Supplementary Table 7.1, Figure 7.1).

University of Ghana http://ugspace.ug.edu.gh

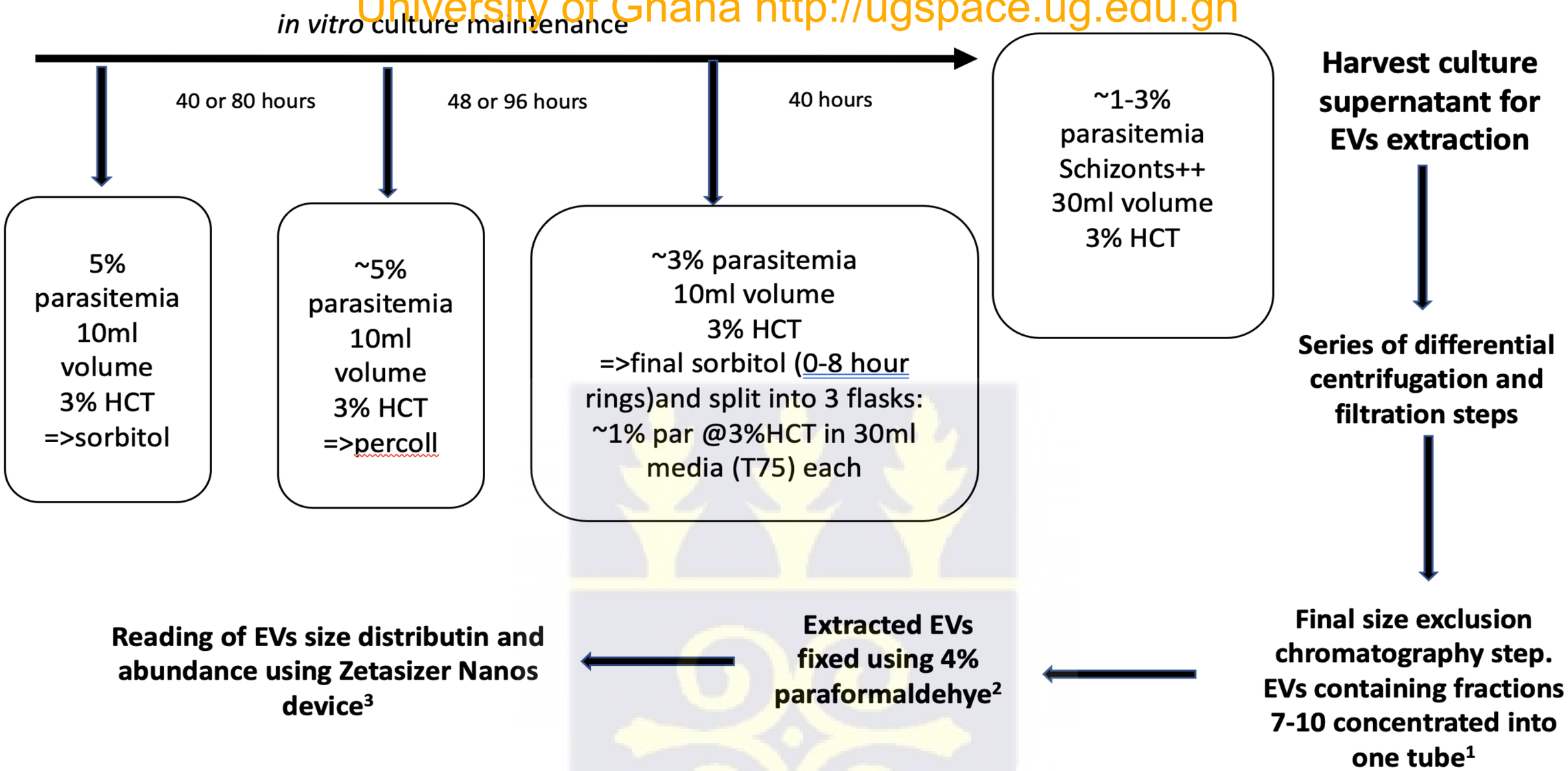

Figure 7.1 Workflow for extracellular vesicles (EVs) extraction, purification, and abundance estimation. Parasite cultures were synchronized to 0–8-hour rings and EVs were harvested from the culture supernatant after 40 hours. A series of centrifugation and filtration steps were used to extract EVs. Finally, a sepharose chromatography column was used to enrich EVs in fractions 7 to 10. Fractions 7-10 were then concentrated using a final filtration step and topped up to 200ul with 1X PBS[1]. After this, EVs were fixed using 4% paraformaldehyde in a 1:2 dilution[2]. EVs size and abundance were then estimated with a Zetasizer Nano device. A 1:9 dilution with 1X PBS was used for loading the fixed EVs unto the Zetasizer Nano device.
[1]first dilution factor; [2]second dilution factor; [3]third dilution factor

University of Ghana http://ugspace.ug.edu.gh

7.3.4 EV size and abundance measurements

Dynamic light scattering was used to measure particle size in the purified EV population as previously described (Hubert et al., 2015). To obtain the optimum light scattering intensity, 100 µl of purified EVs were resuspended in 900 µl of filtered (0.22 µm) PBS after dilution with 1:2 factor in 4% paraformaldehyde (PFA). Mean particle size of vesicle dispersions and the derived count rate (kilo counts per second) were determined in triplicates from light diffusion measured at 25℃ and an attenuator index of 8, using Zetasizer Nano S (Malvern Instruments, Ltd., Malvern, UK) (Avalos-Padilla et al., 2021). The mean EVs abundance was derived from the count rate, duration of count, parasitemia and dilution factors used in the experimental design (Supplementary Table 7.1, Figure 7.1).

University of Ghana http://ugspace.ug.edu.gh

7.4 Results

7.4.1 Determination of parasite sensitivity to artemisinin

We used the RSA assay to establish the sensitivity of the parasite lines (3D7, Vps60 and R561H) to ART. R561H was ARTr with mean RSA survival rate of 12.7% (standard deviation (sd) of 2.4). 3D7 and Vps60 were ART susceptible with a mean survival rate of 0.7% (sd=0.08) and 0.4% (sd=0.09) respectively (Figure 7.2, Supplementary Table 7.2).

7.4.2 Size distribution of enriched EVs is similar among parasite lines for all conditions

Before comparing EVs abundance between parasite and treatment conditions, we determined whether the size distribution of the enriched EVs differed between parasite and treatment conditions. The median EV size was 215.6 (Q1=197.1, Q3= 229.3). EVs size distribution did not differ among the parasite lines and treatment conditions (Kruskal-Wallis, p-value = 0.74). The mean EVs size in Vps60_KO line was 211 + sd = 42, and in 3D7 was 212 + sd=30, and in R561H 214 + sd = 28. (Figure 7.3, Supplementary Table 7.3).

University of Ghana http://ugspace.ug.edu.gh

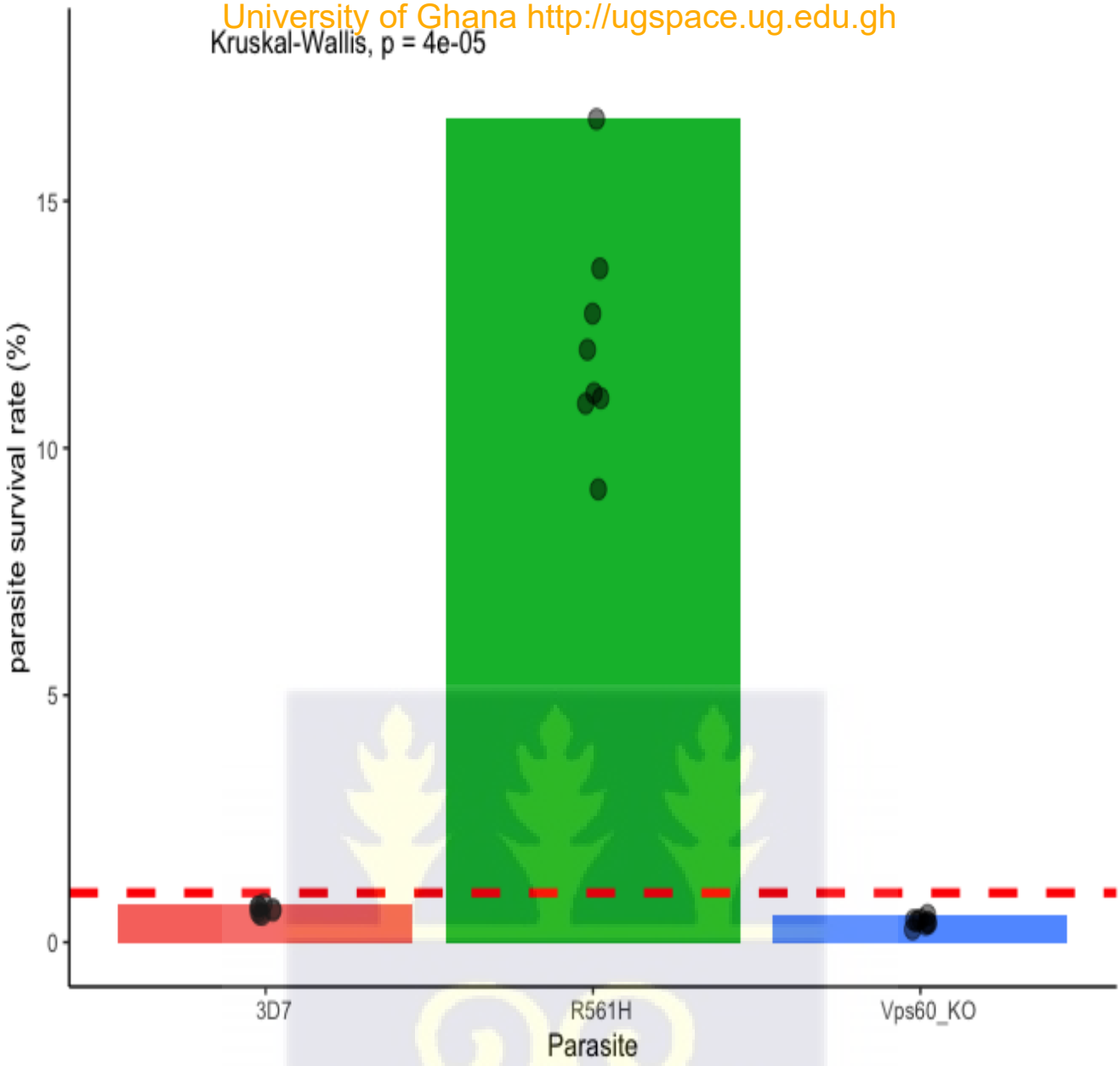

Figure 7.2 ***In vitro*** **RSA0–3 parasite survival rates (%) for the ART susceptible WT** ***Plasmodium falciparum*** **strain (3D7), the** ***P. falciparum PfK13*** **ARTr variants (R561H) and the** ***P. falciparum Vps60*** **knock out (Vps60_KO) used in this study. 3D7 is the wild-type ART susceptible parasite line with normal EVs biogenesis pathway. Vps60 was generated from 3D7 by knocking down the PfVps60 gene resulting in lower constitutive EVs biogenesis. R561H is an ARTr parasite line CRISPR engineered on a 3D7 background. Each bar represents the mean of triplicate experiments. Growth rates for all parasite lines were at least 1.5% in the non-exposed controls. The mutant** ***PfK13*** **parasite, R561H, has significantly higher parasite survival rate compared to 3D7 and Vps60_KO parasite lines (Kruskal-Wallis test = $4x10^{-5}$; 3D7 versus R561H, adjusted p-value = $3.199395\ x10^{-2}$; 3D7 versus Vps60_KO, adjusted p-value = $2.810245\ x\ 10^{-2}$; R561H versus Vps60_KO, adjusted p-value = $2.058283x10^{-5}$). The adjusted p-value was determined using the Dunn post-hoc test. The red dashed line indicates the 1% survival rate above which a parasite line is characterized as ARTr. RSA0–3 - 0-3 hour ring-stage survival assay; ART – artemisinin;** ***PfK13*** **–** ***Plasmodium falciparum*** **kelch 13 gene**

University of Ghana http://ugspace.ug.edu.gh

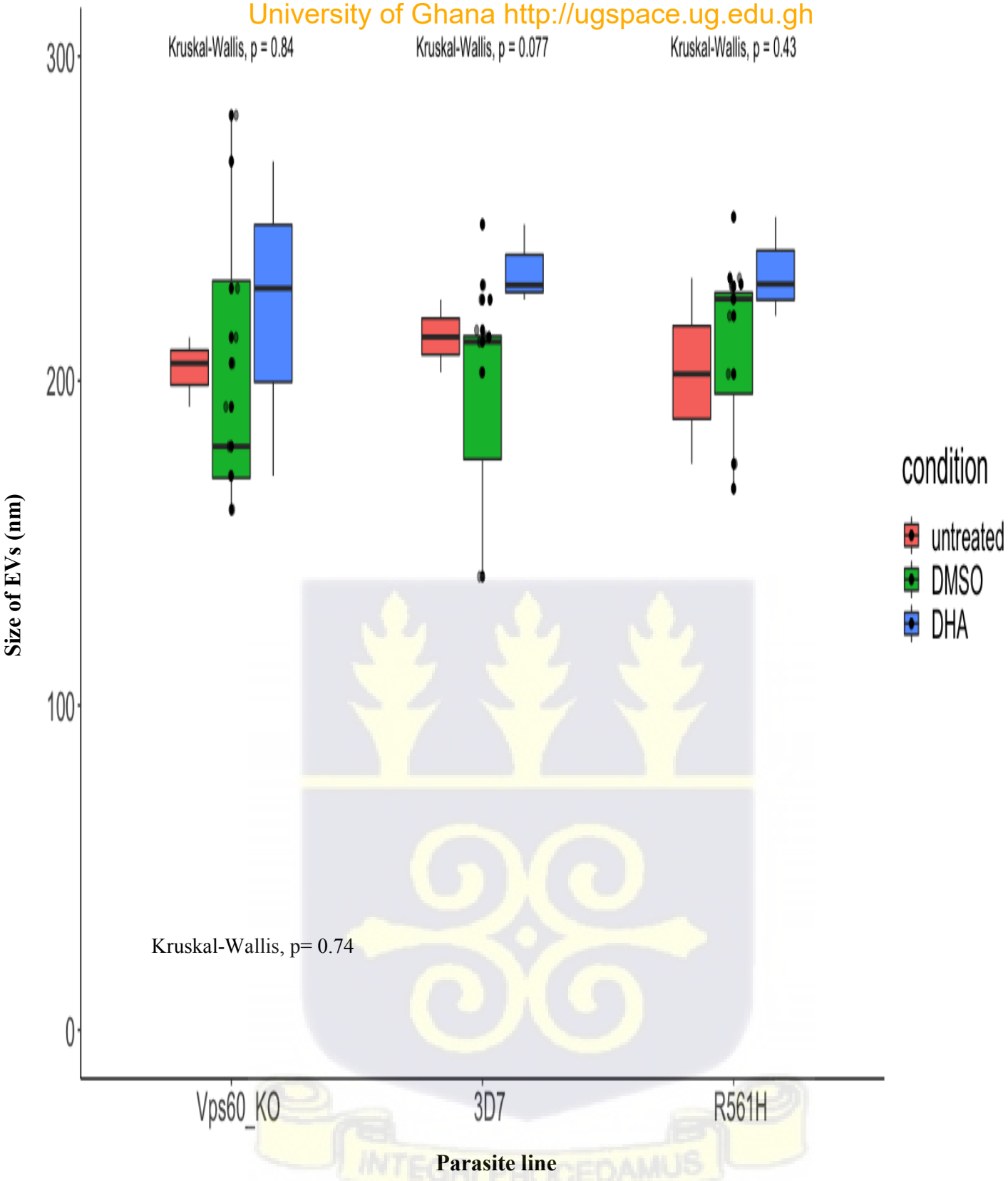

Figure 7.3 Analysis of EVs size by parasite line and treatment condition factors. The comparison of EV size among parasite lines and treatment conditions was done using the Kruskal-Wallis test. The comparison of EVs size among the 3 parasite lines showed no differences in size distribution (Kruskal-Wallis, p= 0.74).

7.4.3 Treatment condition is a better predictor of EVs abundance compared to parasite line

University of Ghana http://ugspace.ug.edu.gh

Next, we considered the independent variables parasite line (3D7, Vps60_KO and R561H) and treatment condition (untreated, DMSO treated, and DHA treated) as predictors of the response variable (Table 1). To determine how much these factors influenced EVs abundance, we conducted a Kruskal-Wallis test to compare EVs abundance using parasite line and treatment condition as categorical factors (Table 7.1, Figure 7.4 and 7.5).

University of Ghana http://ugspace.ug.edu.gh

Table 7.1 Analysis of EVs abundance by parasite line and treatment condition factors. Field values are medians (first quartile, third quartile). The comparison of EVs abundance among parasite lines and treatment conditions was done using the Kruskal-Wallis test with the degree of freedom = 2.

	EVs abundance (mega counts)				
	Untreated (n = 9)	**DMSO (n = 9)**	**DHA (n = 9)**	**KW chi-square**	**p-value**
Vps60_KO (n = 9)	321 (241, 338)	93 (91, 114)	1572 (1222, 3254)	7.2	0.03*
3D7 (n = 9)	414 (358, 563)	400 (369, 1030)	700 (692, 1037)	1.16	0.56
R561H (n = 9)	376 (314, 462)	245 (191, 389)	652 (628,1024)	5.96	0.05*
KW chi-square	1.87	5.96	3.47		
p-value	0.39	0.05*	0.18		

EVs – extracellular vesicles
DMSO – dimethyl sulfoxide
DHA - dihydroartemisinin
KW – Kruskal-Wallis

University of Ghana http://ugspace.ug.edu.gh

Under each of the three treatment condition factors, we compared the contribution of the parasite lines to EVs abundance. We found that EVs abundance was greater in 3D7 compared with Vps60_KO and R561H parasites for untreated and DMSO-treated conditions (Table 1). However, for these control conditions, statistically significant differences in EVs abundance were only seen in the DMSO treated condition (Kruskal-Wallis chi-square = 5.96, p-value = 0.05). EVs abundance in the DHA treated condition was highest in the Vps60_KO line but showed no statistically significant differences in comparison to 3D7 and R561H (Kruskal-Wallis chi-square = 3.47, p-value = 0.18). (Table 7.1 and Figure 7.4). A post-hoc Dunn's test was used to determine that only 3D7 versus Vps60_KO under DMSO condition showed a statistically significant difference in EVs abundance (Dunn's test Z-value = 2.4, p-value = 0.05) (Table 2). Finally, we assumed a linear relationship between parasite line and EVs abundance, for each treatment condition, and used a simple linear regression model to determine the strength of the correlation between parasite line and EVs abundance. We used the EVs deficient parasite line, Vps60_KO as our reference. We found that none of the parasite lines had a statistically significant correlation with EVs abundance (Supplementary Tables 7.4 – 7.6).

University of Ghana http://ugspace.ug.edu.gh

Next, we conducted similar analysis using parasite lines as categorical factors and determined the influence of treatment condition on EVs abundance using a simple linear regression model. Under the parasite line factor and to compare treatment conditions, we found EVs abundance was greater in DHA treated condition compared with untreated and DMSO treated conditions (Table 7.1, Figure 7.5). However, statistically significant differences in EVs abundance was only seen in the Vps60_KO parasite line (Kruskal-Wallis chi-square = 7.2, p-value = 0.03) and R561H (Kruskal-Wallis chi-square = 5.96, p-value = 0.05) (Table 7.1). EVs abundance in the Vps60_KO line showed statistically significant differences between the DHA versus DMSO conditions (Dunn's test Z-value = 2.7, p-value = 0.02), and for the R561H parasite line, statistically significant difference was also seen between the DHA versus DMSO conditions (Dunn's test Z-value = 2.4, p-value = 0.05) (Table 7.2). Finally, following a simple linear regression, we found that treatment condition had a marginally significant correlation with EVs abundance (Supplementary Tables 7.7 – 7.9).

University of Ghana http://ugspace.ug.edu.gh

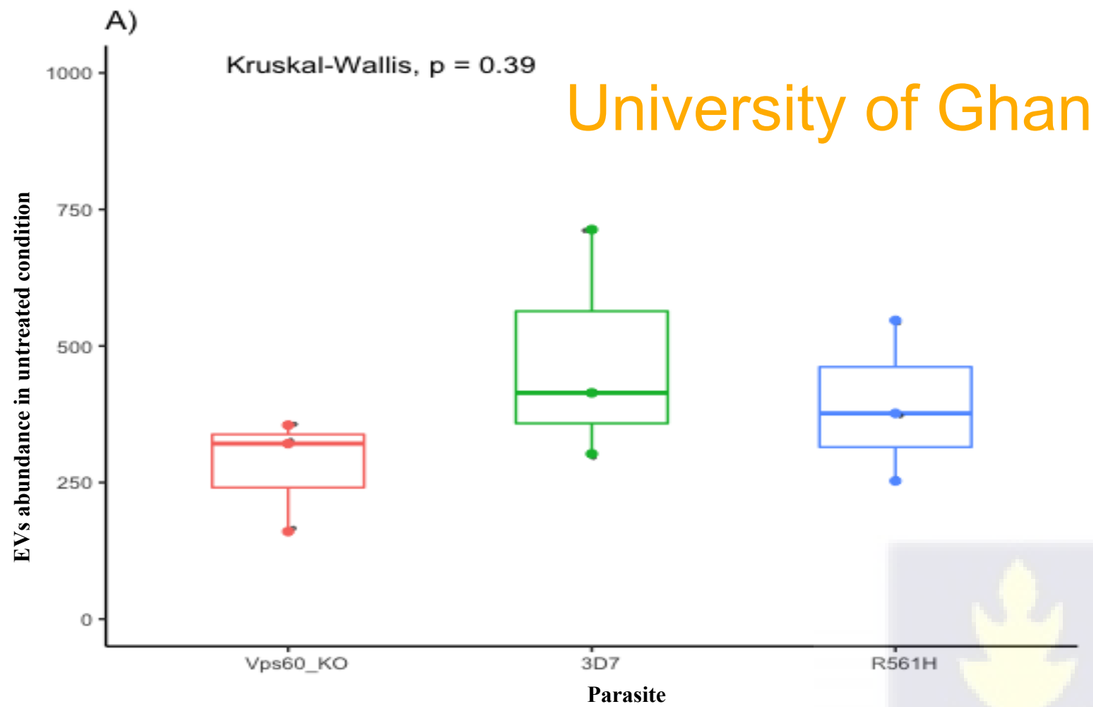

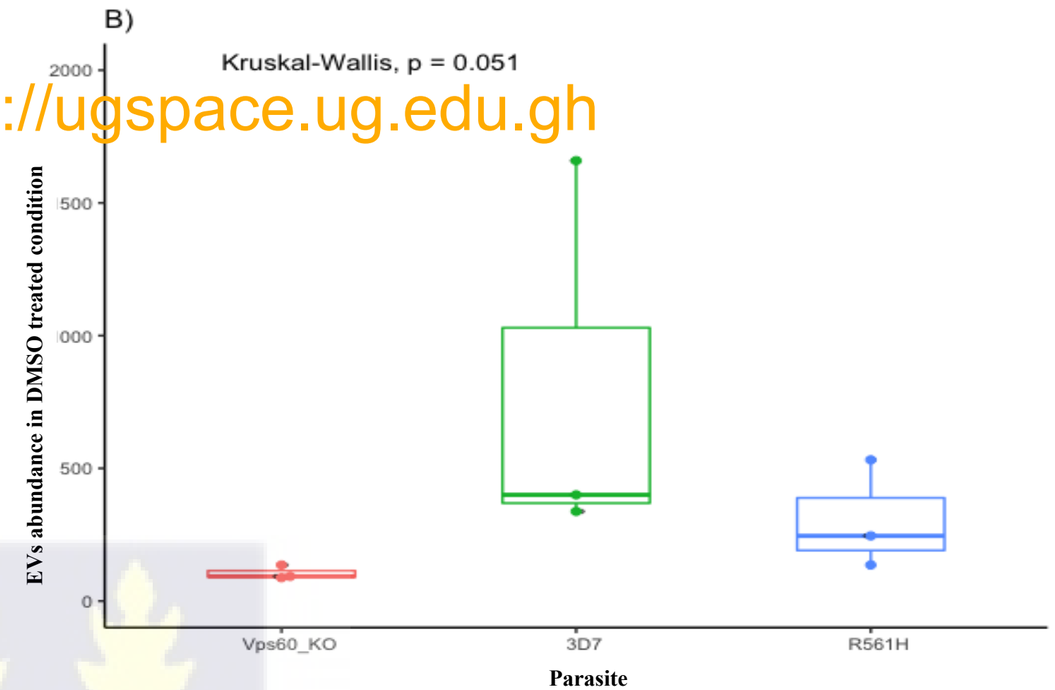

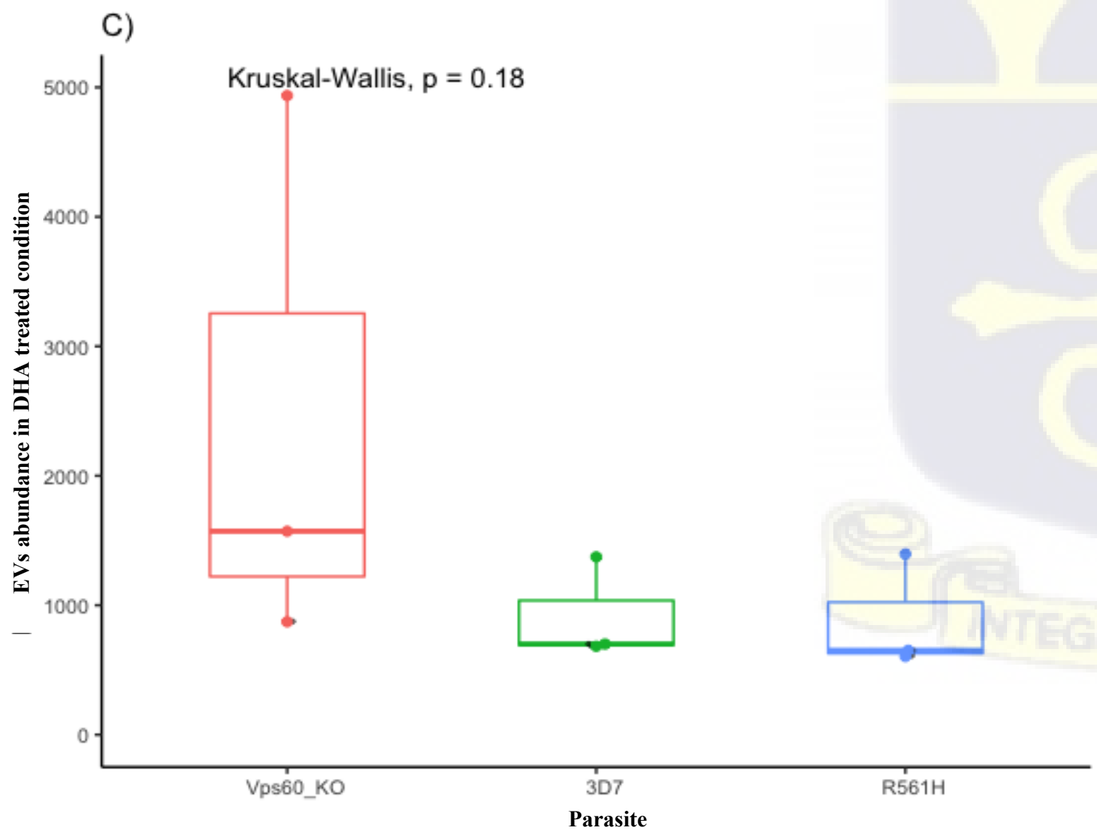

Figure 7.4 Comparison of extracellular vesicles (EVs) abundance among parasite lines for each of the three conditions studied. The objective was to determine the contribution of each parasite's genetic makeup (predictor or independent factor) to EVs abundance (response/dependent factor). We used the null hypothesis that EVs abundance among the 3 parasite lines was equal and the alternate hypothesis that EVs abundance was not equal. 3D7 is the wild-type artemisinin susceptible parasite line with normal EVs biogenesis pathway. Vps60_KO was generated from 3D7 by knocking down the *PfVps60* gene resulting in lower constitutive EVs biogenesis and abundance. R561H is an artemisinin-resistant parasite line CRISPR engineered on a 3D7 background with normal EVs biogenesis pathway. A) In the untreated condition, EVs abundance varied slightly between 3D7 and Vps60, 3D7 and R561H, and Vps60_KO and R561H. None of the paired comparisons yielded a p-value to convincingly reject the null hypothesis. B) In the 0.1% DMSO treated condition, EVs abundance varied between 3D7 and Vps60_KO, 3D7 and R561H, and Vps60_KO and R561H, and yielded a p-value = 0.05. C) In the 700nM DHA treated condition, EVs abundance did not vary between 3D7 and Vps60, 3D7 and R561H, and Vps60 and R561H and was most abundant in Vps60_KO.

University of Ghana http://ugspace.ug.edu.gh

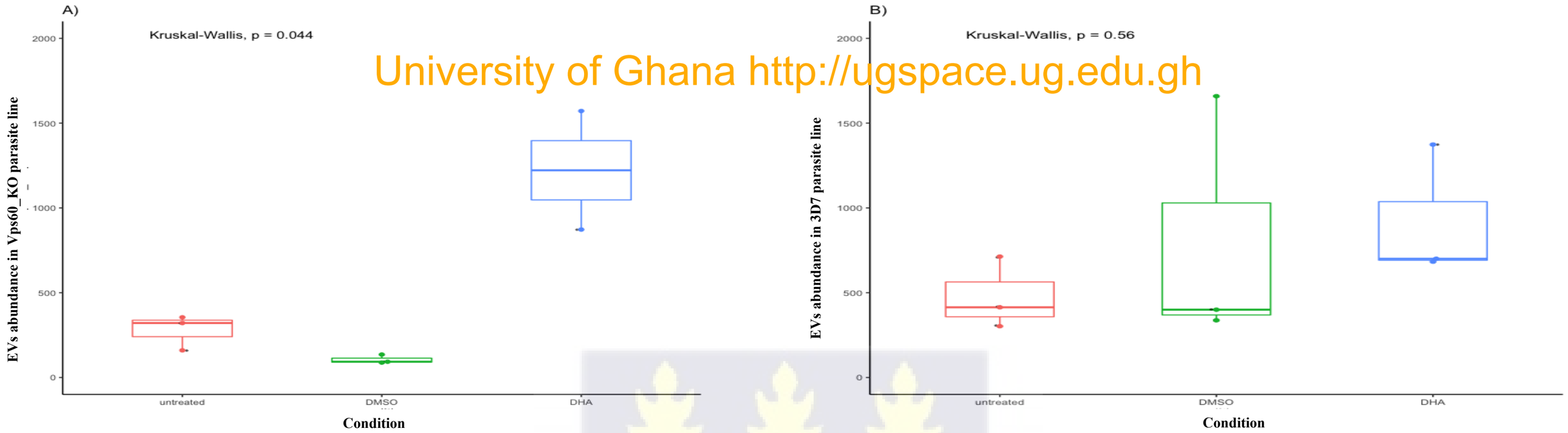

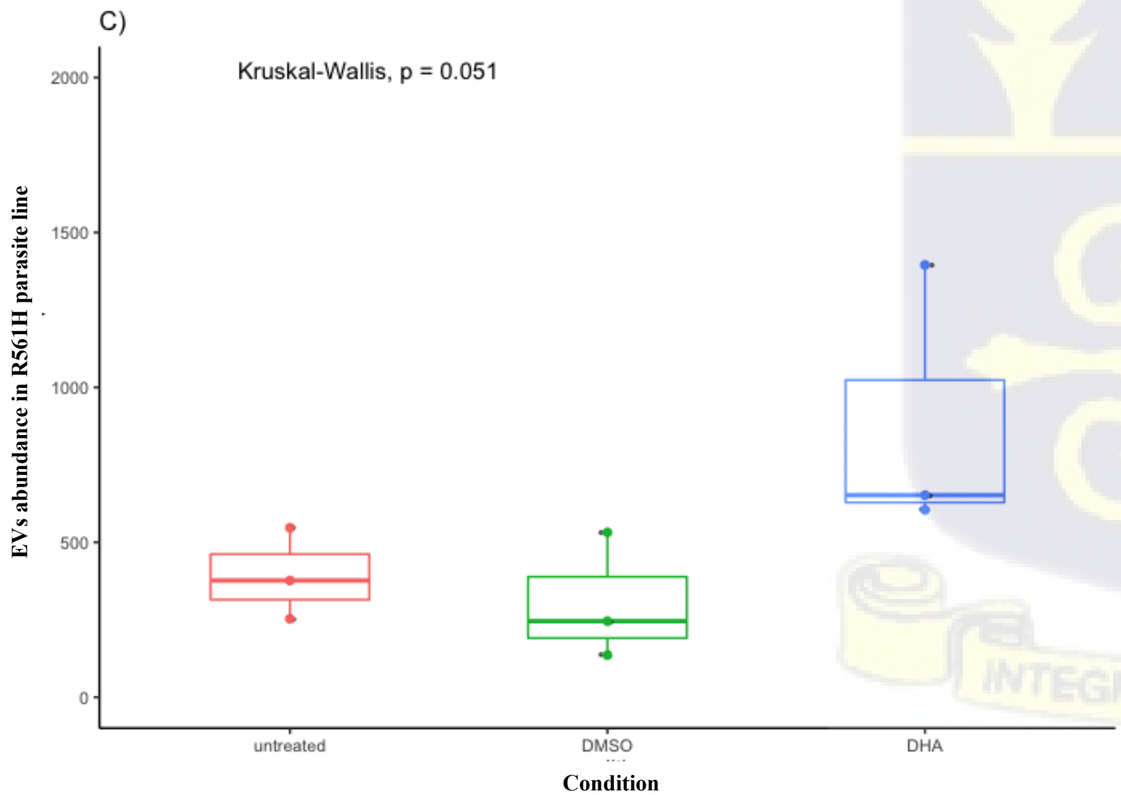

Figure 7.5 Comparison of extracellular vesicles (EVs) abundance between treatment conditions for each parasite line studied. The objective was to determine the contribution of each treatment condition (predictor or independent factor) to EVs abundance (response/dependent factor). We used the null hypothesis that EVs abundance among the 3 conditions was equal and the alternate hypothesis that EVs abundance was not equal. 3D7 is the wild-type artemisinin susceptible parasite line with normal EVs biogenesis pathway. Vps60 was generated from 3D7 by knocking down the *PfVps60* gene resulting in lower constitutive EVs biogenesis and abundance. R561H is an artemisinin-resistant parasite line CRISPR engineered on a 3D7 background with normal EVs biogenesis pathway. A) In the Vps60_KO parasite, EVs abundance varied between untreated versus DMSO treated, untreated versus DHA treated, and DMSO treated versus DHA treated. Paired comparisons yielded a p-value to convincingly reject the null hypothesis. B) In the 3D7 parasite, EVs abundance varied between untreated versus DMSO treated, untreated versus DHA treated, and DMSO treated versus DHA treated although none of the paired comparisons yielded a p-value to convincingly reject the null hypothesis. C) In the R561H parasite, EVs abundance varied between untreated versus DMSO treated, untreated versus DHA treated, and DMSO treated versus DHA treated and yielded a p-value to marginally reject the null hypothesis.

Table 7.2 Post-hoc Dunn's test for the factors: parasite lines (3D7, Vps60 and R561H0) and treatment condition (untreated, DMSO treated, and DHA treated)

University of Ghana http://ugspace.ug.edu.gh

Categorical factor	Comparison	Z	P.unadj	P.adj
Untreated condition	3D7 versus R561H	0.4472136	0.6547208	0.6547208
	3D7 versus Vps60_KO	1.3416408	0.1797125	0.5391375
	R561H versus Vps60_KO	0.8944272	0.3710934	0.5566401
DMSO treated condition	3D7 versus R561H	0.745356	0.45605654	0.45605654
	3D7 versus Vps60_KO	**2.385139**	**0.01707266**	**0.05121798***
	R561H versus Vps60_KO	1.639783	0.10105026	0.15157538
DHA treated condition	3D7 versus R561H	0.4472136	0.6547208	0.6547208
	3D7 versus Vps60_KO	-1.3416408	0.17971249	0.2695687
	R561H versus Vps60_KO	-1.7888544	0.07363827	0.2209148
3D7 parasite line	DHA versus DMSO	0.7453560	0.4560565	0.6840848
	DHA versus untreated	1.0434984	0.2967175	0.8901526
	DMSO versus untreated	0.2981424	0.7655945 5	0.7655945
Vps60 parasite line	**DHA versus DMSO**	**2.683282**	**0.007290358**	**0.02187107***
	DHA versus untreated	1.341641	0.179712495	0.17971249
	DMSO versus untreated	-1.341641	0.179712495	0.26956874
R561H parasite line	**DHA versus DMSO**	**2.385139**	**0.01707266**	**0.05121798***
	DHA versus untreated	1.639783	0.10105026	0.15157538
	DMSO versus untreated	-0.745356	0.45605654	0.45605654

University of Ghana http://ugspace.ug.edu.gh

7.4.4 DHA exposure is the strongest predictor of EVs abundance

Having determined that both parasite line and treatment condition may contribute to EVs abundance, we used both factors as independent predictor variables in a multivariate simple linear regression model to determine the strength and statistical significance of their association with EVs abundance. DHA treated condition was positively correlated with EVs abundance (coefficient estimate = 1038.58, confidence interval of 194.86 – 1882.30 and p-value = 0.018) (Table 7.3, Figure 7.6).

University of Ghana http://ugspace.ug.edu.gh

Table 7.3 Simple linear regression model to determine the strength of the association between parasite line and treatment condition (predictor/independent factors) and EVs abundance (response/dependent factor). The baseline reference to which parasite lines were compared to is Vps60_KO, and untreated for the treatment conditions.

	EVs abundance (mega counts)		
Predictors	**Estimates**	**Confidence interval**	**p**
(Intercept)	595.23	-174.98 – 1365.44	0.123
condition DMSO	20.45	-823.27 – 864.18	0.960
condition DHA	**1038.58**	**194.86 – 1882.30**	**0.018***
parasite 3D7	-216.71	-1060.43 – 627.01	0.600
parasite R561H	-421.42	-1265.14 – 422.30	0.312
Observations	**27**		
R^2 / R^2 adjusted	**0.304 / 0.177**		

University of Ghana http://ugspace.ug.edu.gh

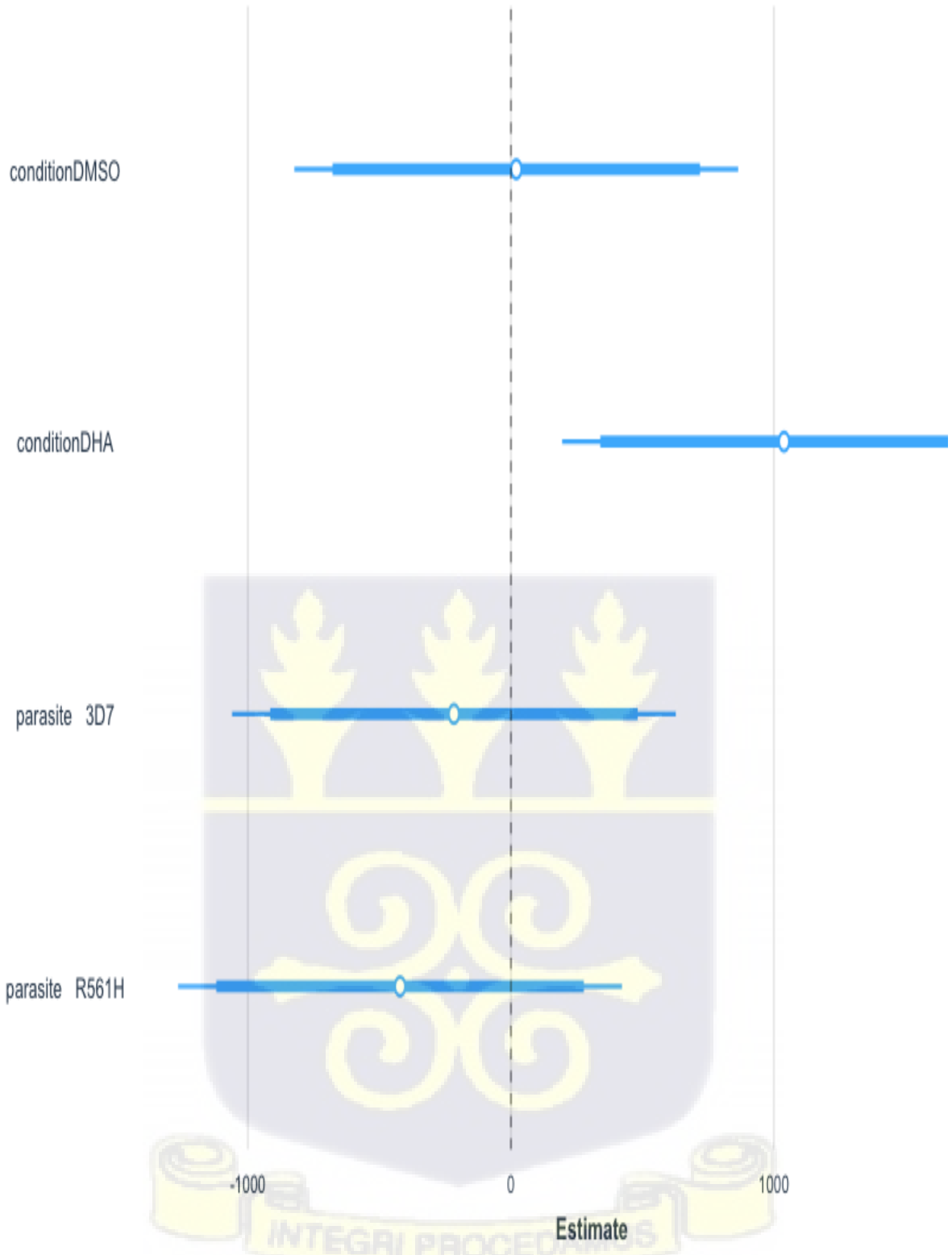

Figure 7.6 The strength of the association between treatment condition and parasite line and EVs abundance. Treatment condition factors were compared to the untreated condition baseline and parasite lines were compared to the 3D7 baseline.

University of Ghana http://ugspace.ug.edu.gh

7.5 Discussion

We hypothesized a role for EVs in the ARTr phenotype within the framework of an EVs export model of ARTr (Tandoh et al., 2022) which predicts that EVs abundance, in an ARTr parasite line, under DHA exposure will be increased. The EVs export model further posits that this increase in EVs biogenesis serves to weather ART-induced proteinopathy and is part of the molecular mechanisms undergirding the ARTr phenotype. To test this hypothesis, we compared EVs abundance between an ARTr line (R561H), an ART-sensitive line (3D7) and an EVs biogenesis deficient line (Vps60_KO). We report that DHA exposure for all parasite lines is positively correlated with EVs abundance and recapitulates the EVs wild-type phenotype in the Vps60_KO line (Figure 7.4, 7.5 and Table 7.1). EVs biogenesis in *P. falciparum* is achieved by an ESCRT-III complex activated by an alternative pathway for the recruitment of PfBro1 and PfVps32/Vps60. In the Vps60_KO line, baseline EVs abundance in the control DMSO condition was lower compared to the wildtype 3D7 (Table 7.1, Figure 7.4) and elevated in the DHA-treated condition compared to both 3D7 and R561H. This finding suggests the induction, by DHA, of an alternative EVs biogenesis pathway in *P. falciparum*.

We sort to ensure the validity of the derived EVs abundance count to enable comparison between parasite lines and treatment conditions. Therefore, we controlled for *in vitro* culture parasitemia, dilution factors during EVs extraction, duration of EVs count during the Zetasizer analysis, and EVs size distribution (Figure 7.1, Supplementary Table 7.1). By controlling for EVs size distribution (Figure 7.3, Supplementary Table 7.3), we effectively controlled for the effect of infected erythrocyte death and cellular debris as confounders of EVs abundance.

University of Ghana http://ugspace.ug.edu.gh

We expected that the comparison between 3D7 and Vps60 for the untreated and DMSO treated conditions will show statistically significant (p-value <0.05) differences with the greater EVs abundance seen in 3D7 (Avalos-Padilla et al., 2021). However, the lack of statistical significance in the comparison of Vps60 and 3D7 EVs abundance for the untreated condition (Figure 7.3, Table 7.2) may be explained by the presence of outliers in the replicates used and their contribution to within-sample variance (Supplementary Table 7.1). This expected difference in EVs abundance between 3D7 and Vps60 was seen, with marginal statistical significance, in the DMSO-treated control arm (Figure 7.4, Table 7.2).

As the EVs biogenesis machinery is similar across the parasite lines used, it was expected that there will be no differences in EVs abundance between 3D7 and R561H for both the untreated and DMSO treated conditions (Table 7.2). Additionally, as DMSO treated condition was used as a solvent/vehicle control for the DHA treated condition, no differences in EVs abundance between both conditions were expected (Table 7.2). We did expect and found differences in EVs abundance between DHA and DMSO treated conditions for Vps60 and R561H parasite lines (Table 7.2, Figure 7.4). 3D7 did show comparable EVs abundance for untreated and DMSO treated conditions and relatively larger EVs abundance under DHA (Table 7.1). However, the difference between EVs abundance in DHA versus DMSO/untreated was not statistically significant (Table 7.2, Figure 7.5).

University of Ghana http://ugspace.ug.edu.gh

Our finding that DHA is positively correlated with EVs abundance suggests a role for the EVs biogenesis pathway in the *P. falciparum* response to DHA. DHA action is known to involve the alkylation of parasite proteins, the induction of a global proteotoxic state and the activation of the unfolded protein response (Tandoh et al., 2022). We hypothesized that, under this DHA-induced effect, EVs biogenesis is induced to affect the removal of accumulating alkylated and ubiquitinated proteins. Thus, our finding of increased EVs abundance in all parasite lines under DHA-treated condition, support the plausibility of the EVs export model of ARTr.

I recognize the following limitations. Although our experimental design and current knowledge on EVs biogenesis in *P. falciparum* did not allow us to control for EVs biogenesis pathways and differentiate exosomes from microvesicles, we are confident in the robustness of our experimental design that showed the enrichment of EVs of similar average size across parasite lines for all conditions (Figure 7.3, Supplementary Table 7.2). Our assumption of a linear relationship between EVs abundance and parasitemia, parasite line and treatment condition was made *a priori* and used downstream. Finally, our study design will have benefitted from more technical replicates of the sample conditions. Our sample size may have hindered the power of our analysis to determine the strength of the association between DHA exposure and EV abundance.

In conclusion, DHA exposure is positively correlated with EVs abundance and recapitulates the wildtype EVs biogenesis phenotype in Vps60_KO. This suggests that EVs play a role in the parasite response to ART and thus the development of the ARTr phenotype. Our testing of the first prediction of the EVs export model showed its plausibility. Further studies testing the other predictions of the EVs export model are merited.

University of Ghana http://ugspace.ug.edu.gh

CHAPTER EIGHT

GENERAL DISCUSSION AND CONCLUSIONS

8.1 General Discussion

In humans, understanding disease and how to design interventions to cure, alleviate or eradicate it is the overarching principle employed in biomedical research. Ergo, understanding disease-causing organisms are vital to humanity's quest to understand disease, mitigate its impact on human life and ultimately cure it. Human parasite infections contribute a huge toll to the disease burden of many populations. In this regard malaria caused by *P. falciparum* can be regarded as perhaps the most important. Malaria parasites, particularly *P. falciparum* has weathered the onslaught of history and modernity's chemotherapeutic and public health intervention assaults to remain intractably relevant today, especially in SSA. This unrelenting relevance stems from the ability of *P. falciparum* populations to survive in human populations by adapting to the harsh milieu enforced by the combination of human immunity and chemotherapeutic pressures. Today, principles and findings in the study of *Plasmodium* genomics and genetics have contributed to the advancement of knowledge on parasite drug resistance, population structure, drug and vaccine targets and host-parasite interactions.

University of Ghana http://ugspace.ug.edu.gh

The emergence of ARTr *P. falciparum* parasites in SEA in 2008 portended the historical spread of it to SSA and evoked a response for risk mitigation interventions. In this regard, molecular surveillance for ARTr parasites in countries with endemic malaria including Ghana is very important. Deepening our understanding of the molecular mechanisms undergirding ARTr in *P. falciparum* also serves as another important risk mitigation approach. The unique genetic architecture of ARTr *P. falciparum* parasites is centered on a loss of function mutation of the *PfK13* gene. Multiple levels of evidence from genetic association studies, genetic editing studies and *PfK13*-interactome studies have unveiled several *PfK13* variants associated with the ARTr phenotype and have also reported *PfK13*-independent ART resistance in *P. falciparum* (Siddiqui et al., 2021). A corollary to this fact about *PfK13*-dependent ARTr is the question of whether a country or regionally defined population of *P. falciparum* parasites will evolve ART resistance via *PfK13*-dependent or *PfK13*-independent pathways. This problem is important because screening for *PfK13* in a population of malaria parasites that may develop ARTr via a *PfK13*-independent path may result in misses at best.

ART was introduced into the vestibule of western medicine following anecdotal success in Chinese herbal medicine practice. Chemotherapy with ACT is arguably the most essential arm of malaria control today. However, the persistent emergence of drug resistance to antimalarial drugs is a constant sword of Damocles for this control strategy. The reason is simple. Drawing from population genetics principles, the presence of a selection pressure like drug exposure will inevitably drive the evolution of parasite strains that have a fitness advantage under the drug pressure. Therefore, this arguably loops malaria chemotherapy and drug resistance in a vicious cycle. The resulting constant evolution of malaria parasites in the human host has spawned the emergence of drug resistance to every known antimalarial drug developed.

University of Ghana http://ugspace.ug.edu.gh

Therefore, unravelling the undercurrents of this evolutionary adaptation and understanding its molecular architecture is a sound strategy to employ in the fight against malaria drug resistance. Furthermore, the central pillar of molecular evolutionary theory sits astride the motif that selection on diversity drives the changes in a population genome pool and reflects an adaptation of the population to the selection pressure. Thus, identifying and predicting the early signature of drug resistance evolution will be a welcome tool in humanity's arsenal in the fight against malaria. To explore this idea, objective one of this thesis was devoted to leveraging the power of NGS, on the unique genomic architecture of ARTr *P. falciparum* parasites, to determine whether parasites in Ghana will evolve PfK13-dependent ART resistance and explore the development of a predictive tool for ARTr. My findings laid the groundwork for future studies in this quest.

One of the main limitations of my analysis of this objective was highlighted as the discord between the positive value of Tajima's D (and my interpretation of these as evidently suggestive of balancing selection) and the other metrics of balancing selection. I defend this by contending that the variance between Tajima's D, MK and HKA reflects the inherent strengths of these tools to detect signatures of balancing selection along a temporal scale. Tajima's D is a site frequency spectrum metric and is a good tool to detect recent or intermediate signatures of balancing selection. HKA looks at trans-species polymorphism and is for detecting the presence of ancient signatures of balancing selection. MK looks at an excess of non-synonymous over synonymous variants and is good for detecting the presence of intermediate and ancient signatures of selection (Casillas et al., 2017).

University of Ghana http://ugspace.ug.edu.gh

My finding of signatures of balancing selection in the two genes that have been reported serving as background loci on which PfK13-driven ART resistance emerges, provides empirical proof to support the use of the *PfK13* molecular marker for molecular surveillance in Ghana. As far as I know, this is the first study to conceptualize this idea and shape its findings into meaningful translational context for molecular surveillance of ARTr malaria parasites. It will be interesting to conduct the same analysis along country lines in the Pf3k dataset to determine the likely path of evolution towards ARTr and corroborate molecular surveillance with the *PfK13* molecular marker. Finally, I have laid the foundations for the future exploration of a predictive forecasting model, that leverages the unique genomic architecture of ARTr *P. falciparum* parasites.

The presence of more than one genetic parasite line of a particular species of *Plasmodium* in a human host constitutes MOI. In *P. falciparum* malaria, high transmission rates in endemic regions drive the phenomenon of MOI in human hosts. The impact of MOI in confounding population genetics metrics is well known and accounted for by filtering out such samples. Whole genome datasets can be used to determine within sample heterozygosity (Fws) indices and the metric is used to identify MOI (Fws < 0.95). Additionally, MOI is considered to delay the emergence of multi-loci genetic variants that confer drug resistance in malaria parasites. This is because a high MOI increases the likelihood of recombination events during the sexual phase in the mosquito vector, breaking down resistance-conferring multi-loci variants. Thus, delaying the emergence of known predisposing background genome variants associated with ART resistance in regions with high MOI such as Ghana. I found fifty-four percent of samples analyzed with MOI in the Ghana cohort. This was expected and is in concordance with studies that report a higher range of MOI in Ghana, compared to the SEA, the ground zero of ART resistance emergence (Lamptey et al., 2018; Abukari et al., 2019).

University of Ghana http://ugspace.ug.edu.gh

The significance of this confirms the importance of the question I posed in objective one. This is because the relatively higher proportion of MOI observed in the Ghana cohort of samples analyzed suggests that MOI may contribute to the delay in the emergence of the variants at the ART resistance predisposing background genetic loci.

Considering the varied ecological belts and transmission rates that define the northern, middle and southern zones of Ghana, these proxies of immune and drug selection pressures may have driven the evolution of different zone-defined populations of malaria parasites. If this initial lack of genetic homogeneity was not accounted for, it will serve as a source of significant confounding in the analysis of population genetics metrics of the Ghana cohort. Therefore, I interrogated this problem using principal component analysis and identified that there was no such expected population structure. The significance of this finding is that the known differences in transmission rates of the three ecological zones of Ghana, as of 2010, did not represent significant differences in the proxy selection pressures of drug and immune pressure. It will be interesting to follow this analysis on a temporal axis to determine whether the pattern changes.

The discovery of chemotherapeutic drugs and their application in modern medicine has been the anchor holding a significant proportion of our successes in the fight against malaria. Purposeful drug discovery is heavily dependent on deepening our understanding and knowledge of the parasite's biology. EVs are ubiquitous vehicles observed in the biology of *P. falciparum* and malaria disease. Whether and how EVs play a role in developing ART resistance was the question explored in objectives 2 and 3 of this thesis.

University of Ghana http://ugspace.ug.edu.gh

Against the backdrop of what we know about the molecular mechanisms undergirding ARTr, I posited that the gene expression profiles of isogenetically similar ARTr parasites with different PfK13 variants will not be the same. I used the spearman correlation coefficient to determine how correlated the gene expression profiles of C580R and R539T are under DHA exposure and compared them to the untreated and DMSO baselines. I found a correlation coefficient that highlights the moderately poor correlation in gene expression profiles between ARTr parasite lines. Additionally, a PCA of the gene expression profile drew the same conclusions. This finding is in concordance with other reports that have intimated the non-homogeneous population of ARTr parasites (Zhu et al., 2022). The significance of this finding lies in the inherent inability of bulk RNA sequencing to provide enough resolution power in gene expression analysis. In this regard, future studies will be better powered to analyze the gene expression profiles of ARTr parasites by utilizing single-cell gene expression techniques. I did not use tightly synchronized cultures during the exposure to the varied conditions (untreated, 0.1%DMSO and DHA). This is a limitation of the experimental design and makes this interpretation of the non-homogeneity in expression profiles a cautious one. Furthermore, this limitation may have accounted for the lack of concordance between my findings and that shared by Mok and others and Zhu and others (Mok et al., 2021; Zhu et al., 2022).

Traditional gene expression analysis identifies differentially expressed genes and relies on known gene ontology libraries to identify biological processes and pathways of interest to the phenotype under investigation. This approach has two weaknesses: first is the reductionist approach that assumes that significant differences in gene expression between and among conditions are entirely driven by highly expressed single gene units. This assumption is fundamentally not foolproof to weakness as we know that genes hardly work individually to affect the emergence of a phenotype and that a gene does not have to be highly expressed to drive the emergence of a phenotype. This is where a systems biology non-reductionist design

University of Ghana http://ugspace.ug.edu.gh

proves the better approach. The second weakness has to do with the reliance on the known in gene ontology analysis.

This means that making discoveries into a little-known process like EVs biogenesis in *P. falciparum* is likely to yield little insight following gene ontology analysis. I demonstrated the validity of this position. To bypass these limitations, I employed the use of a modular analysis approach in the analysis of the gene expression data to interrogate the role of EVs in developing ARTr.

PfVps60 was reported as a gene of importance to developing ARTr by (Avalos-Padilla et al., 2021). It was interesting to find that the PfVps60 module was associated with ARTr following the modular analysis of the gene expression dataset. I think this is the first evidence that implicates EVs in ARTr outside the earlier reported context of parasite-parasite communication. I used this finding to framework the EVs export hypothesis and tested one of its many predictions in my final objective.

The EVs export hypothesis represents the synthesis of my conceptual understanding of ARTr and its amalgamation with the existing body of literature. Its first inkling of veracity came from the findings of the exploratory gene expression analysis conducted in objective 2. Arguably still tenuous at this stage, I sought to test its veracity further. The EVs export hypothesis predicts that EVs abundance will be altered in an ARTr line under DHA pressure. The EVs export hypothesis presents a new paradigm for the interrogation of the molecular mechanisms undergirding ARTr. Our finding of a positive correlation between DHA exposure and nanoparticle EVs abundance in *P. falciparum* suggests a role, albeit tenuous, for EVs in ARTr development. What remains to be explored is the cargo of these EVs and whether they carry the misfolded and ubiquitinated proteins predicted by the EVs export hypothesis.

University of Ghana http://ugspace.ug.edu.gh

A critique of the EVs export hypothesis is the observation of a baseline high level of misfolded proteins with unlikely toxicity to the parasite's viability. Additionally, there is the conceptual argument that ART-induced proteinopathy is unlikely to be singularly offset by an EVs vehicle export. Both arguments make counterarguments to the plausibility of the EVs export hypothesis. In this regard, further wet-lab experiments to provide empirical answers are needed.

In summary, this work makes the following recommendations. Firstly, from objective 1, it is recommended that prospective genomic surveillance studies for signatures of balancing selection in ARTr precursor background genes be done. Such studies could detect the earliest signatures of the evolution of ART-resistant parasites and could serve as a molecular early warning system for ARTr emergence. Secondly, from objectives 2 and 3, further studies investigating the predictions of the EVs export hypothesis are needed to establish the veracity of EVs biogenesis as a potentially novel druggable space for antimalarial drug discovery purposes.

University of Ghana http://ugspace.ug.edu.gh

8.2 General Conclusions and Future Directions

In summary, I have demonstrated the novelty of scanning the genome of malaria parasites for signatures of balancing selection in known ARTr predisposing genes. My finding of signatures of balancing selection in two known PfK13-ARTr predisposing genes suggest a PfK13-dependent evolution of ARTr *P. falciparum* parasites in Ghana. My data provides evidence to support molecular surveillance of ARTr *P. falciparum* parasites in Ghana by searching for PfK13 ARTr-conferring variants. Furthermore, by leveraging the unique genetic architecture of the ARTr phenotype in *P. falciparum*, my approach has the potential to be explored further towards the goal of developing a public health early warning molecular surveillance tool to forecast the emergence of ARTr. This nascent idea that seeks to compliment molecular surveillance from a descriptive to forecasting/predictive motif has the potential to change how we fight malaria. In this vein, input of factors such as local transmission, population MOI, estimated recombination rate in mosquito vector, and estimated sub-lethal ART exposure incorporated into a Bayesian platformed model can be explored.

Searching for novel antimalarial drug targets in the potentially druggable space of *P. falciparum*'s EVs biogenesis pathway is the second future direction I highlight. This recommendation is hinged on my use of a novel transcriptome-module association analysis to show that EVs biogenesis may be part of *P. falciparum*'s response to ART exposure. I proposed a novel hypothetical framework for the role of EVs in developing the ARTr phenotype and tested one of the predictions of this EVs export hypothesis. Overall, by implicating EVs in the mechanistic underpinnings of ARTr development, I posit a potentially new druggable space for novel anti-malarial drug discovery.

University of Ghana http://ugspace.ug.edu.gh

REFERENCES

Abdi, A., Yu, L., Goulding, D., Rono, M. K., Bejon, P., Choudhary, J., & Rayner, J. (2017). Proteomic analysis of extracellular vesicles from a plasmodium falciparum kenyan clinical isolate defines a core parasite secretome. *Wellcome open research, 2*.

Abels, E. R., & Breakefield, X. O. (2016). Introduction to extracellular vesicles: Biogenesis, rna cargo selection, content, release, and uptake. *Cell Mol Neurobiol, 36*(3), 301-312. doi:10.1007/s10571-016-0366-z

Abu Bakar, N., Klonis, N., Hanssen, E., Chan, C., & Tilley, L. (2010). Digestive-vacuole genesis and endocytic processes in the early intraerythrocytic stages of plasmodium falciparum. *J Cell Sci, 123*(Pt 3), 441-450. doi:10.1242/jcs.061499

Abuaku, B., Duah, N., Quaye, L., Quashie, N., & Koram, K. (2012). Therapeutic efficacy of artemether-lumefantrine combination in the treatment of uncomplicated malaria among children under five years of age in three ecological zones in ghana. *Malar J, 11*, 388. doi:10.1186/1475-2875-11-388

Abukari, Z., Okonu, R., Nyarko, S. B., Lo, A. C., Dieng, C. C., Salifu, S. P., Gyan, B. A., Lo, E., & Amoah, L. E. (2019). The diversity, multiplicity of infection and population structure of p. Falciparum parasites circulating in asymptomatic carriers living in high and low malaria transmission settings of ghana. *Genes (Basel), 10*(6). doi:10.3390/genes10060434

Adams, C. J., Kopp, M. C., Larburu, N., Nowak, P. R., & Ali, M. M. U. (2019). Structure and molecular mechanism of er stress signaling by the unfolded protein response signal activator ire1. *Front Mol Biosci, 6*, 11. doi:10.3389/fmolb.2019.00011

University of Ghana http://ugspace.ug.edu.gh

Adams, T., Ennuson, N. A. A., Quashie, N. B., Futagbi, G., Matrevi, S., Hagan, O. C. K., Abuaku, B., Koram, K. A., & Duah, N. O. (2018). Prevalence of plasmodium falciparum delayed clearance associated polymorphisms in adaptor protein complex 2 mu subunit (pfap2mu) and ubiquitin specific protease 1 (pfubp1) genes in ghanaian isolates. *Parasit Vectors, 11*(1), 175. doi:10.1186/s13071-018-2762-3

Aguade, M., Miyashita, N., & Langley, C. H. (1989). Reduced variation in the yellow-achaete-scute region in natural populations of drosophila melanogaster. *Genetics, 122*(3), 607-615. doi:10.1093/genetics/122.3.607

Aguadé, M., Miyashita, N., & Langley, C. H. (1989). Restriction-map variation at the zeste-tko region in natural populations of drosophila melanogaster. *Mol Biol Evol, 6*(2), 123-130. doi:10.1093/oxfordjournals.molbev.a040538

Akers, J. C., Gonda, D., Kim, R., Carter, B. S., & Chen, C. C. (2013). Biogenesis of extracellular vesicles (ev): Exosomes, microvesicles, retrovirus-like vesicles, and apoptotic bodies. *J Neurooncol, 113*(1), 1-11. doi:10.1007/s11060-013-1084-8

Alonso, S., Chaccour, C. J., Elobolobo, E., Nacima, A., Candrinho, B., Saifodine, A., Saute, F., Robertson, M., & Zulliger, R. (2019). The economic burden of malaria on households and the health system in a high transmission district of mozambique. *Malar J, 18*(1), 360. doi:10.1186/s12936-019-2995-4

Amambua-Ngwa, A., Amenga-Etego, L., Kamau, E., Amato, R., Ghansah, A., Golassa, L., Randrianarivelojosia, M., Ishengoma, D., Apinjoh, T., Maïga-Ascofaré, O., Andagalu, B., Yavo, W., Bouyou-Akotet, M., Kolapo, O., Mane, K., Worwui, A., Jeffries, D., Simpson, V., D'Alessandro, U., Kwiatkowski, D., & Djimde, A. A. (2019). Major subpopulations of plasmodium falciparum in sub-saharan africa. *science, 365*(6455), 813-816. doi:10.1126/science.aav5427

University of Ghana http://ugspace.ug.edu.gh

Amambua-Ngwa, A., Tetteh, K. K., Manske, M., Gomez-Escobar, N., Stewart, L. B., Deerhake, M. E., Cheeseman, I. H., Newbold, C. I., Holder, A. A., Knuepfer, E., Janha, O., Jallow, M., Campino, S., Macinnis, B., Kwiatkowski, D. P., & Conway, D. J. (2012). Population genomic scan for candidate signatures of balancing selection to guide antigen characterization in malaria parasites. *PLoS Genet, 8*(11), e1002992. doi:10.1371/journal.pgen.1002992

Amaratunga, C., Lim, P., Suon, S., Sreng, S., Mao, S., Sopha, C., Sam, B., Dek, D., Try, V., Amato, R., Blessborn, D., Song, L., Tullo, G. S., Fay, M. P., Anderson, J. M., Tarning, J., & Fairhurst, R. M. (2016). Dihydroartemisinin-piperaquine resistance in plasmodium falciparum malaria in cambodia: A multisite prospective cohort study. *Lancet Infect Dis, 16*(3), 357-365. doi:10.1016/s1473-3099(15)00487-9

Amaratunga, C., Sreng, S., Suon, S., Phelps, E. S., Stepniewska, K., Lim, P., Zhou, C., Mao, S., Anderson, J. M., Lindegardh, N., Jiang, H., Song, J., Su, X. Z., White, N. J., Dondorp, A. M., Anderson, T. J., Fay, M. P., Mu, J., Duong, S., & Fairhurst, R. M. (2012). Artemisinin-resistant plasmodium falciparum in pursat province, western cambodia: A parasite clearance rate study. *Lancet Infect Dis, 12*(11), 851-858. doi:10.1016/s1473-3099(12)70181-0

Ameme, D. K., Afari, E. A., Nyarko, K. M., Malm, K. L., Sackey, S., & Wurapa, F. (2014). Direct observation of outpatient management of malaria in a rural ghanaian district. *Pan Afr Med J, 19*, 367. doi:10.11604/pamj.2014.19.367.4719

Andaloussi, S. E., Mäger, I., Breakefield, X. O., & Wood, M. J. (2013). Extracellular vesicles: Biology and emerging therapeutic opportunities. *Nature reviews Drug discovery, 12*(5), 347-357.

University of Ghana http://ugspace.ug.edu.gh

Anderson, T. J., Nair, S., Nkhoma, S., Williams, J. T., Imwong, M., Yi, P., Socheat, D., Das, D., Chotivanich, K., Day, N. P., White, N. J., & Dondorp, A. M. (2010). High heritability of malaria parasite clearance rate indicates a genetic basis for artemisinin resistance in western cambodia. *J Infect Dis, 201*(9), 1326-1330. doi:10.1086/651562

Ankarklev, J., Hjelmqvist, D., & Mantel, P.-Y. (2014). Uncovering the role of erythrocyte-derived extracellular vesicles in malaria: From immune regulation to cell communication. *Journal of Circulating Biomarkers, 3*, 3.

Anonymous. (2019). Association of mutations in the plasmodium falciparum kelch13 gene (pf3d7_1343700) with parasite clearance rates after artemisinin-based treatments-a wwarn individual patient data meta-analysis. *BMC Med, 17*(1), 1. doi:10.1186/s12916-018-1207-3

Antwi-Baffour, S., Adjei, J. K., Agyemang-Yeboah, F., Annani-Akollor, M., Kyeremeh, R., Asare, G. A., & Gyan, B. (2016). Proteomic analysis of microparticles isolated from malaria positive blood samples. *Proteome science, 15*(1), 5.

Antwi-Baffour, S., Malibha-Pinchbeck, M., Stratton, D., Jorfi, S., Lange, S., & Inal, J. (2020). Plasma mev levels in ghanain malaria patients with low parasitaemia are higher than those of healthy controls, raising the potential for parasite markers in mevs as diagnostic targets. *J Extracell Vesicles, 9*(1), 1697124. doi:10.1080/20013078.2019.1697124

Aquadro, C. F., Desse, S. F., Bland, M. M., Langley, C. H., & Laurie-Ahlberg, C. C. (1986). Molecular population genetics of the alcohol dehydrogenase gene region of drosophila melanogaster. *Genetics, 114*(4), 1165-1190. doi:10.1093/genetics/114.4.1165

Aravind, L., Iyer, L. M., Wellems, T. E., & Miller, L. H. (2003). Plasmodium biology: Genomic gleanings. *Cell, 115*(7), 771-785. doi:10.1016/s0092-8674(03)01023-7

University of Ghana http://ugspace.ug.edu.gh

Ariey, F., Witkowski, B., Amaratunga, C., Beghain, J., Langlois, A. C., Khim, N., Kim, S., Duru, V., Bouchier, C., Ma, L., Lim, P., Leang, R., Duong, S., Sreng, S., Suon, S., Chuor, C. M., Bout, D. M., Ménard, S., Rogers, W. O., Genton, B., Fandeur, T., Miotto, O., Ringwald, P., Le Bras, J., Berry, A., Barale, J. C., Fairhurst, R. M., Benoit-Vical, F., Mercereau-Puijalon, O., & Ménard, D. (2014). A molecular marker of artemisinin-resistant plasmodium falciparum malaria. *Nature, 505*(7481), 50-55. doi:10.1038/nature12876

Asawamahasakda, W., Ittarat, I., Pu, Y. M., Ziffer, H., & Meshnick, S. R. (1994). Reaction of antimalarial endoperoxides with specific parasite proteins. *Antimicrob Agents Chemother, 38*(8), 1854-1858. doi:10.1128/aac.38.8.1854

Ashley, E. A., Dhorda, M., Fairhurst, R. M., Amaratunga, C., Lim, P., Suon, S., Sreng, S., Anderson, J. M., Mao, S., & Sam, B. (2014). Spread of artemisinin resistance in plasmodium falciparum malaria. *New England journal of medicine, 371*(5), 411-423.

Auburn, S., Campino, S., Miotto, O., Djimde, A. A., Zongo, I., Manske, M., Maslen, G., Mangano, V., Alcock, D., MacInnis, B., Rockett, K. A., Clark, T. G., Doumbo, O. K., Ouédraogo, J. B., & Kwiatkowski, D. P. (2012). Characterization of within-host plasmodium falciparum diversity using next-generation sequence data. *PLoS One, 7*(2), e32891. doi:10.1371/journal.pone.0032891

Avalos-Padilla, Y., Georgiev, V. N., Lantero, E., Pujals, S., Verhoef, R., L, N. B.-C., Albertazzi, L., Dimova, R., & Fernàndez-Busquets, X. (2021). The escrt-iii machinery participates in the production of extracellular vesicles and protein export during plasmodium falciparum infection. *PLoS Pathog, 17*(4), e1009455. doi:10.1371/journal.ppat.1009455

Awine, T., Malm, K., Bart-Plange, C., & Silal, S. P. (2017). Towards malaria control and elimination in ghana: Challenges and decision making tools to guide planning. *Glob Health Action, 10*(1), 1381471. doi:10.1080/16549716.2017.1381471

University of Ghana http://ugspace.ug.edu.gh

Babatunde, K. A., Mbagwu, S., Hernández-Castañeda, M. A., Adapa, S. R., Walch, M., Filgueira, L., Falquet, L., Jiang, R. H., Ghiran, I., & Mantel, P.-Y. (2018). Malaria infected red blood cells release small regulatory rnas through extracellular vesicles. *Scientific reports, 8*(1), 884.

Babatunde, K. A., Subramanian, B. Y., Ahouidi, A. D., Murillo, P. M., Walch, M., & Mantel, P.-Y. (2020). Role of extracellular vesicles in cellular cross talk in malaria. *Frontiers in Immunology, 11*.

Babst, M., Katzmann, D. J., Snyder, W. B., Wendland, B., & Emr, S. D. (2002). Endosome-associated complex, escrt-ii, recruits transport machinery for protein sorting at the multivesicular body. *Dev Cell, 3*(2), 283-289. doi:10.1016/s1534-5807(02)00219-8

Balikagala, B., Fukuda, N., Ikeda, M., Katuro, O. T., Tachibana, S. I., Yamauchi, M., Opio, W., Emoto, S., Anywar, D. A., Kimura, E., Palacpac, N. M. Q., Odongo-Aginya, E. I., Ogwang, M., Horii, T., & Mita, T. (2021). Evidence of artemisinin-resistant malaria in africa. *N Engl J Med, 385*(13), 1163-1171. doi:10.1056/NEJMoa2101746

Barrett, R. D., & Schluter, D. (2008). Adaptation from standing genetic variation. *Trends Ecol Evol, 23*(1), 38-44. doi:10.1016/j.tree.2007.09.008

Bayih, A. G., Getnet, G., Alemu, A., Getie, S., Mohon, A. N., & Pillai, D. R. (2016). A unique plasmodium falciparum k13 gene mutation in northwest ethiopia. *Am J Trop Med Hyg, 94*(1), 132-135. doi:10.4269/ajtmh.15-0477

Bediako, Y., Adams, R., Reid, A. J., Valletta, J. J., Ndungu, F. M., Sodenkamp, J., Mwacharo, J., Ngoi, J. M., Kimani, D., Kai, O., Wambua, J., Nyangweso, G., de Villiers, E. P., Sanders, M., Lotkowska, M. E., Lin, J. W., Manni, S., Addy, J. W. G., Recker, M., Newbold, C., Berriman, M., Bejon, P., Marsh, K., & Langhorne, J. (2019). Repeated clinical malaria episodes are associated with modification of the immune system in children. *BMC Med, 17*(1), 60. doi:10.1186/s12916-019-1292-y

University of Ghana http://ugspace.ug.edu.gh

Beez, D., Sanchez, C. P., Stein, W. D., & Lanzer, M. (2011). Genetic predisposition favors the acquisition of stable artemisinin resistance in malaria parasites. *Antimicrob Agents Chemother, 55*(1), 50-55. doi:10.1128/aac.00916-10

Begun, D. J., & Aquadro, C. F. (1992). Levels of naturally occurring DNA polymorphism correlate with recombination rates in d. Melanogaster. *Nature, 356*(6369), 519-520. doi:10.1038/356519a0

Bejon, P., Andrews, L., Andersen, R. F., Dunachie, S., Webster, D., Walther, M., Gilbert, S. C., Peto, T., & Hill, A. V. (2005). Calculation of liver-to-blood inocula, parasite growth rates, and preerythrocytic vaccine efficacy, from serial quantitative polymerase chain reaction studies of volunteers challenged with malaria sporozoites. *J Infect Dis, 191*(4), 619-626. doi:10.1086/427243

Bennett, P. (2008). Plasmid encoded antibiotic resistance: Acquisition and transfer of antibiotic resistance genes in bacteria. *British journal of pharmacology, 153*(S1), S347-S357.

University of Ghana http://ugspace.ug.edu.gh

Bentley, D. R., Balasubramanian, S., Swerdlow, H. P., Smith, G. P., Milton, J., Brown, C. G., Hall, K. P., Evers, D. J., Barnes, C. L., Bignell, H. R., Boutell, J. M., Bryant, J., Carter, R. J., Keira Cheetham, R., Cox, A. J., Ellis, D. J., Flatbush, M. R., Gormley, N. A., Humphray, S. J., Irving, L. J., Karbelashvili, M. S., Kirk, S. M., Li, H., Liu, X., Maisinger, K. S., Murray, L. J., Obradovic, B., Ost, T., Parkinson, M. L., Pratt, M. R., Rasolonjatovo, I. M., Reed, M. T., Rigatti, R., Rodighiero, C., Ross, M. T., Sabot, A., Sankar, S. V., Scally, A., Schroth, G. P., Smith, M. E., Smith, V. P., Spiridou, A., Torrance, P. E., Tzonev, S. S., Vermaas, E. H., Walter, K., Wu, X., Zhang, L., Alam, M. D., Anastasi, C., Aniebo, I. C., Bailey, D. M., Bancarz, I. R., Banerjee, S., Barbour, S. G., Baybayan, P. A., Benoit, V. A., Benson, K. F., Bevis, C., Black, P. J., Boodhun, A., Brennan, J. S., Bridgham, J. A., Brown, R. C., Brown, A. A., Buermann, D. H., Bundu, A. A., Burrows, J. C., Carter, N. P., Castillo, N., Chiara, E. C. M., Chang, S., Neil Cooley, R., Crake, N. R., Dada, O. O., Diakoumakos, K. D., Dominguez-Fernandez, B., Earnshaw, D. J., Egbujor, U. C., Elmore, D. W., Etchin, S. S., Ewan, M. R., Fedurco, M., Fraser, L. J., Fuentes Fajardo, K. V., Scott Furey, W., George, D., Gietzen, K. J., Goddard, C. P., Golda, G. S., Granieri, P. A., Green, D. E., Gustafson, D. L., Hansen, N. F., Harnish, K., Haudenschild, C. D., Heyer, N. I., Hims, M. M., Ho, J. T., Horgan, A. M., Hoschler, K., Hurwitz, S., Ivanov, D. V., Johnson, M. Q., James, T., Huw Jones, T. A., Kang, G. D., Kerelska, T. H., Kersey, A. D., Khrebtukova, I., Kindwall, A. P., Kingsbury, Z., Kokko-Gonzales, P. I., Kumar, A., Laurent, M. A., Lawley, C. T., Lee, S. E., Lee, X., Liao, A. K., Loch, J. A., Lok, M., Luo, S., Mammen, R. M., Martin, J. W., McCauley, P. G., McNitt, P., Mehta, P., Moon, K. W., Mullens, J. W., Newington, T., Ning, Z., Ling Ng, B., Novo, S. M., O'Neill, M. J., Osborne, M. A., Osnowski, A., Ostadan, O., Paraschos, L. L., Pickering, L., Pike, A. C., Pike, A. C., Chris Pinkard, D., Pliskin, D. P., Podhasky, J., Quijano, V. J., Raczy, C., Rae, V. H., Rawlings, S. R., Chiva Rodriguez, A., Roe, P. M., Rogers, J., Rogert Bacigalupo, M. C., Romanov, N., Romieu, A., Roth, R. K., Rourke, N. J., Ruediger, S. T., Rusman, E., Sanches-Kuiper, R. M., Schenker, M. R., Seoane, J. M., Shaw, R. J., Shiver, M. K., Short, S. W., Sizto, N. L., Sluis, J. P., Smith, M. A., Ernest Sohna Sohna, J., Spence, E. J., Stevens, K., Sutton, N., Szajkowski, L., Tregidgo, C. L.,

University of Ghana http://ugspace.ug.edu.gh

Turcatti, G., Vandevondele, S., Verhovsky, Y., Virk, S. M., Wakelin, S., Walcott, G. C., Wang, J., Worsley, G. J., Yan, J., Yau, L., Zuerlein, M., Rogers, J., Mullikin, J. C., Hurles, M. E., McCooke, N. J., West, J. S., Oaks, F. L., Lundberg, P. L., Klenerman, D., Durbin, R., & Smith, A. J. (2008). Accurate whole human genome sequencing using reversible terminator chemistry. *Nature, 456*(7218), 53-59. doi:10.1038/nature07517

Bergmann, C., van Loon, W., Habarugira, F., Tacoli, C., Jäger, J. C., Savelsberg, D., Nshimiyimana, F., Rwamugema, E., Mbarushimana, D., Ndoli, J., Sendegeya, A., Bayingana, C., & Mockenhaupt, F. P. (2021). Increase in kelch 13 polymorphisms in plasmodium falciparum, southern rwanda. *Emerg Infect Dis, 27*(1), 294-296. doi:10.3201/eid2701.203527

Berry, A. J., Ajioka, J. W., & Kreitman, M. (1991). Lack of polymorphism on the drosophila fourth chromosome resulting from selection. *Genetics, 129*(4), 1111-1117. doi:10.1093/genetics/129.4.1111

Bhanot, P., Schauer, K., Coppens, I., & Nussenzweig, V. (2005). A surface phospholipase is involved in the migration of plasmodium sporozoites through cells. *Journal of Biological Chemistry, 280*(8), 6752-6760.

University of Ghana http://ugspace.ug.edu.gh

Bhattacharjee, S., Coppens, I., Mbengue, A., Suresh, N., Ghorbal, M., Slouka, Z., Safeukui, I., Tang, H.-Y., Speicher, D. W., & Stahelin, R. V. (2018). Remodeling of the malaria parasite and host human red cell by vesicle amplification that induces artemisinin resistance. *Blood*, blood-2017-2011-814665.

Bhisutthibhan, J., & Meshnick, S. R. (2001). Immunoprecipitation of [3h] dihydroartemisinin translationally controlled tumor protein (tctp) adducts from plasmodium falciparum-infected erythrocytes by using anti-tctp antibodies. *Antimicrobial agents and chemotherapy, 45*(8), 2397-2399.

Birnbaum, J., Scharf, S., Schmidt, S., Jonscher, E., Hoeijmakers, W. A. M., Flemming, S., Toenhake, C. G., Schmitt, M., Sabitzki, R., Bergmann, B., Fröhlke, U., Mesén-Ramírez, P., Blancke Soares, A., Herrmann, H., Bártfai, R., & Spielmann, T. (2020). A kelch13-defined endocytosis pathway mediates artemisinin resistance in malaria parasites. *science, 367*(6473), 51-59. doi:10.1126/science.aax4735

Blasco, B., Leroy, D., & Fidock, D. A. (2017). Antimalarial drug resistance: Linking plasmodium falciparum parasite biology to the clinic. *Nat Med, 23*(8), 917-928. doi:10.1038/nm.4381

Borgheti-Cardoso, L. N., & Fernàndez-Busquets, X. (2018). Turning plasmodium survival strategies against itself. *Future Med Chem, 10*(19), 2245-2248. doi:10.4155/fmc-2018-0214

Borrmann, S., Straimer, J., Mwai, L., Abdi, A., Rippert, A., Okombo, J., Muriithi, S., Sasi, P., Kortok, M. M., Lowe, B., Campino, S., Assefa, S., Auburn, S., Manske, M., Maslen, G., Peshu, N., Kwiatkowski, D. P., Marsh, K., Nzila, A., & Clark, T. G. (2013). Genome-wide screen identifies new candidate genes associated with artemisinin susceptibility in plasmodium falciparum in kenya. *Sci Rep, 3*, 3318. doi:10.1038/srep03318

University of Ghana http://ugspace.ug.edu.gh

Botwe, A. K., Asante, K. P., Adjei, G., Assafuah, S., Dosoo, D., & Owusu-Agyei, S. (2017). Dynamics in multiplicity of plasmodium falciparum infection among children with asymptomatic malaria in central ghana. *BMC Genet, 18*(1), 67. doi:10.1186/s12863-017-0536-0

Boudreau, E. F., Webster, H. K., Pavanand, K., & Thosingha, L. (1982). Type ii mefloquine resistance in thailand. *Lancet, 2*(8311), 1335. doi:10.1016/s0140-6736(82)91532-x

Boura, E., Różycki, B., Chung, H. S., Herrick, D. Z., Canagarajah, B., Cafiso, D. S., Eaton, W. A., Hummer, G., & Hurley, J. H. (2012). Solution structure of the escrt-i and -ii supercomplex: Implications for membrane budding and scission. *Structure, 20*(5), 874-886. doi:10.1016/j.str.2012.03.008

Bousema, T., & Drakeley, C. (2011). Epidemiology and infectivity of plasmodium falciparum and plasmodium vivax gametocytes in relation to malaria control and elimination. *Clin Microbiol Rev, 24*(2), 377-410. doi:10.1128/cmr.00051-10

Brancucci, N. M., Gerdt, J. P., Wang, C., De Niz, M., Philip, N., Adapa, S. R., Zhang, M., Hitz, E., Niederwieser, I., & Boltryk, S. D. (2017). Lysophosphatidylcholine regulates sexual stage differentiation in the human malaria parasite plasmodium falciparum. *Cell, 171*(7), 1532-1544. e1515.

Breglio, K. F., Amato, R., Eastman, R., Lim, P., Sa, J. M., Guha, R., Ganesan, S., Dorward, D. W., Klumpp-Thomas, C., & McKnight, C. (2018). A single nucleotide polymorphism in the plasmodium falciparum atg18 gene associates with artemisinin resistance and confers enhanced parasite survival under nutrient deprivation. *Malaria journal, 17*(1), 391.

Bridgford, J. L., Xie, S. C., Cobbold, S. A., Pasaje, C. F. A., Herrmann, S., Yang, T., Gillett, D. L., Dick, L. R., Ralph, S. A., Dogovski, C., Spillman, N. J., & Tilley, L. (2018). Artemisinin kills malaria parasites by damaging proteins and inhibiting the proteasome. *Nat Commun, 9*(1), 3801. doi:10.1038/s41467-018-06221-1

University of Ghana http://ugspace.ug.edu.gh

Bruggeman, F. J., & Westerhoff, H. V. (2007). The nature of systems biology. *Trends Microbiol, 15*(1), 45-50. doi:10.1016/j.tim.2006.11.003

Bushman, M., Antia, R., Udhayakumar, V., & de Roode, J. C. (2018). Within-host competition can delay evolution of drug resistance in malaria. *PLoS Biol, 16*(8), e2005712. doi:10.1371/journal.pbio.2005712

Bushman, M., Morton, L., Duah, N., Quashie, N., Abuaku, B., Koram, K. A., Dimbu, P. R., Plucinski, M., Gutman, J., Lyaruu, P., Kachur, S. P., de Roode, J. C., & Udhayakumar, V. (2016). Within-host competition and drug resistance in the human malaria parasite plasmodium falciparum. *Proc Biol Sci, 283*(1826), 20153038. doi:10.1098/rspb.2015.3038

Bustos, M. D., Wongsrichanalai, C., Delacollette, C., & Burkholder, B. (2013). Monitoring antimalarial drug efficacy in the greater mekong subregion: An overview of in vivo results from 2008 to 2010. *Southeast Asian J Trop Med Public Health, 44 Suppl 1*, 201-230; discussion 306-207.

Carolino, K., & Winzeler, E. A. (2020). The antimalarial resistome - finding new drug targets and their modes of action. *Curr Opin Microbiol, 57*, 49-55. doi:10.1016/j.mib.2020.06.004

Carter, R., & Mendis, K. N. (2002). Evolutionary and historical aspects of the burden of malaria. *Clin Microbiol Rev, 15*(4), 564-594. doi:10.1128/cmr.15.4.564-594.2002

Casillas, S., & Barbadilla, A. (2017). Molecular population genetics. *Genetics, 205*(3), 1003-1035.

Castellini, M. A., Buguliskis, J. S., Casta, L. J., Butz, C. E., Clark, A. B., Kunkel, T. A., & Taraschi, T. F. (2011). Malaria drug resistance is associated with defective DNA mismatch repair. *Mol Biochem Parasitol, 177*(2), 143-147. doi:10.1016/j.molbiopara.2011.02.004

University of Ghana http://ugspace.ug.edu.gh

Cerqueira, G. C., Cheeseman, I. H., Schaffner, S. F., Nair, S., McDew-White, M., Phyo, A. P., Ashley, E. A., Melnikov, A., Rogov, P., Birren, B. W., Nosten, F., Anderson, T. J. C., & Neafsey, D. E. (2017). Longitudinal genomic surveillance of plasmodium falciparum malaria parasites reveals complex genomic architecture of emerging artemisinin resistance. *Genome Biol, 18*(1), 78. doi:10.1186/s13059-017-1204-4

Charlesworth, B. (2010). Molecular population genomics: A short history. *Genetics research, 92*(5-6), 397-411.

Chaussabel, D., & Baldwin, N. (2014). Democratizing systems immunology with modular transcriptional repertoire analyses. *Nat Rev Immunol, 14*(4), 271-280. doi:10.1038/nri3642

Cheeseman, I. H., Miller, B. A., Nair, S., Nkhoma, S., Tan, A., Tan, J. C., Al Saai, S., Phyo, A. P., Moo, C. L., Lwin, K. M., McGready, R., Ashley, E., Imwong, M., Stepniewska, K., Yi, P., Dondorp, A. M., Mayxay, M., Newton, P. N., White, N. J., Nosten, F., Ferdig, M. T., & Anderson, T. J. (2012). A major genome region underlying artemisinin resistance in malaria. *science, 336*(6077), 79-82. doi:10.1126/science.1215966

Chen, N., LaCrue, A. N., Teuscher, F., Waters, N. C., Gatton, M. L., Kyle, D. E., & Cheng, Q. (2014). Fatty acid synthesis and pyruvate metabolism pathways remain active in dihydroartemisinin-induced dormant ring stages of plasmodium falciparum. *Antimicrob Agents Chemother, 58*(8), 4773-4781. doi:10.1128/aac.02647-14

Chenet, S. M., Akinyi Okoth, S., Huber, C. S., Chandrabose, J., Lucchi, N. W., Talundzic, E., Krishnalall, K., Ceron, N., Musset, L., Macedo de Oliveira, A., Venkatesan, M., Rahman, R., Barnwell, J. W., & Udhayakumar, V. (2016). Independent emergence of the plasmodium falciparum kelch propeller domain mutant allele c580y in guyana. *J Infect Dis, 213*(9), 1472-1475. doi:10.1093/infdis/jiv752

University of Ghana http://ugspace.ug.edu.gh

Cheng, Q., Kyle, D. E., & Gatton, M. L. (2012). Artemisinin resistance in plasmodium falciparum: A process linked to dormancy? *Int J Parasitol Drugs Drug Resist, 2*, 249-255. doi:10.1016/j.ijpddr.2012.01.001

Chhibber-Goel, J., & Sharma, A. (2019). Profiles of kelch mutations in plasmodium falciparum across south asia and their implications for tracking drug resistance. *Int J Parasitol Drugs Drug Resist, 11*, 49-58. doi:10.1016/j.ijpddr.2019.10.001

Chiesa, M., Colombo, G. I., & Piacentini, L. (2018). Damirseq-an r/bioconductor package for data mining of rna-seq data: Normalization, feature selection and classification. *Bioinformatics, 34*(8), 1416-1418. doi:10.1093/bioinformatics/btx795

Clark, M., Fisher, N. C., Kasthuri, R., & Cerami Hand, C. (2013). Parasite maturation and host serum iron influence the labile iron pool of erythrocyte stage plasmodium falciparum. *Br J Haematol, 161*(2), 262-269. doi:10.1111/bjh.12234

Coakley, G., Maizels, R. M., & Buck, A. H. (2015). Exosomes and other extracellular vesicles: The new communicators in parasite infections. *Trends Parasitol, 31*(10), 477-489. doi:10.1016/j.pt.2015.06.009

Coelho, C. H., Rappuoli, R., Hotez, P. J., & Duffy, P. E. (2019). Transmission-blocking vaccines for malaria: Time to talk about vaccine introduction. *Trends Parasitol, 35*(7), 483-486. doi:10.1016/j.pt.2019.04.008

Combes, V., Taylor, T. E., Juhan-Vague, I., Mège, J. L., Mwenechanya, J., Tembo, M., Grau, G. E., & Molyneux, M. E. (2004). Circulating endothelial microparticles in malawian children with severe falciparum malaria complicated with coma. *Jama, 291*(21), 2542-2544. doi:10.1001/jama.291.21.2542-b

University of Ghana http://ugspace.ug.edu.gh

Conesa, A., Madrigal, P., Tarazona, S., Gomez-Cabrero, D., Cervera, A., McPherson, A., Szcześniak, M. W., Gaffney, D. J., Elo, L. L., Zhang, X., & Mortazavi, A. (2016). A survey of best practices for rna-seq data analysis. *Genome Biol, 17*, 13. doi:10.1186/s13059-016-0881-8

Conrad, M. D., & Rosenthal, P. J. (2019). Antimalarial drug resistance in africa: The calm before the storm? *Lancet Infect Dis, 19*(10), e338-e351. doi:10.1016/s1473-3099(19)30261-0

Conrad, M. D., Bigira, V., Kapisi, J., Muhindo, M., Kamya, M. R., Havlir, D. V., Dorsey, G., & Rosenthal, P. J. (2014). Polymorphisms in k13 and falcipain-2 associated with artemisinin resistance are not prevalent in plasmodium falciparum isolated from ugandan children. *PLoS One, 9*(8), e105690. doi:10.1371/journal.pone.0105690

Conway, D. (2019). Elementary principles of population genetics. *Lecture Notes*.

Coppée, R., Jeffares, D. C., Miteva, M. A., Sabbagh, A., & Clain, J. (2019). Comparative structural and evolutionary analyses predict functional sites in the artemisinin resistance malaria protein k13. *Sci Rep, 9*(1), 10675. doi:10.1038/s41598-019-47034-6

Core Team, R. (2021). R: A language and environment for statistical computing. *R Foundation for Statistical Computing*.

Correa, R., Coronado, L., Caballero, Z., Faral, P., Robello, C., & Spadafora, C. (2019). Extracellular vesicles carrying lactate dehydrogenase induce suicide in increased population density of plasmodium falciparum in vitro. *Sci Rep, 9*(1), 5042. doi:10.1038/s41598-019-41697-x

Cowell, A. N., Istvan, E. S., Lukens, A. K., Gomez-Lorenzo, M. G., Vanaerschot, M., Sakata-Kato, T., Flannery, E. L., Magistrado, P., Owen, E., & Abraham, M. (2018). Mapping the malaria parasite druggable genome by using in vitro evolution and chemogenomics. *Science, 359*(6372), 191-199.

Cowman, A. F., Healer, J., Marapana, D., & Marsh, K. (2016). Malaria: Biology and disease. *Cell, 167*(3), 610-624.

University of Ghana http://ugspace.ug.edu.gh

Cui, L., Wang, Z., Miao, J., Miao, M., Chandra, R., Jiang, H., Su, X. z., & Cui, L. (2012b). Mechanisms of in vitro resistance to dihydroartemisinin in plasmodium falciparum. *Molecular microbiology, 86*(1), 111-128.

Cui, L., Yan, G., Sattabongkot, J., Cao, Y., Chen, B., Chen, X., Fan, Q., Fang, Q., Jongwutiwes, S., Parker, D., Sirichaisinthop, J., Kyaw, M. P., Su, X. Z., Yang, H., Yang, Z., Wang, B., Xu, J., Zheng, B., Zhong, D., & Zhou, G. (2012a). Malaria in the greater mekong subregion: Heterogeneity and complexity. *Acta Trop, 121*(3), 227-239. doi:10.1016/j.actatropica.2011.02.016

Dai, X., Zhang, X., Chen, W., Chen, Y., Zhang, Q., Mo, S., & Lu, J. (2021). Dihydroartemisinin: A potential natural anticancer drug. *Int J Biol Sci, 17*(2), 603-622. doi:10.7150/ijbs.50364

Demas, A. R., Sharma, A. I., Wong, W., Early, A. M., Redmond, S., Bopp, S., Neafsey, D. E., Volkman, S. K., Hartl, D. L., & Wirth, D. F. (2018). Mutations in plasmodium falciparum actin-binding protein coronin confer reduced artemisinin susceptibility. *Proceedings of the National Academy of Sciences, 115*(50), 12799-12804.

DePristo, M. A., Zilversmit, M. M., & Hartl, D. L. (2006). On the abundance, amino acid composition, and evolutionary dynamics of low-complexity regions in proteins. *Gene, 378*, 19-30. doi:10.1016/j.gene.2006.03.023

Dogovski, C., Xie, S. C., Burgio, G., Bridgford, J., Mok, S., McCaw, J. M., Chotivanich, K., Kenny, S., Gnädig, N., & Straimer, J. (2015). Targeting the cell stress response of plasmodium falciparum to overcome artemisinin resistance. *PLoS biology, 13*(4).

Dondorp, A. M., & Ringwald, P. (2013). Artemisinin resistance is a clear and present danger. *Trends Parasitol, 29*(8), 359-360. doi:10.1016/j.pt.2013.05.005

University of Ghana http://ugspace.ug.edu.gh

Dondorp, A. M., Newton, P. N., Mayxay, M., Van Damme, W., Smithuis, F. M., Yeung, S., Petit, A., Lynam, A. J., Johnson, A., Hien, T. T., McGready, R., Farrar, J. J., Looareesuwan, S., Day, N. P., Green, M. D., & White, N. J. (2004). Fake antimalarials in southeast asia are a major impediment to malaria control: Multinational cross-sectional survey on the prevalence of fake antimalarials. *Trop Med Int Health, 9*(12), 1241-1246. doi:10.1111/j.1365-3156.2004.01342.x

Dondorp, A. M., Nosten, F., Yi, P., Das, D., Phyo, A. P., Tarning, J., Lwin, K. M., Ariey, F., Hanpithakpong, W., Lee, S. J., Ringwald, P., Silamut, K., Imwong, M., Chotivanich, K., Lim, P., Herdman, T., An, S. S., Yeung, S., Singhasivanon, P., Day, N. P., Lindegardh, N., Socheat, D., & White, N. J. (2009). Artemisinin resistance in plasmodium falciparum malaria. *N Engl J Med, 361*(5), 455-467. doi:10.1056/NEJMoa0808859

Dores, M. R., Paing, M. M., Lin, H., Montagne, W. A., Marchese, A., & Trejo, J. (2012). Ap-3 regulates par1 ubiquitin-independent mvb/lysosomal sorting via an alix-mediated pathway. *Mol Biol Cell, 23*(18), 3612-3623. doi:10.1091/mbc.E12-03-0251

Douglas, R. G., Amino, R., Sinnis, P., & Frischknecht, F. (2015). Active migration and passive transport of malaria parasites. *Trends Parasitol, 31*(8), 357-362. doi:10.1016/j.pt.2015.04.010

Duah, N. O., Matrevi, S. A., Quashie, N. B., Abuaku, B., & Koram, K. A. (2016). Genetic diversity of plasmodium falciparum isolates from uncomplicated malaria cases in ghana over a decade. *Parasit Vectors, 9*(1), 416. doi:10.1186/s13071-016-1692-1

Duffy, P. E. (2021). Transmission-blocking vaccines: Harnessing herd immunity for malaria elimination. *Expert Rev Vaccines, 20*(2), 185-198. doi:10.1080/14760584.2021.1878028

Espino, F., & Manderson, L. (2000). Treatment seeking for malaria in morong, bataan, the philippines. *Soc Sci Med, 50*(9), 1309-1316. doi:10.1016/s0277-9536(99)00379-2

University of Ghana http://ugspace.ug.edu.gh

Eyles, D. E., Hoo, C. C., Warren, M., & Sandosham, A. A. (1963). Plasmodium falciparum resistant to chloroquine in cambodia. *Am J Trop Med Hyg, 12*, 840-843. doi:10.4269/ajtmh.1963.12.840

Fairhurst, R. M. (2015). Understanding artemisinin-resistant malaria: What a difference a year makes. *Curr Opin Infect Dis, 28*(5), 417-425. doi:10.1097/qco.0000000000000199

Feng, Z. P., Zhang, X., Han, P., Arora, N., Anders, R. F., & Norton, R. S. (2006). Abundance of intrinsically unstructured proteins in p. Falciparum and other apicomplexan parasite proteomes. *Mol Biochem Parasitol, 150*(2), 256-267. doi:10.1016/j.molbiopara.2006.08.011

Fernando, D., Weerasekera, C. J., Gunasekera, W., Hapuarachchi, H. C., Koo, C., Munas, M., & Ranaweera, P. (2020). Case report: The first case of genotypically confirmed k13 propeller mutation in sri lanka and its implications on the elimination status of malaria. *Am J Trop Med Hyg, 104*(3), 964-967. doi:10.4269/ajtmh.20-1310

Ferreira, P. E., Culleton, R., Gil, J. P., & Meshnick, S. R. (2013). Artemisinin resistance in plasmodium falciparum: What is it really? *Trends Parasitol, 29*(7), 318-320. doi:10.1016/j.pt.2013.05.002

Fisher, R. A. (1930). The genetical theory of natural selection. Clarendon. In: Oxford.

Fowkes, F. J., Boeuf, P., & Beeson, J. G. (2016). Immunity to malaria in an era of declining malaria transmission. *Parasitology, 143*(2), 139-153. doi:10.1017/s0031182015001249

Fu, Y. X., & Li, W. H. (1993). Statistical tests of neutrality of mutations. *Genetics, 133*(3), 693-709.

University of Ghana http://ugspace.ug.edu.gh

Gardner, M. J., Hall, N., Fung, E., White, O., Berriman, M., Hyman, R. W., Carlton, J. M., Pain, A., Nelson, K. E., Bowman, S., Paulsen, I. T., James, K., Eisen, J. A., Rutherford, K., Salzberg, S. L., Craig, A., Kyes, S., Chan, M. S., Nene, V., Shallom, S. J., Suh, B., Peterson, J., Angiuoli, S., Pertea, M., Allen, J., Selengut, J., Haft, D., Mather, M. W., Vaidya, A. B., Martin, D. M., Fairlamb, A. H., Fraunholz, M. J., Roos, D. S., Ralph, S. A., McFadden, G. I., Cummings, L. M., Subramanian, G. M., Mungall, C., Venter, J. C., Carucci, D. J., Hoffman, S. L., Newbold, C., Davis, R. W., Fraser, C. M., & Barrell, B. (2002). Genome sequence of the human malaria parasite plasmodium falciparum. *Nature, 419*(6906), 498-511. doi:10.1038/nature01097

Garrido-Cardenas, J. A., González-Cerón, L., Manzano-Agugliaro, F., & Mesa-Valle, C. (2019). Plasmodium genomics: An approach for learning about and ending human malaria. *Parasitol Res, 118*(1), 1-27. doi:10.1007/s00436-018-6127-9

Ghorbal, M., Gorman, M., Macpherson, C. R., Martins, R. M., Scherf, A., & Lopez-Rubio, J. J. (2014). Genome editing in the human malaria parasite plasmodium falciparum using the crispr-cas9 system. *Nat Biotechnol, 32*(8), 819-821. doi:10.1038/nbt.2925

Gibbons, J., Button-Simons, K. A., Adapa, S. R., Li, S., Pietsch, M., Zhang, M., Liao, X., Adams, J. H., Ferdig, M. T., & Jiang, R. H. Y. (2018). Altered expression of k13 disrupts DNA replication and repair in plasmodium falciparum. *BMC Genomics, 19*(1), 849. doi:10.1186/s12864-018-5207-7

Gill, D. J., Teo, H., Sun, J., Perisic, O., Veprintsev, D. B., Emr, S. D., & Williams, R. L. (2007). Structural insight into the escrt-i/-ii link and its role in mvb trafficking. *Embo j, 26*(2), 600-612. doi:10.1038/sj.emboj.7601501

University of Ghana http://ugspace.ug.edu.gh

Ginsburg, H., Atamna, H., Shalmiev, G., Kanaani, J., & Krugliak, M. (1996). Resistance of glucose-6-phosphate dehydrogenase deficiency to malaria: Effects of fava bean hydroxypyrimidine glucosides on plasmodium falciparum growth in culture and on the phagocytosis of infected cells. *Parasitology, 113 (Pt 1)*, 7-18. doi:10.1017/s0031182000066221

Ginsburg, H., Famin, O., Zhang, J., & Krugliak, M. (1998). Inhibition of glutathione-dependent degradation of heme by chloroquine and amodiaquine as a possible basis for their antimalarial mode of action. *Biochem Pharmacol, 56*(10), 1305-1313. doi:10.1016/s0006-2952(98)00184-1

Gnädig, N. F., Stokes, B. H., Edwards, R. L., Kalantarov, G. F., Heimsch, K. C., Kuderjavy, M., Crane, A., Lee, M. C. S., Straimer, J., Becker, K., Trakht, I. N., Odom John, A. R., Mok, S., & Fidock, D. A. (2020). Insights into the intracellular localization, protein associations and artemisinin resistance properties of plasmodium falciparum k13. *PLoS Pathog, 16*(4), e1008482. doi:10.1371/journal.ppat.1008482

Goodman, C. D., Siregar, J. E., Mollard, V., Vega-Rodríguez, J., Syafruddin, D., Matsuoka, H., Matsuzaki, M., Toyama, T., Sturm, A., Cozijnsen, A., Jacobs-Lorena, M., Kita, K., Marzuki, S., & McFadden, G. I. (2016). Parasites resistant to the antimalarial atovaquone fail to transmit by mosquitoes. *science, 352*(6283), 349-353. doi:10.1126/science.aad9279

Gopalakrishnan, A. M., & Kumar, N. (2015). Antimalarial action of artesunate involves DNA damage mediated by reactive oxygen species. *Antimicrob Agents Chemother, 59*(1), 317-325. doi:10.1128/aac.03663-14

Greening, D. W., & Simpson, R. J. (2018). Understanding extracellular vesicle diversity - current status. *Expert Rev Proteomics, 15*(11), 887-910. doi:10.1080/14789450.2018.1537788

University of Ghana http://ugspace.ug.edu.gh

Group., W. A. b. C. T. A. A. B. S., Dahal, P., d'Alessandro, U., Dorsey, G., Guerin, P. J., Nsanzabana, C., Price, R. N., Sibley, C. H., Stepniewska, K., & Talisuna, A. O. (2015). Clinical determinants of early parasitological response to acts in african patients with uncomplicated falciparum malaria: A literature review and meta-analysis of individual patient data. . *BMC Med, 13*, 212. doi:10.1186/s12916-015-0445-x

Guo, S., Kyaw, M. P., He, L., Min, M., Ning, X., Zhang, W., Wang, B., & Cui, L. (2017). Quality testing of artemisinin-based antimalarial drugs in myanmar. *Am J Trop Med Hyg, 97*(4), 1198-1203. doi:10.4269/ajtmh.17-0305

Gupta, D. K., Patra, A. T., Zhu, L., Gupta, A. P., & Bozdech, Z. (2016). DNA damage regulation and its role in drug-related phenotypes in the malaria parasites. *Sci Rep, 6*, 23603. doi:10.1038/srep23603

Haldane, J. B. S. (1932). 1990. The causes of evolution. In: Princeton (NJ): Princeton University Press.

Haldar, K., Bhattacharjee, S., & Safeukui, I. (2018). Drug resistance in plasmodium. *Nat Rev Microbiol, 16*(3), 156-170. doi:10.1038/nrmicro.2017.161

Halfmann, R., Alberti, S., Krishnan, R., Lyle, N., O'Donnell, C. W., King, O. D., Berger, B., Pappu, R. V., & Lindquist, S. (2011). Opposing effects of glutamine and asparagine govern prion formation by intrinsically disordered proteins. *Mol Cell, 43*(1), 72-84. doi:10.1016/j.molcel.2011.05.013

Hammer, B. K., & Bassler, B. L. (2003). Quorum sensing controls biofilm formation in vibrio cholerae. *Molecular microbiology, 50*(1), 101-104.

Hashimshony, T., Wagner, F., Sher, N., & Yanai, I. (2012). Cel-seq: Single-cell rna-seq by multiplexed linear amplification. *Cell Rep, 2*(3), 666-673. doi:10.1016/j.celrep.2012.08.003

University of Ghana http://ugspace.ug.edu.gh

Hassett, M. R., & Roepe, P. D. (2019). Origin and spread of evolving artemisinin-resistant plasmodium falciparum malarial parasites in southeast asia. *Am J Trop Med Hyg, 101*(6), 1204-1211. doi:10.4269/ajtmh.19-0379

Hassett, M. R., Sternberg, A. R., Riegel, B. E., Thomas, C. J., & Roepe, P. D. (2017). Heterologous expression, purification, and functional analysis of plasmodium falciparum phosphatidylinositol 3'-kinase. *Biochemistry, 56*(33), 4335-4345. doi:10.1021/acs.biochem.7b00416

Hayes, J. D., & McMahon, M. (2006). The double-edged sword of nrf2: Subversion of redox homeostasis during the evolution of cancer. *Mol Cell, 21*(6), 732-734. doi:10.1016/j.molcel.2006.03.004

Haynes, R. K., Cheu, K. W., N'Da, D., Coghi, P., & Monti, D. (2013). Considerations on the mechanism of action of artemisinin antimalarials: Part 1--the 'carbon radical' and 'heme' hypotheses. *Infect Disord Drug Targets, 13*(4), 217-277. doi:10.2174/1871526513666131129155708

Heller, L. E., & Roepe, P. D. (2018b). Quantification of free ferriprotoporphyrin ix heme and hemozoin for artemisinin sensitive versus delayed clearance phenotype plasmodium falciparum malarial parasites. *Biochemistry, 57*(51), 6927-6934. doi:10.1021/acs.biochem.8b00959

Heller, L. E., & Roepe, P. D. (2019). Artemisinin-based antimalarial drug therapy: Molecular pharmacology and evolving resistance. *Trop Med Infect Dis, 4*(2). doi:10.3390/tropicalmed4020089

Heller, L. E., Goggins, E., & Roepe, P. D. (2018a). Dihydroartemisinin-ferriprotoporphyrin ix adduct abundance in plasmodium falciparum malarial parasites and the relationship to emerging artemisinin resistance. *Biochemistry, 57*(51), 6935-6945. doi:10.1021/acs.biochem.8b00960

University of Ghana http://ugspace.ug.edu.gh

Henne, W. M., Stenmark, H., & Emr, S. D. (2013). Molecular mechanisms of the membrane sculpting escrt pathway. *Cold Spring Harb Perspect Biol, 5*(9). doi:10.1101/cshperspect.a016766

Henrici, R. C., Edwards, R. L., Zoltner, M., van Schalkwyk, D. A., Hart, M. N., Mohring, F., Moon, R. W., Nofal, S. D., Patel, A., Flueck, C., Baker, D. A., Odom John, A. R., Field, M. C., & Sutherland, C. J. (2020). The plasmodium falciparum artemisinin susceptibility-associated ap-2 adaptin μ subunit is clathrin independent and essential for schizont maturation. *mBio, 11*(1). doi:10.1128/mBio.02918-19

Henrici, R. C., van Schalkwyk, D. A., & Sutherland, C. J. (2019). Modification of pfap2μ and pfubp1 markedly reduces ring-stage susceptibility of plasmodium falciparum to artemisinin in vitro. *Antimicrob Agents Chemother, 64*(1). doi:10.1128/aac.01542-19

Henriques, G., Hallett, R. L., Beshir, K. B., Gadalla, N. B., Johnson, R. E., Burrow, R., van Schalkwyk, D. A., Sawa, P., Omar, S. A., Clark, T. G., Bousema, T., & Sutherland, C. J. (2014). Directional selection at the pfmdr1, pfcrt, pfubp1, and pfap2mu loci of plasmodium falciparum in kenyan children treated with act. *J Infect Dis, 210*(12), 2001-2008. doi:10.1093/infdis/jiu358

Herrera, R., Anderson, C., Kumar, K., Molina-Cruz, A., Nguyen, V., Burkhardt, M., Reiter, K., Shimp, R., Howard, R. F., & Srinivasan, P. (2015). Reversible conformational change in the plasmodium falciparum circumsporozoite protein masks its adhesion domains. *Infection and immunity*, IAI. 02676-02614.

Hong, Y. L., Yang, Y. Z., & Meshnick, S. R. (1994). The interaction of artemisinin with malarial hemozoin. *Mol Biochem Parasitol, 63*(1), 121-128. doi:10.1016/0166-6851(94)90014-0

Hopp, C. S., Chiou, K., Ragheb, D. R., Salman, A. M., Khan, S. M., Liu, A. J., & Sinnis, P. (2015). Longitudinal analysis of plasmodium sporozoite motility in the dermis reveals component of blood vessel recognition. *Elife, 4*, e07789.

University of Ghana http://ugspace.ug.edu.gh

Howe, R., Kelly, M., Jimah, J., Hodge, D., & Odom, A. R. (2013). Isoprenoid biosynthesis inhibition disrupts rab5 localization and food vacuolar integrity in plasmodium falciparum. *Eukaryot Cell, 12*(2), 215-223. doi:10.1128/ec.00073-12

Huang, F., Takala-Harrison, S., Jacob, C. G., Liu, H., Sun, X., Yang, H., Nyunt, M. M., Adams, M., Zhou, S., Xia, Z., Ringwald, P., Bustos, M. D., Tang, L., & Plowe, C. V. (2015). A single mutation in k13 predominates in southern china and is associated with delayed clearance of plasmodium falciparum following artemisinin treatment. *J Infect Dis, 212*(10), 1629-1635. doi:10.1093/infdis/jiv249

Hubert, A., Subra, C., Jenabian, M. A., Tremblay Labrecque, P. F., Tremblay, C., Laffont, B., Provost, P., Routy, J. P., & Gilbert, C. (2015). Elevated abundance, size, and microrna content of plasma extracellular vesicles in viremic hiv-1+ patients: Correlations with known markers of disease progression. *J Acquir Immune Defic Syndr, 70*(3), 219-227. doi:10.1097/qai.0000000000000756

Hudson, R. R. (1990). Gene genealogies and the coalescent process. *Oxford surveys in evolutionary biology, 7*(1), 44.

Hudson, R. R., Kreitman, M., & Aguadé, M. (1987). A test of neutral molecular evolution based on nucleotide data. *Genetics, 116*(1), 153-159.

Hunt, P., Afonso, A., Creasey, A., Culleton, R., Sidhu, A. B., Logan, J., Valderramos, S. G., McNae, I., Cheesman, S., do Rosario, V., Carter, R., Fidock, D. A., & Cravo, P. (2007). Gene encoding a deubiquitinating enzyme is mutated in artesunate- and chloroquine-resistant rodent malaria parasites. *Mol Microbiol, 65*(1), 27-40. doi:10.1111/j.1365-2958.2007.05753.x

Hurley, J. H. (2015). Escrts are everywhere. *Embo j, 34*(19), 2398-2407. doi:10.15252/embj.201592484

University of Ghana http://ugspace.ug.edu.gh

Hurwitz, E. S., Johnson, D., & Campbell, C. C. (1981). Resistance of plasmodium falciparum malaria to sulfadoxine-pyrimethamine ('fansidar') in a refugee camp in thailand. *Lancet, 1*(8229), 1068-1070. doi:10.1016/s0140-6736(81)92239-x

Hviid, L., & Jensen, A. T. (2015). Pfemp1 - a parasite protein family of key importance in plasmodium falciparum malaria immunity and pathogenesis. *Adv Parasitol, 88*, 51-84. doi:10.1016/bs.apar.2015.02.004

Im, Y. J., Wollert, T., Boura, E., & Hurley, J. H. (2009). Structure and function of the escrt-ii-iii interface in multivesicular body biogenesis. *Dev Cell, 17*(2), 234-243. doi:10.1016/j.devcel.2009.07.008

Imwong, M., Madmanee, W., Suwannasin, K., Kunasol, C., Peto, T. J., Tripura, R., von Seidlein, L., Nguon, C., Davoeung, C., Day, N. P. J., Dondorp, A. M., & White, N. J. (2019). Asymptomatic natural human infections with the simian malaria parasites plasmodium cynomolgi and plasmodium knowlesi. *J Infect Dis, 219*(5), 695-702. doi:10.1093/infdis/jiy519

Innan, H. (2006). Modified hudson-kreitman-aguade test and two-dimensional evaluation of neutrality tests. *Genetics, 173*(3), 1725-1733. doi:10.1534/genetics.106.056242

Ishino, T., Yano, K., Chinzei, Y., & Yuda, M. (2004). Cell-passage activity is required for the malarial parasite to cross the liver sinusoidal cell layer. *PLoS biology, 2*(1), e4.

Ismail, H. M., Barton, V. E., Panchana, M., Charoensutthivarakul, S., Biagini, G. A., Ward, S. A., & O'Neill, P. M. (2016b). A click chemistry-based proteomic approach reveals that 1,2,4-trioxolane and artemisinin antimalarials share a common protein alkylation profile. *Angew Chem Int Ed Engl, 55*(22), 6401-6405. doi:10.1002/anie.201512062

University of Ghana http://ugspace.ug.edu.gh

Ismail, H. M., Barton, V., Phanchana, M., Charoensutthivarakul, S., Wong, M. H., Hemingway, J., Biagini, G. A., O'Neill, P. M., & Ward, S. A. (2016a). Artemisinin activity-based probes identify multiple molecular targets within the asexual stage of the malaria parasites plasmodium falciparum 3d7. *Proc Natl Acad Sci U S A, 113*(8), 2080-2085. doi:10.1073/pnas.1600459113

Jensen, A. R., Adams, Y., & Hviid, L. (2020). Cerebral plasmodium falciparum malaria: The role of pfemp1 in its pathogenesis and immunity, and pfemp1-based vaccines to prevent it. *Immunol Rev, 293*(1), 230-252. doi:10.1111/imr.12807

Jimenez-Ruiz, E., Morlon-Guyot, J., Daher, W., & Meissner, M. (2016). Vacuolar protein sorting mechanisms in apicomplexan parasites. *Mol Biochem Parasitol, 209*(1-2), 18-25. doi:10.1016/j.molbiopara.2016.01.007

Johnson, J. D., Dennull, R. A., Gerena, L., Lopez-Sanchez, M., Roncal, N. E., & Waters, N. C. (2007). Assessment and continued validation of the malaria sybr green i-based fluorescence assay for use in malaria drug screening. *Antimicrobial agents and chemotherapy, 51*(6), 1926-1933.

Joice, R., Nilsson, S. K., Montgomery, J., Dankwa, S., Egan, E., Morahan, B., Seydel, K. B., Bertuccini, L., Alano, P., & Williamson, K. C. (2014). Plasmodium falciparum transmission stages accumulate in the human bone marrow. *Science translational medicine, 6*(244), 244re245-244re245.

Jonscher, E., Flemming, S., Schmitt, M., Sabitzki, R., Reichard, N., Birnbaum, J., Bergmann, B., Höhn, K., & Spielmann, T. (2019). Pfvps45 is required for host cell cytosol uptake by malaria blood stage parasites. *Cell Host Microbe, 25*(1), 166-173.e165. doi:10.1016/j.chom.2018.11.010

University of Ghana http://ugspace.ug.edu.gh

Jourdan, J., Walz, A., Matile, H., Schmidt, A., Wu, J., Wang, X., Dong, Y., Vennerstrom, J. L., Schmidt, R. S., Wittlin, S., & Mäser, P. (2019). Stochastic protein alkylation by antimalarial peroxides. *ACS Infect Dis, 5*(12), 2067-2075. doi:10.1021/acsinfecdis.9b00264

Kafsack, B. F., Rovira-Graells, N., Clark, T. G., Bancells, C., Crowley, V. M., Campino, S. G., Williams, A. E., Drought, L. G., Kwiatkowski, D. P., & Baker, D. A. (2014). A transcriptional switch underlies commitment to sexual development in malaria parasites. *Nature, 507*(7491), 248.

Kariuki, S. N., & Williams, T. N. (2020). Human genetics and malaria resistance. *Hum Genet, 139*(6-7), 801-811. doi:10.1007/s00439-020-02142-6

Katzmann, D. J., Odorizzi, G., & Emr, S. D. (2002). Receptor downregulation and multivesicular-body sorting. *Nat Rev Mol Cell Biol, 3*(12), 893-905. doi:10.1038/nrm973

Katzmann, D. J., Stefan, C. J., Babst, M., & Emr, S. D. (2003). Vps27 recruits escrt machinery to endosomes during mvb sorting. *J Cell Biol, 162*(3), 413-423. doi:10.1083/jcb.200302136

Kavishe, R. A., Koenderink, J. B., & Alifrangis, M. (2017). Oxidative stress in malaria and artemisinin combination therapy: Pros and cons. *Febs j, 284*(16), 2579-2591. doi:10.1111/febs.14097

Keeley, A., & Soldati, D. (2004). The glideosome: A molecular machine powering motility and host-cell invasion by apicomplexa. *Trends Cell Biol, 14*(10), 528-532. doi:10.1016/j.tcb.2004.08.002

Kennedy, K., Cobbold, S. A., Hanssen, E., Birnbaum, J., Spillman, N. J., McHugh, E., Brown, H., Tilley, L., Spielmann, T., McConville, M. J., & Ralph, S. A. (2019). Delayed death in the malaria parasite plasmodium falciparum is caused by disruption of prenylation-dependent intracellular trafficking. *PLoS Biol, 17*(7), e3000376. doi:10.1371/journal.pbio.3000376

University of Ghana http://ugspace.ug.edu.gh

Kimura, M. (1954). *Stochastic processes and distribution of gene frequencies under natural selection*: Citeseer.

Klayman, D. L. (1985). Qinghaosu (artemisinin): An antimalarial drug from china. *science, 228*(4703), 1049-1055. doi:10.1126/science.3887571

Kloch, A., Wenzel, M. A., Laetsch, D. R., Michalski, O., Bajer, A., Behnke, J. M., Welc-Falęciak, R., & Piertney, S. B. (2018). Signatures of balancing selection in toll-like receptor (tlrs) genes - novel insights from a free-living rodent. *Sci Rep, 8*(1), 8361. doi:10.1038/s41598-018-26672-2

Klonis, N., Creek, D. J., & Tilley, L. (2013a). Iron and heme metabolism in plasmodium falciparum and the mechanism of action of artemisinins. *Curr Opin Microbiol, 16*(6), 722-727. doi:10.1016/j.mib.2013.07.005

Klonis, N., Xie, S. C., McCaw, J. M., Crespo-Ortiz, M. P., Zaloumis, S. G., Simpson, J. A., & Tilley, L. (2013b). Altered temporal response of malaria parasites determines differential sensitivity to artemisinin. *Proc Natl Acad Sci U S A, 110*(13), 5157-5162. doi:10.1073/pnas.1217452110

Kobasa, T., Talundzic, E., Sug-Aram, R., Boondat, P., Goldman, I. F., Lucchi, N. W., Dharmarak, P., Sintasath, D., Fukuda, M., Whistler, T., MacArthur, J., Udhayakumar, V., Prempree, P., & Chinanonwait, N. (2018). Emergence and spread of kelch13 mutations associated with artemisinin resistance in plasmodium falciparum parasites in 12 thai provinces from 2007 to 2016. *Antimicrob Agents Chemother, 62*(4). doi:10.1128/aac.02141-17

König, I. R., Fuchs, O., Hansen, G., von Mutius, E., & Kopp, M. V. (2017). What is precision medicine? *European respiratory journal, 50*(4), 1700391.

Koram, K. A., Abuaku, B., Duah, N., & Quashie, N. (2005). Comparative efficacy of antimalarial drugs including acts in the treatment of uncomplicated malaria among children under 5 years in ghana. *Acta Trop, 95*(3), 194-203. doi:10.1016/j.actatropica.2005.06.018

University of Ghana http://ugspace.ug.edu.gh

Kreitman, M. (1983). Nucleotide polymorphism at the alcohol dehydrogenase locus of drosophila melanogaster. *Nature, 304*(5925), 412-417. doi:10.1038/304412a0

Krishna, S., & Kremsner, P. G. (2013). Antidogmatic approaches to artemisinin resistance: Reappraisal as treatment failure with artemisinin combination therapy. *Trends Parasitol, 29*(7), 313-317. doi:10.1016/j.pt.2013.04.001

Krungkrai, S. R., & Yuthavong, Y. (1987). The antimalarial action on plasmodium falciparum of qinghaosu and artesunate in combination with agents which modulate oxidant stress. *Trans R Soc Trop Med Hyg, 81*(5), 710-714. doi:10.1016/0035-9203(87)90003-4

Kümpornsin, K., Kochakarn, T., & Chookajorn, T. (2019). The resistome and genomic reconnaissance in the age of malaria elimination. *Dis Model Mech, 12*(12). doi:10.1242/dmm.040717

Kyaw, M. P., Nyunt, M. H., Chit, K., Aye, M. M., Aye, K. H., Aye, M. M., Lindegardh, N., Tarning, J., Imwong, M., Jacob, C. G., Rasmussen, C., Perin, J., Ringwald, P., & Nyunt, M. M. (2013). Reduced susceptibility of plasmodium falciparum to artesunate in southern myanmar. *PLoS One, 8*(3), e57689. doi:10.1371/journal.pone.0057689

L'Episcopia, M., Kelley, J., Patel, D., Schmedes, S., Ravishankar, S., Menegon, M., Perrotti, E., Nurahmed, A. M., Talha, A. A., Nour, B. Y., Lucchi, N., Severini, C., & Talundzic, E. (2020). Targeted deep amplicon sequencing of kelch 13 and cytochrome b in plasmodium falciparum isolates from an endemic african country using the malaria resistance surveillance (mars) protocol. *Parasit Vectors, 13*(1), 137. doi:10.1186/s13071-020-4005-7

Lambros, C., & Vanderberg, J. P. (1979). Synchronization of plasmodium falciparum erythrocytic stages in culture. *J Parasitol, 65*(3), 418-420.

University of Ghana http://ugspace.ug.edu.gh

Lamptey, H., Ofori, M. F., Kusi, K. A., Adu, B., Owusu-Yeboa, E., Kyei-Baafour, E., Arku, A. T., Bosomprah, S., Alifrangis, M., & Quakyi, I. A. (2018). The prevalence of submicroscopic plasmodium falciparum gametocyte carriage and multiplicity of infection in children, pregnant women and adults in a low malaria transmission area in southern ghana. *Malar J, 17*(1), 331. doi:10.1186/s12936-018-2479-y

Langfelder, P., & Horvath, S. (2008). Wgcna: An r package for weighted correlation network analysis. *BMC bioinformatics, 9*, 559. doi:10.1186/1471-2105-9-559

Langley, C. H., MacDonald, J., Miyashita, N., & Aguadé, M. (1993). Lack of correlation between interspecific divergence and intraspecific polymorphism at the suppressor of forked region in drosophila melanogaster and drosophila simulans. *Proc Natl Acad Sci U S A, 90*(5), 1800-1803. doi:10.1073/pnas.90.5.1800

Langley, C. H., Montgomery, E., & Quattlebaum, W. F. (1982). Restriction map variation in the adh region of drosophila. *Proc Natl Acad Sci U S A, 79*(18), 5631-5635. doi:10.1073/pnas.79.18.5631

Langley, C. H., Shrimpton, A. E., Yamazaki, T., Miyashita, N., Matsuo, Y., & Aquadro, C. F. (1988). Naturally occurring variation in the restriction map of the amy region of drosophila melanogaster. *Genetics, 119*(3), 619-629. doi:10.1093/genetics/119.3.619

Langley, C. H., Stevens, K., Cardeno, C., Lee, Y. C., Schrider, D. R., Pool, J. E., Langley, S. A., Suarez, C., Corbett-Detig, R. B., Kolaczkowski, B., Fang, S., Nista, P. M., Holloway, A. K., Kern, A. D., Dewey, C. N., Song, Y. S., Hahn, M. W., & Begun, D. J. (2012). Genomic variation in natural populations of drosophila melanogaster. *Genetics, 192*(2), 533-598. doi:10.1534/genetics.112.142018

Latifkar, A., Hur, Y. H., Sanchez, J. C., Cerione, R. A., & Antonyak, M. A. (2019). New insights into extracellular vesicle biogenesis and function. *J Cell Sci, 132*(13). doi:10.1242/jcs.222406

University of Ghana http://ugspace.ug.edu.gh

Leang, R., Taylor, W. R., Bouth, D. M., Song, L., Tarning, J., Char, M. C., Kim, S., Witkowski, B., Duru, V., Domergue, A., Khim, N., Ringwald, P., & Menard, D. (2015). Evidence of plasmodium falciparum malaria multidrug resistance to artemisinin and piperaquine in western cambodia: Dihydroartemisinin-piperaquine open-label multicenter clinical assessment. *Antimicrob Agents Chemother, 59*(8), 4719-4726. doi:10.1128/aac.00835-15

Lee, A. H., & Fidock, D. A. (2016). Evidence of a mild mutator phenotype in cambodian plasmodium falciparum malaria parasites. *PLoS One, 11*(4), e0154166. doi:10.1371/journal.pone.0154166

Lee, S., & Bahlo, M. (2016). Moimix: An r package for assessing clonality in high-througput sequencing data (v0.0.1.9001). . *Zenodo. https://doi.org/10.5281/zenodo.58257*.

Leung, K. F., Dacks, J. B., & Field, M. C. (2008). Evolution of the multivesicular body escrt machinery; retention across the eukaryotic lineage. *Traffic, 9*(10), 1698-1716. doi:10.1111/j.1600-0854.2008.00797.x

Li, H., & Durbin, R. (2009). Fast and accurate short read alignment with burrows-wheeler transform. *Bioinformatics, 25*(14), 1754-1760. doi:10.1093/bioinformatics/btp324

Li, W., Zhou, Y., Tang, G., & Xiao, Y. (2016). Characterization of the artemisinin binding site for translationally controlled tumor protein (tctp) by bioorthogonal click chemistry. *Bioconjug Chem, 27*(12), 2828-2833. doi:10.1021/acs.bioconjchem.6b00556

Li, X., Kumar, S., McDew-White, M., Haile, M., Cheeseman, I. H., Emrich, S., Button-Simons, K., Nosten, F., Kappe, S. H. I., Ferdig, M. T., Anderson, T. J. C., & Vaughan, A. M. (2019). Genetic mapping of fitness determinants across the malaria parasite plasmodium falciparum life cycle. *PLoS Genet, 15*(10), e1008453. doi:10.1371/journal.pgen.1008453

Livshits, M. A., Khomyakova, E., Evtushenko, E. G., Lazarev, V. N., Kulemin, N. A., Semina, S. E., Generozov, E. V., & Govorun, V. M. (2015). Isolation of exosomes by differential

University of Ghana http://ugspace.ug.edu.gh

centrifugation: Theoretical analysis of a commonly used protocol. *Sci Rep, 5*, 17319. doi:10.1038/srep17319

Loria, P., Miller, S., Foley, M., & Tilley, L. (1999). Inhibition of the peroxidative degradation of haem as the basis of action of chloroquine and other quinoline antimalarials. *Biochem J, 339 (Pt 2)*(Pt 2), 363-370.

Love, M. I., Huber, W., & Anders, S. (2014). Moderated estimation of fold change and dispersion for rna-seq data with deseq2. *Genome Biol, 15*(12), 550. doi:10.1186/s13059-014-0550-8

Lynch, M., & Walsh, B. (2007). *The origins of genome architecture* (Vol. 98): Sinauer Associates Sunderland, MA.

Maas, S. L. N., Breakefield, X. O., & Weaver, A. M. (2017). Extracellular vesicles: Unique intercellular delivery vehicles. *Trends Cell Biol, 27*(3), 172-188. doi:10.1016/j.tcb.2016.11.003

Machado, M., Murtinheira, F., Lobo, E., & Nogueira, F. (2016). Whole-cell sybr green i assay for antimalarial activity assessment. *Annals of Clinical and Medical Microbiology, 2*.

Mackinnon, M. J. (1997). Survival probability of drug resistant mutants in malaria parasites. *Proc Biol Sci, 264*(1378), 53-59. doi:10.1098/rspb.1997.0008

Mahmoudi, S., & Keshavarz, H. (2017). Efficacy of phase 3 trial of rts, s/as01 malaria vaccine: The need for an alternative development plan. *Hum Vaccin Immunother, 13*(9), 2098-2101. doi:10.1080/21645515.2017.1295906

Maier, A. G., Rug, M., O'Neill, M. T., Brown, M., Chakravorty, S., Szestak, T., Chesson, J., Wu, Y., Hughes, K., Coppel, R. L., Newbold, C., Beeson, J. G., Craig, A., Crabb, B. S., & Cowman, A. F. (2008). Exported proteins required for virulence and rigidity of plasmodium falciparum-infected human erythrocytes. *Cell, 134*(1), 48-61. doi:10.1016/j.cell.2008.04.051

University of Ghana http://ugspace.ug.edu.gh

Manske, M., Miotto, O., Campino, S., Auburn, S., Almagro-Garcia, J., Maslen, G., O'Brien, J., Djimde, A., Doumbo, O., & Zongo, I. (2012). Analysis of plasmodium falciparum diversity in natural infections by deep sequencing. *Nature, 487*(7407), 375-379.

Mantel, P. Y., & Marti, M. (2014). The role of extracellular vesicles in p lasmodium and other protozoan parasites. *Cellular microbiology, 16*(3), 344-354.

Mantel, P.-Y., Hjelmqvist, D., Walch, M., Kharoubi-Hess, S., Nilsson, S., Ravel, D., Ribeiro, M., Grüring, C., Ma, S., & Padmanabhan, P. (2016). Infected erythrocyte-derived extracellular vesicles alter vascular function via regulatory ago2-mirna complexes in malaria. *Nature communications, 7*, 12727.

Mantel, P.-Y., Hoang, A. N., Goldowitz, I., Potashnikova, D., Hamza, B., Vorobjev, I., Ghiran, I., Toner, M., Irimia, D., & Ivanov, A. R. (2013). Malaria-infected erythrocyte-derived microvesicles mediate cellular communication within the parasite population and with the host immune system. *Cell host & microbe, 13*(5), 521-534.

Marti, M., & Johnson, P. J. (2016). Emerging roles for extracellular vesicles in parasitic infections. *Current opinion in microbiology, 32*, 66-70.

Martín-Campos, J. M., Comerón, J. M., Miyashita, N., & Aguadé, M. (1992). Intraspecific and interspecific variation at the y-ac-sc region of drosophila simulans and drosophila melanogaster. *Genetics, 130*(4), 805-816. doi:10.1093/genetics/130.4.805

Mathieu, L. C., Cox, H., Early, A. M., Mok, S., Lazrek, Y., Paquet, J. C., Ade, M. P., Lucchi, N. W., Grant, Q., Udhayakumar, V., Alexandre, J. S., Demar, M., Ringwald, P., Neafsey, D. E., Fidock, D. A., & Musset, L. (2020). Local emergence in amazonia of plasmodium falciparum k13 c580y mutants associated with in vitro artemisinin resistance. *elife, 9*. doi:10.7554/eLife.51015

University of Ghana http://ugspace.ug.edu.gh

Matrevi, S. A., Awandare, G. A., Quashie, N. B., & Quashie, N. (2017). K13 gene polymorphisms in plasmodium falciparum isolates from act post treeatment samples in two ecological zones in ghana. *WACCBIP Research Conference 2017*, 105.

Matrevi, S. A., Opoku-Agyeman, P., Quashie, N. B., Bruku, S., Abuaku, B., Koram, K. A., Fox, A., Letizia, A., & Duah-Quashie, N. O. (2019). Plasmodium falciparum kelch propeller polymorphisms in clinical isolates from ghana from 2007 to 2016. *Antimicrob Agents Chemother, 63*(11). doi:10.1128/aac.00802-19

Mbagwu, S. I., Lannes, N., Walch, M., Filgueira, L., & Mantel, P. Y. (2019). Human microglia respond to malaria-induced extracellular vesicles. *Pathogens, 9*(1). doi:10.3390/pathogens9010021

Mbengue, A., Bhattacharjee, S., Pandharkar, T., Liu, H., Estiu, G., Stahelin, R. V., Rizk, S. S., Njimoh, D. L., Ryan, Y., & Chotivanich, K. (2015). A molecular mechanism of artemisinin resistance in plasmodium falciparum malaria. *Nature, 520*(7549), 683-687.

McDonald, J. H., & Kreitman, M. (1991). Adaptive protein evolution at the adh locus in drosophila. *Nature, 351*(6328), 652-654. doi:10.1038/351652a0

McDonald, L., Cayla, M., Ivens, A., Mony, B. M., MacGregor, P., Silvester, E., McWilliam, K., & Matthews, K. R. (2018). Non-linear hierarchy of the quorum sensing signalling pathway in bloodstream form african trypanosomes. *PLoS Pathog, 14*(6), e1007145. doi:10.1371/journal.ppat.1007145

McLean, K. J., & Jacobs-Lorena, M. (2017). Plasmodium falciparum maf1 confers survival upon amino acid starvation. *mBio, 8*(2). doi:10.1128/mBio.02317-16

Ménard, D., Khim, N., Beghain, J., Adegnika, A. A., Shafiul-Alam, M., Amodu, O., Rahim-Awab, G., Barnadas, C., Berry, A., Boum, Y., Bustos, M. D., Cao, J., Chen, J. H., Collet, L., Cui, L., Thakur, G. D., Dieye, A., Djallé, D., Dorkenoo, M. A., Eboumbou-Moukoko, C. E., Espino,

University of Ghana http://ugspace.ug.edu.gh

F. E., Fandeur, T., Ferreira-da-Cruz, M. F., Fola, A. A., Fuehrer, H. P., Hassan, A. M., Herrera, S., Hongvanthong, B., Houzé, S., Ibrahim, M. L., Jahirul-Karim, M., Jiang, L., Kano, S., Ali-Khan, W., Khanthavong, M., Kremsner, P. G., Lacerda, M., Leang, R., Leelawong, M., Li, M., Lin, K., Mazarati, J. B., Ménard, S., Morlais, I., Muhindo-Mavoko, H., Musset, L., Na-Bangchang, K., Nambozi, M., Niaré, K., Noedl, H., Ouédraogo, J. B., Pillai, D. R., Pradines, B., Quang-Phuc, B., Ramharter, M., Randrianarivelojosia, M., Sattabongkot, J., Sheikh-Omar, A., Silué, K. D., Sirima, S. B., Sutherland, C., Syafruddin, D., Tahar, R., Tang, L. H., Touré, O. A., Tshibangu-wa-Tshibangu, P., Vigan-Womas, I., Warsame, M., Wini, L., Zakeri, S., Kim, S., Eam, R., Berne, L., Khean, C., Chy, S., Ken, M., Loch, K., Canier, L., Duru, V., Legrand, E., Barale, J. C., Stokes, B., Straimer, J., Witkowski, B., Fidock, D. A., Rogier, C., Ringwald, P., Ariey, F., & Mercereau-Puijalon, O. (2016). A worldwide map of plasmodium falciparum k13-propeller polymorphisms. *N Engl J Med, 374*(25), 2453-2464. doi:10.1056/NEJMoa1513137

Meshnick, S. R. (2002). Artemisinin: Mechanisms of action, resistance and toxicity. *Int J Parasitol, 32*(13), 1655-1660. doi:10.1016/s0020-7519(02)00194-7

Meunier, B., & Robert, A. (2010). Heme as trigger and target for trioxane-containing antimalarial drugs. *Acc Chem Res, 43*(11), 1444-1451. doi:10.1021/ar100070k

Ministry of Health, G. (2017). Nmcp: Annual report of the national malaria control programme of ghana,

Miotto, O., Almagro-Garcia, J., Manske, M., MacInnis, B., Campino, S., Rockett, K. A., Amaratunga, C., Lim, P., Suon, S., & Sreng, S. (2013). Multiple populations of artemisinin-resistant plasmodium falciparum in cambodia. *Nature genetics, 45*(6), 648.

Miotto, O., Amato, R., Ashley, E. A., MacInnis, B., Almagro-Garcia, J., Amaratunga, C., Lim, P., Mead, D., Oyola, S. O., Dhorda, M., Imwong, M., Woodrow, C., Manske, M., Stalker, J., Drury, E., Campino, S., Amenga-Etego, L., Thanh, T. N., Tran, H. T., Ringwald, P., Bethell,

University of Ghana http://ugspace.ug.edu.gh

D., Nosten, F., Phyo, A. P., Pukrittayakamee, S., Chotivanich, K., Chuor, C. M., Nguon, C., Suon, S., Sreng, S., Newton, P. N., Mayxay, M., Khanthavong, M., Hongvanthong, B., Htut, Y., Han, K. T., Kyaw, M. P., Faiz, M. A., Fanello, C. I., Onyamboko, M., Mokuolu, O. A., Jacob, C. G., Takala-Harrison, S., Plowe, C. V., Day, N. P., Dondorp, A. M., Spencer, C. C., McVean, G., Fairhurst, R. M., White, N. J., & Kwiatkowski, D. P. (2015). Genetic architecture of artemisinin-resistant plasmodium falciparum. *Nat Genet, 47*(3), 226-234. doi:10.1038/ng.3189

Miotto, O., Sekihara, M., Tachibana, S. I., Yamauchi, M., Pearson, R. D., Amato, R., Gonçalves, S., Mehra, S., Noviyanti, R., Marfurt, J., Auburn, S., Price, R. N., Mueller, I., Ikeda, M., Mori, T., Hirai, M., Tavul, L., Hetzel, M. W., Laman, M., Barry, A. E., Ringwald, P., Ohashi, J., Hombhanje, F., Kwiatkowski, D. P., & Mita, T. (2020). Emergence of artemisinin-resistant plasmodium falciparum with kelch13 c580y mutations on the island of new guinea. *PLoS Pathog, 16*(12), e1009133. doi:10.1371/journal.ppat.1009133

Mita, T., & Tanabe, K. (2012). Evolution of plasmodium falciparum drug resistance: Implications for the development and containment of artemisinin resistance. *Jpn J Infect Dis, 65*(6), 465-475. Retrieved from https://www.ncbi.nlm.nih.gov/pubmed/23183197

Mita, T., Tachibana, S., Hashimoto, M., & Hirai, M. (2016). Plasmodium falciparum kelch 13: A potential molecular marker for tackling artemisinin-resistant malaria parasites. *Expert Rev Anti Infect Ther, 14*(1), 125-135. doi:10.1586/14787210.2016.1106938

Miyashita, N., & Langley, C. H. (1988). Molecular and phenotypic variation of the white locus region in drosophila melanogaster. *Genetics, 120*(1), 199-212. doi:10.1093/genetics/120.1.199

Mockenhaupt, F. P. (1995). Mefloquine resistance in plasmodium falciparum. *Parasitol Today, 11*(7), 248-253. doi:10.1016/0169-4758(95)80201-0

University of Ghana http://ugspace.ug.edu.gh

Mok, S., Ashley, E. A., Ferreira, P. E., Zhu, L., Lin, Z., Yeo, T., Chotivanich, K., Imwong, M., Pukrittayakamee, S., & Dhorda, M. (2015). Population transcriptomics of human malaria parasites reveals the mechanism of artemisinin resistance. *Science, 347*(6220), 431-435.

Mok, S., Imwong, M., Mackinnon, M. J., Sim, J., Ramadoss, R., Yi, P., Mayxay, M., Chotivanich, K., Liong, K. Y., Russell, B., Socheat, D., Newton, P. N., Day, N. P., White, N. J., Preiser, P. R., Nosten, F., Dondorp, A. M., & Bozdech, Z. (2011). Artemisinin resistance in plasmodium falciparum is associated with an altered temporal pattern of transcription. *BMC Genomics, 12*, 391. doi:10.1186/1471-2164-12-391

Mok, S., Stokes, B. H., Gnädig, N. F., Ross, L. S., Yeo, T., Amaratunga, C., Allman, E., Solyakov, L., Bottrill, A. R., & Tripathi, J. (2021). Artemisinin-resistant k13 mutations rewire plasmodium falciparum's intra-erythrocytic metabolic program to enhance survival. *Nature communications, 12*(1), 1-15.

Mvumbi, D. M., Bobanga, T. L., Kayembe, J. N., Mvumbi, G. L., Situakibanza, H. N., Benoit-Vical, F., Melin, P., De Mol, P., & Hayette, M. P. (2017). Molecular surveillance of plasmodium falciparum resistance to artemisinin-based combination therapies in the democratic republic of congo. *PLoS One, 12*(6), e0179142. doi:10.1371/journal.pone.0179142

Nair, S., Li, X., Arya, G. A., McDew-White, M., Ferrari, M., Nosten, F., & Anderson, T. J. C. (2018). Fitness costs and the rapid spread of kelch13-c580y substitutions conferring artemisinin resistance. *Antimicrob Agents Chemother, 62*(9). doi:10.1128/aac.00605-18

Nantakomol, D., Dondorp, A. M., Krudsood, S., Udomsangpetch, R., Pattanapanyasat, K., Combes, V., Grau, G. E., White, N. J., Viriyavejakul, P., Day, N. P., & Chotivanich, K. (2011). Circulating red cell-derived microparticles in human malaria. *J Infect Dis, 203*(5), 700-706. doi:10.1093/infdis/jiq104

University of Ghana http://ugspace.ug.edu.gh

Neafsey, D. E., Schaffner, S. F., Volkman, S. K., Park, D., Montgomery, P., Milner, D. A., Jr., Lukens, A., Rosen, D., Daniels, R., Houde, N., Cortese, J. F., Tyndall, E., Gates, C., Stange-Thomann, N., Sarr, O., Ndiaye, D., Ndir, O., Mboup, S., Ferreira, M. U., Moraes Sdo, L., Dash, A. P., Chitnis, C. E., Wiegand, R. C., Hartl, D. L., Birren, B. W., Lander, E. S., Sabeti, P. C., & Wirth, D. F. (2008). Genome-wide snp genotyping highlights the role of natural selection in plasmodium falciparum population divergence. *Genome Biol, 9*(12), R171. doi:10.1186/gb-2008-9-12-r171

Neafsey, D. E., Taylor, A. R., & MacInnis, B. L. (2021). Advances and opportunities in malaria population genomics. *Nat Rev Genet, 22*(8), 502-517. doi:10.1038/s41576-021-00349-5

Nei, M., & Li, W. H. (1979). Mathematical model for studying genetic variation in terms of restriction endonucleases. *Proc Natl Acad Sci U S A, 76*(10), 5269-5273. doi:10.1073/pnas.76.10.5269

Neves Borgheti-Cardoso, L., San Anselmo, M., Lantero, E., Lancelot, A., Serrano, J. L., Hernández-Ainsa, S., Fernàndez-Busquets, X., & Sierra, T. (2020). Promising nanomaterials in the fight against malaria. *J Mater Chem B, 8*(41), 9428-9448. doi:10.1039/d0tb01398f

Newton, P. N., Fernández, F. M., Plançon, A., Mildenhall, D. C., Green, M. D., Ziyong, L., Christophel, E. M., Phanouvong, S., Howells, S., McIntosh, E., Laurin, P., Blum, N., Hampton, C. Y., Faure, K., Nyadong, L., Soong, C. W., Santoso, B., Zhiguang, W., Newton, J., & Palmer, K. (2008). A collaborative epidemiological investigation into the criminal fake artesunate trade in south east asia. *PLoS Med, 5*(2), e32. doi:10.1371/journal.pmed.0050032

Nkhoma, S. C., Nair, S., Al-Saai, S., Ashley, E., McGready, R., Phyo, A. P., Nosten, F., & Anderson, T. J. (2013). Population genetic correlates of declining transmission in a human pathogen. *Mol Ecol, 22*(2), 273-285. doi:10.1111/mec.12099

University of Ghana http://ugspace.ug.edu.gh

Noedl, H., Se, Y., Schaecher, K., Smith, B. L., Socheat, D., & Fukuda, M. M. (2008). Evidence of artemisinin-resistant malaria in western cambodia. *N Engl J Med, 359*(24), 2619-2620. doi:10.1056/NEJMc0805011

Nonvignon, J., Aryeetey, G. C., Malm, K. L., Agyemang, S. A., Aubyn, V. N., Peprah, N. Y., Bart-Plange, C. N., & Aikins, M. (2016). Economic burden of malaria on businesses in ghana: A case for private sector investment in malaria control. *Malar J, 15*(1), 454. doi:10.1186/s12936-016-1506-0

Nsanzabana, C. (2021). Time to scale up molecular surveillance for anti-malarial drug resistance in sub-saharan africa. *Malar J, 20*(1), 401. doi:10.1186/s12936-021-03942-5

Nsanzabana, C., Djalle, D., Guérin, P. J., Ménard, D., & González, I. J. (2018). Tools for surveillance of anti-malarial drug resistance: An assessment of the current landscape. *Malar J, 17*(1), 75. doi:10.1186/s12936-018-2185-9

Nyunt, M. H., Wang, B., Aye, K. M., Aye, K. H., Han, J. H., Lee, S. K., Han, K. T., Htut, Y., & Han, E. T. (2017). Molecular surveillance of artemisinin resistance falciparum malaria among migrant goldmine workers in myanmar. *Malar J, 16*(1), 97. doi:10.1186/s12936-017-1753-8

O'Neill, P. M., Barton, V. E., & Ward, S. A. (2010). The molecular mechanism of action of artemisinin--the debate continues. *Molecules, 15*(3), 1705-1721. doi:10.3390/molecules15031705

Obita, T., Saksena, S., Ghazi-Tabatabai, S., Gill, D. J., Perisic, O., Emr, S. D., & Williams, R. L. (2007). Structural basis for selective recognition of escrt-iii by the aaa atpase vps4. *Nature, 449*(7163), 735-739. doi:10.1038/nature06171

Ochola-Oyier, L. I., Wamae, K., Omedo, I., Ogola, C., Matharu, A., Musabyimana, J. P., Njogu, F. K., & Marsh, K. (2019). Few plasmodium falciparum merozoite ligand and erythrocyte

University of Ghana http://ugspace.ug.edu.gh

receptor pairs show evidence of balancing selection. *Infect Genet Evol, 69*, 235-245. doi:10.1016/j.meegid.2019.02.004

Ochola, L. I., Tetteh, K. K., Stewart, L. B., Riitho, V., Marsh, K., & Conway, D. J. (2010). Allele frequency–based and polymorphism-versus-divergence indices of balancing selection in a new filtered set of polymorphic genes in plasmodium falciparum. *Molecular biology and evolution, 27*(10), 2344-2351.

Olotu, A., Fegan, G., Wambua, J., Nyangweso, G., Leach, A., Lievens, M., Kaslow, D. C., Njuguna, P., Marsh, K., & Bejon, P. (2016). Seven-year efficacy of rts,s/as01 malaria vaccine among young african children. *N Engl J Med, 374*(26), 2519-2529. doi:10.1056/NEJMoa1515257

Olshina, M. A., Angrisano, F., Marapana, D. S., Riglar, D. T., Bane, K., Wong, W., Catimel, B., Yin, M. X., Holmes, A. B., Frischknecht, F., Kovar, D. R., & Baum, J. (2015). Plasmodium falciparum coronin organizes arrays of parallel actin filaments potentially guiding directional motility in invasive malaria parasites. *Malar J, 14*, 280. doi:10.1186/s12936-015-0801-5

Pandey, A. V., Tekwani, B. L., Singh, R. L., & Chauhan, V. S. (1999). Artemisinin, an endoperoxide antimalarial, disrupts the hemoglobin catabolism and heme detoxification systems in malarial parasite. *J Biol Chem, 274*(27), 19383-19388. doi:10.1074/jbc.274.27.19383

Patel, P. N., & Tolia, N. (2021). Structural vaccinology of malaria transmission-blocking vaccines. *Expert Rev Vaccines, 20*(2), 199-214. doi:10.1080/14760584.2021.1873135

Peatey, C. L., Chavchich, M., Chen, N., Gresty, K. J., Gray, K. A., Gatton, M. L., Waters, N. C., & Cheng, Q. (2015). Mitochondrial membrane potential in a small subset of artemisinin-induced dormant plasmodium falciparum parasites in vitro. *J Infect Dis, 212*(3), 426-434. doi:10.1093/infdis/jiv048

University of Ghana http://ugspace.ug.edu.gh

Pfeifer, B., Wittelsbürger, U., Ramos-Onsins, S. E., & Lercher, M. J. (2014). Popgenome: An efficient swiss army knife for population genomic analyses in r. *Mol Biol Evol, 31*(7), 1929-1936. doi:10.1093/molbev/msu136

Phyo, A. P., Nkhoma, S., Stepniewska, K., Ashley, E. A., Nair, S., McGready, R., ler Moo, C., Al-Saai, S., Dondorp, A. M., Lwin, K. M., Singhasivanon, P., Day, N. P., White, N. J., Anderson, T. J., & Nosten, F. (2012). Emergence of artemisinin-resistant malaria on the western border of thailand: A longitudinal study. *Lancet, 379*(9830), 1960-1966. doi:10.1016/s0140-6736(12)60484-x

Pongtavornpinyo, W., Hastings, I. M., Dondorp, A., White, L. J., Maude, R. J., Saralamba, S., Day, N. P., White, N. J., & Boni, M. F. (2009). Probability of emergence of antimalarial resistance in different stages of the parasite life cycle. *Evol Appl, 2*(1), 52-61. doi:10.1111/j.1752-4571.2008.00067.x

Portugaliza, H. P., Miyazaki, S., Geurten, F. J., Pell, C., Rosanas-Urgell, A., Janse, C. J., & Cortés, A. (2020). Artemisinin exposure at the ring or trophozoite stage impacts plasmodium falciparum sexual conversion differently. *Elife, 9*. doi:10.7554/eLife.60058

Powell, R. D., Brewer, G. J., Alving, A. S., & Millar, J. W. (1964). Studies on a strain of chloroquine-resistant plasmodium falciparum from thailand. *Bull World Health Organ, 30*(1), 29-44.

Project, M. P. f. C. (2016). Genomic epidemiology of artemisinin resistant malaria. *Elife, 5*. doi:10.7554/eLife.08714

Quashie, N. B., Duah, N. O., Abuaku, B., & Koram, K. A. (2007). The in-vitro susceptibilities of ghanaian plasmodium falciparum to antimalarial drugs. *Ann Trop Med Parasitol, 101*(5), 391-398. doi:10.1179/136485907X176553

Quashie, N. B., Duah, N. O., Abuaku, B., Quaye, L., Ayanful-Torgby, R., Akwoviah, G. A., Kweku, M., Johnson, J. D., Lucchi, N. W., Udhayakumar, V., Duplessis, C., Kronmann, K. C., &

University of Ghana http://ugspace.ug.edu.gh

Koram, K. A. (2013). A sybr green 1-based in vitro test of susceptibility of ghanaian plasmodium falciparum clinical isolates to a panel of anti-malarial drugs. *Malar J, 12*, 450. doi:10.1186/1475-2875-12-450

Quashie, N. B., Ranford-Cartwright, L. C., & de Koning, H. P. (2010). Uptake of purines in plasmodium falciparum-infected human erythrocytes is mostly mediated by the human equilibrative nucleoside transporter and the human facilitative nucleobase transporter. *Malar J, 9*, 36. doi:10.1186/1475-2875-9-36

Raiborg, C., & Stenmark, H. (2009). The escrt machinery in endosomal sorting of ubiquitylated membrane proteins. *Nature, 458*(7237), 445-452. doi:10.1038/nature07961

Raman, J., Kagoro, F. M., Mabuza, A., Malatje, G., Reid, A., Frean, J., & Barnes, K. I. (2019). Absence of kelch13 artemisinin resistance markers but strong selection for lumefantrine-tolerance molecular markers following 18 years of artemisinin-based combination therapy use in mpumalanga province, south africa (2001-2018). *Malar J, 18*(1), 280. doi:10.1186/s12936-019-2911-y

Ramírez-Soriano, A., Ramos-Onsins, S. E., Rozas, J., Calafell, F., & Navarro, A. (2008). Statistical power analysis of neutrality tests under demographic expansions, contractions and bottlenecks with recombination. *Genetics, 179*(1), 555-567. doi:10.1534/genetics.107.083006

Raposo, G., & Stoorvogel, W. (2013). Extracellular vesicles: Exosomes, microvesicles, and friends. *J Cell Biol, 200*(4), 373-383. doi:10.1083/jcb.201211138

Rathod, P. K., McErlean, T., & Lee, P. C. (1997). Variations in frequencies of drug resistance in plasmodium falciparum. *Proc Natl Acad Sci U S A, 94*(17), 9389-9393. doi:10.1073/pnas.94.17.9389

University of Ghana http://ugspace.ug.edu.gh

Regev-Rudzki, N., Wilson, D. W., Carvalho, T. G., Sisquella, X., Coleman, B. M., Rug, M., Bursac, D., Angrisano, F., Gee, M., & Hill, A. F. (2013). Cell-cell communication between malaria-infected red blood cells via exosome-like vesicles. *Cell, 153*(5), 1120-1133.

Risco-Castillo, V., Topçu, S., Marinach, C., Manzoni, G., Bigorgne, A. E., Briquet, S., Baudin, X., Lebrun, M., Dubremetz, J.-F., & Silvie, O. (2015). Malaria sporozoites traverse host cells within transient vacuoles. *Cell host & microbe, 18*(5), 593-603.

Ritz, C., Baty, F., Streibig, J. C., & Gerhard, D. (2015). Dose-response analysis using r. *PLoS One, 10*(12), e0146021. doi:10.1371/journal.pone.0146021

Robert, A., Cazelles, J., & Meunier, B. (2001). Characterization of the alkylation product of heme by the antimalarial drug artemisinin. *Angewandte Chemie International Edition, 40*(10), 1954-1957.

Robert, A., Coppel, Y., & Meunier, B. (2002). Alkylation of heme by the antimalarial drug artemisinin. *Chem Commun (Camb)*(5), 414-415. doi:10.1039/b110817b

Roberts, D. J., & Williams, T. N. (2003). Haemoglobinopathies and resistance to malaria. *Redox Rep, 8*(5), 304-310. doi:10.1179/135100003225002998

Rocamora, F., Zhu, L., Liong, K. Y., Dondorp, A., Miotto, O., Mok, S., & Bozdech, Z. (2018). Oxidative stress and protein damage responses mediate artemisinin resistance in malaria parasites. *PLoS pathogens, 14*(3), e1006930.

Roditi, I. (2016). The languages of parasite communication. *Mol Biochem Parasitol, 208*(1), 16-22. doi:10.1016/j.molbiopara.2016.05.008

Rogerson, S. J., Wijesinghe, R. S., & Meshnick, S. R. (2010). Host immunity as a determinant of treatment outcome in plasmodium falciparum malaria. *Lancet Infect Dis, 10*(1), 51-59. doi:10.1016/s1473-3099(09)70322-6

University of Ghana http://ugspace.ug.edu.gh

Roosihermiatie, B., Widjiartini, Paramita, A., Nugroho, A., & Suprapto, A. (2017). Malaria self-care in nimboran subdistrict, jayapura district, papua province, indonesia. *Southeast Asian J Trop Med Public Health, 48*(1), 1-8.

Rossati, A., Bargiacchi, O., Kroumova, V., Zaramella, M., Caputo, A., & Garavelli, P. L. (2016). Climate, environment and transmission of malaria. *Infez Med, 24*(2), 93-104.

Rozas, J., Ferrer-Mata, A., Sánchez-DelBarrio, J. C., Guirao-Rico, S., Librado, P., Ramos-Onsins, S. E., & Sánchez-Gracia, A. (2017). Dnasp 6: DNA sequence polymorphism analysis of large data sets. *Mol Biol Evol, 34*(12), 3299-3302. doi:10.1093/molbev/msx248

Rubert, A., Guillon-Grammatico, L., Chandenier, J., Dimier-Poisson, I., & Desoubeaux, G. (2016). Insecticide resistance in anopheles mosquitoes : Additional obstacles in the battle against malaria. *Med Sante Trop, 26*(4), 423-431. doi:10.1684/mst.2016.0634

Saari, H., Turunen, T., Lõhmus, A., Turunen, M., Jalasvuori, M., Butcher, S. J., Ylä-Herttuala, S., Viitala, T., Cerullo, V., Siljander, P. R. M., & Yliperttula, M. (2020). Extracellular vesicles provide a capsid-free vector for oncolytic adenoviral DNA delivery. *J Extracell Vesicles, 9*(1), 1747206. doi:10.1080/20013078.2020.1747206

Sahu, U., Mohapatra, B. N., Kar, S. K., & Ranjit, M. (2013b). Promoter polymorphisms in the atp binding cassette transporter gene influence production of cell-derived microparticles and are highly associated with susceptibility to severe malaria in humans. *Infect Immun, 81*(4), 1287-1294. doi:10.1128/iai.01175-12

Sahu, U., Sahoo, P. K., Kar, S. K., Mohapatra, B. N., & Ranjit, M. (2013a). Association of tnf level with production of circulating cellular microparticles during clinical manifestation of human cerebral malaria. *Hum Immunol, 74*(6), 713-721. doi:10.1016/j.humimm.2013.02.006

Sampaio, N. G., Cheng, L., & Eriksson, E. M. (2017). The role of extracellular vesicles in malaria biology and pathogenesis. *Malaria journal, 16*(1), 245.

University of Ghana http://ugspace.ug.edu.gh

Sampaio, N. G., Emery, S. J., Garnham, A. L., Tan, Q. Y., Sisquella, X., Pimentel, M. A., Jex, A. R., Regev-Rudzki, N., Schofield, L., & Eriksson, E. M. (2018). Extracellular vesicles from early stage plasmodium falciparum-infected red blood cells contain pfemp1 and induce transcriptional changes in human monocytes. *Cell Microbiol, 20*(5), e12822. doi:10.1111/cmi.12822

Saralamba, S., Pan-Ngum, W., Maude, R. J., Lee, S. J., Tarning, J., Lindegårdh, N., Chotivanich, K., Nosten, F., Day, N. P., Socheat, D., White, N. J., Dondorp, A. M., & White, L. J. (2011). Intrahost modeling of artemisinin resistance in plasmodium falciparum. *Proc Natl Acad Sci U S A, 108*(1), 397-402. doi:10.1073/pnas.1006113108

Saunders, D. L., Vanachayangkul, P., & Lon, C. (2014). Dihydroartemisinin-piperaquine failure in cambodia. *N Engl J Med, 371*(5), 484-485. doi:10.1056/NEJMc1403007

Schaeffer, S. W., Aquadro, C. F., & Langley, C. H. (1988). Restriction-map variation in the notch region of drosophila melanogaster. *Mol Biol Evol, 5*(1), 30-40. doi:10.1093/oxfordjournals.molbev.a040475

Seydel, K. B., Kampondeni, S. D., Valim, C., Potchen, M. J., Milner, D. A., Muwalo, F. W., Birbeck, G. L., Bradley, W. G., Fox, L. L., Glover, S. J., Hammond, C. A., Heyderman, R. S., Chilingulo, C. A., Molyneux, M. E., & Taylor, T. E. (2015). Brain swelling and death in children with cerebral malaria. *N Engl J Med, 372*(12), 1126-1137. doi:10.1056/NEJMoa1400116

Sharma, A. I., Shin, S. H., Bopp, S., Volkman, S. K., Hartl, D. L., & Wirth, D. F. (2020). Genetic background and pfkelch13 affect artemisinin susceptibility of pfcoronin mutants in plasmodium falciparum. *PLoS Genet, 16*(12), e1009266. doi:10.1371/journal.pgen.1009266

Shrivastava, S. K., Dalko, E., Delcroix-Genete, D., Herbert, F., Cazenave, P. A., & Pied, S. (2017). Uptake of parasite-derived vesicles by astrocytes and microglial phagocytosis of infected

University of Ghana http://ugspace.ug.edu.gh

erythrocytes may drive neuroinflammation in cerebral malaria. *Glia, 65*(1), 75-92. doi:10.1002/glia.23075

Siddiqui, F. A., Boonhok, R., Cabrera, M., Mbenda, H. G. N., Wang, M., Min, H., Liang, X., Qin, J., Zhu, X., Miao, J., Cao, Y., & Cui, L. (2020). Role of plasmodium falciparum kelch 13 protein mutations in p. Falciparum populations from northeastern myanmar in mediating artemisinin resistance. *mBio, 11*(1). doi:10.1128/mBio.01134-19

Siddiqui, F. A., Liang, X., & Cui, L. (2021). Plasmodium falciparum resistance to acts: Emergence, mechanisms, and outlook. *Int J Parasitol Drugs Drug Resist, 16*, 102-118. doi:10.1016/j.ijpddr.2021.05.007

Siddiqui, G., Srivastava, A., Russell, A. S., & Creek, D. J. (2017). Multi-omics based identification of specific biochemical changes associated with pfkelch13-mutant artemisinin-resistant plasmodium falciparum. *J Infect Dis, 215*(9), 1435-1444. doi:10.1093/infdis/jix156

Sierro, F., & Grau, G. E. R. (2019). The ins and outs of cerebral malaria pathogenesis: Immunopathology, extracellular vesicles, immunometabolism, and trained immunity. *Front Immunol, 10*, 830. doi:10.3389/fimmu.2019.00830

Silva, M., Ferreira, P. E., Otienoburu, S. D., Calçada, C., Ngasala, B., Björkman, A., Mårtensson, A., Gil, J. P., & Veiga, M. I. (2019). Plasmodium falciparum k13 expression associated with parasite clearance during artemisinin-based combination therapy. *J Antimicrob Chemother, 74*(7), 1890-1893. doi:10.1093/jac/dkz098

Simmini, S., Bialecka, M., Huch, M., Kester, L., van de Wetering, M., Sato, T., Beck, F., van Oudenaarden, A., Clevers, H., & Deschamps, J. (2014). Transformation of intestinal stem cells into gastric stem cells on loss of transcription factor cdx2. *Nat Commun, 5*, 5728. doi:10.1038/ncomms6728

University of Ghana http://ugspace.ug.edu.gh

Simwela, N. V., Hughes, K. R., Roberts, A. B., Rennie, M. T., Barrett, M. P., & Waters, A. P. (2020a). Experimentally engineered mutations in a ubiquitin hydrolase, ubp-1, modulate in vivo susceptibility to artemisinin and chloroquine in plasmodium berghei. *Antimicrob Agents Chemother, 64*(7). doi:10.1128/aac.02484-19

Simwela, N. V., Stokes, B. H., Aghabi, D., Bogyo, M., Fidock, D. A., & Waters, A. P. (2020b). Plasmodium berghei k13 mutations mediate in vivo artemisinin resistance that is reversed by proteasome inhibition. *mBio, 11*(6). doi:10.1128/mBio.02312-20

Singh, G. P., Chandra, B. R., Bhattacharya, A., Akhouri, R. R., Singh, S. K., & Sharma, A. (2004). Hyper-expansion of asparagines correlates with an abundance of proteins with prion-like domains in plasmodium falciparum. *Mol Biochem Parasitol, 137*(2), 307-319. doi:10.1016/j.molbiopara.2004.05.016

Sisquella, X., Ofir-Birin, Y., Pimentel, M. A., Cheng, L., Abou Karam, P., Sampaio, N. G., Penington, J. S., Connolly, D., Giladi, T., Scicluna, B. J., Sharples, R. A., Waltmann, A., Avni, D., Schwartz, E., Schofield, L., Porat, Z., Hansen, D. S., Papenfuss, A. T., Eriksson, E. M., Gerlic, M., Hill, A. F., Bowie, A. G., & Regev-Rudzki, N. (2017). Malaria parasite DNA-harbouring vesicles activate cytosolic immune sensors. *Nat Commun, 8*(1), 1985. doi:10.1038/s41467-017-02083-1

Sondo, P., Derra, K., Rouamba, T., Nakanabo Diallo, S., Taconet, P., Kazienga, A., Ilboudo, H., Tahita, M. C., Valéa, I., Sorgho, H., Lefèvre, T., & Tinto, H. (2020). Determinants of plasmodium falciparum multiplicity of infection and genetic diversity in burkina faso. *Parasit Vectors, 13*(1), 427. doi:10.1186/s13071-020-04302-z

Sonkong, K., Chaiklieng, S., Neave, P., & Suggaravetsiri, P. (2015). Factors affecting delay in seeking treatment among malaria patients along thailand-myanmar border in tak province, thailand. *Malar J, 14*, 3. doi:10.1186/1475-2875-14-3

University of Ghana http://ugspace.ug.edu.gh

Spring, M. D., Lin, J. T., Manning, J. E., Vanachayangkul, P., Somethy, S., Bun, R., Se, Y., Chann, S., Ittiverakul, M., Sia-ngam, P., Kuntawunginn, W., Arsanok, M., Buathong, N., Chaorattanakawee, S., Gosi, P., Ta-aksorn, W., Chanarat, N., Sundrakes, S., Kong, N., Heng, T. K., Nou, S., Teja-isavadharm, P., Pichyangkul, S., Phann, S. T., Balasubramanian, S., Juliano, J. J., Meshnick, S. R., Chour, C. M., Prom, S., Lanteri, C. A., Lon, C., & Saunders, D. L. (2015). Dihydroartemisinin-piperaquine failure associated with a triple mutant including kelch13 c580y in cambodia: An observational cohort study. *Lancet Infect Dis, 15*(6), 683-691. doi:10.1016/s1473-3099(15)70049-6

St Laurent, B., Miller, B., Burton, T. A., Amaratunga, C., Men, S., Sovannaroth, S., Fay, M. P., Miotto, O., Gwadz, R. W., Anderson, J. M., & Fairhurst, R. M. (2015). Artemisinin-resistant plasmodium falciparum clinical isolates can infect diverse mosquito vectors of southeast asia and africa. *Nat Commun, 6*, 8614. doi:10.1038/ncomms9614

Stephan, W., & Langley, C. H. (1989). Molecular genetic variation in the centromeric region of the x chromosome in three drosophila ananassae populations. I. Contrasts between the vermilion and forked loci. *Genetics, 121*(1), 89-99. doi:10.1093/genetics/121.1.89

Stephan, W., & Mitchell, S. J. (1992). Reduced levels of DNA polymorphism and fixed between-population differences in the centromeric region of drosophila ananassae. *Genetics, 132*(4), 1039-1045. doi:10.1093/genetics/132.4.1039

Stepniewska, K., Ashley, E., Lee, S. J., Anstey, N., Barnes, K. I., Binh, T. Q., D'Alessandro, U., Day, N. P., de Vries, P. J., Dorsey, G., Guthmann, J. P., Mayxay, M., Newton, P. N., Olliaro, P., Osorio, L., Price, R. N., Rowland, M., Smithuis, F., Taylor, W. R., Nosten, F., & White, N. J. (2010). In vivo parasitological measures of artemisinin susceptibility. *J Infect Dis, 201*(4), 570-579. doi:10.1086/650301

University of Ghana http://ugspace.ug.edu.gh

Straimer, J., Gnädig, N. F., Stokes, B. H., Ehrenberger, M., Crane, A. A., & Fidock, D. A. (2017). Plasmodium falciparum k13 mutations differentially impact ozonide susceptibility and parasite fitness in vitro. *mBio, 8*(2). doi:10.1128/mBio.00172-17

Straimer, J., Gnädig, N. F., Witkowski, B., Amaratunga, C., Duru, V., Ramadani, A. P., Dacheux, M., Khim, N., Zhang, L., Lam, S., Gregory, P. D., Urnov, F. D., Mercereau-Puijalon, O., Benoit-Vical, F., Fairhurst, R. M., Ménard, D., & Fidock, D. A. (2015). Drug resistance. K13-propeller mutations confer artemisinin resistance in plasmodium falciparum clinical isolates. *science, 347*(6220), 428-431. doi:10.1126/science.1260867

Sturm, A., Amino, R., Van de Sand, C., Regen, T., Retzlaff, S., Rennenberg, A., Krueger, A., Pollok, J.-M., Menard, R., & Heussler, V. T. (2006). Manipulation of host hepatocytes by the malaria parasite for delivery into liver sinusoids. *science, 313*(5791), 1287-1290.

Suazo, K. F., Schaber, C., Palsuledesai, C. C., Odom John, A. R., & Distefano, M. D. (2016). Global proteomic analysis of prenylated proteins in plasmodium falciparum using an alkyne-modified isoprenoid analogue. *Sci Rep, 6*, 38615. doi:10.1038/srep38615

Subramanian, A., Tamayo, P., Mootha, V. K., Mukherjee, S., Ebert, B. L., Gillette, M. A., Paulovich, A., Pomeroy, S. L., Golub, T. R., Lander, E. S., & Mesirov, J. P. (2005). Gene set enrichment analysis: A knowledge-based approach for interpreting genome-wide expression profiles. *Proc Natl Acad Sci U S A, 102*(43), 15545-15550. doi:10.1073/pnas.0506580102

Sultan, A. A., Thathy, V., Frevert, U., Robson, K. J., Crisanti, A., Nussenzweig, V., Nussenzweig, R. S., & Ménard, R. (1997). Trap is necessary for gliding motility and infectivity of plasmodium sporozoites. *Cell, 90*(3), 511-522. doi:10.1016/s0092-8674(00)80511-5

Supek, F., Bošnjak, M., Škunca, N., & Šmuc, T. (2011). Revigo summarizes and visualizes long lists of gene ontology terms. *PLoS One, 6*(7), e21800. doi:10.1371/journal.pone.0021800

University of Ghana http://ugspace.ug.edu.gh

Suresh, N., & Haldar, K. (2018). Mechanisms of artemisinin resistance in plasmodium falciparum malaria. *Current opinion in pharmacology, 42*, 46-54.

Sutherland, C. J., Henrici, R. C., & Artavanis-Tsakonas, K. (2021). Artemisinin susceptibility in the malaria parasite plasmodium falciparum: Propellers, adaptor proteins and the need for cellular healing. *FEMS Microbiol Rev, 45*(3). doi:10.1093/femsre/fuaa056

Sutherland, C. J., Lansdell, P., Sanders, M., Muwanguzi, J., van Schalkwyk, D. A., Kaur, H., Nolder, D., Tucker, J., Bennett, H. M., Otto, T. D., Berriman, M., Patel, T. A., Lynn, R., Gkrania-Klotsas, E., & Chiodini, P. L. (2017). Pfk13-independent treatment failure in four imported cases of plasmodium falciparum malaria treated with artemether-lumefantrine in the united kingdom. *Antimicrob Agents Chemother, 61*(3). doi:10.1128/aac.02382-16

Szatanek, R., Baran, J., Siedlar, M., & Baj-Krzyworzeka, M. (2015). Isolation of extracellular vesicles: Determining the correct approach (review). *Int J Mol Med, 36*(1), 11-17. doi:10.3892/ijmm.2015.2194

Szempruch, A. J., Sykes, S. E., Kieft, R., Dennison, L., Becker, A. C., Gartrell, A., Martin, W. J., Nakayasu, E. S., Almeida, I. C., & Hajduk, S. L. (2016). Extracellular vesicles from trypanosoma brucei mediate virulence factor transfer and cause host anemia. *Cell, 164*(1-2), 246-257.

Tajima, F. (1989). Statistical method for testing the neutral mutation hypothesis by DNA polymorphism. *Genetics, 123*(3), 585-595.

Takala-Harrison, S., Clark, T. G., Jacob, C. G., Cummings, M. P., Miotto, O., Dondorp, A. M., Fukuda, M. M., Nosten, F., Noedl, H., Imwong, M., Bethell, D., Se, Y., Lon, C., Tyner, S. D., Saunders, D. L., Socheat, D., Ariey, F., Phyo, A. P., Starzengruber, P., Fuehrer, H. P., Swoboda, P., Stepniewska, K., Flegg, J., Arze, C., Cerqueira, G. C., Silva, J. C., Ricklefs, S. M., Porcella, S. F., Stephens, R. M., Adams, M., Kenefic, L. J., Campino, S., Auburn, S., MacInnis, B., Kwiatkowski, D. P., Su, X. Z., White, N. J., Ringwald, P., & Plowe, C. V.

University of Ghana http://ugspace.ug.edu.gh

(2013). Genetic loci associated with delayed clearance of plasmodium falciparum following artemisinin treatment in southeast asia. *Proc Natl Acad Sci U S A, 110*(1), 240-245. doi:10.1073/pnas.1211205110

Talisuna, A. O., Karema, C., Ogutu, B., Juma, E., Logedi, J., Nyandigisi, A., Mulenga, M., Mbacham, W. F., Roper, C., Guerin, P. J., D'Alessandro, U., & Snow, R. W. (2012). Mitigating the threat of artemisinin resistance in africa: Improvement of drug-resistance surveillance and response systems. *Lancet Infect Dis, 12*(11), 888-896. doi:10.1016/S1473-3099(12)70241-4

Tandoh, K. Z., Morang'a, C. M., Wilson, M., Quashie, N. B., & Duah-Quashie, N. O. (2022). Malaria artemisinin resistance: An extracellular vesicles export hypothesis. *Trends Parasitol, 38*(8), 614-617. doi:10.1016/j.pt.2022.05.004

Tandoh, K. Z., Wilson, M. D., Quashie, N. B., & Duah-Quashie, N. O. (2021). Implicating extracellular vesicles in plasmodium falciparum artemisinin resistance development. *Traffic, 22*(6), 194-200. doi:10.1111/tra.12787

Tangpukdee, N., Duangdee, C., Wilairatana, P., & Krudsood, S. (2009). Malaria diagnosis: A brief review. *Korean J Parasitol, 47*(2), 93-102. doi:10.3347/kjp.2009.47.2.93

Taraschi, T. F., O'Donnell, M., Martinez, S., Schneider, T., Trelka, D., Fowler, V. M., Tilley, L., & Moriyama, Y. (2003). Generation of an erythrocyte vesicle transport system by plasmodium falciparum malaria parasites. *Blood, 102*(9), 3420-3426. doi:10.1182/blood-2003-05-1448

Tarr, S. J., Díaz-Ingelmo, O., Stewart, L. B., Hocking, S. E., Murray, L., Duffy, C. W., Otto, T. D., Chappell, L., Rayner, J. C., Awandare, G. A., & Conway, D. J. (2018). Schizont transcriptome variation among clinical isolates and laboratory-adapted clones of the malaria parasite plasmodium falciparum. *BMC Genomics, 19*(1), 894. doi:10.1186/s12864-018-5257-x

University of Ghana http://ugspace.ug.edu.gh

Tartaglia, G. G., Cavalli, A., Pellarin, R., & Caflisch, A. (2005). Prediction of aggregation rate and aggregation-prone segments in polypeptide sequences. *Protein Sci, 14*(10), 2723-2734. doi:10.1110/ps.051471205

Tavares, J., Formaglio, P., Thiberge, S., Mordelet, E., Van Rooijen, N., Medvinsky, A., Ménard, R., & Amino, R. (2013). Role of host cell traversal by the malaria sporozoite during liver infection. *Journal of Experimental Medicine, 210*(5), 905-915.

Tawk, L., Chicanne, G., Dubremetz, J. F., Richard, V., Payrastre, B., Vial, H. J., Roy, C., & Wengelnik, K. (2010). Phosphatidylinositol 3-phosphate, an essential lipid in plasmodium, localizes to the food vacuole membrane and the apicoplast. *Eukaryot Cell, 9*(10), 1519-1530. doi:10.1128/ec.00124-10

Taylor, S. M., Parobek, C. M., & Fairhurst, R. M. (2012). Haemoglobinopathies and the clinical epidemiology of malaria: A systematic review and meta-analysis. *Lancet Infect Dis, 12*(6), 457-468. doi:10.1016/s1473-3099(12)70055-5

Taylor, S. M., Parobek, C. M., DeConti, D. K., Kayentao, K., Coulibaly, S. O., Greenwood, B. M., Tagbor, H., Williams, J., Bojang, K., Njie, F., Desai, M., Kariuki, S., Gutman, J., Mathanga, D. P., Mårtensson, A., Ngasala, B., Conrad, M. D., Rosenthal, P. J., Tshefu, A. K., Moormann, A. M., Vulule, J. M., Doumbo, O. K., Ter Kuile, F. O., Meshnick, S. R., Bailey, J. A., & Juliano, J. J. (2015). Absence of putative artemisinin resistance mutations among plasmodium falciparum in sub-saharan africa: A molecular epidemiologic study. *J Infect Dis, 211*(5), 680-688. doi:10.1093/infdis/jiu467

Teis, D., Saksena, S., Judson, B. L., & Emr, S. D. (2010). Escrt-ii coordinates the assembly of escrt-iii filaments for cargo sorting and multivesicular body vesicle formation. *Embo j, 29*(5), 871-883. doi:10.1038/emboj.2009.408

University of Ghana http://ugspace.ug.edu.gh

Teuscher, F., Gatton, M. L., Chen, N., Peters, J., Kyle, D. E., & Cheng, Q. (2010). Artemisinin-induced dormancy in plasmodium falciparum: Duration, recovery rates, and implications in treatment failure. *J Infect Dis, 202*(9), 1362-1368. doi:10.1086/656476

Théry, C., Amigorena, S., Raposo, G., & Clayton, A. (2006). Isolation and characterization of exosomes from cell culture supernatants and biological fluids. *Curr Protoc Cell Biol, Chapter 3*, Unit 3.22. doi:10.1002/0471143030.cb0322s30

Théry, C., Witwer, K. W., Aikawa, E., Alcaraz, M. J., Anderson, J. D., Andriantsitohaina, R., Antoniou, A., Arab, T., Archer, F., & Atkin-Smith, G. K. (2018). Minimal information for studies of extracellular vesicles 2018 (misev2018): A position statement of the international society for extracellular vesicles and update of the misev2014 guidelines. *Journal of extracellular vesicles, 7*(1), 1535750.

Thriemer, K., Van Hong, N., Rosanas-Urgell, A., Phuc, B. Q., Pockele, E., Guetens, P., Van Van, N., Duong, T. T., Amambua, N. A., & D'Alessandro, U. (2014). Delayed parasite clearance after treatment with dihydroartemisinin-piperaquine in plasmodium falciparum malaria patients in central vietnam. *Antimicrobial agents and chemotherapy*, AAC. 02746-02714.

Tilley, L., Straimer, J., Gnädig, N. F., Ralph, S. A., & Fidock, D. A. (2016). Artemisinin action and resistance in plasmodium falciparum. *Trends Parasitol, 32*(9), 682-696. doi:10.1016/j.pt.2016.05.010

Tirrell, A. R., Vendrely, K. M., Checkley, L. A., Davis, S. Z., McDew-White, M., Cheeseman, I. H., Vaughan, A. M., Nosten, F. H., Anderson, T. J. C., & Ferdig, M. T. (2019). Pairwise growth competitions identify relative fitness relationships among artemisinin resistant plasmodium falciparum field isolates. *Malar J, 18*(1), 295. doi:10.1186/s12936-019-2934-4

Tkach, M., & Théry, C. (2016). Communication by extracellular vesicles: Where we are and where we need to go. *Cell, 164*(6), 1226-1232.

University of Ghana http://ugspace.ug.edu.gh

Tong, L., Yang, C., Wu, P. Y., & Wang, M. D. (2016). Evaluating the impact of sequencing error correction for rna-seq data with ercc rna spike-in controls. *IEEE EMBS Int Conf Biomed Health Inform, 2016*, 74-77. doi:10.1109/bhi.2016.7455838

Trager, W., & Jensen, J. B. (1976). Human malaria parasites in continuous culture. *science, 193*(4254), 673-675. doi:10.1126/science.781840

Trotta, R. F., Brown, M. L., Terrell, J. C., & Geyer, J. A. (2004). Defective DNA repair as a potential mechanism for the rapid development of drug resistance in plasmodium falciparum. *Biochemistry, 43*(17), 4885-4891. doi:10.1021/bi0499258

Tu, Y. (2011). The discovery of artemisinin (qinghaosu) and gifts from chinese medicine. *Nat Med, 17*(10), 1217-1220. doi:10.1038/nm.2471

Tu, Y. (2016). Artemisinin-a gift from traditional chinese medicine to the world (nobel lecture). *Angew Chem Int Ed Engl, 55*(35), 10210-10226. doi:10.1002/anie.201601967

Tun, K. M., Imwong, M., Lwin, K. M., Win, A. A., Hlaing, T. M., Hlaing, T., Lin, K., Kyaw, M. P., Plewes, K., Faiz, M. A., Dhorda, M., Cheah, P. Y., Pukrittayakamee, S., Ashley, E. A., Anderson, T. J., Nair, S., McDew-White, M., Flegg, J. A., Grist, E. P., Guerin, P., Maude, R. J., Smithuis, F., Dondorp, A. M., Day, N. P., Nosten, F., White, N. J., & Woodrow, C. J. (2015). Spread of artemisinin-resistant plasmodium falciparum in myanmar: A cross-sectional survey of the k13 molecular marker. *Lancet Infect Dis, 15*(4), 415-421. doi:10.1016/s1473-3099(15)70032-0

Uwimana, A., Legrand, E., Stokes, B. H., Ndikumana, J. M., Warsame, M., Umulisa, N., Ngamije, D., Munyaneza, T., Mazarati, J. B., Munguti, K., Campagne, P., Criscuolo, A., Ariey, F., Murindahabi, M., Ringwald, P., Fidock, D. A., Mbituyumuremyi, A., & Menard, D. (2020). Emergence and clonal expansion of in vitro artemisinin-resistant plasmodium falciparum kelch13 r561h mutant parasites in rwanda. *Nat Med, 26*(10), 1602-1608. doi:10.1038/s41591-020-1005-2

University of Ghana http://ugspace.ug.edu.gh

Uwimana, A., Umulisa, N., Venkatesan, M., Svigel, S. S., Zhou, Z., Munyaneza, T., Habimana, R. M., Rucogoza, A., Moriarty, L. F., Sandford, R., Piercefield, E., Goldman, I., Ezema, B., Talundzic, E., Pacheco, M. A., Escalante, A. A., Ngamije, D., Mangala, J. N., Kabera, M., Munguti, K., Murindahabi, M., Brieger, W., Musanabaganwa, C., Mutesa, L., Udhayakumar, V., Mbituyumuremyi, A., Halsey, E. S., & Lucchi, N. W. (2021). Association of plasmodium falciparum kelch13 r561h genotypes with delayed parasite clearance in rwanda: An open-label, single-arm, multicentre, therapeutic efficacy study. *Lancet Infect Dis*. doi:10.1016/s1473-3099(21)00142-0

Vafa, M., Troye-Blomberg, M., Anchang, J., Garcia, A., & Migot-Nabias, F. (2008). Multiplicity of plasmodium falciparum infection in asymptomatic children in senegal: Relation to transmission, age and erythrocyte variants. *Malar J, 7*, 17. doi:10.1186/1475-2875-7-17

Vaid, A., Ranjan, R., Smythe, W. A., Hoppe, H. C., & Sharma, P. (2010). Pfpi3k, a phosphatidylinositol-3 kinase from plasmodium falciparum, is exported to the host erythrocyte and is involved in hemoglobin trafficking. *Blood, 115*(12), 2500-2507. doi:10.1182/blood-2009-08-238972

Valadi, H., Ekström, K., Bossios, A., Sjöstrand, M., Lee, J. J., & Lötvall, J. O. (2007). Exosome-mediated transfer of mrnas and micrornas is a novel mechanism of genetic exchange between cells. *Nature cell biology, 9*(6), 654.

van Niel, G., D'Angelo, G., & Raposo, G. (2018). Shedding light on the cell biology of extracellular vesicles. *Nat Rev Mol Cell Biol, 19*(4), 213-228. doi:10.1038/nrm.2017.125

Vanaerschot, M., Huijben, S., Van den Broeck, F., & Dujardin, J. C. (2014). Drug resistance in vectorborne parasites: Multiple actors and scenarios for an evolutionary arms race. *FEMS Microbiol Rev, 38*(1), 41-55. doi:10.1111/1574-6976.12032

Verity, R., Aydemir, O., Brazeau, N. F., Watson, O. J., Hathaway, N. J., Mwandagalirwa, M. K., Marsh, P. W., Thwai, K., Fulton, T., Denton, M., Morgan, A. P., Parr, J. B., Tumwebaze, P.

University of Ghana http://ugspace.ug.edu.gh

K., Conrad, M., Rosenthal, P. J., Ishengoma, D. S., Ngondi, J., Gutman, J., Mulenga, M., Norris, D. E., Moss, W. J., Mensah, B. A., Myers-Hansen, J. L., Ghansah, A., Tshefu, A. K., Ghani, A. C., Meshnick, S. R., Bailey, J. A., & Juliano, J. J. (2020). The impact of antimalarial resistance on the genetic structure of plasmodium falciparum in the drc. *Nat Commun, 11*(1), 2107. doi:10.1038/s41467-020-15779-8

Vidal, M. (2019). Exosomes: Revisiting their role as "garbage bags". *Traffic, 20*(11), 815-828. doi:10.1111/tra.12687

Wang, J., Huang, L., Li, J., Fan, Q., Long, Y., Li, Y., & Zhou, B. (2010). Artemisinin directly targets malarial mitochondria through its specific mitochondrial activation. *PLoS One, 5*(3), e9582. doi:10.1371/journal.pone.0009582

Wang, J., Wong, Y. K., & Liao, F. (2018). What has traditional chinese medicine delivered for modern medicine? *Expert Rev Mol Med, 20*, e4. doi:10.1017/erm.2018.3

Wang, J., Zhang, C. J., Chia, W. N., Loh, C. C., Li, Z., Lee, Y. M., He, Y., Yuan, L. X., Lim, T. K., Liu, M., Liew, C. X., Lee, Y. Q., Zhang, J., Lu, N., Lim, C. T., Hua, Z. C., Liu, B., Shen, H. M., Tan, K. S., & Lin, Q. (2015a). Haem-activated promiscuous targeting of artemisinin in plasmodium falciparum. *Nat Commun, 6*, 10111. doi:10.1038/ncomms10111

Wang, Z., Shrestha, S., Li, X., Miao, J., Yuan, L., Cabrera, M., Grube, C., Yang, Z., & Cui, L. (2015b). Prevalence of k13-propeller polymorphisms in plasmodium falciparum from china-myanmar border in 2007-2012. *Malar J, 14*, 168. doi:10.1186/s12936-015-0672-9

Wang, Z., Xi, J., Hao, X., Deng, W., Liu, J., Wei, C., Gao, Y., Zhang, L., & Wang, H. (2017). Red blood cells release microparticles containing human argonaute 2 and mirnas to target genes of plasmodium falciparum. *Emerg Microbes Infect, 6*(8), e75. doi:10.1038/emi.2017.63

Warhurst, D. C., & Williams, J. E. (1996). Acp broadsheet no 148. July 1996. Laboratory diagnosis of malaria. *J Clin Pathol, 49*(7), 533-538. doi:10.1136/jcp.49.7.533

University of Ghana http://ugspace.ug.edu.gh

Warncke, J. D., & Beck, H. P. (2019). Host cytoskeleton remodeling throughout the blood stages of plasmodium falciparum. *Microbiol Mol Biol Rev, 83*(4). doi:10.1128/mmbr.00013-19

Wassmer, S. C., & Grau, G. E. (2017). Severe malaria: What's new on the pathogenesis front? *Int J Parasitol, 47*(2-3), 145-152. doi:10.1016/j.ijpara.2016.08.002

Weiss, G. E., Gilson, P. R., Taechalertpaisarn, T., Tham, W.-H., de Jong, N. W., Harvey, K. L., Fowkes, F. J., Barlow, P. N., Rayner, J. C., & Wright, G. J. (2015). Revealing the sequence and resulting cellular morphology of receptor-ligand interactions during plasmodium falciparum invasion of erythrocytes. *PLoS pathogens, 11*(2), e1004670.

Wellems, T. E., & Plowe, C. V. (2001). Chloroquine-resistant malaria. *The Journal of Infectious Diseases, 184*(6), 770-776. doi:10.1086/322858

Wellems, T. E., Sá, J. M., Su, X. Z., Connelly, S. V., & Ellis, A. C. (2020). 'Artemisinin resistance': Something new or old? Something of a misnomer? *Trends Parasitol, 36*(9), 735-744. doi:10.1016/j.pt.2020.05.013

White, L. J., Flegg, J. A., Phyo, A. P., Wiladpai-ngern, J. H., Bethell, D., Plowe, C., Anderson, T., Nkhoma, S., Nair, S., Tripura, R., Stepniewska, K., Pan-Ngum, W., Silamut, K., Cooper, B. S., Lubell, Y., Ashley, E. A., Nguon, C., Nosten, F., White, N. J., & Dondorp, A. M. (2015). Defining the in vivo phenotype of artemisinin-resistant falciparum malaria: A modelling approach. *PLoS Med, 12*(4), e1001823. doi:10.1371/journal.pmed.1001823

White, N. J. (2004). Antimalarial drug resistance. *J Clin Invest, 113*(8), 1084-1092. doi:10.1172/jci21682

White, N. J. (2008). The role of anti-malarial drugs in eliminating malaria. *Malar J, 7 Suppl 1*(Suppl 1), S8. doi:10.1186/1475-2875-7-s1-s8

White, N. J., Pukrittayakamee, S., Hien, T. T., Faiz, M. A., Mokuolu, O. A., & Dondorp, A. M. (2014). Malaria. *Lancet, 383*(9918), 723-735. doi:10.1016/s0140-6736(13)60024-0

University of Ghana http://ugspace.ug.edu.gh

WHO. (1965). Resistance of malaria parasites to drugs. Report of a who scientific group. *World Health Organ Tech Rep Ser, 296*, 1-65.

WHO. (2006). Guidelines for the treatment of malaria.

WHO. (2015). Global technical strategy for malaria 2016-2030.

WHO. (2020a). Report on antimalarial drug efficacy, resistance and response: 10 years of surveillance

WHO. (2020b). World malaria report 2020.

WHO. (2021a). World malaria report, 2021.

WHO. (2021b). World health organization malaria terminology, 2021 update.

WHO. (2021c). Who guidelines for malaria.

Willms, E., Cabañas, C., Mäger, I., Wood, M. J. A., & Vader, P. (2018). Extracellular vesicle heterogeneity: Subpopulations, isolation techniques, and diverse functions in cancer progression. *Front Immunol, 9*, 738. doi:10.3389/fimmu.2018.00738

Willms, E., Johansson, H. J., Mäger, I., Lee, Y., Blomberg, K. E. M., Sadik, M., Alaarg, A., Smith, C. E., Lehtiö, J., & Andaloussi, S. E. (2016). Cells release subpopulations of exosomes with distinct molecular and biological properties. *Scientific reports, 6*, 22519.

Winter, V., & Hauser, M. T. (2006). Exploring the escrting machinery in eukaryotes. *Trends Plant Sci, 11*(3), 115-123. doi:10.1016/j.tplants.2006.01.008

Witkowski, B., Amaratunga, C., Khim, N., Sreng, S., Chim, P., Kim, S., Lim, P., Mao, S., Sopha, C., & Sam, B. (2013a). Novel phenotypic assays for the detection of artemisinin-resistant plasmodium falciparum malaria in cambodia: In-vitro and ex-vivo drug-response studies. *The Lancet infectious diseases, 13*(12), 1043-1049.

University of Ghana http://ugspace.ug.edu.gh

Witkowski, B., Khim, N., Chim, P., Kim, S., Ke, S., Kloeung, N., Chy, S., Duong, S., Leang, R., Ringwald, P., Dondorp, A. M., Tripura, R., Benoit-Vical, F., Berry, A., Gorgette, O., Ariey, F., Barale, J. C., Mercereau-Puijalon, O., & Menard, D. (2013b). Reduced artemisinin susceptibility of plasmodium falciparum ring stages in western cambodia. *Antimicrob Agents Chemother, 57*(2), 914-923. doi:10.1128/aac.01868-12

Witkowski, B., Lelièvre, J., Barragán, M. J., Laurent, V., Su, X. Z., Berry, A., & Benoit-Vical, F. (2010). Increased tolerance to artemisinin in plasmodium falciparum is mediated by a quiescence mechanism. *Antimicrob Agents Chemother, 54*(5), 1872-1877. doi:10.1128/aac.01636-09

Witmer, K., Dahalan, F. A., Delves, M. J., Yahiya, S., Watson, O. J., Straschil, U., Chiwcharoen, D., Sornboon, B., Pukrittayakamee, S., Pearson, R. D., Howick, V. M., Lawniczak, M. K. N., White, N. J., Dondorp, A. M., Okell, L. C., Chotivanich, K., Ruecker, A., & Baum, J. (2020). Transmission of artemisinin-resistant malaria parasites to mosquitoes under antimalarial drug pressure. *Antimicrob Agents Chemother, 65*(1). doi:10.1128/aac.00898-20

Wongsrichanalai, C., Pickard, A. L., Wernsdorfer, W. H., & Meshnick, S. R. (2002). Epidemiology of drug-resistant malaria. *Lancet Infect Dis, 2*(4), 209-218. doi:10.1016/s1473-3099(02)00239-6

WWARN Artemisinin-based Combination Therapy Africa Baseline Study Group, Dahal, P., d'Alessandro, U., Dorsey, G., Guerin, P. J., Nsanzabana, C., Price, R. N., Sibley, C. H., Stepniewska, K., & Talisuna, A. O. (2015). Clinical determinants of early parasitological response to acts in african patients with uncomplicated falciparum malaria: A literature review and meta-analysis of individual patient data. *BMC Med, 13*, 212. doi:10.1186/s12916-015-0445-x

Xie, S. C., Dogovski, C., Hanssen, E., Chiu, F., Yang, T., Crespo, M. P., Stafford, C., Batinovic, S., Teguh, S., Charman, S., Klonis, N., & Tilley, L. (2016). Haemoglobin degradation underpins

University of Ghana http://ugspace.ug.edu.gh

the sensitivity of early ring stage plasmodium falciparum to artemisinins. *J Cell Sci, 129*(2), 406-416. doi:10.1242/jcs.178830

Xie, S. C., Ralph, S. A., & Tilley, L. (2020). K13, the cytostome, and artemisinin resistance. *Trends Parasitol, 36*(6), 533-544. doi:10.1016/j.pt.2020.03.006

Xiong, A., Prakash, P., Gao, X., Chew, M., Tay, I. J. J., Woodrow, C. J., Engelward, B. P., Han, J., & Preiser, P. R. (2020). K13-mediated reduced susceptibility to artemisinin in plasmodium falciparum is overlaid on a trait of enhanced DNA damage repair. *Cell Rep, 32*(5), 107996. doi:10.1016/j.celrep.2020.107996

Yáñez-Mó, M., Siljander, P. R., Andreu, Z., Zavec, A. B., Borràs, F. E., Buzas, E. I., Buzas, K., Casal, E., Cappello, F., Carvalho, J., Colás, E., Cordeiro-da Silva, A., Fais, S., Falcon-Perez, J. M., Ghobrial, I. M., Giebel, B., Gimona, M., Graner, M., Gursel, I., Gursel, M., Heegaard, N. H., Hendrix, A., Kierulf, P., Kokubun, K., Kosanovic, M., Kralj-Iglic, V., Krämer-Albers, E. M., Laitinen, S., Lässer, C., Lener, T., Ligeti, E., Linē, A., Lipps, G., Llorente, A., Lötvall, J., Manček-Keber, M., Marcilla, A., Mittelbrunn, M., Nazarenko, I., Nolte-'t Hoen, E. N., Nyman, T. A., O'Driscoll, L., Olivan, M., Oliveira, C., Pállinger, É., Del Portillo, H. A., Reventós, J., Rigau, M., Rohde, E., Sammar, M., Sánchez-Madrid, F., Santarém, N., Schallmoser, K., Ostenfeld, M. S., Stoorvogel, W., Stukelj, R., Van der Grein, S. G., Vasconcelos, M. H., Wauben, M. H., & De Wever, O. (2015). Biological properties of extracellular vesicles and their physiological functions. *J Extracell Vesicles, 4*, 27066. doi:10.3402/jev.v4.27066

Yang, M., Coppens, I., Wormsley, S., Baevova, P., Hoppe, H. C., & Joiner, K. A. (2004). The plasmodium falciparum vps4 homolog mediates multivesicular body formation. *J Cell Sci, 117*(Pt 17), 3831-3838. doi:10.1242/jcs.01237

Yang, T., Yeoh, L. M., Tutor, M. V., Dixon, M. W., McMillan, P. J., Xie, S. C., Bridgford, J. L., Gillett, D. L., Duffy, M. F., Ralph, S. A., McConville, M. J., Tilley, L., & Cobbold, S. A.

University of Ghana http://ugspace.ug.edu.gh

(2019). Decreased k13 abundance reduces hemoglobin catabolism and proteotoxic stress, underpinning artemisinin resistance. *Cell Rep, 29*(9), 2917-2928.e2915. doi:10.1016/j.celrep.2019.10.095

Yang, Y. Z., Little, B., & Meshnick, S. R. (1994). Alkylation of proteins by artemisinin. Effects of heme, ph, and drug structure. *Biochem Pharmacol, 48*(3), 569-573. doi:10.1016/0006-2952(94)90287-9

Yap, C. C., & Winckler, B. (2015). Adapting for endocytosis: Roles for endocytic sorting adaptors in directing neural development. *Front Cell Neurosci, 9*, 119. doi:10.3389/fncel.2015.00119

Ye, R., Hu, D., Zhang, Y., Huang, Y., Sun, X., Wang, J., Chen, X., Zhou, H., Zhang, D., Mungthin, M., & Pan, W. (2016). Distinctive origin of artemisinin-resistant plasmodium falciparum on the china-myanmar border. *Sci Rep, 6*, 20100. doi:10.1038/srep20100

Ye, W., Chew, M., Hou, J., Lai, F., Leopold, S. J., Loo, H. L., Ghose, A., Dutta, A. K., Chen, Q., Ooi, E. E., White, N. J., Dondorp, A. M., Preiser, P., & Chen, J. (2018). Microvesicles from malaria-infected red blood cells activate natural killer cells via mda5 pathway. *PLoS Pathog, 14*(10), e1007298. doi:10.1371/journal.ppat.1007298

Zaborowski, M. P., Balaj, L., Breakefield, X. O., & Lai, C. P. (2015). Extracellular vesicles: Composition, biological relevance, and methods of study. *Bioscience, 65*(8), 783-797.

Zhang, M., Gallego-Delgado, J., Fernandez-Arias, C., Waters, N. C., Rodriguez, A., Tsuji, M., Wek, R. C., Nussenzweig, V., & Sullivan, W. J., Jr. (2017). Inhibiting the plasmodium eif2α kinase pk4 prevents artemisinin-induced latency. *Cell Host Microbe, 22*(6), 766-776.e764. doi:10.1016/j.chom.2017.11.005

University of Ghana http://ugspace.ug.edu.gh

Zhang, M., Wang, C., Oberstaller, J., Thomas, P., Otto, T. D., Casandra, D., Boyapalle, S., Adapa, S. R., Xu, S., Button-Simons, K., Mayho, M., Rayner, J. C., Ferdig, M. T., Jiang, R. H. Y., & Adams, J. H. (2021). The apicoplast link to fever-survival and artemisinin-resistance in the malaria parasite. *Nat Commun, 12*(1), 4563. doi:10.1038/s41467-021-24814-1

Zhu, L., van der Pluijm, R. W., Kucharski, M., Nayak, S., Tripathi, J., White, N. J., Day, N. P. J., Faiz, A., Phyo, A. P., Amaratunga, C., Lek, D., Ashley, E. A., Nosten, F., Smithuis, F., Ginsburg, H., von Seidlein, L., Lin, K., Imwong, M., Chotivanich, K., Mayxay, M., Dhorda, M., Nguyen, H. C., Nguyen, T. N. T., Miotto, O., Newton, P. N., Jittamala, P., Tripura, R., Pukrittayakamee, S., Peto, T. J., Hien, T. T., Dondorp, A. M., & Bozdech, Z. (2022). Artemisinin resistance in the malaria parasite, plasmodium falciparum, originates from its initial transcriptional response. *Commun Biol, 5*(1), 274. doi:10.1038/s42003-022-03215-0

University of Ghana http://ugspace.ug.edu.gh

APPENDICES

Appendix I

Supplementary Table 3.1 Genome wide scan of all genes under balancing selection

Chromosomes	GeneID	TajimaD
1	PF3D7_0103600	3.86
1	PF3D7_0103600	3.86
1	PF3D7_0113600	3.85
1	PF3D7_0113600	3.85
1	PF3D7_0113600	3.81
1	PF3D7_0113600	3.81
1	PF3D7_0103600	3.68
1	PF3D7_0103600	3.68
1	PF3D7_0113600	3.60
1	PF3D7_0113600	3.60
1	PF3D7_0113100	3.50
1	PF3D7_0113100	3.50
1	PF3D7_0113100	3.43
1	PF3D7_0113100	3.43
1	PF3D7_0113600	3.19
1	PF3D7_0113600	3.19
1	PF3D7_0102200	3.18
1	PF3D7_0102200	3.18
1	PF3D7_0102200	2.84
1	PF3D7_0102200	2.84
1	PF3D7_0113100	2.78
1	PF3D7_0113100	2.78
1	PF3D7_0103500	2.77
1	PF3D7_0103500	2.77
1	PF3D7_0103700	2.45
1	PF3D7_0103700	2.45
1	PF3D7_0113200	2.43
1	PF3D7_0113200	2.43
1	PF3D7_0113200	2.43
1	PF3D7_0113200	2.43
1	PF3D7_0114500	2.27
1	PF3D7_0114500	2.27
1	PF3D7_0114500	2.27
1	PF3D7_0114500	2.27
1	PF3D7_0103500	2.26
1	PF3D7_0103500	2.26
1	PF3D7_0106700	2.16
1	PF3D7_0106700	2.16
1	PF3D7_0106700	2.16
1	PF3D7_0106700	2.16

University of Ghana http://ugspace.ug.edu.gh

1	PF3D7_0102200	2.10
1	PF3D7_0102200	2.10
1	PF3D7_0103700	1.98
1	PF3D7_0103700	1.98
1	PF3D7_0103600	1.98
1	PF3D7_0103600	1.98
1	PF3D7_0104300	1.80
1	PF3D7_0104300	1.80
1	PF3D7_0104300	1.80
1	PF3D7_0104300	1.80
1	PF3D7_0104500	1.73
1	PF3D7_0104500	1.73
1	PF3D7_0104500	1.73
1	PF3D7_0104500	1.73
1	PF3D7_0114800	1.46
1	PF3D7_0114800	1.46
1	PF3D7_0114800	1.46
1	PF3D7_0114800	1.46
1	PF3D7_0109850	1.23
1	PF3D7_0109850	1.23
1	PF3D7_0109850	1.23
1	PF3D7_0109850	1.23
1	PF3D7_0107200	1.00
1	PF3D7_0107200	1.00
2	PF3D7_0220800	3.67
2	PF3D7_0220800	3.67
2	PF3D7_0220900	3.66
2	PF3D7_0220900	3.66
2	PF3D7_0212500	3.17
2	PF3D7_0212500	3.17
2	PF3D7_0212500	2.94
2	PF3D7_0212500	2.94
2	PF3D7_0212400	2.88
2	PF3D7_0212400	2.88
2	PF3D7_0220000	2.86
2	PF3D7_0220000	2.86
2	PF3D7_0220000	2.86
2	PF3D7_0220000	2.86
2	PF3D7_0211700	2.78
2	PF3D7_0211700	2.78
2	PF3D7_0211700	2.78
2	PF3D7_0221000	2.63
2	PF3D7_0209000	2.47
2	PF3D7_0209000	2.47
2	PF3D7_0207700	2.45
2	PF3D7_0207700	2.45
2	PF3D7_0213600	2.12
2	PF3D7_0213600	2.12

University of Ghana http://ugspace.ug.edu.gh

2	PF3D7_0206700	2.07
2	PF3D7_0206700	2.07
2	PF3D7_0208300	2.03
2	PF3D7_0208300	2.03
2	PF3D7_0212400	2.03
2	PF3D7_0212400	2.03
2	PF3D7_0207900	2.01
2	PF3D7_0207900	2.01
2	PF3D7_0215000	1.98
2	PF3D7_0215000	1.98
2	PF3D7_0221200	1.91
2	PF3D7_0221200	1.91
2	PF3D7_0207300	1.91
2	PF3D7_0207300	1.91
2	PF3D7_0221200	1.82
2	PF3D7_0221200	1.82
2	PF3D7_0204600	1.81
2	PF3D7_0204600	1.81
2	PF3D7_0202100	1.80
2	PF3D7_0202100	1.80
2	PF3D7_0202100	1.80
2	PF3D7_0202100	1.80
2	PF3D7_0218800	1.79
2	PF3D7_0218800	1.79
2	PF3D7_0218800	1.79
2	PF3D7_0220800	1.78
2	PF3D7_0220800	1.78
2	PF3D7_0207300	1.76
2	PF3D7_0207300	1.76
2	PF3D7_0220100	1.75
2	PF3D7_0220100	1.75
2	PF3D7_0220100	1.75
2	PF3D7_0220100	1.75
2	PF3D7_0204000	1.72
2	PF3D7_0204000	1.72
2	PF3D7_0204000	1.72
2	PF3D7_0204000	1.72
2	PF3D7_0207400	1.71
2	PF3D7_0207400	1.71
2	PF3D7_0221300	1.71
2	PF3D7_0221300	1.71
2	PF3D7_0213600	1.70
2	PF3D7_0213600	1.70
2	PF3D7_0207700	1.68
2	PF3D7_0207000	1.68
2	PF3D7_0217000	1.67
2	PF3D7_0207900	1.64
2	PF3D7_0221300	1.64

University of Ghana http://ugspace.ug.edu.gh

2	PF3D7_0221300	1.64
2	PF3D7_0213600	1.61
2	PF3D7_0213600	1.61
2	PF3D7_0217600	1.59
2	PF3D7_0217600	1.59
2	PF3D7_0217600	1.59
2	PF3D7_0217600	1.59
2	PF3D7_0220800	1.58
2	PF3D7_0220800	1.58
2	PF3D7_0207000	1.56
2	PF3D7_0207300	1.53
2	PF3D7_0214800	1.51
2	PF3D7_0214800	1.51
2	PF3D7_0214800	1.51
2	PF3D7_0214800	1.51
2	PF3D7_0204700	1.48
2	PF3D7_0204700	1.48
2	PF3D7_0204700	1.48
2	PF3D7_0204700	1.48
2	PF3D7_0205100	1.46
2	PF3D7_0205100	1.46
2	PF3D7_0208000	1.41
2	PF3D7_0208000	1.41
2	PF3D7_0208000	1.41
2	PF3D7_0208000	1.41
2	PF3D7_0216000	1.36
2	PF3D7_0216000	1.36
2	PF3D7_0216000	1.36
2	PF3D7_0216000	1.36
2	PF3D7_0216500	1.31
2	PF3D7_0216500	1.31
2	PF3D7_0207300	1.28
2	PF3D7_0207100	1.24
2	PF3D7_0207100	1.24
2	PF3D7_0207100	1.24
2	PF3D7_0219700	1.22
2	PF3D7_0211600	1.12
3	PF3D7_0321300	3.27
3	PF3D7_0321300	3.27
3	PF3D7_0315200	3.22
3	PF3D7_0315200	3.22
3	PF3D7_0318200	3.13
3	PF3D7_0318200	3.13
3	PF3D7_0308200	3.07
3	PF3D7_0308200	3.07
3	PF3D7_0308200	3.07
3	PF3D7_0308200	3.07
3	PF3D7_0302600	3.06

University of Ghana http://ugspace.ug.edu.gh

3	PF3D7_0302600	3.06
3	PF3D7_0321200	2.85
3	PF3D7_0321200	2.85
3	PF3D7_0301900	2.84
3	PF3D7_0301900	2.84
3	PF3D7_0321200	2.80
3	PF3D7_0301000	2.61
3	PF3D7_0301000	2.61
3	PF3D7_0301000	2.61
3	PF3D7_0303500	2.46
3	PF3D7_0309900	2.42
3	PF3D7_0309900	2.42
3	PF3D7_0309900	2.42
3	PF3D7_0316600	2.28
3	PF3D7_0311900	2.27
3	PF3D7_0321900	2.25
3	PF3D7_0307600	2.22
3	PF3D7_0307600	2.22
3	PF3D7_0307600	2.22
3	PF3D7_0301600	2.10
3	PF3D7_0319600	2.01
3	PF3D7_0319600	2.01
3	PF3D7_0311800	1.98
3	PF3D7_0302900	1.90
3	PF3D7_0302900	1.90
3	PF3D7_0302900	1.90
3	PF3D7_0321900	1.88
3	PF3D7_0321900	1.88
3	PF3D7_0311700	1.86
3	PF3D7_0311100	1.81
3	PF3D7_0311400	1.79
3	PF3D7_0311400	1.79
3	PF3D7_0311600	1.76
3	PF3D7_0311600	1.76
3	PF3D7_0317500	1.75
3	PF3D7_0317500	1.75
3	PF3D7_0317500	1.75
3	PF3D7_0313900	1.73
3	PF3D7_0311600	1.70
3	PF3D7_0311600	1.70
3	PF3D7_0312500	1.68
3	PF3D7_0304600	1.58
3	PF3D7_0304600	1.58
3	PF3D7_0304600	1.58
3	PF3D7_0321000	1.56
3	PF3D7_0321000	1.56
3	PF3D7_0321000	1.56
3	PF3D7_0321000	1.56

University of Ghana http://ugspace.ug.edu.gh

3	PF3D7_0319200	1.54
3	PF3D7_0319200	1.54
3	PF3D7_0319200	1.54
3	PF3D7_0319200	1.54
3	PF3D7_0306600	1.53
3	PF3D7_0323600	1.44
3	PF3D7_0323600	1.44
3	PF3D7_0323600	1.44
3	PF3D7_0320400	1.39
3	PF3D7_0320400	1.39
3	PF3D7_0320400	1.39
3	PF3D7_0320400	1.39
3	PF3D7_0302500	1.37
3	PF3D7_0321700	1.29
3	PF3D7_0321700	1.29
3	PF3D7_0321700	1.29
3	PF3D7_0304300	1.29
3	PF3D7_0304300	1.29
3	PF3D7_0304300	1.29
3	PF3D7_0304300	1.29
3	PF3D7_0323700	1.23
3	PF3D7_0323700	1.23
3	PF3D7_0323700	1.23
3	PF3D7_0319600	1.21
3	PF3D7_0308900	1.20
3	PF3D7_0308900	1.20
3	PF3D7_0308900	1.20
3	PF3D7_0308900	1.20
3	PF3D7_0321100	1.19
3	PF3D7_0321100	1.19
3	PF3D7_0321100	1.19
3	PF3D7_0306800	1.01
3	PF3D7_0302000	1.01
3	PF3D7_0302000	1.01
3	PF3D7_0302000	1.01
3	PF3D7_0302000	1.01
3	PF3D7_0314500	1.00
4	PF3D7_0420200	4.07
4	PF3D7_0420200	4.07
4	PF3D7_0414100	3.90
4	PF3D7_0414100	3.90
4	PF3D7_0425250	3.86
4	PF3D7_0425250	3.86
4	PF3D7_0414200	3.76
4	PF3D7_0414200	3.76
4	PF3D7_0414200	3.76
4	PF3D7_0424400	3.73
4	PF3D7_0424400	3.73

University of Ghana http://ugspace.ug.edu.gh

4	PF3D7_0418000	3.73
4	PF3D7_0418000	3.73
4	PF3D7_0424400	3.70
4	PF3D7_0424400	3.70
4	PF3D7_0418000	3.65
4	PF3D7_0418000	3.65
4	PF3D7_0422800	3.60
4	PF3D7_0422800	3.60
4	PF3D7_0422800	3.57
4	PF3D7_0422800	3.57
4	PF3D7_0412200	3.47
4	PF3D7_0402300	3.34
4	PF3D7_0422200	3.33
4	PF3D7_0422200	3.33
4	PF3D7_0422200	3.33
4	PF3D7_0422200	3.33
4	PF3D7_0414100	3.23
4	PF3D7_0414100	3.23
4	PF3D7_0425000	3.14
4	PF3D7_0425000	3.14
4	PF3D7_0425000	2.98
4	PF3D7_0414600	2.90
4	PF3D7_0414600	2.90
4	PF3D7_0415700	2.86
4	PF3D7_0414200	2.85
4	PF3D7_0414200	2.85
4	PF3D7_0414200	2.85
4	PF3D7_0414200	2.85
4	PF3D7_0422500	2.83
4	PF3D7_0422500	2.83
4	PF3D7_0422500	2.83
4	PF3D7_0420300	2.80
4	PF3D7_0412300	2.80
4	PF3D7_0412300	2.80
4	PF3D7_0415200	2.80
4	PF3D7_0415200	2.80
4	PF3D7_0415200	2.80
4	PF3D7_0415200	2.80
4	PF3D7_0421600	2.79
4	PF3D7_0421600	2.79
4	PF3D7_0402200	2.78
4	PF3D7_0402200	2.78
4	PF3D7_0424300	2.77
4	PF3D7_0424300	2.77
4	PF3D7_0421600	2.77
4	PF3D7_0421600	2.77
4	PF3D7_0424300	2.73
4	PF3D7_0420000	2.62

University of Ghana http://ugspace.ug.edu.gh

4	PF3D7_0420000	2.62
4	PF3D7_0420000	2.62
4	PF3D7_0420400	2.61
4	PF3D7_0420400	2.61
4	PF3D7_0420400	2.61
4	PF3D7_0420400	2.61
4	PF3D7_0419900	2.60
4	PF3D7_0420100	2.53
4	PF3D7_0420100	2.53
4	PF3D7_0420100	2.53
4	PF3D7_0408700	2.53
4	PF3D7_0401900	2.46
4	PF3D7_0401900	2.46
4	PF3D7_0421700	2.44
4	PF3D7_0421700	2.44
4	PF3D7_0417400	2.37
4	PF3D7_0417400	2.37
4	PF3D7_0405400	2.36
4	PF3D7_0405400	2.36
4	PF3D7_0405400	2.36
4	PF3D7_0405400	2.36
4	PF3D7_0424400	2.34
4	PF3D7_0424400	2.34
4	PF3D7_0401800	2.33
4	PF3D7_0401800	2.33
4	PF3D7_0404500	2.32
4	PF3D7_0404500	2.32
4	PF3D7_0421600	2.17
4	PF3D7_0421600	2.17
4	PF3D7_0407100	2.14
4	PF3D7_0407100	2.14
4	PF3D7_0407100	2.14
4	PF3D7_0407100	2.14
4	PF3D7_0414000	2.14
4	PF3D7_0414000	2.14
4	PF3D7_0404900	2.13
4	PF3D7_0404900	2.13
4	PF3D7_0404900	2.13
4	PF3D7_0404900	2.13
4	PF3D7_0417200	2.12
4	PF3D7_0417200	2.12
4	PF3D7_0417200	2.12
4	PF3D7_0417200	2.12
4	PF3D7_0419400	2.12
4	PF3D7_0419400	2.12
4	PF3D7_0414200	2.11
4	PF3D7_0414200	2.11
4	PF3D7_0414200	2.11

University of Ghana http://ugspace.ug.edu.gh

4	PF3D7_0425200	2.10
4	PF3D7_0425200	2.10
4	PF3D7_0411900	2.09
4	PF3D7_0411900	2.09
4	PF3D7_0414100	2.09
4	PF3D7_0408700	2.07
4	PF3D7_0413900	2.07
4	PF3D7_0413900	2.07
4	PF3D7_0422000	2.06
4	PF3D7_0402900	1.96
4	PF3D7_0409900	1.94
4	PF3D7_0409900	1.94
4	PF3D7_0418500	1.94
4	PF3D7_0418500	1.94
4	PF3D7_0422100	1.93
4	PF3D7_0422100	1.93
4	PF3D7_0422100	1.93
4	PF3D7_0418600	1.84
4	PF3D7_0418600	1.84
4	PF3D7_0418600	1.84
4	PF3D7_0406100	1.81
4	PF3D7_0406100	1.81
4	PF3D7_0406100	1.81
4	PF3D7_0406100	1.81
4	PF3D7_0411900	1.78
4	PF3D7_0411900	1.78
4	PF3D7_0419300	1.78
4	PF3D7_0419300	1.78
4	PF3D7_0424600	1.77
4	PF3D7_0402200	1.73
4	PF3D7_0408700	1.71
4	PF3D7_0408700	1.71
4	PF3D7_0406400	1.68
4	PF3D7_0406400	1.68
4	PF3D7_0406400	1.68
4	PF3D7_0406400	1.68
4	PF3D7_0406500	1.65
4	PF3D7_0411200	1.53
4	PF3D7_0424500	1.49
4	PF3D7_0424500	1.49
4	PF3D7_0424500	1.49
4	PF3D7_0424500	1.49
4	PF3D7_0425200	1.49
4	PF3D7_0425200	1.49
4	PF3D7_0419400	1.48
4	PF3D7_0419400	1.48
4	PF3D7_0403800	1.47
4	PF3D7_0403800	1.47

University of Ghana http://ugspace.ug.edu.gh

4	PF3D7_0425300	1.46
4	PF3D7_0411800	1.44
4	PF3D7_0403400	1.42
4	PF3D7_0403400	1.42
4	PF3D7_0423300	1.41
4	PF3D7_0423300	1.41
4	PF3D7_0423300	1.41
4	PF3D7_0423300	1.41
4	PF3D7_0415300	1.40
4	PF3D7_0421700	1.35
4	PF3D7_0424200	1.34
4	PF3D7_0424200	1.34
4	PF3D7_0424200	1.34
4	PF3D7_0424200	1.34
4	PF3D7_0418000	1.33
4	PF3D7_0418000	1.33
4	PF3D7_0410500	1.32
4	PF3D7_0422800	1.30
4	PF3D7_0418500	1.27
4	PF3D7_0418500	1.27
4	PF3D7_0421700	1.24
4	PF3D7_0421700	1.24
4	PF3D7_0401600	1.18
4	PF3D7_0401600	1.18
4	PF3D7_0401600	1.18
4	PF3D7_0406500	1.15
4	PF3D7_0410800	1.15
4	PF3D7_0410800	1.15
4	PF3D7_0410800	1.15
4	PF3D7_0410800	1.15
4	PF3D7_0401700	1.14
4	PF3D7_0401700	1.14
4	PF3D7_0401700	1.14
4	PF3D7_0401700	1.14
4	PF3D7_0414900	1.07
4	PF3D7_0414900	1.07
4	PF3D7_0407800	1.05
4	PF3D7_0407800	1.05
4	PF3D7_0407800	1.05
4	PF3D7_0414000	1.05
4	PF3D7_0414000	1.05
4	PF3D7_0418700	1.03
4	PF3D7_0418700	1.03
4	PF3D7_0417100	1.03
4	PF3D7_0413500	1.01
4	PF3D7_0413500	1.01
4	PF3D7_0413500	1.01
4	PF3D7_0413500	1.01

University of Ghana http://ugspace.ug.edu.gh

4	PF3D7_0414000	1.01
5	PF3D7_0522400	2.98
5	PF3D7_0522400	2.98
5	PF3D7_0501300	2.90
5	PF3D7_0501300	2.90
5	PF3D7_0529300	2.74
5	PF3D7_0529300	2.74
5	PF3D7_0529800	2.74
5	PF3D7_0529800	2.74
5	PF3D7_0508000	2.66
5	PF3D7_0508000	2.66
5	PF3D7_0511200	2.60
5	PF3D7_0511200	2.60
5	PF3D7_0529800	2.51
5	PF3D7_0529800	2.51
5	PF3D7_0514700	2.47
5	PF3D7_0514700	2.47
5	PF3D7_0529200	2.42
5	PF3D7_0529200	2.42
5	PF3D7_0511400	2.42
5	PF3D7_0503200	2.38
5	PF3D7_0522400	2.35
5	PF3D7_0529400	2.34
5	PF3D7_0529400	2.34
5	PF3D7_0529400	2.34
5	PF3D7_0508500	2.32
5	PF3D7_0508500	2.32
5	PF3D7_0504000	2.31
5	PF3D7_0504000	2.31
5	PF3D7_0504000	2.31
5	PF3D7_0504000	2.31
5	PF3D7_0522400	2.30
5	PF3D7_0522400	2.30
5	PF3D7_0522400	2.21
5	PF3D7_0522400	2.21
5	PF3D7_0511100	2.15
5	PF3D7_0515500	2.13
5	PF3D7_0512200	2.13
5	PF3D7_0512200	2.13
5	PF3D7_0512200	2.13
5	PF3D7_0512200	2.13
5	PF3D7_0524900	2.11
5	PF3D7_0524900	2.11
5	PF3D7_0532100	2.10
5	PF3D7_0532100	2.10
5	PF3D7_0517400	2.10
5	PF3D7_0517400	2.10
5	PF3D7_0529400	2.04

University of Ghana http://ugspace.ug.edu.gh

5	PF3D7_0503800	2.04
5	PF3D7_0519900	2.00
5	PF3D7_0519900	2.00
5	PF3D7_0511200	1.95
5	PF3D7_0520100	1.93
5	PF3D7_0520100	1.93
5	PF3D7_0520100	1.93
5	PF3D7_0522900	1.90
5	PF3D7_0522900	1.90
5	PF3D7_0526400	1.86
5	PF3D7_0526400	1.86
5	PF3D7_0526400	1.86
5	PF3D7_0519600	1.83
5	PF3D7_0519600	1.83
5	PF3D7_0519600	1.83
5	PF3D7_0531100	1.79
5	PF3D7_0524300	1.77
5	PF3D7_0524300	1.77
5	PF3D7_0524300	1.77
5	PF3D7_0523000	1.75
5	PF3D7_0532500	1.74
5	PF3D7_0532500	1.74
5	PF3D7_0504200	1.73
5	PF3D7_0528100	1.72
5	PF3D7_0529500	1.72
5	PF3D7_0529500	1.72
5	PF3D7_0521000	1.72
5	PF3D7_0521000	1.72
5	PF3D7_0529200	1.70
5	PF3D7_0529200	1.70
5	PF3D7_0520400	1.67
5	PF3D7_0520400	1.67
5	PF3D7_0520400	1.67
5	PF3D7_0520400	1.67
5	PF3D7_0519500	1.64
5	PF3D7_0519500	1.64
5	PF3D7_0522100	1.63
5	PF3D7_0512450	1.61
5	PF3D7_0515500	1.61
5	PF3D7_0515500	1.61
5	PF3D7_0514300	1.61
5	PF3D7_0514300	1.61
5	PF3D7_0514300	1.61
5	PF3D7_0514300	1.61
5	PF3D7_0502600	1.55
5	PF3D7_0502600	1.55
5	PF3D7_0530400	1.54
5	PF3D7_0530400	1.54

University of Ghana http://ugspace.ug.edu.gh

5	PF3D7_0530400	1.54
5	PF3D7_0504900	1.41
5	PF3D7_0529400	1.40
5	PF3D7_0529400	1.40
5	PF3D7_0529400	1.40
5	PF3D7_0528700	1.39
5	PF3D7_0528700	1.39
5	PF3D7_0528700	1.39
5	PF3D7_0528700	1.39
5	PF3D7_0500800	1.37
5	PF3D7_0500800	1.37
5	PF3D7_0500800	1.37
5	PF3D7_0500800	1.37
5	PF3D7_0522000	1.36
5	PF3D7_0522000	1.36
5	PF3D7_0522000	1.36
5	PF3D7_0522000	1.36
5	PF3D7_0503900	1.32
5	PF3D7_0503900	1.32
5	PF3D7_0503900	1.32
5	PF3D7_0503900	1.32
5	PF3D7_0526700	1.31
5	PF3D7_0526700	1.31
5	PF3D7_0526700	1.31
5	PF3D7_0526700	1.31
5	PF3D7_0513200	1.31
5	PF3D7_0514200	1.28
5	PF3D7_0514200	1.28
5	PF3D7_0514200	1.28
5	PF3D7_0528400	1.26
5	PF3D7_0528400	1.26
5	PF3D7_0515800	1.25
5	PF3D7_0515800	1.25
5	PF3D7_0515800	1.25
5	PF3D7_0515800	1.25
5	PF3D7_0528500	1.25
5	PF3D7_0528500	1.25
5	PF3D7_0509700	1.23
5	PF3D7_0509700	1.23
5	PF3D7_0528200	1.22
5	PF3D7_0528200	1.22
5	PF3D7_0528200	1.22
5	PF3D7_0528200	1.22
5	PF3D7_0530300	1.21
5	PF3D7_0530300	1.21
5	PF3D7_0530300	1.21
5	PF3D7_0530300	1.21
5	PF3D7_0502600	1.17

University of Ghana http://ugspace.ug.edu.gh

5	PF3D7_0502600	1.17
5	PF3D7_0501200	1.17
5	PF3D7_0501200	1.17
5	PF3D7_0501200	1.17
5	PF3D7_0526200	1.16
5	PF3D7_0526200	1.16
5	PF3D7_0526200	1.16
5	PF3D7_0509100	1.15
5	PF3D7_0528400	1.13
5	PF3D7_0513200	1.11
5	PF3D7_0513200	1.11
6	PF3D7_0619600	4.01
6	PF3D7_0619600	4.01
6	PF3D7_0619600	4.01
6	PF3D7_0619600	4.01
6	PF3D7_0630700	3.91
6	PF3D7_0630700	3.91
6	PF3D7_0630700	3.91
6	PF3D7_0630700	3.91
6	PF3D7_0630800	3.73
6	PF3D7_0630800	3.73
6	PF3D7_0630300	3.69
6	PF3D7_0630300	3.69
6	PF3D7_0630600	3.57
6	PF3D7_0630600	3.57
6	PF3D7_0612900	3.03
6	PF3D7_0612900	3.03
6	PF3D7_0612900	3.03
6	PF3D7_0612900	3.03
6	PF3D7_0602700	2.96
6	PF3D7_0602700	2.96
6	PF3D7_0609700	2.88
6	PF3D7_0609700	2.88
6	PF3D7_0604300	2.83
6	PF3D7_0604300	2.83
6	PF3D7_0623300	2.80
6	PF3D7_0623300	2.80
6	PF3D7_0619200	2.80
6	PF3D7_0619200	2.80
6	PF3D7_0614100	2.78
6	PF3D7_0614100	2.78
6	PF3D7_0614100	2.78
6	PF3D7_0614100	2.78
6	PF3D7_0605600	2.65
6	PF3D7_0605600	2.65
6	PF3D7_0615200	2.64
6	PF3D7_0615200	2.64
6	PF3D7_0601800	2.57

University of Ghana http://ugspace.ug.edu.gh

6	PF3D7_0601800	2.57
6	PF3D7_0601800	2.57
6	PF3D7_0606700	2.56
6	PF3D7_0606700	2.56
6	PF3D7_0606700	2.56
6	PF3D7_0609600	2.55
6	PF3D7_0628900	2.54
6	PF3D7_0628900	2.54
6	PF3D7_0628900	2.54
6	PF3D7_0615100	2.48
6	PF3D7_0615400	2.46
6	PF3D7_0615400	2.46
6	PF3D7_0619100	2.44
6	PF3D7_0619100	2.44
6	PF3D7_0619200	2.42
6	PF3D7_0619200	2.42
6	PF3D7_0615600	2.34
6	PF3D7_0615600	2.34
6	PF3D7_0623300	2.30
6	PF3D7_0623300	2.30
6	PF3D7_0619800	2.30
6	PF3D7_0621700	2.21
6	PF3D7_0615900	2.19
6	PF3D7_0615900	2.19
6	PF3D7_0615900	2.19
6	PF3D7_0615900	2.19
6	PF3D7_0619800	2.19
6	PF3D7_0619800	2.19
6	PF3D7_0613800	2.16
6	PF3D7_0613800	2.16
6	PF3D7_0615400	2.13
6	PF3D7_0615400	2.13
6	PF3D7_0614400	2.13
6	PF3D7_0614400	2.13
6	PF3D7_0630800	2.12
6	PF3D7_0630800	2.12
6	PF3D7_0613800	2.12
6	PF3D7_0613800	2.12
6	PF3D7_0620700	2.06
6	PF3D7_0620700	2.06
6	PF3D7_0620700	2.06
6	PF3D7_0629800	2.02
6	PF3D7_0629800	2.02
6	PF3D7_0629800	2.02
6	PF3D7_0630800	1.99
6	PF3D7_0628700	1.99
6	PF3D7_0628700	1.99
6	PF3D7_0628700	1.99

University of Ghana http://ugspace.ug.edu.gh

6	PF3D7_0609000	1.96
6	PF3D7_0629100	1.94
6	PF3D7_0629100	1.94
6	PF3D7_0629100	1.94
6	PF3D7_0603000	1.92
6	PF3D7_0629500	1.91
6	PF3D7_0616500	1.85
6	PF3D7_0616500	1.85
6	PF3D7_0616500	1.85
6	PF3D7_0619700	1.85
6	PF3D7_0630800	1.84
6	PF3D7_0615200	1.83
6	PF3D7_0619300	1.83
6	PF3D7_0627300	1.79
6	PF3D7_0619300	1.72
6	PF3D7_0615600	1.70
6	PF3D7_0615600	1.70
6	PF3D7_0612200	1.69
6	PF3D7_0612200	1.69
6	PF3D7_0612200	1.69
6	PF3D7_0618200	1.66
6	PF3D7_0618200	1.66
6	PF3D7_0628600	1.66
6	PF3D7_0628600	1.66
6	PF3D7_0628600	1.66
6	PF3D7_0603800	1.63
6	PF3D7_0603600	1.62
6	PF3D7_0603600	1.62
6	PF3D7_0629700	1.60
6	PF3D7_0629700	1.57
6	PF3D7_0625300	1.55
6	PF3D7_0625300	1.55
6	PF3D7_0625300	1.55
6	PF3D7_0625300	1.55
6	PF3D7_0627700	1.54
6	PF3D7_0627700	1.54
6	PF3D7_0627700	1.54
6	PF3D7_0613900	1.53
6	PF3D7_0613900	1.53
6	PF3D7_0624700	1.52
6	PF3D7_0624700	1.52
6	PF3D7_0624700	1.52
6	PF3D7_0613300	1.45
6	PF3D7_0613300	1.45
6	PF3D7_0606600	1.44
6	PF3D7_0606600	1.44
6	PF3D7_0606600	1.44
6	PF3D7_0606600	1.44

University of Ghana http://ugspace.ug.edu.gh

6	PF3D7_0623000	1.42
6	PF3D7_0623000	1.42
6	PF3D7_0623000	1.42
6	PF3D7_0623000	1.42
6	PF3D7_0630100	1.41
6	PF3D7_0630100	1.41
6	PF3D7_0630100	1.41
6	PF3D7_0614900	1.37
6	PF3D7_0603600	1.36
6	PF3D7_0603600	1.35
6	PF3D7_0630400	1.34
6	PF3D7_0630400	1.34
6	PF3D7_0630400	1.34
6	PF3D7_0630400	1.34
6	PF3D7_0609100	1.33
6	PF3D7_0609100	1.33
6	PF3D7_0613300	1.31
6	PF3D7_0613300	1.31
6	PF3D7_0627800	1.31
6	PF3D7_0627800	1.31
6	PF3D7_0627800	1.31
6	PF3D7_0627800	1.31
6	PF3D7_0613500	1.30
6	PF3D7_0613500	1.30
6	PF3D7_0613500	1.30
6	PF3D7_0606200	1.25
6	PF3D7_0606200	1.25
6	PF3D7_0625400	1.25
6	PF3D7_0625400	1.25
6	PF3D7_0625400	1.25
6	PF3D7_0603800	1.24
6	PF3D7_0603800	1.24
6	PF3D7_0628200	1.24
6	PF3D7_0628200	1.24
6	PF3D7_0628200	1.24
6	PF3D7_0628200	1.24
6	PF3D7_0611800	1.22
6	PF3D7_0626000	1.19
6	PF3D7_0626000	1.19
6	PF3D7_0626000	1.19
6	PF3D7_0611800	1.17
6	PF3D7_0616700	1.12
6	PF3D7_0622900	1.09
6	PF3D7_0622900	1.09
6	PF3D7_0622900	1.09
6	PF3D7_0622900	1.09
6	PF3D7_0630900	1.08
6	PF3D7_0630900	1.08

University of Ghana http://ugspace.ug.edu.gh

6	PF3D7_0627200	1.07
6	PF3D7_0627200	1.07
6	PF3D7_0627200	1.07
6	PF3D7_0621300	1.06
6	PF3D7_0621300	1.06
6	PF3D7_0623800	1.05
6	PF3D7_0606000	1.04
6	PF3D7_0606000	1.04
6	PF3D7_0606000	1.04
6	PF3D7_0606000	1.04
6	PF3D7_0624400	1.03
6	PF3D7_0624400	1.03
6	PF3D7_0624400	1.03
6	PF3D7_0624400	1.03
6	PF3D7_0603800	1.03
6	PF3D7_0603800	1.03
6	PF3D7_0602600	1.01
6	PF3D7_0602600	1.01
6	PF3D7_0608300	1.01
6	PF3D7_0608300	1.01
6	PF3D7_0608300	1.01
6	PF3D7_0608300	1.01
7	PF3D7_0710000	4.73
7	PF3D7_0710000	4.73
7	PF3D7_0729700	4.56
7	PF3D7_0729700	4.56
7	PF3D7_0709300	4.27
7	PF3D7_0709300	4.27
7	PF3D7_0713600	3.88
7	PF3D7_0713900	3.78
7	PF3D7_0713900	3.78
7	PF3D7_0713900	3.78
7	PF3D7_0713600	3.74
7	PF3D7_0713600	3.74
7	PF3D7_0711500	3.33
7	PF3D7_0711500	3.33
7	PF3D7_0731500	3.15
7	PF3D7_0720400	3.11
7	PF3D7_0716000	3.07
7	PF3D7_0716000	3.07
7	PF3D7_0716000	3.07
7	PF3D7_0716000	3.07
7	PF3D7_0710400	2.79
7	PF3D7_0710400	2.79
7	PF3D7_0710400	2.79
7	PF3D7_0710400	2.79
7	PF3D7_0701900	2.77
7	PF3D7_0701900	2.77

University of Ghana http://ugspace.ug.edu.gh

7	PF3D7_0719400	2.76
7	PF3D7_0719400	2.76
7	PF3D7_0719400	2.76
7	PF3D7_0719400	2.76
7	PF3D7_0718900	2.72
7	PF3D7_0718900	2.72
7	PF3D7_0731800	2.64
7	PF3D7_0731800	2.64
7	PF3D7_0731800	2.64
7	PF3D7_0731800	2.64
7	PF3D7_0718300	2.59
7	PF3D7_0718300	2.59
7	PF3D7_0720400	2.59
7	PF3D7_0720400	2.59
7	PF3D7_0711200	2.53
7	PF3D7_0711200	2.53
7	PF3D7_0711200	2.53
7	PF3D7_0711200	2.53
7	PF3D7_0705200	2.50
7	PF3D7_0705200	2.50
7	PF3D7_0708300	2.42
7	PF3D7_0708300	2.42
7	PF3D7_0708400	2.39
7	PF3D7_0708400	2.39
7	PF3D7_0710100	2.35
7	PF3D7_0710100	2.35
7	PF3D7_0710100	2.35
7	PF3D7_0710100	2.35
7	PF3D7_0721200	2.14
7	PF3D7_0721200	2.14
7	PF3D7_0721200	2.14
7	PF3D7_0721200	2.14
7	PF3D7_0718900	2.13
7	PF3D7_0718900	2.13
7	PF3D7_0702300	2.11
7	PF3D7_0702300	2.11
7	PF3D7_0702300	2.11
7	PF3D7_0702300	2.11
7	PF3D7_0716200	2.09
7	PF3D7_0716200	2.09
7	PF3D7_0716200	2.09
7	PF3D7_0716200	2.09
7	PF3D7_0731500	2.08
7	PF3D7_0731500	2.08
7	PF3D7_0724700	2.07
7	PF3D7_0724700	2.07
7	PF3D7_0718300	2.06
7	PF3D7_0718300	2.06

University of Ghana http://ugspace.ug.edu.gh

7	PF3D7_0710500	2.05
7	PF3D7_0710500	2.05
7	PF3D7_0717900	2.05
7	PF3D7_0717900	2.05
7	PF3D7_0719200	2.04
7	PF3D7_0719200	2.04
7	PF3D7_0708300	2.02
7	PF3D7_0708300	2.02
7	PF3D7_0710500	1.99
7	PF3D7_0710500	1.99
7	PF3D7_0710000	1.95
7	PF3D7_0710000	1.95
7	PF3D7_0730100	1.94
7	PF3D7_0730100	1.94
7	PF3D7_0718900	1.87
7	PF3D7_0718900	1.87
7	PF3D7_0717300	1.87
7	PF3D7_0717300	1.87
7	PF3D7_0702000	1.86
7	PF3D7_0702000	1.86
7	PF3D7_0716900	1.78
7	PF3D7_0716900	1.78
7	PF3D7_0709400	1.76
7	PF3D7_0709400	1.76
7	PF3D7_0729600	1.76
7	PF3D7_0729600	1.76
7	PF3D7_0713400	1.69
7	PF3D7_0713400	1.69
7	PF3D7_0702000	1.68
7	PF3D7_0702000	1.68
7	PF3D7_0713400	1.66
7	PF3D7_0713400	1.66
7	PF3D7_0716300	1.65
7	PF3D7_0716300	1.65
7	PF3D7_0715200	1.58
7	PF3D7_0715200	1.58
7	PF3D7_0715200	1.58
7	PF3D7_0715200	1.58
7	PF3D7_0731400	1.55
7	PF3D7_0731400	1.55
7	PF3D7_0731400	1.55
7	PF3D7_0731400	1.55
7	PF3D7_0704200	1.51
7	PF3D7_0704200	1.51
7	PF3D7_0704200	1.51
7	PF3D7_0704200	1.51
7	PF3D7_0729500	1.51
7	PF3D7_0729500	1.51

University of Ghana http://ugspace.ug.edu.gh

7	PF3D7_0717300	1.48
7	PF3D7_0709000	1.47
7	PF3D7_0718000	1.42
7	PF3D7_0718000	1.42
7	PF3D7_0708500	1.39
7	PF3D7_0708500	1.39
7	PF3D7_0708500	1.39
7	PF3D7_0708500	1.39
7	PF3D7_0705100	1.38
7	PF3D7_0705100	1.38
7	PF3D7_0703800	1.36
7	PF3D7_0703800	1.36
7	PF3D7_0703800	1.36
7	PF3D7_0703800	1.36
7	PF3D7_0717100	1.33
7	PF3D7_0717100	1.33
7	PF3D7_0717100	1.33
7	PF3D7_0717100	1.33
7	PF3D7_0702000	1.30
7	PF3D7_0702000	1.30
7	PF3D7_0713300	1.29
7	PF3D7_0713300	1.29
7	PF3D7_0718000	1.06
7	PF3D7_0718000	1.06
7	PF3D7_0710300	1.04
7	PF3D7_0710300	1.04
7	PF3D7_0711400	1.03
7	PF3D7_0711400	1.03
7	PF3D7_0711400	1.03
7	PF3D7_0711400	1.03
7	PF3D7_0706500	1.00
8	PF3D7_0830800	4.29
8	PF3D7_0830800	4.29
8	PF3D7_0830800	4.09
8	PF3D7_0830800	4.09
8	PF3D7_0825500	3.89
8	PF3D7_0825500	3.89
8	PF3D7_0825500	3.89
8	PF3D7_0825500	3.89
8	PF3D7_0825800	3.46
8	PF3D7_0825800	3.46
8	PF3D7_0831100	3.22
8	PF3D7_0831100	3.22
8	PF3D7_0827100	3.20
8	PF3D7_0827100	3.20
8	PF3D7_0827100	3.20
8	PF3D7_0827100	3.20
8	PF3D7_0830800	2.95

University of Ghana http://ugspace.ug.edu.gh

8	PF3D7_0830800	2.95
8	PF3D7_0806200	2.92
8	PF3D7_0806200	2.92
8	PF3D7_0806100	2.84
8	PF3D7_0806100	2.84
8	PF3D7_0806100	2.84
8	PF3D7_0806100	2.84
8	PF3D7_0809600	2.44
8	PF3D7_0809600	2.44
8	PF3D7_0830300	2.43
8	PF3D7_0830300	2.43
8	PF3D7_0830300	2.43
8	PF3D7_0830300	2.43
8	PF3D7_0815100	2.42
8	PF3D7_0815100	2.42
8	PF3D7_0815100	2.42
8	PF3D7_0815100	2.42
8	PF3D7_0804500	2.21
8	PF3D7_0804500	2.21
8	PF3D7_0804500	2.21
8	PF3D7_0804500	2.21
8	PF3D7_0827000	2.21
8	PF3D7_0827000	2.21
8	PF3D7_0827000	2.21
8	PF3D7_0827000	2.21
8	PF3D7_0811700	2.16
8	PF3D7_0811700	2.16
8	PF3D7_0811700	2.16
8	PF3D7_0824300	2.16
8	PF3D7_0824300	2.16
8	PF3D7_0822200	2.14
8	PF3D7_0830200	2.13
8	PF3D7_0830200	2.13
8	PF3D7_0830200	2.13
8	PF3D7_0809800	2.13
8	PF3D7_0809800	2.13
8	PF3D7_0822600	2.13
8	PF3D7_0822600	2.13
8	PF3D7_0826900	2.10
8	PF3D7_0813700	2.00
8	PF3D7_0810300	2.00
8	PF3D7_0810300	2.00
8	PF3D7_0810800	1.99
8	PF3D7_0828100	1.95
8	PF3D7_0828100	1.95
8	PF3D7_0828100	1.95
8	PF3D7_0809800	1.95
8	PF3D7_0809800	1.95

University of Ghana http://ugspace.ug.edu.gh

8	PF3D7_0803600	1.92
8	PF3D7_0803600	1.92
8	PF3D7_0817600	1.92
8	PF3D7_0828300	1.89
8	PF3D7_0828300	1.89
8	PF3D7_0828300	1.89
8	PF3D7_0817700	1.87
8	PF3D7_0816300	1.76
8	PF3D7_0816300	1.76
8	PF3D7_0816300	1.76
8	PF3D7_0825700	1.75
8	PF3D7_0825700	1.75
8	PF3D7_0825700	1.75
8	PF3D7_0825700	1.75
8	PF3D7_0827900	1.72
8	PF3D7_0827900	1.72
8	PF3D7_0811300	1.72
8	PF3D7_0811300	1.72
8	PF3D7_0820500	1.71
8	PF3D7_0820500	1.71
8	PF3D7_0820500	1.71
8	PF3D7_0820500	1.71
8	PF3D7_0829800	1.69
8	PF3D7_0820900	1.69
8	PF3D7_0803600	1.67
8	PF3D7_0822200	1.66
8	PF3D7_0822200	1.66
8	PF3D7_0826200	1.65
8	PF3D7_0826200	1.65
8	PF3D7_0826200	1.65
8	PF3D7_0826200	1.65
8	PF3D7_0817700	1.65
8	PF3D7_0817700	1.65
8	PF3D7_0822900	1.65
8	PF3D7_0822900	1.65
8	PF3D7_0822900	1.65
8	PF3D7_0822900	1.65
8	PF3D7_0807700	1.64
8	PF3D7_0807700	1.64
8	PF3D7_0810600	1.63
8	PF3D7_0829600	1.59
8	PF3D7_0829600	1.59
8	PF3D7_0829600	1.59
8	PF3D7_0819800	1.59
8	PF3D7_0819800	1.59
8	PF3D7_0828400	1.58
8	PF3D7_0828400	1.58
8	PF3D7_0828400	1.58

University of Ghana http://ugspace.ug.edu.gh

8	PF3D7_0806000	1.56
8	PF3D7_0806700	1.55
8	PF3D7_0806700	1.55
8	PF3D7_0828500	1.55
8	PF3D7_0828500	1.55
8	PF3D7_0814700	1.54
8	PF3D7_0814700	1.54
8	PF3D7_0814700	1.54
8	PF3D7_0814700	1.54
8	PF3D7_0809700	1.54
8	PF3D7_0809700	1.54
8	PF3D7_0811900	1.52
8	PF3D7_0811900	1.52
8	PF3D7_0802000	1.51
8	PF3D7_0802000	1.51
8	PF3D7_0802000	1.51
8	PF3D7_0824500	1.49
8	PF3D7_0808100	1.46
8	PF3D7_0808100	1.46
8	PF3D7_0817700	1.43
8	PF3D7_0817700	1.43
8	PF3D7_0801000	1.42
8	PF3D7_0801000	1.42
8	PF3D7_0801000	1.42
8	PF3D7_0817100	1.36
8	PF3D7_0823300	1.36
8	PF3D7_0823300	1.36
8	PF3D7_0823300	1.36
8	PF3D7_0826500	1.30
8	PF3D7_0826500	1.30
8	PF3D7_0826500	1.30
8	PF3D7_0806700	1.29
8	PF3D7_0806700	1.29
8	PF3D7_0830600	1.28
8	PF3D7_0830600	1.28
8	PF3D7_0808000	1.23
8	PF3D7_0808000	1.23
8	PF3D7_0808000	1.23
8	PF3D7_0803600	1.22
8	PF3D7_0804400	1.17
8	PF3D7_0804400	1.17
8	PF3D7_0804400	1.17
8	PF3D7_0804400	1.17
8	PF3D7_0800900	1.17
8	PF3D7_0800900	1.17
8	PF3D7_0800900	1.17
8	PF3D7_0830900	1.14
8	PF3D7_0809400	1.14

University of Ghana http://ugspace.ug.edu.gh

8	PF3D7_0809400	1.14
8	PF3D7_0809400	1.14
8	PF3D7_0809400	1.14
8	PF3D7_0809500	1.13
8	PF3D7_0809500	1.13
8	PF3D7_0809500	1.13
8	PF3D7_0809500	1.13
8	PF3D7_0809300	1.12
8	PF3D7_0809300	1.12
8	PF3D7_0809300	1.12
8	PF3D7_0808400	1.06
9	PF3D7_0916000	2.94
9	PF3D7_0916000	2.94
9	PF3D7_0916000	2.94
9	PF3D7_0927300	2.85
9	PF3D7_0927300	2.85
9	PF3D7_0927300	2.85
9	PF3D7_0930200	2.74
9	PF3D7_0930200	2.74
9	PF3D7_0930200	2.74
9	PF3D7_0930200	2.74
9	PF3D7_0922800	2.66
9	PF3D7_0922800	2.66
9	PF3D7_0903400	2.43
9	PF3D7_0903400	2.43
9	PF3D7_0910200	2.40
9	PF3D7_0910200	2.40
9	PF3D7_0933100	2.34
9	PF3D7_0925500	2.27
9	PF3D7_0919800	2.26
9	PF3D7_0925000	2.21
9	PF3D7_0925000	2.21
9	PF3D7_0919400	2.21
9	PF3D7_0919400	2.21
9	PF3D7_0907700	2.19
9	PF3D7_0907700	2.19
9	PF3D7_0907700	2.19
9	PF3D7_0907700	2.19
9	PF3D7_0924700	2.18
9	PF3D7_0924700	2.18
9	PF3D7_0924700	2.18
9	PF3D7_0928800	2.17
9	PF3D7_0930600	2.14
9	PF3D7_0930600	2.14
9	PF3D7_0929900	2.13
9	PF3D7_0929900	2.13
9	PF3D7_0907400	2.13
9	PF3D7_0907400	2.13

University of Ghana http://ugspace.ug.edu.gh

9	PF3D7_0907400	2.13
9	PF3D7_0907800	2.10
9	PF3D7_0907800	2.10
9	PF3D7_0907800	2.10
9	PF3D7_0908500	2.09
9	PF3D7_0907300	2.04
9	PF3D7_0907300	2.04
9	PF3D7_0907300	2.04
9	PF3D7_0903400	2.04
9	PF3D7_0903400	2.04
9	PF3D7_0919400	2.04
9	PF3D7_0919400	2.04
9	PF3D7_0929100	2.03
9	PF3D7_0903400	2.01
9	PF3D7_0908300	2.01
9	PF3D7_0908300	2.01
9	PF3D7_0908300	2.01
9	PF3D7_0920100	2.00
9	PF3D7_0910400	1.98
9	PF3D7_0910400	1.98
9	PF3D7_0910400	1.98
9	PF3D7_0933200	1.93
9	PF3D7_0924900	1.93
9	PF3D7_0924900	1.93
9	PF3D7_0920300	1.93
9	PF3D7_0930100	1.76
9	PF3D7_0930100	1.76
9	PF3D7_0930100	1.76
9	PF3D7_0930100	1.76
9	PF3D7_0925000	1.74
9	PF3D7_0925000	1.74
9	PF3D7_0929600	1.73
9	PF3D7_0929600	1.73
9	PF3D7_0931700	1.73
9	PF3D7_0931700	1.73
9	PF3D7_0931700	1.73
9	PF3D7_0931700	1.73
9	PF3D7_0923200	1.66
9	PF3D7_0923200	1.66
9	PF3D7_0904300	1.65
9	PF3D7_0904300	1.65
9	PF3D7_0911600	1.65
9	PF3D7_0911600	1.65
9	PF3D7_0908500	1.64
9	PF3D7_0926000	1.62
9	PF3D7_0914300	1.45
9	PF3D7_0914300	1.45
9	PF3D7_0930800	1.44

University of Ghana http://ugspace.ug.edu.gh

9	PF3D7_0930800	1.44
9	PF3D7_0930800	1.44
9	PF3D7_0930800	1.44
9	PF3D7_0932800	1.43
9	PF3D7_0909200	1.38
9	PF3D7_0900500	1.37
9	PF3D7_0900500	1.37
9	PF3D7_0900500	1.37
9	PF3D7_0900500	1.37
9	PF3D7_0925500	1.36
9	PF3D7_0925500	1.36
9	PF3D7_0924900	1.36
9	PF3D7_0924900	1.36
9	PF3D7_0914000	1.32
9	PF3D7_0914000	1.32
9	PF3D7_0929400	1.31
9	PF3D7_0929400	1.31
9	PF3D7_0915100	1.30
9	PF3D7_0915100	1.30
9	PF3D7_0929400	1.25
9	PF3D7_0929400	1.25
9	PF3D7_0929300	1.25
9	PF3D7_0929300	1.25
9	PF3D7_0906600	1.21
9	PF3D7_0906600	1.21
9	PF3D7_0928700	1.17
9	PF3D7_0928700	1.17
9	PF3D7_0924200	1.15
9	PF3D7_0924200	1.15
9	PF3D7_0924200	1.15
9	PF3D7_0924200	1.15
9	PF3D7_0916500	1.14
9	PF3D7_0916500	1.14
9	PF3D7_0905200	1.13
9	PF3D7_0905200	1.13
9	PF3D7_0905300	1.08
9	PF3D7_0905300	1.08
9	PF3D7_0929900	1.06
9	PF3D7_0929900	1.06
9	PF3D7_0929000	1.06
9	PF3D7_0929000	1.06
9	PF3D7_0902800	1.04
9	PF3D7_0902800	1.04
9	PF3D7_0922400	1.01
9	PF3D7_0922400	1.01
10	PF3D7_1028500	1.85
10	PF3D7_1028500	1.85
10	PF3D7_1028500	1.85

University of Ghana http://ugspace.ug.edu.gh

10	PF3D7_1028500	1.85
10	PF3D7_1009200	1.63
10	PF3D7_1009200	1.63
10	PF3D7_1009200	1.63
10	PF3D7_1009200	1.63
10	PF3D7_1014800	1.51
10	PF3D7_1014800	1.51
10	PF3D7_1014800	1.99
10	PF3D7_1014800	1.99
10	PF3D7_1004800	5.47
10	PF3D7_1004800	5.47
10	PF3D7_1004800	2.13
10	PF3D7_1004800	2.13
10	PF3D7_1004800	4.56
10	PF3D7_1004800	2.13
10	PF3D7_1004800	2.13
10	PF3D7_1004800	4.56
10	PF3D7_1035500	2.94
10	PF3D7_1035500	2.94
10	PF3D7_1035500	2.94
10	PF3D7_1035500	2.94
10	PF3D7_1021700	1.74
10	PF3D7_1021700	1.74
10	PF3D7_1021700	1.84
10	PF3D7_1021700	1.84
10	PF3D7_1006000	1.05
10	PF3D7_1006000	1.05
10	PF3D7_1006000	1.05
10	PF3D7_1006000	1.05
10	PF3D7_1028000	1.20
10	PF3D7_1028000	1.20
10	PF3D7_1028000	2.13
10	PF3D7_1028000	2.13
10	PF3D7_1029100	1.63
10	PF3D7_1029100	1.63
10	PF3D7_1029100	1.63
10	PF3D7_1029100	1.54
10	PF3D7_1029100	1.54
10	PF3D7_1029100	1.54
10	PF3D7_1003400	1.07
10	PF3D7_1003400	1.07
10	PF3D7_1003400	1.07
10	PF3D7_1003400	1.07
10	PF3D7_1024000	1.06
10	PF3D7_1024000	1.06
10	PF3D7_1024000	1.06
10	PF3D7_1024000	1.06
10	PF3D7_1028600	1.16

University of Ghana http://ugspace.ug.edu.gh

10	PF3D7_1028600	1.16
10	PF3D7_1004600	3.33
10	PF3D7_1004600	3.33
10	PF3D7_1004600	3.23
10	PF3D7_1004600	1.26
10	PF3D7_1004600	1.13
10	PF3D7_1004600	3.23
10	PF3D7_1004600	1.26
10	PF3D7_1004600	1.13
10	PF3D7_1033100	2.04
10	PF3D7_1033100	2.04
10	PF3D7_1033100	2.04
10	PF3D7_1033100	2.04
10	PF3D7_1016700	1.85
10	PF3D7_1016700	1.85
10	PF3D7_1016700	1.85
10	PF3D7_1016700	1.85
10	PF3D7_1035400	2.52
10	PF3D7_1035400	2.52
10	PF3D7_1035400	2.52
10	PF3D7_1035400	2.52
10	PF3D7_1001400	1.92
10	PF3D7_1001400	1.92
10	PF3D7_1001400	1.92
10	PF3D7_1001400	1.92
10	PF3D7_1029200	1.77
10	PF3D7_1029200	1.77
10	PF3D7_1029200	1.77
10	PF3D7_1029200	1.77
10	PF3D7_1026400	1.82
10	PF3D7_1026400	1.82
10	PF3D7_1026400	1.82
10	PF3D7_1026400	1.82
10	PF3D7_1017900	1.54
10	PF3D7_1017900	1.54
10	PF3D7_1017900	1.54
10	PF3D7_1017900	1.54
10	PF3D7_1017800	2.52
10	PF3D7_1017800	2.52
10	PF3D7_1017800	2.52
10	PF3D7_1017800	2.52
10	PF3D7_1018300	1.07
10	PF3D7_1018300	1.07
10	PF3D7_1018300	1.07
10	PF3D7_1018300	1.07
10	PF3D7_1019700	2.39
10	PF3D7_1019700	2.39
10	PF3D7_1019700	2.39

University of Ghana http://ugspace.ug.edu.gh

10	PF3D7_1019700	2.39
10	PF3D7_1035700	3.43
10	PF3D7_1035700	3.43
10	PF3D7_1035700	3.43
10	PF3D7_1035700	3.43
10	PF3D7_1007900	2.13
10	PF3D7_1007900	2.13
10	PF3D7_1007900	2.13
10	PF3D7_1007900	2.13
10	PF3D7_1011500	2.11
10	PF3D7_1011500	2.11
10	PF3D7_1011500	2.11
10	PF3D7_1011500	2.11
10	PF3D7_1036900	1.73
10	PF3D7_1036900	1.73
10	PF3D7_1036900	1.73
10	PF3D7_1036900	1.73
10	PF3D7_1014100	2.36
10	PF3D7_1014100	2.36
10	PF3D7_1014100	2.36
10	PF3D7_1014100	2.36
10	PF3D7_1035300	2.61
10	PF3D7_1035300	2.61
10	PF3D7_1035300	2.61
10	PF3D7_1035300	2.61
10	PF3D7_1021300	1.97
10	PF3D7_1021300	1.97
10	PF3D7_1021300	1.97
10	PF3D7_1021300	1.97
10	PF3D7_1034600	2.76
10	PF3D7_1034600	2.76
10	PF3D7_1034600	2.76
10	PF3D7_1034600	2.76
10	PF3D7_1036400	1.18
10	PF3D7_1036400	1.18
10	PF3D7_1036400	1.18
10	PF3D7_1036400	1.18
10	PF3D7_1030500	1.54
10	PF3D7_1030500	1.54
10	PF3D7_1030500	1.54
10	PF3D7_1030500	1.54
10	PF3D7_1001500	1.06
10	PF3D7_1001500	1.06
10	PF3D7_1001500	1.06
10	PF3D7_1001500	1.06
10	PF3D7_1009100	1.25
10	PF3D7_1009100	1.25
10	PF3D7_1009100	1.25

University of Ghana http://ugspace.ug.edu.gh

10	PF3D7_1009100	1.25
10	PF3D7_1038700	2.01
10	PF3D7_1038700	2.01
10	PF3D7_1038700	2.01
10	PF3D7_1038700	2.01
10	PF3D7_1012200	2.61
10	PF3D7_1012200	2.61
10	PF3D7_1012200	2.06
10	PF3D7_1012200	1.78
10	PF3D7_1012200	2.06
10	PF3D7_1012200	1.78
10	PF3D7_1023800	2.04
10	PF3D7_1023800	2.04
10	PF3D7_1023800	2.04
10	PF3D7_1023800	2.04
10	PF3D7_1003200	2.69
10	PF3D7_1003200	2.69
10	PF3D7_1003200	2.69
10	PF3D7_1003200	2.69
10	PF3D7_1016800	2.32
10	PF3D7_1016800	2.32
10	PF3D7_1016800	2.32
10	PF3D7_1016800	2.32
10	PF3D7_1031700	2.06
10	PF3D7_1031700	2.06
10	PF3D7_1031700	2.06
10	PF3D7_1031700	2.06
10	PF3D7_1032300	2.13
10	PF3D7_1032300	2.13
10	PF3D7_1032300	2.13
10	PF3D7_1032300	2.13
10	PF3D7_1005300	1.70
10	PF3D7_1005300	1.70
10	PF3D7_1005300	1.70
10	PF3D7_1005300	1.70
10	PF3D7_1008500	1.34
10	PF3D7_1008500	1.34
10	PF3D7_1008500	1.34
10	PF3D7_1008500	1.34
10	PF3D7_1008000	1.06
10	PF3D7_1008000	1.06
10	PF3D7_1008000	1.06
10	PF3D7_1008000	1.06
10	PF3D7_1022000	1.62
10	PF3D7_1022000	1.62
10	PF3D7_1022000	1.62
10	PF3D7_1022000	1.62
10	PF3D7_1012000	2.12

University of Ghana http://ugspace.ug.edu.gh

10	PF3D7_1012000	2.12
10	PF3D7_1038400	1.11
10	PF3D7_1038400	1.11
10	PF3D7_1038400	1.11
10	PF3D7_1038400	1.11
10	PF3D7_1032700	2.02
10	PF3D7_1032700	2.02
10	PF3D7_1032700	2.02
10	PF3D7_1032700	2.02
10	PF3D7_1036300	6.21
10	PF3D7_1036300	6.21
10	PF3D7_1036300	6.21
10	PF3D7_1036300	6.21
10	PF3D7_1033000	1.75
10	PF3D7_1033000	1.75
10	PF3D7_1033000	1.75
10	PF3D7_1033000	1.75
10	PF3D7_1019000	1.17
10	PF3D7_1019000	1.17
10	PF3D7_1019000	1.17
10	PF3D7_1019000	1.17
10	PF3D7_1008100	2.57
10	PF3D7_1008100	2.57
10	PF3D7_1008100	2.57
10	PF3D7_1008100	2.57
10	PF3D7_1002800	1.16
10	PF3D7_1002800	1.16
10	PF3D7_1002800	1.16
10	PF3D7_1002800	1.16
10	PF3D7_1034900	2.06
10	PF3D7_1034900	2.06
10	PF3D7_1034900	2.06
10	PF3D7_1034900	2.06
11	PF3D7_1113600	3.38
11	PF3D7_1113600	3.38
11	PF3D7_1113600	3.38
11	PF3D7_1113600	3.38
11	PF3D7_1110300	2.76
11	PF3D7_1110300	2.76
11	PF3D7_1111600	2.10
11	PF3D7_1111600	2.10
11	PF3D7_1106700	1.51
11	PF3D7_1106700	1.51
11	PF3D7_1106700	1.51
11	PF3D7_1106700	1.51
11	PF3D7_1142700	1.45
11	PF3D7_1142700	1.45
11	PF3D7_1142700	1.45

University of Ghana http://ugspace.ug.edu.gh

11	PF3D7_1142700	1.45
12	PF3D7_1225000	3.19
12	PF3D7_1225000	3.19
12	PF3D7_1225000	3.18
12	PF3D7_1225000	3.18
12	PF3D7_1239800	3.08
12	PF3D7_1239800	3.08
12	PF3D7_1251200	2.65
12	PF3D7_1251200	2.65
12	PF3D7_1220400	2.60
12	PF3D7_1220400	2.60
12	PF3D7_1201400	2.60
12	PF3D7_1201400	2.60
12	PF3D7_1252500	2.13
12	PF3D7_1227700	2.12
12	PF3D7_1227700	2.12
12	PF3D7_1220500	2.03
12	PF3D7_1220500	2.03
12	PF3D7_1231800	1.99
12	PF3D7_1231800	1.99
12	PF3D7_1252100	1.97
12	PF3D7_1252100	1.97
12	PF3D7_1211900	1.95
12	PF3D7_1211900	1.95
12	PF3D7_1252600	1.90
12	PF3D7_1252600	1.90
12	PF3D7_1228800	1.88
12	PF3D7_1228800	1.88
12	PF3D7_1208200	1.88
12	PF3D7_1208200	1.88
12	PF3D7_1208200	1.84
12	PF3D7_1208200	1.84
12	PF3D7_1208900	1.71
12	PF3D7_1208900	1.71
12	PF3D7_1218500	1.68
12	PF3D7_1218500	1.68
12	PF3D7_1243900	1.66
12	PF3D7_1243900	1.66
12	PF3D7_1242000	1.61
12	PF3D7_1242000	1.61
12	PF3D7_1252700	1.48
12	PF3D7_1252700	1.48
12	PF3D7_1212400	1.48
12	PF3D7_1212400	1.48
12	PF3D7_1212400	1.48
12	PF3D7_1212400	1.48
12	PF3D7_1235900	1.41
12	PF3D7_1220700	1.38

University of Ghana http://ugspace.ug.edu.gh

12	PF3D7_1252100	1.36
12	PF3D7_1252100	1.36
12	PF3D7_1225500	1.36
12	PF3D7_1225500	1.36
12	PF3D7_1222800	1.24
12	PF3D7_1223400	1.23
12	PF3D7_1223400	1.23
12	PF3D7_1208100	1.22
12	PF3D7_1251100	1.17
12	PF3D7_1251100	1.17
12	PF3D7_1211300	1.14
12	PF3D7_1211300	1.14
12	PF3D7_1246300	1.13
12	PF3D7_1246300	1.13
12	PF3D7_1219000	1.11
12	PF3D7_1219000	1.11
12	PF3D7_1220100	1.09
12	PF3D7_1220100	1.09
12	PF3D7_1241100	1.08
12	PF3D7_1241100	1.08
12	PF3D7_1239900	1.05
12	PF3D7_1239900	1.05
12	PF3D7_1239900	1.05
12	PF3D7_1229300	1.05
12	PF3D7_1229300	1.05
12	PF3D7_1229300	1.05
13	PF3D7_1302900	4.45
13	PF3D7_1302900	4.45
13	PF3D7_1302900	4.45
13	PF3D7_1302900	4.45
13	PF3D7_1319700	3.51
13	PF3D7_1319700	3.51
13	PF3D7_1319700	3.51
13	PF3D7_1319700	3.51
13	PF3D7_1303100	2.42
13	PF3D7_1313600	2.18
13	PF3D7_1317900	2.13
13	PF3D7_1317900	2.13
13	PF3D7_1317900	2.13
13	PF3D7_1301900	2.12
13	PF3D7_1331000	2.12
13	PF3D7_1310900	2.11
13	PF3D7_1310900	2.11
13	PF3D7_1310900	2.11
13	PF3D7_1320700	2.00
13	PF3D7_1320700	2.00
13	PF3D7_1320700	2.00
13	PF3D7_1302500	1.83

University of Ghana http://ugspace.ug.edu.gh

13	PF3D7_1306600	1.80
13	PF3D7_1309700	1.74
13	PF3D7_1309700	1.74
13	PF3D7_1309700	1.74
13	PF3D7_1309700	1.74
13	PF3D7_1308600	1.73
13	PF3D7_1308600	1.73
13	PF3D7_1308600	1.73
13	PF3D7_1308600	1.73
13	PF3D7_1315100	1.72
13	PF3D7_1327500	1.70
13	PF3D7_1306600	1.58
13	PF3D7_1306600	1.58
13	PF3D7_1332200	1.54
13	PF3D7_1321700	1.48
13	PF3D7_1321700	1.48
13	PF3D7_1321700	1.48
13	PF3D7_1309800	1.44
13	PF3D7_1307600	1.40
13	PF3D7_1313800	1.40
13	PF3D7_1313800	1.40
13	PF3D7_1313800	1.40
13	PF3D7_1313800	1.40
13	PF3D7_1303100	1.33
13	PF3D7_1303100	1.33
13	PF3D7_1313200	1.32
13	PF3D7_1328400	1.08
13	PF3D7_1314600	1.07
13	PF3D7_1314600	1.07
13	PF3D7_1314600	1.07
13	PF3D7_1314600	1.07
13	PF3D7_1308200	1.02
13	PF3D7_1308200	1.02
13	PF3D7_1308200	1.02
13	PF3D7_1308200	1.02
13	PF3D7_1314200	1.01
13	PF3D7_1314200	1.01
13	PF3D7_1314200	1.01
14	PF3D7_1401200	2.63
14	PF3D7_1401200	2.63
14	PF3D7_1401200	2.63
14	PF3D7_1401200	2.63
14	PF3D7_1401700	1.98
14	PF3D7_1401700	1.98
14	PF3D7_1401700	1.98
14	PF3D7_1404000	1.96
14	PF3D7_1404000	1.96
14	PF3D7_1404000	1.96

University of Ghana http://ugspace.ug.edu.gh

14	PF3D7_1404000	1.96
14	PF3D7_1407800	1.92
14	PF3D7_1407800	1.92
14	PF3D7_1407800	1.92
14	PF3D7_1407800	1.92
14	PF3D7_1403800	1.84
14	PF3D7_1403800	1.84
14	PF3D7_1401100	1.73
14	PF3D7_1401100	1.73
14	PF3D7_1401100	1.73
14	PF3D7_1401100	1.73
14	PF3D7_1402000	1.59
14	PF3D7_1402000	1.59
14	PF3D7_1405800	1.58
14	PF3D7_1405800	1.58
14	PF3D7_1405800	1.56
14	PF3D7_1405800	1.56
14	PF3D7_1403100	1.53
14	PF3D7_1403100	1.53
14	PF3D7_1403100	1.53
14	PF3D7_1403100	1.53
14	PF3D7_1406500	1.20
14	PF3D7_1406500	1.20
14	PF3D7_1402000	1.01
14	PF3D7_1402000	1.01

University of Ghana http://ugspace.ug.edu.gh

Supplementary Table 3.2 Top ten percent of *P. falciparum* genomic positions under balancing selection

Gene ID	Tajima D	Chromosomes
PF3D7_0103600	3.86	1
PF3D7_0103600	3.86	1
PF3D7_0113600	3.85	1
PF3D7_0113600	3.85	1
PF3D7_0113600	3.81	1
PF3D7_0113600	3.81	1
PF3D7_0103600	3.68	1
PF3D7_0103600	3.68	1
PF3D7_0113600	3.60	1
PF3D7_0113600	3.60	1
PF3D7_0113100	3.50	1
PF3D7_0113100	3.50	1
PF3D7_0113100	3.43	1
PF3D7_0113100	3.43	1
PF3D7_0113600	3.19	1
PF3D7_0113600	3.19	1
PF3D7_0102200	3.18	1
PF3D7_0102200	3.18	1
PF3D7_0220800	3.67	2
PF3D7_0220800	3.67	2
PF3D7_0220900	3.66	2
PF3D7_0220900	3.66	2
PF3D7_0212500	3.17	2
PF3D7_0212500	3.17	2
PF3D7_0212500	2.94	2
PF3D7_0212500	2.94	2
PF3D7_0321300	3.27	3
PF3D7_0321300	3.27	3
PF3D7_0315200	3.22	3
PF3D7_0315200	3.22	3
PF3D7_0318200	3.13	3
PF3D7_0318200	3.13	3
PF3D7_0308200	3.07	3
PF3D7_0308200	3.07	3
PF3D7_0308200	3.07	3
PF3D7_0308200	3.07	3
PF3D7_0302600	3.06	3
PF3D7_0302600	3.06	3
PF3D7_0420200	4.07	4
PF3D7_0420200	4.07	4
PF3D7_0414100	3.90	4
PF3D7_0414100	3.90	4
PF3D7_0425250	3.86	4
PF3D7_0425250	3.86	4
PF3D7_0414200	3.76	4

University of Ghana http://ugspace.ug.edu.gh

PF3D7_0414200	3.76	4
PF3D7_0414200	3.76	4
PF3D7_0424400	3.73	4
PF3D7_0424400	3.73	4
PF3D7_0418000	3.73	4
PF3D7_0418000	3.73	4
PF3D7_0424400	3.70	4
PF3D7_0424400	3.70	4
PF3D7_0418000	3.65	4
PF3D7_0418000	3.65	4
PF3D7_0422800	3.60	4
PF3D7_0422800	3.60	4
PF3D7_0422800	3.57	4
PF3D7_0422800	3.57	4
PF3D7_0412200	3.47	4
PF3D7_0402300	3.34	4
PF3D7_0422200	3.33	4
PF3D7_0422200	3.33	4
PF3D7_0422200	3.33	4
PF3D7_0422200	3.33	4
PF3D7_0414100	3.23	4
PF3D7_0414100	3.23	4
PF3D7_0425000	3.14	4
PF3D7_0425000	3.14	4
PF3D7_0425000	2.98	4
PF3D7_0522400	2.98	5
PF3D7_0522400	2.98	5
PF3D7_0619600	4.01	6
PF3D7_0619600	4.01	6
PF3D7_0619600	4.01	6
PF3D7_0619600	4.01	6
PF3D7_0630700	3.91	6
PF3D7_0630700	3.91	6
PF3D7_0630700	3.91	6
PF3D7_0630700	3.91	6
PF3D7_0630800	3.73	6
PF3D7_0630800	3.73	6
PF3D7_0630300	3.69	6
PF3D7_0630300	3.69	6
PF3D7_0630600	3.57	6
PF3D7_0630600	3.57	6
PF3D7_0612900	3.03	6
PF3D7_0612900	3.03	6
PF3D7_0612900	3.03	6
PF3D7_0612900	3.03	6
PF3D7_0602700	2.96	6
PF3D7_0602700	2.96	6
PF3D7_0710000	4.73	7

University of Ghana http://ugspace.ug.edu.gh

PF3D7_0710000	4.73	7
PF3D7_0729700	4.56	7
PF3D7_0729700	4.56	7
PF3D7_0709300	4.27	7
PF3D7_0709300	4.27	7
PF3D7_0713600	3.88	7
PF3D7_0713900	3.78	7
PF3D7_0713900	3.78	7
PF3D7_0713900	3.78	7
PF3D7_0713600	3.74	7
PF3D7_0713600	3.74	7
PF3D7_0711500	3.33	7
PF3D7_0711500	3.33	7
PF3D7_0731500	3.15	7
PF3D7_0720400	3.11	7
PF3D7_0716000	3.07	7
PF3D7_0716000	3.07	7
PF3D7_0716000	3.07	7
PF3D7_0716000	3.07	7
PF3D7_0830800	4.29	8
PF3D7_0830800	4.29	8
PF3D7_0830800	4.09	8
PF3D7_0830800	4.09	8
PF3D7_0825500	3.89	8
PF3D7_0825500	3.89	8
PF3D7_0825500	3.89	8
PF3D7_0825500	3.89	8
PF3D7_0825800	3.46	8
PF3D7_0825800	3.46	8
PF3D7_0831100	3.22	8
PF3D7_0831100	3.22	8
PF3D7_0827100	3.20	8
PF3D7_0827100	3.20	8
PF3D7_0827100	3.20	8
PF3D7_0827100	3.20	8
PF3D7_0830800	2.95	8
PF3D7_0830800	2.95	8
PF3D7_0916000	2.94	9
PF3D7_0916000	2.94	9
PF3D7_0916000	2.94	9
PF3D7_1004800	5.47	10
PF3D7_1004800	5.47	10
PF3D7_1004800	4.56	10
PF3D7_1004800	4.56	10
PF3D7_1004600	3.33	10
PF3D7_1004600	3.33	10
PF3D7_1004600	3.23	10
PF3D7_1004600	3.23	10

University of Ghana http://ugspace.ug.edu.gh

PF3D7_1035700	3.43	10
PF3D7_1035700	3.43	10
PF3D7_1035700	3.43	10
PF3D7_1035700	3.43	10
PF3D7_1036300	6.21	10
PF3D7_1036300	6.21	10
PF3D7_1036300	6.21	10
PF3D7_1036300	6.21	10
PF3D7_1113600	3.38	11
PF3D7_1113600	3.38	11
PF3D7_1113600	3.38	11
PF3D7_1113600	3.38	11
PF3D7_1225000	3.19	12
PF3D7_1225000	3.19	12
PF3D7_1225000	3.18	12
PF3D7_1225000	3.18	12
PF3D7_1239800	3.08	12
PF3D7_1239800	3.08	12
PF3D7_1302900	4.45	13
PF3D7_1302900	4.45	13
PF3D7_1302900	4.45	13
PF3D7_1302900	4.45	13
PF3D7_1319700	3.51	13
PF3D7_1319700	3.51	13
PF3D7_1319700	3.51	13
PF3D7_1319700	3.51	13

University of Ghana http://ugspace.ug.edu.gh

Supplementary Table 3.3 Variants identified in genes of interest

Gene Name	GENE_ID	SNP	SNP present in Ghana samples	Number of variants found in Ghana samples
ferredoxin	PF3D7_1318100	D193Y	no	0
apicoplast ribosomal protein S10	PF3D7_1460900	V127M	no	0
multidrug resistance protein2	PF3D7_1447900	T484I	no	0
chloroquine resistance transporter	PF3D7_0709000	N326S	no	6
Phosphatidylinositol 4-kinase	PF3D7_0419900	S915G	no	36
Sec14 domain-containing protein	PF3D7_0626400	L498F, N615D	no	4
Ubiquitin-protein ligase	PF3D7_1448400	S57T	no	0
Ubiquitin carboxyl-terminal hydrolase	PF3D7_0104300	R3138H	no	6
Sentrin-specific protease 2, putative protein	PF3D7_0801700	H423Y	no	2

Supplementary Table 3.4 Distribution of polymorphic sites for determination of McDonald–Kreitman test

Gene name	Synonymous		Non-Synonymous	
	Fixed differences	**Polymorphic sites**	**Fixed differences**	**Polymorphic sites**
chloroquine resistance transporter	243	435	785	1352
Phosphatidylinositol 4-kinase	2068	5	7717	31
Ubiquitin carboxyl-terminal hydrolase	1654	2	5092	4
Sentrin-specific protease 2, putative	782	0	0	1

INTEGRI PROCEDAMUS

Supplementary Table 3.5 List of genes reported and known to be under balancing selection in *P. falciparum*.

Gene Name	Genomic length (bp)	sites[1]	π (x 10^{-3})	K (x10^{-3})	T' D	F	D	HKA (π/K)	MK P value
Duffy binding-like merozoite surface protein	2094	22	3.8	240	3.1*	2.8*	1.8*	0.016	0.8
Duffy binding-like merozoite surface protein 2[a]	2289	56	12.8	640	5.6*	4.7*	2.4*	0.02	0.74
surface-associated interspersed protein 4.2[a]	7301	123	5.7	564	3.2*	3.6*	2.9*	0.01	0.004729
erythrocyte binding antigen-175[b]	4875	26	1.7	518	2.7*	2.7*	1.9*	0.003	0.01

INTEGRI PROCEDAMUS

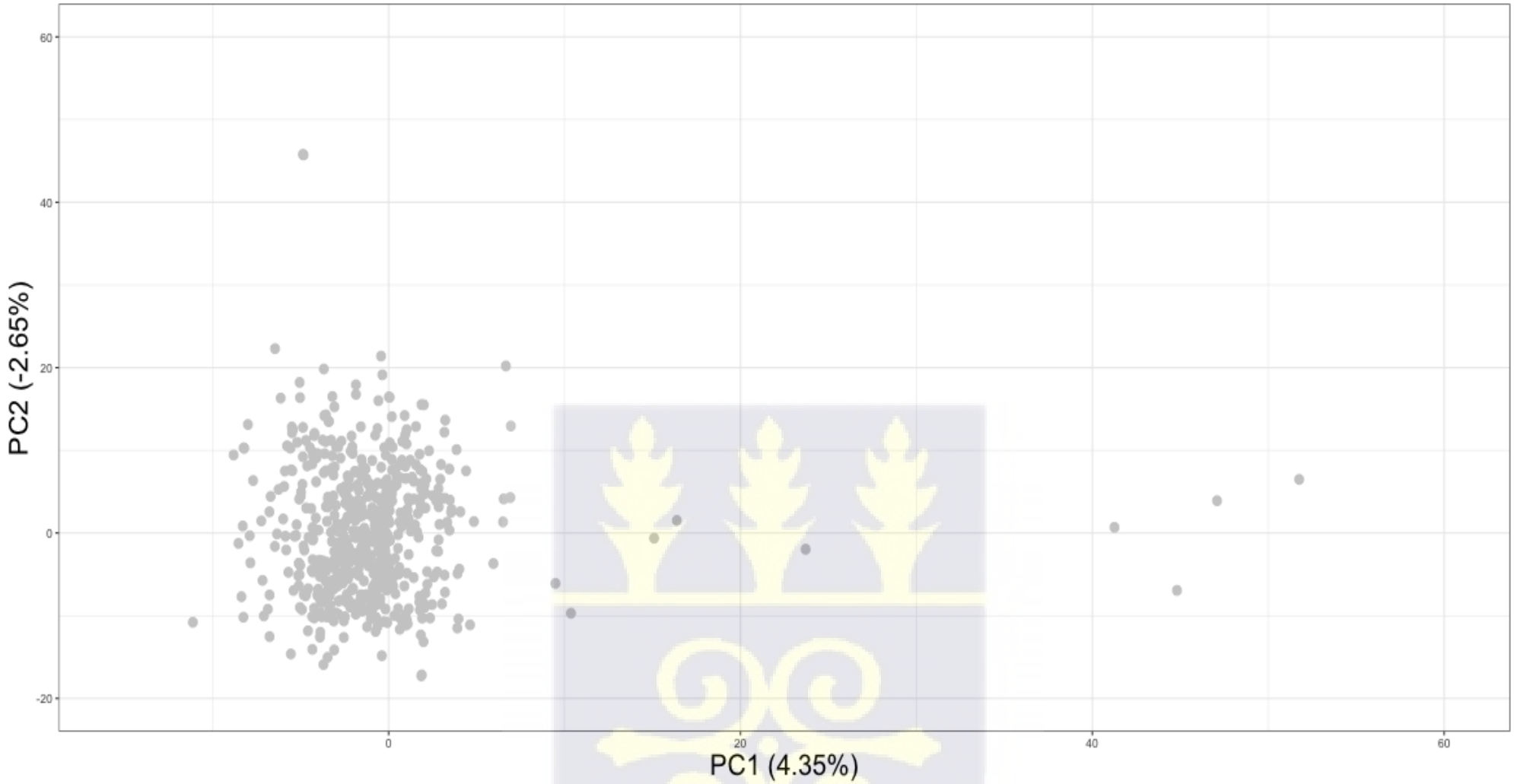

Supplementary Figure 3.1 PCA analysis for all samples (N = 617).

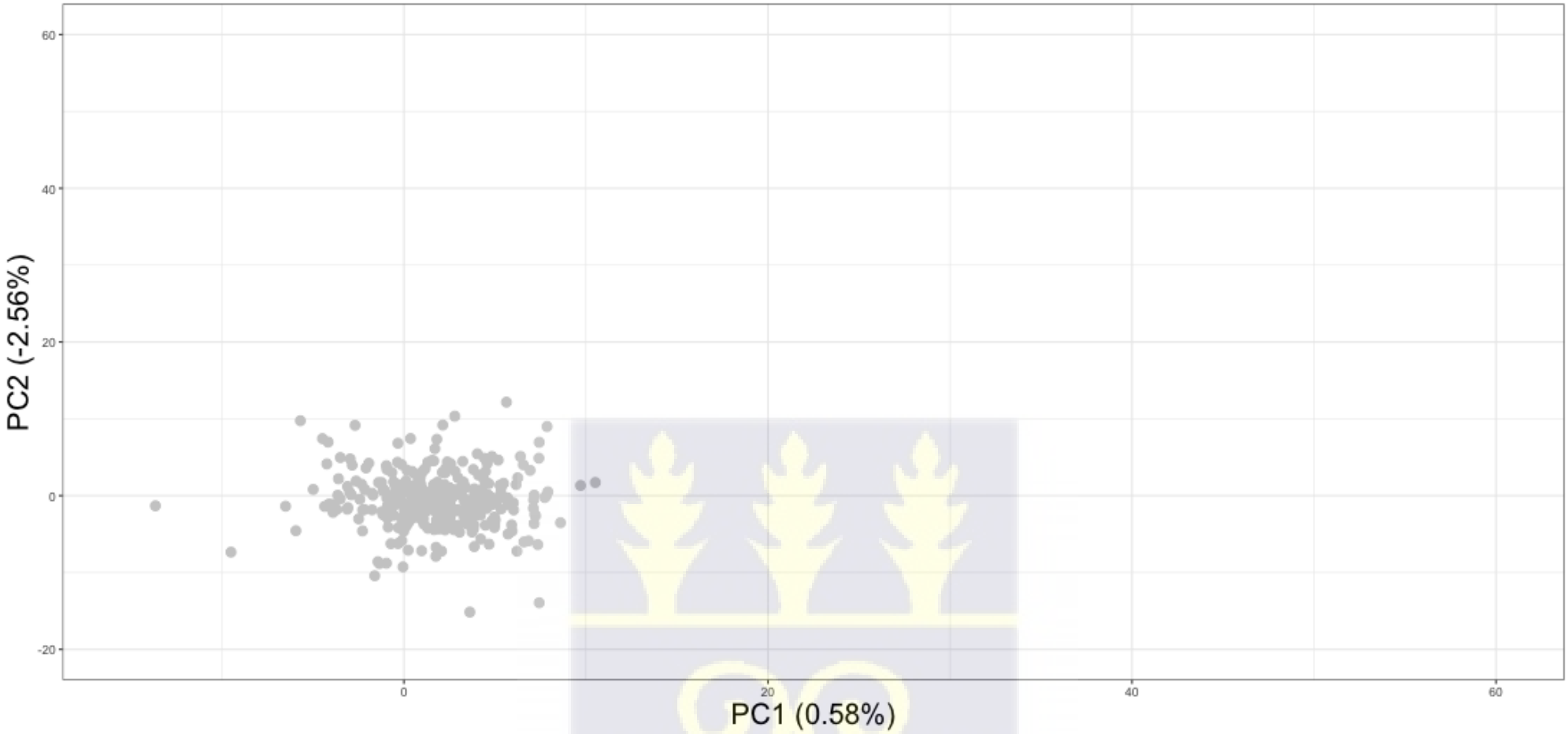

Supplementary Figure 3.2 PCA analysis for samples with multiplicity of infections (N=344)

Appendix II

Supplementary Table 5. 1 Sample annotation file containing phenotype data for the twenty-seven samples used. For each of the 3 parasite lines, the following replicates were used: 4 replicates per parasite line for the 700nM DHA condition, 3 replicates per parasite line for the 0.1% DMSO control condition and 2 replicates per parasite line for the untreated condition.

University of Ghana http://ugspace.ug.edu.gh

sample	parasite	class/condition	sensitivity	batch
C580R_DHA_01	C580R	DHA	Resistant	1
C580R_DHA_02	C580R	DHA	Resistant	2
C580R_DHA_03	C580R	DHA	Resistant	3
C580R_DHA_04	C580R	DHA	Resistant	4
C580R_DMSO_01	C580R	DMSO	Resistant	1
C580R_DMSO_02	C580R	DMSO	Resistant	2
C580R_DMSO_03	C580R	DMSO	Resistant	3
C580R_UNT_01	C580R	Untreated	Resistant	1
C580R_UNT_02	C580R	Untreated	Resistant	2
DD2_DHA_01	DD2	DHA	Susceptible	1
DD2_DHA_02	DD2	DHA	Susceptible	2
DD2_DHA_03	DD2	DHA	Susceptible	3
DD2_DHA_04	DD2	DHA	Susceptible	4
DD2_DMSO_01	DD2	DMSO	Susceptible	1
DD2_DMSO_02	DD2	DMSO	Susceptible	2
DD2_DMSO_03	DD2	DMSO	Susceptible	1
DD2_UNT_01	DD2	Untreated	Susceptible	2
DD2_UNT_02	DD2	Untreated	Susceptible	3
R539T_DHA_01	R539T	DHA	Resistant	1
R539T_DHA_02	R539T	DHA	Resistant	2
R539T_DHA_03	R539T	DHA	Resistant	3
R539T_DHA_04	R539T	DHA	Resistant	4
R539T_DMSO_01	R539T	DMSO	Resistant	1
R539T_DMSO_02	R539T	DMSO	Resistant	2
R539T_DMSO_03	R539T	DMSO	Resistant	3
R539T_UNT_01	R539T	Untreated	Resistant	1
R539T_UNT_02	R539T	Untreated	Resistant	1

Supplementary Table 5.2 Genes composition of modules identified using the WGCNA R package. Modules were selected based on a statistically significant (adjusted p-value < 0.05) expression profile correlation. Modules 0, 1, 3 and 17 contained known EVs biogenesis genes and were designated as EVs modules of interest. This table was also used as the gene set for our gene set enrichment analysis.

University of Ghana http://ugspace.ug.edu.gh

Module 0	Module 1	Module 3	Module 4	Module 5	Module 6	Module 7	Module 9	Module 10	Module 12	Module 14	Module 15	Module 16	Module 17	Module 19	Module 20	Module 21
PF3D7_0312300	PF3D7_0313500	PF3D7_0312400	PF3D7_0311600	PF3D7_0313200	PF3D7_0311200	PF3D7_0314400	PF3D7_0312500	PF3D7_0311900	PF3D7_0113000	PF3D7_0319200	PF3D7_0308200	PF3D7_0319000	PF3D7_0309200	PF3D7_0307600	PF3D7_0314500	PF3D7_0104000
PF3D7_0311800	PF3D7_0311300	PF3D7_0312200	PF3D7_0302100	PF3D7_0303100	PF3D7_0307800	PF3D7_0324500	PF3D7_0308600	PF3D7_0309500	PF3D7_0114800	PF3D7_0316200	PF3D7_0303400	PF3D7_0317200	PF3D7_0317700	PF3D7_0409000	PF3D7_0323500	PF3D7_0416200
PF3D7_0311100	PF3D7_0310700	PF3D7_0312100	PF3D7_0309300	PF3D7_0309800	PF3D7_0310200	PF3D7_0324800	PF3D7_0317400	PF3D7_0315100	PF3D7_0103700	PF3D7_0303500	PF3D7_0321600	PF3D7_0411900	PF3D7_0316400	PF3D7_0404500	PF3D7_0102200	PF3D7_0423300
PF3D7_0311000	PF3D7_0310500	PF3D7_0312800	PF3D7_0319100	PF3D7_0317500	PF3D7_0318200	PF3D7_0324900	PF3D7_0304800	PF3D7_0307300	PF3D7_0103900	PF3D7_0322700	PF3D7_0310000	PF3D7_0405000	PF3D7_0305100	PF3D7_0710000	PF3D7_0107500	PF3D7_0824500
PF3D7_0310900	PF3D7_0302200	PF3D7_0307900	PF3D7_0303700	PF3D7_0317300	PF3D7_0314900	PF3D7_0300100	PF3D7_0320400	PF3D7_0320300	PF3D7_0108800	PF3D7_0301500	PF3D7_0104100	PF3D7_0406200	PF3D7_0106500	PF3D7_0727800	PF3D7_0108500	PF3D7_0823800
PF3D7_0313000	PF3D7_0302500	PF3D7_0309600	PF3D7_0304600	PF3D7_0304000	PF3D7_0319400	PF3D7_0300700	PF3D7_0305900	PF3D7_0322600	PF3D7_0402000	PF3D7_0301800	PF3D7_0105800	PF3D7_0415200	PF3D7_0402100	PF3D7_0814400	PF3D7_0701900	PF3D7_0814700
PF3D7_0302600	PF3D7_0308100	PF3D7_0317600	PF3D7_0307400	PF3D7_0306100	PF3D7_0316100	PF3D7_0300900	PF3D7_0306600	PF3D7_0112200	PF3D7_0716700	PF3D7_0411800	PF3D7_0111200	PF3D7_0705400	PF3D7_0422500	PF3D7_0812100	PF3D7_0702200	PF3D7_0507300
PF3D7_0303300	PF3D7_0308300	PF3D7_0316700	PF3D7_0302000	PF3D7_0321500	PF3D7_0320600	PF3D7_0301000	PF3D7_0306700	PF3D7_0100600	PF3D7_0719400	PF3D7_0102700	PF3D7_0413500	PF3D7_0717700	PF3D7_0423600	PF3D7_0811000	PF3D7_0707500	PF3D7_0510000
PF3D7_0302800	PF3D7_0308700	PF3D7_0316500	PF3D7_0314600	PF3D7_0321700	PF3D7_0106700	PF3D7_0301100	PF3D7_0102800	PF3D7_0104700	PF3D7_0726700	PF3D7_0111300	PF3D7_0415700	PF3D7_0802000	PF3D7_0424600	PF3D7_0502000	PF3D7_0718100	PF3D7_0522800
PF3D7_0308900	PF3D7_0309900	PF3D7_0316800	PF3D7_0407300	PF3D7_0322500	PF3D7_0108300	PF3D7_0409400	PF3D7_0103200	PF3D7_0418200	PF3D7_0728200	PF3D7_0401800	PF3D7_0719000	PF3D7_0509100	PF3D7_0703200	PF3D7_0902500	PF3D7_0726600	PF3D7_0523100
PF3D7_0318800	PF3D7_0318500	PF3D7_0317000	PF3D7_0408600	PF3D7_0323100	PF3D7_0108700	PF3D7_0412400	PF3D7_0107400	PF3D7_0711000	PF3D7_0731300	PF3D7_0414000	PF3D7_0723600	PF3D7_0510100	PF3D7_0709000	PF3D7_0912000	PF3D7_0815300	PF3D7_0906910
PF3D7_0318600	PF3D7_0318100	PF3D7_0315200	PF3D7_0410900	PF3D7_0323700	PF3D7_0403200	PF3D7_0412700	PF3D7_0108000	PF3D7_0715000	PF3D7_0830700	PF3D7_0416000	PF3D7_0824100	PF3D7_0510300	PF3D7_0711100	PF3D7_0934900	PF3D7_0805200	PF3D7_1330500
PF3D7_0318300	PF3D7_0316900	PF3D7_0315400	PF3D7_0113100	PF3D7_0323000	PF3D7_0403700	PF3D7_0100100	PF3D7_0405600	PF3D7_0722100	PF3D7_0814500	PF3D7_0424500	PF3D7_0508400	PF3D7_0511300	PF3D7_0724400	PF3D7_1303800	PF3D7_0801500	PF3D7_1337100
PF3D7_0319300	PF3D7_0316000	PF3D7_0304400	PF3D7_0113400	PF3D7_0301700	PF3D7_0404300	PF3D7_0113800	PF3D7_0418500	PF3D7_0722400	PF3D7_0814200	PF3D7_0702500	PF3D7_0512100	PF3D7_0905800	PF3D7_0726500	PF3D7_1316100	PF3D7_0919500	PF3D7_0621100
PF3D7_0315600	PF3D7_0315500	PF3D7_0304700	PF3D7_0105700	PF3D7_0408100	PF3D7_0405400	PF3D7_0114200	PF3D7_0424700	PF3D7_0724500	PF3D7_0813600	PF3D7_0710100	PF3D7_0513500	PF3D7_0907400	PF3D7_0827800	PF3D7_1324400	PF3D7_1304400	PF3D7_0502700
PF3D7_0315900	PF3D7_0315800	PF3D7_0305700	PF3D7_0107000	PF3D7_0411100	PF3D7_0415300	PF3D7_0114700	PF3D7_0709100	PF3D7_0727500	PF3D7_0501300	PF3D7_0711300	PF3D7_0527000	PF3D7_0917000	PF3D7_0804800	PF3D7_1328200	PF3D7_1347700	PF3D7_0717300
PF3D7_0304300	PF3D7_0303800	PF3D7_0306500	PF3D7_0109700	PF3D7_0412000	PF3D7_0417300	PF3D7_0115700	PF3D7_0709500	PF3D7_0731600	PF3D7_0509500	PF3D7_0719900	PF3D7_0528100	PF3D7_0927100	PF3D7_0513600	PF3D7_1329800	PF3D7_1347900	PF3D7_0906700
PF3D7_0304500	PF3D7_0304200	PF3D7_0306900	PF3D7_0110100	PF3D7_0113300	PF3D7_0420000	PF3D7_0101600	PF3D7_0710700	PF3D7_0823000	PF3D7_0509600	PF3D7_0728100	PF3D7_0528800	PF3D7_0936600	PF3D7_0515300	PF3D7_1334000	PF3D7_0630600	PF3D7_0920100
PF3D7_0323600	PF3D7_0305200	PF3D7_0308500	PF3D7_0110500	PF3D7_0113700	PF3D7_0702600	PF3D7_0111900	PF3D7_0718500	PF3D7_0820200	PF3D7_0512500	PF3D7_0731200	PF3D7_0917300	PF3D7_0937200	PF3D7_0516600	PF3D7_1336600	PF3D7_0632300	PF3D7_0812200
PF3D7_0324100	PF3D7_0305300	PF3D7_0319900	PF3D7_0111500	PF3D7_0105400	PF3D7_0703500	PF3D7_0400100	PF3D7_0721100	PF3D7_0812900	PF3D7_0532200	PF3D7_0830900	PF3D7_0918000	PF3D7_1304100	PF3D7_0519500	PF3D7_0504800	PF3D7_0526200	PF3D7_0209500
PF3D7_0300400	PF3D7_0306200	PF3D7_0322000	PF3D7_0405700	PF3D7_0105900	PF3D7_0705000	PF3D7_0400400	PF3D7_0730900	PF3D7_0501200	PF3D7_0532300	PF3D7_0824800	PF3D7_0935800	PF3D7_1304700	PF3D7_0524100	PF3D7_0724700	PF3D7_0702000	PF3D7_0214000
PF3D7_0300500	PF3D7_0306800	PF3D7_0322900	PF3D7_0409900	PF3D7_0106600	PF3D7_0708800	PF3D7_0400500	PF3D7_0824400	PF3D7_0503100	PF3D7_0902800	PF3D7_0513200	PF3D7_1307900	PF3D7_1317100	PF3D7_0529300	PF3D7_0726400	PF3D7_1369400	PF3D7_1006800
PF3D7_0301900	PF3D7_0307500	PF3D7_0319600	PF3D7_0413600	PF3D7_0109300	PF3D7_0709400	PF3D7_0400900	PF3D7_0813900	PF3D7_0514700	PF3D7_0915400	PF3D7_0514100	PF3D7_1333000	PF3D7_1318400	PF3D7_0904100	PF3D7_1308400	PF3D7_0202500	PF3D7_1015600
PF3D7_0407000	PF3D7_0319700	PF3D7_0321200	PF3D7_0418100	PF3D7_0110200	PF3D7_0709700	PF3D7_0401400	PF3D7_0804400	PF3D7_0518600	PF3D7_0931600	PF3D7_0523200	PF3D7_1335400	PF3D7_1336300	PF3D7_0926900	PF3D7_1320500	PF3D7_0215300	PF3D7_1137800
PF3D7_0410300	PF3D7_0320500	PF3D7_0408700	PF3D7_0419400	PF3D7_0404100	PF3D7_0719300	PF3D7_0402600	PF3D7_0503500	PF3D7_0518900	PF3D7_0933800	PF3D7_0910400	PF3D7_1349800	PF3D7_1339700	PF3D7_0933500	PF3D7_1325900	PF3D7_0221700	PF3D7_1205000
PF3D7_0411300	PF3D7_0320800	PF3D7_0408800	PF3D7_0419800	PF3D7_0404600	PF3D7_0721300	PF3D7_0413100	PF3D7_0515100	PF3D7_0519600	PF3D7_0935900	PF3D7_0913600	PF3D7_1350300	PF3D7_1367300	PF3D7_1302600	PF3D7_0314200	PF3D7_1002100	PF3D7_1206300
PF3D7_0412300	PF3D7_0321100	PF3D7_0409300	PF3D7_0420100	PF3D7_0416300	PF3D7_0721400	PF3D7_0413200	PF3D7_0516800	PF3D7_0520900	PF3D7_0936000	PF3D7_0926800	PF3D7_1355100	PF3D7_1369100	PF3D7_1308700	PF3D7_0721000	PF3D7_1005500	PF3D7_1409700
PF3D7_0302700	PF3D7_0321300	PF3D7_0411200	PF3D7_0422200	PF3D7_0426000	PF3D7_0722900	PF3D7_0413300	PF3D7_0517000	PF3D7_0521900	PF3D7_0936300	PF3D7_1306800	PF3D7_1355900	PF3D7_0617200	PF3D7_1323200	PF3D7_0804500	PF3D7_1102700	PF3D7_1415100
PF3D7_0304900	PF3D7_0323400	PF3D7_0412200	PF3D7_0704200	PF3D7_0702400	PF3D7_0723400	PF3D7_0420700	PF3D7_0519000	PF3D7_0522700	PF3D7_0936800	PF3D7_1312700	PF3D7_1367600	PF3D7_0628500	PF3D7_1324500	PF3D7_0210200	PF3D7_1102800	PF3D7_1416900
PF3D7_0306300	PF3D7_0319500	PF3D7_0312000	PF3D7_0704700	PF3D7_0708400	PF3D7_0723900	PF3D7_0421200	PF3D7_0519800	PF3D7_0532400	PF3D7_1301400	PF3D7_1301500	PF3D7_0604300	PF3D7_0605300	PF3D7_1329000	PF3D7_1004600	PF3D7_1105600	PF3D7_1418300
PF3D7_0100900	PF3D7_0320900	PF3D7_0320700	PF3D7_0705300	PF3D7_0708900	PF3D7_0829000	PF3D7_0421300	PF3D7_0519900	PF3D7_0904700	PF3D7_1301700	PF3D7_1316200	PF3D7_0609800	PF3D7_0611900	PF3D7_1345100	PF3D7_1008800	PF3D7_1115800	PF3D7_1434700
PF3D7_0114500	PF3D7_0300200	PF3D7_0113900	PF3D7_0707900	PF3D7_0711400	PF3D7_0827000	PF3D7_0424400	PF3D7_0523000	PF3D7_0904800	PF3D7_1302000	PF3D7_1322300	PF3D7_0615000	PF3D7_0802900	PF3D7_1352000	PF3D7_1016700	PF3D7_1116700	PF3D7_1445100
PF3D7_0115200	PF3D7_0301300	PF3D7_0103100	PF3D7_0708200	PF3D7_0713100	PF3D7_0826100	PF3D7_0424800	PF3D7_0530200	PF3D7_0914000	PF3D7_1315800	PF3D7_1343200	PF3D7_0707200	PF3D7_0805700	PF3D7_1353300	PF3D7_1106200	PF3D7_1116800	PF3D7_1459500
PF3D7_0115600	PF3D7_0406600	PF3D7_0106900	PF3D7_0708500	PF3D7_0714500	PF3D7_0823300	PF3D7_0425400	PF3D7_0902300	PF3D7_1307400	PF3D7_1323300	PF3D7_1343700	PF3D7_0809500	PF3D7_0807600	PF3D7_1358000	PF3D7_1107500	PF3D7_1149200	
PF3D7_0102900	PF3D7_0407400	PF3D7_0110400	PF3D7_0716000	PF3D7_0715800	PF3D7_0816600	PF3D7_0425500	PF3D7_0907900	PF3D7_1311800	PF3D7_1344700	PF3D7_1361200	PF3D7_0825400	PF3D7_0811900	PF3D7_1368800	PF3D7_1122200	PF3D7_1207500	
PF3D7_0104500	PF3D7_0407700	PF3D7_0413700	PF3D7_0716200	PF3D7_0716900	PF3D7_0814600	PF3D7_0425800	PF3D7_0909400	PF3D7_1314300	PF3D7_1353100	PF3D7_0619700	PF3D7_0920000	PF3D7_1313300	PF3D7_0615900	PF3D7_1134500	PF3D7_1240100	
PF3D7_0105100	PF3D7_0407800	PF3D7_0414400	PF3D7_0718400	PF3D7_0720400	PF3D7_0813700	PF3D7_0701800	PF3D7_0920800	PF3D7_1315300	PF3D7_0617000	PF3D7_0605100	PF3D7_0930100	PF3D7_1326900	PF3D7_0729000	PF3D7_1135000	PF3D7_1245800	
PF3D7_0105500	PF3D7_0407900	PF3D7_0415100	PF3D7_0719700	PF3D7_0722700	PF3D7_0812500	PF3D7_0712000	PF3D7_0926700	PF3D7_1316400	PF3D7_0626400	PF3D7_0605900	PF3D7_0314800	PF3D7_0321900	PF3D7_1302300	PF3D7_1135500	PF3D7_1431600	
PF3D7_0400300	PF3D7_0408000	PF3D7_0415500	PF3D7_0721800	PF3D7_0726100	PF3D7_0807100	PF3D7_0712300	PF3D7_1304500	PF3D7_1319600	PF3D7_0601900	PF3D7_0610100	PF3D7_0719500	PF3D7_0529400	PF3D7_1326600	PF3D7_1208400	PF3D7_1436300	
PF3D7_0401900	PF3D7_0409800	PF3D7_0416100	PF3D7_0722000	PF3D7_0830500	PF3D7_0505100	PF3D7_0712400	PF3D7_1311300	PF3D7_1323400	PF3D7_0602400	PF3D7_0111400	PF3D7_0205900	PF3D7_0625000	PF3D7_1362400	PF3D7_1227500	PF3D7_1455500	

University of Ghana http://ugspace.ug.edu.gh

PF3D7_0403300	PF3D7_0410000	PF3D7_0416800	PF3D7_0723700	PF3D7_0826200	PF3D7_0506000	PF3D7_0712600	PF3D7_1317500	PF3D7_1325100	PF3D7_0613500	PF3D7_0809600	PF3D7_0207800	PF3D7_0704300	PF3D7_0621350	PF3D7_1228300	PF3D7_0220400
PF3D7_0403500	PF3D7_0410400	PF3D7_0417900	PF3D7_0729300	PF3D7_0820600	PF3D7_0508000	PF3D7_0712800	PF3D7_1326000	PF3D7_1327300	PF3D7_0615300	PF3D7_0826500	PF3D7_0209600	PF3D7_0211700	PF3D7_1351800	PF3D7_1419600	PF3D7_0702100
PF3D7_0405800	PF3D7_0410600	PF3D7_0419200	PF3D7_0830600	PF3D7_0818900	PF3D7_0508700	PF3D7_0712900	PF3D7_1330700	PF3D7_1332100	PF3D7_0103500	PF3D7_0829100	PF3D7_0210000	PF3D7_0219100	PF3D7_0729600	PF3D7_1422900	PF3D7_1476400
PF3D7_0406800	PF3D7_0410700	PF3D7_0419300	PF3D7_0828600	PF3D7_0817300	PF3D7_0511000	PF3D7_0713400	PF3D7_1333300	PF3D7_1332700	PF3D7_0503200	PF3D7_0916400	PF3D7_0212900	PF3D7_1004000	PF3D7_0216500	PF3D7_1433400	
PF3D7_0409700	PF3D7_0411400	PF3D7_0419600	PF3D7_0828500	PF3D7_0813000	PF3D7_0511500	PF3D7_0718300	PF3D7_1338900	PF3D7_1334500	PF3D7_0532600	PF3D7_0928300	PF3D7_1009600	PF3D7_1008000	PF3D7_1103800	PF3D7_1457400	
PF3D7_0413800	PF3D7_0412100	PF3D7_0422400	PF3D7_0828400	PF3D7_0802400	PF3D7_0514300	PF3D7_0733000	PF3D7_1346600	PF3D7_1334700	PF3D7_0822700	PF3D7_0933300	PF3D7_1010800	PF3D7_1012700	PF3D7_1104100	PF3D7_1457900	
PF3D7_0418400	PF3D7_0112900	PF3D7_0423100	PF3D7_0824000	PF3D7_0801800	PF3D7_0517400	PF3D7_0809100	PF3D7_1347300	PF3D7_1336700	PF3D7_0902000	PF3D7_0933400	PF3D7_1034500	PF3D7_1033100	PF3D7_1106800		
PF3D7_0419100	PF3D7_0305400	PF3D7_0423700	PF3D7_0823500	PF3D7_0801000	PF3D7_0518500	PF3D7_0808900	PF3D7_1358300	PF3D7_1340000	PF3D7_0930800	PF3D7_1369000	PF3D7_1110300	PF3D7_1106900	PF3D7_1110500		
PF3D7_0422900	PF3D7_0306000	PF3D7_0703800	PF3D7_0822000	PF3D7_0500800	PF3D7_0525400	PF3D7_0808800	PF3D7_1363400	PF3D7_1343000	PF3D7_1322200	PF3D7_0301200	PF3D7_1129300	PF3D7_1128700	PF3D7_1118000		
PF3D7_0423200	PF3D7_0100300	PF3D7_0710600	PF3D7_0820900	PF3D7_0501400	PF3D7_0526500	PF3D7_0808700	PF3D7_0618300	PF3D7_1346900	PF3D7_1369700	PF3D7_0202200	PF3D7_1133300	PF3D7_1140200	PF3D7_1121600		
PF3D7_0424900	PF3D7_0318700	PF3D7_0710900	PF3D7_0816000	PF3D7_0501800	PF3D7_0528000	PF3D7_0808600	PF3D7_0618600	PF3D7_1354500	PF3D7_1370300	PF3D7_0212400	PF3D7_1135700	PF3D7_1142000	PF3D7_1130700		
PF3D7_0425100	PF3D7_0102500	PF3D7_0716800	PF3D7_0814300	PF3D7_0503900	PF3D7_0529800	PF3D7_0800500	PF3D7_0620200	PF3D7_0618200	PF3D7_1371800	PF3D7_0216100	PF3D7_1147400	PF3D7_1145700	PF3D7_1138800		
PF3D7_0425200	PF3D7_0104200	PF3D7_0719600	PF3D7_0811800	PF3D7_0507700	PF3D7_0531300	PF3D7_0800300	PF3D7_0625500	PF3D7_0626500	PF3D7_0202700	PF3D7_1016800	PF3D7_1202000	PF3D7_1203600	PF3D7_1142100		
PF3D7_0425700	PF3D7_0104300	PF3D7_0719800	PF3D7_0811700	PF3D7_0508800	PF3D7_0903500	PF3D7_0800200	PF3D7_0627100	PF3D7_0629100	PF3D7_0217200	PF3D7_1017800	PF3D7_1210100	PF3D7_1219100	PF3D7_1147300		
PF3D7_0701600	PF3D7_0104800	PF3D7_0720100	PF3D7_0810000	PF3D7_0510500	PF3D7_0904600	PF3D7_0502900	PF3D7_0607500	PF3D7_0629200	PF3D7_0223500	PF3D7_1018000	PF3D7_1211500	PF3D7_1220300	PF3D7_1211200		
PF3D7_0703300	PF3D7_0105300	PF3D7_0720600	PF3D7_0809900	PF3D7_0513800	PF3D7_0907500	PF3D7_0511400	PF3D7_0102600	PF3D7_0607800	PF3D7_1001000	PF3D7_1021200	PF3D7_1225500	PF3D7_1220900	PF3D7_1211600		
PF3D7_0708100	PF3D7_0105600	PF3D7_0721200	PF3D7_0806400	PF3D7_0522100	PF3D7_0909900	PF3D7_0522200	PF3D7_0417500	PF3D7_0610800	PF3D7_1001100	PF3D7_1024900	PF3D7_1226800	PF3D7_1222900	PF3D7_1233600		
PF3D7_0710800	PF3D7_0106400	PF3D7_0722500	PF3D7_0802300	PF3D7_0526300	PF3D7_0910200	PF3D7_0529700	PF3D7_0522500	PF3D7_0611000	PF3D7_1001500	PF3D7_1112300	PF3D7_1227900	PF3D7_1225800	PF3D7_1239800		
PF3D7_0711700	PF3D7_0107100	PF3D7_0727200	PF3D7_0502100	PF3D7_0527100	PF3D7_0914500	PF3D7_0532900	PF3D7_0523900	PF3D7_0613200	PF3D7_1014300	PF3D7_1114200	PF3D7_1230500	PF3D7_1228700	PF3D7_1403100		
PF3D7_0713500	PF3D7_0107900	PF3D7_0727400	PF3D7_0505200	PF3D7_0531000	PF3D7_0917600	PF3D7_0900100	PF3D7_0612400	PF3D7_0616600	PF3D7_1030300	PF3D7_1122500	PF3D7_1236900	PF3D7_1230400	PF3D7_1404900		
PF3D7_0715500	PF3D7_0109000	PF3D7_0728600	PF3D7_0509400	PF3D7_0531200	PF3D7_0922100	PF3D7_0900300	PF3D7_0720500	PF3D7_0418000	PF3D7_1031500	PF3D7_1124100	PF3D7_1237200	PF3D7_1239200	PF3D7_1408700		
PF3D7_0718700	PF3D7_0109600	PF3D7_0730000	PF3D7_0509900	PF3D7_0531400	PF3D7_0934100	PF3D7_0901000	PF3D7_0805000	PF3D7_0513400	PF3D7_1039000	PF3D7_1126100	PF3D7_1402000	PF3D7_1244000	PF3D7_1410300		
PF3D7_0720000	PF3D7_0109800	PF3D7_0830400	PF3D7_0511200	PF3D7_0532500	PF3D7_0935600	PF3D7_0901400	PF3D7_0829300	PF3D7_0519700	PF3D7_1106000	PF3D7_1126500	PF3D7_1407100	PF3D7_1248900	PF3D7_1436100		
PF3D7_0720200	PF3D7_0110800	PF3D7_0826700	PF3D7_0522000	PF3D7_0903400	PF3D7_1304600	PF3D7_0902900	PF3D7_0931500	PF3D7_0713700	PF3D7_1116400	PF3D7_1143300	PF3D7_1415800	PF3D7_1252500	PF3D7_1450000		
PF3D7_0720300	PF3D7_0110900	PF3D7_0823900	PF3D7_0522600	PF3D7_0907200	PF3D7_1308900	PF3D7_0911300	PF3D7_1350700	PF3D7_0818200	PF3D7_1126300	PF3D7_1149600	PF3D7_1415900	PF3D7_1403700	PF3D7_1456800		
PF3D7_0720800	PF3D7_0111000	PF3D7_0823200	PF3D7_0524900	PF3D7_0911400	PF3D7_1319400	PF3D7_0917100	PF3D7_1366200	PF3D7_0831400	PF3D7_1127000	PF3D7_1218500	PF3D7_1432200	PF3D7_1419000	PF3D7_1468000		
PF3D7_0722300	PF3D7_0303600	PF3D7_0821700	PF3D7_0525000	PF3D7_0914800	PF3D7_1325600	PF3D7_0927000	PF3D7_0320000	PF3D7_0901800	PF3D7_1131300	PF3D7_1222300	PF3D7_1435800	PF3D7_1421400	PF3D7_1234200		
PF3D7_0723500	PF3D7_0401200	PF3D7_0819800	PF3D7_0526400	PF3D7_0915000	PF3D7_1332900	PF3D7_0937300	PF3D7_0109950	PF3D7_0937000	PF3D7_1132400	PF3D7_1222500	PF3D7_1437200	PF3D7_1422300			
PF3D7_0724100	PF3D7_0402400	PF3D7_0818800	PF3D7_0526600	PF3D7_0931100	PF3D7_1333700	PF3D7_0937500	PF3D7_0529400	PF3D7_0204000	PF3D7_1141700	PF3D7_1223500	PF3D7_1439300	PF3D7_1447400			
PF3D7_0724300	PF3D7_0403100	PF3D7_0814900	PF3D7_0526900	PF3D7_0934300	PF3D7_1334300	PF3D7_0937800	PF3D7_0929700	PF3D7_0204300	PF3D7_1149400	PF3D7_1224800	PF3D7_1440400	PF3D7_1448500			
PF3D7_0725100	PF3D7_0403800	PF3D7_0814000	PF3D7_0904400	PF3D7_0936700	PF3D7_1340300	PF3D7_1300300	PF3D7_0717000	PF3D7_0205600	PF3D7_1200900	PF3D7_1236000	PF3D7_1458300	PF3D7_1466800			
PF3D7_0727000	PF3D7_0403900	PF3D7_0813200	PF3D7_0905200	PF3D7_1307000	PF3D7_1341500	PF3D7_1321900	PF3D7_0810700	PF3D7_0220200	PF3D7_1201000	PF3D7_1241200	PF3D7_1470200	PF3D7_1478000			
PF3D7_0728800	PF3D7_0404000	PF3D7_0812400	PF3D7_0906600	PF3D7_1307100	PF3D7_1341900	PF3D7_1330000	PF3D7_0201000	PF3D7_1001800	PF3D7_1204600	PF3D7_1252800					
PF3D7_0729800	PF3D7_0404400	PF3D7_0810500	PF3D7_0908400	PF3D7_1312000	PF3D7_1349100	PF3D7_1359100	PF3D7_0204800	PF3D7_1008200	PF3D7_1216000	PF3D7_1407200					
PF3D7_0829200	PF3D7_0404700	PF3D7_0807500	PF3D7_0908600	PF3D7_1319100	PF3D7_1349200	PF3D7_1362300	PF3D7_0209300	PF3D7_1016100	PF3D7_1219300	PF3D7_1408300					
PF3D7_0827600	PF3D7_0404800	PF3D7_0807300	PF3D7_0911800	PF3D7_1323600	PF3D7_1354200	PF3D7_1365100	PF3D7_0211600	PF3D7_1016300	PF3D7_1234000	PF3D7_1412400					
PF3D7_0826600	PF3D7_0404900	PF3D7_0804300	PF3D7_0912800	PF3D7_1329500	PF3D7_1359900	PF3D7_1367800	PF3D7_0220700	PF3D7_1016400	PF3D7_1236800	PF3D7_1418000					
PF3D7_0826300	PF3D7_0405200	PF3D7_0803800	PF3D7_0913700	PF3D7_1330600	PF3D7_1361700	PF3D7_1373500	PF3D7_1004300	PF3D7_1024400	PF3D7_1241100	PF3D7_1427000					
PF3D7_0822600	PF3D7_0405900	PF3D7_0802200	PF3D7_0914600	PF3D7_1331200	PF3D7_1366300	PF3D7_0617400	PF3D7_1005000	PF3D7_1032400	PF3D7_1244800	PF3D7_1433900					
PF3D7_0821300	PF3D7_0406000	PF3D7_0503800	PF3D7_0915600	PF3D7_1336000	PF3D7_1366400	PF3D7_0631800	PF3D7_1009900	PF3D7_1034900	PF3D7_1252300	PF3D7_1439100					
PF3D7_0821200	PF3D7_0414100	PF3D7_0504700	PF3D7_0918900	PF3D7_1336900	PF3D7_1366900	PF3D7_0631900	PF3D7_1011400	PF3D7_1037400	PF3D7_1252600	PF3D7_1442200					
PF3D7_0820800	PF3D7_0414600	PF3D7_0505300	PF3D7_0920600	PF3D7_1341600	PF3D7_1367100	PF3D7_0632100	PF3D7_1013600	PF3D7_1102900	PF3D7_1255200	PF3D7_1447900					
PF3D7_0820500	PF3D7_0414700	PF3D7_0505800	PF3D7_0924100	PF3D7_1343400	PF3D7_1367700	PF3D7_0632500	PF3D7_1018500	PF3D7_1105700	PF3D7_1401100	PF3D7_1454600					
PF3D7_0816200	PF3D7_0415400	PF3D7_0507000	PF3D7_0925400	PF3D7_1343500	PF3D7_1369600	PF3D7_0632800	PF3D7_1027400	PF3D7_1109900	PF3D7_1412800	PF3D7_1458000					
PF3D7_0815400	PF3D7_0415800	PF3D7_0507100	PF3D7_0926100	PF3D7_1345800	PF3D7_0621000	PF3D7_0600200	PF3D7_1028200	PF3D7_1112700	PF3D7_1425700	PF3D7_1464900					

PF3D7_0812300	PF3D7_0416600	PF3D7_0508300	PF3D7_0926500	PF3D7_1347000	PF3D7_0622000	PF3D7_1308600	PF3D7_1030800	PF3D7_1114600	PF3D7_1430100	PF3D7_0800900					
PF3D7_0804900	PF3D7_0418600	PF3D7_0510200	PF3D7_0931300	PF3D7_1349700	PF3D7_0622200	PF3D7_1330300	PF3D7_1106400	PF3D7_1124300	PF3D7_1441600						
PF3D7_0803700	PF3D7_0419500	PF3D7_0512200	PF3D7_0932300	PF3D7_1352300	PF3D7_0622800	PF3D7_1372700	PF3D7_1107000	PF3D7_1125200	PF3D7_1446700						
PF3D7_0800100	PF3D7_0419700	PF3D7_0512400	PF3D7_0936200	PF3D7_1355700	PF3D7_0623100	PF3D7_1373300	PF3D7_1117500	PF3D7_1126200	PF3D7_1449700						
PF3D7_0500100	PF3D7_0420400	PF3D7_0512700	PF3D7_0936400	PF3D7_1360800	PF3D7_0623500	PF3D7_1373400	PF3D7_1115500	PF3D7_1126600	PF3D7_1451800						
PF3D7_0501100	PF3D7_0421100	PF3D7_0513300	PF3D7_1302700	PF3D7_1363100	PF3D7_0625700	PF3D7_0313700	PF3D7_1124000	PF3D7_1128400	PF3D7_1456500						
PF3D7_0501900	PF3D7_0422600	PF3D7_0515900	PF3D7_1303600	PF3D7_1367500	PF3D7_0627400	PF3D7_0700100	PF3D7_1127400	PF3D7_1132500	PF3D7_1458700						
PF3D7_0502800	PF3D7_0423400	PF3D7_0516900	PF3D7_1306700	PF3D7_0618800	PF3D7_0629700	PF3D7_0700500	PF3D7_1128100	PF3D7_1134400	PF3D7_1464400						
PF3D7_0504600	PF3D7_0423500	PF3D7_0519400	PF3D7_1310800	PF3D7_0620600	PF3D7_0629900	PF3D7_0831700	PF3D7_1130100	PF3D7_1139900	PF3D7_1468200						
PF3D7_0505600	PF3D7_0423800	PF3D7_0520000	PF3D7_1313500	PF3D7_0621800	PF3D7_0630400	PF3D7_0833000	PF3D7_1130500	PF3D7_1142400	PF3D7_1477700						
PF3D7_0505700	PF3D7_0423900	PF3D7_0521100	PF3D7_1314700	PF3D7_0622900	PF3D7_0603400	PF3D7_0833500	PF3D7_1131000	PF3D7_1143000	PF3D7_0731400						
PF3D7_0506100	PF3D7_0424100	PF3D7_0523300	PF3D7_1319300	PF3D7_0623800	PF3D7_0604500	PF3D7_0200100	PF3D7_1133100	PF3D7_1143400							
PF3D7_0506200	PF3D7_0702300	PF3D7_0523700	PF3D7_1322100	PF3D7_0624600	PF3D7_0606500	PF3D7_0200400	PF3D7_1135800	PF3D7_1144200							
PF3D7_0510400	PF3D7_0703000	PF3D7_0524500	PF3D7_1322500	PF3D7_0629800	PF3D7_0607000	PF3D7_0200500	PF3D7_1137100	PF3D7_1148900							
PF3D7_0511800	PF3D7_0703400	PF3D7_0527500	PF3D7_1322600	PF3D7_0630300	PF3D7_0610200	PF3D7_0200600	PF3D7_1138600	PF3D7_1204100							
PF3D7_0511900	PF3D7_0704800	PF3D7_0528200	PF3D7_1324200	PF3D7_0606000	PF3D7_0611600	PF3D7_0201300	PF3D7_1140100	PF3D7_1209600							
PF3D7_0513900	PF3D7_0704900	PF3D7_0903900	PF3D7_1328900	PF3D7_0606100	PF3D7_0612900	PF3D7_0202300	PF3D7_1140700	PF3D7_1228000							
PF3D7_0514200	PF3D7_0705100	PF3D7_0905300	PF3D7_1328800	PF3D7_0606900	PF3D7_0103000	PF3D7_0219500	PF3D7_1142200	PF3D7_1232100							
PF3D7_0514600	PF3D7_0707700	PF3D7_0906100	PF3D7_1328100	PF3D7_0614600	PF3D7_0406500	PF3D7_1000100	PF3D7_1144300	PF3D7_1237300							
PF3D7_0515200	PF3D7_0708300	PF3D7_0906300	PF3D7_1327400	PF3D7_0111800	PF3D7_0420500	PF3D7_1000400	PF3D7_1147900	PF3D7_1247400							
PF3D7_0516000	PF3D7_0708700	PF3D7_0909600	PF3D7_1330800	PF3D7_0417700	PF3D7_0513100	PF3D7_1000500	PF3D7_1203400	PF3D7_1249500							
PF3D7_0516200	PF3D7_0709200	PF3D7_0909700	PF3D7_1331300	PF3D7_0504900	PF3D7_0527600	PF3D7_1002300	PF3D7_1204500	PF3D7_1250900							
PF3D7_0517700	PF3D7_0709300	PF3D7_0912400	PF3D7_1332400	PF3D7_0522300	PF3D7_0704600	PF3D7_1017200	PF3D7_1205500	PF3D7_1401200							
PF3D7_0519200	PF3D7_0710500	PF3D7_0912900	PF3D7_1332600	PF3D7_0709600	PF3D7_0706000	PF3D7_1021300	PF3D7_1210900	PF3D7_1403300							
PF3D7_0520400	PF3D7_0711200	PF3D7_0913200	PF3D7_1332800	PF3D7_0711500	PF3D7_0706500	PF3D7_1029700	PF3D7_1212100	PF3D7_1407800							
PF3D7_0520800	PF3D7_0713800	PF3D7_0913500	PF3D7_1333200	PF3D7_0724000	PF3D7_0709800	PF3D7_1036400	PF3D7_1215200	PF3D7_1409500							
PF3D7_0521400	PF3D7_0714000	PF3D7_0914700	PF3D7_1333800	PF3D7_0804600	PF3D7_0713900	PF3D7_1040200	PF3D7_1220100	PF3D7_1414800							
PF3D7_0523600	PF3D7_0714400	PF3D7_0915100	PF3D7_1339600	PF3D7_0807000	PF3D7_0727100	PF3D7_1040300	PF3D7_1224500	PF3D7_1417700							
PF3D7_0523800	PF3D7_0716100	PF3D7_0917800	PF3D7_1340800	PF3D7_0818700	PF3D7_0801700	PF3D7_1040800	PF3D7_1225900	PF3D7_1420700							
PF3D7_0524600	PF3D7_0716600	PF3D7_0918300	PF3D7_1344900	PF3D7_0911600	PF3D7_0807400	PF3D7_1041100	PF3D7_1229900	PF3D7_1421300							
PF3D7_0524700	PF3D7_0717400	PF3D7_0919100	PF3D7_1345600	PF3D7_0927400	PF3D7_0816400	PF3D7_1041200	PF3D7_1233100	PF3D7_1428300							
PF3D7_0527300	PF3D7_0717500	PF3D7_0920900	PF3D7_1348300	PF3D7_1333400	PF3D7_0820000	PF3D7_1041300	PF3D7_1239000	PF3D7_1432400							
PF3D7_0527400	PF3D7_0717900	PF3D7_0925300	PF3D7_1350600	PF3D7_1350400	PF3D7_0931200	PF3D7_1100100	PF3D7_1241600	PF3D7_1436000							
PF3D7_0528500	PF3D7_0721500	PF3D7_0929100	PF3D7_1350900	PF3D7_1354600	PF3D7_1346400	PF3D7_1100200	PF3D7_1242500	PF3D7_1437000							
PF3D7_0528700	PF3D7_0722200	PF3D7_0930700	PF3D7_1351000	PF3D7_1364300	PF3D7_0314000	PF3D7_1101300	PF3D7_1247300	PF3D7_1441500							
PF3D7_0529100	PF3D7_0722600	PF3D7_0931000	PF3D7_1354300	PF3D7_1366800	PF3D7_0322400	PF3D7_1118100	PF3D7_1405200	PF3D7_1446300							
PF3D7_0900600	PF3D7_0723000	PF3D7_0931800	PF3D7_1354800	PF3D7_1368300	PF3D7_0215700	PF3D7_1118600	PF3D7_1405600	PF3D7_1448200							
PF3D7_0901900	PF3D7_0724600	PF3D7_0932800	PF3D7_1355300	PF3D7_1372400	PF3D7_0218400	PF3D7_1131600	PF3D7_1406100	PF3D7_1448700							
PF3D7_0903000	PF3D7_0724800	PF3D7_0933600	PF3D7_1356400	PF3D7_0831500	PF3D7_1004400	PF3D7_1131900	PF3D7_1413400	PF3D7_1457300							
PF3D7_0904500	PF3D7_0725200	PF3D7_0936100	PF3D7_1357700	PF3D7_0202400	PF3D7_1004900	PF3D7_1136500	PF3D7_1417800	PF3D7_1460000							
PF3D7_0905900	PF3D7_0725300	PF3D7_1302100	PF3D7_1358100	PF3D7_0206900	PF3D7_1007000	PF3D7_1141200	PF3D7_1419500	PF3D7_1464300							
PF3D7_0908700	PF3D7_0725400	PF3D7_1302800	PF3D7_1358500	PF3D7_0208200	PF3D7_1010000	PF3D7_1149800	PF3D7_1426900	PF3D7_1468700							
PF3D7_0908800	PF3D7_0726300	PF3D7_1305600	PF3D7_1359200	PF3D7_0208800	PF3D7_1010600	PF3D7_1150400	PF3D7_1432700	PF3D7_1471100							
PF3D7_0908900	PF3D7_0726900	PF3D7_1309100	PF3D7_1362200	PF3D7_0215800	PF3D7_1011500	PF3D7_1200100	PF3D7_1435400	PF3D7_1474500							
PF3D7_0910000	PF3D7_0727300	PF3D7_1310900	PF3D7_1364000	PF3D7_0217000	PF3D7_1013000	PF3D7_1200300	PF3D7_1437900								

University of Ghana http://ugspace.ug.edu.gh

University of Ghana http://ugspace.ug.edu.gh

PF3D7_0910600	PF3D7_0727700	PF3D7_1311100	PF3D7_1365900	PF3D7_0218200	PF3D7_1022300	PF3D7_1200400	PF3D7_1438900								
PF3D7_0911900	PF3D7_0727900	PF3D7_1311900	PF3D7_1367000	PF3D7_0218700	PF3D7_1024300	PF3D7_1200500	PF3D7_1439600								
PF3D7_0913300	PF3D7_0730100	PF3D7_1312300	PF3D7_0620000	PF3D7_0219300	PF3D7_1025800	PF3D7_1205300	PF3D7_1439900								
PF3D7_0914200	PF3D7_0730200	PF3D7_1313100	PF3D7_0622700	PF3D7_0219500	PF3D7_1023400	PF3D7_1210300	PF3D7_1442700								
PF3D7_0915900	PF3D7_0730300	PF3D7_1314800	PF3D7_0625600	PF3D7_0219700	PF3D7_1032700	PF3D7_1240300	PF3D7_1446500								
PF3D7_0917500	PF3D7_0730400	PF3D7_1315900	PF3D7_0625800	PF3D7_0220300	PF3D7_1036900	PF3D7_1240600	PF3D7_1449900								
PF3D7_0917700	PF3D7_0730500	PF3D7_1317200	PF3D7_0627900	PF3D7_0220600	PF3D7_1037000	PF3D7_1248600	PF3D7_1454500								
PF3D7_0918800	PF3D7_0731100	PF3D7_1319000	PF3D7_0629400	PF3D7_1000600	PF3D7_1104200	PF3D7_1253700	PF3D7_1455900								
PF3D7_0919300	PF3D7_0731500	PF3D7_1321800	PF3D7_0629600	PF3D7_1002000	PF3D7_1106700	PF3D7_1254000	PF3D7_1456700								
PF3D7_0919600	PF3D7_0831000	PF3D7_1322000	PF3D7_0630900	PF3D7_1002200	PF3D7_1110400	PF3D7_1254100	PF3D7_1458100								
PF3D7_0919700	PF3D7_0830300	PF3D7_1322400	PF3D7_0602100	PF3D7_1002700	PF3D7_1118300	PF3D7_1254300	PF3D7_1459800								
PF3D7_0919800	PF3D7_0828900	PF3D7_1323100	PF3D7_0602200	PF3D7_1003100	PF3D7_1119700	PF3D7_1400700	PF3D7_1460300								
PF3D7_0921500	PF3D7_0828800	PF3D7_1323500	PF3D7_0605000	PF3D7_1003500	PF3D7_1120000	PF3D7_1407700	PF3D7_1460700								
PF3D7_0923600	PF3D7_0828200	PF3D7_1325800	PF3D7_0605500	PF3D7_1003800	PF3D7_1123100	PF3D7_1414100	PF3D7_1466900								
PF3D7_0924700	PF3D7_0827100	PF3D7_1330400	PF3D7_0606600	PF3D7_1013500	PF3D7_1127800	PF3D7_1414600	PF3D7_1469100								
PF3D7_0925700	PF3D7_0826000	PF3D7_1331800	PF3D7_0607300	PF3D7_1015700	PF3D7_1133000	PF3D7_1418100	PF3D7_1470900								
PF3D7_0926000	PF3D7_0825600	PF3D7_1333100	PF3D7_0608900	PF3D7_1016600	PF3D7_1134300	PF3D7_1441000	PF3D7_1471300								
PF3D7_0927700	PF3D7_0825500	PF3D7_1338200	PF3D7_0612600	PF3D7_1017400	PF3D7_1136600	PF3D7_1442600									
PF3D7_0928900	PF3D7_0825200	PF3D7_1338300	PF3D7_0614000	PF3D7_1022000	PF3D7_1138500	PF3D7_1460200									
PF3D7_0937100	PF3D7_0825100	PF3D7_1342000	PF3D7_0614900	PF3D7_1022900	PF3D7_1139300	PF3D7_1468300									
PF3D7_1300100	PF3D7_0824900	PF3D7_1342300	PF3D7_0419900	PF3D7_1026000	PF3D7_1140900	PF3D7_1473000									
PF3D7_1300400	PF3D7_0824300	PF3D7_1342700	PF3D7_0416700	PF3D7_1027500	PF3D7_1144100	PF3D7_1473600									
PF3D7_1300600	PF3D7_0823600	PF3D7_1345500	PF3D7_0418900	PF3D7_1030600	PF3D7_1149000	PF3D7_1475400									
PF3D7_1300700	PF3D7_0822900	PF3D7_1346100	PF3D7_0518200	PF3D7_1031300	PF3D7_1203000	PF3D7_1475900									
PF3D7_1301200	PF3D7_0822500	PF3D7_1346300	PF3D7_0520100	PF3D7_1103100	PF3D7_1207000	PF3D7_1477100									
PF3D7_1302200	PF3D7_0822100	PF3D7_1347200	PF3D7_0614100	PF3D7_1106300	PF3D7_1210400	PF3D7_1479700									
PF3D7_1303100	PF3D7_0821600	PF3D7_1347500	PF3D7_0705900	PF3D7_1107700	PF3D7_1212700	PF3D7_0114300									
PF3D7_1303200	PF3D7_0821500	PF3D7_1349300	PF3D7_0717100	PF3D7_1108000	PF3D7_1217200	PF3D7_0114400									
PF3D7_1304300	PF3D7_0821400	PF3D7_1349600	PF3D7_0729100	PF3D7_1110800	PF3D7_1219000	PF3D7_0114600									
PF3D7_1304900	PF3D7_0820700	PF3D7_1351400	PF3D7_0731800	PF3D7_1112200	PF3D7_1221800	PF3D7_0115150									
PF3D7_1305100	PF3D7_0820300	PF3D7_1352500	PF3D7_0806200	PF3D7_1117000	PF3D7_1225700	PF3D7_0221300									
PF3D7_1305700	PF3D7_0819600	PF3D7_1352900	PF3D7_0808400	PF3D7_1118500	PF3D7_1226700	PF3D7_0221650									
PF3D7_1305900	PF3D7_0819200	PF3D7_1353900	PF3D7_0813300	PF3D7_1119600	PF3D7_1232400	PF3D7_0221900									
PF3D7_1308100	PF3D7_0819100	PF3D7_1358800	PF3D7_0819700	PF3D7_1121700	PF3D7_1232800	PF3D7_0302300									
PF3D7_1308200	PF3D7_0819000	PF3D7_1364100	PF3D7_0824600	PF3D7_1122300	PF3D7_1234100	PF3D7_0401500									
PF3D7_1309000	PF3D7_0818500	PF3D7_1368200	PF3D7_0831200	PF3D7_1124800	PF3D7_1235300	PF3D7_0402800									
PF3D7_1309700	PF3D7_0818100	PF3D7_0620500	PF3D7_0902200	PF3D7_1124900	PF3D7_1248700	PF3D7_0413400									
PF3D7_1309800	PF3D7_0817800	PF3D7_0621500	PF3D7_0902400	PF3D7_1125100	PF3D7_1250800	PF3D7_0421500									
PF3D7_1309900	PF3D7_0817600	PF3D7_0623300	PF3D7_0906000	PF3D7_1126000	PF3D7_1400300	PF3D7_0421600									
PF3D7_1310500	PF3D7_0816100	PF3D7_0623900	PF3D7_0921100	PF3D7_1129400	PF3D7_1402400	PF3D7_0425000									
PF3D7_1311000	PF3D7_0815900	PF3D7_0624000	PF3D7_0924300	PF3D7_1132000	PF3D7_1406200	PF3D7_0632600									
PF3D7_1311600	PF3D7_0815600	PF3D7_0624700	PF3D7_0924500	PF3D7_1133500	PF3D7_1407600	PF3D7_0712500									
PF3D7_1312200	PF3D7_0815100	PF3D7_0626800	PF3D7_0926600	PF3D7_1133600	PF3D7_1408200	PF3D7_0713300									
PF3D7_1313000	PF3D7_0812700	PF3D7_0627600	PF3D7_0930900	PF3D7_1133800	PF3D7_1409100	PF3D7_1000900									
PF3D7_1313700	PF3D7_0812600	PF3D7_0602000	PF3D7_0933700	PF3D7_1133900	PF3D7_1415400	PF3D7_1219400									

PF3D7_1314000	PF3D7_0812000	PF3D7_0603600	PF3D7_1331100	PF3D7_1134000	PF3D7_1417200	PF3D7_1219500										
PF3D7_1314200	PF3D7_0811600	PF3D7_0604000	PF3D7_1331600	PF3D7_1136000	PF3D7_1417600	PF3D7_1240200										
PF3D7_1314400	PF3D7_0811500	PF3D7_0606800	PF3D7_1337500	PF3D7_1136300	PF3D7_1419100	PF3D7_1240700										
PF3D7_1314500	PF3D7_0810900	PF3D7_0608000	PF3D7_1342900	PF3D7_1139100	PF3D7_1422500	PF3D7_1400100										
PF3D7_1314600	PF3D7_0810800	PF3D7_0608500	PF3D7_1362700	PF3D7_1140000	PF3D7_1435900	PF3D7_1401050										
PF3D7_1316500	PF3D7_0810600	PF3D7_0608700	PF3D7_1368000	PF3D7_1143800	PF3D7_1438000	PF3D7_1478400										
PF3D7_1317700	PF3D7_0810200	PF3D7_0608800	PF3D7_1371900	PF3D7_1146000	PF3D7_1441100	PF3D7_1480100										
PF3D7_1318200	PF3D7_0808300	PF3D7_0609500	PF3D7_1372000	PF3D7_1147000	PF3D7_1442800											
PF3D7_1321300	PF3D7_0808200	PF3D7_0612000	PF3D7_0301600	PF3D7_1149300	PF3D7_1442900											
PF3D7_1321700	PF3D7_0807800	PF3D7_0614500	PF3D7_0902600	PF3D7_1200700	PF3D7_1444300											
PF3D7_1323900	PF3D7_0806800	PF3D7_0109850	PF3D7_0703900	PF3D7_1201100	PF3D7_1445500											
PF3D7_1325000	PF3D7_0806500	PF3D7_0114000	PF3D7_0800700	PF3D7_1203200	PF3D7_1450700											
PF3D7_1325500	PF3D7_0804000	PF3D7_0409500	PF3D7_0805900	PF3D7_1204200	PF3D7_1451000											
PF3D7_1329400	PF3D7_0803500	PF3D7_0422800	PF3D7_0203700	PF3D7_1205700	PF3D7_1452600											
PF3D7_1327800	PF3D7_0803300	PF3D7_0611700	PF3D7_0205800	PF3D7_1205900	PF3D7_1458500											
PF3D7_1329600	PF3D7_0803200	PF3D7_0706400	PF3D7_0210100	PF3D7_1207100	PF3D7_1459200											
PF3D7_1334400	PF3D7_0803100	PF3D7_0726200	PF3D7_0213000	PF3D7_1210500	PF3D7_1460100											
PF3D7_1335700	PF3D7_0803000	PF3D7_0801900	PF3D7_0214300	PF3D7_1211300	PF3D7_1461600											
PF3D7_1336200	PF3D7_0802800	PF3D7_0811400	PF3D7_0216800	PF3D7_1214000	PF3D7_1468500											
PF3D7_1336400	PF3D7_0800800	PF3D7_0817000	PF3D7_0220100	PF3D7_1215000	PF3D7_1468800											
PF3D7_1339400	PF3D7_0500900	PF3D7_0819500	PF3D7_1001400	PF3D7_1215600	PF3D7_1469800											
PF3D7_1340600	PF3D7_0501500	PF3D7_0824700	PF3D7_1005900	PF3D7_1216600	PF3D7_1472200											
PF3D7_1342400	PF3D7_0501600	PF3D7_0827900	PF3D7_1008700	PF3D7_1217600	PF3D7_1472900											
PF3D7_1342500	PF3D7_0501700	PF3D7_0903200	PF3D7_1011100	PF3D7_1219600	PF3D7_0206300											
PF3D7_1343300	PF3D7_0503400	PF3D7_0911000	PF3D7_1011300	PF3D7_1220400	PF3D7_0533100											
PF3D7_1343600	PF3D7_0503600	PF3D7_0931400	PF3D7_1012300	PF3D7_1221000												
PF3D7_1344600	PF3D7_0504100	PF3D7_1317800	PF3D7_1016500	PF3D7_1221900												
PF3D7_1344800	PF3D7_0504200	PF3D7_1320900	PF3D7_1020700	PF3D7_1222600												
PF3D7_1348100	PF3D7_0504300	PF3D7_1324700	PF3D7_1021000	PF3D7_1224300												
PF3D7_1348200	PF3D7_0505400	PF3D7_1326500	PF3D7_1022600	PF3D7_1224900												
PF3D7_1349400	PF3D7_0506700	PF3D7_1341300	PF3D7_1024000	PF3D7_1227800												
PF3D7_1350200	PF3D7_0506900	PF3D7_1345900	PF3D7_1024100	PF3D7_1229100												
PF3D7_1351300	PF3D7_0507200	PF3D7_1355800	PF3D7_1025100	PF3D7_1229700												
PF3D7_1352200	PF3D7_0507500	PF3D7_1359000	PF3D7_1027000	PF3D7_1234900												
PF3D7_1353200	PF3D7_0507600	PF3D7_0310300	PF3D7_1027100	PF3D7_1238000												
PF3D7_1353500	PF3D7_0508100	PF3D7_0729900	PF3D7_1028000	PF3D7_1238300												
PF3D7_1354100	PF3D7_0508500	PF3D7_0202900	PF3D7_1032100	PF3D7_1241500												
PF3D7_1356500	PF3D7_0508600	PF3D7_0204700	PF3D7_1033000	PF3D7_1241900												
PF3D7_1357000	PF3D7_0508900	PF3D7_0204900	PF3D7_1033400	PF3D7_1242700												
PF3D7_1357300	PF3D7_0509300	PF3D7_0208600	PF3D7_1037100	PF3D7_1247600												
PF3D7_1357400	PF3D7_0511100	PF3D7_0209400	PF3D7_1037900	PF3D7_1401000												
PF3D7_1357900	PF3D7_0511600	PF3D7_0209800	PF3D7_1038800	PF3D7_1402800												
PF3D7_1358400	PF3D7_0511700	PF3D7_0210900	PF3D7_1102300	PF3D7_1403400												
PF3D7_1359800	PF3D7_0512300	PF3D7_0211200	PF3D7_1102600	PF3D7_1404800												
PF3D7_1360200	PF3D7_0512600	PF3D7_0212000	PF3D7_1113000	PF3D7_1407400												

University of Ghana http://ugspace.ug.edu.gh

PF3D7_1360400	PF3D7_0512900	PF3D7_0213200	PF3D7_1113300	PF3D7_1410200											
PF3D7_1361600	PF3D7_0515700	PF3D7_0214400	PF3D7_1115900	PF3D7_1413300											
PF3D7_1362000	PF3D7_0515800	PF3D7_0217800	PF3D7_1119800	PF3D7_1413600											
PF3D7_1363200	PF3D7_0516100	PF3D7_1001200	PF3D7_1120300	PF3D7_1415500											
PF3D7_1363500	PF3D7_0516700	PF3D7_1001300	PF3D7_1121500	PF3D7_1415600											
PF3D7_1363600	PF3D7_0518100	PF3D7_1002600	PF3D7_1121900	PF3D7_1418200											
PF3D7_1363700	PF3D7_0519300	PF3D7_1002900	PF3D7_1123600	PF3D7_1420400											
PF3D7_1364200	PF3D7_0520200	PF3D7_1003700	PF3D7_1123800	PF3D7_1422200											
PF3D7_1364500	PF3D7_0520300	PF3D7_1004000	PF3D7_1125400	PF3D7_1423000											
PF3D7_1364600	PF3D7_0520500	PF3D7_1005700	PF3D7_1133700	PF3D7_1423200											
PF3D7_1366000	PF3D7_0520700	PF3D7_1006200	PF3D7_1134200	PF3D7_1426600											
PF3D7_1366500	PF3D7_0521300	PF3D7_1007400	PF3D7_1134600	PF3D7_1427300											
PF3D7_1368700	PF3D7_0521500	PF3D7_1007700	PF3D7_1134700	PF3D7_1431500											
PF3D7_0618100	PF3D7_0521700	PF3D7_1009000	PF3D7_1134900	PF3D7_1431900											
PF3D7_0618400	PF3D7_0523400	PF3D7_1010700	PF3D7_1135900	PF3D7_1440200											
PF3D7_0618900	PF3D7_0524200	PF3D7_1012400	PF3D7_1137600	PF3D7_1444500											
PF3D7_0620100	PF3D7_0524300	PF3D7_1013100	PF3D7_1139700	PF3D7_1445000											
PF3D7_0622400	PF3D7_0525100	PF3D7_1013300	PF3D7_1140800	PF3D7_1446900											
PF3D7_0626100	PF3D7_0525600	PF3D7_1015900	PF3D7_1142900	PF3D7_1447500											
PF3D7_0626200	PF3D7_0525800	PF3D7_1017900	PF3D7_1145800	PF3D7_1449300											
PF3D7_0626300	PF3D7_0526000	PF3D7_1020800	PF3D7_1148700	PF3D7_1449500											
PF3D7_0626600	PF3D7_0526800	PF3D7_1020900	PF3D7_1200800	PF3D7_1450500											
PF3D7_0626700	PF3D7_0527200	PF3D7_1021400	PF3D7_1201400	PF3D7_1451200											
PF3D7_0626900	PF3D7_0528300	PF3D7_1022200	PF3D7_1201500	PF3D7_1452200											
PF3D7_0627000	PF3D7_0528400	PF3D7_1023100	PF3D7_1202200	PF3D7_1456000											
PF3D7_0627500	PF3D7_0529000	PF3D7_1024500	PF3D7_1202700	PF3D7_1459000											
PF3D7_0628000	PF3D7_0529500	PF3D7_1024800	PF3D7_1203500	PF3D7_1460400											
PF3D7_0628800	PF3D7_0529900	PF3D7_1025700	PF3D7_1205400	PF3D7_1460500											
PF3D7_0629000	PF3D7_0530000	PF3D7_1029400	PF3D7_1206600	PF3D7_1461900											
PF3D7_0632000	PF3D7_0530100	PF3D7_1030400	PF3D7_1207800	PF3D7_1462300											
PF3D7_0632200	PF3D7_0530400	PF3D7_1034700	PF3D7_1209700	PF3D7_1464000											
PF3D7_0632400	PF3D7_0530600	PF3D7_1036700	PF3D7_1212300	PF3D7_1464500											
PF3D7_0601500	PF3D7_0530700	PF3D7_1037300	PF3D7_1212400	PF3D7_1465100											
PF3D7_0602300	PF3D7_0532100	PF3D7_1038400	PF3D7_1212900	PF3D7_1466400											
PF3D7_0603500	PF3D7_0902100	PF3D7_1102400	PF3D7_1214100	PF3D7_1469700											
PF3D7_0604200	PF3D7_0903700	PF3D7_1105400	PF3D7_1215400	PF3D7_1470800											
PF3D7_0604700	PF3D7_0905000	PF3D7_1105500	PF3D7_1216100	PF3D7_1472500											
PF3D7_0605400	PF3D7_0905100	PF3D7_1107600	PF3D7_1216200	PF3D7_1475600											
PF3D7_0606200	PF3D7_0905400	PF3D7_1108300	PF3D7_1217100	PF3D7_1476200											
PF3D7_0608100	PF3D7_0905500	PF3D7_1108500	PF3D7_1223300	PF3D7_1476800											
PF3D7_0609000	PF3D7_0906200	PF3D7_1108600	PF3D7_1224000	PF3D7_1477800											
PF3D7_0609100	PF3D7_0907100	PF3D7_1108700	PF3D7_1224400	PF3D7_1478600											
PF3D7_0609900	PF3D7_0907300	PF3D7_1109200	PF3D7_1225400	PF3D7_0401700											
PF3D7_0610500	PF3D7_0907600	PF3D7_1111100	PF3D7_1226000	PF3D7_1149500											
PF3D7_0610600	PF3D7_0908200	PF3D7_1111400	PF3D7_1226100												

University of Ghana http://ugspace.ug.edu.gh

PF3D7_0611100	PF3D7_0909300	PF3D7_1113800	PF3D7_1227000												
PF3D7_0611200	PF3D7_0910500	PF3D7_1113900	PF3D7_1227300												
PF3D7_0611400	PF3D7_0911100	PF3D7_1115400	PF3D7_1227600												
PF3D7_0613000	PF3D7_0911200	PF3D7_1117100	PF3D7_1228400												
PF3D7_0613100	PF3D7_0912100	PF3D7_1117500	PF3D7_1229300												
PF3D7_0615600	PF3D7_0913100	PF3D7_1117700	PF3D7_1231100												
PF3D7_0615700	PF3D7_0913800	PF3D7_1119000	PF3D7_1231800												
PF3D7_0615800	PF3D7_0913900	PF3D7_1120100	PF3D7_1232600												
PF3D7_0616000	PF3D7_0914900	PF3D7_1122900	PF3D7_1232700												
PF3D7_0108400	PF3D7_0915300	PF3D7_1126800	PF3D7_1233700												
PF3D7_0407100	PF3D7_0915500	PF3D7_1127100	PF3D7_1237500												
PF3D7_0414300	PF3D7_0916200	PF3D7_1128200	PF3D7_1237600												
PF3D7_0415900	PF3D7_0916300	PF3D7_1128600	PF3D7_1241800												
PF3D7_0416900	PF3D7_0916600	PF3D7_1129000	PF3D7_1246500												
PF3D7_0424000	PF3D7_0916700	PF3D7_1130200	PF3D7_1247900												
PF3D7_0424200	PF3D7_0917200	PF3D7_1134100	PF3D7_1249700												
PF3D7_0507900	PF3D7_0917400	PF3D7_1137700	PF3D7_1401300												
PF3D7_0514000	PF3D7_0917900	PF3D7_1141600	PF3D7_1401500												
PF3D7_0518000	PF3D7_0918700	PF3D7_1144700	PF3D7_1402200												
PF3D7_0519100	PF3D7_0919200	PF3D7_1146500	PF3D7_1402700												
PF3D7_0520600	PF3D7_0920400	PF3D7_1203700	PF3D7_1403500												
PF3D7_0521200	PF3D7_0920500	PF3D7_1204300	PF3D7_1405100												
PF3D7_0521600	PF3D7_0920700	PF3D7_1209900	PF3D7_1405800												
PF3D7_0521800	PF3D7_0921300	PF3D7_1214900	PF3D7_1408400												
PF3D7_0622600	PF3D7_0921400	PF3D7_1216300	PF3D7_1410800												
PF3D7_0705700	PF3D7_0921600	PF3D7_1216400	PF3D7_1411500												
PF3D7_0716500	PF3D7_0922700	PF3D7_1218400	PF3D7_1412900												
PF3D7_0721900	PF3D7_0923000	PF3D7_1223200	PF3D7_1416600												
PF3D7_0726800	PF3D7_0923300	PF3D7_1231500	PF3D7_1421900												
PF3D7_0732500	PF3D7_0923400	PF3D7_1232000	PF3D7_1425600												
PF3D7_0805400	PF3D7_0923500	PF3D7_1234600	PF3D7_1425900												
PF3D7_0807200	PF3D7_0924000	PF3D7_1235100	PF3D7_1426800												
PF3D7_0810100	PF3D7_0924200	PF3D7_1235600	PF3D7_1427200												
PF3D7_0813400	PF3D7_0925200	PF3D7_1235700	PF3D7_1429200												
PF3D7_0815700	PF3D7_0925800	PF3D7_1241400	PF3D7_1431300												
PF3D7_0817400	PF3D7_0927800	PF3D7_1242400	PF3D7_1432300												
PF3D7_0821800	PF3D7_0927900	PF3D7_1245500	PF3D7_1433800												
PF3D7_0821900	PF3D7_0928000	PF3D7_1246100	PF3D7_1435000												
PF3D7_0826900	PF3D7_0928400	PF3D7_1248500	PF3D7_1438500												
PF3D7_0907000	PF3D7_0928700	PF3D7_1249400	PF3D7_1440500												
PF3D7_0908300	PF3D7_0928800	PF3D7_1250500	PF3D7_1442400												
PF3D7_0909800	PF3D7_0929000	PF3D7_1402500	PF3D7_1442500												
PF3D7_0916500	PF3D7_0929300	PF3D7_1406000	PF3D7_1443000												
PF3D7_0916800	PF3D7_0930300	PF3D7_1408000	PF3D7_1443200												
PF3D7_0918200	PF3D7_0930500	PF3D7_1408100	PF3D7_1446400												

University of Ghana http://ugspace.ug.edu.gh

University of Ghana http://ugspace.ug.edu.gh

PF3D7_0921800	PF3D7_0930600	PF3D7_1408600	PF3D7_1448100												
PF3D7_0922600	PF3D7_0932200	PF3D7_1412300	PF3D7_1453900												
PF3D7_0927500	PF3D7_0932500	PF3D7_1414000	PF3D7_1455700												
PF3D7_0929500	PF3D7_0933000	PF3D7_1414300	PF3D7_1457200												
PF3D7_0929800	PF3D7_0934200	PF3D7_1416500	PF3D7_1457700												
PF3D7_0933200	PF3D7_0934400	PF3D7_1419200	PF3D7_1459300												
PF3D7_0935100	PF3D7_0934600	PF3D7_1419900	PF3D7_1462400												
PF3D7_1304000	PF3D7_0934700	PF3D7_1420100	PF3D7_1464200												
PF3D7_1306100	PF3D7_0934800	PF3D7_1420500	PF3D7_1465900												
PF3D7_1313900	PF3D7_0935000	PF3D7_1421200	PF3D7_1466200												
PF3D7_1320300	PF3D7_0935200	PF3D7_1422600	PF3D7_1467600												
PF3D7_1328400	PF3D7_0935300	PF3D7_1424100	PF3D7_1469600												
PF3D7_1336100	PF3D7_0935700	PF3D7_1424400	PF3D7_1471000												
PF3D7_1340700	PF3D7_0936500	PF3D7_1426000	PF3D7_1473500												
PF3D7_1343900	PF3D7_1302500	PF3D7_1426100	PF3D7_1473700												
PF3D7_1344000	PF3D7_1302900	PF3D7_1426200	PF3D7_1473900												
PF3D7_1357600	PF3D7_1303300	PF3D7_1426300	PF3D7_1474000												
PF3D7_1357800	PF3D7_1305400	PF3D7_1427900	PF3D7_1474300												
PF3D7_1365200	PF3D7_1305500	PF3D7_1428000	PF3D7_1477500												
PF3D7_1371500	PF3D7_1305800	PF3D7_1428400	PF3D7_1477600												
PF3D7_1372200	PF3D7_1306000	PF3D7_1431700	PF3D7_0113600												
PF3D7_1372600	PF3D7_1306600	PF3D7_1433300	PF3D7_0731900												
PF3D7_0301400	PF3D7_1307300	PF3D7_1434500	PF3D7_0902700												
PF3D7_0322100	PF3D7_1307500	PF3D7_1435500	PF3D7_0936900												
PF3D7_0107800	PF3D7_1307700	PF3D7_1438700	PF3D7_1301800												
PF3D7_0313700	PF3D7_1307800	PF3D7_1439000	PF3D7_1477900												
PF3D7_0314100	PF3D7_1308300	PF3D7_1440700													
PF3D7_0613000	PF3D7_1309200	PF3D7_1441200													
PF3D7_0613000	PF3D7_1309500	PF3D7_1444100													
PF3D7_0906890	PF3D7_1309600	PF3D7_1445600													
PF3D7_1303200	PF3D7_1310100	PF3D7_1445700													
PF3D7_1372300	PF3D7_1310300	PF3D7_1446200													
PF3D7_0701100	PF3D7_1310700	PF3D7_1447000													
PF3D7_0706200	PF3D7_1311500	PF3D7_1447700													
PF3D7_0710400	PF3D7_1312400	PF3D7_1448400													
PF3D7_0713600	PF3D7_1312600	PF3D7_1451100													
PF3D7_0715300	PF3D7_1312800	PF3D7_1452400													
PF3D7_0716400	PF3D7_1301600	PF3D7_1452800													
PF3D7_0720900	PF3D7_1313400	PF3D7_1453700													
PF3D7_0806100	PF3D7_1314100	PF3D7_1456400													
PF3D7_0806900	PF3D7_1315000	PF3D7_1457000													
PF3D7_0812220	PF3D7_1315100	PF3D7_1458200													
PF3D7_0832900	PF3D7_1315500	PF3D7_1458800													
PF3D7_0203400	PF3D7_1316600	PF3D7_1459900													
PF3D7_0203600	PF3D7_1317900	PF3D7_1460900													

University of Ghana http://ugspace.ug.edu.gh

PF3D7_0204400	PF3D7_1318000	PF3D7_1461300													
PF3D7_0204600	PF3D7_1318100	PF3D7_1462700													
PF3D7_0205500	PF3D7_1318800	PF3D7_1467300													
PF3D7_0205700	PF3D7_1319700	PF3D7_1469000													
PF3D7_0206600	PF3D7_1320000	PF3D7_1470000													
PF3D7_0207300	PF3D7_1320600	PF3D7_1472100													
PF3D7_0208500	PF3D7_1323700	PF3D7_1476100													
PF3D7_0208700	PF3D7_1323800	PF3D7_0402500													
PF3D7_0209100	PF3D7_1324000														
PF3D7_0209200	PF3D7_1326200														
PF3D7_0210100	PF3D7_1329200														
PF3D7_0210700	PF3D7_1328500														
PF3D7_0211900	PF3D7_1328300														
PF3D7_0213100	PF3D7_1328000														
PF3D7_0213300	PF3D7_1327600														
PF3D7_0213400	PF3D7_1327200														
PF3D7_0214200	PF3D7_1329700														
PF3D7_0215100	PF3D7_1330100														
PF3D7_0215900	PF3D7_1331000														
PF3D7_0216400	PF3D7_1331500														
PF3D7_0216700	PF3D7_1332000														
PF3D7_0217400	PF3D7_1332200														
PF3D7_0218500	PF3D7_1332300														
PF3D7_0221200	PF3D7_1333600														
PF3D7_0222500	PF3D7_1334200														
PF3D7_0223100	PF3D7_1335000														
PF3D7_1001100	PF3D7_1335100														
PF3D7_1001900	PF3D7_1335600														
PF3D7_1003200	PF3D7_1336800														
PF3D7_1004800	PF3D7_1337200														
PF3D7_1005400	PF3D7_1337300														
PF3D7_1007100	PF3D7_1337400														
PF3D7_1007500	PF3D7_1337700														
PF3D7_1007600	PF3D7_1337800														
PF3D7_1014000	PF3D7_1338500														
PF3D7_1014400	PF3D7_1339300														
PF3D7_1015000	PF3D7_1339500														
PF3D7_1015300	PF3D7_1339900														
PF3D7_1017300	PF3D7_1340100														
PF3D7_1017600	PF3D7_1340900														
PF3D7_1018600	PF3D7_1342100														
PF3D7_1019400	PF3D7_1342600														
PF3D7_1020000	PF3D7_1343100														
PF3D7_1023500	PF3D7_1344500														
PF3D7_1024600	PF3D7_1346200														

University of Ghana http://ugspace.ug.edu.gh

PF3D7_1024700	PF3D7_1346500														
PF3D7_1025200	PF3D7_1347100														
PF3D7_1025600	PF3D7_1347400														
PF3D7_1026500	PF3D7_1348500														
PF3D7_1028800	PF3D7_1348600														
PF3D7_1029100	PF3D7_1350500														
PF3D7_1030000	PF3D7_1351700														
PF3D7_1030100	PF3D7_1352100														
PF3D7_1031600	PF3D7_1352700														
PF3D7_1032500	PF3D7_1353400														
PF3D7_1033300	PF3D7_1353600														
PF3D7_1033600	PF3D7_1353700														
PF3D7_1034000	PF3D7_1354400														
PF3D7_1034100	PF3D7_1355600														
PF3D7_1034200	PF3D7_1356200														
PF3D7_1034800	PF3D7_1356300														
PF3D7_1035800	PF3D7_1356600														
PF3D7_1037700	PF3D7_1356700														
PF3D7_1038500	PF3D7_1356800														
PF3D7_1038600	PF3D7_1356900														
PF3D7_1038700	PF3D7_1357200														
PF3D7_1038900	PF3D7_1358700														
PF3D7_1039700	PF3D7_1359400														
PF3D7_1040500	PF3D7_1359300														
PF3D7_1101100	PF3D7_1360000														
PF3D7_1103000	PF3D7_1360100														
PF3D7_1103400	PF3D7_1361000														
PF3D7_1103900	PF3D7_1361400														
PF3D7_1104700	PF3D7_1363300														
PF3D7_1105200	PF3D7_1364400														
PF3D7_1106100	PF3D7_1364800														
PF3D7_1107200	PF3D7_1364900														
PF3D7_1107300	PF3D7_1365000														
PF3D7_1108800	PF3D7_1365400														
PF3D7_1110900	PF3D7_1365500														
PF3D7_1111300	PF3D7_1365600														
PF3D7_1111800	PF3D7_1365700														
PF3D7_1111900	PF3D7_1366700														
PF3D7_1112000	PF3D7_1367400														
PF3D7_1112400	PF3D7_1368400														
PF3D7_1112500	PF3D7_1368600														
PF3D7_1112800	PF3D7_0616900														
PF3D7_1113200	PF3D7_0617100														
PF3D7_1114100	PF3D7_0617300														
PF3D7_1114400	PF3D7_0617900														

University of Ghana http://ugspace.ug.edu.gh

PF3D7_1115300	PF3D7_0618000														
PF3D7_1115700	PF3D7_0619100														
PF3D7_1116200	PF3D7_0619200														
PF3D7_1116300	PF3D7_0619600														
PF3D7_1116900	PF3D7_0619900														
PF3D7_1117600	PF3D7_0620300														
PF3D7_1119100	PF3D7_0620400														
PF3D7_1119500	PF3D7_0621300														
PF3D7_1119900	PF3D7_0621700														
PF3D7_1120400	PF3D7_0622300														
PF3D7_1120500	PF3D7_0623400														
PF3D7_1120900	PF3D7_0624500														
PF3D7_1121000	PF3D7_0625000														
PF3D7_1122400	PF3D7_0625200														
PF3D7_1125500	PF3D7_0625400														
PF3D7_1125600	PF3D7_0628100														
PF3D7_1126400	PF3D7_0628300														
PF3D7_1126900	PF3D7_0628700														
PF3D7_1127700	PF3D7_0629300														
PF3D7_1128000	PF3D7_0630100														
PF3D7_1129700	PF3D7_0630500														
PF3D7_1129800	PF3D7_0630700														
PF3D7_1131800	PF3D7_0600300														
PF3D7_1132200	PF3D7_0600400														
PF3D7_1132300	PF3D7_0602600														
PF3D7_1132700	PF3D7_0602900														
PF3D7_1132800	PF3D7_0603000														
PF3D7_1138100	PF3D7_0603800														
PF3D7_1138200	PF3D7_0604100														
PF3D7_1139200	PF3D7_0604600														
PF3D7_1139800	PF3D7_0605200														
PF3D7_1141300	PF3D7_0606300														
PF3D7_1142500	PF3D7_0607600														
PF3D7_1142700	PF3D7_0607900														
PF3D7_1143900	PF3D7_0608400														
PF3D7_1144000	PF3D7_0609200														
PF3D7_1144500	PF3D7_0610400														
PF3D7_1144600	PF3D7_0610900														
PF3D7_1145300	PF3D7_0612700														
PF3D7_1146200	PF3D7_0612800														
PF3D7_1147600	PF3D7_0613300														
PF3D7_1147800	PF3D7_0613400														
PF3D7_1148000	PF3D7_0613600														
PF3D7_1148800	PF3D7_0613700														
PF3D7_1200200	PF3D7_0613900														

University of Ghana http://ugspace.ug.edu.gh

PF3D7_1200600	PF3D7_0614200														
PF3D7_1201300	PF3D7_0614300														
PF3D7_1201800	PF3D7_0614400														
PF3D7_1205100	PF3D7_0614700														
PF3D7_1206400	PF3D7_0615500														
PF3D7_1206800	PF3D7_0616300														
PF3D7_1207200	PF3D7_0616400														
PF3D7_1208000	PF3D7_0616700														
PF3D7_1208600	PF3D7_0104600														
PF3D7_1208700	PF3D7_0106000														
PF3D7_1209200	PF3D7_0106200														
PF3D7_1209500	PF3D7_0107200														
PF3D7_1210700	PF3D7_0113200														
PF3D7_1214400	PF3D7_0402300														
PF3D7_1214700	PF3D7_0403400														
PF3D7_1215300	PF3D7_0403600														
PF3D7_1217000	PF3D7_0406400														
PF3D7_1217800	PF3D7_0406700														
PF3D7_1218600	PF3D7_0407500														
PF3D7_1220500	PF3D7_0408400														
PF3D7_1220600	PF3D7_0414800														
PF3D7_1221200	PF3D7_0414900														
PF3D7_1221500	PF3D7_0422000														
PF3D7_1222000	PF3D7_0505000														
PF3D7_1222100	PF3D7_0507400														
PF3D7_1223600	PF3D7_0517100														
PF3D7_1223700	PF3D7_0517900														
PF3D7_1225200	PF3D7_0528600														
PF3D7_1225600	PF3D7_0702900														
PF3D7_1227400	PF3D7_0704000														
PF3D7_1228200	PF3D7_0704500														
PF3D7_1229400	PF3D7_0705600														
PF3D7_1229500	PF3D7_0706300														
PF3D7_1230300	PF3D7_0706600														
PF3D7_1230600	PF3D7_0707300														
PF3D7_1231600	PF3D7_0717200														
PF3D7_1231700	PF3D7_0728900														
PF3D7_1233000	PF3D7_0729200														
PF3D7_1233200	PF3D7_0802500														
PF3D7_1234500	PF3D7_0802600														
PF3D7_1235000	PF3D7_0806000														
PF3D7_1236300	PF3D7_0806300														
PF3D7_1236600	PF3D7_0806600														
PF3D7_1237100	PF3D7_0808000														
PF3D7_1237800	PF3D7_0810300														

University of Ghana http://ugspace.ug.edu.gh

PF3D7_1238100	PF3D7_0814100														
PF3D7_1238700	PF3D7_0815000														
PF3D7_1239100	PF3D7_0817100														
PF3D7_1239300	PF3D7_0817700														
PF3D7_1239600	PF3D7_0818000														
PF3D7_1239900	PF3D7_0818400														
PF3D7_1240400	PF3D7_0819300														
PF3D7_1242100	PF3D7_0819900														
PF3D7_1242900	PF3D7_0820100														
PF3D7_1243000	PF3D7_0822200														
PF3D7_1243200	PF3D7_0823100														
PF3D7_1243300	PF3D7_0824200														
PF3D7_1244700	PF3D7_0827500														
PF3D7_1245400	PF3D7_0906800														
PF3D7_1245900	PF3D7_0908000														
PF3D7_1247100	PF3D7_0908100														
PF3D7_1247200	PF3D7_0908500														
PF3D7_1248100	PF3D7_0914100														
PF3D7_1248300	PF3D7_0914300														
PF3D7_1249600	PF3D7_0921200														
PF3D7_1251100	PF3D7_0922800														
PF3D7_1252700	PF3D7_0923200														
PF3D7_1252900	PF3D7_0923800														
PF3D7_1253100	PF3D7_0925500														
PF3D7_1254400	PF3D7_0926200														
PF3D7_1254600	PF3D7_0929200														
PF3D7_1254700	PF3D7_0929400														
PF3D7_1400500	PF3D7_0929900														
PF3D7_1400800	PF3D7_0930200														
PF3D7_1401700	PF3D7_0931900														
PF3D7_1402300	PF3D7_0932000														
PF3D7_1403600	PF3D7_0932100														
PF3D7_1403900	PF3D7_1305300														
PF3D7_1404100	PF3D7_1306300														
PF3D7_1404300	PF3D7_1306900														
PF3D7_1404400	PF3D7_1308000														
PF3D7_1404500	PF3D7_1310200														
PF3D7_1404600	PF3D7_1312500														
PF3D7_1406700	PF3D7_1313800														
PF3D7_1408900	PF3D7_1315200														
PF3D7_1411000	PF3D7_1315400														
PF3D7_1411100	PF3D7_1315600														
PF3D7_1411400	PF3D7_1321100														
PF3D7_1411600	PF3D7_1325700														
PF3D7_1411900	PF3D7_1326800														

University of Ghana http://ugspace.ug.edu.gh

PF3D7_1415200	PF3D7_1327000														
PF3D7_1417100	PF3D7_1327500														
PF3D7_1417500	PF3D7_1334600														
PF3D7_1417900	PF3D7_1335300														
PF3D7_1419300	PF3D7_1344100														
PF3D7_1419800	PF3D7_1344300														
PF3D7_1420000	PF3D7_1345300														
PF3D7_1420300	PF3D7_1358900														
PF3D7_1420800	PF3D7_1359700														
PF3D7_1421500	PF3D7_1361500														
PF3D7_1422700	PF3D7_1361800														
PF3D7_1422800	PF3D7_1366100														
PF3D7_1423700	PF3D7_0313300														
PF3D7_1426400	PF3D7_0316300														
PF3D7_1427700	PF3D7_0317100														
PF3D7_1428600	PF3D7_0317900														
PF3D7_1428700	PF3D7_0321400														
PF3D7_1428800	PF3D7_0420600														
PF3D7_1429800	PF3D7_0608310														
PF3D7_1430600	PF3D7_0903600														
PF3D7_1430700	PF3D7_0905700														
PF3D7_1432100	PF3D7_1351800														
PF3D7_1432900	PF3D7_1371700														
PF3D7_1433600	PF3D7_0727600														
PF3D7_1434000	PF3D7_0803600														
PF3D7_1434100	PF3D7_0806700														
PF3D7_1434200	PF3D7_0818600														
PF3D7_1435700	PF3D7_0831600														
PF3D7_1436700	PF3D7_0200700														
PF3D7_1436900	PF3D7_0202100														
PF3D7_1437500	PF3D7_0202800														
PF3D7_1437700	PF3D7_0203300														
PF3D7_1437800	PF3D7_0204200														
PF3D7_1440000	PF3D7_0205200														
PF3D7_1440800	PF3D7_0205400														
PF3D7_1441800	PF3D7_0206000														
PF3D7_1441900	PF3D7_0206100														
PF3D7_1443100	PF3D7_0206200														
PF3D7_1444000	PF3D7_0206500														
PF3D7_1444400	PF3D7_0206700														
PF3D7_1444600	PF3D7_0206800														
PF3D7_1444700	PF3D7_0206900														
PF3D7_1445300	PF3D7_0207000														
PF3D7_1445400	PF3D7_0207100														
PF3D7_1445800	PF3D7_0207200														

University of Ghana http://ugspace.ug.edu.gh

PF3D7_1445900	PF3D7_0207400														
PF3D7_1446800	PF3D7_0207500														
PF3D7_1447100	PF3D7_0207600														
PF3D7_1447200	PF3D7_0207700														
PF3D7_1449800	PF3D7_0209700														
PF3D7_1450100	PF3D7_0210500														
PF3D7_1450200	PF3D7_0210600														
PF3D7_1450600	PF3D7_0211300														
PF3D7_1450800	PF3D7_0211500														
PF3D7_1450900	PF3D7_0212200														
PF3D7_1451900	PF3D7_0212300														
PF3D7_1452300	PF3D7_0212600														
PF3D7_1452700	PF3D7_0213700														
PF3D7_1453200	PF3D7_0213900														
PF3D7_1453300	PF3D7_0214500														
PF3D7_1454100	PF3D7_0214600														
PF3D7_1455400	PF3D7_0214700														
PF3D7_1456100	PF3D7_0214800														
PF3D7_1456900	PF3D7_0214900														
PF3D7_1458400	PF3D7_0215000														
PF3D7_1459700	PF3D7_0215600														
PF3D7_1460800	PF3D7_0216300														
PF3D7_1461200	PF3D7_0216600														
PF3D7_1462100	PF3D7_0217300														
PF3D7_1462200	PF3D7_0217500														
PF3D7_1463200	PF3D7_0217600														
PF3D7_1463800	PF3D7_0217700														
PF3D7_1464700	PF3D7_0218100														
PF3D7_1465000	PF3D7_0218300														
PF3D7_1466300	PF3D7_0219200														
PF3D7_1467700	PF3D7_0219400														
PF3D7_1467800	PF3D7_0219800														
PF3D7_1474800	PF3D7_0219900														
PF3D7_1475100	PF3D7_0220000														
PF3D7_1475200	PF3D7_0220500														
PF3D7_1475300	PF3D7_0220800														
PF3D7_1477200	PF3D7_0221000														
PF3D7_1477400	PF3D7_1002400														
PF3D7_1478100	PF3D7_1002500														
PF3D7_1478800	PF3D7_1002800														
PF3D7_1479600	PF3D7_1003000														
PF3D7_0102100	PF3D7_1003300														
PF3D7_0221100	PF3D7_1003400														
PF3D7_0221500	PF3D7_1003600														
PF3D7_0400200	PF3D7_1004700														

University of Ghana http://ugspace.ug.edu.gh

PF3D7_0402700	PF3D7_1005100														
PF3D7_0424300	PF3D7_1005800														
PF3D7_0425250	PF3D7_1006400														
PF3D7_0425300	PF3D7_1006500														
PF3D7_0500600	PF3D7_1007200														
PF3D7_0500700	PF3D7_1007300														
PF3D7_0532800	PF3D7_1009300														
PF3D7_0533000	PF3D7_1009500														
PF3D7_0601700	PF3D7_1009700														
PF3D7_1000700	PF3D7_1009800														
PF3D7_1000800	PF3D7_1010100														
PF3D7_1129850	PF3D7_1010200														
PF3D7_1219200	PF3D7_1010300														
PF3D7_1220200	PF3D7_1010900														
PF3D7_1253900	PF3D7_1011600														
PF3D7_1334900	PF3D7_1011800														
PF3D7_1372500	PF3D7_1011900														
PF3D7_1463100	PF3D7_1012100														
PF3D7_1477000	PF3D7_1012200														
PF3D7_1478200	PF3D7_1012500														
PF3D7_1478300	PF3D7_1012800														
PF3D7_1478500	PF3D7_1012900														
PF3D7_1478700	PF3D7_1013200														
	PF3D7_1013400														
	PF3D7_1013700														
	PF3D7_1013800														
	PF3D7_1014100														
	PF3D7_1014500														
	PF3D7_1014700														
	PF3D7_1015100														
	PF3D7_1015500														
	PF3D7_1016000														
	PF3D7_1016200														
	PF3D7_1016900														
	PF3D7_1017100														
	PF3D7_1017500														
	PF3D7_1018200														
	PF3D7_1018700														
	PF3D7_1019700														
	PF3D7_1019800														
	PF3D7_1019900														
	PF3D7_1020400														
	PF3D7_1020500														
	PF3D7_1020600														
	PF3D7_1021100														

University of Ghana http://ugspace.ug.edu.gh

	PF3D7_1021500														
	PF3D7_1021600														
	PF3D7_1021700														
	PF3D7_1022100														
	PF3D7_1022500														
	PF3D7_1022700														
	PF3D7_1023000														
	PF3D7_1023400														
	PF3D7_1023800														
	PF3D7_1024200														
	PF3D7_1025000														
	PF3D7_1025900														
	PF3D7_1026200														
	PF3D7_1026300														
	PF3D7_1026600														
	PF3D7_1026800														
	PF3D7_1027200														
	PF3D7_1027300														
	PF3D7_1028600														
	PF3D7_1028700														
	PF3D7_1028900														
	PF3D7_1029200														
	PF3D7_1029300														
	PF3D7_1029500														
	PF3D7_1029900														
	PF3D7_1030200														
	PF3D7_1030500														
	PF3D7_1030700														
	PF3D7_1031100														
	PF3D7_1031400														
	PF3D7_1031400														
	PF3D7_1031700														
	PF3D7_1031800														
	PF3D7_1033700														
	PF3D7_1033900														
	PF3D7_1034600														
	PF3D7_1035100														
	PF3D7_1035200														
	PF3D7_1035300														
	PF3D7_1035400														
	PF3D7_1035500														
	PF3D7_1035600														
	PF3D7_1035700														
	PF3D7_1035900														
	PF3D7_1036000														

University of Ghana http://ugspace.ug.edu.gh

	PF3D7_1036300														
	PF3D7_1036500														
	PF3D7_1037500														
	PF3D7_1038000														
	PF3D7_1038100														
	PF3D7_1102500														
	PF3D7_1103600														
	PF3D7_1104300														
	PF3D7_1104900														
	PF3D7_1105000														
	PF3D7_1105100														
	PF3D7_1105300														
	PF3D7_1106500														
	PF3D7_1106600														
	PF3D7_1107800														
	PF3D7_1108100														
	PF3D7_1108200														
	PF3D7_1108900														
	PF3D7_1110000														
	PF3D7_1110100														
	PF3D7_1110600														
	PF3D7_1111200														
	PF3D7_1111500														
	PF3D7_1111700														
	PF3D7_1112600														
	PF3D7_1113400														
	PF3D7_1113500														
	PF3D7_1114700														
	PF3D7_1115000														
	PF3D7_1116000														
	PF3D7_1116100														
	PF3D7_1116600														
	PF3D7_1117200														
	PF3D7_1117400														
	PF3D7_1118400														
	PF3D7_1118700														
	PF3D7_1119400														
	PF3D7_1120200														
	PF3D7_1120800														
	PF3D7_1121100														
	PF3D7_1121200														
	PF3D7_1121300														
	PF3D7_1122000														
	PF3D7_1122100														
	PF3D7_1122700														

University of Ghana http://ugspace.ug.edu.gh

	PF3D7_1123200														
	PF3D7_1123500														
	PF3D7_1124200														
	PF3D7_1124600														
	PF3D7_1124700														
	PF3D7_1125300														
	PF3D7_1125700														
	PF3D7_1125800														
	PF3D7_1125900														
	PF3D7_1126700														
	PF3D7_1127300														
	PF3D7_1127600														
	PF3D7_1128500														
	PF3D7_1128900														
	PF3D7_1129100														
	PF3D7_1129900														
	PF3D7_1130000														
	PF3D7_1130600														
	PF3D7_1130900														
	PF3D7_1133400														
	PF3D7_1135100														
	PF3D7_1135600														
	PF3D7_1136200														
	PF3D7_1136400														
	PF3D7_1136500														
	PF3D7_1136700														
	PF3D7_1136800														
	PF3D7_1136900														
	PF3D7_1137200														
	PF3D7_1137400														
	PF3D7_1137500														
	PF3D7_1138000														
	PF3D7_1138400														
	PF3D7_1138700														
	PF3D7_1140300														
	PF3D7_1140400														
	PF3D7_1141800														
	PF3D7_1142300														
	PF3D7_1143500														
	PF3D7_1144900														
	PF3D7_1145000														
	PF3D7_1145100														
	PF3D7_1145400														
	PF3D7_1145500														
	PF3D7_1146600														

University of Ghana http://ugspace.ug.edu.gh

	PF3D7_1147500														
	PF3D7_1149100														
	PF3D7_1201200														
	PF3D7_1201900														
	PF3D7_1202400														
	PF3D7_1202800														
	PF3D7_1202900														
	PF3D7_1203900														
	PF3D7_1204700														
	PF3D7_1204900														
	PF3D7_1205200														
	PF3D7_1206000														
	PF3D7_1206700														
	PF3D7_1207600														
	PF3D7_1208100														
	PF3D7_1209400														
	PF3D7_1209800														
	PF3D7_1210600														
	PF3D7_1211800														
	PF3D7_1211900														
	PF3D7_1212200														
	PF3D7_1212800														
	PF3D7_1213600														
	PF3D7_1213900														
	PF3D7_1214200														
	PF3D7_1217400														
	PF3D7_1217500														
	PF3D7_1217900														
	PF3D7_1218000														
	PF3D7_1218100														
	PF3D7_1218300														
	PF3D7_1221300														
	PF3D7_1221600														
	PF3D7_1222700														
	PF3D7_1223000														
	PF3D7_1223100														
	PF3D7_1224100														
	PF3D7_1226500														
	PF3D7_1226600														
	PF3D7_1227100														
	PF3D7_1227700														
	PF3D7_1228100														
	PF3D7_1228500														
	PF3D7_1228600														
	PF3D7_1229000														

University of Ghana http://ugspace.ug.edu.gh

	PF3D7_1229800														
	PF3D7_1230000														
	PF3D7_1230800														
	PF3D7_1230900														
	PF3D7_1231200														
	PF3D7_1231400														
	PF3D7_1231900														
	PF3D7_1232500														
	PF3D7_1233300														
	PF3D7_1233400														
	PF3D7_1234300														
	PF3D7_1234800														
	PF3D7_1235200														
	PF3D7_1235500														
	PF3D7_1237900														
	PF3D7_1238500														
	PF3D7_1238800														
	PF3D7_1238900														
	PF3D7_1239500														
	PF3D7_1240000														
	PF3D7_1241300														
	PF3D7_1241700														
	PF3D7_1242600														
	PF3D7_1243400														
	PF3D7_1243500														
	PF3D7_1243600														
	PF3D7_1243700														
	PF3D7_1243800														
	PF3D7_1244100														
	PF3D7_1244200														
	PF3D7_1244600														
	PF3D7_1244900														
	PF3D7_1245000														
	PF3D7_1245100														
	PF3D7_1245200														
	PF3D7_1245300														
	PF3D7_1246200														
	PF3D7_1246300														
	PF3D7_1246400														
	PF3D7_1246600														
	PF3D7_1246700														
	PF3D7_1247500														
	PF3D7_1247700														
	PF3D7_1249300														
	PF3D7_1250200														

University of Ghana http://ugspace.ug.edu.gh

	PF3D7_1250300														
	PF3D7_1250600														
	PF3D7_1251200														
	PF3D7_1251400														
	PF3D7_1251500														
	PF3D7_1251600														
	PF3D7_1251800														
	PF3D7_1252100														
	PF3D7_1252200														
	PF3D7_1255100														
	PF3D7_1401400														
	PF3D7_1401600														
	PF3D7_1401800														
	PF3D7_1402100														
	PF3D7_1404000														
	PF3D7_1404700														
	PF3D7_1405000														
	PF3D7_1405400														
	PF3D7_1405500														
	PF3D7_1405700														
	PF3D7_1406400														
	PF3D7_1406800														
	PF3D7_1407500														
	PF3D7_1409200														
	PF3D7_1409300														
	PF3D7_1409400														
	PF3D7_1409800														
	PF3D7_1410000														
	PF3D7_1410400														
	PF3D7_1410500														
	PF3D7_1410900														
	PF3D7_1411200														
	PF3D7_1411300														
	PF3D7_1411700														
	PF3D7_1412000														
	PF3D7_1412600														
	PF3D7_1412700														
	PF3D7_1413700														
	PF3D7_1413800														
	PF3D7_1413900														
	PF3D7_1414200														
	PF3D7_1414400														
	PF3D7_1414700														
	PF3D7_1415300														
	PF3D7_1416000														

University of Ghana http://ugspace.ug.edu.gh

	PF3D7_1417300														
	PF3D7_1418900														
	PF3D7_1419400														
	PF3D7_1420200														
	PF3D7_1420900														
	PF3D7_1421000														
	PF3D7_1421100														
	PF3D7_1421600														
	PF3D7_1422000														
	PF3D7_1422100														
	PF3D7_1423100														
	PF3D7_1423300														
	PF3D7_1423500														
	PF3D7_1425300														
	PF3D7_1425400														
	PF3D7_1426700														
	PF3D7_1427800														
	PF3D7_1428100														
	PF3D7_1428200														
	PF3D7_1429000														
	PF3D7_1429400														
	PF3D7_1429500														
	PF3D7_1430000														
	PF3D7_1430200														
	PF3D7_1430300														
	PF3D7_1430900														
	PF3D7_1431400														
	PF3D7_1431800														
	PF3D7_1432600														
	PF3D7_1433000														
	PF3D7_1433100														
	PF3D7_1433500														
	PF3D7_1433700														
	PF3D7_1434400														
	PF3D7_1435300														
	PF3D7_1436200														
	PF3D7_1436400														
	PF3D7_1436500														
	PF3D7_1436600														
	PF3D7_1436800														
	PF3D7_1437100														
	PF3D7_1437300														
	PF3D7_1438400														
	PF3D7_1438600														
	PF3D7_1439200														

University of Ghana http://ugspace.ug.edu.gh

	PF3D7_1439500														
	PF3D7_1440100														
	PF3D7_1440300														
	PF3D7_1440900														
	PF3D7_1441400														
	PF3D7_1442700														
	PF3D7_1443300														
	PF3D7_1443500														
	PF3D7_1443600														
	PF3D7_1444200														
	PF3D7_1444800														
	PF3D7_1445200														
	PF3D7_1446600														
	PF3D7_1447300														
	PF3D7_1447800														
	PF3D7_1448000														
	PF3D7_1448800														
	PF3D7_1449200														
	PF3D7_1449600														
	PF3D7_1450300														
	PF3D7_1451400														
	PF3D7_1451500														
	PF3D7_1451700														
	PF3D7_1452000														
	PF3D7_1452500														
	PF3D7_1452900														
	PF3D7_1454000														
	PF3D7_1454200														
	PF3D7_1455100														
	PF3D7_1455200														
	PF3D7_1455300														
	PF3D7_1455600														
	PF3D7_1456200														
	PF3D7_1456300														
	PF3D7_1456600														
	PF3D7_1457500														
	PF3D7_1457600														
	PF3D7_1458600														
	PF3D7_1459100														
	PF3D7_1460600														
	PF3D7_1461000														
	PF3D7_1461400														
	PF3D7_1462900														
	PF3D7_1463400														
	PF3D7_1463500														

University of Ghana http://ugspace.ug.edu.gh

	PF3D7_1463600														
	PF3D7_1463900														
	PF3D7_1464100														
	PF3D7_1464600														
	PF3D7_1465300														
	PF3D7_1465400														
	PF3D7_1467100														
	PF3D7_1467200														
	PF3D7_1468400														
	PF3D7_1468900														
	PF3D7_1469200														
	PF3D7_1469400														
	PF3D7_1469500														
	PF3D7_1470100														
	PF3D7_1470300														
	PF3D7_1470400														
	PF3D7_1470600														
	PF3D7_1470700														
	PF3D7_1471400														
	PF3D7_1471900														
	PF3D7_1472000														
	PF3D7_1472300														
	PF3D7_1472400														
	PF3D7_1472600														
	PF3D7_1472800														
	PF3D7_1473300														
	PF3D7_1473400														
	PF3D7_1474900														
	PF3D7_1475800														
	PF3D7_1476300														
	PF3D7_1477300														
	PF3D7_1480000														
	PF3D7_0114900														
	PF3D7_0222900														
	PF3D7_0402200														
	PF3D7_0506600														
	PF3D7_0800750														
	PF3D7_1230200														
	PF3D7_1252400														
	PF3D7_1301300														
	PF3D7_1335200														
	PF3D7_1353000														
	PF3D7_1364700														
	PF3D7_1371600														

Supplementary Table 5.3 Gene ontology tabular summary of module 0

University of Ghana http://ugspace.ug.edu.gh

ID	Name	Bgd count	Result count	Result gene list	Pct of bgd	Fold enrichment	Odds ratio	P-value	Benjamini
GO:0043628	ncRNA 3'-end processing	17	7	PF3D7_0206600,PF3D7_0209200,PF3D7_1120500,PF3D7_1144000,PF3D7_1227400,PF3D7_1364500,PF3D7_1417500,	41.2	3.32	4.99	0.0027669 4	0.47482113 9
GO:0016192	vesicle-mediated transport	140	29	PF3D7_0210700,PF3D7_0216400,PF3D7_0314100,PF3D7_0710800,PF3D7_0727000,PF3D7_0804900,PF3D7_0816200,PF3D7_0820500,PF3D7_0822600,PF3D7_0826600,PF3D7_0905900,PF3D7_0910600,PF3D7_1034000,PF3D7_1107200,PF3D7_1111300,PF3D7_1119500,PF3D7_1119900,PF3D7_1239900,PF3D7_1243000,PF3D7_1303200,PF3D7_1309700,PF3D7_1314500,PF3D7_1335700,PF3D7_1359800,PF3D7_1406700,PF3D7_1422800,PF3D7_1429800,PF3D7_1437800,PF3D7_1441800,	20.7	1.67	1.89	0.0032711 4	0.47482113 9
GO:0000375	RNA splicing, via transesterification reactions	104	23	PF3D7_0218500,PF3D7_0308900,PF3D7_0821300,PF3D7_0909800,PF3D7_0924700,PF3D7_1018600,PF3D7_1030000,PF3D7_1030100,PF3D7_1033600,PF3D7_1125500,PF3D7_1126900,PF3D7_1209200,PF3D7_1231600,PF3D7_1237800,PF3D7_1316500,PF3D7_1321700,PF3D7_1325000,PF3D7_1343900,PF3D7_1348200,PF3D7_1350200,PF3D7_1420000,PF3D7_1452700,PF3D7_1475200,	22.1	1.78	2.04	0.0036012 9	0.47482113 9
GO:0006887	exocytosis	10	5	PF3D7_0210700,PF3D7_0216400,PF3D7_1034000,PF3D7_1309700,PF3D7_1422800,	50	4.03	7.11	0.0042649 2	0.47482113 9
GO:0000377	RNA splicing, via transesterification reactions with bulged adenosine as nucleophile	100	22	PF3D7_0218500,PF3D7_0308900,PF3D7_0821300,PF3D7_0909800,PF3D7_0924700,PF3D7_1018600,PF3D7_1030000,PF3D7_1030100,PF3D7_1033600,PF3D7_1125500,PF3D7_1126900,PF3D7_1209200,PF3D7_1231600,PF3D7_1237800,PF3D7_1316500,PF3D7_1325000,PF3D7_1343900,PF3D7_1348200,PF3D7_1350200,PF3D7_1420000,PF3D7_1452700,PF3D7_1475200,	22	1.77	2.03	0.0046649 9	0.47482113 9
GO:0000398	mRNA splicing, via spliceosome	100	22	PF3D7_0218500,PF3D7_0308900,PF3D7_0821300,PF3D7_0909800,PF3D7_0924700,PF3D7_1018600,PF3D7_1030000,PF3D7_1030100,PF3D7_1033600,PF3D7_1125500,PF3D7_1126900,PF3D7_1209200,PF3D7_1231600,PF3D7_1237800,PF3D7_1316500,PF3D7_1325000,PF3D7_1343900,PF3D7_1348200,PF3D7_1350200,PF3D7_1420000,PF3D7_1452700,PF3D7_1475200,	22	1.77	2.03	0.0046649 9	0.47482113 9
GO:0006397	mRNA processing	145	29	PF3D7_0205500,PF3D7_0218500,PF3D7_0308900,PF3D7_0311100,PF3D7_0318600,PF3D7_0322100,PF3D7_0821300,PF3D7_0909800,PF3D7_0924700,PF3D7_1018600,PF3D7_1030000,PF3D7_1030100,PF3D7_1033600,PF3D7_1125500,PF3D7_1126900,PF3D7_1209200,PF3D7_1227400,PF3D7_1231600,PF3D7_1237800,PF3D7_1316500,PF3D7_1321700,PF3D7_1325000,PF3D7_1340600,PF3D7_1343900,PF3D7_1348200,PF3D7_1350200,PF3D7_1420000,PF3D7_1452700,PF3D7_1475200,	20	1.61	1.8	0.0055461 7	0.47482113 9
GO:0006767	water-soluble vitamin metabolic process	15	6	PF3D7_0514600,PF3D7_0616000,PF3D7_0627500,PF3D7_1116200,PF3D7_1239600,PF3D7_1456100,	40	3.22	4.74	0.0066226 9	0.47482113 9
GO:0006766	vitamin metabolic process	15	6	PF3D7_0514600,PF3D7_0616000,PF3D7_0627500,PF3D7_1116200,PF3D7_1239600,PF3D7_1456100,	40	3.22	4.74	0.0066226 9	0.47482113 9
GO:2000582	obsolete positive regulation of microtubule motor activity, plus-end-directed	4	3	PF3D7_0204400,PF3D7_0729800,PF3D7_1357300,	75	6.04	21.28	0.0069024 1	0.47482113 9
GO:0042819	vitamin B6 biosynthetic process	4	3	PF3D7_0514600,PF3D7_0616000,PF3D7_1116200,	75	6.04	21.28	0.0069024 1	0.47482113 9
GO:0042816	vitamin B6 metabolic process	4	3	PF3D7_0514600,PF3D7_0616000,PF3D7_1116200,	75	6.04	21.28	0.0069024 1	0.47482113 9
GO:0009249	protein lipoylation	4	3	PF3D7_0923600,PF3D7_1314600,PF3D7_1344600,	75	6.04	21.28	0.0069024 1	0.47482113 9
GO:0008614	pyridoxine metabolic process	4	3	PF3D7_0514600,PF3D7_0616000,PF3D7_1116200,	75	6.04	21.28	0.0069024 1	0.47482113 9
GO:1901617	organic hydroxy compound biosynthetic process	20	7	PF3D7_0511800,PF3D7_0514600,PF3D7_0616000,PF3D7_0627500,PF3D7_0628000,PF3D7_1116200,PF3D7_1239600,	35	2.82	3.83	0.0079027	0.47482113 9
GO:0006383	transcription by RNA polymerase III	12	5	PF3D7_0206600,PF3D7_0609900,PF3D7_0708100,PF3D7_1104700,PF3D7_1460800,	41.7	3.36	5.08	0.010838	0.47482113 9
GO:0016071	mRNA metabolic process	185	34	PF3D7_0204600,PF3D7_0205500,PF3D7_0209200,PF3D7_0218500,PF3D7_0308900,PF3D7_0311100,PF3D7_0318600,PF3D7_0322100,PF3D7_0821300,PF3D7_0908700,PF3D7_0909800,PF3D7_0924700,PF3D7_1018600,PF3D7_1030000,PF3D7_1030100,PF3D7_1033600,PF3D7_1125500,PF3D7_1126900,PF3D7_1209200,PF3D7_1227400,PF3D7_1231600,PF3D7_1237800,PF3D7_1316500,PF3D7_1321700,PF3D7_1325000,PF3D7_1340600,PF3D7_1343900,PF3D7_1348200,PF3D7_1350200,PF3D7_1364500,PF3D7_1417500,PF3D7_1420000,PF3D7_1452700,PF3D7_1475200,	18.4	1.48	1.62	0.0108576 9	0.47482113 9

GO:0072524	pyridine-containing compound metabolic process	8	4	PF3D7_0514600,PF3D7_0616000,PF3D7_1116200,PF3D7_1143900,	50	4.03	7.1	0.0108854	0.47482113 9
GO:0008033	tRNA processing	65	15	PF3D7_0206600,PF3D7_0908700,PF3D7_0918800,PF3D7_1018600,PF3D7_1119100,PF3D7_1120500,PF3D7_1138100,PF3D7_1206400,PF3D7_1217800,PF3D7_1222000,PF3D7_1248100,PF3D7_1349400,PF3D7_1408900,PF3D7_1434100,PF3D7_1454100,	23.1	1.86	2.15	0.0115707 7	0.47482113 9
GO:0031123	RNA 3'-end processing	32	9	PF3D7_0205500,PF3D7_0206600,PF3D7_0209200,PF3D7_0318600,PF3D7_1120500,PF3D7_1144000,PF3D7_1227400,PF3D7_1364500,PF3D7_1417500,	28.1	2.27	2.79	0.0131510 8	0.47482113 9
GO:1901607	alpha-amino acid biosynthetic process	17	6	PF3D7_0922600,PF3D7_1327800,PF3D7_1357900,PF3D7_1363700,PF3D7_1430700,PF3D7_1456100,	35.3	2.84	3.88	0.0131794	0.47482113 9
GO:0016197	endosomal transport	22	7	PF3D7_0314100,PF3D7_0727000,PF3D7_0816200,PF3D7_1111300,PF3D7_1239900,PF3D7_1406700,PF3D7_1441800,	31.8	2.56	3.32	0.0139405 2	0.47482113 9
GO:1901605	alpha-amino acid metabolic process	38	10	PF3D7_0922600,PF3D7_1116200,PF3D7_1206400,PF3D7_1308200,PF3D7_1327800,PF3D7_1344000,PF3D7_1357900,PF3D7_1363700,PF3D7_1430700,PF3D7_1456100,	26.3	2.12	2.55	0.0148406 1	0.47482113 9
GO:0000162	tryptophan biosynthetic process	2	2	PF3D7_1327800,PF3D7_1363700,	100	8.06	inf	0.0153724 2	0.47482113 9
GO:0072321	obsolete chaperone-mediated protein transport	2	2	PF3D7_1242900,PF3D7_1421500,	100	8.06	inf	0.0153724 2	0.47482113 9
GO:0042430	indole-containing compound metabolic process	2	2	PF3D7_1327800,PF3D7_1363700,	100	8.06	inf	0.0153724 2	0.47482113 9
GO:0046219	indolalkylamine biosynthetic process	2	2	PF3D7_1327800,PF3D7_1363700,	100	8.06	inf	0.0153724 2	0.47482113 9
GO:0006568	tryptophan metabolic process	2	2	PF3D7_1327800,PF3D7_1363700,	100	8.06	inf	0.0153724 2	0.47482113 9
GO:0006586	indolalkylamine metabolic process	2	2	PF3D7_1327800,PF3D7_1363700,	100	8.06	inf	0.0153724 2	0.47482113 9
GO:0042435	indole-containing compound biosynthetic process	2	2	PF3D7_1327800,PF3D7_1363700,	100	8.06	inf	0.0153724 2	0.47482113 9
GO:0046184	aldehyde biosynthetic process	5	3	PF3D7_0318800,PF3D7_0616000,PF3D7_1116200,	60	4.84	10.64	0.0156678 6	0.47482113 9
GO:0006081	cellular aldehyde metabolic process	13	5	PF3D7_0318800,PF3D7_0604700,PF3D7_0616000,PF3D7_0627500,PF3D7_1116200,	38.5	3.1	4.44	0.0158461	0.47482113 9
GO:0042364	water-soluble vitamin biosynthetic process	13	5	PF3D7_0514600,PF3D7_0616000,PF3D7_0627500,PF3D7_1116200,PF3D7_1239600,	38.5	3.1	4.44	0.0158461	0.47482113 9
GO:0000387	spliceosomal snRNP assembly	13	5	PF3D7_0218500,PF3D7_0909800,PF3D7_1125500,PF3D7_1126900,PF3D7_1350200,	38.5	3.1	4.44	0.0158461	0.47482113 9
GO:0009110	vitamin biosynthetic process	13	5	PF3D7_0514600,PF3D7_0616000,PF3D7_0627500,PF3D7_1116200,PF3D7_1239600,	38.5	3.1	4.44	0.0158461	0.47482113 9
GO:1901615	organic hydroxy compound metabolic process	33	9	PF3D7_0318800,PF3D7_0511800,PF3D7_0514600,PF3D7_0604700,PF3D7_0616000,PF3D7_0627500,PF3D7_0628000,PF3D7_1116200,PF3D7_1239600,	27.3	2.2	2.67	0.0161527 4	0.47482113 9
GO:0044283	small molecule biosynthetic process	92	19	PF3D7_0208500,PF3D7_0318800,PF3D7_0511800,PF3D7_0514600,PF3D7_0616000,PF3D7_0626300,PF3D7_0627500,PF3D7_0628000,PF3D7_0724300,PF3D7_0922600,PF3D7_1116200,PF3D7_1239600,PF3D7_1327800,PF3D7_1344600,PF3D7_1357900,PF3D7_1363700,PF3D7_1430700,PF3D7_1456100,PF3D7_1458400,	20.7	1.66	1.86	0.0161771 5	0.47482113 9

University of Ghana http://ugspace.ug.edu.gh

GO:0008652	cellular amino acid biosynthetic process	18	6	PF3D7_0922600,PF3D7_1327800,PF3D7_1357900,PF3D7_1363700,PF3D7_1430700,PF3D7_1456100,	33.3	2.69	3.56	0.0177438 4	0.5071003 24
GO:0016050	vesicle organization	29	8	PF3D7_0210700,PF3D7_0314100,PF3D7_0804900,PF3D7_0822600,PF3D7_1111300,PF3D7_1243000,PF3D7_1309700,PF3D7_1441800,	27.6	2.22	2.71	0.0213403	0.5942451 94
GO:0008380	RNA splicing	129	24	PF3D7_0218500,PF3D7_0308900,PF3D7_0821300,PF3D7_0909800,PF3D7_0924700,PF3D7_1018600,PF3D7_1030000,PF3D7_1030100,PF3D7_1033600,PF3D7_1125500,PF3D7_1126900,PF3D7_1209200,PF3D7_1231600,PF3D7_1237800,PF3D7_1316500,PF3D7_1321700,PF3D7_1325000,PF3D7_1343900,PF3D7_1348200,PF3D7_1350200,PF3D7_1420000,PF3D7_1452700,PF3D7_1454100,PF3D7_1475200,	18.6	1.5	1.64	0.0257326 7	0.6202828 54
GO:0009084	glutamine family amino acid biosynthetic process	6	3	PF3D7_0922600,PF3D7_1357900,PF3D7_1430700,	50	4.03	7.09	0.0284714 6	0.6202828 54
GO:0006904	vesicle docking involved in exocytosis	6	3	PF3D7_0216400,PF3D7_1034000,PF3D7_1309700,	50	4.03	7.09	0.0284714 6	0.6202828 54
GO:0140029	exocytic process	6	3	PF3D7_0216400,PF3D7_1034000,PF3D7_1309700,	50	4.03	7.09	0.0284714 6	0.6202828 54
GO:0048278	vesicle docking	15	5	PF3D7_0210700,PF3D7_0216400,PF3D7_1034000,PF3D7_1243000,PF3D7_1309700,	33.3	2.69	3.55	0.0299699 2	0.6202828 54
GO:0032259	methylation	37	9	PF3D7_0407100,PF3D7_0422900,PF3D7_0724300,PF3D7_1018600,PF3D7_1248100,PF3D7_1303100,PF3D7_1344000,PF3D7_1450600,PF3D7_1456100,	24.3	1.96	2.29	0.0332470 7	0.6202828 54
GO:0006366	transcription by RNA polymerase II	32	8	PF3D7_0205500,PF3D7_0303300,PF3D7_0506200,PF3D7_0708100,PF3D7_0716400,PF3D7_1304900,PF3D7_1441900,PF3D7_1460800,	25	2.01	2.37	0.0375068 6	0.6202828 54
GO:0006396	RNA processing	360	56	PF3D7_0205500,PF3D7_0206600,PF3D7_0209200,PF3D7_0218500,PF3D7_0308900,PF3D7_0311100,PF3D7_0318600,PF3D7_0322100,PF3D7_0720000,PF3D7_0821300,PF3D7_0908700,PF3D7_0909800,PF3D7_0918800,PF3D7_0921800,PF3D7_0924700,PF3D7_1003200,PF3D7_1018600,PF3D7_1030000,PF3D7_1030100,PF3D7_1033600,PF3D7_1119100,PF3D7_1120500,PF3D7_1125500,PF3D7_1126900,PF3D7_1138100,PF3D7_1144000,PF3D7_1206400,PF3D7_1209200,PF3D7_1217800,PF3D7_1220500,PF3D7_1222000,PF3D7_1227400,PF3D7_1230600,PF3D7_1231600,PF3D7_1237800,PF3D7_1248100,PF3D7_1316500,PF3D7_1321700,PF3D7_1325000,PF3D7_1340600,PF3D7_1343900,PF3D7_1348200,PF3D7_1349400,PF3D7_1350200,PF3D7_1364500,PF3D7_1404500,PF3D7_1408900,PF3D7_1417500,PF3D7_1420000,PF3D7_1434100,PF3D7_1450800,PF3D7_1451900,PF3D7_1452700,PF3D7_1454100,PF3D7_1461200,PF3D7_1475200,	15.6	1.25	1.33	0.0388195 9	0.6202828 54
GO:0022406	membrane docking	16	5	PF3D7_0210700,PF3D7_0216400,PF3D7_1034000,PF3D7_1243000,PF3D7_1309700,	31.3	2.52	3.23	0.0392724 2	0.6202828 54
GO:0140056	organelle localization by membrane tethering	16	5	PF3D7_0210700,PF3D7_0216400,PF3D7_1034000,PF3D7_1243000,PF3D7_1309700,	31.3	2.52	3.23	0.0392724 2	0.6202828 54
GO:0006891	intra-Golgi vesicle-mediated transport	16	5	PF3D7_0314100,PF3D7_0905900,PF3D7_1111300,PF3D7_1335700,PF3D7_1429800,	31.3	2.52	3.23	0.0392724 2	0.6202828 54
GO:0016482	cytosolic transport	16	5	PF3D7_0314100,PF3D7_0727000,PF3D7_1111300,PF3D7_1119500,PF3D7_1406700,	31.3	2.52	3.23	0.0392724 2	0.6202828 54
GO:0016053	organic acid biosynthetic process	50	11	PF3D7_0208500,PF3D7_0626300,PF3D7_0627500,PF3D7_0922600,PF3D7_1327800,PF3D7_1344600,PF3D7_1357900,PF3D7_1363700,PF3D7_1430700,PF3D7_1456100,PF3D7_1458400,	22	1.77	2.01	0.0393478	0.6202828 54
GO:0070084	protein initiator methionine removal	3	2	PF3D7_0527300,PF3D7_1015300,	66.7	5.37	14.16	0.0423136 5	0.6202828 54
GO:0050821	protein stabilization	3	2	PF3D7_0933200,PF3D7_1420300,	66.7	5.37	14.16	0.0423136 5	0.6202828 54
GO:0035542	regulation of SNARE complex assembly	3	2	PF3D7_1239900,PF3D7_1309700,	66.7	5.37	14.16	0.0423136 5	0.6202828 54

University of Ghana http://ugspace.ug.edu.gh

University of Ghana http://ugspace.ug.edu.gh

GO:0042823	pyridoxal phosphate biosynthetic process	3	2	PF3D7_0616000,PF3D7_1116200,	66.7	5.37	14.16	0.0423135	0.6202828 54
GO:0042822	pyridoxal phosphate metabolic process	3	2	PF3D7_0616000,PF3D7_1116200,	66.7	5.37	14.16	0.0423135	0.6202828 54
GO:0000390	spliceosomal complex disassembly	3	2	PF3D7_1030100,PF3D7_1475200,	66.7	5.37	14.16	0.0423135	0.6202828 54
GO:0006807	nitrogen compound metabolic process	3	2	PF3D7_0922600,PF3D7_1308200,	66.7	5.37	14.16	0.0423135	0.6202828 54
GO:0006616	SRP-dependent cotranslational protein targeting to membrane, translocation	3	2	PF3D7_0821800,PF3D7_1450100,	66.7	5.37	14.16	0.0423135	0.6202828 54
GO:0032988	ribonucleoprotein complex disassembly	3	2	PF3D7_1030100,PF3D7_1475200,	66.7	5.37	14.16	0.0423135	0.6202828 54
GO:0031647	regulation of protein stability	3	2	PF3D7_0933200,PF3D7_1420300,	66.7	5.37	14.16	0.0423135	0.6202828 54
GO:0000304	response to singlet oxygen	3	2	PF3D7_0616000,PF3D7_1116200,	66.7	5.37	14.16	0.0423135	0.6202828 54
GO:0009154	purine ribonucleotide catabolic process	3	2	PF3D7_1209500,PF3D7_1329400,	66.7	5.37	14.16	0.0423135	0.6202828 54
GO:0009261	ribonucleotide catabolic process	3	2	PF3D7_1209500,PF3D7_1329400,	66.7	5.37	14.16	0.0423135	0.6202828 54
GO:0048193	Golgi vesicle transport	63	13	PF3D7_0314100,PF3D7_0710800,PF3D7_0804900,PF3D7_0820500,PF3D7_0822600,PF3D7_0905900,PF3D7_1034000,PF3D7_1111300,PF3D7_1119500,PF3D7_1314500,PF3D7_1335700,PF3D7_1429800,PF3D7_1437800,	20.6	1.66	1.85	0.0425581	0.6202828 54
GO:0072525	pyridine-containing compound biosynthetic process	7	3	PF3D7_0514600,PF3D7_0616000,PF3D7_1116200,	42.9	3.45	5.32	0.0453028 4	0.6202828 54
GO:1901292	nucleoside phosphate catabolic process	7	3	PF3D7_0720800,PF3D7_1209500,PF3D7_1329400,	42.9	3.45	5.32	0.0453028 4	0.6202828 54
GO:0006888	endoplasmic reticulum to Golgi vesicle-mediated transport	39	9	PF3D7_0314100,PF3D7_0820500,PF3D7_0822600,PF3D7_0905900,PF3D7_1034000,PF3D7_1111300,PF3D7_1314500,PF3D7_1429800,PF3D7_1437800,	23.1	1.86	2.13	0.0453037 1	0.6202828 54
GO:0055085	transmembrane transport	45	10	PF3D7_0302600,PF3D7_0603500,PF3D7_0609100,PF3D7_0721900,PF3D7_0908800,PF3D7_1004800,PF3D7_1132800,PF3D7_1368700,PF3D7_1432100,PF3D7_1440800,	22.2	1.79	2.03	0.0453525 7	0.6202828 54
GO:0006605	protein targeting	70	14	PF3D7_0215900,PF3D7_0314100,PF3D7_0524700,PF3D7_0821800,PF3D7_1111300,PF3D7_1119500,PF3D7_1121000,PF3D7_1208600,PF3D7_1221500,PF3D7_1242900,PF3D7_1420300,PF3D7_1421500,PF3D7_1433600,PF3D7_1450100,	20	1.61	1.78	0.0458054 8	0.6202828 54
GO:0006352	DNA-templated transcription, initiation	22	6	PF3D7_0205500,PF3D7_0506200,PF3D7_0716400,PF3D7_1104700,PF3D7_1428800,PF3D7_1441900,	27.3	2.2	2.66	0.0464479 3	0.6202828 54

Supplementary Table 5.4 Gene ontology tabular summary of module 1

University of Ghana http://ugspace.ug.edu.gh

ID	Name	Bgd count	Result count	Result gene list	Pct of bgd	Fold enrichment	Odds ratio	P-value	Benjamini	Bonferroni
GO:0052126	movement in host environment	120	68	PF3D7_0102500,PF3D7_0206200,PF3D7_0207500,PF3D7_0207600,PF3D7_0210600,PF3D7_0214900,PF3D7_0217500,PF3D7_0316000,PF3D7_0323400,PF3D7_0404400,PF3D7_0404700,PF3D7_0404900,PF3D7_0405200,PF3D7_0423400,PF3D7_0423500,PF3D7_0423800,PF3D7_0424100,PF3D7_0501600,PF3D7_0507500,PF3D7_0612700,PF3D7_0629300,PF3D7_0707300,PF3D7_0722200,PF3D7_0731500,PF3D7_0806300,PF3D7_0808200,PF3D7_0818600,PF3D7_0819200,PF3D7_0828800,PF3D7_0905400,PF3D7_0923300,PF3D7_0929400,PF3D7_0930300,PF3D7_0932200,PF3D7_0934800,PF3D7_1012200,PF3D7_1014100,PF3D7_1017100,PF3D7_1027300,PF3D7_1028700,PF3D7_1030200,PF3D7_1033700,PF3D7_1035400,PF3D7_1035500,PF3D7_1035700,PF3D7_1035900,PF3D7_1116000,PF3D7_1133400,PF3D7_1136700,PF3D7_1136900,PF3D7_1138400,PF3D7_1218000,PF3D7_1222700,PF3D7_1231400,PF3D7_1246200,PF3D7_1252100,PF3D7_1252200,PF3D7_1310700,PF3D7_1335100,PF3D7_1335300,PF3D7_1337700,PF3D7_1337800,PF3D7_1342600,PF3D7_1414400,PF3D7_1430200,PF3D7_1431400,PF3D7_1436600,PF3D7_1451700,	56.7	2.72	5.26	3.19E-18	4.05E-15	4.05E-15
GO:0044409	entry into host	103	61	PF3D7_0102500,PF3D7_0210600,PF3D7_0214900,PF3D7_0217500,PF3D7_0316000,PF3D7_0323400,PF3D7_0404400,PF3D7_0404700,PF3D7_0404900,PF3D7_0405200,PF3D7_0423400,PF3D7_0423500,PF3D7_0423800,PF3D7_0424100,PF3D7_0501600,PF3D7_0612700,PF3D7_0629300,PF3D7_0707300,PF3D7_0722200,PF3D7_0731500,PF3D7_0808200,PF3D7_0818600,PF3D7_0819200,PF3D7_0828800,PF3D7_0905400,PF3D7_0923300,PF3D7_0929400,PF3D7_0930300,PF3D7_0932200,PF3D7_0934800,PF3D7_1012200,PF3D7_1014100,PF3D7_1017100,PF3D7_1027300,PF3D7_1028700,PF3D7_1030200,PF3D7_1033700,PF3D7_1035400,PF3D7_1035500,PF3D7_1035700,PF3D7_1035900,PF3D7_1116000,PF3D7_1133400,PF3D7_1136700,PF3D7_1136900,PF3D7_1218000,PF3D7_1222700,PF3D7_1231400,PF3D7_1246200,PF3D7_1252100,PF3D7_1252200,PF3D7_1310700,PF3D7_1335100,PF3D7_1335300,PF3D7_1337700,PF3D7_1342600,PF3D7_1414400,PF3D7_1430200,PF3D7_1431400,PF3D7_1436600,PF3D7_1451700,	59.2	2.84	5.81	9.48E-18	6.02E-15	1.20E-14
GO:0035890	exit from host	29	16	PF3D7_0206200,PF3D7_0207500,PF3D7_0207600,PF3D7_0217500,PF3D7_0507500,PF3D7_0629300,PF3D7_0806300,PF3D7_0808200,PF3D7_0930300,PF3D7_1014100,PF3D7_1028700,PF3D7_1138400,PF3D7_1231400,PF3D7_1337800,PF3D7_1414400,PF3D7_1436600,	55.2	2.65	4.74	4.80E-05	0.02029993	0.06089817 8
GO:0035891	exit from host cell	28	15	PF3D7_0206200,PF3D7_0207500,PF3D7_0207600,PF3D7_0217500,PF3D7_0507500,PF3D7_0629300,PF3D7_0806300,PF3D7_0808200,PF3D7_0930300,PF3D7_1014100,PF3D7_1028700,PF3D7_1138400,PF3D7_1231400,PF3D7_1337800,PF3D7_1414400,	53.6	2.57	4.44	0.0001300 6	0.0412926 52	0.1651706 09
GO:0030048	actin filament-based movement	9	7	PF3D7_0503400,PF3D7_0503600,PF3D7_0613900,PF3D7_0932200,PF3D7_1229800,PF3D7_1342600,PF3D7_1361400,	77.8	3.73	13.39	0.0004041 9	0.0792962 35	0.5133186 86
GO:0030036	actin cytoskeleton organization	19	11	PF3D7_0105300,PF3D7_0503400,PF3D7_0503600,PF3D7_0613900,PF3D7_0716100,PF3D7_0932200,PF3D7_1229800,PF3D7_1251200,PF3D7_1342600,PF3D7_1361400,PF3D7_1444800,	57.9	2.78	5.27	0.0004370 7	0.0792962 35	0.5550736 43
GO:0030029	actin filament-based process	19	11	PF3D7_0105300,PF3D7_0503400,PF3D7_0503600,PF3D7_0613900,PF3D7_0716100,PF3D7_0932200,PF3D7_1229800,PF3D7_1251200,PF3D7_1342600,PF3D7_1361400,PF3D7_1444800,	57.9	2.78	5.27	0.0004370 7	0.0792962 35	0.5550736 43
GO:0007015	actin filament organization	16	9	PF3D7_0105300,PF3D7_0503400,PF3D7_0503600,PF3D7_0613900,PF3D7_1229800,PF3D7_1251200,PF3D7_1342600,PF3D7_1361400,PF3D7_1444800,	56.3	2.7	4.92	0.0019628 8	0.2935474 78	1
GO:0097435	supramolecular fiber organization	28	13	PF3D7_0105300,PF3D7_0407900,PF3D7_0503400,PF3D7_0503600,PF3D7_0613900,PF3D7_0903700,PF3D7_1126700,PF3D7_1229800,PF3D7_1251200,PF3D7_1342600,PF3D7_1361400,PF3D7_1443600,PF3D7_1444800,	46.4	2.23	3.32	0.0020802 6	0.2935474 78	1
GO:0000209	protein polyubiquitination	22	10	PF3D7_0303800,PF3D7_0707700,PF3D7_0812600,PF3D7_1033900,PF3D7_1119400,PF3D7_1203900,PF3D7_1211800,PF3D7_1243700,PF3D7_1245300,PF3D7_1356300,	45.5	2.18	3.19	0.0081412 3	0.8808546 7	1
GO:0018209	peptidyl-serine modification	19	9	PF3D7_0217500,PF3D7_0717500,PF3D7_0934800,PF3D7_1003300,PF3D7_1104900,PF3D7_1114700,PF3D7_1136500,PF3D7_1238900,PF3D7_1436600,	47.4	2.27	3.44	0.0086585 4	0.8808546 7	1
GO:0070252	actin-mediated cell contraction	3	3	PF3D7_0503400,PF3D7_0932200,PF3D7_1361400,	100	4.8	inf	0.0090166 2	0.8808546 7	1
GO:0060327	cytoplasmic actin-based contraction involved in cell motility	3	3	PF3D7_0503400,PF3D7_0932200,PF3D7_1361400,	100	4.8	inf	0.0090166 2	0.8808546 7	1
GO:0007010	cytoskeleton organization	73	24	PF3D7_0105300,PF3D7_0111000,PF3D7_0407900,PF3D7_0503400,PF3D7_0503600,PF3D7_0607600,PF3D7_0613900,PF3D7_0630500,PF3D7_0716100,PF3D7_0717500,PF3D7_0724800,PF3D7_0903700,PF3D7_0932200,PF3D7_1009700,PF3D7_1126700,PF3D7_1229800,PF3D7_1246200,PF3D7_1251200,PF3D7_1342600,PF3D7_1361400,PF3D7_1443600,PF3D7_1444800,PF3D7_1446600,PF3D7_1470100,	32.9	1.58	1.88	0.0105459 3	0.8960667 75	1
GO:0006470	protein dephosphorylation	26	11	PF3D7_0802800,PF3D7_0810300,PF3D7_1031700,PF3D7_1135100,PF3D7_1249300,PF3D7_1309200,PF3D7_1414400,PF3D7_1423300,PF3D7_1451700,PF3D7_1455100,PF3D7_1464600,	42.3	2.03	2.81	0.0106089 3	0.8960667 75	1

GO:0051205	protein insertion into membrane	11	6	PF3D7_0323400,PF3D7_0424100,PF3D7_0608310,PF3D7_1353700,PF3D7_1368600,PF3D7_1438600,	54.5	2.62	4.58	0.014159	0.89606677 5	1
GO:0006897	endocytosis	21	9	PF3D7_0104300,PF3D7_0217300,PF3D7_0304200,PF3D7_0617100,PF3D7_1025000,PF3D7_1136500,PF3D7_1218300,PF3D7_1246300,PF3D7_1411300,	42.9	2.06	2.87	0.0184713	0.89606677 5	1
GO:0030050	vesicle transport along actin filament	6	4	PF3D7_0503600,PF3D7_0613900,PF3D7_1229800,PF3D7_1342600,	66.7	3.2	7.63	0.0195756 3	0.89606677 5	1
GO:0099515	actin filament-based transport	6	4	PF3D7_0503600,PF3D7_0613900,PF3D7_1229800,PF3D7_1342600,	66.7	3.2	7.63	0.0195756 3	0.89606677 5	1
GO:0008154	actin polymerization or depolymerization	6	4	PF3D7_0105300,PF3D7_0503400,PF3D7_1361400,PF3D7_1444800,	66.7	3.2	7.63	0.0195756 3	0.89606677 5	1
GO:0018105	peptidyl-serine phosphorylation	18	8	PF3D7_0217500,PF3D7_0717500,PF3D7_0934800,PF3D7_1104900,PF3D7_1114700,PF3D7_1136500,PF3D7_1238900,PF3D7_1436600,	44.4	2.13	3.06	0.0204557 3	0.89606677 5	1
GO:0061024	membrane organization	58	19	PF3D7_0323400,PF3D7_0424100,PF3D7_0505000,PF3D7_0530100,PF3D7_0608310,PF3D7_0731100,PF3D7_0806300,PF3D7_0808300,PF3D7_1022700,PF3D7_1138400,PF3D7_1243500,PF3D7_1244600,PF3D7_1326800,PF3D7_1332000,PF3D7_1353700,PF3D7_1368600,PF3D7_1438600,PF3D7_1452500,PF3D7_1455600,	32.8	1.57	1.87	0.0223514 3	0.89606677 5	1
GO:0051650	establishment of vesicle localization	9	5	PF3D7_0503600,PF3D7_0613900,PF3D7_1229800,PF3D7_1244600,PF3D7_1342600,	55.6	2.67	4.77	0.0231141 8	0.89606677 5	1
GO:0051648	vesicle localization	9	5	PF3D7_0503600,PF3D7_0613900,PF3D7_1229800,PF3D7_1244600,PF3D7_1342600,	55.6	2.67	4.77	0.0231141 8	0.89606677 5	1
GO:0007009	plasma membrane organization	4	3	PF3D7_0806300,PF3D7_1022700,PF3D7_1455600,	75	3.6	11.43	0.0304452 3	0.89606677 5	1
GO:0072583	clathrin-dependent endocytosis	4	3	PF3D7_0217300,PF3D7_0617100,PF3D7_1411300,	75	3.6	11.43	0.0304452 3	0.89606677 5	1
GO:0033962	P-body assembly	4	3	PF3D7_0320800,PF3D7_0819900,PF3D7_1474900,	75	3.6	11.43	0.0304452 3	0.89606677 5	1
GO:0080009	mRNA methylation	4	3	PF3D7_0105600,PF3D7_1230800,PF3D7_1235500,	75	3.6	11.43	0.0304452 3	0.89606677 5	1
GO:0006282	regulation of DNA repair	4	3	PF3D7_0216300,PF3D7_0407900,PF3D7_1112600,	75	3.6	11.43	0.0304452 3	0.89606677 5	1
GO:0051261	protein depolymerization	4	3	PF3D7_0503400,PF3D7_1361400,PF3D7_1411300,	75	3.6	11.43	0.0304452 3	0.89606677 5	1
GO:0016567	protein ubiquitination	49	16	PF3D7_0209700,PF3D7_0303800,PF3D7_0315800,PF3D7_0316900,PF3D7_0501700,PF3D7_0624500,PF3D7_0707700,PF3D7_0812600,PF3D7_1033900,PF3D7_1119400,PF3D7_1203900,PF3D7_1211800,PF3D7_1221600,PF3D7_1243700,PF3D7_1245300,PF3D7_1356300,	32.7	1.57	1.86	0.0354236 7	0.89606677 5	1
GO:0030154	cell differentiation	7	4	PF3D7_0507600,PF3D7_0717500,PF3D7_0818600,PF3D7_0934800,	57.1	2.74	5.08	0.0382147 9	0.89606677 5	1
GO:0006698	receptor-mediated endocytosis	7	4	PF3D7_0217300,PF3D7_0617100,PF3D7_1246300,PF3D7_1411300,	57.1	2.74	5.08	0.0382147 9	0.89606677 5	1
GO:0099518	vesicle cytoskeletal trafficking	7	4	PF3D7_0503600,PF3D7_0613900,PF3D7_1229800,PF3D7_1342600,	57.1	2.74	5.08	0.0382147 9	0.89606677 5	1
GO:0030705	cytoskeleton-dependent intracellular transport	10	5	PF3D7_0503600,PF3D7_0613900,PF3D7_1126700,PF3D7_1229800,PF3D7_1342600,	50	2.4	3.81	0.0384326	0.89606677 5	1

University of Ghana http://ugspace.ug.edu.gh

GO:0036211	protein modification process	375	92	PF3D7_0104300,PF3D7_0209700,PF3D7_0214600,PF3D7_0217500,PF3D7_0219400,PF3D7_0303800,PF3D7_0315800,PF3D7_0316900,PF3D7_0321400,PF3D7_0500900,PF3D7_0501700,PF3D7_0516700,PF3D7_0520700,PF3D7_0527200,PF3D7_0528400,PF3D7_0615500,PF3D7_0624500,PF3D7_0704500,PF3D7_0707700,PF3D7_0708300,PF3D7_0717500,PF3D7_0724600,PF3D7_0802800,PF3D7_0803000,PF3D7_0810300,PF3D7_0811500,PF3D7_0812600,PF3D7_0823600,PF3D7_0902100,PF3D7_0916600,PF3D7_0919200,PF3D7_0928800,PF3D7_0930600,PF3D7_0932500,PF3D7_0934800,PF3D7_0935300,PF3D7_1003300,PF3D7_1009700,PF3D7_1012900,PF3D7_1031400,PF3D7_1031700,PF3D7_1033900,PF3D7_1038100,PF3D7_1103600,PF3D7_1104900,PF3D7_1114700,PF3D7_1116600,PF3D7_1119400,PF3D7_1121300,PF3D7_1122100,PF3D7_1135100,PF3D7_1136500,PF3D7_1147500,PF3D7_1202400,PF3D7_1203900,PF3D7_1211800,PF3D7_1214200,PF3D7_1217900,PF3D7_1221600,PF3D7_1238900,PF3D7_1242600,PF3D7_1243700,PF3D7_1243800,PF3D7_1244100,PF3D7_1244200,PF3D7_1245300,PF3D7_1247500,PF3D7_1249300,PF3D7_1309200,PF3D7_1315100,PF3D7_1321100,PF3D7_1331000,PF3D7_1337800,PF3D7_1356300,PF3D7_1356800,PF3D7_1356900,PF3D7_1361000,PF3D7_1371700,PF3D7_1407500,PF3D7_1411700,PF3D7_1412600,PF3D7_1413800,PF3D7_1414400,PF3D7_1414700,PF3D7_1421600,PF3D7_1423300,PF3D7_1429500,PF3D7_1436600,PF3D7_1451400,PF3D7_1451700,PF3D7_1455100,PF3D7_1464600,	24.5	1.18	1.26	0.0398521	0.89606675	1
GO:0006464	cellular protein modification process	375	92	PF3D7_0104300,PF3D7_0209700,PF3D7_0214600,PF3D7_0217500,PF3D7_0219400,PF3D7_0303800,PF3D7_0315800,PF3D7_0316900,PF3D7_0321400,PF3D7_0500900,PF3D7_0501700,PF3D7_0516700,PF3D7_0520700,PF3D7_0527200,PF3D7_0528400,PF3D7_0615500,PF3D7_0624500,PF3D7_0704500,PF3D7_0707700,PF3D7_0708300,PF3D7_0717500,PF3D7_0724600,PF3D7_0802800,PF3D7_0803000,PF3D7_0810300,PF3D7_0811500,PF3D7_0812600,PF3D7_0823600,PF3D7_0902100,PF3D7_0916600,PF3D7_0919200,PF3D7_0928800,PF3D7_0930600,PF3D7_0932500,PF3D7_0934800,PF3D7_0935300,PF3D7_1003300,PF3D7_1009700,PF3D7_1012900,PF3D7_1031400,PF3D7_1031700,PF3D7_1033900,PF3D7_1038100,PF3D7_1103600,PF3D7_1104900,PF3D7_1114700,PF3D7_1116600,PF3D7_1119400,PF3D7_1121300,PF3D7_1122100,PF3D7_1135100,PF3D7_1136500,PF3D7_1147500,PF3D7_1202400,PF3D7_1203900,PF3D7_1211800,PF3D7_1214200,PF3D7_1217900,PF3D7_1221600,PF3D7_1238900,PF3D7_1242600,PF3D7_1243700,PF3D7_1243800,PF3D7_1244100,PF3D7_1244200,PF3D7_1245300,PF3D7_1247500,PF3D7_1249300,PF3D7_1309200,PF3D7_1315100,PF3D7_1321100,PF3D7_1331000,PF3D7_1337800,PF3D7_1356300,PF3D7_1356800,PF3D7_1356900,PF3D7_1361000,PF3D7_1371700,PF3D7_1407500,PF3D7_1411700,PF3D7_1412600,PF3D7_1413800,PF3D7_1414400,PF3D7_1414700,PF3D7_1421600,PF3D7_1423300,PF3D7_1429500,PF3D7_1436600,PF3D7_1451400,PF3D7_1451700,PF3D7_1455100,PF3D7_1464600,	24.5	1.18	1.26	0.0398521	0.89606675	1
GO:0006810	transport	31	11	PF3D7_0218100,PF3D7_0905500,PF3D7_0929900,PF3D7_0932100,PF3D7_1005800,PF3D7_1010300,PF3D7_1021700,PF3D7_1029200,PF3D7_1127600,PF3D7_1204900,PF3D7_1353700,	35.5	1.7	2.1	0.0423012 3	0.89606675	1
GO:0046337	phosphatidylethanolamine metabolic process	2	2	PF3D7_0927900,PF3D7_1124600,	100	4.8	inf	0.0433546 3	0.89606675	1
GO:0030042	actin filament depolymerization	2	2	PF3D7_0503400,PF3D7_1361400,	100	4.8	inf	0.0433546 3	0.89606675	1
GO:0007205	protein kinase C-activating G protein-coupled receptor signaling pathway	2	2	PF3D7_0930500,PF3D7_1471400,	100	4.8	inf	0.0433546 3	0.89606675	1
GO:0006646	phosphatidylethanolamine biosynthetic process	2	2	PF3D7_0927900,PF3D7_1124600,	100	4.8	inf	0.0433546 3	0.89606675	1
GO:0071704	organic substance metabolic process	2	2	PF3D7_1012500,PF3D7_1130000,	100	4.8	inf	0.0433546 3	0.89606675	1
GO:0006509	membrane protein ectodomain proteolysis	2	2	PF3D7_0507500,PF3D7_1136900,	100	4.8	inf	0.0433546 3	0.89606675	1
GO:0006101	citrate metabolic process	2	2	PF3D7_1022500,PF3D7_1342100,	100	4.8	inf	0.0433546 3	0.89606675	1
GO:0098787	mRNA cleavage involved in mRNA processing	2	2	PF3D7_0819000,PF3D7_0933000,	100	4.8	inf	0.0433546 3	0.89606675	1
GO:0098789	pre-mRNA cleavage required for polyadenylation	2	2	PF3D7_0819000,PF3D7_0933000,	100	4.8	inf	0.0433546 3	0.89606675	1
GO:0051123	RNA polymerase II preinitiation complex assembly	2	2	PF3D7_0110800,PF3D7_0929000,	100	4.8	inf	0.0433546 3	0.89606675	1

University of Ghana http://ugspace.ug.edu.gh

Supplementary Table 5.5 Gene ontology tabular summary of module 3

University of Ghana http://ugspace.ug.edu.gh

ID	Name	Bgd count	Result count	Result gene list	Pct of bgd	Fold enrichment	Odds ratio	P-value	Benjamini	Bonferroni
GO:0006412	translation	188	52	PF3D7_0208600,PF3D7_0210900,PF3D7_0217800,PF3D7_0304400,PF3D7_0306900,PF3D7_0312800,PF3D7_0316800,PF3D7_0317600,PF3D7_0322900,PF3D7_0411200,PF3D7_0422400,PF3D7_0503800,PF3D7_0507100,PF3D7_0516900,PF3D7_0519400,PF3D7_0520000,PF3D7_0611700,PF3D7_0614500,PF3D7_0706400,PF3D7_0710600,PF3D7_0710900,PF3D7_0719600,PF3D7_0814000,PF3D7_0821700,PF3D7_0903900,PF3D7_1004000,PF3D7_1105400,PF3D7_1130200,PF3D7_1302800,PF3D7_1309100,PF3D7_1310900,PF3D7_1317800,PF3D7_1323100,PF3D7_1331800,PF3D7_1338200,PF3D7_1341300,PF3D7_1342000,PF3D7_1351400,PF3D7_1358800,PF3D7_1402500,PF3D7_1408600,PF3D7_1414300,PF3D7_1421200,PF3D7_1424100,PF3D7_1424400,PF3D7_1426000,PF3D7_1431700,PF3D7_1441200,PF3D7_1447000,PF3D7_1456400,PF3D7_1460900,PF3D7_1461300,	27.7	3.95	5.81	4.27E-19	3.76E-16	3.76E-16
GO:0010499	proteasomal ubiquitin-independent protein catabolic process	14	7	PF3D7_0317000,PF3D7_0608500,PF3D7_0727400,PF3D7_0803800,PF3D7_0807500,PF3D7_0931800,PF3D7_1353900,	50	7.14	13.53	1.74E-05	0.00766068	0.01532173 6
GO:0051649	establishment of localization in cell	252	34	PF3D7_0103100,PF3D7_0202900,PF3D7_0211200,PF3D7_0214400,PF3D7_0312200,PF3D7_0316500,PF3D7_0320700,PF3D7_0416800,PF3D7_0419600,PF3D7_0423100,PF3D7_0729900,PF3D7_0807300,PF3D7_0812400,PF3D7_0823900,PF3D7_0906100,PF3D7_0932800,PF3D7_0933600,PF3D7_1005700,PF3D7_1020900,PF3D7_1034700,PF3D7_1108600,PF3D7_1117700,PF3D7_1216300,PF3D7_1223200,PF3D7_1235700,PF3D7_1250500,PF3D7_1315900,PF3D7_1324700,PF3D7_1330400,PF3D7_1346100,PF3D7_1368200,PF3D7_1412300,PF3D7_1435500,PF3D7_1462700,	13.5	1.93	2.19	0.0001272 4	0.03463167	0.11209753 9
GO:0002181	cytoplasmic translation	37	10	PF3D7_0312800,PF3D7_0503800,PF3D7_0516900,PF3D7_0528200,PF3D7_0716800,PF3D7_0821700,PF3D7_1130200,PF3D7_1323100,PF3D7_1338200,PF3D7_1351400,	27	3.86	5.04	0.0001572 4	0.03463167	0.13852668 1
GO:0046907	intracellular transport	248	33	PF3D7_0103100,PF3D7_0202900,PF3D7_0211200,PF3D7_0214400,PF3D7_0312200,PF3D7_0320700,PF3D7_0416800,PF3D7_0419600,PF3D7_0423100,PF3D7_0729900,PF3D7_0807300,PF3D7_0812400,PF3D7_0823900,PF3D7_0906100,PF3D7_0932800,PF3D7_0933600,PF3D7_1005700,PF3D7_1020900,PF3D7_1034700,PF3D7_1108600,PF3D7_1117700,PF3D7_1216300,PF3D7_1223200,PF3D7_1235700,PF3D7_1250500,PF3D7_1315900,PF3D7_1324700,PF3D7_1330400,PF3D7_1346100,PF3D7_1368200,PF3D7_1412300,PF3D7_1435500,PF3D7_1462700,	13.3	1.9	2.15	0.0002096 5	0.03693958 3	0.18469794
GO:0042254	ribosome biogenesis	193	27	PF3D7_0214400,PF3D7_0312800,PF3D7_0415100,PF3D7_0422400,PF3D7_0710600,PF3D7_0719600,PF3D7_0720100,PF3D7_0804300,PF3D7_0818800,PF3D7_1013100,PF3D7_1117700,PF3D7_1130200,PF3D7_1232000,PF3D7_1302800,PF3D7_1309100,PF3D7_1317800,PF3D7_1359000,PF3D7_1368200,PF3D7_1408600,PF3D7_1414300,PF3D7_1424100,PF3D7_1424400,PF3D7_1426200,PF3D7_1431700,PF3D7_1434500,PF3D7_1441200,PF3D7_1461300,	14	2	2.26	0.0003574 4	0.04392708 8	0.31490251 5
GO:0051169	nuclear transport	34	9	PF3D7_0214400,PF3D7_0419600,PF3D7_0812400,PF3D7_0932800,PF3D7_1117700,PF3D7_1223200,PF3D7_1315900,PF3D7_1368200,PF3D7_1412300,	26.5	3.78	4.88	0.0003988 8	0.04392708 8	0.35141676 7
GO:0006913	nucleocytoplasmic transport	34	9	PF3D7_0214400,PF3D7_0419600,PF3D7_0812400,PF3D7_0932800,PF3D7_1117700,PF3D7_1223200,PF3D7_1315900,PF3D7_1368200,PF3D7_1412300,	26.5	3.78	4.88	0.0003988 8	0.04392708 8	0.35141676 7
GO:0070925	organelle assembly	84	15	PF3D7_0422400,PF3D7_0719600,PF3D7_0720100,PF3D7_0905300,PF3D7_1015900,PF3D7_1107600,PF3D7_1130200,PF3D7_1309100,PF3D7_1317800,PF3D7_1414300,PF3D7_1424100,PF3D7_1426300,PF3D7_1434500,PF3D7_1461300,PF3D7_1470000,	17.9	2.55	2.97	0.0006091 2	0.05962584	0.53663295 9
GO:0006606	protein import into nucleus	12	5	PF3D7_0419600,PF3D7_0812400,PF3D7_0932800,PF3D7_1117700,PF3D7_1412300,	41.7	5.95	9.61	0.0008592 9	0.06129779	0.75759301
GO:0034504	protein localization to nucleus	12	5	PF3D7_0419600,PF3D7_0812400,PF3D7_0932800,PF3D7_1117700,PF3D7_1412300,	41.7	5.95	9.61	0.0008592 9	0.06129779	0.75759301
GO:0051170	import into nucleus	12	5	PF3D7_0419600,PF3D7_0812400,PF3D7_0932800,PF3D7_1117700,PF3D7_1412300,	41.7	5.95	9.61	0.0008592 9	0.06129779	0.75759301
GO:0022613	ribonucleoprotein complex biogenesis	247	31	PF3D7_0214400,PF3D7_0312800,PF3D7_0415100,PF3D7_0422400,PF3D7_0528200,PF3D7_0710600,PF3D7_0716800,PF3D7_0719600,PF3D7_0720100,PF3D7_0804300,PF3D7_0818800,PF3D7_1013100,PF3D7_1117700,PF3D7_1130200,PF3D7_1231500,PF3D7_1232000,PF3D7_1302800,PF3D7_1309100,PF3D7_1317800,PF3D7_1355800,PF3D7_1359000,PF3D7_1368200,PF3D7_1408600,PF3D7_1414300,PF3D7_1424100,PF3D7_1424400,PF3D7_1426200,PF3D7_1431700,PF3D7_1434500,PF3D7_1441200,PF3D7_1461300,	12.6	1.79	2	0.0009094 9	0.06129779	0.80126279 9
GO:0006508	proteolysis	227	29	PF3D7_0305700,PF3D7_0312200,PF3D7_0317000,PF3D7_0320700,PF3D7_0419300,PF3D7_0505800,PF3D7_0608500,PF3D7_0727400,PF3D7_0803800,PF3D7_0807500,PF3D7_0912900,PF3D7_0913500,PF3D7_0931800,PF3D7_0933600,PF3D7_1005700,PF3D7_1017900,PF3D7_1108600,PF3D7_1115400,PF3D7_1117100,PF3D7_1314800,PF3D7_1323500,PF3D7_1345500,PF3D7_1353900,PF3D7_1402500,PF3D7_1408000,PF3D7_1408100,PF3D7_1414000,PF3D7_1446200,PF3D7_1457000,	12.8	1.82	2.03	0.0010011 1	0.06129779	0.88197352 4

GO:0042255	ribosome assembly	46	10	PF3D7_0422400,PF3D7_0719600,PF3D7_0720100,PF3D7_1130200,PF3D7_1309100,PF3D7_1317800,PF3D7_1414300,PF3D7_1424100,PF3D7_1434500,PF3D7_1461300,	21.7	3.1	3.77	0.001043 66	0.061 2977 79	0.919 4666 92
GO:0006886	intracellular protein transport	166	23	PF3D7_0202900,PF3D7_0214200,PF3D7_0312200,PF3D7_0320700,PF3D7_0416800,PF3D7_0419600,PF3D7_0423100,PF3D7_0807300,PF3D7_0812400,PF3D7_0932800,PF3D7_0933600,PF3D7_1005700,PF3D7_1026900,PF3D7_1034400,PF3D7_1108600,PF3D7_1117700,PF3D7_1216300,PF3D7_1223200,PF3D7_1250500,PF3D7_1324700,PF3D7_1346100,PF3D7_1412300,PF3D7_1435500,	13.9	1.98	2.22	0.001114 41	0.061 3624 18	0.981 7986 91
GO:0051168	nuclear export	25	7	PF3D7_0214400,PF3D7_0419600,PF3D7_0932800,PF3D7_1117700,PF3D7_1223200,PF3D7_1315900,PF3D7_1368200,	28	4	5.25	0.001241 02	0.064 3139 5	1
GO:0065003	protein-containing complex assembly	193	25	PF3D7_0309600,PF3D7_0408700,PF3D7_0422400,PF3D7_0527500,PF3D7_0528200,PF3D7_0626800,PF3D7_0716800,PF3D7_0719600,PF3D7_0720100,PF3D7_0804300,PF3D7_0905300,PF3D7_1130200,PF3D7_1203700,PF3D7_1216300,PF3D7_1231500,PF3D7_1309100,PF3D7_1317800,PF3D7_1355800,PF3D7_1414300,PF3D7_1424100,PF3D7_1426300,PF3D7_1433300,PF3D7_1434500,PF3D7_1453700,PF3D7_1461300,	13	1.85	2.05	0.001825 73	0.089 3591 12	1
GO:0015931	nucleobase-containing compound transport	27	7	PF3D7_0419600,PF3D7_0505300,PF3D7_1037300,PF3D7_1117700,PF3D7_1223200,PF3D7_1315900,PF3D7_1347200,	25.9	3.7	4.72	0.002029 77	0.093 0212 65	1
GO:1901565	organonitrogen compound catabolic process	174	23	PF3D7_0305700,PF3D7_0312200,PF3D7_0317000,PF3D7_0505800,PF3D7_0513300,PF3D7_0608500,PF3D7_0608800,PF3D7_0727400,PF3D7_0803800,PF3D7_0807500,PF3D7_0912900,PF3D7_0931800,PF3D7_1017900,PF3D7_1115400,PF3D7_1117100,PF3D7_1127100,PF3D7_1235600,PF3D7_1314800,PF3D7_1345500,PF3D7_1353900,PF3D7_1402500,PF3D7_1408000,PF3D7_1414000,	13.2	1.89	2.1	0.002111 72	0.093 0212 65	1
GO:0006414	translational elongation	21	6	PF3D7_0309600,PF3D7_0319600,PF3D7_0913200,PF3D7_0931000,PF3D7_1338300,PF3D7_1451100,	28.6	4.08	5.39	0.002488 54	0.104 4001 49	1
GO:0019941	modification-dependent protein catabolic process	116	17	PF3D7_0305700,PF3D7_0312200,PF3D7_0317000,PF3D7_0505800,PF3D7_0608500,PF3D7_0727400,PF3D7_0803800,PF3D7_0807500,PF3D7_0912900,PF3D7_0931800,PF3D7_1017900,PF3D7_1117100,PF3D7_1314800,PF3D7_1345500,PF3D7_1353900,PF3D7_1402500,PF3D7_1414000,	14.7	2.09	2.35	0.002671 18	0.106 9685 94	1
GO:0022618	ribonucleoprotein complex assembly	98	15	PF3D7_0422400,PF3D7_0528200,PF3D7_0716800,PF3D7_0719600,PF3D7_0720100,PF3D7_0804300,PF3D7_1130200,PF3D7_1231500,PF3D7_1309100,PF3D7_1317800,PF3D7_1355800,PF3D7_1414300,PF3D7_1424100,PF3D7_1434500,PF3D7_1461300,	15.3	2.19	2.46	0.003059 56	0.117 1945 03	1
GO:0042273	ribosomal large subunit biogenesis	62	11	PF3D7_0312800,PF3D7_0719600,PF3D7_0804300,PF3D7_1130200,PF3D7_1309100,PF3D7_1414300,PF3D7_1424100,PF3D7_1424400,PF3D7_1431700,PF3D7_1434500,PF3D7_1441200,	17.7	2.53	2.93	0.003377 2	0.123 9711 86	1
GO:0046128	purine ribonucleoside metabolic process	10	4	PF3D7_0513300,PF3D7_1012400,PF3D7_1235700,PF3D7_1311900,	40	5.71	8.94	0.003539 97	0.124 7486 43	1
GO:0043632	modification-dependent macromolecule catabolic process	120	17	PF3D7_0305700,PF3D7_0312200,PF3D7_0317000,PF3D7_0505800,PF3D7_0608500,PF3D7_0727400,PF3D7_0803800,PF3D7_0807500,PF3D7_0912900,PF3D7_0931800,PF3D7_1017900,PF3D7_1117100,PF3D7_1314800,PF3D7_1345500,PF3D7_1353900,PF3D7_1402500,PF3D7_1414000,	14.2	2.02	2.25	0.003836 51	0.129 9985 15	1
GO:0071826	ribonucleoprotein complex subunit organization	101	15	PF3D7_0422400,PF3D7_0528200,PF3D7_0716800,PF3D7_0719600,PF3D7_0720100,PF3D7_0804300,PF3D7_1130200,PF3D7_1231500,PF3D7_1309100,PF3D7_1317800,PF3D7_1355800,PF3D7_1414300,PF3D7_1424100,PF3D7_1434500,PF3D7_1461300,	14.9	2.12	2.38	0.004111 81	0.134 1668 73	1
GO:0036158	outer dynein arm assembly	2	2	PF3D7_0905300,PF3D7_1426300,	100	14.28	inf	0.004893 52	0.138 1427 34	1
GO:0009179	purine ribonucleoside diphosphate metabolic process	17	5	PF3D7_0624000,PF3D7_0626800,PF3D7_1015900,PF3D7_1120100,PF3D7_1214900,	29.4	4.2	5.6	0.005017 67	0.138 1427 34	1
GO:0006096	glycolytic process	17	5	PF3D7_0624000,PF3D7_0626800,PF3D7_1015900,PF3D7_1120100,PF3D7_1214900,	29.4	4.2	5.6	0.005017 67	0.138 1427 34	1
GO:0046031	ADP metabolic process	17	5	PF3D7_0624000,PF3D7_0626800,PF3D7_1015900,PF3D7_1120100,PF3D7_1214900,	29.4	4.2	5.6	0.005017 67	0.138 1427 34	1
GO:0006757	ATP generation from ADP	17	5	PF3D7_0624000,PF3D7_0626800,PF3D7_1015900,PF3D7_1120100,PF3D7_1214900,	29.4	4.2	5.6	0.005017 67	0.138 1427 34	1
GO:0072594	establishment of protein localization to organelle	66	11	PF3D7_0312200,PF3D7_0320700,PF3D7_0419600,PF3D7_0812400,PF3D7_0932800,PF3D7_0933600,PF3D7_1005700,PF3D7_1117700,PF3D7_1216300,PF3D7_1346100,PF3D7_1412300,	16.7	2.38	2.71	0.005550 05	0.144 3888 53	1

University of Ghana http://ugspace.ug.edu.gh

GO:0030163	protein catabolic process	146	19	PF3D7_0305700,PF3D7_0312200,PF3D7_0317000,PF3D7_0505800,PF3D7_0608500,PF3D7_0727400,PF3D7_0803800,PF3D7_0807500,PF3D7_0912900,PF3D7_0931800,PF3D7_1017900,PF3D7_1115400,PF3D7_1117100,PF3D7_1314800,PF3D7_1345500,PF3D7_1353900,PF3D7_1402500,PF3D7_1408000,PF3D7_1414000,	13	1.86	2.04	0.005974	0.1443888	1
GO:0033365	protein localization to organelle	76	12	PF3D7_0312200,PF3D7_0326700,PF3D7_0419600,PF3D7_0812400,PF3D7_0932800,PF3D7_0933600,PF3D7_1005700,PF3D7_1117700,PF3D7_1216300,PF3D7_1330400,PF3D7_1346100,PF3D7_1412300,	15.8	2.25	2.54	0.006020	0.1443888	1
GO:0042274	ribosomal small subunit biogenesis	49	9	PF3D7_0214400,PF3D7_0422400,PF3D7_0720100,PF3D7_0818800,PF3D7_1013100,PF3D7_1302800,PF3D7_1317800,PF3D7_1408600,PF3D7_1461300,	18.4	2.62	3.04	0.006145	0.1443888	1
GO:0009150	purine ribonucleotide metabolic process	67	11	PF3D7_0624000,PF3D7_0626800,PF3D7_1012400,PF3D7_1015900,PF3D7_1102400,PF3D7_1108500,PF3D7_1120100,PF3D7_1214900,PF3D7_1235700,PF3D7_1311900,PF3D7_1462700,	16.4	2.34	2.66	0.006236	0.1443888	1
GO:0043933	protein-containing complex subunit organization	223	26	PF3D7_0309600,PF3D7_0408700,PF3D7_0422400,PF3D7_0527500,PF3D7_0528200,PF3D7_0626800,PF3D7_0716800,PF3D7_0719600,PF3D7_0720100,PF3D7_0804300,PF3D7_0905300,PF3D7_1130200,PF3D7_1203700,PF3D7_1216300,PF3D7_1231500,PF3D7_1309100,PF3D7_1317800,PF3D7_1355800,PF3D7_1368200,PF3D7_1414300,PF3D7_1424100,PF3D7_1426300,PF3D7_1433300,PF3D7_1434500,PF3D7_1453700,PF3D7_1461300,	11.7	1.66	1.81	0.006408	0.1443888	1
GO:0009185	ribonucleoside diphosphate metabolic process	18	5	PF3D7_0624000,PF3D7_0626800,PF3D7_1015900,PF3D7_1120100,PF3D7_1214900,	27.8	3.97	5.17	0.006555	0.1443888	1
GO:0009135	purine nucleoside diphosphate metabolic process	18	5	PF3D7_0624000,PF3D7_0626800,PF3D7_1015900,PF3D7_1120100,PF3D7_1214900,	27.8	3.97	5.17	0.006555	0.1443888	1
GO:0044257	cellular protein catabolic process	138	18	PF3D7_0305700,PF3D7_0312200,PF3D7_0317000,PF3D7_0505800,PF3D7_0608500,PF3D7_0727400,PF3D7_0803800,PF3D7_0807500,PF3D7_0912900,PF3D7_0931800,PF3D7_1017900,PF3D7_1115400,PF3D7_1117100,PF3D7_1314800,PF3D7_1345500,PF3D7_1353900,PF3D7_1402500,PF3D7_1414000,	13	1.86	2.05	0.007192	0.1508690	1
GO:0051603	proteolysis involved in cellular protein catabolic process	138	18	PF3D7_0305700,PF3D7_0312200,PF3D7_0317000,PF3D7_0505800,PF3D7_0608500,PF3D7_0727400,PF3D7_0803800,PF3D7_0807500,PF3D7_0912900,PF3D7_0931800,PF3D7_1017900,PF3D7_1115400,PF3D7_1117100,PF3D7_1314800,PF3D7_1345500,PF3D7_1353900,PF3D7_1402500,PF3D7_1414000,	13	1.86	2.05	0.007192	0.1508690	1
GO:0043161	proteasome-mediated ubiquitin-dependent protein catabolic process	69	11	PF3D7_0312200,PF3D7_0317000,PF3D7_0608500,PF3D7_0727400,PF3D7_0803800,PF3D7_0807500,PF3D7_0912900,PF3D7_0931800,PF3D7_1017900,PF3D7_1345500,PF3D7_1353900,	15.9	2.28	2.57	0.007807	0.1569881	1
GO:0006090	pyruvate metabolic process	26	6	PF3D7_0624000,PF3D7_0626800,PF3D7_1015900,PF3D7_1120100,PF3D7_1214900,PF3D7_1467300,	23.1	3.29	4.04	0.007840	0.1569881	1
GO:0015031	protein transport	60	10	PF3D7_0103100,PF3D7_0320700,PF3D7_0423100,PF3D7_0906100,PF3D7_1020900,PF3D7_1234600,PF3D7_1250500,PF3D7_1321800,PF3D7_1330400,PF3D7_1346100,	16.7	2.38	2.71	0.008041	0.1574419	1
GO:0140694	non-membrane-bounded organelle assembly	61	10	PF3D7_0422400,PF3D7_0719600,PF3D7_0720100,PF3D7_1130200,PF3D7_1309100,PF3D7_1317800,PF3D7_1414300,PF3D7_1424100,PF3D7_1434500,PF3D7_1461300,	16.4	2.34	2.65	0.009038	0.1712899	1
GO:0017038	protein import	27	6	PF3D7_0419600,PF3D7_0812400,PF3D7_0932800,PF3D7_1117700,PF3D7_1144700,PF3D7_1412300,	22.2	3.17	3.84	0.009500	0.1712899	1
GO:0010498	proteasomal protein catabolic process	71	11	PF3D7_0312200,PF3D7_0317000,PF3D7_0608500,PF3D7_0727400,PF3D7_0803800,PF3D7_0807500,PF3D7_0912900,PF3D7_0931800,PF3D7_1017900,PF3D7_1345500,PF3D7_1353900,	15.5	2.21	2.48	0.009671	0.1712899	1
GO:0006405	RNA export from nucleus	13	4	PF3D7_0419600,PF3D7_1117700,PF3D7_1223200,PF3D7_1315900,	30.8	4.39	5.96	0.010187	0.1712899	1
GO:0000028	ribosomal small subunit assembly	13	4	PF3D7_0422400,PF3D7_0720100,PF3D7_1317800,PF3D7_1461300,	30.8	4.39	5.96	0.010187	0.1712899	1
GO:1901135	carbohydrate derivative metabolic process	155	19	PF3D7_0321200,PF3D7_0512700,PF3D7_0513300,PF3D7_0624000,PF3D7_0624700,PF3D7_0626800,PF3D7_0911000,PF3D7_1010700,PF3D7_1012400,PF3D7_1015900,PF3D7_1102400,PF3D7_1108500,PF3D7_1120100,PF3D7_1127100,PF3D7_1141600,PF3D7_1214900,PF3D7_1235700,PF3D7_1462700,PF3D7_1467300,	12.3	1.75	1.91	0.011228	0.1712899	1
GO:0034622	cellular protein-containing complex assembly	177	21	PF3D7_0422400,PF3D7_0528200,PF3D7_0716800,PF3D7_0719600,PF3D7_0720100,PF3D7_0804300,PF3D7_0905300,PF3D7_1130200,PF3D7_1203700,PF3D7_1216300,PF3D7_1231500,PF3D7_1309100,PF3D7_1317800,PF3D7_1355800,PF3D7_1414300,PF3D7_1424100,PF3D7_1426300,PF3D7_1433300,PF3D7_1434500,PF3D7_1453700,PF3D7_1461300,	11.9	1.69	1.84	0.011311	0.1712899	1

University of Ghana http://ugspace.ug.edu.gh

GO:0000027	ribosomal large subunit assembly	28	6	PF3D7_0719600,PF3D7_1130200,PF3D7_1309100,PF3D7_1414300,PF3D7_1424100,PF3D7_1434500,	21.4	3.06	3.67	0.011397 23	0.1712899 66	1
GO:0006511	ubiquitin-dependent protein catabolic process	113	5	PF3D7_0305700,PF3D7_0312200,PF3D7_0317000,PF3D7_0505800,PF3D7_0608500,PF3D7_0727400,PF3D7_0803800,PF3D7_0807500,PF3D7_0912500,PF3D7_0931800,PF3D7_0119900,PF3D7_1111100,PF3D7_1234500,PF3D7_1253900,PF3D7_1414400,	13.3	1.89	2.08	0.011630 08	0.1712899 66	1
GO:0009259	ribonucleotide metabolic process	73	11	PF3D7_0512700,PF3D7_0624000,PF3D7_0626800,PF3D7_1012400,PF3D7_1015900,PF3D7_1102400,PF3D7_1108500,PF3D7_1120100,PF3D7_1214900,PF3D7_1235700,PF3D7_1462700,	15.1	2.15	2.4	0.011860 37	0.1712899 66	1
GO:0051656	establishment of organelle localization	21	5	PF3D7_0214400,PF3D7_0316500,PF3D7_0729900,PF3D7_1117700,PF3D7_1368200,	23.8	3.4	4.2	0.013089 98	0.1712899 66	1
GO:0016052	carbohydrate catabolic process	21	5	PF3D7_0624000,PF3D7_0626800,PF3D7_1015900,PF3D7_1120100,PF3D7_1214900,	23.8	3.4	4.2	0.013089 98	0.1712899 66	1
GO:0006165	nucleoside diphosphate phosphorylation	21	5	PF3D7_0624000,PF3D7_0626800,PF3D7_1015900,PF3D7_1120100,PF3D7_1214900,	23.8	3.4	4.2	0.013089 98	0.1712899 66	1
GO:0046034	ATP metabolic process	46	8	PF3D7_0624000,PF3D7_0626800,PF3D7_1015900,PF3D7_1120100,PF3D7_1214900,PF3D7_1235700,PF3D7_1311900,PF3D7_1462700,	17.4	2.48	2.84	0.013307 3	0.1712899 66	1
GO:1904659	glucose transmembrane transport	3	2	PF3D7_0204700,PF3D7_0508300,	66.7	9.52	26.7	0.013998 73	0.1712899 66	1
GO:0008216	spermidine metabolic process	3	2	PF3D7_0409300,PF3D7_1129000,	66.7	9.52	26.7	0.013998 73	0.1712899 66	1
GO:0044088	regulation of vacuole organization	3	2	PF3D7_0211200,PF3D7_1015900,	66.7	9.52	26.7	0.013998 73	0.1712899 66	1
GO:0034219	carbohydrate transmembrane transport	3	2	PF3D7_0204700,PF3D7_0508300,	66.7	9.52	26.7	0.013998 73	0.1712899 66	1
GO:0006596	polyamine biosynthetic process	3	2	PF3D7_0409300,PF3D7_1129000,	66.7	9.52	26.7	0.013998 73	0.1712899 66	1
GO:0006595	polyamine metabolic process	3	2	PF3D7_0409300,PF3D7_1129000,	66.7	9.52	26.7	0.013998 73	0.1712899 66	1
GO:0008295	spermidine biosynthetic process	3	2	PF3D7_0409300,PF3D7_1129000,	66.7	9.52	26.7	0.013998 73	0.1712899 66	1
GO:0006493	protein O-linked glycosylation	3	2	PF3D7_1010700,PF3D7_1141600,	66.7	9.52	26.7	0.013998 73	0.1712899 66	1
GO:0051262	protein tetramerization	3	2	PF3D7_0309600,PF3D7_0626800,	66.7	9.52	26.7	0.013998 73	0.1712899 66	1
GO:0015749	monosaccharide transmembrane transport	3	2	PF3D7_0204700,PF3D7_0508300,	66.7	9.52	26.7	0.013998 73	0.1712899 66	1
GO:0072530	purine-containing compound transmembrane transport	3	2	PF3D7_1037300,PF3D7_1347200,	66.7	9.52	26.7	0.013998 73	0.1712899 66	1
GO:0032889	regulation of vacuole fusion, non-autophagic	3	2	PF3D7_0211200,PF3D7_1015900,	66.7	9.52	26.7	0.013998 73	0.1712899 66	1
GO:0008645	hexose transmembrane transport	3	2	PF3D7_0204700,PF3D7_0508300,	66.7	9.52	26.7	0.013998 73	0.1712899 66	1

University of Ghana http://ugspace.ug.edu.gh

GO:0019693	ribose phosphate metabolic process	75	11	PF3D7_0512700,PF3D7_0624000,PF3D7_0626800,PF3D7_1012400,PF3D7_1015900,PF3D7_1102400,PF3D7_1108500,PF3D7_1120100,PF3D7_1214900,PF3D7_1235700,PF3D7_1462700,	14.7	2.09	2.32	0.014408 87	0.1738933 78	1
GO:1901264	carbohydrate derivative transport	8	3	PF3D7_0505300,PF3D7_1037300,PF3D7_1347200,	37.5	5.35	8.03	0.014637 98	0.1742710 35	1
GO:0042592	homeostatic process	68	10	PF3D7_0624000,PF3D7_0802200,PF3D7_0827900,PF3D7_1036700,PF3D7_1108700,PF3D7_1134100,PF3D7_1223200,PF3D7_1311900,PF3D7_1352500,PF3D7_1439000,	14.7	2.1	2.33	0.018880 88	0.2200110 94	1
GO:0072521	purine-containing compound metabolic process	78	11	PF3D7_0513300,PF3D7_0624000,PF3D7_0626800,PF3D7_1012400,PF3D7_1015900,PF3D7_1102400,PF3D7_1108500,PF3D7_1120100,PF3D7_1214900,PF3D7_1235700,PF3D7_1462700,	14.1	2.01	2.22	0.018979 39	0.2200110 94	1
GO:0046939	nucleotide phosphorylation	23	5	PF3D7_0624000,PF3D7_0626800,PF3D7_1015900,PF3D7_1120100,PF3D7_1214900,	21.7	3.1	3.73	0.019292 77	0.2207393 43	1
GO:0009119	ribonucleoside metabolic process	9	3	PF3D7_0512700,PF3D7_0513300,PF3D7_1012400,	33.3	4.76	6.69	0.020833 43	0.2294281	1
GO:0035082	axoneme assembly	9	3	PF3D7_0905300,PF3D7_1107600,PF3D7_1426300,	33.3	4.76	6.69	0.020833 43	0.2294281	1
GO:0001578	microtubule bundle formation	9	3	PF3D7_0905300,PF3D7_1107600,PF3D7_1426300,	33.3	4.76	6.69	0.020833 43	0.2294281	1
GO:0043648	dicarboxylic acid metabolic process	16	4	PF3D7_0608800,PF3D7_1214900,PF3D7_1235600,PF3D7_1416500,	25	3.57	4.47	0.021947 59	0.2358027 72	1
GO:0090502	RNA phosphodiester bond hydrolysis, endonucleolytic	16	4	PF3D7_0621500,PF3D7_0623900,PF3D7_0720100,PF3D7_1013100,	25	3.57	4.47	0.021947 59	0.2358027 72	1
GO:0070972	protein localization to endoplasmic reticulum	24	5	PF3D7_0312200,PF3D7_0320700,PF3D7_1216300,PF3D7_1330400,PF3D7_1346100,	20.8	2.97	3.53	0.023011 46	0.2442541 22	1
GO:0006611	protein export from nucleus	4	2	PF3D7_0932800,PF3D7_1223200,	50	7.14	13.35	0.026704 84	0.2643479 05	1
GO:0006627	protein processing involved in protein targeting to mitochondrion	4	2	PF3D7_0933600,PF3D7_1005700,	50	7.14	13.35	0.026704 84	0.2643479 05	1
GO:0000967	rRNA 5'-end processing	4	2	PF3D7_0720100,PF3D7_1013100,	50	7.14	13.35	0.026704 84	0.2643479 05	1
GO:0000472	endonucleolytic cleavage to generate mature 5'-end of SSU-rRNA from (SSU-rRNA, 5.8S rRNA, LSU-rRNA)	4	2	PF3D7_0720100,PF3D7_1013100,	50	7.14	13.35	0.026704 84	0.2643479 05	1
GO:0042776	mitochondrial ATP synthesis coupled proton transport	4	2	PF3D7_1235700,PF3D7_1462700,	50	7.14	13.35	0.026704 84	0.2643479 05	1
GO:0000480	endonucleolytic cleavage in 5'-ETS of tricistronic rRNA transcript (SSU-rRNA, 5.8S rRNA, LSU-rRNA)	4	2	PF3D7_0720100,PF3D7_1013100,	50	7.14	13.35	0.026704 84	0.2643479 05	1
GO:0019725	cellular homeostasis	62	9	PF3D7_0624000,PF3D7_0802200,PF3D7_0827900,PF3D7_1036700,PF3D7_1108700,PF3D7_1134100,PF3D7_1311900,PF3D7_1352500,PF3D7_1439000,	14.5	2.07	2.29	0.027294 23	0.2648645 27	1
GO:0009116	nucleoside metabolic process	10	3	PF3D7_0512700,PF3D7_0513300,PF3D7_1012400,	30	4.28	5.73	0.028244 91	0.2648645 27	1
GO:0033750	ribosome localization	10	3	PF3D7_0214400,PF3D7_1117700,PF3D7_1368200,	30	4.28	5.73	0.028244 91	0.2648645 27	1

University of Ghana http://ugspace.ug.edu.gh

GO:0000054	ribosomal subunit export from nucleus	10	3	PF3D7_0214400,PF3D7_1117700,PF3D7_1368200,	30	4.28	5.73	0.0282449 1	0.2648645 27	1
GO:0019752	carboxylic acid metabolic process	161	8	PF3D7_0409500,PF3D7_0416100,PF3D7_0608800,PF3D7_0624000,PF3D7_0626800,PF3D7_0727200,PF3D7_0925300,PF3D7_1001200,PF3D7_1015900,PF3D7_1020800,PF3D7_1117500,PF3D7_1120100,PF3D7_1214900,PF3D7_1232000,PF3D7_1235600,PF3D7_1416500,PF3D7_1456400,PF3D7_1467300,	11.2	1.6	1.71	0.0313636 3	0.2648645 27	1
GO:0009132	nucleoside diphosphate metabolic process	26	5	PF3D7_0624000,PF3D7_0626800,PF3D7_1015900,PF3D7_1120100,PF3D7_1214900,	19.2	2.75	3.19	0.0317652 6	0.2648645 27	1
GO:0006163	purine nucleotide metabolic process	74	10	PF3D7_0624000,PF3D7_0626800,PF3D7_1012400,PF3D7_1015900,PF3D7_1102400,PF3D7_1108500,PF3D7_1120100,PF3D7_1214900,PF3D7_1235700,PF3D7_1462700,	13.5	1.93	2.11	0.0322224 3	0.2648645 27	1
GO:0006082	organic acid metabolic process	164	18	PF3D7_0409500,PF3D7_0416100,PF3D7_0608800,PF3D7_0624000,PF3D7_0626800,PF3D7_0727200,PF3D7_0925300,PF3D7_1001200,PF3D7_1015900,PF3D7_1020800,PF3D7_1117500,PF3D7_1120100,PF3D7_1214900,PF3D7_1232000,PF3D7_1235600,PF3D7_1416500,PF3D7_1456400,PF3D7_1467300,	11	1.57	1.67	0.0367936	0.2648645 27	1
GO:0043436	oxoacid metabolic process	164	18	PF3D7_0409500,PF3D7_0416100,PF3D7_0608800,PF3D7_0624000,PF3D7_0626800,PF3D7_0727200,PF3D7_0925300,PF3D7_1001200,PF3D7_1015900,PF3D7_1020800,PF3D7_1117500,PF3D7_1120100,PF3D7_1214900,PF3D7_1232000,PF3D7_1235600,PF3D7_1416500,PF3D7_1456400,PF3D7_1467300,	11	1.57	1.67	0.0367936	0.2648645 27	1
GO:0006403	RNA localization	27	5	PF3D7_0419600,PF3D7_0804300,PF3D7_1117700,PF3D7_1223200,PF3D7_1315900,	18.5	2.64	3.05	0.0368253 9	0.2648645 27	1
GO:0031503	protein-containing complex localization	11	3	PF3D7_0214400,PF3D7_1117700,PF3D7_1368200,	27.3	3.89	5.01	0.0368648 8	0.2648645 27	1
GO:1901657	glycosyl compound metabolic process	11	3	PF3D7_0512700,PF3D7_0513300,PF3D7_1012400,	27.3	3.89	5.01	0.0368648 8	0.2648645 27	1
GO:0009117	nucleotide metabolic process	98	12	PF3D7_0512700,PF3D7_0624000,PF3D7_0626800,PF3D7_1012400,PF3D7_1015900,PF3D7_1102400,PF3D7_1108500,PF3D7_1120100,PF3D7_1127100,PF3D7_1214900,PF3D7_1235700,PF3D7_1462700,	12.2	1.75	1.88	0.0397057 5	0.2648645 27	1
GO:0032259	methylation	37	6	PF3D7_0204900,PF3D7_0409300,PF3D7_0608000,PF3D7_0801900,PF3D7_1009000,PF3D7_1235600,	16.2	2.31	2.6	0.0414792 1	0.2648645 27	1
GO:0045454	cell redox homeostasis	37	6	PF3D7_0802200,PF3D7_0827900,PF3D7_1036700,PF3D7_1108700,PF3D7_1134100,PF3D7_1352500,	16.2	2.31	2.6	0.0414792 1	0.2648645 27	1
GO:0032787	monocarboxylic acid metabolic process	67	9	PF3D7_0409500,PF3D7_0624000,PF3D7_0626800,PF3D7_1001200,PF3D7_1015900,PF3D7_1020800,PF3D7_1120100,PF3D7_1214900,PF3D7_1467300,	13.4	1.92	2.09	0.0424243 1	0.2648645 27	1
GO:0006753	nucleoside phosphate metabolic process	99	12	PF3D7_0512700,PF3D7_0624000,PF3D7_0626800,PF3D7_1012400,PF3D7_1015900,PF3D7_1102400,PF3D7_1108500,PF3D7_1120100,PF3D7_1127100,PF3D7_1214900,PF3D7_1235700,PF3D7_1462700,	12.1	1.73	1.86	0.0424584 7	0.2648645 27	1
GO:0042401	cellular biogenic amine biosynthetic process	5	2	PF3D7_0409300,PF3D7_1129000,	40	5.71	8.9	0.0424654 58	0.2648645 27	1
GO:0070286	axonemal dynein complex assembly	5	2	PF3D7_0905300,PF3D7_1426300,	40	5.71	8.9	0.0424654 58	0.2648645 27	1
GO:0009309	amine biosynthetic process	5	2	PF3D7_0409300,PF3D7_1129000,	40	5.71	8.9	0.0424654 58	0.2648645 27	1
GO:0060271	cilium assembly	12	3	PF3D7_0905300,PF3D7_1107600,PF3D7_1426300,	25	3.57	4.46	0.0466668 1	0.2648645 27	1
GO:0006720	isoprenoid metabolic process	12	3	PF3D7_0106900,PF3D7_1141600,PF3D7_1467300,	25	3.57	4.46	0.0466668 1	0.2648645 27	1
GO:0044782	cilium organization	12	3	PF3D7_0905300,PF3D7_1107600,PF3D7_1426300,	25	3.57	4.46	0.0466668 1	0.2648645 27	1

University of Ghana http://ugspace.ug.edu.gh

GO:0045047	protein targeting to ER	20	4	PF3D7_0312200,PF3D7_0320700,PF3D7_1216300,PF3D7_1346100,	20	2.86	3.35	0.046877 65	0.2648645 27	1
GO:0050657	nucleic acid transport	20	4	PF3D7_0419600,PF3D7_1117700,PF3D7_1223200,PF3D7_1315900,	20	2.86	3.35	0.046877 65	0.2648645 27	1
GO:0050658	RNA transport	20	4	PF3D7_0419600,PF3D7_1117700,PF3D7_1223200,PF3D7_1315900,	20	2.86	3.35	0.046877 65	0.2648645 27	1
GO:0051236	establishment of RNA localization	20	4	PF3D7_0419600,PF3D7_1117700,PF3D7_1223200,PF3D7_1315900,	20	2.86	3.35	0.046877 65	0.2648645 27	1
GO:0072599	establishment of protein localization to endoplasmic reticulum	20	4	PF3D7_0312200,PF3D7_0320700,PF3D7_1216300,PF3D7_1346100,	20	2.86	3.35	0.046877 65	0.2648645 27	1
GO:0006839	mitochondrial transport	29	5	PF3D7_0823900,PF3D7_0933600,PF3D7_1005700,PF3D7_1235700,PF3D7_1462700,	17.2	2.46	2.79	0.048354 71	0.2648645 27	1
GO:0016485	protein processing	29	5	PF3D7_0320700,PF3D7_0913500,PF3D7_0933600,PF3D7_1005700,PF3D7_1457000,	17.2	2.46	2.79	0.048354 71	0.2648645 27	1
GO:0009410	response to xenobiotic stimulus	135	15	PF3D7_0106900,PF3D7_0204700,PF3D7_0312400,PF3D7_0513300,PF3D7_0624000,PF3D7_0909700,PF3D7_1007700,PF3D7_1012400,PF3D7_1323500,PF3D7_1347200,PF3D7_1408000,PF3D7_1408100,PF3D7_1451100,PF3D7_1457000,PF3D7_1467300,	11.1	1.59	1.69	0.049062 82	0.2648645 27	1

University of Ghana http://ugspace.ug.edu.gh

Supplementary Table 5.6 Gene ontology tabular summary of module 17

University of Ghana http://ugspace.ug.edu.gh

ID	Name	Bgd count	Result count	Result gene list	Pct of bgd	Fold enrichment	Odds ratio	P-value	Benjamini	Bonferroni
GO:0022402	cell cycle process	81	7	PF3D7_0309200,PF3D7_0926900,PF3D7_0933500,PF3D7_1130700,PF3D7_1324500,PF3D7_1368800,PF3D7_1403100,	8.6	6.57	7.85	7.87E-05	0.022655472	0.022655472
GO:0098813	nuclear chromosome segregation	25	4	PF3D7_1130700,PF3D7_1324500,PF3D7_1368800,PF3D7_1403100,	16	12.17	15.18	0.00027941	0.040235406	0.080470812
GO:0022414	reproductive process	33	4	PF3D7_0926900,PF3D7_0933500,PF3D7_1368800,PF3D7_1403100,	12.1	9.22	10.98	0.00083532	0.048114532	0.24057266
GO:0007059	chromosome segregation	33	4	PF3D7_1130700,PF3D7_1324500,PF3D7_1368800,PF3D7_1403100,	12.1	9.22	10.98	0.00083532	0.048114532	0.24057266
GO:0000003	reproduction	33	4	PF3D7_0926900,PF3D7_0933500,PF3D7_1368800,PF3D7_1403100,	12.1	9.22	10.98	0.00083532	0.048114532	0.24057266
GO:0000819	sister chromatid segregation	19	3	PF3D7_1130700,PF3D7_1324500,PF3D7_1403100,	15.8	12.01	14.72	0.00180732	0.08675113	0.520506781
GO:0000278	mitotic cell cycle	73	5	PF3D7_0309200,PF3D7_0926900,PF3D7_0933500,PF3D7_1130700,PF3D7_1403100,	6.8	5.21	5.9	0.00253204	0.099874406	0.729228195
GO:1903047	mitotic cell cycle process	52	4	PF3D7_0309200,PF3D7_0926900,PF3D7_1130700,PF3D7_1403100,	7.7	5.85	6.61	0.00458615	0.099874406	1
GO:0051304	chromosome separation	9	2	PF3D7_1368800,PF3D7_1403100,	22.2	16.9	22.11	0.00577231	0.099874406	1
GO:0051321	meiotic cell cycle	30	3	PF3D7_0933500,PF3D7_1368800,PF3D7_1403100,	10	7.61	8.7	0.00683224	0.099874406	1
GO:0055067	monovalent inorganic cation homeostasis	11	2	PF3D7_1323200,PF3D7_1456800,	18.2	13.83	17.19	0.00867065	0.099874406	1
GO:0006885	regulation of pH	11	2	PF3D7_1323200,PF3D7_1456800,	18.2	13.83	17.19	0.00867065	0.099874406	1
GO:0000280	nuclear division	33	3	PF3D7_1130700,PF3D7_1368800,PF3D7_1403100,	9.1	6.91	7.83	0.00892837	0.099874406	1
GO:0000288	nuclear-transcribed mRNA catabolic process, deadenylation-dependent decay	12	2	PF3D7_0519500,PF3D7_1103800,	16.7	12.68	15.46	0.01031714	0.099874406	1
GO:0050779	RNA destabilization	13	2	PF3D7_0519500,PF3D7_1103800,	15.4	11.7	14.06	0.01209038	0.099874406	1
GO:0061157	mRNA destabilization	13	2	PF3D7_0519500,PF3D7_1103800,	15.4	11.7	14.06	0.01209038	0.099874406	1
GO:1902979	mitotic DNA replication termination	1	1	PF3D7_0926900,	100	76.06	inf	0.01314708	0.099874406	1
GO:0032505	reproduction of a single-celled organism	1	1	PF3D7_0926900,	100	76.06	inf	0.01314708	0.099874406	1
GO:0034085	establishment of sister chromatid cohesion	1	1	PF3D7_1324500,	100	76.06	inf	0.01314708	0.099874406	1
GO:1902294	cell cycle DNA replication termination	1	1	PF3D7_0926900,	100	76.06	inf	0.01314708	0.099874406	1
GO:0036092	phosphatidylinositol-3-phosphate biosynthetic process	1	1	PF3D7_0515300,	100	76.06	inf	0.01314708	0.099874406	1
GO:0042939	tripeptide transport	1	1	PF3D7_0709000,	100	76.06	inf	0.01314708	0.099874406	1
GO:0071514	genetic imprinting	1	1	PF3D7_0926900,	100	76.06	inf	0.01314708	0.099874406	1
GO:0071515	genetic imprinting at mating-type locus	1	1	PF3D7_0926900,	100	76.06	inf	0.01314708	0.099874406	1
GO:0071947	protein deubiquitination involved in ubiquitin-dependent protein catabolic process	1	1	PF3D7_1408700,	100	76.06	inf	0.01314708	0.099874406	1
GO:0071516	establishment of imprinting at mating-type locus	1	1	PF3D7_0926900,	100	76.06	inf	0.01314708	0.099874406	1
GO:0022413	reproductive process in single-celled organism	1	1	PF3D7_0926900,	100	76.06	inf	0.01314708	0.099874406	1

University of Ghana http://ugspace.ug.edu.gh

GO:0071170	site-specific DNA replication termination	1	1	PF3D7_0926900,	100	76.06	inf	0.01314708	0.099874406	1
GO:0071171	site-specific DNA replication termination at RTS1 barrier	1	1	PF3D7_0926900,	100	76.06	inf	0.01314708	0.099874406	1
GO:0045165	cell fate commitment	1	1	PF3D7_0926900,	100	76.06	inf	0.01314708	0.099874406	1
GO:1902317	nuclear DNA replication termination	1	1	PF3D7_0926900,	100	76.06	inf	0.01314708	0.099874406	1
GO:0034635	glutathione transport	1	1	PF3D7_0709000,	100	76.06	inf	0.01314708	0.099874406	1
GO:0015833	peptide transport	1	1	PF3D7_0709000,	100	76.06	inf	0.01314708	0.099874406	1
GO:0000719	photoreactive repair	1	1	PF3D7_0513600,	100	76.06	inf	0.01314708	0.099874406	1
GO:0006274	DNA replication termination	1	1	PF3D7_0926900,	100	76.06	inf	0.01314708	0.099874406	1
GO:0007533	mating type switching	1	1	PF3D7_0926900,	100	76.06	inf	0.01314708	0.099874406	1
GO:0007531	mating type determination	1	1	PF3D7_0926900,	100	76.06	inf	0.01314708	0.099874406	1
GO:0048285	organelle fission	38	3	PF3D7_1130700,PF3D7_1368800,PF3D7_1403100,	7.9	6	6.7	0.01317787	0.099874406	1
GO:0061014	positive regulation of mRNA catabolic process	14	2	PF3D7_0519500,PF3D7_1103800,	14.3	10.87	12.88	0.01398685	0.103287495	1
GO:1903313	positive regulation of mRNA metabolic process	15	2	PF3D7_0519500,PF3D7_1103800,	13.3	10.14	11.89	0.01600312	0.112412134	1
GO:0000070	mitotic sister chromatid segregation	15	2	PF3D7_1130700,PF3D7_1403100,	13.3	10.14	11.89	0.01600312	0.112412134	1
GO:0007051	spindle organization	16	2	PF3D7_0309200,PF3D7_0933500,	12.5	9.51	11.04	0.01813581	0.121467714	1
GO:0016482	cytosolic transport	16	2	PF3D7_0621350,PF3D7_1110500,	12.5	9.51	11.04	0.01813581	0.121467714	1
GO:0140014	mitotic nuclear division	17	2	PF3D7_1130700,PF3D7_1403100,	11.8	8.95	10.3	0.0203816	0.13044226	1
GO:0043488	regulation of mRNA stability	17	2	PF3D7_0519500,PF3D7_1103800,	11.8	8.95	10.3	0.0203816	0.13044226	1
GO:0043487	regulation of RNA stability	18	2	PF3D7_0519500,PF3D7_1103800,	11.1	8.45	9.65	0.02273727	0.139326232	1
GO:0061013	regulation of mRNA catabolic process	18	2	PF3D7_0519500,PF3D7_1103800,	11.1	8.45	9.65	0.02273727	0.139326232	1
GO:0007530	sex determination	2	1	PF3D7_0926900,	50	38.03	76.24	0.02612399	0.139327925	1
GO:0072337	modified amino acid transport	2	1	PF3D7_0709000,	50	38.03	76.24	0.02612399	0.139327925	1
GO:0008612	peptidyl-lysine modification to peptidyl-hypusine	2	1	PF3D7_1302600,	50	38.03	76.24	0.02612399	0.139327925	1
GO:0006290	pyrimidine dimer repair	2	1	PF3D7_0513600,	50	38.03	76.24	0.02612399	0.139327925	1
GO:1901255	nucleotide-excision repair involved in interstrand cross-link repair	2	1	PF3D7_1368800,	50	38.03	76.24	0.02612399	0.139327925	1
GO:0000289	nuclear-transcribed mRNA poly(A) tail shortening	2	1	PF3D7_0519500,	50	38.03	76.24	0.02612399	0.139327925	1
GO:0003006	developmental process involved in reproduction	2	1	PF3D7_0926900,	50	38.03	76.24	0.02612399	0.139327925	1
GO:0006417	regulation of translation	20	2	PF3D7_0422500,PF3D7_1103800,	10	7.61	8.58	0.02776553	0.145390389	1
GO:0006897	endocytosis	21	2	PF3D7_0515300,PF3D7_0904100,	9.5	7.24	8.12	0.03043194	0.156018195	1
GO:0009410	response to xenobiotic stimulus	135	5	PF3D7_0515300,PF3D7_0709000,PF3D7_0827800,PF3D7_1121600,PF3D7_1302600,	3.7	2.82	3.05	0.03143876	0.156018195	1

GO:0016579	protein deubiquitination	22	2	PF3D7_0726500,PF3D7_1408700,	9.1	6.91	7.72	0.03319587	0.156018195	1
GO:0016192	vesicle-mediated transport	140	5	PF3D7_0515300,PF3D7_0621350,PF3D7_0904100,PF3D7_1104100,PF3D7_1110500,	3.6	2.72	2.93	0.03597966	0.156018195	1
GO:0006289	nucleotide-excision repair	23	2	PF3D7_0317700,PF3D7_1368800,	8.7	6.61	7.35	0.03605436	0.156018195	1
GO:0006893	Golgi to plasma membrane transport	3	1	PF3D7_0621350,	33.3	25.35	38.11	0.03893288	0.156018195	1
GO:0030242	autophagy of peroxisome	3	1	PF3D7_0515300,	33.3	25.35	38.11	0.03893288	0.156018195	1
GO:0010032	meiotic chromosome condensation	3	1	PF3D7_1403100,	33.3	25.35	38.11	0.03893288	0.156018195	1
GO:0043001	Golgi to plasma membrane protein transport	3	1	PF3D7_0621350,	33.3	25.35	38.11	0.03893288	0.156018195	1
GO:0006895	Golgi to endosome transport	3	1	PF3D7_0621350,	33.3	25.35	38.11	0.03893288	0.156018195	1
GO:0007062	sister chromatid cohesion	3	1	PF3D7_1324500,	33.3	25.35	38.11	0.03893288	0.156018195	1
GO:0072348	sulfur compound transport	3	1	PF3D7_0709000,	33.3	25.35	38.11	0.03893288	0.156018195	1
GO:0006296	nucleotide-excision repair, DNA incision, 5'-to lesion	3	1	PF3D7_1368800,	33.3	25.35	38.11	0.03893288	0.156018195	1
GO:0006857	oligopeptide transport	3	1	PF3D7_0709000,	33.3	25.35	38.11	0.03893288	0.156018195	1
GO:0061951	establishment of protein localization to plasma membrane	3	1	PF3D7_0621350,	33.3	25.35	38.11	0.03893288	0.156018195	1
GO:0070646	protein modification by small protein removal	24	2	PF3D7_0726500,PF3D7_1408700,	8.3	6.34	7.01	0.03900455	0.156018195	1
GO:1903046	meiotic cell cycle process	24	2	PF3D7_1368800,PF3D7_1403100,	8.3	6.34	7.01	0.03900455	0.156018195	1
GO:0042493	response to drug	25	2	PF3D7_0709000,PF3D7_1121600,	8	6.08	6.71	0.0420436	0.165870643	1
GO:0046907	intracellular transport	248	7	PF3D7_0515300,PF3D7_0621350,PF3D7_0724400,PF3D7_0729000,PF3D7_0904100,PF3D7_1104100,PF3D7_1110500,	2.8	2.15	2.33	0.04273491	0.166319629	1
GO:0015031	protein transport	60	3	PF3D7_0529300,PF3D7_0904100,PF3D7_1110500,	5	3.8	4.1	0.04363352	0.166776932	1
GO:0098771	inorganic ion homeostasis	26	2	PF3D7_1323200,PF3D7_1456800,	7.7	5.85	6.42	0.04516875	0.166776932	1
GO:0050801	ion homeostasis	26	2	PF3D7_1323200,PF3D7_1456800,	7.7	5.85	6.42	0.04516875	0.166776932	1
GO:0055080	cation homeostasis	26	2	PF3D7_1323200,PF3D7_1456800,	7.7	5.85	6.42	0.04516875	0.166776932	1
GO:0051649	establishment of localization in cell	252	7	PF3D7_0515300,PF3D7_0621350,PF3D7_0724400,PF3D7_0729000,PF3D7_0904100,PF3D7_1104100,PF3D7_1110500,	2.8	2.11	2.29	0.04595008	0.167514219	1
GO:1902600	proton transmembrane transport	27	2	PF3D7_1323200,PF3D7_1456800,	7.4	5.63	6.17	0.04837729	0.174158255	1

University of Ghana http://ugspace.ug.edu.gh

Supplementary Table 5.7 Gene ontology tabular summary of module 7

University of Ghana http://ugspace.ug.edu.gh

ID	Name	Bgd count	Result count	Result gene list	Pct of bgd	Fold enrichment	Odds ratio	P-value	Benjamini
GO:0020013	modulation by symbiont of host erythrocyte aggregation	190	77	PF3D7_0100100,PF3D7_0101600,PF3D7_0115700,PF3D7_0200400,PF3D7_0200500,PF3D7_0200600,PF3D7_0201300,PF3D7_0300700,PF3D7_0324800,PF3D7_0400100,PF3D7_0400400,PF3D7_0400500,PF3D7_0400900,PF3D7_0401400,PF3D7_0402600,PF3D7_0412400,PF3D7_0412700,PF3D7_0413100,PF3D7_0413200,PF3D7_0413300,PF3D7_0420700,PF3D7_0421300,PF3D7_0425500,PF3D7_0425800,PF3D7_0600200,PF3D7_0617400,PF3D7_0631900,PF3D7_0632100,PF3D7_0632500,PF3D7_0632800,PF3D7_0700500,PF3D7_0701800,PF3D7_0712000,PF3D7_0712300,PF3D7_0712400,PF3D7_0712600,PF3D7_0712800,PF3D7_0712900,PF3D7_0713000,PF3D7_0733000,PF3D7_0800200,PF3D7_0800300,PF3D7_0800500,PF3D7_0808600,PF3D7_0808700,PF3D7_0808800,PF3D7_0808900,PF3D7_0809100,PF3D7_0833000,PF3D7_0901400,PF3D7_0937300,PF3D7_0937500,PF3D7_0937800,PF3D7_1000100,PF3D7_1000400,PF3D7_1000500,PF3D7_1040200,PF3D7_1040300,PF3D7_1041200,PF3D7_1041300,PF3D7_1100100,PF3D7_1100200,PF3D7_1101300,PF3D7_1150400,PF3D7_1200100,PF3D7_1200400,PF3D7_1200500,PF3D7_1240300,PF3D7_1240600,PF3D7_1253700,PF3D7_1254100,PF3D7_1254300,PF3D7_1300300,PF3D7_1372700,PF3D7_1373400,PF3D7_1400700,PF3D7_1479700,	40.5	12.98	41.82	5.78E-73	1.17E-70
GO:0044068	modulation by symbiont of host cellular process	192	77	PF3D7_0100100,PF3D7_0101600,PF3D7_0115700,PF3D7_0200400,PF3D7_0200500,PF3D7_0200600,PF3D7_0201300,PF3D7_0300700,PF3D7_0324800,PF3D7_0400100,PF3D7_0400400,PF3D7_0400500,PF3D7_0400900,PF3D7_0401400,PF3D7_0402600,PF3D7_0412400,PF3D7_0412700,PF3D7_0413100,PF3D7_0413200,PF3D7_0413300,PF3D7_0420700,PF3D7_0421300,PF3D7_0425500,PF3D7_0425800,PF3D7_0600200,PF3D7_0617400,PF3D7_0631900,PF3D7_0632100,PF3D7_0632500,PF3D7_0632800,PF3D7_0700500,PF3D7_0701800,PF3D7_0712000,PF3D7_0712300,PF3D7_0712400,PF3D7_0712600,PF3D7_0712800,PF3D7_0712900,PF3D7_0713000,PF3D7_0733000,PF3D7_0800200,PF3D7_0800300,PF3D7_0800500,PF3D7_0808600,PF3D7_0808700,PF3D7_0808800,PF3D7_0808900,PF3D7_0809100,PF3D7_0833000,PF3D7_0901400,PF3D7_0937300,PF3D7_0937500,PF3D7_0937800,PF3D7_1000100,PF3D7_1000400,PF3D7_1000500,PF3D7_1040200,PF3D7_1040300,PF3D7_1041200,PF3D7_1041300,PF3D7_1100100,PF3D7_1100200,PF3D7_1101300,PF3D7_1150400,PF3D7_1200100,PF3D7_1200400,PF3D7_1200500,PF3D7_1240300,PF3D7_1240600,PF3D7_1253700,PF3D7_1254100,PF3D7_1254300,PF3D7_1300300,PF3D7_1372700,PF3D7_1373400,PF3D7_1400700,PF3D7_1479700,	40.1	12.84	41.08	1.57E-72	1.58E-70
GO:0020033	antigenic variation	202	78	PF3D7_0100100,PF3D7_0101600,PF3D7_0114700,PF3D7_0115700,PF3D7_0200100,PF3D7_0200500,PF3D7_0200600,PF3D7_0300700,PF3D7_0324800,PF3D7_0400100,PF3D7_0400400,PF3D7_0400500,PF3D7_0400900,PF3D7_0401400,PF3D7_0412400,PF3D7_0412700,PF3D7_0413100,PF3D7_0413200,PF3D7_0413300,PF3D7_0420700,PF3D7_0421200,PF3D7_0421300,PF3D7_0425800,PF3D7_0532900,PF3D7_0600200,PF3D7_0617400,PF3D7_0631800,PF3D7_0632100,PF3D7_0632500,PF3D7_0632800,PF3D7_0700500,PF3D7_0701800,PF3D7_0712000,PF3D7_0712300,PF3D7_0712400,PF3D7_0712600,PF3D7_0712800,PF3D7_0712900,PF3D7_0713000,PF3D7_0733000,PF3D7_0800200,PF3D7_0800300,PF3D7_0800500,PF3D7_0808600,PF3D7_0808700,PF3D7_0808800,PF3D7_0808900,PF3D7_0809100,PF3D7_0833000,PF3D7_0901400,PF3D7_0937300,PF3D7_0937500,PF3D7_0937800,PF3D7_1000100,PF3D7_1000400,PF3D7_1000500,PF3D7_1040300,PF3D7_1040800,PF3D7_1041100,PF3D7_1041200,PF3D7_1041300,PF3D7_1100100,PF3D7_1100200,PF3D7_1101300,PF3D7_1149800,PF3D7_1150400,PF3D7_1200100,PF3D7_1200300,PF3D7_1200400,PF3D7_1200500,PF3D7_1240300,PF3D7_1240600,PF3D7_1253700,PF3D7_1254000,PF3D7_1300300,PF3D7_1372700,PF3D7_1373400,PF3D7_1479700,	38.6	12.37	39.03	4.89E-72	3.29E-70
GO:0042783	evasion of host immune response	205	78	PF3D7_0100100,PF3D7_0101600,PF3D7_0114700,PF3D7_0115700,PF3D7_0200100,PF3D7_0200500,PF3D7_0200600,PF3D7_0300700,PF3D7_0324800,PF3D7_0400100,PF3D7_0400400,PF3D7_0400500,PF3D7_0400900,PF3D7_0401400,PF3D7_0412400,PF3D7_0412700,PF3D7_0413100,PF3D7_0413200,PF3D7_0413300,PF3D7_0420700,PF3D7_0421200,PF3D7_0421300,PF3D7_0425800,PF3D7_0532900,PF3D7_0600200,PF3D7_0617400,PF3D7_0631800,PF3D7_0632100,PF3D7_0632500,PF3D7_0632800,PF3D7_0700500,PF3D7_0701800,PF3D7_0712000,PF3D7_0712300,PF3D7_0712400,PF3D7_0712600,PF3D7_0712800,PF3D7_0712900,PF3D7_0713000,PF3D7_0733000,PF3D7_0800200,PF3D7_0800300,PF3D7_0800500,PF3D7_0808600,PF3D7_0808700,PF3D7_0808800,PF3D7_0808900,PF3D7_0809100,PF3D7_0833000,PF3D7_0901400,PF3D7_0937300,PF3D7_0937500,PF3D7_0937800,PF3D7_1000100,PF3D7_1000400,PF3D7_1000500,PF3D7_1040300,PF3D7_1040800,PF3D7_1041100,PF3D7_1041200,PF3D7_1041300,PF3D7_1100100,PF3D7_1100200,PF3D7_1101300,PF3D7_1149800,PF3D7_1150400,PF3D7_1200100,PF3D7_1200300,PF3D7_1200400,PF3D7_1200500,PF3D7_1240300,PF3D7_1240600,PF3D7_1253700,PF3D7_1254000,PF3D7_1300300,PF3D7_1372700,PF3D7_1373400,PF3D7_1479700,	38	12.19	38.09	1.98E-71	1.00E-69
GO:0052220	response to host defenses	208	78	PF3D7_0100100,PF3D7_0101600,PF3D7_0114700,PF3D7_0115700,PF3D7_0200100,PF3D7_0200500,PF3D7_0200600,PF3D7_0300700,PF3D7_0324800,PF3D7_0400100,PF3D7_0400400,PF3D7_0400500,PF3D7_0400900,PF3D7_0401400,PF3D7_0412400,PF3D7_0412700,PF3D7_0413100,PF3D7_0413200,PF3D7_0413300,PF3D7_0420700,PF3D7_0421200,PF3D7_0421300,PF3D7_0425800,PF3D7_0532900,PF3D7_0600200,PF3D7_0617400,PF3D7_0631800,PF3D7_0632100,PF3D7_0632500,PF3D7_0632800,PF3D7_0700500,PF3D7_0701800,PF3D7_0712000,PF3D7_0712300,PF3D7_0712400,PF3D7_0712600,PF3D7_0712800,PF3D7_0712900,PF3D7_0713000,PF3D7_0733000,PF3D7_0800200,PF3D7_0800300,PF3D7_0800500,PF3D7_0808600,PF3D7_0808700,PF3D7_0808800,PF3D7_0808900,PF3D7_0809100,PF3D7_0833000,PF3D7_0901400,PF3D7_0937300,PF3D7_0937500,PF3D7_0937800,PF3D7_1000100,PF3D7_1000400,PF3D7_1000500,PF3D7_1040300,PF3D7_1040800,PF3D7_1041100,PF3D7_1041200,PF3D7_1041300,PF3D7_1100100,PF3D7_1100200,PF3D7_1101300,PF3D7_1149800,PF3D7_1150400,PF3D7_1200100,PF3D7_1200300,PF3D7_1200400,PF3D7_1200500,PF3D7_1240300,PF3D7_1240600,PF3D7_1253700,PF3D7_1254000,PF3D7_1300300,PF3D7_1372700,PF3D7_1373400,PF3D7_1479700,	37.5	12.01	37.18	7.80E-71	1.58E-69
GO:0052173	response to defenses of other organism	208	78	PF3D7_0100100,PF3D7_0101600,PF3D7_0114700,PF3D7_0115700,PF3D7_0200100,PF3D7_0200500,PF3D7_0200600,PF3D7_0300700,PF3D7_0324800,PF3D7_0400100,PF3D7_0400400,PF3D7_0400500,PF3D7_0400900,PF3D7_0401400,PF3D7_0412400,PF3D7_0412700,PF3D7_0413100,PF3D7_0413200,PF3D7_0413300,PF3D7_0420700,PF3D7_0421200,PF3D7_0421300,PF3D7_0425800,PF3D7_0532900,PF3D7_0600200,PF3D7_0617400,PF3D7_0631800,PF3D7_0632100,PF3D7_0632500,PF3D7_0632800,PF3D7_0700500,PF3D7_0701800,PF3D7_0712000,PF3D7_0712300,PF3D7_0712400,PF3D7_0712600,PF3D7_0712800,PF3D7_0712900,PF3D7_0713000,PF3D7_0733000,PF3D7_0800200,PF3D7_0800300,PF3D7_0800500,PF3D7_0808600,PF3D7_0808700,PF3D7_0808800,PF3D7_0808900,PF3D7_0809100,PF3D7_0833000,PF3D7_0901400,PF3D7_0937300,PF3D7_0937500,PF3D7_0937800,PF3D7_1000100,PF3D7_1000400,PF3D7_1000500,PF3D7_1040300,PF3D7_1040800,PF3D7_1041100,PF3D7_1041200,PF3D7_1041300,PF3D7_1100100,PF3D7_1100200,PF3D7_1101300,PF3D7_1149800,PF3D7_1150400,PF3D7_1200100,PF3D7_1200300,PF3D7_1200400,PF3D7_1200500,PF3D7_1240300,PF3D7_1240600,PF3D7_1253700,PF3D7_1254000,PF3D7_1300300,PF3D7_1372700,PF3D7_1373400,PF3D7_1479700,	37.5	12.01	37.18	7.80E-71	1.58E-69

GO:0052572	response to host immune response	208	78	PF3D7_0100100,PF3D7_0101600,PF3D7_0114700,PF3D7_0115700,PF3D7_0200100,PF3D7_0200500,PF3D7_0200600,PF3D7_0300700,PF3D7_0324800,PF3D7_0400100,PF3D7_0400400,PF3D7_0400500,PF3D7_0400900,PF3D7_0401400,PF3D7_0412400,PF3D7_0412700,PF3D7_0413100,PF3D7_0413200,PF3D7_0413300,PF3D7_0420700,PF3D7_0421200,PF3D7_0421300,PF3D7_0425800,PF3D7_0532900,PF3D7_0600200,PF3D7_0617400,PF3D7_0631800,PF3D7_0632100,PF3D7_0632500,PF3D7_0632800,PF3D7_0700500,PF3D7_0701800,PF3D7_0712000,PF3D7_0712300,PF3D7_0712400,PF3D7_0712600,PF3D7_0712800,PF3D7_0712900,PF3D7_0713000,PF3D7_0733000,PF3D7_0800200,PF3D7_0800300,PF3D7_0800500,PF3D7_0808600,PF3D7_0808700,PF3D7_0808800,PF3D7_0808900,PF3D7_0809100,PF3D7_0833000,PF3D7_0901400,PF3D7_0937300,PF3D7_0937500,PF3D7_0937800,PF3D7_1000100,PF3D7_1000400,PF3D7_1000500,PF3D7_1040300,PF3D7_1040800,PF3D7_1041100,PF3D7_1041200,PF3D7_1041300,PF3D7_1100100,PF3D7_1100200,PF3D7_1101300,PF3D7_1149800,PF3D7_1150400,PF3D7_1200100,PF3D7_1200300,PF3D7_1200400,PF3D7_1200500,PF3D7_1240300,PF3D7_1240600,PF3D7_1253700,PF3D7_1254000,PF3D7_1300300,PF3D7_1372700,PF3D7_1373400,PF3D7_1479700,	37.5	12.01	37.18	7.80E-71	1.58E-69
GO:0075136	response to host	208	78	PF3D7_0100100,PF3D7_0101600,PF3D7_0114700,PF3D7_0115700,PF3D7_0200100,PF3D7_0200500,PF3D7_0200600,PF3D7_0300700,PF3D7_0324800,PF3D7_0400100,PF3D7_0400400,PF3D7_0400500,PF3D7_0400900,PF3D7_0401400,PF3D7_0412400,PF3D7_0412700,PF3D7_0413100,PF3D7_0413200,PF3D7_0413300,PF3D7_0420700,PF3D7_0421200,PF3D7_0421300,PF3D7_0425800,PF3D7_0532900,PF3D7_0600200,PF3D7_0617400,PF3D7_0631800,PF3D7_0632100,PF3D7_0632500,PF3D7_0632800,PF3D7_0700500,PF3D7_0701800,PF3D7_0712000,PF3D7_0712300,PF3D7_0712400,PF3D7_0712600,PF3D7_0712800,PF3D7_0712900,PF3D7_0713000,PF3D7_0733000,PF3D7_0800200,PF3D7_0800300,PF3D7_0800500,PF3D7_0808600,PF3D7_0808700,PF3D7_0808800,PF3D7_0808900,PF3D7_0809100,PF3D7_0833000,PF3D7_0901400,PF3D7_0937300,PF3D7_0937500,PF3D7_0937800,PF3D7_1000100,PF3D7_1000400,PF3D7_1000500,PF3D7_1040300,PF3D7_1040800,PF3D7_1041100,PF3D7_1041200,PF3D7_1041300,PF3D7_1100100,PF3D7_1100200,PF3D7_1101300,PF3D7_1149800,PF3D7_1150400,PF3D7_1200100,PF3D7_1200300,PF3D7_1200400,PF3D7_1200500,PF3D7_1240300,PF3D7_1240600,PF3D7_1253700,PF3D7_1254000,PF3D7_1300300,PF3D7_1372700,PF3D7_1373400,PF3D7_1479700,	37.5	12.01	37.18	7.80E-71	1.58E-69
GO:0051707	response to other organism	208	78	PF3D7_0100100,PF3D7_0101600,PF3D7_0114700,PF3D7_0115700,PF3D7_0200100,PF3D7_0200500,PF3D7_0200600,PF3D7_0300700,PF3D7_0324800,PF3D7_0400100,PF3D7_0400400,PF3D7_0400500,PF3D7_0400900,PF3D7_0401400,PF3D7_0412400,PF3D7_0412700,PF3D7_0413100,PF3D7_0413200,PF3D7_0413300,PF3D7_0420700,PF3D7_0421200,PF3D7_0421300,PF3D7_0425800,PF3D7_0532900,PF3D7_0600200,PF3D7_0617400,PF3D7_0631800,PF3D7_0632100,PF3D7_0632500,PF3D7_0632800,PF3D7_0700500,PF3D7_0701800,PF3D7_0712000,PF3D7_0712300,PF3D7_0712400,PF3D7_0712600,PF3D7_0712800,PF3D7_0712900,PF3D7_0713000,PF3D7_0733000,PF3D7_0800200,PF3D7_0800300,PF3D7_0800500,PF3D7_0808600,PF3D7_0808700,PF3D7_0808800,PF3D7_0808900,PF3D7_0809100,PF3D7_0833000,PF3D7_0901400,PF3D7_0937300,PF3D7_0937500,PF3D7_0937800,PF3D7_1000100,PF3D7_1000400,PF3D7_1000500,PF3D7_1040300,PF3D7_1040800,PF3D7_1041100,PF3D7_1041200,PF3D7_1041300,PF3D7_1100100,PF3D7_1100200,PF3D7_1101300,PF3D7_1149800,PF3D7_1150400,PF3D7_1200100,PF3D7_1200300,PF3D7_1200400,PF3D7_1200500,PF3D7_1240300,PF3D7_1240600,PF3D7_1253700,PF3D7_1254000,PF3D7_1300300,PF3D7_1372700,PF3D7_1373400,PF3D7_1479700,	37.5	12.01	37.18	7.80E-71	1.58E-69
GO:0043207	response to external biotic stimulus	208	78	PF3D7_0100100,PF3D7_0101600,PF3D7_0114700,PF3D7_0115700,PF3D7_0200100,PF3D7_0200500,PF3D7_0200600,PF3D7_0300700,PF3D7_0324800,PF3D7_0400100,PF3D7_0400400,PF3D7_0400500,PF3D7_0400900,PF3D7_0401400,PF3D7_0412400,PF3D7_0412700,PF3D7_0413100,PF3D7_0413200,PF3D7_0413300,PF3D7_0420700,PF3D7_0421200,PF3D7_0421300,PF3D7_0425800,PF3D7_0532900,PF3D7_0600200,PF3D7_0617400,PF3D7_0631800,PF3D7_0632100,PF3D7_0632500,PF3D7_0632800,PF3D7_0700500,PF3D7_0701800,PF3D7_0712000,PF3D7_0712300,PF3D7_0712400,PF3D7_0712600,PF3D7_0712800,PF3D7_0712900,PF3D7_0713000,PF3D7_0733000,PF3D7_0800200,PF3D7_0800300,PF3D7_0800500,PF3D7_0808600,PF3D7_0808700,PF3D7_0808800,PF3D7_0808900,PF3D7_0809100,PF3D7_0833000,PF3D7_0901400,PF3D7_0937300,PF3D7_0937500,PF3D7_0937800,PF3D7_1000100,PF3D7_1000400,PF3D7_1000500,PF3D7_1040300,PF3D7_1040800,PF3D7_1041100,PF3D7_1041200,PF3D7_1041300,PF3D7_1100100,PF3D7_1100200,PF3D7_1101300,PF3D7_1149800,PF3D7_1150400,PF3D7_1200100,PF3D7_1200300,PF3D7_1200400,PF3D7_1200500,PF3D7_1240300,PF3D7_1240600,PF3D7_1253700,PF3D7_1254000,PF3D7_1300300,PF3D7_1372700,PF3D7_1373400,PF3D7_1479700,	37.5	12.01	37.18	7.80E-71	1.58E-69
GO:0044003	modulation by symbiont of host process	205	77	PF3D7_0100100,PF3D7_0101600,PF3D7_0115700,PF3D7_0200400,PF3D7_0200500,PF3D7_0200600,PF3D7_0201300,PF3D7_0300700,PF3D7_0324800,PF3D7_0400100,PF3D7_0400400,PF3D7_0400500,PF3D7_0400900,PF3D7_0401400,PF3D7_0402600,PF3D7_0412400,PF3D7_0412700,PF3D7_0413100,PF3D7_0413200,PF3D7_0413300,PF3D7_0420700,PF3D7_0421300,PF3D7_0425500,PF3D7_0425800,PF3D7_0600200,PF3D7_0617400,PF3D7_0631900,PF3D7_0632100,PF3D7_0632500,PF3D7_0632800,PF3D7_0700500,PF3D7_0701800,PF3D7_0712000,PF3D7_0712300,PF3D7_0712400,PF3D7_0712600,PF3D7_0712800,PF3D7_0712900,PF3D7_0713000,PF3D7_0733000,PF3D7_0800200,PF3D7_0800300,PF3D7_0800500,PF3D7_0808600,PF3D7_0808700,PF3D7_0808800,PF3D7_0808900,PF3D7_0809100,PF3D7_0833000,PF3D7_0901400,PF3D7_0937300,PF3D7_0937500,PF3D7_0937800,PF3D7_1000100,PF3D7_1000400,PF3D7_1000500,PF3D7_1040200,PF3D7_1040300,PF3D7_1041200,PF3D7_1041300,PF3D7_1100100,PF3D7_1100200,PF3D7_1101300,PF3D7_1150400,PF3D7_1200100,PF3D7_1200400,PF3D7_1200500,PF3D7_1240300,PF3D7_1240600,PF3D7_1253700,PF3D7_1254100,PF3D7_1254300,PF3D7_1300300,PF3D7_1372700,PF3D7_1373400,PF3D7_1400700,PF3D7_1479700,	37.6	12.03	36.8	7.39E-70	1.36E-68
GO:0044406	adhesion of symbiont to host	176	70	PF3D7_0100100,PF3D7_0101600,PF3D7_0115700,PF3D7_0200100,PF3D7_0200500,PF3D7_0200600,PF3D7_0300700,PF3D7_0324800,PF3D7_0400100,PF3D7_0400400,PF3D7_0400500,PF3D7_0400900,PF3D7_0401400,PF3D7_0412400,PF3D7_0412700,PF3D7_0413100,PF3D7_0413200,PF3D7_0413300,PF3D7_0420700,PF3D7_0421300,PF3D7_0425800,PF3D7_0600200,PF3D7_0617400,PF3D7_0632100,PF3D7_0632500,PF3D7_0632800,PF3D7_0700500,PF3D7_0701800,PF3D7_0712000,PF3D7_0712300,PF3D7_0712400,PF3D7_0712600,PF3D7_0712800,PF3D7_0712900,PF3D7_0713000,PF3D7_0733000,PF3D7_0800200,PF3D7_0800300,PF3D7_0800500,PF3D7_0808600,PF3D7_0808700,PF3D7_0808800,PF3D7_0808900,PF3D7_0809100,PF3D7_0831700,PF3D7_0833000,PF3D7_0901400,PF3D7_0937300,PF3D7_0937500,PF3D7_0937800,PF3D7_1000100,PF3D7_1000400,PF3D7_1000500,PF3D7_1040300,PF3D7_1041200,PF3D7_1041300,PF3D7_1100100,PF3D7_1100200,PF3D7_1101300,PF3D7_1150400,PF3D7_1200100,PF3D7_1200400,PF3D7_1200500,PF3D7_1240300,PF3D7_1240600,PF3D7_1253700,PF3D7_1300300,PF3D7_1372700,PF3D7_1373400,PF3D7_1479700,	39.8	12.74	37.13	8.14E-65	1.26E-63
GO:0020035	cytoadherence to microvasculature, mediated by symbiont protein	176	70	PF3D7_0100100,PF3D7_0101600,PF3D7_0115700,PF3D7_0200100,PF3D7_0200500,PF3D7_0200600,PF3D7_0300700,PF3D7_0324800,PF3D7_0400100,PF3D7_0400400,PF3D7_0400500,PF3D7_0400900,PF3D7_0401400,PF3D7_0412400,PF3D7_0412700,PF3D7_0413100,PF3D7_0413200,PF3D7_0413300,PF3D7_0420700,PF3D7_0421300,PF3D7_0425800,PF3D7_0600200,PF3D7_0617400,PF3D7_0632100,PF3D7_0632500,PF3D7_0632800,PF3D7_0700500,PF3D7_0701800,PF3D7_0712000,PF3D7_0712300,PF3D7_0712400,PF3D7_0712600,PF3D7_0712800,PF3D7_0712900,PF3D7_0713000,PF3D7_0733000,PF3D7_0800200,PF3D7_0800300,PF3D7_0800500,PF3D7_0808600,PF3D7_0808700,PF3D7_0808800,PF3D7_0808900,PF3D7_0809100,PF3D7_0831700,PF3D7_0833000,PF3D7_0901400,PF3D7_0937300,PF3D7_0937500,PF3D7_0937800,PF3D7_1000100,PF3D7_1000400,PF3D7_1000500,PF3D7_1040300,PF3D7_1041200,PF3D7_1041300,PF3D7_1100100,PF3D7_1100200,PF3D7_1101300,PF3D7_1150400,PF3D7_1200100,PF3D7_1200400,PF3D7_1200500,PF3D7_1240300,PF3D7_1240600,PF3D7_1253700,PF3D7_1300300,PF3D7_1372700,PF3D7_1373400,PF3D7_1479700,	39.8	12.74	37.13	8.14E-65	1.26E-63

University of Ghana http://ugspace.ug.edu.gh

GO:0022610	biological adhesion	195	71	PF3D7_0100100,PF3D7_0101600,PF3D7_0115700,PF3D7_0200100,PF3D7_0200500,PF3D7_0200600,PF3D7_0300700,PF3D7_0324800,PF3D7_0400100,PF3D7_0400400,PF3D7_0400500,PF3D7_0400900,PF3D7_0401400,PF3D7_0412400,PF3D7_0412700,PF3D7_0413100,PF3D7_0413200,PF3D7_0413300,PF3D7_0420700,PF3D7_0421300,PF3D7_0425800,PF3D7_0600200,PF3D7_0617400,PF3D7_0632100,PF3D7_0632500,PF3D7_0632800,PF3D7_0700500,PF3D7_0701800,PF3D7_0712000,PF3D7_0712300,PF3D7_0712400,PF3D7_0712600,PF3D7_0712800,PF3D7_0712900,PF3D7_0713000,PF3D7_0733000,PF3D7_0800200,PF3D7_0800300,PF3D7_0800500,PF3D7_0808600,PF3D7_0808700,PF3D7_0808800,PF3D7_0808900,PF3D7_0809100,PF3D7_0831700,PF3D7_0833000,PF3D7_0900100,PF3D7_0901400,PF3D7_0937300,PF3D7_0937500,PF3D7_0937800,PF3D7_1000100,PF3D7_1000400,PF3D7_1000500,PF3D7_1040300,PF3D7_1041200,PF3D7_1041300,PF3D7_1100100,PF3D7_1100200,PF3D7_1101300,PF3D7_1150400,PF3D7_1200100,PF3D7_1200400,PF3D7_1200500,PF3D7_1240300,PF3D7_1240600,PF3D7_1253700,PF3D7_1300300,PF3D7_1372700,PF3D7_1373400,PF3D7_1479700,	36.4	11.66	32.46	1.46E-62	2.11E-61
GO:0051701	biological process involved in interaction with host	382	89	PF3D7_0100100,PF3D7_0101600,PF3D7_0114700,PF3D7_0115700,PF3D7_0200100,PF3D7_0200400,PF3D7_0200500,PF3D7_0200600,PF3D7_0201300,PF3D7_0300700,PF3D7_0324800,PF3D7_0400100,PF3D7_0400400,PF3D7_0400500,PF3D7_0400900,PF3D7_0401400,PF3D7_0402600,PF3D7_0412400,PF3D7_0412700,PF3D7_0413100,PF3D7_0413200,PF3D7_0413300,PF3D7_0420700,PF3D7_0421200,PF3D7_0421300,PF3D7_0424400,PF3D7_0425500,PF3D7_0425800,PF3D7_0532900,PF3D7_0600200,PF3D7_0617400,PF3D7_0631800,PF3D7_0631900,PF3D7_0632100,PF3D7_0632500,PF3D7_0632800,PF3D7_0700500,PF3D7_0701800,PF3D7_0712000,PF3D7_0712300,PF3D7_0712400,PF3D7_0712600,PF3D7_0712800,PF3D7_0712900,PF3D7_0713000,PF3D7_0733000,PF3D7_0800200,PF3D7_0800300,PF3D7_0800500,PF3D7_0808600,PF3D7_0808700,PF3D7_0808800,PF3D7_0808900,PF3D7_0809100,PF3D7_0833000,PF3D7_0901400,PF3D7_0937300,PF3D7_0937500,PF3D7_0937800,PF3D7_1000100,PF3D7_1000400,PF3D7_1000500,PF3D7_1040200,PF3D7_1040300,PF3D7_1040800,PF3D7_1041100,PF3D7_1041200,PF3D7_1041300,PF3D7_1100100,PF3D7_1100200,PF3D7_1101300,PF3D7_1149800,PF3D7_1150400,PF3D7_1200100,PF3D7_1200300,PF3D7_1200400,PF3D7_1200500,PF3D7_1240300,PF3D7_1240600,PF3D7_1253700,PF3D7_1254000,PF3D7_1254100,PF3D7_1254300,PF3D7_1300300,PF3D7_1372700,PF3D7_1373400,PF3D7_1400700,PF3D7_1418100,PF3D7_1479700,	23.3	7.46	21.33	1.05E-61	1.41E-60
GO:0044403	biological process involved in symbiotic interaction	397	90	PF3D7_0100100,PF3D7_0101600,PF3D7_0114700,PF3D7_0115700,PF3D7_0200100,PF3D7_0200400,PF3D7_0200500,PF3D7_0200600,PF3D7_0201300,PF3D7_0300700,PF3D7_0324800,PF3D7_0400100,PF3D7_0400400,PF3D7_0400500,PF3D7_0400900,PF3D7_0401400,PF3D7_0402600,PF3D7_0412400,PF3D7_0412700,PF3D7_0413100,PF3D7_0413200,PF3D7_0413300,PF3D7_0420700,PF3D7_0421200,PF3D7_0421300,PF3D7_0424400,PF3D7_0425500,PF3D7_0425800,PF3D7_0532900,PF3D7_0600200,PF3D7_0617400,PF3D7_0631800,PF3D7_0631900,PF3D7_0632100,PF3D7_0632500,PF3D7_0632800,PF3D7_0700500,PF3D7_0701800,PF3D7_0712000,PF3D7_0712300,PF3D7_0712400,PF3D7_0712600,PF3D7_0712800,PF3D7_0712900,PF3D7_0713000,PF3D7_0733000,PF3D7_0800200,PF3D7_0800300,PF3D7_0800500,PF3D7_0808600,PF3D7_0808700,PF3D7_0808800,PF3D7_0808900,PF3D7_0809100,PF3D7_0831700,PF3D7_0833000,PF3D7_0901400,PF3D7_0937300,PF3D7_0937500,PF3D7_0937800,PF3D7_1000100,PF3D7_1000400,PF3D7_1000500,PF3D7_1040200,PF3D7_1040300,PF3D7_1040800,PF3D7_1041100,PF3D7_1041200,PF3D7_1041300,PF3D7_1100100,PF3D7_1100200,PF3D7_1101300,PF3D7_1149800,PF3D7_1150400,PF3D7_1200100,PF3D7_1200300,PF3D7_1200400,PF3D7_1200500,PF3D7_1240300,PF3D7_1240600,PF3D7_1253700,PF3D7_1254000,PF3D7_1254100,PF3D7_1254300,PF3D7_1300300,PF3D7_1372700,PF3D7_1373400,PF3D7_1400700,PF3D7_1418100,PF3D7_1479700,	22.7	7.26	20.85	2.02E-61	2.55E-60
GO:0044419	biological process involved in interspecies interaction between organisms	399	90	PF3D7_0100100,PF3D7_0101600,PF3D7_0114700,PF3D7_0115700,PF3D7_0200100,PF3D7_0200400,PF3D7_0200500,PF3D7_0200600,PF3D7_0201300,PF3D7_0300700,PF3D7_0324800,PF3D7_0400100,PF3D7_0400400,PF3D7_0400500,PF3D7_0400900,PF3D7_0401400,PF3D7_0402600,PF3D7_0412400,PF3D7_0412700,PF3D7_0413100,PF3D7_0413200,PF3D7_0413300,PF3D7_0420700,PF3D7_0421200,PF3D7_0421300,PF3D7_0424400,PF3D7_0425500,PF3D7_0425800,PF3D7_0532900,PF3D7_0600200,PF3D7_0617400,PF3D7_0631800,PF3D7_0631900,PF3D7_0632100,PF3D7_0632500,PF3D7_0632800,PF3D7_0700500,PF3D7_0701800,PF3D7_0712000,PF3D7_0712300,PF3D7_0712400,PF3D7_0712600,PF3D7_0712800,PF3D7_0712900,PF3D7_0713000,PF3D7_0733000,PF3D7_0800200,PF3D7_0800300,PF3D7_0800500,PF3D7_0808600,PF3D7_0808700,PF3D7_0808800,PF3D7_0808900,PF3D7_0809100,PF3D7_0831700,PF3D7_0833000,PF3D7_0901400,PF3D7_0937300,PF3D7_0937500,PF3D7_0937800,PF3D7_1000100,PF3D7_1000400,PF3D7_1000500,PF3D7_1040200,PF3D7_1040300,PF3D7_1040800,PF3D7_1041100,PF3D7_1041200,PF3D7_1041300,PF3D7_1100100,PF3D7_1100200,PF3D7_1101300,PF3D7_1149800,PF3D7_1150400,PF3D7_1200100,PF3D7_1200300,PF3D7_1200400,PF3D7_1200500,PF3D7_1240300,PF3D7_1240600,PF3D7_1253700,PF3D7_1254000,PF3D7_1254100,PF3D7_1254300,PF3D7_1300300,PF3D7_1372700,PF3D7_1373400,PF3D7_1400700,PF3D7_1418100,PF3D7_1479700,	22.6	7.22	20.7	3.27E-61	3.89E-60
GO:0009405	obsolete pathogenesis	75	45	PF3D7_0100100,PF3D7_0113800,PF3D7_0115700,PF3D7_0200100,PF3D7_0300100,PF3D7_0324900,PF3D7_0400100,PF3D7_0400400,PF3D7_0412400,PF3D7_0412700,PF3D7_0413100,PF3D7_0420700,PF3D7_0421300,PF3D7_0425800,PF3D7_0600200,PF3D7_0617400,PF3D7_0632500,PF3D7_0632800,PF3D7_0700100,PF3D7_0712000,PF3D7_0712300,PF3D7_0712400,PF3D7_0712600,PF3D7_0712800,PF3D7_0712900,PF3D7_0733000,PF3D7_0800200,PF3D7_0800300,PF3D7_0808600,PF3D7_0808700,PF3D7_0809100,PF3D7_0833500,PF3D7_0900100,PF3D7_0937800,PF3D7_1000100,PF3D7_1041300,PF3D7_1100100,PF3D7_1100200,PF3D7_1150400,PF3D7_1200100,PF3D7_1200400,PF3D7_1240300,PF3D7_1240600,PF3D7_1300300,PF3D7_1373500,	60	19.22	65.69	6.21E-51	6.97E-50
GO:0008150	biological process	662	95	PF3D7_0100100,PF3D7_0101600,PF3D7_0114700,PF3D7_0115700,PF3D7_0200100,PF3D7_0200400,PF3D7_0200500,PF3D7_0200600,PF3D7_0201300,PF3D7_0300700,PF3D7_0324800,PF3D7_0400100,PF3D7_0400400,PF3D7_0400500,PF3D7_0400900,PF3D7_0401400,PF3D7_0402600,PF3D7_0412400,PF3D7_0412700,PF3D7_0413100,PF3D7_0413200,PF3D7_0413300,PF3D7_0420700,PF3D7_0421200,PF3D7_0421300,PF3D7_0424400,PF3D7_0425500,PF3D7_0425800,PF3D7_0532900,PF3D7_0600200,PF3D7_0617400,PF3D7_0631800,PF3D7_0631900,PF3D7_0632100,PF3D7_0632500,PF3D7_0632800,PF3D7_0700500,PF3D7_0701800,PF3D7_0712000,PF3D7_0712300,PF3D7_0712400,PF3D7_0712600,PF3D7_0712800,PF3D7_0712900,PF3D7_0713000,PF3D7_0718300,PF3D7_0733000,PF3D7_0800200,PF3D7_0800300,PF3D7_0800500,PF3D7_0808600,PF3D7_0808700,PF3D7_0808800,PF3D7_0808900,PF3D7_0809100,PF3D7_0831700,PF3D7_0833000,PF3D7_0900100,PF3D7_0901400,PF3D7_0911300,PF3D7_0927000,PF3D7_0937300,PF3D7_0937500,PF3D7_0937800,PF3D7_1000100,PF3D7_1000400,PF3D7_1000500,PF3D7_1040200,PF3D7_1040300,PF3D7_1040800,PF3D7_1041100,PF3D7_1041200,PF3D7_1041300,PF3D7_1100100,PF3D7_1100200,PF3D7_1101300,PF3D7_1149800,PF3D7_1150400,PF3D7_1200100,PF3D7_1200300,PF3D7_1200400,PF3D7_1200500,PF3D7_1240300,PF3D7_1240600,PF3D7_1253700,PF3D7_1254000,PF3D7_1254100,PF3D7_1254300,PF3D7_1300300,PF3D7_1372700,PF3D7_1373400,PF3D7_1400700,PF3D7_1418100,PF3D7_1475400,PF3D7_1479700,	14.4	4.6	12.2	2.44E-46	2.59E-45
GO:0098609	cell-cell adhesion	62	39	PF3D7_0100100,PF3D7_0115700,PF3D7_0200100,PF3D7_0400100,PF3D7_0400400,PF3D7_0412400,PF3D7_0412700,PF3D7_0413100,PF3D7_0420700,PF3D7_0421300,PF3D7_0425800,PF3D7_0600200,PF3D7_0617400,PF3D7_0632500,PF3D7_0632800,PF3D7_0712000,PF3D7_0712300,PF3D7_0712400,PF3D7_0712600,PF3D7_0712800,PF3D7_0712900,PF3D7_0733000,PF3D7_0800200,PF3D7_0800300,PF3D7_0808600,PF3D7_0808700,PF3D7_0809100,PF3D7_0900100,PF3D7_0937800,PF3D7_1000100,PF3D7_1041300,PF3D7_1100100,PF3D7_1100200,PF3D7_1150400,PF3D7_1200100,PF3D7_1200400,PF3D7_1240300,PF3D7_1240600,PF3D7_1300300,	62.9	20.15	70.42	3.75E-45	3.78E-44

University of Ghana http://ugspace.ug.edu.gh

GO:0007155	cell adhesion	70	39	PF3D7_0100100,PF3D7_0115700,PF3D7_0200100,PF3D7_0400100,PF3D7_0400400,PF3D7_0412400,PF3D7_0412700,PF3D7_0413100,PF3D7_0420700,PF3D7_0421300,PF3D7_0425800,PF3D7_0600200,PF3D7_0617400,PF3D7_0632500,PF3D7_0632800,PF3D7_0712000,PF3D7_0712300,PF3D7_0712400,PF3D7_0712600,PF3D7_0712800,PF3D7_0712900,PF3D7_0733000,PF3D7_0800200,PF3D7_0800300,PF3D7_0808600,PF3D7_0808700,PF3D7_0809100,PF3D7_0900100,PF3D7_0937800,PF3D7_1000100,PF3D7_1041300,PF3D7_1100100,PF3D7_1100200,PF3D7_1150400,PF3D7_1200100,PF3D7_1200400,PF3D7_1240300,PF3D7_1240600,PF3D7_1300300,	55.7	17.84	52.16	3.72E-42	3.58E-41
GO:0030522	intracellular receptor signaling pathway	4	3	PF3D7_0718300,PF3D7_0911300,PF3D7_1475400,	75	24.02	94.93	0.0001167 1	0.00107157 9
GO:0042026	protein refolding	9	2	PF3D7_0409400,PF3D7_0831700,	22.2	7.12	8.97	0.0301898 7	0.20346171 2
GO:0061572	actin filament bundle organization	1	1	PF3D7_1036400,	100	32.03	inf	0.0312243 2	0.20346171 2
GO:0006771	riboflavin metabolic process	1	1	PF3D7_1359100,	100	32.03	inf	0.0312243 2	0.20346171 2
GO:0046444	FMN metabolic process	1	1	PF3D7_1359100,	100	32.03	inf	0.0312243 2	0.20346171 2
GO:0032469	endoplasmic reticulum calcium ion homeostasis	1	1	PF3D7_1362300,	100	32.03	inf	0.0312243 2	0.20346171 2
GO:0009398	FMN biosynthetic process	1	1	PF3D7_1359100,	100	32.03	inf	0.0312243 2	0.20346171 2
GO:0009231	riboflavin biosynthetic process	1	1	PF3D7_1359100,	100	32.03	inf	0.0312243 2	0.20346171 2
GO:0051017	actin filament bundle assembly	1	1	PF3D7_1036400,	100	32.03	inf	0.0312243 2	0.20346171 2
GO:0043984	histone H4-K16 acetylation	1	1	PF3D7_1118600,	100	32.03	inf	0.0312243 2	0.20346171 2

University of Ghana http://ugspace.ug.edu.gh

Supplementary Table 5.8 List of differentially expressed genes (up- and down-regulated) between the conditions R539T_DMSO treated compared with R539T_DHA treated

Gene ID	source_id	Input Order	Organism	Genomic Location (Gene)	Product Description	Gene Type	Input ID	differentially expressed
PF3D7_0113400	PF3D7_0113400.1	4	Plasmodium falciparum 3D7	Pf3D7_01_v3:507,977..510,158(-)	Plasmodium exported protein, unknown function	protein coding gene	PF3D7_0113400	Down
PF3D7_0113700	PF3D7_0113700.1	5	Plasmodium falciparum 3D7	Pf3D7_01_v3:519,756..523,106(+)	heat shock protein 40, type II	protein coding gene	PF3D7_0113700	Down
PF3D7_0301700	PF3D7_0301700.1	3	Plasmodium falciparum 3D7	Pf3D7_03_v3:95,216..99,115(-)	Plasmodium exported protein, unknown function	protein coding gene	PF3D7_0301700	Down
PF3D7_0304000	PF3D7_0304000.1	2	Plasmodium falciparum 3D7	Pf3D7_03_v3:198,542..201,584(-)	inner membrane complex protein 1a, putative	protein coding gene	PF3D7_0304000	Down
PF3D7_0315900	PF3D7_0315900.1	1	Plasmodium falciparum 3D7	Pf3D7_03_v3:644,186..645,268(+)	conserved Plasmodium protein, unknown function	protein coding gene	PF3D7_0315900	Up
PF3D7_0426000	PF3D7_0426000.1	6	Plasmodium falciparum 3D7	Pf3D7_04_v3:1,173,053..1,180,226(-)	erythrocyte membrane protein 1, PfEMP1	protein coding gene	PF3D7_0426000	Down
PF3D7_0529400	PF3D7_0529400.1	12	Plasmodium falciparum 3D7	Pf3D7_05_v3:1,198,563..1,205,743(+)	conserved Plasmodium protein, unknown function	protein coding gene	PF3D7_0529400	Down
PF3D7_0529400	PF3D7_0529400.2	12	Plasmodium falciparum 3D7	Pf3D7_05_v3:1,198,563..1,205,743(+)	conserved Plasmodium protein, unknown function	protein coding gene	PF3D7_0529400	Down
PF3D7_0617300	PF3D7_0617300.1	10	Plasmodium falciparum 3D7	Pf3D7_06_v3:720,336..721,721(+)	RNA-binding protein, putative	protein coding gene	PF3D7_0617300	Down
PF3D7_0722700	PF3D7_0722700.1	7	Plasmodium falciparum 3D7	Pf3D7_07_v3:961,629..963,030(+)	respiratory chain complex 3 associated protein 1	protein coding gene	PF3D7_0722700	Down
PF3D7_0731900	PF3D7_0731900.1	17	Plasmodium falciparum 3D7	Pf3D7_07_v3:1,382,410..1,383,524(+)	rifin, pseudogene	pseudogene	PF3D7_0731900	Down
PF3D7_0900300	PF3D7_0900300.1	8	Plasmodium falciparum 3D7	Pf3D7_09_v3:33,553..34,795(-)	rifin	protein coding gene	PF3D7_0900300	Down
PF3D7_1000600	PF3D7_1000600.1	13	Plasmodium falciparum 3D7	Pf3D7_10_v3:50,964..53,006(-)	rifin	protein coding gene	PF3D7_1000600	Down
PF3D7_1001200	PF3D7_1001200.1	14	Plasmodium falciparum 3D7	Pf3D7_10_v3:69,800..71,269(-)	acyl-CoA binding protein, isoform 2, ACBP2	protein coding gene	PF3D7_1001200	Up
PF3D7_1201100	PF3D7_1201100.1	15	Plasmodium falciparum 3D7	Pf3D7_12_v3:80,874..84,922(-)	RESA-like protein with PHIST and DnaJ domains	protein coding gene	PF3D7_1201100	Down
PF3D7_1350600	PF3D7_1350600.1	9	Plasmodium falciparum 3D7	Pf3D7_13_v3:2,021,350..2,022,307(+)	conserved Plasmodium protein, unknown function	protein coding gene	PF3D7_1350600	Down
PF3D7_1372000	PF3D7_1372000.1	11	Plasmodium falciparum 3D7	Pf3D7_13_v3:2,832,623..2,835,439(+)	Plasmodium exported protein (PHISTa), unknown function	protein coding gene	PF3D7_1372000	Down
PF3D7_1401000	PF3D7_1401000.1	16	Plasmodium falciparum 3D7	Pf3D7_14_v3:34,693..35,773(-)	GBPH protein	protein coding gene	PF3D7_1401000	Down

University of Ghana http://ugspace.ug.edu.gh

Supplementary Table 5.9 Gene ontology enrichment analysis for up/down-regulated genes between R539T DMSO_treated and DHA_treated condition

University of Ghana http://ugspace.ug.edu.gh

Gene ontology term	Differential expression	ID	Name	Bgd count	Result count	Result gene list	Pct of bgd	Fold enrichment	Odds ratio	P-value	Benjamini	Bonferroni
Biological process	Upregulated	GO:0006631	fatty acid metabolic process	39	1	PF3D7_1001200,	2.6	62.41	127.05	0.01596046	0.066250513	0.111723193
		GO:0032787	monocarboxylic acid metabolic process	67	1	PF3D7_1001200,	1.5	36.33	72.73	0.02734006	0.066250513	0.191380449
		GO:0044255	cellular lipid metabolic process	123	1	PF3D7_1001200,	0.8	19.79	38.89	0.04990074	0.066250513	0.349305157
	Downregulated	GO:0017062	respiratory chain complex III assembly	5	1	PF3D7_0722700,	20	69.54	93.27	0.01430299	0.177137409	0.557816761
		GO:0034551	mitochondrial respiratory chain complex III assembly	5	1	PF3D7_0722700,	20	69.54	93.27	0.01430299	0.177137409	0.557816761
		GO:0044403	biological process involved in symbiotic interaction	397	4	PF3D7_0113700,PF3D7_0304000,PF3D7_0426000,PF3D7_1000600,	1	3.5	4.54	0.02258201	0.177137409	0.880698306
		GO:0044419	biological process involved in interspecies interaction between organisms	399	4	PF3D7_0113700,PF3D7_0304000,PF3D7_0426000,PF3D7_1000600,	1	3.49	4.52	0.02296367	0.177137409	0.895583268
		GO:0033108	mitochondrial respiratory chain complex assembly	9	1	PF3D7_0722700,	11.1	38.63	46.6	0.02560836	0.177137409	0.998726156
		GO:0017004	cytochrome complex assembly	13	1	PF3D7_0722700,	7.7	26.75	31.04	0.03679323	0.177137409	1
		GO:0051084	'de novo' posttranslational protein folding	15	1	PF3D7_0113700,	6.7	23.18	26.59	0.04234084	0.177137409	1
		GO:0051085	chaperone cofactor-dependent protein refolding	15	1	PF3D7_0113700,	6.7	23.18	26.59	0.04234084	0.177137409	1
		GO:0061077	chaperone-mediated protein folding	17	1	PF3D7_0113700,	5.9	20.45	23.26	0.04785878	0.177137409	1

University of Ghana http://ugspace.ug.edu.gh

Molecular function	Upregulated	GO:0120227	acyl-CoA binding	5	1	PF3D7_1001200,	20	486.8	1215.5	0.00205339	0.010266938	0.030800814
		GO:0000062	fatty-acyl-CoA binding	5	1	PF3D7_1001200,	20	486.8	1215.5	0.00205339	0.010266938	0.030800814
		GO:1901567	fatty acid derivative binding	5	1	PF3D7_1001200,	20	486.8	1215.5	0.00205339	0.010266938	0.030800814
		GO:1901681	sulfur compound binding	26	1	PF3D7_1001200,	3.8	93.62	193.64	0.01065457	0.03295972	0.159818552
		GO:0032559	adenyl ribonucleotide binding	577	2	PF3D7_0315900,PF3D7_1001200,	0.3	8.44	inf	0.0140277	0.03295972	0.210415457
		GO:0030554	adenyl nucleotide binding	579	2	PF3D7_0315900,PF3D7_1001200,	0.3	8.41	inf	0.0141252	0.03295972	0.211877942
		GO:0032555	purine ribonucleotide binding	680	2	PF3D7_0315900,PF3D7_1001200,	0.3	7.16	inf	0.01948798	0.03295972	0.292319664
		GO:0017076	purine nucleotide binding	683	2	PF3D7_0315900,PF3D7_1001200,	0.3	7.13	inf	0.01966044	0.03295972	0.294906552
		GO:0032553	ribonucleotide binding	685	2	PF3D7_0315900,PF3D7_1001200,	0.3	7.11	inf	0.01977583	0.03295972	0.296637476
		GO:0000166	nucleotide binding	806	2	PF3D7_0315900,PF3D7_1001200,	0.2	6.04	inf	0.02738539	0.03734372	0.410780922
		GO:1901265	nucleoside phosphate binding	806	2	PF3D7_0315900,PF3D7_1001200,	0.2	6.04	inf	0.02738539	0.03734372	0.410780922
	Downregulated	GO:0015485	cholesterol binding	1	1	PF3D7_0113700,	100	347.71	inf	0.00287592	0.022976668	0.034511093
		GO:0005496	steroid binding	2	1	PF3D7_0113700,	50	173.86	373.31	0.00574417	0.022976668	0.068930005
		GO:0032934	sterol binding	2	1	PF3D7_0113700,	50	173.86	373.31	0.00574417	0.022976668	0.068930005
		GO:0043178	alcohol binding	3	1	PF3D7_0113700,	33.3	115.9	186.62	0.00860475	0.025814241	0.103256963

		GO:0051087	chaperone binding	17	1	PF3D7_0113700,	5.9	20.45	23.26	0.04785878	0.11486107	0.574305348
Cellular component	Downregulated	GO:0044217	other organism part	116	4	PF3D7_0113400,PF3D7_0301700,PF3D7_1372000,PF3D7_1401000,	3.4	11.99	16.94	0.00025479	0.004134581	0.011720454
		GO:0018995	host cellular component	713	8	PF3D7_0113400,PF3D7_0113700,PF3D7_0301700,PF3D7_0426000,PF3D7_1000600, PF3D7_1201100,PF3D7_1372000,PF3D7_1401000,	1.1	3.9	7.85	0.00026965	0.004134581	0.012403744
		GO:0043657	host cell	713	8	PF3D7_0113400,PF3D7_0113700,PF3D7_0301700,PF3D7_0426000,PF3D7_1000600, PF3D7_1201100,PF3D7_1372000,PF3D7_1401000,	1.1	3.9	7.85	0.00026965	0.004134581	0.012403744
		GO:0016021	integral component of membrane	1297	8	PF3D7_0113400,PF3D7_0113700,PF3D7_0301700,PF3D7_0426000,PF3D7_0722700, PF3D7_0900300,PF3D7_1350600,PF3D7_1372000,	0.6	2.14	3.69	0.01522829	0.140148292	0.700501167
		GO:0031224	intrinsic component of membrane	1314	8	PF3D7_0113400,PF3D7_0113700,PF3D7_0301700,PF3D7_0426000,PF3D7_0722700, PF3D7_0900300,PF3D7_1350600,PF3D7_1372000,	0.6	2.12	3.62	0.01650757	0.140148292	0.759348135
		GO:0005750	mitochondrial respiratory chain complex III	9	1	PF3D7_0722700,	11.1	38.63	46.6	0.02560836	0.140148292	1
		GO:0045275	respiratory chain complex III	9	1	PF3D7_0722700,	11.1	38.63	46.6	0.02560836	0.140148292	1
		GO:0033643	host cell part	630	5	PF3D7_0113700,PF3D7_0301700,PF3D7_0426000,PF3D7_1000600,PF3D7_1201100,	0.8	2.76	3.76	0.02624729	0.140148292	1
		GO:0016020	membrane	637	5	PF3D7_0529400,PF3D7_1000600,PF3D7_1201100,PF3D7_1350600,PF3D7_1401000,	0.8	2.73	3.71	0.02742032	0.140148292	1
		GO:1902495	transmembrane transporter complex	15	1	PF3D7_0722700,	6.7	23.18	26.59	0.04234084	0.184833339	1
		GO:0005575	cellular component	723	5	PF3D7_0529400,PF3D7_1000600,PF3D7_1201100,PF3D7_1350600,PF3D7_1401000,	0.7	2.4	3.2	0.04478113	0.184833339	1

University of Ghana http://ugspace.ug.edu.gh

Supplementary Table 5.10 List of differentially expressed genes (up- and down-regulated) between the conditions R539T_untreated compared with R539T_DHA treated

GeneID	source_id	Input.Order	Organism	Genomic.Location..Gene.	Product.Description	Gene.Type	differentially expressed
PF3D7_0102200	PF3D7_0102200.1	14	Plasmodium falciparum 3D7	Pf3D7_01_v3:97,590..103,615(+)	ring-infected erythrocyte surface antigen	protein coding gene	DOWN
PF3D7_0102500	PF3D7_0102500.1	15	Plasmodium falciparum 3D7	Pf3D7_01_v3:109,005..117,516(-)	erythrocyte binding antigen-181	protein coding gene	DOWN
PF3D7_0104800	PF3D7_0104800.1	16	Plasmodium falciparum 3D7	Pf3D7_01_v3:215,143..217,616(+)	novel putative transporter 1, putative	protein coding gene	DOWN
PF3D7_0105300	PF3D7_0105300.1	17	Plasmodium falciparum 3D7	Pf3D7_01_v3:224,638..226,017(-)	cyclase-associated protein	protein coding gene	DOWN
PF3D7_0106600	PF3D7_0106600.1	18	Plasmodium falciparum 3D7	Pf3D7_01_v3:279,115..280,014(+)	conserved Plasmodium protein, unknown function	protein coding gene	DOWN
PF3D7_0108500	PF3D7_0108500.1	19	Plasmodium falciparum 3D7	Pf3D7_01_v3:347,246..350,568(+)	ELM2 domain-containing protein, putative	protein coding gene	DOWN
PF3D7_0110000	PF3D7_0110000.1	20	Plasmodium falciparum 3D7	Pf3D7_01_v3:388,192..389,559(+)	conserved Plasmodium protein, unknown function	protein coding gene	UP
PF3D7_0113000	PF3D7_0113000.1	11	Plasmodium falciparum 3D7	Pf3D7_01_v3:487,239..490,901(-)	glutamic acid-rich protein GARP	protein coding gene	DOWN
PF3D7_0113200	PF3D7_0113200.1	123	Plasmodium falciparum 3D7	Pf3D7_01_v3:500,888..503,795(-)	Plasmodium exported protein, unknown function	protein coding gene	DOWN
PF3D7_0114500	PF3D7_0114500.1	13	Plasmodium falciparum 3D7	Pf3D7_01_v3:557,700..558,946(-)	Plasmodium exported protein (hyp10), unknown function	protein coding gene	DOWN
PF3D7_0202100	PF3D7_0202100.1	153	Plasmodium falciparum 3D7	Pf3D7_02_v3:108,217..111,658(-)	liver stage associated protein 2	protein coding gene	DOWN
PF3D7_0202500	PF3D7_0202500.1	154	Plasmodium falciparum 3D7	Pf3D7_02_v3:127,203..129,089(+)	early transcribed membrane protein 2	protein coding gene	DOWN
PF3D7_0204200	PF3D7_0204200.1	155	Plasmodium falciparum 3D7	Pf3D7_02_v3:192,755..194,248(+)	translocation protein SEC66, putative	protein coding gene	DOWN
PF3D7_0206200	PF3D7_0206200.1	156	Plasmodium falciparum 3D7	Pf3D7_02_v3:248,880..251,521(+)	pantothenate transporter	protein coding gene	DOWN
PF3D7_0206800	PF3D7_0206800.1	157	Plasmodium falciparum 3D7	Pf3D7_02_v3:271,576..274,917(-)	merozoite surface protein 2	protein coding gene	DOWN
PF3D7_0207400	PF3D7_0207400.1	158	Plasmodium falciparum 3D7	Pf3D7_02_v3:293,896..297,980(-)	serine repeat antigen 7	protein coding gene	DOWN
PF3D7_0207500	PF3D7_0207500.1	159	Plasmodium falciparum 3D7	Pf3D7_02_v3:298,380..302,820(-)	serine repeat antigen 6	protein coding gene	DOWN
PF3D7_0207600	PF3D7_0207600.1	160	Plasmodium falciparum 3D7	Pf3D7_02_v3:303,409..307,376(-)	serine repeat antigen 5	protein coding gene	DOWN
PF3D7_0207700	PF3D7_0207700.1	161	Plasmodium falciparum 3D7	Pf3D7_02_v3:308,628..312,348(-)	serine repeat antigen 4	protein coding gene	DOWN
PF3D7_0207800	PF3D7_0207800.1	162	Plasmodium falciparum 3D7	Pf3D7_02_v3:312,990..316,944(-)	serine repeat antigen 3	protein coding gene	DOWN
PF3D7_0209000	PF3D7_0209000.1	163	Plasmodium falciparum 3D7	Pf3D7_02_v3:369,351..380,156(+)	6-cysteine protein P230	protein coding gene	UP
PF3D7_0212600	PF3D7_0212600.1	164	Plasmodium falciparum 3D7	Pf3D7_02_v3:522,339..524,405(+)	secreted protein with altered thrombospondin repeat domain	protein coding gene	DOWN
PF3D7_0214600	PF3D7_0214600.1	165	Plasmodium falciparum 3D7	Pf3D7_02_v3:593,374..600,035(+)	serine/threonine protein kinase STK2, putative	protein coding gene	DOWN
PF3D7_0214900	PF3D7_0214900.1	166	Plasmodium falciparum 3D7	Pf3D7_02_v3:609,924..616,306(+)	rhoptry neck protein 6	protein coding gene	DOWN
PF3D7_0215300	PF3D7_0215300.1	167	Plasmodium falciparum 3D7	Pf3D7_02_v3:628,091..632,681(-)	acyl-CoA synthetase	protein coding gene	DOWN
PF3D7_0217500	PF3D7_0217500.1	168	Plasmodium falciparum 3D7	Pf3D7_02_v3:719,266..723,617(+)	calcium-dependent protein kinase 1	protein coding gene	DOWN
PF3D7_0220000	PF3D7_0220000.1	169	Plasmodium falciparum 3D7	Pf3D7_02_v3:794,978..801,981(+)	liver stage antigen 3	protein coding gene	DOWN
PF3D7_0220300	PF3D7_0220300.1	170	Plasmodium falciparum 3D7	Pf3D7_02_v3:812,892..815,853(-)	Plasmodium exported protein, unknown function	protein coding gene	DOWN
PF3D7_0220800	PF3D7_0220800.1	171	Plasmodium falciparum 3D7	Pf3D7_02_v3:838,594..844,668(+)	cytoadherence linked asexual protein 2	protein coding gene	DOWN
PF3D7_0221500	PF3D7_0221500.1	282	Plasmodium falciparum 3D7	Pf3D7_02_v3:863,079..863,842(-)	Pfmc-2TM Maurer's cleft two transmembrane protein, pseudogene	pseudogene	DOWN
PF3D7_0221700	PF3D7_0221700.1	172	Plasmodium falciparum 3D7	Pf3D7_02_v3:868,884..871,778(-)	Plasmodium exported protein, unknown function	protein coding gene	DOWN
PF3D7_0301700	PF3D7_0301700.1	9	Plasmodium falciparum 3D7	Pf3D7_03_v3:95,216..99,115(-)	Plasmodium exported protein, unknown function	protein coding gene	DOWN
PF3D7_0301800	PF3D7_0301800.1	8	Plasmodium falciparum 3D7	Pf3D7_03_v3:103,118..105,748(+)	Plasmodium exported protein, unknown function	protein coding gene	DOWN
PF3D7_0302200	PF3D7_0302200.1	1	Plasmodium falciparum 3D7	Pf3D7_03_v3:119,098..124,924(+)	cytoadherence linked asexual protein 3.2	protein coding gene	DOWN
PF3D7_0302500	PF3D7_0302500.1	2	Plasmodium falciparum 3D7	Pf3D7_03_v3:134,486..141,185(+)	cytoadherence linked asexual protein 3.1	protein coding gene	DOWN
PF3D7_0304000	PF3D7_0304000.1	5	Plasmodium falciparum 3D7	Pf3D7_03_v3:198,542..201,584(-)	inner membrane complex protein 1a, putative	protein coding gene	DOWN
PF3D7_0308100	PF3D7_0308100.1	3	Plasmodium falciparum 3D7	Pf3D7_03_v3:355,867..361,936(+)	zinc finger protein, putative	protein coding gene	DOWN
PF3D7_0308300	PF3D7_0308300.1	4	Plasmodium falciparum 3D7	Pf3D7_03_v3:365,177..366,948(-)	PhIL1-interacting candidate PIC4	protein coding gene	DOWN
PF3D7_0318700	PF3D7_0318700.1	12	Plasmodium falciparum 3D7	Pf3D7_03_v3:788,145..789,211(+)	conserved Plasmodium protein, unknown function	protein coding gene	DOWN
PF3D7_0320500	PF3D7_0320500.1	6	Plasmodium falciparum 3D7	Pf3D7_03_v3:860,221..862,776(+)	nicotinamidase, putative	protein coding gene	DOWN
PF3D7_0321100	PF3D7_0321100.1	7	Plasmodium falciparum 3D7	Pf3D7_03_v3:879,438..885,952(-)	conserved Plasmodium protein, unknown function	protein coding gene	DOWN
PF3D7_0321400	PF3D7_0321400.1	148	Plasmodium falciparum 3D7	Pf3D7_03_v3:894,149..896,220(+)	pseudo protein kinase 1, putative	protein coding gene	DOWN

University of Ghana http://ugspace.ug.edu.gh

PF3D7_0401800	PF3D7_0401800.1	21	Plasmodium falciparum 3D7	Pf3D7_04_v3:103,078..106,145(-)	Plasmodium exported protein (PHISTb), unknown function	protein coding gene	DOWN
PF3D7_0404700	PF3D7_0404700.1	22	Plasmodium falciparum 3D7	Pf3D7_04_v3:259,944..263,782(-)	dipeptidyl aminopeptidase 3	protein coding gene	DOWN
PF3D7_0404900	PF3D7_0404900.1	23	Plasmodium falciparum 3D7	Pf3D7_04_v3:266,566..268,913(-)	6-cysteine protein P41	protein coding gene	DOWN
PF3D7_0405900	PF3D7_0405900.1	24	Plasmodium falciparum 3D7	Pf3D7_04_v3:315,974..319,564(-)	apical sushi protein	protein coding gene	DOWN
PF3D7_0406200	PF3D7_0406200.1	25	Plasmodium falciparum 3D7	Pf3D7_04_v3:328,473..330,639(+)	parasitophorous vacuole membrane protein S16	protein coding gene	UP
PF3D7_0411700	PF3D7_0411700.1	10	Plasmodium falciparum 3D7	Pf3D7_04_v3:518,685..519,101(-)	conserved Plasmodium protein, unknown function	protein coding gene	UP
PF3D7_0414800	PF3D7_0414800.1	124	Plasmodium falciparum 3D7	Pf3D7_04_v3:663,115..664,901(-)	conserved Plasmodium protein, unknown function	protein coding gene	DOWN
PF3D7_0414900	PF3D7_0414900.1	125	Plasmodium falciparum 3D7	Pf3D7_04_v3:665,765..668,508(+)	armadillo-domain containing rhoptry protein	protein coding gene	DOWN
PF3D7_0418800	PF3D7_0418800.1	126	Plasmodium falciparum 3D7	Pf3D7_04_v3:843,562..845,169(+)	MOLO1 domain-containing protein, putative	protein coding gene	UP
PF3D7_0419700	PF3D7_0419700.1	26	Plasmodium falciparum 3D7	Pf3D7_04_v3:872,600..876,321(+)	apical merozoite protein	protein coding gene	DOWN
PF3D7_0421900	PF3D7_0421900.1	27	Plasmodium falciparum 3D7	Pf3D7_04_v3:997,240..997,455(+)	conserved Plasmodium protein, unknown function	protein coding gene	UP
PF3D7_0423400	PF3D7_0423400.1	28	Plasmodium falciparum 3D7	Pf3D7_04_v3:1,055,314..1,056,674(+)	apical asparagine-rich protein AARP	protein coding gene	DOWN
PF3D7_0423800	PF3D7_0423800.1	29	Plasmodium falciparum 3D7	Pf3D7_04_v3:1,075,910..1,077,829(+)	cysteine-rich protective antigen	protein coding gene	DOWN
PF3D7_0424100	PF3D7_0424100.1	30	Plasmodium falciparum 3D7	Pf3D7_04_v3:1,082,005..1,084,464(-)	reticulocyte binding protein homologue 5	protein coding gene	DOWN
PF3D7_0425100	PF3D7_0425100.1	31	Plasmodium falciparum 3D7	Pf3D7_04_v3:1,134,415..1,135,394(-)	Plasmodium exported protein (hyp6), unknown function	protein coding gene	DOWN
PF3D7_0426000	PF3D7_0426000.1	32	Plasmodium falciparum 3D7	Pf3D7_04_v3:1,173,053..1,180,226(-)	erythrocyte membrane protein 1, PfEMP1	protein coding gene	DOWN
PF3D7_0500900	PF3D7_0500900.1	54	Plasmodium falciparum 3D7	Pf3D7_05_v3:50,081..52,576(-)	serine/threonine protein kinase, FIKK family	protein coding gene	DOWN
PF3D7_0501300	PF3D7_0501300.1	55	Plasmodium falciparum 3D7	Pf3D7_05_v3:67,224..70,944(+)	skeleton-binding protein 1	protein coding gene	DOWN
PF3D7_0501400	PF3D7_0501400.1	56	Plasmodium falciparum 3D7	Pf3D7_05_v3:73,163..80,813(+)	interspersed repeat antigen	protein coding gene	DOWN
PF3D7_0501500	PF3D7_0501500.1	57	Plasmodium falciparum 3D7	Pf3D7_05_v3:80,570..82,763(-)	rhoptry-associated protein 3	protein coding gene	DOWN
PF3D7_0501600	PF3D7_0501600.1	58	Plasmodium falciparum 3D7	Pf3D7_05_v3:83,760..85,512(-)	rhoptry-associated protein 2	protein coding gene	DOWN
PF3D7_0505300	PF3D7_0505300.1	59	Plasmodium falciparum 3D7	Pf3D7_05_v3:233,139..235,836(+)	UDP-N-acetylglucosamine transporter, putative	protein coding gene	DOWN
PF3D7_0507200	PF3D7_0507200.1	60	Plasmodium falciparum 3D7	Pf3D7_05_v3:298,070..301,000(-)	subtilisin-like protease 3	protein coding gene	DOWN
PF3D7_0507400	PF3D7_0507400.1	127	Plasmodium falciparum 3D7	Pf3D7_05_v3:305,282..306,963(-)	subtilisin propeptide-like protein	protein coding gene	DOWN
PF3D7_0507500	PF3D7_0507500.1	61	Plasmodium falciparum 3D7	Pf3D7_05_v3:307,090..310,120(-)	subtilisin-like protease 1	protein coding gene	DOWN
PF3D7_0508900	PF3D7_0508900.1	62	Plasmodium falciparum 3D7	Pf3D7_05_v3:366,627..376,779(+)	protein AAP6	protein coding gene	DOWN
PF3D7_0511600	PF3D7_0511600.1	63	Plasmodium falciparum 3D7	Pf3D7_05_v3:517,088..518,520(-)	apical rhoptry neck protein	protein coding gene	DOWN
PF3D7_0513000	PF3D7_0513000.1	64	Plasmodium falciparum 3D7	Pf3D7_05_v3:555,264..556,651(+)	conserved protein, unknown function	protein coding gene	UP
PF3D7_0513300	PF3D7_0513300.1	65	Plasmodium falciparum 3D7	Pf3D7_05_v3:568,594..570,527(-)	purine nucleoside phosphorylase	protein coding gene	DOWN
PF3D7_0518800	PF3D7_0518800.1	128	Plasmodium falciparum 3D7	Pf3D7_05_v3:783,638..784,991(-)	secreted ookinete protein, putative	protein coding gene	UP
PF3D7_0525800	PF3D7_0525800.1	66	Plasmodium falciparum 3D7	Pf3D7_05_v3:1,071,094..1,072,988(+)	inner membrane complex protein 1g, putative	protein coding gene	DOWN
PF3D7_0528300	PF3D7_0528300.1	67	Plasmodium falciparum 3D7	Pf3D7_05_v3:1,166,047..1,169,378(-)	conserved protein, unknown function	protein coding gene	DOWN
PF3D7_0529400	PF3D7_0529400.1	149	Plasmodium falciparum 3D7	Pf3D7_05_v3:1,198,563..1,205,743(+)	conserved Plasmodium protein, unknown function	protein coding gene	DOWN
PF3D7_0529400	PF3D7_0529400.2	149	Plasmodium falciparum 3D7	Pf3D7_05_v3:1,198,563..1,205,743(+)	conserved Plasmodium protein, unknown function	protein coding gene	DOWN
PF3D7_0530800	PF3D7_0530800.1	129	Plasmodium falciparum 3D7	Pf3D7_05_v3:1,255,012..1,257,579(+)	CPW-WPC family protein	protein coding gene	UP
PF3D7_0532300	PF3D7_0532300.1	68	Plasmodium falciparum 3D7	Pf3D7_05_v3:1,307,099..1,310,572(+)	Plasmodium exported protein (PHISTb), unknown function	protein coding gene	DOWN
PF3D7_0532600	PF3D7_0532600.1	130	Plasmodium falciparum 3D7	Pf3D7_05_v3:1,317,882..1,319,382(-)	Plasmodium exported protein, unknown function	protein coding gene	DOWN
PF3D7_0604100	PF3D7_0604100.1	114	Plasmodium falciparum 3D7	Pf3D7_06_v3:170,776..178,985(-)	AP2 domain transcription factor	protein coding gene	DOWN
PF3D7_0604800	PF3D7_0604800.1	115	Plasmodium falciparum 3D7	Pf3D7_06_v3:206,807..211,802(-)	RAP protein, putative	protein coding gene	UP
PF3D7_0606200	PF3D7_0606200.1	116	Plasmodium falciparum 3D7	Pf3D7_06_v3:260,228..262,593(-)	ubiquitin-conjugating enzyme E2 PEX4, putative	protein coding gene	DOWN
PF3D7_0611300	PF3D7_0611300.1	117	Plasmodium falciparum 3D7	Pf3D7_06_v3:469,685..471,521(+)	ATP synthase-associated protein, putative	protein coding gene	UP
PF3D7_0612500	PF3D7_0612500.1	118	Plasmodium falciparum 3D7	Pf3D7_06_v3:522,300..522,665(-)	conserved Plasmodium protein, unknown function	protein coding gene	UP
PF3D7_0612700	PF3D7_0612700.1	119	Plasmodium falciparum 3D7	Pf3D7_06_v3:525,736..527,850(-)	6-cysteine protein P12	protein coding gene	DOWN
PF3D7_0613300	PF3D7_0613300.1	120	Plasmodium falciparum 3D7	Pf3D7_06_v3:539,725..545,452(-)	rhoptry protein ROP14	protein coding gene	DOWN
PF3D7_0613800	PF3D7_0613800.1	121	Plasmodium falciparum 3D7	Pf3D7_06_v3:565,925..579,231(+)	AP2 domain transcription factor, putative	protein coding gene	DOWN

University of Ghana http://ugspace.ug.edu.gh

PF3D7_0613900	PF3D7_0613900.1	122	Plasmodium falciparum 3D7	Pf3D7_06_v3:579,250..586,589(-)	myosin E, putative	protein coding gene	DOWN
PF3D7_0617300	PF3D7_0617300.1	106	Plasmodium falciparum 3D7	Pf3D7_06_v3:720,336..721,721(+)	RNA-binding protein, putative	protein coding gene	DOWN
PF3D7_0617800	PF3D7_0617800.1	107	Plasmodium falciparum 3D7	Pf3D7_06_v3:747,329..749,285(-)	histone H2A	protein coding gene	DOWN
PF3D7_0618000	PF3D7_0618000.1	108	Plasmodium falciparum 3D7	Pf3D7_06_v3:757,278..761,654(+)	conserved Plasmodium membrane protein, unknown function	protein coding gene	DOWN
PF3D7_0620300	PF3D7_0620300.1	109	Plasmodium falciparum 3D7	Pf3D7_06_v3:848,035..850,864(-)	conserved Plasmodium protein, unknown function	protein coding gene	DOWN
PF3D7_0620400	PF3D7_0620400.1	110	Plasmodium falciparum 3D7	Pf3D7_06_v3:851,162..853,200(-)	merozoite surface protein 10	protein coding gene	DOWN
PF3D7_0628300	PF3D7_0628300.1	111	Plasmodium falciparum 3D7	Pf3D7_06_v3:1,169,270..1,174,371(-)	choline/ethanolaminephosphotransferase, putative	protein coding gene	DOWN
PF3D7_0630000	PF3D7_0630000.1	112	Plasmodium falciparum 3D7	Pf3D7_06_v3:1,252,052..1,253,985(-)	CPW-WPC family protein	protein coding gene	UP
PF3D7_0632200	PF3D7_0632200.1	113	Plasmodium falciparum 3D7	Pf3D7_06_v3:1,341,307..1,342,595(-)	rifin	protein coding gene	DOWN
PF3D7_0701900	PF3D7_0701900.1	33	Plasmodium falciparum 3D7	Pf3D7_07_v3:79,450..83,836(-)	Plasmodium exported protein, unknown function	protein coding gene	DOWN
PF3D7_0702000	PF3D7_0702000.1	131	Plasmodium falciparum 3D7	Pf3D7_07_v3:83,838..86,436(+)	Plasmodium exported protein (hyp12), unknown function	protein coding gene	DOWN
PF3D7_0702100	PF3D7_0702100.1	283	Plasmodium falciparum 3D7	Pf3D7_07_v3:88,685..90,886(+)	Plasmodium exported protein (PHISTb), unknown function, pseudogene	pseudogene	DOWN
PF3D7_0702200	PF3D7_0702200.1	34	Plasmodium falciparum 3D7	Pf3D7_07_v3:91,731..95,602(-)	lysophospholipase LPL20	protein coding gene	DOWN
PF3D7_0703400	PF3D7_0703400.1	35	Plasmodium falciparum 3D7	Pf3D7_07_v3:129,160..132,186(-)	conserved Plasmodium protein, unknown function	protein coding gene	UP
PF3D7_0706300	PF3D7_0706300.1	132	Plasmodium falciparum 3D7	Pf3D7_07_v3:305,264..306,466(+)	conserved Plasmodium protein, unknown function	protein coding gene	DOWN
PF3D7_0706700	PF3D7_0706700.1	133	Plasmodium falciparum 3D7	Pf3D7_07_v3:322,907..325,528(+)	DNA mismatch repair protein MSH2, putative	protein coding gene	UP
PF3D7_0707300	PF3D7_0707300.1	134	Plasmodium falciparum 3D7	Pf3D7_07_v3:337,720..343,059(+)	rhoptry-associated membrane antigen	protein coding gene	DOWN
PF3D7_0713800	PF3D7_0713800.1	36	Plasmodium falciparum 3D7	Pf3D7_07_v3:623,870..625,625(-)	negative elongation factor A, putative	protein coding gene	DOWN
PF3D7_0722200	PF3D7_0722200.1	37	Plasmodium falciparum 3D7	Pf3D7_07_v3:946,077..949,317(+)	rhoptry-associated leucine zipper-like protein 1	protein coding gene	DOWN
PF3D7_0725400	PF3D7_0725400.1	38	Plasmodium falciparum 3D7	Pf3D7_07_v3:1,078,691..1,080,123(+)	conserved Plasmodium protein, unknown function	protein coding gene	DOWN
PF3D7_0731500	PF3D7_0731500.1	39	Plasmodium falciparum 3D7	Pf3D7_07_v3:1,357,251..1,363,653(+)	erythrocyte binding antigen-175	protein coding gene	DOWN
PF3D7_0800800	PF3D7_0800800.1	53	Plasmodium falciparum 3D7	Pf3D7_08_v3:79,126..80,766(+)	Plasmodium exported protein (hyp7), unknown function	protein coding gene	DOWN
PF3D7_0800900	PF3D7_0800900.1	284	Plasmodium falciparum 3D7	Pf3D7_08_v3:83,128..83,904(+)	Plasmodium exported protein (hyp7), unknown function, pseudogene	pseudogene	DOWN
PF3D7_0801400	PF3D7_0801400.1	52	Plasmodium falciparum 3D7	Pf3D7_08_v3:104,442..105,517(-)	conserved Plasmodium protein, unknown function	protein coding gene	UP
PF3D7_0802600	PF3D7_0802600.1	135	Plasmodium falciparum 3D7	Pf3D7_08_v3:180,040..188,229(+)	adenylyl cyclase beta	protein coding gene	DOWN
PF3D7_0808200	PF3D7_0808200.1	51	Plasmodium falciparum 3D7	Pf3D7_08_v3:415,549..419,066(-)	plasmepsin X	protein coding gene	DOWN
PF3D7_0817600	PF3D7_0817600.1	50	Plasmodium falciparum 3D7	Pf3D7_08_v3:800,326..804,715(-)	conserved protein, unknown function	protein coding gene	DOWN
PF3D7_0817700	PF3D7_0817700.1	136	Plasmodium falciparum 3D7	Pf3D7_08_v3:804,723..814,055(-)	rhoptry neck protein 5	protein coding gene	DOWN
PF3D7_0818100	PF3D7_0818100.1	49	Plasmodium falciparum 3D7	Pf3D7_08_v3:823,912..827,305(+)	zinc finger protein, putative	protein coding gene	DOWN
PF3D7_0818900	PF3D7_0818900.1	48	Plasmodium falciparum 3D7	Pf3D7_08_v3:858,550..862,980(+)	heat shock protein 70	protein coding gene	DOWN
PF3D7_0819400	PF3D7_0819400.1	47	Plasmodium falciparum 3D7	Pf3D7_08_v3:878,495..880,459(+)	perforin-like protein 4	protein coding gene	UP
PF3D7_0821400	PF3D7_0821400.1	46	Plasmodium falciparum 3D7	Pf3D7_08_v3:964,289..967,130(+)	conserved Plasmodium protein, unknown function	protein coding gene	DOWN
PF3D7_0822900	PF3D7_0822900.1	45	Plasmodium falciparum 3D7	Pf3D7_08_v3:1,006,504..1,011,755(-)	PhIL1-interacting candidate PIC2	protein coding gene	DOWN
PF3D7_0825700	PF3D7_0825700.1	44	Plasmodium falciparum 3D7	Pf3D7_08_v3:1,101,887..1,102,804(-)	crystalloid-specific PH domain-containing protein, putative	protein coding gene	UP
PF3D7_0825800	PF3D7_0825800.1	137	Plasmodium falciparum 3D7	Pf3D7_08_v3:1,103,768..1,105,108(+)	PH-like domain-containing protein, putative	protein coding gene	UP
PF3D7_0825900	PF3D7_0825900.1	43	Plasmodium falciparum 3D7	Pf3D7_08_v3:1,105,631..1,108,315(+)	conserved Plasmodium protein, unknown function	protein coding gene	UP
PF3D7_0827200	PF3D7_0827200.1	42	Plasmodium falciparum 3D7	Pf3D7_08_v3:1,177,310..1,180,324(+)	conserved Plasmodium protein, unknown function	protein coding gene	UP
PF3D7_0827400	PF3D7_0827400.1	41	Plasmodium falciparum 3D7	Pf3D7_08_v3:1,184,595..1,185,251(+)	conserved protein, unknown function	protein coding gene	UP
PF3D7_0830500	PF3D7_0830500.1	40	Plasmodium falciparum 3D7	Pf3D7_08_v3:1,295,569..1,299,431(-)	sporozoite and liver stage tryptophan-rich protein, putative	protein coding gene	DOWN
PF3D7_0831600	PF3D7_0831600.1	152	Plasmodium falciparum 3D7	Pf3D7_08_v3:1,358,188..1,363,639(+)	cytoadherence linked asexual protein 8	protein coding gene	DOWN
PF3D7_0902100	PF3D7_0902100.1	69	Plasmodium falciparum 3D7	Pf3D7_09_v3:93,768..95,820(-)	serine/threonine protein kinase, FIKK family	protein coding gene	DOWN
PF3D7_0903800	PF3D7_0903800.1	70	Plasmodium falciparum 3D7	Pf3D7_09_v3:179,187..183,991(+)	LCCL domain-containing protein	protein coding gene	UP
PF3D7_0904200	PF3D7_0904200.1	71	Plasmodium falciparum 3D7	Pf3D7_09_v3:197,658..198,894(+)	PH domain-containing protein, putative	protein coding gene	UP
PF3D7_0905400	PF3D7_0905400.1	72	Plasmodium falciparum 3D7	Pf3D7_09_v3:270,371..275,833(-)	high molecular weight rhoptry protein 3	protein coding gene	DOWN
PF3D7_0905500	PF3D7_0905500.1	73	Plasmodium falciparum 3D7	Pf3D7_09_v3:276,467..279,624(+)	conserved protein, unknown function	protein coding gene	DOWN

University of Ghana http://ugspace.ug.edu.gh

PF3D7_0916300	PF3D7_0916300.1	74	Plasmodium falciparum 3D7	Pf3D7_09_v3:680,231..681,984(-)	conserved Plasmodium protein, unknown function	protein coding gene	DOWN
PF3D7_0918700	PF3D7_0918700.1	75	Plasmodium falciparum 3D7	Pf3D7_09_v3:769,319..772,498(+)	conserved Plasmodium protein, unknown function	protein coding gene	DOWN
PF3D7_0919200	PF3D7_0919200.1	76	Plasmodium falciparum 3D7	Pf3D7_09_v3:788,717..791,151(-)	PPPDE peptidase, putative	protein coding gene	DOWN
PF3D7_0920500	PF3D7_0920500.1	77	Plasmodium falciparum 3D7	Pf3D7_09_v3:840,386..842,993(+)	ADP-ribosylation factor, putative	protein coding gene	DOWN
PF3D7_0922200	PF3D7_0922200.1	78	Plasmodium falciparum 3D7	Pf3D7_09_v3:901,584..905,953(+)	S-adenosylmethionine synthetase	protein coding gene	DOWN
PF3D7_0923100	PF3D7_0923100.1	79	Plasmodium falciparum 3D7	Pf3D7_09_v3:941,830..942,498(-)	OTU domain-containing protein, putative	protein coding gene	UP
PF3D7_0929400	PF3D7_0929400.1	138	Plasmodium falciparum 3D7	Pf3D7_09_v3:1,173,579..1,181,380(+)	high molecular weight rhoptry protein 2	protein coding gene	DOWN
PF3D7_0930000	PF3D7_0930000.1	80	Plasmodium falciparum 3D7	Pf3D7_09_v3:1,189,646..1,191,322(+)	procollagen lysine 5-dioxygenase, putative	protein coding gene	UP
PF3D7_0930300	PF3D7_0930300.1	81	Plasmodium falciparum 3D7	Pf3D7_09_v3:1,201,305..1,207,576(+)	merozoite surface protein 1	protein coding gene	DOWN
PF3D7_0930700	PF3D7_0930700.1	82	Plasmodium falciparum 3D7	Pf3D7_09_v3:1,221,470..1,224,028(+)	conserved Plasmodium protein, unknown function	protein coding gene	UP
PF3D7_0932100	PF3D7_0932100.1	139	Plasmodium falciparum 3D7	Pf3D7_09_v3:1,278,479..1,284,699(-)	protein MAM3, putative	protein coding gene	DOWN
PF3D7_0934800	PF3D7_0934800.1	83	Plasmodium falciparum 3D7	Pf3D7_09_v3:1,360,721..1,364,051(+)	cAMP-dependent protein kinase catalytic subunit	protein coding gene	DOWN
PF3D7_0936000	PF3D7_0936000.1	84	Plasmodium falciparum 3D7	Pf3D7_09_v3:1,426,152..1,428,942(-)	ring-exported protein 2	protein coding gene	DOWN
PF3D7_0936500	PF3D7_0936500.1	85	Plasmodium falciparum 3D7	Pf3D7_09_v3:1,443,260..1,445,400(-)	virulence-associated protein 1	protein coding gene	UP
PF3D7_0936600	PF3D7_0936600.1	86	Plasmodium falciparum 3D7	Pf3D7_09_v3:1,445,945..1,448,525(+)	gametocyte exported protein 5	protein coding gene	UP
PF3D7_1000600	PF3D7_1000600.1	173	Plasmodium falciparum 3D7	Pf3D7_10_v3:50,964..53,006(-)	rifin	protein coding gene	DOWN
PF3D7_1001600	PF3D7_1001600.1	174	Plasmodium falciparum 3D7	Pf3D7_10_v3:85,910..91,177(-)	exported lipase 2	protein coding gene	DOWN
PF3D7_1003600	PF3D7_1003600.1	175	Plasmodium falciparum 3D7	Pf3D7_10_v3:164,213..166,726(+)	inner membrane complex protein 1c, putative	protein coding gene	DOWN
PF3D7_1005200	PF3D7_1005200.1	176	Plasmodium falciparum 3D7	Pf3D7_10_v3:232,315..233,024(-)	conserved Plasmodium protein, unknown function	protein coding gene	UP
PF3D7_1005300	PF3D7_1005300.1	177	Plasmodium falciparum 3D7	Pf3D7_10_v3:233,285..234,473(-)	conserved Plasmodium protein, unknown function	protein coding gene	UP
PF3D7_1006300	PF3D7_1006300.1	178	Plasmodium falciparum 3D7	Pf3D7_10_v3:265,750..266,836(-)	conserved Plasmodium protein, unknown function	protein coding gene	UP
PF3D7_1007300	PF3D7_1007300.1	179	Plasmodium falciparum 3D7	Pf3D7_10_v3:292,725..296,323(+)	RING zinc finger protein, putative	protein coding gene	DOWN
PF3D7_1010300	PF3D7_1010300.1	180	Plasmodium falciparum 3D7	Pf3D7_10_v3:412,469..415,659(+)	succinate dehydrogenase subunit 4, putative	protein coding gene	DOWN
PF3D7_1012200	PF3D7_1012200.1	181	Plasmodium falciparum 3D7	Pf3D7_10_v3:470,483..472,274(+)	rhoptry associated adhesin	protein coding gene	DOWN
PF3D7_1013800	PF3D7_1013800.1	182	Plasmodium falciparum 3D7	Pf3D7_10_v3:542,175..545,149(+)	conserved Plasmodium protein, unknown function	protein coding gene	DOWN
PF3D7_1014100	PF3D7_1014100.1	183	Plasmodium falciparum 3D7	Pf3D7_10_v3:554,233..560,227(+)	merozoite surface protein MSA180	protein coding gene	DOWN
PF3D7_1016900	PF3D7_1016900.1	184	Plasmodium falciparum 3D7	Pf3D7_10_v3:680,750..683,255(-)	early transcribed membrane protein 10.3	protein coding gene	UP
PF3D7_1017500	PF3D7_1017500.1	185	Plasmodium falciparum 3D7	Pf3D7_10_v3:701,258..703,707(+)	myosin essential light chain ELC	protein coding gene	DOWN
PF3D7_1021500	PF3D7_1021500.1	186	Plasmodium falciparum 3D7	Pf3D7_10_v3:867,337..870,148(-)	ATP-dependent RNA helicase ROK1, putative	protein coding gene	UP
PF3D7_1021600	PF3D7_1021600.1	187	Plasmodium falciparum 3D7	Pf3D7_10_v3:870,416..873,015(+)	deoxyribose-phosphate aldolase, putative	protein coding gene	UP
PF3D7_1022700	PF3D7_1022700.1	188	Plasmodium falciparum 3D7	Pf3D7_10_v3:951,189..953,537(-)	phospholipid scramblase	protein coding gene	DOWN
PF3D7_1026600	PF3D7_1026600.1	189	Plasmodium falciparum 3D7	Pf3D7_10_v3:1,113,232..1,119,224(-)	conserved Plasmodium protein, unknown function	protein coding gene	DOWN
PF3D7_1027300	PF3D7_1027300.1	190	Plasmodium falciparum 3D7	Pf3D7_10_v3:1,139,669..1,144,013(-)	peroxiredoxin	protein coding gene	DOWN
PF3D7_1028700	PF3D7_1028700.1	191	Plasmodium falciparum 3D7	Pf3D7_10_v3:1,179,469..1,183,381(+)	merozoite TRAP-like protein	protein coding gene	DOWN
PF3D7_1028900	PF3D7_1028900.1	192	Plasmodium falciparum 3D7	Pf3D7_10_v3:1,184,559..1,186,461(-)	inner membrane complex protein 1m, putative	protein coding gene	DOWN
PF3D7_1031000	PF3D7_1031000.1	193	Plasmodium falciparum 3D7	Pf3D7_10_v3:1,253,373..1,254,412(-)	ookinete surface protein P25	protein coding gene	UP
PF3D7_1031800	PF3D7_1031800.1	194	Plasmodium falciparum 3D7	Pf3D7_10_v3:1,282,058..1,284,276(-)	conserved protein, unknown function	protein coding gene	DOWN
PF3D7_1035100	PF3D7_1035100.1	195	Plasmodium falciparum 3D7	Pf3D7_10_v3:1,391,390..1,393,405(+)	probable protein, unknown function	protein coding gene	DOWN
PF3D7_1035200	PF3D7_1035200.1	196	Plasmodium falciparum 3D7	Pf3D7_10_v3:1,393,856..1,397,323(+)	S-antigen	protein coding gene	DOWN
PF3D7_1035300	PF3D7_1035300.1	197	Plasmodium falciparum 3D7	Pf3D7_10_v3:1,398,801..1,403,741(+)	glutamate-rich protein GLURP	protein coding gene	DOWN
PF3D7_1035400	PF3D7_1035400.1	198	Plasmodium falciparum 3D7	Pf3D7_10_v3:1,403,807..1,406,234(+)	merozoite surface protein 3	protein coding gene	DOWN
PF3D7_1035500	PF3D7_1035500.1	199	Plasmodium falciparum 3D7	Pf3D7_10_v3:1,406,658..1,409,053(+)	merozoite surface protein 6	protein coding gene	DOWN
PF3D7_1035700	PF3D7_1035700.1	200	Plasmodium falciparum 3D7	Pf3D7_10_v3:1,412,641..1,416,363(+)	duffy binding-like merozoite surface protein	protein coding gene	DOWN
PF3D7_1035900	PF3D7_1035900.1	201	Plasmodium falciparum 3D7	Pf3D7_10_v3:1,423,666..1,425,959(+)	merozoites-associated armadillo repeats protein	protein coding gene	DOWN
PF3D7_1036000	PF3D7_1036000.1	202	Plasmodium falciparum 3D7	Pf3D7_10_v3:1,426,843..1,429,332(+)	merozoite surface protein 11	protein coding gene	DOWN

University of Ghana http://ugspace.ug.edu.gh

PF3D7_1036500	PF3D7_1036500.1	203	Plasmodium falciparum 3D7	Pf3D7_10_v3:1,440,686..1,443,875(+)	conserved Plasmodium protein, unknown function	protein coding gene	DOWN
PF3D7_1102700	PF3D7_1102700.1	204	Plasmodium falciparum 3D7	Pf3D7_11_v3:127,762..130,186(+)	early transcribed membrane protein 11.1	protein coding gene	DOWN
PF3D7_1102800	PF3D7_1102800.1	205	Plasmodium falciparum 3D7	Pf3D7_11_v3:129,265..132,824(-)	early transcribed membrane protein 11.2	protein coding gene	DOWN
PF3D7_1103500	PF3D7_1103500.1	206	Plasmodium falciparum 3D7	Pf3D7_11_v3:151,196..154,519(-)	CPW-WPC family protein	protein coding gene	UP
PF3D7_1104900	PF3D7_1104900.1	207	Plasmodium falciparum 3D7	Pf3D7_11_v3:212,772..220,288(+)	calcium/calmodulin-dependent protein kinase, putative	protein coding gene	DOWN
PF3D7_1105000	PF3D7_1105000.1	208	Plasmodium falciparum 3D7	Pf3D7_11_v3:219,926..223,878(-)	histone H4	protein coding gene	DOWN
PF3D7_1106900	PF3D7_1106900.1	209	Plasmodium falciparum 3D7	Pf3D7_11_v3:289,667..290,290(+)	conserved Plasmodium protein, unknown function	protein coding gene	UP
PF3D7_1115100	PF3D7_1115100.1	210	Plasmodium falciparum 3D7	Pf3D7_11_v3:570,914..573,409(-)	conserved protein, unknown function	protein coding gene	UP
PF3D7_1115800	PF3D7_1115800.1	211	Plasmodium falciparum 3D7	Pf3D7_11_v3:595,116..598,541(-)	conserved Plasmodium protein, unknown function	protein coding gene	DOWN
PF3D7_1116000	PF3D7_1116000.1	212	Plasmodium falciparum 3D7	Pf3D7_11_v3:602,440..607,471(-)	rhoptry neck protein 4	protein coding gene	DOWN
PF3D7_1117300	PF3D7_1117300.1	213	Plasmodium falciparum 3D7	Pf3D7_11_v3:661,949..662,633(+)	conserved protein, unknown function	protein coding gene	DOWN
PF3D7_1117400	PF3D7_1117400.1	214	Plasmodium falciparum 3D7	Pf3D7_11_v3:663,535..665,778(+)	conserved Plasmodium protein, unknown function	protein coding gene	DOWN
PF3D7_1121300	PF3D7_1121300.1	215	Plasmodium falciparum 3D7	Pf3D7_11_v3:801,809..808,198(-)	tyrosine kinase-like protein	protein coding gene	DOWN
PF3D7_1122700	PF3D7_1122700.1	216	Plasmodium falciparum 3D7	Pf3D7_11_v3:868,275..869,789(-)	conserved Plasmodium protein, unknown function	protein coding gene	DOWN
PF3D7_1125700	PF3D7_1125700.1	217	Plasmodium falciparum 3D7	Pf3D7_11_v3:1,004,021..1,007,682(-)	kelch domain-containing protein, putative	protein coding gene	DOWN
PF3D7_1125800	PF3D7_1125800.1	218	Plasmodium falciparum 3D7	Pf3D7_11_v3:1,007,693..1,011,537(-)	kelch domain-containing protein, putative	protein coding gene	DOWN
PF3D7_1126700	PF3D7_1126700.1	219	Plasmodium falciparum 3D7	Pf3D7_11_v3:1,040,447..1,048,468(-)	conserved Plasmodium protein, unknown function	protein coding gene	DOWN
PF3D7_1133400	PF3D7_1133400.1	220	Plasmodium falciparum 3D7	Pf3D7_11_v3:1,292,966..1,296,696(+)	apical membrane antigen 1	protein coding gene	DOWN
PF3D7_1136200	PF3D7_1136200.1	221	Plasmodium falciparum 3D7	Pf3D7_11_v3:1,417,279..1,420,432(-)	conserved Plasmodium protein, unknown function	protein coding gene	DOWN
PF3D7_1136500	PF3D7_1136500.1	222	Plasmodium falciparum 3D7	Pf3D7_11_v3:1,431,881..1,435,170(-)	casein kinase 1	protein coding gene	DOWN
PF3D7_1136500	PF3D7_1136500.2	222	Plasmodium falciparum 3D7	Pf3D7_11_v3:1,431,881..1,435,170(-)	casein kinase 1	protein coding gene	DOWN
PF3D7_1136700	PF3D7_1136700.1	223	Plasmodium falciparum 3D7	Pf3D7_11_v3:1,446,063..1,449,550(+)	armadillo-interacting protein AIP	protein coding gene	DOWN
PF3D7_1136700	PF3D7_1136700.2	223	Plasmodium falciparum 3D7	Pf3D7_11_v3:1,446,063..1,449,550(+)	armadillo-interacting protein AIP	protein coding gene	DOWN
PF3D7_1137900	PF3D7_1137900.1	224	Plasmodium falciparum 3D7	Pf3D7_11_v3:1,483,375..1,485,858(+)	conserved Plasmodium protein, unknown function	protein coding gene	UP
PF3D7_1140400	PF3D7_1140400.1	225	Plasmodium falciparum 3D7	Pf3D7_11_v3:1,607,519..1,608,723(+)	conserved Plasmodium protein, unknown function	protein coding gene	DOWN
PF3D7_1141800	PF3D7_1141800.1	226	Plasmodium falciparum 3D7	Pf3D7_11_v3:1,672,402..1,675,566(-)	EELM2 domain-containing protein, putative	protein coding gene	DOWN
PF3D7_1149100	PF3D7_1149100.1	227	Plasmodium falciparum 3D7	Pf3D7_11_v3:1,970,810..1,974,642(+)	Plasmodium exported protein, unknown function	protein coding gene	UP
PF3D7_1149100	PF3D7_1149100.2	227	Plasmodium falciparum 3D7	Pf3D7_11_v3:1,970,810..1,974,642(+)	Plasmodium exported protein, unknown function	protein coding gene	UP
PF3D7_1149300	PF3D7_1149300.1	228	Plasmodium falciparum 3D7	Pf3D7_11_v3:1,982,068..1,984,327(+)	serine/threonine protein kinase, FIKK family	protein coding gene	DOWN
PF3D7_1149400	PF3D7_1149400.1	229	Plasmodium falciparum 3D7	Pf3D7_11_v3:1,985,056..1,987,411(-)	Plasmodium exported protein, unknown function	protein coding gene	DOWN
PF3D7_1206500	PF3D7_1206500.1	230	Plasmodium falciparum 3D7	Pf3D7_12_v3:292,233..294,941(+)	Tat binding protein 1(TBP-1)-interacting protein, putative	protein coding gene	UP
PF3D7_1207700	PF3D7_1207700.1	231	Plasmodium falciparum 3D7	Pf3D7_12_v3:351,850..354,006(-)	41-3 protein	protein coding gene	UP
PF3D7_1210200	PF3D7_1210200.1	232	Plasmodium falciparum 3D7	Pf3D7_12_v3:458,672..462,423(-)	zinc finger protein, putative	protein coding gene	UP
PF3D7_1213500	PF3D7_1213500.1	233	Plasmodium falciparum 3D7	Pf3D7_12_v3:583,089..585,323(+)	integral membrane protein GPR180, putative	protein coding gene	UP
PF3D7_1214800	PF3D7_1214800.1	234	Plasmodium falciparum 3D7	Pf3D7_12_v3:616,536..617,998(+)	conserved Plasmodium protein, unknown function	protein coding gene	UP
PF3D7_1218000	PF3D7_1218000.1	235	Plasmodium falciparum 3D7	Pf3D7_12_v3:703,859..706,124(+)	thrombospondin-related apical membrane protein	protein coding gene	DOWN
PF3D7_1221100	PF3D7_1221100.1	236	Plasmodium falciparum 3D7	Pf3D7_12_v3:846,961..849,446(+)	conserved Plasmodium protein, unknown function	protein coding gene	UP
PF3D7_1222600	PF3D7_1222600.1	237	Plasmodium falciparum 3D7	Pf3D7_12_v3:906,714..914,983(+)	AP2 domain transcription factor AP2-G	protein coding gene	DOWN
PF3D7_1222700	PF3D7_1222700.1	238	Plasmodium falciparum 3D7	Pf3D7_12_v3:918,280..920,560(+)	glideosome-associated protein 45	protein coding gene	DOWN
PF3D7_1228600	PF3D7_1228600.1	239	Plasmodium falciparum 3D7	Pf3D7_12_v3:1,160,654..1,163,264(-)	merozoite surface protein 9	protein coding gene	DOWN
PF3D7_1229800	PF3D7_1229800.1	240	Plasmodium falciparum 3D7	Pf3D7_12_v3:1,218,464..1,227,615(-)	myosin J, putative	protein coding gene	DOWN
PF3D7_1232500	PF3D7_1232500.1	241	Plasmodium falciparum 3D7	Pf3D7_12_v3:1,339,320..1,343,378(-)	CG2-related protein, putative	protein coding gene	DOWN
PF3D7_1234700	PF3D7_1234700.1	242	Plasmodium falciparum 3D7	Pf3D7_12_v3:1,446,207..1,450,552(-)	upregulated in late gametocytes ULG8	protein coding gene	UP
PF3D7_1235200	PF3D7_1235200.1	243	Plasmodium falciparum 3D7	Pf3D7_12_v3:1,463,659..1,468,189(-)	V-type K+-independent H+-translocating inorganic pyrophosphatase	protein coding gene	DOWN
PF3D7_1238900	PF3D7_1238900.1	244	Plasmodium falciparum 3D7	Pf3D7_12_v3:1,612,601..1,618,965(-)	protein kinase 2	protein coding gene	DOWN

University of Ghana http://ugspace.ug.edu.gh

PF3D7_1240100	PF3D7_1240100.1	245	Plasmodium falciparum 3D7	Pf3D7_12_v3:1,684,977..1,686,307(-)	early transcribed membrane protein 12	protein coding gene	DOWN
PF3D7_1243400	PF3D7_1243400.1	246	Plasmodium falciparum 3D7	Pf3D7_12_v3:1,818,146..1,820,497(+)	conserved Plasmodium protein, unknown function	protein coding gene	DOWN
PF3D7_1243500	PF3D7_1243500.1	247	Plasmodium falciparum 3D7	Pf3D7_12_v3:1,820,308..1,822,837(-)	vacuolar-sorting protein SNF7, putative	protein coding gene	DOWN
PF3D7_1246400	PF3D7_1246400.1	248	Plasmodium falciparum 3D7	Pf3D7_12_v3:1,931,257..1,933,545(+)	myosin A-tail interacting protein	protein coding gene	DOWN
PF3D7_1248400	PF3D7_1248400.1	249	Plasmodium falciparum 3D7	Pf3D7_12_v3:1,981,753..1,982,857(+)	conserved Plasmodium protein, unknown function	protein coding gene	UP
PF3D7_1250400	PF3D7_1250400.1	250	Plasmodium falciparum 3D7	Pf3D7_12_v3:2,067,229..2,069,794(+)	conserved Plasmodium protein, unknown function	protein coding gene	UP
PF3D7_1251200	PF3D7_1251200.1	251	Plasmodium falciparum 3D7	Pf3D7_12_v3:2,091,731..2,094,720(+)	coronin	protein coding gene	DOWN
PF3D7_1252100	PF3D7_1252100.1	252	Plasmodium falciparum 3D7	Pf3D7_12_v3:2,113,980..2,123,174(-)	rhoptry neck protein 3	protein coding gene	DOWN
PF3D7_1252400	PF3D7_1252400.1	285	Plasmodium falciparum 3D7	Pf3D7_12_v3:2,136,053..2,144,874(+)	reticulocyte binding protein homologue 3, pseudogene	pseudogene	DOWN
PF3D7_1252500	PF3D7_1252500.1	253	Plasmodium falciparum 3D7	Pf3D7_12_v3:2,145,008..2,147,250(-)	Plasmodium exported protein, unknown function	protein coding gene	UP
PF3D7_1252600	PF3D7_1252600.1	254	Plasmodium falciparum 3D7	Pf3D7_12_v3:2,147,509..2,152,520(+)	esterase, putative	protein coding gene	DOWN
PF3D7_1300300	PF3D7_1300300.1	87	Plasmodium falciparum 3D7	Pf3D7_13_v3:33,358..45,388(-)	erythrocyte membrane protein 1, PfEMP1	protein coding gene	UP
PF3D7_1301600	PF3D7_1301600.1	91	Plasmodium falciparum 3D7	Pf3D7_13_v3:88,139..93,987(-)	erythrocyte binding antigen-140	protein coding gene	DOWN
PF3D7_1302400	PF3D7_1302400.1	140	Plasmodium falciparum 3D7	Pf3D7_13_v3:129,717..131,086(-)	conserved protein, unknown function	protein coding gene	UP
PF3D7_1306000	PF3D7_1306000.1	88	Plasmodium falciparum 3D7	Pf3D7_13_v3:283,370..287,947(+)	conserved Plasmodium protein, unknown function	protein coding gene	DOWN
PF3D7_1307500	PF3D7_1307500.1	89	Plasmodium falciparum 3D7	Pf3D7_13_v3:337,467..339,281(-)	conserved Plasmodium protein, unknown function	protein coding gene	DOWN
PF3D7_1309600	PF3D7_1309600.1	90	Plasmodium falciparum 3D7	Pf3D7_13_v3:438,135..439,566(+)	ribosomal RNA methyltransferase, putative	protein coding gene	UP
PF3D7_1310200	PF3D7_1310200.1	141	Plasmodium falciparum 3D7	Pf3D7_13_v3:453,771..455,266(+)	conserved Plasmodium protein, unknown function	protein coding gene	DOWN
PF3D7_1318000	PF3D7_1318000.1	92	Plasmodium falciparum 3D7	Pf3D7_13_v3:745,720..747,765(-)	conserved protein, unknown function	protein coding gene	DOWN
PF3D7_1321100	PF3D7_1321100.1	142	Plasmodium falciparum 3D7	Pf3D7_13_v3:861,001..872,925(-)	protein kinase domain-containing protein, putative	protein coding gene	DOWN
PF3D7_1322900	PF3D7_1322900.1	143	Plasmodium falciparum 3D7	Pf3D7_13_v3:961,213..963,561(+)	conserved protein, unknown function	protein coding gene	UP
PF3D7_1323700	PF3D7_1323700.1	93	Plasmodium falciparum 3D7	Pf3D7_13_v3:981,651..984,211(+)	glideosome associated protein with multiple membrane spans 1	protein coding gene	DOWN
PF3D7_1327500	PF3D7_1327500.1	144	Plasmodium falciparum 3D7	Pf3D7_13_v3:1,154,684..1,158,545(+)	conserved protein, unknown function	protein coding gene	DOWN
PF3D7_1331000	PF3D7_1331000.1	94	Plasmodium falciparum 3D7	Pf3D7_13_v3:1,297,070..1,299,355(-)	protein kinase, putative	protein coding gene	DOWN
PF3D7_1332200	PF3D7_1332200.1	95	Plasmodium falciparum 3D7	Pf3D7_13_v3:1,332,221..1,335,647(+)	conserved protein, unknown function	protein coding gene	DOWN
PF3D7_1335100	PF3D7_1335100.1	96	Plasmodium falciparum 3D7	Pf3D7_13_v3:1,418,213..1,421,552(-)	merozoite surface protein 7	protein coding gene	DOWN
PF3D7_1335300	PF3D7_1335300.1	145	Plasmodium falciparum 3D7	Pf3D7_13_v3:1,428,350..1,439,462(-)	reticulocyte binding protein 2 homologue b	protein coding gene	DOWN
PF3D7_1335400	PF3D7_1335400.1	97	Plasmodium falciparum 3D7	Pf3D7_13_v3:1,440,169..1,451,101(+)	reticulocyte binding protein 2 homologue a	protein coding gene	DOWN
PF3D7_1342600	PF3D7_1342600.1	98	Plasmodium falciparum 3D7	Pf3D7_13_v3:1,673,239..1,677,299(+)	myosin A	protein coding gene	DOWN
PF3D7_1343000	PF3D7_1343000.1	99	Plasmodium falciparum 3D7	Pf3D7_13_v3:1,695,462..1,699,267(+)	phosphoethanolamine N-methyltransferase	protein coding gene	DOWN
PF3D7_1348100	PF3D7_1348100.1	100	Plasmodium falciparum 3D7	Pf3D7_13_v3:1,925,011..1,927,105(+)	GTPase, putative	protein coding gene	DOWN
PF3D7_1351700	PF3D7_1351700.1	101	Plasmodium falciparum 3D7	Pf3D7_13_v3:2,058,839..2,064,747(+)	inner membrane complex protein 1f, putative	protein coding gene	DOWN
PF3D7_1354700	PF3D7_1354700.1	102	Plasmodium falciparum 3D7	Pf3D7_13_v3:2,178,639..2,179,862(-)	conserved Plasmodium protein, unknown function	protein coding gene	UP
PF3D7_1361400	PF3D7_1361400.1	103	Plasmodium falciparum 3D7	Pf3D7_13_v3:2,463,755..2,464,745(-)	actin-depolymerizing factor 2	protein coding gene	DOWN
PF3D7_1361500	PF3D7_1361500.1	146	Plasmodium falciparum 3D7	Pf3D7_13_v3:2,464,790..2,468,539(-)	PH domain-containing protein, putative	protein coding gene	DOWN
PF3D7_1361500	PF3D7_1361500.2	146	Plasmodium falciparum 3D7	Pf3D7_13_v3:2,464,790..2,468,539(-)	PH domain-containing protein, putative	protein coding gene	DOWN
PF3D7_1362600	PF3D7_1362600.1	104	Plasmodium falciparum 3D7	Pf3D7_13_v3:2,505,912..2,507,356(+)	conserved protein, unknown function	protein coding gene	UP
PF3D7_1367300	PF3D7_1367300.1	105	Plasmodium falciparum 3D7	Pf3D7_13_v3:2,685,059..2,686,331(-)	conserved Plasmodium protein, unknown function	protein coding gene	UP
PF3D7_1369400	PF3D7_1369400.1	147	Plasmodium falciparum 3D7	Pf3D7_13_v3:2,759,048..2,768,913(+)	conserved Plasmodium protein, unknown function	protein coding gene	UP
PF3D7_1371600	PF3D7_1371600.1	286	Plasmodium falciparum 3D7	Pf3D7_13_v3:2,811,706..2,820,270(+)	erythrocyte binding like protein 1, pseudogene	pseudogene	DOWN
PF3D7_1371700	PF3D7_1371700.1	150	Plasmodium falciparum 3D7	Pf3D7_13_v3:2,821,078..2,824,446(+)	serine/threonine protein kinase, FIKK family	protein coding gene	DOWN
PF3D7_1371800	PF3D7_1371800.1	151	Plasmodium falciparum 3D7	Pf3D7_13_v3:2,823,251..2,825,967(-)	Plasmodium exported protein, unknown function	protein coding gene	DOWN
PF3D7_1401100	PF3D7_1401100.1	255	Plasmodium falciparum 3D7	Pf3D7_14_v3:39,940..43,736(-)	DnaJ protein, putative	protein coding gene	DOWN
PF3D7_1403200	PF3D7_1403200.1	256	Plasmodium falciparum 3D7	Pf3D7_14_v3:119,995..121,405(-)	EGF domain-containing protein, putative	protein coding gene	UP
PF3D7_1404300	PF3D7_1404300.1	257	Plasmodium falciparum 3D7	Pf3D7_14_v3:150,000..150,608(+)	secreted ookinete adhesive protein, putative	protein coding gene	DOWN

University of Ghana http://ugspace.ug.edu.gh

PF3D7_1408300	PF3D7_1408300.1	258	Plasmodium falciparum 3D7	Pf3D7_14_v3:312,569..313,296(+)	conserved Plasmodium protein, unknown function	protein coding gene	DOWN
PF3D7_1408800	PF3D7_1408800.1	259	Plasmodium falciparum 3D7	Pf3D7_14_v3:348,831..350,857(+)	conserved Plasmodium protein, unknown function	protein coding gene	UP
PF3D7_1410400	PF3D7_1410400.1	260	Plasmodium falciparum 3D7	Pf3D7_14_v3:419,442..423,481(+)	rhoptry-associated protein 1	protein coding gene	DOWN
PF3D7_1413700	PF3D7_1413700.1	261	Plasmodium falciparum 3D7	Pf3D7_14_v3:540,168..546,533(-)	DET1 domain-containing protein, putative	protein coding gene	DOWN
PF3D7_1423300	PF3D7_1423300.1	262	Plasmodium falciparum 3D7	Pf3D7_14_v3:935,849..941,730(+)	serine/threonine protein phosphatase 7	protein coding gene	DOWN
PF3D7_1426500	PF3D7_1426500.1	263	Plasmodium falciparum 3D7	Pf3D7_14_v3:1,027,682..1,030,025(-)	ABC transporter G family member 2	protein coding gene	UP
PF3D7_1429400	PF3D7_1429400.1	264	Plasmodium falciparum 3D7	Pf3D7_14_v3:1,154,726..1,163,789(+)	rRNA (adenosine-2'-O-)-methyltransferase, putative	protein coding gene	UP
PF3D7_1431400	PF3D7_1431400.1	265	Plasmodium falciparum 3D7	Pf3D7_14_v3:1,232,648..1,237,614(-)	surface-related antigen SRA	protein coding gene	DOWN
PF3D7_1433700	PF3D7_1433700.1	266	Plasmodium falciparum 3D7	Pf3D7_14_v3:1,341,313..1,349,600(-)	conserved Plasmodium protein, unknown function	protein coding gene	DOWN
PF3D7_1437300	PF3D7_1437300.1	267	Plasmodium falciparum 3D7	Pf3D7_14_v3:1,513,414..1,515,796(-)	conserved Plasmodium protein, unknown function	protein coding gene	DOWN
PF3D7_1440900	PF3D7_1440900.1	268	Plasmodium falciparum 3D7	Pf3D7_14_v3:1,668,319..1,670,272(+)	conserved Plasmodium protein, unknown function	protein coding gene	DOWN
PF3D7_1449200	PF3D7_1449200.1	269	Plasmodium falciparum 3D7	Pf3D7_14_v3:2,013,486..2,015,102(+)	conserved Plasmodium protein, unknown function	protein coding gene	DOWN
PF3D7_1453500	PF3D7_1453500.1	270	Plasmodium falciparum 3D7	Pf3D7_14_v3:2,194,694..2,198,480(-)	NAD(P) transhydrogenase, putative	protein coding gene	UP
PF3D7_1455300	PF3D7_1455300.1	271	Plasmodium falciparum 3D7	Pf3D7_14_v3:2,258,680..2,262,632(+)	conserved protein, unknown function	protein coding gene	DOWN
PF3D7_1455600	PF3D7_1455600.1	272	Plasmodium falciparum 3D7	Pf3D7_14_v3:2,271,364..2,277,727(-)	ferlin, putative	protein coding gene	DOWN
PF3D7_1460600	PF3D7_1460600.1	273	Plasmodium falciparum 3D7	Pf3D7_14_v3:2,473,732..2,475,410(+)	inner membrane complex sub-compartment protein 3	protein coding gene	DOWN
PF3D7_1461800	PF3D7_1461800.1	274	Plasmodium falciparum 3D7	Pf3D7_14_v3:2,503,209..2,514,031(+)	conserved Plasmodium protein, unknown function	protein coding gene	UP
PF3D7_1463900	PF3D7_1463900.1	275	Plasmodium falciparum 3D7	Pf3D7_14_v3:2,584,086..2,590,847(-)	rhoptry neck protein 11, putative	protein coding gene	DOWN
PF3D7_1466800	PF3D7_1466800.1	276	Plasmodium falciparum 3D7	Pf3D7_14_v3:2,731,557..2,735,622(+)	NOC3 domain-containing protein, putative	protein coding gene	UP
PF3D7_1468400	PF3D7_1468400.1	277	Plasmodium falciparum 3D7	Pf3D7_14_v3:2,809,460..2,812,520(+)	zinc finger protein, putative	protein coding gene	DOWN
PF3D7_1471600	PF3D7_1471600.1	278	Plasmodium falciparum 3D7	Pf3D7_14_v3:2,925,721..2,929,673(+)	apical polar ring protein APR2, putative	protein coding gene	UP
PF3D7_1471700	PF3D7_1471700.1	279	Plasmodium falciparum 3D7	Pf3D7_14_v3:2,929,823..2,931,547(+)	conserved Plasmodium protein, unknown function	protein coding gene	UP
PF3D7_1471800	PF3D7_1471800.1	280	Plasmodium falciparum 3D7	Pf3D7_14_v3:2,931,759..2,932,950(+)	conserved Plasmodium protein, unknown function	protein coding gene	UP
PF3D7_1478400	PF3D7_1478400.1	287	Plasmodium falciparum 3D7	Pf3D7_14_v3:3,223,288..3,224,632(-)	Plasmodium exported protein, unknown function, pseudogene	pseudogene	UP
PF3D7_1479600	PF3D7_1479600.1	281	Plasmodium falciparum 3D7	Pf3D7_14_v3:3,272,578..3,273,848(+)	rifin	protein coding gene	DOWN

University of Ghana http://ugspace.ug.edu.gh

Supplementary Table 5.11 Gene ontology enrichment analysis for up/down-regulated genes between R539T untreated and DHA_treated condition

University of Ghana http://ugspace.ug.edu.gh

Gene ontology term	Differential expression	ID	Name	Bgd count	Result count	Result gene list	Per of bgd	Fold enrichment	Odds ratio	P-value	Benjamini	Bonferroni
Biological process	Upregulated	GO:0006740	NADPH regeneration	10	2	PF3D7_1021600,PF3D7_1453500,	20	19.47	25.05	0.00441466	0.254619392	0.41939295
		GO:0006739	NADP metabolic process	11	2	PF3D7_1021600,PF3D7_1453500,	18.2	17.7	22.26	0.00536041	0.254619392	0.509238784
		GO:0019236	response to pheromone	2	1	PF3D7_1213500,	50	48.68	98.31	0.02043891	0.407794864	1
		GO:0006869	lipid transport	3	1	PF3D7_1426500,	33.3	32.45	49.14	0.03050427	0.407794864	1
		GO:0009264	deoxyribonucleotide catabolic process	3	1	PF3D7_1021600,	33.3	32.45	49.14	0.03050427	0.407794864	1
		GO:0043570	maintenance of DNA repeat elements	3	1	PF3D7_0706700,	33.3	32.45	49.14	0.03050427	0.407794864	1
		GO:0046386	deoxyribose phosphate catabolic process	3	1	PF3D7_1021600,	33.3	32.45	49.14	0.03050427	0.407794864	1
		GO:0045910	negative regulation of DNA recombination	4	1	PF3D7_0706700,	25	24.34	32.76	0.04046826	0.407794864	1

		GO:0 0094 05	obsolete pathogenesis	75	3	PF3D7_0209000,PF3D7_0936500,PF3D7_1300300,	4	3.89	4.21	0.0410 7038	0.407794864	1
	Downreg ulated	GO:0 0521 26	movement in host environment	120	42	PF3D7_0102500,PF3D7_0206200,PF3D7_0207500,PF3D7_0207600,PF3D7_0214900,PF3D7_0217500,PF3D7_0304000,PF3D7_0404700,PF3D7_0404900,PF3D7_0423400,PF3D7_0423800,PF3D7_0424100,PF3D7_0501600,PF3D7_0507500,PF3D7_0612700,PF3D7_0707300,PF3D7_0722200,PF3D7_0731500,PF3D7_0808200,PF3D7_0905400,PF3D7_0929400,PF3D7_0930300,PF3D7_0934800,PF3D7_1012200,PF3D7_1014100,PF3D7_1027300,PF3D7_1028700,PF3D7_1035400,PF3D7_1035500,PF3D7_1035700,PF3D7_1035900,PF3D7_1116000,PF3D7_1133400,PF3D7_1136700,PF3D7_1218000,PF3D7_1222700,PF3D7_1252100,PF3D7_1335100,PF3D7_1335300,PF3D7_1335400,PF3D7_1342600,PF3D7_1431400,	35	8.43	15.44	3.47E- 29	9.66E-27	9.66E-27
		GO:0 0444 09	entry into host	103	38	PF3D7_0102500,PF3D7_0214900,PF3D7_0217500,PF3D7_0304000,PF3D7_0404700,PF3D7_0404900,PF3D7_0423400,PF3D7_0423800,PF3D7_0424100,PF3D7_0501600,PF3D7_0612700,PF3D7_0707300,PF3D7_0722200,PF3D7_0731500,PF3D7_0808200,PF3D7_0905400,PF3D7_0929400,PF3D7_0930300,PF3D7_0934800,PF3D7_1012200,PF3D7_1014100,PF3D7_1027300,PF3D7_1028700,PF3D7_1035400,PF3D7_1035500,PF3D7_1035700,PF3D7_1035900,PF3D7_1116000,PF3D7_1133400,PF3D7_1136700,PF3D7_1218000,PF3D7_1222700,PF3D7_1252100,PF3D7_1335100,PF3D7_1335300,PF3D7_1335400,PF3D7_1342600,PF3D7_1431400,	36.9	8.89	16.4	2.18E- 27	3.03E-25	6.05E-25
		GO:0 0444 03	biological process involved in symbiotic interaction	397	54	PF3D7_0102500,PF3D7_0113000,PF3D7_0206200,PF3D7_0207500,PF3D7_0207600,PF3D7_0214900,PF3D7_0217500,PF3D7_0220800,PF3D7_0302200,PF3D7_0302500,PF3D7_0304000,PF3D7_0404700,PF3D7_0404900,PF3D7_0423400,PF3D7_0423800,PF3D7_0424100,PF3D7_0426000,PF3D7_0500900,PF3D7_0501600,PF3D7_0507500,PF3D7_0612700,PF3D7_0632200,PF3D7_0707300,PF3D7_0722200,PF3D7_0731500,PF3D7_0808200,PF3D7_0831600,PF3D7_0905400,PF3D7_0929400,PF3D7_0930300,PF3D7_0934800,PF3D7_1000600,PF3D7_1012200,PF3D7_1014100,PF3D7_1027300,PF3D7_1028700,PF3D7_1035400,PF3D7_1035500,PF3D7_1035700,PF3D7_1035900,PF3D7_1116000,PF3D7_1133400,PF3D7_1136700,PF3D7_1149300,PF3D7_1218000,PF3D7_1222700,PF3D7_1252100,PF3D7_1335100,PF3D7_1335300,PF3D7_1335400,PF3D7_1342600,PF3D7_1371700,PF3D7_1431400,PF3D7_1479600,	13.6	3.28	4.6	5.19E- 16	4.52E-14	1.44E-13

University of Ghana http://ugspace.ug.edu.gh

		GO:0044419	biological process involved in interspecies interaction between organisms	399	54	PF3D7_0102500,PF3D7_0113000,PF3D7_0206200,PF3D7_0207500,PF3D7_0207600,PF3D7_0214900,PF3D7_0217500,PF3D7_0220800,PF3D7_0302200,PF3D7_0302500,PF3D7_0304000,PF3D7_0404700,PF3D7_0404900,PF3D7_0423400,PF3D7_0423800,PF3D7_0424100,PF3D7_0426000,PF3D7_0500900,PF3D7_0501600,PF3D7_0507500,PF3D7_0612700,PF3D7_0632200,PF3D7_0707300,PF3D7_0722200,PF3D7_0731500,PF3D7_0808200,PF3D7_0831600,PF3D7_0905400,PF3D7_0929400,PF3D7_0930300,PF3D7_0934800,PF3D7_1000600,PF3D7_1012200,PF3D7_1014100,PF3D7_1027300,PF3D7_1028700,PF3D7_1035400,PF3D7_1035500,PF3D7_1035700,PF3D7_1035900,PF3D7_1116000,PF3D7_1133400,PF3D7_1136700,PF3D7_1149300,PF3D7_1218000,PF3D7_1222700,PF3D7_1252100,PF3D7_1335100,PF3D7_1335300,PF3D7_1335400,PF3D7_1342600,PF3D7_1371700,PF3D7_1431400,PF3D7_1479600,	13.5	3.26	4.57	6.50E-16	4.52E-14	1.81E-13
		GO:0051701	biological process involved in interaction with host	382	50	PF3D7_0102500,PF3D7_0113000,PF3D7_0206200,PF3D7_0207500,PF3D7_0207600,PF3D7_0214900,PF3D7_0217500,PF3D7_0304000,PF3D7_0404700,PF3D7_0404900,PF3D7_0423400,PF3D7_0423800,PF3D7_0424100,PF3D7_0426000,PF3D7_0500900,PF3D7_0501600,PF3D7_0507500,PF3D7_0612700,PF3D7_0632200,PF3D7_0707300,PF3D7_0722200,PF3D7_0731500,PF3D7_0808200,PF3D7_0905400,PF3D7_0929400,PF3D7_0930300,PF3D7_0934800,PF3D7_1000600,PF3D7_1012200,PF3D7_1014100,PF3D7_1027300,PF3D7_1028700,PF3D7_1035400,PF3D7_1035500,PF3D7_1035700,PF3D7_1035900,PF3D7_1116000,PF3D7_1133400,PF3D7_1136700,PF3D7_1149300,PF3D7_1218000,PF3D7_1222700,PF3D7_1252100,PF3D7_1335100,PF3D7_1335300,PF3D7_1335400,PF3D7_1342600,PF3D7_1371700,PF3D7_1431400,PF3D7_1479600,	13.1	3.15	4.29	4.10E-14	2.28E-12	1.14E-11
		GO:0008150	biological process	662	68	PF3D7_0102500,PF3D7_0113000,PF3D7_0206200,PF3D7_0206800,PF3D7_0207400,PF3D7_0207500,PF3D7_0207600,PF3D7_0207700,PF3D7_0207800,PF3D7_0212600,PF3D7_0214900,PF3D7_0217500,PF3D7_0220800,PF3D7_0302200,PF3D7_0302500,PF3D7_0304000,PF3D7_0320500,PF3D7_0404700,PF3D7_0404900,PF3D7_0423400,PF3D7_0423800,PF3D7_0424100,PF3D7_0426000,PF3D7_0500900,PF3D7_0501600,PF3D7_0507500,PF3D7_0612700,PF3D7_0617800,PF3D7_0632200,PF3D7_0707300,PF3D7_0722200,PF3D7_0731500,PF3D7_0802600,PF3D7_0808200,PF3D7_0831600,PF3D7_0902100,PF3D7_0905400,PF3D7_0929400,PF3D7_0930300,PF3D7_0934800,PF3D7_1000600,PF3D7_1012200,PF3D7_1014100,PF3D7_1027300,PF3D7_1028700,PF3D7_1035400,PF3D7_1035500,PF3D7_103	10.3	2.48	3.48	7.68E-14	3.56E-12	2.13E-11

University of Ghana http://ugspace.ug.edu.gh

						5700,PF3D7_1035900,PF3D7_1104900,PF3D7_1105000,PF3D7_1116000,PF3D7_1133400,PF3D7_1136700,PF3D7_1149300,PF3D7_1218000,PF3D7_1222700,PF3D7_1238900,PF3D7_1251100,PF3D7_1301600,PF3D7_1325100,PF3D7_1335300,PF3D7_1335400,PF3D7_1342600,PF3D7_1348100,PF3D7_1371700,PF3D7_1431400,PF3D7_1479600,						
		GO:0035891	exit from host cell	28	9	PF3D7_0206200,PF3D7_0207500,PF3D7_0207600,PF3D7_0217500,PF3D7_0507500,PF3D7_0808200,PF3D7_0930300,PF3D7_1014100,PF3D7_1028700,	32.1	7.75	11.41	1.06E-06	4.22E-05	0.000295268
		GO:0035890	exit from host	29	9	PF3D7_0206200,PF3D7_0207500,PF3D7_0207600,PF3D7_0217500,PF3D7_0507500,PF3D7_0808200,PF3D7_0930300,PF3D7_1014100,PF3D7_1028700,	31	7.48	10.83	1.49E-06	5.16E-05	0.000412895
		GO:0050776	regulation of immune response	12	6	PF3D7_0102200,PF3D7_0207400,PF3D7_0207500,PF3D7_0207600,PF3D7_0207700,PF3D7_0207800,	50	12.05	23.78	3.56E-06	0.000109843	0.000988591
		GO:0002377	immunoglobulin production	8	5	PF3D7_0207400,PF3D7_0207500,PF3D7_0207600,PF3D7_0207700,PF3D7_0207800,	62.5	15.06	39.45	5.93E-06	0.000147728	0.001647263
		GO:0002440	production of molecular mediator of immune response	8	5	PF3D7_0207400,PF3D7_0207500,PF3D7_0207600,PF3D7_0207700,PF3D7_0207800,	62.5	15.06	39.45	5.93E-06	0.000147728	0.001647263
		GO:0002682	regulation of immune system process	13	6	PF3D7_0102200,PF3D7_0207400,PF3D7_0207500,PF3D7_0207600,PF3D7_0207700,PF3D7_0207800,	46.2	11.12	20.37	6.38E-06	0.000147728	0.001772737
		GO:0002376	immune system process	14	6	PF3D7_0207400,PF3D7_0207500,PF3D7_0207600,PF3D7_0207700,PF3D7_0207800,PF3D7_1301600,	42.9	10.33	17.82	1.08E-05	0.000230426	0.002995532
		GO:0007015	actin filament organization	16	6	PF3D7_0105300,PF3D7_0613900,PF3D7_1229800,PF3D7_1251200,PF3D7_1342600,PF3D7_1361400,	37.5	9.04	14.25	2.68E-05	0.000532018	0.00744825

University of Ghana http://ugspace.ug.edu.gh

		GO:0030029	actin filament-based process	19	6	PF3D7_0105300,PF3D7_0613900,PF3D7_1229800,PF3D7_1251200,PF3D7_1342600,PF3D7_1361400,	31.6	7.61	10.96	8.17E-05	0.001420305	0.022724887
		GO:0030036	actin cytoskeleton organization	19	6	PF3D7_0105300,PF3D7_0613900,PF3D7_1229800,PF3D7_1251200,PF3D7_1342600,PF3D7_1361400,	31.6	7.61	10.96	8.17E-05	0.001420305	0.022724887
		GO:0097435	supramolecular fiber organization	28	7	PF3D7_0105300,PF3D7_0613900,PF3D7_1126700,PF3D7_1229800,PF3D7_1251200,PF3D7_1342600,PF3D7_1361400,	25	6.02	7.94	0.00010743	0.0017568	0.029865596
		GO:0006468	protein phosphorylation	110	14	PF3D7_0214600,PF3D7_0217500,PF3D7_0321400,PF3D7_0500900,PF3D7_0902100,PF3D7_0934800,PF3D7_1104900,PF3D7_1121300,PF3D7_1136500,PF3D7_1149300,PF3D7_1238900,PF3D7_1321100,PF3D7_1331000,PF3D7_1371700,	12.7	3.07	3.54	0.00015466	0.002388613	0.042995042
		GO:0030048	actin filament-based movement	9	4	PF3D7_0613900,PF3D7_1229800,PF3D7_1342600,PF3D7_1361400,	44.4	10.71	18.83	0.00030777	0.004503129	0.085559456
		GO:0030705	cytoskeleton-dependent intracellular transport	10	4	PF3D7_0613900,PF3D7_1126700,PF3D7_1229800,PF3D7_1342600,	40	9.64	15.69	0.00049635	0.006899219	0.137984384
		GO:0018105	peptidyl-serine phosphorylation	18	5	PF3D7_0217500,PF3D7_0934800,PF3D7_1104900,PF3D7_1136500,PF3D7_1238900,	27.8	6.69	9.08	0.00064452	0.008532252	0.179177295
		GO:0018209	peptidyl-serine modification	19	5	PF3D7_0217500,PF3D7_0934800,PF3D7_1104900,PF3D7_1136500,PF3D7_1238900,	26.3	6.34	8.43	0.00084551	0.010684234	0.235053155
		GO:0016310	phosphorylation	135	14	PF3D7_0214600,PF3D7_0217500,PF3D7_0321400,PF3D7_0500900,PF3D7_0902100,PF3D7_0934800,PF3D7_1104900,PF3D7_1121300,PF3D7_1136500,PF3D7_1149300,PF3D7_1238900,PF3D7_1321100,PF3D7_1331000,PF3D7_1371700,	10.4	2.5	2.8	0.00128241	0.014269623	0.356508971
		GO:0030050	vesicle transport along actin filament	6	3	PF3D7_0613900,PF3D7_1229800,PF3D7_1342600,	50	12.05	23.43	0.00128324	0.014269623	0.356740563

University of Ghana http://ugspace.ug.edu.gh

University of Ghana http://ugspace.ug.edu.gh

		GO:0099515	actin filament-based transport	6	3	PF3D7_0613900,PF3D7_1229800,PF3D7_1342600,	50	12.05	23.43	0.00128324	0.014269623	0.356740563
		GO:0099518	vesicle cytoskeletal trafficking	7	3	PF3D7_0613900,PF3D7_1229800,PF3D7_1342600,	42.9	10.33	17.57	0.00217718	0.023279094	0.605256453
		GO:0048870	cell motility	16	4	PF3D7_0613900,PF3D7_1251200,PF3D7_1342600,PF3D7_1361400,	25	6.02	7.84	0.00353442	0.036391409	0.982568056
		GO:0051648	vesicle localization	9	3	PF3D7_0613900,PF3D7_1229800,PF3D7_1342600,	33.3	8.03	11.71	0.00491231	0.047090463	1
		GO:0051650	establishment of vesicle localization	9	3	PF3D7_0613900,PF3D7_1229800,PF3D7_1342600,	33.3	8.03	11.71	0.00491231	0.047090463	1
		GO:0035556	intracellular signal transduction	81	9	PF3D7_0217500,PF3D7_0500900,PF3D7_0802600,PF3D7_0902100,PF3D7_1104900,PF3D7_1149300,PF3D7_1238900,PF3D7_1348100,PF3D7_1371700,	11.1	2.68	2.98	0.00595952	0.055224864	1
		GO:0007155	cell adhesion	70	8	PF3D7_0102500,PF3D7_0206800,PF3D7_0212600,PF3D7_0423400,PF3D7_0426000,PF3D7_0707300,PF3D7_1301600,PF3D7_1335400,	11.4	2.75	3.06	0.00790978	0.070932886	1
		GO:0007009	plasma membrane organization	4	2	PF3D7_1022700,PF3D7_1455600,	50	12.05	23.32	0.00972737	0.084506561	1
		GO:0046777	protein autophosphorylation	12	3	PF3D7_0217500,PF3D7_1104900,PF3D7_1238900,	25	6.02	7.8	0.01173301	0.098841758	1
		GO:0098609	cell-cell adhesion	62	7	PF3D7_0102500,PF3D7_0212600,PF3D7_0423400,PF3D7_0426000,PF3D7_0707300,PF3D7_1301600,PF3D7_1335400,	11.3	2.72	3.01	0.01354166	0.110723007	1

		GO:0 0081 54	actin polymerization or depolymerization	6	2	PF3D7_0105300,PF3D7_1361400,	33.3	8.03	11.65	0.0230 1497	0.174783994	1
		GO:0 0071 65	signal transduction	119	10	PF3D7_0217500,PF3D7_0500900,PF3D7_0802600,PF3D7_0902100,PF3D7_0934800,PF3D7_1104900,PF3D7_1149300,PF3D7_1238900,PF3D7_1348100,PF3D7_1371700,	8.4	2.03	2.18	0.0251 1068	0.174783994	1
		GO:0 0230 52	signaling	119	10	PF3D7_0217500,PF3D7_0500900,PF3D7_0802600,PF3D7_0902100,PF3D7_0934800,PF3D7_1104900,PF3D7_1149300,PF3D7_1238900,PF3D7_1348100,PF3D7_1371700,	8.4	2.03	2.18	0.0251 1068	0.174783994	1
		GO:0 0070 10	cytoskeleton organization	73	7	PF3D7_0105300,PF3D7_0613900,PF3D7_1126700,PF3D7_1229800,PF3D7_1251200,PF3D7_1342600,PF3D7_1361400,	9.6	2.31	2.5	0.0306 7452	0.174783994	1
		GO:0 0094 05	obsolete pathogenesis	75	7	PF3D7_0102500,PF3D7_0426000,PF3D7_0731500,PF3D7_0930300,PF3D7_1035700,PF3D7_1133400,PF3D7_1301600,	9.3	2.25	2.43	0.0348 8273	0.174783994	1
		GO:0 0071 54	cell communication	127	10	PF3D7_0217500,PF3D7_0500900,PF3D7_0802600,PF3D7_0902100,PF3D7_0934800,PF3D7_1104900,PF3D7_1149300,PF3D7_1238900,PF3D7_1348100,PF3D7_1371700,	7.9	1.9	2.03	0.0371 5137	0.174783994	1
		GO:0 0065 56	S-adenosylmethionine biosynthetic process	1	1	PF3D7_0922200,	100	24.1	inf	0.0414 9548	0.174783994	1
		GO:0 0061 48	inosine catabolic process	1	1	PF3D7_0513300,	100	24.1	inf	0.0414 9548	0.174783994	1
		GO:0 0511 80	vitamin transport	1	1	PF3D7_0206200,	100	24.1	inf	0.0414 9548	0.174783994	1
		GO:0 0513 39	regulation of lyase activity	1	1	PF3D7_0105300,	100	24.1	inf	0.0414 9548	0.174783994	1

University of Ghana http://ugspace.ug.edu.gh

		GO:0075109	modulation by symbiont of host receptor-mediated signal transduction	1	1	PF3D7_0731500,	100	24.1	inf	0.04149548	0.174783994	1
		GO:0052027	modulation by symbiont of host signal transduction pathway	1	1	PF3D7_0731500,	100	24.1	inf	0.04149548	0.174783994	1
		GO:0050900	leukocyte migration	1	1	PF3D7_1301600,	100	24.1	inf	0.04149548	0.174783994	1
		GO:0045861	negative regulation of proteolysis	1	1	PF3D7_0507400,	100	24.1	inf	0.04149548	0.174783994	1
		GO:0015819	lysine transport	1	1	PF3D7_0104800,	100	24.1	inf	0.04149548	0.174783994	1
		GO:0044501	modulation of signal transduction in other organism	1	1	PF3D7_0731500,	100	24.1	inf	0.04149548	0.174783994	1
		GO:0017121	plasma membrane phospholipid scrambling	1	1	PF3D7_1022700,	100	24.1	inf	0.04149548	0.174783994	1
		GO:0015809	arginine transport	1	1	PF3D7_0104800,	100	24.1	inf	0.04149548	0.174783994	1
		GO:0015802	basic amino acid transport	1	1	PF3D7_0104800,	100	24.1	inf	0.04149548	0.174783994	1
		GO:0012501	programmed cell death	1	1	PF3D7_0113000,	100	24.1	inf	0.04149548	0.174783994	1

University of Ghana http://ugspace.ug.edu.gh

		GO:0010951	negative regulation of endopeptidase activity	1	1	PF3D7_0507400,	100	24.1	inf	0.04149548	0.174783994	1
		GO:0010466	negative regulation of peptidase activity	1	1	PF3D7_0507400,	100	24.1	inf	0.04149548	0.174783994	1
		GO:0045761	regulation of adenylate cyclase activity	1	1	PF3D7_0105300,	100	24.1	inf	0.04149548	0.174783994	1
		GO:0030581	symbiont intracellular protein transport in host	1	1	PF3D7_1252100,	100	24.1	inf	0.04149548	0.174783994	1
		GO:0031279	regulation of cyclase activity	1	1	PF3D7_0105300,	100	24.1	inf	0.04149548	0.174783994	1
		GO:0035461	vitamin transmembrane transport	1	1	PF3D7_0206200,	100	24.1	inf	0.04149548	0.174783994	1
		GO:0035821	modulation of process of other organism	1	1	PF3D7_0731500,	100	24.1	inf	0.04149548	0.174783994	1
		GO:0043112	receptor metabolic process	1	1	PF3D7_1361500,	100	24.1	inf	0.04149548	0.174783994	1
		GO:0007163	establishment or maintenance of cell polarity	1	1	PF3D7_0105300,	100	24.1	inf	0.04149548	0.174783994	1
		GO:0015887	pantothenate transmembrane transport	1	1	PF3D7_0206200,	100	24.1	inf	0.04149548	0.174783994	1

University of Ghana http://ugspace.ug.edu.gh

University of Ghana http://ugspace.ug.edu.gh

		GO:0009268	response to pH	1	1	PF3D7_0802600,	100	24.1	inf	0.04149548	0.174783994	1
		GO:0001881	receptor recycling	1	1	PF3D7_1361500,	100	24.1	inf	0.04149548	0.174783994	1
Molecular function	Upregulated	GO:0004139	deoxyribose-phosphate aldolase activity	1	1	PF3D7_1021600,	100	97.36	inf	0.01027116	0.178718159	0.893590797
		GO:0008475	procollagen-lysine 5-dioxygenase activity	1	1	PF3D7_0930000,	100	97.36	inf	0.01027116	0.178718159	0.893590797
		GO:0008746	NAD(P)+ transhydrogenase activity	1	1	PF3D7_1453500,	100	97.36	inf	0.01027116	0.178718159	0.893590797
		GO:0016652	oxidoreductase activity, acting on NAD(P)H, NAD(P) as acceptor	1	1	PF3D7_1453500,	100	97.36	inf	0.01027116	0.178718159	0.893590797
		GO:0070815	peptidyl-lysine 5-dioxygenase activity	1	1	PF3D7_0930000,	100	97.36	inf	0.01027116	0.178718159	0.893590797
		GO:0000406	double-strand/single-strand DNA junction binding	2	1	PF3D7_0706700,	50	48.68	98.31	0.02043891	0.222273137	1
		GO:0008650	rRNA (uridine-2'-O-)-methyltransferase activity	2	1	PF3D7_1309600,	50	48.68	98.31	0.02043891	0.222273137	1
		GO:0016832	aldehyde-lyase activity	2	1	PF3D7_1021600,	50	48.68	98.31	0.02043891	0.222273137	1

University of Ghana http://ugspace.ug.edu.gh

		GO:0004482	mRNA (guanine-N7-)-methyltransferase activity	3	1	PF3D7_1309600,	33.3	32.45	49.14	0.03050427	0.294874627	1
		GO:005201	extracellular matrix structural constituent	4	1	PF3D7_0827200,	25	24.34	32.76	0.04046826	0.345086731	1
	Downregulated	GO:004681 2	host cell surface binding	107	23	PF3D7_0102500,PF3D7_0113000,PF3D7_0423400,PF3D7_0424100,PF3D7_0426000,PF3D7_0620400,PF3D7_0722200,PF3D7_0731500,PF3D7_0817700,PF3D7_0905400,PF3D7_0930300,PF3D7_1012200,PF3D7_1028700,PF3D7_1035500,PF3D7_1035700,PF3D7_1036000,PF3D7_1133400,PF3D7_1252100,PF3D7_1301600,PF3D7_1335100,PF3D7_1335300,PF3D7_1335400,PF3D7_1431400,	21.5	5.18	7.01	3.20E-11	6.62E-09	6.62E-09
		GO:008201	heparin binding	9	6	PF3D7_0102500,PF3D7_0424100,PF3D7_0731500,PF3D7_1301600,PF3D7_1335300,PF3D7_1335400,	66.7	16.07	47.58	3.59E-07	3.72E-05	7.43E-05
		GO:005539	glycosaminoglycan binding	10	6	PF3D7_0102500,PF3D7_0424100,PF3D7_0731500,PF3D7_1301600,PF3D7_1335300,PF3D7_1335400,	60	14.46	35.68	8.67E-07	5.98E-05	0.000179454
		GO:005515	protein binding	605	49	PF3D7_0102200,PF3D7_0207500,PF3D7_0207600,PF3D7_0217500,PF3D7_0301700,PF3D7_0302200,PF3D7_0302500,PF3D7_0401800,PF3D7_0404900,PF3D7_0423800,PF3D7_0424100,PF3D7_0501300,PF3D7_0501600,PF3D7_0507200,PF3D7_0532300,PF3D7_0612700,PF3D7_0701900,PF3D7_0707300,PF3D7_0818900,PF3D7_0830500,PF3D7_0905400,PF3D7_0922200,PF3D7_0929400,PF3D7_0930300,PF3D7_0934800,PF3D7_0936000,PF3D7_1003600,PF3D7_1014100,PF3D7_1017500,PF3D7_1035300,PF3D7_1035400,PF3D7_1035500,PF3D7_1035700,PF3D7_1116000,PF3D7_1125700,PF3D7_1125800,PF3D7_1133400,PF3D7_1136500,PF3D7_1222600,PF3D7_1222700,PF3D7_1246400,PF3D7_1251200,PF3D7_1252100,PF3D7_1323700,PF3D7_1335100,PF3D7_1342600,PF3D7_1343000,PF3D7_1410400,PF3D7_1423300,	8.1	1.95	2.37	1.67E-06	8.65E-05	0.000345917
		GO:004678 9	host cell surface receptor binding	88	13	PF3D7_0102500,PF3D7_0113000,PF3D7_0423400,PF3D7_0424100,PF3D7_0426000,PF3D7_0722200,PF3D7_0731500,PF3D7_0905400,PF3D7_1028700,PF3D7_1035700,PF3D7_1301600,PF3D7_1335100,PF3D7_1335300,	14.8	3.56	4.21	5.64E-05	0.002334097	0.011670484

		GO:0004672	protein kinase activity	108	14	PF3D7_0214600,PF3D7_0217500,PF3D7_0321400,PF3D7_0500900,PF3D7_0902100,PF3D7_0934800,PF3D7_1104900,PF3D7_1121300,PF3D7_1136500,PF3D7_1149300,PF3D7_1238900,PF3D7_1321100,PF3D7_1331000,PF3D7_1371700,	13	3.12	3.62	0.00012661	0.004368018	0.026208106
		GO:0051015	actin filament binding	14	5	PF3D7_0613900,PF3D7_1229800,PF3D7_1251200,PF3D7_1342600,PF3D7_1361400,	35.7	8.61	13.13	0.00017256	0.005102737	0.03571916
		GO:1901681	sulfur compound binding	26	6	PF3D7_0102500,PF3D7_0424100,PF3D7_0731500,PF3D7_1301600,PF3D7_1335300,PF3D7_1335400,	23.1	5.56	7.11	0.00054362	0.014066213	0.112529705
		GO:0004197	cysteine-type endopeptidase activity	27	6	PF3D7_0207400,PF3D7_0207500,PF3D7_0207600,PF3D7_0207700,PF3D7_0207800,PF3D7_0404700,	22.2	5.36	6.77	0.00067509	0.015527108	0.139743969
		GO:0003779	actin binding	30	6	PF3D7_0105300,PF3D7_0613900,PF3D7_1229800,PF3D7_1251200,PF3D7_1342600,PF3D7_1361400,	20	4.82	5.92	0.00122041	0.024148233	0.252625504
		GO:0030898	actin-dependent ATPase activity	6	3	PF3D7_0613900,PF3D7_1229800,PF3D7_1342600,	50	12.05	23.43	0.00128324	0.024148233	0.265630563
		GO:0004867	serine-type endopeptidase inhibitor activity	2	2	PF3D7_0501400,PF3D7_0507400,	100	24.1	inf	0.0017137	0.029561374	0.354736483
		GO:0016773	phosphotransferase activity, alcohol group as acceptor	141	14	PF3D7_0214600,PF3D7_0217500,PF3D7_0321400,PF3D7_0500900,PF3D7_0902100,PF3D7_0934800,PF3D7_1104900,PF3D7_1121300,PF3D7_1136500,PF3D7_1149300,PF3D7_1238900,PF3D7_1321100,PF3D7_1331000,PF3D7_1371700,	9.9	2.39	2.66	0.00195116	0.031068403	0.403889236
		GO:0000146	microfilament motor activity	7	3	PF3D7_0613900,PF3D7_1229800,PF3D7_1342600,	42.9	10.33	17.57	0.00217718	0.032191183	0.450676567
		GO:0044877	protein-containing complex binding	101	11	PF3D7_0613900,PF3D7_0905400,PF3D7_0929400,PF3D7_0930300,PF3D7_1035400,PF3D7_1035500,PF3D7_1035700,PF3D7_1229800,PF3D7_1251200,PF3D7_1342600,PF3D7_1361400,	10.9	2.62	2.93	0.00286278	0.039506325	0.592594872

University of Ghana http://ugspace.ug.edu.gh

		GO:0 0046 74	protein serine/threonine kinase activity	93	10	PF3D7_0214600,PF3D7_0217500,PF3D7_0500900,PF3D7_0902100,PF3D7_0934800,PF3D7_1104900,PF3D7_1136500,PF3D7_1149300,PF3D7_1238900,PF3D7_1371700,	10.8	2.59	2.88	0.0048 3149	0.051752452	1
		GO:0 0108 57	calcium-dependent protein kinase activity	9	3	PF3D7_0217500,PF3D7_1104900,PF3D7_1238900,	33.3	8.03	11.71	0.0049 1231	0.051752452	1
		GO:0 0099 31	calcium-dependent protein serine/threonine kinase activity	9	3	PF3D7_0217500,PF3D7_1104900,PF3D7_1238900,	33.3	8.03	11.71	0.0049 1231	0.051752452	1
		GO:0 0048 66	endopeptidase inhibitor activity	3	2	PF3D7_0501400,PF3D7_0507400,	66.7	16.07	46.65	0.0050 0024	0.051752452	1
		GO:0 0304 14	peptidase inhibitor activity	3	2	PF3D7_0501400,PF3D7_0507400,	66.7	16.07	46.65	0.0050 0024	0.051752452	1
		GO:0 0082 34	cysteine-type peptidase activity	55	7	PF3D7_0207400,PF3D7_0207500,PF3D7_0207600,PF3D7_0207700,PF3D7_0207800,PF3D7_0404700,PF3D7_0919200,	12.7	3.07	3.45	0.0071 281	0.070262686	1
		GO:0 0052 53	anion channel activity	4	2	PF3D7_0302200,PF3D7_0302500,	50	12.05	23.32	0.0097 2737	0.087546366	1
		GO:0 0037 85	actin monomer binding	4	2	PF3D7_0105300,PF3D7_1361400,	50	12.05	23.32	0.0097 2737	0.087546366	1
		GO:0 0611 35	endopeptidase regulator activity	5	2	PF3D7_0501400,PF3D7_0507400,	40	9.64	15.54	0.0157 7106	0.136025395	1
		GO:0 0055 16	calmodulin binding	14	3	PF3D7_0217500,PF3D7_1104900,PF3D7_1238900,	21.4	5.16	6.38	0.0182 621	0.15121018	1

University of Ghana http://ugspace.ug.edu.gh

		GO:0005509	calcium ion binding	52	6	PF3D7_0217500,PF3D7_1022700,PF3D7_1238900,PF3D7_1246400,PF3D7_1423300,PF3D7_1463900,	11.5	2.78	3.07	0.01965929	0.156518186	1
		GO:0061134	peptidase regulator activity	6	2	PF3D7_0501400,PF3D7_0507400,	33.3	8.03	11.65	0.02301497	0.176448108	1
		GO:0004175	endopeptidase activity	107	9	PF3D7_0207400,PF3D7_0207500,PF3D7_0207600,PF3D7_0207700,PF3D7_0207800,PF3D7_0404700,PF3D7_0507200,PF3D7_0507500,PF3D7_0808200,	8.4	2.03	2.17	0.03260241	0.190879211	1
		GO:0008092	cytoskeletal protein binding	74	7	PF3D7_0105300,PF3D7_0613900,PF3D7_1126700,PF3D7_1229800,PF3D7_1251200,PF3D7_1342600,PF3D7_1361400,	9.5	2.28	2.46	0.03273336	0.190879211	1
		GO:0004857	enzyme inhibitor activity	8	2	PF3D7_0501400,PF3D7_0507400,	25	6.02	7.77	0.04067429	0.190879211	1
		GO:0015103	inorganic anion transmembrane transporter activity	8	2	PF3D7_0302200,PF3D7_0302500,	25	6.02	7.77	0.04067429	0.190879211	1
		GO:0015136	sialic acid transmembrane transporter activity	1	1	PF3D7_0505300,	100	24.1	inf	0.04149548	0.190879211	1
		GO:0015181	arginine transmembrane transporter activity	1	1	PF3D7_0104800,	100	24.1	inf	0.04149548	0.190879211	1
		GO:0015233	pantothenate transmembrane transporter activity	1	1	PF3D7_0206200,	100	24.1	inf	0.04149548	0.190879211	1
		GO:0004307	ethanolaminephosphotransferase activity	1	1	PF3D7_0628300,	100	24.1	inf	0.04149548	0.190879211	1

University of Ghana http://ugspace.ug.edu.gh

		GO:0017128	phospholipid scramblase activity	1	1	PF3D7_1022700,	100	24.1	inf	0.04149548	0.190879211	1
		GO:0008179	adenylate cyclase binding	1	1	PF3D7_0105300,	100	24.1	inf	0.04149548	0.190879211	1
		GO:0004142	diacylglycerol cholinephosphotransferase activity	1	1	PF3D7_0628300,	100	24.1	inf	0.04149548	0.190879211	1
		GO:0033691	sialic acid binding	1	1	PF3D7_0102500,	100	24.1	inf	0.04149548	0.190879211	1
		GO:0004478	methionine adenosyltransferase activity	1	1	PF3D7_0922200,	100	24.1	inf	0.04149548	0.190879211	1
		GO:0003823	antigen binding	1	1	PF3D7_1116000,	100	24.1	inf	0.04149548	0.190879211	1
		GO:0005488	binding	1	1	PF3D7_0405900,	100	24.1	inf	0.04149548	0.190879211	1
		GO:0000234	phosphoethanolamine N-methyltransferase activity	1	1	PF3D7_1343000,	100	24.1	inf	0.04149548	0.190879211	1
		GO:0004731	purine-nucleoside phosphorylase activity	1	1	PF3D7_0513300,	100	24.1	inf	0.04149548	0.190879211	1
		GO:0008936	nicotinamidase activity	1	1	PF3D7_0320500,	100	24.1	inf	0.04149548	0.190879211	1

University of Ghana http://ugspace.ug.edu.gh

Cellular component	Upregulated	GO:004431 2	crystalloid	17	7	PF3D7_0418800,PF3D7_0825700,PF3D7_0825800,PF3D7_0903800,PF3D7_0904200,PF3D7_1103500,PF3D7_1453500,	41.2	40.09	78.27	1.40E-10	9.13E-09	9.13E-09
		GO:003126	intrinsic component of plasma membrane	51	3	PF3D7_0209000,PF3D7_0418800,PF3D7_1031000,	5.9	5.73	6.34	0.01502557	0.194852754	0.976661925
		GO:000589 2	acetylcholine-gated channel complex	2	1	PF3D7_0418800,	50	48.68	98.31	0.02043891	0.194852754	1
		GO:003230 2	MutSbeta complex	2	1	PF3D7_0706700,	50	48.68	98.31	0.02043891	0.194852754	1
		GO:004323 5	receptor complex	2	1	PF3D7_0418800,	50	48.68	98.31	0.02043891	0.194852754	1
		GO:009880 2	plasma membrane signaling receptor complex	2	1	PF3D7_0418800,	50	48.68	98.31	0.02043891	0.194852754	1
		GO:005581	collagen trimer	3	1	PF3D7_0827200,	33.3	32.45	49.14	0.03050427	0.194852754	1
		GO:005882	intermediate filament	3	1	PF3D7_1408800,	33.3	32.45	49.14	0.03050427	0.194852754	1
		GO:003230 1	MutSalpha complex	3	1	PF3D7_0706700,	33.3	32.45	49.14	0.03050427	0.194852754	1
		GO:045111	intermediate filament cytoskeleton	3	1	PF3D7_1408800,	33.3	32.45	49.14	0.03050427	0.194852754	1

University of Ghana http://ugspace.ug.edu.gh

University of Ghana http://ugspace.ug.edu.gh

		GO:0046658	anchored component of plasma membrane	28	2	PF3D7_0209000,PF3D7_1031000,	7.1	6.95	7.68	0.03297508	0.194852754	1
		GO:031225	anchored component of membrane	30	2	PF3D7_0209000,PF3D7_1031000,	6.7	6.49	7.13	0.03745918	0.202903891	1
	Downregulated	GO:020007	apical complex	104	42	PF3D7_0102500,PF3D7_0206200,PF3D7_0212600,PF3D7_0214900,PF3D7_0220800,PF3D7_0302200,PF3D7_0302500,PF3D7_0405900,PF3D7_0414900,PF3D7_0419700,PF3D7_0423400,PF3D7_0423800,PF3D7_0424100,PF3D7_0501500,PF3D7_0501600,PF3D7_0507500,PF3D7_0511600,PF3D7_0612700,PF3D7_0613300,PF3D7_0707300,PF3D7_0722200,PF3D7_0731500,PF3D7_0802600,PF3D7_0808200,PF3D7_0817700,PF3D7_0905400,PF3D7_0929400,PF3D7_1012200,PF3D7_1028700,PF3D7_1116000,PF3D7_1133400,PF3D7_1136500,PF3D7_1136700,PF3D7_1218000,PF3D7_1252100,PF3D7_1301600,PF3D7_1332200,PF3D7_1335300,PF3D7_1335400,PF3D7_1404300,PF3D7_1410400,PF3D7_1463900,	40.4	9.73	19.49	3.28E-32	4.59E-30	4.59E-30
		GO:045177	apical part of cell	147	47	PF3D7_0102500,PF3D7_0206200,PF3D7_0212600,PF3D7_0214900,PF3D7_0220800,PF3D7_0302200,PF3D7_0302500,PF3D7_0404700,PF3D7_0405900,PF3D7_0414900,PF3D7_0419700,PF3D7_0423400,PF3D7_0423800,PF3D7_0424100,PF3D7_0501500,PF3D7_0501600,PF3D7_0507500,PF3D7_0508900,PF3D7_0511600,PF3D7_0612700,PF3D7_0613300,PF3D7_0707300,PF3D7_0722200,PF3D7_0731500,PF3D7_0802600,PF3D7_0808200,PF3D7_0817700,PF3D7_0905400,PF3D7_0929400,PF3D7_1012200,PF3D7_1028700,PF3D7_1035900,PF3D7_1116000,PF3D7_1133400,PF3D7_1136500,PF3D7_1136700,PF3D7_1218000,PF3D7_1243400,PF3D7_1252100,PF3D7_1301600,PF3D7_1318000,PF3D7_1332200,PF3D7_1335300,PF3D7_1335400,PF3D7_1404300,PF3D7_1410400,PF3D7_1463900,	32	7.71	13.85	1.17E-30	8.20E-29	1.64E-28
		GO:020008	rhoptry	52	30	PF3D7_0212600,PF3D7_0214900,PF3D7_0220800,PF3D7_0302200,PF3D7_0302500,PF3D7_0405900,PF3D7_0414900,PF3D7_0419700,PF3D7_0423400,PF3D7_0424100,PF3D7_0501500,PF3D7_0501600,PF3D7_0511600,PF3D7_0612700,PF3D7_0613300,PF3D7_0707300,PF3D7_0722200,PF3D7_0802600,PF3D7_0817700,PF3D7_0905400,PF3D7_0929400,PF3D7_1012200,PF3D7_1116000,PF3D7_1136700,PF3D7_1218000,PF3D7_1252100,PF3D7_1335300,PF3D7_1335400,PF3D7_1410400,PF3D7_1463900,	57.7	13.9	36.82	4.92E-29	2.29E-27	6.88E-27

		GO:199902 25	rhoptry neck	14	11	PF3D7_0214900,PF3D7_0405900,PF3D7_0419700,PF3D7_0423400,PF3D7_0511600,PF3D7_0722200,PF3D7_0817700,PF3D7_1116000,PF3D7_1335300,PF3D7_1335400,PF3D7_1463900,	78.6	18.93	89.52	1.57E-13	5.49E-12	2.20E-11
		GO:190350 61	extracellular vesicle	91	23	PF3D7_0102200,PF3D7_0102500,PF3D7_0202500,PF3D7_0207600,PF3D7_0301700,PF3D7_0302500,PF3D7_0501300,PF3D7_0501500,PF3D7_0501600,PF3D7_0731500,PF3D7_0818900,PF3D7_0905400,PF3D7_0922200,PF3D7_0929400,PF3D7_0930300,PF3D7_1014100,PF3D7_1035300,PF3D7_1035700,PF3D7_1105000,PF3D7_1228600,PF3D7_1252100,PF3D7_1343000,PF3D7_1410400,	25.3	6.09	8.69	8.43E-13	2.14E-11	1.18E-10
		GO:000998 6	cell surface	159	30	PF3D7_0212600,PF3D7_0308300,PF3D7_0404900,PF3D7_0423800,PF3D7_0424100,PF3D7_0612700,PF3D7_0818900,PF3D7_0905400,PF3D7_0922200,PF3D7_1012200,PF3D7_1014100,PF3D7_1017500,PF3D7_1028700,PF3D7_1028900,PF3D7_1035300,PF3D7_1035400,PF3D7_1035500,PF3D7_1035700,PF3D7_1035900,PF3D7_1036000,PF3D7_1115800,PF3D7_1140400,PF3D7_1218000,PF3D7_1228600,PF3D7_1252100,PF3D7_1323700,PF3D7_1342600,PF3D7_1431400,PF3D7_1437300,PF3D7_1440900,	18.9	4.55	6.13	9.15E-13	2.14E-11	1.28E-10
		GO:005576	extracellular region	334	43	PF3D7_0102200,PF3D7_0102500,PF3D7_0202500,PF3D7_0207400,PF3D7_0207500,PF3D7_0207600,PF3D7_0207700,PF3D7_0207800,PF3D7_0214900,PF3D7_0217500,PF3D7_0301700,PF3D7_0302500,PF3D7_0404700,PF3D7_0404900,PF3D7_0423800,PF3D7_0424100,PF3D7_0501300,PF3D7_0501400,PF3D7_0501500,PF3D7_0501600,PF3D7_0507200,PF3D7_0507400,PF3D7_0507500,PF3D7_0612700,PF3D7_0632200,PF3D7_0707300,PF3D7_0731500,PF3D7_0818900,PF3D7_0905400,PF3D7_0922200,PF3D7_0929400,PF3D7_0930300,PF3D7_1014100,PF3D7_1035200,PF3D7_1035300,PF3D7_1035700,PF3D7_1102700,PF3D7_1102800,PF3D7_1105000,PF3D7_1228600,PF3D7_1252100,PF3D7_1343000,PF3D7_1410400,	12.9	3.1	4.07	6.63E-12	1.33E-10	9.28E-10
		GO:004365 7	host cell	713	66	PF3D7_0102200,PF3D7_0106600,PF3D7_0108500,PF3D7_0113000,PF3D7_0113200,PF3D7_0114500,PF3D7_0202100,PF3D7_0202500,PF3D7_0207500,PF3D7_0207600,PF3D7_0207700,PF3D7_0214900,PF3D7_0217500,PF3D7_0220000,PF3D7_0220300,PF3D7_0221700,PF3D7_0301700,PF3D7_0301800,PF3D7_0302200,PF3D7_0302500,PF3D7_0401800,PF3D7_0404700,PF3D7_0404900,PF3D7_0423800,PF3D7_0424100,PF3D7_0425100,PF3D7_0426000,PF3D7_0501300,PF3D7_0501400,PF3D7_0507400,PF3D7_0507500,PF3D7_0532300,PF3D7_0532600,PF3D7_0612700,PF3D7_0632200,PF3D7_0701900,PF3D7_0702000,P	9.3	2.23	3.01	3.01E-11	4.68E-10	4.21E-09

University of Ghana http://ugspace.ug.edu.gh

						F3D7_0707300,PF3D7_0800800,PF3D7_0830500,PF3D7_0905400,PF3D7_0922200,PF3D7_0929400,PF3D7_0936000,PF3D7_1000600,PF3D7_1001600,PF3D7_1014100,PF3D7_1035200,PF3D7_1035300,PF3D7_1102700,PF3D7_1102800,PF3D7_1105000,PF3D7_1115800,PF3D7_1121300,PF3D7_1136500,PF3D7_1149300,PF3D7_1149400,PF3D7_1222700,PF3D7_1228600,PF3D7_1252100,PF3D7_1252600,PF3D7_1371800,PF3D7_1401100,PF3D7_1410400,PF3D7_1463900,PF3D7_1479600,						
		GO:0018995	host cellular component	713	66	PF3D7_0102200,PF3D7_0106600,PF3D7_0108500,PF3D7_0113000,PF3D7_0113200,PF3D7_0114500,PF3D7_0202100,PF3D7_0202500,PF3D7_0207500,PF3D7_0207600,PF3D7_0207700,PF3D7_0214900,PF3D7_0217500,PF3D7_0220000,PF3D7_0220300,PF3D7_0221700,PF3D7_0301700,PF3D7_0301800,PF3D7_0302200,PF3D7_0302500,PF3D7_0401800,PF3D7_0404700,PF3D7_0404900,PF3D7_0423800,PF3D7_0424100,PF3D7_0425100,PF3D7_0426000,PF3D7_0501300,PF3D7_0501400,PF3D7_0507400,PF3D7_0507500,PF3D7_0532300,PF3D7_0532600,PF3D7_0612700,PF3D7_0632200,PF3D7_0701900,PF3D7_0702000,PF3D7_0707300,PF3D7_0800800,PF3D7_0830500,PF3D7_0905400,PF3D7_0922200,PF3D7_0929400,PF3D7_0936000,PF3D7_1000600,PF3D7_1001600,PF3D7_1014100,PF3D7_1035200,PF3D7_1035300,PF3D7_1102700,PF3D7_1102800,PF3D7_1105000,PF3D7_1115800,PF3D7_1121300,PF3D7_1136500,PF3D7_1149300,PF3D7_1149400,PF3D7_1222700,PF3D7_1228600,PF3D7_1252100,PF3D7_1252600,PF3D7_1371800,PF3D7_1401100,PF3D7_1410400,PF3D7_1463900,PF3D7_1479600,	9.3	2.23	3.01	3.01E-11	4.68E-10	4.21E-09
		GO:0006501 0	extracellular membrane-bounded organelle	280	37	PF3D7_0102200,PF3D7_0102500,PF3D7_0202500,PF3D7_0207500,PF3D7_0207600,PF3D7_0207700,PF3D7_0214900,PF3D7_0217500,PF3D7_0301700,PF3D7_0302500,PF3D7_0404700,PF3D7_0404900,PF3D7_0501300,PF3D7_0501500,PF3D7_0501600,PF3D7_0507400,PF3D7_0507500,PF3D7_0612700,PF3D7_0632200,PF3D7_0707300,PF3D7_0731500,PF3D7_0818900,PF3D7_0905400,PF3D7_0922200,PF3D7_0929400,PF3D7_0930300,PF3D7_1014100,PF3D7_1035200,PF3D7_1035300,PF3D7_1035700,PF3D7_1102700,PF3D7_1102800,PF3D7_1105000,PF3D7_1228600,PF3D7_1252100,PF3D7_1343000,PF3D7_1410400,	13.2	3.18	4.08	1.19E-10	1.67E-09	1.67E-08
		GO:0043230	extracellular organelle	282	37	PF3D7_0102200,PF3D7_0102500,PF3D7_0202500,PF3D7_0207500,PF3D7_0207600,PF3D7_0207700,PF3D7_0214900,PF3D7_0217500,PF3D7_0301700,PF3D7_0302500,PF3D7_0404700,PF3D7_0404900,PF3D7_0501300,PF3D7_0501500,PF3D7_0501600,PF3D7_0507400,PF3D7_0507500,PF3D7_0612700,PF3D7_0632200,PF3D7_0707300,PF3D7_0731500,PF	13.1	3.16	4.05	1.47E-10	1.87E-09	2.06E-08

University of Ghana http://ugspace.ug.edu.gh

						3D7_0818900,PF3D7_0905400,PF3D7_0922200,PF3D7_0929400,PF3D7_0930300,PF3D7_1014100,PF3D7_1035200,PF3D7_1035300,PF3D7_1035700,PF3D7_1102700,PF3D7_1102800,PF3D7_1105000,PF3D7_1228600,PF3D7_1232100,PF3D7_1343000,PF3D7_1410400,						
		GO:0031982	vesicle	288	37	PF3D7_0102200,PF3D7_0102500,PF3D7_0202500,PF3D7_0206200,PF3D7_0207600,PF3D7_0220000,PF3D7_0301700,PF3D7_0302500,PF3D7_0423800,PF3D7_0424100,PF3D7_0501300,PF3D7_0501500,PF3D7_0501600,PF3D7_0507500,PF3D7_0613900,PF3D7_0618000,PF3D7_0702200,PF3D7_0731500,PF3D7_0818900,PF3D7_0905400,PF3D7_0922200,PF3D7_0929400,PF3D7_0930300,PF3D7_1014100,PF3D7_1035300,PF3D7_1035700,PF3D7_1105000,PF3D7_1116000,PF3D7_1228600,PF3D7_1229800,PF3D7_1243500,PF3D7_1252100,PF3D7_1342600,PF3D7_1343000,PF3D7_1348100,PF3D7_1361500,PF3D7_1410400,	12.8	3.1	3.94	2.74E-10	3.20E-09	3.84E-08
		GO:0033643	host cell part	630	59	PF3D7_0102200,PF3D7_0106600,PF3D7_0108500,PF3D7_0113000,PF3D7_0202100,PF3D7_0202500,PF3D7_0207500,PF3D7_0207600,PF3D7_0207700,PF3D7_0214900,PF3D7_0217500,PF3D7_0220000,PF3D7_0221700,PF3D7_0301700,PF3D7_0301800,PF3D7_0302200,PF3D7_0302500,PF3D7_0401800,PF3D7_0404700,PF3D7_0404900,PF3D7_0423800,PF3D7_0424100,PF3D7_0426000,PF3D7_0501300,PF3D7_0501400,PF3D7_0507400,PF3D7_0507500,PF3D7_0532300,PF3D7_0532600,PF3D7_0612700,PF3D7_0632200,PF3D7_0701900,PF3D7_0702000,PF3D7_0707300,PF3D7_0830500,PF3D7_0905400,PF3D7_0922200,PF3D7_0929400,PF3D7_0936000,PF3D7_1000600,PF3D7_1001600,PF3D7_1014100,PF3D7_1035200,PF3D7_1035300,PF3D7_1102700,PF3D7_1102800,PF3D7_1105000,PF3D7_1115800,PF3D7_1121300,PF3D7_1136500,PF3D7_1149300,PF3D7_1222700,PF3D7_1228600,PF3D7_1252100,PF3D7_1252600,PF3D7_1401100,PF3D7_1410400,PF3D7_1463900,PF3D7_1479600,	9.4	2.26	2.96	3.29E-10	3.54E-09	4.61E-08
		GO:0020004	symbiont-containing vacuolar space	6	6	PF3D7_0207600,PF3D7_0217500,PF3D7_0404900,PF3D7_0501300,PF3D7_0507500,PF3D7_0612700,	100	24.1	inf	4.75E-09	4.75E-08	6.65E-07
		GO:0031225	anchored component of membrane	30	11	PF3D7_0206800,PF3D7_0404900,PF3D7_0405900,PF3D7_0414900,PF3D7_0419700,PF3D7_0423800,PF3D7_0612700,PF3D7_0620400,PF3D7_0707300,PF3D7_0930300,PF3D7_1136200,	36.7	8.84	14.09	1.31E-08	1.22E-07	1.83E-06

University of Ghana http://ugspace.ug.edu.gh

		GO:0020009	microneme	40	12	PF3D7_0102500,PF3D7_0206200,PF3D7_0212600,PF3D7_0405900,PF3D7_0423800,PF3D7_0731500,PF3D7_1028700,PF3D7_1133400,PF3D7_1136500,PF3D7_1218000,PF3D7_1301600,PF3D7_1404300,	30	7.23	10.46	3.78E-08	3.31E-07	5.29E-06
		GO:0020039	pellicle	65	14	PF3D7_0304000,PF3D7_0308300,PF3D7_0525800,PF3D7_0822900,PF3D7_1003600,PF3D7_1017500,PF3D7_1028900,PF3D7_1222700,PF3D7_1246400,PF3D7_1251200,PF3D7_1323700,PF3D7_1342600,PF3D7_1351700,PF3D7_1460600,	21.5	5.19	6.74	2.69E-07	2.21E-06	3.76E-05
		GO:0033646	host intracellular part	549	47	PF3D7_0102200,PF3D7_0108500,PF3D7_0202100,PF3D7_0202500,PF3D7_0207500,PF3D7_0207600,PF3D7_0207700,PF3D7_0214900,PF3D7_0217500,PF3D7_0221700,PF3D7_0301700,PF3D7_0301800,PF3D7_0401800,PF3D7_0404700,PF3D7_0404900,PF3D7_0426000,PF3D7_0501300,PF3D7_0501400,PF3D7_0507400,PF3D7_0507500,PF3D7_0532300,PF3D7_0532600,PF3D7_0612700,PF3D7_0632200,PF3D7_0701900,PF3D7_0702000,PF3D7_0707300,PF3D7_0830500,PF3D7_0905400,PF3D7_0922200,PF3D7_0929400,PF3D7_0936000,PF3D7_1001600,PF3D7_1014100,PF3D7_1035200,PF3D7_1035300,PF3D7_1102700,PF3D7_1102800,PF3D7_1105000,PF3D7_1115800,PF3D7_1121300,PF3D7_1228600,PF3D7_1252100,PF3D7_1252600,PF3D7_1401100,PF3D7_1410400,PF3D7_1463900,	8.6	2.06	2.52	5.79E-07	4.51E-06	8.11E-05
		GO:0043656	host intracellular region	550	47	PF3D7_0102200,PF3D7_0108500,PF3D7_0202100,PF3D7_0202500,PF3D7_0207500,PF3D7_0207600,PF3D7_0207700,PF3D7_0214900,PF3D7_0217500,PF3D7_0221700,PF3D7_0301700,PF3D7_0301800,PF3D7_0401800,PF3D7_0404700,PF3D7_0404900,PF3D7_0426000,PF3D7_0501300,PF3D7_0501400,PF3D7_0507400,PF3D7_0507500,PF3D7_0532300,PF3D7_0532600,PF3D7_0612700,PF3D7_0632200,PF3D7_0701900,PF3D7_0702000,PF3D7_0707300,PF3D7_0830500,PF3D7_0905400,PF3D7_0922200,PF3D7_0929400,PF3D7_0936000,PF3D7_1001600,PF3D7_1014100,PF3D7_1035200,PF3D7_1035300,PF3D7_1102700,PF3D7_1102800,PF3D7_1105000,PF3D7_1115800,PF3D7_1121300,PF3D7_1228600,PF3D7_1252100,PF3D7_1252600,PF3D7_1401100,PF3D7_1410400,PF3D7_1463900,	8.5	2.06	2.51	6.12E-07	4.51E-06	8.56E-05
		GO:0030430	host cell cytoplasm	540	46	PF3D7_0102200,PF3D7_0108500,PF3D7_0202100,PF3D7_0202500,PF3D7_0207500,PF3D7_0207600,PF3D7_0207700,PF3D7_0214900,PF3D7_0217500,PF3D7_0221700,PF3D7_0301700,PF3D7_0301800,PF3D7_0401800,PF3D7_0404700,PF3D7_0404900,PF3D7_0426000,PF3D7_0501300,PF3D7_0501400,PF3D7_0507400,PF3D7_0507500,PF3D7_0532300,PF3D7_0532600,PF3D7_0612700,PF3D7_0632200,PF3D7_0701900,PF3D7_0702000,PF3D7_0707300,PF3D7_0830500,PF3D7_0905400,PF3D7_0922200,PF3D7_0929400,PF3D7_0936	8.5	2.05	2.49	9.15E-07	6.40E-06	0.000128071

University of Ghana http://ugspace.ug.edu.gh

						000,PF3D7_1001600,PF3D7_1014100,PF3D7_1035200,PF3D7_1035300,PF3D7_1102700,PF3D7_1102800,PF3D7_1115800,PF3D7_1121300,PF3D7_1228600,PF3D7_1252100,PF3D7_1252600,PF3D7_1401100,PF3D7_1410400,PF3D7_1463900,						
		GO:0033655	host cell cytoplasm part	524	45	PF3D7_0102200,PF3D7_0108500,PF3D7_0202100,PF3D7_0202500,PF3D7_0207500,PF3D7_0207600,PF3D7_0207700,PF3D7_0214900,PF3D7_0217500,PF3D7_0221700,PF3D7_0301700,PF3D7_0301800,PF3D7_0401800,PF3D7_0404700,PF3D7_0404900,PF3D7_0426000,PF3D7_0501300,PF3D7_0501400,PF3D7_0507400,PF3D7_0507500,PF3D7_0532300,PF3D7_0532600,PF3D7_0612700,PF3D7_0632200,PF3D7_0701900,PF3D7_0702000,PF3D7_0707300,PF3D7_0830500,PF3D7_0905400,PF3D7_0922200,PF3D7_0936000,PF3D7_1001600,PF3D7_1014100,PF3D7_1035200,PF3D7_1035300,PF3D7_1102700,PF3D7_1102800,PF3D7_1115800,PF3D7_1121300,PF3D7_1228600,PF3D7_1252100,PF3D7_1252600,PF3D7_1401100,PF3D7_1410400,PF3D7_1463900,	8.6	2.07	2.51	9.88E-07	6.59E-06	0.000138332
		GO:0046658	anchored component of plasma membrane	28	9	PF3D7_0206800,PF3D7_0404900,PF3D7_0405900,PF3D7_0419700,PF3D7_0423800,PF3D7_0612700,PF3D7_0620400,PF3D7_0930300,PF3D7_1136200,	32.1	7.75	11.41	1.06E-06	6.76E-06	0.000148696
		GO:0070258	inner membrane pellicle complex	63	13	PF3D7_0304000,PF3D7_0308300,PF3D7_0525800,PF3D7_0822900,PF3D7_1003600,PF3D7_1017500,PF3D7_1028900,PF3D7_1222700,PF3D7_1246400,PF3D7_1323700,PF3D7_1342600,PF3D7_1351700,PF3D7_1460600,	20.6	4.97	6.35	1.23E-06	7.50E-06	0.000172415
		GO:0005615	extracellular space	22	8	PF3D7_0207400,PF3D7_0207500,PF3D7_0207600,PF3D7_0207700,PF3D7_0207800,PF3D7_0404700,PF3D7_0501400,PF3D7_0507200,	36.4	8.76	13.7	1.48E-06	8.65E-06	0.000207622
		GO:0020003	symbiont-containing vacuole	205	23	PF3D7_0102200,PF3D7_0202500,PF3D7_0207500,PF3D7_0207600,PF3D7_0207700,PF3D7_0214900,PF3D7_0217500,PF3D7_0404700,PF3D7_0404900,PF3D7_0501300,PF3D7_0507400,PF3D7_0507500,PF3D7_0612700,PF3D7_0632200,PF3D7_0707300,PF3D7_1014100,PF3D7_1035200,PF3D7_1035300,PF3D7_1102700,PF3D7_1102800,PF3D7_1228600,PF3D7_1252100,PF3D7_1410400,	11.2	2.7	3.17	9.81E-06	5.49E-05	0.001372809
		GO:0000323	lytic vacuole	111	16	PF3D7_0102200,PF3D7_0207400,PF3D7_0207500,PF3D7_0207600,PF3D7_0207700,PF3D7_0207800,PF3D7_0404700,PF3D7_0501500,PF3D7_0501600,PF3D7_0618000,PF3D7_0818900,PF3D7_0922200,PF3D7_0930300,PF3D7_1116000,PF3D7_1343000,PF3D7_1410400,	14.4	3.47	4.14	1.06E-05	5.51E-05	0.001486625

University of Ghana http://ugspace.ug.edu.gh

		GO:0005764	lysosome	111	16	PF3D7_0102200,PF3D7_0207400,PF3D7_0207500,PF3D7_0207600,PF3D7_0207700,PF3D7_0207800,PF3D7_0404700,PF3D7_0501500,PF3D7_0501600,PF3D7_0618000,PF3D7_0818900,PF3D7_0922200,PF3D7_0930300,PF3D7_1116000,PF3D7_1343000,PF3D7_1410400,	14.4	3.47	4.14	1.06E-05	5.51E-05	0.001486625
		GO:0005773	vacuole	126	17	PF3D7_0102200,PF3D7_0207400,PF3D7_0207500,PF3D7_0207600,PF3D7_0207700,PF3D7_0207800,PF3D7_0404700,PF3D7_0501500,PF3D7_0501600,PF3D7_0618000,PF3D7_0818900,PF3D7_0922200,PF3D7_0930300,PF3D7_1035200,PF3D7_1116000,PF3D7_1343000,PF3D7_1410400,	13.5	3.25	3.84	1.38E-05	6.90E-05	0.001931831
		GO:0031226	intrinsic component of plasma membrane	51	9	PF3D7_0206800,PF3D7_0404900,PF3D7_0405900,PF3D7_0419700,PF3D7_0423800,PF3D7_0612700,PF3D7_0620400,PF3D7_0930300,PF3D7_1136200,	17.6	4.25	5.13	0.0002037	0.000983391	0.02851834
		GO:0032991	protein-containing complex	16	5	PF3D7_0423800,PF3D7_0424100,PF3D7_0817700,PF3D7_1116000,PF3D7_1323700,	31.3	7.53	10.74	0.0003517	0.00164125	0.049237505
		GO:0044538	host cell periphery	26	6	PF3D7_0106600,PF3D7_0113000,PF3D7_0401800,PF3D7_0701900,PF3D7_1136500,PF3D7_1149300,	23.1	5.56	7.11	0.00054362	0.002455066	0.076107047
		GO:0044217	other organism part	116	13	PF3D7_0113200,PF3D7_0114500,PF3D7_0202100,PF3D7_0220300,PF3D7_0221700,PF3D7_0301700,PF3D7_0301800,PF3D7_0425100,PF3D7_0702000,PF3D7_0800800,PF3D7_1149400,PF3D7_1371800,PF3D7_1401100,	11.2	2.7	3.05	0.00092617	0.004051997	0.129663906
		GO:0005886	plasma membrane	140	14	PF3D7_0104800,PF3D7_0206200,PF3D7_0206800,PF3D7_0207600,PF3D7_0217500,PF3D7_0507400,PF3D7_0932100,PF3D7_1022700,PF3D7_1035400,PF3D7_1133400,PF3D7_1218000,PF3D7_1301600,PF3D7_1335400,PF3D7_1342600,	10	2.41	2.68	0.00182298	0.007733856	0.255217245
		GO:0020005	symbiont-containing vacuole membrane	44	7	PF3D7_0202500,PF3D7_0207500,PF3D7_0217500,PF3D7_0404700,PF3D7_0501300,PF3D7_1102700,PF3D7_1102800,	15.9	3.83	4.49	0.00197787	0.008144164	0.276901593
		GO:0031410	cytoplasmic vesicle	210	18	PF3D7_0102200,PF3D7_0206200,PF3D7_0220000,PF3D7_0423800,PF3D7_0424100,PF3D7_0501500,PF3D7_0501600,PF3D7_0507500,PF3D7_0618000,PF3D7_0818900,PF3D7_0922200,PF3D7_0930300,PF3D7_1116000,PF3D7_1243500,PF3D7_1343000,PF3D7_1348100,PF3D7_1361500,PF3D7_1410400,	8.6	2.07	2.28	0.00249706	0.00995577	0.349587864

University of Ghana http://ugspace.ug.edu.gh

		GO:0 0055 75	cellular component	723	45	PF3D7_0106600,PF3D7_0114500,PF3D7_0202100,PF3D7_0207500,PF3D7_0215300,PF3D7_0217500,PF3D7_0220000,PF3D7_0220300,PF3D7_0301800,PF3D7_0308100,PF3D7_0423800,PF3D7_0424100,PF3D7_0501200,PF3D7_0507500,PF3D7_0529400,PF3D7_0620300,PF3D7_0628300,PF3D7_0702200,PF3D7_0817700,PF3D7_0905500,PF3D7_0918700,PF3D7_0930300,PF3D7_1000600,PF3D7_1001600,PF3D7_1007300,PF3D7_1013800,PF3D7_1022700,PF3D7_1116000,PF3D7_1117400,PF3D7_1122700,PF3D7_1133400,PF3D7_1136200,PF3D7_1228600,PF3D7_1235200,PF3D7_1238900,PF3D7_1240100,PF3D7_1252600,PF3D7_1310200,PF3D7_1321100,PF3D7_1323700,PF3D7_1335100,PF3D7_1335400,PF3D7_1348100,PF3D7_1455600,PF3D7_1479600,	6.2	1.5	1.69	0.0025 8965	0.00995577	0.362551501
		GO:0 0977 08	intracellular vesicle	211	18	PF3D7_0102200,PF3D7_0206200,PF3D7_0220000,PF3D7_0423800,PF3D7_0424100,PF3D7_0501500,PF3D7_0501600,PF3D7_0507500,PF3D7_0618000,PF3D7_0818900,PF3D7_0922200,PF3D7_0930300,PF3D7_1116000,PF3D7_1243500,PF3D7_1343000,PF3D7_1348100,PF3D7_1361500,PF3D7_1410400,	8.5	2.06	2.27	0.0026 3117	0.00995577	0.368363493
		GO:0 0160 20	membrane	637	40	PF3D7_0114500,PF3D7_0202100,PF3D7_0207500,PF3D7_0215300,PF3D7_0217500,PF3D7_0220000,PF3D7_0220300,PF3D7_0301800,PF3D7_0308100,PF3D7_0424100,PF3D7_0507200,PF3D7_0507500,PF3D7_0529400,PF3D7_0620300,PF3D7_0628300,PF3D7_0702200,PF3D7_0905500,PF3D7_0918700,PF3D7_0930300,PF3D7_1000600,PF3D7_1001600,PF3D7_1007300,PF3D7_1013800,PF3D7_1022700,PF3D7_1117400,PF3D7_1122700,PF3D7_1133400,PF3D7_1136200,PF3D7_1228600,PF3D7_1235200,PF3D7_1238900,PF3D7_1240100,PF3D7_1252600,PF3D7_1310200,PF3D7_1321100,PF3D7_1335100,PF3D7_1335400,PF3D7_1348100,PF3D7_1455600,PF3D7_1479600,	6.3	1.51	1.68	0.0039 9522	0.014719226	0.5593306
		GO:0 0444 21	obsolete extracellular region part	3	2	PF3D7_0423800,PF3D7_0424100,	66.7	16.07	46.65	0.0050 0024	0.01707398	0.700033162
		GO:0 0443 11	exoneme	3	2	PF3D7_0507500,PF3D7_0808200,	66.7	16.07	46.65	0.0050 0024	0.01707398	0.700033162
		GO:0 0436 55	host extracellular space	3	2	PF3D7_0423800,PF3D7_0424100,	66.7	16.07	46.65	0.0050 0024	0.01707398	0.700033162

University of Ghana http://ugspace.ug.edu.gh

University of Ghana http://ugspace.ug.edu.gh

		GO:0015629	actin cytoskeleton	29	5	PF3D7_0105300,PF3D7_0613900,PF3D7_1229800,PF3D7_1342600,PF3D7_1361400,	17.2	4.16	4.91	0.00616083	0.019826914	0.862516409
		GO:0005767	secondary lysosome	97	10	PF3D7_0102200,PF3D7_0501500,PF3D7_0501600,PF3D7_0618000,PF3D7_0818900,PF3D7_0922200,PF3D7_0930300,PF3D7_1116000,PF3D7_1343000,PF3D7_1410400,	10.3	2.48	2.74	0.00651456	0.019826914	0.912038041
		GO:0032010	phagolysosome	97	10	PF3D7_0102200,PF3D7_0501500,PF3D7_0501600,PF3D7_0618000,PF3D7_0818900,PF3D7_0922200,PF3D7_0930300,PF3D7_1116000,PF3D7_1343000,PF3D7_1410400,	10.3	2.48	2.74	0.00651456	0.019826914	0.912038041
		GO:0020020	food vacuole	97	10	PF3D7_0102200,PF3D7_0501500,PF3D7_0501600,PF3D7_0618000,PF3D7_0818900,PF3D7_0922200,PF3D7_0930300,PF3D7_1116000,PF3D7_1343000,PF3D7_1410400,	10.3	2.48	2.74	0.00651456	0.019826914	0.912038041
		GO:0045335	phagocytic vesicle	97	10	PF3D7_0102200,PF3D7_0501500,PF3D7_0501600,PF3D7_0618000,PF3D7_0818900,PF3D7_0922200,PF3D7_0930300,PF3D7_1116000,PF3D7_1343000,PF3D7_1410400,	10.3	2.48	2.74	0.00651456	0.019826914	0.912038041
		GO:0020026	merozoite dense granule	10	3	PF3D7_0102200,PF3D7_0220000,PF3D7_0507500,	30	7.23	10.03	0.00680487	0.019847543	0.952682088
		GO:0016459	myosin complex	10	3	PF3D7_0613900,PF3D7_1229800,PF3D7_1342600,	30	7.23	10.03	0.00680487	0.019847543	0.952682088
		GO:0044164	host cell cytosol	30	5	PF3D7_0404700,PF3D7_0532600,PF3D7_1001600,PF3D7_1121300,PF3D7_1463900,	16.7	4.02	4.71	0.00714892	0.020425472	1
		GO:0044228	host cell surface	31	5	PF3D7_0102200,PF3D7_0113000,PF3D7_0220000,PF3D7_0401800,PF3D7_0532300,	16.1	3.89	4.53	0.00824259	0.023079246	1
		GO:0030139	endocytic vesicle	102	10	PF3D7_0102200,PF3D7_0501500,PF3D7_0501600,PF3D7_0618000,PF3D7_0818900,PF3D7_0922200,PF3D7_0930300,PF3D7_1116000,PF3D7_1343000,PF3D7_1410400,	9.8	2.36	2.59	0.00922314	0.025318422	1

		GO:0071944	cell periphery	23	4	PF3D7_0104800,PF3D7_0702200,PF3D7_1342600,PF3D7_1460600,	17.4	4.19	4.94	0.01370256	0.036891511	1
		GO:030864	cortical actin cytoskeleton	1	1	PF3D7_0105300,	100	24.1	inf	0.04149548	0.10562486	1
		GO:009898	cytoplasmic side of plasma membrane	1	1	PF3D7_1243500,	100	24.1	inf	0.04149548	0.10562486	1
		GO:034591	rhoptry lumen	1	1	PF3D7_0424100,	100	24.1	inf	0.04149548	0.10562486	1

University of Ghana http://ugspace.ug.edu.gh

Supplementary Table 5.12 List of differentially expressed genes (up- and down-regulated) between the conditions C580R_DMSO treated compared with C580R_DHA treated

University of Ghana http://ugspace.ug.edu.gh

Gene ID	source_id	Input Order	Organism	Genomic Location (Gene)	Product Description	Gene Type	differentially expressed
PF3D7_0102600	PF3D7_0102600.1	10	Plasmodium falciparum 3D7	Pf3D7_01_v3:118,812..122,534(-)	serine/threonine protein kinase, NEK family	protein coding gene	Down
PF3D7_0113700	PF3D7_0113700.1	2	Plasmodium falciparum 3D7	Pf3D7_01_v3:519,766..523,106(+)	heat shock protein 40, type II	protein coding gene	Down
PF3D7_0202200	PF3D7_0202200.1	13	Plasmodium falciparum 3D7	Pf3D7_02_v3:111,818..115,064(-)	EMP1-trafficking protein	protein coding gene	Down
PF3D7_0210100	PF3D7_0210100.1	14	Plasmodium falciparum 3D7	Pf3D7_02_v3:411,419..412,963(+)	60S ribosomal protein L37ae, putative	protein coding gene	Down
PF3D7_0210100	PF3D7_0210100.2	14	Plasmodium falciparum 3D7	Pf3D7_02_v3:411,419..412,963(+)	60S ribosomal protein L37ae, putative	protein coding gene	Up
PF3D7_0304000	PF3D7_0304000.1	1	Plasmodium falciparum 3D7	Pf3D7_03_v3:198,542..201,584(-)	inner membrane complex protein 1a, putative	protein coding gene	Down
PF3D7_0401500	PF3D7_0401500.1	21	Plasmodium falciparum 3D7	Pf3D7_04_v3:89,153..90,184(+)	stevor, pseudogene	pseudogene	Down
PF3D7_0426000	PF3D7_0426000.1	3	Plasmodium falciparum 3D7	Pf3D7_04_v3:1,173,053..1,180,226(-)	erythrocyte membrane protein 1, PfEMP1	protein coding gene	Down
PF3D7_0500600	PF3D7_0500600.1	22	Plasmodium falciparum 3D7	Pf3D7_05_v3:39,443..40,488(-)	stevor, pseudogene	pseudogene	Down
PF3D7_0529400	PF3D7_0529400.1	12	Plasmodium falciparum 3D7	Pf3D7_05_v3:1,198,563..1,205,743(+)	conserved Plasmodium protein, unknown function	protein coding gene	Down
PF3D7_0529400	PF3D7_0529400.2	12	Plasmodium falciparum 3D7	Pf3D7_05_v3:1,198,563..1,205,743(+)	conserved Plasmodium protein, unknown function	protein coding gene	Down
PF3D7_0816500	PF3D7_0816500.1	5	Plasmodium falciparum 3D7	Pf3D7_08_v3:760,138..761,031(+)	small heat shock protein HSP20, putative	protein coding gene	Down
PF3D7_0818900	PF3D7_0818900.1	4	Plasmodium falciparum 3D7	Pf3D7_08_v3:858,550..862,980(+)	heat shock protein 70	protein coding gene	Down
PF3D7_0900300	PF3D7_0900300.1	6	Plasmodium falciparum 3D7	Pf3D7_09_v3:33,553..34,795(-)	rifin	protein coding gene	Down
PF3D7_0935600	PF3D7_0935600.1	7	Plasmodium falciparum 3D7	Pf3D7_09_v3:1,403,986..1,407,459(+)	gametocytogenesis-implicated protein	protein coding gene	Down
PF3D7_1121200	PF3D7_1121200.1	15	Plasmodium falciparum 3D7	Pf3D7_11_v3:800,552..801,465(-)	conserved protein, unknown function	protein coding gene	Down
PF3D7_1201100	PF3D7_1201100.1	16	Plasmodium falciparum 3D7	Pf3D7_12_v3:80,874..84,922(-)	RESA-like protein with PHIST and DnaJ domains	protein coding gene	Down
PF3D7_1212400	PF3D7_1212400.1	17	Plasmodium falciparum 3D7	Pf3D7_12_v3:549,734..551,279(+)	tetratricopeptide repeat protein, putative	protein coding gene	Down
PF3D7_1350600	PF3D7_1350600.1	8	Plasmodium falciparum 3D7	Pf3D7_13_v3:2,021,350..2,022,307(+)	conserved Plasmodium protein, unknown function	protein coding gene	Down
PF3D7_1367800	PF3D7_1367800.1	9	Plasmodium falciparum 3D7	Pf3D7_13_v3:2,701,228..2,704,776(+)	secreted ookinete protein, putative	protein coding gene	Down
PF3D7_1372000	PF3D7_1372000.1	11	Plasmodium falciparum 3D7	Pf3D7_13_v3:2,832,623..2,835,439(+)	Plasmodium exported protein (PHISTa), unknown function	protein coding gene	Down
PF3D7_1400700	PF3D7_1400700.1	18	Plasmodium falciparum 3D7	Pf3D7_14_v3:24,337..25,320(-)	stevor	protein coding gene	Down
PF3D7_1401000	PF3D7_1401000.1	19	Plasmodium falciparum 3D7	Pf3D7_14_v3:34,693..35,773(-)	GBPH protein	protein coding gene	Down
PF3D7_1416600	PF3D7_1416600.1	20	Plasmodium falciparum 3D7	Pf3D7_14_v3:669,374..679,741(-)	conserved Plasmodium protein, unknown function	protein coding gene	Down

Supplementary Table 5.13 Functional prediction and gene ontology enrichment analysis for up/down-regulated genes between C580R DMSO_treated and DHA_treated condition

University of Ghana http://ugspace.ug.edu.gh

Gene ID	Ontology	go_id	Is Not	GO Term Name	Slim go_id	GO Slim Term Name						
PF3D7_0210100	Biological Process	GO:0006412	N/A	translation	N/A	N/A						
PF3D7_0210100	Cellular Component	GO:0005634	N/A	nucleus	GO:0005634	nucleus						
PF3D7_0210100	Cellular Component	GO:0005840	N/A	ribosome	GO:0005840	ribosome						
PF3D7_0210100	Molecular Function	GO:0003735	N/A	structural constituent of ribosome	GO:0003735	structural constituent of ribosome						
PF3D7_0210100	Molecular Function	GO:0046872	N/A	metal ion binding	GO:0043167	ion binding						
Gene ontology term	Differential expression	ID	Name	Bgd count	Result count	Result gene list	Pct of bgd	Fold enrichment	Odds ratio	P-value	Benjamini	Bonferroni
Biological process	Downregulated	GO:0009408	response to heat	29	3	PF3D7_0113700,PF3D7_0816500,PF3D7_0818900,	10.3	27.98	37.11	0.00014611	0.00445416	0.00803608
		GO:0009266	response to temperature stimulus	30	3	PF3D7_0113700,PF3D7_0816500,PF3D7_0818900,	10	27.04	35.73	0.00016197	0.00445416	0.00890833
		GO:0009628	response to abiotic stimulus	40	3	PF3D7_0113700,PF3D7_0816500,PF3D7_0818900,	7.5	20.28	26.02	0.00038513	0.00706072	0.02118216
		GO:0051084	'de novo' posttranslational protein folding	15	2	PF3D7_0113700,PF3D7_0818900,	13.3	36.06	46.51	0.00131801	0.01449809	0.07249046
		GO:0051085	chaperone cofactor-dependent protein refolding	15	2	PF3D7_0113700,PF3D7_0818900,	13.3	36.06	46.51	0.00131801	0.01449809	0.07249046
		GO:0061077	chaperone-mediated protein folding	17	2	PF3D7_0113700,PF3D7_0818900,	11.8	31.82	40.29	0.00169967	0.014991	0.09348189

University of Ghana http://ugspace.ug.edu.gh

		GO:0006458	'de novo' protein folding	18	2	PF3D7_0113700,PF3D7_0818900,	11.1	30.05	37.77	0.00190795	0.014991	0.10493702
		GO:0006986	response to unfolded protein	22	2	PF3D7_0816500,PF3D7_0818900,	9.1	24.59	30.19	0.0028555	0.01963158	0.15705265
		GO:0035966	response to topologically incorrect protein	29	2	PF3D7_0816500,PF3D7_0818900,	6.9	18.65	22.33	0.00494247	0.030204	0.27183598
		GO:0006457	protein folding	103	3	PF3D7_0113700,PF3D7_0816500,PF3D7_0818900,	2.9	7.88	9.5	0.00595795	0.03276874	0.32768741
		GO:0006970	response to osmotic stress	3	1	PF3D7_0816500,	33.3	90.15	142.59	0.01105415	0.04629114	0.60797811
		GO:0042542	response to hydrogen peroxide	3	1	PF3D7_0816500,	33.3	90.15	142.59	0.01105415	0.04629114	0.60797811
		GO:0009651	response to salt stress	3	1	PF3D7_0816500,	33.3	90.15	142.59	0.01105415	0.04629114	0.60797811
		GO:0044403	biological process involved in symbiotic interaction	397	5	PF3D7_0102600,PF3D7_0113700,PF3D7_0304000,PF3D7_0426000,PF3D7_1400700,	1.3	3.41	4.37	0.01236735	0.04629114	0.68020418
		GO:0044419	biological process involved in interspecies interaction between organisms	399	5	PF3D7_0102600,PF3D7_0113700,PF3D7_0304000,PF3D7_0426000,PF3D7_1400700,	1.3	3.39	4.35	0.01262486	0.04629114	0.69436712
		GO:0000302	response to reactive oxygen species	7	1	PF3D7_0816500,	14.3	38.63	47.49	0.02561358	0.08804667	1
		GO:0010035	response to inorganic substance	9	1	PF3D7_0816500,	11.1	30.05	35.6	0.03281715	0.09499701	1
		GO:0042026	protein refolding	9	1	PF3D7_0818900,	11.1	30.05	35.6	0.03281715	0.09499701	1
		GO:0034620	cellular response to unfolded protein	9	1	PF3D7_0818900,	11.1	30.05	35.6	0.03281715	0.09499701	1
		GO:0051259	protein complex oligomerization	10	1	PF3D7_0816500,	10	27.04	31.64	0.03640004	0.09859332	1

University of Ghana http://ugspace.ug.edu.gh

		GO:0044003	modulation by symbiont of host process	205	3	PF3D7_0102600,PF3D7_0426000,PF3D7_1400700,	1.5	3.96	4.6	0.03764472	0.09859332	1
		GO:0051701	biological process involved in interaction with host	382	4	PF3D7_0102600,PF3D7_0204000,PF3D7_0426000,PF3D7_1400700,	1	2.83	3.38	0.04733923	0.11834808	1
Molecular function	Downregulated	GO:0051082	unfolded protein binding	65	3	PF3D7_0113700,PF3D7_0816500,PF3D7_0818900,	4.6	12.48	15.45	0.0016069	0.06909685	0.06909685
		GO:0015485	cholesterol binding	1	1	PF3D7_0113700,	100	270.44	inf	0.00369762	0.07922139	0.15899753
		GO:0005496	steroid binding	2	1	PF3D7_0113700,	50	135.22	285.24	0.00738232	0.07922139	0.31743971
		GO:0032934	sterol binding	2	1	PF3D7_0113700,	50	135.22	285.24	0.00738232	0.07922139	0.31743971
		GO:0043621	protein self-association	3	1	PF3D7_0816500,	33.3	90.15	142.59	0.01105415	0.07922139	0.47532834
		GO:0043178	alcohol binding	3	1	PF3D7_0113700,	33.3	90.15	142.59	0.01105415	0.07922139	0.47532834
		GO:0032266	phosphatidylinositol-3-phosphate binding	5	1	PF3D7_0818900,	20	54.09	71.26	0.01835935	0.1050768	0.78945226
		GO:0044183	protein folding chaperone	6	1	PF3D7_0818900,	16.7	45.07	57	0.02199282	0.1050768	0.94569118
		GO:1901981	phosphatidylinositol phosphate binding	6	1	PF3D7_0818900,	16.7	45.07	57	0.02199282	0.1050768	0.94569118
		GO:0051787	misfolded protein binding	8	1	PF3D7_0818900,	12.5	33.81	40.7	0.02922167	0.12565319	1
		GO:0035091	phosphatidylinositol binding	10	1	PF3D7_0818900,	10	27.04	31.64	0.03640004	0.14229108	1
Cellular component	Downregulated	GO:0018995	host cellular component	713	9	PF3D7_0102600,PF3D7_0113700,PF3D7_0202200,PF3D7_0426000,PF3D7_0935600,PF3D7_1201100,PF3D7_1372000,PF3D7_1400700,PF3D7_1401000,	1.3	3.41	5.89	0.00041387	0.00869131	0.01738262
		GO:0043657	host cell	713	9	PF3D7_0102600,PF3D7_0113700,PF3D7_0202200,PF3D7_0426000,PF3D7_0935600,PF3D7_1201100,PF3D7_1372000,PF3D7_1400700,PF3D7_1401000,	1.3	3.41	5.89	0.00041387	0.00869131	0.01738262

University of Ghana http://ugspace.ug.edu.gh

		GO:0030430	host cell cytoplasm	540	7	PF3D7_0102600,PF3D7_0113700,PF3D7_0202200,PF3D7_0426000,PF3D7_0935600,PF3D7_1201100,PF3D7_1400700,	1.3	3.51	5.15	0.00211443	0.01748958	0.08880618
		GO:0033646	host intracellular part	549	7	PF3D7_0102600,PF3D7_0113700,PF3D7_0202200,PF3D7_0426000,PF3D7_0935600,PF3D7_1201100,PF3D7_1400700,	1.3	3.45	5.06	0.00232982	0.01748958	0.09785227
		GO:0043656	host intracellular region	550	7	PF3D7_0102600,PF3D7_0113700,PF3D7_0202200,PF3D7_0426000,PF3D7_0935600,PF3D7_1201100,PF3D7_1400700,	1.3	3.44	5.05	0.00235478	0.01748958	0.09890075
		GO:0005575	cellular component	723	8	PF3D7_0202200,PF3D7_0529400,PF3D7_1201100,PF3D7_1212400,PF3D7_1350600,PF3D7_1367800,PF3D7_1400700,PF3D7_1401000,	1.1	2.99	4.63	0.00249851	0.01748958	0.10493748
		GO:0033643	host cell part	630	7	PF3D7_0102600,PF3D7_0113700,PF3D7_0202200,PF3D7_0426000,PF3D7_0935600,PF3D7_1201100,PF3D7_1400700,	1.1	3	4.32	0.00514908	0.02877533	0.21626154
		GO:0016020	membrane	637	7	PF3D7_0529400,PF3D7_1201100,PF3D7_1212400,PF3D7_1350600,PF3D7_1367800,PF3D7_1400700,PF3D7_1401000,	1.1	2.97	4.26	0.00548102	0.02877533	0.23020268
		GO:0033655	host cell cytoplasm part	524	6	PF3D7_0102600,PF3D7_0113700,PF3D7_0202200,PF3D7_0426000,PF3D7_0935600,PF3D7_1400700,	1.1	3.1	4.18	0.00904201	0.0388128	0.37976458
		GO:0020036	Maurer's cleft	370	5	PF3D7_0102600,PF3D7_0113700,PF3D7_0202200,PF3D7_0935600,PF3D7_1400700,	1.4	3.65	4.73	0.00924114	0.0388128	0.38812804
		GO:0070258	inner membrane pellicle complex	63	2	PF3D7_0304000,PF3D7_0816500,	3.2	8.59	9.81	0.02207474	0.08192825	0.92713894
		GO:0020039	pellicle	65	2	PF3D7_0304000,PF3D7_0816500,	3.1	8.32	9.5	0.02340807	0.08192825	0.98313903

Supplementary Table 5.14 List of differentially expressed genes (up- and down-regulated) between the conditions C580R_untreated compared with C580R_DHA treated

Gene_ID	source_id	Input.Order	Organism	Genomic.Location..Gene.	Product.Description	Gene.Type	differentially expressed
PF3D7_0100100	PF3D7_0100100.1	18	Plasmodium falciparum 3D7	Pf3D7_01_v3:29,510..37,126(+)	erythrocyte membrane protein 1, PfEMP1	protein coding gene	UP
PF3D7_0100500	PF3D7_0100500.1	404	Plasmodium falciparum 3D7	Pf3D7_01_v3:53,169..53,280(-)	erythrocyte membrane protein 1 (PfEMP1), exon 1, pseudogene	pseudogene	UP
PF3D7_0102100	PF3D7_0102100.1	405	Plasmodium falciparum 3D7	Pf3D7_01_v3:95,050..95,899(+)	stevor, pseudogene	pseudogene	UP
PF3D7_0102200	PF3D7_0102200.1	24	Plasmodium falciparum 3D7	Pf3D7_01_v3:97,590..103,615(+)	ring-infected erythrocyte surface antigen	protein coding gene	DOWN
PF3D7_0102500	PF3D7_0102500.1	25	Plasmodium falciparum 3D7	Pf3D7_01_v3:109,005..117,516(-)	erythrocyte binding antigen-181	protein coding gene	DOWN
PF3D7_0102700	PF3D7_0102700.1	26	Plasmodium falciparum 3D7	Pf3D7_01_v3:124,394..126,213(+)	merozoite-associated tryptophan-rich antigen	protein coding gene	DOWN
PF3D7_0104100	PF3D7_0104100.1	27	Plasmodium falciparum 3D7	Pf3D7_01_v3:177,187..181,825(+)	protein E140, putative	protein coding gene	DOWN
PF3D7_0104200	PF3D7_0104200.1	28	Plasmodium falciparum 3D7	Pf3D7_01_v3:182,205..184,820(-)	StAR-related lipid transfer protein	protein coding gene	DOWN
PF3D7_0104700	PF3D7_0104700.1	29	Plasmodium falciparum 3D7	Pf3D7_01_v3:210,870..213,005(+)	major facilitator superfamily-related transporter, putative	protein coding gene	UP
PF3D7_0104800	PF3D7_0104800.1	30	Plasmodium falciparum 3D7	Pf3D7_01_v3:215,143..217,616(+)	novel putative transporter 1, putative	protein coding gene	DOWN
PF3D7_0105300	PF3D7_0105300.1	31	Plasmodium falciparum 3D7	Pf3D7_01_v3:224,638..226,017(-)	cyclase-associated protein	protein coding gene	DOWN
PF3D7_0107200	PF3D7_0107200.1	196	Plasmodium falciparum 3D7	Pf3D7_01_v3:297,189..299,513(+)	CCR4 domain-containing protein 3, putative	protein coding gene	DOWN
PF3D7_0108500	PF3D7_0108500.1	32	Plasmodium falciparum 3D7	Pf3D7_01_v3:347,246..350,568(+)	ELM2 domain-containing protein, putative	protein coding gene	DOWN
PF3D7_0109000	PF3D7_0109000.1	33	Plasmodium falciparum 3D7	Pf3D7_01_v3:362,217..365,209(+)	photosensitized INA-labeled protein PHIL1	protein coding gene	DOWN
PF3D7_0111900	PF3D7_0111900.1	34	Plasmodium falciparum 3D7	Pf3D7_01_v3:449,966..450,646(-)	mitochondrial distribution and morphology protein, putative	protein coding gene	DOWN
PF3D7_0114200	PF3D7_0114200.1	20	Plasmodium falciparum 3D7	Pf3D7_01_v3:550,576..551,713(-)	exported protein family 3	protein coding gene	UP
PF3D7_0114600	PF3D7_0114600.1	406	Plasmodium falciparum 3D7	Pf3D7_01_v3:560,474..561,534(-)	stevor, pseudogene	pseudogene	UP
PF3D7_0114700	PF3D7_0114700.1	21	Plasmodium falciparum 3D7	Pf3D7_01_v3:563,703..564,842(-)	rifin	protein coding gene	UP
PF3D7_0115000	PF3D7_0115000.1	22	Plasmodium falciparum 3D7	Pf3D7_01_v3:577,704..583,789(+)	surface-associated interspersed protein 1.3 (SURFIN 1.3)	protein coding gene	UP
PF3D7_0115700	PF3D7_0115700.1	23	Plasmodium falciparum 3D7	Pf3D7_01_v3:607,390..614,893(-)	erythrocyte membrane protein 1, PfEMP1	protein coding gene	UP
PF3D7_0202100	PF3D7_0202100.1	231	Plasmodium falciparum 3D7	Pf3D7_02_v3:108,217..111,658(-)	liver stage associated protein 2	protein coding gene	DOWN
PF3D7_0202200	PF3D7_0202200.1	232	Plasmodium falciparum 3D7	Pf3D7_02_v3:111,818..115,064(-)	EMP1-trafficking protein	protein coding gene	DOWN
PF3D7_0202500	PF3D7_0202500.1	233	Plasmodium falciparum 3D7	Pf3D7_02_v3:127,203..129,089(+)	early transcribed membrane protein 2	protein coding gene	DOWN
PF3D7_0204200	PF3D7_0204200.1	234	Plasmodium falciparum 3D7	Pf3D7_02_v3:192,755..194,248(+)	translocation protein SEC66, putative	protein coding gene	DOWN
PF3D7_0206200	PF3D7_0206200.1	235	Plasmodium falciparum 3D7	Pf3D7_02_v3:248,880..251,521(+)	pantothenate transporter	protein coding gene	DOWN
PF3D7_0206800	PF3D7_0206800.1	236	Plasmodium falciparum 3D7	Pf3D7_02_v3:271,576..274,917(-)	merozoite surface protein 2	protein coding gene	DOWN
PF3D7_0207000	PF3D7_0207000.1	237	Plasmodium falciparum 3D7	Pf3D7_02_v3:276,725..279,258(-)	merozoite surface protein 4	protein coding gene	DOWN
PF3D7_0207400	PF3D7_0207400.1	238	Plasmodium falciparum 3D7	Pf3D7_02_v3:293,896..297,980(-)	serine repeat antigen 7	protein coding gene	DOWN
PF3D7_0207500	PF3D7_0207500.1	239	Plasmodium falciparum 3D7	Pf3D7_02_v3:298,380..302,820(-)	serine repeat antigen 6	protein coding gene	DOWN
PF3D7_0207600	PF3D7_0207600.1	240	Plasmodium falciparum 3D7	Pf3D7_02_v3:303,409..307,376(-)	serine repeat antigen 5	protein coding gene	DOWN
PF3D7_0207700	PF3D7_0207700.1	241	Plasmodium falciparum 3D7	Pf3D7_02_v3:308,628..312,348(-)	serine repeat antigen 4	protein coding gene	DOWN
PF3D7_0207800	PF3D7_0207800.1	242	Plasmodium falciparum 3D7	Pf3D7_02_v3:312,990..316,944(-)	serine repeat antigen 3	protein coding gene	DOWN
PF3D7_0208900	PF3D7_0208900.1	243	Plasmodium falciparum 3D7	Pf3D7_02_v3:360,828..368,354(+)	6-cysteine protein P230p	protein coding gene	UP
PF3D7_0210600	PF3D7_0210600.1	244	Plasmodium falciparum 3D7	Pf3D7_02_v3:431,716..434,231(-)	protein CERLI1	protein coding gene	DOWN
PF3D7_0212600	PF3D7_0212600.1	245	Plasmodium falciparum 3D7	Pf3D7_02_v3:522,339..524,405(+)	secreted protein with altered thrombospondin repeat domain	protein coding gene	DOWN
PF3D7_0214600	PF3D7_0214600.1	246	Plasmodium falciparum 3D7	Pf3D7_02_v3:593,374..600,035(+)	serine/threonine protein kinase STK2, putative	protein coding gene	DOWN
PF3D7_0214700	PF3D7_0214700.1	247	Plasmodium falciparum 3D7	Pf3D7_02_v3:599,425..601,740(-)	conserved Plasmodium protein, unknown function	protein coding gene	DOWN
PF3D7_0214900	PF3D7_0214900.1	248	Plasmodium falciparum 3D7	Pf3D7_02_v3:609,924..616,306(+)	rhoptry neck protein 6	protein coding gene	DOWN
PF3D7_0217500	PF3D7_0217500.1	249	Plasmodium falciparum 3D7	Pf3D7_02_v3:719,266..723,617(+)	calcium-dependent protein kinase 1	protein coding gene	DOWN
PF3D7_0218100	PF3D7_0218100.1	250	Plasmodium falciparum 3D7	Pf3D7_02_v3:740,884..742,775(+)	conserved protein, unknown function	protein coding gene	DOWN
PF3D7_0220300	PF3D7_0220300.1	251	Plasmodium falciparum 3D7	Pf3D7_02_v3:812,892..815,853(-)	Plasmodium exported protein, unknown function	protein coding gene	DOWN
PF3D7_0220800	PF3D7_0220800.1	252	Plasmodium falciparum 3D7	Pf3D7_02_v3:838,594..844,668(+)	cytoadherence linked asexual protein 2	protein coding gene	DOWN

University of Ghana http://ugspace.ug.edu.gh

PF3D7_0300100	PF3D7_0300100.1	10	Plasmodium falciparum 3D7	Pf3D7_03_v3:36,965..44,482(+)	erythrocyte membrane protein 1, PfEMP1	protein coding gene	UP
PF3D7_0300900	PF3D7_0300900.1	11	Plasmodium falciparum 3D7	Pf3D7_03_v3:67,870..68,761(+)	stevor	protein coding gene	UP
PF3D7_0301000	PF3D7_0301000.1	12	Plasmodium falciparum 3D7	Pf3D7_03_v3:69,460..71,919(-)	acyl-CoA synthetase	protein coding gene	UP
PF3D7_0301300	PF3D7_0301300.1	13	Plasmodium falciparum 3D7	Pf3D7_03_v3:81,939..84,290(-)	epoxide hydrolase 1	protein coding gene	DOWN
PF3D7_0302200	PF3D7_0302200.1	2	Plasmodium falciparum 3D7	Pf3D7_03_v3:119,098..124,924(+)	cytoadherence linked asexual protein 3.2	protein coding gene	DOWN
PF3D7_0302300	PF3D7_0302300.1	407	Plasmodium falciparum 3D7	Pf3D7_03_v3:125,687..130,112(-)	erythrocyte membrane protein 1 (PfEMP1), pseudogene	pseudogene	UP
PF3D7_0302500	PF3D7_0302500.1	3	Plasmodium falciparum 3D7	Pf3D7_03_v3:134,486..141,185(+)	cytoadherence linked asexual protein 3.1	protein coding gene	DOWN
PF3D7_0302700	PF3D7_0302700.1	17	Plasmodium falciparum 3D7	Pf3D7_03_v3:146,052..147,270(-)	CDGSH iron-sulfur domain-containing protein, putative	protein coding gene	DOWN
PF3D7_0304000	PF3D7_0304000.1	6	Plasmodium falciparum 3D7	Pf3D7_03_v3:198,542..201,584(-)	inner membrane complex protein 1a, putative	protein coding gene	DOWN
PF3D7_0308300	PF3D7_0308300.1	4	Plasmodium falciparum 3D7	Pf3D7_03_v3:365,177..366,948(-)	PhIL1-interacting candidate PIC4	protein coding gene	DOWN
PF3D7_0308700	PF3D7_0308700.1	5	Plasmodium falciparum 3D7	Pf3D7_03_v3:375,388..377,772(+)	conserved protein, unknown function	protein coding gene	DOWN
PF3D7_0313500	PF3D7_0313500.1	1	Plasmodium falciparum 3D7	Pf3D7_03_v3:548,576..551,854(+)	Ras-like G protein	protein coding gene	UP
PF3D7_0318700	PF3D7_0318700.1	19	Plasmodium falciparum 3D7	Pf3D7_03_v3:788,145..789,211(+)	conserved Plasmodium protein, unknown function	protein coding gene	DOWN
PF3D7_0320900	PF3D7_0320900.1	9	Plasmodium falciparum 3D7	Pf3D7_03_v3:874,313..876,685(+)	histone H2A.Z	protein coding gene	DOWN
PF3D7_0321400	PF3D7_0321400.1	226	Plasmodium falciparum 3D7	Pf3D7_03_v3:894,149..896,220(+)	pseudo protein kinase 1, putative	protein coding gene	DOWN
PF3D7_0324800	PF3D7_0324800.1	7	Plasmodium falciparum 3D7	Pf3D7_03_v3:1,027,571..1,028,929(+)	rifin	protein coding gene	UP
PF3D7_0324900	PF3D7_0324900.1	8	Plasmodium falciparum 3D7	Pf3D7_03_v3:1,030,822..1,038,254(-)	erythrocyte membrane protein 1, PfEMP1	protein coding gene	UP
PF3D7_0400100	PF3D7_0400100.1	35	Plasmodium falciparum 3D7	Pf3D7_04_v3:28,706..37,677(+)	erythrocyte membrane protein 1, PfEMP1	protein coding gene	UP
PF3D7_0400400	PF3D7_0400400.1	36	Plasmodium falciparum 3D7	Pf3D7_04_v3:45,555..56,860(-)	erythrocyte membrane protein 1, PfEMP1	protein coding gene	UP
PF3D7_0401800	PF3D7_0401800.1	37	Plasmodium falciparum 3D7	Pf3D7_04_v3:103,078..106,145(-)	Plasmodium exported protein (PHISTb), unknown function	protein coding gene	DOWN
PF3D7_0402100	PF3D7_0402100.1	38	Plasmodium falciparum 3D7	Pf3D7_04_v3:123,068..125,848(-)	Plasmodium exported protein (PHISTb), unknown function	protein coding gene	DOWN
PF3D7_0402600	PF3D7_0402600.1	39	Plasmodium falciparum 3D7	Pf3D7_04_v3:159,279..160,314(-)	stevor	protein coding gene	UP
PF3D7_0402800	PF3D7_0402800.1	408	Plasmodium falciparum 3D7	Pf3D7_04_v3:167,245..171,985(+)	erythrocyte membrane protein 1 (PfEMP1), pseudogene	pseudogene	UP
PF3D7_0403800	PF3D7_0403800.1	40	Plasmodium falciparum 3D7	Pf3D7_04_v3:209,977..216,599(-)	alpha/beta hydrolase, putative	protein coding gene	DOWN
PF3D7_0404700	PF3D7_0404700.1	41	Plasmodium falciparum 3D7	Pf3D7_04_v3:259,944..263,782(-)	dipeptidyl aminopeptidase 3	protein coding gene	DOWN
PF3D7_0404800	PF3D7_0404800.1	42	Plasmodium falciparum 3D7	Pf3D7_04_v3:264,062..266,503(-)	sporozoite-specific protein S10, putative	protein coding gene	DOWN
PF3D7_0404900	PF3D7_0404900.1	43	Plasmodium falciparum 3D7	Pf3D7_04_v3:266,566..268,913(-)	6-cysteine protein P41	protein coding gene	DOWN
PF3D7_0405200	PF3D7_0405200.1	44	Plasmodium falciparum 3D7	Pf3D7_04_v3:277,684..281,983(+)	protein CERLI2	protein coding gene	DOWN
PF3D7_0405300	PF3D7_0405300.1	45	Plasmodium falciparum 3D7	Pf3D7_04_v3:282,403..288,297(-)	liver specific protein 2, putative	protein coding gene	UP
PF3D7_0405900	PF3D7_0405900.1	46	Plasmodium falciparum 3D7	Pf3D7_04_v3:315,974..319,564(-)	apical sushi protein	protein coding gene	DOWN
PF3D7_0408000	PF3D7_0408000.1	14	Plasmodium falciparum 3D7	Pf3D7_04_v3:394,047..394,714(-)	conserved Plasmodium protein, unknown function	protein coding gene	DOWN
PF3D7_0411100	PF3D7_0411100.1	15	Plasmodium falciparum 3D7	Pf3D7_04_v3:504,413..505,095(-)	mediator of RNA polymerase II transcription subunit 8, putative	protein coding gene	UP
PF3D7_0412400	PF3D7_0412400.1	16	Plasmodium falciparum 3D7	Pf3D7_04_v3:545,623..554,633(-)	erythrocyte membrane protein 1, PfEMP1	protein coding gene	UP
PF3D7_0413200	PF3D7_0413200.1	47	Plasmodium falciparum 3D7	Pf3D7_04_v3:603,166..604,456(-)	rifin	protein coding gene	UP
PF3D7_0413400	PF3D7_0413400.1	409	Plasmodium falciparum 3D7	Pf3D7_04_v3:612,798..614,069(+)	erythrocyte membrane protein 1 (PfEMP1), exon 1, pseudogene	pseudogene	UP
PF3D7_0414800	PF3D7_0414800.1	197	Plasmodium falciparum 3D7	Pf3D7_04_v3:663,115..664,901(-)	conserved Plasmodium protein, unknown function	protein coding gene	DOWN
PF3D7_0414900	PF3D7_0414900.1	198	Plasmodium falciparum 3D7	Pf3D7_04_v3:665,765..668,508(+)	armadillo-domain containing rhoptry protein	protein coding gene	DOWN
PF3D7_0418600	PF3D7_0418600.1	48	Plasmodium falciparum 3D7	Pf3D7_04_v3:833,620..840,678(+)	regulator of chromosome condensation, putative	protein coding gene	DOWN
PF3D7_0418800	PF3D7_0418800.1	199	Plasmodium falciparum 3D7	Pf3D7_04_v3:843,562..845,169(+)	MOLO1 domain-containing protein, putative	protein coding gene	UP
PF3D7_0419700	PF3D7_0419700.1	49	Plasmodium falciparum 3D7	Pf3D7_04_v3:872,600..875,321(+)	apical merozoite protein	protein coding gene	DOWN
PF3D7_0420200	PF3D7_0420200.1	50	Plasmodium falciparum 3D7	Pf3D7_04_v3:909,409..912,119(+)	holo-[acyl-carrier-protein] synthase, putative	protein coding gene	UP
PF3D7_0420700	PF3D7_0420700.1	51	Plasmodium falciparum 3D7	Pf3D7_04_v3:935,031..941,875(-)	erythrocyte membrane protein 1, PfEMP1	protein coding gene	UP
PF3D7_0421100	PF3D7_0421100.1	52	Plasmodium falciparum 3D7	Pf3D7_04_v3:958,067..965,611(-)	erythrocyte membrane protein 1, PfEMP1	protein coding gene	UP
PF3D7_0421600	PF3D7_0421600.1	410	Plasmodium falciparum 3D7	Pf3D7_04_v3:986,135..987,447(+)	erythrocyte membrane protein 1 (PfEMP1)-like pseudogene	pseudogene	UP
PF3D7_0423400	PF3D7_0423400.1	53	Plasmodium falciparum 3D7	Pf3D7_04_v3:1,055,314..1,056,674(+)	apical asparagine-rich protein AARP	protein coding gene	DOWN

University of Ghana http://ugspace.ug.edu.gh

PF3D7_0423900	PF3D7_0423900.1	54	Plasmodium falciparum 3D7	Pf3D7_04_v3:1,077,575..1,078,515(-)	probable protein, unknown function	protein coding gene	DOWN
PF3D7_0424100	PF3D7_0424100.1	55	Plasmodium falciparum 3D7	Pf3D7_04_v3:1,082,005..1,084,464(-)	reticulocyte binding protein homologue 5	protein coding gene	DOWN
PF3D7_0424300	PF3D7_0424300.1	411	Plasmodium falciparum 3D7	Pf3D7_04_v3:1,093,138..1,097,835(+)	erythrocyte binding antigen-165, pseudogene	pseudogene	UP
PF3D7_0424400	PF3D7_0424400.1	56	Plasmodium falciparum 3D7	Pf3D7_04_v3:1,099,303..1,107,445(+)	surface-associated interspersed protein 4.2 (SURFIN 4.2)	protein coding gene	UP
PF3D7_0425000	PF3D7_0425000.1	412	Plasmodium falciparum 3D7	Pf3D7_04_v3:1,129,660..1,130,893(-)	Plasmodium exported protein, unknown function, pseudogene	pseudogene	UP
PF3D7_0425800	PF3D7_0425800.1	57	Plasmodium falciparum 3D7	Pf3D7_04_v3:1,156,423..1,167,821(+)	erythrocyte membrane protein 1, PfEMP1	protein coding gene	UP
PF3D7_0500900	PF3D7_0500900.1	100	Plasmodium falciparum 3D7	Pf3D7_05_v3:50,081..52,576(-)	serine/threonine protein kinase, FIKK family	protein coding gene	DOWN
PF3D7_0501300	PF3D7_0501300.1	101	Plasmodium falciparum 3D7	Pf3D7_05_v3:67,224..70,944(+)	skeleton-binding protein 1	protein coding gene	DOWN
PF3D7_0501400	PF3D7_0501400.1	102	Plasmodium falciparum 3D7	Pf3D7_05_v3:73,163..80,813(+)	interspersed repeat antigen	protein coding gene	DOWN
PF3D7_0501500	PF3D7_0501500.1	103	Plasmodium falciparum 3D7	Pf3D7_05_v3:80,570..82,703(-)	rhoptry-associated protein 3	protein coding gene	DOWN
PF3D7_0501600	PF3D7_0501600.1	104	Plasmodium falciparum 3D7	Pf3D7_05_v3:83,760..85,512(-)	rhoptry-associated protein 2	protein coding gene	DOWN
PF3D7_0503400	PF3D7_0503400.1	105	Plasmodium falciparum 3D7	Pf3D7_05_v3:139,481..142,206(+)	actin-depolymerizing factor 1	protein coding gene	DOWN
PF3D7_0503600	PF3D7_0503600.1	106	Plasmodium falciparum 3D7	Pf3D7_05_v3:146,352..150,733(-)	myosin B	protein coding gene	DOWN
PF3D7_0506900	PF3D7_0506900.1	107	Plasmodium falciparum 3D7	Pf3D7_05_v3:288,024..291,540(-)	rhomboid protease ROM4	protein coding gene	DOWN
PF3D7_0507200	PF3D7_0507200.1	108	Plasmodium falciparum 3D7	Pf3D7_05_v3:298,070..301,000(-)	subtilisin-like protease 3	protein coding gene	DOWN
PF3D7_0507400	PF3D7_0507400.1	200	Plasmodium falciparum 3D7	Pf3D7_05_v3:305,282..306,963(-)	subtilisin propeptide-like protein	protein coding gene	DOWN
PF3D7_0507500	PF3D7_0507500.1	109	Plasmodium falciparum 3D7	Pf3D7_05_v3:307,090..310,120(-)	subtilisin-like protease 1	protein coding gene	DOWN
PF3D7_0510300	PF3D7_0510300.1	110	Plasmodium falciparum 3D7	Pf3D7_05_v3:440,724..442,007(-)	stripes inner membrane complex protein, putative	protein coding gene	UP
PF3D7_0511600	PF3D7_0511600.1	111	Plasmodium falciparum 3D7	Pf3D7_05_v3:517,088..518,520(-)	apical rhoptry neck protein	protein coding gene	DOWN
PF3D7_0513000	PF3D7_0513000.1	112	Plasmodium falciparum 3D7	Pf3D7_05_v3:555,264..556,651(+)	conserved protein, unknown function	protein coding gene	UP
PF3D7_0515700	PF3D7_0515700.1	113	Plasmodium falciparum 3D7	Pf3D7_05_v3:653,317..656,149(-)	glideosome-associated protein 40, putative	protein coding gene	DOWN
PF3D7_0518800	PF3D7_0518800.1	201	Plasmodium falciparum 3D7	Pf3D7_05_v3:783,638..784,991(-)	secreted ookinete protein, putative	protein coding gene	UP
PF3D7_0525800	PF3D7_0525800.1	114	Plasmodium falciparum 3D7	Pf3D7_05_v3:1,071,094..1,072,988(+)	inner membrane complex protein 1g, putative	protein coding gene	DOWN
PF3D7_0528300	PF3D7_0528300.1	115	Plasmodium falciparum 3D7	Pf3D7_05_v3:1,166,047..1,169,378(-)	conserved protein, unknown function	protein coding gene	DOWN
PF3D7_0528400	PF3D7_0528400.1	116	Plasmodium falciparum 3D7	Pf3D7_05_v3:1,170,170..1,174,394(+)	palmitoyltransferase DHHC7	protein coding gene	DOWN
PF3D7_0600200	PF3D7_0600200.1	189	Plasmodium falciparum 3D7	Pf3D7_06_v3:3,503..12,835(+)	erythrocyte membrane protein 1, PfEMP1	protein coding gene	UP
PF3D7_0604100	PF3D7_0604100.1	190	Plasmodium falciparum 3D7	Pf3D7_06_v3:170,776..178,985(-)	AP2 domain transcription factor	protein coding gene	DOWN
PF3D7_0604800	PF3D7_0604800.1	191	Plasmodium falciparum 3D7	Pf3D7_06_v3:206,807..211,802(-)	RAP protein, putative	protein coding gene	UP
PF3D7_0612700	PF3D7_0612700.1	192	Plasmodium falciparum 3D7	Pf3D7_06_v3:525,736..527,850(-)	6-cysteine protein P12	protein coding gene	DOWN
PF3D7_0613300	PF3D7_0613300.1	193	Plasmodium falciparum 3D7	Pf3D7_06_v3:539,725..545,452(-)	rhoptry protein ROP14	protein coding gene	DOWN
PF3D7_0613800	PF3D7_0613800.1	194	Plasmodium falciparum 3D7	Pf3D7_06_v3:565,925..579,231(+)	AP2 domain transcription factor, putative	protein coding gene	DOWN
PF3D7_0613900	PF3D7_0613900.1	195	Plasmodium falciparum 3D7	Pf3D7_06_v3:579,250..586,589(-)	myosin E, putative	protein coding gene	DOWN
PF3D7_0617300	PF3D7_0617300.1	177	Plasmodium falciparum 3D7	Pf3D7_06_v3:720,336..721,721(+)	RNA-binding protein, putative	protein coding gene	DOWN
PF3D7_0617400	PF3D7_0617400.1	178	Plasmodium falciparum 3D7	Pf3D7_06_v3:722,377..731,499(-)	erythrocyte membrane protein 1, PfEMP1	protein coding gene	UP
PF3D7_0617800	PF3D7_0617800.1	179	Plasmodium falciparum 3D7	Pf3D7_06_v3:747,329..749,285(-)	histone H2A	protein coding gene	DOWN
PF3D7_0618000	PF3D7_0618000.1	180	Plasmodium falciparum 3D7	Pf3D7_06_v3:757,278..761,654(+)	conserved Plasmodium membrane protein, unknown function	protein coding gene	DOWN
PF3D7_0618400	PF3D7_0618400.1	181	Plasmodium falciparum 3D7	Pf3D7_06_v3:770,147..772,506(-)	LMBR1 domain-containing protein, putative	protein coding gene	UP
PF3D7_0620400	PF3D7_0620400.1	182	Plasmodium falciparum 3D7	Pf3D7_06_v3:851,162..853,200(-)	merozoite surface protein 10	protein coding gene	DOWN
PF3D7_0625900	PF3D7_0625900.1	183	Plasmodium falciparum 3D7	Pf3D7_06_v3:1,046,986..1,048,052(+)	conserved Plasmodium protein, unknown function	protein coding gene	UP
PF3D7_0628100	PF3D7_0628100.1	184	Plasmodium falciparum 3D7	Pf3D7_06_v3:1,122,322..1,154,481(-)	HECT domain-containing protein 1, putative	protein coding gene	DOWN
PF3D7_0628300	PF3D7_0628300.1	185	Plasmodium falciparum 3D7	Pf3D7_06_v3:1,169,270..1,174,371(-)	choline/ethanolaminephosphotransferase, putative	protein coding gene	DOWN
PF3D7_0631800	PF3D7_0631800.1	186	Plasmodium falciparum 3D7	Pf3D7_06_v3:1,329,771..1,330,963(+)	rifin	protein coding gene	UP
PF3D7_0632500	PF3D7_0632500.1	187	Plasmodium falciparum 3D7	Pf3D7_06_v3:1,353,946..1,366,430(-)	erythrocyte membrane protein 1, PfEMP1	protein coding gene	UP
PF3D7_0632800	PF3D7_0632800.1	188	Plasmodium falciparum 3D7	Pf3D7_06_v3:1,374,797..1,382,627(-)	erythrocyte membrane protein 1, PfEMP1	protein coding gene	UP
PF3D7_0702000	PF3D7_0702000.1	202	Plasmodium falciparum 3D7	Pf3D7_07_v3:83,838..86,436(+)	Plasmodium exported protein (hyp12), unknown function	protein coding gene	DOWN

University of Ghana http://ugspace.ug.edu.gh

PF3D7_0702100	PF3D7_0702100.1	413	Plasmodium falciparum 3D7	Pf3D7_07_v3:88,685..90,886(+)	Plasmodium exported protein (PHISTb), unknown function, pseudogene	pseudogene	DOWN
PF3D7_0702200	PF3D7_0702200.1	58	Plasmodium falciparum 3D7	Pf3D7_07_v3:91,731..95,602(-)	lysophospholipase LPL20	protein coding gene	DOWN
PF3D7_0703600	PF3D7_0703600.1	203	Plasmodium falciparum 3D7	Pf3D7_07_v3:143,601..146,565(+)	conserved protein, unknown function	protein coding gene	DOWN
PF3D7_0706300	PF3D7_0706300.1	204	Plasmodium falciparum 3D7	Pf3D7_07_v3:305,264..306,466(+)	conserved Plasmodium protein, unknown function	protein coding gene	DOWN
PF3D7_0707300	PF3D7_0707300.1	205	Plasmodium falciparum 3D7	Pf3D7_07_v3:337,720..343,059(+)	rhoptry-associated membrane antigen	protein coding gene	DOWN
PF3D7_0711700	PF3D7_0711700.1	59	Plasmodium falciparum 3D7	Pf3D7_07_v3:511,950..519,425(-)	erythrocyte membrane protein 1, PfEMP1	protein coding gene	UP
PF3D7_0712000	PF3D7_0712000.1	60	Plasmodium falciparum 3D7	Pf3D7_07_v3:527,338..535,131(-)	erythrocyte membrane protein 1, PfEMP1	protein coding gene	UP
PF3D7_0712300	PF3D7_0712300.1	61	Plasmodium falciparum 3D7	Pf3D7_07_v3:542,906..550,520(-)	erythrocyte membrane protein 1, PfEMP1	protein coding gene	UP
PF3D7_0712400	PF3D7_0712400.1	62	Plasmodium falciparum 3D7	Pf3D7_07_v3:552,158..559,078(-)	erythrocyte membrane protein 1, PfEMP1	protein coding gene	UP
PF3D7_0712500	PF3D7_0712500.1	414	Plasmodium falciparum 3D7	Pf3D7_07_v3:562,906..564,160(-)	rifin, pseudogene	pseudogene	UP
PF3D7_0712600	PF3D7_0712600.1	63	Plasmodium falciparum 3D7	Pf3D7_07_v3:566,726..574,308(-)	erythrocyte membrane protein 1, PfEMP1	protein coding gene	UP
PF3D7_0712800	PF3D7_0712800.1	64	Plasmodium falciparum 3D7	Pf3D7_07_v3:581,386..588,923(-)	erythrocyte membrane protein 1, PfEMP1	protein coding gene	UP
PF3D7_0712900	PF3D7_0712900.1	65	Plasmodium falciparum 3D7	Pf3D7_07_v3:590,326..597,733(-)	erythrocyte membrane protein 1, PfEMP1	protein coding gene	UP
PF3D7_0713000	PF3D7_0713000.1	66	Plasmodium falciparum 3D7	Pf3D7_07_v3:602,141..603,381(+)	rifin	protein coding gene	UP
PF3D7_0713800	PF3D7_0713800.1	67	Plasmodium falciparum 3D7	Pf3D7_07_v3:623,870..625,625(-)	negative elongation factor A, putative	protein coding gene	DOWN
PF3D7_0714000	PF3D7_0714000.1	68	Plasmodium falciparum 3D7	Pf3D7_07_v3:642,200..643,997(-)	histone H2B variant	protein coding gene	DOWN
PF3D7_0715700	PF3D7_0715700.1	69	Plasmodium falciparum 3D7	Pf3D7_07_v3:694,095..695,200(+)	conserved protein, unknown function	protein coding gene	UP
PF3D7_0722200	PF3D7_0722200.1	70	Plasmodium falciparum 3D7	Pf3D7_07_v3:946,077..949,317(+)	rhoptry-associated leucine zipper-like protein 1	protein coding gene	DOWN
PF3D7_0723200	PF3D7_0723200.1	71	Plasmodium falciparum 3D7	Pf3D7_07_v3:972,658..974,272(+)	conserved Plasmodium protein, unknown function	protein coding gene	UP
PF3D7_0725400	PF3D7_0725400.1	72	Plasmodium falciparum 3D7	Pf3D7_07_v3:1,078,691..1,080,123(+)	conserved Plasmodium protein, unknown function	protein coding gene	DOWN
PF3D7_0726200	PF3D7_0726200.1	206	Plasmodium falciparum 3D7	Pf3D7_07_v3:1,099,013..1,103,615(+)	serine/threonine protein kinase, FIKK family	protein coding gene	UP
PF3D7_0731500	PF3D7_0731500.1	73	Plasmodium falciparum 3D7	Pf3D7_07_v3:1,357,251..1,363,653(+)	erythrocyte binding antigen-175	protein coding gene	DOWN
PF3D7_0800200	PF3D7_0800200.1	99	Plasmodium falciparum 3D7	Pf3D7_08_v3:29,147..39,682(-)	erythrocyte membrane protein 1, PfEMP1	protein coding gene	UP
PF3D7_0800300	PF3D7_0800300.1	98	Plasmodium falciparum 3D7	Pf3D7_08_v3:40,302..51,425(+)	erythrocyte membrane protein 1, PfEMP1	protein coding gene	UP
PF3D7_0800800	PF3D7_0800800.1	97	Plasmodium falciparum 3D7	Pf3D7_08_v3:79,126..80,766(+)	Plasmodium exported protein (hyp7), unknown function	protein coding gene	DOWN
PF3D7_0802600	PF3D7_0802600.1	207	Plasmodium falciparum 3D7	Pf3D7_08_v3:180,040..188,229(+)	adenylyl cyclase beta	protein coding gene	DOWN
PF3D7_0802800	PF3D7_0802800.1	96	Plasmodium falciparum 3D7	Pf3D7_08_v3:191,422..194,498(+)	serine/threonine protein phosphatase 2B catalytic subunit A	protein coding gene	DOWN
PF3D7_0805200	PF3D7_0805200.1	95	Plasmodium falciparum 3D7	Pf3D7_08_v3:290,626..291,907(+)	gamete release protein, putative	protein coding gene	DOWN
PF3D7_0805600	PF3D7_0805600.1	227	Plasmodium falciparum 3D7	Pf3D7_08_v3:310,797..313,261(+)	phosphatidic acid phosphatase 2	protein coding gene	DOWN
PF3D7_0808200	PF3D7_0808200.1	94	Plasmodium falciparum 3D7	Pf3D7_08_v3:415,549..419,066(-)	plasmepsin X	protein coding gene	DOWN
PF3D7_0808600	PF3D7_0808600.1	93	Plasmodium falciparum 3D7	Pf3D7_08_v3:430,405..439,297(+)	erythrocyte membrane protein 1, PfEMP1	protein coding gene	UP
PF3D7_0808700	PF3D7_0808700.1	92	Plasmodium falciparum 3D7	Pf3D7_08_v3:440,408..448,062(+)	erythrocyte membrane protein 1, PfEMP1	protein coding gene	UP
PF3D7_0809100	PF3D7_0809100.1	91	Plasmodium falciparum 3D7	Pf3D7_08_v3:459,071..467,014(+)	erythrocyte membrane protein 1, PfEMP1	protein coding gene	UP
PF3D7_0816100	PF3D7_0816100.1	90	Plasmodium falciparum 3D7	Pf3D7_08_v3:748,331..750,033(+)	phosphopantothenoylcysteine decarboxylase, putative	protein coding gene	DOWN
PF3D7_0816500	PF3D7_0816500.1	89	Plasmodium falciparum 3D7	Pf3D7_08_v3:760,138..761,031(+)	small heat shock protein HSP20, putative	protein coding gene	DOWN
PF3D7_0817600	PF3D7_0817600.1	88	Plasmodium falciparum 3D7	Pf3D7_08_v3:800,326..804,715(-)	conserved protein, unknown function	protein coding gene	DOWN
PF3D7_0817700	PF3D7_0817700.1	208	Plasmodium falciparum 3D7	Pf3D7_08_v3:804,723..814,055(-)	rhoptry neck protein 5	protein coding gene	DOWN
PF3D7_0817800	PF3D7_0817800.1	87	Plasmodium falciparum 3D7	Pf3D7_08_v3:814,303..815,974(+)	respiratory chain complex 3 associated protein 3	protein coding gene	DOWN
PF3D7_0818100	PF3D7_0818100.1	86	Plasmodium falciparum 3D7	Pf3D7_08_v3:823,912..827,305(+)	zinc finger protein, putative	protein coding gene	DOWN
PF3D7_0818900	PF3D7_0818900.1	85	Plasmodium falciparum 3D7	Pf3D7_08_v3:858,550..862,980(+)	heat shock protein 70	protein coding gene	DOWN
PF3D7_0819200	PF3D7_0819200.1	84	Plasmodium falciparum 3D7	Pf3D7_08_v3:871,410..873,440(+)	perforin-like protein 5	protein coding gene	UP
PF3D7_0819300	PF3D7_0819300.1	209	Plasmodium falciparum 3D7	Pf3D7_08_v3:873,926..877,521(+)	conserved Plasmodium protein, unknown function	protein coding gene	UP
PF3D7_0820200	PF3D7_0820200.1	83	Plasmodium falciparum 3D7	Pf3D7_08_v3:911,627..915,386(-)	phosphatidylglycerophosphate synthase	protein coding gene	DOWN
PF3D7_0821000	PF3D7_0821000.1	82	Plasmodium falciparum 3D7	Pf3D7_08_v3:948,437..951,284(+)	conserved Plasmodium protein, unknown function	protein coding gene	DOWN
PF3D7_0821400	PF3D7_0821400.1	81	Plasmodium falciparum 3D7	Pf3D7_08_v3:964,289..967,130(+)	conserved Plasmodium protein, unknown function	protein coding gene	DOWN

University of Ghana http://ugspace.ug.edu.gh

PF3D7_0822900	PF3D7_0822900.1	80	Plasmodium falciparum 3D7	Pf3D7_08_v3:1,006,504..1,011,755(-)	PhIL1-interacting candidate PIC2	protein coding gene	DOWN
PF3D7_0825200	PF3D7_0825200.1	79	Plasmodium falciparum 3D7	Pf3D7_08_v3:1,093,439..1,094,936(+)	translation initiation factor IF-3	protein coding gene	DOWN
PF3D7_0825900	PF3D7_0825900.1	78	Plasmodium falciparum 3D7	Pf3D7_08_v3:1,105,631..1,108,315(+)	conserved Plasmodium protein, unknown function	protein coding gene	UP
PF3D7_0827200	PF3D7_0827200.1	77	Plasmodium falciparum 3D7	Pf3D7_08_v3:1,177,310..1,180,324(+)	conserved Plasmodium protein, unknown function	protein coding gene	UP
PF3D7_0827700	PF3D7_0827700.1	76	Plasmodium falciparum 3D7	Pf3D7_08_v3:1,193,847..1,196,678(-)	magnesium transporter, putative	protein coding gene	UP
PF3D7_0828800	PF3D7_0828800.1	75	Plasmodium falciparum 3D7	Pf3D7_08_v3:1,237,184..1,241,229(-)	GPI-anchored micronemal antigen	protein coding gene	DOWN
PF3D7_0830500	PF3D7_0830500.1	74	Plasmodium falciparum 3D7	Pf3D7_08_v3:1,295,569..1,299,431(-)	sporozoite and liver stage tryptophan-rich protein, putative	protein coding gene	DOWN
PF3D7_0831100	PF3D7_0831100.1	210	Plasmodium falciparum 3D7	Pf3D7_08_v3:1,324,597..1,331,626(+)	surface-associated interspersed protein 8.1 (SURFIN 8.1)	protein coding gene	UP
PF3D7_0831600	PF3D7_0831600.1	228	Plasmodium falciparum 3D7	Pf3D7_08_v3:1,358,188..1,363,639(+)	cytoadherence linked asexual protein 8	protein coding gene	DOWN
PF3D7_0833000	PF3D7_0833000.1	229	Plasmodium falciparum 3D7	Pf3D7_08_v3:1,417,438..1,418,625(+)	rifin	protein coding gene	UP
PF3D7_0833500	PF3D7_0833500.1	230	Plasmodium falciparum 3D7	Pf3D7_08_v3:1,435,794..1,443,449(-)	erythrocyte membrane protein 1, PfEMP1	protein coding gene	UP
PF3D7_0900100	PF3D7_0900100.1	117	Plasmodium falciparum 3D7	Pf3D7_09_v3:20,080..27,885(+)	erythrocyte membrane protein 1, PfEMP1	protein coding gene	UP
PF3D7_0902100	PF3D7_0902100.1	118	Plasmodium falciparum 3D7	Pf3D7_09_v3:93,768..95,820(-)	serine/threonine protein kinase, FIKK family	protein coding gene	DOWN
PF3D7_0903800	PF3D7_0903800.1	119	Plasmodium falciparum 3D7	Pf3D7_09_v3:179,187..183,991(+)	LCCL domain-containing protein	protein coding gene	UP
PF3D7_0905400	PF3D7_0905400.1	120	Plasmodium falciparum 3D7	Pf3D7_09_v3:270,371..275,833(-)	high molecular weight rhoptry protein 3	protein coding gene	DOWN
PF3D7_0905500	PF3D7_0905500.1	121	Plasmodium falciparum 3D7	Pf3D7_09_v3:276,467..279,624(+)	conserved protein, unknown function	protein coding gene	DOWN
PF3D7_0905600	PF3D7_0905600.1	122	Plasmodium falciparum 3D7	Pf3D7_09_v3:280,207..284,102(+)	WD repeat-containing protein 66, putative	protein coding gene	UP
PF3D7_0909000	PF3D7_0909000.1	123	Plasmodium falciparum 3D7	Pf3D7_09_v3:410,326..413,841(-)	conserved Plasmodium protein, unknown function	protein coding gene	UP
PF3D7_0913800	PF3D7_0913800.1	124	Plasmodium falciparum 3D7	Pf3D7_09_v3:592,048..593,728(+)	conserved Plasmodium protein, unknown function	protein coding gene	DOWN
PF3D7_0916300	PF3D7_0916300.1	125	Plasmodium falciparum 3D7	Pf3D7_09_v3:680,231..681,984(-)	conserved Plasmodium protein, unknown function	protein coding gene	DOWN
PF3D7_0917900	PF3D7_0917900.1	126	Plasmodium falciparum 3D7	Pf3D7_09_v3:736,669..741,656(+)	heat shock protein 70	protein coding gene	DOWN
PF3D7_0918000	PF3D7_0918000.1	127	Plasmodium falciparum 3D7	Pf3D7_09_v3:741,677..745,333(-)	glideosome-associated protein 50	protein coding gene	DOWN
PF3D7_0919200	PF3D7_0919200.1	128	Plasmodium falciparum 3D7	Pf3D7_09_v3:788,717..791,151(-)	PPPDE peptidase, putative	protein coding gene	DOWN
PF3D7_0920500	PF3D7_0920500.1	129	Plasmodium falciparum 3D7	Pf3D7_09_v3:840,386..842,993(+)	ADP-ribosylation factor, putative	protein coding gene	DOWN
PF3D7_0921300	PF3D7_0921300.1	130	Plasmodium falciparum 3D7	Pf3D7_09_v3:871,334..873,544(+)	RAP protein, putative	protein coding gene	UP
PF3D7_0922200	PF3D7_0922200.1	131	Plasmodium falciparum 3D7	Pf3D7_09_v3:901,584..905,953(+)	S-adenosylmethionine synthetase	protein coding gene	DOWN
PF3D7_0923300	PF3D7_0923300.1	132	Plasmodium falciparum 3D7	Pf3D7_09_v3:947,033..949,498(+)	perforin-like protein 3	protein coding gene	UP
PF3D7_0925100	PF3D7_0925100.1	133	Plasmodium falciparum 3D7	Pf3D7_09_v3:1,014,478..1,015,518(-)	conserved Plasmodium protein, unknown function	protein coding gene	UP
PF3D7_0925900	PF3D7_0925900.1	134	Plasmodium falciparum 3D7	Pf3D7_09_v3:1,039,462..1,042,118(+)	lipocalin	protein coding gene	DOWN
PF3D7_0927900	PF3D7_0927900.1	135	Plasmodium falciparum 3D7	Pf3D7_09_v3:1,130,507..1,134,907(-)	phosphatidylserine decarboxylase	protein coding gene	DOWN
PF3D7_0928100	PF3D7_0928100.1	136	Plasmodium falciparum 3D7	Pf3D7_09_v3:1,136,403..1,138,628(-)	conserved Plasmodium protein, unknown function	protein coding gene	UP
PF3D7_0929400	PF3D7_0929400.1	211	Plasmodium falciparum 3D7	Pf3D7_09_v3:1,173,579..1,181,380(+)	high molecular weight rhoptry protein 2	protein coding gene	DOWN
PF3D7_0930300	PF3D7_0930300.1	137	Plasmodium falciparum 3D7	Pf3D7_09_v3:1,201,305..1,207,576(+)	merozoite surface protein 1	protein coding gene	DOWN
PF3D7_0931900	PF3D7_0931900.1	212	Plasmodium falciparum 3D7	Pf3D7_09_v3:1,274,656..1,277,085(-)	adenylate kinase-like protein 2	protein coding gene	DOWN
PF3D7_0932100	PF3D7_0932100.1	213	Plasmodium falciparum 3D7	Pf3D7_09_v3:1,278,479..1,284,699(-)	protein MAM3, putative	protein coding gene	DOWN
PF3D7_0932200	PF3D7_0932200.1	138	Plasmodium falciparum 3D7	Pf3D7_09_v3:1,286,481..1,289,644(+)	profilin	protein coding gene	DOWN
PF3D7_0934800	PF3D7_0934800.1	139	Plasmodium falciparum 3D7	Pf3D7_09_v3:1,360,721..1,364,051(+)	cAMP-dependent protein kinase catalytic subunit	protein coding gene	DOWN
PF3D7_0935300	PF3D7_0935300.1	140	Plasmodium falciparum 3D7	Pf3D7_09_v3:1,372,874..1,374,250(+)	phosphatidylinositol N-acetylglucosaminyltransferase subunit P, putative	protein coding gene	DOWN
PF3D7_0935800	PF3D7_0935800.1	141	Plasmodium falciparum 3D7	Pf3D7_09_v3:1,412,562..1,419,940(+)	cytoadherence linked asexual protein 9	protein coding gene	DOWN
PF3D7_0936000	PF3D7_0936000.1	142	Plasmodium falciparum 3D7	Pf3D7_09_v3:1,426,152..1,428,942(-)	ring-exported protein 2	protein coding gene	DOWN
PF3D7_0936500	PF3D7_0936500.1	143	Plasmodium falciparum 3D7	Pf3D7_09_v3:1,443,260..1,445,400(-)	virulence-associated protein 1	protein coding gene	UP
PF3D7_0937200	PF3D7_0937200.1	144	Plasmodium falciparum 3D7	Pf3D7_09_v3:1,471,599..1,473,298(+)	lysophospholipase, putative	protein coding gene	UP
PF3D7_0937300	PF3D7_0937300.1	145	Plasmodium falciparum 3D7	Pf3D7_09_v3:1,474,431..1,475,704(+)	rifin	protein coding gene	UP
PF3D7_0937800	PF3D7_0937800.1	146	Plasmodium falciparum 3D7	Pf3D7_09_v3:1,495,579..1,503,336(-)	erythrocyte membrane protein 1, PfEMP1	protein coding gene	UP
PF3D7_1000100	PF3D7_1000100.1	253	Plasmodium falciparum 3D7	Pf3D7_10_v3:28,490..36,164(+)	erythrocyte membrane protein 1, PfEMP1	protein coding gene	UP

University of Ghana http://ugspace.ug.edu.gh

PF3D7_1000500	PF3D7_1000500.1	254	Plasmodium falciparum 3D7	Pf3D7_10_v3:48,052..49,384(-)	rifin	protein coding gene	UP
PF3D7_1001000	PF3D7_1001000.1	255	Plasmodium falciparum 3D7	Pf3D7_10_v3:62,926..64,808(+)	chondroitin sulfate A ligand	protein coding gene	DOWN
PF3D7_1001600	PF3D7_1001600.1	256	Plasmodium falciparum 3D7	Pf3D7_10_v3:85,910..91,177(-)	exported lipase 2	protein coding gene	DOWN
PF3D7_1003600	PF3D7_1003600.1	257	Plasmodium falciparum 3D7	Pf3D7_10_v3:164,213..166,726(+)	inner membrane complex protein 1c, putative	protein coding gene	DOWN
PF3D7_1005200	PF3D7_1005200.1	258	Plasmodium falciparum 3D7	Pf3D7_10_v3:232,315..233,024(-)	conserved Plasmodium protein, unknown function	protein coding gene	UP
PF3D7_1006200	PF3D7_1006200.1	259	Plasmodium falciparum 3D7	Pf3D7_10_v3:261,496..263,974(-)	DNA/RNA-binding protein Alba 3	protein coding gene	DOWN
PF3D7_1006300	PF3D7_1006300.1	260	Plasmodium falciparum 3D7	Pf3D7_10_v3:265,750..266,836(-)	conserved Plasmodium protein, unknown function	protein coding gene	UP
PF3D7_1007300	PF3D7_1007300.1	261	Plasmodium falciparum 3D7	Pf3D7_10_v3:292,725..296,323(+)	RING zinc finger protein, putative	protein coding gene	DOWN
PF3D7_1009100	PF3D7_1009100.1	262	Plasmodium falciparum 3D7	Pf3D7_10_v3:372,519..374,072(+)	conserved Plasmodium membrane protein, unknown function	protein coding gene	UP
PF3D7_1010300	PF3D7_1010300.1	263	Plasmodium falciparum 3D7	Pf3D7_10_v3:412,469..415,059(+)	succinate dehydrogenase subunit 4, putative	protein coding gene	DOWN
PF3D7_1012200	PF3D7_1012200.1	264	Plasmodium falciparum 3D7	Pf3D7_10_v3:470,483..472,274(+)	rhoptry associated adhesin	protein coding gene	DOWN
PF3D7_1012800	PF3D7_1012800.1	265	Plasmodium falciparum 3D7	Pf3D7_10_v3:492,014..496,309(+)	conserved Plasmodium protein, unknown function	protein coding gene	UP
PF3D7_1013800	PF3D7_1013800.1	266	Plasmodium falciparum 3D7	Pf3D7_10_v3:542,175..545,149(+)	conserved Plasmodium protein, unknown function	protein coding gene	DOWN
PF3D7_1014100	PF3D7_1014100.1	267	Plasmodium falciparum 3D7	Pf3D7_10_v3:554,233..560,227(+)	merozoite surface protein MSA180	protein coding gene	DOWN
PF3D7_1017100	PF3D7_1017100.1	268	Plasmodium falciparum 3D7	Pf3D7_10_v3:689,308..692,024(-)	rhoptry neck protein 12	protein coding gene	DOWN
PF3D7_1017500	PF3D7_1017500.1	269	Plasmodium falciparum 3D7	Pf3D7_10_v3:701,258..703,707(+)	myosin essential light chain ELC	protein coding gene	DOWN
PF3D7_1019900	PF3D7_1019900.1	270	Plasmodium falciparum 3D7	Pf3D7_10_v3:808,483..810,465(-)	autophagy-related protein 8	protein coding gene	DOWN
PF3D7_1022700	PF3D7_1022700.1	271	Plasmodium falciparum 3D7	Pf3D7_10_v3:951,189..953,537(-)	phospholipid scramblase	protein coding gene	DOWN
PF3D7_1023000	PF3D7_1023000.1	272	Plasmodium falciparum 3D7	Pf3D7_10_v3:960,653..962,723(-)	conserved Plasmodium protein, unknown function	protein coding gene	DOWN
PF3D7_1023100	PF3D7_1023100.1	273	Plasmodium falciparum 3D7	Pf3D7_10_v3:963,497..980,560(-)	dynein heavy chain, putative	protein coding gene	UP
PF3D7_1023700	PF3D7_1023700.1	274	Plasmodium falciparum 3D7	Pf3D7_10_v3:991,147..993,420(+)	conserved Plasmodium protein, unknown function	protein coding gene	UP
PF3D7_1026600	PF3D7_1026600.1	275	Plasmodium falciparum 3D7	Pf3D7_10_v3:1,113,232..1,119,224(-)	conserved Plasmodium protein, unknown function	protein coding gene	DOWN
PF3D7_1026900	PF3D7_1026900.1	276	Plasmodium falciparum 3D7	Pf3D7_10_v3:1,125,283..1,126,167(+)	biotin--protein ligase 1	protein coding gene	UP
PF3D7_1027300	PF3D7_1027300.1	277	Plasmodium falciparum 3D7	Pf3D7_10_v3:1,139,669..1,144,013(-)	peroxiredoxin	protein coding gene	DOWN
PF3D7_1028600	PF3D7_1028600.1	278	Plasmodium falciparum 3D7	Pf3D7_10_v3:1,176,028..1,177,887(-)	conserved Plasmodium protein, unknown function	protein coding gene	DOWN
PF3D7_1028700	PF3D7_1028700.1	279	Plasmodium falciparum 3D7	Pf3D7_10_v3:1,179,469..1,183,381(+)	merozoite TRAP-like protein	protein coding gene	DOWN
PF3D7_1028900	PF3D7_1028900.1	280	Plasmodium falciparum 3D7	Pf3D7_10_v3:1,184,559..1,186,461(-)	inner membrane complex protein 1m, putative	protein coding gene	DOWN
PF3D7_1029900	PF3D7_1029900.1	281	Plasmodium falciparum 3D7	Pf3D7_10_v3:1,216,830..1,222,661(+)	ORC3 domain-containing protein, putative	protein coding gene	DOWN
PF3D7_1030200	PF3D7_1030200.1	282	Plasmodium falciparum 3D7	Pf3D7_10_v3:1,229,987..1,233,020(-)	claudin-like apicomplexan microneme protein, putative	protein coding gene	DOWN
PF3D7_1035100	PF3D7_1035100.1	283	Plasmodium falciparum 3D7	Pf3D7_10_v3:1,391,390..1,393,405(+)	probable protein, unknown function	protein coding gene	DOWN
PF3D7_1035200	PF3D7_1035200.1	284	Plasmodium falciparum 3D7	Pf3D7_10_v3:1,393,856..1,397,323(+)	S-antigen	protein coding gene	DOWN
PF3D7_1035300	PF3D7_1035300.1	285	Plasmodium falciparum 3D7	Pf3D7_10_v3:1,398,801..1,403,741(+)	glutamate-rich protein GLURP	protein coding gene	DOWN
PF3D7_1035400	PF3D7_1035400.1	286	Plasmodium falciparum 3D7	Pf3D7_10_v3:1,403,807..1,406,234(+)	merozoite surface protein 3	protein coding gene	DOWN
PF3D7_1035500	PF3D7_1035500.1	287	Plasmodium falciparum 3D7	Pf3D7_10_v3:1,406,658..1,409,053(+)	merozoite surface protein 6	protein coding gene	DOWN
PF3D7_1035700	PF3D7_1035700.1	288	Plasmodium falciparum 3D7	Pf3D7_10_v3:1,412,641..1,416,363(+)	duffy binding-like merozoite surface protein	protein coding gene	DOWN
PF3D7_1035900	PF3D7_1035900.1	289	Plasmodium falciparum 3D7	Pf3D7_10_v3:1,423,666..1,425,959(+)	merozoites-associated armadillo repeats protein	protein coding gene	DOWN
PF3D7_1036000	PF3D7_1036000.1	290	Plasmodium falciparum 3D7	Pf3D7_10_v3:1,426,843..1,429,332(+)	merozoite surface protein 11	protein coding gene	DOWN
PF3D7_1036500	PF3D7_1036500.1	291	Plasmodium falciparum 3D7	Pf3D7_10_v3:1,440,686..1,443,875(+)	conserved Plasmodium protein, unknown function	protein coding gene	DOWN
PF3D7_1041300	PF3D7_1041300.1	292	Plasmodium falciparum 3D7	Pf3D7_10_v3:1,642,401..1,649,948(-)	erythrocyte membrane protein 1, PfEMP1	protein coding gene	UP
PF3D7_1100100	PF3D7_1100100.1	293	Plasmodium falciparum 3D7	Pf3D7_11_v3:24,160..31,598(+)	erythrocyte membrane protein 1, PfEMP1	protein coding gene	UP
PF3D7_1100200	PF3D7_1100200.1	294	Plasmodium falciparum 3D7	Pf3D7_11_v3:32,666..42,386(-)	erythrocyte membrane protein 1, PfEMP1	protein coding gene	UP
PF3D7_1102700	PF3D7_1102700.1	295	Plasmodium falciparum 3D7	Pf3D7_11_v3:127,762..130,186(+)	early transcribed membrane protein 11.1	protein coding gene	DOWN
PF3D7_1102800	PF3D7_1102800.1	296	Plasmodium falciparum 3D7	Pf3D7_11_v3:129,265..132,824(-)	early transcribed membrane protein 11.2	protein coding gene	DOWN
PF3D7_1104900	PF3D7_1104900.1	297	Plasmodium falciparum 3D7	Pf3D7_11_v3:212,772..220,288(+)	calcium/calmodulin-dependent protein kinase, putative	protein coding gene	DOWN
PF3D7_1105000	PF3D7_1105000.1	298	Plasmodium falciparum 3D7	Pf3D7_11_v3:219,926..223,878(-)	histone H4	protein coding gene	DOWN

University of Ghana http://ugspace.ug.edu.gh

PF3D7_1105100	PF3D7_1105100.1	299	Plasmodium falciparum 3D7	Pf3D7_11_v3:225,227..226,943(+)	histone H2B	protein coding gene	DOWN
PF3D7_1111000	PF3D7_1111000.1	300	Plasmodium falciparum 3D7	Pf3D7_11_v3:434,474..436,923(+)	RNA cytosine C(5)-methyltransferase NSUN2	protein coding gene	UP
PF3D7_1115800	PF3D7_1115800.1	301	Plasmodium falciparum 3D7	Pf3D7_11_v3:595,116..598,541(-)	conserved Plasmodium protein, unknown function	protein coding gene	DOWN
PF3D7_1116000	PF3D7_1116000.1	302	Plasmodium falciparum 3D7	Pf3D7_11_v3:602,440..607,471(-)	rhoptry neck protein 4	protein coding gene	DOWN
PF3D7_1116600	PF3D7_1116600.1	303	Plasmodium falciparum 3D7	Pf3D7_11_v3:626,070..629,940(-)	dolichyl-diphosphooligosaccharide--protein glycosyltransferase subunit STT3, putative	protein coding gene	DOWN
PF3D7_1116800	PF3D7_1116800.1	304	Plasmodium falciparum 3D7	Pf3D7_11_v3:635,806..641,374(-)	heat shock protein 101	protein coding gene	DOWN
PF3D7_1117400	PF3D7_1117400.1	305	Plasmodium falciparum 3D7	Pf3D7_11_v3:663,535..665,778(+)	conserved Plasmodium protein, unknown function	protein coding gene	DOWN
PF3D7_1118700	PF3D7_1118700.1	306	Plasmodium falciparum 3D7	Pf3D7_11_v3:707,860..713,551(-)	myosin light chain B	protein coding gene	DOWN
PF3D7_1120200	PF3D7_1120200.1	307	Plasmodium falciparum 3D7	Pf3D7_11_v3:764,390..766,081(+)	conserved Plasmodium protein, unknown function	protein coding gene	DOWN
PF3D7_1121300	PF3D7_1121300.1	308	Plasmodium falciparum 3D7	Pf3D7_11_v3:801,809..808,198(-)	tyrosine kinase-like protein	protein coding gene	DOWN
PF3D7_1122700	PF3D7_1122700.1	309	Plasmodium falciparum 3D7	Pf3D7_11_v3:868,275..869,789(-)	conserved Plasmodium protein, unknown function	protein coding gene	DOWN
PF3D7_1122800	PF3D7_1122800.1	310	Plasmodium falciparum 3D7	Pf3D7_11_v3:871,050..877,707(+)	calcium-dependent protein kinase 6	protein coding gene	DOWN
PF3D7_1123900	PF3D7_1123900.1	311	Plasmodium falciparum 3D7	Pf3D7_11_v3:944,850..946,524(+)	13 kDa ribonucleoprotein-associated protein, putative	protein coding gene	DOWN
PF3D7_1125700	PF3D7_1125700.1	312	Plasmodium falciparum 3D7	Pf3D7_11_v3:1,004,021..1,007,682(-)	kelch domain-containing protein, putative	protein coding gene	DOWN
PF3D7_1125800	PF3D7_1125800.1	313	Plasmodium falciparum 3D7	Pf3D7_11_v3:1,007,693..1,011,537(-)	kelch domain-containing protein, putative	protein coding gene	DOWN
PF3D7_1129300	PF3D7_1129300.1	314	Plasmodium falciparum 3D7	Pf3D7_11_v3:1,131,284..1,137,072(-)	conserved Plasmodium protein, unknown function	protein coding gene	DOWN
PF3D7_1133300	PF3D7_1133300.1	315	Plasmodium falciparum 3D7	Pf3D7_11_v3:1,289,824..1,292,127(+)	LEM3/CDC50 family protein, putative	protein coding gene	DOWN
PF3D7_1133400	PF3D7_1133400.1	316	Plasmodium falciparum 3D7	Pf3D7_11_v3:1,292,966..1,296,696(+)	apical membrane antigen 1	protein coding gene	DOWN
PF3D7_1136200	PF3D7_1136200.1	317	Plasmodium falciparum 3D7	Pf3D7_11_v3:1,417,279..1,420,432(-)	conserved Plasmodium protein, unknown function	protein coding gene	DOWN
PF3D7_1137900	PF3D7_1137900.1	318	Plasmodium falciparum 3D7	Pf3D7_11_v3:1,483,375..1,485,858(+)	conserved Plasmodium protein, unknown function	protein coding gene	UP
PF3D7_1139600	PF3D7_1139600.1	319	Plasmodium falciparum 3D7	Pf3D7_11_v3:1,580,594..1,582,483(+)	conserved Plasmodium protein, unknown function	protein coding gene	UP
PF3D7_1140400	PF3D7_1140400.1	320	Plasmodium falciparum 3D7	Pf3D7_11_v3:1,607,519..1,608,723(+)	conserved Plasmodium protein, unknown function	protein coding gene	DOWN
PF3D7_1141800	PF3D7_1141800.1	321	Plasmodium falciparum 3D7	Pf3D7_11_v3:1,672,402..1,675,566(-)	EELM2 domain-containing protein, putative	protein coding gene	DOWN
PF3D7_1144400	PF3D7_1144400.1	322	Plasmodium falciparum 3D7	Pf3D7_11_v3:1,762,256..1,766,650(+)	conserved Plasmodium protein, unknown function	protein coding gene	UP
PF3D7_1200100	PF3D7_1200100.1	323	Plasmodium falciparum 3D7	Pf3D7_12_v3:16,973..24,497(+)	erythrocyte membrane protein 1, PfEMP1	protein coding gene	UP
PF3D7_1200400	PF3D7_1200400.1	324	Plasmodium falciparum 3D7	Pf3D7_12_v3:32,703..41,940(+)	erythrocyte membrane protein 1, PfEMP1	protein coding gene	UP
PF3D7_1200600	PF3D7_1200600.1	325	Plasmodium falciparum 3D7	Pf3D7_12_v3:45,887..58,295(-)	erythrocyte membrane protein 1, PfEMP1	protein coding gene	UP
PF3D7_1202900	PF3D7_1202900.1	326	Plasmodium falciparum 3D7	Pf3D7_12_v3:161,330..163,926(-)	high mobility group protein B1	protein coding gene	DOWN
PF3D7_1204900	PF3D7_1204900.1	327	Plasmodium falciparum 3D7	Pf3D7_12_v3:216,812..219,272(+)	conserved Plasmodium protein, unknown function	protein coding gene	DOWN
PF3D7_1206500	PF3D7_1206500.1	328	Plasmodium falciparum 3D7	Pf3D7_12_v3:292,233..294,941(+)	Tat binding protein 1(TBP-1)-interacting protein, putative	protein coding gene	UP
PF3D7_1207300	PF3D7_1207300.1	329	Plasmodium falciparum 3D7	Pf3D7_12_v3:343,326..344,361(-)	LIMP protein, putative	protein coding gene	UP
PF3D7_1207700	PF3D7_1207700.1	330	Plasmodium falciparum 3D7	Pf3D7_12_v3:351,850..354,006(-)	41-3 protein	protein coding gene	UP
PF3D7_1207800	PF3D7_1207800.1	331	Plasmodium falciparum 3D7	Pf3D7_12_v3:354,195..357,606(-)	conserved Plasmodium protein, unknown function	protein coding gene	UP
PF3D7_1208500	PF3D7_1208500.1	332	Plasmodium falciparum 3D7	Pf3D7_12_v3:395,960..401,562(-)	conserved Plasmodium protein, unknown function	protein coding gene	UP
PF3D7_1213600	PF3D7_1213600.1	333	Plasmodium falciparum 3D7	Pf3D7_12_v3:586,314..587,973(+)	dynein light chain 1, putative	protein coding gene	UP
PF3D7_1217600	PF3D7_1217600.1	334	Plasmodium falciparum 3D7	Pf3D7_12_v3:695,559..696,455(+)	anaphase-promoting complex subunit 10, putative	protein coding gene	UP
PF3D7_1218000	PF3D7_1218000.1	335	Plasmodium falciparum 3D7	Pf3D7_12_v3:703,859..706,124(+)	thrombospondin-related apical membrane protein	protein coding gene	DOWN
PF3D7_1218100	PF3D7_1218100.1	336	Plasmodium falciparum 3D7	Pf3D7_12_v3:706,227..708,196(+)	conserved Plasmodium protein, unknown function	protein coding gene	DOWN
PF3D7_1219400	PF3D7_1219400.1	415	Plasmodium falciparum 3D7	Pf3D7_12_v3:776,510..779,933(-)	erythrocyte membrane protein 1 (PfEMP1), pseudogene	pseudogene	UP
PF3D7_1219700	PF3D7_1219700.1	337	Plasmodium falciparum 3D7	Pf3D7_12_v3:792,877..793,449(-)	raf kinase inhibitor	protein coding gene	UP
PF3D7_1221300	PF3D7_1221300.1	338	Plasmodium falciparum 3D7	Pf3D7_12_v3:850,987..855,507(-)	conserved Plasmodium protein, unknown function	protein coding gene	DOWN
PF3D7_1222700	PF3D7_1222700.1	339	Plasmodium falciparum 3D7	Pf3D7_12_v3:918,280..920,560(+)	glideosome-associated protein 45	protein coding gene	DOWN
PF3D7_1223100	PF3D7_1223100.1	340	Plasmodium falciparum 3D7	Pf3D7_12_v3:927,063..930,026(-)	cAMP-dependent protein kinase regulatory subunit	protein coding gene	DOWN
PF3D7_1224100	PF3D7_1224100.1	341	Plasmodium falciparum 3D7	Pf3D7_12_v3:975,744..979,052(-)	conserved protein, unknown function	protein coding gene	DOWN
PF3D7_1228600	PF3D7_1228600.1	342	Plasmodium falciparum 3D7	Pf3D7_12_v3:1,160,654..1,163,264(-)	merozoite surface protein 9	protein coding gene	DOWN

University of Ghana http://ugspace.ug.edu.gh

PF3D7_1229800	PF3D7_1229800.1	343	Plasmodium falciparum 3D7	Pf3D7_12_v3:1,218,464..1,227,615(-)	myosin J, putative	protein coding gene	DOWN
PF3D7_1232500	PF3D7_1232500.1	344	Plasmodium falciparum 3D7	Pf3D7_12_v3:1,339,320..1,343,378(-)	CG2-related protein, putative	protein coding gene	DOWN
PF3D7_1237700	PF3D7_1237700.1	345	Plasmodium falciparum 3D7	Pf3D7_12_v3:1,571,678..1,574,455(+)	conserved protein, unknown function	protein coding gene	DOWN
PF3D7_1238900	PF3D7_1238900.1	346	Plasmodium falciparum 3D7	Pf3D7_12_v3:1,612,601..1,618,965(-)	protein kinase 2	protein coding gene	DOWN
PF3D7_1240100	PF3D7_1240100.1	347	Plasmodium falciparum 3D7	Pf3D7_12_v3:1,684,977..1,686,307(-)	early transcribed membrane protein 12	protein coding gene	DOWN
PF3D7_1240300	PF3D7_1240300.1	348	Plasmodium falciparum 3D7	Pf3D7_12_v3:1,694,150..1,703,087(+)	erythrocyte membrane protein 1, PfEMP1	protein coding gene	UP
PF3D7_1240600	PF3D7_1240600.1	349	Plasmodium falciparum 3D7	Pf3D7_12_v3:1,719,574..1,727,456(+)	erythrocyte membrane protein 1, PfEMP1	protein coding gene	UP
PF3D7_1240700	PF3D7_1240700.1	416	Plasmodium falciparum 3D7	Pf3D7_12_v3:1,728,774..1,730,007(+)	rifin, pseudogene	pseudogene	UP
PF3D7_1240900	PF3D7_1240900.1	350	Plasmodium falciparum 3D7	Pf3D7_12_v3:1,734,992..1,744,191(+)	erythrocyte membrane protein 1, PfEMP1	protein coding gene	UP
PF3D7_1243400	PF3D7_1243400.1	351	Plasmodium falciparum 3D7	Pf3D7_12_v3:1,818,146..1,820,497(+)	conserved Plasmodium protein, unknown function	protein coding gene	DOWN
PF3D7_1245300	PF3D7_1245300.1	352	Plasmodium falciparum 3D7	Pf3D7_12_v3:1,892,918..1,894,243(+)	NEDD8-conjugating enzyme UBC12, putative	protein coding gene	UP
PF3D7_1245600	PF3D7_1245600.1	353	Plasmodium falciparum 3D7	Pf3D7_12_v3:1,900,249..1,905,066(-)	kinesin-15, putative	protein coding gene	UP
PF3D7_1246200	PF3D7_1246200.1	354	Plasmodium falciparum 3D7	Pf3D7_12_v3:1,919,898..1,923,323(+)	actin I	protein coding gene	DOWN
PF3D7_1246300	PF3D7_1246300.1	355	Plasmodium falciparum 3D7	Pf3D7_12_v3:1,925,058..1,929,618(+)	protein KIC4	protein coding gene	DOWN
PF3D7_1246400	PF3D7_1246400.1	356	Plasmodium falciparum 3D7	Pf3D7_12_v3:1,931,257..1,933,545(+)	myosin A-tail interacting protein	protein coding gene	DOWN
PF3D7_1250400	PF3D7_1250400.1	357	Plasmodium falciparum 3D7	Pf3D7_12_v3:2,067,229..2,069,794(+)	conserved Plasmodium protein, unknown function	protein coding gene	UP
PF3D7_1251200	PF3D7_1251200.1	358	Plasmodium falciparum 3D7	Pf3D7_12_v3:2,091,731..2,094,720(+)	coronin	protein coding gene	DOWN
PF3D7_1252100	PF3D7_1252100.1	359	Plasmodium falciparum 3D7	Pf3D7_12_v3:2,113,980..2,123,174(-)	rhoptry neck protein 3	protein coding gene	DOWN
PF3D7_1253700	PF3D7_1253700.1	360	Plasmodium falciparum 3D7	Pf3D7_12_v3:2,190,483..2,191,770(-)	rifin	protein coding gene	UP
PF3D7_1300100	PF3D7_1300100.1	147	Plasmodium falciparum 3D7	Pf3D7_13_v3:21,364..28,787(+)	erythrocyte membrane protein 1, PfEMP1	protein coding gene	UP
PF3D7_1300300	PF3D7_1300300.1	148	Plasmodium falciparum 3D7	Pf3D7_13_v3:33,358..45,388(-)	erythrocyte membrane protein 1, PfEMP1	protein coding gene	UP
PF3D7_1301600	PF3D7_1301600.1	151	Plasmodium falciparum 3D7	Pf3D7_13_v3:88,139..93,987(-)	erythrocyte binding antigen-140	protein coding gene	DOWN
PF3D7_1307500	PF3D7_1307500.1	149	Plasmodium falciparum 3D7	Pf3D7_13_v3:337,467..339,281(-)	conserved Plasmodium protein, unknown function	protein coding gene	DOWN
PF3D7_1308000	PF3D7_1308000.1	214	Plasmodium falciparum 3D7	Pf3D7_13_v3:355,912..359,788(+)	conserved Plasmodium membrane protein, unknown function	protein coding gene	DOWN
PF3D7_1310200	PF3D7_1310200.1	215	Plasmodium falciparum 3D7	Pf3D7_13_v3:453,771..455,266(+)	conserved Plasmodium protein, unknown function	protein coding gene	DOWN
PF3D7_1310700	PF3D7_1310700.1	150	Plasmodium falciparum 3D7	Pf3D7_13_v3:467,319..469,389(-)	PhIL1-interacting candidate PIC5	protein coding gene	DOWN
PF3D7_1314100	PF3D7_1314100.1	152	Plasmodium falciparum 3D7	Pf3D7_13_v3:606,945..610,544(+)	conserved Plasmodium protein, unknown function	protein coding gene	UP
PF3D7_1318000	PF3D7_1318000.1	153	Plasmodium falciparum 3D7	Pf3D7_13_v3:745,720..747,765(-)	conserved protein, unknown function	protein coding gene	DOWN
PF3D7_1320100	PF3D7_1320100.1	154	Plasmodium falciparum 3D7	Pf3D7_13_v3:833,359..835,735(-)	ATP-dependent Clp protease adapter protein ClpS	protein coding gene	DOWN
PF3D7_1323700	PF3D7_1323700.1	155	Plasmodium falciparum 3D7	Pf3D7_13_v3:981,651..984,211(+)	glideosome associated protein with multiple membrane spans 1	protein coding gene	DOWN
PF3D7_1327500	PF3D7_1327500.1	216	Plasmodium falciparum 3D7	Pf3D7_13_v3:1,154,684..1,158,545(+)	conserved protein, unknown function	protein coding gene	DOWN
PF3D7_1328300	PF3D7_1328300.1	156	Plasmodium falciparum 3D7	Pf3D7_13_v3:1,195,364..1,199,554(-)	conserved protein, unknown function	protein coding gene	DOWN
PF3D7_1330100	PF3D7_1330100.1	157	Plasmodium falciparum 3D7	Pf3D7_13_v3:1,274,448..1,275,008(+)	conserved Plasmodium protein, unknown function	protein coding gene	DOWN
PF3D7_1331000	PF3D7_1331000.1	158	Plasmodium falciparum 3D7	Pf3D7_13_v3:1,297,070..1,299,355(-)	protein kinase, putative	protein coding gene	DOWN
PF3D7_1332200	PF3D7_1332200.1	159	Plasmodium falciparum 3D7	Pf3D7_13_v3:1,332,221..1,335,647(+)	conserved protein, unknown function	protein coding gene	DOWN
PF3D7_1332500	PF3D7_1332500.1	160	Plasmodium falciparum 3D7	Pf3D7_13_v3:1,340,768..1,341,856(+)	SAM-dependent RNA methyltransferase, putative	protein coding gene	UP
PF3D7_1335100	PF3D7_1335100.1	161	Plasmodium falciparum 3D7	Pf3D7_13_v3:1,418,213..1,421,552(-)	merozoite surface protein 7	protein coding gene	DOWN
PF3D7_1335300	PF3D7_1335300.1	217	Plasmodium falciparum 3D7	Pf3D7_13_v3:1,428,350..1,439,462(-)	reticulocyte binding protein 2 homologue b	protein coding gene	DOWN
PF3D7_1335400	PF3D7_1335400.1	162	Plasmodium falciparum 3D7	Pf3D7_13_v3:1,440,169..1,451,101(+)	reticulocyte binding protein 2 homologue a	protein coding gene	DOWN
PF3D7_1342600	PF3D7_1342600.1	163	Plasmodium falciparum 3D7	Pf3D7_13_v3:1,673,239..1,677,299(+)	myosin A	protein coding gene	DOWN
PF3D7_1342700	PF3D7_1342700.1	164	Plasmodium falciparum 3D7	Pf3D7_13_v3:1,677,300..1,678,286(-)	DNA-directed RNA polymerases I, II, and III subunit RPABC4, putative	protein coding gene	UP
PF3D7_1343000	PF3D7_1343000.1	165	Plasmodium falciparum 3D7	Pf3D7_13_v3:1,695,462..1,699,267(+)	phosphoethanolamine N-methyltransferase	protein coding gene	DOWN
PF3D7_1343100	PF3D7_1343100.1	166	Plasmodium falciparum 3D7	Pf3D7_13_v3:1,699,588..1,702,492(-)	conserved Plasmodium protein, unknown function	protein coding gene	DOWN
PF3D7_1343200	PF3D7_1343200.1	167	Plasmodium falciparum 3D7	Pf3D7_13_v3:1,703,564..1,707,279(+)	tRNA guanosine-2'-O-methyltransferase, putative	protein coding gene	DOWN
PF3D7_1344300	PF3D7_1344300.1	218	Plasmodium falciparum 3D7	Pf3D7_13_v3:1,773,639..1,781,932(-)	zinc finger protein, putative	protein coding gene	DOWN

University of Ghana http://ugspace.ug.edu.gh

PF3D7_1348600	PF3D7_1348600.1	168	Plasmodium falciparum 3D7	Pf3D7_13_v3:1,952,854..1,954,954(+)	conserved Plasmodium protein, unknown function	protein coding gene	DOWN
PF3D7_1351700	PF3D7_1351700.1	169	Plasmodium falciparum 3D7	Pf3D7_13_v3:2,058,839..2,064,747(+)	inner membrane complex protein 1f, putative	protein coding gene	DOWN
PF3D7_1356300	PF3D7_1356300.1	170	Plasmodium falciparum 3D7	Pf3D7_13_v3:2,231,116..2,233,675(+)	ubiquitin-conjugating enzyme E2, putative	protein coding gene	DOWN
PF3D7_1356900	PF3D7_1356900.1	171	Plasmodium falciparum 3D7	Pf3D7_13_v3:2,262,738..2,265,705(-)	protein kinase 5	protein coding gene	UP
PF3D7_1360500	PF3D7_1360500.1	172	Plasmodium falciparum 3D7	Pf3D7_13_v3:2,413,324..2,425,261(+)	guanylyl cyclase beta	protein coding gene	UP
PF3D7_1361400	PF3D7_1361400.1	173	Plasmodium falciparum 3D7	Pf3D7_13_v3:2,463,755..2,464,745(-)	actin-depolymerizing factor 2	protein coding gene	DOWN
PF3D7_1361500	PF3D7_1361500.1	219	Plasmodium falciparum 3D7	Pf3D7_13_v3:2,464,790..2,468,539(-)	PH domain-containing protein, putative	protein coding gene	DOWN
PF3D7_1361500	PF3D7_1361500.2	219	Plasmodium falciparum 3D7	Pf3D7_13_v3:2,464,790..2,468,539(-)	PH domain-containing protein, putative	protein coding gene	DOWN
PF3D7_1361800	PF3D7_1361800.1	220	Plasmodium falciparum 3D7	Pf3D7_13_v3:2,473,498..2,482,244(+)	glideosome-associated connector	protein coding gene	DOWN
PF3D7_1367300	PF3D7_1367300.1	174	Plasmodium falciparum 3D7	Pf3D7_13_v3:2,685,059..2,686,331(-)	conserved Plasmodium protein, unknown function	protein coding gene	UP
PF3D7_1369300	PF3D7_1369300.1	175	Plasmodium falciparum 3D7	Pf3D7_13_v3:2,755,662..2,758,407(-)	conserved Plasmodium protein, unknown function	protein coding gene	UP
PF3D7_1369400	PF3D7_1369400.1	221	Plasmodium falciparum 3D7	Pf3D7_13_v3:2,759,048..2,768,913(+)	conserved Plasmodium protein, unknown function	protein coding gene	UP
PF3D7_1371600	PF3D7_1371600.1	417	Plasmodium falciparum 3D7	Pf3D7_13_v3:2,811,706..2,820,270(+)	erythrocyte binding like protein 1, pseudogene	pseudogene	DOWN
PF3D7_1371900	PF3D7_1371900.1	222	Plasmodium falciparum 3D7	Pf3D7_13_v3:2,829,530..2,830,830(+)	Plasmodium exported protein, unknown function	protein coding gene	UP
PF3D7_1372100	PF3D7_1372100.1	223	Plasmodium falciparum 3D7	Pf3D7_13_v3:2,835,756..2,839,580(+)	Plasmodium exported protein (PHISTb), unknown function	protein coding gene	UP
PF3D7_1372500	PF3D7_1372500.1	418	Plasmodium falciparum 3D7	Pf3D7_13_v3:2,854,544..2,855,568(-)	stevor, pseudogene	pseudogene	DOWN
PF3D7_1372600	PF3D7_1372600.1	224	Plasmodium falciparum 3D7	Pf3D7_13_v3:2,856,586..2,858,026(+)	rifin	protein coding gene	DOWN
PF3D7_1373300	PF3D7_1373300.1	225	Plasmodium falciparum 3D7	Pf3D7_13_v3:2,877,908..2,879,141(+)	rifin	protein coding gene	UP
PF3D7_1373500	PF3D7_1373500.1	176	Plasmodium falciparum 3D7	Pf3D7_13_v3:2,884,786..2,892,340(-)	erythrocyte membrane protein 1, PfEMP1	protein coding gene	UP
PF3D7_1401400	PF3D7_1401400.1	361	Plasmodium falciparum 3D7	Pf3D7_14_v3:52,256..54,457(-)	early transcribed membrane protein 14.1	protein coding gene	DOWN
PF3D7_1401600	PF3D7_1401600.1	362	Plasmodium falciparum 3D7	Pf3D7_14_v3:60,100..64,491(-)	Plasmodium exported protein (PHISTb), unknown function	protein coding gene	DOWN
PF3D7_1403200	PF3D7_1403200.1	363	Plasmodium falciparum 3D7	Pf3D7_14_v3:119,995..121,405(-)	EGF domain-containing protein, putative	protein coding gene	UP
PF3D7_1406300	PF3D7_1406300.1	364	Plasmodium falciparum 3D7	Pf3D7_14_v3:227,948..230,574(+)	glycerophosphodiester phosphodiesterase	protein coding gene	DOWN
PF3D7_1407200	PF3D7_1407200.1	365	Plasmodium falciparum 3D7	Pf3D7_14_v3:260,615..262,717(-)	conserved Plasmodium protein, unknown function	protein coding gene	DOWN
PF3D7_1408800	PF3D7_1408800.1	366	Plasmodium falciparum 3D7	Pf3D7_14_v3:348,831..350,857(+)	conserved Plasmodium protein, unknown function	protein coding gene	UP
PF3D7_1409400	PF3D7_1409400.1	367	Plasmodium falciparum 3D7	Pf3D7_14_v3:365,269..367,978(-)	conserved protein, unknown function	protein coding gene	DOWN
PF3D7_1410400	PF3D7_1410400.1	368	Plasmodium falciparum 3D7	Pf3D7_14_v3:419,442..423,481(+)	rhoptry-associated protein 1	protein coding gene	DOWN
PF3D7_1411200	PF3D7_1411200.1	369	Plasmodium falciparum 3D7	Pf3D7_14_v3:451,761..456,500(-)	rhomboid protease ROM8	protein coding gene	DOWN
PF3D7_1412000	PF3D7_1412000.1	370	Plasmodium falciparum 3D7	Pf3D7_14_v3:482,070..484,006(+)	p1/s1 nuclease, putative	protein coding gene	DOWN
PF3D7_1413000	PF3D7_1413000.1	371	Plasmodium falciparum 3D7	Pf3D7_14_v3:523,890..525,305(-)	conserved Plasmodium protein, unknown function	protein coding gene	UP
PF3D7_1413700	PF3D7_1413700.1	372	Plasmodium falciparum 3D7	Pf3D7_14_v3:540,168..546,533(-)	DET1 domain-containing protein, putative	protein coding gene	DOWN
PF3D7_1416700	PF3D7_1416700.1	373	Plasmodium falciparum 3D7	Pf3D7_14_v3:680,612..682,264(-)	conserved protein, unknown function	protein coding gene	UP
PF3D7_1420100	PF3D7_1420100.1	374	Plasmodium falciparum 3D7	Pf3D7_14_v3:831,758..837,178(-)	conserved Plasmodium protein, unknown function	protein coding gene	UP
PF3D7_1423300	PF3D7_1423300.1	375	Plasmodium falciparum 3D7	Pf3D7_14_v3:935,849..941,730(+)	serine/threonine protein phosphatase 7	protein coding gene	DOWN
PF3D7_1431400	PF3D7_1431400.1	376	Plasmodium falciparum 3D7	Pf3D7_14_v3:1,232,648..1,237,614(-)	surface-related antigen SRA	protein coding gene	DOWN
PF3D7_1433700	PF3D7_1433700.1	377	Plasmodium falciparum 3D7	Pf3D7_14_v3:1,341,313..1,349,600(-)	conserved Plasmodium protein, unknown function	protein coding gene	DOWN
PF3D7_1434400	PF3D7_1434400.1	378	Plasmodium falciparum 3D7	Pf3D7_14_v3:1,375,352..1,377,636(-)	conserved protein, unknown function	protein coding gene	DOWN
PF3D7_1437300	PF3D7_1437300.1	379	Plasmodium falciparum 3D7	Pf3D7_14_v3:1,513,414..1,515,796(-)	conserved Plasmodium protein, unknown function	protein coding gene	DOWN
PF3D7_1439500	PF3D7_1439500.1	380	Plasmodium falciparum 3D7	Pf3D7_14_v3:1,606,643..1,611,876(+)	oocyst rupture protein 2, putative	protein coding gene	DOWN
PF3D7_1440900	PF3D7_1440900.1	381	Plasmodium falciparum 3D7	Pf3D7_14_v3:1,668,319..1,670,272(+)	conserved Plasmodium protein, unknown function	protein coding gene	DOWN
PF3D7_1442600	PF3D7_1442600.1	382	Plasmodium falciparum 3D7	Pf3D7_14_v3:1,730,087..1,740,916(+)	TRAP-like protein	protein coding gene	UP
PF3D7_1444800	PF3D7_1444800.1	383	Plasmodium falciparum 3D7	Pf3D7_14_v3:1,843,368..1,846,989(-)	fructose-bisphosphate aldolase	protein coding gene	DOWN
PF3D7_1448000	PF3D7_1448000.1	384	Plasmodium falciparum 3D7	Pf3D7_14_v3:1,959,368..1,964,665(-)	U3 small nucleolar RNA-associated protein 12, putative	protein coding gene	UP
PF3D7_1449200	PF3D7_1449200.1	385	Plasmodium falciparum 3D7	Pf3D7_14_v3:2,013,486..2,015,102(+)	conserved Plasmodium protein, unknown function	protein coding gene	DOWN
PF3D7_1452000	PF3D7_1452000.1	386	Plasmodium falciparum 3D7	Pf3D7_14_v3:2,133,266..2,141,180(+)	rhoptry neck protein 2	protein coding gene	DOWN

University of Ghana http://ugspace.ug.edu.gh

PF3D7_1455300	PF3D7_1455300.1	387	Plasmodium falciparum 3D7	Pf3D7_14_v3:2,258,680..2,262,632(+)	conserved protein, unknown function	protein coding gene	DOWN
PF3D7_1456400	PF3D7_1456400.1	388	Plasmodium falciparum 3D7	Pf3D7_14_v3:2,309,181..2,312,472(-)	conserved Plasmodium protein, unknown function	protein coding gene	UP
PF3D7_1459100	PF3D7_1459100.1	389	Plasmodium falciparum 3D7	Pf3D7_14_v3:2,423,624..2,426,573(+)	GTP-binding protein, putative	protein coding gene	UP
PF3D7_1460600	PF3D7_1460600.1	390	Plasmodium falciparum 3D7	Pf3D7_14_v3:2,473,732..2,475,410(+)	inner membrane complex sub-compartment protein 3	protein coding gene	DOWN
PF3D7_1461800	PF3D7_1461800.1	391	Plasmodium falciparum 3D7	Pf3D7_14_v3:2,503,209..2,514,031(+)	conserved Plasmodium protein, unknown function	protein coding gene	UP
PF3D7_1463900	PF3D7_1463900.1	392	Plasmodium falciparum 3D7	Pf3D7_14_v3:2,584,086..2,590,847(-)	rhoptry neck protein 11, putative	protein coding gene	DOWN
PF3D7_1467700	PF3D7_1467700.1	393	Plasmodium falciparum 3D7	Pf3D7_14_v3:2,765,528..2,766,792(+)	conserved Plasmodium protein, unknown function	protein coding gene	DOWN
PF3D7_1468400	PF3D7_1468400.1	394	Plasmodium falciparum 3D7	Pf3D7_14_v3:2,809,460..2,812,520(+)	zinc finger protein, putative	protein coding gene	DOWN
PF3D7_1469200	PF3D7_1469200.1	395	Plasmodium falciparum 3D7	Pf3D7_14_v3:2,838,446..2,840,316(-)	shewanella-like protein phosphatase 1, putative	protein coding gene	DOWN
PF3D7_1470400	PF3D7_1470400.1	396	Plasmodium falciparum 3D7	Pf3D7_14_v3:2,879,948..2,881,746(+)	mitochondrial pyruvate carrier protein 2, putative	protein coding gene	DOWN
PF3D7_1471600	PF3D7_1471600.1	397	Plasmodium falciparum 3D7	Pf3D7_14_v3:2,925,721..2,929,673(+)	apical polar ring protein APR2, putative	protein coding gene	UP
PF3D7_1471700	PF3D7_1471700.1	398	Plasmodium falciparum 3D7	Pf3D7_14_v3:2,929,823..2,931,547(+)	conserved Plasmodium protein, unknown function	protein coding gene	UP
PF3D7_1471800	PF3D7_1471800.1	399	Plasmodium falciparum 3D7	Pf3D7_14_v3:2,931,759..2,932,950(+)	conserved Plasmodium protein, unknown function	protein coding gene	UP
PF3D7_1475400	PF3D7_1475400.1	400	Plasmodium falciparum 3D7	Pf3D7_14_v3:3,087,061..3,105,071(-)	cysteine repeat modular protein 4	protein coding gene	UP
PF3D7_1475800	PF3D7_1475800.1	401	Plasmodium falciparum 3D7	Pf3D7_14_v3:3,120,854..3,121,849(+)	conserved Plasmodium protein, unknown function	protein coding gene	UP
PF3D7_1475900	PF3D7_1475900.1	402	Plasmodium falciparum 3D7	Pf3D7_14_v3:3,124,298..3,126,709(+)	KELT protein	protein coding gene	UP
PF3D7_1476300	PF3D7_1476300.1	403	Plasmodium falciparum 3D7	Pf3D7_14_v3:3,137,437..3,142,012(+)	Plasmodium exported protein (PHISTb), unknown function	protein coding gene	DOWN
PF3D7_1478400	PF3D7_1478400.1	419	Plasmodium falciparum 3D7	Pf3D7_14_v3:3,223,288..3,224,632(-)	Plasmodium exported protein, unknown function, pseudogene	pseudogene	UP

University of Ghana http://ugspace.ug.edu.gh

Supplementary Table 5.15 Gene ontology enrichment analysis for up/down-regulated genes between C580R untreated and DHA_treated condition

University of Ghana http://ugspace.ug.edu.gh

Gene ontology term	Differential expression	ID	Name	Bgl count	Result count	Result gene list	Pct of bgd	Fold enrichment	Odds ratio	P-value	Benjamini	Bonferroni
Biological process	Upregulated	GO:0009405	obsolete pathogenesis	75	43	PF3D7_0100100,PF3D7_0115700,PF3D7_0300100,PF3D7_0324900,PF3D7_0400100,PF3D7_0400400,PF3D7_0412400,PF3D7_0420700,PF3D7_0421100,PF3D7_0425800,PF3D7_0600200,PF3D7_0617400,PF3D7_0632500,PF3D7_0632800,PF3D7_0711700,PF3D7_0712000,PF3D7_0712300,PF3D7_0712400,PF3D7_0712600,PF3D7_0712800,PF3D7_0712900,PF3D7_0800200,PF3D7_0800300,PF3D7_0808600,PF3D7_0808700,PF3D7_0809100,PF3D7_0833500,PF3D7_0900100,PF3D7_0936500,PF3D7_0937800,PF3D7_1000100,PF3D7_1041300,PF3D7_1100100,PF3D7_1100200,PF3D7_1200100,PF3D7_1200400,PF3D7_1200600,PF3D7_1240300,PF3D7_1240600,PF3D7_1240900,PF3D7_1300100,PF3D7_1300300,PF3D7_1373500,	57.3	23.26	82.3	1.45E-52	1.99E-50	1.99E-50
		GO:0098609	cell-cell adhesion	62	36	PF3D7_0100100,PF3D7_0115700,PF3D7_0400100,PF3D7_0400400,PF3D7_0412400,PF3D7_0420700,PF3D7_0421100,PF3D7_0425800,PF3D7_0600200,PF3D7_0617400,PF3D7_0632500,PF3D7_0632800,PF3D7_0711700,PF3D7_0712000,PF3D7_0712300,PF3D7_0712400,PF3D7_0712600,PF3D7_0712800,PF3D7_0712900,PF3D7_0800200,PF3D7_0800300,PF3D7_0808600,PF3D7_0808700,PF3D7_0809100,PF3D7_0900100,PF3D7_0937800,PF3D7_1000100,PF3D7_1041300,PF3D7_1100100,PF3D7_1100200,PF3D7_1200100,PF3D7_1200400,PF3D7_1200600,PF3D7_1240300,PF3D7_1240600,PF3D7_1300300,	58.1	23.55	77.84	5.56E-44	3.81E-42	7.62E-42
		GO:0007155	cell adhesion	70	36	PF3D7_0100100,PF3D7_0115700,PF3D7_0400100,PF3D7_0400400,PF3D7_0412400,PF3D7_0420700,PF3D7_0421100,PF3D7_0425800,PF3D7_0600200,PF3D7_0617400,PF3D7_0632500,PF3D7_0632800,PF3D7_0711700,PF3D7_0712000,PF3D7_0712300,PF3D7_0712400,PF3D7_0712600,PF3D7_0712800,PF3D7_0712900,PF3D7_0800200,PF3D7_0800300,PF3D7_0808600,PF3D7_0808700,PF3D7_0809100,PF3D7_0900100,PF3D7_0937800,PF3D7_1000100,PF3D7_1041300,PF3D7_1100100,PF3D7_1100200,PF3D7_1200100,PF3D7_1200400,PF3D7_1200600,PF3D7_1240300,PF3D7_1240600,PF3D7_1300300,	51.4	20.86	59.42	2.52E-41	1.15E-39	3.46E-39
		GO:0020035	cytoadherence to microvasculature, mediated by symbiont protein	176	42	PF3D7_0100100,PF3D7_0115700,PF3D7_0324800,PF3D7_0400100,PF3D7_0400400,PF3D7_0412400,PF3D7_0413200,PF3D7_0420700,PF3D7_0421100,PF3D7_0425800,PF3D7_0600200,PF3D7_0617400,PF3D7_0632500,PF3D7_0632800,PF3D7_0711700,PF3D7_0712000,PF3D7_0712300,PF3D7_0712400,PF3D7_0712600,PF3D7_0712800,PF3D7_0712900,PF3D7_0713000,PF3D7_0800200,PF3D7_0800300,PF3D7_0808600,PF3D7_0808700,PF3D7_0809100,PF3D7_0833000,PF3D7_0937300,PF3D7_0937800,PF3D7_1000100,PF3D7_1000500,PF3D7_1041300,PF3D7_1100100,PF3D7_1100200,PF3D7_1200100,PF3D7_1200400,PF3D7_1200600,PF3D7_1240300,PF3D7_1240600,PF3D7_1253700,PF3D7_1300300,	23.9	9.68	18.54	7.78E-32	2.13E-30	1.07E-29

		GO: 0044406	adhesion of symbiont to host	176	42	PF3D7_0100100,PF3D7_0115700,PF3D7_0324800,PF3D7_0400100,PF3D7_0400400,PF3D7_0412400,PF3D7_0413200,PF3D7_0420700,PF3D7_0421100,PF3D7_0425800,PF3D7_0600200,PF3D7_0617400,PF3D7_0632500,PF3D7_0632800,PF3D7_0711700,PF3D7_0712000,PF3D7_0712300,PF3D7_0712400,PF3D7_0712600,PF3D7_0712800,PF3D7_0712900,PF3D7_0713000,PF3D7_0800200,PF3D7_0800300,PF3D7_0808600,PF3D7_0808700,PF3D7_0809100,PF3D7_0833000,PF3D7_0937300,PF3D7_0937800,PF3D7_1000100,PF3D7_1000500,PF3D7_1041300,PF3D7_1100100,PF3D7_1100200,PF3D7_1200100,PF3D7_1200400,PF3D7_1200600,PF3D7_1240300,PF3D7_1240600,PF3D7_1253700,PF3D7_1300300,	23.9	9.68	18.54	7.78E-32	2.13E-30	1.07E-29
		GO: 0020033	antigenic variation	202	44	PF3D7_0100100,PF3D7_0114700,PF3D7_0115700,PF3D7_0324800,PF3D7_0400100,PF3D7_0400400,PF3D7_0412400,PF3D7_0413200,PF3D7_0420700,PF3D7_0421100,PF3D7_0425800,PF3D7_0600200,PF3D7_0617400,PF3D7_0631800,PF3D7_0632500,PF3D7_0632800,PF3D7_0711700,PF3D7_0712000,PF3D7_0712300,PF3D7_0712400,PF3D7_0712600,PF3D7_0712800,PF3D7_0712900,PF3D7_0713000,PF3D7_0800200,PF3D7_0800300,PF3D7_0808600,PF3D7_0808700,PF3D7_0809100,PF3D7_0833000,PF3D7_0937300,PF3D7_0937800,PF3D7_1000100,PF3D7_1000500,PF3D7_1041300,PF3D7_1100100,PF3D7_1100200,PF3D7_1200100,PF3D7_1200400,PF3D7_1200600,PF3D7_1240300,PF3D7_1240600,PF3D7_1253700,PF3D7_1300300,	21.8	8.84	16.82	1.32E-31	2.69E-30	1.81E-29
		GO: 0020013	modulation by symbiont of host erythrocyte aggregation	190	43	PF3D7_0100100,PF3D7_0115700,PF3D7_0324800,PF3D7_0400100,PF3D7_0400400,PF3D7_0402600,PF3D7_0412400,PF3D7_0413200,PF3D7_0420700,PF3D7_0421100,PF3D7_0425800,PF3D7_0600200,PF3D7_0617400,PF3D7_0632500,PF3D7_0632800,PF3D7_0711700,PF3D7_0712000,PF3D7_0712300,PF3D7_0712400,PF3D7_0712600,PF3D7_0712800,PF3D7_0712900,PF3D7_0713000,PF3D7_0800200,PF3D7_0800300,PF3D7_0808600,PF3D7_0808700,PF3D7_0809100,PF3D7_0833000,PF3D7_0937300,PF3D7_0937800,PF3D7_1000100,PF3D7_1000500,PF3D7_1041300,PF3D7_1100100,PF3D7_1100200,PF3D7_1200100,PF3D7_1200400,PF3D7_1200600,PF3D7_1240300,PF3D7_1240600,PF3D7_1253700,PF3D7_1300300,	22.6	9.18	17.48	1.37E-31	2.69E-30	1.88E-29
		GO: 0044068	modulation by symbiont of host cellular process	192	43	PF3D7_0100100,PF3D7_0115700,PF3D7_0324800,PF3D7_0400100,PF3D7_0400400,PF3D7_0402600,PF3D7_0412400,PF3D7_0413200,PF3D7_0420700,PF3D7_0421100,PF3D7_0425800,PF3D7_0600200,PF3D7_0617400,PF3D7_0632500,PF3D7_0632800,PF3D7_0711700,PF3D7_0712000,PF3D7_0712300,PF3D7_0712400,PF3D7_0712600,PF3D7_0712800,PF3D7_0712900,PF3D7_0713000,PF3D7_0800200,PF3D7_0800300,PF3D7_0808600,PF3D7_0808700,PF3D7_0809100,PF3D7_0833000,PF3D7_0937300,PF3D7_0937800,PF3D7_1000100,PF3D7_1000500,PF3D7_1041300,PF3D7_1100100,PF3D7_1100200,PF3D7_1200100,PF3D7_1200400,PF3D7_1200600,PF3D7_1240300,PF3D7_1240600,PF3D7_1253700,PF3D7_1300300,	22.4	9.09	17.24	2.21E-31	3.58E-30	3.03E-29
		GO: 0042783	evasion of host immune response	205	44	PF3D7_0100100,PF3D7_0114700,PF3D7_0115700,PF3D7_0324800,PF3D7_0400100,PF3D7_0400400,PF3D7_0412400,PF3D7_0413200,PF3D7_0420700,PF3D7_0421100,PF3D7_0425800,PF3D7_0600200,PF3D7_0617400,PF3D7_0631800,PF3D7_0632500,PF3D7_0632800,PF3D7_0711700,PF3D7_0712000,PF3D7_0712300,PF3D7_0712400,PF3D7_0712600,PF3D7_0712800,PF3D7_0712900,PF3D7_0713000,PF3D7_0800200,PF3D7_0800300,PF3D7_0808600,PF3D7_0808700,PF3D7_0809100,PF3D7_0833000,PF3D7_0937300,PF3D7_0937800,PF3D7_1000100,PF3D7_1000500,PF3D7_1041300,PF3D7_1100100,PF3D7_1100200,PF3D7_1200100,PF3D7_1200400,PF3D7_1200600,PF3D7_1240300,PF3D7_1240600,PF3D7_1253700,PF3D7_1300300,	21.5	8.71	16.49	2.62E-31	3.58E-30	3.58E-29

University of Ghana http://ugspace.ug.edu.gh

		GO: 0044003	modulation by symbiont of host process	205	44	PF3D7_0100100,PF3D7_0115700,PF3D7_0324800,PF3D7_0400100,PF3D7_0400400,PF3D7_0402600,PF3D7_0412400,PF3D7_0413200,PF3D7_0420700,PF3D7_0421100,PF3D7_0425800,PF3D7_0600200,PF3D7_0617400,PF3D7_0632500,PF3D7_0632800,PF3D7_0711700,PF3D7_0712000,PF3D7_0712300,PF3D7_0712400,PF3D7_0712600,PF3D7_0712800,PF3D7_0712900,PF3D7_0713000,PF3D7_0726200,PF3D7_0800200,PF3D7_0800300,PF3D7_0808600,PF3D7_0808700,PF3D7_0809100,PF3D7_0833000,PF3D7_0937300,PF3D7_0937800,PF3D7_1000100,PF3D7_1000500,PF3D7_1041300,PF3D7_1100100,PF3D7_1100200,PF3D7_1200100,PF3D7_1200400,PF3D7_1200600,PF3D7_1240300,PF3D7_1240600,PF3D7_1253700,PF3D7_1300300,	21.5	8.71	16.49	2.62E-31	3.58E-30	3.58E-29
		GO: 0022610	biological adhesion	195	43	PF3D7_0100100,PF3D7_0115700,PF3D7_0324800,PF3D7_0400100,PF3D7_0400400,PF3D7_0412400,PF3D7_0413200,PF3D7_0420700,PF3D7_0421100,PF3D7_0425800,PF3D7_0600200,PF3D7_0617400,PF3D7_0632500,PF3D7_0632800,PF3D7_0711700,PF3D7_0712000,PF3D7_0712300,PF3D7_0712400,PF3D7_0712600,PF3D7_0712800,PF3D7_0712900,PF3D7_0713000,PF3D7_0800200,PF3D7_0800300,PF3D7_0808600,PF3D7_0808700,PF3D7_0809100,PF3D7_0833000,PF3D7_0900100,PF3D7_0937300,PF3D7_0937800,PF3D7_1000100,PF3D7_1000500,PF3D7_1041300,PF3D7_1100100,PF3D7_1100200,PF3D7_1200100,PF3D7_1200400,PF3D7_1200600,PF3D7_1240300,PF3D7_1240600,PF3D7_1253700,PF3D7_1300300,	22.1	8.95	16.89	4.46E-31	4.12E-30	6.12E-29
		GO: 0052572	response to host immune response	208	44	PF3D7_0100100,PF3D7_0114700,PF3D7_0115700,PF3D7_0324800,PF3D7_0400100,PF3D7_0400400,PF3D7_0412400,PF3D7_0413200,PF3D7_0420700,PF3D7_0421100,PF3D7_0425800,PF3D7_0600200,PF3D7_0617400,PF3D7_0631800,PF3D7_0632500,PF3D7_0632800,PF3D7_0711700,PF3D7_0712000,PF3D7_0712300,PF3D7_0712400,PF3D7_0712600,PF3D7_0712800,PF3D7_0712900,PF3D7_0713000,PF3D7_0800200,PF3D7_0800300,PF3D7_0808600,PF3D7_0808700,PF3D7_0809100,PF3D7_0833000,PF3D7_0937300,PF3D7_0937800,PF3D7_1000100,PF3D7_1000500,PF3D7_1041300,PF3D7_1100100,PF3D7_1100200,PF3D7_1200100,PF3D7_1200400,PF3D7_1200600,PF3D7_1240300,PF3D7_1240600,PF3D7_1253700,PF3D7_1300300,	21.2	8.58	16.18	5.11E-31	4.12E-30	7.00E-29
		GO: 0052200	response to host defenses	208	44	PF3D7_0100100,PF3D7_0114700,PF3D7_0115700,PF3D7_0324800,PF3D7_0400100,PF3D7_0400400,PF3D7_0412400,PF3D7_0413200,PF3D7_0420700,PF3D7_0421100,PF3D7_0425800,PF3D7_0600200,PF3D7_0617400,PF3D7_0631800,PF3D7_0632500,PF3D7_0632800,PF3D7_0711700,PF3D7_0712000,PF3D7_0712300,PF3D7_0712400,PF3D7_0712600,PF3D7_0712800,PF3D7_0712900,PF3D7_0713000,PF3D7_0800200,PF3D7_0800300,PF3D7_0808600,PF3D7_0808700,PF3D7_0809100,PF3D7_0833000,PF3D7_0937300,PF3D7_0937800,PF3D7_1000100,PF3D7_1000500,PF3D7_1041300,PF3D7_1100100,PF3D7_1100200,PF3D7_1200100,PF3D7_1200400,PF3D7_1200600,PF3D7_1240300,PF3D7_1240600,PF3D7_1253700,PF3D7_1300300,	21.2	8.58	16.18	5.11E-31	4.12E-30	7.00E-29
		GO: 0052173	response to defenses of other organism	208	44	PF3D7_0100100,PF3D7_0114700,PF3D7_0115700,PF3D7_0324800,PF3D7_0400100,PF3D7_0400400,PF3D7_0412400,PF3D7_0413200,PF3D7_0420700,PF3D7_0421100,PF3D7_0425800,PF3D7_0600200,PF3D7_0617400,PF3D7_0631800,PF3D7_0632500,PF3D7_0632800,PF3D7_0711700,PF3D7_0712000,PF3D7_0712300,PF3D7_0712400,PF3D7_0712600,PF3D7_0712800,PF3D7_0712900,PF3D7_0713000,PF3D7_0800200,PF3D7_0800300,PF3D7_0808600,PF3D7_0808700,PF3D7_0809100,PF3D7_0833000,PF3D7_0937300,PF3D7_0937800,PF3D7_1000100,PF3D7_1000500,PF3D7_1041300,PF3D7_1100100,PF3D7_1100200,PF3D7_1200100,PF3D7_1200400,PF3D7_1200600,PF3D7_1240300,PF3D7_1240600,PF3D7_1253700,PF3D7_1300300,	21.2	8.58	16.18	5.11E-31	4.12E-30	7.00E-29

University of Ghana http://ugspace.ug.edu.gh

		GO: 0051707	response to other organism	208	44	PF3D7_0100100,PF3D7_0114700,PF3D7_0115700,PF3D7_0324800,PF3D7_0400100,PF3D7_0400400,PF3D7_0412400,PF3D7_0413200,PF3D7_0420700,PF3D7_0421100,PF3D7_0425800,PF3D7_0600200,PF3D7_0617400,PF3D7_0631800,PF3D7_0632500,PF3D7_0632800,PF3D7_0711700,PF3D7_0712000,PF3D7_0712300,PF3D7_0712400,PF3D7_0712600,PF3D7_0712800,PF3D7_0712900,PF3D7_0713000,PF3D7_0800200,PF3D7_0800300,PF3D7_0808600,PF3D7_0808700,PF3D7_0809100,PF3D7_0833000,PF3D7_0937300,PF3D7_0937800,PF3D7_1000100,PF3D7_1000500,PF3D7_1041300,PF3D7_1100100,PF3D7_1100200,PF3D7_1200100,PF3D7_1200400,PF3D7_1200600,PF3D7_1240300,PF3D7_1240600,PF3D7_1253700,PF3D7_1300300,	21.2	8.58	16.18	5.11E-31	4.12E-30	7.00E-29
		GO: 0043207	response to external biotic stimulus	208	44	PF3D7_0100100,PF3D7_0114700,PF3D7_0115700,PF3D7_0324800,PF3D7_0400100,PF3D7_0400400,PF3D7_0412400,PF3D7_0413200,PF3D7_0420700,PF3D7_0421100,PF3D7_0425800,PF3D7_0600200,PF3D7_0617400,PF3D7_0631800,PF3D7_0632500,PF3D7_0632800,PF3D7_0711700,PF3D7_0712000,PF3D7_0712300,PF3D7_0712400,PF3D7_0712600,PF3D7_0712800,PF3D7_0712900,PF3D7_0713000,PF3D7_0800200,PF3D7_0800300,PF3D7_0808600,PF3D7_0808700,PF3D7_0809100,PF3D7_0833000,PF3D7_0937300,PF3D7_0937800,PF3D7_1000100,PF3D7_1000500,PF3D7_1041300,PF3D7_1100100,PF3D7_1100200,PF3D7_1200100,PF3D7_1200400,PF3D7_1200600,PF3D7_1240300,PF3D7_1240600,PF3D7_1253700,PF3D7_1300300,	21.2	8.58	16.18	5.11E-31	4.12E-30	7.00E-29
		GO: 0075136	response to host	208	44	PF3D7_0100100,PF3D7_0114700,PF3D7_0115700,PF3D7_0324800,PF3D7_0400100,PF3D7_0400400,PF3D7_0412400,PF3D7_0413200,PF3D7_0420700,PF3D7_0421100,PF3D7_0425800,PF3D7_0600200,PF3D7_0617400,PF3D7_0631800,PF3D7_0632500,PF3D7_0632800,PF3D7_0711700,PF3D7_0712000,PF3D7_0712300,PF3D7_0712400,PF3D7_0712600,PF3D7_0712800,PF3D7_0712900,PF3D7_0713000,PF3D7_0800200,PF3D7_0800300,PF3D7_0808600,PF3D7_0808700,PF3D7_0809100,PF3D7_0833000,PF3D7_0937300,PF3D7_0937800,PF3D7_1000100,PF3D7_1000500,PF3D7_1041300,PF3D7_1100100,PF3D7_1100200,PF3D7_1200100,PF3D7_1200400,PF3D7_1200600,PF3D7_1240300,PF3D7_1240600,PF3D7_1253700,PF3D7_1300300,	21.2	8.58	16.18	5.11E-31	4.12E-30	7.00E-29
		GO: 0051701	biological process involved in interaction with host	382	51	PF3D7_0100100,PF3D7_0114700,PF3D7_0115700,PF3D7_0208900,PF3D7_0324800,PF3D7_0400100,PF3D7_0400400,PF3D7_0402600,PF3D7_0412400,PF3D7_0413200,PF3D7_0420700,PF3D7_0421100,PF3D7_0424400,PF3D7_0425800,PF3D7_0600200,PF3D7_0617400,PF3D7_0631800,PF3D7_0632500,PF3D7_0632800,PF3D7_0711700,PF3D7_0712000,PF3D7_0712300,PF3D7_0712400,PF3D7_0712600,PF3D7_0712800,PF3D7_0712900,PF3D7_0713000,PF3D7_0726200,PF3D7_0800200,PF3D7_0800300,PF3D7_0808600,PF3D7_0808700,PF3D7_0809100,PF3D7_0819200,PF3D7_0833000,PF3D7_0923300,PF3D7_0937300,PF3D7_0937800,PF3D7_1000100,PF3D7_1000500,PF3D7_1041300,PF3D7_1100100,PF3D7_1100200,PF3D7_1200100,PF3D7_1200400,PF3D7_1200600,PF3D7_1207300,PF3D7_1240300,PF3D7_1240600,PF3D7_1253700,PF3D7_1300300,	13.4	5.42	9.86	3.34E-26	2.54E-25	4.58E-24
		GO: 0044403	biological process involved in symbiotic interaction	397	51	PF3D7_0100100,PF3D7_0114700,PF3D7_0115700,PF3D7_0208900,PF3D7_0324800,PF3D7_0400100,PF3D7_0400400,PF3D7_0402600,PF3D7_0412400,PF3D7_0413200,PF3D7_0420700,PF3D7_0421100,PF3D7_0424400,PF3D7_0425800,PF3D7_0600200,PF3D7_0617400,PF3D7_0631800,PF3D7_0632500,PF3D7_0632800,PF3D7_0711700,PF3D7_0712000,PF3D7_0712300,PF3D7_0712400,PF3D7_0712600,PF3D7_0712800,PF3D7_0712900,PF3D7_0713000,PF3D7_0726200,PF3D7_0800200,PF3D7_0800300,PF3D7_0808600,PF3D7_0808700,PF3D7_0809100,PF3D7_0819200,PF3D7_0833000,PF3D7_0923300,PF3D7_0937300,PF3D7_0937800,PF3D7_1	12.8	5.21	9.4	2.18E-25	1.57E-24	2.99E-23

University of Ghana http://ugspace.ug.edu.gh

						000100,PF3D7_1000500,PF3D7_1041300,PF3D7_1100100,PF3D7_1100200,PF3D7_1200100,PF3D7_1200400,PF3D7_1200600,PF3D7_1207300,PF3D7_1240300,PF3D7_1240600,PF3D7_1253700,PF3D7_1300300,						
		GO:0044419	biological process involved in interspecies interaction between organisms	399	51	PF3D7_0100100,PF3D7_0114700,PF3D7_0115700,PF3D7_0208900,PF3D7_0324800,PF3D7_0400100,PF3D7_0400400,PF3D7_0402600,PF3D7_0412400,PF3D7_0413200,PF3D7_0420700,PF3D7_0421100,PF3D7_0424400,PF3D7_0425800,PF3D7_0600200,PF3D7_0617400,PF3D7_0631800,PF3D7_0632500,PF3D7_0632800,PF3D7_0711700,PF3D7_0712000,PF3D7_0712300,PF3D7_0712400,PF3D7_0712600,PF3D7_0712800,PF3D7_0712900,PF3D7_0713000,PF3D7_0726200,PF3D7_0800200,PF3D7_0800300,PF3D7_0808600,PF3D7_0808700,PF3D7_0809100,PF3D7_0819200,PF3D7_0833000,PF3D7_0923300,PF3D7_0937300,PF3D7_0937800,PF3D7_1000100,PF3D7_1000500,PF3D7_1041300,PF3D7_1100100,PF3D7_1100200,PF3D7_1200100,PF3D7_1200400,PF3D7_1200600,PF3D7_1207300,PF3D7_1240300,PF3D7_1240600,PF3D7_1253700,PF3D7_1300300,	12.8	5.19	9.35	2.78E-25	1.90E-24	3.81E-23
		GO:0008150	biological process	662	56	PF3D7_0100100,PF3D7_0114700,PF3D7_0115700,PF3D7_0208900,PF3D7_0324800,PF3D7_0400100,PF3D7_0400400,PF3D7_0402600,PF3D7_0412400,PF3D7_0413200,PF3D7_0420700,PF3D7_0421100,PF3D7_0424400,PF3D7_0425800,PF3D7_0600200,PF3D7_0617400,PF3D7_0631800,PF3D7_0632500,PF3D7_0632800,PF3D7_0711700,PF3D7_0712000,PF3D7_0712300,PF3D7_0712400,PF3D7_0712600,PF3D7_0712800,PF3D7_0712900,PF3D7_0713000,PF3D7_0726200,PF3D7_0800200,PF3D7_0800300,PF3D7_0808600,PF3D7_0808700,PF3D7_0809100,PF3D7_0819200,PF3D7_0833000,PF3D7_0900100,PF3D7_0923300,PF3D7_0937300,PF3D7_0937800,PF3D7_1000100,PF3D7_1000500,PF3D7_1041300,PF3D7_1100100,PF3D7_1100200,PF3D7_1200100,PF3D7_1200400,PF3D7_1200600,PF3D7_1206500,PF3D7_1207300,PF3D7_1217600,PF3D7_1240300,PF3D7_1240600,PF3D7_1253700,PF3D7_1300300,PF3D7_1360500,PF3D7_1475400,	8.5	3.43	5.98	5.68E-19	3.71E-18	7.78E-17
		GO:0000083	regulation of transcription involved in G1/S transition of mitotic cell cycle	1	1	PF3D7_1356900,	100	40.57	inf	0.024650 78	0.153507 13	1
		GO:0071976	cell gliding	11	2	PF3D7_1207300,PF3D7_1360500,	18.2	7.38	8.92	0.028659 34	0.170710 01	1
		GO:0007018	microtubule-based movement	32	3	PF3D7_1023100,PF3D7_1213600,PF3D7_1245600,	9.4	3.8	4.17	0.043119 7	0.238276 47	1
		GO:0042966	biotin carboxyl carrier protein biosynthetic process	2	1	PF3D7_1026900,	50	20.28	39.89	0.048698 84	0.238276 47	1

University of Ghana http://ugspace.ug.edu.gh

University of Ghana http://ugspace.ug.edu.gh

		GO:0009305	protein biotinylation	2	1	PF3D7_1026900,	50	20.28	39.89	0.048698 84	0.238276 47	1
		GO:0006426	glycyl-tRNA aminoacylation	2	1	PF3D7_1456400,	50	20.28	39.89	0.048698 84	0.238276 47	1
		GO:0070979	protein K11-linked ubiquitination	2	1	PF3D7_1217600,	50	20.28	39.89	0.048698 84	0.238276 47	1
	Downregulated	GO:0052126	movement in host environment	120	49	PF3D7_0102500,PF3D7_0206200,PF3D7_0207500,PF3D7_0207600,PF3D7_0210600,PF3D7_0214900,PF3D7_0217500,PF3D7_0304000,PF3D7_0404700,PF3D7_0404900,PF3D7_0405200,PF3D7_0423400,PF3D7_0424100,PF3D7_0501600,PF3D7_0507500,PF3D7_0612700,PF3D7_0707300,PF3D7_0722200,PF3D7_0731500,PF3D7_0805600,PF3D7_0808200,PF3D7_0828800,PF3D7_0905400,PF3D7_0929400,PF3D7_0930300,PF3D7_0932200,PF3D7_0934800,PF3D7_1012200,PF3D7_1014100,PF3D7_1017100,PF3D7_1027300,PF3D7_1028700,PF3D7_1030200,PF3D7_1035400,PF3D7_1035500,PF3D7_1035700,PF3D7_1035900,PF3D7_1116000,PF3D7_1133400,PF3D7_1218000,PF3D7_1222700,PF3D7_1246200,PF3D7_1252100,PF3D7_1310700,PF3D7_1335100,PF3D7_1335300,PF3D7_1335400,PF3D7_1342600,PF3D7_1431400,	40.8	7.83	15.29	7.93E-33	3.25E-30	3.25E-30
		GO:0044409	entry into host	103	44	PF3D7_0102500,PF3D7_0210600,PF3D7_0214900,PF3D7_0217500,PF3D7_0304000,PF3D7_0404700,PF3D7_0404900,PF3D7_0405200,PF3D7_0423400,PF3D7_0424100,PF3D7_0501600,PF3D7_0612700,PF3D7_0707300,PF3D7_0722200,PF3D7_0731500,PF3D7_0808200,PF3D7_0828800,PF3D7_0905400,PF3D7_0929400,PF3D7_0930300,PF3D7_0932200,PF3D7_0934800,PF3D7_1012200,PF3D7_1014100,PF3D7_1017100,PF3D7_1027300,PF3D7_1028700,PF3D7_1030200,PF3D7_1035400,PF3D7_1035500,PF3D7_1035700,PF3D7_1035900,PF3D7_1116000,PF3D7_1133400,PF3D7_1218000,PF3D7_1222700,PF3D7_1246200,PF3D7_1252100,PF3D7_1310700,PF3D7_1335100,PF3D7_1335300,PF3D7_1335400,PF3D7_1342600,PF3D7_1431400,	42.7	8.19	16.18	1.75E-30	3.59E-28	7.19E-28
		GO:0044403	biological process involved in symbiotic interaction	397	57	PF3D7_0102500,PF3D7_0104100,PF3D7_0206200,PF3D7_0207500,PF3D7_0207600,PF3D7_0210600,PF3D7_0214900,PF3D7_0217500,PF3D7_0220800,PF3D7_0302200,PF3D7_0302500,PF3D7_0304000,PF3D7_0404700,PF3D7_0404900,PF3D7_0405200,PF3D7_0423400,PF3D7_0424100,PF3D7_0500900,PF3D7_0501600,PF3D7_0507500,PF3D7_0612700,PF3D7_0707300,PF3D7_0722200,PF3D7_0731500,PF3D7_0805600,PF3D7_0808200,PF3D7_0828800,PF3D7_0831600,PF3D7_0905400,PF3D7_0929400,PF3D7_0930300,PF3D7_0932200,PF3D7_0934800,PF3D7_0935800,PF3D7_1012200,PF3D7_1014100,PF3D7_1017100,PF3D7_1027300,PF3D7_1028700,PF3D7_1030200,PF3D7_1035400,PF3D7_1035500,PF3D7_1035700,PF3D7_1035900,PF3D7_1116000,PF3D7_1116800,PF3D7_1133400,PF3D7_1218000,PF3D7_1222700,PF3D7_1246200,PF3D7_1252100,PF3D7_1310700,PF3D7_1335100,PF3D7_1335300,PF3D7_1335400,PF3D7_1342600,PF3D7_1431400,	14.4	2.75	3.64	3.15E-13	4.03E-11	1.29E-10

		GO: 0044419	biological process involved in interspecies interaction between organisms	399	57	PF3D7_0102500,PF3D7_0104100,PF3D7_0206200,PF3D7_0207500,PF3D7_0207600,PF3D7_0210600,PF3D7_0214900,PF3D7_0217500,PF3D7_0220800,PF3D7_0302200,PF3D7_0302500,PF3D7_0304000,PF3D7_0404700,PF3D7_0404900,PF3D7_0405200,PF3D7_0423400,PF3D7_0424100,PF3D7_0500900,PF3D7_0501600,PF3D7_0507500,PF3D7_0507600,PF3D7_0612700,PF3D7_0707300,PF3D7_0722200,PF3D7_0731500,PF3D7_0805600,PF3D7_0808200,PF3D7_0828800,PF3D7_0831600,PF3D7_0905400,PF3D7_0929400,PF3D7_0930300,PF3D7_0932200,PF3D7_0934800,PF3D7_0935800,PF3D7_1012200,PF3D7_1014100,PF3D7_1017100,PF3D7_1027300,PF3D7_1028700,PF3D7_1030200,PF3D7_1035400,PF3D7_1035500,PF3D7_1035700,PF3D7_1035900,PF3D7_1116000,PF3D7_1116800,PF3D7_1133400,PF3D7_1218000,PF3D7_1222700,PF3D7_1246200,PF3D7_1252100,PF3D7_1310700,PF3D7_1335100,PF3D7_1335300,PF3D7_1335400,PF3D7_1342600,PF3D7_1431400,	14.3	2.74	3.61	3.93 E-13	4.03 E-11	1.61 E-10
		GO: 0008150	biological process	662	76	PF3D7_0102500,PF3D7_0104100,PF3D7_0206200,PF3D7_0206800,PF3D7_0207400,PF3D7_0207500,PF3D7_0207600,PF3D7_0207700,PF3D7_0207800,PF3D7_0210600,PF3D7_0212600,PF3D7_0214900,PF3D7_0217500,PF3D7_0220800,PF3D7_0302200,PF3D7_0302500,PF3D7_0304000,PF3D7_0404700,PF3D7_0404900,PF3D7_0405200,PF3D7_0418600,PF3D7_0423400,PF3D7_0424100,PF3D7_0500900,PF3D7_0501600,PF3D7_0507500,PF3D7_0612700,PF3D7_0617800,PF3D7_0707300,PF3D7_0722200,PF3D7_0731500,PF3D7_0802600,PF3D7_0802800,PF3D7_0805600,PF3D7_0808200,PF3D7_0828800,PF3D7_0831600,PF3D7_0902100,PF3D7_0905400,PF3D7_0917900,PF3D7_0925900,PF3D7_0929400,PF3D7_0930300,PF3D7_0932200,PF3D7_0934800,PF3D7_0935800,PF3D7_1012200,PF3D7_1014100,PF3D7_1017100,PF3D7_1027300,PF3D7_1028700,PF3D7_1029900,PF3D7_1030200,PF3D7_1035400,PF3D7_1035500,PF3D7_1035700,PF3D7_1035900,PF3D7_1104900,PF3D7_1105000,PF3D7_1105100,PF3D7_1116000,PF3D7_1116800,PF3D7_1122800,PF3D7_1133400,PF3D7_1218000,PF3D7_1222700,PF3D7_1238900,PF3D7_1246200,PF3D7_1252100,PF3D7_1301600,PF3D7_1310700,PF3D7_1335100,PF3D7_1335300,PF3D7_1335400,PF3D7_1342600,PF3D7_1431400,	11.5	2.2	2.93	2.48 E-12	2.03 E-10	1.01 E-09
		GO: 0051701	biological process involved in interaction with host	382	52	PF3D7_0102500,PF3D7_0104100,PF3D7_0206200,PF3D7_0207500,PF3D7_0207600,PF3D7_0210600,PF3D7_0214900,PF3D7_0217500,PF3D7_0304000,PF3D7_0404700,PF3D7_0404900,PF3D7_0405200,PF3D7_0423400,PF3D7_0424100,PF3D7_0500900,PF3D7_0501600,PF3D7_0507500,PF3D7_0612700,PF3D7_0707300,PF3D7_0722200,PF3D7_0731500,PF3D7_0805600,PF3D7_0808200,PF3D7_0828800,PF3D7_0905400,PF3D7_0929400,PF3D7_0930300,PF3D7_0932200,PF3D7_0934800,PF3D7_1012200,PF3D7_1014100,PF3D7_1017100,PF3D7_1027300,PF3D7_1028700,PF3D7_1030200,PF3D7_1035400,PF3D7_1035500,PF3D7_1035700,PF3D7_1035900,PF3D7_1116000,PF3D7_1116800,PF3D7_1133400,PF3D7_1218000,PF3D7_1222700,PF3D7_1246200,PF3D7_1252100,PF3D7_1310700,PF3D7_1335100,PF3D7_1335300,PF3D7_1335400,PF3D7_1342600,PF3D7_1431400,	13.6	2.61	3.34	3.58 E-11	2.44 E-09	1.47 E-08
		GO: 0030029	actin filament-based process	19	10	PF3D7_0105300,PF3D7_0503400,PF3D7_0503600,PF3D7_0613900,PF3D7_0932200,PF3D7_1229800,PF3D7_1251200,PF3D7_1342600,PF3D7_1361400,PF3D7_1444800,	52.6	10.09	20.97	7.66 E-09	3.92 E-07	3.14 E-06

University of Ghana http://ugspace.ug.edu.gh

		GO:0030036	actin cytoskeleton organization	19	10	PF3D7_0105300,PF3D7_0503400,PF3D7_0503600,PF3D7_0613900,PF3D7_0932200,PF3D7_1229800,PF3D7_1251200,PF3D7_1342600,PF3D7_1361400,PF3D7_1444800,	52.6	10.09	20.97	7.66E-09	3.92E-07	3.14E-06
		GO:0007015	actin filament organization	16	9	PF3D7_0105300,PF3D7_0503400,PF3D7_0503600,PF3D7_0613900,PF3D7_1229800,PF3D7_1251200,PF3D7_1342600,PF3D7_1361400,PF3D7_1444800,	56.3	10.78	24.18	2.07E-08	9.42E-07	8.48E-06
		GO:0030048	actin filament-based movement	9	7	PF3D7_0503400,PF3D7_0503600,PF3D7_0613900,PF3D7_0932200,PF3D7_1229800,PF3D7_1342600,PF3D7_1361400,	77.8	14.91	65.35	3.20E-08	1.31E-06	1.31E-05
		GO:0035891	exit from host cell	28	10	PF3D7_0206200,PF3D7_0207500,PF3D7_0207600,PF3D7_0217500,PF3D7_0507500,PF3D7_0805600,PF3D7_0808200,PF3D7_0930300,PF3D7_1014100,PF3D7_1028700,	35.7	6.84	10.46	7.15E-07	2.67E-05	0.000293174
		GO:0035890	exit from host	29	10	PF3D7_0206200,PF3D7_0207500,PF3D7_0207600,PF3D7_0217500,PF3D7_0507500,PF3D7_0805600,PF3D7_0808200,PF3D7_0930300,PF3D7_1014100,PF3D7_1028700,	34.5	6.61	9.91	1.04E-06	3.56E-05	0.000427132
		GO:0097435	supramolecular fiber organization	28	9	PF3D7_0105300,PF3D7_0503400,PF3D7_0503600,PF3D7_0613900,PF3D7_1229800,PF3D7_1251200,PF3D7_1342600,PF3D7_1361400,PF3D7_1444800,	32.1	6.16	8.88	7.17E-06	0.000216 66	0.002939 52
		GO:0048870	cell motility	16	7	PF3D7_0503400,PF3D7_0613900,PF3D7_0805200,PF3D7_0932200,PF3D7_1251200,PF3D7_1342600,PF3D7_1361400,	43.8	8.38	14.5	7.40E-06	0.000216 66	0.003033205
		GO:0050776	regulation of immune response	12	6	PF3D7_0102200,PF3D7_0207400,PF3D7_0207500,PF3D7_0207600,PF3D7_0207700,PF3D7_0207800,	50	9.58	18.58	1.35E-05	0.000368 56	0.005528416
		GO:0002440	production of molecular mediator of immune response	8	5	PF3D7_0207400,PF3D7_0207500,PF3D7_0207600,PF3D7_0207700,PF3D7_0207800,	62.5	11.98	30.86	1.83E-05	0.000441 45	0.007504646
		GO:0002377	immunoglobulin production	8	5	PF3D7_0207400,PF3D7_0207500,PF3D7_0207600,PF3D7_0207700,PF3D7_0207800,	62.5	11.98	30.86	1.83E-05	0.000441 45	0.007504646

University of Ghana http://ugspace.ug.edu.gh

University of Ghana http://ugspace.ug.edu.gh

		GO:0002682	regulation of immune system process	13	6	PF3D7_0102200,PF3D7_0207400,PF3D7_0207500,PF3D7_0207600,PF3D7_0207700,PF3D7_0207800,	46.2	8.85	15.92	2.40E-05	0.000545 57	0.009820318
		GO:0002376	immune system process	14	6	PF3D7_0207400,PF3D7_0207500,PF3D7_0207600,PF3D7_0207700,PF3D7_0207800,PF3D7_1301600,	42.9	8.21	13.93	4.01E-05	0.000865 18	0.016438399
		GO:0008154	actin polymerization or depolymerization	6	4	PF3D7_0105300,PF3D7_0503400,PF3D7_1361400,PF3D7_1444800,	66.7	12.78	36.9	1.00E-04	0.001862 83	0.040982346
		GO:0099515	actin filament-based transport	6	4	PF3D7_0503600,PF3D7_0613900,PF3D7_1229800,PF3D7_1342600,	66.7	12.78	36.9	1.00E-04	0.001862 83	0.040982346
		GO:0030050	vesicle transport along actin filament	6	4	PF3D7_0503600,PF3D7_0613900,PF3D7_1229800,PF3D7_1342600,	66.7	12.78	36.9	1.00E-04	0.001862 83	0.040982346
		GO:0060327	cytoplasmic actin-based contraction involved in cell motility	3	3	PF3D7_0503400,PF3D7_0932200,PF3D7_1361400,	100	19.17	inf	0.000140 47	0.002399 62	0.057590999
		GO:0070252	actin-mediated cell contraction	3	3	PF3D7_0503400,PF3D7_0932200,PF3D7_1361400,	100	19.17	inf	0.000140 47	0.002399 62	0.057590999
		GO:0099518	vesicle cytoskeletal trafficking	7	4	PF3D7_0503600,PF3D7_0613900,PF3D7_1229800,PF3D7_1342600,	57.1	10.95	24.59	0.000223 67	0.003668 25	0.091706293
		GO:0051650	establishment of vesicle localization	9	4	PF3D7_0503600,PF3D7_0613900,PF3D7_1229800,PF3D7_1342600,	44.4	8.52	14.75	0.000740 73	0.011248 16	0.303700401
		GO:0051648	vesicle localization	9	4	PF3D7_0503600,PF3D7_0613900,PF3D7_1229800,PF3D7_1342600,	44.4	8.52	14.75	0.000740 73	0.011248 16	0.303700401

University of Ghana http://ugspace.ug.edu.gh

		GO:0030705	cytoskeleton-dependent intracellular transport	10	4	PF3D7_0503600,PF3D7_0613900,PF3D7_1229800,PF3D7_1342600,	40	7.67	12.29	0.001184	0.017340	0.485526
		GO:0007010	cytoskeleton organization	73	11	PF3D7_0105300,PF3D7_0503400,PF3D7_0503600,PF3D7_0613900,PF3D7_0932200,PF3D7_1229800,PF3D7_1246200,PF3D7_1251200,PF3D7_1342600,PF3D7_1361400,PF3D7_1444800,	15.1	2.89	3.32	0.001250	0.017674	0.512572
		GO:0018105	peptidyl-serine phosphorylation	18	5	PF3D7_0217500,PF3D7_0934800,PF3D7_1104900,PF3D7_1122800,PF3D7_1238900,	27.8	5.32	7.11	0.001817	0.024841	0.745257
		GO:0018209	peptidyl-serine modification	19	5	PF3D7_0217500,PF3D7_0934800,PF3D7_1104900,PF3D7_1122800,PF3D7_1238900,	26.3	5.04	6.6	0.002363	0.031255	0.968923
		GO:0046777	protein autophosphorylation	12	4	PF3D7_0217500,PF3D7_1104900,PF3D7_1122800,PF3D7_1238900,	33.3	6.39	9.21	0.002568	0.031772	1
		GO:0009395	phospholipid catabolic process	2	2	PF3D7_0702200,PF3D7_1406300,	100	19.17	inf	0.002712	0.031772	1
		GO:0046475	glycerophospholipid catabolic process	2	2	PF3D7_0702200,PF3D7_1406300,	100	19.17	inf	0.002712	0.031772	1
		GO:0030042	actin filament depolymerization	2	2	PF3D7_0503400,PF3D7_1361400,	100	19.17	inf	0.002712	0.031772	1
		GO:0006342	chromatin silencing	3	2	PF3D7_0320900,PF3D7_0617800,	66.7	12.78	36.61	0.007856	0.089471	1
		GO:0006650	glycerophospholipid metabolic process	47	7	PF3D7_0702200,PF3D7_0805600,PF3D7_0820200,PF3D7_0927900,PF3D7_0935300,PF3D7_1343000,PF3D7_1406300,	14.9	2.85	3.24	0.010156	0.112548	1

University of Ghana http://ugspace.ug.edu.gh

		GO:0006333	chromatin assembly or disassembly	18	4	PF3D7_0320900,PF3D7_0714000,PF3D7_1105000,PF3D7_1105100,	22.2	4.26	5.26	0.012400 93	0.131354 84	1
		GO:0051276	chromosome organization	10	3	PF3D7_0617800,PF3D7_1105000,PF3D7_1105100,	30	5.75	7.87	0.012815 11	0.131354 84	1
		GO:0006334	nucleosome assembly	10	3	PF3D7_0714000,PF3D7_1105000,PF3D7_1105100,	30	5.75	7.87	0.012815 11	0.131354 84	1
		GO:0046503	glycerolipid catabolic process	4	2	PF3D7_0702200,PF3D7_1406300,	50	9.58	18.3	0.015171 99	0.148107 49	1
		GO:0051261	protein depolymerization	4	2	PF3D7_0503400,PF3D7_1361400,	50	9.58	18.3	0.015171 99	0.148107 49	1
		GO:0046486	glycerolipid metabolic process	51	7	PF3D7_0702200,PF3D7_0805600,PF3D7_0820200,PF3D7_0927900,PF3D7_0935300,PF3D7_1343000,PF3D7_1406300,	13.7	2.63	2.94	0.015672 6	0.149436 46	1
		GO:0006644	phospholipid metabolic process	65	8	PF3D7_0628300,PF3D7_0702200,PF3D7_0805600,PF3D7_0820200,PF3D7_0927900,PF3D7_0935300,PF3D7_1343000,PF3D7_1406300,	12.3	2.36	2.6	0.018793 03	0.175116 83	1
		GO:0006810	transport	31	5	PF3D7_0218100,PF3D7_0905500,PF3D7_0932100,PF3D7_1010300,PF3D7_1204900,	16.1	3.09	3.54	0.020725 35	0.188830 96	1
		GO:0051656	establishment of organelle localization	21	4	PF3D7_0503600,PF3D7_0613900,PF3D7_1229800,PF3D7_1342600,	19	3.65	4.33	0.021456 22	0.191240 24	1
		GO:0006986	response to unfolded protein	22	4	PF3D7_0816500,PF3D7_0818900,PF3D7_0917900,PF3D7_1116800,	18.2	3.48	4.09	0.025178 29	0.219640 36	1

University of Ghana http://ugspace.ug.edu.gh

		GO:0006468	protein phosphorylation	110	11	PF3D7_0214600,PF3D7_0217500,PF3D7_0321400,PF3D7_0500900,PF3D7_0902100,PF3D7_0934800,PF3D7_1104900,PF3D7_1121300,PF3D7_1122800,PF3D7_1238900,PF3D7_1331000,	10	1.92	2.06	0.027396	0.234010	1
		GO:0007155	cell adhesion	70	8	PF3D7_0102500,PF3D7_0206800,PF3D7_0212600,PF3D7_0423400,PF3D7_0707300,PF3D7_0935800,PF3D7_1301600,PF3D7_1335400,	11.4	2.19	2.39	0.028146	0.235085	1
		GO:0031497	chromatin assembly	15	3	PF3D7_0714000,PF3D7_1105000,PF3D7_1105100,	20	3.83	4.58	0.040079	0.235085	1
		GO:0098609	cell-cell adhesion	62	7	PF3D7_0102500,PF3D7_0212600,PF3D7_0423400,PF3D7_0707300,PF3D7_0935800,PF3D7_1301600,PF3D7_1335400,	11.3	2.16	2.35	0.041122	0.235085	1
		GO:0044242	cellular lipid catabolic process	7	2	PF3D7_0702200,PF3D7_1406300,	28.6	5.48	7.32	0.047856	0.235085	1
		GO:0016310	phosphorylation	135	12	PF3D7_0214600,PF3D7_0217500,PF3D7_0321400,PF3D7_0500900,PF3D7_0902100,PF3D7_0934800,PF3D7_1104900,PF3D7_1121300,PF3D7_1122800,PF3D7_1238900,PF3D7_1331000,PF3D7_1444800,	8.9	1.7	1.81	0.048042	0.235085	1
Molecular function	Upregulated	GO:0050839	cell adhesion molecule binding	55	37	PF3D7_0100100,PF3D7_0115700,PF3D7_0400100,PF3D7_0400400,PF3D7_0412400,PF3D7_0420700,PF3D7_0421100,PF3D7_0425800,PF3D7_0600200,PF3D7_0617400,PF3D7_0632500,PF3D7_0632800,PF3D7_0711700,PF3D7_0712000,PF3D7_0712300,PF3D7_0712400,PF3D7_0712600,PF3D7_0712800,PF3D7_0712900,PF3D7_0800200,PF3D7_0800300,PF3D7_0808600,PF3D7_0808700,PF3D7_0809100,PF3D7_0900100,PF3D7_0936500,PF3D7_0937800,PF3D7_1000100,PF3D7_1041300,PF3D7_1100100,PF3D7_1100200,PF3D7_1200100,PF3D7_1200400,PF3D7_1200600,PF3D7_1240300,PF3D7_1240600,PF3D7_1300300,	67.3	27.29	117.14	7.65E-49	1.02E-46	1.02E-46
		GO:0046789	host cell surface receptor binding	88	42	PF3D7_0100100,PF3D7_0115700,PF3D7_0300100,PF3D7_0324900,PF3D7_0400100,PF3D7_0400400,PF3D7_0412400,PF3D7_0420700,PF3D7_0421100,PF3D7_0425800,PF3D7_0600200,PF3D7_0617400,PF3D7_0632500,PF3D7_0632800,PF3D7_0711700,PF3D7_0712000,PF3D7_0712300,PF3D7_0712400,PF3D7_0712600,PF3D7_0712800,PF3D7_0712900,PF3D7_0800200,PF3D7_0800300,PF3D7_0808600,PF3D7_0808700,PF3D7_0809100,PF3D7_0833500,PF3D7_0900100,PF3D7_0937800,PF3D7_1000100,PF3D7_1041300,PF3D7_1100100,PF3D7_1100200,PF3D7_1200100,PF3D7_1200400,PF3D7_1200600,PF3D7_1240300,PF3D7_1240600,PF3D7_1240900,PF3D7_1300100,PF3D7_1300300,PF3D7_1373500,	47.7	19.36	55.04	1.10E-46	7.30E-45	1.46E-44

		GO: 0046812	host cell surface binding	107	43	PF3D7_0100100,PF3D7_0115700,PF3D7_0300100,PF3D7_0324900,PF3D7_0400100,PF3D7_0400400,PF3D7_0412400,PF3D7_0420700,PF3D7_0421100,PF3D7_0424400,PF3D7_0425800,PF3D7_0600200,PF3D7_0617400,PF3D7_0632500,PF3D7_0632800,PF3D7_0711700,PF3D7_0712000,PF3D7_0712300,PF3D7_0712400,PF3D7_0712600,PF3D7_0712800,PF3D7_0712900,PF3D7_0800200,PF3D7_0800300,PF3D7_0808600,PF3D7_0808700,PF3D7_0809100,PF3D7_0833500,PF3D7_0900100,PF3D7_0937800,PF3D7_1000100,PF3D7_1041300,PF3D7_1100100,PF3D7_1100200,PF3D7_1200100,PF3D7_1200400,PF3D7_1200600,PF3D7_1240300,PF3D7_1240600,PF3D7_1240900,PF3D7_1300100,PF3D7_1300300,PF3D7_1373500,	40.2	16.3	40.87	8.97E-44	3.98E-42	1.19E-41
		GO: 0003777	microtubule motor activity	22	3	PF3D7_1023100,PF3D7_1213600,PF3D7_1245600,	13.6	5.53	6.38	0.015982 6	0.327855 38	1
		GO: 0035373	chondroitin sulfate proteoglycan binding	1	1	PF3D7_1200600,	100	40.57	inf	0.024650 78	0.327855 38	1
		GO: 0008429	phosphatidylethanolamine binding	1	1	PF3D7_1219700,	100	40.57	inf	0.024650 78	0.327855 38	1
		GO: 0035241	protein-arginine omega-N monomethyltransferase activity	1	1	PF3D7_1332500,	100	40.57	inf	0.024650 78	0.327855 38	1
		GO: 0016427	tRNA (cytosine) methyltransferase activity	1	1	PF3D7_1111000,	100	40.57	inf	0.024650 78	0.327855 38	1
		GO: 0016428	tRNA (cytosine-5-)-methyltransferase activity	1	1	PF3D7_1111000,	100	40.57	inf	0.024650 78	0.327855 38	1
		GO: 0019788	NEDD8 transferase activity	1	1	PF3D7_1245300,	100	40.57	inf	0.024650 78	0.327855 38	1
		GO: 0051959	dynein light intermediate chain binding	12	2	PF3D7_1023100,PF3D7_1213600,	16.7	6.76	8.03	0.033844 9	0.380996 81	1

University of Ghana http://ugspace.ug.edu.gh

University of Ghana http://ugspace.ug.edu.gh

		GO: 0045505	dynein intermediate chain binding	13	2	PF3D7_1023100,PF3D7_1213600,	15.4	6.24	7.3	0.039364	0.380996 81	1
		GO: 0004820	glycine-tRNA ligase activity	2	1	PF3D7_1456400,	50	20.28	39.89	0.048698 84	0.380996 81	1
		GO: 0004383	guanylate cyclase activity	2	1	PF3D7_1360500,	50	20.28	39.89	0.048698 84	0.380996 81	1
		GO: 0004077	biotin-[acetyl-CoA-carboxylase] ligase activity	2	1	PF3D7_1026900,	50	20.28	39.89	0.048698 84	0.380996 81	1
		GO: 0008897	holo-[acyl-carrier-protein] synthase activity	2	1	PF3D7_0420200,	50	20.28	39.89	0.048698 84	0.380996 81	1
		GO: 0018271	biotin-protein ligase activity	2	1	PF3D7_1026900,	50	20.28	39.89	0.048698 84	0.380996 81	1
	Downregulated	GO: 0046812	host cell surface binding	107	23	PF3D7_0102500,PF3D7_0423400,PF3D7_0424100,PF3D7_0620400,PF3D7_0722200,PF3D7_0731500,PF3D7_0817700,PF3D7_0828800,PF3D7_0905400,PF3D7_0930300,PF3D7_0935800,PF3D7_1012200,PF3D7_1028700,PF3D7_1035500,PF3D7_1035700,PF3D7_1036000,PF3D7_1133400,PF3D7_1252100,PF3D7_1301600,PF3D7_1335100,PF3D7_1335300,PF3D7_1335400,PF3D7_1431400,	21.5	4.12	5.37	3.32E-09	9.12E-07	9.12E-07
		GO: 0003779	actin binding	30	12	PF3D7_0105300,PF3D7_0503400,PF3D7_0503600,PF3D7_0613900,PF3D7_0932200,PF3D7_1118700,PF3D7_1229800,PF3D7_1251200,PF3D7_1342600,PF3D7_1361400,PF3D7_1361800,PF3D7_1444800,	40	7.67	12.66	1.18E-08	1.62E-06	3.23E-06
		GO: 0005515	protein binding	605	63	PF3D7_0102200,PF3D7_0109000,PF3D7_0207500,PF3D7_0207600,PF3D7_0217500,PF3D7_0302200,PF3D7_0302500,PF3D7_0401800,PF3D7_0402100,PF3D7_0404900,PF3D7_0424100,PF3D7_0501300,PF3D7_0501600,PF3D7_0503600,PF3D7_0507200,PF3D7_0612700,PF3D7_0628100,PF3D7_0707300,PF3D7_0818900,PF3D7_0830500,PF3D7_0905400,PF3D7_0917900,PF3D7_0918000,PF3D7_0922200,PF3D7_0929400,PF3D7_0930300,PF3D7_0932200,PF3D7_0934800,PF3D7_0935800,PF3D7_0936000,PF3D7_1001000,PF3D7_1003600,PF3D7_1006200,PF3D7_1014100,PF3D7_1017500,PF3D7_1019900,PF3D7_1035300,PF3D7_1035400,PF3D7_1035500,PF3D7_1035700,PF3D7_1116000,PF3D7_1116800,PF3D7_1118700,PF3D7_1125700,PF3D7_1125800,PF3D7_1133400,PF3	10.4	2	2.48	1.98E-08	1.82E-06	5.46E-06

University of Ghana http://ugspace.ug.edu.gh

						D7_1222700,PF3D7_1223100,PF3D7_1246200,PF3D7_1246400,PF3D7_1251200,PF3D7_1252100,PF3D7_1310700,PF3D7_1323700,PF3D7_1335100,PF3D7_1342600,PF3D7_1343000,PF3D7_1344300,PF3D7_1356300,PF3D7_1361800,PF3D7_1410400,PF3D7_1423360,PF3D7_1452000,						
		GO: 0051015	actin filament binding	14	8	PF3D7_0503400,PF3D7_0503600,PF3D7_0613900,PF3D7_1229800,PF3D7_1251200,PF3D7_1342600,PF3D7_1361400,PF3D7_1361800,	57.1	10.95	24.98	1.13E-07	7.74E-06	3.10E-05
		GO: 0008201	heparin binding	9	6	PF3D7_0102500,PF3D7_0424100,PF3D7_0731500,PF3D7_1301600,PF3D7_1335300,PF3D7_1335400,	66.7	12.78	37.19	1.40E-06	7.71E-05	0.000385314
		GO: 0005539	glycosaminoglycan binding	10	6	PF3D7_0102500,PF3D7_0424100,PF3D7_0731500,PF3D7_1301600,PF3D7_1335300,PF3D7_1335400,	60	11.5	27.88	3.35E-06	0.000153 54	0.000921269
		GO: 0003785	actin monomer binding	4	4	PF3D7_0105300,PF3D7_0503400,PF3D7_0932200,PF3D7_1361400,	100	19.17	inf	7.25E-06	0.000284 71	0.001992 94
		GO: 0044877	protein-containing complex binding	101	17	PF3D7_0202200,PF3D7_0301300,PF3D7_0503400,PF3D7_0503600,PF3D7_0613900,PF3D7_0825200,PF3D7_0905400,PF3D7_0929400,PF3D7_0930300,PF3D7_1035400,PF3D7_1035500,PF3D7_1035700,PF3D7_1229800,PF3D7_1251200,PF3D7_1342600,PF3D7_1361400,PF3D7_1361800,	16.8	3.23	3.87	1.41E-05	0.000485 18	0.003881415
		GO: 0046982	protein heterodimerization activity	15	6	PF3D7_0320900,PF3D7_0617800,PF3D7_0714000,PF3D7_1105000,PF3D7_1105100,PF3D7_1439500,	40	7.67	12.38	6.39E-05	0.001953 11	0.017578007
		GO: 0008092	cytoskeletal protein binding	74	13	PF3D7_0105300,PF3D7_0301300,PF3D7_0503400,PF3D7_0503600,PF3D7_0613900,PF3D7_0932200,PF3D7_1118700,PF3D7_1229800,PF3D7_1251200,PF3D7_1342600,PF3D7_1361400,PF3D7_1361800,PF3D7_1444800,	17.6	3.37	4.03	9.37E-05	0.002498 92	0.025768259
		GO: 0030898	actin-dependent ATPase activity	6	4	PF3D7_0503600,PF3D7_0613900,PF3D7_1229800,PF3D7_1342600,	66.7	12.78	36.9	1.00E-04	0.002498 92	0.027488159
		GO: 0000146	microfilament motor activity	7	4	PF3D7_0503600,PF3D7_0613900,PF3D7_1229800,PF3D7_1342600,	57.1	10.95	24.59	0.000223 67	0.005125 86	0.061510319

		GO: 0005516	calmodulin binding	14	5	PF3D7_0217500,PF3D7_0802800,PF3D7_1104900,PF3D7_1122800,PF3D7_1238900,	35.7	6.84	10.27	0.000504 56	0.010673 48	0.138755199
		GO: 0046789	host cell surface receptor binding	88	13	PF3D7_0102500,PF3D7_0423400,PF3D7_0424100,PF3D7_0722200,PF3D7_0731500,PF3D7_0828800,PF3D7_0905400,PF3D7_0935800,PF3D7_1028700,PF3D7_1035700,PF3D7_1301600,PF3D7_1335100,PF3D7_1335300,	14.8	2.83	3.26	0.000558 28	0.010966 2	0.153526763
		GO: 0008236	serine-type peptidase activity	30	7	PF3D7_0207600,PF3D7_0506900,PF3D7_0507200,PF3D7_0507500,PF3D7_1308000,PF3D7_1320100,PF3D7_1411200,	23.3	4.47	5.66	0.000700 78	0.011316 75	0.192713396
		GO: 0017171	serine hydrolase activity	30	7	PF3D7_0207600,PF3D7_0506900,PF3D7_0507200,PF3D7_0507500,PF3D7_1308000,PF3D7_1320100,PF3D7_1411200,	23.3	4.47	5.66	0.000700 78	0.011316 75	0.192713396
		GO: 0010857	calcium-dependent protein kinase activity	9	4	PF3D7_0217500,PF3D7_1104900,PF3D7_1122800,PF3D7_1238900,	44.4	8.52	14.75	0.000740 73	0.011316 75	0.203701488
		GO: 0009931	calcium-dependent protein serine/threonine kinase activity	9	4	PF3D7_0217500,PF3D7_1104900,PF3D7_1122800,PF3D7_1238900,	44.4	8.52	14.75	0.000740 73	0.011316 75	0.203701488
		GO: 0046983	protein dimerization activity	40	8	PF3D7_0105300,PF3D7_0320900,PF3D7_0617800,PF3D7_0714000,PF3D7_0922200,PF3D7_1105000,PF3D7_1105100,PF3D7_1439500,	20	3.83	4.66	0.000880 67	0.012746 53	0.242184053
		GO: 1901681	sulfur compound binding	26	6	PF3D7_0102500,PF3D7_0424100,PF3D7_0731500,PF3D7_1301600,PF3D7_1335300,PF3D7_1335400,	23.1	4.42	5.56	0.001808 77	0.024870 65	0.497412939
		GO: 0004197	cysteine-type endopeptidase activity	27	6	PF3D7_0207400,PF3D7_0207500,PF3D7_0207600,PF3D7_0207700,PF3D7_0207800,PF3D7_0404700,	22.2	4.26	5.29	0.002225 64	0.029145 35	0.612052341
		GO: 0004252	serine-type endopeptidase activity	28	6	PF3D7_0506900,PF3D7_0507200,PF3D7_0507500,PF3D7_1308000,PF3D7_1320100,PF3D7_1411200,	21.4	4.11	5.05	0.002711 05	0.031078 77	0.745538537

University of Ghana http://ugspace.ug.edu.gh

University of Ghana http://ugspace.ug.edu.gh

		GO: 0004867	serine-type endopeptidase inhibitor activity	2	2	PF3D7_0501400,PF3D7_0507400,	100	19.17	inf	0.002712 33	0.031078 77	0.745890 397
		GO: 0004679	AMP-activated protein kinase activity	2	2	PF3D7_0934800,PF3D7_1223100,	100	19.17	inf	0.002712 33	0.031078 77	0.745890 397
		GO: 0004175	endopeptidase activity	107	13	PF3D7_0207400,PF3D7_0207500,PF3D7_0207600,PF3D7_0207700,PF3D7_0207800,PF3D7_0404700,PF3D7_0506900,PF3D7_0507200,PF3D7_0507500,PF3D7_0808200,PF3D7_1308000,PF3D7_1320100,PF3D7_1411200,	12.1	2.33	2.59	0.003473 29	0.038206 21	0.955155 256
		GO: 0004866	endopeptidase inhibitor activity	3	2	PF3D7_0501400,PF3D7_0507400,	66.7	12.78	36.61	0.007856 05	0.080015 37	1
		GO: 0030414	peptidase inhibitor activity	3	2	PF3D7_0501400,PF3D7_0507400,	66.7	12.78	36.61	0.007856 05	0.080015 37	1
		GO: 0004672	protein kinase activity	108	12	PF3D7_0214600,PF3D7_0217500,PF3D7_0321400,PF3D7_0500900,PF3D7_0902100,PF3D7_0934800,PF3D7_1104900,PF3D7_1121300,PF3D7_1122800,PF3D7_1223100,PF3D7_1238900,PF3D7_1331000,	11.1	2.13	2.33	0.009985 08	0.098067 73	1
		GO: 0004690	cyclic nucleotide-dependent protein kinase activity	4	2	PF3D7_0934800,PF3D7_1223100,	50	9.58	18.3	0.015171 99	0.126433 22	1
		GO: 0005253	anion channel activity	4	2	PF3D7_0302200,PF3D7_0302500,	50	9.58	18.3	0.015171 99	0.126433 22	1
		GO: 0071889	14-3-3 protein binding	4	2	PF3D7_0217500,PF3D7_1223100,	50	9.58	18.3	0.015171 99	0.126433 22	1
		GO: 0017169	CDP-alcohol phosphatidyltransferase activity	4	2	PF3D7_0628300,PF3D7_0820200,	50	9.58	18.3	0.015171 99	0.126433 22	1

University of Ghana http://ugspace.ug.edu.gh

		GO: 0004691	cAMP-dependent protein kinase activity	4	2	PF3D7_0934800,PF3D7_1223100,	50	9.58	18.3	0.015171 99	0.126433 22	1
		GO: 0005509	calcium ion binding	52	7	PF3D7_0217500,PF3D7_1022700,PF3D7_1122800,PF3D7_1238900,PF3D7_1246400,PF3D7_1423300,PF3D7_1463900,	13.5	2.58	2.88	0.017330 72	0.140174 93	1
		GO: 0008234	cysteine-type peptidase activity	55	7	PF3D7_0207400,PF3D7_0207500,PF3D7_0207600,PF3D7_0207700,PF3D7_0207800,PF3D7_0404700,PF3D7_0919200,	12.7	2.44	2.7	0.023041 77	0.181042 48	1
		GO: 0061135	endopeptidase regulator activity	5	2	PF3D7_0501400,PF3D7_0507400,	40	7.67	12.2	0.024421 19	0.186550 73	1
		GO: 0044183	protein folding chaperone	6	2	PF3D7_0818900,PF3D7_0917900,	33.3	6.39	9.15	0.035383 57	0.214161 32	1
		GO: 0061134	peptidase regulator activity	6	2	PF3D7_0501400,PF3D7_0507400,	33.3	6.39	9.15	0.035383 57	0.214161 32	1
		GO: 0008233	peptidase activity	159	14	PF3D7_0207400,PF3D7_0207500,PF3D7_0207600,PF3D7_0207700,PF3D7_0207800,PF3D7_0404700,PF3D7_0506900,PF3D7_0507200,PF3D7_0507500,PF3D7_0808200,PF3D7_0919200,PF3D7_1308000,PF3D7_1320100,PF3D7_1411200,	8.8	1.69	1.8	0.036828 48	0.214161 32	1
		GO: 0140096	catalytic activity, acting on a protein	482	34	PF3D7_0207400,PF3D7_0207500,PF3D7_0207600,PF3D7_0207700,PF3D7_0207800,PF3D7_0214600,PF3D7_0217500,PF3D7_0321400,PF3D7_0404700,PF3D7_0500900,PF3D7_0501300,PF3D7_0506900,PF3D7_0507200,PF3D7_0507500,PF3D7_0528400,PF3D7_0628100,PF3D7_0802800,PF3D7_0808200,PF3D7_0902100,PF3D7_0918000,PF3D7_0919200,PF3D7_0934800,PF3D7_1104900,PF3D7_1121300,PF3D7_1122800,PF3D7_1223100,PF3D7_1238900,PF3D7_1308000,PF3D7_1320100,PF3D7_1331000,PF3D7_1356300,PF3D7_1411200,PF3D7_1423300,PF3D7_1469200,	7.1	1.35	1.44	0.039840 64	0.214161 32	1
		GO: 0016830	carbon-carbon lyase activity	16	3	PF3D7_0816100,PF3D7_0927900,PF3D7_1444800,	18.8	3.59	4.23	0.047481 06	0.214161 32	1

Cellular component	Upregulated	GO:0020030	infected host cell surface knob	61	36	PF3D7_0100100,PF3D7_0115700,PF3D7_0400100,PF3D7_0400400,PF3D7_0412400,PF3D7_0420700,PF3D7_0421100,PF3D7_0425800,PF3D7_0600200,PF3D7_0617400,PF3D7_0632500,PF3D7_0632800,PF3D7_0711700,PF3D7_0712000,PF3D7_0712300,PF3D7_0712400,PF3D7_0712600,PF3D7_0712800,PF3D7_0712900,PF3D7_0800200,PF3D7_0800300,PF3D7_0808600,PF3D7_0808700,PF3D7_0809100,PF3D7_0900100,PF3D7_0937800,PF3D7_1000100,PF3D7_1041300,PF3D7_1100100,PF3D7_1100200,PF3D7_1200100,PF3D7_1200400,PF3D7_1200600,PF3D7_1240300,PF3D7_1240600,PF3D7_1300300,	59	23.94	80.97	2.37E-44	2.78E-42	2.78E-42
		GO:0020002	host cell plasma membrane	219	45	PF3D7_0100100,PF3D7_0114700,PF3D7_0115700,PF3D7_0324800,PF3D7_0400100,PF3D7_0400400,PF3D7_0412400,PF3D7_0413200,PF3D7_0420700,PF3D7_0421100,PF3D7_0425800,PF3D7_0600200,PF3D7_0617400,PF3D7_0631800,PF3D7_0632500,PF3D7_0632800,PF3D7_0711700,PF3D7_0712000,PF3D7_0712300,PF3D7_0712400,PF3D7_0712600,PF3D7_0712800,PF3D7_0712900,PF3D7_0713000,PF3D7_0800200,PF3D7_0800300,PF3D7_0808600,PF3D7_0808700,PF3D7_0809100,PF3D7_0833000,PF3D7_0900100,PF3D7_0937300,PF3D7_0937800,PF3D7_1000100,PF3D7_1000500,PF3D7_1041300,PF3D7_1100100,PF3D7_1100200,PF3D7_1200100,PF3D7_1200400,PF3D7_1200600,PF3D7_1240300,PF3D7_1240600,PF3D7_1253700,PF3D7_1300300,	20.5	8.34	15.77	3.47E-31	2.03E-29	4.06E-29
		GO:0033644	host cell membrane	242	46	PF3D7_0100100,PF3D7_0114700,PF3D7_0115700,PF3D7_0324800,PF3D7_0400100,PF3D7_0400400,PF3D7_0412400,PF3D7_0413200,PF3D7_0420700,PF3D7_0421100,PF3D7_0425800,PF3D7_0600200,PF3D7_0617400,PF3D7_0631800,PF3D7_0632500,PF3D7_0632800,PF3D7_0711700,PF3D7_0712000,PF3D7_0712300,PF3D7_0712400,PF3D7_0712600,PF3D7_0712800,PF3D7_0712900,PF3D7_0713000,PF3D7_0800200,PF3D7_0800300,PF3D7_0808600,PF3D7_0808700,PF3D7_0809100,PF3D7_0833000,PF3D7_0900100,PF3D7_0936500,PF3D7_0937300,PF3D7_0937800,PF3D7_1000100,PF3D7_1000500,PF3D7_1041300,PF3D7_1100100,PF3D7_1100200,PF3D7_1200100,PF3D7_1200400,PF3D7_1200600,PF3D7_1240300,PF3D7_1240600,PF3D7_1253700,PF3D7_1300300,	19	7.71	14.44	2.49E-30	9.69E-29	2.91E-28
		GO:0033643	host cell part	630	55	PF3D7_0100100,PF3D7_0114200,PF3D7_0114700,PF3D7_0115000,PF3D7_0115700,PF3D7_0313500,PF3D7_0324800,PF3D7_0400100,PF3D7_0400400,PF3D7_0402600,PF3D7_0405300,PF3D7_0412400,PF3D7_0413200,PF3D7_0420700,PF3D7_0421100,PF3D7_0424400,PF3D7_0425800,PF3D7_0600200,PF3D7_0617400,PF3D7_0631800,PF3D7_0632500,PF3D7_0632800,PF3D7_0711700,PF3D7_0712000,PF3D7_0712300,PF3D7_0712400,PF3D7_0712600,PF3D7_0712800,PF3D7_0712900,PF3D7_0713000,PF3D7_0726200,PF3D7_0800200,PF3D7_0800300,PF3D7_0808600,PF3D7_0808700,PF3D7_0809100,PF3D7_0831100,PF3D7_0833000,PF3D7_0900100,PF3D7_0903800,PF3D7_0936500,PF3D7_0937300,PF3D7_0937800,PF3D7_1000100,PF3D7_1000500,PF3D7_1041300,PF3D7_1100100,PF3D7_1100200,PF3D7_1200100,PF3D7_1200400,PF3D7_1200600,PF3D7_1240300,PF3D7_1240600,PF3D7_1253700,PF3D7_1300300,	8.7	3.54	6.14	3.17E-19	9.27E-18	3.71E-17
		GO:0033655	host cell cytoplasm part	524	50	PF3D7_0100100,PF3D7_0114200,PF3D7_0115700,PF3D7_0313500,PF3D7_0324800,PF3D7_0400100,PF3D7_0400400,PF3D7_0402600,PF3D7_0405300,PF3D7_0412400,PF3D7_0413200,PF3D7_0420700,PF3D7_0421100,PF3D7_0424400,PF3D7_0425800,PF3D7_0600200,PF3D7_0617400,PF3D7_0632500,PF3D7_0632800,PF3D7_0711700,PF3D7_0712000,PF3D7_0712300,PF3D7_0712400,PF3D7_0712600,PF3D7_0712800,PF3D7_0712900,PF3D7_0713000,PF3D7_0800200,PF3D7_0800300,PF3D7_0808600,PF3D7_0808700,PF3D7_0809100,PF3D7_0833000,PF3D7_0900100,PF3D7_0903800,PF3D7_0936500,PF3D7_0937300,PF3D7_0937800,PF3D7_1	9.5	3.87	6.44	6.65E-19	1.56E-17	7.78E-17

University of Ghana http://ugspace.ug.edu.gh

						000100,PF3D7_1000500,PF3D7_1041300,PF3D7_1100100,PF3D7_1100200,PF3D7_1200100,PF3D7_1200400,PF3D7_1200600,PF3D7_1240300,PF3D7_1240600,PF3D7_1253700,PF3D7_1300300,						
		GO: 0030430	host cell cytoplasm	540	50	PF3D7_0100100,PF3D7_0114200,PF3D7_0115700,PF3D7_0313500,PF3D7_0324800,PF3D7_0400100,PF3D7_0400400,PF3D7_0402600,PF3D7_0405300,PF3D7_0412400,PF3D7_0413200,PF3D7_0420700,PF3D7_0421100,PF3D7_0424400,PF3D7_0425800,PF3D7_0600200,PF3D7_0617400,PF3D7_0632500,PF3D7_0632800,PF3D7_0711700,PF3D7_0712000,PF3D7_0712300,PF3D7_0712400,PF3D7_0712600,PF3D7_0712800,PF3D7_0712900,PF3D7_0713000,PF3D7_0800200,PF3D7_0800300,PF3D7_0808600,PF3D7_0808700,PF3D7_0809100,PF3D7_0833000,PF3D7_0900100,PF3D7_0903800,PF3D7_0936500,PF3D7_0937300,PF3D7_0937800,PF3D7_1000100,PF3D7_1000500,PF3D7_1041300,PF3D7_1100100,PF3D7_1100200,PF3D7_1200100,PF3D7_1200400,PF3D7_1200600,PF3D7_1240300,PF3D7_1240600,PF3D7_1253700,PF3D7_1300300,	9.3	3.76	6.21	2.50 E-18	4.87 E-17	2.92 E-16
		GO: 0043657	host cell	713	57	PF3D7_0100100,PF3D7_0114200,PF3D7_0114700,PF3D7_0115000,PF3D7_0115700,PF3D7_0313500,PF3D7_0324800,PF3D7_0400100,PF3D7_0400400,PF3D7_0402600,PF3D7_0405300,PF3D7_0412400,PF3D7_0413200,PF3D7_0420700,PF3D7_0421100,PF3D7_0424400,PF3D7_0425800,PF3D7_0600200,PF3D7_0617400,PF3D7_0631800,PF3D7_0632500,PF3D7_0632800,PF3D7_0711700,PF3D7_0712000,PF3D7_0712300,PF3D7_0712400,PF3D7_0712600,PF3D7_0712800,PF3D7_0712900,PF3D7_0713000,PF3D7_0726200,PF3D7_0800200,PF3D7_0800300,PF3D7_0808600,PF3D7_0808700,PF3D7_0809100,PF3D7_0831100,PF3D7_0833000,PF3D7_0900100,PF3D7_0903800,PF3D7_0936500,PF3D7_0937300,PF3D7_0937800,PF3D7_1000100,PF3D7_1000500,PF3D7_1041300,PF3D7_1100100,PF3D7_1100200,PF3D7_1200100,PF3D7_1200400,PF3D7_1200600,PF3D7_1240300,PF3D7_1240600,PF3D7_1253700,PF3D7_1300300,PF3D7_1371900,PF3D7_1372100,	8	3.24	5.64	3.59 E-18	5.25 E-17	4.20 E-16
		GO: 0018995	host cellular component	713	57	PF3D7_0100100,PF3D7_0114200,PF3D7_0114700,PF3D7_0115000,PF3D7_0115700,PF3D7_0313500,PF3D7_0324800,PF3D7_0400100,PF3D7_0400400,PF3D7_0402600,PF3D7_0405300,PF3D7_0412400,PF3D7_0413200,PF3D7_0420700,PF3D7_0421100,PF3D7_0424400,PF3D7_0425800,PF3D7_0600200,PF3D7_0617400,PF3D7_0631800,PF3D7_0632500,PF3D7_0632800,PF3D7_0711700,PF3D7_0712000,PF3D7_0712300,PF3D7_0712400,PF3D7_0712600,PF3D7_0712800,PF3D7_0712900,PF3D7_0713000,PF3D7_0726200,PF3D7_0800200,PF3D7_0800300,PF3D7_0808600,PF3D7_0808700,PF3D7_0809100,PF3D7_0831100,PF3D7_0833000,PF3D7_0900100,PF3D7_0903800,PF3D7_0936500,PF3D7_0937300,PF3D7_0937800,PF3D7_1000100,PF3D7_1000500,PF3D7_1041300,PF3D7_1100100,PF3D7_1100200,PF3D7_1200100,PF3D7_1200400,PF3D7_1200600,PF3D7_1240300,PF3D7_1240600,PF3D7_1253700,PF3D7_1300300,PF3D7_1371900,PF3D7_1372100,	8	3.24	5.64	3.59 E-18	5.25 E-17	4.20 E-16
		GO: 0033646	host intracellular part	549	50	PF3D7_0100100,PF3D7_0114200,PF3D7_0115700,PF3D7_0313500,PF3D7_0324800,PF3D7_0400100,PF3D7_0400400,PF3D7_0402600,PF3D7_0405300,PF3D7_0412400,PF3D7_0413200,PF3D7_0420700,PF3D7_0421100,PF3D7_0424400,PF3D7_0425800,PF3D7_0600200,PF3D7_0617400,PF3D7_0632500,PF3D7_0632800,PF3D7_0711700,PF3D7_0712000,PF3D7_0712300,PF3D7_0712400,PF3D7_0712600,PF3D7_0712800,PF3D7_0712900,PF3D7_0713000,PF3D7_0800200,PF3D7_0800300,PF3D7_0808600,PF3D7_0808700,PF3D7_0809100,PF3D7_0833000,PF3D7_0900100,PF3D7_0903800,PF3D7_0936500,PF3D7_0937300,PF3D7_0937800,PF3D7_1	9.1	3.69	6.08	5.15 E-18	6.52 E-17	6.02 E-16

University of Ghana http://ugspace.ug.edu.gh

						000100,PF3D7_1000500,PF3D7_1041300,PF3D7_1100100,PF3D7_1100200,PF3D7_1200100,PF3D7_1200400,PF3D7_1200600,PF3D7_1240300,PF3D7_1240600,PF3D7_1253700,PF3D7_1300300,						
		GO:0043656	host intracellular region	550	50	PF3D7_0400100,PF3D7_0114200,PF3D7_0115700,PF3D7_0335500,PF3D7_0324300,PF3D7_0400100,PF3D7_0400400,PF3D7_0402600,PF3D7_0405300,PF3D7_0412400,PF3D7_0413200,PF3D7_0420700,PF3D7_0421100,PF3D7_0424400,PF3D7_0425800,PF3D7_0600200,PF3D7_0617400,PF3D7_0632500,PF3D7_0632800,PF3D7_0711700,PF3D7_0712000,PF3D7_0712300,PF3D7_0712400,PF3D7_0712600,PF3D7_0712800,PF3D7_0712900,PF3D7_0713000,PF3D7_0800200,PF3D7_0800300,PF3D7_0808600,PF3D7_0808700,PF3D7_0809100,PF3D7_0833000,PF3D7_0900100,PF3D7_0903800,PF3D7_0936500,PF3D7_0937300,PF3D7_0937800,PF3D7_1000100,PF3D7_1000500,PF3D7_1041300,PF3D7_1100100,PF3D7_1100200,PF3D7_1200100,PF3D7_1200400,PF3D7_1200600,PF3D7_1240300,PF3D7_1240600,PF3D7_1253700,PF3D7_1300300,	9.1	3.69	6.07	5.57E-18	6.52E-17	6.52E-16
		GO:0016021	integral component of membrane	1297	71	PF3D7_0100100,PF3D7_0104700,PF3D7_0114200,PF3D7_0114700,PF3D7_0115000,PF3D7_0115700,PF3D7_0208900,PF3D7_0300100,PF3D7_0324800,PF3D7_0324900,PF3D7_0400100,PF3D7_0400400,PF3D7_0402600,PF3D7_0405300,PF3D7_0412400,PF3D7_0413200,PF3D7_0418800,PF3D7_0420700,PF3D7_0421100,PF3D7_0425800,PF3D7_0600200,PF3D7_0617400,PF3D7_0618400,PF3D7_0631800,PF3D7_0632500,PF3D7_0632800,PF3D7_0711700,PF3D7_0712000,PF3D7_0712300,PF3D7_0712400,PF3D7_0712600,PF3D7_0712800,PF3D7_0712900,PF3D7_0713000,PF3D7_0726200,PF3D7_0800200,PF3D7_0800300,PF3D7_0808600,PF3D7_0808700,PF3D7_0809100,PF3D7_0827700,PF3D7_0831100,PF3D7_0833000,PF3D7_0833500,PF3D7_0900100,PF3D7_0923300,PF3D7_0925100,PF3D7_0936500,PF3D7_0937300,PF3D7_0937800,PF3D7_1000100,PF3D7_1000500,PF3D7_1041300,PF3D7_1100100,PF3D7_1100200,PF3D7_1200100,PF3D7_1200400,PF3D7_1200600,PF3D7_1240300,PF3D7_1240600,PF3D7_1240900,PF3D7_1300100,PF3D7_1300300,PF3D7_1360500,PF3D7_1369400,PF3D7_1372100,PF3D7_1373300,PF3D7_1373500,PF3D7_1442600,PF3D7_1475400,PF3D7_1475800,	5.5	2.22	4.16	3.18E-14	3.38E-13	3.72E-12
		GO:0031224	intrinsic component of membrane	1314	71	PF3D7_0100100,PF3D7_0104700,PF3D7_0114200,PF3D7_0114700,PF3D7_0115000,PF3D7_0115700,PF3D7_0208900,PF3D7_0300100,PF3D7_0324800,PF3D7_0324900,PF3D7_0400100,PF3D7_0400400,PF3D7_0402600,PF3D7_0405300,PF3D7_0412400,PF3D7_0413200,PF3D7_0418800,PF3D7_0420700,PF3D7_0421100,PF3D7_0425800,PF3D7_0600200,PF3D7_0617400,PF3D7_0618400,PF3D7_0631800,PF3D7_0632500,PF3D7_0632800,PF3D7_0711700,PF3D7_0712000,PF3D7_0712300,PF3D7_0712400,PF3D7_0712600,PF3D7_0712800,PF3D7_0712900,PF3D7_0713000,PF3D7_0726200,PF3D7_0800200,PF3D7_0800300,PF3D7_0808600,PF3D7_0808700,PF3D7_0809100,PF3D7_0827700,PF3D7_0831100,PF3D7_0833000,PF3D7_0833500,PF3D7_0900100,PF3D7_0923300,PF3D7_0925100,PF3D7_0936500,PF3D7_0937300,PF3D7_0937800,PF3D7_1000100,PF3D7_1000500,PF3D7_1041300,PF3D7_1100100,PF3D7_1100200,PF3D7_1200100,PF3D7_1200400,PF3D7_1200600,PF3D7_1240300,PF3D7_1240600,PF3D7_1240900,PF3D7_1300100,PF3D7_1300300,PF3D7_1360500,PF3D7_1369400,PF3D7_1372100,PF3D7_1373300,PF3D7_1373500,PF3D7_1442600,PF3D7_1475400,PF3D7_1475800,	5.4	2.19	4.09	6.53E-14	6.37E-13	7.64E-12

University of Ghana http://ugspace.ug.edu.gh

University of Ghana http://ugspace.ug.edu.gh

		GO:0044312	crystalloid	17	3	PF3D7_0418800,PF3D7_0903800,PF3D7_1207300,	17.6	7.16	8.67	0.007717 1	0.069453 92	0.902900975
		GO:0020003	symbiont-containing vacuole	205	11	PF3D7_0324800,PF3D7_0405300,PF3D7_0413200,PF3D7_0424400,PF3D7_0713000,PF3D7_0833000,PF3D7_0903800,PF3D7_0936500,PF3D7_0937300,PF3D7_1000500,PF3D7_1253700,	5.4	2.18	2.37	0.011683 7	0.097642 33	1
		GO:0005576	extracellular region	334	14	PF3D7_0324800,PF3D7_0405300,PF3D7_0413200,PF3D7_0424400,PF3D7_0713000,PF3D7_0827200,PF3D7_0833000,PF3D7_0903800,PF3D7_0909000,PF3D7_0936500,PF3D7_0937300,PF3D7_1000500,PF3D7_1253700,PF3D7_1403200,	4.2	1.7	1.83	0.034118 26	0.266122 45	1
		GO:0044228	host cell surface	31	3	PF3D7_0115000,PF3D7_0424400,PF3D7_0831100,	9.7	3.93	4.32	0.039771 66	0.290830 29	1
		GO:0005892	acetylcholine-gated channel complex	2	1	PF3D7_0418800,	50	20.28	39.89	0.048698 84	0.299882 33	1
		GO:0043235	receptor complex	2	1	PF3D7_0418800,	50	20.28	39.89	0.048698 84	0.299882 33	1
		GO:0098802	plasma membrane signaling receptor complex	2	1	PF3D7_0418800,	50	20.28	39.89	0.048698 84	0.299882 33	1
	Downregulated	GO:0045177	apical part of cell	147	57	PF3D7_0102500,PF3D7_0104100,PF3D7_0206200,PF3D7_0210600,PF3D7_0212600,PF3D7_0214900,PF3D7_0220800,PF3D7_0302200,PF3D7_0302500,PF3D7_0404700,PF3D7_0405200,PF3D7_0405900,PF3D7_0414900,PF3D7_0419700,PF3D7_0423400,PF3D7_0424100,PF3D7_0501500,PF3D7_0501600,PF3D7_0503600,PF3D7_0507500,PF3D7_0511600,PF3D7_0528400,PF3D7_0612700,PF3D7_0613300,PF3D7_0707300,PF3D7_0722200,PF3D7_0731500,PF3D7_0802600,PF3D7_0808200,PF3D7_0817700,PF3D7_0828800,PF3D7_0905400,PF3D7_0929400,PF3D7_0935800,PF3D7_1012200,PF3D7_1017100,PF3D7_1023000,PF3D7_1028700,PF3D7_1030200,PF3D7_1035900,PF3D7_1116000,PF3D7_1116800,PF3D7_1118700,PF3D7_1133400,PF3D7_1218000,PF3D7_1243400,PF3D7_1252100,PF3D7_1301600,PF3D7_1318000,PF3D7_1332200,PF3D7_1335300,PF3D7_1335400,PF3D7_1361800,PF3D7_1410400,PF3D7_1412000,PF3D7_1452000,PF3D7_1463900,	38.8	7.43	14.54	8.32E-37	1.72E-34	1.72E-34

		GO: 0020007	apical complex	104	47	PF3D7_0102500,PF3D7_0206200,PF3D7_0210600,PF3D7_0212600,PF3D7_0214900,PF3D7_0220800,PF3D7_0302200,PF3D7_0302500,PF3D7_0405200,PF3D7_0405900,PF3D7_0414900,PF3D7_0419700,PF3D7_0423400,PF3D7_0424100,PF3D7_0501500,PF3D7_0501600,PF3D7_0507500,PF3D7_0511600,PF3D7_0528400,PF3D7_0612700,PF3D7_0613300,PF3D7_0707300,PF3D7_0722200,PF3D7_0731500,PF3D7_0802600,PF3D7_0808200,PF3D7_0817700,PF3D7_0828800,PF3D7_0905400,PF3D7_0929400,PF3D7_0935800,PF3D7_1012200,PF3D7_1017100,PF3D7_1028700,PF3D7_1030200,PF3D7_1116000,PF3D7_1116800,PF3D7_1133400,PF3D7_1218000,PF3D7_1252100,PF3D7_1301600,PF3D7_1332200,PF3D7_1335300,PF3D7_1335400,PF3D7_1410400,PF3D7_1452000,PF3D7_1463900,	45.2	8.66	18.15	5.88E-34	6.08E-32	1.22E-31
		GO: 0020008	rhoptry	52	35	PF3D7_0210600,PF3D7_0212600,PF3D7_0214900,PF3D7_0220800,PF3D7_0302200,PF3D7_0302500,PF3D7_0405200,PF3D7_0405900,PF3D7_0414900,PF3D7_0419700,PF3D7_0423400,PF3D7_0424100,PF3D7_0501500,PF3D7_0501600,PF3D7_0511600,PF3D7_0528400,PF3D7_0612700,PF3D7_0613300,PF3D7_0707300,PF3D7_0722200,PF3D7_0802600,PF3D7_0817700,PF3D7_0905400,PF3D7_0929400,PF3D7_0935800,PF3D7_1012200,PF3D7_1017100,PF3D7_1116000,PF3D7_1218000,PF3D7_1252100,PF3D7_1335300,PF3D7_1335400,PF3D7_1410400,PF3D7_1452000,PF3D7_1463900,	67.3	12.9	43.22	1.28E-33	8.82E-32	2.65E-31
		GO: 0009986	cell surface	159	46	PF3D7_0102700,PF3D7_0104100,PF3D7_0212600,PF3D7_0308300,PF3D7_0404900,PF3D7_0424100,PF3D7_0506900,PF3D7_0515700,PF3D7_0612700,PF3D7_0816500,PF3D7_0818900,PF3D7_0828800,PF3D7_0905400,PF3D7_0917900,PF3D7_0918000,PF3D7_0922200,PF3D7_1012200,PF3D7_1014100,PF3D7_1017100,PF3D7_1017500,PF3D7_1028600,PF3D7_1028700,PF3D7_1028900,PF3D7_1035300,PF3D7_1035400,PF3D7_1035500,PF3D7_1035700,PF3D7_1035900,PF3D7_1036000,PF3D7_1115800,PF3D7_1140400,PF3D7_1218000,PF3D7_1228600,PF3D7_1237700,PF3D7_1246200,PF3D7_1252100,PF3D7_1323700,PF3D7_1342600,PF3D7_1361800,PF3D7_1409400,PF3D7_1431400,PF3D7_1434400,PF3D7_1437300,PF3D7_1440900,PF3D7_1444800,PF3D7_1452000,	28.9	5.54	8.81	2.83E-23	1.47E-21	5.86E-21
		GO: 1903561	extracellular vesicle	91	31	PF3D7_0102200,PF3D7_0102500,PF3D7_0202500,PF3D7_0207600,PF3D7_0302500,PF3D7_0501300,PF3D7_0501500,PF3D7_0501600,PF3D7_0714000,PF3D7_0731500,PF3D7_0818900,PF3D7_0905400,PF3D7_0917900,PF3D7_0918000,PF3D7_0922200,PF3D7_0929400,PF3D7_0930300,PF3D7_1006200,PF3D7_1014100,PF3D7_1035300,PF3D7_1035700,PF3D7_1105000,PF3D7_1116800,PF3D7_1122800,PF3D7_1223100,PF3D7_1228600,PF3D7_1246200,PF3D7_1252100,PF3D7_1343000,PF3D7_1410400,PF3D7_1444800,	34.1	6.53	10.55	3.58E-18	1.48E-16	7.42E-16
		GO: 1990225	rhoptry neck	14	13	PF3D7_0214900,PF3D7_0405900,PF3D7_0419700,PF3D7_0423400,PF3D7_0511600,PF3D7_0722200,PF3D7_0817700,PF3D7_1017100,PF3D7_1116000,PF3D7_1335300,PF3D7_1335400,PF3D7_1452000,PF3D7_1463900,	92.9	17.8	248.83	2.11E-16	7.28E-15	4.37E-14
		GO: 0065010	extracellular membrane-bounded organelle	280	51	PF3D7_0102200,PF3D7_0102500,PF3D7_0104100,PF3D7_0104200,PF3D7_0202500,PF3D7_0207500,PF3D7_0207600,PF3D7_0207700,PF3D7_0214900,PF3D7_0217500,PF3D7_0302500,PF3D7_0404700,PF3D7_0404900,PF3D7_0501300,PF3D7_0501500,PF3D7_0501600,PF3D7_0503600,PF3D7_0507400,PF3D7_0507500,PF3D7_0612700,PF3D7_0707300,PF3D7_0714000,PF3D7_0731500,PF3D7_0818900,PF3D7_0905400,PF3D7_0917900,PF3D7_0918000,PF3D7_0922200,PF3D7_0925900,PF3D7_0929400,PF3D7_09303	18.2	3.49	4.81	3.80E-16	1.12E-14	7.87E-14

University of Ghana http://ugspace.ug.edu.gh

						00,PF3D7_1006200,PF3D7_1014100,PF3D7_1017100,PF3D7_1035200,PF3D7_1035300,PF3D7_1035700,PF3D7_1102700,PF3D7_1102800,PF3D7_1105000,PF3D7_1116800,PF3D7_1122800,PF3D7_1223100,PF3D7_1228600,PF3D7_1246200,PF3D7_1252100,PF3D7_1343000,PF3D7_1401400,PF3D7_1406300,PF3D7_1410400,PF3D7_1444800,						
		GO: 0005576	extracellular region	334	56	PF3D7_0102200,PF3D7_0102500,PF3D7_0104100,PF3D7_0104200,PF3D7_0202500,PF3D7_0207400,PF3D7_0207500,PF3D7_0207600,PF3D7_0207700,PF3D7_0207800,PF3D7_0214900,PF3D7_0217500,PF3D7_0302500,PF3D7_0404700,PF3D7_0404900,PF3D7_0424100,PF3D7_0501300,PF3D7_0501400,PF3D7_0501500,PF3D7_0501600,PF3D7_0503600,PF3D7_0507200,PF3D7_0507400,PF3D7_0507500,PF3D7_0612700,PF3D7_0707300,PF3D7_0714000,PF3D7_0731500,PF3D7_0818900,PF3D7_0905400,PF3D7_0917900,PF3D7_0918000,PF3D7_0922200,PF3D7_0925900,PF3D7_0929400,PF3D7_0930300,PF3D7_1006200,PF3D7_1014100,PF3D7_1017100,PF3D7_1035200,PF3D7_1035300,PF3D7_1035700,PF3D7_1102700,PF3D7_1102800,PF3D7_1105000,PF3D7_1116800,PF3D7_1122800,PF3D7_1223100,PF3D7_1228600,PF3D7_1246200,PF3D7_1252100,PF3D7_1343000,PF3D7_1401400,PF3D7_1406300,PF3D7_1410400,PF3D7_1444800,	16.8	3.21	4.41	5.04 E-16	1.19 E-14	1.04 E-13
		GO: 0043230	extracellular organelle	282	51	PF3D7_0102200,PF3D7_0102500,PF3D7_0104100,PF3D7_0104200,PF3D7_0202500,PF3D7_0207500,PF3D7_0207600,PF3D7_0207700,PF3D7_0214900,PF3D7_0217500,PF3D7_0302500,PF3D7_0404700,PF3D7_0404900,PF3D7_0501300,PF3D7_0501500,PF3D7_0501600,PF3D7_0503600,PF3D7_0507400,PF3D7_0507500,PF3D7_0612700,PF3D7_0707300,PF3D7_0714000,PF3D7_0731500,PF3D7_0818900,PF3D7_0905400,PF3D7_0917900,PF3D7_0918000,PF3D7_0922200,PF3D7_0925900,PF3D7_0929400,PF3D7_0930300,PF3D7_1006200,PF3D7_1014100,PF3D7_1017100,PF3D7_1035200,PF3D7_1035300,PF3D7_1035700,PF3D7_1102700,PF3D7_1102800,PF3D7_1105000,PF3D7_1116800,PF3D7_1122800,PF3D7_1223100,PF3D7_1228600,PF3D7_1246200,PF3D7_1252100,PF3D7_1343000,PF3D7_1401400,PF3D7_1406300,PF3D7_1410400,PF3D7_1444800,	18.1	3.47	4.77	5.19 E-16	1.19 E-14	1.07 E-13
		GO: 0031982	vesicle	288	48	PF3D7_0102200,PF3D7_0102500,PF3D7_0202500,PF3D7_0206200,PF3D7_0207600,PF3D7_0302500,PF3D7_0424100,PF3D7_0501300,PF3D7_0501500,PF3D7_0501600,PF3D7_0503600,PF3D7_0507500,PF3D7_0613900,PF3D7_0618000,PF3D7_0702200,PF3D7_0714000,PF3D7_0731500,PF3D7_0818900,PF3D7_0828800,PF3D7_0905400,PF3D7_0917900,PF3D7_0918000,PF3D7_0922200,PF3D7_0925900,PF3D7_0929400,PF3D7_0930300,PF3D7_1006200,PF3D7_1014100,PF3D7_1019900,PF3D7_1035300,PF3D7_1035700,PF3D7_1105000,PF3D7_1116000,PF3D7_1116800,PF3D7_1122800,PF3D7_1223100,PF3D7_1228600,PF3D7_1229800,PF3D7_1237700,PF3D7_1246200,PF3D7_1246300,PF3D7_1252100,PF3D7_1342600,PF3D7_1343000,PF3D7_1361500,PF3D7_1406300,PF3D7_1410400,PF3D7_1444800,	16.7	3.19	4.25	1.18 E-13	2.45 E-12	2.45 E-11
		GO: 0020039	pellicle	65	20	PF3D7_0109000,PF3D7_0304000,PF3D7_0308300,PF3D7_0515700,PF3D7_0525800,PF3D7_0805200,PF3D7_0816500,PF3D7_0822900,PF3D7_0918000,PF3D7_1003600,PF3D7_1017500,PF3D7_1028900,PF3D7_1222700,PF3D7_1246400,PF3D7_1251200,PF3D7_1310700,PF3D7_1323700,PF3D7_1342600,PF3D7_1351700,PF3D7_1460600,	30.8	5.9	8.68	3.67 E-11	6.90 E-10	7.59 E-09

University of Ghana http://ugspace.ug.edu.gh

		GO:0070258	inner membrane pellicle complex	63	19	PF3D7_0109000,PF3D7_0304000,PF3D7_0308300,PF3D7_0515700,PF3D7_0525800,PF3D7_0805200,PF3D7_0816500,PF3D7_0822900,PF3D7_0918000,PF3D7_1003600,PF3D7_1017500,PF3D7_1028900,PF3D7_1222700,PF3D7_1246400,PF3D7_1310700,PF3D7_1323700,PF3D7_1342600,PF3D7_1351700,PF3D7_1460600,	30.2	5.78	8.4	1.71E-10	2.95E-09	3.54E-08
		GO:0000323	lytic vacuole	111	23	PF3D7_0102200,PF3D7_0207400,PF3D7_0207500,PF3D7_0207600,PF3D7_0207700,PF3D7_0207800,PF3D7_0404700,PF3D7_0501500,PF3D7_0501600,PF3D7_0618000,PF3D7_0818900,PF3D7_0917900,PF3D7_0918000,PF3D7_0922200,PF3D7_0925900,PF3D7_0930300,PF3D7_1006200,PF3D7_1116000,PF3D7_1237700,PF3D7_1246200,PF3D7_1343000,PF3D7_1406300,PF3D7_1410400,	20.7	3.97	5.12	7.06E-09	1.04E-07	1.46E-06
		GO:0005764	lysosome	111	23	PF3D7_0102200,PF3D7_0207400,PF3D7_0207500,PF3D7_0207600,PF3D7_0207700,PF3D7_0207800,PF3D7_0404700,PF3D7_0501500,PF3D7_0501600,PF3D7_0618000,PF3D7_0818900,PF3D7_0917900,PF3D7_0918000,PF3D7_0922200,PF3D7_0925900,PF3D7_0930300,PF3D7_1006200,PF3D7_1116000,PF3D7_1237700,PF3D7_1246200,PF3D7_1343000,PF3D7_1406300,PF3D7_1410400,	20.7	3.97	5.12	7.06E-09	1.04E-07	1.46E-06
		GO:0031225	anchored component of membrane	30	12	PF3D7_0206800,PF3D7_0207000,PF3D7_0404900,PF3D7_0405900,PF3D7_0414900,PF3D7_0419700,PF3D7_0612700,PF3D7_0620400,PF3D7_0707300,PF3D7_0828800,PF3D7_0930300,PF3D7_1136200,	40	7.67	12.66	1.18E-08	1.62E-07	2.43E-06
		GO:0005773	vacuole	126	24	PF3D7_0102200,PF3D7_0207400,PF3D7_0207500,PF3D7_0207600,PF3D7_0207700,PF3D7_0207800,PF3D7_0404700,PF3D7_0501500,PF3D7_0501600,PF3D7_0618000,PF3D7_0818900,PF3D7_0917900,PF3D7_0918000,PF3D7_0922200,PF3D7_0925900,PF3D7_0930300,PF3D7_1006200,PF3D7_1035200,PF3D7_1116000,PF3D7_1237700,PF3D7_1246200,PF3D7_1343000,PF3D7_1406300,PF3D7_1410400,	19	3.65	4.62	1.90E-08	2.32E-07	3.93E-06
		GO:0020004	symbiont-containing vacuolar space	6	6	PF3D7_0207600,PF3D7_0217500,PF3D7_0404900,PF3D7_0501300,PF3D7_0507500,PF3D7_0612700,	100	19.17	inf	1.91E-08	2.32E-07	3.95E-06
		GO:0020003	symbiont-containing vacuole	205	30	PF3D7_0102200,PF3D7_0104100,PF3D7_0104200,PF3D7_0202500,PF3D7_0207500,PF3D7_0207600,PF3D7_0207700,PF3D7_0214900,PF3D7_0217500,PF3D7_0404700,PF3D7_0404900,PF3D7_0501300,PF3D7_0503600,PF3D7_0507400,PF3D7_0507500,PF3D7_0612700,PF3D7_0707300,PF3D7_0925900,PF3D7_1014100,PF3D7_1017100,PF3D7_1035200,PF3D7_1035300,PF3D7_1102700,PF3D7_1102800,PF3D7_1116800,PF3D7_1228600,PF3D7_1252100,PF3D7_1401400,PF3D7_1406300,PF3D7_1410400,	14.6	2.8	3.4	1.66E-07	1.91E-06	3.44E-05
		GO:0020009	microneme	40	12	PF3D7_0102500,PF3D7_0206200,PF3D7_0212600,PF3D7_0405900,PF3D7_0731500,PF3D7_0828800,PF3D7_1017100,PF3D7_1028700,PF3D7_1030200,PF3D7_1133400,PF3D7_1218000,PF3D7_1301600,	30	5.75	8.12	4.75E-07	5.17E-06	9.83E-05
		GO:0046658	anchored component of plasma membrane	28	10	PF3D7_0206800,PF3D7_0207000,PF3D7_0404900,PF3D7_0405900,PF3D7_0419700,PF3D7_0612700,PF3D7_0620400,PF3D7_0828800,PF3D7_0930300,PF3D7_1136200,	35.7	6.84	10.46	7.15E-07	7.40E-06	0.000148017

University of Ghana http://ugspace.ug.edu.gh

University of Ghana http://ugspace.ug.edu.gh

		GO:0015629	actin cytoskeleton	29	10	PF3D7_0105300,PF3D7_0503400,PF3D7_0503600,PF3D7_0613900,PF3D7_0932200,PF3D7_1118700,PF3D7_1229800,PF3D7_1246200,PF3D7_1342600,PF3D7_1361400,	34.5	6.61	9.91	1.04E-06	1.03E-05	0.000215649
		GO:0000786	nucleosome	9	6	PF3D7_0320900,PF3D7_0617800,PF3D7_0714000,PF3D7_1105000,PF3D7_1105100,PF3D7_1439500,	66.7	12.78	37.19	1.40E-06	1.32E-05	0.000290037
		GO:0005767	secondary lysosome	97	17	PF3D7_0102200,PF3D7_0501500,PF3D7_0501600,PF3D7_0618000,PF3D7_0818900,PF3D7_0917900,PF3D7_0918000,PF3D7_0922200,PF3D7_0925900,PF3D7_0930300,PF3D7_1006200,PF3D7_1116000,PF3D7_1237700,PF3D7_1246200,PF3D7_1343000,PF3D7_1406300,PF3D7_1410400,	17.5	3.36	4.07	8.06E-06	6.37E-05	0.001668058
		GO:0020020	food vacuole	97	17	PF3D7_0102200,PF3D7_0501500,PF3D7_0501600,PF3D7_0618000,PF3D7_0818900,PF3D7_0917900,PF3D7_0918000,PF3D7_0922200,PF3D7_0925900,PF3D7_0930300,PF3D7_1006200,PF3D7_1116000,PF3D7_1237700,PF3D7_1246200,PF3D7_1343000,PF3D7_1406300,PF3D7_1410400,	17.5	3.36	4.07	8.06E-06	6.37E-05	0.001668058
		GO:0045335	phagocytic vesicle	97	17	PF3D7_0102200,PF3D7_0501500,PF3D7_0501600,PF3D7_0618000,PF3D7_0818900,PF3D7_0917900,PF3D7_0918000,PF3D7_0922200,PF3D7_0925900,PF3D7_0930300,PF3D7_1006200,PF3D7_1116000,PF3D7_1237700,PF3D7_1246200,PF3D7_1343000,PF3D7_1406300,PF3D7_1410400,	17.5	3.36	4.07	8.06E-06	6.37E-05	0.001668058
		GO:0032010	phagolysosome	97	17	PF3D7_0102200,PF3D7_0501500,PF3D7_0501600,PF3D7_0618000,PF3D7_0818900,PF3D7_0917900,PF3D7_0918000,PF3D7_0922200,PF3D7_0925900,PF3D7_0930300,PF3D7_1006200,PF3D7_1116000,PF3D7_1237700,PF3D7_1246200,PF3D7_1343000,PF3D7_1406300,PF3D7_1410400,	17.5	3.36	4.07	8.06E-06	6.37E-05	0.001668058
		GO:0005615	extracellular space	22	8	PF3D7_0207400,PF3D7_0207500,PF3D7_0207600,PF3D7_0207700,PF3D7_0207800,PF3D7_0404700,PF3D7_0501400,PF3D7_0507200,	36.4	6.97	10.69	8.31E-06	6.37E-05	0.001720685
		GO:0020005	symbiont-containing vacuole membrane	44	11	PF3D7_0104100,PF3D7_0202500,PF3D7_0207500,PF3D7_0217500,PF3D7_0404700,PF3D7_0501300,PF3D7_0503600,PF3D7_1102700,PF3D7_1102800,PF3D7_1116800,PF3D7_1401400,	25	4.79	6.28	1.04E-05	7.67E-05	0.002146213
		GO:0030139	endocytic vesicle	102	17	PF3D7_0102200,PF3D7_0501500,PF3D7_0501600,PF3D7_0618000,PF3D7_0818900,PF3D7_0917900,PF3D7_0918000,PF3D7_0922200,PF3D7_0925900,PF3D7_0930300,PF3D7_1006200,PF3D7_1116000,PF3D7_1237700,PF3D7_1246200,PF3D7_1343000,PF3D7_1406300,PF3D7_1410400,	16.7	3.19	3.82	1.62E-05	0.001153 1	0.003344135
		GO:0033646	host intracellular part	549	50	PF3D7_0102200,PF3D7_0104100,PF3D7_0104200,PF3D7_0108500,PF3D7_0202100,PF3D7_0202200,PF3D7_0202500,PF3D7_0207000,PF3D7_0207500,PF3D7_0207600,PF3D7_0207700,PF3D7_0214900,PF3D7_0217500,PF3D7_0301300,PF3D7_0401800,PF3D7_0402100,PF3D7_0404700,PF3D7_0404900,PF3D7_0501300,PF3D7_0501400,PF3D7_0503600,PF3D7_0507400,PF3D7_0507500,P	9.1	1.75	2.02	4.02E-05	0.000277 51	0.008325166

University of Ghana http://ugspace.ug.edu.gh

						F3D7_0612700,PF3D7_0702000,PF3D7_0707300,PF3D7_0830500,PF3D7_0905400,PF3D7_0922200,PF3D7_0925900,PF3D7_0929400,PF3D7_0936000,PF3D7_1001000,PF3D7_1001600,PF3D7_1014100,PF3D7_1017100,PF3D7_1035200,PF3D7_1035300,PF3D7_1102700,PF3D7_1102800,PF3D7_1105000,PF3D7_1115800,PF3D7_1116800,PF3D7_1121300,PF3D7_1228600,PF3D7_1252100,PF3D7_1401400,PF3D7_1406300,PF3D7_1410400,PF3D7_1463900,						
		GO:0043656	host intracellular region	550	50	PF3D7_0102200,PF3D7_0104100,PF3D7_0104200,PF3D7_0108500,PF3D7_0202100,PF3D7_0202200,PF3D7_0202500,PF3D7_0207000,PF3D7_0207500,PF3D7_0207600,PF3D7_0207700,PF3D7_0214900,PF3D7_0217500,PF3D7_0301300,PF3D7_0401800,PF3D7_0402100,PF3D7_0404700,PF3D7_0404900,PF3D7_0501300,PF3D7_0501400,PF3D7_0503600,PF3D7_0507400,PF3D7_0507500,PF3D7_0612700,PF3D7_0702000,PF3D7_0707300,PF3D7_0830500,PF3D7_0905400,PF3D7_0922200,PF3D7_0925900,PF3D7_0929400,PF3D7_0936000,PF3D7_1001000,PF3D7_1001600,PF3D7_1014100,PF3D7_1017100,PF3D7_1035200,PF3D7_1035300,PF3D7_1102700,PF3D7_1102800,PF3D7_1105000,PF3D7_1115800,PF3D7_1116800,PF3D7_1121300,PF3D7_1228600,PF3D7_1252100,PF3D7_1401400,PF3D7_1406300,PF3D7_1410400,PF3D7_1463900,	9.1	1.74	2.02	4.22E-05	0.000282 01	0.008742205
		GO:0031226	intrinsic component of plasma membrane	51	11	PF3D7_0206800,PF3D7_0207000,PF3D7_0404900,PF3D7_0405900,PF3D7_0419700,PF3D7_0612700,PF3D7_0620400,PF3D7_0828800,PF3D7_0930300,PF3D7_1116600,PF3D7_1136200,	21.6	4.13	5.18	4.65E-05	0.000300 54	0.009617322
		GO:0033655	host cell cytoplasm part	524	48	PF3D7_0102200,PF3D7_0104100,PF3D7_0104200,PF3D7_0108500,PF3D7_0202100,PF3D7_0202200,PF3D7_0202500,PF3D7_0207000,PF3D7_0207500,PF3D7_0207600,PF3D7_0207700,PF3D7_0214900,PF3D7_0217500,PF3D7_0301300,PF3D7_0401800,PF3D7_0402100,PF3D7_0404700,PF3D7_0404900,PF3D7_0501300,PF3D7_0501400,PF3D7_0503600,PF3D7_0507400,PF3D7_0507500,PF3D7_0612700,PF3D7_0702000,PF3D7_0707300,PF3D7_0830500,PF3D7_0905400,PF3D7_0922200,PF3D7_0925900,PF3D7_0936000,PF3D7_1001000,PF3D7_1001600,PF3D7_1014100,PF3D7_1017100,PF3D7_1035200,PF3D7_1035300,PF3D7_1102700,PF3D7_1102800,PF3D7_1115800,PF3D7_1116800,PF3D7_1121300,PF3D7_1228600,PF3D7_1252100,PF3D7_1401400,PF3D7_1406300,PF3D7_1410400,PF3D7_1463900,	9.2	1.76	2.03	5.11E-05	0.000311 51	0.010581327
		GO:0033643	host cell part	630	55	PF3D7_0102200,PF3D7_0104100,PF3D7_0104200,PF3D7_0108500,PF3D7_0202100,PF3D7_0202200,PF3D7_0202500,PF3D7_0207000,PF3D7_0207500,PF3D7_0207600,PF3D7_0207700,PF3D7_0214900,PF3D7_0217500,PF3D7_0301300,PF3D7_0302200,PF3D7_0302500,PF3D7_0401800,PF3D7_0402100,PF3D7_0404700,PF3D7_0404900,PF3D7_0424100,PF3D7_0501300,PF3D7_0501400,PF3D7_0503600,PF3D7_0507400,PF3D7_0507500,PF3D7_0612700,PF3D7_0702000,PF3D7_0707300,PF3D7_0830500,PF3D7_0905400,PF3D7_0922200,PF3D7_0925900,PF3D7_0929400,PF3D7_0936000,PF3D7_1001000,PF3D7_1001600,PF3D7_1014100,PF3D7_1017100,PF3D7_1035200,PF3D7_1035300,PF3D7_1102700,PF3D7_1102800,PF3D7_1105000,PF3D7_1115800,PF3D7_1116800,PF3D7_1121300,PF3D7_1222700,PF3D7_1228600,PF3D7_1252100,PF3D7_1401400,PF3D7_1406300,PF3D7_1410400,PF3D7_1463900,PF3D7_1476300,	8.7	1.67	1.94	5.12E-05	0.000311 51	0.010591475

		GO:0030430	host cell cytoplasm	540	49	PF3D7_0102200,PF3D7_0104100,PF3D7_0104200,PF3D7_0108500,PF3D7_0202100,PF3D7_0202200,PF3D7_0202500,PF3D7_0207000,PF3D7_0207500,PF3D7_0207600,PF3D7_0207700,PF3D7_0214900,PF3D7_0217500,PF3D7_0301300,PF3D7_0401800,PF3D7_0402100,PF3D7_0404700,PF3D7_0404900,PF3D7_0501300,PF3D7_0501400,PF3D7_0503600,PF3D7_0507400,PF3D7_0507500,PF3D7_0612700,PF3D7_0702000,PF3D7_0707300,PF3D7_0830500,PF3D7_0905400,PF3D7_0922200,PF3D7_0925900,PF3D7_0929400,PF3D7_0936000,PF3D7_1001000,PF3D7_1001600,PF3D7_1014100,PF3D7_1017100,PF3D7_1035200,PF3D7_1035300,PF3D7_1102700,PF3D7_1102800,PF3D7_1115800,PF3D7_1116800,PF3D7_1121300,PF3D7_1228600,PF3D7_1252100,PF3D7_1401400,PF3D7_1406300,PF3D7_1410400,PF3D7_1463900,	9.1	1.74	2.01	5.38E-05	0.000318 36	0.011142 7
		GO:0031410	cytoplasmic vesicle	210	25	PF3D7_0102200,PF3D7_0206200,PF3D7_0424100,PF3D7_0501500,PF3D7_0501600,PF3D7_0507500,PF3D7_0618000,PF3D7_0818900,PF3D7_0828800,PF3D7_0917900,PF3D7_0918000,PF3D7_0922200,PF3D7_0925900,PF3D7_0930300,PF3D7_1006200,PF3D7_1019900,PF3D7_1116000,PF3D7_1116800,PF3D7_1237700,PF3D7_1246200,PF3D7_1246300,PF3D7_1343000,PF3D7_1361500,PF3D7_1406300,PF3D7_1410400,	11.9	2.28	2.61	7.51E-05	0.000422 48	0.015552 303
		GO:0016459	myosin complex	10	5	PF3D7_0503600,PF3D7_0613900,PF3D7_1118700,PF3D7_1229800,PF3D7_1342600,	50	9.58	18.51	7.55E-05	0.000422 48	0.015631 633
		GO:0097708	intracellular vesicle	211	25	PF3D7_0102200,PF3D7_0206200,PF3D7_0424100,PF3D7_0501500,PF3D7_0501600,PF3D7_0507500,PF3D7_0618000,PF3D7_0818900,PF3D7_0828800,PF3D7_0917900,PF3D7_0918000,PF3D7_0922200,PF3D7_0925900,PF3D7_0930300,PF3D7_1006200,PF3D7_1019900,PF3D7_1116000,PF3D7_1116800,PF3D7_1237700,PF3D7_1246200,PF3D7_1246300,PF3D7_1343000,PF3D7_1361500,PF3D7_1406300,PF3D7_1410400,	11.8	2.27	2.6	8.13E-05	0.000442 81	0.016826 624
		GO:0032991	protein-containing complex	16	6	PF3D7_0202200,PF3D7_0424100,PF3D7_0817700,PF3D7_1116000,PF3D7_1323700,PF3D7_1452000,	37.5	7.19	11.14	9.78E-05	0.000516 94	0.020251 474
		GO:0005886	plasma membrane	140	19	PF3D7_0104800,PF3D7_0206200,PF3D7_0206800,PF3D7_0207600,PF3D7_0217500,PF3D7_0506900,PF3D7_0507400,PF3D7_0805600,PF3D7_0918000,PF3D7_0932100,PF3D7_1022700,PF3D7_1035400,PF3D7_1133300,PF3D7_1133400,PF3D7_1218000,PF3D7_1301600,PF3D7_1308000,PF3D7_1335400,PF3D7_1342600,	13.6	2.6	3	9.99E-05	0.000516 94	0.020677 641
		GO:0033016	rhoptry membrane	3	3	PF3D7_0210600,PF3D7_0405200,PF3D7_0707300,	100	19.17	inf	0.000140 47	0.000709 18	0.029076 431
		GO:0044815	DNA packaging complex	17	6	PF3D7_0320900,PF3D7_0617800,PF3D7_0714000,PF3D7_1105000,PF3D7_1105100,PF3D7_1439500,	35.3	6.76	10.12	0.000144 64	0.000712 87	0.029940 512

University of Ghana http://ugspace.ug.edu.gh

		GO: 0018995	host cellular component	713	58	PF3D7_0102200,PF3D7_0104100,PF3D7_0104200,PF3D7_0108500,PF3D7_0202100,PF3D7_0202200,PF3D7_0202500,PF3D7_0207000,PF3D7_0207500,PF3D7_0207600,PF3D7_0207700,PF3D7_0214900,PF3D7_0217500,PF3D7_0220300,PF3D7_0301300,PF3D7_0302200,PF3D7_0302500,PF3D7_0401800,PF3D7_0402100,PF3D7_0404700,PF3D7_0404900,PF3D7_0424100,PF3D7_0501300,PF3D7_0501400,PF3D7_0503600,PF3D7_0507400,PF3D7_0507500,PF3D7_0612700,PF3D7_0702000,PF3D7_0707300,PF3D7_0800800,PF3D7_0830500,PF3D7_0905400,PF3D7_0922200,PF3D7_0925900,PF3D7_0929400,PF3D7_0936000,PF3D7_1001000,PF3D7_1001600,PF3D7_1014100,PF3D7_1017100,PF3D7_1035200,PF3D7_1035300,PF3D7_1102700,PF3D7_1102800,PF3D7_1105000,PF3D7_1115800,PF3D7_1116800,PF3D7_1121300,PF3D7_1222700,PF3D7_1228600,PF3D7_1252100,PF3D7_1401400,PF3D7_1401600,PF3D7_1406300,PF3D7_1410400,PF3D7_1463900,PF3D7_1476300,	8.1	1.56	1.79	0.000229 07	0.001077 65	0.047416 697
		GO: 0043657	host cell	713	58	PF3D7_0102200,PF3D7_0104100,PF3D7_0104200,PF3D7_0108500,PF3D7_0202100,PF3D7_0202200,PF3D7_0202500,PF3D7_0207000,PF3D7_0207500,PF3D7_0207600,PF3D7_0207700,PF3D7_0214900,PF3D7_0217500,PF3D7_0220300,PF3D7_0301300,PF3D7_0302200,PF3D7_0302500,PF3D7_0401800,PF3D7_0402100,PF3D7_0404700,PF3D7_0404900,PF3D7_0424100,PF3D7_0501300,PF3D7_0501400,PF3D7_0503600,PF3D7_0507400,PF3D7_0507500,PF3D7_0612700,PF3D7_0702000,PF3D7_0707300,PF3D7_0800800,PF3D7_0830500,PF3D7_0905400,PF3D7_0922200,PF3D7_0925900,PF3D7_0929400,PF3D7_0936000,PF3D7_1001000,PF3D7_1001600,PF3D7_1014100,PF3D7_1017100,PF3D7_1035200,PF3D7_1035300,PF3D7_1102700,PF3D7_1102800,PF3D7_1105000,PF3D7_1115800,PF3D7_1116800,PF3D7_1121300,PF3D7_1222700,PF3D7_1228600,PF3D7_1252100,PF3D7_1401400,PF3D7_1401600,PF3D7_1406300,PF3D7_1410400,PF3D7_1463900,PF3D7_1476300,	8.1	1.56	1.79	0.000229 07	0.001077 65	0.047416 697
		GO: 0032993	protein-DNA complex	26	6	PF3D7_0320900,PF3D7_0617800,PF3D7_0714000,PF3D7_1105000,PF3D7_1105100,PF3D7_1439500,	23.1	4.42	5.56	0.001808 77	0.008320 36	0.374416 285
		GO: 0044164	host cell cytosol	30	6	PF3D7_0104200,PF3D7_0301300,PF3D7_0404700,PF3D7_1001600,PF3D7_1121300,PF3D7_1463900,	20	3.83	4.63	0.003914 43	0.017614 92	0.810286 532
		GO: 0071944	cell periphery	23	5	PF3D7_0104800,PF3D7_0702200,PF3D7_1342600,PF3D7_1439500,PF3D7_1460600,	21.7	4.17	5.13	0.005763 04	0.025381 88	1
		GO: 0044311	exoneme	3	2	PF3D7_0507500,PF3D7_0808200,	66.7	12.78	36.61	0.007856 05	0.033879 23	1

University of Ghana http://ugspace.ug.edu.gh

		GO: 0045178	basal part of cell	10	3	PF3D7_0104100,PF3D7_0613900,PF3D7_1351700,	30	5.75	7.87	0.012815 11	0.053054 54	1
		GO: 0020026	merozoite dense granule	10	3	PF3D7_0102200,PF3D7_0507500,PF3D7_1116800,	30	5.75	7.87	0.012815 11	0.053054 54	1
		GO: 0005952	cAMP-dependent protein kinase complex	5	2	PF3D7_0934800,PF3D7_1223100,	40	7.67	12.2	0.024421 19	0.099121 28	1
		GO: 0019898	extrinsic component of membrane	13	3	PF3D7_0828800,PF3D7_1036000,PF3D7_1222700,	23.1	4.42	5.5	0.027201 1	0.108281 28	1
		GO: 0005938	cell cortex	7	2	PF3D7_0105300,PF3D7_0932200,	28.6	5.48	7.32	0.047856 61	0.180012 33	1

University of Ghana http://ugspace.ug.edu.gh

Supplementary Table 5.16 List of differentially expressed genes (up- and down-regulated) between the conditions DD2_DMSO_treated compared with DD2_DHA treated

GeneID	source_id	Input.Order	Organism	Genomic.Location..Gene.	Product.Description	Gene.Type	Differentially.expressed
PF3D7_0102600	PF3D7_0102600.1	28	Plasmodium falciparum 3D7	Pf3D7_01_v3:118,812..122,534(-)	serine/threonine protein kinase, FIKK family	protein coding gene	DOWN
PF3D7_0113400	PF3D7_0113400.1	3	Plasmodium falciparum 3D7	Pf3D7_01_v3:507,977..510,158(-)	Plasmodium exported protein, unknown function	protein coding gene	DOWN
PF3D7_0113700	PF3D7_0113700.1	4	Plasmodium falciparum 3D7	Pf3D7_01_v3:519,766..523,106(+)	heat shock protein 40, type II	protein coding gene	DOWN
PF3D7_0113900	PF3D7_0113900.1	5	Plasmodium falciparum 3D7	Pf3D7_01_v3:536,783..538,156(-)	CX3CL1-binding protein 1	protein coding gene	DOWN
PF3D7_0201000	PF3D7_0201000.1	37	Plasmodium falciparum 3D7	Pf3D7_02_v3:57,344..58,421(-)	rifin	protein coding gene	DOWN
PF3D7_0207900	PF3D7_0207900.1	38	Plasmodium falciparum 3D7	Pf3D7_02_v3:317,422..321,552(-)	serine repeat antigen 2	protein coding gene	DOWN
PF3D7_0220300	PF3D7_0220300.1	39	Plasmodium falciparum 3D7	Pf3D7_02_v3:812,892..815,853(-)	Plasmodium exported protein, unknown function	protein coding gene	DOWN
PF3D7_0301700	PF3D7_0301700.1	2	Plasmodium falciparum 3D7	Pf3D7_03_v3:95,216..99,115(-)	Plasmodium exported protein, unknown function	protein coding gene	DOWN
PF3D7_0304000	PF3D7_0304000.1	1	Plasmodium falciparum 3D7	Pf3D7_03_v3:198,542..201,584(-)	inner membrane complex protein 1a, putative	protein coding gene	DOWN
PF3D7_0401700	PF3D7_0401700.1	62	Plasmodium falciparum 3D7	Pf3D7_04_v3:100,684..102,110(+)	Plasmodium exported protein, unknown function, pseudogene	pseudo gene	DOWN
PF3D7_0401800	PF3D7_0401800.1	6	Plasmodium falciparum 3D7	Pf3D7_04_v3:103,078..106,145(-)	Plasmodium exported protein (PHISTb), unknown function	protein	DOWN

University of Ghana http://ugspace.ug.edu.gh

						coding gene	
PF3D7_0424700	PF3D7_0424700.1	7	Plasmodium falciparum 3D7	Pf3D7_04_v3:1,115,896..1,123,289(+)	serine/threonine protein kinase, FIKK family	protein coding gene	DOWN
PF3D7_0426000	PF3D7_0426000.1	8	Plasmodium falciparum 3D7	Pf3D7_04_v3:1,173,053..1,180,226(-)	erythrocyte membrane protein 1, PfEMP1	protein coding gene	DOWN
PF3D7_0500800	PF3D7_0500800.1	16	Plasmodium falciparum 3D7	Pf3D7_05_v3:42,114..48,258(-)	mature parasite-infected erythrocyte surface antigen	protein coding gene	DOWN
PF3D7_0501300	PF3D7_0501300.1	17	Plasmodium falciparum 3D7	Pf3D7_05_v3:67,224..70,944(+)	skeleton-binding protein 1	protein coding gene	DOWN
PF3D7_0501400	PF3D7_0501400.1	18	Plasmodium falciparum 3D7	Pf3D7_05_v3:73,163..80,813(+)	interspersed repeat antigen	protein coding gene	DOWN
PF3D7_0511200	PF3D7_0511200.1	19	Plasmodium falciparum 3D7	Pf3D7_05_v3:470,506..474,400(+)	stearoyl-CoA desaturase	protein coding gene	UP
PF3D7_0529400	PF3D7_0529400.1	35	Plasmodium falciparum 3D7	Pf3D7_05_v3:1,198,563..1,205,743(+)	conserved Plasmodium protein, unknown function	protein coding gene	DOWN
PF3D7_0529400	PF3D7_0529400.2	35	Plasmodium falciparum 3D7	Pf3D7_05_v3:1,198,563..1,205,743(+)	conserved Plasmodium protein, unknown function	protein coding gene	DOWN
PF3D7_0532600	PF3D7_0532600.1	29	Plasmodium falciparum 3D7	Pf3D7_05_v3:1,317,882..1,319,382(-)	Plasmodium exported protein, unknown function	protein coding gene	DOWN
PF3D7_0620000	PF3D7_0620000.1	26	Plasmodium falciparum 3D7	Pf3D7_06_v3:841,846..843,363(-)	PIMMS43 protein	protein coding gene	DOWN
PF3D7_0625700	PF3D7_0625700.1	27	Plasmodium falciparum 3D7	Pf3D7_06_v3:1,042,132..1,043,395(-)	conserved protein, unknown function	protein coding gene	UP

University of Ghana http://ugspace.ug.edu.gh

PF3D7_0702400	PF3D7_0702400.1	9	Plasmodium falciparum 3D7	Pf3D7_07_v3:100,338..103,399(+)	small exported membrane protein 1	protein coding gene	DOWN
PF3D7_0713100	PF3D7_0713100.1	10	Plasmodium falciparum 3D7	Pf3D7_07_v3:605,369..606,780(+)	Pfmc-2TM Maurer's cleft two transmembrane protein	protein coding gene	DOWN
PF3D7_0718700	PF3D7_0718700.1	11	Plasmodium falciparum 3D7	Pf3D7_07_v3:831,360..833,140(-)	conserved Plasmodium membrane protein, unknown function	protein coding gene	UP
PF3D7_0730900	PF3D7_0730900.1	12	Plasmodium falciparum 3D7	Pf3D7_07_v3:1,324,452..1,333,940(+)	EMP1-trafficking protein	protein coding gene	DOWN
PF3D7_0731900	PF3D7_0731900.1	63	Plasmodium falciparum 3D7	Pf3D7_07_v3:1,382,410..1,383,524(+)	rifin, pseudogene	pseudogene	DOWN
PF3D7_0800900	PF3D7_0800900.1	64	Plasmodium falciparum 3D7	Pf3D7_08_v3:83,128..83,904(+)	Plasmodium exported protein (hyp7), unknown function, pseudogene	pseudogene	DOWN
PF3D7_0808800	PF3D7_0808800.1	15	Plasmodium falciparum 3D7	Pf3D7_08_v3:450,615..451,899(+)	rifin	protein coding gene	DOWN
PF3D7_0815700	PF3D7_0815700.1	30	Plasmodium falciparum 3D7	Pf3D7_08_v3:732,891..735,068(-)	ubiquitin	protein coding gene	UP
PF3D7_0818900	PF3D7_0818900.1	14	Plasmodium falciparum 3D7	Pf3D7_08_v3:858,550..862,980(+)	heat shock protein 70	protein coding gene	DOWN
PF3D7_0828000	PF3D7_0828000.1	31	Plasmodium falciparum 3D7	Pf3D7_08_v3:1,210,692..1,211,860(+)	rhomboid protease ROM3	protein coding gene	UP
PF3D7_0830500	PF3D7_0830500.1	13	Plasmodium falciparum 3D7	Pf3D7_08_v3:1,295,569..1,299,431(-)	sporozoite and liver stage tryptophan-rich protein, putative	protein coding gene	DOWN
PF3D7_0831700	PF3D7_0831700.1	36	Plasmodium falciparum 3D7	Pf3D7_08_v3:1,364,640..1,369,862(-)	heat shock protein 70	protein coding gene	DOWN
PF3D7_0902300	PF3D7_0902300.1	20	Plasmodium falciparum 3D7	Pf3D7_09_v3:101,962..105,349(-)	serine/threonine protein kinase, FIKK family	protein	DOWN

University of Ghana http://ugspace.ug.edu.gh

						coding gene	
PF3D7_0902400	PF3D7_0902400.1	32	Plasmodium falciparum 3D7	Pf3D7_09_v3:106,514..108,406(-)	serine/threonine protein kinase, FIKK family	protein coding gene	DOWN
PF3D7_0908400	PF3D7_0908400.1	21	Plasmodium falciparum 3D7	Pf3D7_09_v3:387,511..389,444(+)	conserved Plasmodium protein, unknown function	protein coding gene	UP
PF3D7_0931300	PF3D7_0931300.1	22	Plasmodium falciparum 3D7	Pf3D7_09_v3:1,260,984..1,261,969(+)	conserved Plasmodium protein, unknown function	protein coding gene	DOWN
PF3D7_0935600	PF3D7_0935600.1	23	Plasmodium falciparum 3D7	Pf3D7_09_v3:1,403,986..1,407,459(+)	gametocytogenesis-implicated protein	protein coding gene	DOWN
PF3D7_1000600	PF3D7_1000600.1	40	Plasmodium falciparum 3D7	Pf3D7_10_v3:50,964..53,006(-)	rifin	protein coding gene	DOWN
PF3D7_1000700	PF3D7_1000700.1	65	Plasmodium falciparum 3D7	Pf3D7_10_v3:54,542..55,498(-)	Plasmodium exported protein (PHISTa), unknown function, pseudogene	pseudogene	DOWN
PF3D7_1000800	PF3D7_1000800.1	66	Plasmodium falciparum 3D7	Pf3D7_10_v3:57,968..58,980(+)	stevor, pseudogene	pseudogene	DOWN
PF3D7_1002000	PF3D7_1002000.1	41	Plasmodium falciparum 3D7	Pf3D7_10_v3:102,837..105,100(-)	Plasmodium exported protein (hyp2), unknown function	protein coding gene	DOWN
PF3D7_1003300	PF3D7_1003300.1	42	Plasmodium falciparum 3D7	Pf3D7_10_v3:150,176..151,598(-)	N-terminal acetyltransferase A complex catalytic subunit ARD1, putative	protein coding gene	DOWN
PF3D7_1016500	PF3D7_1016500.1	43	Plasmodium falciparum 3D7	Pf3D7_10_v3:660,965..664,407(-)	Plasmodium exported protein (PHISTc), unknown function	protein coding gene	DOWN
PF3D7_1038800	PF3D7_1038800.1	44	Plasmodium falciparum 3D7	Pf3D7_10_v3:1,556,587..1,561,332(+)	RESA-like protein with PHIST and DnaJ domains	protein coding gene	DOWN
PF3D7_1102300	PF3D7_1102300.1	45	Plasmodium falciparum 3D7	Pf3D7_11_v3:109,829..111,884(-)	Plasmodium exported protein, unknown function	protein coding gene	DOWN

University of Ghana http://ugspace.ug.edu.gh

PF3D7_1113300	PF3D7_1113300.1	46	Plasmodium falciparum 3D7	Pf3D7_11_v3:518,688..520,690(+)	UDP-galactose transporter, putative	protein coding gene	UP
PF3D7_1147000	PF3D7_1147000.1	47	Plasmodium falciparum 3D7	Pf3D7_11_v3:1,858,329..1,867,357(-)	sporozoite and liver stage asparagine-rich protein	protein coding gene	DOWN
PF3D7_1149300	PF3D7_1149300.1	48	Plasmodium falciparum 3D7	Pf3D7_11_v3:1,982,068..1,984,327(+)	serine/threonine protein kinase, FIKK family	protein coding gene	DOWN
PF3D7_1149500	PF3D7_1149500.1	67	Plasmodium falciparum 3D7	Pf3D7_11_v3:1,991,359..1,994,018(-)	ring-infected erythrocyte surface antigen 2, pseudogene	pseudogene	DOWN
PF3D7_1201100	PF3D7_1201100.1	49	Plasmodium falciparum 3D7	Pf3D7_12_v3:80,874..84,922(-)	RESA-like protein with PHIST and DnaJ domains	protein coding gene	DOWN
PF3D7_1217800	PF3D7_1217800.1	50	Plasmodium falciparum 3D7	Pf3D7_12_v3:698,771..699,388(-)	diphthamide biosynthesis protein 3, putative	protein coding gene	DOWN
PF3D7_1238000	PF3D7_1238000.1	51	Plasmodium falciparum 3D7	Pf3D7_12_v3:1,581,356..1,583,229(+)	COPI associated protein, putative	protein coding gene	UP
PF3D7_1254700	PF3D7_1254700.1	52	Plasmodium falciparum 3D7	Pf3D7_12_v3:2,224,997..2,226,201(-)	rifin	protein coding gene	UP
PF3D7_1301500	PF3D7_1301500.1	24	Plasmodium falciparum 3D7	Pf3D7_13_v3:85,156..87,187(-)	Plasmodium exported protein (PHISTa), unknown function	protein coding gene	DOWN
PF3D7_1301800	PF3D7_1301800.1	68	Plasmodium falciparum 3D7	Pf3D7_13_v3:102,842..109,471(+)	surface-associated interspersed protein 13.1 (SURFIN 13.1), pseudogene	pseudogene	DOWN
PF3D7_1350600	PF3D7_1350600.1	25	Plasmodium falciparum 3D7	Pf3D7_13_v3:2,021,350..2,022,307(+)	conserved Plasmodium protein, unknown function	protein coding gene	DOWN
PF3D7_1371900	PF3D7_1371900.1	33	Plasmodium falciparum 3D7	Pf3D7_13_v3:2,829,530..2,830,830(+)	Plasmodium exported protein, unknown function	protein coding gene	DOWN
PF3D7_1372000	PF3D7_1372000.1	34	Plasmodium falciparum 3D7	Pf3D7_13_v3:2,832,623..2,835,439(+)	Plasmodium exported protein (PHISTa), unknown function	protein	DOWN

University of Ghana http://ugspace.ug.edu.gh

						coding gene	
PF3D7_1400500	PF3D7_1400500.1	53	Plasmodium falciparum 3D7	Pf3D7_14_v3:17,469..18,808(-)	rifin	protein coding gene	DOWN
PF3D7_1401000	PF3D7_1401000.1	54	Plasmodium falciparum 3D7	Pf3D7_14_v3:34,693..35,773(-)	GBPH protein	protein coding gene	DOWN
PF3D7_1415500	PF3D7_1415500.1	55	Plasmodium falciparum 3D7	Pf3D7_14_v3:623,840..628,505(-)	conserved Plasmodium membrane protein, unknown function	protein coding gene	UP
PF3D7_1416600	PF3D7_1416600.1	56	Plasmodium falciparum 3D7	Pf3D7_14_v3:669,374..679,741(-)	conserved Plasmodium protein, unknown function	protein coding gene	DOWN
PF3D7_1421900	PF3D7_1421900.1	57	Plasmodium falciparum 3D7	Pf3D7_14_v3:890,541..891,622(-)	copper transporter, putative	protein coding gene	UP
PF3D7_1429200	PF3D7_1429200.1	58	Plasmodium falciparum 3D7	Pf3D7_14_v3:1,144,128..1,148,920(-)	AP2 domain transcription factor AP2-O3, putative	protein coding gene	DOWN
PF3D7_1454800	PF3D7_1454800.1	59	Plasmodium falciparum 3D7	Pf3D7_14_v3:2,243,873..2,244,367(+)	conserved Plasmodium protein, unknown function	protein coding gene	UP
PF3D7_1457200	PF3D7_1457200.1	60	Plasmodium falciparum 3D7	Pf3D7_14_v3:2,343,508..2,344,657(-)	thioredoxin 1	protein coding gene	UP
PF3D7_1478600	PF3D7_1478600.1	61	Plasmodium falciparum 3D7	Pf3D7_14_v3:3,231,222..3,237,075(+)	EMP1-trafficking protein	protein coding gene	DOWN

University of Ghana http://ugspace.ug.edu.gh

Supplementary Table 5.17 Gene ontology enrichment analysis for up/down-regulated genes between DD2 DMSO_treated and DHA_treated condition

University of Ghana http://ugspace.ug.edu.gh

Gene ontology term	Differential expression	ID	Name	Bg count	Result count	Result genes list	Pct of bgd	Fold enrichment	Odds ratio	P-value	Benjamini	Bonferroni
Biological process	Upregulated	GO:0006636	unsaturated fatty acid biosynthetic process	1	1	PF3D7_0511200,	100	405.67	inf	0.00246508	0.05293929	0.211996713
		GO:0072334	UDP-galactose transmembrane transport	1	1	PF3D7_1113300,	100	405.67	inf	0.00246508	0.05293929	0.211996713
		GO:0033559	unsaturated fatty acid metabolic process	1	1	PF3D7_0511200,	100	405.67	inf	0.00246508	0.05293929	0.211996713
		GO:0015780	nucleotide-sugar transmembrane transport	2	1	PF3D7_1113300,	50	202.83	441.36	0.00492458	0.05293929	0.423514289
		GO:0090481	pyrimidine nucleotide-sugar transmembrane transport	2	1	PF3D7_1113300,	50	202.83	441.36	0.00492458	0.05293929	0.423514289
		GO:0035434	copper ion transmembrane transport	2	1	PF3D7_1421900,	50	202.83	441.36	0.00492458	0.05293929	0.423514289
		GO:0018904	ether metabolic process	2	1	PF3D7_1457200,	50	202.83	441.36	0.00492458	0.05293929	0.423514289
		GO:0006662	glycerol ether metabolic process	2	1	PF3D7_1457200,	50	202.83	441.36	0.00492458	0.05293929	0.423514289
		GO:0006878	cellular copper ion homeostasis	3	1	PF3D7_1421900,	33.3	135.22	220.64	0.00737853	0.06345537	0.634553711
		GO:0055070	copper ion homeostasis	3	1	PF3D7_1421900,	33.3	135.22	220.64	0.00737853	0.06345537	0.634553711
		GO:0019725	cellular homeostasis	62	2	PF3D7_1421900,PF3D7_1457200,	3.2	13.09	15.99	0.00970397	0.07586744	0.834541848
		GO:0042592	homeostatic process	68	2	PF3D7_1421900,PF3D7_1457200,	2.9	11.93	14.52	0.01159429	0.08116939	0.997108885
		GO:0006825	copper ion transport	5	1	PF3D7_1421900,	20	81.13	110.27	0.01226979	0.08116939	1
		GO:0055076	transition metal ion homeostasis	6	1	PF3D7_1421900,	16.7	67.61	88.2	0.01470713	0.08432086	1
		GO:0046916	cellular transition metal ion homeostasis	6	1	PF3D7_1421900,	16.7	67.61	88.2	0.01470713	0.08432086	1
		GO:1901264	carbohydrate derivative transport	8	1	PF3D7_1113300,	12.5	50.71	62.97	0.01956527	0.1051633	1
		GO:0006465	signal peptide processing	10	1	PF3D7_0828000,	10	40.57	48.96	0.02440144	0.11658465	1

University of Ghana http://ugspace.ug.edu.gh

		GO: 0098656	anion transmembrane transport	10	1	PF3D7_1113300,	10	40.57	48.96	0.02440144	0.11658465	1
		GO: 0000041	transition metal ion transport	11	1	PF3D7_1421900,	9.1	35.88	44.05	0.02681132	0.12135648	1
		GO: 0006875	cellular metal ion homeostasis	13	1	PF3D7_1421900,	7.7	31.21	36.7	0.03161471	0.13594324	1
		GO: 0055065	metal ion homeostasis	15	1	PF3D7_1421900,	6.7	27.04	31.44	0.03639636	0.14905175	1
	Downregulated	**GO: 0044403**	**biological process involved in symbiotic interaction**	**397**	**14**	**PF3D7_0102600,PF3D7_0113700,PF3D7_0113900,PF3D7_0201000,PF3D7_0304000,PF3D7_0424700,PF3D7_0426000,PF3D7_0620000,PF3D7_0713100,PF3D7_0808800,PF3D7_0831700,PF3D7_1000600,PF3D7_1149300,PF3D7_1400500,**	**3.5**	**3.73**	**5.07**	**9.73E-06**	**0.00044848**	**0.000846094**
		GO: 0044419	**biological process involved in interspecies interaction between organisms**	**399**	**14**	**PF3D7_0102600,PF3D7_0113700,PF3D7_0113900,PF3D7_0201000,PF3D7_0304000,PF3D7_0424700,PF3D7_0426000,PF3D7_0620000,PF3D7_0713100,PF3D7_0808800,PF3D7_0831700,PF3D7_1000600,PF3D7_1149300,PF3D7_1400500,**	**3.5**	**3.71**	**5.04**	**1.03E-05**	**0.00044848**	**0.00089696**
		GO: 0008150	**biological process**	**662**	**17**	**PF3D7_0102600,PF3D7_0113700,PF3D7_0113900,PF3D7_0201000,PF3D7_0207900,PF3D7_0304000,PF3D7_0424700,PF3D7_0426000,PF3D7_0620000,PF3D7_0713100,PF3D7_0808800,PF3D7_0831700,PF3D7_0902300,PF3D7_0902400,PF3D7_1000600,PF3D7_1149300,PF3D7_1400500,**	**2.6**	**2.72**	**3.8**	**5.66E-05**	**0.00164104**	**0.004923111**
		GO: 0051085	**chaperone cofactor-dependent protein refolding**	**15**	**3**	**PF3D7_0113700,PF3D7_0818900,PF3D7_0831700,**	**20**	**21.17**	**27.97**	**0.00033193**	**0.00577553**	**0.028877646**
		GO: 0051084	**'de novo' posttranslational protein folding**	**15**	**3**	**PF3D7_0113700,PF3D7_0818900,PF3D7_0831700,**	**20**	**21.17**	**27.97**	**0.00033193**	**0.00577553**	**0.028877646**
		GO: 0061077	**chaperone-mediated protein folding**	**17**	**3**	**PF3D7_0113700,PF3D7_0818900,PF3D7_0831700,**	**17.6**	**18.68**	**23.96**	**0.00048954**	**0.00707527**	**0.042589548**
		GO: 0006458	'de novo' protein folding	18	3	PF3D7_0113700,PF3D7_0818900,PF3D7_0831700,	16.7	17.64	22.36	0.00058356	0.00707527	0.050770029
		GO: 0051701	biological process involved in interaction with host	382	11	PF3D7_0102600,PF3D7_0201000,PF3D7_0304000,PF3D7_0424700,PF3D7_0426000,PF3D7_0620000,PF3D7_0713100,PF3D7_0808800,PF3D7_1000600,PF3D7_1149300,PF3D7_1400500,	2.9	3.05	3.77	0.0006506	0.00707527	0.05660213
		GO: 0035556	intracellular signal transduction	81	5	PF3D7_0102600,PF3D7_0424700,PF3D7_0902300,PF3D7_0902400,PF3D7_1149300,	6.2	6.53	7.62	0.00090467	0.00874517	0.078706532
		GO: 0042026	protein refolding	9	2	PF3D7_0818900,PF3D7_0831700,	22.2	23.52	31.27	0.00301518	0.02384731	0.262320431
		GO: 0034620	cellular response to unfolded protein	9	2	PF3D7_0818900,PF3D7_0831700,	22.2	23.52	31.27	0.00301518	0.02384731	0.262320431
		GO: 0006468	protein phosphorylation	110	5	PF3D7_0102600,PF3D7_0424700,PF3D7_0902300,PF3D7_0902400,PF3D7_1149300,	4.5	4.81	5.48	0.00352537	0.02555893	0.306707134
		GO: 0007165	signal transduction	119	5	PF3D7_0102600,PF3D7_0424700,PF3D7_0902300,PF3D7_0902400,PF3D7_1149300,	4.2	4.45	5.04	0.00493896	0.0306921	0.429689405
		GO: 0023052	signaling	119	5	PF3D7_0102600,PF3D7_0424700,PF3D7_0902300,PF3D7_0902400,PF3D7_1149300,	4.2	4.45	5.04	0.00493896	0.0306921	0.429689405

		GO:0007154	cell communication	127	5	PF3D7_0102600,PF3D7_0424700,PF3D7_0902300,PF3D7_0902400,PF3D7_1149300,	3.9	4.17	4.7	0.00650025	0.03770146	0.565521878
		GO:0016310	phosphorylation	135	5	PF3D7_0102600,PF3D7_0424700,PF3D7_0902300,PF3D7_0902400,PF3D7_1149300,	3.7	3.92	4.4	0.00838157	0.04094767	0.72919624
		GO:0017198	N-terminal peptidyl-serine acetylation	1	1	PF3D7_1003300,	100	105.83	inf	0.00944947	0.04094767	0.822103533
		GO:0018002	N-terminal peptidyl-glutamic acid acetylation	1	1	PF3D7_1003300,	100	105.83	inf	0.00944947	0.04094767	0.822103533
		GO:0030920	peptidyl-serine acetylation	1	1	PF3D7_1003300,	100	105.83	inf	0.00944947	0.04094767	0.822103533
		GO:0035967	cellular response to topologically incorrect protein	16	2	PF3D7_0818900,PF3D7_0831700,	12.5	13.23	15.61	0.00963657	0.04094767	0.838381911
		GO:0042783	evasion of host immune response	205	6	PF3D7_0201000,PF3D7_0426000,PF3D7_0620000,PF3D7_0808800,PF3D7_1000600,PF3D7_1400500,	2.9	3.1	3.48	0.01188421	0.04094767	1
		GO:0043207	response to external biotic stimulus	208	6	PF3D7_0201000,PF3D7_0426000,PF3D7_0620000,PF3D7_0808800,PF3D7_1000600,PF3D7_1400500,	2.9	3.05	3.43	0.0127079	0.04094767	1
		GO:0075136	response to host	208	6	PF3D7_0201000,PF3D7_0426000,PF3D7_0620000,PF3D7_0808800,PF3D7_1000600,PF3D7_1400500,	2.9	3.05	3.43	0.0127079	0.04094767	1
		GO:0052572	response to host immune response	208	6	PF3D7_0201000,PF3D7_0426000,PF3D7_0620000,PF3D7_0808800,PF3D7_1000600,PF3D7_1400500,	2.9	3.05	3.43	0.0127079	0.04094767	1
		GO:0051707	response to other organism	208	6	PF3D7_0201000,PF3D7_0426000,PF3D7_0620000,PF3D7_0808800,PF3D7_1000600,PF3D7_1400500,	2.9	3.05	3.43	0.0127079	0.04094767	1
		GO:0052173	response to defenses of other organism	208	6	PF3D7_0201000,PF3D7_0426000,PF3D7_0620000,PF3D7_0808800,PF3D7_1000600,PF3D7_1400500,	2.9	3.05	3.43	0.0127079	0.04094767	1
		GO:0052200	response to host defenses	208	6	PF3D7_0201000,PF3D7_0426000,PF3D7_0620000,PF3D7_0808800,PF3D7_1000600,PF3D7_1400500,	2.9	3.05	3.43	0.0127079	0.04094767	1
		GO:0006986	response to unfolded protein	22	2	PF3D7_0818900,PF3D7_0831700,	9.1	9.62	10.91	0.01789609	0.05560571	1
		GO:0020035	cytoadherence to microvasculature, mediated by symbiont protein	176	5	PF3D7_0113700,PF3D7_0113900,PF3D7_0426000,PF3D7_0808800,PF3D7_0831700,	2.8	3.01	3.32	0.02412482	0.06996197	1
		GO:0044406	adhesion of symbiont to host	176	5	PF3D7_0113700,PF3D7_0113900,PF3D7_0426000,PF3D7_0808800,PF3D7_0831700,	2.8	3.01	3.32	0.02412482	0.06996197	1
		GO:0035966	response to topologically incorrect protein	29	2	PF3D7_0818900,PF3D7_0831700,	6.9	7.3	8.07	0.03016849	0.08202058	1
		GO:0009408	response to heat	29	2	PF3D7_0113700,PF3D7_0818900,	6.9	7.3	8.07	0.03016849	0.08202058	1
		GO:0009266	response to temperature stimulus	30	2	PF3D7_0113700,PF3D7_0818900,	6.7	7.06	7.78	0.03213181	0.08471113	1
		GO:0022610	biological adhesion	195	5	PF3D7_0113700,PF3D7_0113900,PF3D7_0426000,PF3D7_0808800,PF3D7_0831700,	2.6	2.71	2.97	0.03548579	0.09080188	1

University of Ghana http://ugspace.ug.edu.gh

		GO: 0018200	peptidyl-glutamic acid modification	4	1	PF3D7_1003300,	25	26.46	35.7	0.0372768	0.09265948	1
		GO: 0020033	antigenic variation	202	5	PF3D7_0201000,PF3D7_0426000,PF3D7_0808800,PF3D7_1000600,PF3D7_1400300,	2.5	2.62	2.86	0.04039099	0.09761157	1
		GO: 0044003	modulation by symbiont of host process	205	5	PF3D7_0102600,PF3D7_0424700,PF3D7_0426000,PF3D7_0808800,PF3D7_1149300,	2.4	2.58	2.82	0.04261507	0.09841929	1
		GO: 0017182	peptidyl-diphthamide metabolic process	5	1	PF3D7_1217800,	20	21.17	26.77	0.0463815	0.09841929	1
		GO: 0017183	peptidyl-diphthamide biosynthetic process from peptidyl-histidine	5	1	PF3D7_1217800,	20	21.17	26.77	0.0463815	0.09841929	1
		GO: 0018202	peptidyl-histidine modification	5	1	PF3D7_1217800,	20	21.17	26.77	0.0463815	0.09841929	1
		GO: 1900247	regulation of cytoplasmic translational elongation	5	1	PF3D7_1217800,	20	21.17	26.77	0.0463815	0.09841929	1
Molecular function	Upregulated	GO: 0005460	UDP-glucose transmembrane transporter activity	1	1	PF3D7_1113300,	100	405.67	inf	0.00246508	0.02021364	0.1010682
		GO: 0005459	UDP-galactose transmembrane transporter activity	1	1	PF3D7_1113300,	100	405.67	inf	0.00246508	0.02021364	0.1010682
		GO: 0004768	stearoyl-CoA 9-desaturase activity	1	1	PF3D7_0511200,	100	405.67	inf	0.00246508	0.02021364	0.1010682
		GO: 0016717	oxidoreductase activity, acting on paired donors, with oxidation of a pair of donors resulting in the reduction of molecular oxygen to two molecules of water	1	1	PF3D7_0511200,	100	405.67	inf	0.00246508	0.02021364	0.1010682
		GO: 0016215	acyl-CoA desaturase activity	1	1	PF3D7_0511200,	100	405.67	inf	0.00246508	0.02021364	0.1010682
		GO: 0005375	copper ion transmembrane transporter activity	2	1	PF3D7_1421900,	50	202.83	441.36	0.00492458	0.028844	0.201907975
		GO: 0015165	pyrimidine nucleotide-sugar transmembrane transporter activity	2	1	PF3D7_1113300,	50	202.83	441.36	0.00492458	0.028844	0.201907975
		GO: 0005338	nucleotide-sugar transmembrane transporter activity	4	1	PF3D7_1113300,	25	101.42	147.06	0.00982693	0.05036302	0.402904122
		GO: 0046915	transition metal ion transmembrane transporter activity	11	1	PF3D7_1421900,	9.1	36.88	44.05	0.02681132	0.09310774	1
		GO: 0015035	protein-disulfide reductase activity	12	1	PF3D7_1457200,	8.3	33.81	40.04	0.02921573	0.09310774	1
		GO: 0015036	disulfide oxidoreductase activity	13	1	PF3D7_1457200,	7.7	31.21	36.7	0.03161471	0.09310774	1
		GO: 0005506	iron ion binding	14	1	PF3D7_0511200,	7.1	28.98	33.87	0.03400824	0.09310774	1

University of Ghana http://ugspace.ug.edu.gh

		GO:0016705	oxidoreductase activity, acting on paired donors, with incorporation or reduction of molecular oxygen	14	1	PF3D7_0511200,	7.1	28.98	33.87	0.03400824	0.09310774	1
		GO:1901505	carbohydrate derivative transmembrane transporter activity	14	1	PF3D7_1113300,	7.1	28.98	33.87	0.03400824	0.09310774	1
		GO:0008514	organic anion transmembrane transporter activity	15	1	PF3D7_1113300,	6.7	27.04	31.44	0.03639636	0.09310774	1
		GO:0015932	nucleobase-containing compound transmembrane transporter activity	15	1	PF3D7_1113300,	6.7	27.04	31.44	0.03639636	0.09310774	1
		GO:0016667	oxidoreductase activity, acting on a sulfur group of donors	16	1	PF3D7_1457200,	6.3	25.35	29.34	0.03877906	0.09310774	1
		GO:0016491	oxidoreductase activity	133	2	PF3D7_0511200,PF3D7_1457200,	1.5	6.1	7.21	0.04087657	0.09310774	1
	Downregulated	GO:0044183	protein folding chaperone	6	2	PF3D7_0818900,PF3D7_0831700,	33.3	35.28	54.75	0.00127925	0.06763351	0.110015511
		GO:0004674	protein serine/threonine kinase activity	93	5	PF3D7_0102600,PF3D7_0424700,PF3D7_0902300,PF3D7_0902400,PF3D7_1149300,	5.4	5.69	6.56	0.00168669	0.06763351	0.145055395
		GO:0051787	misfolded protein binding	8	2	PF3D7_0818900,PF3D7_0831700,	25	26.46	36.48	0.00235931	0.06763351	0.202900532
		GO:0004672	protein kinase activity	108	5	PF3D7_0102600,PF3D7_0424700,PF3D7_0902300,PF3D7_0902400,PF3D7_1149300,	4.6	4.9	5.59	0.00325613	0.0700067	0.280026793
		GO:1990190	peptide-glutamate-N-acetyltransferase activity	1	1	PF3D7_1003300,	100	105.83	inf	0.00944947	0.11555674	0.812654067
		GO:0015485	cholesterol binding	1	1	PF3D7_0113700,	100	105.83	inf	0.00944947	0.11555674	0.812654067
		GO:0016773	phosphotransferase activity, alcohol group as acceptor	141	5	PF3D7_0102600,PF3D7_0424700,PF3D7_0902300,PF3D7_0902400,PF3D7_1149300,	3.5	3.75	4.2	0.0100211	0.11555674	0.861814858
		GO:0031072	heat shock protein binding	22	2	PF3D7_0818900,PF3D7_0831700,	9.1	9.62	10.91	0.01789609	0.11555674	1
		GO:0032934	sterol binding	2	1	PF3D7_0113700,	50	52.91	107.13	0.01881156	0.11555674	1
		GO:0019956	chemokine binding	2	1	PF3D7_0113900,	50	52.91	107.13	0.01881156	0.11555674	1
		GO:1990189	peptide-serine-N-acetyltransferase activity	2	1	PF3D7_1003300,	50	52.91	107.13	0.01881156	0.11555674	1
		GO:0019955	cytokine binding	2	1	PF3D7_0113900,	50	52.91	107.13	0.01881156	0.11555674	1
		GO:0005496	steroid binding	2	1	PF3D7_0113700,	50	52.91	107.13	0.01881156	0.11555674	1
		GO:0004867	serine-type endopeptidase inhibitor activity	2	1	PF3D7_0501400,	50	52.91	107.13	0.01881156	0.11555674	1

University of Ghana http://ugspace.ug.edu.gh

		GO: 0005515	protein binding	605	11	PF3D7_0113700,PF3D7_0113900,PF3D7_0301700,PF3D7_0401800,PF3D7_0500800,PF3D7_0501300,PF3D7_0702400,PF3D7_0818900,PF3D7_0830500,PF3D7_0831700,PF3D7_1038800,	1.8	1.92	2.24	0.0224164	0.12077444	1
		GO: 0051082	unfolded protein binding	65	3	PF3D7_0113700,PF3D7_0818900,PF3D7_0831700,	4.6	4.88	5.36	0.02293403	0.12077444	1
		GO: 0030414	peptidase inhibitor activity	3	1	PF3D7_0501400,	33.3	35.28	53.56	0.02808708	0.12077444	1
		GO: 0043178	alcohol binding	3	1	PF3D7_0113700,	33.3	35.28	53.56	0.02808708	0.12077444	1
		GO: 0004866	endopeptidase inhibitor activity	3	1	PF3D7_0501400,	33.3	35.28	53.56	0.02808708	0.12077444	1
		GO: 0017178	diphthine-ammonia ligase activity	3	1	PF3D7_1217800,	33.3	35.28	53.56	0.02808708	0.12077444	1
		GO: 0016880	acid-ammonia (or amide) ligase activity	4	1	PF3D7_1217800,	25	26.46	35.7	0.0372768	0.14571841	1
		GO: 0004596	peptide alpha-N-acetyltransferase activity	4	1	PF3D7_1003300,	25	26.46	35.7	0.0372768	0.14571841	1
		GO: 0032266	phosphatidylinositol-3-phosphate binding	5	1	PF3D7_0818900,	20	21.17	26.77	0.0463815	0.16620038	1
		GO: 0061135	endopeptidase regulator activity	5	1	PF3D7_0501400,	20	21.17	26.77	0.0463815	0.16620038	1
Cellular component	Upregulated	GO: 0016021	integral component of membrane	1297	9	PF3D7_0511200,PF3D7_0718700,PF3D7_0815700,PF3D7_0828000,PF3D7_0908400,PF3D7_1113300,PF3D7_1238000,PF3D7_1415500,PF3D7_1421900,	0.7	2.81	8.31	0.00064564	0.015063	0.027116912
		GO: 0031224	intrinsic component of membrane	1314	9	PF3D7_0511200,PF3D7_0718700,PF3D7_0815700,PF3D7_0828000,PF3D7_0908400,PF3D7_1113300,PF3D7_1238000,PF3D7_1415500,PF3D7_1421900,	0.7	2.78	8.16	0.00071729	0.015063	0.030125993
		GO: 0030173	integral component of Golgi membrane	10	1	PF3D7_1113300,	10	40.57	48.96	0.02440144	0.18469789	1
		GO: 0031228	intrinsic component of Golgi membrane	10	1	PF3D7_1113300,	10	40.57	48.96	0.02440144	0.18469789	1
		GO: 0005789	endoplasmic reticulum membrane	113	2	PF3D7_0511200,PF3D7_1113300,	1.8	7.18	8.55	0.03028431	0.18469789	1
		GO: 0098827	endoplasmic reticulum subcompartment	113	2	PF3D7_0511200,PF3D7_1113300,	1.8	7.18	8.55	0.03028431	0.18469789	1
		GO: 0042175	nuclear outer membrane-endoplasmic reticulum membrane network	114	2	PF3D7_0511200,PF3D7_1113300,	1.8	7.12	8.47	0.03078298	0.18469789	1
		GO: 0031984	organelle subcompartment	130	2	PF3D7_0511200,PF3D7_1113300,	1.5	6.24	7.39	0.03920688	0.20583612	1
	Downregulated	**GO: 0018995**	**host cellular component**	**713**	**34**	**PF3D7_0102600,PF3D7_0113400,PF3D7_0113700,PF3D7_0113900,PF3D7_0201000,PF3D7_0220300,PF3D7_0301700,PF3D7_0401800,PF3D7_0424700,PF3D7_0426000,PF3D7_0500800,PF3D7_0501300,PF3D7_0501400,PF3D7_0532600,PF3D7_0702400,PF3D7_0713100,PF3D7_0730900,PF3D7_0808800,PF3D7_0830500,**	**4.8**	**5.05**	**17.29**	**1.46E-19**	**4.01E-18**	**8.01E-18**

University of Ghana http://ugspace.ug.edu.gh

						PF3D7_0831700,PF3D7_0935600,PF3D7_1000600,PF3D7_1002000,PF3D7_1016500,PF3D7_1038800,PF3D7_1102300,PF3D7_1149300,PF3D7_1201100,PF3D7_1301500,PF3D7_1371900,PF3D7_1372000,PF3D7_1400500,PF3D7_1401000,PF3D7_1478600,						
		GO:0043657	**host cell**	**713**	**34**	**PF3D7_0102600,PF3D7_0113400,PF3D7_0113700,PF3D7_0113900,PF3D7_0201000,PF3D7_0220300,PF3D7_0301700,PF3D7_0401800,PF3D7_0424700,PF3D7_0426000,PF3D7_0500800,PF3D7_0501300,PF3D7_0501400,PF3D7_0532600,PF3D7_0702400,PF3D7_0713100,PF3D7_0730900,PF3D7_0808800,PF3D7_0830500,PF3D7_0831700,PF3D7_0935600,PF3D7_1000600,PF3D7_1002000,PF3D7_1016500,PF3D7_1038800,PF3D7_1102300,PF3D7_1149300,PF3D7_1201100,PF3D7_1301500,PF3D7_1371900,PF3D7_1372000,PF3D7_1400500,PF3D7_1401000,PF3D7_1478600,**	**4.8**	**5.05**	**17.29**	**1.46E-19**	**4.01E-18**	**8.01E-18**
		GO:0033643	**host cell part**	**630**	**25**	**PF3D7_0102600,PF3D7_0113700,PF3D7_0113900,PF3D7_0201000,PF3D7_0301700,PF3D7_0401800,PF3D7_0424700,PF3D7_0426000,PF3D7_0500800,PF3D7_0501300,PF3D7_0501400,PF3D7_0532600,PF3D7_0702400,PF3D7_0713100,PF3D7_0808800,PF3D7_0830500,PF3D7_0831700,PF3D7_0935600,PF3D7_1000600,PF3D7_1038800,PF3D7_1102300,PF3D7_1149300,PF3D7_1201100,PF3D7_1400500,PF3D7_1478600,**	**4**	**4.2**	**8.3**	**1.96E-11**	**3.59E-10**	**1.08E-09**
		GO:0030430	**host cell cytoplasm**	**540**	**20**	**PF3D7_0102600,PF3D7_0113700,PF3D7_0113900,PF3D7_0301700,PF3D7_0401800,PF3D7_0424700,PF3D7_0426000,PF3D7_0500800,PF3D7_0501300,PF3D7_0501400,PF3D7_0532600,PF3D7_0702400,PF3D7_0713100,PF3D7_0808800,PF3D7_0830500,PF3D7_0831700,PF3D7_0935600,PF3D7_1038800,PF3D7_1201100,PF3D7_1478600,**	**3.7**	**3.92**	**6.36**	**1.98E-08**	**2.49E-07**	**1.09E-06**
		GO:0033646	**host intracellular part**	**549**	**20**	**PF3D7_0102600,PF3D7_0113700,PF3D7_0113900,PF3D7_0301700,PF3D7_0401800,PF3D7_0424700,PF3D7_0426000,PF3D7_0500800,PF3D7_0501300,PF3D7_0501400,PF3D7_0532600,PF3D7_0702400,PF3D7_0713100,PF3D7_0808800,PF3D7_0830500,PF3D7_0831700,PF3D7_0935600,PF3D7_1038800,PF3D7_1201100,PF3D7_1478600,**	**3.6**	**3.86**	**6.24**	**2.63E-08**	**2.49E-07**	**1.45E-06**
		GO:0043656	**host intracellular region**	**550**	**20**	**PF3D7_0102600,PF3D7_0113700,PF3D7_0113900,PF3D7_0301700,PF3D7_0401800,PF3D7_0424700,PF3D7_0426000,PF3D7_0500800,PF3D7_0501300,PF3D7_0501400,PF3D7_0532600,PF3D7_0702400,PF3D7_0713100,PF3D7_0808800,PF3D7_0830500,PF3D7_0831700,PF3D7_0935600,PF3D7_1038800,PF3D7_1201100,PF3D7_1478600,**	**3.6**	**3.85**	**6.23**	**2.72E-08**	**2.49E-07**	**1.49E-06**
		GO:0044217	**other organism part**	**116**	**10**	**PF3D7_0113400,PF3D7_0220300,PF3D7_0301700,PF3D7_0730900,PF3D7_1002000,PF3D7_1016500,PF3D7_1301500,PF3D7_1371900,PF3D7_1372000,PF3D7_1401000,**	**8.6**	**9.12**	**12.36**	**7.92E-08**	**6.22E-07**	**4.36E-06**
		GO:0020036	**Maurer's cleft**	**370**	**16**	**PF3D7_0102600,PF3D7_0113700,PF3D7_0113900,PF3D7_0301700,PF3D7_0401800,PF3D7_0424700,PF3D7_0500800,PF3D7_0501300,PF3D7_0501400,PF3D7_0532600,PF3D7_0702400,PF3D7_0713100,PF3D7_0808800,PF3D7_0830500,PF3D7_0831700,PF3D7_0935600,**	**4.3**	**4.58**	**6.73**	**1.08E-07**	**7.40E-07**	**5.92E-06**
		GO:0033655	**host cell cytoplasm part**	**524**	**17**	**PF3D7_0102600,PF3D7_0113700,PF3D7_0113900,PF3D7_0301700,PF3D7_0401800,PF3D7_0424700,PF3D7_0426000,PF3D7_0500800,PF3D7_0501300,PF3D7_0501400,PF3D7_0532600,PF3D7_0702400,PF3D7_0713100,PF3D7_0808800,PF3D7_0830500,PF3D7_0831700,PF3D7_0935600,**	**3.2**	**3.43**	**4.99**	**2.40E-06**	**1.46E-05**	**0.00013178**
		GO:0044538	**host cell periphery**	**26**	**4**	**PF3D7_0401800,PF3D7_0424700,PF3D7_1102300,PF3D7_1149300,**	**15.4**	**16.28**	**20.78**	**8.96E-05**	**0.00049304**	**0.004930421**
		GO:1903561	extracellular vesicle	91	5	PF3D7_0301700,PF3D7_0501300,PF3D7_0702400,PF3D7_0818900,PF3D7_0831700,	5.5	5.81	6.72	0.00153062	0.00765309	0.084184
		GO:0044164	host cell cytosol	30	3	PF3D7_0113700,PF3D7_0532600,PF3D7_0831700,	10	10.58	12.39	0.00268206	0.01229279	0.147513476

University of Ghana http://ugspace.ug.edu.gh

		GO:0016021	integral component of membrane	1297	21	PF3D7_0102600,PF3D7_0113400,PF3D7_0113700,PF3D7_0113900,PF3D7_0301700,PF3D7_0401800,PF3D7_0424700,PF3D7_0426000,PF3D7_0501300,PF3D7_0620000,PF3D7_0702400,PF3D7_0713100,PF3D7_0730900,PF3D7_0808800,PF3D7_0830500,PF3D7_0902300,PF3D7_1102300,PF3D7_1301500,PF3D7_1350600,PF3D7_1372000,PF3D7_1478600,	1.6	1.71	2.33	0.00411724	0.01741908	0.226448025
		GO:0031224	intrinsic component of membrane	1314	21	PF3D7_0102600,PF3D7_0113400,PF3D7_0113700,PF3D7_0113900,PF3D7_0301700,PF3D7_0401800,PF3D7_0424700,PF3D7_0426000,PF3D7_0501300,PF3D7_0620000,PF3D7_0702400,PF3D7_0713100,PF3D7_0730900,PF3D7_0808800,PF3D7_0830500,PF3D7_0902300,PF3D7_1102300,PF3D7_1301500,PF3D7_1350600,PF3D7_1372000,PF3D7_1478600,	1.6	1.69	2.29	0.00486436	0.01910998	0.26753972
		GO:0033644	host cell membrane	242	7	PF3D7_0201000,PF3D7_0426000,PF3D7_0500800,PF3D7_0702400,PF3D7_0808800,PF3D7_1000600,PF3D7_1400500,	2.9	3.06	3.5	0.0069837	0.02560692	0.384103743
		GO:0031415	NatA complex	1	1	PF3D7_1003300,	100	105.83	inf	0.00944947	0.03248254	0.519720624
		GO:0005576	extracellular region	334	8	PF3D7_0207900,PF3D7_0301700,PF3D7_0501300,PF3D7_0501400,PF3D7_0702400,PF3D7_0808800,PF3D7_0818900,PF3D7_0831700,	2.4	2.53	2.9	0.01182951	0.03827193	0.650622839
		GO:0020002	host cell plasma membrane	219	6	PF3D7_0201000,PF3D7_0426000,PF3D7_0500800,PF3D7_0808800,PF3D7_1000600,PF3D7_1400500,	2.7	2.9	3.25	0.01607538	0.04911922	0.884145914
		GO:0005615	extracellular space	22	2	PF3D7_0207900,PF3D7_0501400,	9.1	9.62	10.91	0.01789609	0.05180448	0.984285047
		GO:0031414	N-terminal protein acetyltransferase complex	3	1	PF3D7_1003300,	33.3	35.28	53.56	0.02808708	0.07723947	1
		GO:0044228	host cell surface	31	2	PF3D7_0113900,PF3D7_0401800,	6.5	6.83	7.51	0.03414435	0.08942568	1
		GO:0065010	extracellular membrane-bounded organelle	280	6	PF3D7_0301700,PF3D7_0501300,PF3D7_0702400,PF3D7_0808800,PF3D7_0818900,PF3D7_0831700,	2.1	2.27	2.49	0.04633839	0.11406901	1
		GO:0043230	extracellular organelle	282	6	PF3D7_0301700,PF3D7_0501300,PF3D7_0702400,PF3D7_0808800,PF3D7_0818900,PF3D7_0831700,	2.1	2.25	2.47	0.04770158	0.11406901	1

University of Ghana http://ugspace.ug.edu.gh

Supplementary Table 5.18 List of differentially expressed genes (up- and down-regulated) between the conditions DD2 untreated compared with DD2_DHA treated

GeneID	source_id	Input.Order	Organism	Genomic.Location..Gene.	Product.Description	Gene.Type	differentially.expressed
PF3D7_0102200	PF3D7_0102200.1	24	Plasmodium falciparum 3D7	Pf3D7_01_v3:97,590..103,615(+)	ring-infected erythrocyte surface antigen	protein coding gene	DOWN
PF3D7_0102400	PF3D7_0102400.1	635	Plasmodium falciparum 3D7	Pf3D7_01_v3:107,197..108,348(-)	lysophospholipase, putative, pseudogene	pseudogene	UP
PF3D7_0102500	PF3D7_0102500.1	25	Plasmodium falciparum 3D7	Pf3D7_01_v3:109,005..117,516(-)	erythrocyte binding antigen-181	protein coding gene	DOWN
PF3D7_0102600	PF3D7_0102600.1	258	Plasmodium falciparum 3D7	Pf3D7_01_v3:118,812..122,534(-)	serine/threonine protein kinase, FIKK family	protein coding gene	DOWN
PF3D7_0104200	PF3D7_0104200.1	26	Plasmodium falciparum 3D7	Pf3D7_01_v3:182,205..184,820(-)	StAR-related lipid transfer protein	protein coding gene	DOWN
PF3D7_0104700	PF3D7_0104700.1	27	Plasmodium falciparum 3D7	Pf3D7_01_v3:210,870..213,005(+)	major facilitator superfamily-related transporter, putative	protein coding gene	UP
PF3D7_0107300	PF3D7_0107300.1	28	Plasmodium falciparum 3D7	Pf3D7_01_v3:299,464..301,151(-)	conserved Plasmodium protein, unknown function	protein coding gene	UP
PF3D7_0107500	PF3D7_0107500.1	29	Plasmodium falciparum 3D7	Pf3D7_01_v3:303,437..311,928(-)	Niemann-Pick type C1-related protein	protein coding gene	DOWN
PF3D7_0108500	PF3D7_0108500.1	30	Plasmodium falciparum 3D7	Pf3D7_01_v3:347,246..350,568(+)	ELM2 domain-containing protein, putative	protein coding gene	DOWN
PF3D7_0109100	PF3D7_0109100.1	31	Plasmodium falciparum 3D7	Pf3D7_01_v3:365,266..369,336(+)	LCCL domain-containing protein	protein coding gene	UP
PF3D7_0110000	PF3D7_0110000.1	32	Plasmodium falciparum 3D7	Pf3D7_01_v3:388,192..389,559(+)	conserved Plasmodium protein, unknown function	protein coding gene	UP
PF3D7_0112200	PF3D7_0112200.1	15	Plasmodium falciparum 3D7	Pf3D7_01_v3:463,764..471,891(+)	multidrug resistance-associated protein 1	protein coding gene	DOWN
PF3D7_0112800	PF3D7_0112800.1	16	Plasmodium falciparum 3D7	Pf3D7_01_v3:481,231..483,218(-)	Plasmodium exported protein (hyp11), unknown function	protein coding gene	UP
PF3D7_0113000	PF3D7_0113000.1	17	Plasmodium falciparum 3D7	Pf3D7_01_v3:487,239..490,901(-)	glutamic acid-rich protein GARP	protein coding gene	DOWN
PF3D7_0113200	PF3D7_0113200.1	259	Plasmodium falciparum 3D7	Pf3D7_01_v3:500,888..503,795(-)	Plasmodium exported protein, unknown function	protein coding gene	DOWN
PF3D7_0113700	PF3D7_0113700.1	21	Plasmodium falciparum 3D7	Pf3D7_01_v3:519,766..523,106(+)	heat shock protein 40, type II	protein coding gene	DOWN
PF3D7_0114200	PF3D7_0114200.1	22	Plasmodium falciparum 3D7	Pf3D7_01_v3:550,576..551,713(-)	exported protein family 3	protein coding gene	UP
PF3D7_0114800	PF3D7_0114800.1	23	Plasmodium falciparum 3D7	Pf3D7_01_v3:569,485..570,272(-)	Plasmodium exported protein (hyp7), unknown function	protein coding gene	DOWN
PF3D7_0202200	PF3D7_0202200.1	341	Plasmodium falciparum 3D7	Pf3D7_02_v3:111,818..115,064(-)	EMP1-trafficking protein	protein coding gene	DOWN
PF3D7_0202500	PF3D7_0202500.1	342	Plasmodium falciparum 3D7	Pf3D7_02_v3:127,203..129,089(+)	early transcribed membrane protein 2	protein coding gene	DOWN
PF3D7_0203800	PF3D7_0203800.1	343	Plasmodium falciparum 3D7	Pf3D7_02_v3:171,277..175,196(-)	conserved Plasmodium protein, unknown function	protein coding gene	UP
PF3D7_0206800	PF3D7_0206800.1	344	Plasmodium falciparum 3D7	Pf3D7_02_v3:271,576..274,917(-)	merozoite surface protein 2	protein coding gene	DOWN
PF3D7_0207400	PF3D7_0207400.1	345	Plasmodium falciparum 3D7	Pf3D7_02_v3:293,896..297,980(-)	serine repeat antigen 7	protein coding gene	DOWN
PF3D7_0207500	PF3D7_0207500.1	346	Plasmodium falciparum 3D7	Pf3D7_02_v3:298,380..302,820(-)	serine repeat antigen 6	protein coding gene	DOWN
PF3D7_0207600	PF3D7_0207600.1	347	Plasmodium falciparum 3D7	Pf3D7_02_v3:303,409..307,376(-)	serine repeat antigen 5	protein coding gene	DOWN
PF3D7_0207700	PF3D7_0207700.1	348	Plasmodium falciparum 3D7	Pf3D7_02_v3:308,628..312,348(-)	serine repeat antigen 4	protein coding gene	DOWN
PF3D7_0207800	PF3D7_0207800.1	349	Plasmodium falciparum 3D7	Pf3D7_02_v3:312,990..316,944(-)	serine repeat antigen 3	protein coding gene	DOWN
PF3D7_0208900	PF3D7_0208900.1	350	Plasmodium falciparum 3D7	Pf3D7_02_v3:360,828..368,354(+)	6-cysteine protein P230p	protein coding gene	UP
PF3D7_0209000	PF3D7_0209000.1	351	Plasmodium falciparum 3D7	Pf3D7_02_v3:369,351..380,156(+)	6-cysteine protein P230	protein coding gene	UP
PF3D7_0212600	PF3D7_0212600.1	352	Plasmodium falciparum 3D7	Pf3D7_02_v3:522,339..524,405(+)	secreted protein with altered thrombospondin repeat domain	protein coding gene	DOWN
PF3D7_0213600	PF3D7_0213600.1	353	Plasmodium falciparum 3D7	Pf3D7_02_v3:546,482..555,294(-)	conserved Plasmodium protein, unknown function	protein coding gene	UP
PF3D7_0213800	PF3D7_0213800.1	354	Plasmodium falciparum 3D7	Pf3D7_02_v3:558,585..560,594(+)	conserved protein, unknown function	protein coding gene	UP
PF3D7_0214200	PF3D7_0214200.1	355	Plasmodium falciparum 3D7	Pf3D7_02_v3:574,898..576,521(-)	ribosomal protein L13, mitochondrial	protein coding gene	DOWN
PF3D7_0215300	PF3D7_0215300.1	356	Plasmodium falciparum 3D7	Pf3D7_02_v3:628,091..632,681(-)	acyl-CoA synthetase	protein coding gene	DOWN
PF3D7_0216000	PF3D7_0216000.1	357	Plasmodium falciparum 3D7	Pf3D7_02_v3:657,770..664,734(+)	DEAD/DEAH box helicase, putative	protein coding gene	UP
PF3D7_0219100	PF3D7_0219100.1	358	Plasmodium falciparum 3D7	Pf3D7_02_v3:769,194..771,126(+)	saccharopine dehydrogenase, putative	protein coding gene	UP
PF3D7_0219300	PF3D7_0219300.1	359	Plasmodium falciparum 3D7	Pf3D7_02_v3:773,171..774,191(-)	conserved Plasmodium protein, unknown function	protein coding gene	UP
PF3D7_0220000	PF3D7_0220000.1	360	Plasmodium falciparum 3D7	Pf3D7_02_v3:794,978..801,981(+)	liver stage antigen 3	protein coding gene	DOWN
PF3D7_0220200	PF3D7_0220200.1	361	Plasmodium falciparum 3D7	Pf3D7_02_v3:809,073..812,695(-)	Plasmodium exported protein, unknown function	protein coding gene	DOWN
PF3D7_0220300	PF3D7_0220300.1	362	Plasmodium falciparum 3D7	Pf3D7_02_v3:812,892..815,853(-)	Plasmodium exported protein, unknown function	protein coding gene	DOWN
PF3D7_0220500	PF3D7_0220500.1	363	Plasmodium falciparum 3D7	Pf3D7_02_v3:823,293..825,588(-)	Plasmodium exported protein (hyp2), unknown function	protein coding gene	DOWN
PF3D7_0220600	PF3D7_0220600.1	364	Plasmodium falciparum 3D7	Pf3D7_02_v3:830,123..833,035(+)	Plasmodium exported protein (hyp9), unknown function	protein coding gene	DOWN
PF3D7_0220800	PF3D7_0220800.1	365	Plasmodium falciparum 3D7	Pf3D7_02_v3:838,594..844,668(+)	cytoadherence linked asexual protein 2	protein coding gene	DOWN

University of Ghana http://ugspace.ug.edu.gh

PF3D7_0221100	PF3D7_0221100.1	636	Plasmodium falciparum 3D7	Pf3D7_02_v3:851,052..851,962(+)	Plasmodium exported protein, unknown function, pseudogene	pseudogene	UP
PF3D7_0221700	PF3D7_0221700.1	366	Plasmodium falciparum 3D7	Pf3D7_02_v3:868,884..871,778(-)	Plasmodium exported protein, unknown function	protein coding gene	DOWN
PF3D7_0223500	PF3D7_0223500.1	367	Plasmodium falciparum 3D7	Pf3D7_02_v3:916,352..923,648(-)	erythrocyte membrane protein 1, PfEMP1	protein coding gene	DOWN
PF3D7_0301200	PF3D7_0301200.1	330	Plasmodium falciparum 3D7	Pf3D7_03_v3:78,154..81,283(-)	serine/threonine protein kinase, FIKK family	protein coding gene	DOWN
PF3D7_0301500	PF3D7_0301500.1	11	Plasmodium falciparum 3D7	Pf3D7_03_v3:87,480..90,921(-)	Plasmodium exported protein, unknown function	protein coding gene	DOWN
PF3D7_0301700	PF3D7_0301700.1	13	Plasmodium falciparum 3D7	Pf3D7_03_v3:95,216..99,115(-)	Plasmodium exported protein, unknown function	protein coding gene	DOWN
PF3D7_0301800	PF3D7_0301800.1	12	Plasmodium falciparum 3D7	Pf3D7_03_v3:103,118..105,748(+)	Plasmodium exported protein, unknown function	protein coding gene	DOWN
PF3D7_0302200	PF3D7_0302200.1	3	Plasmodium falciparum 3D7	Pf3D7_03_v3:119,098..124,924(+)	cytoadherence linked asexual protein 3.2	protein coding gene	DOWN
PF3D7_0302500	PF3D7_0302500.1	4	Plasmodium falciparum 3D7	Pf3D7_03_v3:134,486..141,185(+)	cytoadherence linked asexual protein 3.1	protein coding gene	DOWN
PF3D7_0303900	PF3D7_0303900.1	18	Plasmodium falciparum 3D7	Pf3D7_03_v3:196,570..197,601(-)	phosphatidylethanolamine-binding protein, putative	protein coding gene	UP
PF3D7_0304100	PF3D7_0304100.1	6	Plasmodium falciparum 3D7	Pf3D7_03_v3:203,251..206,328(+)	inner membrane complex protein 1e, putative	protein coding gene	UP
PF3D7_0307300	PF3D7_0307300.1	7	Plasmodium falciparum 3D7	Pf3D7_03_v3:318,804..320,336(+)	microtubule-associated protein RP/EB family, putative	protein coding gene	UP
PF3D7_0311000	PF3D7_0311000.1	2	Plasmodium falciparum 3D7	Pf3D7_03_v3:469,287..470,118(+)	conserved Plasmodium protein, unknown function	protein coding gene	UP
PF3D7_0311700	PF3D7_0311700.1	1	Plasmodium falciparum 3D7	Pf3D7_03_v3:502,698..505,935(+)	plasmepsin VI	protein coding gene	UP
PF3D7_0318000	PF3D7_0318000.1	5	Plasmodium falciparum 3D7	Pf3D7_03_v3:742,191..742,799(+)	conserved Plasmodium protein, unknown function	protein coding gene	UP
PF3D7_0318700	PF3D7_0318700.1	19	Plasmodium falciparum 3D7	Pf3D7_03_v3:788,145..789,211(+)	conserved Plasmodium protein, unknown function	protein coding gene	DOWN
PF3D7_0320200	PF3D7_0320200.1	331	Plasmodium falciparum 3D7	Pf3D7_03_v3:842,496..844,477(+)	CPW-WPC family protein	protein coding gene	UP
PF3D7_0320500	PF3D7_0320500.1	8	Plasmodium falciparum 3D7	Pf3D7_03_v3:860,221..862,776(+)	nicotinamidase, putative	protein coding gene	DOWN
PF3D7_0320900	PF3D7_0320900.1	10	Plasmodium falciparum 3D7	Pf3D7_03_v3:874,313..876,685(+)	histone H2A.Z	protein coding gene	DOWN
PF3D7_0321100	PF3D7_0321100.1	9	Plasmodium falciparum 3D7	Pf3D7_03_v3:879,438..885,952(-)	conserved Plasmodium protein, unknown function	protein coding gene	DOWN
PF3D7_0322800	PF3D7_0322800.1	20	Plasmodium falciparum 3D7	Pf3D7_03_v3:964,101..965,203(+)	conserved Plasmodium protein, unknown function	protein coding gene	UP
PF3D7_0401700	PF3D7_0401700.1	637	Plasmodium falciparum 3D7	Pf3D7_04_v3:100,684..102,110(+)	Plasmodium exported protein, unknown function, pseudogene	pseudogene	DOWN
PF3D7_0401800	PF3D7_0401800.1	33	Plasmodium falciparum 3D7	Pf3D7_04_v3:103,078..106,145(-)	Plasmodium exported protein (PHISTb), unknown function	protein coding gene	DOWN
PF3D7_0401900	PF3D7_0401900.1	34	Plasmodium falciparum 3D7	Pf3D7_04_v3:108,357..111,662(-)	acyl-CoA synthetase	protein coding gene	DOWN
PF3D7_0402000	PF3D7_0402000.1	35	Plasmodium falciparum 3D7	Pf3D7_04_v3:113,655..116,953(-)	Plasmodium exported protein (PHISTa), unknown function	protein coding gene	DOWN
PF3D7_0402100	PF3D7_0402100.1	36	Plasmodium falciparum 3D7	Pf3D7_04_v3:123,068..125,848(-)	Plasmodium exported protein (PHISTb), unknown function	protein coding gene	DOWN
PF3D7_0402400	PF3D7_0402400.1	37	Plasmodium falciparum 3D7	Pf3D7_04_v3:146,710..149,188(-)	Plasmodium exported protein, unknown function	protein coding gene	DOWN
PF3D7_0402500	PF3D7_0402500.1	638	Plasmodium falciparum 3D7	Pf3D7_04_v3:155,877..156,984(+)	rifin, pseudogene	pseudogene	UP
PF3D7_0402800	PF3D7_0402800.1	639	Plasmodium falciparum 3D7	Pf3D7_04_v3:167,245..171,985(+)	erythrocyte membrane protein 1 (PfEMP1), pseudogene	pseudogene	UP
PF3D7_0404700	PF3D7_0404700.1	38	Plasmodium falciparum 3D7	Pf3D7_04_v3:259,944..263,782(-)	dipeptidyl aminopeptidase 3	protein coding gene	DOWN
PF3D7_0405500	PF3D7_0405500.1	39	Plasmodium falciparum 3D7	Pf3D7_04_v3:301,259..302,267(-)	conserved Plasmodium protein, unknown function	protein coding gene	UP
PF3D7_0406900	PF3D7_0406900.1	260	Plasmodium falciparum 3D7	Pf3D7_04_v3:353,655..359,878(-)	conserved Plasmodium protein, unknown function	protein coding gene	UP
PF3D7_0411700	PF3D7_0411700.1	14	Plasmodium falciparum 3D7	Pf3D7_04_v3:518,685..519,101(-)	conserved Plasmodium protein, unknown function	protein coding gene	UP
PF3D7_0414300	PF3D7_0414300.1	261	Plasmodium falciparum 3D7	Pf3D7_04_v3:649,273..650,954(-)	Rab5-interacting protein, putative	protein coding gene	UP
PF3D7_0417100	PF3D7_0417100.1	40	Plasmodium falciparum 3D7	Pf3D7_04_v3:743,611..745,637(-)	mRNA-binding protein PUF2	protein coding gene	UP
PF3D7_0417700	PF3D7_0417700.1	262	Plasmodium falciparum 3D7	Pf3D7_04_v3:784,194..786,430(+)	conserved Plasmodium protein, unknown function	protein coding gene	UP
PF3D7_0418800	PF3D7_0418800.1	263	Plasmodium falciparum 3D7	Pf3D7_04_v3:843,562..845,169(+)	MOLO1 domain-containing protein, putative	protein coding gene	UP
PF3D7_0420200	PF3D7_0420200.1	41	Plasmodium falciparum 3D7	Pf3D7_04_v3:909,409..912,119(+)	holo-[acyl-carrier-protein] synthase, putative	protein coding gene	UP
PF3D7_0421700	PF3D7_0421700.1	264	Plasmodium falciparum 3D7	Pf3D7_04_v3:987,842..994,360(-)	conserved Plasmodium protein, unknown function	protein coding gene	UP
PF3D7_0421900	PF3D7_0421900.1	42	Plasmodium falciparum 3D7	Pf3D7_04_v3:997,240..997,455(+)	conserved Plasmodium protein, unknown function	protein coding gene	UP
PF3D7_0423400	PF3D7_0423400.1	43	Plasmodium falciparum 3D7	Pf3D7_04_v3:1,055,314..1,056,674(+)	apical asparagine-rich protein AARP	protein coding gene	DOWN
PF3D7_0424000	PF3D7_0424000.1	265	Plasmodium falciparum 3D7	Pf3D7_04_v3:1,080,176..1,082,321(+)	Plasmodium exported protein (PHISTc), unknown function	protein coding gene	DOWN
PF3D7_0424500	PF3D7_0424500.1	44	Plasmodium falciparum 3D7	Pf3D7_04_v3:1,108,275..1,112,724(+)	serine/threonine protein kinase, FIKK family	protein coding gene	DOWN
PF3D7_0424600	PF3D7_0424600.1	45	Plasmodium falciparum 3D7	Pf3D7_04_v3:1,112,736..1,117,250(-)	Plasmodium exported protein (PHISTb)	protein coding gene	DOWN
PF3D7_0424700	PF3D7_0424700.1	46	Plasmodium falciparum 3D7	Pf3D7_04_v3:1,115,896..1,123,289(+)	serine/threonine protein kinase, FIKK family	protein coding gene	DOWN

University of Ghana http://ugspace.ug.edu.gh

PF3D7_0426000	PF3D7_0426000.1	47	Plasmodium falciparum 3D7	Pf3D7_04_v3:1,173,053..1,180,226(-)	erythrocyte membrane protein 1, PfEMP1	protein coding gene	DOWN
PF3D7_0500800	PF3D7_0500800.1	101	Plasmodium falciparum 3D7	Pf3D7_05_v3:42,114..48,258(-)	mature parasite-infected erythrocyte surface antigen	protein coding gene	DOWN
PF3D7_0500900	PF3D7_0500900.1	102	Plasmodium falciparum 3D7	Pf3D7_05_v3:50,081..52,576(-)	serine/threonine protein kinase, FIKK family	protein coding gene	DOWN
PF3D7_0501000	PF3D7_0501000.1	103	Plasmodium falciparum 3D7	Pf3D7_05_v3:55,122..57,159(+)	Plasmodium exported protein, unknown function	protein coding gene	DOWN
PF3D7_0501300	PF3D7_0501300.1	104	Plasmodium falciparum 3D7	Pf3D7_05_v3:67,224..70,944(+)	skeleton-binding protein 1	protein coding gene	DOWN
PF3D7_0501400	PF3D7_0501400.1	105	Plasmodium falciparum 3D7	Pf3D7_05_v3:73,163..80,813(+)	interspersed repeat antigen	protein coding gene	DOWN
PF3D7_0501500	PF3D7_0501500.1	106	Plasmodium falciparum 3D7	Pf3D7_05_v3:80,570..82,763(-)	rhoptry-associated protein 3	protein coding gene	DOWN
PF3D7_0501600	PF3D7_0501600.1	107	Plasmodium falciparum 3D7	Pf3D7_05_v3:83,760..85,512(-)	rhoptry-associated protein 2	protein coding gene	DOWN
PF3D7_0501700	PF3D7_0501700.1	108	Plasmodium falciparum 3D7	Pf3D7_05_v3:86,820..89,201(-)	anaphase-promoting complex subunit 3, putative	protein coding gene	UP
PF3D7_0502300	PF3D7_0502300.1	109	Plasmodium falciparum 3D7	Pf3D7_05_v3:106,583..108,202(-)	conserved Plasmodium protein, unknown function	protein coding gene	UP
PF3D7_0503100	PF3D7_0503100.1	110	Plasmodium falciparum 3D7	Pf3D7_05_v3:126,662..128,917(-)	4-diphosphocytidyl-2-C-methyl-D-erythritol kinase, putative	protein coding gene	DOWN
PF3D7_0503200	PF3D7_0503200.1	111	Plasmodium falciparum 3D7	Pf3D7_05_v3:130,209..133,825(+)	cell division control protein 6, putative	protein coding gene	UP
PF3D7_0504500	PF3D7_0504500.1	112	Plasmodium falciparum 3D7	Pf3D7_05_v3:174,882..176,765(+)	MOLO1 domain-containing protein, putative	protein coding gene	UP
PF3D7_0504900	PF3D7_0504900.1	266	Plasmodium falciparum 3D7	Pf3D7_05_v3:206,397..208,680(+)	transmembrane protein TMEM222, putative	protein coding gene	UP
PF3D7_0506400	PF3D7_0506400.1	267	Plasmodium falciparum 3D7	Pf3D7_05_v3:262,672..263,925(-)	conserved Plasmodium protein, unknown function	protein coding gene	UP
PF3D7_0507500	PF3D7_0507500.1	113	Plasmodium falciparum 3D7	Pf3D7_05_v3:307,090..310,120(-)	subtilisin-like protease 1	protein coding gene	DOWN
PF3D7_0508300	PF3D7_0508300.1	114	Plasmodium falciparum 3D7	Pf3D7_05_v3:340,652..344,452(+)	triose phosphate transporter	protein coding gene	DOWN
PF3D7_0509700	PF3D7_0509700.1	115	Plasmodium falciparum 3D7	Pf3D7_05_v3:405,961..407,897(-)	conserved Plasmodium protein, unknown function	protein coding gene	UP
PF3D7_0510300	PF3D7_0510300.1	116	Plasmodium falciparum 3D7	Pf3D7_05_v3:440,724..442,007(-)	stripes inner membrane complex protein, putative	protein coding gene	UP
PF3D7_0510700	PF3D7_0510700.1	117	Plasmodium falciparum 3D7	Pf3D7_05_v3:459,301..460,344(+)	conserved Plasmodium protein, unknown function	protein coding gene	UP
PF3D7_0510800	PF3D7_0510800.1	268	Plasmodium falciparum 3D7	Pf3D7_05_v3:461,017..464,399(+)	WD repeat-containing protein, putative	protein coding gene	UP
PF3D7_0511600	PF3D7_0511600.1	118	Plasmodium falciparum 3D7	Pf3D7_05_v3:517,088..518,520(-)	apical rhoptry neck protein	protein coding gene	DOWN
PF3D7_0513000	PF3D7_0513000.1	119	Plasmodium falciparum 3D7	Pf3D7_05_v3:555,264..556,651(+)	conserved protein, unknown function	protein coding gene	UP
PF3D7_0513700	PF3D7_0513700.1	269	Plasmodium falciparum 3D7	Pf3D7_05_v3:580,815..584,424(+)	secreted ookinete protein, putative	protein coding gene	UP
PF3D7_0514500	PF3D7_0514500.1	270	Plasmodium falciparum 3D7	Pf3D7_05_v3:604,633..606,347(-)	conserved Plasmodium membrane protein, unknown function	protein coding gene	UP
PF3D7_0514700	PF3D7_0514700.1	120	Plasmodium falciparum 3D7	Pf3D7_05_v3:610,089..614,771(+)	MORN repeat protein, putative	protein coding gene	UP
PF3D7_0515500	PF3D7_0515500.1	121	Plasmodium falciparum 3D7	Pf3D7_05_v3:641,137..644,685(-)	gametogenesis essential protein 1, putative	protein coding gene	UP
PF3D7_0515600	PF3D7_0515600.1	122	Plasmodium falciparum 3D7	Pf3D7_05_v3:646,042..652,163(+)	gamete egress protein GEP, putative	protein coding gene	UP
PF3D7_0516500	PF3D7_0516500.1	271	Plasmodium falciparum 3D7	Pf3D7_05_v3:683,708..685,859(+)	major facilitator superfamily domain-containing protein, putative	protein coding gene	UP
PF3D7_0517500	PF3D7_0517500.1	272	Plasmodium falciparum 3D7	Pf3D7_05_v3:735,386..738,469(-)	UTP--glucose-1-phosphate uridylyltransferase, putative	protein coding gene	UP
PF3D7_0517800	PF3D7_0517800.1	273	Plasmodium falciparum 3D7	Pf3D7_05_v3:745,798..746,634(-)	apicortin	protein coding gene	UP
PF3D7_0518400	PF3D7_0518400.1	123	Plasmodium falciparum 3D7	Pf3D7_05_v3:762,103..762,792(-)	cyclin, putative	protein coding gene	UP
PF3D7_0518700	PF3D7_0518700.1	124	Plasmodium falciparum 3D7	Pf3D7_05_v3:774,052..780,916(-)	mRNA-binding protein PUF1	protein coding gene	UP
PF3D7_0518800	PF3D7_0518800.1	274	Plasmodium falciparum 3D7	Pf3D7_05_v3:783,638..784,991(-)	secreted ookinete protein, putative	protein coding gene	UP
PF3D7_0520900	PF3D7_0520900.1	125	Plasmodium falciparum 3D7	Pf3D7_05_v3:856,500..859,367(+)	adenosylhomocysteinase	protein coding gene	DOWN
PF3D7_0521900	PF3D7_0521900.1	126	Plasmodium falciparum 3D7	Pf3D7_05_v3:888,657..895,144(+)	conserved Plasmodium protein, unknown function	protein coding gene	UP
PF3D7_0522900	PF3D7_0522900.1	127	Plasmodium falciparum 3D7	Pf3D7_05_v3:948,230..953,960(+)	zinc finger protein, putative	protein coding gene	UP
PF3D7_0525800	PF3D7_0525800.1	128	Plasmodium falciparum 3D7	Pf3D7_05_v3:1,071,094..1,072,988(+)	inner membrane complex protein 1g, putative	protein coding gene	DOWN
PF3D7_0525900	PF3D7_0525900.1	275	Plasmodium falciparum 3D7	Pf3D7_05_v3:1,073,417..1,075,644(+)	NIMA related kinase 2	protein coding gene	UP
PF3D7_0526100	PF3D7_0526100.1	129	Plasmodium falciparum 3D7	Pf3D7_05_v3:1,079,225..1,081,313(+)	conserved Plasmodium membrane protein, unknown function	protein coding gene	UP
PF3D7_0527100	PF3D7_0527100.1	130	Plasmodium falciparum 3D7	Pf3D7_05_v3:1,129,570..1,131,702(-)	ubiquitin-conjugating enzyme E2 13	protein coding gene	UP
PF3D7_0527200	PF3D7_0527200.1	131	Plasmodium falciparum 3D7	Pf3D7_05_v3:1,132,901..1,135,534(-)	ubiquitin carboxyl-terminal hydrolase 14	protein coding gene	DOWN
PF3D7_0528900	PF3D7_0528900.1	276	Plasmodium falciparum 3D7	Pf3D7_05_v3:1,183,850..1,186,249(-)	conserved protein, unknown function	protein coding gene	UP
PF3D7_0530500	PF3D7_0530500.1	277	Plasmodium falciparum 3D7	Pf3D7_05_v3:1,244,751..1,248,359(+)	conserved Plasmodium membrane protein, unknown function	protein coding gene	UP
PF3D7_0530800	PF3D7_0530800.1	278	Plasmodium falciparum 3D7	Pf3D7_05_v3:1,255,012..1,257,579(+)	CPW-WPC family protein	protein coding gene	UP

University of Ghana http://ugspace.ug.edu.gh

PF3D7_0532100	PF3D7_0532100.1	132	Plasmodium falciparum 3D7	Pf3D7_05_v3:1,300,188..1,302,740(+)	early transcribed membrane protein 5	protein coding gene	DOWN
PF3D7_0532300	PF3D7_0532300.1	133	Plasmodium falciparum 3D7	Pf3D7_05_v3:1,307,099..1,310,572(+)	Plasmodium exported protein (PHISTb), unknown function	protein coding gene	DOWN
PF3D7_0532400	PF3D7_0532400.1	134	Plasmodium falciparum 3D7	Pf3D7_05_v3:1,311,992..1,315,355(+)	lysine-rich membrane-associated PHISTb protein	protein coding gene	DOWN
PF3D7_0532600	PF3D7_0532600.1	279	Plasmodium falciparum 3D7	Pf3D7_05_v3:1,317,882..1,319,382(-)	Plasmodium exported protein, unknown function	protein coding gene	DOWN
PF3D7_0601900	PF3D7_0601900.1	239	Plasmodium falciparum 3D7	Pf3D7_06_v3:76,204..79,596(+)	conserved Plasmodium protein, unknown function	protein coding gene	DOWN
PF3D7_0602700	PF3D7_0602700.1	240	Plasmodium falciparum 3D7	Pf3D7_06_v3:113,592..115,478(-)	conserved Plasmodium protein, unknown function	protein coding gene	UP
PF3D7_0604100	PF3D7_0604100.1	241	Plasmodium falciparum 3D7	Pf3D7_06_v3:170,776..178,985(-)	AP2 domain transcription factor	protein coding gene	DOWN
PF3D7_0604400	PF3D7_0604400.1	242	Plasmodium falciparum 3D7	Pf3D7_06_v3:184,892..185,843(+)	conserved protein, unknown function	protein coding gene	UP
PF3D7_0604800	PF3D7_0604800.1	243	Plasmodium falciparum 3D7	Pf3D7_06_v3:206,807..211,802(-)	RAP protein, putative	protein coding gene	UP
PF3D7_0605600	PF3D7_0605600.1	244	Plasmodium falciparum 3D7	Pf3D7_06_v3:228,132..234,835(-)	nucleoside diphosphate kinase, putative	protein coding gene	UP
PF3D7_0606400	PF3D7_0606400.1	245	Plasmodium falciparum 3D7	Pf3D7_06_v3:263,936..264,830(-)	conserved Plasmodium protein, unknown function	protein coding gene	UP
PF3D7_0607100	PF3D7_0607100.1	246	Plasmodium falciparum 3D7	Pf3D7_06_v3:297,941..301,197(+)	MYND-type zinc finger protein, putative	protein coding gene	UP
PF3D7_0607700	PF3D7_0607700.1	247	Plasmodium falciparum 3D7	Pf3D7_06_v3:319,519..329,442(+)	conserved Plasmodium protein, unknown function	protein coding gene	UP
PF3D7_0608600	PF3D7_0608600.1	248	Plasmodium falciparum 3D7	Pf3D7_06_v3:354,683..356,424(+)	conserved Plasmodium protein, unknown function	protein coding gene	UP
PF3D7_0609600	PF3D7_0609600.1	249	Plasmodium falciparum 3D7	Pf3D7_06_v3:408,041..412,002(+)	conserved Plasmodium protein, unknown function	protein coding gene	UP
PF3D7_0611000	PF3D7_0611000.1	250	Plasmodium falciparum 3D7	Pf3D7_06_v3:463,021..465,127(-)	SNARE associated Golgi protein, putative	protein coding gene	UP
PF3D7_0611500	PF3D7_0611500.1	251	Plasmodium falciparum 3D7	Pf3D7_06_v3:482,825..483,907(-)	conserved protein, unknown function	protein coding gene	UP
PF3D7_0611900	PF3D7_0611900.1	252	Plasmodium falciparum 3D7	Pf3D7_06_v3:505,314..507,593(+)	lsm12, putative	protein coding gene	UP
PF3D7_0612500	PF3D7_0612500.1	253	Plasmodium falciparum 3D7	Pf3D7_06_v3:522,300..522,665(-)	conserved Plasmodium protein, unknown function	protein coding gene	UP
PF3D7_0613200	PF3D7_0613200.1	254	Plasmodium falciparum 3D7	Pf3D7_06_v3:539,074..539,954(+)	conserved Plasmodium protein, unknown function	protein coding gene	UP
PF3D7_0613500	PF3D7_0613500.1	255	Plasmodium falciparum 3D7	Pf3D7_06_v3:547,900..552,544(-)	AP-3 complex subunit beta, putative	protein coding gene	UP
PF3D7_0615200	PF3D7_0615200.1	256	Plasmodium falciparum 3D7	Pf3D7_06_v3:625,120..627,612(+)	conserved protein, unknown function	protein coding gene	UP
PF3D7_0616500	PF3D7_0616500.1	257	Plasmodium falciparum 3D7	Pf3D7_06_v3:684,742..688,857(+)	TRAP-like protein	protein coding gene	UP
PF3D7_0617700	PF3D7_0617700.1	222	Plasmodium falciparum 3D7	Pf3D7_06_v3:741,269..742,406(-)	rifin	protein coding gene	DOWN
PF3D7_0617800	PF3D7_0617800.1	223	Plasmodium falciparum 3D7	Pf3D7_06_v3:747,329..749,285(-)	histone H2A	protein coding gene	DOWN
PF3D7_0618000	PF3D7_0618000.1	224	Plasmodium falciparum 3D7	Pf3D7_06_v3:757,278..761,654(+)	conserved Plasmodium membrane protein, unknown function	protein coding gene	DOWN
PF3D7_0618900	PF3D7_0618900.1	225	Plasmodium falciparum 3D7	Pf3D7_06_v3:784,019..788,588(+)	phosphatidylinositol N-acetylglucosaminyltransferase subunit GPI1	protein coding gene	UP
PF3D7_0618900	PF3D7_0618900.2	225	Plasmodium falciparum 3D7	Pf3D7_06_v3:784,019..788,588(+)	phosphatidylinositol N-acetylglucosaminyltransferase subunit GPI1	protein coding gene	UP
PF3D7_0619500	PF3D7_0619500.1	226	Plasmodium falciparum 3D7	Pf3D7_06_v3:819,576..824,325(-)	acyl-CoA synthetase	protein coding gene	DOWN
PF3D7_0620300	PF3D7_0620300.1	227	Plasmodium falciparum 3D7	Pf3D7_06_v3:848,035..850,864(-)	conserved Plasmodium protein, unknown function	protein coding gene	DOWN
PF3D7_0620400	PF3D7_0620400.1	228	Plasmodium falciparum 3D7	Pf3D7_06_v3:851,162..853,200(-)	merozoite surface protein 10	protein coding gene	DOWN
PF3D7_0620700	PF3D7_0620700.1	229	Plasmodium falciparum 3D7	Pf3D7_06_v3:858,689..860,721(-)	DnaJ protein, putative	protein coding gene	UP
PF3D7_0621400	PF3D7_0621400.1	230	Plasmodium falciparum 3D7	Pf3D7_06_v3:878,363..880,852(+)	Pf77 protein	protein coding gene	UP
PF3D7_0622100	PF3D7_0622100.1	231	Plasmodium falciparum 3D7	Pf3D7_06_v3:897,970..902,735(-)	conserved Plasmodium protein, unknown function	protein coding gene	UP
PF3D7_0623200	PF3D7_0623200.1	232	Plasmodium falciparum 3D7	Pf3D7_06_v3:945,100..947,629(+)	ferredoxin--NADP reductase	protein coding gene	UP
PF3D7_0624100	PF3D7_0624100.1	233	Plasmodium falciparum 3D7	Pf3D7_06_v3:983,297..985,562(+)	conserved protein, unknown function	protein coding gene	UP
PF3D7_0624300	PF3D7_0624300.1	234	Plasmodium falciparum 3D7	Pf3D7_06_v3:987,808..989,636(+)	CPW-WPC family protein	protein coding gene	UP
PF3D7_0625100	PF3D7_0625100.1	235	Plasmodium falciparum 3D7	Pf3D7_06_v3:1,023,015..1,024,214(+)	sphingomyelin synthase 2, putative	protein coding gene	UP
PF3D7_0625400	PF3D7_0625400.1	236	Plasmodium falciparum 3D7	Pf3D7_06_v3:1,031,969..1,034,471(-)	conserved Plasmodium protein, unknown function	protein coding gene	DOWN
PF3D7_0628400	PF3D7_0628400.1	280	Plasmodium falciparum 3D7	Pf3D7_06_v3:1,175,869..1,178,588(+)	protease, putative	protein coding gene	UP
PF3D7_0630000	PF3D7_0630000.1	237	Plasmodium falciparum 3D7	Pf3D7_06_v3:1,252,052..1,253,985(-)	CPW-WPC family protein	protein coding gene	UP
PF3D7_0630200	PF3D7_0630200.1	238	Plasmodium falciparum 3D7	Pf3D7_06_v3:1,258,880..1,259,939(+)	secreted ookinete protein, putative	protein coding gene	UP
PF3D7_0701900	PF3D7_0701900.1	48	Plasmodium falciparum 3D7	Pf3D7_07_v3:79,450..83,835(-)	Plasmodium exported protein, unknown function	protein coding gene	DOWN
PF3D7_0702000	PF3D7_0702000.1	281	Plasmodium falciparum 3D7	Pf3D7_07_v3:83,838..86,436(+)	Plasmodium exported protein (hyp12), unknown function	protein coding gene	DOWN

University of Ghana http://ugspace.ug.edu.gh

PF3D7_0702100	PF3D7_0702100.1	640	Plasmodium falciparum 3D7	Pf3D7_07_v3:88,685..90,886(+)	Plasmodium exported protein (PHISTb), unknown function, pseudogene	pseudogene	DOWN
PF3D7_0702200	PF3D7_0702200.1	49	Plasmodium falciparum 3D7	Pf3D7_07_v3:91,731..95,602(-)	lysophospholipase LPL20	protein coding gene	DOWN
PF3D7_0702400	PF3D7_0702400.1	50	Plasmodium falciparum 3D7	Pf3D7_07_v3:100,338..103,399(+)	small exported membrane protein 1	protein coding gene	DOWN
PF3D7_0702500	PF3D7_0702500.1	51	Plasmodium falciparum 3D7	Pf3D7_07_v3:104,012..106,731(-)	Plasmodium exported protein, unknown function	protein coding gene	DOWN
PF3D7_0703700	PF3D7_0703700.1	52	Plasmodium falciparum 3D7	Pf3D7_07_v3:146,573..148,237(-)	conserved protein, unknown function	protein coding gene	DOWN
PF3D7_0704100	PF3D7_0704100.1	282	Plasmodium falciparum 3D7	Pf3D7_07_v3:179,797..191,155(+)	basal complex transmembrane protein 2	protein coding gene	UP
PF3D7_0705800	PF3D7_0705800.1	337	Plasmodium falciparum 3D7	Pf3D7_07_v3:287,597..289,088(-)	cysteine-rich secretory protein	protein coding gene	UP
PF3D7_0707300	PF3D7_0707300.1	283	Plasmodium falciparum 3D7	Pf3D7_07_v3:337,720..343,059(+)	rhoptry-associated membrane antigen	protein coding gene	DOWN
PF3D7_0708000	PF3D7_0708000.1	284	Plasmodium falciparum 3D7	Pf3D7_07_v3:368,274..372,081(+)	cytoskeleton associated protein, putative	protein coding gene	UP
PF3D7_0708600	PF3D7_0708600.1	53	Plasmodium falciparum 3D7	Pf3D7_07_v3:389,473..390,365(-)	inner membrane complex protein 1d, putative	protein coding gene	UP
PF3D7_0711700	PF3D7_0711700.1	54	Plasmodium falciparum 3D7	Pf3D7_07_v3:511,950..519,425(-)	erythrocyte membrane protein 1, PfEMP1	protein coding gene	DOWN
PF3D7_0713100	PF3D7_0713100.1	55	Plasmodium falciparum 3D7	Pf3D7_07_v3:605,369..606,780(+)	Pfmc-2TM Maurer's cleft two transmembrane protein	protein coding gene	DOWN
PF3D7_0714000	PF3D7_0714000.1	56	Plasmodium falciparum 3D7	Pf3D7_07_v3:642,200..643,997(-)	histone H2B variant	protein coding gene	DOWN
PF3D7_0714100	PF3D7_0714100.1	57	Plasmodium falciparum 3D7	Pf3D7_07_v3:646,719..648,767(-)	MAATS1 domain-containing protein, putative	protein coding gene	UP
PF3D7_0714400	PF3D7_0714400.1	58	Plasmodium falciparum 3D7	Pf3D7_07_v3:662,068..664,084(-)	calmodulin, putative	protein coding gene	UP
PF3D7_0715200	PF3D7_0715200.1	59	Plasmodium falciparum 3D7	Pf3D7_07_v3:675,522..682,899(-)	conserved Plasmodium protein, unknown function	protein coding gene	UP
PF3D7_0715400	PF3D7_0715400.1	338	Plasmodium falciparum 3D7	Pf3D7_07_v3:687,618..689,135(-)	secreted ookinete protein, putative	protein coding gene	UP
PF3D7_0715700	PF3D7_0715700.1	60	Plasmodium falciparum 3D7	Pf3D7_07_v3:694,095..695,200(+)	conserved protein, unknown function	protein coding gene	UP
PF3D7_0717800	PF3D7_0717800.1	61	Plasmodium falciparum 3D7	Pf3D7_07_v3:767,357..771,949(-)	conserved Plasmodium protein, unknown function	protein coding gene	UP
PF3D7_0718000	PF3D7_0718000.1	285	Plasmodium falciparum 3D7	Pf3D7_07_v3:776,141..795,637(-)	dynein heavy chain, putative	protein coding gene	UP
PF3D7_0718700	PF3D7_0718700.1	62	Plasmodium falciparum 3D7	Pf3D7_07_v3:831,360..833,140(-)	conserved Plasmodium membrane protein, unknown function	protein coding gene	UP
PF3D7_0718800	PF3D7_0718800.1	286	Plasmodium falciparum 3D7	Pf3D7_07_v3:833,630..835,051(-)	conserved protein, unknown function	protein coding gene	UP
PF3D7_0719100	PF3D7_0719100.1	63	Plasmodium falciparum 3D7	Pf3D7_07_v3:838,686..840,277(-)	ATP synthase F0 subunit a-like protein, putative	protein coding gene	UP
PF3D7_0719200	PF3D7_0719200.1	287	Plasmodium falciparum 3D7	Pf3D7_07_v3:840,693..843,025(+)	NIMA related kinase 4	protein coding gene	UP
PF3D7_0721700	PF3D7_0721700.1	64	Plasmodium falciparum 3D7	Pf3D7_07_v3:935,116..937,312(+)	secreted ookinete protein, putative	protein coding gene	UP
PF3D7_0722200	PF3D7_0722200.1	65	Plasmodium falciparum 3D7	Pf3D7_07_v3:946,077..949,317(+)	rhoptry-associated leucine zipper-like protein 1	protein coding gene	DOWN
PF3D7_0722800	PF3D7_0722800.1	66	Plasmodium falciparum 3D7	Pf3D7_07_v3:963,370..965,109(+)	conserved protein, unknown function	protein coding gene	UP
PF3D7_0723100	PF3D7_0723100.1	67	Plasmodium falciparum 3D7	Pf3D7_07_v3:970,492..971,877(-)	protein CPH1, putative	protein coding gene	UP
PF3D7_0724900	PF3D7_0724900.1	68	Plasmodium falciparum 3D7	Pf3D7_07_v3:1,052,392..1,058,413(+)	kinesin-20, putative	protein coding gene	UP
PF3D7_0728700	PF3D7_0728700.1	69	Plasmodium falciparum 3D7	Pf3D7_07_v3:1,225,499..1,229,857(-)	alpha/beta hydrolase, putative	protein coding gene	UP
PF3D7_0730900	PF3D7_0730900.1	70	Plasmodium falciparum 3D7	Pf3D7_07_v3:1,324,452..1,333,940(+)	EMP1-trafficking protein	protein coding gene	DOWN
PF3D7_0731200	PF3D7_0731200.1	71	Plasmodium falciparum 3D7	Pf3D7_07_v3:1,342,335..1,344,508(-)	Plasmodium exported protein, unknown function	protein coding gene	DOWN
PF3D7_0731300	PF3D7_0731300.1	72	Plasmodium falciparum 3D7	Pf3D7_07_v3:1,348,427..1,351,829(+)	Plasmodium exported protein (PHISTb), unknown function	protein coding gene	DOWN
PF3D7_0731400	PF3D7_0731400.1	641	Plasmodium falciparum 3D7	Pf3D7_07_v3:1,353,758..1,355,482(+)	serine/threonine protein kinase, FIKK family, pseudogene	pseudogene	DOWN
PF3D7_0731500	PF3D7_0731500.1	73	Plasmodium falciparum 3D7	Pf3D7_07_v3:1,357,251..1,363,653(+)	erythrocyte binding antigen-175	protein coding gene	DOWN
PF3D7_0731600	PF3D7_0731600.1	74	Plasmodium falciparum 3D7	Pf3D7_07_v3:1,366,407..1,370,816(+)	acyl-CoA synthetase	protein coding gene	DOWN
PF3D7_0731700	PF3D7_0731700.1	75	Plasmodium falciparum 3D7	Pf3D7_07_v3:1,371,309..1,372,884(+)	Plasmodium exported protein (hyp9), unknown function	protein coding gene	DOWN
PF3D7_0732200	PF3D7_0732200.1	76	Plasmodium falciparum 3D7	Pf3D7_07_v3:1,390,711..1,392,043(+)	rifin	protein coding gene	DOWN
PF3D7_0800100	PF3D7_0800100.1	100	Plasmodium falciparum 3D7	Pf3D7_08_v3:21,361..28,653(+)	erythrocyte membrane protein 1, PfEMP1	protein coding gene	DOWN
PF3D7_0800800	PF3D7_0800800.1	99	Plasmodium falciparum 3D7	Pf3D7_08_v3:79,126..80,766(+)	Plasmodium exported protein (hyp7), unknown function	protein coding gene	DOWN
PF3D7_0800900	PF3D7_0800900.1	642	Plasmodium falciparum 3D7	Pf3D7_08_v3:83,128..83,904(+)	Plasmodium exported protein (hyp7), unknown function, pseudogene	pseudogene	DOWN
PF3D7_0801400	PF3D7_0801400.1	98	Plasmodium falciparum 3D7	Pf3D7_08_v3:104,442..105,517(-)	conserved Plasmodium protein, unknown function	protein coding gene	UP
PF3D7_0801600	PF3D7_0801600.1	97	Plasmodium falciparum 3D7	Pf3D7_08_v3:108,965..109,811(-)	conserved protein, unknown function	protein coding gene	UP
PF3D7_0804700	PF3D7_0804700.1	339	Plasmodium falciparum 3D7	Pf3D7_08_v3:271,417..277,413(-)	conserved Plasmodium protein, unknown function	protein coding gene	UP
PF3D7_0805300	PF3D7_0805300.1	96	Plasmodium falciparum 3D7	Pf3D7_08_v3:293,097..297,324(-)	zinc finger protein, putative	protein coding gene	UP

University of Ghana http://ugspace.ug.edu.gh

PF3D7_0805800	PF3D7_0805800.1	340	Plasmodium falciparum 3D7	Pf3D7_08_v3:322,367..323,677(-)	conserved Plasmodium protein, unknown function	protein coding gene	UP
PF3D7_0809200	PF3D7_0809200.1	95	Plasmodium falciparum 3D7	Pf3D7_08_v3:467,507..472,481(-)	asparagine-rich antigen Pfa55-14	protein coding gene	UP
PF3D7_0813500	PF3D7_0813500.1	94	Plasmodium falciparum 3D7	Pf3D7_08_v3:665,548..667,095(-)	PUB domain-containing protein, putative	protein coding gene	UP
PF3D7_0813800	PF3D7_0813800.1	93	Plasmodium falciparum 3D7	Pf3D7_08_v3:676,314..677,698(+)	GDP-mannose 4,6-dehydratase	protein coding gene	UP
PF3D7_0816500	PF3D7_0816500.1	92	Plasmodium falciparum 3D7	Pf3D7_08_v3:760,138..761,031(+)	small heat shock protein HSP20, putative	protein coding gene	UP
PF3D7_0816800	PF3D7_0816800.1	91	Plasmodium falciparum 3D7	Pf3D7_08_v3:767,916..769,803(-)	meiotic recombination protein DMC1, putative	protein coding gene	UP
PF3D7_0817900	PF3D7_0817900.1	90	Plasmodium falciparum 3D7	Pf3D7_08_v3:816,742..818,583(-)	high mobility group protein B2	protein coding gene	UP
PF3D7_0818100	PF3D7_0818100.1	89	Plasmodium falciparum 3D7	Pf3D7_08_v3:823,912..827,305(+)	zinc finger protein, putative	protein coding gene	DOWN
PF3D7_0818900	PF3D7_0818900.1	88	Plasmodium falciparum 3D7	Pf3D7_08_v3:858,550..862,980(+)	heat shock protein 70	protein coding gene	DOWN
PF3D7_0820200	PF3D7_0820200.1	87	Plasmodium falciparum 3D7	Pf3D7_08_v3:911,627..915,386(-)	phosphatidylglycerophosphate synthase	protein coding gene	DOWN
PF3D7_0821400	PF3D7_0821400.1	86	Plasmodium falciparum 3D7	Pf3D7_08_v3:964,289..967,130(+)	conserved Plasmodium protein, unknown function	protein coding gene	DOWN
PF3D7_0822400	PF3D7_0822400.1	288	Plasmodium falciparum 3D7	Pf3D7_08_v3:989,973..992,608(+)	conserved Plasmodium protein, unknown function	protein coding gene	UP
PF3D7_0822900	PF3D7_0822900.1	85	Plasmodium falciparum 3D7	Pf3D7_08_v3:1,006,504..1,011,755(-)	PhIL1-interacting candidate PIC2	protein coding gene	DOWN
PF3D7_0825000	PF3D7_0825000.1	289	Plasmodium falciparum 3D7	Pf3D7_08_v3:1,085,451..1,091,286(+)	conserved Plasmodium protein, unknown function	protein coding gene	UP
PF3D7_0825300	PF3D7_0825300.1	84	Plasmodium falciparum 3D7	Pf3D7_08_v3:1,094,794..1,095,972(-)	SAYSvFN domain-containing protein, putative	protein coding gene	UP
PF3D7_0825700	PF3D7_0825700.1	83	Plasmodium falciparum 3D7	Pf3D7_08_v3:1,101,887..1,102,804(-)	crystalloid-specific PH domain-containing protein, putative	protein coding gene	UP
PF3D7_0825800	PF3D7_0825800.1	290	Plasmodium falciparum 3D7	Pf3D7_08_v3:1,103,768..1,105,108(+)	PH-like domain-containing protein, putative	protein coding gene	UP
PF3D7_0825900	PF3D7_0825900.1	82	Plasmodium falciparum 3D7	Pf3D7_08_v3:1,105,631..1,108,315(+)	conserved Plasmodium protein, unknown function	protein coding gene	UP
PF3D7_0827200	PF3D7_0827200.1	81	Plasmodium falciparum 3D7	Pf3D7_08_v3:1,177,310..1,180,324(+)	conserved Plasmodium protein, unknown function	protein coding gene	UP
PF3D7_0827400	PF3D7_0827400.1	80	Plasmodium falciparum 3D7	Pf3D7_08_v3:1,184,595..1,185,251(+)	conserved protein, unknown function	protein coding gene	UP
PF3D7_0827700	PF3D7_0827700.1	79	Plasmodium falciparum 3D7	Pf3D7_08_v3:1,193,847..1,196,678(-)	magnesium transporter, putative	protein coding gene	UP
PF3D7_0828000	PF3D7_0828000.1	291	Plasmodium falciparum 3D7	Pf3D7_08_v3:1,210,692..1,211,860(+)	rhomboid protease ROM3	protein coding gene	UP
PF3D7_0828100	PF3D7_0828100.1	78	Plasmodium falciparum 3D7	Pf3D7_08_v3:1,211,965..1,215,795(-)	conserved Plasmodium protein, unknown function	protein coding gene	UP
PF3D7_0830500	PF3D7_0830500.1	77	Plasmodium falciparum 3D7	Pf3D7_08_v3:1,295,569..1,299,431(-)	sporozoite and liver stage tryptophan-rich protein, putative	protein coding gene	DOWN
PF3D7_0831300	PF3D7_0831300.1	292	Plasmodium falciparum 3D7	Pf3D7_08_v3:1,337,791..1,342,328(+)	Plasmodium exported protein, unknown function	protein coding gene	UP
PF3D7_0831400	PF3D7_0831400.1	293	Plasmodium falciparum 3D7	Pf3D7_08_v3:1,343,563..1,345,903(-)	Plasmodium exported protein, unknown function	protein coding gene	DOWN
PF3D7_0901700	PF3D7_0901700.1	294	Plasmodium falciparum 3D7	Pf3D7_09_v3:81,122..83,382(-)	Plasmodium exported protein (hyp5), unknown function	protein coding gene	DOWN
PF3D7_0901800	PF3D7_0901800.1	295	Plasmodium falciparum 3D7	Pf3D7_09_v3:83,928..85,972(+)	Plasmodium exported protein, unknown function	protein coding gene	DOWN
PF3D7_0902100	PF3D7_0902100.1	135	Plasmodium falciparum 3D7	Pf3D7_09_v3:93,768..95,820(-)	serine/threonine protein kinase, FIKK family	protein coding gene	DOWN
PF3D7_0902800	PF3D7_0902800.1	136	Plasmodium falciparum 3D7	Pf3D7_09_v3:120,969..125,252(-)	serine repeat antigen 9	protein coding gene	DOWN
PF3D7_0903800	PF3D7_0903800.1	137	Plasmodium falciparum 3D7	Pf3D7_09_v3:179,187..183,991(+)	LCCL domain-containing protein	protein coding gene	UP
PF3D7_0904200	PF3D7_0904200.1	138	Plasmodium falciparum 3D7	Pf3D7_09_v3:197,658..198,894(+)	PH domain-containing protein, putative	protein coding gene	UP
PF3D7_0904300	PF3D7_0904300.1	296	Plasmodium falciparum 3D7	Pf3D7_09_v3:199,051..207,458(-)	conserved protein, unknown function	protein coding gene	UP
PF3D7_0905400	PF3D7_0905400.1	139	Plasmodium falciparum 3D7	Pf3D7_09_v3:270,371..275,833(-)	high molecular weight rhoptry protein 3	protein coding gene	DOWN
PF3D7_0906400	PF3D7_0906400.1	140	Plasmodium falciparum 3D7	Pf3D7_09_v3:312,356..315,110(-)	dynein intermediate light chain, putative	protein coding gene	UP
PF3D7_0907700	PF3D7_0907700.1	141	Plasmodium falciparum 3D7	Pf3D7_09_v3:363,574..365,642(-)	proteasome activator 28	protein coding gene	DOWN
PF3D7_0909000	PF3D7_0909000.1	142	Plasmodium falciparum 3D7	Pf3D7_09_v3:410,326..413,841(-)	conserved Plasmodium protein, unknown function	protein coding gene	UP
PF3D7_0909100	PF3D7_0909100.1	297	Plasmodium falciparum 3D7	Pf3D7_09_v3:414,632..417,901(+)	conserved Plasmodium membrane protein, unknown function	protein coding gene	UP
PF3D7_0909200	PF3D7_0909200.1	143	Plasmodium falciparum 3D7	Pf3D7_09_v3:418,208..419,895(-)	GDP-fucose protein O-fucosyltransferase 2	protein coding gene	UP
PF3D7_0911500	PF3D7_0911500.1	298	Plasmodium falciparum 3D7	Pf3D7_09_v3:526,449..528,094(-)	conserved Plasmodium protein, unknown function	protein coding gene	UP
PF3D7_0911500	PF3D7_0911500.2	298	Plasmodium falciparum 3D7	Pf3D7_09_v3:526,449..528,094(-)	conserved Plasmodium protein, unknown function	protein coding gene	UP
PF3D7_0912200	PF3D7_0912200.1	144	Plasmodium falciparum 3D7	Pf3D7_09_v3:549,085..550,446(-)	conserved protein, unknown function	protein coding gene	UP
PF3D7_0912700	PF3D7_0912700.1	145	Plasmodium falciparum 3D7	Pf3D7_09_v3:562,269..563,000(+)	conserved Plasmodium protein, unknown function	protein coding gene	UP
PF3D7_0913400	PF3D7_0913400.1	146	Plasmodium falciparum 3D7	Pf3D7_09_v3:580,760..581,468(-)	elongation factor, putative	protein coding gene	UP
PF3D7_0914400	PF3D7_0914400.1	147	Plasmodium falciparum 3D7	Pf3D7_09_v3:617,808..619,842(+)	protein KIC3	protein coding gene	UP

University of Ghana http://ugspace.ug.edu.gh

PF3D7_0915800	PF3D7_0915800.1	148	Plasmodium falciparum 3D7	Pf3D7_09_v3:663,573..664,607(+)	glycolipid transfer protein, putative	protein coding gene	UP
PF3D7_0917900	PF3D7_0917900.1	149	Plasmodium falciparum 3D7	Pf3D7_09_v3:736,669..741,656(+)	heat shock protein 70	protein coding gene	DOWN
PF3D7_0918700	PF3D7_0918700.1	150	Plasmodium falciparum 3D7	Pf3D7_09_v3:769,319..772,498(+)	conserved Plasmodium protein, unknown function	protein coding gene	DOWN
PF3D7_0919200	PF3D7_0919200.1	151	Plasmodium falciparum 3D7	Pf3D7_09_v3:788,717..791,151(-)	PPPDE peptidase, putative	protein coding gene	DOWN
PF3D7_0920300	PF3D7_0920300.1	152	Plasmodium falciparum 3D7	Pf3D7_09_v3:831,524..832,780(+)	conserved Plasmodium protein, unknown function	protein coding gene	UP
PF3D7_0922200	PF3D7_0922200.1	153	Plasmodium falciparum 3D7	Pf3D7_09_v3:901,584..905,953(+)	S-adenosylmethionine synthetase	protein coding gene	DOWN
PF3D7_0922300	PF3D7_0922300.1	299	Plasmodium falciparum 3D7	Pf3D7_09_v3:905,998..908,357(+)	conserved protein, unknown function	protein coding gene	UP
PF3D7_0922400	PF3D7_0922400.1	154	Plasmodium falciparum 3D7	Pf3D7_09_v3:908,583..912,061(+)	para-aminobenzoic acid synthetase	protein coding gene	UP
PF3D7_0923700	PF3D7_0923700.1	300	Plasmodium falciparum 3D7	Pf3D7_09_v3:960,181..961,390(-)	CFAP298 domain-containing protein, putative	protein coding gene	UP
PF3D7_0924600	PF3D7_0924600.1	155	Plasmodium falciparum 3D7	Pf3D7_09_v3:998,794..1,006,187(+)	conserved Plasmodium protein, unknown function	protein coding gene	UP
PF3D7_0924800	PF3D7_0924800.1	301	Plasmodium falciparum 3D7	Pf3D7_09_v3:1,009,063..1,009,755(+)	telomeric repeat binding factor 1, putative	protein coding gene	UP
PF3D7_0924900	PF3D7_0924900.1	302	Plasmodium falciparum 3D7	Pf3D7_09_v3:1,010,380..1,011,822(+)	alpha-tubulin N-acetyltransferase, putative	protein coding gene	UP
PF3D7_0925100	PF3D7_0925100.1	156	Plasmodium falciparum 3D7	Pf3D7_09_v3:1,014,478..1,015,518(-)	conserved Plasmodium protein, unknown function	protein coding gene	UP
PF3D7_0926400	PF3D7_0926400.1	303	Plasmodium falciparum 3D7	Pf3D7_09_v3:1,070,433..1,073,592(-)	monocarboxylate transporter, putative	protein coding gene	UP
PF3D7_0927100	PF3D7_0927100.1	157	Plasmodium falciparum 3D7	Pf3D7_09_v3:1,099,900..1,101,387(-)	conserved protein, unknown function	protein coding gene	UP
PF3D7_0928100	PF3D7_0928100.1	158	Plasmodium falciparum 3D7	Pf3D7_09_v3:1,136,403..1,138,628(-)	conserved Plasmodium protein, unknown function	protein coding gene	UP
PF3D7_0929400	PF3D7_0929400.1	304	Plasmodium falciparum 3D7	Pf3D7_09_v3:1,173,579..1,181,380(+)	high molecular weight rhoptry protein 2	protein coding gene	DOWN
PF3D7_0930000	PF3D7_0930000.1	159	Plasmodium falciparum 3D7	Pf3D7_09_v3:1,189,646..1,191,322(+)	procollagen lysine 5-dioxygenase, putative	protein coding gene	UP
PF3D7_0930300	PF3D7_0930300.1	160	Plasmodium falciparum 3D7	Pf3D7_09_v3:1,201,305..1,207,576(+)	merozoite surface protein 1	protein coding gene	DOWN
PF3D7_0931700	PF3D7_0931700.1	305	Plasmodium falciparum 3D7	Pf3D7_09_v3:1,270,155..1,272,656(+)	PIH1 domain-containing protein, putative	protein coding gene	UP
PF3D7_0934800	PF3D7_0934800.1	161	Plasmodium falciparum 3D7	Pf3D7_09_v3:1,360,721..1,364,051(+)	cAMP-dependent protein kinase catalytic subunit	protein coding gene	DOWN
PF3D7_0935900	PF3D7_0935900.1	162	Plasmodium falciparum 3D7	Pf3D7_09_v3:1,419,960..1,424,840(-)	ring-exported protein 1	protein coding gene	DOWN
PF3D7_0936000	PF3D7_0936000.1	163	Plasmodium falciparum 3D7	Pf3D7_09_v3:1,426,152..1,428,942(-)	ring-exported protein 2	protein coding gene	DOWN
PF3D7_0936300	PF3D7_0936300.1	164	Plasmodium falciparum 3D7	Pf3D7_09_v3:1,435,767..1,439,273(-)	ring-exported protein 3	protein coding gene	DOWN
PF3D7_0936500	PF3D7_0936500.1	165	Plasmodium falciparum 3D7	Pf3D7_09_v3:1,443,260..1,445,400(-)	virulence-associated protein 1	protein coding gene	UP
PF3D7_0936600	PF3D7_0936600.1	166	Plasmodium falciparum 3D7	Pf3D7_09_v3:1,445,945..1,448,525(+)	gametocyte exported protein 5	protein coding gene	UP
PF3D7_0936800	PF3D7_0936800.1	167	Plasmodium falciparum 3D7	Pf3D7_09_v3:1,457,833..1,460,579(+)	Plasmodium exported protein (PHISTc), unknown function	protein coding gene	DOWN
PF3D7_0936900	PF3D7_0936900.1	643	Plasmodium falciparum 3D7	Pf3D7_09_v3:1,462,400..1,463,659(+)	Plasmodium exported protein (PHISTb), unknown function, pseudogene	pseudogene	DOWN
PF3D7_1000600	PF3D7_1000600.1	368	Plasmodium falciparum 3D7	Pf3D7_10_v3:50,964..53,006(-)	rifin	protein coding gene	DOWN
PF3D7_1000700	PF3D7_1000700.1	644	Plasmodium falciparum 3D7	Pf3D7_10_v3:54,542..55,498(-)	Plasmodium exported protein (PHISTa), unknown function, pseudogene	pseudogene	DOWN
PF3D7_1000800	PF3D7_1000800.1	645	Plasmodium falciparum 3D7	Pf3D7_10_v3:57,968..58,980(+)	stevor, pseudogene	pseudogene	DOWN
PF3D7_1001000	PF3D7_1001000.1	369	Plasmodium falciparum 3D7	Pf3D7_10_v3:62,926..64,808(+)	chondroitin sulfate A ligand	protein coding gene	DOWN
PF3D7_1001500	PF3D7_1001500.1	370	Plasmodium falciparum 3D7	Pf3D7_10_v3:80,302..82,576(-)	early transcribed membrane protein 10.1	protein coding gene	DOWN
PF3D7_1001600	PF3D7_1001600.1	371	Plasmodium falciparum 3D7	Pf3D7_10_v3:85,910..91,177(-)	exported lipase 2	protein coding gene	DOWN
PF3D7_1001700	PF3D7_1001700.1	372	Plasmodium falciparum 3D7	Pf3D7_10_v3:92,437..94,615(-)	Plasmodium exported protein (PHISTc), unknown function	protein coding gene	DOWN
PF3D7_1001800	PF3D7_1001800.1	373	Plasmodium falciparum 3D7	Pf3D7_10_v3:95,930..97,877(-)	Plasmodium exported protein (PHISTc), unknown function	protein coding gene	DOWN
PF3D7_1002000	PF3D7_1002000.1	374	Plasmodium falciparum 3D7	Pf3D7_10_v3:102,837..105,100(-)	Plasmodium exported protein (hyp2), unknown function	protein coding gene	DOWN
PF3D7_1002100	PF3D7_1002100.1	375	Plasmodium falciparum 3D7	Pf3D7_10_v3:106,648..109,855(-)	EMP1-trafficking protein	protein coding gene	DOWN
PF3D7_1002200	PF3D7_1002200.1	376	Plasmodium falciparum 3D7	Pf3D7_10_v3:110,388..116,655(+)	tryptophan-rich antigen 3	protein coding gene	DOWN
PF3D7_1003500	PF3D7_1003500.1	377	Plasmodium falciparum 3D7	Pf3D7_10_v3:159,811..163,428(-)	40S ribosomal protein S20e, putative	protein coding gene	DOWN
PF3D7_1005200	PF3D7_1005200.1	378	Plasmodium falciparum 3D7	Pf3D7_10_v3:232,315..233,024(-)	conserved Plasmodium protein, unknown function	protein coding gene	UP
PF3D7_1005300	PF3D7_1005300.1	379	Plasmodium falciparum 3D7	Pf3D7_10_v3:233,285..234,473(-)	conserved Plasmodium protein, unknown function	protein coding gene	UP
PF3D7_1006000	PF3D7_1006000.1	380	Plasmodium falciparum 3D7	Pf3D7_10_v3:255,990..258,116(-)	IMP1-like protein, putative	protein coding gene	UP
PF3D7_1006300	PF3D7_1006300.1	381	Plasmodium falciparum 3D7	Pf3D7_10_v3:265,750..266,836(-)	conserved Plasmodium protein, unknown function	protein coding gene	UP
PF3D7_1007800	PF3D7_1007800.1	382	Plasmodium falciparum 3D7	Pf3D7_10_v3:310,582..314,699(-)	conserved Plasmodium protein, unknown function	protein coding gene	UP

University of Ghana http://ugspace.ug.edu.gh

PF3D7_1009100	PF3D7_1009100.1	383	Plasmodium falciparum 3D7	Pf3D7_10_v3:372,519..374,072(+)	conserved Plasmodium membrane protein, unknown function	protein coding gene	UP
PF3D7_1010300	PF3D7_1010300.1	384	Plasmodium falciparum 3D7	Pf3D7_10_v3:412,469..415,659(+)	succinate dehydrogenase subunit 4, putative	protein coding gene	DOWN
PF3D7_1010400	PF3D7_1010400.1	385	Plasmodium falciparum 3D7	Pf3D7_10_v3:415,404..417,471(-)	MORN repeat protein, putative	protein coding gene	UP
PF3D7_1010500	PF3D7_1010500.1	386	Plasmodium falciparum 3D7	Pf3D7_10_v3:417,705..419,318(+)	ankyrin-repeat protein, putative	protein coding gene	UP
PF3D7_1014100	PF3D7_1014100.1	387	Plasmodium falciparum 3D7	Pf3D7_10_v3:554,233..560,227(+)	merozoite surface protein MSA180	protein coding gene	DOWN
PF3D7_1016300	PF3D7_1016300.1	388	Plasmodium falciparum 3D7	Pf3D7_10_v3:648,012..654,565(-)	GBP130 protein	protein coding gene	DOWN
PF3D7_1016600	PF3D7_1016600.1	389	Plasmodium falciparum 3D7	Pf3D7_10_v3:665,222..667,054(-)	Plasmodium exported protein (PHISTc), unknown function	protein coding gene	DOWN
PF3D7_1018400	PF3D7_1018400.1	390	Plasmodium falciparum 3D7	Pf3D7_10_v3:734,360..735,786(+)	conserved Plasmodium protein, unknown function	protein coding gene	UP
PF3D7_1018900	PF3D7_1018900.1	391	Plasmodium falciparum 3D7	Pf3D7_10_v3:752,748..755,185(-)	conserved Plasmodium protein, unknown function	protein coding gene	UP
PF3D7_1019100	PF3D7_1019100.1	392	Plasmodium falciparum 3D7	Pf3D7_10_v3:765,846..772,370(-)	conserved Plasmodium protein, unknown function	protein coding gene	UP
PF3D7_1019200	PF3D7_1019200.1	393	Plasmodium falciparum 3D7	Pf3D7_10_v3:773,531..774,490(+)	conserved Plasmodium protein, unknown function	protein coding gene	UP
PF3D7_1020200	PF3D7_1020200.1	394	Plasmodium falciparum 3D7	Pf3D7_10_v3:816,038..818,991(-)	conserved Plasmodium protein, unknown function	protein coding gene	UP
PF3D7_1020300	PF3D7_1020300.1	395	Plasmodium falciparum 3D7	Pf3D7_10_v3:819,637..822,447(+)	cytoplasmic dynein intermediate chain, putative	protein coding gene	UP
PF3D7_1021500	PF3D7_1021500.1	396	Plasmodium falciparum 3D7	Pf3D7_10_v3:867,337..870,148(-)	ATP-dependent RNA helicase ROK1, putative	protein coding gene	UP
PF3D7_1022900	PF3D7_1022900.1	397	Plasmodium falciparum 3D7	Pf3D7_10_v3:958,464..960,482(-)	cytochrome c oxidase subunit ApiCOX13, putative	protein coding gene	UP
PF3D7_1023100	PF3D7_1023100.1	398	Plasmodium falciparum 3D7	Pf3D7_10_v3:963,497..980,560(-)	dynein heavy chain, putative	protein coding gene	UP
PF3D7_1026100	PF3D7_1026100.1	399	Plasmodium falciparum 3D7	Pf3D7_10_v3:1,101,024..1,103,427(+)	conserved Plasmodium protein, unknown function	protein coding gene	UP
PF3D7_1026400	PF3D7_1026400.1	400	Plasmodium falciparum 3D7	Pf3D7_10_v3:1,109,794..1,111,976(-)	cell division cycle protein 20 homolog, putative	protein coding gene	UP
PF3D7_1026900	PF3D7_1026900.1	401	Plasmodium falciparum 3D7	Pf3D7_10_v3:1,125,283..1,126,167(+)	biotin--protein ligase 1	protein coding gene	UP
PF3D7_1027600	PF3D7_1027600.1	402	Plasmodium falciparum 3D7	Pf3D7_10_v3:1,148,267..1,150,490(-)	meiotic recombination protein SPO11-2, putative	protein coding gene	UP
PF3D7_1027900	PF3D7_1027900.1	403	Plasmodium falciparum 3D7	Pf3D7_10_v3:1,156,648..1,158,980(+)	palmitoyltransferase DHHC10, putative	protein coding gene	UP
PF3D7_1029500	PF3D7_1029500.1	404	Plasmodium falciparum 3D7	Pf3D7_10_v3:1,204,346..1,204,762(-)	conserved Plasmodium protein, unknown function	protein coding gene	UP
PF3D7_1031000	PF3D7_1031000.1	405	Plasmodium falciparum 3D7	Pf3D7_10_v3:1,253,373..1,254,412(-)	ookinete surface protein P25	protein coding gene	UP
PF3D7_1032000	PF3D7_1032000.1	406	Plasmodium falciparum 3D7	Pf3D7_10_v3:1,287,320..1,290,508(-)	ribosome maturation factor RimM, putative	protein coding gene	UP
PF3D7_1032200	PF3D7_1032200.1	407	Plasmodium falciparum 3D7	Pf3D7_10_v3:1,298,327..1,299,141(-)	conserved Plasmodium protein, unknown function	protein coding gene	UP
PF3D7_1033800	PF3D7_1033800.1	408	Plasmodium falciparum 3D7	Pf3D7_10_v3:1,351,197..1,353,284(+)	plasmepsin VII	protein coding gene	UP
PF3D7_1034300	PF3D7_1034300.1	409	Plasmodium falciparum 3D7	Pf3D7_10_v3:1,365,099..1,366,691(+)	thioredoxin-like associated protein 2, putative	protein coding gene	UP
PF3D7_1035200	PF3D7_1035200.1	410	Plasmodium falciparum 3D7	Pf3D7_10_v3:1,393,856..1,397,323(+)	S-antigen	protein coding gene	DOWN
PF3D7_1035300	PF3D7_1035300.1	411	Plasmodium falciparum 3D7	Pf3D7_10_v3:1,398,801..1,403,741(+)	glutamate-rich protein GLURP	protein coding gene	DOWN
PF3D7_1035400	PF3D7_1035400.1	412	Plasmodium falciparum 3D7	Pf3D7_10_v3:1,403,807..1,406,234(+)	merozoite surface protein 3	protein coding gene	DOWN
PF3D7_1035500	PF3D7_1035500.1	413	Plasmodium falciparum 3D7	Pf3D7_10_v3:1,406,658..1,409,053(+)	merozoite surface protein 6	protein coding gene	DOWN
PF3D7_1035700	PF3D7_1035700.1	414	Plasmodium falciparum 3D7	Pf3D7_10_v3:1,412,641..1,416,363(+)	duffy binding-like merozoite surface protein	protein coding gene	DOWN
PF3D7_1035900	PF3D7_1035900.1	415	Plasmodium falciparum 3D7	Pf3D7_10_v3:1,423,666..1,425,959(+)	merozoites-associated armadillo repeats protein	protein coding gene	DOWN
PF3D7_1036000	PF3D7_1036000.1	416	Plasmodium falciparum 3D7	Pf3D7_10_v3:1,426,843..1,429,332(+)	merozoite surface protein 11	protein coding gene	DOWN
PF3D7_1036500	PF3D7_1036500.1	417	Plasmodium falciparum 3D7	Pf3D7_10_v3:1,440,686..1,443,875(+)	conserved Plasmodium protein, unknown function	protein coding gene	DOWN
PF3D7_1039000	PF3D7_1039000.1	418	Plasmodium falciparum 3D7	Pf3D7_10_v3:1,567,784..1,572,695(+)	serine/threonine protein kinase, FIKK family	protein coding gene	DOWN
PF3D7_1102700	PF3D7_1102700.1	419	Plasmodium falciparum 3D7	Pf3D7_11_v3:127,762..130,186(+)	early transcribed membrane protein 11.1	protein coding gene	DOWN
PF3D7_1102800	PF3D7_1102800.1	420	Plasmodium falciparum 3D7	Pf3D7_11_v3:129,265..132,824(-)	early transcribed membrane protein 11.2	protein coding gene	DOWN
PF3D7_1103500	PF3D7_1103500.1	421	Plasmodium falciparum 3D7	Pf3D7_11_v3:151,196..154,519(-)	CPW-WPC family protein	protein coding gene	UP
PF3D7_1104500	PF3D7_1104500.1	422	Plasmodium falciparum 3D7	Pf3D7_11_v3:199,103..201,037(-)	WD repeat-containing protein, putative	protein coding gene	UP
PF3D7_1104600	PF3D7_1104600.1	423	Plasmodium falciparum 3D7	Pf3D7_11_v3:202,330..204,261(+)	radial spoke head protein, putative	protein coding gene	UP
PF3D7_1105900	PF3D7_1105900.1	424	Plasmodium falciparum 3D7	Pf3D7_11_v3:254,523..254,921(+)	conserved Plasmodium membrane protein, unknown function	protein coding gene	UP
PF3D7_1106900	PF3D7_1106900.1	425	Plasmodium falciparum 3D7	Pf3D7_11_v3:289,667..290,290(+)	conserved Plasmodium protein, unknown function	protein coding gene	UP
PF3D7_1107400	PF3D7_1107400.1	426	Plasmodium falciparum 3D7	Pf3D7_11_v3:317,615..319,552(-)	DNA repair protein RAD51	protein coding gene	UP
PF3D7_1107500	PF3D7_1107500.1	427	Plasmodium falciparum 3D7	Pf3D7_11_v3:319,592..321,540(-)	prefoldin, putative	protein coding gene	DOWN

University of Ghana http://ugspace.ug.edu.gh

PF3D7_1107900	PF3D7_1107900.1	428	Plasmodium falciparum 3D7	Pf3D7_11_v3:343,913..349,351(-)	mechanosensitive ion channel protein, putative	protein coding gene	UP
PF3D7_1109100	PF3D7_1109100.1	429	Plasmodium falciparum 3D7	Pf3D7_11_v3:382,557..387,277(-)	conserved Plasmodium protein, unknown function	protein coding gene	UP
PF3D7_1112200	PF3D7_1112200.1	430	Plasmodium falciparum 3D7	Pf3D7_11_v3:470,541..471,608(+)	ubiquinone biosynthesis protein COQ4, putative	protein coding gene	UP
PF3D7_1115100	PF3D7_1115100.1	431	Plasmodium falciparum 3D7	Pf3D7_11_v3:570,914..573,409(-)	conserved protein, unknown function	protein coding gene	UP
PF3D7_1115200	PF3D7_1115200.1	432	Plasmodium falciparum 3D7	Pf3D7_11_v3:574,690..580,622(+)	histone-lysine N-methyltransferase SET7	protein coding gene	UP
PF3D7_1115800	PF3D7_1115800.1	433	Plasmodium falciparum 3D7	Pf3D7_11_v3:595,116..598,541(-)	conserved Plasmodium protein, unknown function	protein coding gene	DOWN
PF3D7_1116000	PF3D7_1116000.1	434	Plasmodium falciparum 3D7	Pf3D7_11_v3:602,440..607,471(-)	rhoptry neck protein 4	protein coding gene	DOWN
PF3D7_1116500	PF3D7_1116500.1	435	Plasmodium falciparum 3D7	Pf3D7_11_v3:622,544..626,072(+)	folate transporter 2	protein coding gene	UP
PF3D7_1116600	PF3D7_1116600.1	436	Plasmodium falciparum 3D7	Pf3D7_11_v3:626,070..629,940(-)	dolichyl-diphosphooligosaccharide--protein glycosyltransferase subunit STT3, putative	protein coding gene	DOWN
PF3D7_1116800	PF3D7_1116800.1	437	Plasmodium falciparum 3D7	Pf3D7_11_v3:635,898..641,374(-)	heat shock protein 101	protein coding gene	DOWN
PF3D7_1117300	PF3D7_1117300.1	438	Plasmodium falciparum 3D7	Pf3D7_11_v3:661,949..662,633(+)	conserved protein, unknown function	protein coding gene	DOWN
PF3D7_1118800	PF3D7_1118800.1	439	Plasmodium falciparum 3D7	Pf3D7_11_v3:714,095..716,553(-)	actin-related protein 2/3 complex subunit 1, putative	protein coding gene	UP
PF3D7_1118900	PF3D7_1118900.1	440	Plasmodium falciparum 3D7	Pf3D7_11_v3:716,730..718,412(+)	conserved protein, unknown function	protein coding gene	UP
PF3D7_1120700	PF3D7_1120700.1	441	Plasmodium falciparum 3D7	Pf3D7_11_v3:783,924..789,129(-)	conserved Plasmodium protein, unknown function	protein coding gene	UP
PF3D7_1121800	PF3D7_1121800.1	442	Plasmodium falciparum 3D7	Pf3D7_11_v3:823,239..829,313(-)	peptidase M16, putative	protein coding gene	UP
PF3D7_1123900	PF3D7_1123900.1	443	Plasmodium falciparum 3D7	Pf3D7_11_v3:944,850..946,524(+)	13 kDa ribonucleoprotein-associated protein, putative	protein coding gene	DOWN
PF3D7_1124400	PF3D7_1124400.1	444	Plasmodium falciparum 3D7	Pf3D7_11_v3:964,315..965,485(-)	U6 snRNA-associated Sm-like protein LSm1, putative	protein coding gene	UP
PF3D7_1125700	PF3D7_1125700.1	445	Plasmodium falciparum 3D7	Pf3D7_11_v3:1,004,021..1,007,682(-)	kelch domain-containing protein, putative	protein coding gene	DOWN
PF3D7_1125800	PF3D7_1125800.1	446	Plasmodium falciparum 3D7	Pf3D7_11_v3:1,007,693..1,011,537(-)	kelch domain-containing protein, putative	protein coding gene	DOWN
PF3D7_1127200	PF3D7_1127200.1	447	Plasmodium falciparum 3D7	Pf3D7_11_v3:1,062,718..1,063,072(+)	conserved Plasmodium protein, unknown function	protein coding gene	UP
PF3D7_1128300	PF3D7_1128300.1	448	Plasmodium falciparum 3D7	Pf3D7_11_v3:1,097,880..1,103,771(-)	ATP-dependent 6-phosphofructokinase	protein coding gene	UP
PF3D7_1129600	PF3D7_1129600.1	449	Plasmodium falciparum 3D7	Pf3D7_11_v3:1,144,744..1,148,981(+)	phosphatidylinositol-4-phosphate 5-kinase, putative	protein coding gene	UP
PF3D7_1130800	PF3D7_1130800.1	450	Plasmodium falciparum 3D7	Pf3D7_11_v3:1,187,604..1,189,562(+)	armadillo repeat protein PF16, putative	protein coding gene	UP
PF3D7_1131300	PF3D7_1131300.1	451	Plasmodium falciparum 3D7	Pf3D7_11_v3:1,201,675..1,204,113(-)	conserved Plasmodium protein, unknown function	protein coding gene	UP
PF3D7_1131500	PF3D7_1131500.1	452	Plasmodium falciparum 3D7	Pf3D7_11_v3:1,210,686..1,211,456(-)	conserved Plasmodium protein, unknown function	protein coding gene	UP
PF3D7_1131700	PF3D7_1131700.1	453	Plasmodium falciparum 3D7	Pf3D7_11_v3:1,225,688..1,226,474(-)	conserved Plasmodium protein, unknown function	protein coding gene	UP
PF3D7_1132400	PF3D7_1132400.1	454	Plasmodium falciparum 3D7	Pf3D7_11_v3:1,254,662..1,260,426(-)	conserved Plasmodium membrane protein, unknown function	protein coding gene	UP
PF3D7_1133400	PF3D7_1133400.1	455	Plasmodium falciparum 3D7	Pf3D7_11_v3:1,292,966..1,296,696(+)	apical membrane antigen 1	protein coding gene	DOWN
PF3D7_1136100	PF3D7_1136100.1	456	Plasmodium falciparum 3D7	Pf3D7_11_v3:1,415,406..1,417,214(+)	conserved Plasmodium protein, unknown function	protein coding gene	UP
PF3D7_1136500	PF3D7_1136500.1	457	Plasmodium falciparum 3D7	Pf3D7_11_v3:1,431,881..1,435,170(-)	casein kinase 1	protein coding gene	DOWN
PF3D7_1136500	PF3D7_1136500.2	457	Plasmodium falciparum 3D7	Pf3D7_11_v3:1,431,881..1,435,170(-)	casein kinase 1	protein coding gene	DOWN
PF3D7_1138300	PF3D7_1138300.1	458	Plasmodium falciparum 3D7	Pf3D7_11_v3:1,498,612..1,499,571(-)	conserved protein, unknown function	protein coding gene	UP
PF3D7_1139500	PF3D7_1139500.1	459	Plasmodium falciparum 3D7	Pf3D7_11_v3:1,576,132..1,578,978(-)	AAA family ATPase, putative	protein coding gene	UP
PF3D7_1139600	PF3D7_1139600.1	460	Plasmodium falciparum 3D7	Pf3D7_11_v3:1,580,594..1,582,483(+)	conserved Plasmodium protein, unknown function	protein coding gene	UP
PF3D7_1140200	PF3D7_1140200.1	461	Plasmodium falciparum 3D7	Pf3D7_11_v3:1,600,448..1,603,560(-)	conserved Plasmodium protein, unknown function	protein coding gene	DOWN
PF3D7_1140400	PF3D7_1140400.1	462	Plasmodium falciparum 3D7	Pf3D7_11_v3:1,607,519..1,608,723(+)	conserved Plasmodium protein, unknown function	protein coding gene	DOWN
PF3D7_1141100	PF3D7_1141100.1	463	Plasmodium falciparum 3D7	Pf3D7_11_v3:1,649,321..1,657,012(+)	conserved Plasmodium protein, unknown function	protein coding gene	UP
PF3D7_1141700	PF3D7_1141700.1	464	Plasmodium falciparum 3D7	Pf3D7_11_v3:1,669,907..1,671,894(+)	OTU domain-containing protein, putative	protein coding gene	DOWN
PF3D7_1141900	PF3D7_1141900.1	465	Plasmodium falciparum 3D7	Pf3D7_11_v3:1,676,182..1,677,783(-)	inner membrane complex protein 1b, putative	protein coding gene	UP
PF3D7_1144400	PF3D7_1144400.1	466	Plasmodium falciparum 3D7	Pf3D7_11_v3:1,762,256..1,766,650(+)	conserved Plasmodium protein, unknown function	protein coding gene	UP
PF3D7_1144800	PF3D7_1144800.1	467	Plasmodium falciparum 3D7	Pf3D7_11_v3:1,774,605..1,776,787(+)	conserved Plasmodium protein, unknown function	protein coding gene	UP
PF3D7_1146100	PF3D7_1146100.1	468	Plasmodium falciparum 3D7	Pf3D7_11_v3:1,823,963..1,826,025(-)	PH-like domain-containing protein, putative	protein coding gene	UP
PF3D7_1146300	PF3D7_1146300.1	469	Plasmodium falciparum 3D7	Pf3D7_11_v3:1,828,240..1,829,054(-)	conserved Plasmodium protein, unknown function	protein coding gene	UP
PF3D7_1146700	PF3D7_1146700.1	470	Plasmodium falciparum 3D7	Pf3D7_11_v3:1,839,423..1,842,878(-)	kinesin-X4, putative	protein coding gene	UP
PF3D7_1146800	PF3D7_1146800.1	471	Plasmodium falciparum 3D7	Pf3D7_11_v3:1,843,205..1,854,563(-)	conserved Plasmodium protein, unknown function	protein coding gene	UP

University of Ghana http://ugspace.ug.edu.gh

PF3D7_1147100	PF3D7_1147100.1	472	Plasmodium falciparum 3D7	Pf3D7_11_v3:1,870,415..1,871,077(-)	dynein light chain, putative	protein coding gene	UP
PF3D7_1147200	PF3D7_1147200.1	473	Plasmodium falciparum 3D7	Pf3D7_11_v3:1,872,795..1,881,752(+)	tubulin--tyrosine ligase, putative	protein coding gene	UP
PF3D7_1148900	PF3D7_1148900.1	474	Plasmodium falciparum 3D7	Pf3D7_11_v3:1,944,702..1,946,935(+)	Plasmodium exported protein, unknown function	protein coding gene	DOWN
PF3D7_1149000	PF3D7_1149000.1	475	Plasmodium falciparum 3D7	Pf3D7_11_v3:1,948,696..1,969,412(+)	antigen 332, DBL-like protein	protein coding gene	DOWN
PF3D7_1149300	PF3D7_1149300.1	476	Plasmodium falciparum 3D7	Pf3D7_11_v3:1,982,068..1,984,327(+)	serine/threonine protein kinase, FIKK family	protein coding gene	DOWN
PF3D7_1149400	PF3D7_1149400.1	477	Plasmodium falciparum 3D7	Pf3D7_11_v3:1,985,056..1,987,411(-)	Plasmodium exported protein, unknown function	protein coding gene	DOWN
PF3D7_1149500	PF3D7_1149500.1	646	Plasmodium falciparum 3D7	Pf3D7_11_v3:1,991,359..1,994,018(-)	ring-infected erythrocyte surface antigen 2, pseudogene	pseudogene	DOWN
PF3D7_1149600	PF3D7_1149600.1	478	Plasmodium falciparum 3D7	Pf3D7_11_v3:2,000,342..2,003,996(+)	DnaJ protein, putative	protein coding gene	DOWN
PF3D7_1149800	PF3D7_1149800.1	479	Plasmodium falciparum 3D7	Pf3D7_11_v3:2,006,706..2,007,829(+)	rifin	protein coding gene	UP
PF3D7_1200700	PF3D7_1200700.1	480	Plasmodium falciparum 3D7	Pf3D7_12_v3:60,857..65,703(-)	acyl-CoA synthetase	protein coding gene	DOWN
PF3D7_1201000	PF3D7_1201000.1	481	Plasmodium falciparum 3D7	Pf3D7_12_v3:76,048..79,299(-)	Plasmodium exported protein (PHISTb), unknown function	protein coding gene	DOWN
PF3D7_1201100	PF3D7_1201100.1	482	Plasmodium falciparum 3D7	Pf3D7_12_v3:80,874..84,922(-)	RESA-like protein with PHIST and DnaJ domains	protein coding gene	DOWN
PF3D7_1201600	PF3D7_1201600.1	483	Plasmodium falciparum 3D7	Pf3D7_12_v3:101,030..102,674(-)	NIMA related kinase 3	protein coding gene	UP
PF3D7_1202900	PF3D7_1202900.1	484	Plasmodium falciparum 3D7	Pf3D7_12_v3:161,330..163,926(-)	high mobility group protein B1	protein coding gene	DOWN
PF3D7_1204400	PF3D7_1204400.1	485	Plasmodium falciparum 3D7	Pf3D7_12_v3:208,165..210,893(-)	sexual stage-specific protein G37, putative	protein coding gene	UP
PF3D7_1205700	PF3D7_1205700.1	486	Plasmodium falciparum 3D7	Pf3D7_12_v3:252,516..254,143(+)	targeted glyoxalase II	protein coding gene	UP
PF3D7_1206100	PF3D7_1206100.1	487	Plasmodium falciparum 3D7	Pf3D7_12_v3:272,320..275,022(-)	IMP-specific 5'-nucleotidase 1	protein coding gene	UP
PF3D7_1206500	PF3D7_1206500.1	488	Plasmodium falciparum 3D7	Pf3D7_12_v3:292,233..294,941(+)	Tat binding protein 1(TBP-1)-interacting protein, putative	protein coding gene	UP
PF3D7_1206900	PF3D7_1206900.1	489	Plasmodium falciparum 3D7	Pf3D7_12_v3:310,831..313,357(+)	conserved Plasmodium protein, unknown function	protein coding gene	UP
PF3D7_1207300	PF3D7_1207300.1	490	Plasmodium falciparum 3D7	Pf3D7_12_v3:343,326..344,361(-)	LIMP protein, putative	protein coding gene	UP
PF3D7_1207400	PF3D7_1207400.1	491	Plasmodium falciparum 3D7	Pf3D7_12_v3:345,922..347,239(+)	conserved Plasmodium protein, unknown function	protein coding gene	UP
PF3D7_1207700	PF3D7_1207700.1	492	Plasmodium falciparum 3D7	Pf3D7_12_v3:351,850..354,006(-)	41-3 protein	protein coding gene	UP
PF3D7_1208300	PF3D7_1208300.1	493	Plasmodium falciparum 3D7	Pf3D7_12_v3:387,833..389,498(+)	acyl carrier protein, mitochondrial	protein coding gene	DOWN
PF3D7_1210200	PF3D7_1210200.1	494	Plasmodium falciparum 3D7	Pf3D7_12_v3:458,672..462,423(-)	zinc finger protein, putative	protein coding gene	UP
PF3D7_1211000	PF3D7_1211000.1	495	Plasmodium falciparum 3D7	Pf3D7_12_v3:484,065..489,902(+)	kinesin-X3, putative	protein coding gene	UP
PF3D7_1212600	PF3D7_1212600.1	496	Plasmodium falciparum 3D7	Pf3D7_12_v3:555,503..556,924(-)	SND2 domain-containing protein, putative	protein coding gene	UP
PF3D7_1213400	PF3D7_1213400.1	497	Plasmodium falciparum 3D7	Pf3D7_12_v3:579,595..581,325(-)	kelch domain-containing protein, putative	protein coding gene	UP
PF3D7_1213500	PF3D7_1213500.1	498	Plasmodium falciparum 3D7	Pf3D7_12_v3:583,089..585,323(+)	integral membrane protein GPR180, putative	protein coding gene	UP
PF3D7_1214500	PF3D7_1214500.1	499	Plasmodium falciparum 3D7	Pf3D7_12_v3:611,272..613,482(+)	conserved Plasmodium protein, unknown function	protein coding gene	UP
PF3D7_1214800	PF3D7_1214800.1	500	Plasmodium falciparum 3D7	Pf3D7_12_v3:616,536..617,998(+)	conserved Plasmodium protein, unknown function	protein coding gene	UP
PF3D7_1215700	PF3D7_1215700.1	501	Plasmodium falciparum 3D7	Pf3D7_12_v3:635,538..638,879(-)	conserved Plasmodium protein, unknown function	protein coding gene	UP
PF3D7_1216500	PF3D7_1216500.1	502	Plasmodium falciparum 3D7	Pf3D7_12_v3:656,653..658,519(-)	male development gene 1	protein coding gene	UP
PF3D7_1216700	PF3D7_1216700.1	503	Plasmodium falciparum 3D7	Pf3D7_12_v3:663,061..666,282(+)	perforin-like protein 2	protein coding gene	UP
PF3D7_1217600	PF3D7_1217600.1	504	Plasmodium falciparum 3D7	Pf3D7_12_v3:695,559..696,455(+)	anaphase-promoting complex subunit 10, putative	protein coding gene	UP
PF3D7_1218700	PF3D7_1218700.1	505	Plasmodium falciparum 3D7	Pf3D7_12_v3:736,335..737,825(-)	conserved Plasmodium protein, unknown function	protein coding gene	UP
PF3D7_1218800	PF3D7_1218800.1	506	Plasmodium falciparum 3D7	Pf3D7_12_v3:737,900..740,324(-)	secreted ookinete protein, putative	protein coding gene	UP
PF3D7_1220000	PF3D7_1220000.1	507	Plasmodium falciparum 3D7	Pf3D7_12_v3:798,304..799,611(-)	zinc finger protein, putative	protein coding gene	UP
PF3D7_1220700	PF3D7_1220700.1	508	Plasmodium falciparum 3D7	Pf3D7_12_v3:822,958..827,712(-)	conserved Plasmodium protein, unknown function	protein coding gene	UP
PF3D7_1221100	PF3D7_1221100.1	509	Plasmodium falciparum 3D7	Pf3D7_12_v3:846,961..849,446(+)	conserved Plasmodium protein, unknown function	protein coding gene	UP
PF3D7_1221400	PF3D7_1221400.1	510	Plasmodium falciparum 3D7	Pf3D7_12_v3:856,817..859,199(+)	inner membrane complex protein 1h, putative	protein coding gene	UP
PF3D7_1221900	PF3D7_1221900.1	511	Plasmodium falciparum 3D7	Pf3D7_12_v3:871,737..876,247(-)	conserved Plasmodium membrane protein, unknown function	protein coding gene	DOWN
PF3D7_1222600	PF3D7_1222600.1	512	Plasmodium falciparum 3D7	Pf3D7_12_v3:906,714..914,983(+)	AP2 domain transcription factor AP2-G	protein coding gene	DOWN
PF3D7_1222700	PF3D7_1222700.1	513	Plasmodium falciparum 3D7	Pf3D7_12_v3:918,280..920,560(+)	glideosome-associated protein 45	protein coding gene	DOWN
PF3D7_1222800	PF3D7_1222800.1	514	Plasmodium falciparum 3D7	Pf3D7_12_v3:919,948..922,798(-)	conserved Plasmodium protein, unknown function	protein coding gene	UP
PF3D7_1222900	PF3D7_1222900.1	515	Plasmodium falciparum 3D7	Pf3D7_12_v3:923,314..925,896(+)	conserved Plasmodium protein, unknown function	protein coding gene	UP

University of Ghana http://ugspace.ug.edu.gh

PF3D7_1226200	PF3D7_1226200.1	516	Plasmodium falciparum 3D7	Pf3D7_12_v3:1,059,280..1,064,008(-)	conserved Plasmodium protein, unknown function	protein coding gene	UP
PF3D7_1228600	PF3D7_1228600.1	517	Plasmodium falciparum 3D7	Pf3D7_12_v3:1,160,654..1,163,264(-)	merozoite surface protein 9	protein coding gene	DOWN
PF3D7_1230100	PF3D7_1230100.1	518	Plasmodium falciparum 3D7	Pf3D7_12_v3:1,241,879..1,243,601(-)	thioredoxin-like associated protein 1, putative	protein coding gene	UP
PF3D7_1231000	PF3D7_1231000.1	519	Plasmodium falciparum 3D7	Pf3D7_12_v3:1,270,895..1,274,974(+)	conserved Plasmodium protein, unknown function	protein coding gene	UP
PF3D7_1232200	PF3D7_1232200.1	520	Plasmodium falciparum 3D7	Pf3D7_12_v3:1,332,463..1,334,896(+)	dihydrolipoyl dehydrogenase, mitochondrial	protein coding gene	UP
PF3D7_1232300	PF3D7_1232300.1	521	Plasmodium falciparum 3D7	Pf3D7_12_v3:1,335,579..1,337,655(+)	cytochrome b5, putative	protein coding gene	UP
PF3D7_1234000	PF3D7_1234000.1	522	Plasmodium falciparum 3D7	Pf3D7_12_v3:1,411,288..1,413,290(-)	conserved Plasmodium protein, unknown function	protein coding gene	UP
PF3D7_1234400	PF3D7_1234400.1	523	Plasmodium falciparum 3D7	Pf3D7_12_v3:1,436,790..1,439,349(-)	microgamete surface protein MiGS, putative	protein coding gene	UP
PF3D7_1234700	PF3D7_1234700.1	524	Plasmodium falciparum 3D7	Pf3D7_12_v3:1,446,207..1,450,552(-)	upregulated in late gametocytes ULG8	protein coding gene	UP
PF3D7_1236500	PF3D7_1236500.1	525	Plasmodium falciparum 3D7	Pf3D7_12_v3:1,525,407..1,526,216(-)	conserved Plasmodium protein, unknown function	protein coding gene	UP
PF3D7_1236800	PF3D7_1236800.1	526	Plasmodium falciparum 3D7	Pf3D7_12_v3:1,531,958..1,534,077(+)	protein-S-isoprenylcysteine O-methyltransferase	protein coding gene	UP
PF3D7_1238000	PF3D7_1238000.1	527	Plasmodium falciparum 3D7	Pf3D7_12_v3:1,581,356..1,583,229(+)	COPI associated protein, putative	protein coding gene	UP
PF3D7_1238200	PF3D7_1238200.1	528	Plasmodium falciparum 3D7	Pf3D7_12_v3:1,586,261..1,587,466(-)	conserved Plasmodium protein, unknown function	protein coding gene	UP
PF3D7_1239400	PF3D7_1239400.1	529	Plasmodium falciparum 3D7	Pf3D7_12_v3:1,646,612..1,647,151(-)	conserved protein, unknown function	protein coding gene	UP
PF3D7_1240100	PF3D7_1240100.1	530	Plasmodium falciparum 3D7	Pf3D7_12_v3:1,684,977..1,686,307(-)	early transcribed membrane protein 12	protein coding gene	DOWN
PF3D7_1241100	PF3D7_1241100.1	531	Plasmodium falciparum 3D7	Pf3D7_12_v3:1,746,049..1,748,494(-)	polyadenylation factor subunit 2, putative	protein coding gene	DOWN
PF3D7_1243400	PF3D7_1243400.1	532	Plasmodium falciparum 3D7	Pf3D7_12_v3:1,818,146..1,820,497(+)	conserved Plasmodium protein, unknown function	protein coding gene	DOWN
PF3D7_1245600	PF3D7_1245600.1	533	Plasmodium falciparum 3D7	Pf3D7_12_v3:1,900,249..1,905,066(-)	kinesin-15, putative	protein coding gene	UP
PF3D7_1246000	PF3D7_1246000.1	534	Plasmodium falciparum 3D7	Pf3D7_12_v3:1,912,457..1,914,595(+)	conserved Plasmodium protein, unknown function	protein coding gene	UP
PF3D7_1247800	PF3D7_1247800.1	535	Plasmodium falciparum 3D7	Pf3D7_12_v3:1,967,712..1,971,234(+)	dipeptidyl aminopeptidase 2	protein coding gene	UP
PF3D7_1248400	PF3D7_1248400.1	536	Plasmodium falciparum 3D7	Pf3D7_12_v3:1,981,753..1,982,857(+)	conserved Plasmodium protein, unknown function	protein coding gene	UP
PF3D7_1248800	PF3D7_1248800.1	537	Plasmodium falciparum 3D7	Pf3D7_12_v3:2,001,987..2,002,271(+)	conserved Plasmodium protein, unknown function	protein coding gene	UP
PF3D7_1250100	PF3D7_1250100.1	538	Plasmodium falciparum 3D7	Pf3D7_12_v3:2,045,070..2,054,429(-)	osmiophilic body protein G377	protein coding gene	UP
PF3D7_1250400	PF3D7_1250400.1	539	Plasmodium falciparum 3D7	Pf3D7_12_v3:2,067,229..2,069,794(+)	conserved Plasmodium protein, unknown function	protein coding gene	UP
PF3D7_1251000	PF3D7_1251000.1	540	Plasmodium falciparum 3D7	Pf3D7_12_v3:2,085,370..2,086,959(-)	HSP20-like chaperone, putative	protein coding gene	UP
PF3D7_1251200	PF3D7_1251200.1	541	Plasmodium falciparum 3D7	Pf3D7_12_v3:2,091,731..2,094,720(+)	coronin	protein coding gene	DOWN
PF3D7_1252100	PF3D7_1252100.1	542	Plasmodium falciparum 3D7	Pf3D7_12_v3:2,113,980..2,123,174(-)	rhoptry neck protein 3	protein coding gene	DOWN
PF3D7_1252300	PF3D7_1252300.1	543	Plasmodium falciparum 3D7	Pf3D7_12_v3:2,127,090..2,130,230(-)	conserved Plasmodium protein, unknown function	protein coding gene	DOWN
PF3D7_1252400	PF3D7_1252400.1	647	Plasmodium falciparum 3D7	Pf3D7_12_v3:2,136,053..2,144,874(+)	reticulocyte binding protein homologue 3, pseudogene	pseudogene	DOWN
PF3D7_1252600	PF3D7_1252600.1	544	Plasmodium falciparum 3D7	Pf3D7_12_v3:2,147,509..2,152,520(+)	esterase, putative	protein coding gene	DOWN
PF3D7_1253700	PF3D7_1253700.1	545	Plasmodium falciparum 3D7	Pf3D7_12_v3:2,190,483..2,191,770(-)	rifin	protein coding gene	UP
PF3D7_1254700	PF3D7_1254700.1	546	Plasmodium falciparum 3D7	Pf3D7_12_v3:2,224,997..2,226,201(-)	rifin	protein coding gene	UP
PF3D7_1255200	PF3D7_1255200.1	547	Plasmodium falciparum 3D7	Pf3D7_12_v3:2,241,271..2,248,962(-)	erythrocyte membrane protein 1, PfEMP1	protein coding gene	DOWN
PF3D7_1300100	PF3D7_1300100.1	168	Plasmodium falciparum 3D7	Pf3D7_13_v3:21,364..28,787(+)	erythrocyte membrane protein 1, PfEMP1	protein coding gene	DOWN
PF3D7_1301400	PF3D7_1301400.1	172	Plasmodium falciparum 3D7	Pf3D7_13_v3:82,128..84,689(+)	Plasmodium exported protein (hyp12), unknown function	protein coding gene	DOWN
PF3D7_1301500	PF3D7_1301500.1	173	Plasmodium falciparum 3D7	Pf3D7_13_v3:85,156..87,187(-)	Plasmodium exported protein (PHISTa), unknown function	protein coding gene	DOWN
PF3D7_1301600	PF3D7_1301600.1	174	Plasmodium falciparum 3D7	Pf3D7_13_v3:88,139..93,987(-)	erythrocyte binding antigen-140	protein coding gene	DOWN
PF3D7_1301700	PF3D7_1301700.1	175	Plasmodium falciparum 3D7	Pf3D7_13_v3:98,252..101,166(+)	CX3CL1-binding protein 2	protein coding gene	DOWN
PF3D7_1301900	PF3D7_1301900.1	176	Plasmodium falciparum 3D7	Pf3D7_13_v3:109,507..110,463(-)	Plasmodium exported protein, unknown function	protein coding gene	UP
PF3D7_1302000	PF3D7_1302000.1	177	Plasmodium falciparum 3D7	Pf3D7_13_v3:112,224..115,251(-)	EMP1-trafficking protein	protein coding gene	DOWN
PF3D7_1303900	PF3D7_1303900.1	306	Plasmodium falciparum 3D7	Pf3D7_13_v3:215,291..216,331(+)	GINS complex subunit Psf3, putative	protein coding gene	UP
PF3D7_1306500	PF3D7_1306500.1	307	Plasmodium falciparum 3D7	Pf3D7_13_v3:299,720..314,523(+)	MORN repeat protein, putative	protein coding gene	UP
PF3D7_1307100	PF3D7_1307100.1	169	Plasmodium falciparum 3D7	Pf3D7_13_v3:327,138..331,324(+)	U3 small nucleolar RNA-associated protein 6, putative	protein coding gene	DOWN
PF3D7_1309400	PF3D7_1309400.1	170	Plasmodium falciparum 3D7	Pf3D7_13_v3:431,848..436,382(+)	HORMA domain protein, putative	protein coding gene	UP
PF3D7_1310000	PF3D7_1310000.1	171	Plasmodium falciparum 3D7	Pf3D7_13_v3:448,789..449,862(+)	ATP synthase subunit O, mitochondrial, putative	protein coding gene	UP

University of Ghana http://ugspace.ug.edu.gh

PF3D7_1312450	PF3D7_1312450.1	332	Plasmodium falciparum 3D7	Pf3D7_13_v3:525,028..525,219(-)	apical ring associated protein 1, putative	protein coding gene	UP
PF3D7_1315300	PF3D7_1315300.1	178	Plasmodium falciparum 3D7	Pf3D7_13_v3:644,504..646,683(+)	conserved protein, unknown function	protein coding gene	UP
PF3D7_1316000	PF3D7_1316000.1	308	Plasmodium falciparum 3D7	Pf3D7_13_v3:668,118..670,953(-)	protein kinase, putative	protein coding gene	UP
PF3D7_1316200	PF3D7_1316200.1	179	Plasmodium falciparum 3D7	Pf3D7_13_v3:679,376..681,341(+)	ADP-ribosylation factor, putative	protein coding gene	DOWN
PF3D7_1316300	PF3D7_1316300.1	309	Plasmodium falciparum 3D7	Pf3D7_13_v3:681,363..682,149(-)	conserved Plasmodium protein, unknown function	protein coding gene	UP
PF3D7_1316400	PF3D7_1316400.1	180	Plasmodium falciparum 3D7	Pf3D7_13_v3:683,084..684,476(+)	SAS6-like protein, putative	protein coding gene	UP
PF3D7_1316700	PF3D7_1316700.1	181	Plasmodium falciparum 3D7	Pf3D7_13_v3:695,732..697,985(+)	conserved protein, unknown function	protein coding gene	UP
PF3D7_1318300	PF3D7_1318300.1	182	Plasmodium falciparum 3D7	Pf3D7_13_v3:752,413..759,638(+)	conserved Plasmodium protein, unknown function	protein coding gene	UP
PF3D7_1319600	PF3D7_1319600.1	183	Plasmodium falciparum 3D7	Pf3D7_13_v3:808,286..815,634(+)	ACDC domain-containing protein, putative	protein coding gene	UP
PF3D7_1319800	PF3D7_1319800.1	184	Plasmodium falciparum 3D7	Pf3D7_13_v3:819,978..821,239(+)	conserved Plasmodium protein, unknown function	protein coding gene	UP
PF3D7_1319900	PF3D7_1319900.1	185	Plasmodium falciparum 3D7	Pf3D7_13_v3:822,078..826,547(-)	conserved Plasmodium protein, unknown function	protein coding gene	UP
PF3D7_1321000	PF3D7_1321000.1	186	Plasmodium falciparum 3D7	Pf3D7_13_v3:859,299..861,347(+)	conserved Plasmodium protein, unknown function	protein coding gene	UP
PF3D7_1321400	PF3D7_1321400.1	187	Plasmodium falciparum 3D7	Pf3D7_13_v3:886,652..889,804(+)	palmitoyltransferase DHHC8, putative	protein coding gene	UP
PF3D7_1322900	PF3D7_1322900.1	310	Plasmodium falciparum 3D7	Pf3D7_13_v3:961,213..963,561(+)	conserved protein, unknown function	protein coding gene	UP
PF3D7_1326900	PF3D7_1326900.1	311	Plasmodium falciparum 3D7	Pf3D7_13_v3:1,129,282..1,133,343(-)	conserved Plasmodium membrane protein, unknown function	protein coding gene	UP
PF3D7_1327100	PF3D7_1327100.1	312	Plasmodium falciparum 3D7	Pf3D7_13_v3:1,138,558..1,141,561(-)	conserved protein, unknown function	protein coding gene	UP
PF3D7_1327900	PF3D7_1327900.1	333	Plasmodium falciparum 3D7	Pf3D7_13_v3:1,165,307..1,166,558(+)	conserved Plasmodium protein, unknown function	protein coding gene	UP
PF3D7_1328600	PF3D7_1328600.1	313	Plasmodium falciparum 3D7	Pf3D7_13_v3:1,209,744..1,211,772(-)	conserved Plasmodium protein, unknown function	protein coding gene	UP
PF3D7_1329900	PF3D7_1329900.1	314	Plasmodium falciparum 3D7	Pf3D7_13_v3:1,269,178..1,271,461(+)	conserved Plasmodium protein, unknown function	protein coding gene	UP
PF3D7_1331400	PF3D7_1331400.1	188	Plasmodium falciparum 3D7	Pf3D7_13_v3:1,310,771..1,312,216(+)	CPW-WPC family protein	protein coding gene	UP
PF3D7_1332200	PF3D7_1332200.1	189	Plasmodium falciparum 3D7	Pf3D7_13_v3:1,332,221..1,335,647(+)	conserved protein, unknown function	protein coding gene	DOWN
PF3D7_1334500	PF3D7_1334500.1	190	Plasmodium falciparum 3D7	Pf3D7_13_v3:1,405,046..1,408,182(-)	MSP7-like protein	protein coding gene	DOWN
PF3D7_1334700	PF3D7_1334700.1	191	Plasmodium falciparum 3D7	Pf3D7_13_v3:1,410,493..1,412,171(-)	MSP7-like protein	protein coding gene	DOWN
PF3D7_1335100	PF3D7_1335100.1	192	Plasmodium falciparum 3D7	Pf3D7_13_v3:1,418,213..1,421,552(-)	merozoite surface protein 7	protein coding gene	DOWN
PF3D7_1335300	PF3D7_1335300.1	315	Plasmodium falciparum 3D7	Pf3D7_13_v3:1,428,350..1,439,462(-)	reticulocyte binding protein 2 homologue b	protein coding gene	DOWN
PF3D7_1336300	PF3D7_1336300.1	193	Plasmodium falciparum 3D7	Pf3D7_13_v3:1,476,333..1,477,407(+)	conserved Plasmodium membrane protein, unknown function	protein coding gene	UP
PF3D7_1338800	PF3D7_1338800.1	316	Plasmodium falciparum 3D7	Pf3D7_13_v3:1,564,491..1,567,716(-)	CPW-WPC family protein	protein coding gene	UP
PF3D7_1340400	PF3D7_1340400.1	194	Plasmodium falciparum 3D7	Pf3D7_13_v3:1,610,715..1,611,989(-)	conserved Plasmodium protein, unknown function	protein coding gene	UP
PF3D7_1340500	PF3D7_1340500.1	195	Plasmodium falciparum 3D7	Pf3D7_13_v3:1,613,155..1,616,805(-)	conserved Plasmodium protein, unknown function	protein coding gene	UP
PF3D7_1341700	PF3D7_1341700.1	317	Plasmodium falciparum 3D7	Pf3D7_13_v3:1,645,048..1,645,868(+)	conserved Plasmodium protein, unknown function	protein coding gene	UP
PF3D7_1342600	PF3D7_1342600.1	196	Plasmodium falciparum 3D7	Pf3D7_13_v3:1,673,239..1,677,299(+)	myosin A	protein coding gene	DOWN
PF3D7_1342800	PF3D7_1342800.1	197	Plasmodium falciparum 3D7	Pf3D7_13_v3:1,678,802..1,682,001(+)	phosphoenolpyruvate carboxykinase	protein coding gene	UP
PF3D7_1343000	PF3D7_1343000.1	198	Plasmodium falciparum 3D7	Pf3D7_13_v3:1,695,462..1,699,267(+)	phosphoethanolamine N-methyltransferase	protein coding gene	DOWN
PF3D7_1343100	PF3D7_1343100.1	199	Plasmodium falciparum 3D7	Pf3D7_13_v3:1,699,588..1,702,492(-)	conserved Plasmodium protein, unknown function	protein coding gene	DOWN
PF3D7_1344400	PF3D7_1344400.1	334	Plasmodium falciparum 3D7	Pf3D7_13_v3:1,785,041..1,787,409(-)	conserved Plasmodium protein, unknown function	protein coding gene	UP
PF3D7_1345000	PF3D7_1345000.1	318	Plasmodium falciparum 3D7	Pf3D7_13_v3:1,806,661..1,809,617(+)	RING zinc finger protein, putative	protein coding gene	UP
PF3D7_1346700	PF3D7_1346700.1	200	Plasmodium falciparum 3D7	Pf3D7_13_v3:1,875,452..1,878,087(-)	6-cysteine protein	protein coding gene	UP
PF3D7_1346800	PF3D7_1346800.1	201	Plasmodium falciparum 3D7	Pf3D7_13_v3:1,878,475..1,880,618(-)	6-cysteine protein P47	protein coding gene	UP
PF3D7_1347000	PF3D7_1347000.1	202	Plasmodium falciparum 3D7	Pf3D7_13_v3:1,882,964..1,884,946(-)	WD repeat-containing protein 92, putative	protein coding gene	UP
PF3D7_1347600	PF3D7_1347600.1	319	Plasmodium falciparum 3D7	Pf3D7_13_v3:1,902,723..1,905,355(+)	conserved protein, unknown function	protein coding gene	UP
PF3D7_1348400	PF3D7_1348400.1	203	Plasmodium falciparum 3D7	Pf3D7_13_v3:1,935,006..1,947,401(-)	conserved Plasmodium membrane protein, unknown function	protein coding gene	UP
PF3D7_1349000	PF3D7_1349000.1	320	Plasmodium falciparum 3D7	Pf3D7_13_v3:1,966,890..1,969,427(-)	conserved Plasmodium protein, unknown function	protein coding gene	UP
PF3D7_1349700	PF3D7_1349700.1	204	Plasmodium falciparum 3D7	Pf3D7_13_v3:1,998,716..1,999,945(+)	peptidase, putative	protein coding gene	UP
PF3D7_1349900	PF3D7_1349900.1	205	Plasmodium falciparum 3D7	Pf3D7_13_v3:2,002,379..2,002,989(-)	conserved Plasmodium protein, unknown function	protein coding gene	UP
PF3D7_1350000	PF3D7_1350000.1	206	Plasmodium falciparum 3D7	Pf3D7_13_v3:2,003,004..2,005,374(-)	conserved Plasmodium protein, unknown function	protein coding gene	UP

University of Ghana http://ugspace.ug.edu.gh

PF3D7_1350500	PF3D7_1350500.1	207	Plasmodium falciparum 3D7	Pf3D7_13_v3:2,014,953..2,019,472(-)	conserved Plasmodium protein, unknown function	protein coding gene	DOWN
PF3D7_1350800	PF3D7_1350800.1	208	Plasmodium falciparum 3D7	Pf3D7_13_v3:2,025,366..2,026,106(-)	conserved Plasmodium protein, unknown function	protein coding gene	UP
PF3D7_1351600	PF3D7_1351600.1	209	Plasmodium falciparum 3D7	Pf3D7_13_v3:2,055,161..2,057,075(+)	glycerol kinase	protein coding gene	UP
PF3D7_1353100	PF3D7_1353100.1	210	Plasmodium falciparum 3D7	Pf3D7_13_v3:2,124,264..2,126,527(-)	Plasmodium exported protein, unknown function	protein coding gene	DOWN
PF3D7_1354000	PF3D7_1354000.1	211	Plasmodium falciparum 3D7	Pf3D7_13_v3:2,155,755..2,157,542(-)	conserved Plasmodium protein, unknown function	protein coding gene	UP
PF3D7_1354600	PF3D7_1354600.1	321	Plasmodium falciparum 3D7	Pf3D7_13_v3:2,175,867..2,177,361(-)	60S ribosomal protein L7-2, putative	protein coding gene	DOWN
PF3D7_1354700	PF3D7_1354700.1	212	Plasmodium falciparum 3D7	Pf3D7_13_v3:2,178,639..2,179,862(-)	conserved Plasmodium protein, unknown function	protein coding gene	UP
PF3D7_1356000	PF3D7_1356000.1	213	Plasmodium falciparum 3D7	Pf3D7_13_v3:2,218,743..2,222,939(+)	conserved Plasmodium protein, unknown function	protein coding gene	UP
PF3D7_1358600	PF3D7_1358600.1	214	Plasmodium falciparum 3D7	Pf3D7_13_v3:2,322,060..2,325,077(+)	zinc finger protein, putative	protein coding gene	UP
PF3D7_1359500	PF3D7_1359500.1	322	Plasmodium falciparum 3D7	Pf3D7_13_v3:2,364,426..2,365,235(+)	conserved Plasmodium protein, unknown function	protein coding gene	UP
PF3D7_1360500	PF3D7_1360500.1	215	Plasmodium falciparum 3D7	Pf3D7_13_v3:2,413,324..2,425,261(+)	guanylyl cyclase beta	protein coding gene	UP
PF3D7_1361300	PF3D7_1361300.1	323	Plasmodium falciparum 3D7	Pf3D7_13_v3:2,461,591..2,463,928(+)	conserved Plasmodium protein, unknown function	protein coding gene	UP
PF3D7_1361900	PF3D7_1361900.1	216	Plasmodium falciparum 3D7	Pf3D7_13_v3:2,481,776..2,484,101(-)	proliferating cell nuclear antigen 1	protein coding gene	DOWN
PF3D7_1362600	PF3D7_1362600.1	217	Plasmodium falciparum 3D7	Pf3D7_13_v3:2,505,912..2,507,356(+)	conserved protein, unknown function	protein coding gene	UP
PF3D7_1362900	PF3D7_1362900.1	218	Plasmodium falciparum 3D7	Pf3D7_13_v3:2,526,360..2,531,483(+)	conserved Plasmodium protein, unknown function	protein coding gene	UP
PF3D7_1363800	PF3D7_1363800.1	219	Plasmodium falciparum 3D7	Pf3D7_13_v3:2,556,025..2,559,547(+)	nuclear fusion protein, putative	protein coding gene	UP
PF3D7_1367200	PF3D7_1367200.1	324	Plasmodium falciparum 3D7	Pf3D7_13_v3:2,683,581..2,684,967(+)	CLAMP domain-containing protein, putative	protein coding gene	UP
PF3D7_1368900	PF3D7_1368900.1	220	Plasmodium falciparum 3D7	Pf3D7_13_v3:2,738,083..2,741,740(+)	conserved protein, unknown function	protein coding gene	UP
PF3D7_1369300	PF3D7_1369300.1	221	Plasmodium falciparum 3D7	Pf3D7_13_v3:2,755,662..2,758,407(-)	conserved Plasmodium protein, unknown function	protein coding gene	UP
PF3D7_1369400	PF3D7_1369400.1	325	Plasmodium falciparum 3D7	Pf3D7_13_v3:2,759,048..2,768,913(+)	conserved Plasmodium protein, unknown function	protein coding gene	UP
PF3D7_1370300	PF3D7_1370300.1	326	Plasmodium falciparum 3D7	Pf3D7_13_v3:2,786,609..2,789,345(+)	membrane associated histidine-rich protein 1	protein coding gene	DOWN
PF3D7_1371600	PF3D7_1371600.1	648	Plasmodium falciparum 3D7	Pf3D7_13_v3:2,811,706..2,820,270(+)	erythrocyte binding like protein 1, pseudogene	pseudogene	DOWN
PF3D7_1371700	PF3D7_1371700.1	335	Plasmodium falciparum 3D7	Pf3D7_13_v3:2,821,078..2,824,446(+)	serine/threonine protein kinase, FIKK family	protein coding gene	DOWN
PF3D7_1371800	PF3D7_1371800.1	336	Plasmodium falciparum 3D7	Pf3D7_13_v3:2,823,251..2,825,967(-)	Plasmodium exported protein, unknown function	protein coding gene	DOWN
PF3D7_1372000	PF3D7_1372000.1	327	Plasmodium falciparum 3D7	Pf3D7_13_v3:2,832,623..2,835,439(+)	Plasmodium exported protein (PHISTa), unknown function	protein coding gene	DOWN
PF3D7_1372400	PF3D7_1372400.1	328	Plasmodium falciparum 3D7	Pf3D7_13_v3:2,850,369..2,853,482(+)	acyl-CoA synthetase	protein coding gene	DOWN
PF3D7_1372600	PF3D7_1372600.1	329	Plasmodium falciparum 3D7	Pf3D7_13_v3:2,856,586..2,858,026(+)	rifin	protein coding gene	DOWN
PF3D7_1400500	PF3D7_1400500.1	548	Plasmodium falciparum 3D7	Pf3D7_14_v3:17,469..18,808(-)	rifin	protein coding gene	DOWN
PF3D7_1401000	PF3D7_1401000.1	549	Plasmodium falciparum 3D7	Pf3D7_14_v3:34,693..35,773(-)	GBPH protein	protein coding gene	DOWN
PF3D7_1401100	PF3D7_1401100.1	550	Plasmodium falciparum 3D7	Pf3D7_14_v3:39,940..43,736(-)	DnaJ protein, putative	protein coding gene	DOWN
PF3D7_1401200	PF3D7_1401200.1	551	Plasmodium falciparum 3D7	Pf3D7_14_v3:46,160..48,541(+)	Plasmodium exported protein, unknown function	protein coding gene	DOWN
PF3D7_1401400	PF3D7_1401400.1	552	Plasmodium falciparum 3D7	Pf3D7_14_v3:52,256..54,457(-)	early transcribed membrane protein 14.1	protein coding gene	DOWN
PF3D7_1402800	PF3D7_1402800.1	553	Plasmodium falciparum 3D7	Pf3D7_14_v3:100,564..106,014(+)	conserved Plasmodium protein, unknown function	protein coding gene	DOWN
PF3D7_1403000	PF3D7_1403000.1	554	Plasmodium falciparum 3D7	Pf3D7_14_v3:110,031..112,645(+)	radial spoke protein 3, putative	protein coding gene	UP
PF3D7_1403200	PF3D7_1403200.1	555	Plasmodium falciparum 3D7	Pf3D7_14_v3:119,995..121,405(-)	EGF domain-containing protein, putative	protein coding gene	UP
PF3D7_1403300	PF3D7_1403300.1	556	Plasmodium falciparum 3D7	Pf3D7_14_v3:121,855..125,340(-)	tetratricopeptide repeat protein, putative	protein coding gene	UP
PF3D7_1404200	PF3D7_1404200.1	557	Plasmodium falciparum 3D7	Pf3D7_14_v3:147,447..148,737(+)	conserved Plasmodium protein, unknown function	protein coding gene	UP
PF3D7_1407000	PF3D7_1407000.1	558	Plasmodium falciparum 3D7	Pf3D7_14_v3:253,542..257,360(+)	LCCL domain-containing protein	protein coding gene	UP
PF3D7_1408300	PF3D7_1408300.1	559	Plasmodium falciparum 3D7	Pf3D7_14_v3:312,569..313,296(+)	conserved Plasmodium protein, unknown function	protein coding gene	DOWN
PF3D7_1408800	PF3D7_1408800.1	560	Plasmodium falciparum 3D7	Pf3D7_14_v3:348,831..350,857(+)	conserved Plasmodium protein, unknown function	protein coding gene	UP
PF3D7_1410100	PF3D7_1410100.1	561	Plasmodium falciparum 3D7	Pf3D7_14_v3:395,877..398,406(+)	alpha/beta hydrolase, putative	protein coding gene	UP
PF3D7_1410400	PF3D7_1410400.1	562	Plasmodium falciparum 3D7	Pf3D7_14_v3:419,442..423,481(+)	rhoptry-associated protein 1	protein coding gene	DOWN
PF3D7_1412500	PF3D7_1412500.1	563	Plasmodium falciparum 3D7	Pf3D7_14_v3:506,478..509,453(+)	actin II	protein coding gene	UP
PF3D7_1412800	PF3D7_1412800.1	564	Plasmodium falciparum 3D7	Pf3D7_14_v3:515,932..519,380(-)	glycylpeptide N-tetradecanoyltransferase	protein coding gene	DOWN
PF3D7_1413300	PF3D7_1413300.1	565	Plasmodium falciparum 3D7	Pf3D7_14_v3:532,707..533,532(-)	conserved Plasmodium protein, unknown function	protein coding gene	UP

University of Ghana http://ugspace.ug.edu.gh

PF3D7_1415700	PF3D7_1415700.1	566	Plasmodium falciparum 3D7	Pf3D7_14_v3:634,236..637,046(-)	serine palmitoyltransferase, putative	protein coding gene	UP
PF3D7_1416400	PF3D7_1416400.1	567	Plasmodium falciparum 3D7	Pf3D7_14_v3:661,098..665,295(-)	conserved protein, unknown function	protein coding gene	UP
PF3D7_1416700	PF3D7_1416700.1	568	Plasmodium falciparum 3D7	Pf3D7_14_v3:680,612..682,264(-)	conserved protein, unknown function	protein coding gene	UP
PF3D7_1417000	PF3D7_1417000.1	569	Plasmodium falciparum 3D7	Pf3D7_14_v3:688,592..689,740(+)	inner membrane complex protein 11	protein coding gene	UP
PF3D7_1421300	PF3D7_1421300.1	570	Plasmodium falciparum 3D7	Pf3D7_14_v3:877,441..881,450(-)	conserved Plasmodium protein, unknown function	protein coding gene	UP
PF3D7_1421800	PF3D7_1421800.1	571	Plasmodium falciparum 3D7	Pf3D7_14_v3:888,580..890,032(-)	conserved Plasmodium protein, unknown function	protein coding gene	UP
PF3D7_1423300	PF3D7_1423300.1	572	Plasmodium falciparum 3D7	Pf3D7_14_v3:935,849..941,730(+)	serine/threonine protein phosphatase 7	protein coding gene	DOWN
PF3D7_1423600	PF3D7_1423600.1	573	Plasmodium falciparum 3D7	Pf3D7_14_v3:953,981..958,714(+)	calcium-dependent protein kinase, putative	protein coding gene	UP
PF3D7_1425500	PF3D7_1425500.1	574	Plasmodium falciparum 3D7	Pf3D7_14_v3:993,652..994,661(+)	conserved Plasmodium protein, unknown function	protein coding gene	UP
PF3D7_1426500	PF3D7_1426500.1	575	Plasmodium falciparum 3D7	Pf3D7_14_v3:1,027,682..1,030,025(+)	ABC transporter G family member 2	protein coding gene	UP
PF3D7_1427300	PF3D7_1427300.1	576	Plasmodium falciparum 3D7	Pf3D7_14_v3:1,064,142..1,069,386(+)	conserved Plasmodium protein, unknown function	protein coding gene	UP
PF3D7_1429300	PF3D7_1429300.1	577	Plasmodium falciparum 3D7	Pf3D7_14_v3:1,150,188..1,153,847(-)	CPW-WPC family protein	protein coding gene	UP
PF3D7_1429600	PF3D7_1429600.1	578	Plasmodium falciparum 3D7	Pf3D7_14_v3:1,167,130..1,168,075(+)	conserved Plasmodium protein, unknown function	protein coding gene	UP
PF3D7_1430100	PF3D7_1430100.1	579	Plasmodium falciparum 3D7	Pf3D7_14_v3:1,184,314..1,187,350(+)	serine/threonine protein phosphatase 2A activator	protein coding gene	UP
PF3D7_1430400	PF3D7_1430400.1	580	Plasmodium falciparum 3D7	Pf3D7_14_v3:1,200,622..1,204,458(+)	autophagy protein 5, putative	protein coding gene	UP
PF3D7_1435200	PF3D7_1435200.1	581	Plasmodium falciparum 3D7	Pf3D7_14_v3:1,418,686..1,421,491(+)	conserved protein, unknown function	protein coding gene	UP
PF3D7_1436300	PF3D7_1436300.1	582	Plasmodium falciparum 3D7	Pf3D7_14_v3:1,476,538..1,483,887(+)	translocon component PTEX150	protein coding gene	DOWN
PF3D7_1437300	PF3D7_1437300.1	583	Plasmodium falciparum 3D7	Pf3D7_14_v3:1,513,414..1,515,796(-)	conserved Plasmodium protein, unknown function	protein coding gene	DOWN
PF3D7_1437600	PF3D7_1437600.1	584	Plasmodium falciparum 3D7	Pf3D7_14_v3:1,522,980..1,525,078(+)	conserved protein, unknown function	protein coding gene	UP
PF3D7_1438100	PF3D7_1438100.1	585	Plasmodium falciparum 3D7	Pf3D7_14_v3:1,540,920..1,543,553(-)	translocation protein SEC62, putative	protein coding gene	DOWN
PF3D7_1438800	PF3D7_1438800.1	586	Plasmodium falciparum 3D7	Pf3D7_14_v3:1,570,403..1,574,738(+)	OST-HTH associated domain protein, putative	protein coding gene	UP
PF3D7_1440200	PF3D7_1440200.1	587	Plasmodium falciparum 3D7	Pf3D7_14_v3:1,638,717..1,647,251(+)	stromal-processing peptidase, putative	protein coding gene	DOWN
PF3D7_1443700	PF3D7_1443700.1	588	Plasmodium falciparum 3D7	Pf3D7_14_v3:1,791,629..1,793,782(-)	dephospho-CoA kinase	protein coding gene	DOWN
PF3D7_1444800	PF3D7_1444800.1	589	Plasmodium falciparum 3D7	Pf3D7_14_v3:1,843,368..1,846,989(-)	fructose-bisphosphate aldolase	protein coding gene	DOWN
PF3D7_1446100	PF3D7_1446100.1	590	Plasmodium falciparum 3D7	Pf3D7_14_v3:1,889,978..1,892,108(-)	conserved Plasmodium protein, unknown function	protein coding gene	UP
PF3D7_1447600	PF3D7_1447600.1	591	Plasmodium falciparum 3D7	Pf3D7_14_v3:1,942,151..1,942,963(-)	conserved protein, unknown function	protein coding gene	UP
PF3D7_1448800	PF3D7_1448800.1	592	Plasmodium falciparum 3D7	Pf3D7_14_v3:2,001,083..2,002,106(-)	Appr-1-p processing domain protein	protein coding gene	UP
PF3D7_1448900	PF3D7_1448900.1	593	Plasmodium falciparum 3D7	Pf3D7_14_v3:2,002,360..2,003,426(-)	mitochondrial respiratory chain complex II subunit, putative	protein coding gene	UP
PF3D7_1449000	PF3D7_1449000.1	594	Plasmodium falciparum 3D7	Pf3D7_14_v3:2,004,406..2,005,456(-)	gamete egress and sporozoite traversal protein, putative	protein coding gene	UP
PF3D7_1449200	PF3D7_1449200.1	595	Plasmodium falciparum 3D7	Pf3D7_14_v3:2,013,486..2,015,102(+)	conserved Plasmodium protein, unknown function	protein coding gene	DOWN
PF3D7_1451600	PF3D7_1451600.1	596	Plasmodium falciparum 3D7	Pf3D7_14_v3:2,115,436..2,118,190(-)	LCCL domain-containing protein	protein coding gene	UP
PF3D7_1452900	PF3D7_1452900.1	597	Plasmodium falciparum 3D7	Pf3D7_14_v3:2,171,480..2,172,584(-)	conserved protein, unknown function	protein coding gene	UP
PF3D7_1453500	PF3D7_1453500.1	598	Plasmodium falciparum 3D7	Pf3D7_14_v3:2,194,694..2,198,480(-)	NAD(P) transhydrogenase, putative	protein coding gene	UP
PF3D7_1454800	PF3D7_1454800.1	599	Plasmodium falciparum 3D7	Pf3D7_14_v3:2,243,873..2,244,367(+)	conserved Plasmodium protein, unknown function	protein coding gene	UP
PF3D7_1454900	PF3D7_1454900.1	600	Plasmodium falciparum 3D7	Pf3D7_14_v3:2,244,961..2,245,795(-)	conserved protein, unknown function	protein coding gene	UP
PF3D7_1455800	PF3D7_1455800.1	601	Plasmodium falciparum 3D7	Pf3D7_14_v3:2,285,113..2,290,227(+)	LCCL domain-containing protein	protein coding gene	UP
PF3D7_1456400	PF3D7_1456400.1	602	Plasmodium falciparum 3D7	Pf3D7_14_v3:2,309,181..2,312,472(-)	conserved Plasmodium protein, unknown function	protein coding gene	UP
PF3D7_1457100	PF3D7_1457100.1	603	Plasmodium falciparum 3D7	Pf3D7_14_v3:2,339,830..2,343,206(+)	conserved Plasmodium protein, unknown function	protein coding gene	UP
PF3D7_1457800	PF3D7_1457800.1	604	Plasmodium falciparum 3D7	Pf3D7_14_v3:2,372,222..2,374,557(-)	conserved Plasmodium protein, unknown function	protein coding gene	UP
PF3D7_1458900	PF3D7_1458900.1	605	Plasmodium falciparum 3D7	Pf3D7_14_v3:2,418,138..2,419,436(+)	golgi apparatus membrane protein TVP23, putative	protein coding gene	DOWN
PF3D7_1460000	PF3D7_1460000.1	606	Plasmodium falciparum 3D7	Pf3D7_14_v3:2,452,076..2,453,357(+)	biotin--protein ligase 2	protein coding gene	UP
PF3D7_1461500	PF3D7_1461500.1	607	Plasmodium falciparum 3D7	Pf3D7_14_v3:2,496,050..2,497,400(-)	meiotic nuclear division protein 1, putative	protein coding gene	UP
PF3D7_1461700	PF3D7_1461700.1	608	Plasmodium falciparum 3D7	Pf3D7_14_v3:2,500,927..2,502,802(-)	conserved Plasmodium protein, unknown function	protein coding gene	UP
PF3D7_1461800	PF3D7_1461800.1	609	Plasmodium falciparum 3D7	Pf3D7_14_v3:2,503,209..2,514,031(+)	conserved Plasmodium protein, unknown function	protein coding gene	UP
PF3D7_1462600	PF3D7_1462600.1	610	Plasmodium falciparum 3D7	Pf3D7_14_v3:2,550,692..2,552,432(+)	conserved Plasmodium membrane protein, unknown function	protein coding gene	UP

University of Ghana http://ugspace.ug.edu.gh

PF3D7_1463900	PF3D7_1463900.1	611	Plasmodium falciparum 3D7	Pf3D7_14_v3:2,584,086..2,590,847(-)	rhoptry neck protein 11, putative	protein coding gene	DOWN
PF3D7_1465600	PF3D7_1465600.1	612	Plasmodium falciparum 3D7	Pf3D7_14_v3:2,655,491..2,657,965(-)	conserved Plasmodium protein, unknown function	protein coding gene	UP
PF3D7_1465700	PF3D7_1465700.1	613	Plasmodium falciparum 3D7	Pf3D7_14_v3:2,658,255..2,660,911(-)	plasmepsin VIII, putative	protein coding gene	UP
PF3D7_1466000	PF3D7_1466000.1	614	Plasmodium falciparum 3D7	Pf3D7_14_v3:2,686,224..2,688,303(-)	conserved protein, unknown function	protein coding gene	UP
PF3D7_1466500	PF3D7_1466500.1	615	Plasmodium falciparum 3D7	Pf3D7_14_v3:2,725,021..2,726,694(+)	conserved Plasmodium protein, unknown function	protein coding gene	UP
PF3D7_1466600	PF3D7_1466600.1	616	Plasmodium falciparum 3D7	Pf3D7_14_v3:2,726,800..2,727,642(-)	enkurin domain-containing protein, putative	protein coding gene	UP
PF3D7_1466800	PF3D7_1466800.1	617	Plasmodium falciparum 3D7	Pf3D7_14_v3:2,731,557..2,735,622(+)	NOC3 domain-containing protein, putative	protein coding gene	UP
PF3D7_1467000	PF3D7_1467000.1	618	Plasmodium falciparum 3D7	Pf3D7_14_v3:2,742,387..2,745,257(+)	magnesium transporter, putative	protein coding gene	UP
PF3D7_1467800	PF3D7_1467800.1	619	Plasmodium falciparum 3D7	Pf3D7_14_v3:2,767,400..2,768,020(+)	conserved Plasmodium protein, unknown function	protein coding gene	DOWN
PF3D7_1468400	PF3D7_1468400.1	620	Plasmodium falciparum 3D7	Pf3D7_14_v3:2,809,460..2,812,520(+)	zinc finger protein, putative	protein coding gene	DOWN
PF3D7_1469900	PF3D7_1469900.1	621	Plasmodium falciparum 3D7	Pf3D7_14_v3:2,866,150..2,868,183(+)	protein MGET	protein coding gene	UP
PF3D7_1470500	PF3D7_1470500.1	622	Plasmodium falciparum 3D7	Pf3D7_14_v3:2,881,612..2,886,576(+)	cGMP-specific 3',5'-cyclic phosphodiesterase delta	protein coding gene	UP
PF3D7_1471100	PF3D7_1471100.1	623	Plasmodium falciparum 3D7	Pf3D7_14_v3:2,903,947..2,907,414(-)	exported protein 2	protein coding gene	DOWN
PF3D7_1471500	PF3D7_1471500.1	624	Plasmodium falciparum 3D7	Pf3D7_14_v3:2,922,351..2,924,557(-)	transmembrane protein 43, putative	protein coding gene	UP
PF3D7_1471600	PF3D7_1471600.1	625	Plasmodium falciparum 3D7	Pf3D7_14_v3:2,925,721..2,929,673(+)	apical polar ring protein APR2, putative	protein coding gene	UP
PF3D7_1471700	PF3D7_1471700.1	626	Plasmodium falciparum 3D7	Pf3D7_14_v3:2,929,823..2,931,547(+)	conserved Plasmodium protein, unknown function	protein coding gene	UP
PF3D7_1471800	PF3D7_1471800.1	627	Plasmodium falciparum 3D7	Pf3D7_14_v3:2,931,759..2,932,950(+)	conserved Plasmodium protein, unknown function	protein coding gene	UP
PF3D7_1473200	PF3D7_1473200.1	628	Plasmodium falciparum 3D7	Pf3D7_14_v3:2,979,847..2,983,715(+)	DnaJ protein, putative	protein coding gene	DOWN
PF3D7_1475400	PF3D7_1475400.1	629	Plasmodium falciparum 3D7	Pf3D7_14_v3:3,087,061..3,105,071(-)	cysteine repeat modular protein 4	protein coding gene	UP
PF3D7_1475500	PF3D7_1475500.1	630	Plasmodium falciparum 3D7	Pf3D7_14_v3:3,106,516..3,111,987(+)	LCCL domain-containing protein	protein coding gene	UP
PF3D7_1476100	PF3D7_1476100.1	631	Plasmodium falciparum 3D7	Pf3D7_14_v3:3,131,104..3,131,637(+)	early transcribed membrane protein 14.2	protein coding gene	UP
PF3D7_1476400	PF3D7_1476400.1	649	Plasmodium falciparum 3D7	Pf3D7_14_v3:3,142,075..3,144,341(+)	serine/threonine protein kinase, FIKK family, pseudogene	pseudogene	DOWN
PF3D7_1476700	PF3D7_1476700.1	632	Plasmodium falciparum 3D7	Pf3D7_14_v3:3,156,572..3,158,056(+)	lysophospholipase LPL1	protein coding gene	UP
PF3D7_1477000	PF3D7_1477000.1	650	Plasmodium falciparum 3D7	Pf3D7_14_v3:3,168,563..3,171,692(+)	Plasmodium exported protein (hyp17), unknown function, pseudogene	pseudogene	DOWN
PF3D7_1477500	PF3D7_1477500.1	633	Plasmodium falciparum 3D7	Pf3D7_14_v3:3,187,707..3,191,551(+)	Plasmodium exported protein (PHISTb), unknown function	protein coding gene	DOWN
PF3D7_1478600	PF3D7_1478600.1	634	Plasmodium falciparum 3D7	Pf3D7_14_v3:3,231,222..3,237,075(+)	EMP1-trafficking protein	protein coding gene	DOWN

University of Ghana http://ugspace.ug.edu.gh

Supplementary Table 5.19 Gene ontology enrichment analysis for up/down-regulated genes between DD2 untreated and DHA_treated condition

University of Ghana http://ugspace.ug.edu.gh

Gene ontology term	Differential expression	ID	Name	Bgd count	Result count	Result gene list	Pct of bgd	Fold enrichment	Odds ratio	P-value	Benjamini	Bonferroni
Biological process	Upregulated	GO:0007127	meiosis I	13	6	PF3D7_0816800,PF3D7_1027600,PF3D7_1107400,PF3D7_1139500,PF3D7_1206500,PF3D7_1461500,	46.2	7.09	12.52	8.44E-05	0.014862285	0.05944914
		GO:0140527	reciprocal homologous recombination	13	6	PF3D7_0816800,PF3D7_1027600,PF3D7_1107400,PF3D7_1139500,PF3D7_1206500,PF3D7_1461500,	46.2	7.09	12.52	8.44E-05	0.014862285	0.05944914
		GO:0035825	homologous recombination	13	6	PF3D7_0816800,PF3D7_1027600,PF3D7_1107400,PF3D7_1139500,PF3D7_1206500,PF3D7_1461500,	46.2	7.09	12.52	8.44E-05	0.014862285	0.05944914
		GO:0007131	reciprocal meiotic recombination	13	6	PF3D7_0816800,PF3D7_1027600,PF3D7_1107400,PF3D7_1139500,PF3D7_1206500,PF3D7_1461500,	46.2	7.09	12.52	8.44E-05	0.014862285	0.05944914
		GO:0007018	microtubule-based movement	32	9	PF3D7_0718000,PF3D7_0724900,PF3D7_0906400,PF3D7_1020300,PF3D7_1023100,PF3D7_1104600,PF3D7_1146700,PF3D7_1211000,PF3D7_1245600,	28.1	4.32	5.75	0.00013839	0.019485694	0.097428469
		GO:0140013	meiotic nuclear division	16	6	PF3D7_0816800,PF3D7_1027600,PF3D7_1107400,PF3D7_1139500,PF3D7_1206500,PF3D7_1461500,	37.5	5.76	8.76	0.00033325	0.033515121	0.234605846
		GO:0061982	meiosis I cell cycle process	16	6	PF3D7_0816800,PF3D7_1027600,PF3D7_1107400,PF3D7_1139500,PF3D7_1206500,PF3D7_1461500,	37.5	5.76	8.76	0.00033325	0.033515121	0.234605846
		GO:0007017	microtubule-based process	75	13	PF3D7_0307300,PF3D7_0708000,PF3D7_0718000,PF3D7_0724900,PF3D7_0906400,PF3D7_1020300,PF3D7_1023100,PF3D7_1104600,PF3D7_1146700,PF3D7_1147200,PF3D7_1211000,PF3D7_1245600,PF3D7_1430100,	17.3	2.66	3.1	0.00094561	0.083213374	0.665706988

		GO: 1903046	meiotic cell cycle process	24	6	PF3D7_0816800,PF3D7_1027600,PF3D7_1107400,PF3D7_1139500,PF3D7_1206500,PF3D7_1461500,	25	3.84	4.86	0.00359269	0.186031765	1
		GO: 0090735	DNA repair complex assembly	2	2	PF3D7_0816800,PF3D7_1107400,	100	15.36	inf	0.00422799	0.186031765	1
		GO: 0006004	fucose metabolic process	2	2	PF3D7_0813800,PF3D7_0909200,	100	15.36	inf	0.00422799	0.186031765	1
		GO: 0042966	biotin carboxyl carrier protein biosynthetic process	2	2	PF3D7_1026900,PF3D7_1460000,	100	15.36	inf	0.00422799	0.186031765	1
		GO: 0042148	strand invasion	2	2	PF3D7_0816800,PF3D7_1107400,	100	15.36	inf	0.00422799	0.186031765	1
		GO: 0000730	DNA recombinase assembly	2	2	PF3D7_0816800,PF3D7_1107400,	100	15.36	inf	0.00422799	0.186031765	1
		GO: 0009305	protein biotinylation	2	2	PF3D7_1026900,PF3D7_1460000,	100	15.36	inf	0.00422799	0.186031765	1
		GO: 0010212	response to ionizing radiation	2	2	PF3D7_0816800,PF3D7_1107400,	100	15.36	inf	0.00422799	0.186031765	1
		GO: 0031145	anaphase-promoting complex-dependent catabolic process	6	3	PF3D7_0501700,PF3D7_1026400,PF3D7_1217600,	50	7.68	14.48	0.00471923	0.195431806	1
		GO: 0006259	DNA metabolic process	7	3	PF3D7_0816800,PF3D7_1027600,PF3D7_1107400,	42.9	6.58	10.86	0.0078628	0.307522997	1

University of Ghana http://ugspace.ug.edu.gh

		GO: 0051321	meiotic cell cycle	30	6	PF3D7_0816800,PF3D7_1027600,PF3D7_1107400,PF3D7_1139500,PF3D7_1206500,PF3D7_1461500,	20	3.07	3.64	0.01139514	0.422219959	1
		GO: 0010608	posttranscriptional regulation of gene expression	3	2	PF3D7_0417100,PF3D7_0518700,	66.7	10.24	28.89	0.01213659	0.42720784	1
		GO: 0022402	cell cycle process	81	11	PF3D7_0307300,PF3D7_0501700,PF3D7_0503200,PF3D7_0816800,PF3D7_1027600,PF3D7_1107400,PF3D7_1139500,PF3D7_1206500,PF3D7_1423600,PF3D7_1430100,PF3D7_1461500,	13.6	2.09	2.3	0.01502344	0.432489419	1
		GO: 0009187	cyclic nucleotide metabolic process	9	3	PF3D7_0515500,PF3D7_1360500,PF3D7_1470500,	33.3	5.12	7.24	0.01711383	0.432489419	1
		GO: 0045786	negative regulation of cell cycle	16	4	PF3D7_0503200,PF3D7_0518400,PF3D7_1139500,PF3D7_1423600,	25	3.84	4.83	0.01718491	0.432489419	1
		GO: 0022414	reproductive process	33	6	PF3D7_0816800,PF3D7_1027600,PF3D7_1107400,PF3D7_1139500,PF3D7_1206500,PF3D7_1461500,	18.2	2.79	3.23	0.01804219	0.432489419	1
		GO: 0000003	reproduction	33	6	PF3D7_0816800,PF3D7_1027600,PF3D7_1107400,PF3D7_1139500,PF3D7_1206500,PF3D7_1461500,	18.2	2.79	3.23	0.01804219	0.432489419	1
		GO: 0000280	nuclear division	33	6	PF3D7_0816800,PF3D7_1027600,PF3D7_1107400,PF3D7_1139500,PF3D7_1206500,PF3D7_1461500,	18.2	2.79	3.23	0.01804219	0.432489419	1
		GO: 0018410	C-terminal protein amino acid modification	4	2	PF3D7_1236800,PF3D7_1430400,	50	7.68	14.44	0.02323137	0.432489419	1
		GO: 0006672	ceramide metabolic process	4	2	PF3D7_0625100,PF3D7_1415700,	50	7.68	14.44	0.02323137	0.432489419	1

University of Ghana http://ugspace.ug.edu.gh

University of Ghana http://ugspace.ug.edu.gh

		GO:0046513	ceramide biosynthetic process	4	2	PF3D7_0625100,PF3D7_1415700,	50	7.68	14.44	0.02323137	0.432489419	1
		GO:0045003	double-strand break repair via synthesis-dependent strand annealing	4	2	PF3D7_0816800,PF3D7_1107400,	50	7.68	14.44	0.02323137	0.432489419	1
		GO:0043687	post-translational protein modification	4	2	PF3D7_1236800,PF3D7_1430400,	50	7.68	14.44	0.02323137	0.432489419	1
		GO:0019318	hexose metabolic process	10	3	PF3D7_0813800,PF3D7_0909200,PF3D7_1342800,	30	4.61	6.2	0.0232885	0.432489419	1
		GO:0071976	cell gliding	11	3	PF3D7_1207300,PF3D7_1360500,PF3D7_1465700,	27.3	4.19	5.43	0.03050796	0.432489419	1
		GO:0005996	monosaccharide metabolic process	11	3	PF3D7_0813800,PF3D7_0909200,PF3D7_1342800,	27.3	4.19	5.43	0.03050796	0.432489419	1
		GO:0035891	exit from host cell	28	5	PF3D7_1216500,PF3D7_1247800,PF3D7_1250100,PF3D7_1449000,PF3D7_1465700,	17.9	2.74	3.15	0.03229174	0.432489419	1
		GO:0048285	organelle fission	38	6	PF3D7_0816800,PF3D7_1027600,PF3D7_1107400,PF3D7_1139500,PF3D7_1206500,PF3D7_1461500,	15.8	2.42	2.72	0.03427956	0.432489419	1
		GO:0007154	cell communication	127	14	PF3D7_0503200,PF3D7_0517800,PF3D7_0530500,PF3D7_0714400,PF3D7_0719200,PF3D7_1129600,PF3D7_1139500,PF3D7_1213500,PF3D7_1316000,PF3D7_1360500,PF3D7_1423600,PF3D7_1430400,PF3D7_1470500,PF3D7_1475400,	11	1.69	1.81	0.03544703	0.432489419	1
		GO:0035890	exit from host	29	5	PF3D7_1216500,PF3D7_1247800,PF3D7_1250100,PF3D7_1449000,PF3D7_1465700,	17.2	2.65	3.02	0.03701303	0.432489419	1

University of Ghana http://ugspace.ug.edu.gh

		GO:0009073	aromatic amino acid family biosynthetic process	5	2	PF3D7_0922400,PF3D7_1236500,	40	6.14	9.63	0.0370664	0.432489419	1
		GO:0009190	cyclic nucleotide biosynthetic process	5	2	PF3D7_0515500,PF3D7_1360500,	40	6.14	9.63	0.0370664	0.432489419	1
		GO:0006638	neutral lipid metabolic process	5	2	PF3D7_1351600,PF3D7_1476700,	40	6.14	9.63	0.0370664	0.432489419	1
		GO:0006312	mitotic recombination	5	2	PF3D7_0816800,PF3D7_1107400,	40	6.14	9.63	0.0370664	0.432489419	1
		GO:0009072	aromatic amino acid family metabolic process	5	2	PF3D7_0922400,PF3D7_1236500,	40	6.14	9.63	0.0370664	0.432489419	1
		GO:0051301	cell division	30	5	PF3D7_0307300,PF3D7_0501700,PF3D7_1026400,PF3D7_1217600,PF3D7_1455800,	16.7	2.56	2.9	0.04213661	0.432489419	1
		GO:1901987	regulation of cell cycle phase transition	21	4	PF3D7_0501700,PF3D7_0503200,PF3D7_1139500,PF3D7_1423600,	19	2.93	3.41	0.04376529	0.432489419	1
		GO:0007165	signal transduction	119	13	PF3D7_0503200,PF3D7_0517800,PF3D7_0530500,PF3D7_0714400,PF3D7_0719200,PF3D7_1129600,PF3D7_1139500,PF3D7_1213500,PF3D7_1316000,PF3D7_1360500,PF3D7_1423600,PF3D7_1470500,PF3D7_1475400,	10.9	1.68	1.79	0.0444436	0.432489419	1
		GO:0023052	signaling	119	13	PF3D7_0503200,PF3D7_0517800,PF3D7_0530500,PF3D7_0714400,PF3D7_0719200,PF3D7_1129600,PF3D7_1139500,PF3D7_1213500,PF3D7_1316000,PF3D7_1360500,PF3D7_1423600,PF3D7_1470500,PF3D7_1475400,	10.9	1.68	1.79	0.0444436	0.432489419	1
	Downregulated	GO:0044403	biological process involved in symbiotic interaction	397	56	PF3D7_0102500,PF3D7_0102600,PF3D7_0113000,PF3D7_0113700,PF3D7_0207500,PF3D7_0207600,PF3D7_0220800,PF3D7_0223500,PF3D7_0301200,PF3D7_0302200,PF3D7_0302500,PF3D7_0404700,PF3D7_0423400,PF3D7_0424500,PF3D7_0424600,PF3D7_0424700,PF3D7_0426000,	14.1	3.01	4.1	8.32E-15	1.79E-12	2.86E-12

University of Ghana http://ugspace.ug.edu.gh

						PF3D7_0500900,PF3D7_0501600,PF3D7_0507500,PF3D7_0532400,PF3D7_0617700,PF3D7_0707300,PF3D7_0711700,PF3D7_0713100,PF3D7_0722200,PF3D7_0731500,PF3D7_0732200,PF3D7_0800100,PF3D7_0905400,PF3D7_0929400,PF3D7_0930300,PF3D7_0934800,PF3D7_1000600,PF3D7_1014100,PF3D7_1035400,PF3D7_1035500,PF3D7_1035700,PF3D7_1035900,PF3D7_1039000,PF3D7_1116000,PF3D7_1116800,PF3D7_1133400,PF3D7_1149300,PF3D7_1222700,PF3D7_1252100,PF3D7_1255200,PF3D7_1301700,PF3D7_1335100,PF3D7_1335300,PF3D7_1342600,PF3D7_1371700,PF3D7_1400500,PF3D7_1412800,PF3D7_1436300,PF3D7_1471100,						
		GO:0044419	biological process involved in interspecies interaction between organisms	399	56	PF3D7_0102500,PF3D7_0102600,PF3D7_0113000,PF3D7_0113700,PF3D7_0207500,PF3D7_0207600,PF3D7_0220800,PF3D7_0223500,PF3D7_0301200,PF3D7_0302200,PF3D7_0302500,PF3D7_0404700,PF3D7_0423400,PF3D7_0424500,PF3D7_0424600,PF3D7_0424700,PF3D7_0426000,PF3D7_0500900,PF3D7_0501600,PF3D7_0507500,PF3D7_0532400,PF3D7_0617700,PF3D7_0707300,PF3D7_0711700,PF3D7_0713100,PF3D7_0722200,PF3D7_0731500,PF3D7_0732200,PF3D7_0800100,PF3D7_0905400,PF3D7_0929400,PF3D7_0930300,PF3D7_0934800,PF3D7_1000600,PF3D7_1014100,PF3D7_1035400,PF3D7_1035500,PF3D7_1035700,PF3D7_1035900,PF3D7_1039000,PF3D7_1116000,PF3D7_1116800,PF3D7_1133400,PF3D7_1149300,PF3D7_1222700,PF3D7_1252100,PF3D7_1255200,PF3D7_1301700,PF3D7_1335100,PF3D7_1335300,PF3D7_1342600,PF3D7_1371700,PF3D7_1400500,PF3D7_1412800,PF3D7_1436300,PF3D7_1471100,	14	3	4.08	1.04E-14	1.79E-12	3.59E-12
		GO:0052126	movement in host environment	120	28	PF3D7_0102500,PF3D7_0207500,PF3D7_0207600,PF3D7_0404700,PF3D7_0423400,PF3D7_0501600,PF3D7_0507500,PF3D7_0707300,PF3D7_0722200,PF3D7_0731500,PF3D7_0905400,PF3D7_0929400,PF3D7_0930300,PF3D7_0934800,PF3D7_1014100,PF3D7_1035400,PF3D7_1035500,PF3D7_1035700,PF3D7_1035900,PF3D7_1116000,PF3D7_1133400,PF3D7_1222700,PF3D7_1252100,PF3D7_1335100,PF3D7_1335300,PF3D7_1342600,PF3D7_1412800,PF3D7_1471100,	23.3	4.98	6.92	4.66E-13	5.34E-11	1.60E-10
		GO:0044409	entry into host	103	25	PF3D7_0102500,PF3D7_0404700,PF3D7_0423400,PF3D7_0501600,PF3D7_0707300,PF3D7_0722200,PF3D7_0731500,PF3D7_0905400,PF3D7_0929400,PF3D7_0930300,PF3D7_0934800,PF3D7_1014100,PF3D7_1035400,PF3D7_1035500,PF3D7_1035700,PF3D7_1035900,PF3D7_1116000,PF3D7_1133400,PF3D7_1222700,PF3D7_1252100,PF3D7_1335100,PF3D7_1335300,PF3D7_1342600,PF3D7_1412800,PF3D7_1471100,	24.3	5.18	7.2	3.54E-12	3.04E-10	1.22E-09
		GO:0008150	biological process	662	70	PF3D7_0102500,PF3D7_0102600,PF3D7_0113000,PF3D7_0113700,PF3D7_0206800,PF3D7_0207400,PF3D7_0207500,PF3D7_0207600,PF3D7_0207700,PF3D7_0207800,PF3D7_0212600,PF3D7_0220800,PF3D7_0223500,PF3D7_0301200,PF3D7_0302200,PF3D7_0302500,PF3D7_0320500,	10.6	2.26	3.03	5.15E-12	3.54E-10	1.77E-09

University of Ghana http://ugspace.ug.edu.gh

						PF3D7_0404700,PF3D7_0423400,PF3D7_0424500,PF3D7_0424600,PF3D7_0424700,PF3D7_0426000,PF3D7_0500900,PF3D7_0501600,PF3D7_0507500,PF3D7_0532400,PF3D7_0617700,PF3D7_0617800,PF3D7_0707300,PF3D7_0711700,PF3D7_0713100,PF3D7_0722200,PF3D7_0731500,PF3D7_0732200,PF3D7_0800100,PF3D7_0902100,PF3D7_0902800,PF3D7_0905400,PF3D7_0917900,PF3D7_0929400,PF3D7_0930300,PF3D7_0934800,PF3D7_1000600,PF3D7_1014100,PF3D7_1035400,PF3D7_1035500,PF3D7_1035700,PF3D7_1035900,PF3D7_1039000,PF3D7_1116000,PF3D7_1116800,PF3D7_1133400,PF3D7_1149000,PF3D7_1149300,PF3D7_1222700,PF3D7_1252100,PF3D7_1255200,PF3D7_1301600,PF3D7_1301700,PF3D7_1335100,PF3D7_1335300,PF3D7_1342600,PF3D7_1361900,PF3D7_1371700,PF3D7_1400500,PF3D7_1412800,PF3D7_1436300,PF3D7_1438100,PF3D7_1471100,						
		GO:0051701	biological process involved in interaction with host	382	49	PF3D7_0102500,PF3D7_0102600,PF3D7_0113000,PF3D7_0207500,PF3D7_0207600,PF3D7_0223500,PF3D7_0301200,PF3D7_0404700,PF3D7_0423400,PF3D7_0424500,PF3D7_0424700,PF3D7_0426000,PF3D7_0500900,PF3D7_0501600,PF3D7_0507500,PF3D7_0617700,PF3D7_0707300,PF3D7_0711700,PF3D7_0713100,PF3D7_0722200,PF3D7_0731500,PF3D7_0732200,PF3D7_0800100,PF3D7_0905400,PF3D7_0929400,PF3D7_0930300,PF3D7_0934800,PF3D7_1000600,PF3D7_1014100,PF3D7_1035400,PF3D7_1035500,PF3D7_1035700,PF3D7_1035900,PF3D7_1039000,PF3D7_1116000,PF3D7_1116800,PF3D7_1133400,PF3D7_1149300,PF3D7_1222700,PF3D7_1252100,PF3D7_1255200,PF3D7_1335100,PF3D7_1335300,PF3D7_1342600,PF3D7_1371700,PF3D7_1400500,PF3D7_1412800,PF3D7_1436300,PF3D7_1471100,	12.8	2.74	3.54	2.23E-11	1.28E-09	7.67E-09
		GO:0002377	immunoglobulin production	8	6	PF3D7_0207400,PF3D7_0207500,PF3D7_0207600,PF3D7_0207700,PF3D7_0207800,PF3D7_0902800,	75	16.01	62.68	2.56E-07	1.10E-05	8.81E-05
		GO:0002440	production of molecular mediator of immune response	8	6	PF3D7_0207400,PF3D7_0207500,PF3D7_0207600,PF3D7_0207700,PF3D7_0207800,PF3D7_0902800,	75	16.01	62.68	2.56E-07	1.10E-05	8.81E-05
		GO:0050776	regulation of immune response	12	7	PF3D7_0102200,PF3D7_0207400,PF3D7_0207500,PF3D7_0207600,PF3D7_0207700,PF3D7_0207800,PF3D7_0902800,	58.3	12.45	29.36	2.93E-07	1.12E-05	0.000100647

University of Ghana http://ugspace.ug.edu.gh

		GO:0002682	regulation of immune system process	13	7	PF3D7_0102200,PF3D7_0207400,PF3D7_0207500,PF3D7_0207600,PF3D7_0207700,PF3D7_0207800,PF3D7_0902800,	53.8	11.5	24.46	6.09E-07	2.09E-05	0.000209414
		GO:0002376	immune system process	14	7	PF3D7_0207400,PF3D7_0207500,PF3D7_0207600,PF3D7_0207700,PF3D7_0207800,PF3D7_0902800,PF3D7_1301600,	50	10.68	20.96	1.17E-06	3.66E-05	0.000402216
		GO:0009405	obsolete pathogenesis	75	13	PF3D7_0102500,PF3D7_0223500,PF3D7_0426000,PF3D7_0711700,PF3D7_0731500,PF3D7_0800100,PF3D7_0930300,PF3D7_1035700,PF3D7_1133400,PF3D7_1149000,PF3D7_1255200,PF3D7_1300100,PF3D7_1301600,	17.3	3.7	4.46	3.52E-05	0.001010054	0.012120652
		GO:0007155	cell adhesion	70	12	PF3D7_0102500,PF3D7_0206800,PF3D7_0212600,PF3D7_0223500,PF3D7_0423400,PF3D7_0426000,PF3D7_0707300,PF3D7_0711700,PF3D7_0800100,PF3D7_1149000,PF3D7_1255200,PF3D7_1301600,	17.1	3.66	4.39	7.92E-05	0.002096068	0.02724888
		GO:0022610	biological adhesion	195	22	PF3D7_0102500,PF3D7_0113700,PF3D7_0206800,PF3D7_0212600,PF3D7_0220800,PF3D7_0223500,PF3D7_0302200,PF3D7_0302500,PF3D7_0423400,PF3D7_0424500,PF3D7_0424600,PF3D7_0426000,PF3D7_0532400,PF3D7_0617700,PF3D7_0707300,PF3D7_0711700,PF3D7_0732200,PF3D7_0800100,PF3D7_1149000,PF3D7_1255200,PF3D7_1301600,PF3D7_1301700,	11.3	2.41	2.76	9.32E-05	0.002289657	0.032055202
		GO:0098609	cell-cell adhesion	62	11	PF3D7_0102500,PF3D7_0212600,PF3D7_0223500,PF3D7_0423400,PF3D7_0426000,PF3D7_0707300,PF3D7_0711700,PF3D7_0800100,PF3D7_1149000,PF3D7_1255200,PF3D7_1301600,	17.7	3.79	4.56	0.00011434	0.002622275	0.039334118
		GO:0035891	exit from host cell	28	6	PF3D7_0207500,PF3D7_0207600,PF3D7_0507500,PF3D7_0930300,PF3D7_1014100,PF3D7_1412800,	21.4	4.58	5.67	0.00156159	0.03357427	0.537188316
		GO:0035890	exit from host	29	6	PF3D7_0207500,PF3D7_0207600,PF3D7_0507500,PF3D7_0930300,PF3D7_1014100,PF3D7_1412800,	20.7	4.42	5.43	0.00189318	0.038308956	0.651252253
		GO:0046500	S-adenosylmethionine metabolic process	2	2	PF3D7_0520900,PF3D7_0922200,	100	21.35	inf	0.00218448	0.041747909	0.751462358

		GO: 0035556	intracellular signal transduction	81	10	PF3D7_0102600,PF3D7_0301200,PF3D7_0424500,PF3D7_0424700,PF3D7_0500900,PF3D7_0902100,PF3D7_1039000,PF3D7_1149300,PF3D7_1371700,PF3D7_1438100,	12.3	2.64	2.95	0.00419723	0.075992042	1
		GO: 0006342	chromatin silencing	3	2	PF3D7_0320900,PF3D7_0617800,	66.7	14.23	41.05	0.00635054	0.109229208	1
		GO: 0023052	signaling	119	12	PF3D7_0102600,PF3D7_0301200,PF3D7_0424500,PF3D7_0424700,PF3D7_0500900,PF3D7_0902100,PF3D7_0917900,PF3D7_0934800,PF3D7_1039000,PF3D7_1149300,PF3D7_1371700,PF3D7_1438100,	10.1	2.15	2.35	0.00928299	0.145152219	1
		GO: 0007165	signal transduction	119	12	PF3D7_0102600,PF3D7_0301200,PF3D7_0424500,PF3D7_0424700,PF3D7_0500900,PF3D7_0902100,PF3D7_0917900,PF3D7_0934800,PF3D7_1039000,PF3D7_1149300,PF3D7_1371700,PF3D7_1438100,	10.1	2.15	2.35	0.00928299	0.145152219	1
		GO: 0044053	translocation of peptides or proteins into host cell cytoplasm	4	2	PF3D7_1116800,PF3D7_1436300,	50	10.68	20.52	0.01230932	0.184104562	1
		GO: 0006468	protein phosphorylation	110	11	PF3D7_0102600,PF3D7_0301200,PF3D7_0424500,PF3D7_0424700,PF3D7_0500900,PF3D7_0902100,PF3D7_0934800,PF3D7_1039000,PF3D7_1136500,PF3D7_1149300,PF3D7_1371700,	10	2.14	2.33	0.01328353	0.190397228	1
		GO: 0044003	modulation by symbiont of host process	205	17	PF3D7_0102600,PF3D7_0223500,PF3D7_0301200,PF3D7_0424500,PF3D7_0424700,PF3D7_0426000,PF3D7_0500900,PF3D7_0617700,PF3D7_0711700,PF3D7_0731500,PF3D7_0732200,PF3D7_0800100,PF3D7_1039000,PF3D7_1149300,PF3D7_1255200,PF3D7_1371700,PF3D7_1471100,	8.3	1.77	1.91	0.01483786	0.200348143	1
		GO: 0007154	cell communication	127	12	PF3D7_0102600,PF3D7_0301200,PF3D7_0424500,PF3D7_0424700,PF3D7_0500900,PF3D7_0902100,PF3D7_0917900,PF3D7_0934800,PF3D7_1039000,PF3D7_1149300,PF3D7_1371700,PF3D7_1438100,	9.4	2.02	2.19	0.01514259	0.200348143	1
		GO: 0020035	cytoadherence to microvasculature, mediated by symbiont protein	176	15	PF3D7_0113700,PF3D7_0220800,PF3D7_0223500,PF3D7_0302200,PF3D7_0302500,PF3D7_0424500,PF3D7_0424600,PF3D7_0426000,PF3D7_0532400,PF3D7_0617700,PF3D7_0711700,PF3D7_0732200,PF3D7_0800100,PF3D7_1255200,PF3D7_1301700,	8.5	1.82	1.96	0.01715224	0.210727751	1
		GO: 0044406	adhesion of symbiont to host	176	15	PF3D7_0113700,PF3D7_0220800,PF3D7_0223500,PF3D7_0302200,PF3D7_0302500,PF3D7_0424500,PF3D7_0424600,PF3D7_0426000,PF3D7_0532400,PF3D7_0617700,PF3D7_0711700,PF3D7_0732200,PF3D7_0800100,PF3D7_1255200,PF3D7_1301700,	8.5	1.82	1.96	0.01715224	0.210727751	1

University of Ghana http://ugspace.ug.edu.gh

		GO: 0016310	phosphorylation	135	12	PF3D7_0102600,PF3D7_0301200,PF3D7_0424500,PF3D7_0424700,PF3D7_0500900,PF3D7_0902100,PF3D7_0934800,PF3D7_1039000,PF3D7_1136500,PF3D7_1149300,PF3D7_1371700,PF3D7_1444800,	8.9	1.9	2.04	0.02346484	0.251746097	1
		GO: 0042000	translocation of peptides or proteins into host	14	3	PF3D7_0713100,PF3D7_1116800,PF3D7_1436300,	21.4	4.58	5.61	0.02515984	0.251746097	1
		GO: 0044417	translocation of molecules into host	14	3	PF3D7_0713100,PF3D7_1116800,PF3D7_1436300,	21.4	4.58	5.61	0.02515984	0.251746097	1
		GO: 0051084	'de novo' posttranslational protein folding	15	3	PF3D7_0113700,PF3D7_0818900,PF3D7_0917900,	20	4.27	5.14	0.03038695	0.251746097	1
		GO: 0051085	chaperone cofactor-dependent protein refolding	15	3	PF3D7_0113700,PF3D7_0818900,PF3D7_0917900,	20	4.27	5.14	0.03038695	0.251746097	1
		GO: 0007015	actin filament organization	16	3	PF3D7_1251200,PF3D7_1342600,PF3D7_1444800,	18.8	4	4.75	0.03613861	0.251746097	1
		GO: 0061077	chaperone-mediated protein folding	17	3	PF3D7_0113700,PF3D7_0818900,PF3D7_0917900,	17.6	3.77	4.41	0.04240711	0.251746097	1
		GO: 0046471	phosphatidylglycerol metabolic process	1	1	PF3D7_0820200,	100	21.35	inf	0.04683648	0.251746097	1
		GO: 0044658	pore formation in membrane of host by symbiont	1	1	PF3D7_1471100,	100	21.35	inf	0.04683648	0.251746097	1
		GO: 0044501	modulation of signal transduction in other organism	1	1	PF3D7_0731500,	100	21.35	inf	0.04683648	0.251746097	1

University of Ghana http://ugspace.ug.edu.gh

		GO: 0052027	modulation by symbiont of host signal transduction pathway	1	1	PF3D7_0731500,	100	21.35	inf	0.04683648	0.251746097	1
		GO: 0052111	modification by symbiont of host structure	1	1	PF3D7_1471100,	100	21.35	inf	0.04683648	0.251746097	1
		GO: 0075109	modulation by symbiont of host receptor-mediated signal transduction	1	1	PF3D7_0731500,	100	21.35	inf	0.04683648	0.251746097	1
		GO: 1902806	regulation of cell cycle G1/S phase transition	1	1	PF3D7_0907700,	100	21.35	inf	0.04683648	0.251746097	1
		GO: 2000045	regulation of G1/S transition of mitotic cell cycle	1	1	PF3D7_0907700,	100	21.35	inf	0.04683648	0.251746097	1
		GO: 0050900	leukocyte migration	1	1	PF3D7_1301600,	100	21.35	inf	0.04683648	0.251746097	1
		GO: 0001819	positive regulation of cytokine production	1	1	PF3D7_1202900,	100	21.35	inf	0.04683648	0.251746097	1
		GO: 0032049	cardiolipin biosynthetic process	1	1	PF3D7_0820200,	100	21.35	inf	0.04683648	0.251746097	1
		GO: 0033353	S-adenosylmethionine cycle	1	1	PF3D7_0520900,	100	21.35	inf	0.04683648	0.251746097	1
		GO: 0006498	N-terminal protein lipidation	1	1	PF3D7_1412800,	100	21.35	inf	0.04683648	0.251746097	1

University of Ghana http://ugspace.ug.edu.gh

		GO: 0006499	N-terminal protein myristoylation	1	1	PF3D7_1412800,	100	21.35	inf	0.04683648	0.251746097	1
		GO: 0006556	S-adenosylmethionine biosynthetic process	1	1	PF3D7_0922200,	100	21.35	inf	0.04683648	0.251746097	1
		GO: 0006655	phosphatidylglycerol biosynthetic process	1	1	PF3D7_0820200,	100	21.35	inf	0.04683648	0.251746097	1
		GO: 0010950	positive regulation of endopeptidase activity	1	1	PF3D7_0907700,	100	21.35	inf	0.04683648	0.251746097	1
		GO: 0010952	positive regulation of peptidase activity	1	1	PF3D7_0907700,	100	21.35	inf	0.04683648	0.251746097	1
		GO: 0035821	modulation of process of other organism	1	1	PF3D7_0731500,	100	21.35	inf	0.04683648	0.251746097	1
		GO: 0012501	programmed cell death	1	1	PF3D7_0113000,	100	21.35	inf	0.04683648	0.251746097	1
		GO: 0018008	N-terminal peptidyl-glycine N-myristoylation	1	1	PF3D7_1412800,	100	21.35	inf	0.04683648	0.251746097	1
		GO: 0018201	peptidyl-glycine modification	1	1	PF3D7_1412800,	100	21.35	inf	0.04683648	0.251746097	1
		GO: 0018377	protein myristoylation	1	1	PF3D7_1412800,	100	21.35	inf	0.04683648	0.251746097	1

University of Ghana http://ugspace.ug.edu.gh

University of Ghana http://ugspace.ug.edu.gh

		GO: 0030388	fructose 1,6-bisphosphate metabolic process	1	1	PF3D7_1444800,	100	21.35	inf	0.04683648	0.251746097	1
		GO: 0030581	symbiont intracellular protein transport in host	1	1	PF3D7_1252100,	100	21.35	inf	0.04683648	0.251746097	1
		GO: 0032048	cardiolipin metabolic process	1	1	PF3D7_0820200,	100	21.35	inf	0.04683648	0.251746097	1
		GO: 2001138	regulation of phospholipid transport	1	1	PF3D7_0104200,	100	21.35	inf	0.04683648	0.251746097	1
		GO: 0015908	fatty acid transport	1	1	PF3D7_0401900,	100	21.35	inf	0.04683648	0.251746097	1
		GO: 2001139	negative regulation of phospholipid transport	1	1	PF3D7_0104200,	100	21.35	inf	0.04683648	0.251746097	1
		GO: 0006458	'de novo' protein folding	18	3	PF3D7_0113700,PF3D7_0818900,PF3D7_0917900,	16.7	3.56	4.11	0.0491819	0.260285728	1
Molecular function	Upregulated	GO: 0003777	microtubule motor activity	22	7	PF3D7_0718000,PF3D7_0724900,PF3D7_1020300,PF3D7_1023100,PF3D7_1146700,PF3D7_1211000,PF3D7_1245600,	31.8	4.89	6.83	0.00033792	0.11556946	0.11556946
		GO: 0003774	cytoskeletal motor activity	42	9	PF3D7_0718000,PF3D7_0724900,PF3D7_0931700,PF3D7_1020300,PF3D7_1023100,PF3D7_1146700,PF3D7_1211000,PF3D7_1245600,PF3D7_1412500,	21.4	3.29	4	0.0012332	0.210877445	0.421754889
		GO: 0000150	DNA strand exchange activity	2	2	PF3D7_0816800,PF3D7_1107400,	100	15.36	inf	0.00422799	0.242550346	1

University of Ghana http://ugspace.ug.edu.gh

		GO:0004077	biotin-[acetyl-CoA-carboxylase] ligase activity	2	2	PF3D7_1026900,PF3D7_1460000,	100	15.36	inf	0.00422799	0.242550346	1
		GO:0018271	biotin-protein ligase activity	2	2	PF3D7_1026900,PF3D7_1460000,	100	15.36	inf	0.00422799	0.242550346	1
		GO:0015631	tubulin binding	41	8	PF3D7_0307300,PF3D7_0517800,PF3D7_0708000,PF3D7_0724900,PF3D7_1146700,PF3D7_1147200,PF3D7_1211000,PF3D7_1245600,	19.5	3	3.54	0.00425527	0.242550346	1
		GO:0008017	microtubule binding	27	6	PF3D7_0307300,PF3D7_0517800,PF3D7_0724900,PF3D7_1146700,PF3D7_1211000,PF3D7_1245600,	22.2	3.41	4.16	0.00669727	0.327209385	1
		GO:0008092	cytoskeletal protein binding	74	11	PF3D7_0307300,PF3D7_0517800,PF3D7_0708000,PF3D7_0724900,PF3D7_0931700,PF3D7_1118800,PF3D7_1146700,PF3D7_1147200,PF3D7_1211000,PF3D7_1238200,PF3D7_1245600,	14.9	2.28	2.56	0.00776705	0.33204124	1
		GO:0005201	extracellular matrix structural constituent	4	2	PF3D7_0607700,PF3D7_0827200,	50	7.68	14.44	0.02323137	0.365094225	1
		GO:0016409	palmitoyltransferase activity	13	3	PF3D7_1027900,PF3D7_1321400,PF3D7_1415700,	23.1	3.54	4.34	0.04802488	0.365094225	1
	Downregulated	GO:0005515	protein binding	605	70	PF3D7_0102200,PF3D7_0113700,PF3D7_0207500,PF3D7_0207600,PF3D7_0301700,PF3D7_0302200,PF3D7_0302500,PF3D7_0401800,PF3D7_0402000,PF3D7_0402100,PF3D7_0424000,PF3D7_0500800,PF3D7_0501300,PF3D7_0501600,PF3D7_0520900,PF3D7_0527200,PF3D7_0532100,PF3D7_0532300,PF3D7_0532400,PF3D7_0601900,PF3D7_0701900,PF3D7_0702400,PF3D7_0702500,PF3D7_0707300,PF3D7_0818900,PF3D7_0830500,PF3D7_0905400,PF3D7_0917900,PF3D7_0922200,PF3D7_0929400,PF3D7_0930300,PF3D7_0934800,PF3D7_0935900,PF3D7_0936000,PF3D7_0936800,PF3D7_1001000,PF3D7_1002100,PF3D7_1014100,PF3D7_1016300,PF3D7_1035300,PF3D7_1035400,PF3D7_1035500,PF3D7_1035700,PF3D7_1116000,PF3D7_1116800,PF3D7_1125700,PF3D7_1125800,PF3D7_1133400,PF3D7_1136500,PF3D7_1149000,PF3D7_1201000,	11.6	2.47	3.4	5.41E-14	1.20E-11	1.20E-11

						PF3D7_1208300,PF3D7_1222600,PF3D7_1222700,PF3D7_1241100,PF3D7_1251200,PF3D7_1252100,PF3D7_1301700,PF3D7_1335100,PF3D7_1342600,PF3D7_1343000,PF3D7_1353100,PF3D7_1370300,PF3D7_1401100,PF3D7_1410400,PF3D7_1412300,PF3D7_1423300,PF3D7_1436300,PF3D7_1438100,PF3D7_1471100,						
		GO:0046812	host cell surface binding	107	23	PF3D7_0102500,PF3D7_0113000,PF3D7_0223500,PF3D7_0423400,PF3D7_0426000,PF3D7_0620400,PF3D7_0711700,PF3D7_0722200,PF3D7_0731500,PF3D7_0800100,PF3D7_0905400,PF3D7_0930300,PF3D7_1035500,PF3D7_1035700,PF3D7_1036000,PF3D7_1133400,PF3D7_1149000,PF3D7_1252100,PF3D7_1255200,PF3D7_1300100,PF3D7_1301600,PF3D7_1335100,PF3D7_1335300,	21.5	4.59	6.09	3.85E-10	4.28E-08	8.55E-08
		GO:0046789	host cell surface receptor binding	88	17	PF3D7_0102500,PF3D7_0113000,PF3D7_0223500,PF3D7_0423400,PF3D7_0426000,PF3D7_0711700,PF3D7_0722200,PF3D7_0731500,PF3D7_0800100,PF3D7_0905400,PF3D7_1035700,PF3D7_1149000,PF3D7_1255200,PF3D7_1300100,PF3D7_1301600,PF3D7_1335100,PF3D7_1335300,	19.3	4.12	5.18	4.35E-07	3.22E-05	9.66E-05
		GO:0004467	long-chain fatty acid-CoA ligase activity	12	6	PF3D7_0215300,PF3D7_0401900,PF3D7_0619500,PF3D7_0731600,PF3D7_1200700,PF3D7_1372400,	50	10.68	20.87	7.21E-06	0.000320069	0.001600343
		GO:0102391	decanoate-CoA ligase activity	12	6	PF3D7_0215300,PF3D7_0401900,PF3D7_0619500,PF3D7_0731600,PF3D7_1200700,PF3D7_1372400,	50	10.68	20.87	7.21E-06	0.000320069	0.001600343
		GO:0015645	fatty acid ligase activity	13	6	PF3D7_0215300,PF3D7_0401900,PF3D7_0619500,PF3D7_0731600,PF3D7_1200700,PF3D7_1372400,	46.2	9.85	17.89	1.29E-05	0.000408032	0.002856226
		GO:0031956	medium-chain fatty acid-CoA ligase activity	13	6	PF3D7_0215300,PF3D7_0401900,PF3D7_0619500,PF3D7_0731600,PF3D7_1200700,PF3D7_1372400,	46.2	9.85	17.89	1.29E-05	0.000408032	0.002856226
		GO:0016405	CoA-ligase activity	15	6	PF3D7_0215300,PF3D7_0401900,PF3D7_0619500,PF3D7_0731600,PF3D7_1200700,PF3D7_1372400,	40	8.54	13.91	3.47E-05	0.000961825	0.007694599
		GO:0016878	acid-thiol ligase activity	17	6	PF3D7_0215300,PF3D7_0401900,PF3D7_0619500,PF3D7_0731600,PF3D7_1200700,PF3D7_1372400,	35.3	7.54	11.37	7.92E-05	0.00195289	0.017576011

University of Ghana http://ugspace.ug.edu.gh

		GO:0004197	cysteine-type endopeptidase activity	27	7	PF3D7_0207400,PF3D7_0207500,PF3D7_0207600,PF3D7_0207700,PF3D7_0207800,PF3D7_0404700,PF3D7_0902800,	25.9	5.54	7.32	0.00017912	0.003834731	0.039765151
		GO:0008234	cysteine-type peptidase activity	55	10	PF3D7_0207400,PF3D7_0207500,PF3D7_0207600,PF3D7_0207700,PF3D7_0207800,PF3D7_0404700,PF3D7_0527200,PF3D7_0902800,PF3D7_0919200,PF3D7_1141700,	18.2	3.88	4.68	0.00019001	0.003834731	0.042182036
		GO:0008201	heparin binding	9	4	PF3D7_0102500,PF3D7_0731500,PF3D7_1301600,PF3D7_1335300,	44.4	9.49	16.55	0.00049032	0.009070964	0.108851567
		GO:0005539	glycosaminoglycan binding	10	4	PF3D7_0102500,PF3D7_0731500,PF3D7_1301600,PF3D7_1335300,	40	8.54	13.79	0.00078732	0.01344492	0.17478396
		GO:0016877	ligase activity, forming carbon-sulfur bonds	26	6	PF3D7_0215300,PF3D7_0401900,PF3D7_0619500,PF3D7_0731600,PF3D7_1200700,PF3D7_1372400,	23.1	4.93	6.24	0.00103235	0.015278788	0.229181826
		GO:1901681	sulfur compound binding	26	6	PF3D7_0102500,PF3D7_0112200,PF3D7_0619500,PF3D7_0731500,PF3D7_1301600,PF3D7_1335300,	23.1	4.93	6.24	0.00103235	0.015278788	0.229181826
		GO:0044877	protein-containing complex binding	101	12	PF3D7_0202200,PF3D7_0424000,PF3D7_0527200,PF3D7_0905400,PF3D7_0929400,PF3D7_0930300,PF3D7_1035400,PF3D7_1035500,PF3D7_1035700,PF3D7_1251200,PF3D7_1255200,PF3D7_1342600,	11.9	2.54	2.84	0.00245076	0.034004304	0.544068859
		GO:0004674	protein serine/threonine kinase activity	93	11	PF3D7_0102600,PF3D7_0301200,PF3D7_0424500,PF3D7_0424700,PF3D7_0500900,PF3D7_0902100,PF3D7_0934800,PF3D7_1039000,PF3D7_1136500,PF3D7_1149300,PF3D7_1371700,	11.8	2.53	2.82	0.00381237	0.049785077	0.846346317
		GO:0004672	protein kinase activity	108	11	PF3D7_0102600,PF3D7_0301200,PF3D7_0424500,PF3D7_0424700,PF3D7_0500900,PF3D7_0902100,PF3D7_0934800,PF3D7_1039000,PF3D7_1136500,PF3D7_1149300,PF3D7_1371700,	10.2	2.17	2.37	0.01166413	0.143824647	1
		GO:0005253	anion channel activity	4	2	PF3D7_0302200,PF3D7_0302500,	50	10.68	20.52	0.01230932	0.143824647	1

University of Ghana http://ugspace.ug.edu.gh

University of Ghana http://ugspace.ug.edu.gh

		GO:0050839	cell adhesion molecule binding	55	7	PF3D7_0223500,PF3D7_0302200,PF3D7_0302500,PF3D7_0426000,PF3D7_0711700,PF3D7_0800100,PF3D7_1255200,	12.7	2.72	3.03	0.01343179	0.149092854	1
		GO:0016773	phosphotransferase activity, alcohol group as acceptor	141	13	PF3D7_0102600,PF3D7_0301200,PF3D7_0424500,PF3D7_0424700,PF3D7_0500900,PF3D7_0503100,PF3D7_0902100,PF3D7_0934800,PF3D7_1039000,PF3D7_1136500,PF3D7_1149300,PF3D7_1371700,PF3D7_1443700,	9.2	1.97	2.13	0.01416903	0.149786845	1
		GO:0061135	endopeptidase regulator activity	5	2	PF3D7_0501400,PF3D7_0907700,	40	8.54	13.68	0.0198852	0.20065976	1
		GO:0061134	peptidase regulator activity	6	2	PF3D7_0501400,PF3D7_0907700,	33.3	7.12	10.26	0.02891496	0.247564268	1
		GO:0044183	protein folding chaperone	6	2	PF3D7_0818900,PF3D7_0917900,	33.3	7.12	10.26	0.02891496	0.247564268	1
		GO:0046982	protein heterodimerization activity	15	3	PF3D7_0320900,PF3D7_0617800,PF3D7_0714000,	20	4.27	5.14	0.03038695	0.247564268	1
		GO:0016298	lipase activity	28	4	PF3D7_0702200,PF3D7_1001600,PF3D7_1221900,PF3D7_1252600,	14.3	3.05	3.43	0.03966127	0.247564268	1
		GO:0005178	integrin binding	1	1	PF3D7_1255200,	100	21.35	inf	0.04683648	0.247564268	1
		GO:0050515	4-(cytidine 5'-diphospho)-2-C-methyl-D-erythritol kinase activity	1	1	PF3D7_0503100,	100	21.35	inf	0.04683648	0.247564268	1
		GO:0003823	antigen binding	1	1	PF3D7_1116000,	100	21.35	inf	0.04683648	0.247564268	1

University of Ghana http://ugspace.ug.edu.gh

		GO:0004013	adenosylhomocysteinase activity	1	1	PF3D7_0520900,	100	21.35	inf	0.04683648	0.247564268	1
		GO:0019237	centromeric DNA binding	1	1	PF3D7_1202900,	100	21.35	inf	0.04683648	0.247564268	1
		GO:0004140	dephospho-CoA kinase activity	1	1	PF3D7_1443700,	100	21.35	inf	0.04683648	0.247564268	1
		GO:0019107	myristoyltransferase activity	1	1	PF3D7_1412800,	100	21.35	inf	0.04683648	0.247564268	1
		GO:0004332	fructose-bisphosphate aldolase activity	1	1	PF3D7_1444800,	100	21.35	inf	0.04683648	0.247564268	1
		GO:0004379	glycylpeptide N-tetradecanoyltransferase activity	1	1	PF3D7_1412800,	100	21.35	inf	0.04683648	0.247564268	1
		GO:0016802	trialkylsulfonium hydrolase activity	1	1	PF3D7_0520900,	100	21.35	inf	0.04683648	0.247564268	1
		GO:0004478	methionine adenosyltransferase activity	1	1	PF3D7_0922200,	100	21.35	inf	0.04683648	0.247564268	1
		GO:0015485	cholesterol binding	1	1	PF3D7_0113700,	100	21.35	inf	0.04683648	0.247564268	1
		GO:0008936	nicotinamidase activity	1	1	PF3D7_0320500,	100	21.35	inf	0.04683648	0.247564268	1

University of Ghana http://ugspace.ug.edu.gh

		GO:0008444	CDP-diacylglycerol-glycerol-3-phosphate 3-phosphatidyltransferase activity	1	1	PF3D7_0820200,	100	21.35	inf	0.04683648	0.247564268	1
		GO:0033691	sialic acid binding	1	1	PF3D7_0102500,	100	21.35	inf	0.04683648	0.247564268	1
		GO:0000234	phosphoethanolamine N-methyltransferase activity	1	1	PF3D7_1343000,	100	21.35	inf	0.04683648	0.247564268	1
Cellular component	Upregulated	GO:0044312	crystalloid	17	17	PF3D7_0109100,PF3D7_0418800,PF3D7_0504500,PF3D7_0825700,PF3D7_0825800,PF3D7_0903800,PF3D7_0904200,PF3D7_1027900,PF3D7_1103500,PF3D7_1146100,PF3D7_1207300,PF3D7_1407000,PF3D7_1429300,PF3D7_1451600,PF3D7_1453500,PF3D7_1455800,PF3D7_1475500,	100	15.36	inf	4.52E-21	1.04E-18	1.04E-18
		GO:0044310	osmiophilic body	21	8	PF3D7_0311700,PF3D7_0515600,PF3D7_1214800,PF3D7_1216500,PF3D7_1234400,PF3D7_1247800,PF3D7_1250100,PF3D7_1449000,	38.1	5.85	9.04	2.85E-05	0.003262924	0.006525847
		GO:0005856	cytoskeleton	130	20	PF3D7_0307300,PF3D7_0718000,PF3D7_0724900,PF3D7_0906400,PF3D7_0911500,PF3D7_0924900,PF3D7_1020300,PF3D7_1023100,PF3D7_1034300,PF3D7_1104600,PF3D7_1118800,PF3D7_1146700,PF3D7_1211000,PF3D7_1230100,PF3D7_1238200,PF3D7_1316400,PF3D7_1340500,PF3D7_1403000,PF3D7_1408800,PF3D7_1412500,	15.4	2.36	2.72	0.00023664	0.018063786	0.054191357
		GO:0099513	polymeric cytoskeletal fiber	51	10	PF3D7_0307300,PF3D7_0718000,PF3D7_0724900,PF3D7_0911500,PF3D7_0924900,PF3D7_1023100,PF3D7_1146700,PF3D7_1230100,PF3D7_1408800,PF3D7_1412500,	19.6	3.01	3.58	0.00138103	0.052709191	0.316255144
		GO:0099081	supramolecular polymer	51	10	PF3D7_0307300,PF3D7_0718000,PF3D7_0724900,PF3D7_0911500,PF3D7_0924900,PF3D7_1023100,PF3D7_1146700,PF3D7_1230100,PF3D7_1408800,PF3D7_1412500,	19.6	3.01	3.58	0.00138103	0.052709191	0.316255144
		GO:0099512	supramolecular fiber	51	10	PF3D7_0307300,PF3D7_0718000,PF3D7_0724900,PF3D7_0911500,PF3D7_0924900,PF3D7_1023100,PF3D7_1146700,PF3D7_1230100,PF3D7_1408800,PF3D7_1412500,	19.6	3.01	3.58	0.00138103	0.052709191	0.316255144

		GO: 0005886	plasma membrane	140	18	PF3D7_0104700,PF3D7_0209000,PF3D7_0219100,PF3D7_0825300,PF3D7_1031000,PF3D7_1105900,PF3D7_1107900,PF3D7_1116500,PF3D7_1204400,PF3D7_1216500,PF3D7_1321000,PF3D7_1346700,PF3D7_1346800,PF3D7_1360500,PF3D7_1421300,PF3D7_1425500,PF3D7_1438300,PF3D7_1461700,	12.9	1.97	2.19	0.00392093	0.096821077	0.897892613
		GO: 0098802	plasma membrane signaling receptor complex	2	2	PF3D7_0418800,PF3D7_0504500,	100	15.36	inf	0.00422799	0.096821077	0.968210775
		GO: 0043235	receptor complex	2	2	PF3D7_0418800,PF3D7_0504500,	100	15.36	inf	0.00422799	0.096821077	0.968210775
		GO: 0005892	acetylcholine-gated channel complex	2	2	PF3D7_0418800,PF3D7_0504500,	100	15.36	inf	0.00422799	0.096821077	0.968210775
		GO: 0031226	intrinsic component of plasma membrane	51	9	PF3D7_0208900,PF3D7_0209000,PF3D7_0418800,PF3D7_0504500,PF3D7_0625100,PF3D7_1031000,PF3D7_1346700,PF3D7_1346800,PF3D7_1475400,	17.6	2.71	3.14	0.00501437	0.104390098	1
		GO: 0005875	microtubule associated complex	44	8	PF3D7_0718000,PF3D7_0724900,PF3D7_0906400,PF3D7_1020300,PF3D7_1023100,PF3D7_1034300,PF3D7_1146700,PF3D7_1211000,	18.2	2.79	3.25	0.00665786	0.12317196	1
		GO: 0000152	nuclear ubiquitin ligase complex	7	3	PF3D7_0501700,PF3D7_1026400,PF3D7_1217600,	42.9	6.58	10.86	0.0078628	0.12317196	1
		GO: 0005680	anaphase-promoting complex	7	3	PF3D7_0501700,PF3D7_1026400,PF3D7_1217600,	42.9	6.58	10.86	0.0078628	0.12317196	1
		GO: 0046658	anchored component of plasma membrane	28	6	PF3D7_0208900,PF3D7_0209000,PF3D7_1031000,PF3D7_1346700,PF3D7_1346800,PF3D7_1475400,	21.4	3.29	3.97	0.00806803	0.12317196	1

University of Ghana http://ugspace.ug.edu.gh

		GO:0016020	membrane	637	56	PF3D7_0311000,PF3D7_0414300,PF3D7_0504900,PF3D7_0514500,PF3D7_0526100,PF3D7_0606400,PF3D7_0622100,PF3D7_0624300,PF3D7_0718800,PF3D7_0719100,PF3D7_0728700,PF3D7_0801600,PF3D7_0827700,PF3D7_0909000,PF3D7_0909100,PF3D7_0918800,PF3D7_0925100,PF3D7_1009100,PF3D7_1020200,PF3D7_1027900,PF3D7_1029500,PF3D7_1031000,PF3D7_1107900,PF3D7_1120700,PF3D7_1127200,PF3D7_1132400,PF3D7_1146300,PF3D7_1149800,PF3D7_1206900,PF3D7_1212600,PF3D7_1216700,PF3D7_1232300,PF3D7_1234000,PF3D7_1234400,PF3D7_1246000,PF3D7_1315300,PF3D7_1348400,PF3D7_1349700,PF3D7_1354000,PF3D7_1361300,PF3D7_1369400,PF3D7_1403000,PF3D7_1403200,PF3D7_1407000,PF3D7_1415700,PF3D7_1426500,PF3D7_1429600,PF3D7_1452900,PF3D7_1454900,PF3D7_1457100,PF3D7_1461800,PF3D7_1462600,PF3D7_1467000,PF3D7_1470500,PF3D7_1471500,PF3D7_1476700,	8.8	1.35	1.47	0.00968912	0.132346585	1
		GO:0031225	anchored component of membrane	30	6	PF3D7_0208900,PF3D7_0209000,PF3D7_1031000,PF3D7_1346700,PF3D7_1346800,PF3D7_1475400,	20	3.07	3.64	0.01139514	0.132346585	1
		GO:0005871	kinesin complex	8	3	PF3D7_0724900,PF3D7_1146700,PF3D7_1211000,	37.5	5.76	8.69	0.01197952	0.132346585	1
		GO:0005882	intermediate filament	3	2	PF3D7_0911500,PF3D7_1408800,	66.7	10.24	28.89	0.01213659	0.132346585	1
		GO:0045111	intermediate filament cytoskeleton	3	2	PF3D7_0911500,PF3D7_1408800,	66.7	10.24	28.89	0.01213659	0.132346585	1
		GO:0005581	collagen trimer	3	2	PF3D7_0607700,PF3D7_0827200,	66.7	10.24	28.89	0.01213659	0.132346585	1
		GO:0015630	microtubule cytoskeleton	90	12	PF3D7_0307300,PF3D7_0718000,PF3D7_0724900,PF3D7_0906400,PF3D7_0924900,PF3D7_1020300,PF3D7_1023100,PF3D7_1034300,PF3D7_1146700,PF3D7_1211000,PF3D7_1230100,PF3D7_1340500,	13.3	2.05	2.26	0.01303211	0.135652469	1

University of Ghana http://ugspace.ug.edu.gh

		GO: 0009986	cell surface	159	18	PF3D7_0208900,PF3D7_0209000,PF3D7_0513700,PF3D7_0517800,PF3D7_0816500,PF3D7_0904200,PF3D7_0904300,PF3D7_1031000,PF3D7_1146300,PF3D7_1204400,PF3D7_1207300,PF3D7_1234400,PF3D7_1238000,PF3D7_1338800,PF3D7_1346700,PF3D7_1345800,PF3D7_1349000,PF3D7_1475400,	11.3	1.74	1.88	0.014418	0.143553147	1
		GO: 0005575	cellular component	723	61	PF3D7_0311000,PF3D7_0414300,PF3D7_0504900,PF3D7_0514500,PF3D7_0526100,PF3D7_0606400,PF3D7_0622100,PF3D7_0624300,PF3D7_0718800,PF3D7_0719100,PF3D7_0728700,PF3D7_0801600,PF3D7_0817900,PF3D7_0827700,PF3D7_0909000,PF3D7_0909100,PF3D7_0915800,PF3D7_0925100,PF3D7_1009100,PF3D7_1020200,PF3D7_1027600,PF3D7_1027900,PF3D7_1029500,PF3D7_1031000,PF3D7_1107900,PF3D7_1120700,PF3D7_1127200,PF3D7_1132400,PF3D7_1139500,PF3D7_1146300,PF3D7_1149800,PF3D7_1206900,PF3D7_1212600,PF3D7_1216700,PF3D7_1232300,PF3D7_1234000,PF3D7_1234400,PF3D7_1238200,PF3D7_1246000,PF3D7_1315300,PF3D7_1348400,PF3D7_1349700,PF3D7_1354000,PF3D7_1361300,PF3D7_1369400,PF3D7_1403000,PF3D7_1403200,PF3D7_1407000,PF3D7_1415700,PF3D7_1426500,PF3D7_1429600,PF3D7_1452900,PF3D7_1454900,PF3D7_1455800,PF3D7_1457100,PF3D7_1461800,PF3D7_1462600,PF3D7_1467000,PF3D7_1470500,PF3D7_1471500,PF3D7_1476700,	8.4	1.3	1.4	0.01631787	0.155699689	1
		GO: 0070258	inner membrane pellicle complex	63	9	PF3D7_0304100,PF3D7_0510300,PF3D7_0621400,PF3D7_0704100,PF3D7_0708600,PF3D7_0816500,PF3D7_1141900,PF3D7_1221400,PF3D7_1417000,	14.3	2.19	2.43	0.01967454	0.180218756	1
		GO: 0099080	supramolecular complex	85	11	PF3D7_0307300,PF3D7_0718000,PF3D7_0724900,PF3D7_0911500,PF3D7_0924900,PF3D7_1023100,PF3D7_1124400,PF3D7_1146700,PF3D7_1230100,PF3D7_1408800,PF3D7_1412500,	12.9	1.99	2.17	0.02098993	0.184872821	1
		GO: 0044424	obsolete intracellular part	1005	80	PF3D7_0208900,PF3D7_0322800,PF3D7_0411700,PF3D7_0417100,PF3D7_0421900,PF3D7_0501700,PF3D7_0517500,PF3D7_0517800,PF3D7_0518700,PF3D7_0606400,PF3D7_0607100,PF3D7_0607700,PF3D7_0622100,PF3D7_0630200,PF3D7_0708000,PF3D7_0714100,PF3D7_0717800,PF3D7_0718000,PF3D7_0813800,PF3D7_0816500,PF3D7_0822400,PF3D7_0825700,PF3D7_0827200,PF3D7_0827400,PF3D7_0906400,PF3D7_0913400,PF3D7_0915800,PF3D7_0920300,PF3D7_0922400,PF3D7_0928100,PF3D7_0931700,PF3D7_1007800,PF3D7_1019100,PF3D7_1026400,PF3D7_1026900,PF3D7_1104500,PF3D7_1106900,PF3D7_1115200,PF3D7_1118800,PF3D7_1131500,PF3D7_1136100,PF3D7_1139600,PF3D7_1141100,PF3D7_1146300,PF3D7_1146800,PF3D7_1147200,PF3D7_1213400,PF3D7_1220700,PF3D7_1222800,PF3D7_1222900,PF3D7_1238200,	8	1.22	1.32	0.02364969	0.194035269	1

University of Ghana http://ugspace.ug.edu.gh

University of Ghana http://ugspace.ug.edu.gh

						PF3D7_1239400,PF3D7_1247800,PF3D7_1248800,PF3D7_1251000,PF3D7_1316000,PF3D7_1316400,PF3D7_1328600,PF3D7_1340500,PF3D7_1349000,PF3D7_1350000,PF3D7_1360500,PF3D7_1369300,PF3D7_1403000,PF3D7_1410100,PF3D7_1412500,PF3D7_1415700,PF3D7_1416700,PF3D7_1423600,PF3D7_1430100,PF3D7_1430400,PF3D7_1438800,PF3D7_1452900,PF3D7_1456400,PF3D7_1457800,PF3D7_1460000,PF3D7_1461700,PF3D7_1465600,PF3D7_1465700,PF3D7_1475500,						
		GO:0020039	pellicle	65	9	PF3D7_0304100,PF3D7_0510300,PF3D7_0621400,PF3D7_0704100,PF3D7_0708600,PF3D7_0816500,PF3D7_1141900,PF3D7_1221400,PF3D7_1417000,	13.8	2.13	2.35	0.02372484	0.194035269	1
		GO:0005874	microtubule	45	7	PF3D7_0307300,PF3D7_0718000,PF3D7_0724900,PF3D7_0924900,PF3D7_1023100,PF3D7_1146700,PF3D7_1230100,	15.6	2.39	2.68	0.02478772	0.195737533	1
		GO:0043232	intracellular non-membrane-bounded organelle	502	43	PF3D7_0109100,PF3D7_0219100,PF3D7_0307300,PF3D7_0418800,PF3D7_0504500,PF3D7_0718000,PF3D7_0724900,PF3D7_0817900,PF3D7_0825700,PF3D7_0825800,PF3D7_0903800,PF3D7_0904200,PF3D7_0906400,PF3D7_0911500,PF3D7_0924900,PF3D7_1020300,PF3D7_1023100,PF3D7_1027600,PF3D7_1027900,PF3D7_1032000,PF3D7_1034300,PF3D7_1103500,PF3D7_1104600,PF3D7_1118800,PF3D7_1124400,PF3D7_1139500,PF3D7_1146100,PF3D7_1146700,PF3D7_1207300,PF3D7_1211000,PF3D7_1230100,PF3D7_1238200,PF3D7_1316400,PF3D7_1340500,PF3D7_1403000,PF3D7_1407000,PF3D7_1408800,PF3D7_1412500,PF3D7_1429300,PF3D7_1451600,PF3D7_1453500,PF3D7_1455800,PF3D7_1475500,	8.6	1.32	1.4	0.03391829	0.258909607	1
		GO:0043228	non-membrane-bounded organelle	504	43	PF3D7_0109100,PF3D7_0219100,PF3D7_0307300,PF3D7_0418800,PF3D7_0504500,PF3D7_0718000,PF3D7_0724900,PF3D7_0817900,PF3D7_0825700,PF3D7_0825800,PF3D7_0903800,PF3D7_0904200,PF3D7_0906400,PF3D7_0911500,PF3D7_0924900,PF3D7_1020300,PF3D7_1023100,PF3D7_1027600,PF3D7_1027900,PF3D7_1032000,PF3D7_1034300,PF3D7_1103500,PF3D7_1104600,PF3D7_1118800,PF3D7_1124400,PF3D7_1139500,PF3D7_1146100,PF3D7_1146700,PF3D7_1207300,PF3D7_1211000,PF3D7_1230100,PF3D7_1238200,PF3D7_1316400,PF3D7_1340500,PF3D7_1403000,PF3D7_1407000,PF3D7_1408800,PF3D7_1412500,PF3D7_1429300,PF3D7_1451600,PF3D7_1453500,PF3D7_1455800,PF3D7_1475500,	8.5	1.31	1.39	0.0359283	0.265256442	1

University of Ghana http://ugspace.ug.edu.gh

		GO: 0034702	ion channel complex	5	2	PF3D7_0418800,PF3D7_0504500,	40	6.14	9.63	0.0370664	0.265256442	1
	Downregulated	GO: 0018995	host cellular component	713	130	PF3D7_0102200,PF3D7_0102600,PF3D7_0104200,PF3D7_0108500,PF3D7_0112200,PF3D7_0113000,PF3D7_0113200,PF3D7_0113700,PF3D7_0114800,PF3D7_0202200,PF3D7_0202500,PF3D7_0207500,PF3D7_0207600,PF3D7_0207700,PF3D7_0220000,PF3D7_0220200,PF3D7_0220300,PF3D7_0220500,PF3D7_0220600,PF3D7_0221700,PF3D7_0223500,PF3D7_0301500,PF3D7_0301700,PF3D7_0301800,PF3D7_0302200,PF3D7_0302500,PF3D7_0401800,PF3D7_0401900,PF3D7_0402000,PF3D7_0402100,PF3D7_0402400,PF3D7_0404700,PF3D7_0424000,PF3D7_0424500,PF3D7_0424600,PF3D7_0424700,PF3D7_0426000,PF3D7_0500800,PF3D7_0501000,PF3D7_0501300,PF3D7_0501400,PF3D7_0507500,PF3D7_0520900,PF3D7_0532100,PF3D7_0532300,PF3D7_0532400,PF3D7_0532600,PF3D7_0601900,PF3D7_0617700,PF3D7_0701900,PF3D7_0702000,PF3D7_0702400,PF3D7_0702500,PF3D7_0707300,PF3D7_0711700,PF3D7_0713100,PF3D7_0730900,PF3D7_0731200,PF3D7_0731300,PF3D7_0731600,PF3D7_0731700,PF3D7_0732200,PF3D7_0800100,PF3D7_0800800,PF3D7_0830500,PF3D7_0831400,PF3D7_0901700,PF3D7_0901800,PF3D7_0905400,PF3D7_0922200,PF3D7_0929400,PF3D7_0935900,PF3D7_0936000,PF3D7_0936300,PF3D7_0936800,PF3D7_1000600,PF3D7_1001000,PF3D7_1001500,PF3D7_1001600,PF3D7_1001700,PF3D7_1001800,PF3D7_1002000,PF3D7_1002100,PF3D7_1014100,PF3D7_1016300,PF3D7_1016600,PF3D7_1035200,PF3D7_1035300,PF3D7_1039000,PF3D7_1102700,PF3D7_1102800,PF3D7_1115800,PF3D7_1116800,PF3D7_1136500,PF3D7_1148900,PF3D7_1149000,PF3D7_1149300,PF3D7_1149400,PF3D7_1149600,PF3D7_1200700,PF3D7_1201000,PF3D7_1201100,PF3D7_1222700,PF3D7_1228600,PF3D7_1252100,PF3D7_1252300,PF3D7_1252600,PF3D7_1255200,PF3D7_1301400,PF3D7_1301500,PF3D7_1301700,PF3D7_1302000,PF3D7_1334500,PF3D7_1334700,PF3D7_1353100,PF3D7_1370300,PF3D7_1371800,PF3D7_1372000,PF3D7_1400500,PF3D7_1401000,PF3D7_1401100,PF3D7_1401200,PF3D7_1401400,PF3D7_1410400,PF3D7_1436300,PF3D7_1463900,PF3D7_1471100,PF3D7_1473200,PF3D7_1477500,PF3D7_1478600,	18.2	3.89	9.23	4.31E-53	3.90E-51	7.81E-51
		GO: 0043657	host cell	713	130	PF3D7_0102200,PF3D7_0102600,PF3D7_0104200,PF3D7_0108500,PF3D7_0112200,PF3D7_0113000,PF3D7_0113200,PF3D7_0113700,PF3D7_0114800,PF3D7_0202200,PF3D7_0202500,PF3D7_0207500,PF3D7_0207600,PF3D7_0207700,PF3D7_0220000,PF3D7_0220200,PF3D7_0220300,PF3D7_0220500,PF3D7_0220600,PF3D7_0221700,PF3D7_0223500,PF3D7_0301500,PF3D7_030	18.2	3.89	9.23	4.31E-53	3.90E-51	7.81E-51

						1700,PF3D7_0301800,PF3D7_0302200,PF3D7_0302500,PF3D7_0401800,PF3D7_0401900,PF3D7_0402000,PF3D7_0402100,PF3D7_0402400,PF3D7_0404700,PF3D7_0424000,PF3D7_0424500,PF3D7_0424600,PF3D7_0424700,PF3D7_0426000,PF3D7_0500800,PF3D7_0501000,PF3D7_0501300,PF3D7_0501400,PF3D7_0507500,PF3D7_0520900,PF3D7_0532100,PF3D7_0532300,PF3D7_0532400,PF3D7_0532600,PF3D7_0601900,PF3D7_0617700,PF3D7_0701900,PF3D7_0702000,PF3D7_0702400,PF3D7_0702500,PF3D7_0707300,PF3D7_0711700,PF3D7_0713100,PF3D7_0730900,PF3D7_0731200,PF3D7_0731300,PF3D7_0731600,PF3D7_0731700,PF3D7_0732200,PF3D7_0800100,PF3D7_0800800,PF3D7_0830500,PF3D7_0831400,PF3D7_0901700,PF3D7_0901800,PF3D7_0905400,PF3D7_0922200,PF3D7_0929400,PF3D7_0935900,PF3D7_0936000,PF3D7_0936300,PF3D7_0936800,PF3D7_1000600,PF3D7_1001000,PF3D7_1001500,PF3D7_1001600,PF3D7_1001700,PF3D7_1001800,PF3D7_1002000,PF3D7_1002100,PF3D7_1014100,PF3D7_1016300,PF3D7_1016600,PF3D7_1035200,PF3D7_1035300,PF3D7_1039000,PF3D7_1102700,PF3D7_1102800,PF3D7_1115800,PF3D7_1116800,PF3D7_1136500,PF3D7_1148900,PF3D7_1149000,PF3D7_1149300,PF3D7_1149400,PF3D7_1149600,PF3D7_1200700,PF3D7_1201000,PF3D7_1201100,PF3D7_1222700,PF3D7_1228600,PF3D7_1252100,PF3D7_1252300,PF3D7_1252600,PF3D7_1255200,PF3D7_1301400,PF3D7_1301500,PF3D7_1301700,PF3D7_1302000,PF3D7_1334500,PF3D7_1334700,PF3D7_1353100,PF3D7_1370300,PF3D7_1371800,PF3D7_1372000,PF3D7_1400500,PF3D7_1401000,PF3D7_1401100,PF3D7_1401200,PF3D7_1401400,PF3D7_1410400,PF3D7_1436300,PF3D7_1463900,PF3D7_1471100,PF3D7_1473200,PF3D7_1477500,PF3D7_1478600,						
		GO:0033643	host cell part	630	107	PF3D7_0102200,PF3D7_0102600,PF3D7_0104200,PF3D7_0108500,PF3D7_0112200,PF3D7_0113000,PF3D7_0113700,PF3D7_0202200,PF3D7_0202500,PF3D7_0207500,PF3D7_0207600,PF3D7_0207700,PF3D7_0220000,PF3D7_0220200,PF3D7_0221700,PF3D7_0223500,PF3D7_0301700,PF3D7_0301800,PF3D7_0302200,PF3D7_0302500,PF3D7_0401800,PF3D7_0401900,PF3D7_0402000,PF3D7_0402100,PF3D7_0404700,PF3D7_0424000,PF3D7_0424500,PF3D7_0424600,PF3D7_0424700,PF3D7_0426000,PF3D7_0500800,PF3D7_0501000,PF3D7_0501300,PF3D7_0501400,PF3D7_0507500,PF3D7_0520900,PF3D7_0532100,PF3D7_0532300,PF3D7_0532400,PF3D7_0532600,PF3D7_0601900,PF3D7_0617700,PF3D7_0701900,PF3D7_0702000,PF3D7_0702400,PF3D7_0702500,PF3D7_0707300,PF3D7_0711700,PF3D7_0713100,PF3D7_0731200,PF3D7_0731300,PF3D7_0731600,PF3D7_0732200,PF3D7_0800100,PF3D7_0830500,PF3D7_0905400,PF3D7_0922200,PF3D7_0929400,PF3D7_0935900,PF3D7_0936000,PF3D7_0936300,PF3D7_0936800,PF3D	17	3.63	6.96	2.41E-38	1.45E-36	4.36E-36

University of Ghana http://ugspace.ug.edu.gh

University of Ghana http://ugspace.ug.edu.gh

						7_1000600,PF3D7_1001000,PF3D7_1001500,PF3D7_1001600,PF3D7_1002100,PF3D7_1014100,PF3D7_1016300,PF3D7_1035200,PF3D7_1035300,PF3D7_1039000,PF3D7_1102700,PF3D7_1102900,PF3D7_1115800,PF3D7_1116800,PF3D7_1136500,PF3D7_1148900,PF3D7_1149000,PF3D7_1149300,PF3D7_1149600,PF3D7_1200700,PF3D7_1201000,PF3D7_1201100,PF3D7_1222700,PF3D7_1228600,PF3D7_1252100,PF3D7_1252300,PF3D7_1252600,PF3D7_1255200,PF3D7_1301400,PF3D7_1301700,PF3D7_1302000,PF3D7_1334500,PF3D7_1334700,PF3D7_1353100,PF3D7_1370300,PF3D7_1400500,PF3D7_1401100,PF3D7_1401200,PF3D7_1401400,PF3D7_1410400,PF3D7_1436300,PF3D7_1463900,PF3D7_1471100,PF3D7_1473200,PF3D7_1478600,						
		GO:0030430	host cell cytoplasm	540	97	PF3D7_0102200,PF3D7_0102600,PF3D7_0104200,PF3D7_0108500,PF3D7_0112200,PF3D7_0113700,PF3D7_0202200,PF3D7_0202500,PF3D7_0207500,PF3D7_0207600,PF3D7_0207700,PF3D7_0220200,PF3D7_0221700,PF3D7_0223500,PF3D7_0301700,PF3D7_0301800,PF3D7_0401800,PF3D7_0401900,PF3D7_0402000,PF3D7_0402100,PF3D7_0404700,PF3D7_0424000,PF3D7_0424500,PF3D7_0424700,PF3D7_0426000,PF3D7_0500800,PF3D7_0501000,PF3D7_0501300,PF3D7_0501400,PF3D7_0507500,PF3D7_0520900,PF3D7_0532100,PF3D7_0532300,PF3D7_0532400,PF3D7_0532600,PF3D7_0601900,PF3D7_0617700,PF3D7_0701900,PF3D7_0702000,PF3D7_0702400,PF3D7_0702500,PF3D7_0707300,PF3D7_0711700,PF3D7_0713100,PF3D7_0731200,PF3D7_0731300,PF3D7_0731600,PF3D7_0732200,PF3D7_0800100,PF3D7_0830500,PF3D7_0905400,PF3D7_0922200,PF3D7_0929400,PF3D7_0935900,PF3D7_0936000,PF3D7_0936300,PF3D7_0936800,PF3D7_1001000,PF3D7_1001500,PF3D7_1001600,PF3D7_1002100,PF3D7_1014100,PF3D7_1016300,PF3D7_1035200,PF3D7_1035300,PF3D7_1039000,PF3D7_1102700,PF3D7_1102800,PF3D7_1115800,PF3D7_1116800,PF3D7_1148900,PF3D7_1149000,PF3D7_1149600,PF3D7_1200700,PF3D7_1201000,PF3D7_1201100,PF3D7_1228600,PF3D7_1252100,PF3D7_1252300,PF3D7_1252600,PF3D7_1255200,PF3D7_1301400,PF3D7_1301700,PF3D7_1302000,PF3D7_1334500,PF3D7_1334700,PF3D7_1353100,PF3D7_1370300,PF3D7_1401100,PF3D7_1401200,PF3D7_1401400,PF3D7_1410400,PF3D7_1436300,PF3D7_1463900,PF3D7_1471100,PF3D7_1473200,PF3D7_1478600,	18	3.84	7.02	3.13E-36	1.42E-34	5.66E-34
		GO:0033646	host intracellular part	549	97	PF3D7_0102200,PF3D7_0102600,PF3D7_0104200,PF3D7_0108500,PF3D7_0112200,PF3D7_0113700,PF3D7_0202200,PF3D7_0202500,PF3D7_0207500,PF3D7_0207600,PF3D7_0207700,PF3D7_0220200,PF3D7_0221700,PF3D7_0223500,PF3D7_0301700,PF3D7_0301800,PF3D7_0401800,PF3D7_0401900,PF3D7_0402000,PF3D7_0402100,PF3D7_0404700,PF3D7_0424000,PF3D7_042	17.7	3.77	6.86	1.39E-35	4.93E-34	2.51E-33

University of Ghana http://ugspace.ug.edu.gh

						4500,PF3D7_0424700,PF3D7_0426000,PF3D7_0500800,PF3D7_0501000,PF3D7_0501300,PF3D7_0501400,PF3D7_0507500,PF3D7_0520900,PF3D7_0532100,PF3D7_0532300,PF3D7_0532400,PF3D7_0532600,PF3D7_0601900,PF3D7_0617700,PF3D7_0701900,PF3D7_0702000,PF3D7_0702400,PF3D7_0702500,PF3D7_0707300,PF3D7_0711700,PF3D7_0713100,PF3D7_0731200,PF3D7_0731300,PF3D7_0731600,PF3D7_0732200,PF3D7_0800100,PF3D7_0830500,PF3D7_0905400,PF3D7_0922200,PF3D7_0929400,PF3D7_0935900,PF3D7_0936000,PF3D7_0936300,PF3D7_0936800,PF3D7_1001000,PF3D7_1001500,PF3D7_1001600,PF3D7_1002100,PF3D7_1014100,PF3D7_1016300,PF3D7_1035200,PF3D7_1035300,PF3D7_1039000,PF3D7_1102700,PF3D7_1102800,PF3D7_1115800,PF3D7_1116800,PF3D7_1148900,PF3D7_1149000,PF3D7_1149600,PF3D7_1200700,PF3D7_1201000,PF3D7_1201100,PF3D7_1228600,PF3D7_1252100,PF3D7_1252300,PF3D7_1252600,PF3D7_1255200,PF3D7_1301400,PF3D7_1301700,PF3D7_1302000,PF3D7_1334500,PF3D7_1334700,PF3D7_1353100,PF3D7_1370300,PF3D7_1401100,PF3D7_1401200,PF3D7_1401400,PF3D7_1410400,PF3D7_1436300,PF3D7_1463900,PF3D7_1471100,PF3D7_1473200,PF3D7_1478600,						
		GO:0043656	host intracellular region	550	97	PF3D7_0102200,PF3D7_0102600,PF3D7_0104200,PF3D7_0108500,PF3D7_0112200,PF3D7_0113700,PF3D7_0202200,PF3D7_0202500,PF3D7_0207500,PF3D7_0207600,PF3D7_0207700,PF3D7_0220200,PF3D7_0221700,PF3D7_0223500,PF3D7_0301700,PF3D7_0301800,PF3D7_0401800,PF3D7_0401900,PF3D7_0402000,PF3D7_0402100,PF3D7_0404700,PF3D7_0424000,PF3D7_0424500,PF3D7_0424700,PF3D7_0426000,PF3D7_0500800,PF3D7_0501000,PF3D7_0501300,PF3D7_0501400,PF3D7_0507500,PF3D7_0520900,PF3D7_0532100,PF3D7_0532300,PF3D7_0532400,PF3D7_0532600,PF3D7_0601900,PF3D7_0617700,PF3D7_0701900,PF3D7_0702000,PF3D7_0702400,PF3D7_0702500,PF3D7_0707300,PF3D7_0711700,PF3D7_0713100,PF3D7_0731200,PF3D7_0731300,PF3D7_0731600,PF3D7_0732200,PF3D7_0800100,PF3D7_0830500,PF3D7_0905400,PF3D7_0922200,PF3D7_0929400,PF3D7_0935900,PF3D7_0936000,PF3D7_0936300,PF3D7_0936800,PF3D7_1001000,PF3D7_1001500,PF3D7_1001600,PF3D7_1002100,PF3D7_1014100,PF3D7_1016300,PF3D7_1035200,PF3D7_1035300,PF3D7_1039000,PF3D7_1102700,PF3D7_1102800,PF3D7_1115800,PF3D7_1116800,PF3D7_1148900,PF3D7_1149000,PF3D7_1149600,PF3D7_1200700,PF3D7_1201000,PF3D7_1201100,PF3D7_1228600,PF3D7_1252100,PF3D7_1252300,PF3D7_1252600,PF3D7_1255200,PF3D7_1301400,PF3D7_1301700,PF3D7_1302000,PF3D7_1334500,PF3D7_1334700,PF3D7_1353100,PF3D7_1370300,PF3D7_1401100,PF3D7_1401200,PF3D7_1401400	17.6	3.77	6.84	1.64E-35	4.93E-34	2.96E-33

						1400,PF3D7_1410400,PF3D7_1436300,PF3D7_1463900,PF3D7_1471100,PF3D7_1473200,PF3D7_1478600,						
		GO:0033655	host cell cytoplasm part	524	93	PF3D7_0102200,PF3D7_0102500,PF3D7_0104200,PF3D7_0185900,PF3D7_0112200,PF3D7_0113700,PF3D7_0202200,PF3D7_0202500,PF3D7_0207500,PF3D7_0207600,PF3D7_0207700,PF3D7_0220200,PF3D7_0221700,PF3D7_0223500,PF3D7_0301700,PF3D7_0301800,PF3D7_0401800,PF3D7_0401900,PF3D7_0402000,PF3D7_0402100,PF3D7_0404700,PF3D7_0424000,PF3D7_0424500,PF3D7_0424700,PF3D7_0426000,PF3D7_0500800,PF3D7_0501000,PF3D7_0501300,PF3D7_0501400,PF3D7_0507500,PF3D7_0520900,PF3D7_0532100,PF3D7_0532300,PF3D7_0532400,PF3D7_0532600,PF3D7_0601900,PF3D7_0617700,PF3D7_0701900,PF3D7_0702000,PF3D7_0702400,PF3D7_0702500,PF3D7_0707300,PF3D7_0711700,PF3D7_0713100,PF3D7_0731200,PF3D7_0731300,PF3D7_0731600,PF3D7_0732200,PF3D7_0800100,PF3D7_0830500,PF3D7_0905400,PF3D7_0922200,PF3D7_0935900,PF3D7_0936000,PF3D7_0936800,PF3D7_1001000,PF3D7_1001500,PF3D7_1001600,PF3D7_1002100,PF3D7_1014100,PF3D7_1016300,PF3D7_1035200,PF3D7_1035300,PF3D7_1039000,PF3D7_1102700,PF3D7_1102800,PF3D7_1115800,PF3D7_1116800,PF3D7_1148900,PF3D7_1149000,PF3D7_1149600,PF3D7_1200700,PF3D7_1201000,PF3D7_1228600,PF3D7_1252100,PF3D7_1252300,PF3D7_1252600,PF3D7_1255200,PF3D7_1301400,PF3D7_1301700,PF3D7_1302000,PF3D7_1334500,PF3D7_1334700,PF3D7_1353100,PF3D7_1370300,PF3D7_1401100,PF3D7_1401200,PF3D7_1401400,PF3D7_1410400,PF3D7_1436300,PF3D7_1463900,PF3D7_1471100,PF3D7_1473200,	17.7	3.79	6.73	4.99E-34	1.29E-32	9.03E-32
		GO:1903561	extracellular vesicle	91	36	PF3D7_0102200,PF3D7_0102500,PF3D7_0202500,PF3D7_0207600,PF3D7_0301700,PF3D7_0302500,PF3D7_0424600,PF3D7_0501000,PF3D7_0501300,PF3D7_0501500,PF3D7_0501600,PF3D7_0601900,PF3D7_0702400,PF3D7_0702500,PF3D7_0714000,PF3D7_0731500,PF3D7_0818900,PF3D7_0905400,PF3D7_0917900,PF3D7_0922200,PF3D7_0929400,PF3D7_0930300,PF3D7_0935900,PF3D7_1014100,PF3D7_1035300,PF3D7_1035700,PF3D7_1116800,PF3D7_1228600,PF3D7_1252100,PF3D7_1343000,PF3D7_1353100,PF3D7_1370300,PF3D7_1410400,PF3D7_1436300,PF3D7_1444800,PF3D7_1471100,	39.6	8.45	15.63	2.76E-25	6.23E-24	4.99E-23
		GO:0005576	extracellular region	334	57	PF3D7_0102200,PF3D7_0102500,PF3D7_0104200,PF3D7_0202500,PF3D7_0207400,PF3D7_0207500,PF3D7_0207600,PF3D7_0207700,PF3D7_0207800,PF3D7_0301700,PF3D7_0302500,PF3D7_0402000,PF3D7_0404700,PF3D7_0424600,PF3D7_0501000,PF3D7_0501300,PF3D7_0501400,PF3D7_0501500,PF3D7_0501600,PF3D7_0507500,PF3D7_0532100,PF3D7_0601900,PF3D7_061	17.1	3.64	5.25	4.83E-19	9.10E-18	8.75E-17

University of Ghana http://ugspace.ug.edu.gh

						7700,PF3D7_0702400,PF3D7_0702500,PF3D7_0707300,PF3D7_0714000,PF3D7_0731500,PF3D7_0732200,PF3D7_0818900,PF3D7_0902800,PF3D7_0905400,PF3D7_0917900,PF3D7_0922200,PF3D7_0929400,PF3D7_0930300,PF3D7_0935900,PF3D7_1001500,PF3D7_1014100,PF3D7_1035200,PF3D7_1035300,PF3D7_1035700,PF3D7_1102700,PF3D7_1102800,PF3D7_1116800,PF3D7_1201000,PF3D7_1221900,PF3D7_1228600,PF3D7_1252100,PF3D7_1343000,PF3D7_1353100,PF3D7_1370300,PF3D7_1401400,PF3D7_1410400,PF3D7_1436300,PF3D7_1444800,PF3D7_1471100,						
		GO: 0065010	extracellular membrane-bounded organelle	280	52	PF3D7_0102200,PF3D7_0102500,PF3D7_0104200,PF3D7_0202500,PF3D7_0207500,PF3D7_0207600,PF3D7_0207700,PF3D7_0301700,PF3D7_0302500,PF3D7_0402000,PF3D7_0404700,PF3D7_0424600,PF3D7_0501000,PF3D7_0501300,PF3D7_0501500,PF3D7_0501600,PF3D7_0507500,PF3D7_0532100,PF3D7_0601900,PF3D7_0617700,PF3D7_0702400,PF3D7_0702500,PF3D7_0707300,PF3D7_0714000,PF3D7_0731500,PF3D7_0732200,PF3D7_0818900,PF3D7_0905400,PF3D7_0917900,PF3D7_0922200,PF3D7_0929400,PF3D7_0930300,PF3D7_0935900,PF3D7_1001500,PF3D7_1014100,PF3D7_1035200,PF3D7_1035300,PF3D7_1035700,PF3D7_1102700,PF3D7_1102800,PF3D7_1116800,PF3D7_1201000,PF3D7_1228600,PF3D7_1252100,PF3D7_1343000,PF3D7_1353100,PF3D7_1370300,PF3D7_1401400,PF3D7_1410400,PF3D7_1436300,PF3D7_1444800,PF3D7_1471100,	18.6	3.97	5.72	5.03E-19	9.10E-18	9.10E-17
		GO: 0043230	extracellular organelle	282	52	PF3D7_0102200,PF3D7_0102500,PF3D7_0104200,PF3D7_0202500,PF3D7_0207500,PF3D7_0207600,PF3D7_0207700,PF3D7_0301700,PF3D7_0302500,PF3D7_0402000,PF3D7_0404700,PF3D7_0424600,PF3D7_0501000,PF3D7_0501300,PF3D7_0501500,PF3D7_0501600,PF3D7_0507500,PF3D7_0532100,PF3D7_0601900,PF3D7_0617700,PF3D7_0702400,PF3D7_0702500,PF3D7_0707300,PF3D7_0714000,PF3D7_0731500,PF3D7_0732200,PF3D7_0818900,PF3D7_0905400,PF3D7_0917900,PF3D7_0922200,PF3D7_0929400,PF3D7_0930300,PF3D7_0935900,PF3D7_1001500,PF3D7_1014100,PF3D7_1035200,PF3D7_1035300,PF3D7_1035700,PF3D7_1102700,PF3D7_1102800,PF3D7_1116800,PF3D7_1201000,PF3D7_1228600,PF3D7_1252100,PF3D7_1343000,PF3D7_1353100,PF3D7_1370300,PF3D7_1401400,PF3D7_1410400,PF3D7_1436300,PF3D7_1444800,PF3D7_1471100,	18.4	3.94	5.67	7.01E-19	1.15E-17	1.27E-16
		GO: 0020036	Maurer's cleft	370	59	PF3D7_0102600,PF3D7_0108500,PF3D7_0112200,PF3D7_0113700,PF3D7_0202200,PF3D7_0220200,PF3D7_0221700,PF3D7_0301700,PF3D7_0301800,PF3D7_0401800,PF3D7_0401900,PF3D7_0402000,PF3D7_0402100,PF3D7_0424000,PF3D7_0424500,PF3D7_0424700,PF3D7_0500800,	15.9	3.4	4.86	3.13E-18	4.72E-17	5.67E-16

University of Ghana http://ugspace.ug.edu.gh

University of Ghana http://ugspace.ug.edu.gh

						PF3D7_0501000,PF3D7_0501300,PF3D7_0501400,PF3D7_0520900,PF3D7_0532300,PF3D7_0532400,PF3D7_0532600,PF3D7_0601900,PF3D7_0617700,PF3D7_0701900,PF3D7_0702000,PF3D7_0702400,PF3D7_0702500,PF3D7_0713100,PF3D7_0731200,PF3D7_0731300,PF3D7_0732200,PF3D7_0830500,PF3D7_0922200,PF3D7_0935900,PF3D7_0936000,PF3D7_0936800,PF3D7_1001000,PF3D7_1002100,PF3D7_1039000,PF3D7_1115800,PF3D7_1116800,PF3D7_1148900,PF3D7_1149000,PF3D7_1149600,PF3D7_1200700,PF3D7_1252300,PF3D7_1252600,PF3D7_1301400,PF3D7_1301700,PF3D7_1302000,PF3D7_1334500,PF3D7_1353100,PF3D7_1370300,PF3D7_1401100,PF3D7_1401200,PF3D7_1473200,						
		GO:0044217	other organism part	116	33	PF3D7_0113200,PF3D7_0114800,PF3D7_0220200,PF3D7_0220300,PF3D7_0220500,PF3D7_0220600,PF3D7_0221700,PF3D7_0301500,PF3D7_0301700,PF3D7_0301800,PF3D7_0402100,PF3D7_0402400,PF3D7_0702000,PF3D7_0730900,PF3D7_0731200,PF3D7_0731700,PF3D7_0800800,PF3D7_0831400,PF3D7_0901700,PF3D7_0901800,PF3D7_1001700,PF3D7_1001800,PF3D7_1002000,PF3D7_1016600,PF3D7_1149400,PF3D7_1149600,PF3D7_1301500,PF3D7_1371800,PF3D7_1372000,PF3D7_1401000,PF3D7_1401100,PF3D7_1401200,PF3D7_1477500,	28.4	6.07	9.29	4.63E-18	6.45E-17	8.38E-16
		GO:0020007	apical complex	104	27	PF3D7_0102500,PF3D7_0212600,PF3D7_0220800,PF3D7_0301200,PF3D7_0302200,PF3D7_0302500,PF3D7_0423400,PF3D7_0501500,PF3D7_0501600,PF3D7_0507500,PF3D7_0511600,PF3D7_0707300,PF3D7_0722200,PF3D7_0731500,PF3D7_0905400,PF3D7_0929400,PF3D7_1116000,PF3D7_1116800,PF3D7_1133400,PF3D7_1136500,PF3D7_1252100,PF3D7_1301600,PF3D7_1332200,PF3D7_1335300,PF3D7_1410400,PF3D7_1436300,PF3D7_1463900,	26	5.54	7.96	7.60E-14	9.83E-13	1.38E-11
		GO:0031982	vesicle	288	44	PF3D7_0102200,PF3D7_0102500,PF3D7_0202500,PF3D7_0207600,PF3D7_0220000,PF3D7_0301700,PF3D7_0302500,PF3D7_0424600,PF3D7_0501000,PF3D7_0501300,PF3D7_0501500,PF3D7_0501600,PF3D7_0507500,PF3D7_0601900,PF3D7_0618000,PF3D7_0702200,PF3D7_0702400,PF3D7_0702500,PF3D7_0714000,PF3D7_0731500,PF3D7_0818900,PF3D7_0905400,PF3D7_0917900,PF3D7_0922200,PF3D7_0929400,PF3D7_0930300,PF3D7_0935900,PF3D7_1014100,PF3D7_1035300,PF3D7_1035700,PF3D7_1116000,PF3D7_1116800,PF3D7_1228600,PF3D7_1252100,PF3D7_1301400,PF3D7_1334700,PF3D7_1342600,PF3D7_1343000,PF3D7_1353100,PF3D7_1370300,PF3D7_1410400,PF3D7_1436300,PF3D7_1444800,PF3D7_1471100,	15.3	3.26	4.31	6.70E-13	8.08E-12	1.21E-10
		GO:0045177	apical part of cell	147	30	PF3D7_0102500,PF3D7_0212600,PF3D7_0220800,PF3D7_0301200,PF3D7_0302200,PF3D7_0302500,PF3D7_0404700,PF3D7_0423400,PF3D7_0501500,PF3D7_0501600,PF3D7_0507500,PF3D7_0511600,PF3D7_0707300,PF3D7_0722200,PF3D7_0731500,PF3D7_0905400,PF3D7_0929400,	20.4	4.36	5.86	2.71E-12	3.06E-11	4.90E-10

University of Ghana http://ugspace.ug.edu.gh

						PF3D7_1035900,PF3D7_1116000,PF3D7_1116800,PF3D7_1133400,PF3D7_1136500,PF3D7_1243400,PF3D7_1252100,PF3D7_1301600,PF3D7_1332200,PF3D7_1335300,PF3D7_1410400,PF3D7_1436300,PF3D7_1463900,						
		GO:0020008	rhoptry	52	18	PF3D7_0212600,PF3D7_0220800,PF3D7_0301200,PF3D7_0302200,PF3D7_0302500,PF3D7_0423400,PF3D7_0501500,PF3D7_0501600,PF3D7_0511600,PF3D7_0707300,PF3D7_0722200,PF3D7_0905400,PF3D7_0929400,PF3D7_1116000,PF3D7_1252100,PF3D7_1335300,PF3D7_1410400,PF3D7_1463900,	34.6	7.39	11.61	6.25E-12	6.66E-11	1.13E-09
		GO:0044538	host cell periphery	26	12	PF3D7_0113000,PF3D7_0401800,PF3D7_0402000,PF3D7_0424500,PF3D7_0424600,PF3D7_0424700,PF3D7_0532400,PF3D7_0701900,PF3D7_1136500,PF3D7_1149300,PF3D7_1201000,PF3D7_1401200,	46.2	9.85	18.36	4.52E-10	4.54E-09	8.18E-08
		GO:0020005	symbiont-containing vacuole membrane	44	13	PF3D7_0202500,PF3D7_0207500,PF3D7_0402000,PF3D7_0404700,PF3D7_0501300,PF3D7_0532100,PF3D7_1001500,PF3D7_1102700,PF3D7_1102800,PF3D7_1116800,PF3D7_1401400,PF3D7_1436300,PF3D7_1471100,	29.5	6.31	8.99	5.29E-08	5.04E-07	9.58E-06
		GO:0000323	lytic vacuole	111	20	PF3D7_0102200,PF3D7_0207400,PF3D7_0207500,PF3D7_0207600,PF3D7_0207700,PF3D7_0207800,PF3D7_0404700,PF3D7_0501500,PF3D7_0501600,PF3D7_0618000,PF3D7_0818900,PF3D7_0902800,PF3D7_0917900,PF3D7_0922200,PF3D7_0930300,PF3D7_1116000,PF3D7_1301400,PF3D7_1334700,PF3D7_1343000,PF3D7_1410400,	18	3.85	4.81	1.35E-07	1.16E-06	2.44E-05
		GO:0005764	lysosome	111	20	PF3D7_0102200,PF3D7_0207400,PF3D7_0207500,PF3D7_0207600,PF3D7_0207700,PF3D7_0207800,PF3D7_0404700,PF3D7_0501500,PF3D7_0501600,PF3D7_0618000,PF3D7_0818900,PF3D7_0902800,PF3D7_0917900,PF3D7_0922200,PF3D7_0930300,PF3D7_1116000,PF3D7_1301400,PF3D7_1334700,PF3D7_1343000,PF3D7_1410400,	18	3.85	4.81	1.35E-07	1.16E-06	2.44E-05
		GO:0020003	symbiont-containing vacuole	205	28	PF3D7_0102200,PF3D7_0104200,PF3D7_0202500,PF3D7_0207500,PF3D7_0207600,PF3D7_0207700,PF3D7_0402000,PF3D7_0404700,PF3D7_0501300,PF3D7_0507500,PF3D7_0532100,PF3D7_0617700,PF3D7_0707300,PF3D7_0732200,PF3D7_1001500,PF3D7_1014100,PF3D7_1035200,PF3D7_1035300,PF3D7_1102700,PF3D7_1102800,PF3D7_1116800,PF3D7_1201000,PF3D7_1228600,PF3D7_1252100,PF3D7_1401400,PF3D7_1410400,PF3D7_1436300,PF3D7_1471100,	13.7	2.92	3.53	1.97E-07	1.62E-06	3.57E-05
		GO:0005773	vacuole	126	21	PF3D7_0102200,PF3D7_0207400,PF3D7_0207500,PF3D7_0207600,PF3D7_0207700,PF3D7_0207800,PF3D7_0404700,PF3D7_0501500,PF3D7_0501600,PF3D7_0618000,PF3D7_0818900,PF3D7_0902800,PF3D7_0917900,PF3D7_0922200,PF3D7_0930300,PF3D7_1035200,PF3D7_1116000,PF3D7_1301400,PF3D7_1334700,PF3D7_1343000,PF3D7_1410400,	16.7	3.56	4.38	2.59E-07	2.04E-06	4.69E-05

University of Ghana http://ugspace.ug.edu.gh

		GO:0044164	host cell cytosol	30	10	PF3D7_0104200,PF3D7_0113700,PF3D7_0404700,PF3D7_0532400,PF3D7_0532600,PF3D7_0936800,PF3D7_1001600,PF3D7_1002100,PF3D7_1334700,PF3D7_1463900,	33.3	7.12	10.6	5.49E-07	4.14E-06	9.94E-05
		GO:0044228	host cell surface	31	10	PF3D7_0102200,PF3D7_0113000,PF3D7_0220000,PF3D7_0401800,PF3D7_0424600,PF3D7_0532300,PF3D7_0532400,PF3D7_1001000,PF3D7_1201000,PF3D7_1301700,	32.3	6.89	10.09	7.77E-07	5.63E-06	0.000140724
		GO:0020026	merozoite dense granule	10	6	PF3D7_0102200,PF3D7_0220000,PF3D7_0507500,PF3D7_1116800,PF3D7_1436300,PF3D7_1471100,	60	12.81	31.32	1.77E-06	1.24E-05	0.000321111
		GO:0005615	extracellular space	22	8	PF3D7_0207400,PF3D7_0207500,PF3D7_0207600,PF3D7_0207700,PF3D7_0207800,PF3D7_0404700,PF3D7_0501400,PF3D7_0902800,	36.4	7.76	12.02	3.71E-06	2.48E-05	0.000670875
		GO:0020030	infected host cell surface knob	61	12	PF3D7_0223500,PF3D7_0426000,PF3D7_0500800,PF3D7_0532400,PF3D7_0711700,PF3D7_0731600,PF3D7_0800100,PF3D7_0905400,PF3D7_1001000,PF3D7_1016300,PF3D7_1201000,PF3D7_1255200,	19.7	4.2	5.21	1.89E-05	0.000122005	0.003416128
		GO:1990225	rhoptry neck	14	6	PF3D7_0423400,PF3D7_0511600,PF3D7_0722200,PF3D7_1116000,PF3D7_1335300,PF3D7_1463900,	42.9	9.15	15.65	2.16E-05	0.000135053	0.003916545
		GO:0009986	cell surface	159	20	PF3D7_0212600,PF3D7_0818900,PF3D7_0905400,PF3D7_0917900,PF3D7_0922200,PF3D7_1002200,PF3D7_1014100,PF3D7_1035300,PF3D7_1035400,PF3D7_1035500,PF3D7_1035700,PF3D7_1035900,PF3D7_1036000,PF3D7_1115800,PF3D7_1140400,PF3D7_1228600,PF3D7_1252100,PF3D7_1342600,PF3D7_1437300,PF3D7_1444800,	12.6	2.69	3.11	4.21E-05	0.000253769	0.007613071
		GO:0045335	phagocytic vesicle	97	13	PF3D7_0102200,PF3D7_0501500,PF3D7_0501600,PF3D7_0618000,PF3D7_0818900,PF3D7_0917900,PF3D7_0922200,PF3D7_0930300,PF3D7_1116000,PF3D7_1301400,PF3D7_1334700,PF3D7_1343000,PF3D7_1410400,	13.4	2.86	3.28	0.00051793	0.002757198	0.093744717
		GO:0032010	phagolysosome	97	13	PF3D7_0102200,PF3D7_0501500,PF3D7_0501600,PF3D7_0618000,PF3D7_0818900,PF3D7_0917900,PF3D7_0922200,PF3D7_0930300,PF3D7_1116000,PF3D7_1301400,PF3D7_1334700,PF3D7_1343000,PF3D7_1410400,	13.4	2.86	3.28	0.00051793	0.002757198	0.093744717

		GO: 0005767	secondary lysosome	97	13	PF3D7_0102200,PF3D7_0501500,PF3D7_0501600,PF3D7_0618000,PF3D7_0818900,PF3D7_0917900,PF3D7_0922200,PF3D7_0930300,PF3D7_1116000,PF3D7_1301400,PF3D7_1334700,PF3D7_1343000,PF3D7_1410400,	13.4	2.86	3.28	0.00051793	0.002757198	0.093744717
		GO: 0020020	food vacuole	97	13	PF3D7_0102200,PF3D7_0501500,PF3D7_0501600,PF3D7_0618000,PF3D7_0818900,PF3D7_0917900,PF3D7_0922200,PF3D7_0930300,PF3D7_1116000,PF3D7_1301400,PF3D7_1334700,PF3D7_1343000,PF3D7_1410400,	13.4	2.86	3.28	0.00051793	0.002757198	0.093744717
		GO: 0030139	endocytic vesicle	102	13	PF3D7_0102200,PF3D7_0501500,PF3D7_0501600,PF3D7_0618000,PF3D7_0818900,PF3D7_0917900,PF3D7_0922200,PF3D7_0930300,PF3D7_1116000,PF3D7_1301400,PF3D7_1334700,PF3D7_1343000,PF3D7_1410400,	12.7	2.72	3.09	0.00084395	0.004364441	0.152755452
		GO: 0031224	intrinsic component of membrane	1314	83	PF3D7_0102500,PF3D7_0102600,PF3D7_0104200,PF3D7_0107500,PF3D7_0112200,PF3D7_0113200,PF3D7_0113700,PF3D7_0114800,PF3D7_0202200,PF3D7_0206800,PF3D7_0223500,PF3D7_0301500,PF3D7_0301700,PF3D7_0301800,PF3D7_0401800,PF3D7_0402000,PF3D7_0402100,PF3D7_0402400,PF3D7_0424500,PF3D7_0424700,PF3D7_0426000,PF3D7_0501000,PF3D7_0501300,PF3D7_0503100,PF3D7_0508300,PF3D7_0511600,PF3D7_0532100,PF3D7_0532400,PF3D7_0601900,PF3D7_0617700,PF3D7_0618000,PF3D7_0620400,PF3D7_0701900,PF3D7_0702400,PF3D7_0702500,PF3D7_0707300,PF3D7_0711700,PF3D7_0713100,PF3D7_0730900,PF3D7_0731200,PF3D7_0731300,PF3D7_0731500,PF3D7_0732200,PF3D7_0800100,PF3D7_0800800,PF3D7_0830500,PF3D7_0901700,PF3D7_0901800,PF3D7_0902100,PF3D7_0930300,PF3D7_0935900,PF3D7_0936000,PF3D7_0936300,PF3D7_0936800,PF3D7_1002200,PF3D7_1010300,PF3D7_1016300,PF3D7_1035700,PF3D7_1116600,PF3D7_1133400,PF3D7_1149000,PF3D7_1252100,PF3D7_1255200,PF3D7_1300100,PF3D7_1301500,PF3D7_1301600,PF3D7_1301700,PF3D7_1302000,PF3D7_1307100,PF3D7_1350500,PF3D7_1353100,PF3D7_1370300,PF3D7_1371700,PF3D7_1371800,PF3D7_1372000,PF3D7_1372600,PF3D7_1401100,PF3D7_1408300,PF3D7_1438100,PF3D7_1458900,PF3D7_1463900,PF3D7_1477500,PF3D7_1478600,	6.3	1.35	1.59	0.00090258	0.004537959	0.163366527
		GO: 0097619	PTEX complex	5	3	PF3D7_1116800,PF3D7_1436300,PF3D7_1471100,	60	12.81	30.92	0.00094549	0.004580036	0.171133594
		GO: 0016021	integral component of membrane	1297	82	PF3D7_0102500,PF3D7_0102600,PF3D7_0104200,PF3D7_0107500,PF3D7_0112200,PF3D7_0113200,PF3D7_0113700,PF3D7_0114800,PF3D7_0202200,PF3D7_0206800,PF3D7_0223500,PF3D7_0301500,PF3D7_0301700,PF3D7_0301800,PF3D7_0401800,PF3D7_0402000,PF3D7_0402100,	6.3	1.35	1.58	0.00096155	0.004580036	0.174041365

University of Ghana http://ugspace.ug.edu.gh

University of Ghana http://ugspace.ug.edu.gh

						PF3D7_0402400,PF3D7_0424500,PF3D7_0424700,PF3D7_0426000,PF3D7_0501000,PF3D7_0501300,PF3D7_0503100,PF3D7_0508300,PF3D7_0511600,PF3D7_0532100,PF3D7_0532400,PF3D7_0601900,PF3D7_0617700,PF3D7_0618000,PF3D7_0620400,PF3D7_0701900,PF3D7_0702400,PF3D7_0702500,PF3D7_0711700,PF3D7_0713100,PF3D7_0730900,PF3D7_0731200,PF3D7_0731300,PF3D7_0731500,PF3D7_0732200,PF3D7_0800100,PF3D7_0800800,PF3D7_0830500,PF3D7_0901700,PF3D7_0901800,PF3D7_0902100,PF3D7_0930300,PF3D7_0935900,PF3D7_0936000,PF3D7_0936300,PF3D7_0936800,PF3D7_1002200,PF3D7_1010300,PF3D7_1016300,PF3D7_1035700,PF3D7_1116600,PF3D7_1133400,PF3D7_1149000,PF3D7_1252100,PF3D7_1255200,PF3D7_1300100,PF3D7_1301500,PF3D7_1301600,PF3D7_1301700,PF3D7_1302000,PF3D7_1307100,PF3D7_1350500,PF3D7_1353100,PF3D7_1370300,PF3D7_1371700,PF3D7_1371800,PF3D7_1372000,PF3D7_1372600,PF3D7_1401100,PF3D7_1408300,PF3D7_1438100,PF3D7_1458900,PF3D7_1463900,PF3D7_1477500,PF3D7_1478600,						
		GO:0020004	symbiont-containing vacuolar space	6	3	PF3D7_0207600,PF3D7_0501300,PF3D7_0507500,	50	10.68	20.61	0.00182568	0.008473036	0.330448391
		GO:0000786	nucleosome	9	3	PF3D7_0320900,PF3D7_0617800,PF3D7_0714000,	33.3	7.12	10.3	0.00690405	0.031240808	1
		GO:0033644	host cell membrane	242	20	PF3D7_0102200,PF3D7_0223500,PF3D7_0302200,PF3D7_0302500,PF3D7_0426000,PF3D7_0500800,PF3D7_0532400,PF3D7_0617700,PF3D7_0702400,PF3D7_0711700,PF3D7_0732200,PF3D7_0800100,PF3D7_0929400,PF3D7_0935900,PF3D7_0936800,PF3D7_1000600,PF3D7_1149000,PF3D7_1222700,PF3D7_1255200,PF3D7_1400500,	8.3	1.76	1.91	0.00884535	0.038421375	1
		GO:0031410	cytoplasmic vesicle	210	18	PF3D7_0102200,PF3D7_0220000,PF3D7_0501500,PF3D7_0501600,PF3D7_0507500,PF3D7_0618000,PF3D7_0818900,PF3D7_0917900,PF3D7_0922200,PF3D7_0930300,PF3D7_1116000,PF3D7_1116800,PF3D7_1301400,PF3D7_1334700,PF3D7_1343000,PF3D7_1410400,PF3D7_1436300,PF3D7_1471100,	8.6	1.83	1.99	0.00891546	0.038421375	1
		GO:0097708	intracellular vesicle	211	18	PF3D7_0102200,PF3D7_0220000,PF3D7_0501500,PF3D7_0501600,PF3D7_0507500,PF3D7_0618000,PF3D7_0818900,PF3D7_0917900,PF3D7_0922200,PF3D7_0930300,PF3D7_1116000,PF3D7_1116800,PF3D7_1301400,PF3D7_1334700,PF3D7_1343000,PF3D7_1410400,PF3D7_1436300,PF3D7_1471100,	8.5	1.82	1.97	0.00934733	0.039345736	1

		GO:0020009	microneme	40	6	PF3D7_0102500,PF3D7_0212600,PF3D7_0731500,PF3D7_1133400,PF3D7_1136500,PF3D7_1301600,	15	3.2	3.66	0.00995674	0.040958414	1
		GO:0005634	nucleus	1519	84	PF3D7_0102600,PF3D7_0108500,PF3D7_0202500,PF3D7_0206800,PF3D7_0207500,PF3D7_0207600,PF3D7_0301200,PF3D7_0302200,PF3D7_0302500,PF3D7_0320500,PF3D7_0320900,PF3D7_0401800,PF3D7_0402000,PF3D7_0424500,PF3D7_0424600,PF3D7_0424700,PF3D7_0500800,PF3D7_0500900,PF3D7_0501000,PF3D7_0501300,PF3D7_0501500,PF3D7_0501600,PF3D7_0527200,PF3D7_0532300,PF3D7_0532400,PF3D7_0601900,PF3D7_0604100,PF3D7_0617800,PF3D7_0702400,PF3D7_0702500,PF3D7_0703700,PF3D7_0707300,PF3D7_0714000,PF3D7_0730900,PF3D7_0731300,PF3D7_0731600,PF3D7_0818900,PF3D7_0821400,PF3D7_0822900,PF3D7_0902100,PF3D7_0905400,PF3D7_0907700,PF3D7_0917900,PF3D7_0918700,PF3D7_0922200,PF3D7_0929400,PF3D7_0930300,PF3D7_0934800,PF3D7_0936300,PF3D7_0936800,PF3D7_1003500,PF3D7_1016300,PF3D7_1039000,PF3D7_1115800,PF3D7_1116000,PF3D7_1116800,PF3D7_1123900,PF3D7_1136500,PF3D7_1140200,PF3D7_1140400,PF3D7_1149000,PF3D7_1149300,PF3D7_1201000,PF3D7_1202900,PF3D7_1222600,PF3D7_1228600,PF3D7_1251200,PF3D7_1252100,PF3D7_1301700,PF3D7_1332200,PF3D7_1335100,PF3D7_1342600,PF3D7_1353100,PF3D7_1361900,PF3D7_1371700,PF3D7_1402800,PF3D7_1410400,PF3D7_1412800,PF3D7_1423300,PF3D7_1436300,PF3D7_1438100,PF3D7_1444800,PF3D7_1471100,PF3D7_1473200,	5.5	1.18	1.3	0.03655358	0.147026618	1
		GO:0044815	DNA packaging complex	17	3	PF3D7_0320900,PF3D7_0617800,PF3D7_0714000,	17.6	3.77	4.41	0.04240711	0.166862757	1
		GO:0031355	integral component of plastid outer membrane	1	1	PF3D7_0508300,	100	21.35	inf	0.04683648	0.169548069	1
		GO:0009527	plastid outer membrane	1	1	PF3D7_0508300,	100	21.35	inf	0.04683648	0.169548069	1
		GO:0008537	proteasome activator complex	1	1	PF3D7_0907700,	100	21.35	inf	0.04683648	0.169548069	1

University of Ghana http://ugspace.ug.edu.gh

		GO: 0031354	intrinsic component of plastid outer membrane	1	1	PF3D7_0508300,	100	21.35	inf	0.04683648	0.169548069	1
		GO: 0031225	anchored component of membrane	30	4	PF3D7_0206800,PF3D7_0620400,PF3D7_0707300,PF3D7_0930300,	13.3	2.85	3.17	0.04939321	0.175297456	1

University of Ghana http://ugspace.ug.edu.gh

University of Ghana http://ugspace.ug.edu.gh

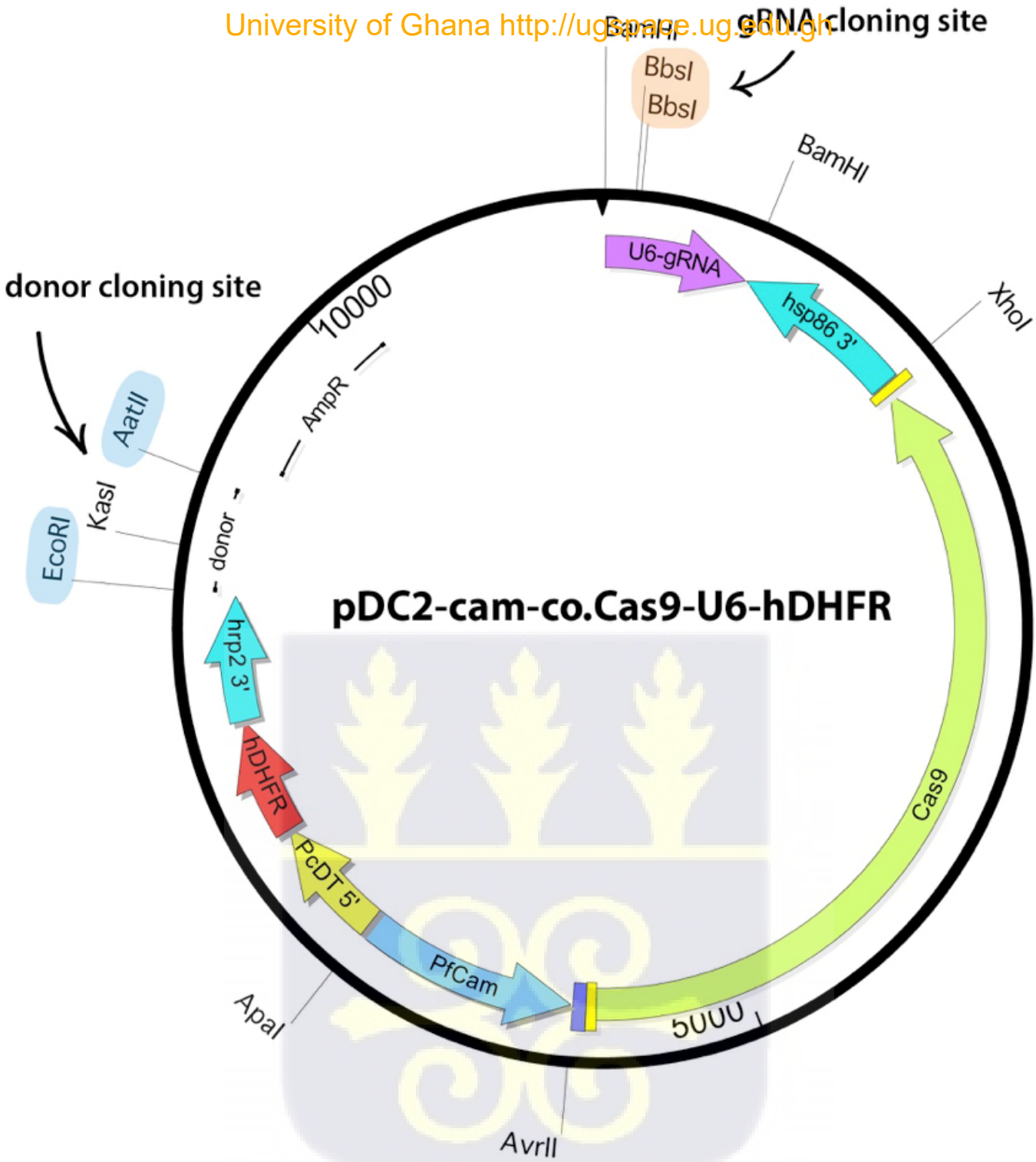

Supplementary Figure 5.1 Map of the plasmid vector pDC2-cam-co.Cas9-U6-hDHFR. It was approximately 10, 000 base pairs in size and contained a Cas9 codon-optimised sequence under *Pfcam* promoter with NLS to localise it to the *P. falciparum* nucleus. The U6 cassette has *BbsI* restriction site for cloning in the gRNA. The AatII and the EcoRI restriction sites serve as the site for the donor DNA insertion. The ampicillin resistance cassette was for selection after the *E. coli* transformation and the *hDHFR* gene was for selection after the transfection. *Pfcam* - ; NLS - nuclear localisation sequences; hDHFR - human dihydrofolate reductase. This was done by Oheneba Charles Kofi Hagan during his PhD work.

University of Ghana http://ugspace.ug.edu.gh

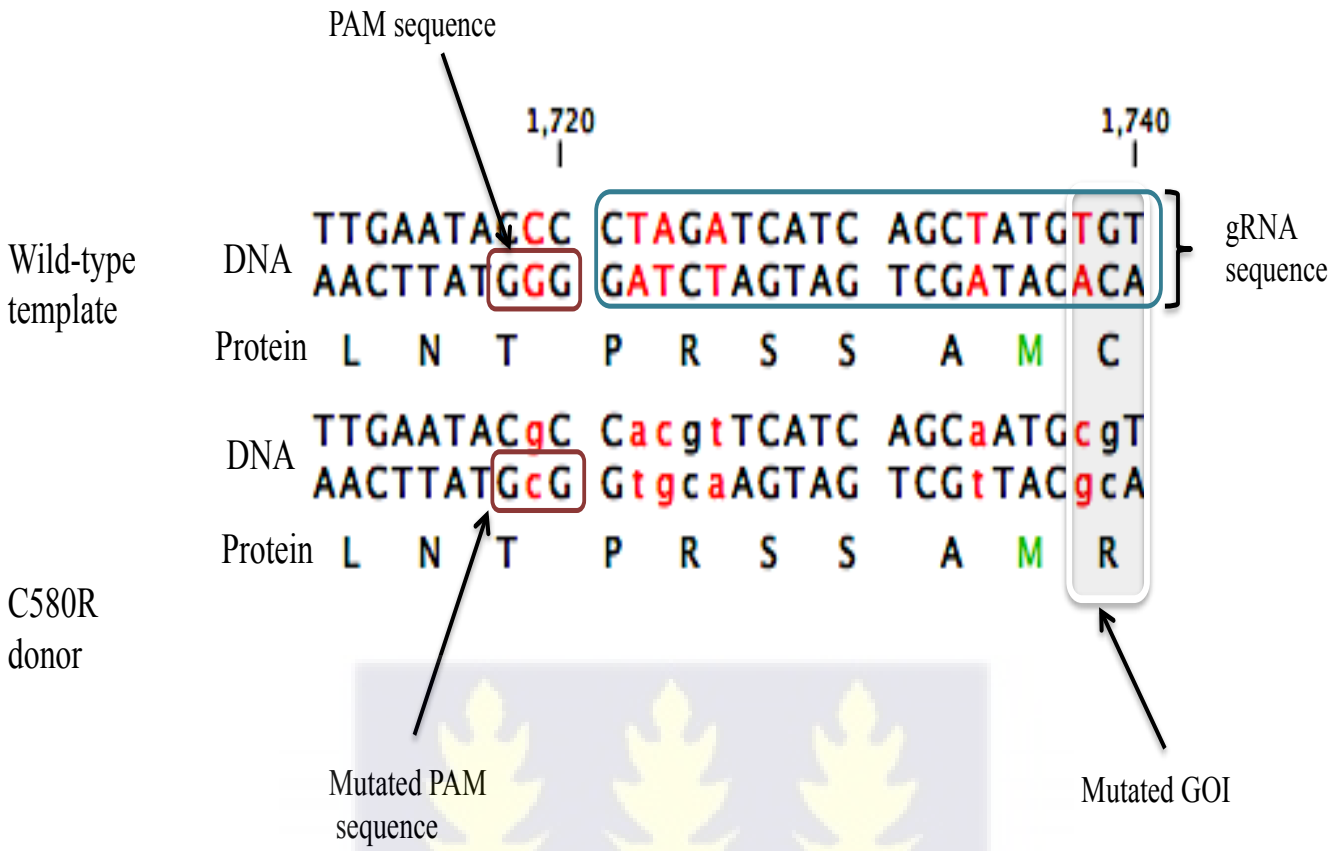

Supplementary Figure 5.2 Design of donor DNA for *PfK13* genome editing. Alignment of the designed C580R donor DNA and the wild-type template (3D7), as performed with CLC Workbench, and showing the wild-type NGG PAM (GGG) sequence and the mutated PAM sequence (GCG), the gRNA sequence and the mutated GOI (gene of interest). Additional mutations were made in the donor DNA within the gRNA sequence to reduce the chance of re-cleavages. This was done by Oheneba Charles Kofi Hagan during his PhD work.

University of Ghana http://ugspace.ug.edu.gh

C580R

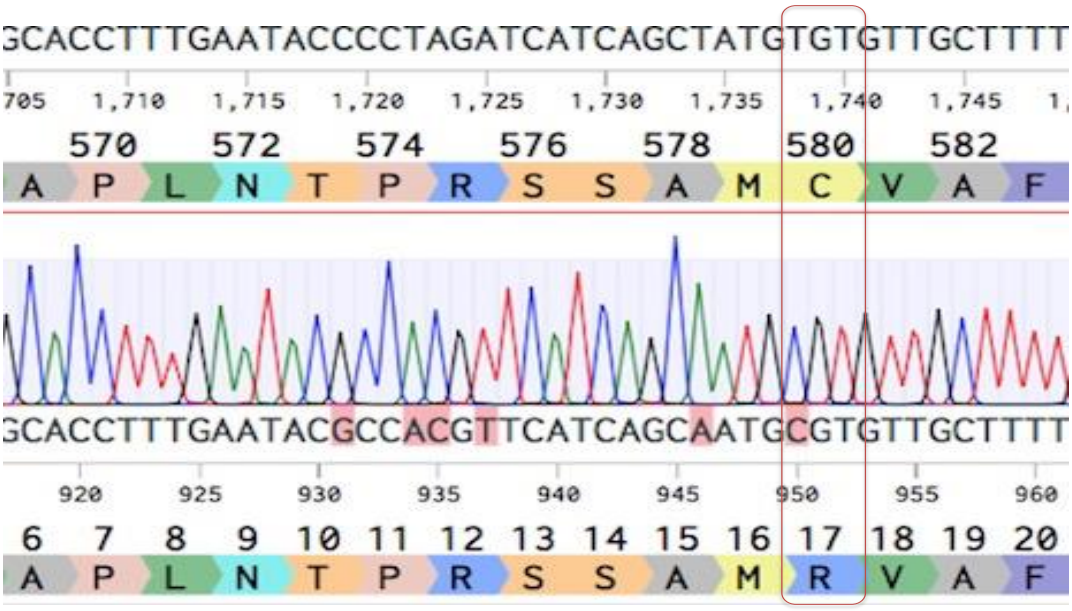

R539T

Supplementary Figure 5.3 Chromatographs showing analyses of genotyped transfectants. Genotyped sequences were aligned to the 3D7 *PfK13* template using (https://www.benchling.com). Mutations seen are : AGA (R539R) to ACA (R539T); and (C580C) to CGT (C580R).

This was done by Oheneba Charles Kofi Hagan during his PhD work.

University of Ghana http://ugspace.ug.edu.gh

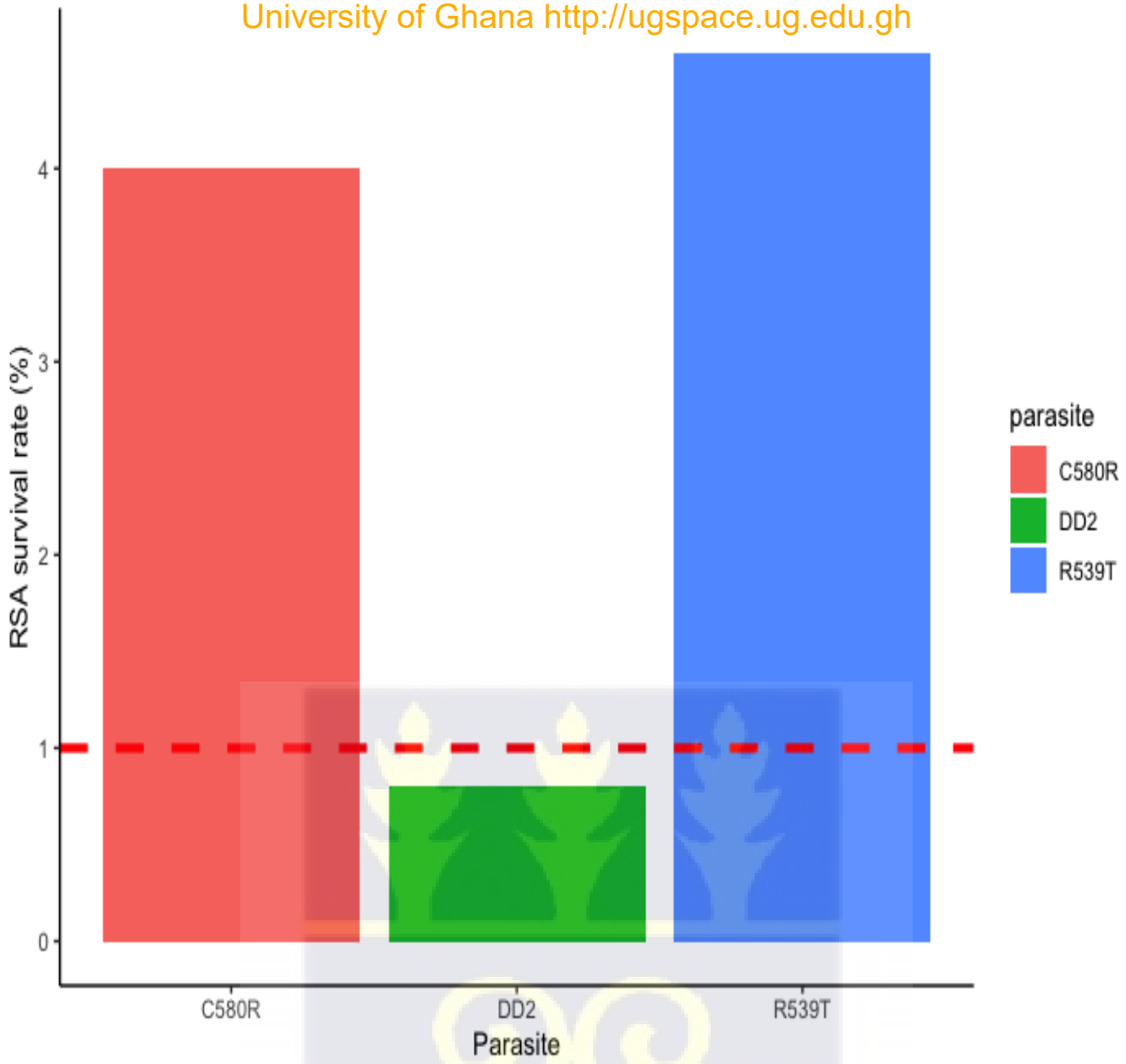

Supplementary Figure 5.4 ***In vitro*** **RSA_{0-3} survival rates (%) for the ART susceptible WT** ***Plasmodium falciparum*** **strain (DD2) and two** ***P. falciparum PfK13*** **ARTr variants (C580R and R539T) used in this study. C580R and R539T are ARTr parasites generated by CRISPR/Cas9 genetic engineering of a wild type DD2 ART susceptible parasite line at the** ***PfK13*** **gene. Each bar represents the mean of triplicate experiments. Growth rates for all parasite lines were at least 1.5% in the non-exposed controls. Mutant** ***PfK13*** **parasites have significantly higher survival rates compared to wild type DD2 parasite line (DD2 versus C580R : p-value, Kruskal-Wallis test = 0.04; DD2 versus R539T, p-value Kruskal-Wallis test = 0.04). The red dashed line indicates the 1% survival rate above which a parasite line is characterized as ARTr. RSA_{0-3} - 0-3 hour ring stage survival assay; ART – artemisinin;** ***PfK13 – Plasmodium falciparum*** **kelch 13 gene**

University of Ghana http://ugspace.ug.edu.gh

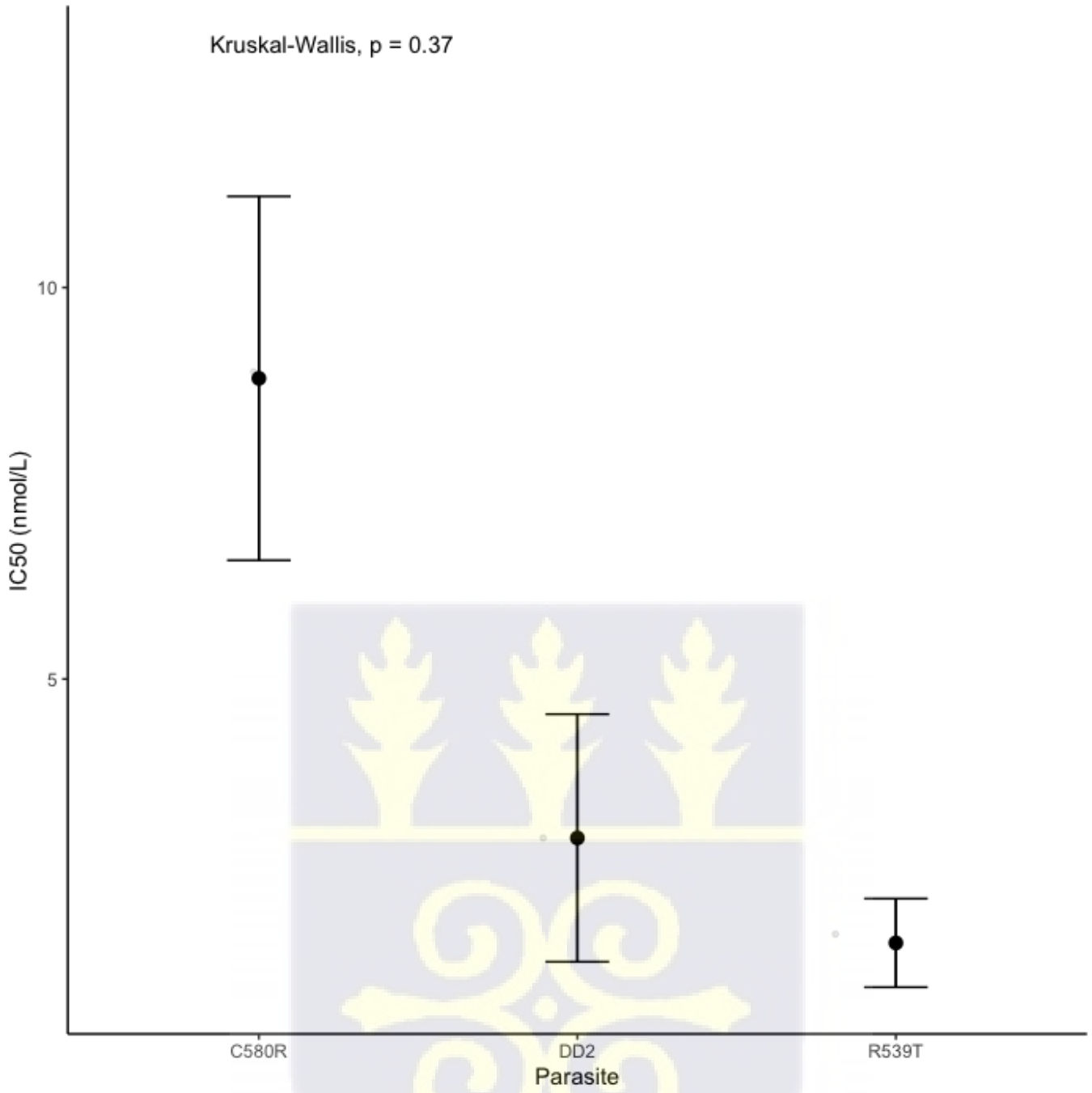

Supplementary Figure 5.5 IC50 values for DHA for the ART susceptible WT *Plasmodium falciparum* strain (DD2) and two P. falciparum *PfK13* ARTr variants (C580R and R539T) used in this study. The data point displays the median IC50 value + SD (C580R: 8.84+2.32; R539T:1.63+0.57; DD2: 2.97+1.58). P-values were determined by Kruskal-Wallis test. Assay was done in triplicates for each parasite line. WT – wild type; IC50 - 50% inhibitory concentration; ART – artemisinin; *PfK13* – *Plasmodium falciparum* kelch 13 gene; SD – standard deviation

University of Ghana http://ugspace.ug.edu.gh

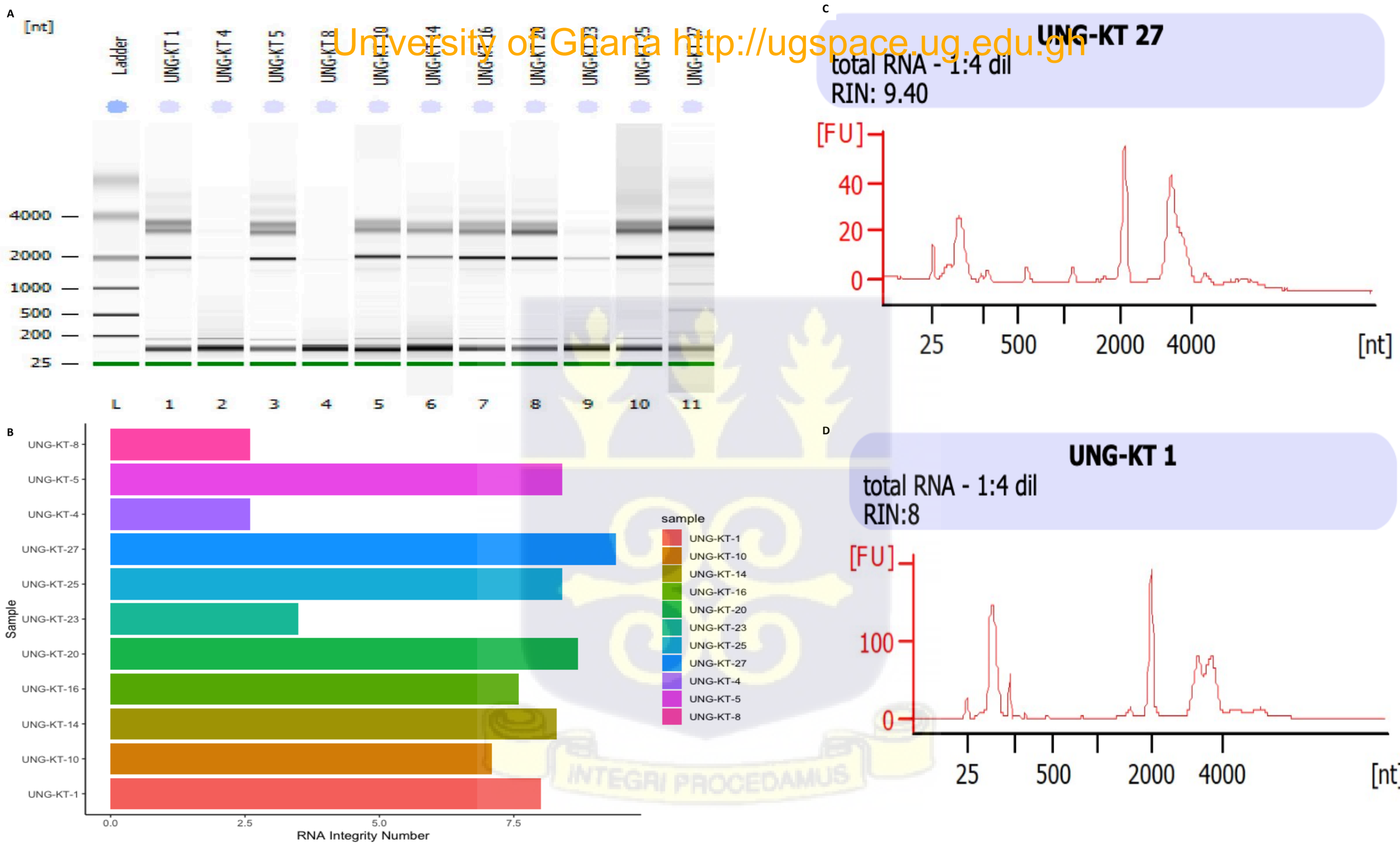

Supplementary Figure 5.6 Quality of extracted RNA integrity from the 27 samples used in this study. RNA extraction was done using TRIzol method. A) Agarose electrophoretic gel to visualize 18s and 28s ribosomal RNA bands indicative of good RNA quality. B) RIN for 11 of the 27 samples analyzed. C) and D) Electropherograms for samples 27 and 1 showing good 18s and 28s peaks indicative of good RNA quality. RNA – ribonucleic acid; RIN – RNA integrity number

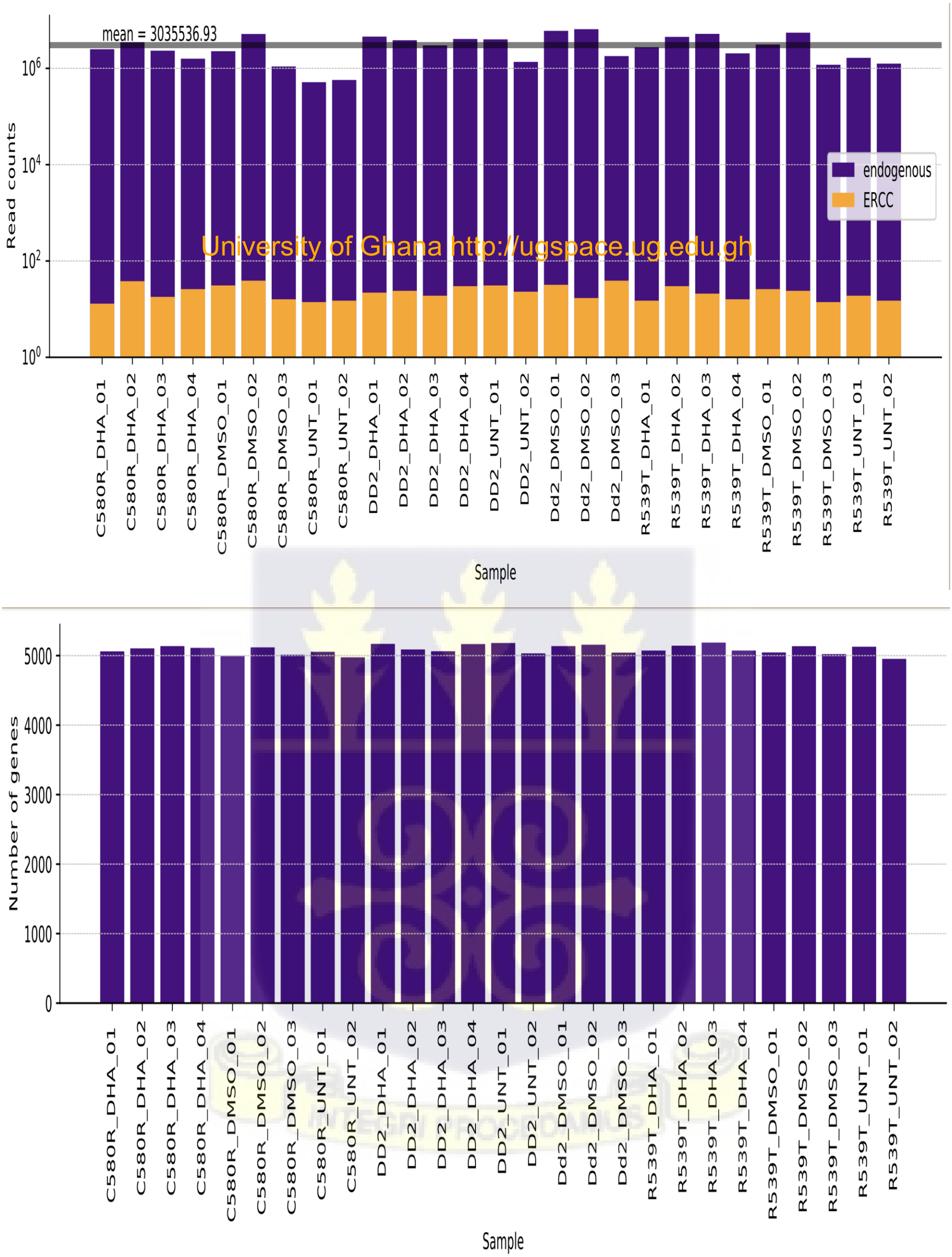

University of Ghana http://ugspace.ug.edu.gh

Supplementary Figure 5.7 Quality of reads mapped to reference genome for all samples. Mapping quality metrics for each sample was obtained and summarised using customised R scripts. A) The mean overall alignment reads alignment to the reference *P. falciparum* transcriptome was 3035536.93 External RNA Controls Consortium (ERCC) spike-in control levels were similar across all samples. B) For each sample the number of genes, mapped to by reads, was at least 5000.

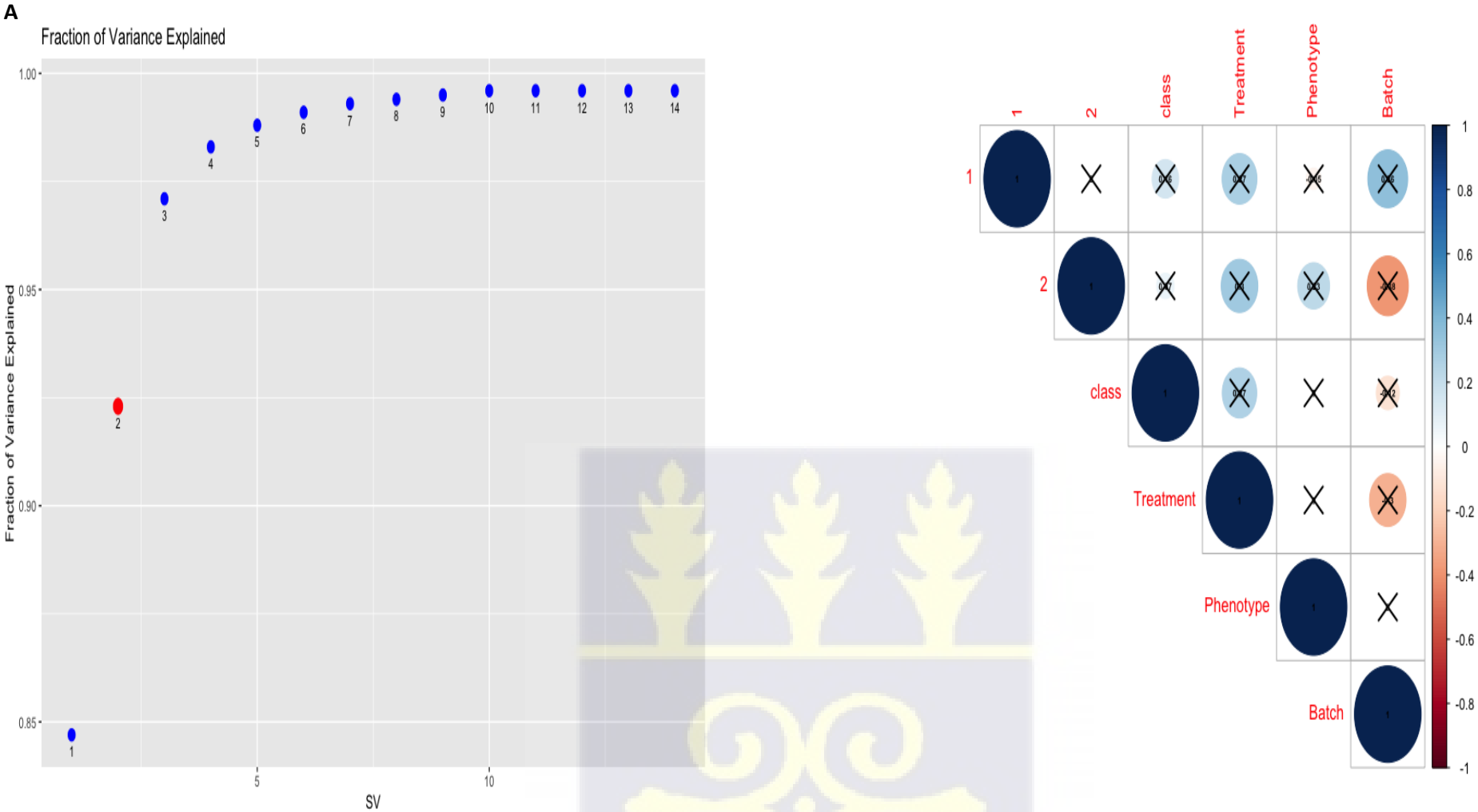

Supplementary Figure 5.8 Identification of surrogate variable (Sv) using the DaMiR.SV() function in the filtered and normalized expression dataset. A) Plot showing relationship between each Sv and the fraction of the variance it explains in the data. Each blue dot represents the cumulative proportion of variance explained by a Sv. The red dot marks the Sv that corresponds to ≤ 95% of variance explained and was used to adjust the data set. B) Correlation plot between surrogate variables and known the known covariates: treatment class, parasite strain, parasite sensitivity to ART and experimental batch. This plot shows the correlation between surrogate variables and known covariates, using both color gradient and circle size. The color ranges from correlation of -1 to +1 (dark red to dark blue). The circle size is maximum for a correlation equal to 1 or -1 and decreases up to zero. Black crosses indicate non-significant correlations. This plot shows no significant correlation between all seven surrogate variables and the known covariates.

University of Ghana http://ugspace.ug.edu.gh

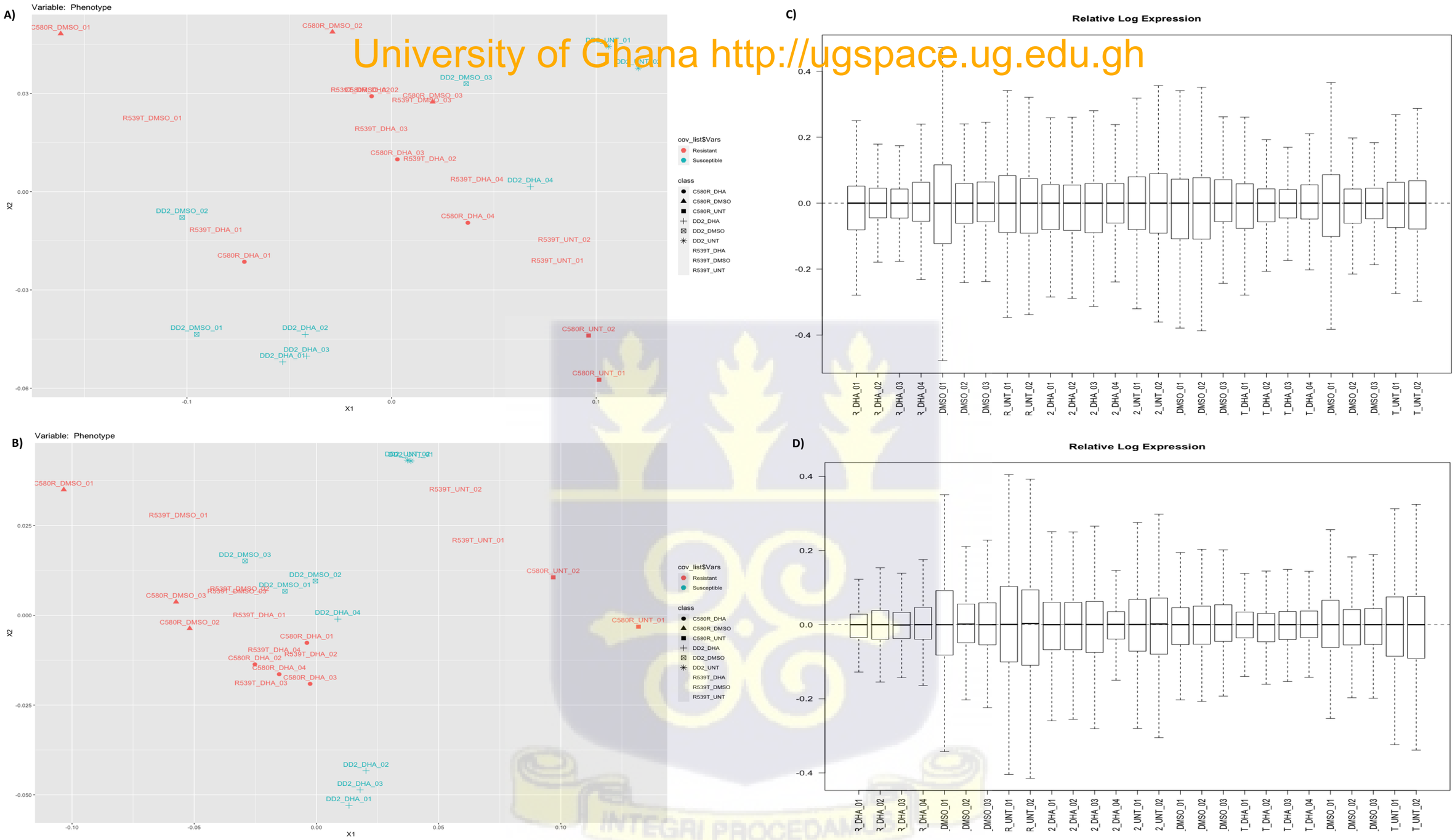

Supplementary Figure 5.9 Summary findings following interrogation of validity of RNA sequenced data. The R package DaMiRseq was used to filter, normalize and adjust the raw count data. Final adjustment for hidden sources of variation in the count data was done using surrogate variables (Svs). Top row indicate graphical summaries of count data structure before Svs adjustment and bottom row shows summaries following Svs adjustment. A) and B) Multidimensional scaling plot of count data showing parasite lines, technical replicates and treatment conditions. Following adjustment for Svs (B), parasite treatment conditions largely clustered together. C) and D) Following adjustment for Svs, relative log expression across samples was minimally affected.

University of Ghana http://ugspace.ug.edu.gh

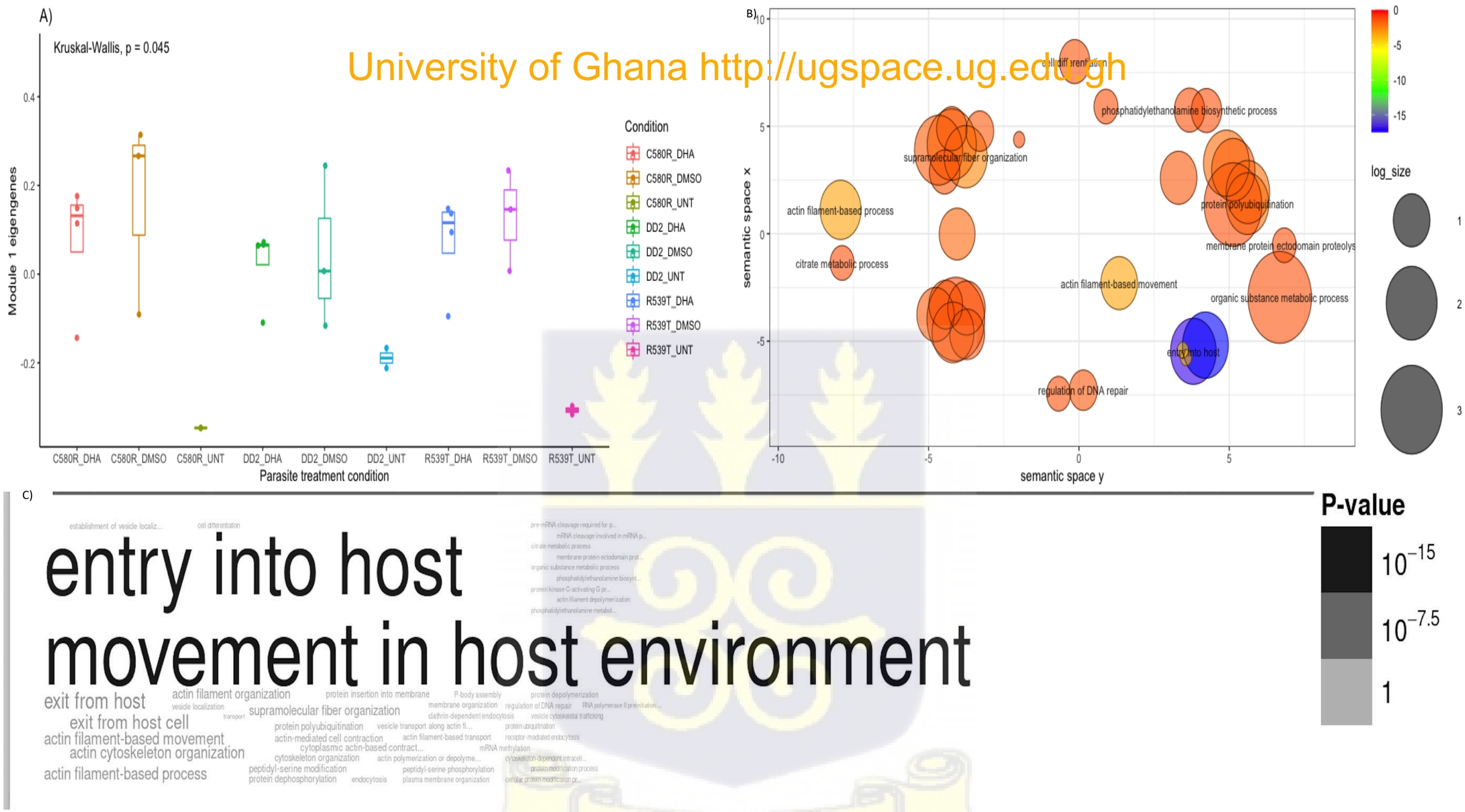

Supplementary Figure 5.10 Properties of EVs module of interest module 1 (ME1). ME1 was uploaded to plasmodb (https://plasmodb.org/plasmo/app) and analyzed with the platform's gene ontology (GO) pipeline. A) Comparison of ME3 between the three treatment conditions pooled for all parasite lines (DD2, C580R and R539T). The Kruskal-Wallis test was used to determine the statistical significance of the difference in expression of ME1 among the conditions (0.05 < p-value < 0.1). B) GO (biological processes) output for ME1 summarized using REVIGO (http://revigo.irb.hr) scatterplot visualization option. Each circle denotes the representative cluster of the GO biological process associated with the ARTr phenotype and is derived by multidimensional scaling and redundancy reduction of the GO sematic similarities. The size of the circles denote the frequency of the GO term in the *P. falciparum* GO database (updated in November 2021) with larger circles denoting more general terms. The colors (red to blue range) indicate the statistical significance of the association's strength. "Movement in host environment and entry into host" were two of the biological processes enriched. C) Word cloud summary of the GO biological processes associated with the ARTr phenotype. EVs – extracellular vesicles, ARTr – artemisinin resistance

University of Ghana http://ugspace.ug.edu.gh

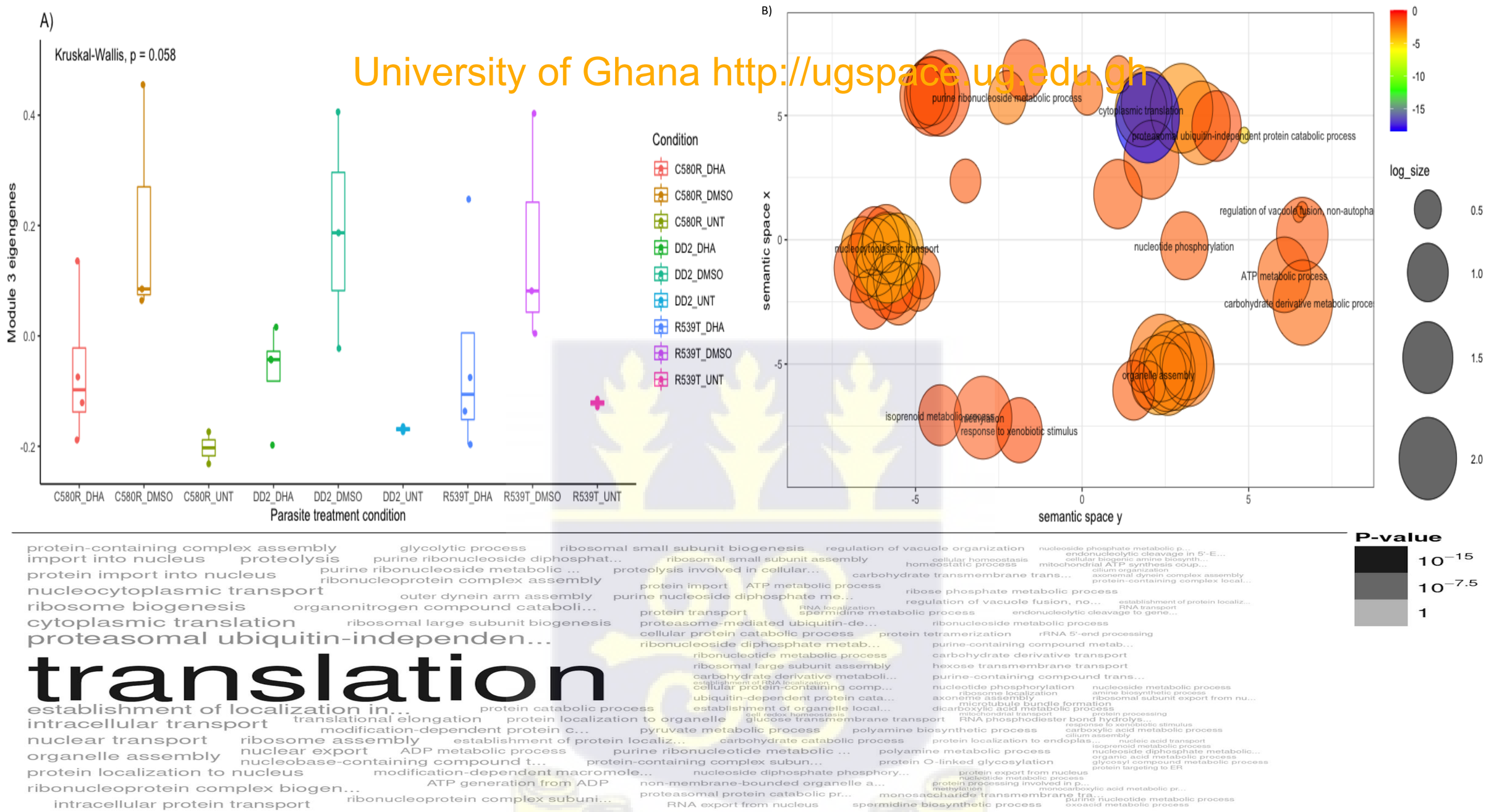

Supplementary Figure 5.11 Properties of EVs module of interest module 3 (ME3). ME3 was uploaded to plasmodb (https://plasmodb.org/plasmo/app) and analyzed with the platform's gene ontology (GO) pipeline. A) Comparison of ME3 between the three treatment conditions pooled for all parasite lines (DD2, C580R and R539T). The Kruskal-Wallis test was used to determine the statistical significance of the difference in expression of ME1 among the conditions (0.05 < p-value < 0.1). B) GO (biological processes) output for ME3 summarized using REVIGO (http://revigo.irb.hr) scatterplot visualization option. Each circle denotes the representative cluster of the GO biological process associated with the ARTr phenotype and is derived by multidimensional scaling and redundancy reduction of the GO sematic similarities. The size of the circles denote the frequency of the GO term in the *P. falciparum* GO database (updated in November 2021) with larger circles denoting more general terms. The colors (red to blue range) indicate the statistical significance of the association's strength. "translation and proteasomal ubiquitin-independent protein catabolic process" had the strongest statistical significance at p-value = 3.76 x10^{-16} and 0.015321736 respectively. C) Word cloud summary of the GO biological processes associated with the ARTr phenotype. EVs – extracellular vesicles, ARTr – artemisinin resistance

University of Ghana http://ugspace.ug.edu.gh

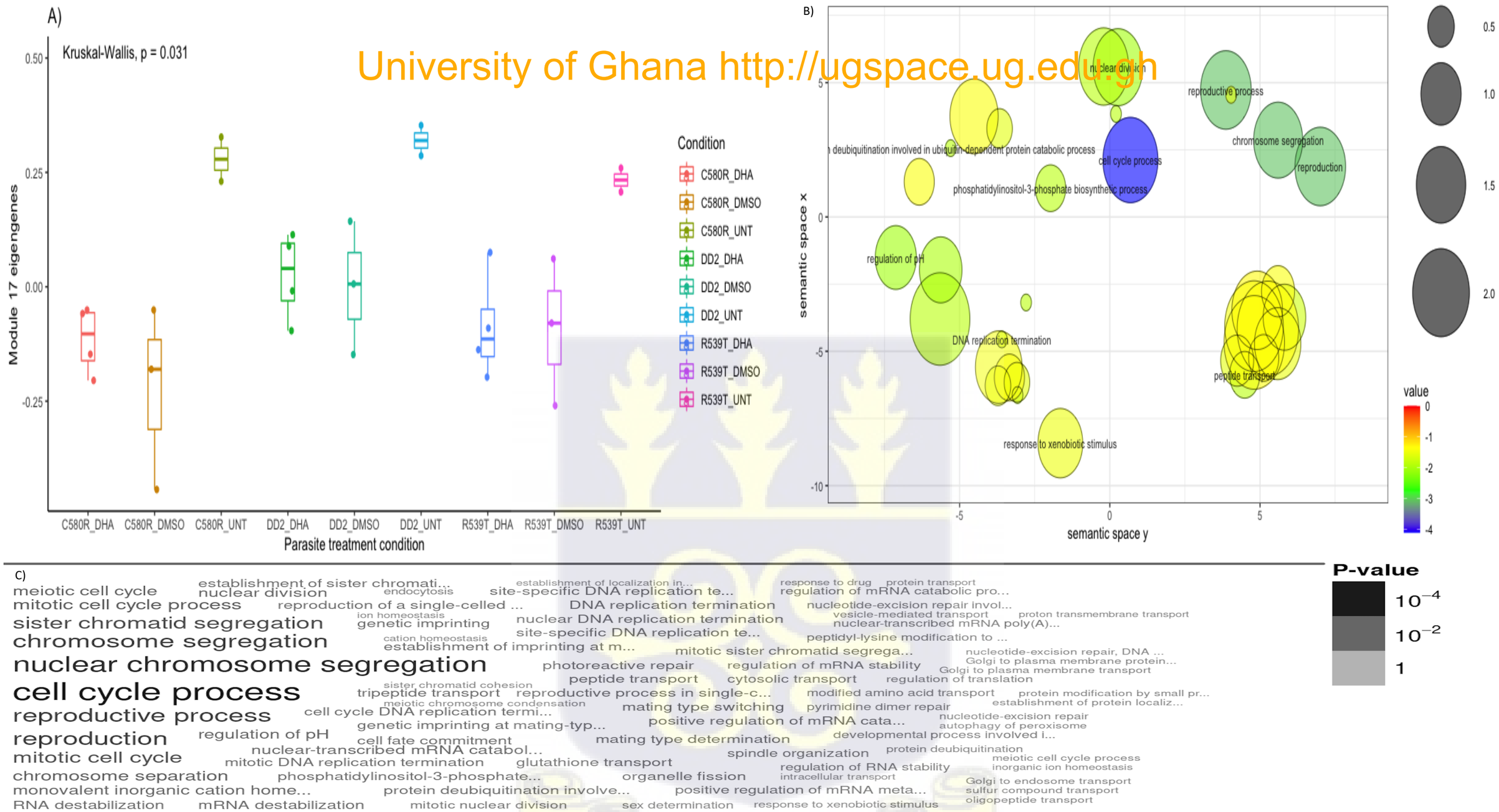

Supplementary Figure 5.12 Properties of EVs module of interest module 17 (ME17). ME17 was uploaded to plasmodb (https://plasmodb.org/plasmo/app) and analyzed with the platform's gene ontology (GO) pipeline. A) Comparison of ME3 between the three treatment conditions pooled for all parasite lines (DD2, C580R and R539T). The Kruskal-Wallis test was used to determine the statistical significance of the difference in expression of ME17 among the conditions (0.05 < p-value < 0.1). B) GO (biological processes) output for ME17 summarized using REVIGO (http://revigo.irb.hr) scatterplot visualization option. Each circle denotes the representative cluster of the GO biological process associated with the ARTr phenotype and is derived by multidimensional scaling and redundancy reduction of the GO sematic similarities. The size of the circles denote the frequency of the GO term in the *P. falciparum* GO database (updated in November 2021) with larger circles denoting more general terms. The colors (red to blue range) indicate the statistical significance of the association's strength. "cell cycle, nuclear chromosome segregation processes and phosphatidylinositol-3-phosphate biosynthetic process" were some of the top biological processes enriched in ME17. C) Word cloud summary of the GO biological processes associated with the ARTr phenotype. EVs – extracellular vesicles, ARTr – artemisinin resistance

Supplementary Data 5.1 Summary of GSEA output for R539T_DHA_treated versus R539T_untreated showing association with module 0

Table: GSEA Results Summary

Dataset	Expression_dataset_dataset_collapsed_to_symbols.PhenotypeData.cls #R539T_DHA_versus_R539T_UNT.PhenotypeData.cls #R539T_DHA_versus_R539T_UNT_repos
Phenotype	PhenotypeData.cls#R539T_DHA_versus_R539T_UNT_repos
Upregulated in class	R539T_DHA
GeneSet	ME0
Enrichment Score (ES)	0.41410053
Normalized Enrichment Score (NES)	1.1830174
Nominal p-value	0.23866348
FDR q-value	0.23794872
FWER p-Value	0.373

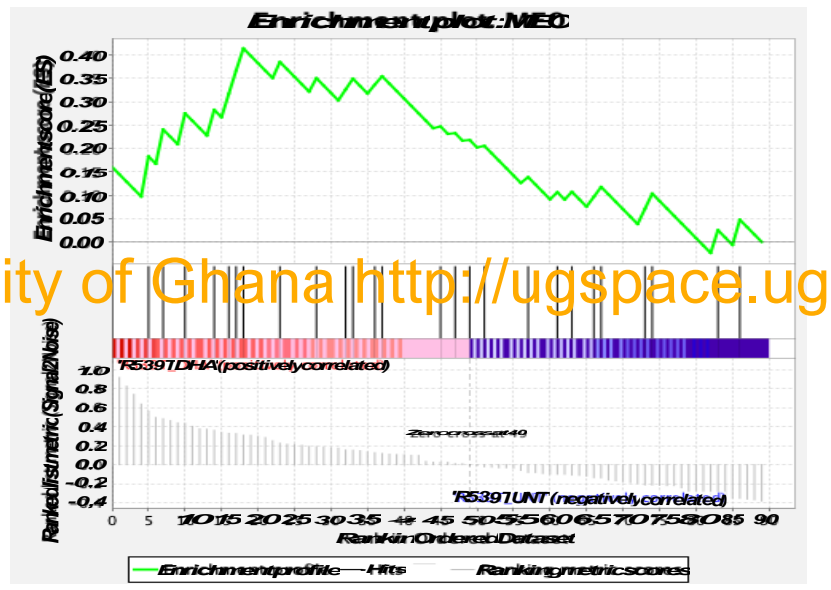

University of Ghana http://ugspace.ug.edu.gh

Fig 1: Enrichment plot: ME0
Profile of the Running ES Score & Positions of GeneSet Members on the Rank Ordered List

Table: GSEA details [plain text format]

	SYMBOL	TITLE	RANK IN GENE LIST	RANK METRIC SCORE	RUNNING ES	CORE ENRICHMENT
1	PF3D7_0221500	NA	0	1.051	0.1606	Yes
2	PF3D7_0400200	NA	5	0.562	0.1831	Yes
3	PF3D7_0500600	NA	7	0.481	0.2408	Yes
4	PF3D7_1477000	NA	10	0.433	0.2753	Yes
5	PF3D7_1478700	NA	14	0.360	0.2827	Yes
6	PF3D7_1000700	NA	16	0.328	0.3170	Yes
7	PF3D7_0102100	NA	17	0.326	0.3668	Yes
8	PF3D7_1372500	NA	18	0.309	0.4141	Yes
9	PF3D7_1000800	NA	23	0.225	0.3851	No
10	PF3D7_1219200	NA	28	0.189	0.3504	No
11	PF3D7_0533000	NA	32	0.153	0.3262	No
12	PF3D7_0601700	NA	33	0.151	0.3493	No
13	PF3D7_0221100	NA	36	0.125	0.3366	No
14	PF3D7_1334900	NA	37	0.117	0.3545	No
15	PF3D7_0500700	NA	45	0.025	0.2471	No
16	PF3D7_1129850	NA	47	0.010	0.2328	No
17	PF3D7_1463100	NA	49	-0.008	0.2181	No
18	PF3D7_1220200	NA	51	-0.022	0.2056	No
19	PF3D7_0425250	NA	57	-0.082	0.1388	No
20	PF3D7_0425300	NA	61	-0.100	0.1065	No
21	PF3D7_1253900	NA	63	-0.109	0.1073	No
22	PF3D7_0424300	NA	66	-0.137	0.0965	No
23	PF3D7_1478200	NA	67	-0.139	0.1177	No
24	PF3D7_1478300	NA	73	-0.213	0.0708	No
25	PF3D7_0402700	NA	74	-0.214	0.1035	No
26	PF3D7_0532800	NA	83	-0.319	0.0253	No
27	PF3D7_1478500	NA	86	-0.353	0.0476	No

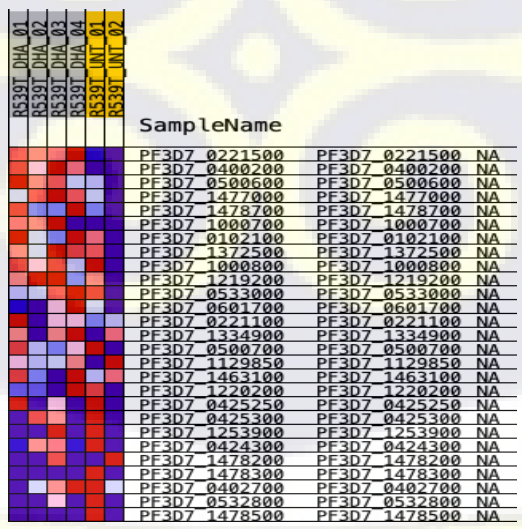

Fig 2: ME0
Blue-Pink O' Gram in the Space of the Analyzed GeneSet

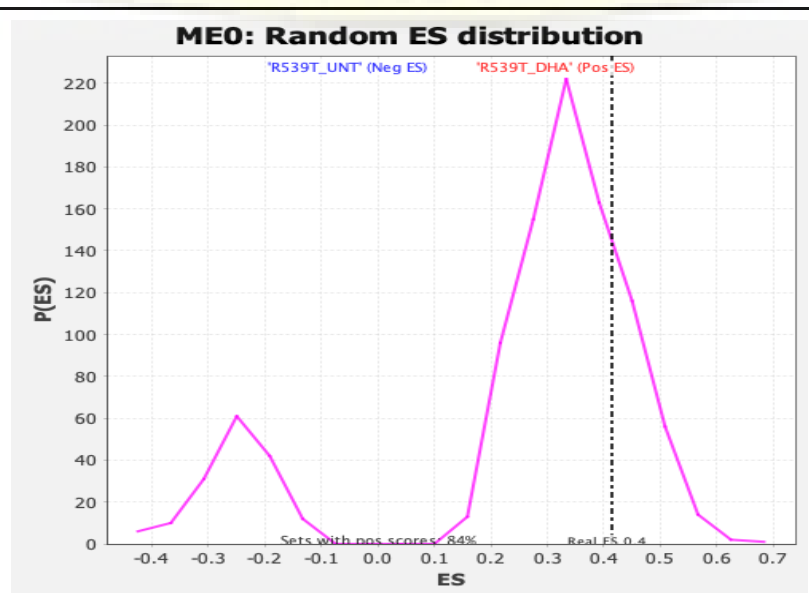

Fig 3: ME0: Random ES distribution
Gene set null distribution of ES for ME0

Supplementary Data 5.2 Summary of GSEA output for R539T_DHA_treated versus R539T_DMSO_treated showing association with module 0

Table: GSEA Results Summary

Dataset	Expression_dataset_dataset_collapsed_to_symbols.PhenotypeData.cls #R539T_DHA_versus_R539T_DMSO.PhenotypeData.cls #R539T_DHA_versus_R539T_DMSO_repos
Phenotype	PhenotypeData.cls#R539T_DHA_versus_R539T_DMSO_repos
Upregulated in class	R539T_DMSO
GeneSet	ME0
Enrichment Score (ES)	-0.20600075
Normalized Enrichment Score (NES)	-0.78877187
Nominal p-value	0.85714287
FDR q-value	0.859322
FWER p-Value	0.255

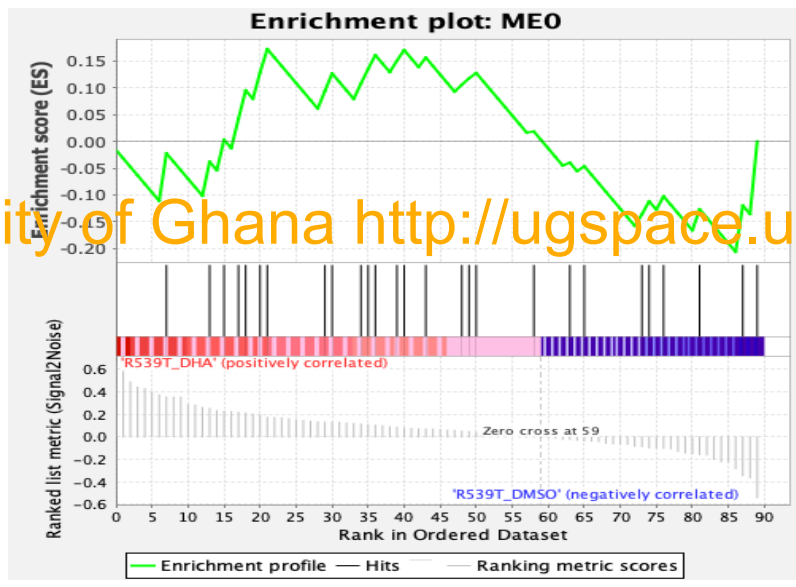

University of Ghana http://ugspace.ug.edu.gh

Fig 1: Enrichment plot: ME0
Profile of the Running ES Score & Positions of GeneSet Members on the Rank Ordered List

Table: GSEA details [plain text format]

	SYMBOL	TITLE	RANK IN GENE LIST	RANK METRIC SCORE	RUNNING ES	CORE ENRICHMENT
1	PF3D7_0221500	NA	7	0.355	-0.0222	Yes
2	PF3D7_0425300	NA	13	0.254	-0.0380	Yes
3	PF3D7_0500600	NA	15	0.227	0.0030	Yes
4	PF3D7_0500700	NA	17	0.219	0.0420	Yes
5	PF3D7_0425250	NA	18	0.212	0.0951	Yes
6	PF3D7_0533000	NA	20	0.197	0.1285	Yes
7	PF3D7_1478700	NA	21	0.174	0.1721	Yes
8	PF3D7_1129850	NA	29	0.131	0.0939	No
9	PF3D7_1477000	NA	30	0.131	0.1266	No
10	PF3D7_1000800	NA	34	0.114	0.1077	No
11	PF3D7_0400200	NA	35	0.108	0.1348	No
12	PF3D7_1253900	NA	36	0.104	0.1608	No
13	PF3D7_1372500	NA	39	0.085	0.1504	No
14	PF3D7_1463100	NA	40	0.079	0.1703	No
15	PF3D7_0601700	NA	43	0.070	0.1562	No
16	PF3D7_1220200	NA	48	0.051	0.1055	No
17	PF3D7_1334900	NA	49	0.047	0.1174	No
18	PF3D7_0221100	NA	50	0.040	0.1275	No
19	PF3D7_1478200	NA	58	0.008	0.0184	No
20	PF3D7_0532800	NA	63	-0.022	-0.0397	No
21	PF3D7_0102100	NA	65	-0.036	-0.0464	No
22	PF3D7_0424300	NA	73	-0.086	-0.1360	No
23	PF3D7_1219200	NA	74	-0.097	-0.1117	No
24	PF3D7_1000700	NA	76	-0.101	-0.1024	No
25	PF3D7_0402700	NA	81	-0.157	-0.1266	No
26	PF3D7_1478300	NA	87	-0.345	-0.1197	No
27	PF3D7_1478500	NA	89	-0.541	0.0000	No

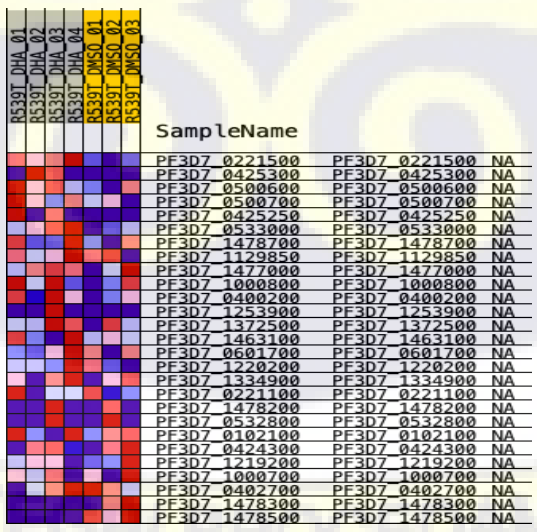

Fig 2: ME0
Blue-Pink O' Gram in the Space of the Analyzed GeneSet

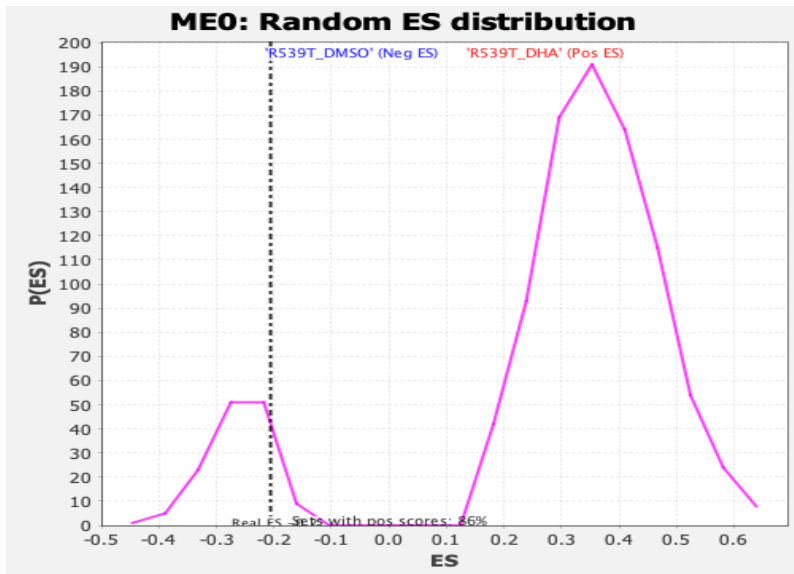

Fig 3: ME0: Random ES distribution
Gene set null distribution of ES for ME0

Supplementary Data 5.3 Summary of GSEA output for R539T_DHA_treated versus DD2_DHA_treated showing association with module 0

Table: GSEA Results Summary

Dataset	Expression_dataset_dataset_collapsed_to_symbols.PhenotypeData.cls #R539T_DHA_versus_DD2_DHA.PhenotypeData.cls #R539T_DHA_versus_DD2_DHA_repos
Phenotype	PhenotypeData.cls#R539T_DHA_versus_DD2_DHA_repos
Upregulated in class	DD2_DHA
GeneSet	ME0
Enrichment Score (ES)	-0.41499826
Normalized Enrichment Score (NES)	-1.1220989
Nominal p-value	0.28860295
FDR q-value	0.28233033
FWER p-Value	0.275

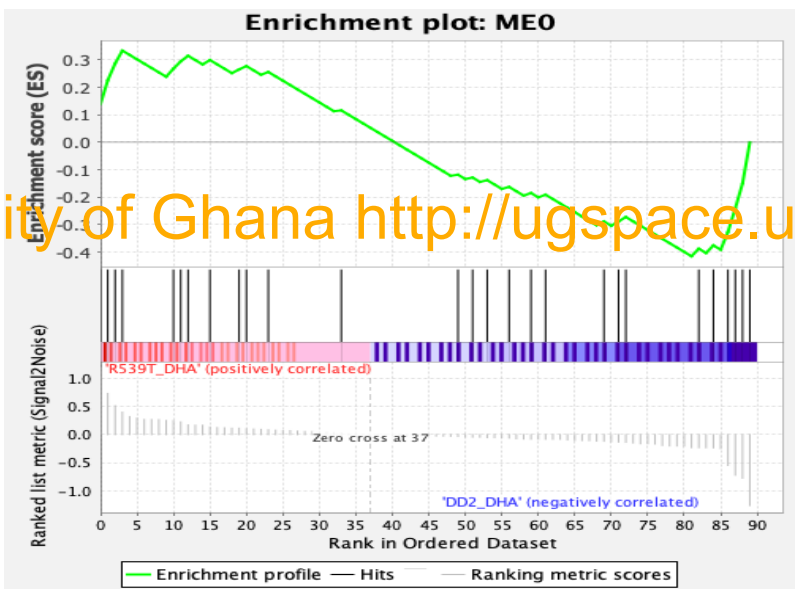

University of Ghana http://ugspace.ug.edu.gh

Fig 1: Enrichment plot: ME0
Profile of the Running ES Score & Positions of GeneSet Members on the Rank Ordered List

Table: GSEA details [plain text format]

	SYMBOL	TITLE	RANK IN GENE LIST	RANK METRIC SCORE	RUNNING ES	CORE ENRICHMENT
1	PF3D7_0221500	NA	0	1.179	0.1391	No
2	PF3D7_0102100	NA	1	0.734	0.2257	No
3	PF3D7_0221100	NA	2	0.514	0.2865	No
4	PF3D7_0500600	NA	3	0.401	0.3338	No
5	PF3D7_0400200	NA	10	0.249	0.2680	No
6	PF3D7_1463100	NA	11	0.226	0.2946	No
7	PF3D7_0425300	NA	12	0.173	0.3150	No
8	PF3D7_1220200	NA	15	0.136	0.2994	No
9	PF3D7_1334900	NA	19	0.114	0.2652	No
10	PF3D7_1478200	NA	20	0.104	0.2774	No
11	PF3D7_1129850	NA	23	0.087	0.2559	No
12	PF3D7_0425250	NA	33	0.025	0.1161	No
13	PF3D7_1219200	NA	49	-0.033	-0.1181	No
14	PF3D7_1478700	NA	51	-0.046	-0.1285	No
15	PF3D7_1372500	NA	53	-0.054	-0.1380	No
16	PF3D7_0500700	NA	56	-0.061	-0.1625	No
17	PF3D7_1478500	NA	59	-0.081	-0.1847	No
18	PF3D7_1253900	NA	61	-0.082	-0.1910	No
19	PF3D7_0533000	NA	69	-0.117	-0.2882	No
20	PF3D7_0601700	NA	71	-0.133	-0.2884	No
21	PF3D7_1478300	NA	72	-0.138	-0.2721	No
22	PF3D7_0532800	NA	82	-0.233	-0.3875	Yes
23	PF3D7_0402700	NA	84	-0.237	-0.3755	Yes
24	PF3D7_0424300	NA	86	-0.549	-0.3265	Yes
25	PF3D7_1000700	NA	87	-0.724	-0.2411	Yes
26	PF3D7_1477000	NA	88	-0.778	-0.1493	Yes
27	PF3D7_1000800	NA	89	-1.265	0.0000	Yes

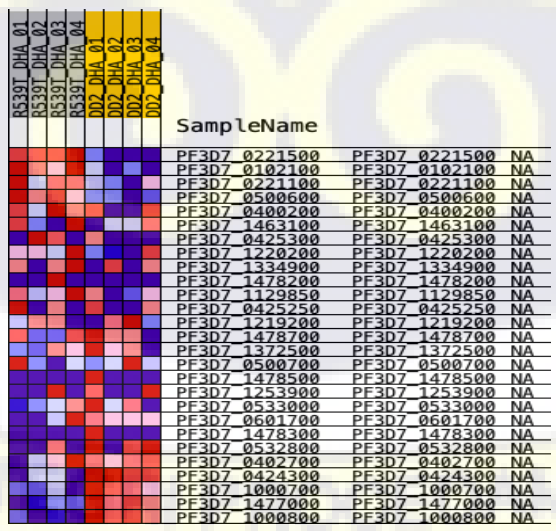

Fig 2: ME0
Blue-Pink O' Gram in the Space of the Analyzed GeneSet

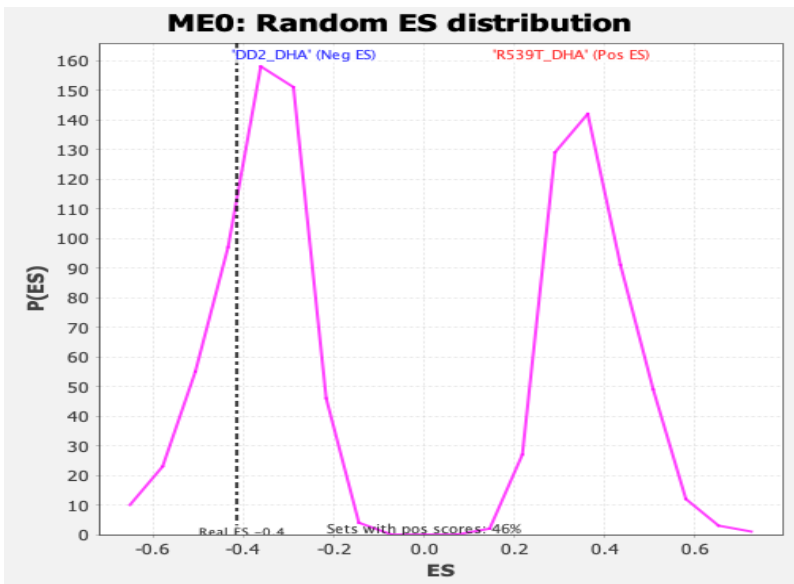

Fig 3: ME0: Random ES distribution
Gene set null distribution of ES for ME0

Supplementary Data 5.4 Summary of GSEA output for C580R_DHA_treated versus C580R_untreated showing association with module 0

Table: GSEA Results Summary

Dataset	Expression_dataset_dataset_collapsed_to_symbols.PhenotypeData.cls #C580R_DHA_versus_C580R_UNT.PhenotypeData.cls #C580R_DHA_versus_C580R_UNT_repos
Phenotype	PhenotypeData.cls#C580R_DHA_versus_C580R_UNT_repos
Upregulated in class	C580R_DHA
GeneSet	ME0
Enrichment Score (ES)	0.309629
Normalized Enrichment Score (NES)	1.2457103
Nominal p-value	0.11764706
FDR q-value	0.14403293
FWER p-Value	0.037

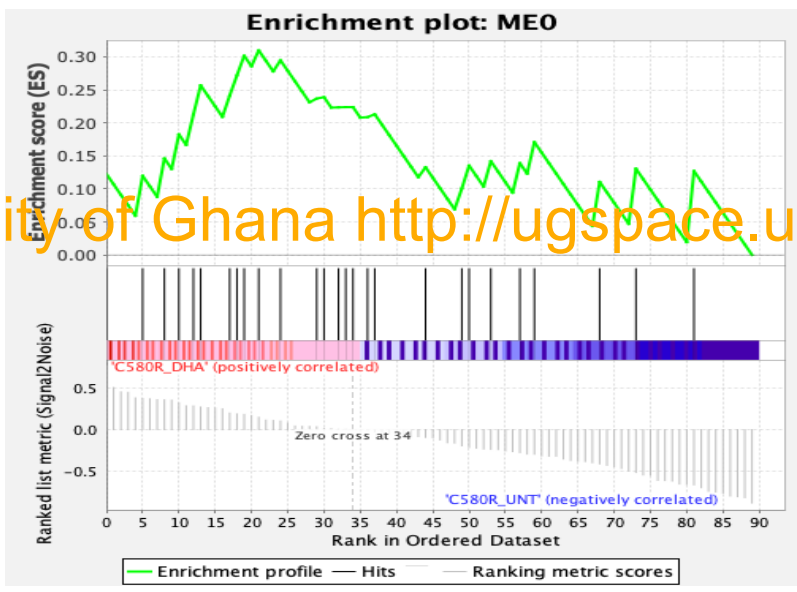

University of Ghana http://ugspace.ug.edu.gh

Fig 1: Enrichment plot: ME0
Profile of the Running ES Score & Positions of GeneSet Members on the Rank Ordered List

Table: GSEA details [plain text format]

	SYMBOL	TITLE	RANK IN GENE LIST	RANK METRIC SCORE	RUNNING ES	CORE ENRICHMENT
1	PF3D7_1372500	NA	0	0.754	0.1228	Yes
2	PF3D7_1478700	NA	5	0.371	0.1197	Yes
3	PF3D7_0533000	NA	8	0.357	0.1461	Yes
4	PF3D7_1478500	NA	10	0.321	0.1825	Yes
5	PF3D7_0425250	NA	12	0.283	0.2126	Yes
6	PF3D7_0500700	NA	13	0.270	0.2566	Yes
7	PF3D7_0601700	NA	17	0.198	0.2412	Yes
8	PF3D7_0532800	NA	18	0.188	0.2718	Yes
9	PF3D7_1220200	NA	19	0.182	0.3015	Yes
10	PF3D7_0500600	NA	21	0.148	0.3096	Yes
11	PF3D7_1478200	NA	24	0.103	0.2946	No
12	PF3D7_0425300	NA	29	0.034	0.2367	No
13	PF3D7_0221500	NA	30	0.013	0.2389	No
14	PF3D7_1000800	NA	32	0.002	0.2234	No
15	PF3D7_0400200	NA	33	0.002	0.2237	No
16	PF3D7_1253900	NA	34	0.000	0.2237	No
17	PF3D7_0402700	NA	36	-0.005	0.2086	No
18	PF3D7_1000700	NA	37	-0.026	0.2129	No
19	PF3D7_1477000	NA	44	-0.092	0.1327	No
20	PF3D7_1334900	NA	49	-0.193	0.1006	No
21	PF3D7_1129850	NA	50	-0.213	0.1353	No
22	PF3D7_1478300	NA	53	-0.236	0.1419	No
23	PF3D7_1463100	NA	57	-0.274	0.1389	No
24	PF3D7_1219200	NA	59	-0.293	0.1708	No
25	PF3D7_0102100	NA	68	-0.410	0.1105	No
26	PF3D7_0221100	NA	73	-0.513	0.1305	No
27	PF3D7_0424300	NA	81	-0.661	0.1270	No

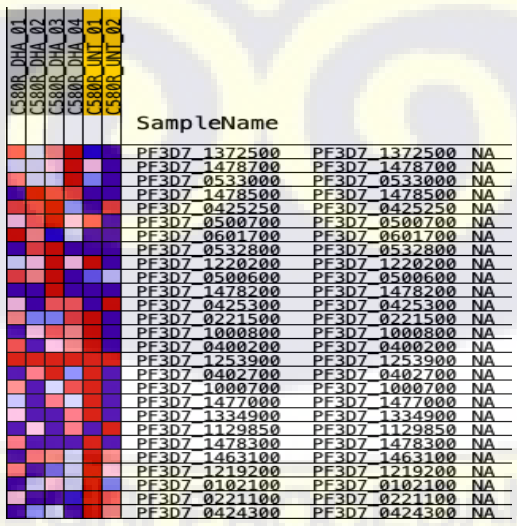

Fig 2: ME0
Blue-Pink O' Gram in the Space of the Analyzed GeneSet

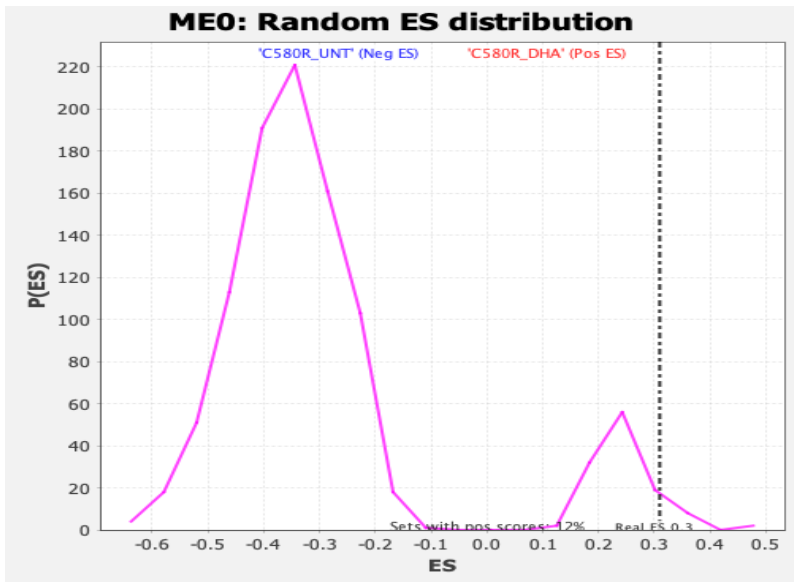

Fig 3: ME0: Random ES distribution
Gene set null distribution of ES for ME0

Supplementary Data 5.5 Summary of GSEA output for C580R_DHA_treated versus C580R_DMSO_treated showing association with module 0

Table: GSEA Results Summary

Dataset	Expression_dataset_dataset_collapsed_to_symbols.PhenotypeData.cls #C580R_DHA_versus_C580R_DMSO.PhenotypeData.cls #C580R_DHA_versus_C580R_DMSO_repos
Phenotype	PhenotypeData.cls#C580R_DHA_versus_C580R_DMSO_repos
Upregulated in class	C580R_DHA
GeneSet	ME0
Enrichment Score (ES)	0.312271
Normalized Enrichment Score (NES)	0.7299921
Nominal p-value	0.8987854
FDR q-value	0.891
FWER p-Value	0.984

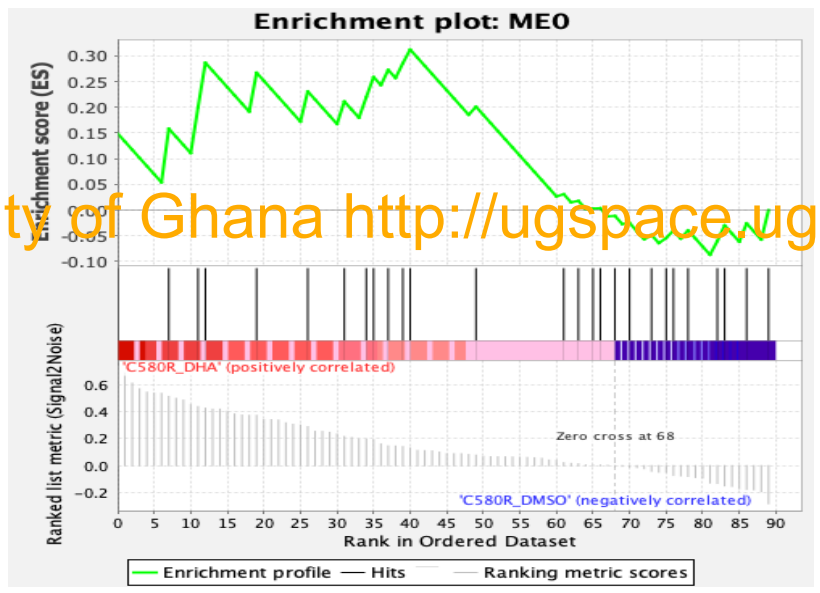

Fig 1: Enrichment plot: ME0
Profile of the Running ES Score & Positions of GeneSet Members on the Rank Ordered List

University of Ghana http://ugspace.ug.edu.gh

Table: GSEA details [plain text format]

	SYMBOL	TITLE	RANK IN GENE LIST	RANK METRIC SCORE	RUNNING ES	CORE ENRICHMENT
1	PF3D7_0500600	NA	0	0.730	0.1491	Yes
2	PF3D7_0221500	NA	7	0.512	0.1584	Yes
3	PF3D7_1000700	NA	11	0.437	0.1999	Yes
4	PF3D7_0533000	NA	12	0.424	0.2866	Yes
5	PF3D7_1000800	NA	19	0.372	0.2673	Yes
6	PF3D7_0500700	NA	26	0.288	0.2309	Yes
7	PF3D7_1477000	NA	31	0.215	0.2113	Yes
8	PF3D7_0425300	NA	34	0.196	0.2196	Yes
9	PF3D7_0425250	NA	35	0.192	0.2588	Yes
10	PF3D7_1478700	NA	37	0.146	0.2727	Yes
11	PF3D7_1478500	NA	39	0.141	0.2856	Yes
12	PF3D7_1463100	NA	40	0.131	0.3123	Yes
13	PF3D7_1372500	NA	49	0.078	0.2011	No
14	PF3D7_1220200	NA	61	0.022	0.0310	No
15	PF3D7_0601700	NA	63	0.014	0.0179	No
16	PF3D7_1219200	NA	65	0.004	0.0029	No
17	PF3D7_0221100	NA	66	0.004	0.0037	No
18	PF3D7_1478200	NA	68	-0.004	-0.0113	No
19	PF3D7_0402700	NA	70	-0.010	-0.0251	No
20	PF3D7_0400200	NA	73	-0.041	-0.0484	No
21	PF3D7_0102100	NA	75	-0.048	-0.0543	No
22	PF3D7_0532800	NA	76	-0.072	-0.0397	No
23	PF3D7_1478300	NA	78	-0.079	-0.0394	No
24	PF3D7_0424300	NA	82	-0.131	-0.0602	No
25	PF3D7_1253900	NA	83	-0.149	-0.0298	No
26	PF3D7_1334900	NA	86	-0.175	-0.0257	No
27	PF3D7_1129850	NA	89	-0.281	-0.0000	No

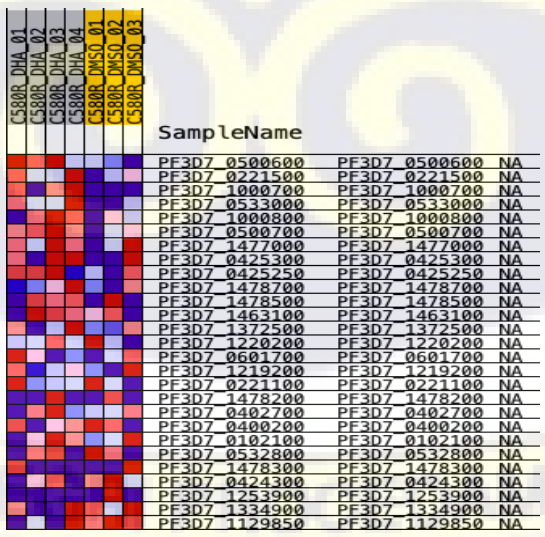

Fig 2: ME0
Blue-Pink O' Gram in the Space of the Analyzed GeneSet

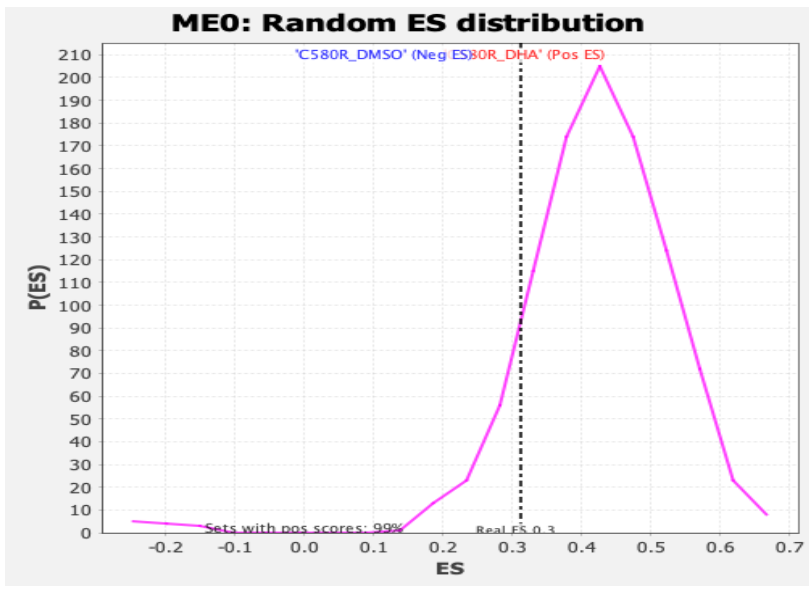

Fig 3: ME0: Random ES distribution
Gene set null distribution of ES for ME0

Supplementary Data 5.6 Summary of GSEA output for C580R_DHA_treated versus DD2_DHA_treated showing association with module 0

Table: GSEA Results Summary

Dataset	Expression_dataset_dataset_collapsed_to_symbols.PhenotypeData.cls #C580R_DHA_versus_DD2_DHA.PhenotypeData.cls #C580R_DHA_versus_DD2_DHA_repos
Phenotype	PhenotypeData.cls#C580R_DHA_versus_DD2_DHA_repos
Upregulated in class	C580R_DHA
GeneSet	ME0
Enrichment Score (ES)	0.40779817
Normalized Enrichment Score (NES)	1.0806667
Nominal p-value	0.34814814
FDR q-value	0.35456595
FWER p-Value	0.416

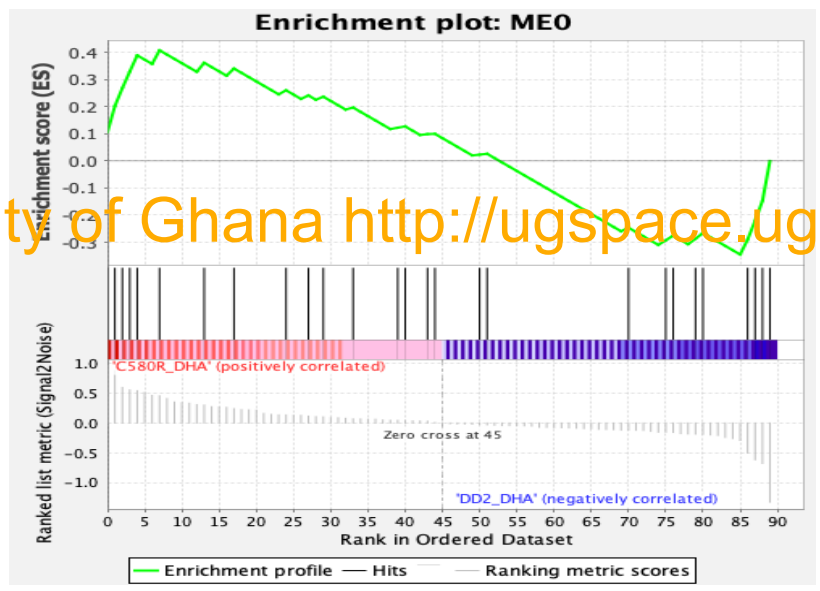

University of Ghana http://ugspace.ug.edu.gh

Fig 1: Enrichment plot: ME0
Profile of the Running ES Score & Positions of GeneSet Members on the Rank Ordered List

Table: GSEA details [plain text format]

	SYMBOL	TITLE	RANK IN GENE LIST	RANK METRIC SCORE	RUNNING ES	CORE ENRICHMENT
1	PF3D7_1372500	NA	0	0.958	0.1057	Yes
2	PF3D7_0533000	NA	1	0.875	0.2023	Yes
3	PF3D7_0425250	NA	2	0.596	0.2681	Yes
4	PF3D7_0500600	NA	3	0.556	0.3294	Yes
5	PF3D7_0221100	NA	4	0.542	0.3892	Yes
6	PF3D7_0221500	NA	7	0.456	0.4078	Yes
7	PF3D7_0425300	NA	13	0.302	0.3617	No
8	PF3D7_1478500	NA	17	0.241	0.3407	No
9	PF3D7_1463100	NA	24	0.135	0.2604	No
10	PF3D7_1220200	NA	27	0.115	0.2414	No
11	PF3D7_1478200	NA	29	0.103	0.2368	No
12	PF3D7_1219200	NA	33	0.069	0.1968	No
13	PF3D7_0500700	NA	39	0.045	0.1224	No
14	PF3D7_0102100	NA	40	0.044	0.1273	No
15	PF3D7_0400200	NA	43	0.030	0.0989	No
16	PF3D7_1334900	NA	44	0.008	0.0998	No
17	PF3D7_1478700	NA	50	-0.024	0.0230	No
18	PF3D7_1478300	NA	51	-0.030	0.0263	No
19	PF3D7_0532800	NA	70	-0.119	-0.2462	No
20	PF3D7_0402700	NA	75	-0.154	-0.2927	No
21	PF3D7_0601700	NA	76	-0.158	-0.2753	No
22	PF3D7_1253900	NA	79	-0.185	-0.2866	No
23	PF3D7_1129850	NA	80	-0.189	-0.2658	No
24	PF3D7_0424300	NA	86	-0.503	-0.2897	No
25	PF3D7_1000700	NA	87	-0.617	-0.2216	No
26	PF3D7_1477000	NA	88	-0.678	-0.1467	No
27	PF3D7_1000800	NA	89	-1.329	0.0000	No

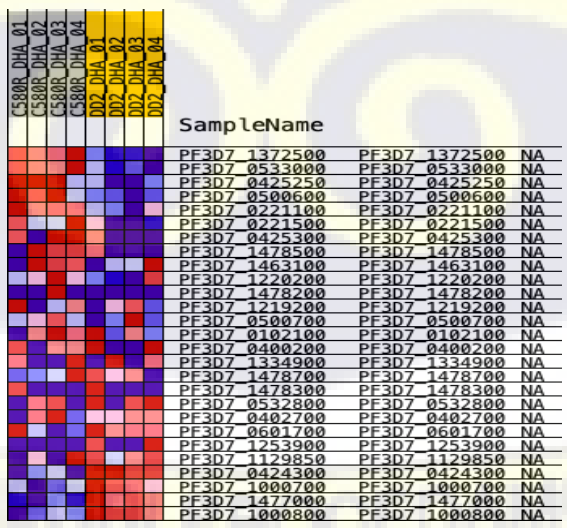

Fig 2: ME0
Blue-Pink O' Gram in the Space of the Analyzed GeneSet

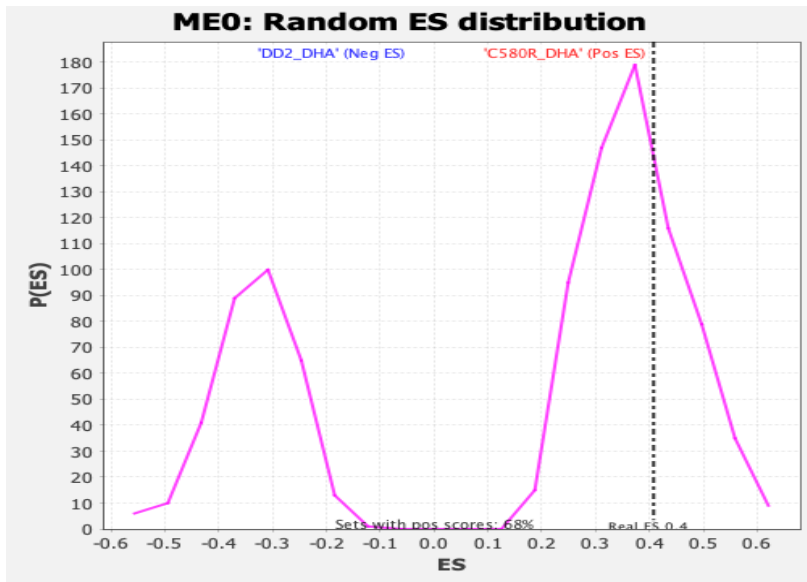

Fig 3: ME0: Random ES distribution
Gene set null distribution of ES for ME0

Supplementary Data 5.7 Summary of GSEA output for DD2_DHA_treated versus DD2_untreated showing association with module 0

Table: GSEA Results Summary

Dataset	Expression_dataset_dataset_collapsed_to_symbols.PhenotypeData.cls #DD2_DHA_versus_DD2_UNT.PhenotypeData.cls #DD2_DHA_versus_DD2_UNT_repos
Phenotype	PhenotypeData.cls#DD2_DHA_versus_DD2_UNT_repos
Upregulated in class	DD2_DHA
GeneSet	ME0
Enrichment Score (ES)	0.37629843
Normalized Enrichment Score (NES)	1.1802711
Nominal p-value	0.22782874
FDR q-value	0.22940503
FWER p-Value	0.282

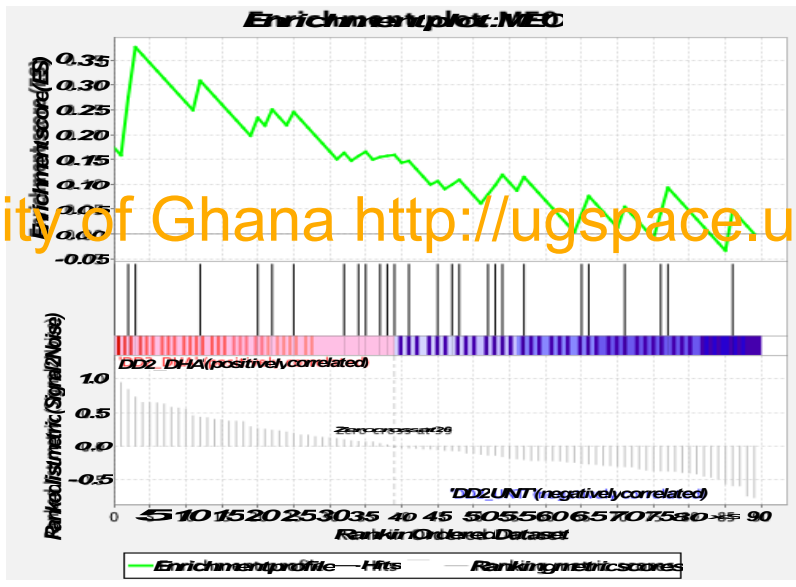

University of Ghana http://ugspace.ug.edu.gh

Fig 1: Enrichment plot: ME0
Profile of the Running ES Score & Positions of GeneSet Members on the Rank Ordered List

Table: GSEA details [plain text format]

	SYMBOL	TITLE	RANK IN GENE LIST	RANK METRIC SCORE	RUNNING ES	CORE ENRICHMENT
1	PF3D7_1000800	NA	0	1.254	0.1743	Yes
2	PF3D7_1477000	NA	2	0.840	0.2752	Yes
3	PF3D7_1000700	NA	3	0.728	0.3763	Yes
4	PF3D7_0424300	NA	12	0.428	0.3088	No
5	PF3D7_0402700	NA	20	0.262	0.2340	No
6	PF3D7_1372500	NA	22	0.234	0.2507	No
7	PF3D7_1478700	NA	25	0.192	0.2456	No
8	PF3D7_1334900	NA	32	0.093	0.1634	No
9	PF3D7_0601700	NA	34	0.069	0.1570	No
10	PF3D7_0500600	NA	35	0.062	0.1657	No
11	PF3D7_1220200	NA	37	0.037	0.1549	No
12	PF3D7_0500700	NA	38	0.017	0.1572	No
13	PF3D7_1478300	NA	39	-0.014	0.1592	No
14	PF3D7_1253900	NA	41	-0.026	0.1470	No
15	PF3D7_1463100	NA	45	-0.050	0.1064	No
16	PF3D7_0221500	NA	47	-0.064	0.0994	No
17	PF3D7_0533000	NA	48	-0.069	0.1090	No
18	PF3D7_1478500	NA	52	-0.131	0.0796	No
19	PF3D7_1219200	NA	53	-0.133	0.0980	No
20	PF3D7_1478200	NA	54	-0.152	0.1191	No
21	PF3D7_0102100	NA	57	-0.197	0.1147	No
22	PF3D7_1129850	NA	65	-0.261	0.0398	No
23	PF3D7_0400200	NA	66	-0.262	0.0762	No
24	PF3D7_0425250	NA	71	-0.302	0.0548	No
25	PF3D7_0532800	NA	76	-0.366	0.0421	No
26	PF3D7_0425300	NA	77	-0.368	0.0932	No
27	PF3D7_0221100	NA	86	-0.586	0.0476	No

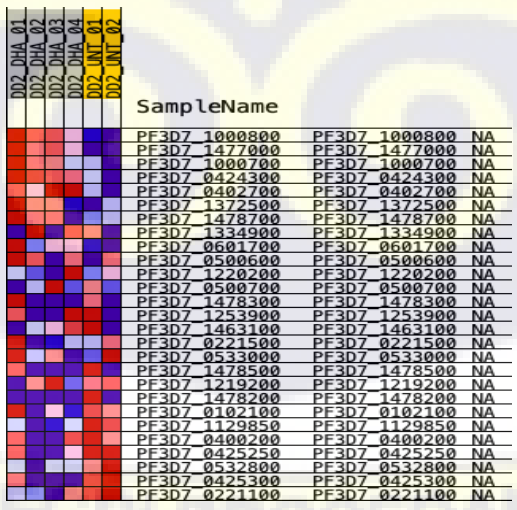

Fig 2: ME0
Blue-Pink O' Gram in the Space of the Analyzed GeneSet

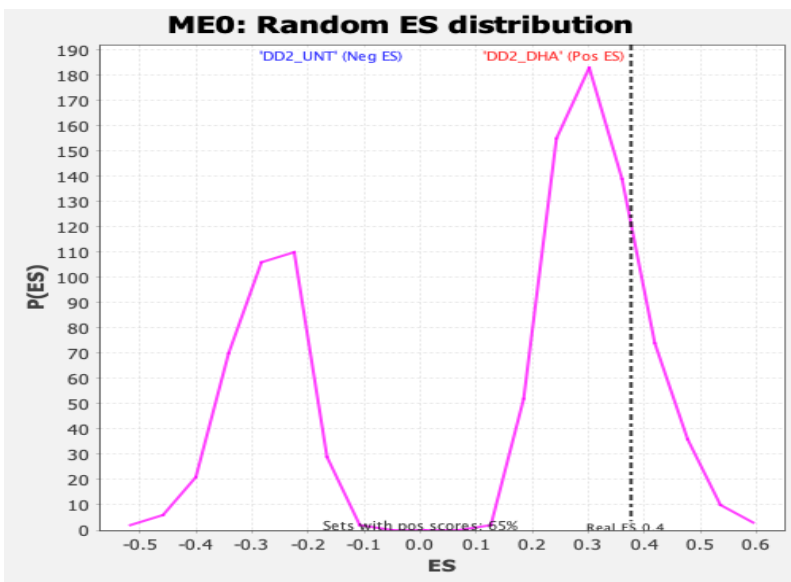

Fig 3: ME0: Random ES distribution
Gene set null distribution of ES for ME0

Supplementary Data 5.8 Summary of GSEA output for DD2_DHA_treated versus DD2_DMSO_treated showing association with module 0

Table: GSEA Results Summary

Dataset	Expression_dataset_dataset_collapsed_to_symbols.PhenotypeData.cls #DD2_DHA_versus_DD2_DMSO.PhenotypeData.cls #DD2_DHA_versus_DD2_DMSO_repos
Phenotype	PhenotypeData.cls#DD2_DHA_versus_DD2_DMSO_repos
Upregulated in class	DD2_DMSO
GeneSet	ME0
Enrichment Score (ES)	-0.26537684
Normalized Enrichment Score (NES)	-1.1928045
Nominal p-value	0.16071428
FDR q-value	0.33333334
FWER p-Value	0.017

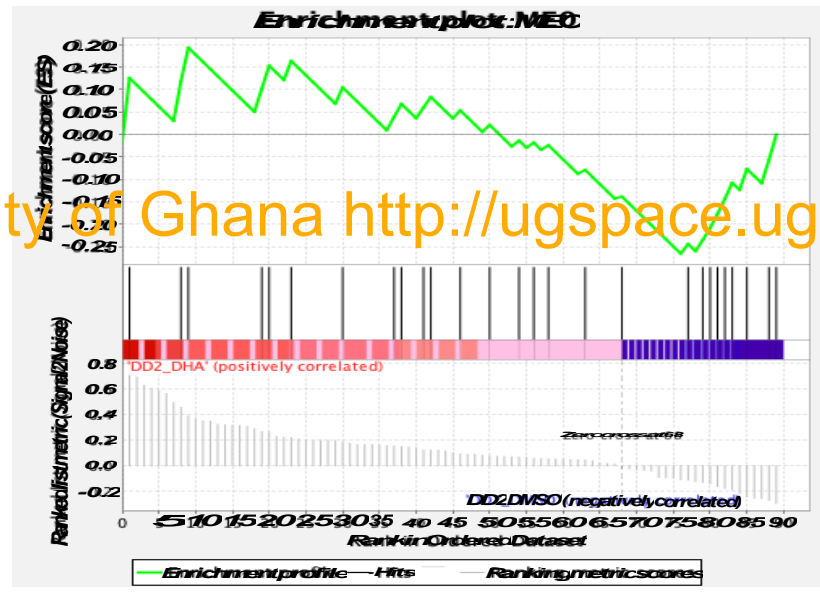

University of Ghana http://ugspace.ug.edu.gh

Fig 1: Enrichment plot: ME0
Profile of the Running ES Score & Positions of GeneSet Members on the Rank Ordered List

Table: GSEA details [plain text format]

	SYMBOL	TITLE	RANK IN GENE LIST	RANK METRIC SCORE	RUNNING ES	CORE ENRICHMENT
1	PF3D7_1000800	NA	1	0.730	0.1257	No
2	PF3D7_1000700	NA	8	0.453	0.1182	No
3	PF3D7_0533000	NA	9	0.387	0.1932	No
4	PF3D7_1478700	NA	19	0.265	0.1019	No
5	PF3D7_1477000	NA	20	0.264	0.1531	No
6	PF3D7_1372500	NA	23	0.218	0.1636	No
7	PF3D7_0500700	NA	30	0.187	0.1046	No
8	PF3D7_0601700	NA	37	0.152	0.0390	No
9	PF3D7_0402700	NA	38	0.149	0.0679	No
10	PF3D7_0221500	NA	41	0.122	0.0600	No
11	PF3D7_1129850	NA	42	0.121	0.0834	No
12	PF3D7_1253900	NA	46	0.092	0.0535	No
13	PF3D7_1219200	NA	50	0.078	0.0210	No
14	PF3D7_0500600	NA	54	0.068	-0.0135	No
15	PF3D7_0424300	NA	56	0.057	-0.0183	No
16	PF3D7_0532800	NA	58	0.052	-0.0240	No
17	PF3D7_1478300	NA	63	0.044	-0.0790	No
18	PF3D7_0102100	NA	68	-0.021	-0.1384	No
19	PF3D7_0221100	NA	77	-0.110	-0.2440	Yes
20	PF3D7_1334900	NA	79	-0.129	-0.2349	Yes
21	PF3D7_0425300	NA	80	-0.138	-0.2081	Yes
22	PF3D7_1478200	NA	81	-0.160	-0.1771	Yes
23	PF3D7_1220200	NA	82	-0.173	-0.1435	Yes
24	PF3D7_1463100	NA	83	-0.185	-0.1076	Yes
25	PF3D7_0425250	NA	85	-0.241	-0.0768	Yes
26	PF3D7_1478500	NA	88	-0.267	-0.0568	Yes
27	PF3D7_0400200	NA	89	-0.293	0.0000	Yes

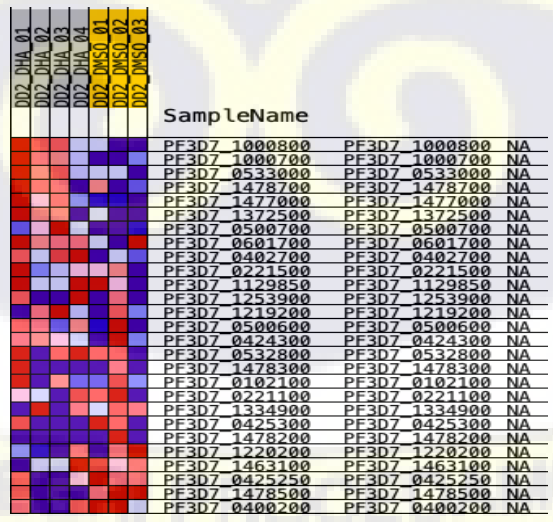

Fig 2: ME0
Blue-Pink O' Gram in the Space of the Analyzed GeneSet

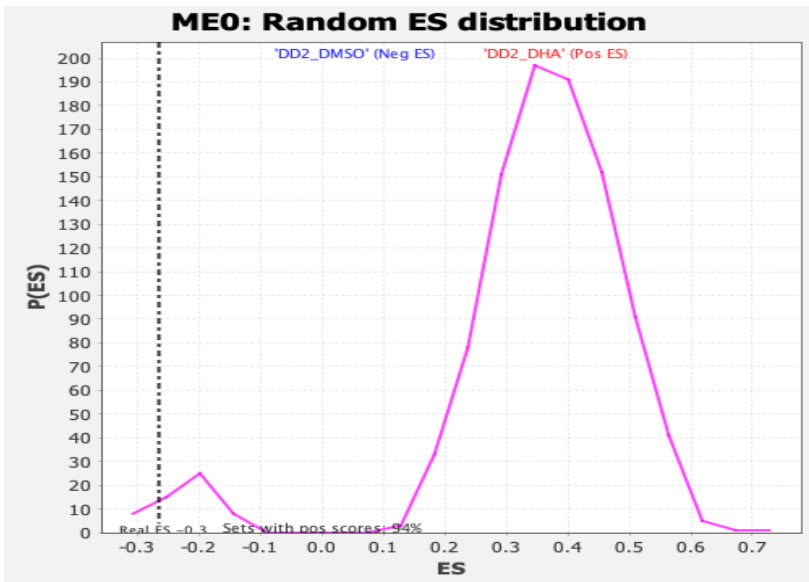

Fig 3: ME0: Random ES distribution
Gene set null distribution of ES for ME0

Supplementary Data 5.9 Summary of GSEA output for R539T_DHA_treated versus R539T_untreated showing association with module 7

Table: GSEA Results Summary

Dataset	Expression_dataset_dataset_collapsed_to_symbols.PhenotypeData.cls #R539T_DHA_versus_R539T_UNT.PhenotypeData.cls #R539T_DHA_versus_R539T_UNT_repos
Phenotype	PhenotypeData.cls#R539T_DHA_versus_R539T_UNT_repos
Upregulated in class	R539T_UNT
GeneSet	ME7
Enrichment Score (ES)	-0.34375
Normalized Enrichment Score (NES)	-1.2690192
Nominal p-value	0.14084508
FDR q-value	0.14516129
FWER p-Value	0.044

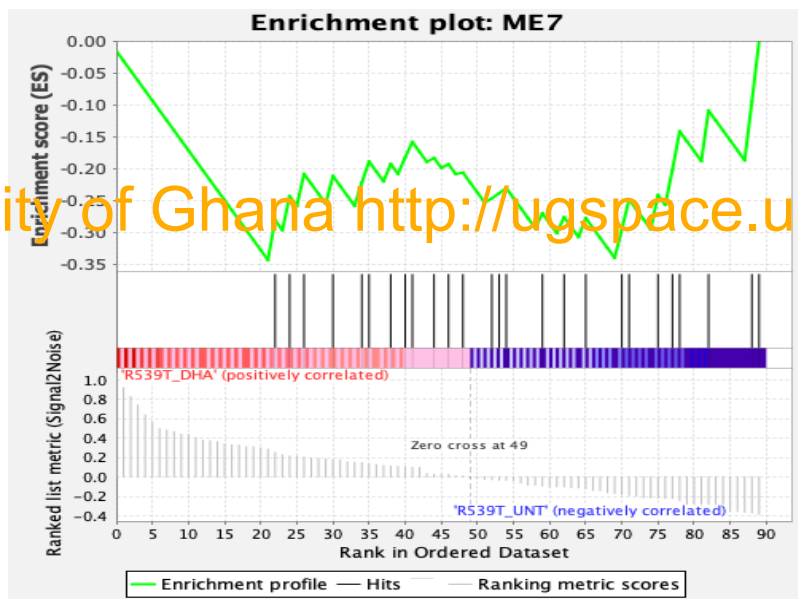

University of Ghana http://ugspace.ug.edu.gh

Fig 1: Enrichment plot: ME7
Profile of the Running ES Score & Positions of GeneSet Members on the Rank Ordered List

Table: GSEA details [plain text format]

	SYMBOL	TITLE	RANK IN GENE LIST	RANK METRIC SCORE	RUNNING ES	CORE ENRICHMENT
1	PF3D7_0115150	NA	22	0.250	-0.2813	No
2	PF3D7_0401500	NA	24	0.214	-0.2436	No
3	PF3D7_1240700	NA	26	0.202	-0.2087	No
4	PF3D7_1480100	NA	30	0.175	-0.2120	No
5	PF3D7_1400100	NA	34	0.146	-0.2223	No
6	PF3D7_0221650	NA	35	0.132	-0.1892	No
7	PF3D7_0114400	NA	38	0.109	-0.1932	No
8	PF3D7_0712500	NA	40	0.104	-0.1828	No
9	PF3D7_0413400	NA	41	0.097	-0.1586	No
10	PF3D7_0425000	NA	44	0.025	-0.1837	No
11	PF3D7_1240200	NA	46	0.024	-0.1934	No
12	PF3D7_0302300	NA	48	0.009	-0.2067	No
13	PF3D7_0402800	NA	52	-0.026	-0.2471	No
14	PF3D7_0632600	NA	53	-0.032	-0.2391	No
15	PF3D7_0713300	NA	54	-0.032	-0.2310	No
16	PF3D7_1219400	NA	59	-0.093	-0.2704	No
17	PF3D7_1000900	NA	62	-0.101	-0.2766	No
18	PF3D7_1219500	NA	65	-0.120	-0.2779	No
19	PF3D7_0114300	NA	70	-0.180	-0.2956	Yes
20	PF3D7_1401050	NA	71	-0.188	-0.2487	Yes
21	PF3D7_0421600	NA	75	-0.215	-0.2418	Yes
22	PF3D7_0221300	NA	77	-0.220	-0.2024	Yes
23	PF3D7_0421500	NA	78	-0.243	-0.1418	Yes
24	PF3D7_0221900	NA	82	-0.318	-0.1093	Yes
25	PF3D7_1478400	NA	88	-0.369	-0.0954	Yes
26	PF3D7_0114600	NA	89	-0.382	-0.0000	Yes

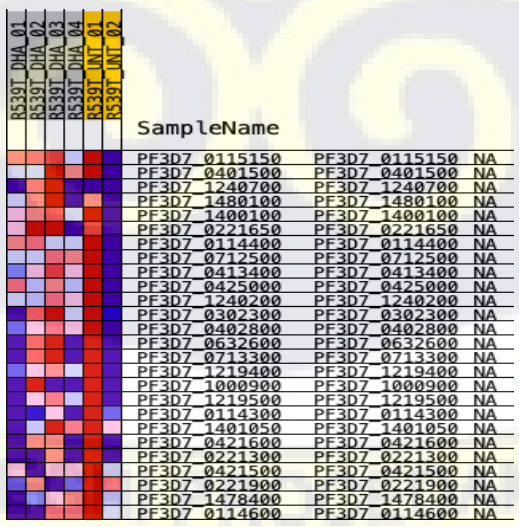

Fig 2: ME7
Blue-Pink O' Gram in the Space of the Analyzed GeneSet

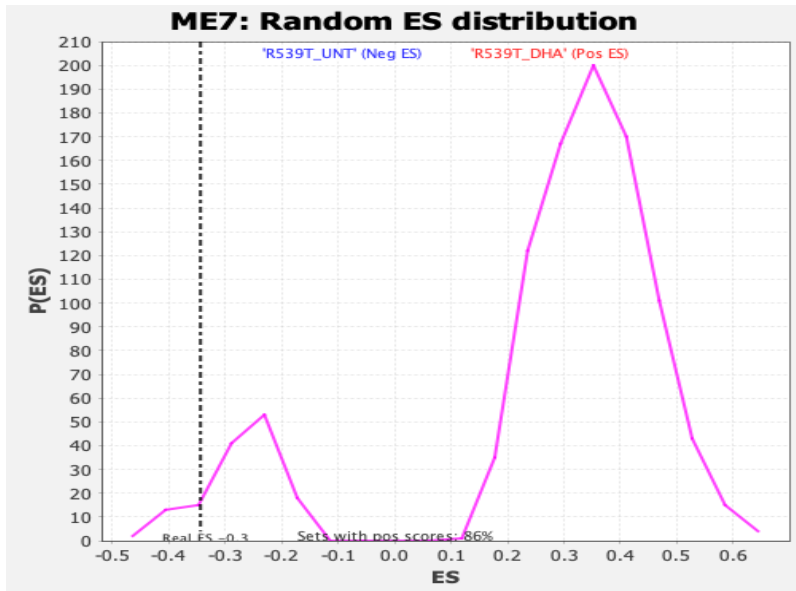

Fig 3: ME7: Random ES distribution
Gene set null distribution of ES for ME7

Supplementary Data 5.10 Summary of GSEA output for R539T_DHA_treated versus R539T_DMSO_treated showing association with module 7

Table: GSEA Results Summary

Dataset	Expression_dataset_dataset_collapsed_to_symbols.PhenotypeData.cls #R539T_DHA_versus_R539T_DMSO.PhenotypeData.cls #R539T_DHA_versus_R539T_DMSO_repos
Phenotype	PhenotypeData.cls#R539T_DHA_versus_R539T_DMSO_repos
Upregulated in class	R539T_DMSO
GeneSet	ME7
Enrichment Score (ES)	-0.31506842
Normalized Enrichment Score (NES)	-1.141659
Nominal p-value	0.19767442
FDR q-value	0.43728814
FWER p-Value	0.066

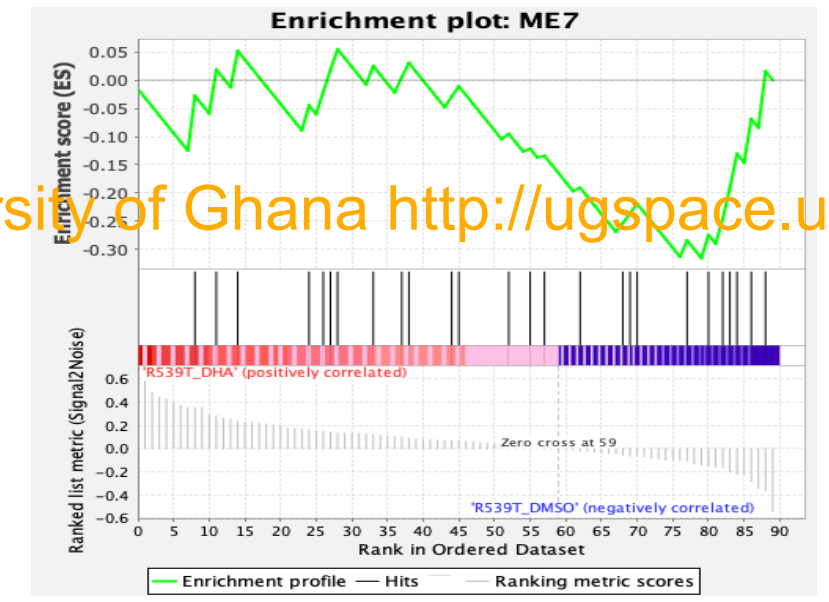

University of Ghana http://ugspace.ug.edu.gh

Fig 1: Enrichment plot: ME7
Profile of the Running ES Score & Positions of GeneSet Members on the Rank Ordered List

Table: GSEA details [plain text format]

	SYMBOL	TITLE	RANK IN GENE LIST	RANK METRIC SCORE	RUNNING ES	CORE ENRICHMENT
1	PF3D7_1240200	NA	8	0.353	-0.0279	No
2	PF3D7_1480100	NA	11	0.282	0.0185	No
3	PF3D7_1400100	NA	14	0.234	0.0516	No
4	PF3D7_0115150	NA	24	0.161	-0.0447	No
5	PF3D7_0425000	NA	26	0.146	-0.0203	No
6	PF3D7_0302300	NA	27	0.139	0.0179	No
7	PF3D7_1219500	NA	28	0.133	0.0546	No
8	PF3D7_0413400	NA	33	0.119	0.0249	No
9	PF3D7_0114300	NA	37	0.099	0.0054	No
10	PF3D7_0402800	NA	38	0.091	0.0303	No
11	PF3D7_1240700	NA	44	0.068	-0.0291	No
12	PF3D7_1401050	NA	45	0.066	-0.0110	No
13	PF3D7_0401500	NA	52	0.035	-0.0951	No
14	PF3D7_0632600	NA	55	0.018	-0.1215	No
15	PF3D7_0114400	NA	57	0.012	-0.1339	No
16	PF3D7_0221300	NA	62	-0.022	-0.1904	No
17	PF3D7_1478400	NA	68	-0.057	-0.2528	No
18	PF3D7_0221900	NA	69	-0.061	-0.2360	No
19	PF3D7_1219400	NA	70	-0.062	-0.2191	No
20	PF3D7_0712500	NA	77	-0.105	-0.2838	Yes
21	PF3D7_0221650	NA	80	-0.149	-0.2742	Yes
22	PF3D7_0114600	NA	82	-0.160	-0.2458	Yes
23	PF3D7_1000900	NA	83	-0.199	-0.1910	Yes
24	PF3D7_0421500	NA	84	-0.220	-0.1305	Yes
25	PF3D7_0713300	NA	86	-0.282	-0.0687	Yes
26	PF3D7_0421600	NA	88	-0.363	0.0156	Yes

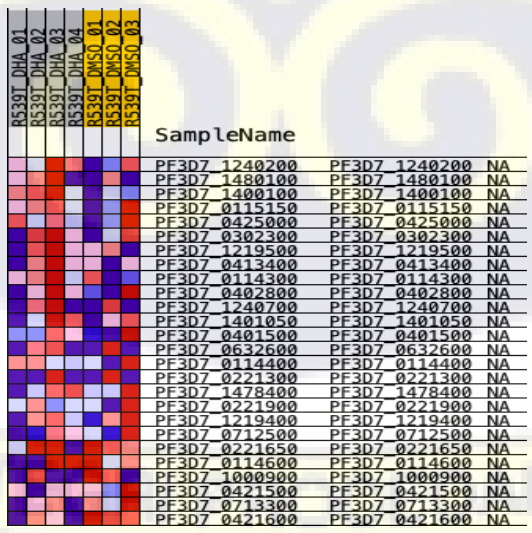

Fig 2: ME7
Blue-Pink O' Gram in the Space of the Analyzed GeneSet

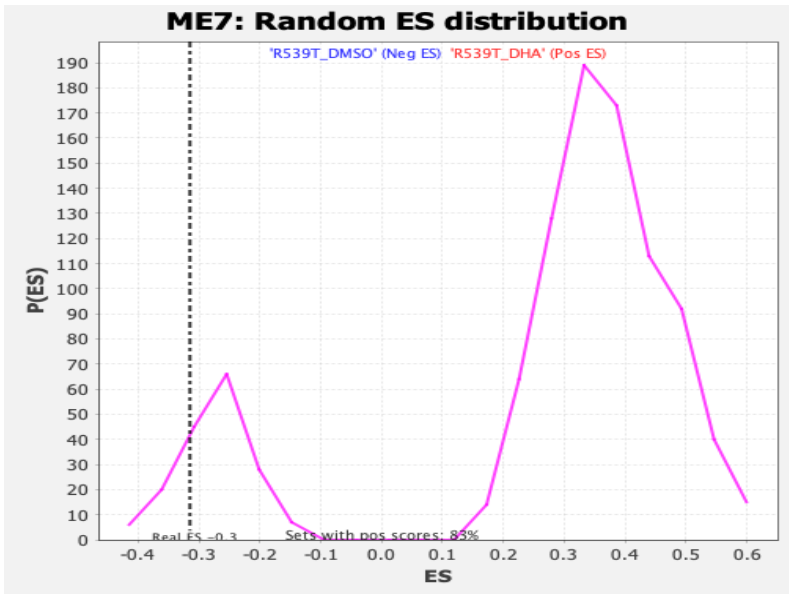

Fig 3: ME7: Random ES distribution
Gene set null distribution of ES for ME7

Supplementary Data 5.11 Summary of GSEA output for R539T_DHA_treated versus DD2_DHA_treated

Table: GSEA Results Summary

Dataset	Expression_dataset_dataset_collapsed_to_symbols.PhenotypeData.cls #R539T_DHA_versus_DD2_DHA.PhenotypeData.cls #R539T_DHA_versus_DD2_DHA_repos
Phenotype	PhenotypeData.cls#R539T_DHA_versus_DD2_DHA_repos
Upregulated in class	R539T_DHA
GeneSet	ME7
Enrichment Score (ES)	0.25544685
Normalized Enrichment Score (NES)	0.6829786
Nominal p-value	0.9445585
FDR q-value	0.9447514
FWER p-Value	0.7

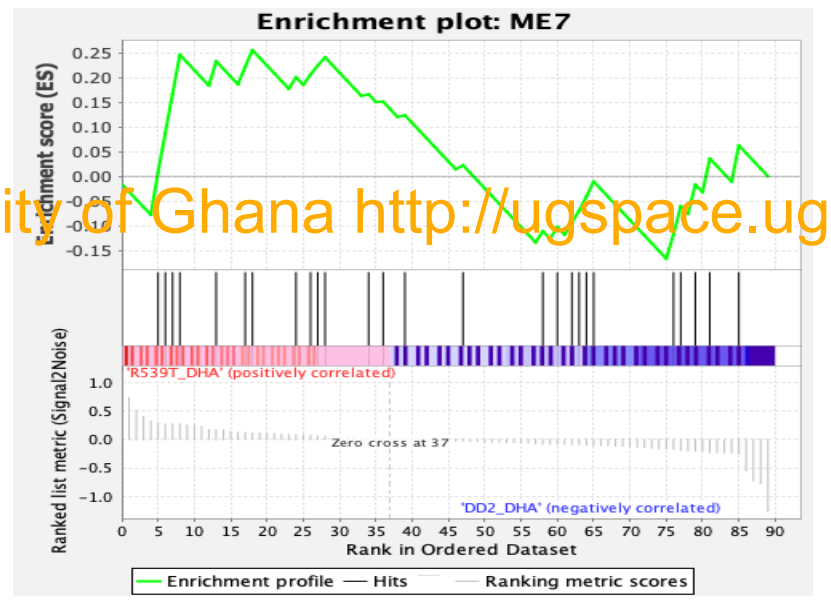

University of Ghana http://ugspace.ug.edu.gh

Fig 1: Enrichment plot: ME7
Profile of the Running ES Score & Positions of GeneSet Members on the Rank Ordered List

Table: GSEA details [plain text format]

	SYMBOL	TITLE	RANK IN GENE LIST	RANK METRIC SCORE	RUNNING ES	CORE ENRICHMENT
1	PF3D7_0221900	NA	5	0.295	0.0086	Yes
2	PF3D7_0115150	NA	6	0.270	0.0882	Yes
3	PF3D7_0402800	NA	7	0.269	0.1675	Yes
4	PF3D7_0401500	NA	8	0.267	0.2461	Yes
5	PF3D7_0425000	NA	13	0.168	0.2331	Yes
6	PF3D7_0413400	NA	17	0.121	0.2218	Yes
7	PF3D7_1240200	NA	18	0.114	0.2554	Yes
8	PF3D7_0421500	NA	24	0.079	0.2007	No
9	PF3D7_1400100	NA	26	0.072	0.2062	No
10	PF3D7_1401050	NA	27	0.062	0.2245	No
11	PF3D7_1480100	NA	28	0.056	0.2410	No
12	PF3D7_1219400	NA	34	0.011	0.1660	No
13	PF3D7_1219500	NA	36	0.003	0.1512	No
14	PF3D7_0114400	NA	39	-0.012	0.1236	No
15	PF3D7_0632600	NA	47	-0.027	0.0223	No
16	PF3D7_0114600	NA	58	-0.078	-0.1110	No
17	PF3D7_0221300	NA	60	-0.082	-0.1026	No
18	PF3D7_0114300	NA	62	-0.083	-0.0939	No
19	PF3D7_0713300	NA	63	-0.083	-0.0694	No
20	PF3D7_1240700	NA	64	-0.096	-0.0412	No
21	PF3D7_0712500	NA	65	-0.104	-0.0105	No
22	PF3D7_1478400	NA	76	-0.167	-0.1176	No
23	PF3D7_0221650	NA	77	-0.194	-0.0606	No
24	PF3D7_1000900	NA	79	-0.202	-0.0167	No
25	PF3D7_0302300	NA	81	-0.232	0.0360	No
26	PF3D7_0421600	NA	85	-0.249	0.0625	No

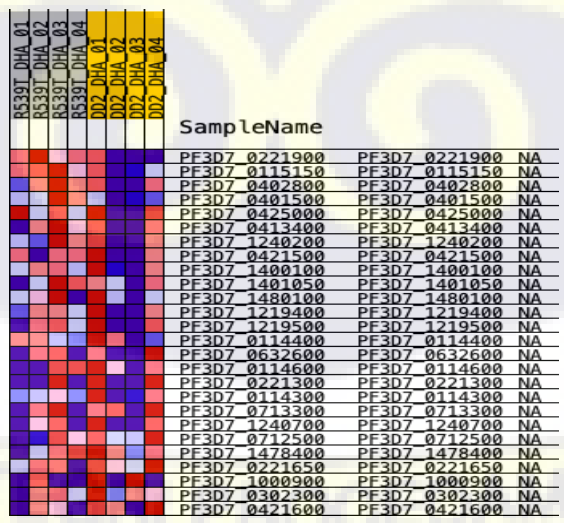

Fig 2: ME7
Blue-Pink O' Gram in the Space of the Analyzed GeneSet

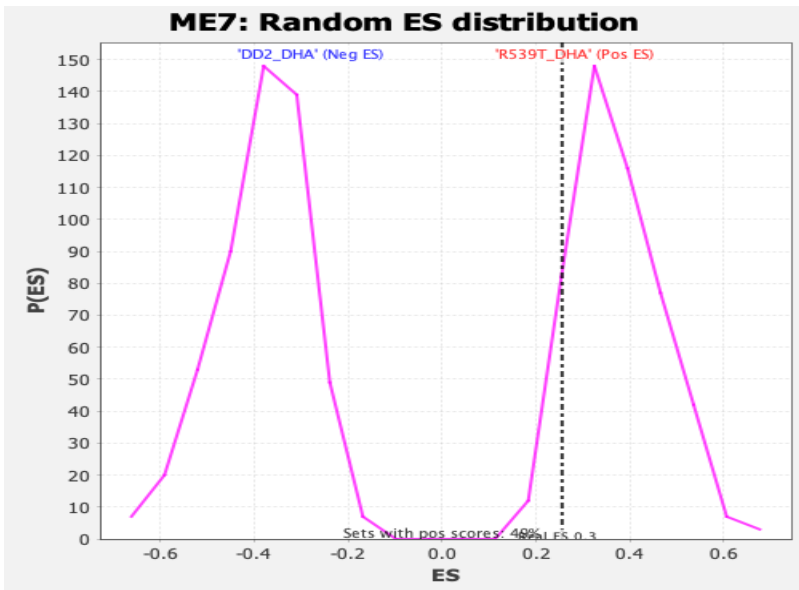

Fig 3: ME7: Random ES distribution
Gene set null distribution of ES for ME7

Supplementary Data 5.12 Summary of GSEA output for C580R_DHA_treated versus C580R_untreated showing association with module 7

Table: GSEA Results Summary

Dataset	Expression_dataset_dataset_collapsed_to_symbols.PhenotypeData.cls #C580R_DHA_versus_C580R_UNT.PhenotypeData.cls #C580R_DHA_versus_C580R_UNT_repos
Phenotype	PhenotypeData.cls#C580R_DHA_versus_C580R_UNT_repos
Upregulated in class	C580R_UNT
GeneSet	ME7
Enrichment Score (ES)	-0.8752158
Normalized Enrichment Score (NES)	-2.4335837
Nominal p-value	0.0
FDR q-value	0.0
FWER p-Value	0.0

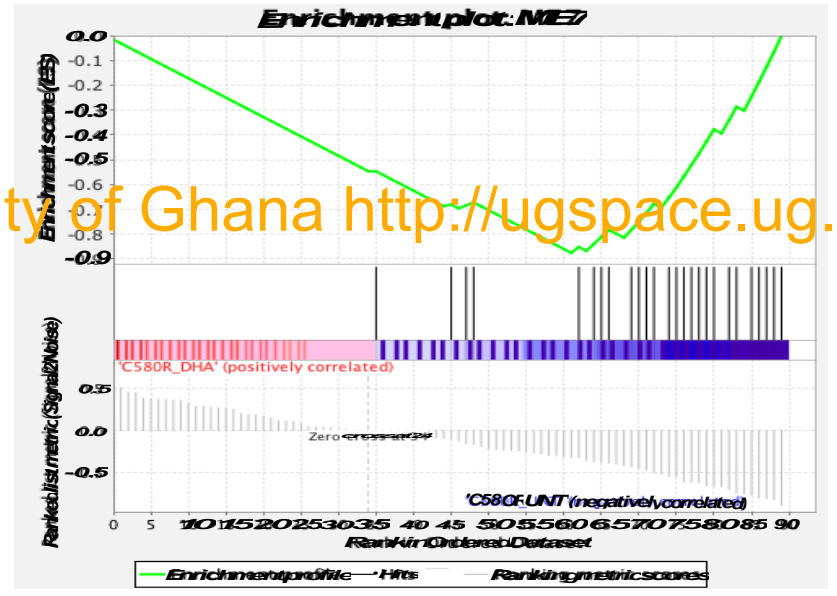

University of Ghana http://ugspace.ug.edu.gh

Fig 1: Enrichment plot: ME7
Profile of the Running ES Score & Positions of GeneSet Members on the Rank Ordered List

Table: GSEA details [plain text format]

	SYMBOL	TITLE	RANK IN GENE LIST	RANK METRIC SCORE	RUNNING ES	CORE ENRICHMENT
1	PF3D7_0114400	NA	35	-0.001	-0.5468	No
2	PF3D7_0221300	NA	45	-0.097	-0.6801	No
3	PF3D7_0401500	NA	47	-0.156	-0.6841	No
4	PF3D7_1219500	NA	48	-0.160	-0.6721	No
5	PF3D7_1000900	NA	62	-0.318	-0.8515	Yes
6	PF3D7_0421500	NA	64	-0.368	-0.8396	Yes
7	PF3D7_0114300	NA	65	-0.379	-0.8113	Yes
8	PF3D7_1240200	NA	66	-0.381	-0.7829	Yes
9	PF3D7_0425000	NA	69	-0.427	-0.7822	Yes
10	PF3D7_0221900	NA	70	-0.442	-0.7493	Yes
11	PF3D7_0115150	NA	71	-0.464	-0.7146	Yes
12	PF3D7_0302300	NA	72	-0.495	-0.6777	Yes
13	PF3D7_0221650	NA	74	-0.542	-0.6528	Yes
14	PF3D7_0632600	NA	75	-0.545	-0.6121	Yes
15	PF3D7_0713300	NA	76	-0.607	-0.5668	Yes
16	PF3D7_1480100	NA	77	-0.609	-0.5213	Yes
17	PF3D7_1219400	NA	78	-0.615	-0.4754	Yes
18	PF3D7_1240700	NA	79	-0.650	-0.4269	Yes
19	PF3D7_1400100	NA	80	-0.655	-0.3780	Yes
20	PF3D7_0114600	NA	82	-0.695	-0.3417	Yes
21	PF3D7_0413400	NA	83	-0.738	-0.2867	Yes
22	PF3D7_1478400	NA	85	-0.761	-0.2455	Yes
23	PF3D7_0402800	NA	86	-0.794	-0.1862	Yes
24	PF3D7_0421600	NA	87	-0.802	-0.1263	Yes
25	PF3D7_0712500	NA	88	-0.814	-0.0656	Yes
26	PF3D7_1401050	NA	89	-0.878	-0.0000	Yes

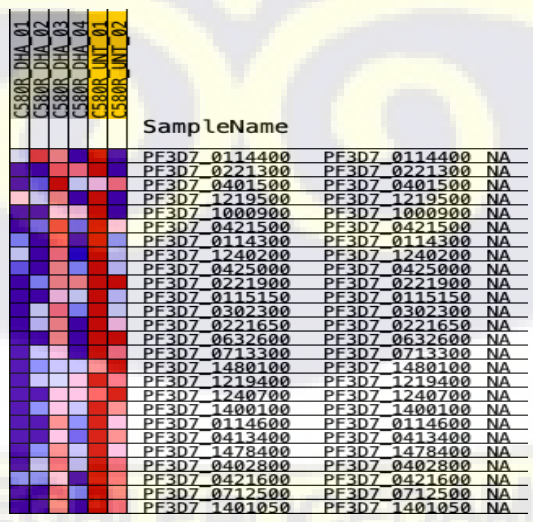

Fig 2: ME7
Blue-Pink O' Gram in the Space of the Analyzed GeneSet

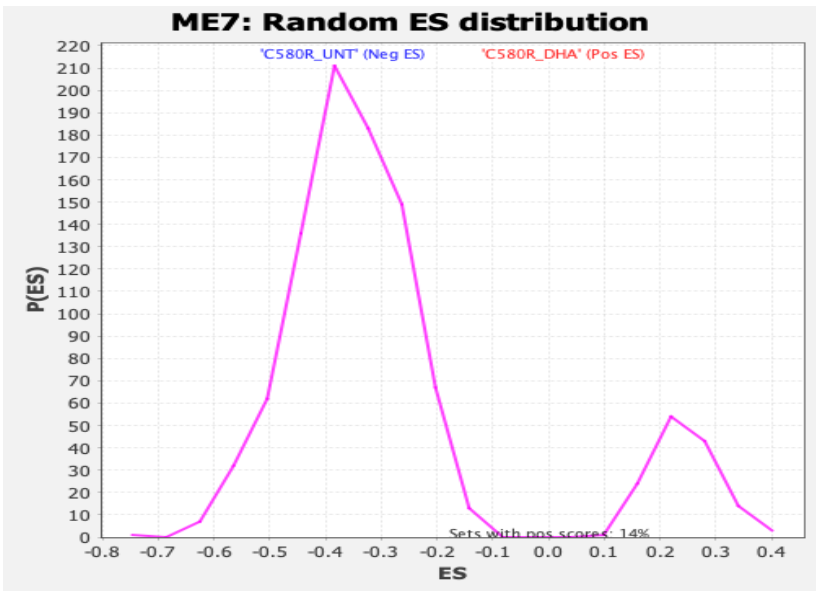

Fig 3: ME7: Random ES distribution
Gene set null distribution of ES for ME7

Supplementary Data 5.13 Summary of GSEA output for C580R_DHA_treated versus C580R_DMSO_treated

Table: GSEA Results Summary

Dataset	Expression_dataset_dataset_collapsed_to_symbols.PhenotypeData.cls #C580R_DHA_versus_C580R_DMSO.PhenotypeData.cls #C580R_DHA_versus_C580R_DMSO_repos
Phenotype	PhenotypeData.cls#C580R_DHA_versus_C580R_DMSO_repos
Upregulated in class	C580R_DHA
GeneSet	ME7
Enrichment Score (ES)	0.5312583
Normalized Enrichment Score (NES)	1.2448145
Nominal p-value	0.120080724
FDR q-value	0.253
FWER p-Value	0.237

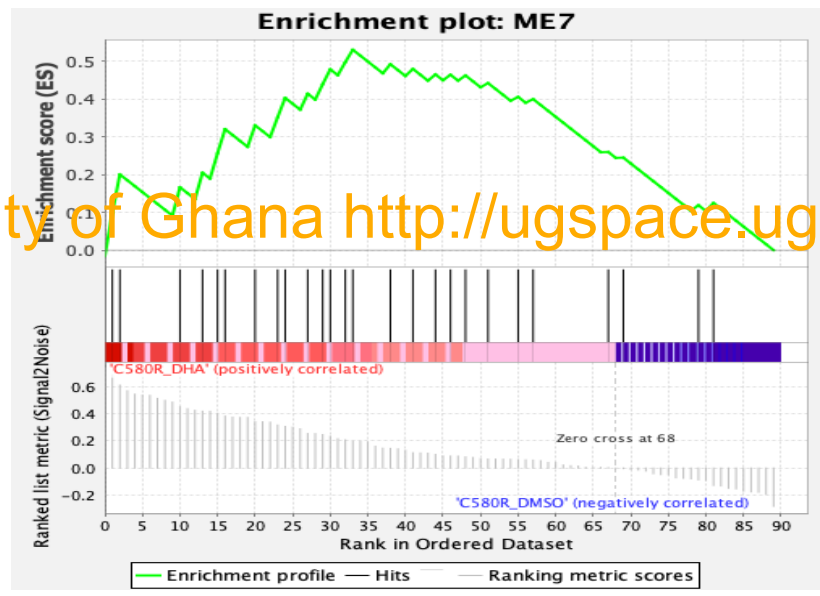

University of Ghana http://ugspace.ug.edu.gh

Fig 1: Enrichment plot: ME7
Profile of the Running ES Score & Positions of GeneSet Members on the Rank Ordered List

Table: GSEA details [plain text format]

	SYMBOL	TITLE	RANK IN GENE LIST	RANK METRIC SCORE	RUNNING ES	CORE ENRICHMENT
1	PF3D7_0401500	NA	1	0.685	0.0988	Yes
2	PF3D7_0115150	NA	2	0.610	0.2008	Yes
3	PF3D7_1478400	NA	10	0.450	0.1667	Yes
4	PF3D7_0421500	NA	13	0.418	0.2053	Yes
5	PF3D7_0221650	NA	15	0.402	0.2570	Yes
6	PF3D7_0114400	NA	16	0.382	0.3208	Yes
7	PF3D7_0402800	NA	20	0.341	0.3309	Yes
8	PF3D7_0221900	NA	23	0.316	0.3525	Yes
9	PF3D7_1240200	NA	24	0.306	0.4036	Yes
10	PF3D7_1219400	NA	27	0.254	0.4148	Yes
11	PF3D7_0221300	NA	29	0.246	0.4403	Yes
12	PF3D7_1219500	NA	30	0.234	0.4794	Yes
13	PF3D7_1000900	NA	32	0.207	0.4984	Yes
14	PF3D7_0413400	NA	33	0.197	0.5313	Yes
15	PF3D7_0302300	NA	38	0.144	0.4929	No
16	PF3D7_0114300	NA	41	0.112	0.4804	No
17	PF3D7_1240700	NA	44	0.100	0.4659	No
18	PF3D7_0114600	NA	46	0.088	0.4650	No
19	PF3D7_1480100	NA	48	0.082	0.4631	No
20	PF3D7_0712500	NA	51	0.066	0.4429	No
21	PF3D7_0425000	NA	55	0.062	0.4064	No
22	PF3D7_1401050	NA	57	0.058	0.4004	No
23	PF3D7_1400100	NA	67	0.003	0.2602	No
24	PF3D7_0632600	NA	69	-0.004	0.2453	No
25	PF3D7_0421600	NA	79	-0.087	0.1192	No
26	PF3D7_0713300	NA	81	-0.128	0.1250	No

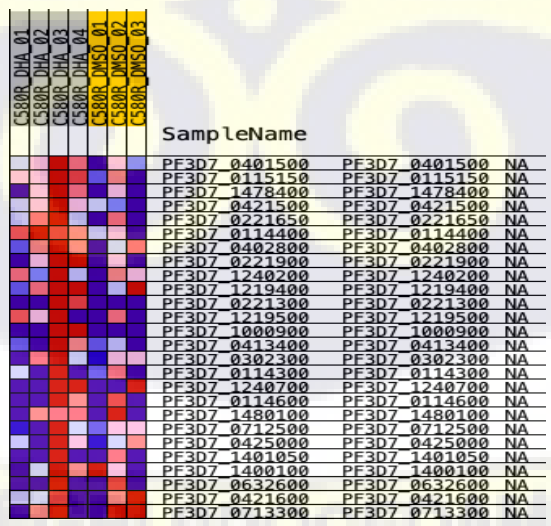

Fig 2: ME7
Blue-Pink O' Gram in the Space of the Analyzed GeneSet

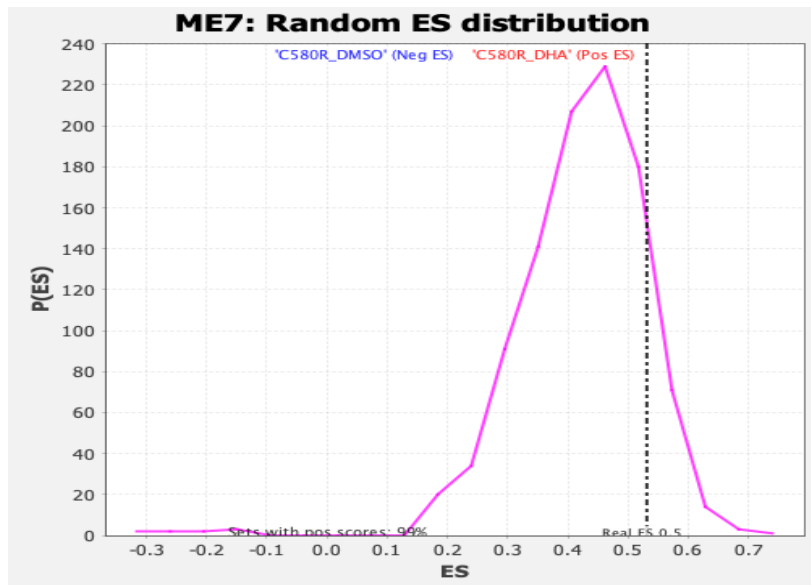

Fig 3: ME7: Random ES distribution
Gene set null distribution of ES for ME7

Supplementary Data 5.14 Summary of GSEA output for C580R_DHA_treated versus DD2_DHA_treated showing association with module 7

Table: GSEA Results Summary

Dataset	Expression_dataset_dataset_collapsed_to_symbols.PhenotypeData.cls #C580R_DHA_versus_DD2_DHA.PhenotypeData.cls #C580R_DHA_versus_DD2_DHA_repos
Phenotype	PhenotypeData.cls#C580R_DHA_versus_DD2_DHA_repos
Upregulated in class	C580R_DHA
GeneSet	ME7
Enrichment Score (ES)	0.41607258
Normalized Enrichment Score (NES)	1.088161
Nominal p-value	0.3448795
FDR q-value	0.686584
FWER p-Value	0.406

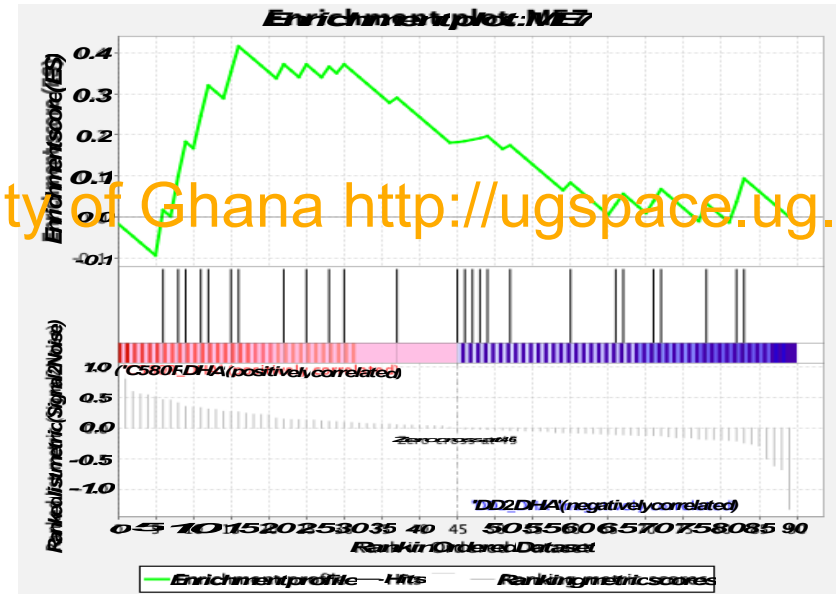

University of Ghana http://ugspace.ug.edu.gh

Fig 1: Enrichment plot: ME7
Profile of the Running ES Score & Positions of GeneSet Members on the Rank Ordered List

Table: GSEA details [plain text format]

	SYMBOL	TITLE	RANK IN GENE LIST	RANK METRIC SCORE	RUNNING ES	CORE ENRICHMENT
1	PF3D7_0425000	NA	6	0.464	0.0169	Yes
2	PF3D7_0401500	NA	8	0.411	0.0994	Yes
3	PF3D7_0421500	NA	9	0.352	0.1832	Yes
4	PF3D7_0402800	NA	11	0.332	0.2469	Yes
5	PF3D7_0221900	NA	12	0.309	0.3206	Yes
6	PF3D7_0115150	NA	15	0.268	0.3533	Yes
7	PF3D7_1240200	NA	16	0.263	0.4161	Yes
8	PF3D7_0413400	NA	22	0.144	0.3723	No
9	PF3D7_1219400	NA	25	0.130	0.3720	No
10	PF3D7_0114400	NA	28	0.107	0.3662	No
11	PF3D7_0221300	NA	30	0.091	0.3722	No
12	PF3D7_0221650	NA	37	0.051	0.2906	No
13	PF3D7_1219500	NA	45	-0.005	0.1823	No
14	PF3D7_1240700	NA	46	-0.011	0.1850	No
15	PF3D7_0114300	NA	47	-0.015	0.1885	No
16	PF3D7_0421600	NA	48	-0.015	0.1922	No
17	PF3D7_1478400	NA	49	-0.021	0.1972	No
18	PF3D7_0713300	NA	52	-0.037	0.1747	No
19	PF3D7_1401050	NA	60	-0.077	0.0837	No
20	PF3D7_0632600	NA	66	-0.105	0.0307	No
21	PF3D7_1000900	NA	67	-0.107	0.0564	No
22	PF3D7_0114600	NA	71	-0.121	0.0383	No
23	PF3D7_1480100	NA	72	-0.124	0.0679	No
24	PF3D7_0712500	NA	78	-0.183	0.0335	No
25	PF3D7_1400100	NA	82	-0.208	0.0362	No
26	PF3D7_0302300	NA	83	-0.241	0.0938	No

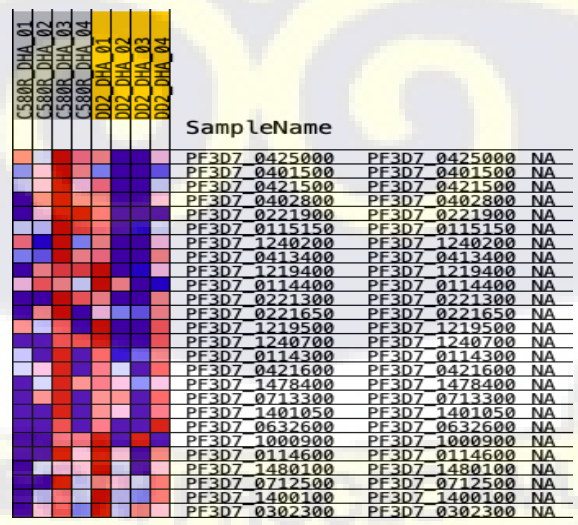

Fig 2: ME7
Blue-Pink O' Gram in the Space of the Analyzed GeneSet

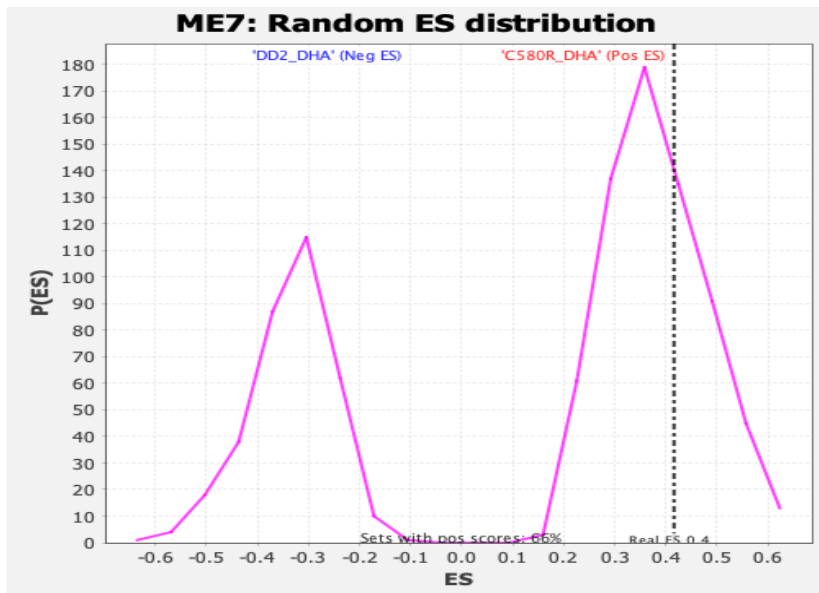

Fig 3: ME7: Random ES distribution
Gene set null distribution of ES for ME7

Supplementary Data 5.15 Summary of GSEA output for DD2_DHA_treated versus DD2_untreated

Table: GSEA Results Summary

Dataset	Expression_dataset_dataset_collapsed_to_symbols.PhenotypeData.cls #DD2_DHA_versus_DD2_UNT.PhenotypeData.cls #DD2_DHA_versus_DD2_UNT_repos
Phenotype	PhenotypeData.cls#DD2_DHA_versus_DD2_UNT_repos
Upregulated in class	DD2_UNT
GeneSet	ME7
Enrichment Score (ES)	-0.6388882
Normalized Enrichment Score (NES)	-2.2366247
Nominal p-value	0.0
FDR q-value	0.0
FWER p-Value	0.0

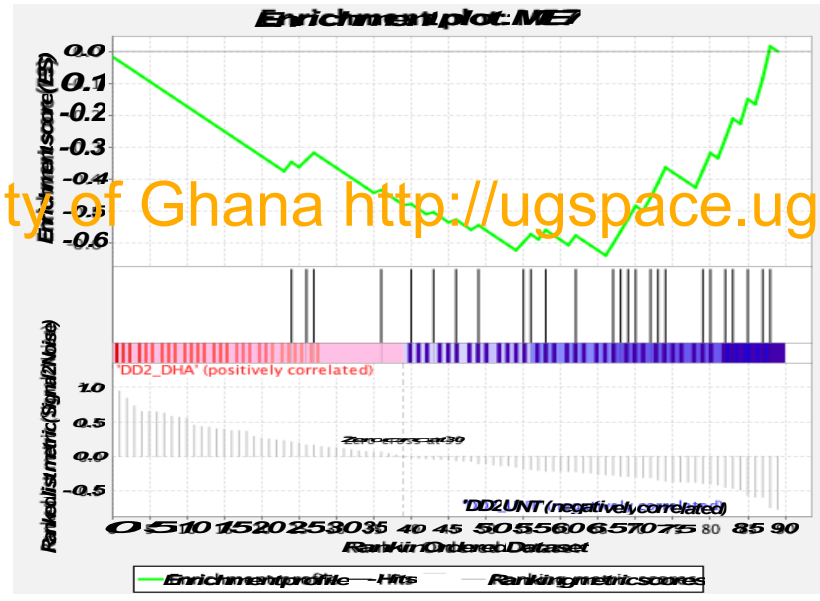

Fig 1: Enrichment plot: ME7
Profile of the Running ES Score & Positions of GeneSet Members on the Rank Ordered List

Table: GSEA details [plain text format]

	SYMBOL	TITLE	RANK IN GENE LIST	RANK METRIC SCORE	RUNNING ES	CORE ENRICHMENT
1	PF3D7_0632600	NA	24	0.208	-0.3466	No
2	PF3D7_1401050	NA	26	0.163	-0.3398	No
3	PF3D7_1000900	NA	27	0.163	-0.3176	No
4	PF3D7_0302300	NA	36	0.061	-0.4342	No
5	PF3D7_0114400	NA	40	-0.022	-0.4780	No
6	PF3D7_0221650	NA	43	-0.039	-0.5039	No
7	PF3D7_0401500	NA	46	-0.060	-0.5270	No
8	PF3D7_0221300	NA	49	-0.101	-0.5445	No
9	PF3D7_0421600	NA	55	-0.181	-0.5979	No
10	PF3D7_0713300	NA	56	-0.185	-0.5726	No
11	PF3D7_0114300	NA	58	-0.211	-0.5593	No
12	PF3D7_1219400	NA	62	-0.218	-0.5764	No
13	PF3D7_1478400	NA	67	-0.268	-0.6022	Yes
14	PF3D7_0114600	NA	68	-0.283	-0.5635	Yes
15	PF3D7_1400100	NA	69	-0.286	-0.5244	Yes
16	PF3D7_0115150	NA	70	-0.296	-0.4839	Yes
17	PF3D7_0712500	NA	72	-0.305	-0.4578	Yes
18	PF3D7_0221900	NA	73	-0.336	-0.4119	Yes
19	PF3D7_1219500	NA	74	-0.354	-0.3635	Yes
20	PF3D7_1480100	NA	79	-0.388	-0.3729	Yes
21	PF3D7_0421500	NA	80	-0.397	-0.3185	Yes
22	PF3D7_1240700	NA	82	-0.443	-0.2736	Yes
23	PF3D7_0425000	NA	83	-0.459	-0.2108	Yes
24	PF3D7_0413400	NA	85	-0.560	-0.1499	Yes
25	PF3D7_1240200	NA	87	-0.587	-0.0852	Yes
26	PF3D7_0402800	NA	88	-0.738	0.0156	Yes

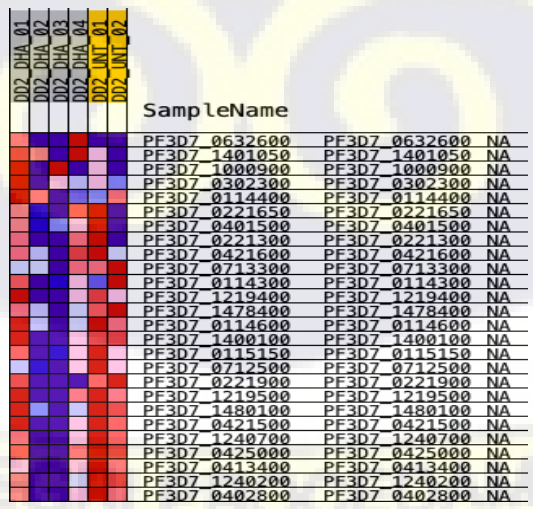

Fig 2: ME7
Blue-Pink O' Gram in the Space of the Analyzed GeneSet

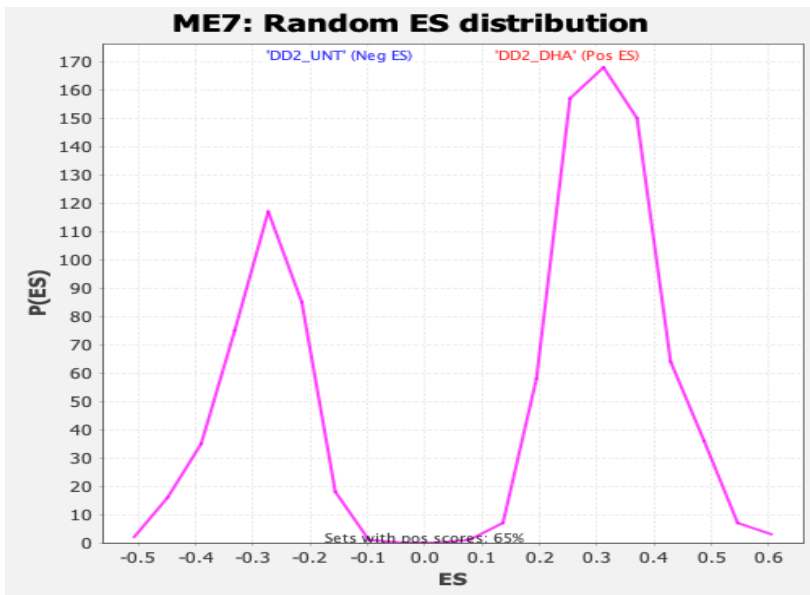

Fig 3: ME7: Random ES distribution
Gene set null distribution of ES for ME7

University of Ghana http://ugspace.ug.edu.gh

Supplementary Data 5.16 Summary of GSEA output for DD2_DHA_treated versus DD2_DMSO_treated showing association with module 7

Table: GSEA Results Summary

Dataset	Expression_dataset_dataset_collapsed_to_symbols.PhenotypeData.cls #DD2_DHA_versus_DD2_DMSO.PhenotypeData.cls #DD2_DHA_versus_DD2_DMSO_repos
Phenotype	PhenotypeData.cls#DD2_DHA_versus_DD2_DMSO_repos
Upregulated in class	DD2_DMSO
GeneSet	ME7
Enrichment Score (ES)	-0.21875
Normalized Enrichment Score (NES)	-0.9836254
Nominal p-value	0.42857143
FDR q-value	0.51960784
FWER p-Value	0.05

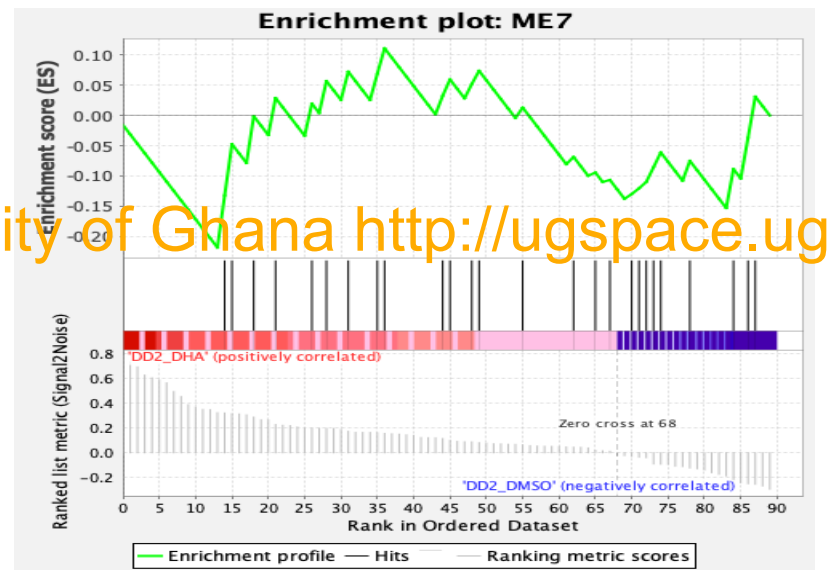

University of Ghana http://ugspace.ug.edu.gh

Fig 1: Enrichment plot: ME7
Profile of the Running ES Score & Positions of GeneSet Members on the Rank Ordered List

Table: GSEA details [plain text format]

	SYMBOL	TITLE	RANK IN GENE LIST	RANK METRIC SCORE	RUNNING ES	CORE ENRICHMENT
1	PF3D7_1480100	NA	14	0.320	-0.1323	Yes
2	PF3D7_1000900	NA	15	0.314	-0.0474	Yes
3	PF3D7_0114300	NA	18	0.287	-0.0012	Yes
4	PF3D7_1219400	NA	21	0.227	0.0290	Yes
5	PF3D7_0114400	NA	26	0.197	0.0197	Yes
6	PF3D7_0421500	NA	28	0.196	0.0571	Yes
7	PF3D7_1240200	NA	31	0.173	0.0725	Yes
8	PF3D7_1478400	NA	35	0.161	0.0692	Yes
9	PF3D7_1401050	NA	36	0.156	0.1113	Yes
10	PF3D7_0632600	NA	44	0.114	0.0328	Yes
11	PF3D7_0401500	NA	45	0.100	0.0597	Yes
12	PF3D7_0712500	NA	48	0.088	0.0521	Yes
13	PF3D7_0221650	NA	49	0.081	0.0740	Yes
14	PF3D7_0302300	NA	55	0.064	0.0131	Yes
15	PF3D7_0713300	NA	62	0.045	-0.0686	Yes
16	PF3D7_0413400	NA	65	0.020	-0.0945	Yes
17	PF3D7_1219500	NA	67	0.013	-0.1068	Yes
18	PF3D7_0425000	NA	70	-0.029	-0.1301	Yes
19	PF3D7_0421600	NA	71	-0.035	-0.1206	Yes
20	PF3D7_1240700	NA	72	-0.039	-0.1101	Yes
21	PF3D7_0114600	NA	73	-0.090	-0.0858	Yes
22	PF3D7_0221300	NA	74	-0.091	-0.0612	Yes
23	PF3D7_1400100	NA	78	-0.122	-0.0751	Yes
24	PF3D7_0115150	NA	84	-0.239	-0.0887	Yes
25	PF3D7_0402800	NA	86	-0.249	-0.0370	Yes
26	PF3D7_0221900	NA	87	-0.253	0.0312	Yes

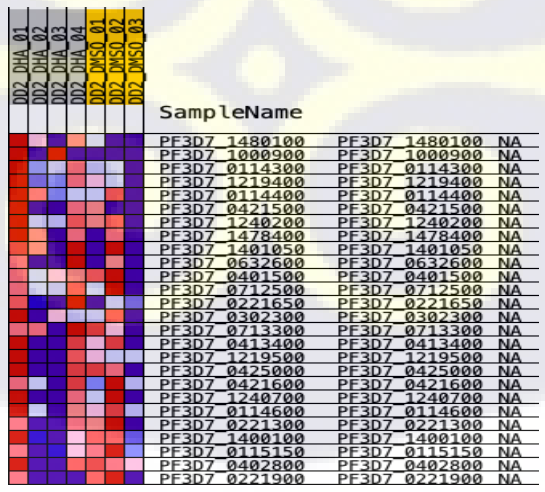

Fig 2: ME7
Blue-Pink O' Gram in the Space of the Analyzed GeneSet

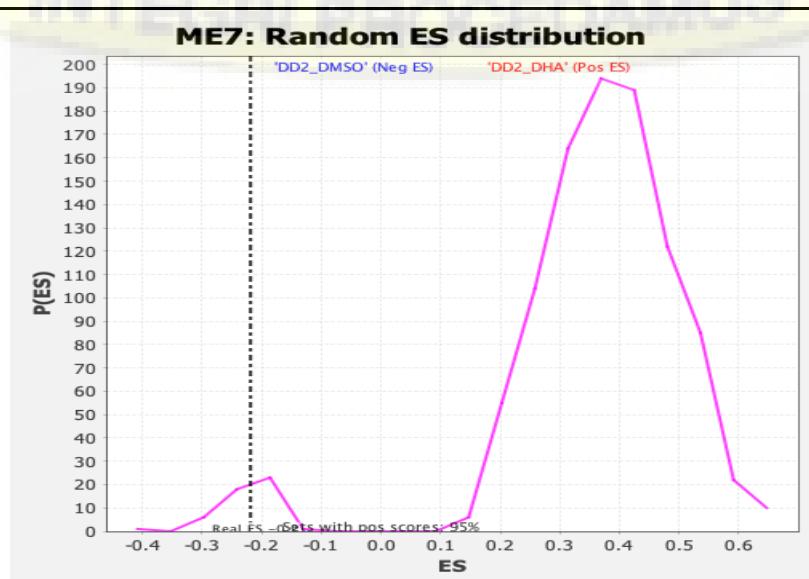

Fig 3: ME7: Random ES distribution
Gene set null distribution of ES for ME7

Supplementary Data 5.17 Summary of gene ontology enrichment in the biological processes terms for DHA_treated condition compared to the untreated condition baseline

	UP regulated	DOWN regulated
DD2	Nil significantly enriched biological processes	biological process involved in symbiotic interaction biological process involved in interspecies interaction between organisms movement in host environment entry into host biological process biological process involved in interaction with host immunoglobulin production production of molecular mediator of immune response regulation of immune response regulation of immune system process immune system process obsolete pathogenesis cell adhesion biological adhesion cell-cell adhesion
C580R	obsolete pathogenesis cell-cell adhesion cell adhesion cytoadherence to microvasculature, mediated by symbiont protein adhesion of symbiont to host antigenic variation modulation by symbiont of host erythrocyte aggregation modulation by symbiont of host cellular process evasion of host immune response modulation by symbiont of host process biological adhesion response to host immune response response to host defenses response to defenses of other organism response to other organism response to external biotic stimulus response to host biological process involved in interaction with host biological process involved in symbiotic interaction biological process involved in interspecies interaction between organisms biological process	movement in host environment entry into host biological process involved in symbiotic interaction biological process involved in interspecies interaction between organisms biological process biological process involved in interaction with host actin filament-based process actin cytoskeleton organization actin filament organization actin filament-based movement exit from host cell exit from host supramolecular fiber organization cell motility regulation of immune response production of molecular mediator of immune response immunoglobulin production regulation of immune system process immune system process actin polymerization or depolymerization actin filament-based transport vesicle transport along actin filament
R539T	Nil significantly enriched biological processes	movement in host environment entry into host biological process involved in symbiotic interaction biological process involved in interspecies interaction between organisms biological process involved in interaction with host biological process exit from host cell exit from host regulation of immune response immunoglobulin production production of molecular mediator of immune response regulation of immune system process immune system process actin filament organization actin filament-based process actin cytoskeleton organization supramolecular fiber organization protein phosphorylation

University of Ghana http://ugspace.ug.edu.gh

Appendix III

Supplementary Table 7.1 Summary data of EVs extraction experiment for all parasite lines and treatment conditions.

University of Ghana http://ugspace.ug.edu.gh

parasite	condition	replicate	sensitivity	parasitemia	mean_kcps	duration	kc_count	df1	df2	df3	kc_total	kc_norm	EV size (nm)	Intensity/100	EVs_count (x10^6)
Vps60_KO	untreated	1	sensitive	4.2	147.9	80	11832	0.25	0.3	0.1	1577600	375619.0476	213.4	0.945	354.96
Vps60_KO	untreated	2	sensitive	4.4	117.8	90	10602	0.25	0.3	0.1	1413600	321272.7273	192	1	321.2727273
Vps60_KO	untreated	3	sensitive	4.5	137.4	80	10992	0.5	0.3	0.1	732800	162844.4444	205.4	0.984	160.2389333
Vps60_KO	DMSO	1	sensitive	4.1	19.9	130	2587	0.2	0.3	0.1	431166.667	105162.6016	281.8	0.838	88.12626016
Vps60_KO	DMSO	2	sensitive	4.3	25.2	240	6048	0.25	0.3	0.1	806400	187534.8837	160.3	0.723	135.5877209
Vps60_KO	DMSO	3	sensitive	4.4	24.8	170	4216	0.25	0.3	0.1	562133.333	127757.5758	179.8	0.728	93.00751515
Vps60_KO	DHA	1	sensitive	0.2	93	50	4650	0.05	0.3	0.1	3100000	3100000	267.6	0.507	1571.7
Vps60_KO	DHA	2	sensitive	0.1	93.5	90	8415	0.05	0.3	0.1	5610000	5610000	170.7	0.88	4936.8
Vps60_KO	DHA	3	sensitive	0.2	39.3	180	7074	0.2	0.3	0.1	1179000	1179000	228.5	0.74	872.46
3D7	untreated	1	sensitive	2.4	183.4	70	12838	0.25	0.3	0.1	1711733.33	713222.2222	213.5	1	713.2222222
3D7	untreated	2	sensitive	2.5	82.7	100	8270	0.35	0.3	0.1	787619.048	315047.619	225	0.96	302.4457143
3D7	untreated	3	sensitive	2.1	149.6	80	11968	0.45	0.3	0.1	886518.519	422151.6755	202.6	0.981	414.1307937
3D7	DMSO	1	sensitive	2.2	29.7	100	2970	0.1	0.3	0.1	990000	450000	215.6	0.889	400.05
3D7	DMSO	2	sensitive	2.3	117.9	100	11790	0.5	0.3	0.1	786000	341739.1304	212	0.988	337.6382609
3D7	DMSO	3	sensitive	2.2	219	50	10950	0.1	0.3	0.1	3650000	1659090.909	139.7	1	1659.090909
3D7	DHA	1	sensitive	0.5	49.9	140	6986	0.3	0.3	0.1	776222.222	776222.2222	225	0.88	683.0755556
3D7	DHA	2	sensitive	0.6	74.9	90	6741	0.3	0.3	0.1	749000	749000	248.2	0.935	700.315
3D7	DHA	3	sensitive	0.5	113.6	80	9088	0.2	0.3	0.1	1514666.67	1514666.667	229.5	0.907	1373.802667
R561H	untreated	1	resistant	2.4	152.7	80	12216	0.3	0.3	0.1	1357333.33	565555.5556	231.7	0.967	546.8922222

R561H	untreated	2	resistant	2.9	98.4	110	10824	0.4	0.3	0.1	902000	311034.4828	202.1	0.813	252.8710345
R561H	untreated	3	resistant	2.6	42.6	160	6816	0.2	0.3	0.1	1136000	436923.0769	174.4	0.862	376.6276923
R561H	DMSO	1	resistant	3	20.1	210	4221	0.15	0.3	0.1	938000	312666.6667	166.8	0.785	245.4433333
R561H	DMSO	2	resistant	2.8	65.6	120	7872	0.6	0.3	0.1	437333.333	156190.4762	229.1	0.87	135.8857143
R561H	DMSO	3	resistant	2.6	54.9	130	7137	0.15	0.3	0.1	1586000	610000	225.2	0.872	531.92
R561H	DHA	1	resistant	0.7	56.4	110	6204	0.3	0.3	0.1	689333.333	689333.3333	229.8	0.877	604.5453333
R561H	DHA	2	resistant	0.6	114.6	80	9168	0.2	0.3	0.1	1528000	1528000	250.5	0.913	1395.064
R561H	DHA	3	resistant	0.8	65.5	100	6550	0.3	0.3	0.1	727777.778	727777.7778	220	0.896	652.0888889

kc_count = mean_kcps x duration; kc_total = kc_count/ (df1 x df2 x df3); kc_norm = kc_total/ parasitemia for untreated and DMSO treated conditions; and is equal to kc_total for DHA treated conditions;EVs_count ($x10^6$) = kc_norm x Intensity/100

University of Ghana http://ugspace.ug.edu.gh

University of Ghana http://ugspace.ug.edu.gh

Supplementary Table 7.2 Post-hoc Dunn's test for the RSA analysis for 3D7, Vps60 and R561H. The p-values were adjusted for multiple testing with the Benjamini-Hochberg method.

Comparison	Z value	Unadjusted P-value	Adjusted P-value
3D7 versus R561H	-2.302104	2.132930e-02	3.199395e-02
3D7 versus Vps60_KO	2.195853	2.810245e-02	2.810245e-02
R561H versus Vps60_KO	4.497957	6.860944e-06	2.058283e-05

University of Ghana http://ugspace.ug.edu.gh

Supplementary Table 7.3 Analysis of EVs size distribution by parasite lines.

Parasite (n = 9)	mean	sd	min	Q1	median	Q3	max
Vps60_KO	211.0556	41.96511	160.3	179.8	205.4	228.5	281.8
3D7	212.3444	30.17549	139.7	212.0	215.6	225.0	248.2
R561H	214.4000	27.88548	166.8	202.1	225.2	229.8	250.5

University of Ghana http://ugspace.ug.edu.gh

Supplementary Table 7.4 Tabular summary of simple linear regression model to determine strength of the association between parasite line (predictor/independent factors) and EVs abundance (response/dependent factor) for the untreated condition. Baseline reference to which parasite lines were compared to is Vps60_KO.

	EVs abundance (mega counts)		
Predictors	**Estimates**	**Confidence interval**	**P-value**
(Intercept)	278.82	51.42 – 506.23	**0.024**
parasite 3D7	197.78	-123.83 – 519.38	0.183
parasite R561H	113.31	-208.29 – 434.91	0.422
Observations	9		
R^2 / R^2 adjusted	0.275 / 0.034		

University of Ghana http://ugspace.ug.edu.gh

Supplementary Table 7.5 Tabular summary of simple linear regression model to determine strength of the association between parasite line (predictor/independent factors) and EVs abundance (response/dependent factor) for the 0.1% DMSO treated condition. Baseline reference to which parasite lines were compared to is Vps60_KO.

	EVs abundance (mega counts)		
Predictors	**Estimates**	**Confidence interval**	**P-value**
(Intercept)	105.57	-525.37 – 736.51	0.696
parasite 3D7	693.35	-198.93 – 1585.64	0.106
parasite R561H	198.84	-693.44 – 1091.13	0.605
Observations	9		
R^2 / R^2 adjusted	0.390 / 0.187		

University of Ghana http://ugspace.ug.edu.gh

Supplementary Table 7.6 Tabular summary of simple linear regression model to determine strength of the association between parasite line (predictor/independent factors) and EVs abundance (response/dependent factor) for the 700nM DHA treated condition. Baseline reference to which parasite lines were compared to is Vps60_KO.

	EVs abundance (mega counts)		
Predictors	**Estimates**	**Confidence interval**	**P-value**
(Intercept)	2460.32	623.12 – 4297.52	**0.017**
parasite 3D7	-1541.26	-4139.45 – 1056.94	0.197
parasite R561H	-1576.42	-4174.62 – 1021.78	0.188
Observations	9		
R^2 / R^2 adjusted	0.324 / 0.099		

University of Ghana http://ugspace.ug.edu.gh

Supplementary Table 7.7 Tabular summary of simple linear regression model to determine strength of the association between treatment condition (predictor/independent factors) and EVs abundance (response/dependent factor) for the Vps60_KO parasite line. Baseline reference to which treatment conditions were compared to is the untreated condition.

	EVs abundance (mega counts)		
Predictors	**Estimates**	**Confidence interval**	**P-value**
(Intercept)	278.82	-1495.72 – 2053.37	0.714
condition DMSO	-173.25	-2682.83 – 2336.33	0.871
condition DHA	2181.50	-328.09 – 4691.08	0.078
Observations	9		
R^2 / R^2 adjusted	0.522 / 0.363		

University of Ghana http://ugspace.ug.edu.gh

Supplementary Table 7.8 Tabular summary of simple linear regression model to determine strength of the association between treatment condition (predictor/independent factors) and EVs abundance (response/dependent factor) for the 3D7 parasite line. Baseline reference to which treatment conditions were compared to is the untreated condition.

	EVs abundance (mega counts)		
Predictors	**Estimates**	**Confidence interval**	**P-value**
(Intercept)	476.60	-232.66 – 1185.86	0.151
condition DMSO	322.33	-680.72 – 1325.37	0.462
condition DHA	442.46	-560.58 – 1445.51	0.322
Observations	9		
R^2 / R^2 adjusted	0.172 / -0.104		

University of Ghana http://ugspace.ug.edu.gh

Supplementary Table 7.9 Tabular summary of simple linear regression model to determine strength of the association between treatment condition (predictor/independent factors) and EVs abundance (response/dependent factor) for the R561H parasite line. Baseline reference to which treatment conditions were compared to is the untreated condition.

	EVs abundance (mega counts)		
Predictors	**Estimates**	**Confidence interval**	**P-value**
(Intercept)	392.13	-23.88 – 808.14	0.061
condition DMSO	-87.71	-676.04 – 500.61	0.728
condition DHA	491.77	-96.56 – 1080.10	0.087
Observations	9		
R^2 / R^2 adjusted	0.529 / 0.373		